Reaction of Aromatic *N*-Oxides with Dipolarophiles. XVI.[1] Cycloaddition Behavior of Aromatic *N*-Oxides toward Electron-Deficient Allenes and X-Ray Structure of the 1,4-Dipolar Cycloadduct

Takuzo HISANO,* Kazunobu HARANO, Toshikazu MATSUOKA, Tatsuya MATSUZAKI and Masashi ETO

Faculty of Pharmaceutical Sciences, Kumamoto University, 5–1 Oe-honmachi, Kumamoto 862, Japan. *Received May 23, 1990*

In connection with the pericyclic reaction of pyridine *N*-oxides with dipolarophiles, the cycloaddition behavior of some aromatic *N*-oxides toward electron-deficient allenes was investigated. In the reaction of 2-phenylpyridine *N*-oxide with dimethyl 2,3-pentadienedioate, the 2,3-dihydropyridine type 1 : 1 cycloadducts, which resulted from 1,5-sigmatropic rearrangement of the primary cycloadduct, were isolated. The reaction of 3,5-dihalogenopyridine *N*-oxides with the allene gave the dehydrohalogenated cycloadducts of the 1,5-sigmatropic rearrangement products. The reaction of 3,5-dimethylpyridine *N*-oxide with the allene caused deoxygenation to give 3,5-dimethylpyridine, which in turn reacted with two molecules of the allene to give the 1 : 2 cycloadduct (1,4-dipolar cycloaddition product). The structure of the cycloadduct was determined by single crystal X-ray analysis.

The observed reaction behaviors are discussed in terms of frontier molecular orbital considerations.

Keywords pericyclic reaction; frontier molecular orbital; 1,3-dipolar cycloaddition; 1,4-dipolar cycloaddition; allene; reactivity; X-ray analysis; pyridine *N*-oxide; 1,5-sigmatropy

During the course of an investigation of the 1,3-dipolar cycloaddition reaction of pyridine *N*-oxides with *N*-substituted maleimides, an important question arose concerning the cycloaddition reactivity, *i.e.*, why does only 3,5-dimethylpyridine *N*-oxide show reactivity toward *N*-substituted maleimides?[2a,b] We concluded that the inertness of other types of pyridine *N*-oxides such as unsubstituted pyridine *N*-oxide or 3-methylpyridine *N*-oxide might be attributable to their high degree of aromaticity and stabilization of the ground state by charge-transfer (CT) complex formation[3] between the dipoles and dipolarophiles.

It is well known that cyclic planar addends are prone to form the coplanar π,π-complex at an early point in the reaction coordinate, leading to the formation of the CT complex, which stabilize the ground state energy of the reaction system prior to cycloaddition. In order to avoid such a ground-state stabilization, we tried to use electron-deficient allenes which do not have a cyclic planar π-electron system, but have an orthogonal π-electron system.

This paper describes the results of cycloaddition of pyridine *N*-oxides (I) with dimethyl 2,3-pentadienedioate (II).

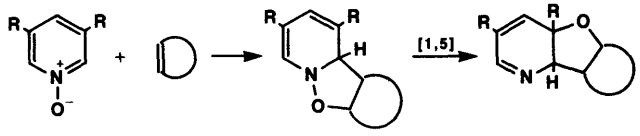

Chart 1

Results

Cycloaddition of 2-Phenylpyridine *N*-Oxide (Ia) with Dimethyl 2,3-Pentadienedioate (II) Pyridine *N*-oxide bearing a phenyl substituent at the 2-position (Ia) readily reacted with II to give a mixture of 1 : 1 cycloadducts assignable to the isomers due to the *exo* and *endo* cycloadditions (IIIa and III'a) (Charts 2 and 3). The pericyclic reaction pathways leading to the 1,5-sigmatropic rearrangement products are depicted in Chart 3. The products were separated by chromatography on silica gel. The infrared (IR) spectra of the isolated crystals (IIIa and III'a) showed conjugated and unconjugated carbonyl absorption bands at *ca.* 1700 and 1740 cm^{-1}, respectively. The carbon nuclear magnetic resonance (^{13}C-NMR) spectra showed three sp^3 carbons, suggesting that the products are not the primary adducts (two sp^3 carbons) but the 1,5-sigmatropically rearranged products, and also showed signals due to an olefinic carbon attached to an oxygen atom (*ca.* 158 ppm, –O–C=) and a carbon ascribable to >C=CH–COOMe (*ca.* 90 ppm).

The stereochemistries of IIIa and III'a were determined by careful inspection of their proton nuclear magnetic resonance (^{1}H-NMR) spectral data. The proton on the exocyclic double bond [–O–C(R)=CH(COOMe)] of IIIa and III'a resonated at 5.36 and 5.31 ppm, respectively. The configuration of the proton is considered to be *trans* with

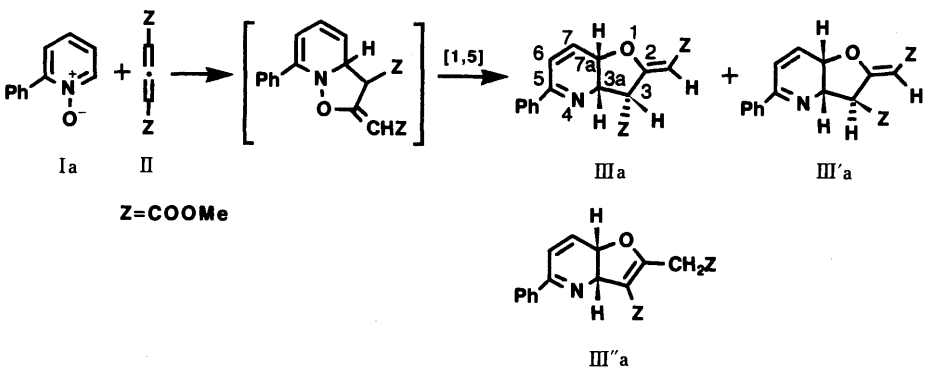

Ia II IIIa III'a

Z=COOMe

III"a

Chart 2

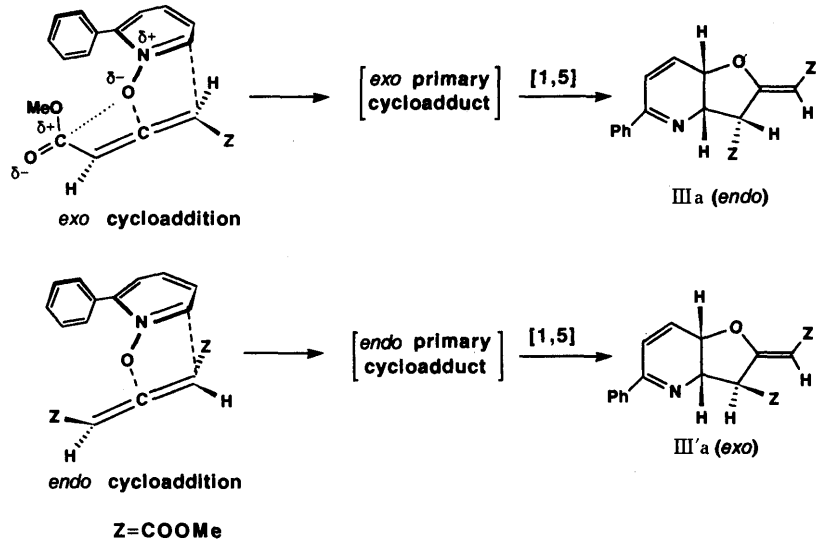

Chart 3

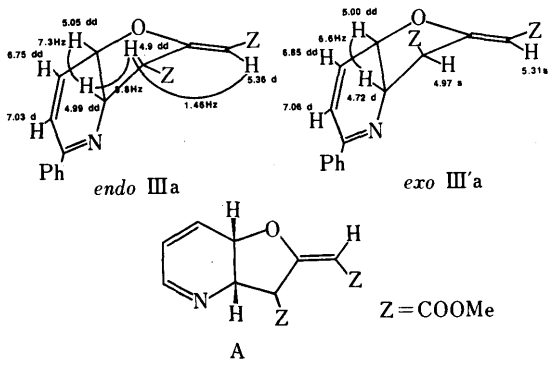

Fig. 1. ^{1}H-NMR Spectral Data of IIIa and III'a Formed by Cycloaddition of 2-Phenylpyridine *N*-Oxide (Ia) with the Allene (II)

respect to the ether group in each case on the basis of the chemical shifts of structurally similar compounds.[4a] This observation rules out the possibility that the ether group and the olefinic proton of the double bond are *cis*-oriented (see structure A in Fig. 1).[4b]

Next, the configuration of the methoxycarbonyl group on C_3, which reflects the stereochemistry of the cycloaddition (*endo–exo* nature of IIIa and III'a) was determined on the basis of the coupling constant between the C_3- and C_{3a}-protons. The ^{1}H-NMR spectral data are shown in Fig. 1. The C_3-proton of IIIa appeared as a weakly split doublet, whereas the proton of III'a appeared as a singlet. Molecular models, which satisfy the above spectral behaviors, suggest that the tetrahydrofuran rings takes a puckered conformation as depicted in Fig. 1.

Inspection of the correlation[4c] between the angle between the plane of the exocyclic double bond and the adjacent σ-bond (C_3-H) and the allylic coupling constant (J_{al}) also supports the assignments. In IIIa, the C_3 proton resonance occurs as a doulbet of doublet ($J_{al}=1.46$ Hz), indicating that the C_3 proton is approximately parallel with the π-orbital of the double bond. However, in III'a, the olefinic resonance appears as a singlet, since allylic coupling to the exocyclic proton is very small ($J_{al}<0.2$ Hz), indicating that the C_3 proton lies nearly in the plane of the double bond.

In the *endo* adduct (IIIa), there appears to be a sizable amount of van der Waals compression between the methoxycarbonyl group and its environment, whereas, in the case of *exo* adduct (III'a), such an interaction must not be serious. This would be consistent with the fact that compound IIIa exhibited the unconjugated ester carbonyl absorption at 1748 cm^{-1}, which is 10 cm^{-1} higher than that of III'a.

It should be noted that the exocyclic double bonds of IIIa and III'a did not isomerize to the endocyclic form (III''a) under the reaction conditions used (see Chart 2).

Cycloaddition of 3,5-Dichloropyridine *N*-Oxide (Ib) and 3,5-Dibromopyridine *N*-Oxide (Ic) with II The 1,3-dipole (Ib) showed high reactivity toward the allene (II), giving the cycloadduct IIIb as a sole product. The mass spectrum (MS) of IIIb showed an M^+ peak suggesting the formation of the furopyridine-type compound through elimination of HCl from the 1,5-sigmatropically rearranged product. The IR spectrum of IIIb exhibited two carbonyl absorption bands at 1740 and 1712 cm^{-1}. The adduct IIIb showed a simple ^{1}H-NMR spectral pattern consisting of a singlet peak due to Ar–CH_2COO– and two aromatic protons having a *meta* coupling. The alternative structure of III'b can be excluded based on the chemical shift of the α-carbon of the furan ring and the other examples of the cycloaddition studied in this work. The presence of triethylamine as a trapping agent for HCl gave a higher yield as compared with the reaction carried out without the base.

In the case of the reaction of 3,5-dibromopyridine *N*-oxide (Ic) with II, a similar result was obtained to give IIIc.

Cycloaddition of Quinoline *N*-Oxide (Id) with II The reaction of Id with II gave pale yellow crystals (IIId). The MS suggested formation of the 1 : 1 adduct. The ^{1}H-NMR spectrum exhibited a broad signal at 17.28 ppm due to a hydrogen-bonded proton. These results indicate that the primary adduct underwent ring cleavage to give the 2-methylene-type compound, which transformed into the 2-vinyl-type compound (see Chart 5). In this reaction, the 1,5-sigmatropic rearrangement could not be observed.

Cycloaddition of 3,5-Dimethylpyridine *N*-Oxide (Ie) with II When II was added to a solution of Ie in $CHCl_3$, the reaction mixture showed a red color. Purification of the product by silica gel chromatography gave unstable orange crystals. When a solution of the crystals in benzene was

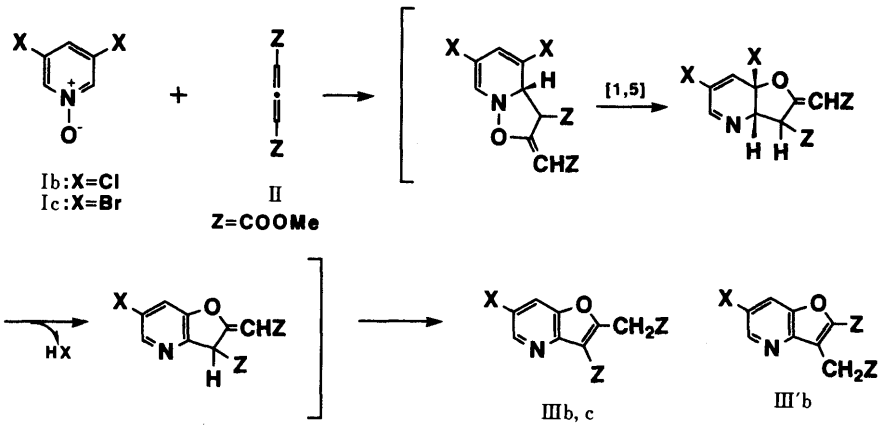

Chart 4

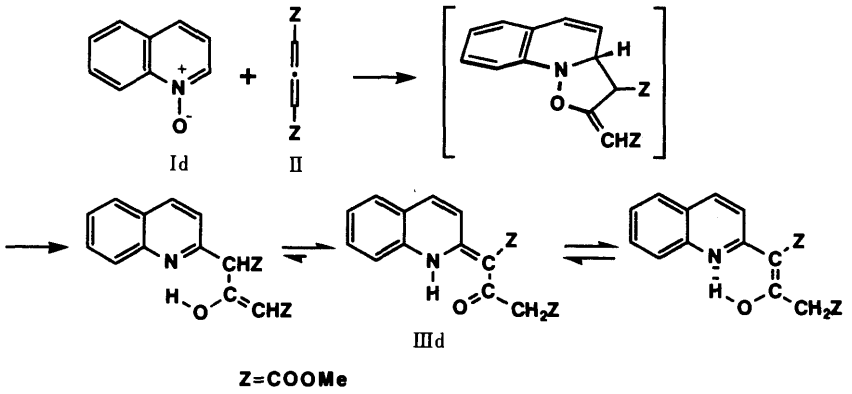

Chart 5

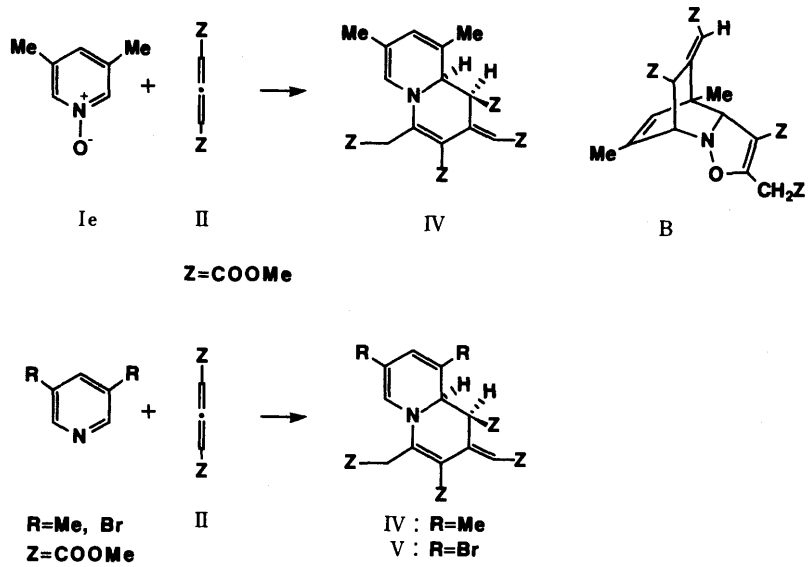

Chart 6

allowed to stand overnight at room temperature, several spots were recognized on a thin layer chromatogram. The MS of the product suggested that the cycloaddition of Ie with II gave a 1 : 2 cycloadduct (IV). However, the high resolution MS (HRMS) did not give definitive evidence for the 1 : 2 adduct because the product contained a small amount of impurities. The IR spectrum of IV showed three carbonyl absorption bands at 1760, 1741 and 1708 cm^{-1}. From these observations, we considered the product to be the [4+2]π cycloadduct (B) of the 1,5-sigmatropically rearranged product and II. However, the visible absorption spectrum of IV exhibited an absorption maximum at 480 nm due to a highly conjugated structure and a ^{1}H-NMR study of IV was in apparent disagreement with the structure B. Therefore, we performed a single crystal X-ray analysis.

Fortunately, single crystals of the adduct could be obtained by slow evaporation of a solution in benzene. The structure was solved by the direct method using the

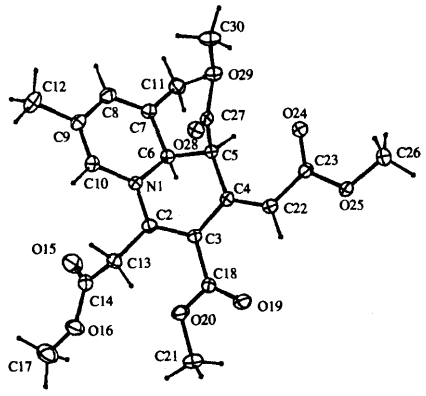

Fig. 2. ORTEP Perspective View of the Cycloadduct (IV), Showing the Atomic Numbering Used in Tables I—III

Table I. Fractional Atomic Coordinates[a] and Isotropic Temperature Factors (B) for Non-hydrogen Atoms with Their Estimated Standard Deviations in Parentheses

Atom	x/a	y/b	z/c	B[b]
N1	2746 (4)	3803 (3)	5538 (3)	3.07 (13)
C2	3238 (5)	2789 (4)	6383 (4)	3.20 (17)
C3	2585 (5)	1486 (4)	6103 (4)	3.23 (17)
C4	1778 (5)	1311 (4)	4713 (4)	3.02 (16)
C5	1218 (5)	2451 (4)	3802 (4)	2.89 (16)
C6	1301 (5)	3335 (4)	4699 (4)	2.97 (16)
C7	698 (5)	4469 (4)	3932 (4)	3.14 (17)
C8	1506 (5)	5760 (4)	3927 (4)	3.95 (19)
C9	2974 (5)	6166 (4)	4655 (4)	3.70 (19)
C10	3537 (5)	5211 (4)	5429 (4)	3.49 (18)
C11	−837 (5)	4013 (5)	3252 (5)	4.21 (20)
C12	3830 (6)	7650 (5)	4568 (6)	5.39 (23)
C13	4509 (5)	3101 (4)	7544 (4)	3.31 (17)
C14	4187 (5)	3226 (4)	8759 (4)	3.93 (19)
O15	3342 (4)	3692 (4)	8687 (3)	5.86 (17)
O16	5019 (4)	2777 (3)	9920 (3)	5.19 (15)
C17	4825 (8)	2825 (7)	11186 (5)	7.34 (31)
C18	2786 (5)	293 (4)	7186 (4)	4.04 (19)
O19	2816 (5)	−726 (4)	7047 (3)	7.48 (19)
O20	2892 (4)	429 (3)	8423 (3)	4.71 (13)
C21	2972 (6)	−736 (5)	9546 (5)	5.77 (24)
C22	1574 (5)	232 (4)	4256 (4)	3.75 (18)
C23	837 (5)	51 (4)	2856 (4)	3.73 (18)
O24	468 (4)	874 (3)	1898 (3)	5.08 (14)
O25	624 (4)	−1214 (3)	2764 (3)	4.84 (14)
C26	−120 (7)	−1530 (5)	1425 (5)	6.13 (25)
C27	1994 (5)	3322 (4)	2690 (4)	3.24 (17)
O28	3206 (3)	3587 (3)	2800 (3)	4.35 (13)
O29	1128 (3)	3831 (3)	1587 (3)	4.02 (12)
C30	1752 (6)	4706 (6)	459 (5)	5.95 (25)

a) Positional parameters are multiplied by 10^4. *b*) Thermal parameters are given by the equivalent temperature factors (Å^2).

MULTAN78 program[5] and refined by the block-diagonal least-square method. The final *R* value obtained was 0.05. The ORTEP[6] drawing shown in Fig. 2 reveals the product to have a 9*H*-quinolizine-type structure, presumably derived from deoxygenation of 3,5-dimethylpyridine *N*-oxide (Ie) followed by cycloaddition with two molecules of II. The sum of the angles around the N_1 nitrogen atom is about 360, indicating that the N_1 is an sp^2 nitrogen. The atoms of C_7, C_8, C_9, C_{10}, N_1, C_2 and C_3 make a planar structure with which the π-plane defined by the C_4 and C_{22} atoms makes an angle of 25°. The bond lengths indicate that the 14π-electrons form a resonance structure consistent with

Table II. Bond Distances (Å) for Non-hydrogen Atoms with Their Estimated Standard Deviations in Parentheses

Atom 1	Atom 2	Distance	Atom 1	Atom 2	Distance
N1	–C2	1.352 (6)	N1	–C6	1.478 (5)
N1	–C10	1.416 (5)	C2	–C3	1.399 (6)
C2	–C13	1.503 (6)	C3	–C4	1.468 (6)
C3	–C18	1.468 (6)	C4	–C5	1.515 (6)
C4	–C22	1.341 (8)	C5	–C6	1.539 (8)
C5	–C27	1.515 (6)	C6	–C7	1.509 (7)
C7	–C8	1.327 (6)	C7	–C11	1.501 (7)
C8	–C9	1.454 (7)	C9	–C10	1.326 (7)
C9	–C12	1.499 (6)	C13	–C14	1.515 (8)
C14	–O15	1.191 (8)	C14	–O16	1.331 (5)
O16	–C17	1.459 (9)	C18	–O19	1.196 (8)
C18	–O20	1.339 (7)	O20	–C21	1.442 (6)
C22	–C23	1.467 (6)	C23	–O24	1.192 (5)
C23	–O25	1.348 (6)	O25	–C26	1.456 (6)
C27	–O28	1.190 (7)	C27	–O29	1.343 (5)
O29	–C30	1.442 (6)			

Table III. Bond Angles (°) of IV for Non-hydrogen Atoms with Their Estimated Standard Deviations in Parentheses

Atom 2–atom 1–atom 3			Angle	Atom 2–atom 1–atom 3			Angle
C2	–N1	–C6	114.8 (3)	C2	–N1	–C10	123.8 (4)
C6	–N1	–C10	121.5 (4)	N1	–C2	–C3	118.6 (4)
N1	–C2	–C13	119.6 (4)	C3	–C2	–C13	121.8 (4)
C2	–C3	–C4	120.6 (4)	C2	–C3	–C18	119.6 (4)
C4	–C3	–C18	119.7 (4)	C3	–C4	–C5	115.7 (4)
C3	–C4	–C22	122.6 (4)	C5	–C4	–C22	121.6 (4)
C4	–C5	–C6	108.9 (3)	C4	–C5	–C27	112.4 (5)
C6	–C5	–C27	110.7 (3)	N1	–C6	–C5	109.6 (5)
N1	–C6	–C7	113.7 (3)	C5	–C6	–C7	114.7 (3)
C6	–C7	–C8	112.0 (4)	C6	–C7	–C11	115.3 (4)
C8	–C7	–C11	124.7 (5)	C7	–C8	–C9	123.4 (5)
C8	–C9	–C10	119.4 (4)	C8	–C9	–C12	120.3 (5)
C10	–C9	–C12	120.3 (4)	N1	–C10	–C9	121.4 (4)
C2	–C13	–C14	112.9 (5)	C13	–C14	–O15	125.1 (4)
C13	–C14	–O16	110.0 (5)	O15	–C14	–O16	124.8 (5)
C14	–O16	–C17	116.4 (6)	C3	–C18	–O19	127.0 (5)
C3	–C18	–O20	112.0 (5)	O19	–C18	–O20	120.9 (4)
C18	–O20	–C21	116.4 (5)	C4	–C22	–C23	124.4 (4)
C22	–C23	–O24	127.2 (5)	C22	–C23	–O25	110.4 (4)
O24	–C23	–O25	122.4 (4)	C23	–O25	–C26	115.8 (4)
C5	–C27	–O28	125.5 (4)	C5	–C27	–O29	109.5 (4)
O28	–C27	–O29	124.8 (4)	C27	–O29	–C30	115.1 (4)

the visible absorption spectrum observed at 480 nm. The stereochemistry of the two hydrogen atoms on C_5 and C_6 is revealed to be *cis*.

1,4-Dipolar Reactions of 3,5-Dimethylpyridine and 3,5-Dibromopyridine with II In order to clarify the formation mechanism of IV, the reaction of 3,5-dimethylpyridine with II was carried out. When 3,5-dimethylpyridine was mixed with II at room temperature, an exothermic reaction took place to afford IV in 63% yield. In the case of 3,5-dibromopyridine, a similar reaction occurred to afford the 1 : 2 adduct (V).

The structure of V was determined by comparison of the IR and ^{1}H-NMR spectral data with those of IV.

Reactions of Other Pyridine *N*-Oxides with II The allene (II) showed moderate cycloaddition reactivity toward both unsubstituted and electron-deficient pyridine *N*-oxides even at room temperature.

In the reaction of 3-methoxycarbonylpyridine *N*-oxide

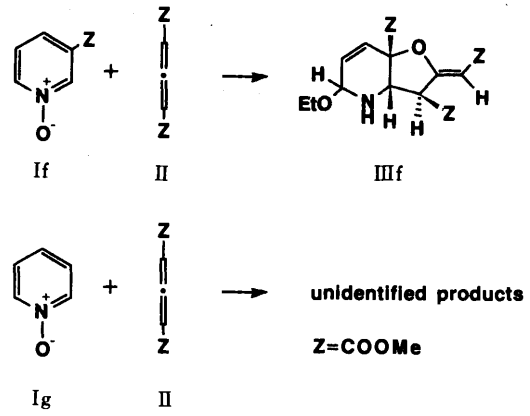

Chart 7

(If) with II, the reaction solution turned red, indicating that the 1,4-dipolar cycloaddition took place. However, the corresponding 1,4-dipolar cycloadduct could not be isolated. The thin-layer chromatogram of the reaction mixture showed the presence of several products. The product isolated was colorless crystals (IIIf), and was determined to be an addition compound of the 1,5-sigmatropic rearrangement product and ethanol. The stereochemistry was confirmed by comparison of the ^{1}H-NMR spectral data with those of IIIa and III'a (Chart 7).

The reaction of pyridine *N*-oxide (Ig) with II gave not only the 1,5-sigmatropic rearrangement product but also the 1,4-dipolar cycloaddition product, though their structures have not yet been determined by spectroscopic methods. A coherent interpretation of the spectral data and suitable single crystals for X-ray analysis have not yet been obtained. 3-Methylpyridine *N*-oxide showed similar reaction behavior.

Discussion

As mentioned above, the dimethyl pentadienedioate (II) showed high reactivity toward aromatic *N*-oxides bearing both electron-donating and accepting substituents and the reactions proceeded at room temperature to give the cycloadducts. This is in sharp contrast to the reaction conditions (100—130 °C) required in the 1,3-dipolar cycloaddition reaction with dipolarophiles such as phenyl isocyanate,[7] *N*-substituted maleimides[2a] or epoxynaphthalene.[3b]

As far as we know, there has been no report concerned with the cycloadducts formed by the 1,3-dipolar cycloaddition of aromatic *N*-oxides with allenes.[8] In order to understand the reaction behavior, modified neglect of diatomic overlap (MNDO)[9] calculations were performed. The calculated orbital energy levels and coefficients are listed in Table IV.

As can be seen in Fig. 3, the reaction of pyridine *N*-oxides with II falls into the category of a "normal-type" reaction in Sustmann's classification[10] for cycloadditions, wherein the dominant interaction is the one between the highest occupied molecular orbital (HOMO) of the 1,3-dipole and the lowest unoccupied molecular orbital (LUMO) of the dipolarophile. In the case of 3,5-dichloropyridine *N*-oxide (Ib), the frontier molecular orbital (FMO) energy levels lie between the FMO energy levels of the allene (II), indicating that the "inverse-type" interaction also plays an important role in determining the cycloaddition reactivity. A similar argument may be applied to the reaction behavior of 2-phenylpyridine *N*-oxide (Ia) because phenyl groups compress the FMO energy levels.[11b]

The LUMO energy level (−1.16 eV) of maleimide is considerably lower than that of II (−0.45 eV) implying that maleimides would show higher cycloaddition reactivity toward I than the allene (II) if only FMO separation was considered. Contrary to expectation, the experimental results are inconsistent with the FMO prediction. This indicates that the primary FMO interaction energy between I and II is perhaps not the sole factor responsible for the high reactivity. Inspection of the MNDO calculation data of pyridine *N*-oxides (I) and II suggests that the huge lobe of the p_y orbital (in the molecular plane) exists on the oxygen atom of I in the next HOMO (NHOMO), which can strongly interact with the p_y orbital of the central carbon atom of II, stabilizing the transition state (Fig. 4). This interaction may contribute to the formation of the $=C=\cdots O\leftarrow N\lesssim$ bond, building up the resonance structure

TABLE IV. MNDO Calculation Data for Pyridine *N*-Oxide (Ig), 3,5-Dichloropyridine *N*-Oxide (Ib), 3,5-Dimethylpyridine *N*-Oxide (Ie) and Dimethyl 2,3-Pentadienedioate (II)

Calcd values		Ig[a]	Ib	Ie	II
LUMO (eV),		−0.474	−1.148	−0.473	−0.45
Coefficients (p_z)	O	−0.393	0.393	0.379	
	N	0.529	−0.511	−0.512	
	C	−0.287	0.225	0.254	
					C_1 −0.459
					C_2 0.536
HOMO[a] (eV),		−8.769	−9.351	−8.737	−10.9
Coefficients (p_z)	O	−0.646	0.640	0.649	
	N	0.226	−0.214	−0.227	
	C	0.379	−0.388	−0.376	
					C_1 0.620
					C_2 0.544
Net charges	O	−0.421	−0.394	−0.429	
	N	0.263	0.267	0.261	
	C	−0.080	−0.063	−0.063	
					C_1 −0.026
					C_2 −0.034

a) The large in-plane coefficient (p_y −0.922) was on oxygen in NHOMO (−10.698 eV).

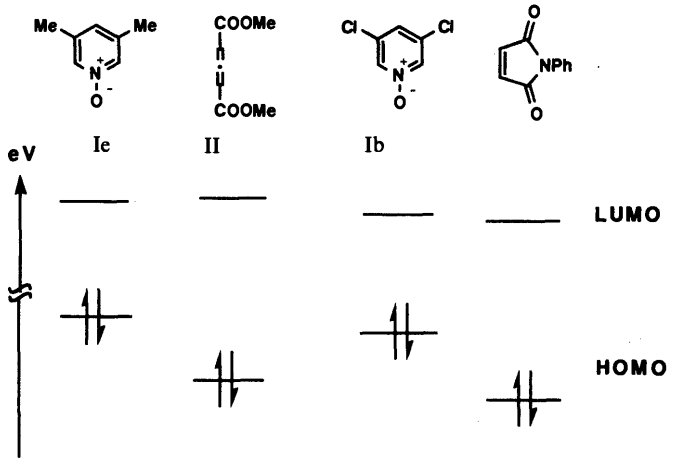

Fig. 3. FMO Interactions of 3,5-Dichloropyridine *N*-Oxide (Ib) and 3,5-Dimethylpyridine *N*-Oxide (Ie) with the Allene (II) and Maleimide

of the enol ether moiety in the primary cycloadduct.[12]

As regards the regiochemistry of the 1,3-dipolar reaction, the observed regiochemistry of the reaction of I with the allene (II) follows the principle of maximum overlap of the FMO theory[11] as exemplified in Fig. 4. Bonding occurs between the central carbon of II and the oxygen atom of I where the largest coefficients of the interacting frontier orbitals are found. The net charges of II are very small, indicating that the coulombic interaction may be unimportant as a controlling factor in the early stage of the reaction.

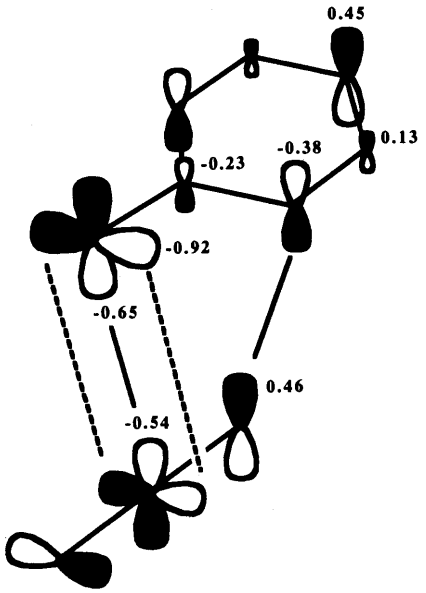

Fig. 4. Secondary Interactions in the Cycloaddition of Pyridine *N*-Oxide (Ig) with Allenes

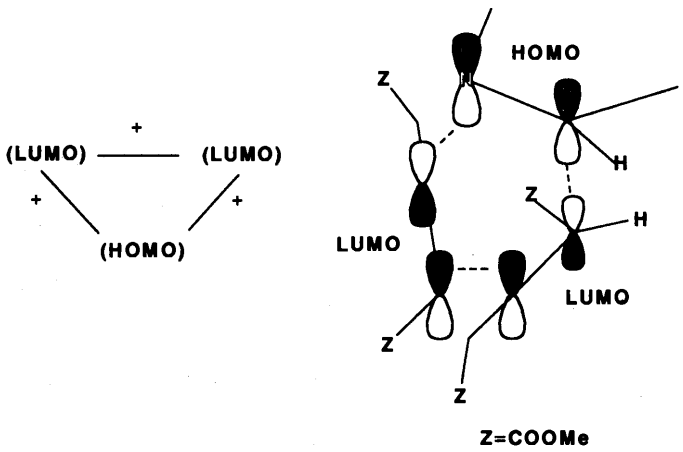

Fig. 5. Three System Interaction for the 1,4-Dipolar Cycloaddition of Pyridines with II

The *endo*-selectivity could not be observed, as exemplified in the 1,3-dipolar reaction of 2-phenylpyridine *N*-oxide (Ia) with II, in which a 1:1 mixture of the *endo* and *exo* cycloadducts was obtained. In the reaction, the secondary orbital overlap[2] between the nitrogen of Ia and the carbonyl carbon of II is considered to be poor.

The configuration of the exocyclic double bonds of IIIa and III'a reflected the stereochemistry of the primary cycloaddition, in which the coulombic attraction of the oxygen atom of Ia and the carbonyl carbon of II may be operative (see Chart 3).

Though the deoxygenation mechanism is still obscure, the formation reaction of 9*H*-quinolizine-type compounds is formally considered to be a so-called "1,4-dipolar cycloaddition"[14] wherein 1,4-dipoles formed from pyridines plus allene react with an additional allene to give $[2\pi+2\pi+2\pi]$ cycloadducts. Taking into consideration that the reactions readily took place in a nonpolar solvent such as benzene, and the central allene carbon (C_β) has a small negative net charge (C_α -0.026, C_β -0.034), the reaction should proceed *via* a nonionic concerted transition state (Fig. 5) rather than *via* an ionic intermediate (see Chart 8). The formation of 9*H*-quinolizine-type compounds can be account for in terms of the three system interaction,[15] in which pyridines act as HOMO[16] and two molecules of allenes act as LUMO's. The structures of the cycloadducts follow the principle that the larger lobe should unite with the larger one (large–large/small–small interaction) according to the perturbation theory.[11b]

An important factor which must be taken into consideration in the interpretation of the cycloaddition behavior of I toward dipolarophiles is the stability of the reactants, *e.g.*, the high degree of aromaticity of I.[7] It is worth mentioning that in the reaction of I with II, the orbital interaction energy overcomes the aromaticity of I.

Experimental

All melting points are uncorrected. ^{1}H-NMR spectra were taken with Hitachi R-600 and JEOL GX-400 spectrometers for *ca.* 10% (w/v) solutions, with tetramethylsilane (TMS) as an internal standard; chemical shifts are expressed in δ values. IR spectra were recorded on a Hitachi 270-30 infrared spectrophotometer. Visible absorption spectra were taken with a Hitachi 150-20 spectrometer. MS were taken with a JEOL JMS-DX303HF double-focussing spectrometer operating at an ionization

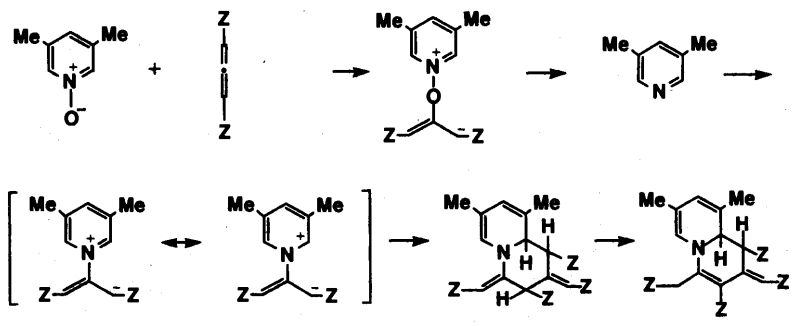

Chart 8

potential of 75 eV. Flash chromatography was carried out with Merck Silica Gel 60.

Molecular orbital (MO) calculations were performed on a FACOM M-360 computer at the Information Processing Center of Kumamoto University. Graphic analysis of the MO calculation and X-ray data were performed on a FACOM G-150 work station and a Fujitsu FMR-60HD personal computer.

Materials Dimethyl 2,3-pentadienedioate (II),[17] 2-phenylpyridine *N*-oxide (Ia),[18] 3,5-dichloropyridine *N*-oxide (Ib),[18] 3,5-dibromopyridine *N*-oxide (Ic),[18] quinoline *N*-oxide (Id),[18] 3,5-dimethylpyridine *N*-oxide (Ie),[18] 3-methoxycarbonylpyridine *N*-oxide (If)[18] and pyridine *N*-oxide (Ig)[18] were prepared according to the established methods.

Cycloaddition of 2-Phenylpyridine *N*-Oxide (Ia) with Dimethyl 2,3-Pentadienedioate (II) Compound II (13 mmol) was added to a solution containing Ia (10 mmol) in CH_2Cl_2. After the addition was complete, the mixture was stirred at room temperature for 12 h. The solvent was evaporated off. The residue was submitted to silica gel chromatography using a benzene : ethyl acetate (4 : 1) mixture as the eluent to give IIIa (yield 8.6%) and III'a (yield 8.3%).

exo Adduct (IIIa): mp 144—146 °C (colorless prisms from benzene). IR (KBr): 1738, 1700 (C=O) cm^{-1}. ^{1}H-NMR (in $CDCl_3$) δ: 3.58 (3H, s, COOMe), 3.78 (3H, s, COOMe), 4.72 (1H, d, J=6.6 Hz, C_{3a}-H), 4.97 (1H, s, C_3-H), 5.00 (1H, dd, J=6.6, 5.8 Hz, C_{7a}-H), 5.31 (1H, s, $C_{2'}$-H), 6.85 (1H, dd, J=5.8, 10.2 Hz, C_7-H), 7.06 (1H, d, J=10.2 Hz, C_6-H), 7.49—7.92 (5H, m, Ar). ^{13}C-NMR (in Acetone-d_6) δ: 51.0 (q, OMe), 52.9 (q, OMe), 58.5 (d, C_3), 63.7 (d, C_{3a}), 73.3 (d, C_{7a}), 90.0 (d, $C_{2'}$), 123.7 (d, C_6), 127.6 (d, Ar), 129.3 (d, Ar), 130.3 (d, C_7), 131.4 (d, Ar), 138.8 (s, Ar), 158.0 (s, C_2), 168.3 (s, C_5), 170.5 (s, C=O), 171.3 (s, C=O). MS m/z: 327 (M^+). HRMS, M^+ for $C_{15}H_{17}NO_5$ m/z: 327.1107. Found: 327.1102.

endo Adduct (III'a): mp 119—122 °C (colorless needles from benzene). IR (KBr): 1748, 1704 (C=O) cm^{-1}. ^{1}H-NMR (in $CDCl_3$) δ: 3.57 (3H, s, COOMe), 3.66 (3H, s, COOMe), 4.90 (1H, d, J=8.8 Hz, C_3-H), 4.99 (1H, dd, J=7.3, 8.8 Hz, C_{3a}-H), 5.05 (1H, dd, J=5.1, 10.2 Hz, C_{7a}-H), 5.36 (1H, d, J=1.46 Hz, $C_{2'}$-H), 6.75 (1H, dd, J=5.1, 10.2 Hz, C_7-H), 7.03 (1H, d, J=10.2 Hz, C_6-H), 7.49—7.92 (5H, m, Ar). ^{13}C-NMR (in acetone-d_6) δ: 50.9 (q, OMe), 51.9 (q, OMe), 56.3 (d, C_3), 60.5 (d, C_{3a}), 72.9 (d, C_{7a}), 92.6 (d, $C_{2'}$), 122.9 (d, C_6), 127.5 (d, Ar), 129.1 (d, Ar), 129.3 (d, Ar), 130.5 (d, C_7), 131.2 (d, Ar), 138.5 (s, Ar), 158.5 (s, C_2), 168.3 (s, C_5), 168.5 (s, C=O), 170.2 (s, C=O). MS m/z: 327 (M^+). HRMS, M^+ for $C_{15}H_{17}NO_5$ m/z: 327.1107. Found: 327.1095.

Cycloadditions of 3,5-Dichloropyridine *N*-Oxide (Ib) or 3,5-Dibromopyridine *N*-Oxide (Ic) with II Compound II (6 mmol) was added to a solution containing Ib or Ic (3 mmol) in tetrahydrofuran (THF) (10 ml). After the addition was complete, the mixture was stirred at room temperature for 24 h. The solvent was evaporated off. The residue was submitted to silica gel chromatography using a hexane : ethyl acetate (1 : 1) mixture as the eluent to give IIIb (yield 38%) or IIIc (yield 17%). The reaction of Ib with II in the presence of triethylamine gave IIIb in 69% yield.

Adduct (IIIb): mp 111—112 °C (colorless needles from benzene). IR (KBr): 1740, 1712 (C=O) cm^{-1}. ^{1}H-NMR (in $CDCl_3$) δ: 3.76 (3H, s, COOMe), 4.02 (3H, s, COOMe), 4.32 (2H, s, $-CH_2-$), 7.82 (1H, d, J=2.0 Hz, Ar), 8.86 (1H, J=2.0 Hz, Ar). MS m/z: 283, 285 (M^+, relative intensity 3 : 1). HRMS, M^+ for $C_{12}H_{10}{}^{35}ClNO_5$ m/z: 283.6247. Found: 283.0252. M^+ for $C_{12}H_{10}{}^{37}ClNO_5$ m/z: 285.0222. Found: 285.0243.

Adduct (IIIc): mp 109—111 °C (colorless prisms from benzene). IR (KBr): 1738, 1710 (C=O) cm^{-1}. ^{1}H-NMR (in $CDCl_3$) δ: 3.73 (3H, s, COOMe), 4.02 (3H, s, COOMe), 4.31 (2H, s, $-CH_2-$), 7.96 (1H, d, J=2.0 Hz, Ar), 8.76 (1H, J=2.0 Hz, Ar). MS m/z: 327, 330 (M^+, relative intensity 1 : 0.88). HRMS, M^+ for $C_{12}H_{10}{}^{79}BrNO_5$ m/z: 326.9742. Found: 326.9720. M^+ for $C_{12}H_{10}{}^{81}BrNO_5$ m/z: 328.9724. Found: 328.9723.

Reaction of Quinoline *N*-Oxide (Id) with II A solution of II (10 mmol) in absolute benzene (5 ml) was added to a solution containing Id (10 mmol) in absolute benzene was added. After the addition was complete, the mixture was stirred at room temperature for 2 h. The solvent was evaporated off. The solid was recrystallized from benzene–MeOH to give IIId in 37% yield. mp 116—118 °C (pale yellow prisms from benzene–MeOH). IR (KBr): 1738, 1680, 1634 (C=O) cm^{-1}. ^{1}H-NMR (in $CDCl_3$) δ: 3.77 (3H, s, COOMe), 3.82 (3H, s, COOMe), 3.86 (2H, s, $-CH_2-$), 7.39—8.13 (5H, m, Ar), 17.28 (1H, br, NH). MS m/z: 301 (M^+). HRMS, M^+ for $C_{16}H_{15}NO_5$ m/z: 301.0950. Found: 301.0937.

Cycloaddition of 3,5-Dimethylpyridine *N*-Oxide (Ie) with II Compound II (4 mmol) was added to a solution containing Ie (4 mmol) in $CHCl_3$. After the addition was complete, the mixture was stirred at room temperature for 0.5 h. The solvent was evaporated off. The residue was submitted to silica gel chromatography using a hexane : ethyl acetate (1 : 1) mixture as the eluent to give IV. The crude product was dissolved in ether (20 ml). The ether solution was chilled in a refrigerator for 6 h to give red needles in 17% yield. mp 142—144 °C (red needles from ether). IR (KBr): 1760, 1741, 1708 (C=O) cm^{-1}. UV $\lambda_{max}^{cyclohexane}$ nm (ε): 288 (20000), 480 (16000). ^{1}H-NMR (in $CDCl_3$) δ: 1.67 (3H, s, C_1-Me), 1.91 (3H, C_3-Me), 3.53 (1H, d, J=17.5 Hz, $-CH_2-$), 3.57 (1H, d, J=17.5 Hz, $-CH_2-$), 3.63 (3H, s, COOMe), 3.67 (3H, s, COOMe), 3.75 (3H, s, –COOMe), 3.80 (3H, s, COOMe), 4.55 (1H, d, J=3 Hz, C_{9a}-H), 5.09 (1H, d, J=3 Hz, C_9-H), 5.67 (1H, s, C_2-H), 5.94 (1H, s, =CHCOO–), 6.06 (1H, s, C_4-H). ^{13}C-NMR (in $CDCl_3$) δ: 18.3 (q, OMe), 19.9 (q, C_3-Me), 36.6 (t, $-CH_2-$), 44.0 (d, C_9), 51.1, 51.8, 52.0, 52.5 (q, OMe), 106.9 (d, $C_{8'}$), 109.6 (s, C_1), 118.2 (d, C_4), 122.3 (d, C_2), 128.2 (s, C_3), 144.0 (s, C_7), 145.5 (s, C_6), 167.5, 168.2, 168.7, 169.0 (s, C=O). MS m/z: 419 (M^+). HRMS, M^+ for $C_{21}H_{25}NO_5$ m/z: 419.1580. Found: 419.1551.

Cycloaddition of 3,5-Dimethylpyridine with II 3,5-Dimethylpyridine (2.56 mmol) was added to a solution containing II (5.12 mmol) in $CHCl_3$ (10 ml) under ice-cooling. After the addition was complete, the mixture was stirred at room temperature for 0.5 h. The solvent was evaporated off. The residue was submitted to silica gel chromatography using a hexane : ethyl acetate (1 : 1) mixture as the eluent to give a red solid. The crude product was dissolved in ether (20 ml). The ether solution was chilled in a refrigerator for 6 h to give IV as orange needles in 63% yield. This compound was identical with the material obtained from the reaction of Ie and II.

Cycloaddition of 3,5-Dibromopyridine with II A solution containing 3,5-dibromopyridine (2 mmol) and II (6 mmol) in benzene (5 ml) was refluxed for 8 h. After cooling, the mixture was stirred at room temperature for 12 h. The solvent was evaporated off. The residue was submitted to silica gel chromatography using a hexane : ethyl acetate (1 : 4) mixture as the eluent to give red solid, which was dissolved in ether (20 ml). The ether solution was chilled in a refrigerator to give crude V (mp 116—121 °C) in 60% yield. The crude product was again purified by chromatography on silica gel to give a pure sample, mp 120—123 °C, in 36% yield. IR (KBr): 1746, 1728, 1704 (C=O) cm^{-1}. ^{1}H-NMR (in $CDCl_3$) δ: 3.46 (1H, d, J=17.6 Hz, $-CH_2-$), 3.65 (1H, d, J=17.6 Hz, $-CH_2-$), 3.70, 3.72, 3.77, 3.83 (3H, s, COOMe), 4.82 (1H, d, J=2.9 Hz, C_{9a}-H), 5.36 (1H, d, J=2.9 Hz, C_9-H), 5.88 (1H, s, $C_{8'}$-H), 6.43 (1H, split s, C_2-H), 6.62 (1H, split s, C_4-H). MS m/z: 547, 549, 551 (M^+, relative intensity 1 : 3 : 1).

Cycloaddition of 3-Methoxycarbonylpyridine *N*-Oxide (If) with Dimethyl 2,3-Pentadienedioate (II) Compound II (6.6 mmol) was added to a solution containing If (3.3 mmol) in $CHCl_3$. After the addition was complete, the mixture was stirred at 0 °C to room temperature for 48 h. The solvent was evaporated off. The residue was submitted to silica gel chromatography using a benzene : ethyl acetate (1 : 1) mixture as the eluent to give IIIf (yield 21%). mp 168—172 °C (colorless needles from benzene). IR (KBr): 1740, 1712 (C=O) cm^{-1}. ^{1}H-NMR (in DMSO-d_6) δ: 1.07 (3H, t, J=7.0 Hz, Me of ethyl), 3.54 (2H, q, J=7.0 Hz, methylene of ethyl), 3.57 (6H, s, two COOMe), 3.70 (3H, s, COOMe), 4.09 (1H, d, J=3.3 Hz, C_{3a}-H), 4.41 (d, J=3.3 Hz, N-H), 4.58 (1H, br s, C_3-H), 4.62 (1H, br s, C_5-H), 5.44 (1H, br s, >C=CZ–H), 7.43 (1H, br dd, J=6.8 Hz, C_6-H), 7.50 (1H, d, J=6.8 Hz, C_7-H). MS m/z: 355 (M^+ + EtOH), 324 (M^+ − OMe), 310 (M^+ − OEt), 138 (methyl nicotinate + H^+). HRMS, M^+ for $C_{16}H_{21}NO_6$ m/z: 355.1267. Found: 355.1250.

X-Ray Crystallography Crystal Data. $C_{21}H_{25}NO_5$ (IV) M=419.2: triclinic, a=10.818 (11) Å, b=11.026 (11) Å, c=10.677 (10) Å, α=70.36 (8)°, β=110.31 (8)°, γ=114.43 (8)°, V=1059 (2) Å^3, D_m=1.307 g cm^{-3} (aq. KI), D_c=1.315 g cm^{-3}, Z=2, MoK_α radiation (40 kV-20 mA), λ=0.7107 Å.

The cell constants were determined by a least-squares procedure using the value of the Bragg angles of 17 reflections measured on a Rigaku AFC-6 four-circle autodiffractometer equipped with a graphite monochromated MoK_α source. The apparatus was interfaced to a PANAFACOM U-1200 minicomputer.

The space group $P\bar{1}$ (No. 2) was selected from the number of molecules per unit cell (Z=2) and was later confirmed in the course of the structure refinement. Intensity data were collected in the range of $2\theta < 55°$ using the θ—2θ scan technique. A variable scan rate was adopted. Two reflections were monitored after measurement of every 100 reflections. Of the 2372 independent reflections, 1627 were treated as observed ($F_o > 3\sigma$ F). The intensities were corrected for Lorentz and polarization effects, but no correction was applied for absorption.

Structure Solution and Refinement An overall temperature factor obtained from a Wilson plot did not give the correct solution. Therefore, the value of 5.0 Å^2 was used to calculate the normalized structure factor. The structure was solved by the direct method using the MULTAN78

series of programs.[5] An E map calculated with 390 signed E's ($E>1.2$), which gave a combined figure of merit of 2.255, revealed the positions of all the expected nonhydrogen atoms. Refinements were carried out by the block-diagonal least-squares method. Six cycles of isotropic refinement and 6 cycles of anisotropic refinement led to an R index of 0.094. All the hydrogens were located at calculated positions. After adding the hydrogens but keeping their thermal parameters fixed ($B(H)=B(C)+1.0$), we obtained a final R of 0.0501. Thermal parameters of the hydrogens attached to the methyl and methoxy groups were fixed for their anisotropic vibration. In final refinements, the following weights were used for the observed reflections: $w=1.0$ for $F_o<20.0$, $w=400/F_o^2$ for $F_o>20.0$.

All structure-solving programs were from the Information Processing Center of Kumamoto University with the Universal Crystallographic Computation Program System (UNICS III).[19]

Acknowledgment The authors are grateful to Professor Shigeaki Kawano of Junior College of Kyushu Jogakuin for the use of the crystallographic programs. We also thank Miss Yasuko Miyata for experimental assistance and the members of the Analytical Department of this Faculty for microanalyses and spectral measurements.

The authors are also grateful to Eisai Co., Ltd., for financial support of this work.

References and Notes

1) Part XV: T. Matsuoka, K. Ono, K. Harano and T. Hisano, *Chem. Pharm. Bull.*, **39**, 10 (1991).
2) *a*) T. Hisano, K. Harano, T. Matsuoka, H. Yamada and M. Kurihara, *Chem. Pharm. Bull.*, **35**, 1049 (1987); *b*) T. Hisano, K. Harano, T. Matsuoka, S. Watanabe and T. Matsuzaki, *ibid.*, **37**, 907 (1989).
3) *a*) K. Harano, R. Kondo, M. Murase, T. Matsuoka and T. Hisano, *Chem. Pharm. Bull.*, **34**, 966 (1986); *b*) T. Hisano, K. Harano, T. Matsuoka, T. Suzuki and Y. Murayama, *ibid.*, **38**, 605 (1990).
4) *a*) The olefinic proton of *trans* $(MeO)_2P(=O)OC(Me)=CH$-(COOMe) resonates at 5.47 ppm, upfield by about 0.3 ppm from the position of the *cis*-isomer; L. M. Jackmann and S. Sternhell, "Applications of Nuclear Magnetic Resonance Spectroscopy in Organic Chemistry," Pergamon Press, Inc., London, 1969, pp. 184—192 and references cited therein; *b*) A referee pointed out that the geometric assignment of IIIa should be made by comparison of the ^{1}H-NMR spectra of the two isomers. However, we could not recognize any signals due to the geometric isomer (A). Suitable single crystals of IIIa (or III'a) for X-ray analysis have not yet been obtained; *c*) A. P. Marchand, "Stereochemical Applications of NMR Studies in Rigid Bicyclic Systems," Verlag Chemie International Inc., Florida, 1982, pp. 108—110.
5) P. Main, S. E. Hull, L. Lessinger, G. Germain, J. P. Declercq and M. M. Woolfson, "MULTAN78, a System of Computer Programs for Automatic Solution of Crystal Structures from X-ray Diffraction Data," University of York, York, England, 1978.
6) C. K. Johnson, "ORTEP," Report ORNL-3794, Oak Ridge National Laboratory, Oak Ridge, TN, 1965.
7) T. Matsuoka, M. Shinada, F. Suematsu, K. Harano and T. Hisano, *Chem. Pharm. Bull.*, **32**, 2077 (1984).
8) A. Padwa, M. Matzinger, Y. Tomioka and M. K. Venkatramanan, *J. Org. Chem.*, **53**, 955 (1988) and references cited therein; H. F. Schuster and G. M. Coppola, "Allenes in Organic Synthesis," Wiley-Interscience, New York, 1984.
9) M. J. S. Dewar and W. Thiel, *J. Am. Chem. Soc.*, **99**, 4899, 4907 (1977); M. J. S. Dewar and J. J. P. Stewart, "Quantum Chemistry Program Exchange (QCPE), Program No. 464," Indiana University, 1984.
10) R. Sustmann, *Tetrahedron Lett.*, **1971**, 2717, 2721.
11) *a*) K. Fukui, "Kagaku Hanno To Densi No Kido (Chemical Reactions and Electron Orbitals)," Maruzen, Tokyo, 1976. *b*) I. Fleming, "Frontier Orbitals and Organic Chemical Reactions," John Wiley & Sons, Ltd., London, 1976, Chapters 2 and 4.
12) The release of the strain involved in the allene system is also an important driving force for the cycloaddition. The MNDO calculations and experimental data for heat of formation of simple unsaturated compounds indicate that $\Delta\Delta Hf$ of the allene-to-propene conversion is about 10 kcal larger than that of the propene to propane conversion.[13]
13) R. C. Bingham, M. J. S. Dewar and D. H. Lo, *J. Am. Chem. Soc.*, **97**, 1296 (1975); R. L. Deming and C. A. Wulff, "The Chemistry of Ketenes, Allenes, and Related Compounds: The Thermodynamics of Allenes, Ketenes and Related Compouds," ed. by S. Patai, John Wiley & Sons, Ltd., New York, 1980, Chapter 4.
14) R. Huisgen, "Topics in Heterocyclic Chemistry," ed. by R. N. Castle, Wiley-Interscience, New York, 1969, Capter 8.
15) S. Inagaki, H. Fujimoto and J. Fukui, *J. Am. Chem. Soc.*, **98**, 4693 (1976).
16) The HOMO of 3,5-dimethylpyridine has a node close to the N atom. The NHOMO (−10.35 eV) is considered to play an important role in the cycloaddition. The NHOMO coefficients of N and C_2 and C_2 are −0.461 and −0.144, respectively.
17) T. A. Bryson and T. M. Dolak, "Organic Syntheses," Coll. Vol. VI, Ed. by W. E. Noland, John Wiley and Sons, Inc., New York, 1988, p. 505.
18) E. Ochiai, "Aromatic Amine Oxides," Elsevier Publishing Co., Amsterdam, 1967.
19) T. Sakurai and K. Kobayashi, *Rikagaku Kenkyusho Hokoku*, **55**, 69 (1979); S. Kawano, *Koho, Comput. Center Kyushu Univ.*, **16**, 113 (1983).

Mechanism of Decomposition of Cyclic Peroxides, 4-Alkoxy-1,4-dihydro-2,3-benzodioxin-1-ols, to Afford Hydroxyl Radical

Seiichi MATSUGO,*[,a] Nobuko KAYAMORI,[b] Tatsuo OHTA[b] and Tetsuya KONISHI*[,b]

Department of Chemistry, Kobe University of Mercantile Marine,[a] Fukae-minami 5–1–1, Kobe 658, Japan and Niigata College of Pharmacy,[b] Kamishin-ei-cho 5–13–2, Niigata 950–21, Japan. *Received June 25, 1990*

The decomposition of 4-alkoxy-1,4-dihydro-2,3-benzodioxin-1-ols (1, Bd) in aqueous media was examined. Increasing the water content of the medium accelerated the decomposition of 1 and increased the formation of the corresponding 2-formyl benzoic acid ester (2) as the decomposition product. Electron spin resonance (ESR) studies using dimethylpyrroline *N*-oxide (DMPO) as a spin trapping reagent had revealed that hydroxyl radicals are formed during the decomposition of 1 (Matsugo *et al.*, *FEBS Lett.*, 184, 25 (1985)). Thus, water-mediated decomposition of 1 was suggested to occur, affording the ester 2 and hydroxyl radical. Direct involvement of water was confirmed by an ^{18}O isotopic tracer experiment which revealed that ^{18}O was incorporated exclusively into the formyl position of the ester 2. It is plausible that a hydrated hydroperoxide (5) is formed by the addition of water at the formyl position of the ring-opened structure of 1 at the initial stage of the decomposition of 1. Preliminary studies on the antibacterial activities of 1 showed moderate cell-killing activity, especially to *Pseudomonas* strains, and the activity was found to be related to the decomposition of 1.

Keywords hydroxyl radical; 4-alkoxy-1,4-dihydro-2,3-benzodioxin-1-ol; antibacterial activity; cyclic peroxide; minimum inhibitory concentration; decomposition kinetics; ESR spectrum; dimethylpyrroline *N*-oxide

The toxicity of peroxides, typically lipid peroxides, has been widely recognized and is considered to be due to active oxygen species generated by their decomposition.[1] In the action mechanism of certain anti-tumor drugs such as adriamycin[2] or bleomycin,[3] hydroxyl radicals are considered to play a significant role in tumor cell killing. These facts suggest that if one could develop a chemical system to generate active oxygen radicals in a specified site, a strong cell toxicity would be produced at that site. As candidate compounds, we chose cyclic peroxides, such as 4-methoxy- and 4-ethoxy-1,4-dihydro-2,3-benzodioxin-1-ols (**1a, b** Bd), and studied their reactions with cytochrome c.[4–6] These studies indicated that Bd generated active oxygen radicals including hydroxyl radical on its decomposition in aqueous media and indeed the generation of hydroxyl radical was confirmed by electron spin resonance (ESR) using dimethylpyrroline *N*-oxide (DMPO) as a spin trapping reagent.[7] We have studied the precise decomposition path of Bd in aqueous media using ^{18}O as a tracer and we propose here a water-mediated Bd decomposition which accompanied with hydroxyl radical generation. Preliminary studies on the antibacterial activity of Bd are also described and the antibacterial activities of cyclic peroxides are discussed in relation to the mechanism of hydroxyl radical generation.

Results and Discussion

Decomposition of Bd in an Aqueous Medium The decomposition of 4-methoxy-1,4-dihydro-2,3-benzodioxin-1-ol (**1a**) and 4-ethoxy-1,4-dihydro-2,3-benzodioxin-1-ol (**1b**) was quite slow in aprotic media such as acetonitrile, chloroform, and acetone at 30 °C, but, in aqueous media, **1a** and **1b** smoothly decomposed to afford 2-formyl-benzoic acid (**3**) and corresponding esters (**2a, b**). The product distribution studies revealed that as the water content in the medium was increased, the formation of esters (**2a, b**) increased, while the formation of the acid **3** was low in every case (Figs. 1 and 2).

The rate constant for the decomposition of **1a** and **1b** became larger with increasing water content in the medium.

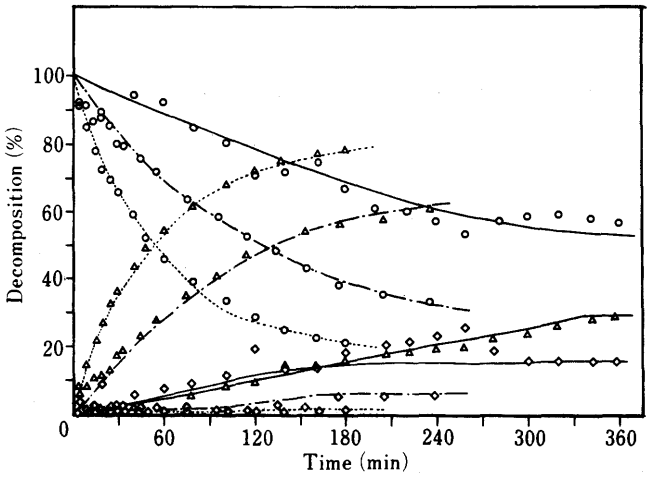

Fig. 1. Decomposition Profiles of 4-Methoxy-1,4-dihydro-2,3-benzodioxin-1-ol (**1a**) in Aqueous MeCN (90, 70, 50%) Solutions at 29.5±0.5 °C

○, peroxide, △, ester; ◇, acid. —, $CH_3CN:H_2O$ (9:1); ———, $CH_3CN:H_2O$ (7:3); – – –, $CH_3CN:H_2O$ (5:5).

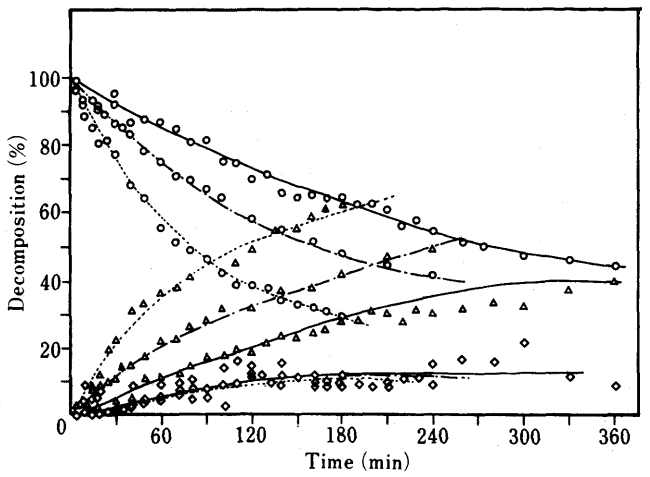

Fig. 2. Decomposition Profiles of 4-Ethoxy-1,4-dihydro-2,3-benzodioxin-1-ol (**1b**) in Aqueous MeCN (90, 70, 50%) Solutions at 29.5±0.5 °C

○, peroxide; △, ester; ◇, acid. —, $CH_3CN:H_2O$ (9:1); ———, $CH_3CN:H_2O$ (7:3); – – –, $CH_3CN:H_2O$ (5:5).

TABLE I. Thermal Decomposition Kinetics of 4-Methoxy-1,4-dihydro-2,3-benzodioxin-1-ol (**1a**) and 4-Ethoxy-1,4-dihydro-2,3-benzodioxin-1-ol (**1b**) in Various Aqueous Solvent Media[a]

Solvent MeCN : H_2O	Peroxide	Temp. (°C)	K_{obsd} ($\times 10^6 h^{-1}$)
9 : 1	**1a**	30.3	2.602±0.30
8 : 2	**1a**	30.3	6.600±0.25
7 : 3	**1a**	29.6	10.384±0.30
6 : 4	**1a**	29.6	17.287±0.50
5 : 5	**1a**	29.6	23.956±0.50
9 : 1	**1b**	29.6	1.894±0.50
8 : 2	**1b**	29.6	4.029±0.20
7 : 3	**1b**	29.6	7.460±0.30
6 : 4	**1b**	29.6	11.072±0.40
5 : 5	**1b**	29.6	15.525±0.30

a) Peroxides (**1a**, **b**) did not decompose at all in 100% MeCN even if the sample solution was heated at 60 °C for 3 h.

Fig. 3. Effect of D_2O on DMPO-OH Adduct Formation Mediated by the Decomposition of 4-Ethoxy-1,4-dihydro-2,3-benzodioxin-1-ol (**1b**)

The reaction mixture, containing 40 μl of DMPO aqueous solution (50 mM), 60 μl of (H_2O + various volumes of D_2O) and 10 μl of **1b** in acetonitrile (10 mM), was heated for 3 min, at 40 °C. The ESR measurement conditions were as described in the experimental section.

For example, the rate constant of **1a** in MeCN–H_2O (1 : 1) was *ca.* ten times larger than that of **1a** in MeCN–H_2O (9 : 1) (Table I). Increasing the temperature up to 65 °C accelerate the decomposition reaction without producing any significant change in ester/acid ratio in 50% aqueous solution.[8]

In an aqueous Bd solution, a typical DMPO-OH adduct signal ($A_N = A_H^\beta = 14.86$ G) was detected after heat treatment at temperatures above 30 °C, when ESR spectra were recorded in the presence of DMPO as a spin trapping reagent (see also refs. 5 and 7). Although increasing the concentration of acetonitrile decreased the DMPO-OH formation (not shown), participation of H_2O in hydroxyl radical generation is not conclusive, because acetonitrile itself is a quencher of hydroxyl radical. Therefore, the effect of D_2O on the DMPO-OH formation was measured to clarify the direct participation of H_2O in Bd decomposition. As is shown in Fig. 3, DMPO-OH formation decreased as the concentration of D_2O was increased, as expected.

We showed previously that the DMPO-OH signal increased at higher temperatures concomitantly with Bd decomposition, and the presence of a hydroxyl radical scavenger such as ethyl alcohol caused disappearance of the signals.[5]

The above experimental results suggest that water in the medium favors the formation of the ester **2** and hydroxyl

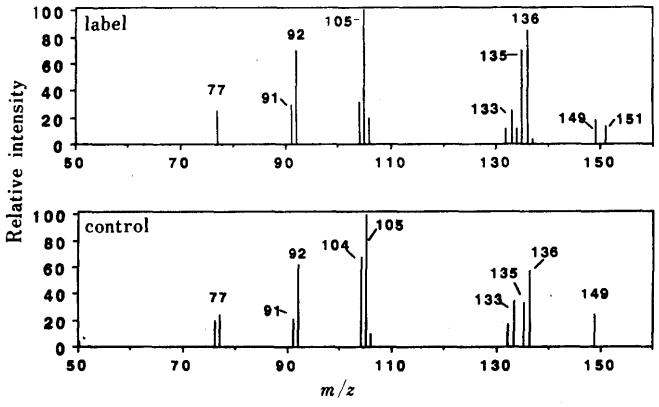

Fig. 4. GC-MS of Methyl 2-Formyl-benzoate **2a** Obtained by the Decomposition of **1a** in MeCN–$H_2{}^{18}O$ (v/v = 1 : 1, Label) at Room Temperature and **2a** Obtained by the Decomposition of **1a** in MeCN–H_2O (v/v = 1 : 1, Control) at Room Temperature

TABLE II. GC-MS Data for **2a** Obtained during the Decomposition of **1a** in MeCN–$H_2{}^{18}O$ (1 : 1) and MeCN–H_2O (1 : 1)

	Peaks
Labeling experiment **2a**	151 (M^+ – Me, 13.33), 135[a] (M^+ – CHO(^{18}O), M^+ – OMe, 69.30), 149 (M^+ – Me, 16.27), 133 (M^+ – OMe, 26.67), 136 (M^+ – CO(^{18}O), 84.44), 105 (M^+ – CO(^{18}O) – OMe, 100)
Control experiment **2a**	149 (M^+ – Me, 26.67), 135 (M^+ – CHO, 34.67), 136 (M^+ – CO, 61.33), 133 (M^+ – OMe, 37.86), 105 (M^+ – COOMe, 100)

a) This peak corresponds to the sum of labeled $M^+ - CH^{18}O$, non-labeled $M^+ - CHO$ and labeled $M^+ - OMe$.

radical, and thus presumably participates in the decomposition of **1**. In order to know how the water molecule is involved in the peroxide decomposition, we examined the decomposition of **1a** in MeCN–$H_2{}^{18}O$ (v/v, 1 : 1) solvent. If water in the medium participates directly in the decomposition of **1a**, ^{18}O should be incorporated into the ester **2a**. In the gas chromatography–mass spectrometry (GC-MS) analysis of the ester **2a**, the signal corresponding to $M^+ - Me$ was observed as a doublet at *m/z* 151 and 149 although M^+ of **2a** could not be detected under the measuring conditions; the relative intensity was 46 : 54. Further, the signal corresponding to $M^+ - OMe$ was observed as a doublet at *m/z* 133 and 135. Since the signal due to $M^+ - CHO(^{18}O)$ might also appear at *m/z* 135, the fraction corresponding to ^{18}O labeled ion (labeled $M^+ - OMe$) in the *m/z* 135 signal was calculated by subtracting the fraction corresponding to $M^+ - CHO(^{18}O)$ from the value at *m/z* 135 according to Eq. 1.

$$135_{labeled}(M^+ - OMe) = 135_{labeled} - 136_{labeled} \times 135_{control}/136_{control} \quad (1)$$

Finally, $135_{labeled}(M^+ - OMe) : 133_{labeled}(M^+ - OMe) = 44.7 : 55.3$ was obtained. Thus, it is clear that ^{18}O label incorporation in ester **2a** is *ca.* 50%. On the other hand, the deformyl ion, $M^+ - CO$, appeared as a singlet at 136, indicating the absence of ^{18}O label in the fragment ion. Thus, ^{18}O is concluded to be incorporated exclusively into the formyl position of the ester **2a** (Fig. 4, Table II).

Based on these experimental results, a plausible decomposition pathway of **1** in an aqueous medium is as follows.

As the cyclic peroxide **1a** has a partial structure resembling to a hemiacetal, the ring structure may easily open to afford the non-cyclic hydroperoxide **4** by analogy with carbohydrates. This structure could be the precursor of **1a**. So, in an aqueous medium, the cyclic peroxide **1a** is in equilibrium with its non-cyclic hydroperoxide **4**. Since **3** does not incorporate any ^{18}O of $H_2{}^{18}O$ at neutral pH, water in the medium would initially add to the aldehyde portion of **4** to produce the hydrated hydroperoxide **5**. Hydrogen abstraction by **8**, **9**, or hydroxyl radical (spontaneously produced to a slight extent by the O–O homolytic scission of **1a**) gives the carbon-centered radical **6**. Successive decomposition of **6** generates hydroxyl radical to afford the hydrated ester **7**.[9] Dehydration of **7** results in the formation of the ester **2a** as a final product. Here, the possibility of losing H_2O or $H_2{}^{18}O$ from **7** is expected to be about the same. Namely, 50% loss of the label would be expected. This was actually the case in our present study.

Direct attack of H_2O on cyclic peroxide was reported[10] only in strongly alkaline solution, but not at neutral pH. Further, hydrolysis and methanolysis of endoperoxide have also been reported only under acidic conditions.[11] Thus, a direct attack of water to **1a** under our mild reaction conditions is unlikely. This view is consistent with the non-linear correlation of the $k_{decomp.}$ of **1** to the molar concentration of water. If direct attack of water played a central role in the decomposition of **1**, a linear correlation would be expected between water content and the decomposition rate, which is not the case. As for the formation of **3**, we did not detect any ^{18}O incorporation into **3** under the same conditions as those where we observed *ca.* 50% ^{18}O incorporation in **2a**, so it would be reasonable to consider a different pathway for the formation of **3**, namely, O–O homolytic scission. The O–O homolytic scission of **1a** gives the biradical **8**, which equilibrates with **9**. Intramolecular hydrogen abstraction would afford hemiacetal **10**, which excludes methanol to afford **3** as a final product. The mechanism proposed here well explains the 50% incorporation of ^{18}O in **2a** at its formyl position and is also consistent with the observation that hydroxyl radical is generated from **1** in an aqueous medium[7] (see also Fig. 3).

Antibacterial Activity of Bd Active oxygen species such as hydroxyl radical are well known to possess cell-killing activity. Thus, it is of interest to know if hydroxyl radical-generating cyclic peroxides have biological effects. We examined the antibacterial activities of **1b** toward fifteen different gram-positive or gram-negative bacterial strains by the broth dilution method. It was found that **1b** had moderate but reproducible antibacterial activities toward *Pseudomonas* strains and *Proteus rettgeri* (Table III).

The antibacterial activity of **1b** was dependent on the preincubation time, namely, the antibacterial activity became lower if *Ps. maltophilia* was inoculated with a lag period after the addition of peroxide in the culture medium (Table IV); presumably some of the peroxide (**1b**) would

Table III. Antibacterial Activity Spectrum of **1b**

Strains	MIC (μg/ml)
Alcaligenes faecalis	100
Pseudomonas aeruginosa	100
Ps. maltophilia 2491	25
Ps. pseudoalcaligenes	50
Ps. putida	200
Ps. stutzeri	50
Staphylococcus aureus ATCC 25923	100
Bacillus subtilis ATCC 6633	400
Escherichia coli K12	200
E. coli 15	400
Enterobacter cloacae	400
Proteus rettgeri	25
Pr. vulgaris	100
Salmonella typhimurium	200
Shigella sonnei	400

Table IV. Effect of Preincubation of **1b** Containing Culture Medium on MIC for *Ps. maltophila* 2491

Preincubation (h)	MIC (μg/ml) **1b**
0	25
20	100
46	200

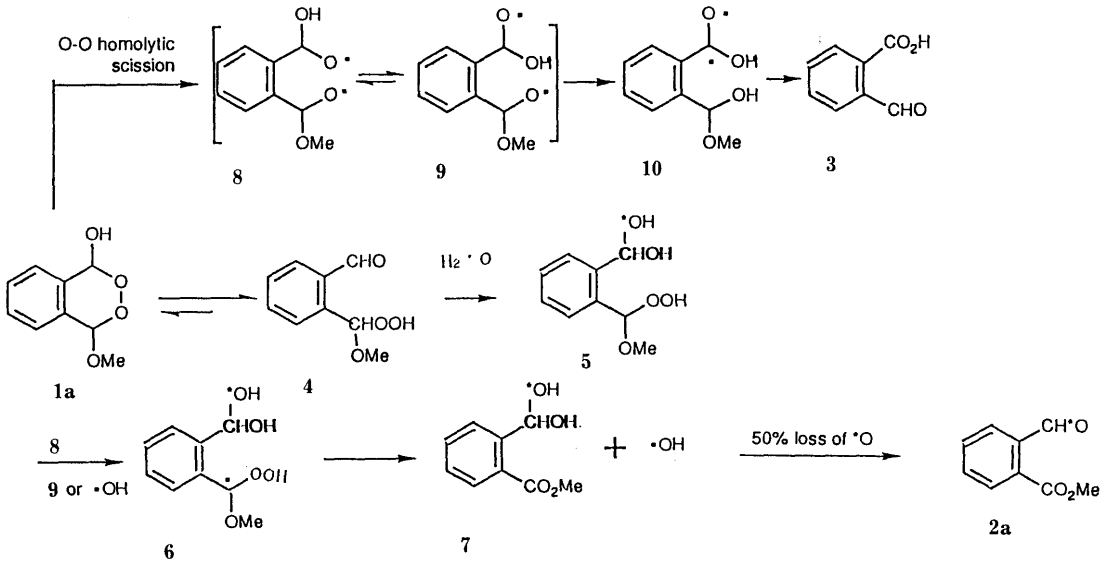

Chart 1

have decomposed. In addition, the antimicrobial activity of **1a**, which is less stable in an aqueous medium than **1b**, were rather low and more variable (not shown).

Therefore, it appears that the antibacterial activity of **1b** is related to the peroxide decomposition, and the radicals generated, including hydroxyl radical, are the reactive species responsible for the antibacterial activity.

Based on the above experimental results, we have reached the following conclusions.

1) In an aqueous medium, the decomposition of 4-alkoxy-1,4-dihydro-2,3-benzodioxin-1-ol (**1**) proceeds through two different pathways, namely that involving water participation and the O–O homolytic path.

2) Hydrogen abstraction from the hydrated non-cyclic hydroperoxide **5** exclusively affords the ester **2** accompanied with the hydroxyl radical.

3) The synthetic cyclic peroxide **1b** showed moderate antibacterial activities especially toward *Pseudomonas* strains, and the antibacterial activity is related to the generation of active oxygen radicals by the water-mediated decomposition of **1b**.

Experimental

Melting points were recorded on a Yanagimoto melting point apparatus. Proton and carbon-13 nuclear magnetic resonance (^{1}H- and ^{13}C-NMR) spectra were measured with a JEOL JNM-FX-200 spectrometer using tetramethylsilane as an internal standard. Infrared (IR) spectra were measured with a Jasco A-3 spectrometer. GC-MS was measured with a Hitachi RMU-7M mass spectrometer. ESR spectra were obtained using a Varian model X-4 ESR spectrometer. DMPO (Aldrich) was purified by passing it through a charcoal column and dissolved in distilled water to prepare a 0.5 M solution. Compound **1b** was dissolved in MeCN to prepare a 50 mM solution. The reaction mixtures containing 40 μl of DMPO solution, 60 μl of (H_2O+D_2O) and 10 μl of Bd solution were heated at 40 °C for 3 min. ESR spectra were measured under the following conditions: field setting, 3380 G; modulation amplitude, 0.5 × 1 G; time constant, 0.28 × 0.3 s; scan range, 200 G; microwave power, 10 mW; modulation frequency, 100 MHz.

Degradation kinetics were followed by high performance liquid chromatography (HPLC) using a Nippon Bunko Twincle model equipped with ODS-120A reverse-phase column (Toyo Soda). Acetonitrile–water (v/v, 80 : 20) was used as an eluent. Elution peaks were detected at 254 nm using a model UVidec 100 III UV detector (Nippon Bunko). Alliquots of 10 μl of 1 mM aqueous reaction solution of 4-alkoxy-1,4-dihydro-2,3-benzodioxin-1-ols (**1a, b**) were injected for analysis before or after heat treatment at 30 °C.

Synthesis of 4-Methoxy-1,4-dihydro-2,3-benzodioxin-1-ol (1a) A solution of naphthalene (1.28 g, 0.01 mol) in 200 ml of distilled methanol was ozonized at −70 °C for 1 h. The reaction mixture was evaporated *in vacuo* at 0 °C to give an oily residue, which was then dissolved in 10 ml of ether solution and allowed to stand for 24 h at −20 °C. A white powder was precipitated, and was further washed with 1 ml of cold ether to afford analytically pure **1a** as a white powder. **1a** (1.76 g, 0.0092 mol), 126—128 °C (dec.) (lit. 126—127 °C[12]). ^{1}H-NMR ($CDCl_3$) δ: 3.66 (s, 3H), 5.07 (br s, 1H, OH), 5.53 (s, 1H), 5.95 (s, 1H), 7.28—7.42 (m, 4H). ^{13}C-NMR ($CDCl_3$) δ: 56.14 (q), 93.94 (d), 99.83 (d), 126.93 (d), 126.98 (d), 129.12 (d), 130.14 (s), 131.82 (s). IR (KBr): 3350, 3050, 2970, 2920, 1600, 1460, 1350, 1330, 1285 cm^{-1}. *Anal.* Calcd for $C_9H_{10}O_4$: C, 59.33; H, 5.53. Found: C, 59.45; H, 5.81.

4-Ethoxy-1,4-dihydro-2,3-benzodioxin-1-ol (**1b**) was obtained analogously in 88% yield using ethanol instead of methanol.

1b: 130—132 °C (dec. point). ^{1}H-NMR ($CDCl_3$) δ: 1.26 (t, 3H, J=7.0 Hz), 3.55 (q, 2H, J=7.0 Hz), 5.04 (br s, 1H, OH), 5.69 (s, 1H), 5.91 (s, 1H), 7.30—7.42 (m, 4H). ^{13}C-NMR ($CDCl_3$) δ: 15.07 (q), 64.65 (t), 93.94 (d), 98.70 (d), 126.96 (d, 2C), 129.06 (d, 2C), 130.41 (s), 131.90 (s). IR (KBr) 3400, 3070, 2990, 1600, 1450, 1340, 1320, 1260, 1200 cm^{-1}. *Anal.* Calcd for $C_{10}H_{12}O_4$: C, 61.21; H, 6.17. Found: C, 60.89; H, 5.96.

o-Formylbenzoic acid (**3**) was purchased from Tokyo Kasei Co., Ltd. and was used for the identification of the decomposition product. Methyl *o*-formylbenzoic acid (**2a**) and ethyl *o*-formyl benzoic acid (**2b**) were synthesized by the esterification of **3** with the corresponding alcohols. They were identical with the decomposition products **2a** and **2b**, respectively, on their IR and NMR spectral comparison.

Decomposition of 1a in MeCN–$H_2{}^{18}O$ The peroxide **1a** (20 mg) was dissolved in 1 ml of dry MeCN, to which 1 ml of $H_2{}^{18}O$ (^{18}O content 99.8%) was added. The mixed solution was kept at room temperature for 24 h. GC analysis revealed the reaction mixture contained **2a** (88%) and **3** (*ca.* 5%) under these reaction conditions. The reaction mixture was analyzed by GC-MS and the results were listed on Table II and Fig. 4.

Determination of Minimum Inhibitory Concentrations (MICs) MIC was determined by the broth dilution method. Serial two-fold dilutions of **1b** with nutrient broth (Difco) were inoculated with test organisms and incubated at 37 °C for 18 h (except *Ps. stuzeri*; 48 h). The minimum concentration of serial dilutions which inhibited bacterial growth was regarded as the MIC.

References

1) H. S. Kappus and H. Sies, *Experientia*, **37**, 1233 (1981).
2) J. V. Bennister and P. J. Thornalley, *FEBS Lett.*, **157**, 170 (1983).
3) T. Takita, Y. Muraoka, T. Nakatani, A. Fujii, Y. Iitaka and H. Umezawa, *J. Antibiot.*, **31**, 1073 (1978).
4) S. Matsugo, T. Ohta, Y. Hatano and T. Konishi, *J. Pharmacobio-Dyn.*, **8**, s-142 (1985).
5) S. Matsugo, N. Kayamori and T. Konishi, *Chem. Pharm. Bull.*, **34**, 2144 (1986).
6) T. Konishi and S. Matsugo, *Biochim. Biophys. Acta*, **967**, 267 (1988).
7) S. Matsugo, N. Kayamori, Y. Hatano, T. Ohta and T. Konishi, *FEBS Lett.*, **184**, 25 (1985).
8) S. Matsugo, N. Kayamori and T. Konishi, *Radioisotopes*, **38**, 123 (1989).
9) J. A. Howard and J. H. B. Chenier, *Can. J. Chem.*, **58**, 2808 (1980).
10) W. D. Crow, W. Nicholls and M. Sterns, *Tetrahedron Lett.*, **1971**, 1353.
11) J. Rigaudy and D. Sparfel, *Bull. Soc. Chim. Fr.*, **1972**, 3441.
12) P. S. Bailey, D. S. Bath, F. Dobinson, F. J. Garcia-Sharp and D. D. Johnson, *J. Org. Chem.*, **29**, 697 (1964).

Studies on the Constituents of *Veratrum* Plants. II.[1] Constituents of *Veratrum nigrum* L. var. *ussuriense*. (1). Structure and ^{1}H- and ^{13}C-Nuclear Magnetic Resonance Spectra of a New Alkaloid, Verussurinine, and Related Alkaloids

Weijie ZHAO,[a] Yasuhiro TEZUKA,[a] Tohru KIKUCHI,*[,a] Jun CHEN,[b] and Yongtian GUO[b]

Research Institute for Wakan-Yaku (Oriental Medicines), Toyama Medical and Pharmaceutical University,[a] Sugitani 2630, Toyama 930-01, Japan and Research Institute for Medical and Pharmaceutical Science, Dalian,[b] Chunyangjie 21, Dalian, China. *Received July 19, 1990*

Alkaloidal constituents of the roots and rhizoma of *Veratrum nigrum* L. var. *ussuriense* (Liliaceae), which are used as a source of the Chinese crude drug "Li-lu," were examined and a new alkaloid named verussurinine and six known alkaloids have been isolated. The structure of verussurinine was determined to be 16-*O*-(2-methylbutyroyl)germine (1) by means of spectroscopic methods, and six other alkaloids were identified as germidine (2), germerine (3), 15-*O*-(2-methylbutyroyl)germine (4), verazine (5), jervine (6), and neogermbudine (7). Complete assignments of the proton and carbon-13 nuclear magnetic resonance (^{1}H- and ^{13}C-NMR) signals of these alkaloids are also presented.

Keywords *Veratrum nigrum* var. *ussuriense*; steroidal alkaloid; verussurinine; 15-*O*-(2-methylbutyroyl)germine; germidine; germerine; ^{1}H-NMR; ^{13}C-NMR; 2D NMR

The Chinese crude drug "Li-lu (藜蘆)" is prepared from dried roots and rhizoma of several plants of *Veratrum* species (Liliaceae) such as *V. nigrum* L., *V. maackii* REG., *V. dahuricum* LOES. f., and so on, and is used to treat aphasia arising from apoplexy, wind type dysentery, jaundice, headache, scabies, chronic malaria, *etc.*[2] Constituents of *Veratrum* plants have been examined extensively and more than ninety steroidal alkaloids have been isolated so far.[3] In the preceding paper,[1] we have reported the isolation and structure elucidation of a new alkaloid named maackinine (**8**) together with five known steroidal alkaloids from *V. maackii* REG. We have also examined the constituents of *Veratrum nigrum* L. var. *ussuriense*,[4] and isolated a new alkaloid named verussurinine (**1**) along with six known alkaloids. In this paper, we wish to report the structure elucidation of this new compound and the proton and carbon-13 nuclear magnetic resonance (^{1}H- and ^{13}C-NMR) signal assignments of related alkaloids.

Dried roots and rhizoma of *V. nigrum* L. var. *ussuriense* were cut into small pieces and extracted with ethanol. The ethanol extract was treated as shown in Chart 2 to give four fractions A, B, C, and D. Among these, fractions B and C were separated by a combination of column chromatography over alkali-treated silica gel and preparative thin-layer chromatography (TLC) to give verussurinine (U_{11}, **1**) together with seven alkaloids, U_5, U_6 (unidentified), U_7, U_8, U_9, U_{10}, and U_{12}, among which U_5, U_8, and U_{12} were identified as verazine (**5**), jervine (**6**), and neogermbudine (**7**),[4] respectively.

Verussurinine (U_{11}, **1**) was obtained as a colorless amorphous powder, $[\alpha]_D^{23}$ −28.40° (pyridine), and its molecular formula was determined to be $C_{32}H_{51}NO_9$ by mass spectral (MS) and high-resolution MS (HR-MS) measurements. It showed infrared (IR) absorptions at ν 3230 (br, OH), 2880, 2820, 2760 (*trans*-quinolizidine),[5] and 1740 (ester CO) cm^{-1}. The ^{1}H-NMR spectrum of **1** showed signals due to two *tert*-methyls (δ 0.77 and 1.33, 19- and 21-H_3, respectively), a *sec*-methyl (δ 1.01, d, J=7 Hz, 27-H_3), and a 2-methylbutyroyl group (δ 0.88, 3H, t, J=7 Hz, 4′-H_3; 1.30, 3H, d, J=7 Hz, 5′-H_3; 1.44 and 1.81, each 1H, dqd, J=14, 7, and 7 Hz, 3′-H_2; 2.42, 1H, sextet, J=7 Hz, 2′-H) (Table I), and the ^{13}C-NMR spectrum showed thirty-two signals including a carbonyl carbon signal (δ 175.3) and eleven oxygen- or nitrogen-substituted carbon signals (Table II).

Detailed analyses of the ^{1}H- and ^{13}C-NMR spectra by means of ^{1}H–^{1}H shift correlation spectroscopy (COSY) (Fig. 1) and ^{1}H–^{13}C COSY indicated the presence in **1** of the partial structures shown in Chart 3.

These partial structures, coupled with the similarity of the ^{13}C-NMR spectral pattern to that of maackinine (**8**)[1] (Table II), suggested that **1** might be a monoester alkaloid

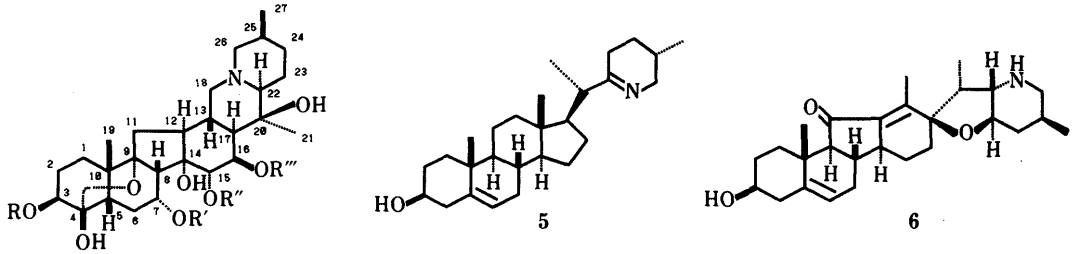

5 **6**

1 : R=R′=R″=H, R‴=2-methylbutyroyl
2 : R=acetyl, R′=R‴=H, R″=2-methylbutyroyl
3 : R=2-hudroxy-2-methylbutyroyl, R′=R‴=H, R″=2-methylbutyroyl
4 : R=R′=R‴=H, R″=2-methylbutyroyl
7 : R=2,3-dihydroxy-2-methylbutyroyl, R′=R‴=H, R″=2-methylbutyroyl
8 : R=R″=angeloyl, R′=acetyl, R‴=H

Chart 1

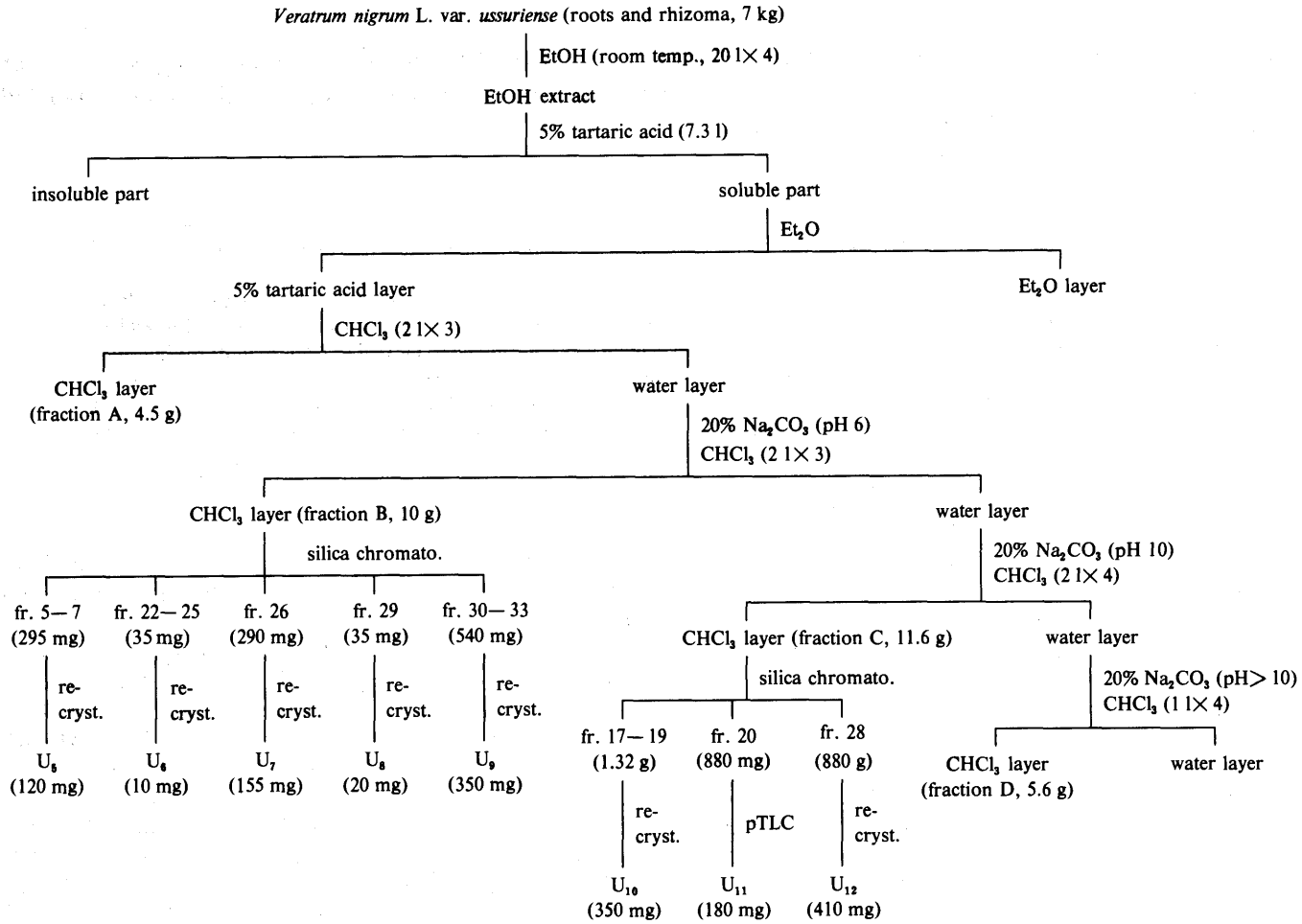

Chart 2

of the germine series. Furthermore, the ^{1}H-signal assignable to 16-H was shifted markedly down-field (δ 6.27) when compared with that of **8** (δ 4.31), indicating the location of the 2-methylbutyroyl group to be at the C-16 position.

Based on these spectral data, verussurinine was concluded to be 16-*O*-(2-methylbutyroyl)germine (**1**).

Compound U_7 (**2**) was obtained as colorless prisms, mp 231—233 °C, $[\alpha]_D^{23}$ +6.85° ($CHCl_3$), and its molecular formula was determined to be $C_{34}H_{53}NO_{10}$ by MS and HR-MS measurements. It showed IR absorptions at ν 3450, 2860, 2830, 2780, and 1735 cm^{-1}, suggesting the presence of hydroxyl, *trans*-quinolizidine,[5] and ester groups in the molecule. In the ^{1}H-NMR spectrum, **2** showed signals due to two *tert*-methyls (δ 0.97 and 1.20, 19- and 21-H_3, respectively), a *sec*-methyl (δ 1.08, d, J=7 Hz, 27-H_3), an acetyl methyl (δ 2.08), and a 2-methylbutyroyl group (δ 0.91, 3H, t, J=7 Hz, 4″-H_3; 1.14, 3H, d, J=7 Hz, 5″-H_3; 1.47 and 1.66, each 1H, dqd, J=14, 7, and 7 Hz, 3″-H_2; 2.40, 1H, sextet, J=7 Hz, 2″-H) (Table I), and in the ^{13}C-NMR spectrum, **2** showed signals due to two carbonyl carbons at δ 170.5 and 175.7 (Table II). Extensive analyses of these ^{1}H- and ^{13}C-NMR spectra with the aid of ^{1}H–^{1}H and ^{1}H–^{13}C COSY led to unambiguous assignments of all the ^{1}H- and ^{13}C-signals except for quaternary carbon signals.

These spectral data suggested that **2** is also an ester alkaloid of the germine type. This was supported by the long-range ^{1}H–^{13}C COSY spectrum (Fig. 2), in which connectivities of all the quaternary carbons (C_4, C_9, C_{10}, C_{14}, and C_{20}) with relevant protons were observed as shown by arrows in the formula in Fig. 2. The positions of the acetyl and the 2-methylbutyroyl groups were also elucidated by long-range ^{1}H–^{13}C COSY. As can be seen in Fig. 2a, the carbonyl carbons at δ 170.5 and 175.7 showed long-range correlations with the protons at δ 2.08 (acetyl methyl) and 4.92 (3-H) and with the protons at δ 1.14 (5″-H_3), 2.40 (2″-H), and 5.34 (15-H), respectively (Fig. 2a and Table II).

From the foregoing evidence, compound U_7 (**2**) was determined to be germidine [3-*O*-acetyl-15-*O*-(2-methylbutyroyl)germine].[6]

Compound U_9 (**3**), $C_{37}H_{59}NO_{11}$, mp 207—209 °C, $[\alpha]_D^{23}$ +5.16° ($CHCl_3$), and compound U_{10} (**4**), $C_{32}H_{51}NO_9$, mp 221—223 °C, $[\alpha]_D^{23}$ −24.10° ($CHCl_3$), were also believed to be germine-type alkaloids. Extensive analyses of their ^{1}H- and ^{13}C-NMR spectra by means of ^{1}H–^{1}H COSY, ^{1}H–^{13}C COSY, and long-range ^{1}H–^{13}C COSY led to exact assignments of all the ^{1}H- and ^{13}C-signals as shown in Tables I and II. Finally, compounds U_9 and U_{10} were determined to be germerine (**3**) [3-*O*-(2-hydroxy-2-methylbutyroyl)-15-*O*-(2-methylbutyroyl)germine][6] and 15-*O*-(2-methylbutyroyl)germine (**4**),[7] respectively, on the basis of the above-mentioned spectral data.

Verussurinine (**1**) has the interesting structural feature of

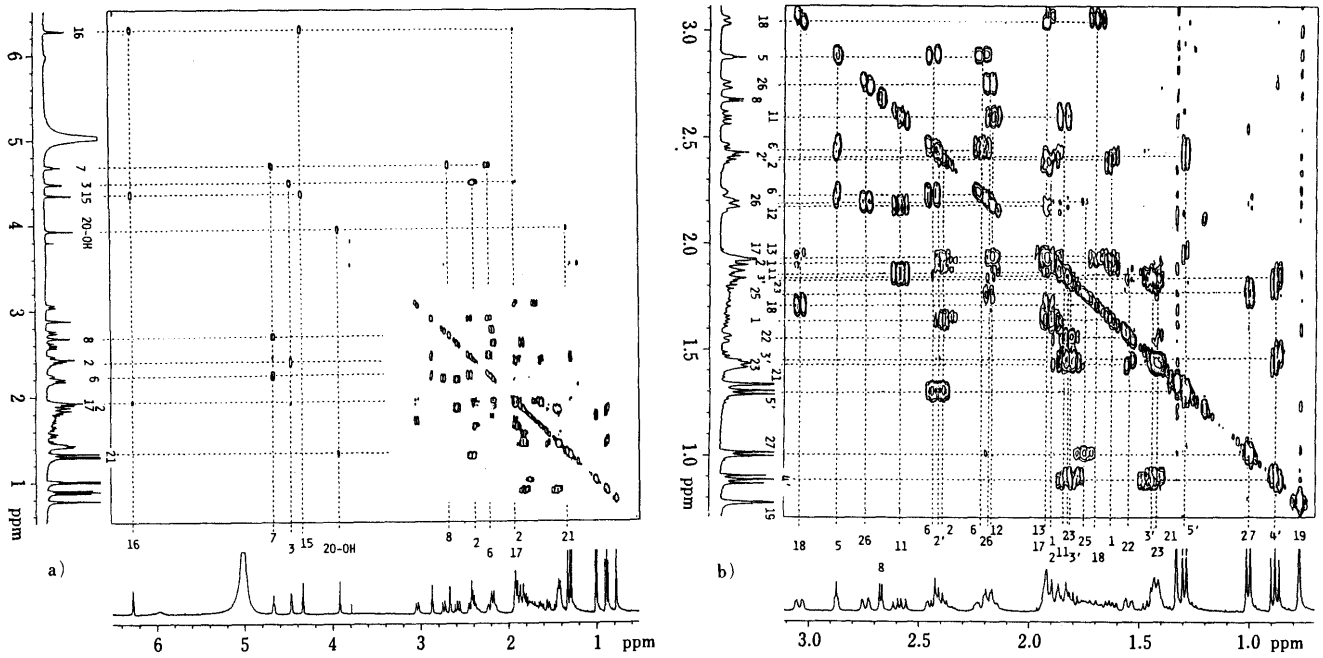

Fig. 1. ^1H–^1H COSY Spectrum of Verussurinine (**1**) in C_5D_5N
a) Whole region, b) high-field region.

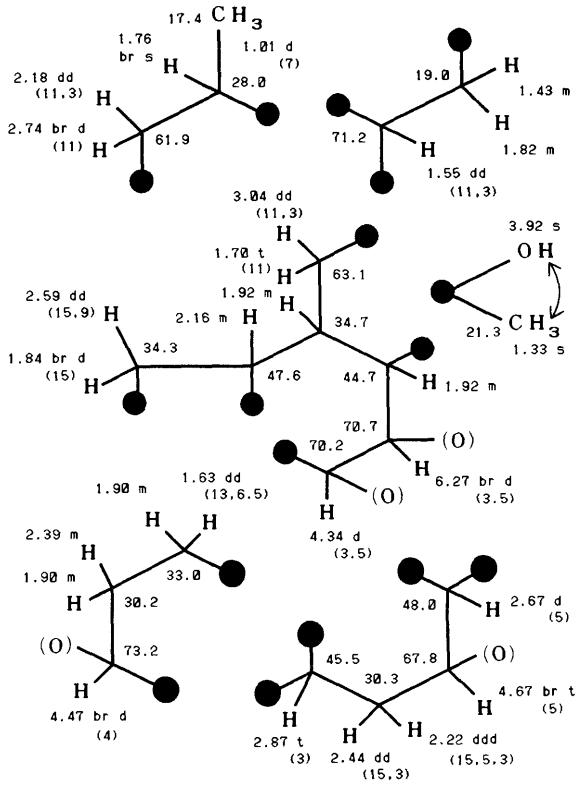

Chart 3. Partial Structures of Verussurinine (**1**) Deduced from the ^1H- and ^{13}C-NMR Data

⌒ : Long-range coupling observed in ^1H–^1H COSY.

an ester group at the C-16β position, which is considered to be sterically hindered. To our knowledge, this is only the second example of a natural germine-type alkaloid carrying a 16-*O*-acyl group.[8] Structure elucidation of U_6 and purification of fractions A and D are now under investigation and will be reported in forthcoming papers.

Experimental

Melting points were determined on a Kofler-type apparatus and are uncorrected. Optical rotations were measured on a JASCO DIP-4 polarimeter at 23 °C, and IR spectra were recorded on a JASCO IRA-2 spectrometer. MS and HR-MS were taken on a JEOL D-300 mass spectrometer in the electron impact mode at the ionization potential of 70 eV, and NMR spectra were recorded with a JEOL JNM-GX400 spectrometer with tetramethylsilane as an internal standard. Column chromatography was done over alkali-treated silica gel,[1] and preparative TLC was carried out with precoated Merck Kieselgel GF_{254} plates. For drying organic solvents, anhydrous $MgSO_4$ was used.

Isolation of Alkaloids Dried roots and rhizoma (7 kg) of *Veratrum nigrum* L. var. *ussuriense*, collected at Qianshan in Liaoning Province, China in 1985, were cut into small pieces and extracted with EtOH (20 l × 4) at room temperature. The EtOH solutions were combined and concentrated *in vacuo*. The residue was dissolved in 5% aqueous tartaric acid solution (7.3 l) and insoluble material was removed by filtration. The filtrate was defatted with ether (1 l × 4) and then extracted with $CHCl_3$ (2 l × 3). The $CHCl_3$ layer was dried and concentrated to give fraction A (4.5 g). The 5% tartaric acid layer was adjusted to pH 6 by careful addition of 20% aqueous Na_2CO_3 solution and extracted with $CHCl_3$ (2 l × 3). The $CHCl_3$ layer was dried and concentrated to give fraction B (10 g). The residual aqueous solution was then adjusted to pH 10 with 20% aqueous Na_2CO_3 solution and extracted with $CHCl_3$ (2 l × 4). Drying and concentration of the $CHCl_3$ layer gave fraction C (11.6 g). Then, the aqueous solution was further basified (pH > 10) by addition of 20% aqueous Na_2CO_3 solution and extracted with $CHCl_3$ (1 l × 4). The $CHCl_3$ layer was dried and concentrated to give fraction D (5.6 g).

Treatment of Fraction B Fraction B (10 g) was chromatographed over alkali-treated silica gel (520 g) with MeOH–$CHCl_3$ (2 : 98, 4 : 96, and then 6 : 94). The eluates were monitored by TLC and separated into fifty-one fractions.

Fractions 5—7 (295 mg) were combined and recrystallized from acetone to give U_5 (120 mg), mp 178—180 °C, which was identified as verazine (**5**) by comparison with an authentic sample.[4]

Fractions 22—25 (35 mg) and fraction 26 (290 mg) were recrystallized from acetone to give U_6 (10 mg) and U_7 (155 mg), respectively.

Fraction 29 (35 mg) was also recrystallized from acetone to afford U_8 (20 mg), mp 236.5—238 °C, which was identified as jervine (**6**).[4]

Combined fractions 30—33 (540 mg) were recrystallized from acetone to give U_9 (350 mg).

Treatment of Fraction C Fraction C (11.6 g) was also chromatographed over alkali-treated silica gel (670 g) with MeOH–$CHCl_3$ (2 : 98, 4 : 96, and then 8 : 92), and separated into fifty fractions on the basis of TLC

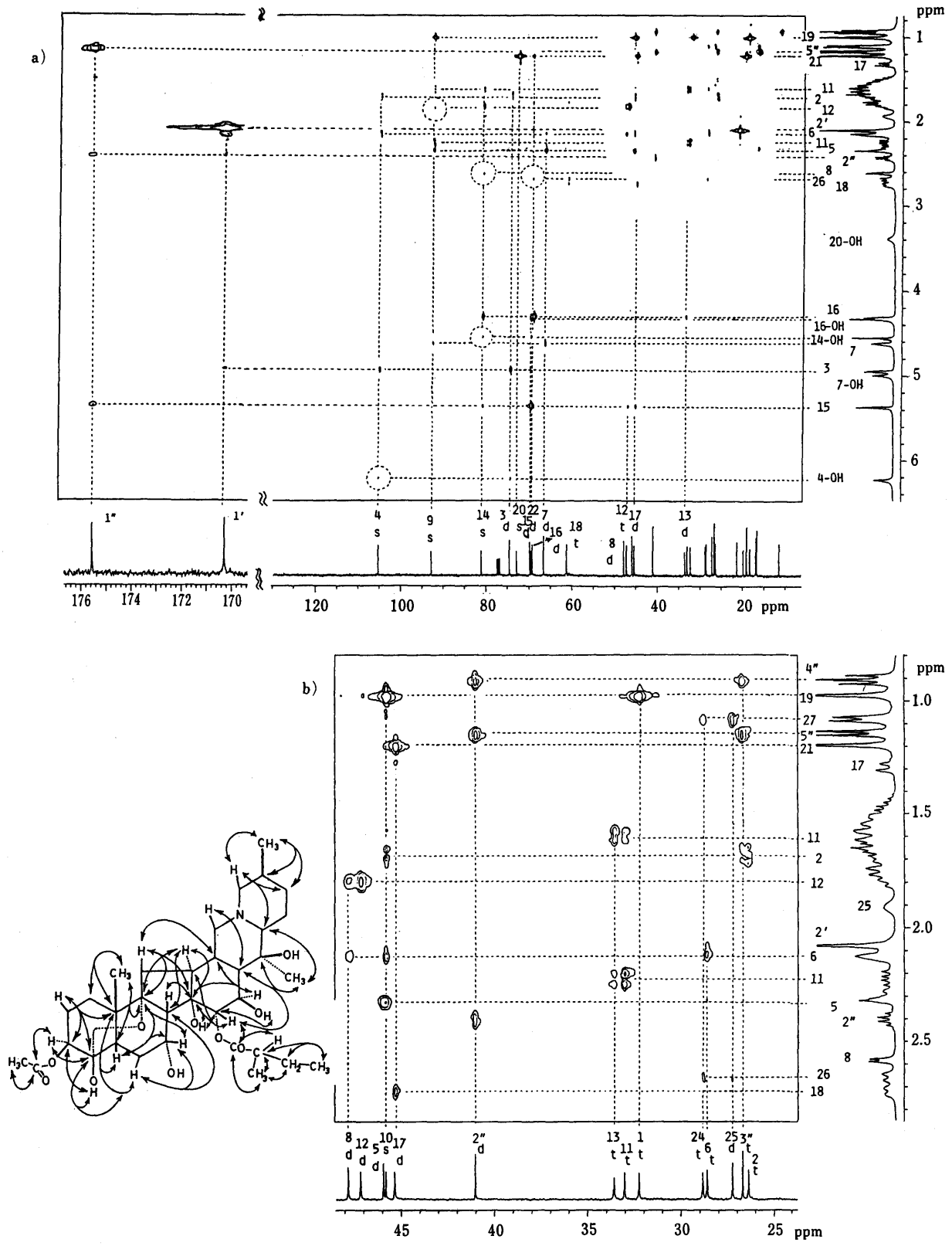

Fig. 2. Long-Range ^{1}H–^{13}C COSY Spectrum of **2** in $CDCl_3$ (Sample *ca.* 80 mg, $J_{CH}=10$ Hz, 12 h Run)

a) Whole region, b) high-field region. Dotted circles indicate the correlation peaks, which are significant but weak at this threshold level.

monitoring.

Fractions 17—19 (1.32 g) were combined and recrystallized from acetone to give U_{10} (350 mg).

Fraction 20 (880 mg) was further purified by preparative TLC with MeOH–$CHCl_3$ (5:95) to give U_{11} (180 mg), while fraction 28 (880 mg) was recrystallized from acetone to give U_{12} (410 mg), mp 147—149 °C, which was identified as neogermbudine (7).[4]

Verussurinine (U_{11}, 1) Colorless amorphous powder, $[\alpha]_D$ −28.40° ($c=0.48$, pyridine). IR ν_{max} (KBr) cm^{-1}: 3230, 2880, 2820, 2760, 1740. ^{1}H- and ^{13}C-NMR: Tables I and II. MS *m/z* (%): 593 (M^+, 100), 575 (M^+-H_2O, 25), 550 (15), 492 (32), 474 (15), 331 (8), 154 (17), 112 (100), 98 (61). HR-MS: Found 593.3561, Calcd for $C_{32}H_{51}NO_9$ (M^+) 593.3563.

TABLE I. ^1H Chemical Shifts (in ppm) and Coupling Constants (in Hz, in Parentheses) for the Alkaloids from *V. nigrum* L. var. *ussuriense*

^1H	1[a]	2[b]	3[b]	4[b]
1-H	1.90 m	1.66 m	1.70 m	1.70 m
	1.63 dd (13, 6.5)	1.56 m	1.61 m	1.57 m
2-H	2.39 m	2.11 m	2.15 m	2.02 m
	1.90 m	1.68 m	1.65 m	1.59 m
3-H	4.47 br d (4)	4.92 br d (4)	5.03 br d (4)	3.85 br d (4.5)
5-H	2.87 t (3)	2.32 t (3)	2.22 t (3)	2.37 t (3)
6-H	2.44 dd (15, 3)	2.14 br s	2.17 m	2.13 m
	2.22 ddd (15, 5, 3)		2.08 dd (17, 5)	2.07 m
7-H	4.67 br t (5)	4.59 br t (5)	4.60 br t (5)	4.59 br t (5)
8-H	2.67 d (5)	2.58 d (5)	2.60 d (5)	2.56 d (5)
11-H	2.59 dd (15, 9)	2.22 dd (15, 8.5)	2.22 dd (15, 9)	2.18 dd (15, 8.5)
	1.84 br d (15)	1.59 m	1.59 m	1.58 m
12-H	2.16 m	1.79 ddd (11.5, 8.5, 2)	1.79 ddd (11.5, 8.5, 2)	1.77 ddd (11.5, 8.5, 2)
13-H	1.92 m	1.54 m	1.52 m	1.53 m
15-H	4.34 d (3.5)	5.34 d (3.5)	5.34 d (3)	5.34 d (3.5)
16-H	6.27 br d (3.5)	4.29 dd (3.5, 2)	4.29 dd (3, 2)	4.28 dd (3.5, 2)
17-H	1.92 m	1.29 dd (12, 2)	1.28 dd (12, 2)	1.28 dd (12, 2)
18-H	3.04 dd (11, 3)	2.72 dd (11.5, 4)	2.72 dd (11.5, 4)	2.73 dd (11.5, 4)
	1.70 t (11)	1.74 t (11.5)	1.74 t (11.5)	1.73 t (11.5)
22-H	1.55 dd (11, 3)	1.75 m	1.77 m	1.74 m
23-H	1.82 m	1.54 m	ca. 1.5	1.54 m
	1.43 m			
24-H	1.43 m	1.60 m	1.58 m	1.61 m
		1.51 m	1.51 m	1.51 m
25-H	1.76 br s	1.90 br s	1.91 br s	1.91 br s
26-H	2.74 br d (11)	2.65 br d (11.5)	2.66 br d (11.5)	2.67 br d (11.5)
	2.18 dd (11, 3)	2.29 dd (11.5, 3.5)	2.29 dd (11.5, 3.5)	2.28 dd (11.5, 3.5)
19-H_3	0.77 s	0.97 s	0.98 s	0.94 s
21-H_3	1.33 s	1.20 s	1.20 s	1.20 s
27-H_3	1.01 d (7)	1.08 d (7)	1.08 d (7)	1.08 d (7)
4-OH	6.71 br s	6.21 br s	6.12 br s	6.34 br s
7-OH	Not observed	4.97 br s	4.90 br s	5.07 br s
14-OH	Not observed	4.53 s	4.43 s	4.63 s
15-OH	5.97 br s			
16-OH		4.31 s	4.29 s	4.32 s
20-OH	3.92 s	3.36 br s	3.30 br s	Not observed
2'-H(H_3)	2.42 sextet (7)	2.08 s		2.40 sextet (7)
3'-H	1.81 dqd (14, 7, 7)		1.77 m	1.67 dqd (14, 7, 7)
	1.44 dqd (14, 7, 7)		1.67 m	1.47 dqd (14, 7, 7)
4'-H_3	0.88 t (7)		0.90 t (7)	0.91 t (7)
5'-H_3	1.30 d (7)		1.40 s	1.14 d (7)
2''-H		2.40 sextet (7)	2.40 sextet (7)	
3''-H		1.66 dqd (14, 7, 7)	1.67 m	
		1.47 dqd (14, 7, 7)	1.47 dqd (14, 7, 7)	
4''-H_3		0.91 t (7)	0.91 t (7)	
5''-H_3		1.14 d (7)	1.15 d (7)	

a, b) Measured in C_5D_5N and $CDCl_3$, respectively.

U_6 Colorless amorphous powder, $[\alpha]_D$ −62.8° (c=1.0, $CHCl_3$).

Germidine (U_7, 2) Colorless prisms, mp 231—233 °C, $[\alpha]_D$ +6.85° (c=0.62, $CHCl_3$). [Lit.,[6a] mp 230—231 °C, $[\alpha]_D$ +13° (c=1.67, $CHCl_3$)]. IR ν_{max} ($CHCl_3$) cm^{-1}: 3450, 2860, 2830, 2780, 1735. ^1H- and ^{13}C-NMR: Tables I and II. MS m/z (%): 635 (M^+, 17), 617 (M^+-H_2O, 4), 575 ($M^+-CH_3CO_2H$, 6), 557 ($M^+-H_2O-CH_3CO_2H$, 3), 535 (4), 472 (3), 112 (100), 98 (10). HR-MS: Found 635.3667, Calcd for $C_{34}H_{53}NO_{10}$ (M^+) 635.3668.

Germerine (U_9, 3) Colorless prisms, mp 207—209 °C, $[\alpha]_D$ +5.16° (c=0.63, $CHCl_3$). [Lit.,[6a] mp 200—203 °C, $[\alpha]_D$ +15.7° (c=1.02, $CHCl_3$)]. IR ν_{max} ($CHCl_3$) cm^{-1}: 3450, 2860, 2820, 2770, 1770. ^1H- and ^{13}C-NMR: Tables I and II. MS m/z (%): 693 (M^+, 4), 635 (3), 575 ($M^+-C_4H_8(OH)CO_2H$, 20), 557 ($M^+-C_4H_8(OH)CO_2H-H_2O$, 5), 473 (3), 456 (12), 112 (100), 98 (11), 73 (31). HR-MS: Found 693.4056, Calcd for $C_{37}H_{59}NO_{11}$ (M^+) 693.4087.

15-*O*-(2-Methylbutyroyl)germine (U_{10}, 4) Colorless prisms, mp 221—223 °C, $[\alpha]_D$ −24.10° (c=0.77, $CHCl_3$). [Lit.,[7] mp 224—226 °C, $[\alpha]_D$ −21.48° (pyridine)]. IR ν_{max} ($CHCl_3$) cm^{-1}: 3450, 2860, 2820, 2790, 1730. ^1H- and ^{13}C-NMR: Tables I and II. MS m/z (%): 593 (M^+, 100), 575 (M^+-H_2O, 49), 535 (4), 491 (14), 474 (12), 331 (10), 154 (8), 112 (100), 98 (31). HR-MS: Found 593.3561, Calcd for $C_{32}H_{51}NO_9$ (M^+) 593.3563.

Acknowledgements This study was supported in part by a Grant-in-Aid for Scientific Research to T. K. (No. 01571145) from the Ministry of Education, Science and Culture of Japan. One of the authors (W. Z.) is grateful to Dr. M. Sasa, former President of Toyama Medical and Pharmaceutical University, and to the Fujisawa Foundation for a fellowship.

References and Notes

1) Part I: W. Zhao, Y. Tezuka, T. Kikuchi, J. Chen, and Y. Guo, *Chem. Pharm. Bull.*, **37**, 2920 (1989).
2) Chiang Su New Medical College ed., "Dictionary of Chinese Crude Drugs," Shanghai Scientific Technologic Publisher, Shanghai, 1977, p. 2692.
3) D. M. Harrison, *Nat. Prod. Rep.*, **1**, 221 (1984); *idem, ibid.*, **3**, 446 (1986); J. Tomko and Z. Voticky, "The Alkaloids," Vol. XIV, ed. by R. H. F. Manske, Academic Press, Inc., New York, 1973, p. 5; and references cited therein.
4) The Chinese group of the present authors has reported the isolation of verazine, jervine, and neogermbudine from the same plant; see W. Zhao, J. Chen, and Y. Guo, *Zhongyao Tongbao*, **12**, 34 (1987).
5) F. Bohlmann, *Chem. Ber.*, **91**, 2157 (1958).

TABLE II. ^{13}C Chemical Shifts (in ppm) for the Alkaloids from *V. nigrum* L. var. *ussuriense*

^{13}C	**1**[a] δ	**8**[b] δ	**2**[b] δ	^1H L.r. coupled $^3J_{CH}$[c]	^1H L.r. coupled $^2J_{CH}$[c]	**3**[b] δ	^1H L.r. coupled $^3J_{CH}$[c]	^1H L.r. coupled $^2J_{CH}$[c]	**4**[b] δ
1	33.0 t	32.7 t	32.4 t	19		32.4 t	3, 19		32.1 t
2	30.2 t	26.5 t	26.6 t			26.5 t			27.9 t
3	73.2 d	74.2 d	74.6 d	2, 4-OH		75.5 d			72.7 d
4	107.4 s	105.0 s	105.4 s	2, 6	3, 4-OH	105.2 s	6		107.0 s
5	45.5 d	46.2 d	46.0 d	19		46.3 d			44.5 d
6	30.3 t	27.8 t	28.6 t			28.6 t			28.6 t
7	67.8 d	67.9 d	66.7 d	5	6	66.6 d	5	6	66.8 d
8	48.0 d	47.9 d	47.9 d	6, 12		47.9 d	6, 14-OH		47.8 d
9	93.0 s	92.5 s	92.9 s	5, 7, 12, 19	11	92.9 s	5, 7, 19	11	92.6 s
10	47.0 s	45.8 s	45.9 s	2, 6	5, 19	45.9 s	6	1, 19	46.2 s
11	34.3 t	32.9 t	33.1 t			33.1 t			33.1 t
12	47.6 d	46.8 d	47.3 d	15		47.2 d	15		47.2 d
13	34.7 d	33.3 d	33.7 d	11, 16		33.6 d	11, 16		33.6 d
14	82.5 s	80.0 s	81.2 s	8, 11, 16	12, 15, 14-OH	81.1 s	11, 16	8, 12, 15, 14-OH	81.1 s
15	70.2 d	69.7 d	69.71 d	14-OH, 16-OH		69.8 d	14-OH	16	69.9 d
16	70.7 d	69.4 d	69.3 d			69.3 d			69.3 d
17	44.7 d	45.8 d	45.5 d	15, 18, 21		45.4 d	15, 18, 21		45.4 d
18	63.1 t	61.6 t	61.4 t			61.4 t			61.3 t
19	19.2 q	19.4 q	19.1 q			19.1 q			19.2 q
20	73.2 s	72.9 s	73.0 s		21	72.9 s		21	72.9 s
21	21.3 q	19.9 q	19.9 q			19.9 q			20.0 q
22	71.2 d	69.8 d	69.65 d	21, 26		69.6 d	18, 21, 26		69.7 d
23	19.0 t	18.4 t	18.4 t			18.3 t			18.3 t
24	29.6 t	29.0 t	28.9 t	26, 27		28.9 t	26		28.9 t
25	28.0 d	27.4 d	27.3 d		27	27.3 d		27	27.3 d
26	61.9 t	61.4 t	61.3 t			61.3 t			61.2 t
27	17.4 q	17.1 q	17.1 q	26		17.0 q	26		17.1 q
1′	175.3 s	167.2 s	170.5 s	3	2′	176.4 s	3, 5′		175.7 s
2′	42.1 d	127.9 s	21.5 q			74.8 s	4′	5′	41.1 d
3′	26.9 t	138.2 d				33.2 t	5′	4′	26.7 t
4′	12.0 q	15.7 q				7.7 q			11.5 q
5′	16.7 q	20.7 q				25.6 q			16.8 q
1″		169.4 s	175.7 s	15, 5″	2″	175.6 s	15, 5″		
2″		21.6 q	41.2 d	4″	5″	41.1 d	4″	5″	
3″			26.8 t	5″	4″	26.7 t	5″	4″	
4″			11.6 q			11.5 q			
5″			16.8 q			16.8 q			
1‴		166.8 s							
2‴		128.4 s							
3‴		136.3 d							
4‴		15.9 q							
5‴		20.7 q							

a, b) Measured in C_5D_5N and $CDCl_3$, respectively. *c*) $^2J_{CH}$ and $^3J_{CH}$ indicate the protons coupled with the carbon through two and three bonds, respectively, observed in the long-range ^1H–^{13}C COSY.

6) *a*) J. Fried, H. L. White, and O. Wintersteiner, *J. Am. Chem. Soc.*, **72**, 4621 (1950); *b*) S. M. Kupchan, *ibid.*, **81**, 1921 (1959).
7) I. Nakhatov, R. Shakirov, and S. Yu. Yunusov, *Khim. Prir. Soedin.*, **1983**, 118 [*Chem. Nat. Prod.*, **1983**, 120].
8) Germinaline [16-*O*-acetyl-3,15-*O*,*O*-bis(2-methylbutyroyl)germine] has been isolated from *V. lobelianum*; see K. Samikov, R. Shakirov, and S. Yu. Yunusov, *Khim. Prir. Soedin.*, **1971**, 790. It was reported that synthetic 3,16-*O*,*O*-diacetylgermine is unstable and degraded rapidly in aqueous solution above pH 7 at room temperature, but is stable in nonaqueous systems (CH_2Cl_2, $CHCl_3$, acetonitrile, acetone, and pyridine). See E. M. Cohen and R. Aczel, *J. Pharmaceut. Sci.*, **60**, 193 (1971); E. M. Cohen, R. Aczel, M. Torchiana, R. Tull, and E. J. J. Grabowski, *J. Med. Chem.*, **17**, 769 (1974).

Incarnal. A New Antibacterial Sesquiterpene from Basidiomycetes

Hideki TAKAZAWA*,[a] and Setsuo KASHINO[b]

The Mushroom Research Institute of Japan,[a] 8–1 Hirai-cho, Kiryu, Gumma, 376 Japan and Department of Chemistry, Faculty of Science, Okayama University,[b] Tsushima, Okayama 700, Japan. *Received July 23, 1990*

A new sesquiterpene, incarnal, was isolated from culture fluid of *Gloeostereum incarnatum* (Japanese name: Nikawaurokotake). Incarnal inhibited the growth of gram-positive bacteria at 6.25—12.5 μg/ml. The structure of incarnal has been determined to be (1-hydroxy-2,10,10-trimethyl)-3-methylene-tricyclo[6.3.0.0^{2,6}]undec-5,7-diene-4,9-dione by X-ray diffraction and spectroscopic methods.

Keywords sesquiterpene; X-ray diffraction; antibiotic; basidiomycetes; *Gloeostereum incarnatum*; incarnal

An extract of basidioma of *G. incarnatum* inhibits the growth of *Shigella dysenteriae*, *Pseudomonas pyocynea*, *Staphylococcus aureus*, *Escherichia coli* and *Bacillus subtilis*.[1] In the present paper, we describe the isolation, antibacterial activities and three dimensional structure of a new hirsutane-type sesquiterpene, incarnal (**1**), which was isolated from culture fluid of *G. incarnatum*.

Experimental

The melting point was determined with a Yazawa micro melting point apparatus and is uncorrected. Proton and carbon-13 nuclear magnetic resonance (^{1}H- and ^{13}C-NMR) spectra were obtained on a JEOL JNM-GX270 spectrometer. Chemical shifts (δ) are reported in ppm from internal tetramethylsilane. The mass spectrum (MS) was determined with a JEOL JMS-D300 mass spectrometer. The infrared (IR) spectrum was measured on a JASCO IR-810 spectrometer, and the ultraviolet (UV) spectrum on a Hitachi U-3200.

Fermentation and Isolation Procedure *G. incarnatum* was grown in 10 l of GYP medium composed of (g/l): glucose 50.0, polypeptone 2.5, yeast extract 2.5, KH_2PO_4 1.0, $MgSO_4 \cdot 7H_2O$ 0.5, $CaCl_2$ 0.5, pH 5.0, 121 °C, 15 min. The shaken culture obtained from the spores was kept at 25 °C for 10 d. After fermentation, the mycelia were separated from the culture fluid by filtration. Incarnal was extracted from the culture fluid (9.5 l) with ethyl acetate (4 l). After evaporation of the solvent, the crude product (2.1 g) was applied to a column on silica gel (Fuji Davison 4B) and eluted with *n*-hexane–ether. The fractions containing incarnal were combined to yield 0.70 g of a yellow solid. Pure incarnal (0.57 g) was obtained by crystallization from ether.

A mycelial culture of *G. incarnatum* was also tested for the production of antibacterial activity. For maintenance on agar slants, the strain was grown in potato dextrose agar medium (Difco).

X-Ray Crystallographic Analysis Single crystals were grown from an ether solution by slow evaporation. A yellow prism elongated along *c*, with dimensions of 0.11 × 0.08 × 0.30 mm, was mounted on a Rigaku AFC-5 four-circle diffractometer equipped with a rotating anode (Ni-filtered CuK_α, 40 kV, 200 mA). The lattice parameters were determined with 20 reflections in the range of $36 < 2\theta < 41°$. Systematic absences were $h00$ for h odd, $0k0$ for k odd, $00l$ for l odd.

Crystal data: $C_{15}H_{16}O_3$, $M_r = 244.29$, mp = 405—406 K, orthorhombic, $P2_12_12_1$, $a = 12.019$ (1), $b = 17.690$ (1), $c = 6.282$ (1) Å, $V = 1335.6$ (3) Å^3, $Z = 4$, $D_x = 1.215$ Mg·m^{-3}, CuK_α ($\lambda = 1.54178$ Å), $\mu = 0.64$ mm^{-1}, $F(000) = 520$.

Intensity data were collected at 25 °C within $2\theta_{max} = 120°$ ($0 \leqq h \leqq 13$, $0 \leqq k \leqq 19$, $0 \leqq l \leqq 7$) by the ω-2θ scan method [scan speed 4° min^{-1} in ω, scan range in ω 1.2° + 0.15° tan θ]. Background was measured for 4 s on either side of the peak; three standard reflections were recorded after every 97 reflections, fluctuations being within 0.8%. Lorentz and polarization corrections were applied, but no absorption correction was made. In total, 1174 unique reflections were measured, 1099 reflections being larger than $\sigma(F_o)$. All unique reflections were used in structure analysis. The structure was solved by MULTAN78 and refined by the block-diagonal least-squares method (non-H atoms anisotropically). The H atoms were determined from a difference Fourier map and refined isotropically; $\Sigma w(|F_o| - |F_c|)^2$ was minimized with $w = 1.0/[\sigma(F_o)^2 - 0.0922|F_o| + 0.0055|F_o|^2]$ for $|F_o| > 0$, $w = 0.6347$ for $|F_o| = 0$. Final $R = 0.050$ for 1174 reflections, $wR = 0.044$, $S = 1.79$. $(\Delta/\sigma)_{max} = 0.21$ for non-H atoms and 0.74 for H atoms. The residual electron density in the final difference map was within ± 0.16 eÅ^{-3}. Atomic scattering factors were taken from "International Tables for X-Ray Crystallography".[2] Programs: MULTAN78,[3] HBLS-V and DAPH,[4] MOLCON[5] and ORTEP.[6] Computations were carried out at the Research Center for Protein Engineering, Institute for Protein Research, Osaka University, and at the Okayama University Computer Center.

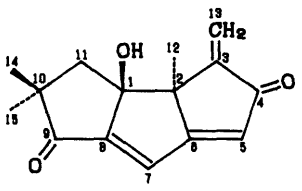

Chart 1. Incarnal (**1**)

Results and Discussion

Physical and Spectroscopic Data Soluble in dimethyl sulfoxide (DMSO), methanol, acetone, ethyl acetate, ether and chloroform; insoluble in water and *n*-hexane; mp 132—133 °C; *Rf* 0.35 (chloroform : ether : acetic acid = 50 : 50 : 1). *Anal.* Calcd for $C_{15}H_{16}O_3$: C, 73.77; H, 6.56. Found:

Table I. ^{1}H- and ^{13}C-NMR Data (in $CDCl_3$, 270 and 67.9 MHz)

H-atom	δ multiplicity, J [Hz]		C-atom	δ multiplicity, J [Hz]	
5	6.41 s		1	83.67 s	
7	7.33 s		2	63.22 s	
11	2.04 d	5.1	3	147.60 s	
	2.17 d	5.1	4	207.44 s	
12	1.29 s		5	128.34 D	78.2
13	5.41 s		6	184.52 s	
	5.92 s		7	126.49 D	88.1
14	1.18 s		8	157.40 s	
15	1.11 s		9	195.45 s	
OH	5.13 s		10	51.10 s	
			11	42.52 T	28.8
			13	116.66 T	62.9
			$-CH_3$	26.01 Q	22.5
				26.50 Q	22.5
				27.35 Q	23.3

Table II. Antibacterial Spectra

Test organism[a)]	MIC (μg/ml)
Staphylococcus aureus FDA 209P	6.25
Bacillus subtilis ATCC 6633	12.5
Escherichia coli NIHJ JC-2	>100
Pseudomonas aeruginosa	>100

a) Mueller Hintone agar, 36 °C, 18 h. MIC, minimal inhibitory concentration.

TABLE III. Final Atomic Coordinates ($\times 10^4$) and Equivalent Isotropic Thermal Parameters (Å^2) with e. s. d.'s in Parentheses

Atoms	x	y	z	B_{eq}
O(1)	1014 (1)	3687 (1)	754 (3)	4.59 (8)
O(2)	4180 (2)	2122 (1)	669 (4)	8.0 (1)
O(3)	743 (2)	5654 (1)	3561 (4)	7.4 (1)
C(1)	1147 (2)	3669 (1)	3019 (4)	3.8 (1)
C(2)	2107 (2)	3127 (1)	3664 (5)	4.4 (1)
C(3)	2425 (2)	2478 (1)	2261 (5)	4.8 (1)
C(4)	3624 (2)	2572 (2)	1695 (5)	5.6 (2)
C(5)	3967 (2)	3309 (2)	2464 (5)	5.7 (2)
C(6)	3100 (2)	3650 (1)	3389 (5)	4.5 (1)
C(7)	2737 (2)	4424 (2)	3787 (5)	4.9 (1)
C(8)	1629 (2)	4429 (1)	3546 (5)	4.3 (1)
C(9)	701 (2)	4965 (1)	3743 (5)	5.0 (1)
C(10)	−354 (2)	4513 (2)	4185 (5)	5.1 (2)
C(11)	27 (2)	3682 (2)	4146 (5)	4.9 (1)
C(12)	2030 (2)	2870 (2)	5996 (5)	6.2 (2)
C(13)	1809 (3)	1906 (2)	1579 (7)	7.8 (2)
C(14)	−1224 (3)	4682 (2)	2492 (7)	8.0 (2)
C(15)	−775 (3)	4746 (2)	6392 (7)	7.5 (2)

$B_{eq}=(4/3)\Sigma\beta_{ij}/a_i$*2

TABLE IV. Bond Lengths (Å) and Angles (°) for the Non-Hydrogen Atoms with e. s. d.'s in Parentheses

O(1)–C(1)	1.432 (4)	C(3)–C(15)	1.325 (6)
O(2)–C(4)	1.223 (4)	C(4)–C(5)	1.450 (4)
O(3)–C(9)	1.225 (4)	C(5)–C(6)	1.337 (4)
C(1)–C(2)	1.554 (4)	C(6)–C(7)	1.459 (4)
C(1)–C(8)	1.501 (4)	C(7)–C(8)	1.340 (4)
C(1)–C(11)	1.521 (4)	C(8)–C(9)	1.469 (4)
C(2)–C(3)	1.497 (4)	C(9)–C(10)	1.525 (4)
C(2)–C(6)	1.520 (4)	C(10)–C(11)	1.540 (4)
C(2)–C(12)	1.537 (4)	C(10)–C(14)	1.521 (5)
C(3)–C(4)	1.494 (4)	C(10)–C(15)	1.532 (5)
O(1)–C(1)–C(2)	110.8 (2)	C(4)–C(5)–C(6)	109.2 (3)
O(1)–C(1)–C(8)	104.0 (2)	C(2)–C(6)–C(5)	112.8 (3)
O(1)–C(1)–C(11)	111.3 (2)	C(2)–C(6)–C(7)	108.5 (3)
C(2)–C(1)–C(8)	102.0 (2)	C(5)–C(6)–C(7)	137.0 (3)
C(2)–C(1)–C(11)	123.0 (3)	C(6)–C(7)–C(8)	106.5 (3)
C(8)–C(1)–C(11)	103.0 (2)	C(1)–C(8)–C(7)	113.7 (3)
C(1)–C(2)–C(3)	120.6 (3)	C(1)–C(8)–C(9)	107.7 (3)
C(1)–C(2)–C(6)	100.2 (2)	C(7)–C(8)–C(9)	138.5 (3)
C(1)–C(2)–C(12)	112.7 (2)	O(3)–C(9)–C(8)	127.1 (3)
C(3)–C(2)–C(6)	101.5 (2)	O(3)–C(9)–C(10)	125.0 (3)
C(3)–C(2)–C(12)	110.5 (3)	C(8)–C(9)–C(10)	108.0 (3)
C(6)–C(2)–C(12)	109.6 (2)	C(9)–C(10)–C(11)	104.5 (2)
C(2)–C(3)–C(4)	107.5 (3)	C(9)–C(10)–C(14)	110.0 (3)
C(2)–C(3)–C(13)	129.3 (3)	C(9)–C(10)–C(15)	107.4 (3)
C(4)–C(3)–C(13)	123.2 (3)	C(11)–C(10)–C(14)	112.4 (3)
O(2)–C(4)–C(3)	125.5 (3)	C(11)–C(10)–C(15)	111.7 (3)
O(2)–C(4)–C(5)	127.3 (3)	C(14)–C(10)–C(15)	110.7 (3)
C(3)–C(4)–C(5)	107.2 (3)	C(1)–C(11)–C(10)	106.6 (2)

C, 73.86; H, 6.55. UV λ_{max}^{EtOH} nm (log ε): 314.4 (4.21). IR ν_{max}^{KBr} cm^{-1}: 3340 (st), 2950—2870 (m), 1720 (st), 1690 (st), 1650 (st), 1600 (st), 1160 (m), 1000 (m), 940 (m), 860 (m). ^{1}H- and ^{13}C-NMR spectral data are listed in Table I. MS m/z: 244 (100, M$^+$), 229 (50.6), 160 (71.5), 132 (99.7), 104 (88.7). The IR, ^{1}H- and ^{13}C-NMR spectra showed the presence of ≥C–OH, 2 ≥C=CH–, ≥C=CH$_2$, 2 ≥C=O and 3 –CH$_3$ groups.

Biogical Assays The antibacterial spectra obtained by the agar dilution method are shown in Table II. Incarnal inhibited the growth of gram-positive bacteria at 6.25—12.5 μg/ml, but it had no antibacterial activity against gram-negative bacteria.

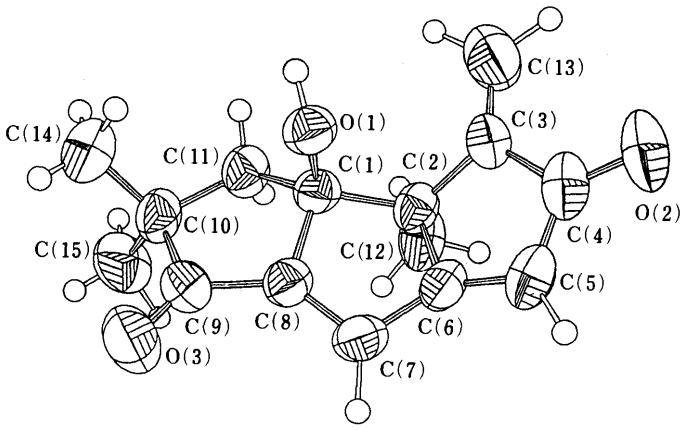

Fig. 1. ORTEP Drawing with Atomic Numbering

Ellipsoids of 50% probability are drawn for the non-H atoms; the H atoms are represented as spheres equivalent to $B=1.0$ Å^2.

Three Dimensional Structure The final positional and thermal parameters for non-hydrogen atoms are given in Table III. Bond lengths and angles are listed in Table IV. An ORTEP drawing of the molecule with the atomic numbering is shown in Fig. 1.

The molecular skeleton is composed of three five-membered rings. The largest distortions in the skeleton are found around the ring-junction bonds C(2)–C(6) and C(1)–C(8): C(1)–C(2)–C(6)–C(7) 29.4 (3)° and C(11)–C(1)–C(8)–C(9) −31.8 (3)°. The C(1)–C(2) bond is lengthened by a short 1,4-contact, C(11)···C(12) 3.035 (4) Å. The double bond character of the C(5)–C(6) and C(7)–C(8) bonds is clearly evidenced by their short bond lengths. In the crystal, the molecules related by a 2_1 axis along ***a*** are linked by an O–H···O hydrogen bond [O(1)···O(2) 2.776 (4), H(1)···O(2) 1.86 (4) Å, O(1)–H(1)···O(2) 172 (4)°].

Sesquiterpenes comprise the majority of the isoprene metabolites isolated from basidiomycetes.[7] They are classified into hirsutanes, protoilludanes, illudanes, marasmanes, sterpranes, fomannosanes, illudalanes, secoilludalanes, lactalanes, secolactalanes and isolactalanes. The structure determination revealed that incarnal is a hirsutane-type compound, a category which includes coriolins,[8] complicatic acid,[9] hypnophilin[10] and pleuroteic acid.[10] The X-ray structure determination of hexahydrocoriolin has been reported.[11] However, the present work is the first to elucidate a sesquiterpene structure composed of highly conjugated five-membered rings. Substances like incarnal have been detected during the synthesis of *dl*-coriolins[12] and among terpenoid metabolites of mushrooms.[7] Therefore, it can be assumed that incarnal is also a terpenoid metabolite.

Acknowledgments The authors thank Dr. Toshiyuki Chikuma of Showa College of Pharmaceutical Sciences for measuring ^{1}H- and ^{13}C-NMR spectra and MS, Mr. Atsushi Zennyoji of The Mushroom Research Institute of Japan for his valuable suggestions, Mr. Takashi Suda of Mori & Company, Ltd. for supplying the strain of *Gloeostereum incarnatum*. The Research Center for Protein Engineering, Institute for Protein Research, Osaka University, is gratefully acknowledged for the use of the diffractometer.

References

1) L. Ruijun and L. Fengzhen, *Edible Fungi of China*, **9**, 9 (1989).

2) "International Tables for X-Ray Crystallography," Vol. IV, Kynoch Press, Birmingham, 1974.
3) P. Main, S. E. Hull, L. Lessinger, G. Germain, J.-P. Declercq and M. M. Woolfson, "MULTAN78, A System of Computer Programs for the Automatic Solution of Crystal Structures from X-Ray Diffraction Data," Univs. of York, England, and Louvain, Belgium, 1978.
4) T. Ashida, "The Universal Crystallographic Computing System, Osaka," The Computation Center, Osaka Univ., 1973.
5) S. Fujii, "The Universal Crystallographic Computing System, Osaka," The Computation Center, Osaka Univ., 1979.
6) C. K. Johnson ORTEP. Report ORNL-3794, revised. Oak Ridge National Laboratory, Tennessee, U.S.A., 1971.
7) W. A. Ayer and L. M. Browne, *Tetrahedron*, **37**, 2199 (1981).
8) T. Takeuchi, H. Iimura, J. Iwanaga, S. Takahashi, T. Takita and H. Umezawa, *J. Antibiot.*, **22**, 215 (1969).
9) P. G. Mantle and G. Mellows, *Trans. Br. Mycol. Soc.*, **61**, 513 (1973).
10) B. M. Giannetti, B. Steffan and W. Steglich, *Tetrahedron*, **42**, 3587 (1986).
11) H. Nakayama, T. Takita, H. Umezawa, M. Kunishima, Y. Nakayama and Y. Iitaka, *J. Antibiot.*, **27** 301 (1974).
12) B. M. Trost and D. P. Curran, *J. Am. Chem. Soc.*, **103**, 7380 (1981).

Amidines. VIII. A Kinetic Study of Alcoholysis of N^1-Arenesulfonyl-N^1,N^2-diarylacetamidines

Machiko ONO, Reiko TODORIKI, and Shinzo TAMURA*

School of Pharmaceutical Sciences, Toho University, 2-2-1, Miyama, Funabashi, Chiba 274, Japan. *Received July 25, 1990*

Alcoholysis of N^1-arenesulfonyl-N^1,N^2-diarylacetamidines (1—30) was studied kinetically. The rate of the reaction between the substrates and ethoxide ion depended on the electron-withdrawing resonance effect of the substituents on both the N^1-aryl and N^2-aryl groups to a similar extent. The rate of the neutral alcoholysis depended on the resonance effect of the N^1-aryl substituent to a larger extent than in the former reaction, and depended hardly at all on the electron-releasing resonance effect of the N^2-aryl substituent, showing that the reaction does not proceed by the solvolysis mechanism.

A reaction mechanism is proposed in which the rate-determining attack of the nucleophile is accompanied by the concerted departure of the *N*-arylarenesulfonamide group.

Keywords kinetic study; alcoholysis; N^1-arenesulfonyl-N^1,N^2-diarylacetamidine; concerted mechanism; tetrahedral intermediate; Hammett's plot; Yukawa–Tsuno equation

In previous papers we reported the reactions between N^1-arenesulfonyl-N^1,N^2-diarylamidines and various nucleophiles, *i.e.*, ethoxide ion,[1,2] *p*-nitroaniline[3] and amides.[2,4] The reactions took place at the amidine central carbon, and gave imidates, unsymmetrical amidines and acylamidines, respectively, with departure of *N*-arylarenesulfonamides.

In this work, we studied the alcoholysis of N^1-arenesulfonyl-N^1,N^2-diarylacetamidines (**1—30**) kinetically to elucidate the electronic effect of the three substituents X, Y and Z on the reaction rate (Chart 1).

The reaction was allowed to proceed in the presence of sodium ethoxide. The second-order rate constant, k^{EtO}, was correlated to the nucleophilic substituent constant, σ^-, of the substituents X and Y to a moderate extent in Hammett's relation.

The attack of ethoxide ion on the amidine central carbon is expected to be rate-determining on the basis that the *N*-arylarenesulfonamide group is a better leaving group than the ethoxide group if the metastable tetrahedral intermediate exists. The contribution of the resonance effect of the substituent X to the reaction rate suggests that there is a significant change in the charge of the sulfonamide nitrogen in the transition state. This implies that the rate-determining attack of ethoxide ion is accompanied by the concerted departure of the sulfonamide group.

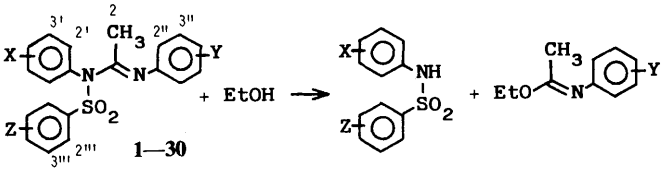

	X	Y	Z		X	Y	Z
1	*p*-Cl	*m*-NO_2	*p*-Cl	**16**	*p*-NO_2	*m*-CH_3O	*p*-CH_3
2	*m*-Cl	*m*-NO_2	*p*-Cl	**17**	*p*-NO_2	*m*-Cl	*p*-CH_3
3	*p*-CF_3	*m*-NO_2	*p*-Cl	**18**	*p*-NO_2	*m*-NO_2	*p*-CH_3
4	*p*-CN	*m*-NO_2	*p*-Cl	**19**	*p*-NO_2	*p*-CN	*p*-CH_3
5	*p*-NO_2	*m*-NO_2	*p*-Cl	**20**	*p*-NO_2	*p*-NO_2	*p*-CH_3
6	*p*-NO_2	*p*-Cl	*p*-CH_3	**21**	*p*-NO_2	*p*-CH_3O	*m*-NO_2
7	*p*-NO_2	*p*-Cl	H	**22**	*p*-NO_2	*p*-CH_3	*m*-NO_2
8	*p*-NO_2	*p*-Cl	*p*-Cl	**23**	*p*-NO_2	*p*-isoPr	*m*-NO_2
9	*p*-NO_2	*p*-Cl	*m*-NO_2	**24**	*p*-NO_2	*p*-(*tert*-Bu)	*m*-NO_2
10	*p*-NO_2	H	*p*-CH_3	**25**	*p*-NO_2	*p*-CH_3S	*m*-NO_2
11	*p*-NO_2	H	H	**26**	*p*-CF_3	*p*-CH_3O	*m*-NO_2
12	*p*-NO_2	H	*p*-Cl	**27**	*m*-NO_2	*p*-CH_3O	*m*-NO_2
13	*p*-NO_2	H	*m*-NO_2	**28**	*p*-CN	*p*-CH_3O	*m*-NO_2
14	*p*-NO_2	*p*-CH_3O	*p*-CH_3	**29**	*p*-NO_2	*p*-CH_3O	H
15	*p*-NO_2	*p*-CH_3	*p*-CH_3	**30**	*p*-NO_2	*p*-CH_3O	*p*-Cl

Chart 1

Experimental

All melting points are uncorrected. The ultraviolet (UV) spectra were measured on a Hitachi spectrophotometer, model 139. Proton nuclear magnetic resonance (^{1}H-NMR) spectra were recorded on JEOL PMX 60 and JEOL GX 400 NMR spectrometers with tetramethylsilane as an internal standard. The following abbreviations are used: singlet (s), doublet (d), triplet (t), quartet (q), double double doublet (ddd) and broad (br).

Materials N^1-Tosyl-N^1-(*p*-nitrophenyl)-N^2-(*p*-chlorophenyl)acetamidine (**6**),[1] N^1-tosyl-N^1-(*p*-nitrophenyl)-N^2-(*p*-methoxyphenyl)acetamidine (**14**),[4] N^1-tosyl-N^1-(*p*-nitrophenyl)-N^2-(*p*-methylphenyl)acetamidine (**15**),[4] N^1-tosyl-N^1-(*p*-nitrophenyl)-N^2-(*m*-nitrophenyl)acetamidine (**18**),[4] N^1-tosyl-N^1,N^2-di(*p*-nitrophenyl)acetamidine (**20**)[3] and N^1-(*p*-methoxyphenyl)-N^2-(*p*-nitrophenyl)acetamidine[3] were prepared according to the cited references.

Preparation of N^1-Arenesulfonyl-N^1,N^2-diarylacetamidines by Beckmann Rearrangement N^1-Arenesulfonyl-N^1,N^2-diarylacetamidines were prepared according to the previous papers[1,4] by method A and method B. Method A: Substituted acetophenoxime tosylate (0.01 mol) and the sodium salt of *N*-arylarenesulfonamide (0.01 mol) were heated with an appropriate solvent. Method B: Substituted acetophenoxime (0.01 mol), tosyl chloride (0.01 mol) and Et_3N (0.01 mol) were dissolved in an appropriate solvent under ice-cooling. The mixture was kept for 1 d in an ice-box, and filtered. The sodium salt of substituted *N*-arylarenesulfonamide (0.01 mol) was added to the filtrate, and the mixture was heated under reflux. The results are shown in Table I. ^{1}H-NMR data for N^1-arenesulfonyl-N^1,N^2-diarylacetamidines ($CDCl_3$, 400 MHz) are shown in Table II.

Preparation of N^1-Mesyl-N^1-(*p*-nitrophenyl)-N^2-(*p*-methoxyphenyl)acetamidine (31) *p*-Methoxyacetophenoxime (1.65 g, 0.01 mol), tosyl chloride (1.91 g, 0.01 mol) and Et_3N (1.01 g, 0.01 mol) were dissolved in 20 ml of anhydrous tetrahydrofuran (THF) under ice-cooling. The mixture was kept for 1 d in an ice-box and filtered. The sodium salt of *N*-(*p*-nitrophenyl)methanesulfonamide (2.38 g, 0.01 mol) and 50 ml of anhydrous THF were added to the filtrate. The whole was stirred for 5.5 h at room temperature, and filtered. The filtrate was concentrated under reduced pressure. The residue was dissolved in 50 ml of $CHCl_3$. The $CHCl_3$ solution was washed successively with 1 N NaOH and H_2O, dried over Na_2SO_4, and concentrated under reduced pressure. The residue was washed with a small amount of AcOEt, and recrystallized from AcOEt to give 1.08 g (30%) of **31**, mp 141 °C. *Anal.* Calcd for $C_{16}H_{17}N_3O_5S$: C, 52.88; H, 4.72; N, 11.56. Found: C, 53.04; H, 4.75; N, 11.45. ^{1}H-NMR ($CDCl_3$, 400 MHz) δ: 1.81 (3H, s, 2-position), 3.46 (3H, s, CH_3SO_2), 3.81 (3H, s, OCH_3), 6.80 (2H, d, J=9 Hz, 2″- and 6″-positions), 6.90 (2H, d, J=9 Hz, 3″- and 5″-positions), 7.63 (2H, d, J=9 Hz, 2′- and 6′-positions), 8.33 (2H, d, J=9 Hz, 3′- and 5′-positions).

Preparation of Ethyl *N*-Arylacetimidates Ethyl *N*-(*p*-methoxyphenyl)-acetimidate,[1] ethyl *N*-(*p*-methylphenyl)acetimidate,[5] ethyl *N*-phenylacetimidate,[5] ethyl *N*-(*p*-chlorophenyl)acetimidate,[5] ethyl *N*-(*m*-chlorophenyl)acetimidate[5] and ethyl *N*-(*p*-nitrophenyl)acetimidate[6] were prepared

TABLE I. Preparation of N^1-Arenesulfonyl-N^1,N^2-diarylacetamidines[a)]

Compd. No.	Method	React. solvent	React. time (h)	Yield (%)	mp (°C)	Molecular formula	Analysis (%) Calcd C	Calcd H	Calcd N	Found C	Found H	Found N
1	A	Xylene	8	50	178	$C_{20}H_{15}Cl_2N_3O_4S$	51.73	3.26	9.05	51.66	3.24	9.07
2	A	Xylene	8	41	211	$C_{20}H_{15}Cl_2N_3O_4S$	51.73	3.26	9.05	51.48	3.30	9.14
3	A	Toluene	17	28	166	$C_{21}H_{15}ClF_3N_3O_4S$	50.66	3.04	8.44	50.71	3.02	8.41
4	A	Toluene	13	22	222	$C_{21}H_{15}ClN_4O_4S$	55.45	3.32	12.32	55.42	3.22	12.17
5	A	Toluene	7	29	203	$C_{20}H_{15}ClN_4O_6S \cdot 1/2AcOEt$	50.92	3.69	10.80	50.78	3.64	10.89
7	A	Dioxane	2	30	193	$C_{20}H_{16}ClN_3O_4S$	55.88	3.75	9.77	55.87	3.73	9.73
8	A	Dioxane	1.5	42	184	$C_{20}H_{15}Cl_2N_3O_4S$	51.73	3.26	9.05	51.71	3.22	9.02
9	A	Dioxane	2	46	192	$C_{20}H_{15}ClN_4O_6S$	50.59	3.18	11.80	50.77	3.15	11.87
10	B	Dioxane	2.5	62	218	$C_{21}H_{19}N_3O_4S$	61.60	4.68	10.26	61.59	4.63	10.26
11	B	Dioxane	4	70	190	$C_{20}H_{17}N_3O_4S$	60.75	4.33	10.63	60.84	4.26	10.61
12	B	Dioxane	4	57	185	$C_{20}H_{16}ClN_3O_4S$	55.88	3.75	9.77	55.88	3.71	9.75
13	B	Dioxane	2	59	158	$C_{20}H_{16}N_4O_6S$	54.54	3.66	12.72	54.59	3.59	12.64
16	B	THF	2	53	178	$C_{22}H_{21}N_3O_5S$	60.12	4.82	9.56	60.04	4.74	9.50
17	B	Dioxane	12	24	183	$C_{21}H_{18}ClN_3O_4S$	56.82	4.09	9.47	56.83	4.07	9.39
19	A	Toluene	6.5	25	198	$C_{22}H_{18}N_4O_4S \cdot 1/2AcOEt$	60.24	4.63	11.71	60.28	4.55	11.72
21	B	THF	7	23	152	$C_{21}H_{18}N_4O_7S$	53.61	3.86	11.91	53.61	3.80	11.72
22	B	THF	10	57	152	$C_{21}H_{18}N_4O_6S$	55.50	3.99	12.33	55.48	3.93	12.20
23	B	THF	5	23	155	$C_{23}H_{22}N_4O_6S$	57.25	4.60	11.61	57.12	4.58	11.51
24	B	THF	7	34	162	$C_{24}H_{24}N_4O_6S$	58.05	4.87	11.28	57.89	4.83	11.26
25	B	THF	7	29	164	$C_{21}H_{18}N_4O_6S_2$	51.84	3.73	11.52	51.73	3.84	11.41
26	B	THF	2	11	132	$C_{22}H_{18}F_3N_3O_5S$	53.55	3.68	8.52	53.53	3.68	8.42
27	B	THF	3	22	133	$C_{21}H_{18}N_4O_7S$	53.61	3.86	11.91	53.72	3.86	11.84
28	B	THF	2	24	150	$C_{22}H_{18}N_4O_5S$	58.66	4.03	12.44	58.69	3.96	12.18
29	B	THF	1	23	165	$C_{21}H_{19}N_3O_5S$	59.28	4.50	9.88	59.20	4.53	9.87
30	B	THF	4	33	170	$C_{21}H_{18}ClN_3O_5S$	54.84	3.95	9.14	54.90	3.92	9.19

a) All samples were recrystallized from ethyl acetate except for **22**, **27** and **28**. Compounds **22** and **27** were recrystallized from a mixture of ethyl acetate and petroleum benzin (4 : 1), and compound **28** was recrystallized from benzene.

TABLE II. ^{1}H-NMR Spectral Data for N^1-Arenesulfonyl-N^1,N^2-diarylacetamidines (δ, $CDCl_3$)

Compd. No.	2	2′	3′	4′	5′	6′	2″	3″	4″	5″	6″	2‴	3‴	4‴	5‴	6‴	Other signals
1	1.69	7.47	7.27				7.49		7.94	7.47	7.02	7.84	7.47				
2	1.69	7.36		7.24	7.44	7.49	7.50		7.94	7.47	7.02	7.85	7.49				
3	1.71	7.49	7.77				7.51		7.95	7.48	7.03	7.84	7.49				
4	1.72	7.49	7.81				7.50		7.96	7.48	7.02	7.81	7.49				
5	1.76	7.53	8.36				7.51		7.96	7.50	7.03	7.82	7.49				
7	1.76	7.53	8.32				6.57	7.25				7.87	7.50	7.64			
8	1.73	7.46	8.33				6.62	7.28				7.79	7.46				
9	1.75	7.55	8.37				6.63	7.29				8.75		8.48	7.70	8.20	
10	1.78	7.52	8.30				6.66	7.30	7.07			7.75	7.28				CH_3 (Ts), 2.44
11	1.77	7.54	8.31				6.64	7.29	7.08			7.88	7.49	7.62			
12	1.74	7.53	8.32				6.69	7.32	7.10			7.81	7.45				
13	1.76	7.56	8.36				6.68	7.32	7.11			8.73		8.46	7.69	8.23	
16	1.78	7.52	8.30				6.20		6.62	7.19	6.24	7.75	7.28				CH_3 (Ts), 2.44; CH_3O, 3.78
17	1.77	7.51	8.32				6.64		7.04	7.21	6.55	7.74	7.29				CH_3 (Ts), 2.46
19	1.76	7.52	8.33				6.72	7.58				7.75	7.31				CH_3 (Ts), 2.48
21	1.79	7.55	8.35				6.65	6.86				8.76		8.45	7.68	8.19	CH_3O, 3.80
22	1.76	7.56	8.35				6.59	7.12				8.73		8.45	7.68	8.21	CH_3, 2.32
23	1.78	7.56	8.35				6.62	7.13				8.72		8.45	7.68	8.22	CH_3, 1.24; CH, 2.89
24	1.78	7.56	8.35				6.63	7.33				8.72		8.46	7.69	8.23	CH_3, 1.31
25	1.77	7.55	8.36				6.64	7.23				8.75		8.46	7.69	8.20	CH_3S, 2.48
26	1.75	7.49	7.76				6.64	6.86				8.79		8.44	7.67	8.21	CH_3O, 3.79
27	1.79	8.19		8.37	7.71	7.75	6.65	6.86				8.75		8.47	7.70	8.22	CH_3O, 3.80
28	1.77	7.49	7.79				6.64	6.86				8.74		8.45	7.68	8.19	CH_3O, 3.80
29	1.80	7.54	8.31				6.60	6.84				7.87	7.48	7.61			CH_3O, 3.79
30	1.77	7.53	8.31				6.64	6.87				7.80	7.44				CH_3O, 3.79

according to the cited references. The following imidates were prepared by the reaction of ethyl orthoacetate and arylamines.[7] Ethyl *N*-(*p*-isopropylphenyl)acetimidate, bp 131 °C/13 mmHg, yield 88%. *Anal.* Calcd for $C_{13}H_{19}NO$: C, 76.06; H, 9.33; N, 6.82. Found: C, 75.66; H, 9.51; N, 6.74. ^{1}H-NMR ($CDCl_3$, 400 MHz) δ: 1.23 (6H, d, J=7 Hz, CH_3 of isopropyl), 1.33 (3H, t, J=7 Hz, CH_2CH_3), 1.83 (3H, s, 2-position), 2.86 (1H, septet, J=7 Hz, CH of isopropyl), 4.21 (2H, q, J=7 Hz, CH_2CH_3), 6.68 (2H, d, J=9 Hz, 2′- and 6′-positions), 7.12 (2H, d, J=9 Hz, 3′-

and 5'-positions). Ethyl *N*-(*p*-(*tert*-butyl)phenyl)acetimidate, bp 139 °C/18 mmHg, yield 78%. *Anal.* Calcd for $C_{14}H_{21}NO$: C, 76.67; H, 9.65; N, 6.39. Found: C, 76.53; H, 9.84; N, 6.43. ^{1}H-NMR ($CDCl_3$, 400 MHz) δ: 1.30 (9H, s, *tert*-Bu), 1.33 (3H, t, J=7 Hz, $CH_2C\underline{H}_3$), 1.83 (3H, s, 2-position), 4.22 (2H, q, J=7 Hz, $C\underline{H}_2CH_3$), 6.68 (2H, d, J=9 Hz, 2'- and 6'-positions), 7.28 (2H, d, J=9 Hz, 3'- and 5'-positions). Ethyl *N*-(*p*-methylthiophenyl)acetimidate, bp 156 °C/15 mmHg, yield 80%. *Anal.* Calcd for $C_{11}H_{15}NOS$: C, 63.12; H, 7.22; N, 6.69. Found: C, 63.03; H, 7.45; N, 6.78. ^{1}H-NMR ($CDCl_3$, 60 MHz) δ: 1.30 (3H, t, J=7 Hz, $CH_2C\underline{H}_3$), 1.80 (3H, s, 2-position), 2.42 (3H, s, SCH_3), 4.25 (2H, q, J=7 Hz, $C\underline{H}_2CH_3$), 6.73 (2H, d, J=9 Hz, 2'- and 6'-positions), 7.28 (2H, d, J=9 Hz, 3'- and 5'-positions). Ethyl *N*-(*p*-cyanophenyl)acetimidate, bp 164 °C/13 mmHg, mp 75 °C (petroleum ether), yield 82%. *Anal.* Calcd for $C_{11}H_{12}N_2O$: C, 70.19; H, 6.43; N, 14.88. Found: C, 70.15; H, 6.43; N, 14.77. ^{1}H-NMR ($CDCl_3$, 60 MHz) δ: 1.33 (3H, t, J=7 Hz, $CH_2C\underline{H}_3$), 1.80 (3H, s, 2-position), 4.23 (2H, q, J=7 Hz, $C\underline{H}_2CH_3$), 6.83 (2H, d, J=9 Hz, 2'- and 6'-positions), 7.58 (2H, d, J=9 Hz, 3'- and 5'-positions). Ethyl *N*-(*m*-nitrophenyl)acetimidate, bp 169 °C/22 mmHg, yield 64%. *Anal.* Calcd for $C_{10}H_{12}N_2O_3$: C, 57.68; H, 5.81; N, 13.45. Found: C, 57.77; H, 5.85; N, 13.28. ^{1}H-NMR ($CDCl_3$, 400 MHz) δ: 1.36 (3H, t, J=7 Hz, $CH_2C\underline{H}_3$), 1.85 (3H, s, 2-position), 4.24 (2H, q, J=7 Hz, $C\underline{H}_2CH_3$), 7.10 (1H, ddd, J=8, 2, 1 Hz, 6'-position), 7.44 (1H, t, J=8 Hz, 5'-position), 7.62 (1H, t, J=2 Hz, 2'-position), 7.90 (1H, ddd, J=8, 2, 1 Hz, 4'-position). Ethyl *N*-(*m*-methoxyphenyl)acetimidate, bp 141 °C/22 mmHg, yield 91%. *Anal.* Calcd for $C_{11}H_{15}NO_2$: C, 68.37; H, 7.82; N, 7.25. Found: C, 68.46; H, 7.98; N, 7.58. ^{1}H-NMR ($CDCl_3$, 400 MHz) δ: 1.33 (3H, t, J=7 Hz, $CH_2C\underline{H}_3$), 1.83 (3H, s, 2-position), 3.78 (3H, s, OCH_3), 4.21 (2H, q, J=7 Hz, $C\underline{H}_2CH_3$), 6.32 (1H, t, J=2 Hz, 2'-position), 6.35 (1H, ddd, J=8, 2, 1 Hz, 6'-position), 6.59 (1H, ddd, J=8, 2, 1 Hz, 4'-position), 7.17 (1H, t, J=8 Hz, 5'-position).

Preparation of *N*-Arylarenesulfonamides *N*-(*p*-Chlorophenyl)-*p*-chlorobenzenesulfonamide,[8] *N*-(*m*-chlorophenyl)-*p*-chlorobenzenesulfonamide,[8] *N*-(*p*-nitrophenyl)-*p*-chlorobenzenesulfonamide,[8] *N*-(*p*-trifluoromethylphenyl)-*p*-chlorobenzenesulfonamide,[9] *N*-(*p*-nitrophenyl)-*m*-nitrobenzenesulfonamide,[10] *N*-(*p*-trifluoromethylphenyl)-*m*-nitrobenzenesulfonamide,[11] *N*-(*m*-nitrophenyl)-*m*-nitrobenzenesulfonamide[12] and *N*-(*p*-nitrophenyl)methanesulfonamide[13] were prepared according to the cited references.

N-(*p*-Cyanophenyl)-*p*-chlorobenzenesulfonamide was prepared by the usual method. mp 181.5 °C (AcOEt), yield 66%. *Anal.* Calcd for $C_{13}H_9ClN_2O_2S$: C, 53.34; H, 3.10; N, 9.57. Found: C, 53.33; H, 3.05; N, 9.51. ^{1}H-NMR ($CDCl_3$, 400 MHz) δ: 7.18 (2H, d, J=8 Hz, 2'- and 6'-positions), 7.19 (1H, br s, NH), 7.48 (2H, d, J=8 Hz, 3- and 5-positions), 7.56 (2H, d, J=8 Hz, 3'- and 5'-positions), 7.78 (2H, d, J=8 Hz, 2- and 6-positions). *N*-(*p*-Cyanophenyl)-*m*-nitrobenzenesulfonamide, mp 195 °C (AcOEt), yield 75%. *Anal.* Calcd for $C_{13}H_9N_3O_4S$: C, 51.48; H, 2.99; N, 13.85. Found: C, 51.61; H, 2.99; N, 13.74. ^{1}H-NMR (DMSO-d_6, 400 MHz) δ: 7.29 (2H, d, J=9 Hz, 2'- and 6'-positions), 7.75 (2H, d, J=9 Hz, 3'- and 5'-positions), 7.90 (1H, t, J=8 Hz, 5-position), 8.25 (1H, ddd, J=8, 2, 1 Hz, 6-position), 8.49 (1H, ddd, J=8, 2, 1 Hz, 4-position), 8.56 (1H, t, J=2 Hz, 2-position), 11.31 (1H, br s, NH).

Preparation of *p*-Cyanoacetophenoxime Tosylate The compound was prepared by the same method as used for the preparation of *m*-nitroacetophenoxime tosylate.[4] mp 120 °C (AcOEt), yield 85%. *Anal.* Calcd for $C_{16}H_{14}N_2O_3S$: C, 61.13; H, 4.49; N, 8.91. Found: C, 60.92; H, 4.42; N, 8.84. ^{1}H-NMR ($CDCl_3$, 400 MHz) δ: 2.36 (3H, s, 2-position), 2.45 (3H, s, CH_3 of Ts), 7.38 (2H, d, J=8 Hz, 3''- and 5''-positions), 7.67 (2H, d, J=9 Hz, 3'- and 5'-positions), 7.71 (2H, d, J=9 Hz, 2'- and 6'-positions), 7.92 (2H, d, J=8 Hz, 2''- and 6''-positions).

Kinetic Runs The alcoholysis reaction was allowed to proceed in EtOH–THF (99 : 1, v/v) solution in the presence or absence of NaOEt at 25 °C unless otherwise noted. The ionic strength was maintained at 0.02 by the addition of NaBr unless otherwise noted.

Preparation of the Reaction Solution A THF solution (1 ml) of the substrate (2 to 8 × 10^{-3} M) was added to EtOH or EtOH containing NaOEt in a 100 ml volumetric flask which had been prewarmed to the desired temperature, and the mixture was diluted to the mark with the same EtOH solution.

Alcoholysis in the Presence of NaOEt The UV spectra of **15** and *N*-(*p*-nitrophenyl)-*p*-toluenesulfonamide in the presence of NaOEt and ethyl *N*-(*p*-methylphenyl)acetimidate in EtOH–THF (99 : 1, v/v) are shown in Fig. 1. The proportion of *N*-(*p*-nitrophenyl)-*p*-toluenesulfonamide was calculated from the absorbance of the reaction solution at 390 nm. The reactions of **5**—**20** were followed in the same manner. The UV spectra of N^1-(*p*-chlorobenzenesulfonyl)-N^1-(*p*-trifluoromethylphenyl)-N^2-(*m*-nitrophenyl)acetamidine (**3**), *N*-(*p*-trifluoromethylphenyl)-*p*-chlorobenzenesulfonamide and ethyl *N*-(*m*-nitrophenyl)acetimidate are shown in Fig. 2. The proportions of **3** and the sum of sulfonamide and imidate were calculated from the absorbancies of the reaction solution at 235, 240, 245, 250, 255 and 260 nm by the least-squares method for two variables. The reactions of **1**—**4** were followed in the same manner.

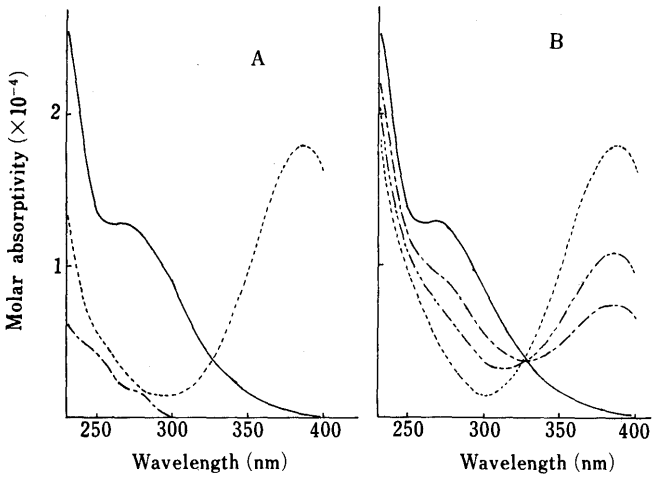

Fig. 1. A: Absorption Spectra of **15** (——) and *N*-(*p*-Nitrophenyl)-*p*-methylbenzenesulfonamide (– – –) in EtOH–THF (99 : 1, v/v) in the Presence of 0.02 M NaOEt, and Ethyl *N*-(*p*-Methylphenyl)acetimidate (—·—) in EtOH–THF (99 : 1, v/v) at 25 °C

B: Absorption Spectra of **15** in EtOH–THF (99 : 1, v/v) in the Presence of 0.02 M NaOEt, Immediately after Dissolution (——), at 990 min after Dissolution (—·—), at 1840 min after Dissolution (— – —) and the Sum of the Spectra of *N*-(*p*-Nitrophenyl)-*p*-methylbenzenesulfonamide and Ethyl *N*-(*p*-Methylphenyl)acetimidate (– – –) at 25 °C

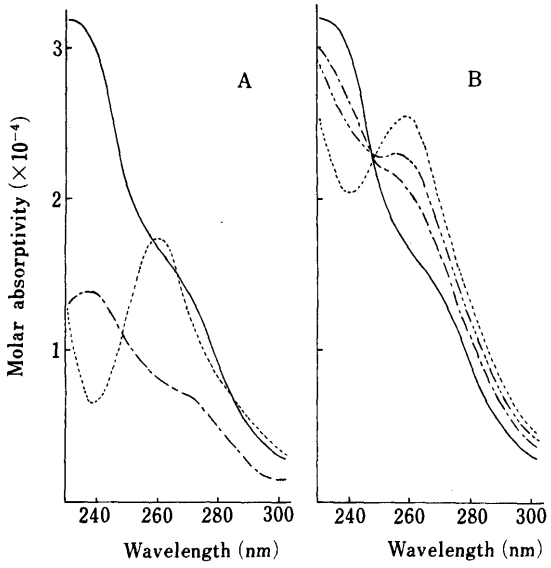

Fig. 2. A: Absorption Spectra of **3** (——) and *N*-(*p*-Trifluoromethylphenyl)-*p*-chlorobenzenesulfonamide (– – –) in EtOH–THF (99 : 1, v/v) in the Presence of 0.02 M NaOEt, and Ethyl *N*-(*m*-Nitrophenyl)acetimidate (—·—) in EtOH–THF (99 : 1, v/v) at 25 °C

B: Absorption Spectra of **3** in EtOH–THF (99 : 1, v/v) in the Presence of 0.02 M NaOEt, Immediately after Dissolution (——), at 160 min after Dissolution (—·—), at 320 min after Dissolution (—··—), and the Sum of the Spectra of *N*-(*p*-Trifluoromethylphenl)-*p*-chlorobenzenesulfonamide and Ethyl *N*-(*m*-Nitrophenyl)acetimidate (– – –) at 25 °C

Alcoholysis under Neutral Conditions The UV spectra of N^1-(*m*-nitrobenzenesulfonyl)-N^1-(*p*-nitrophenyl)-N^2-(*p*-methoxyphenyl)acetamidine (**21**), *N*-(*p*-nitrophenyl)-*m*-nitrobenzenesulfonamide and ethyl *N*-(*p*-methoxyphenyl)acetimidate are shown in Fig. 3. The proportions of **21** and the sum of sulfonamide and imidate were calculated from the absorbancies of the reaction solution at 265, 270, 305 and 310 nm by the

TABLE III. Second-Order Rate Constants, k^{EtO}, of Alcoholysis of **1**—**20** in 1% THF–EtOH in the Presence of EtONa at 25 °C; Ionic Strength 0.02[a,b]

Compd. No.	X	Y	Z	$10^4 k^{EtO}$ ($M^{-1}s^{-1}$)	Compd. No.	X	Y	Z	$10^4 k^{EtO}$ ($M^{-1}s^{-1}$)
1	*p*-Cl	*m*-NO_2	*p*-Cl	3.77 (0.206)	**11**	*p*-NO_2	H	H	4.70 (0.122)
2	*m*-Cl	*m*-NO_2	*p*-Cl	10.2 (0.323)	**12**	*p*-NO_2	H	*p*-Cl	8.74 (0.610)
3	*p*-CF_3	*m*-NO_2	*p*-Cl	22.9 (0.622)	**13**	*p*-NO_2	H	*m*-NO_2	43.4 (3.49)
4	*p*-CN	*m*-NO_2	*p*-Cl	117 (4.4)	**15**	*p*-NO_2	*p*-CH_3	*p*-CH_3	1.68 (0.301)
5	*p*-NO_2	*m*-NO_2	*p*-Cl	259 (4.9)	**16**	*p*-NO_2	*m*-CH_3O	*p*-CH_3	4.69 (0.154)
6	*p*-NO_2	*p*-Cl	*p*-CH_3	12.8 (0.71)	**17**	*p*-NO_2	*m*-Cl	*p*-CH_3	16.0 (0.69)
7	*p*-NO_2	*p*-Cl	H	20.8 (0.62)	**18**	*p*-NO_2	*m*-NO_2	*p*-CH_3	75.9 (2.26)
8	*p*-NO_2	*p*-Cl	*p*-Cl	41.6 (1.00)	**19**	*p*-NO_2	*p*-CN	*p*-CH_3	136 (6.2)
9	*p*-NO_2	*p*-Cl	*m*-NO_2	187 (7.7)	**20**	*p*-NO_2	*p*-NO_2	*p*-CH_3	284 (5.5)
10	*p*-NO_2	H	*p*-CH_3	3.05 (0.102)					

a) The precise k^{EtO} for **14** could not be obtained. *b*) Standard deviations are shown in parentheses.

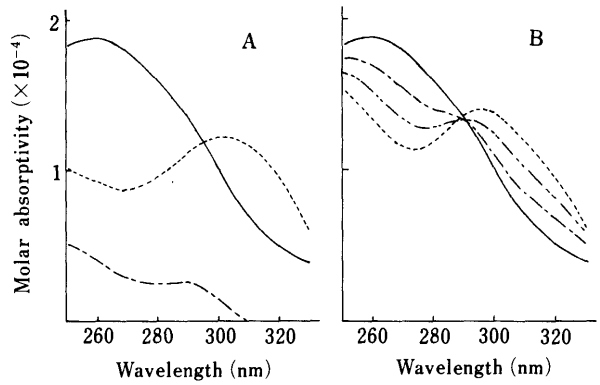

Fig. 3. A: Absorption Spectra of **21** (——), *N*-(*p*-Nitrophenyl)-*m*-nitrobenzenesulfonamide (– – –) and Ethyl *N*-(*p*-Methoxyphenyl)acetimidate (—·—) in EtOH–THF (99:1, v/v) at 25 °C

B: Absorption Spectra of **21** in EtOH–THF (99:1, v/v), Immediately after Dissolution (——), at 45 min after Dissolution (—·—), at 130 min after Dissolution (—··—), and the Sum of the Spectra of *N*-(*p*-Nitrophenyl)-*m*-nitrobenzenesulfonamide and Ethyl *N*-(*p*-Methoxyphenyl)acetimidate (– – –) at 25 °C

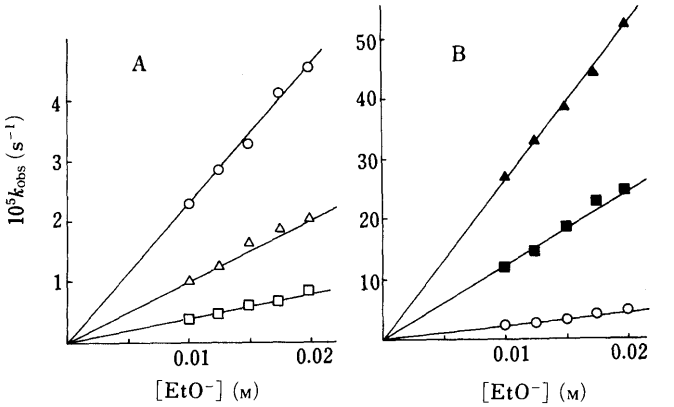

Fig. 4. Plots of the Apparent Rate Constants, k_{obs}, of Alcoholysis of **1**—**5** in EtOH–THF (99:1, v/v) in the Presence of NaOEt *versus* [EtO^-] at 25 °C

Ionic strength 0.02. A: □, **1**; △, **2**; ○, **3**. B: ○, **3**; ■, **4**; ▲, **5**.

least-squares method for two variables. The reactions of **14**, **21**—**25**, **29** and **30** were followed in the same manner. The reactions of **26**—**28** were followed in the same manner as those of **1**—**4** after the addition of NaOEt to the reaction solution immediately before UV measurement.

Alcoholysis of 31 under Neutral Conditions The reaction proceeded in two ways; by alcoholysis at the amidine central carbon to give *N*-(*p*-nitrophenyl)methanesulfonamide and ethyl *N*-(*p*-methoxyphenyl)acetimidate (k_1^0), and by alcoholysis at the sulfonamide nitrogen to give N^1-(*p*-methoxyphenyl)-N^2-(*p*-nitrophenyl)acetamidine and ethyl methanesulfonate (k_2^0). The alcoholysis of **31** was carried out by allowing an EtOH–THF (60:40, v/v) solution of **31** to stand for 8 d at 25 °C. The ^{1}H-NMR (DMSO-d_6) spectrum of the crude product showed the presence of all the substances mentioned above. In the kinetic runs (25 °C, EtOH–THF (99:1, v/v)), the proportions of **31**, amidine, and the sum of sulfonamide and imidate were calculated from the absorbancies at 275, 280, 305, 310, 355 and 360 nm (near λ_{max} of each substance) by the least-squares method for three variables. The value of k_1^0 was 5.78 (0.062) × 10^{-6} s^{-1}, and k_2^0 was 1.03 (0.106) × 10^{-6} s^{-1}. Standard deviations are shown in parentheses.

Alcoholysis of 21 in the Presence of HCl Ionic strength of the reaction solution was maintained at 0.02 by the addition of LiCl. The proportions of **21** and *N*-(*p*-nitrophenyl)-*m*-nitrobenzenesulfonamide were calculated from the absorbancies at 300, 320, 325 and 375 nm of the reaction solution, to which NaOEt was added immediately before the UV measurement, by the least-squares method for two variables (absorption by imidate could be neglected at the cited wavelengths).

Results

The Effect of the Substituent X on the Reaction Rate The apparent rate constant of alcoholysis in the presence of NaOEt k_{obs}, is represented by Eq. 1.

$$k_{obs} = k^0 + k^{EtO}[EtO^-] \quad (1)$$

Plots of k_{obs} *vs.* [EtO^-] were linear (Fig. 4), and the second-order rate constants, k^{EtO}, are shown in Table III. The k^{EtO} values for **1**—**5** (Y = *m*-NO_2, Z = *p*-Cl) showed a linear logarithmic relation with the corrected Hammett's substituent constant[14] according to the Yukawa–Tsuno equation (2),[15] $\sigma + r(\sigma^- - \sigma)$, with a ρ value of 2.50 and an r value of 0.41 (Fig. 5). The correlation coefficient, R, was 0.9983.

$$\log k^{EtO} = \rho\{\sigma + r(\sigma^- - \sigma)\} + \log k_H^{EtO} \quad (2)$$

Willi[16] reported that the dissociation constant of *N*-arylarenesulfonamides correlated well with σ^- of the aryl substituents ($\rho^- = 1.74$). The r value of 0.41 in Fig. 5 suggests that the resonance effect of the substituent X plays a role to in stabilizing the transition state to a moderate extent.

The Effect of the Substituent Z on the Reaction Rate Plots of k_{obs} *vs.* [EtO^-] for **6**—**13** are shown in Fig. 6. The k^{EtO} values for **6**—**9** (X = *p*-NO_2, Y = *p*-Cl) (Table III) showed a linear logarithmic relation with σ of the substituent Z with a ρ value of 1.33, R = 0.9999 (Eq. 3).

$$\log k^{EtO} = \rho\sigma + \log k_H^{EtO} \quad (3)$$

The effect of the substituent Z on the reaction rate was less than that of X. In these experiments, substrates carrying a

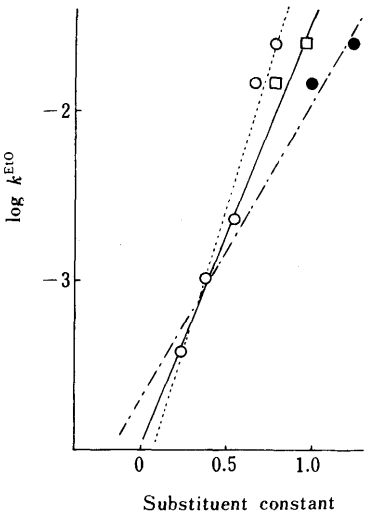

Fig. 5. Hammett's Plots of k^{EtO} for the Substituent X (**1**—**5**) (Y=*m*-NO_2, Z=*p*-Cl)

○, σ; ●, σ^-; □, $\sigma+r(\sigma^- -\sigma)$. ——, log k^{EtO} *versus* $\sigma+r(\sigma^- -\sigma)$ ($\rho=2.50$, $R=0.9983$); – – –, log k^{EtO} *versus* σ ($\rho=3.38$, $R=0.9869$); —·—, log k^{EtO} *versus* σ^- ($\rho^-=1.76$, $R=0.9921$).

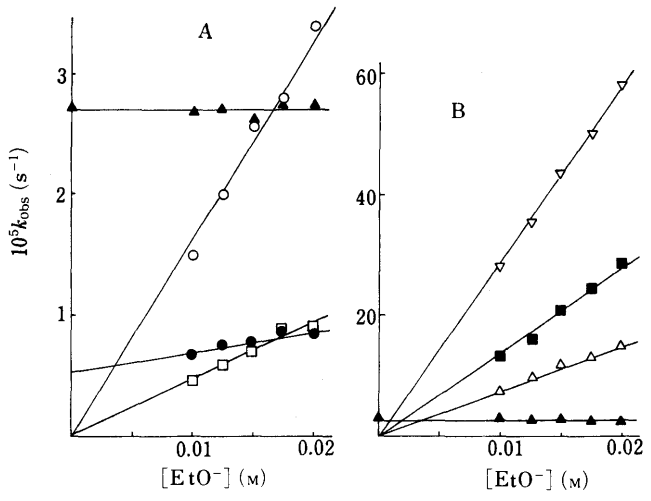

Fig. 7. Plots of the Apparent Rate Constants, k_{obs}, of Alcoholysis of **14**—**20**, in EtOH–THF (99 : 1, v/v) in the Presence of NaOEt *versus* [EtO^-] at 25 °C

Ionic strength 0.02. A: ▲, **14**; ●, **15**; □, **16**; ○, **17**. B: ▲, **14**; △, **18**; ■, **19**; ▽, **20**.

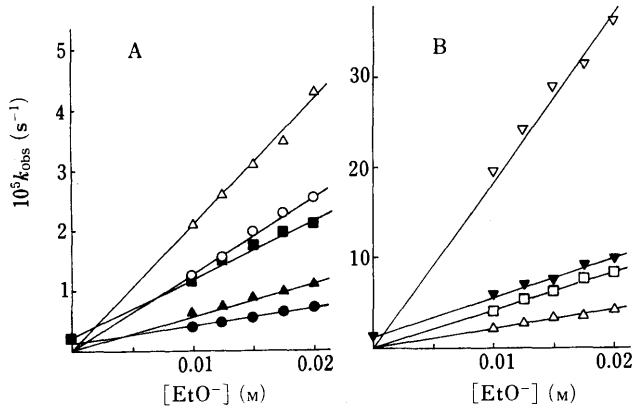

Fig. 6. Plots of the Apparent Rate Constants, k_{obs}, of Alcoholysis of **6**—**13** in EtOH–THF (99 : 1, v/v) in the Presence of NaOEt *versus* [EtO^-] at 25 °C

Ionic strength 0.02. A: ○, **6**; △, **7**; ●, **10**; ▲, **11**; ■, **12**. B: △, **7**; □, **8**; ▽, **9**; ▼, **13**.

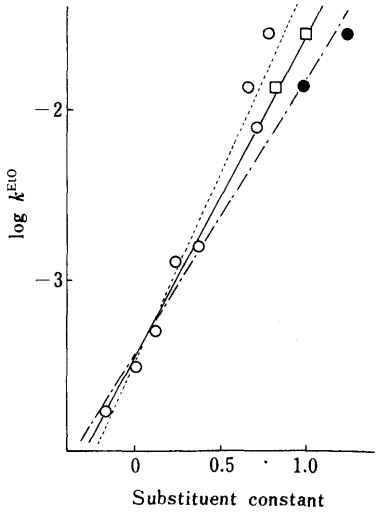

Fig. 8. Hammett's Plots of k^{EtO} for the Substituent Y (**6**, **10** and **15**—**20**) (X=*p*-NO_2, Z=*p*-CH_3)

○, σ; ●, σ^-; □, $\sigma+r(\sigma^- -\sigma)$. ——, log k^{EtO} *versus* $\sigma+r(\sigma^- -\sigma)$ ($\rho=1.92$, $R=0.9965$); – – –, log k^{EtO} *versus* σ ($\rho=2.26$, $R=0.9829$); —·—, log k^{EtO} *versus* σ^- ($\rho^-=1.62$, $R=0.9901$).

strongly electron-withdrawing Z at the para position to the sulfonyl group were not examined because these compounds readily undergo Smiles rearrangement to give trisubstituted amidines.[2]

The k^{EtO} values of **10**—**13** (X=*p*-NO_2, Y=H) (Table III) also correlated well with σ of the substituent Z ($\rho=1.32$, $R=0.9982$). The electronic properties of the substituents Y (Y=H and *p*-Cl) do not affect the sensitivity of the reaction rate to the electronic effect of Z.

The Effect of the Substituent Y on the Reaction Rate Plots of k_{obs} *vs.* [EtO^-] for **14**—**20** are shown in Fig. 7. The k^{EtO} values of **6**, **10** and **15**—**20** (X=*p*-NO_2, Z=*p*-CH_3) (Table III) were analyzed by the use of Eq. 2 to give a ρ value of 1.92 and an r value of 0.51, with $R=0.9965$ (Fig. 8). The results showed that the resonance effect of the substituent Y plays a role in stabilizing the transition state to a similar extent to that of the substituent X.

A remarkable contribution of the term k^0 to the reaction rate of N^1-tosyl-N^1-(*p*-nitrophenyl)-N^2-(*p*-methoxyphenyl)acetamidine (**14**), which carries electron-releasing Y and electron-withdrawing X, was observed (Fig. 7), while the k^{EtO} value for the same substrate was too small to allow us to obtain a precise value. The alcoholysis of **14** proceeded in EtOH–THF (99 : 1, v/v) solution without any added catalyst. The k^0 value was evaluated to be 2.72 (0.029) × 10^{-5} s^{-1} at 25 °C (standard deviation in parenthesis).

Alcoholysis under Neutral Conditions Alcoholysis of the substrates carrying electron-releasing Y and electron-withdrawing X and Z (**9**, **13**, **21**—**25** and **26**—**28**) proceeded with measurable rates under neutral conditions (Table IV).

The reaction of **21** was also undertaken in the presence of hydrogen chloride for the purpose of discriminating whether the reaction proceeds *via* the conjugate acid of **21** or not. The apparent rate constants, k_{obs}, are represented by Eq. 4

TABLE IV. Pseudo First-Order Rate Constants, k^0, of Alcoholysis of **9**, **13**, **14** and **21**—**30**; Ionic Strength 0.02[a]

Compd. No.	X	Y	Z	10^5k^0 (s^{-1}) 18 °C	25 °C	32 °C	39 °C	46 °C	$\Delta H^{\ddagger}$ (kcal mol^{-1})	$\Delta S^{\ddagger}$ (cal K^{-1} mol^{-1})
9	p-NO_2	p-Cl	m-NO_2		0.202 (0.0021)					
13	p-NO_2	H	m-NO_2		1.14 (0.083)	3.26 (0.071)	8.29 (0.413)	18.6 (1.05)	24.5 (0.67)	0.60 (2.16)
14	p-NO_2	p-CH_3O	p-CH_3		2.72 (0.029)					
21	p-NO_2	p-CH_3O	m-NO_2	5.18 (0.189)	14.2 (0.42)	33.3 (2.59)	73.2 (3.63)		22.1 (0.99)	−2.1 (1.98)
22	p-NO_2	p-CH_3	m-NO_2		4.31 (0.128)					
23	p-NO_2	p-isoPr	m-NO_2		4.21 (0.207)					
24	p-NO_2	p-(*tert*-Bu)	m-NO_2		3.86 (0.250)					
25	p-NO_2	p-CH_3S	m-NO_2		1.86 (0.129)					
26	p-CF_3	p-CH_3O	m-NO_2		1.04 (0.023)					
27	m-NO_2	p-CH_3O	m-NO_2		2.74 (0.038)					
28	p-CN	p-CH_3O	m-NO_2		6.04 (0.026)					
29	p-NO_2	p-CH_3O	H		3.18 (0.108)					
30	p-NO_2	p-CH_3O	p-Cl		4.81 (0.134)					

a) Standard deviations are shown in parentheses.

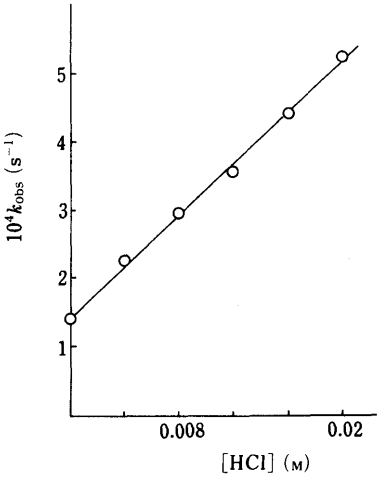

Fig. 9. Plot of the Apparent Rate Constants, k_{obs}, of Alcoholysis of **21** in EtOH–THF (99 : 1, v/v) in the Presence of HCl *versus* [HCl] at 25 °C
Ionic strength 0.02.

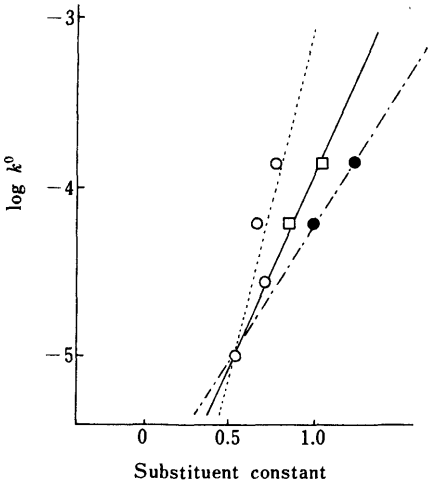

Fig. 10. Hammett's Plots of k^0 for the Substituent X (**21** and **26**—**28**) (Y = p-CH_3O, Z = m-NO_2)
○, σ; ●, σ^-; □, $\sigma+r(\sigma^- -\sigma)$. ——, log k^0 *versus* $\sigma+r(\sigma^- -\sigma)$ (ρ = 2.26, R = 0.9973); – – –, log k^0 *versus* σ (ρ = 4.22, R = 0.8719); — · —, log k^0 *versus* σ^- (ρ^- = 1.57, R = 0.9928).

$$k_{obs}=k^0+\frac{[H^+]k^H}{[H^+]+K_{BH^+}} \quad (4)$$

where K_{BH^+} and k^H are the dissociation constant of the conjugate acid of the substrate and the rate constant of the reaction between the conjugate acid and ethanol, respectively. If the basicity of the substrate is low enough, $K_{BH^+} \gg [H^+]$, Eq. 4 reduces to Eq. 5.

$$k_{obs}=k^0+\frac{k^H}{K_{BH^+}}[H^+] \quad (5)$$

The plot of k_{obs} *vs.* [HCl] was linear showing that Eq. 5 is valid under these conditions (Fig. 9). The value of k^H/K_{BH^+} was calculated to be 1.90 (0.066) × 10^{-2} M^{-1} s^{-1} (standard deviation in parenthesis). Based on the autoprotolysis constant of ethanol (pK_s = 19.1), the value of k^0 is estimated to be 5.36 × 10^{-12} s^{-1} if the reaction proceeds *via* the conjugate acid of the substrate under neutral conditions. Since k^0 = 1.42 × 10^{-4} s^{-1} experimentally (Table IV), the reaction must proceed between the neutral substrate and ethanol. The k^0 values of **9**, **13**, and **21**—**25** (X = p-NO_2, Z = m-NO_2) (Table IV) were analyzed according to Yukawa–Tsuno equation (6) to give a ρ value of −3.37, and an r value of 0.09, with R = −0.9926.

$$\log k^0=\rho\{\sigma+r(\sigma^+-\sigma)\}+\log k^0_H \quad (6)$$

The reaction rate hardly depends at all on the resonance effect of the substituent Y. The k^0 values of **21** and **26**—**28** (Y = p-CH_3O, Z = m-NO_2) (Table IV) were analyzed according to Eq. 2 to give a ρ value of 2.26 and an r value of 0.58, with R = 0.9973 (Fig. 10). The enhanced r value of the substituent X as compared with that of the same substituent for the term k^{EtO} suggests that there is a larger change in the charge of sulfonamide nitrogen in the transition state of the neutral alcoholysis as compared with that of the attack of ethoxide ion.

The k^0 values of **14**, **21**, **29** and **30** (X = p-NO_2, Y = p-CH_3O) (Table IV) showed a linear logarithmic relation with σ of the substituent Z with a ρ value of 0.84. R = 0.9917. The effect of the substituent Z on the reaction rate was reasonably less than those of X and Y.

Discussion

Schmir *et al.*[17] reported that the rate constants of the

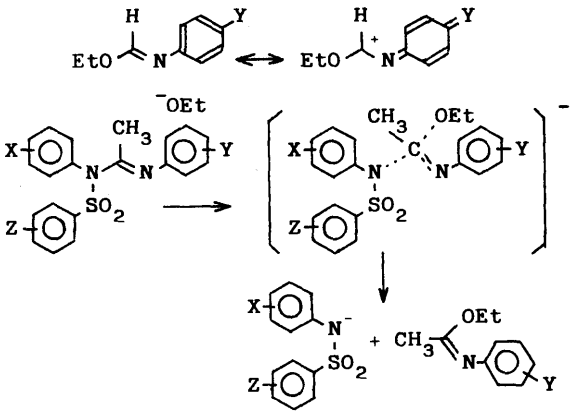

Chart 2

step of hydroxide ion attack in the alkaline hydrolysis of ethyl *N*-arylformimidates were well correlated with σ^- of aryl substituents with a ρ^- value of 1.68.[18] As is shown in Chart 2, the resonance effect of electron-withdrawing aryl substituents enhances the electrophilicity of the reaction site. In the present reaction, the resonance effect of the substituent Y influenced the second-order rate constant, k^{EtO}, to a moderate extent ($r=0.51$), while that of X also did so to a similar extent ($r=0.41$). Probably the attack of ethoxide ion on the amidine central carbon is accompanied by the concerted departure of the arenesulfonamide group so that the negative charge on the sulfonamide nitrogen increases in the transition state (Chart 2).

From a study on the exchange of isotopic carbonyl oxygen with oxygen of the medium, Bender[19] proposed that the hydrolysis of the ester proceeds through a tetrahedral intermediate. Since his proposal, it has been widely accepted that the carbonyl addition and related reactions proceed not by a nucleophilic substitution on the sp^2 carbon but by an addition and subsequent elimination mechanism. If the tetrahedral intermediate is too unstable to have a sufficient lifetime, however, the possibility remains that the reaction proceeds by a concerted mechanism with properties similar to those expected for the first step. Jencks and Gilchrist[20] claimed that the tetrahedral intermediate in the aminolysis of aryl acetate does not have a sufficient lifetime to reach equilibrium with respect to proton transfer on the basis of the fact that tertiary amines react with aryl acetate with the same reaction characteristics as primary and secondary amines.

In the alcoholysis under neutral conditions, the reaction rate hardly depends on the electron-releasing resonance effect of the substituent Y ($r=0.09$). The reaction would not, therefore, proceed by a solvolysis mechanism (Chart 3). Heck and Winstein[21] reported that the rate of acetolysis of neophyl *p*-bromobenzenesulfonate correlated with σ^+ of the substituents on the neophyl group. They proposed a mechanism in which the reaction proceeds with anchimeric assistance, and the existence of the cationic three-membered ring intermediate was proved. The possibility can not be ruled out that the cationic intermediate formed by the solvolysis mechanism reacts directly with ethanol without forming the three-membered structure so that the rate of reaction does not correlate with σ^+ of the substituent Y. However, the situation requires that the rate of reaction should be correlated with σ^- of the substituent X, *i.e.*, the

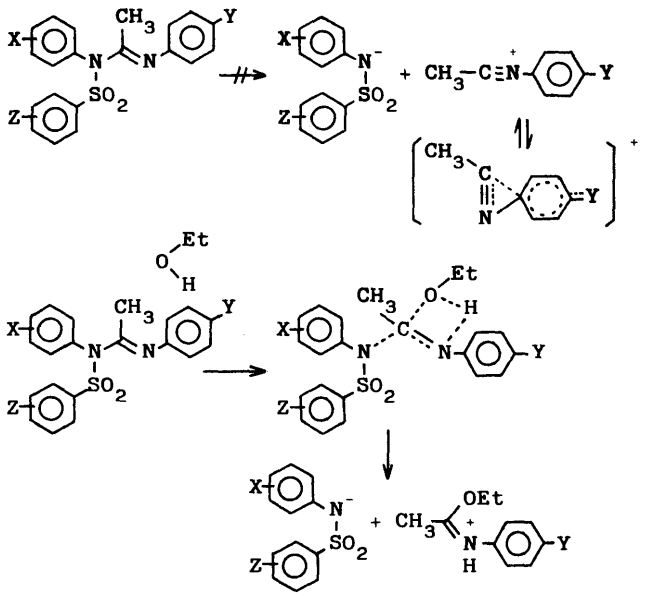

Chart 3

r value should be unity or near to it. The *r* value for the substituent X (0.58) is only slightly greater than that for the attack of ethoxide ion (0.41) suggesting that the two reactions proceed by similar mechanisms. The tetrahedral intermediate of the alcoholysis, if it exists at all, is structurally crowded, and is expected to readily expel the *N*-arylarenesulfonamide group to release the steric strain. As a result, the rate-determining attack of ethoxide ion or ethanol is accompanied by the concerted departure of the sulfonamide group (Charts 2 and 3). Jencks and Gilchrist[20] pointed out that the rate of the reaction between the esters and nucleophiles depends sharply on the basicity of both the attacking nucleophile and the leaving group as the basicity of the nucleophile decreases. The situation accords with the results that the *r* value for X in the neutral reaction (0.58) was greater than in the attack of ethoxide ion (0.41). In the neutral alcoholysis, the imino nitrogen probably assists the attack of ethanol on the amidine central carbon as an intramolecular general base catalyst as judged from the large negative value (-3.37) of ρ for substituent Y (Chart 3).[22]

Fersht and Kirby[23] reported that the activation entropy, $\Delta S^{\neq}$, is -22.5 eu for the intramolecular general base-catalyzed hydrolysis of acetylsalicylic acid. The values of $\Delta S^{\neq}$ for the neutral alcoholysis of **13** and **21** were nearly zero (Table IV). The large difference in the activation entropies of the two reactions would be attributable to the structural features of their transition states. Probably the eight-membered chelate structure for the intramolecular general base catalysis of acetylsalicylic acid hydrolysis requires a large negative activation entropy, while the present reaction proceeds *via* the four-membered chelate intermediate which would be expected to require a less negative activation entropy (Chart 3).

References and Notes

1) M. Ono and S. Tamura, *Chem. Pharm. Bull.*, **38**, 590 (1990).
2) M. Ono, I. Araya, and S. Tamura, *Chem. Pharm. Bull.*, **38**, 1373 (1990).
3) M. Ono, R. Todoriki, and S. Tamura, *Chem. Pharm. Bull.*, **38**, 866 (1990).

4) M. Ono, K. Aoki, and S. Tamura, *Chem. Pharm. Bull.*, **38**, 1379 (1990).
5) R. H. DeWolfe, *J. Org. Chem.*, **36**, 162 (1971).
6) T. Kato, Y. Yamamoto, and S. Takeda, *Yakugaku Zasshi*, **93**, 1034 (1973).
7) R. H. DeWolfe, *J. Org. Chem.*, **27**, 490 (1962).
8) R. R. Baxter and F. D. Chattaway, *J. Chem. Soc.*, **107**, 1814 (1915).
9) K. Igarashi, Y. Enomoto, H. Yanagida, M. Gohara, N. Iida, S. Ozawa, and T. Kuwazuka, Japan. Kokai Tokkyo Koho 61257960 (1986) [*Chem. Abstr.*, **106**, P133792*p* (1987)].
10) F. Bell, *J. Chem. Soc.*, **1929**, 2787.
11) A. Burger and E. D. Hornbaker, *J. Org. Chem.*, **18**, 192 (1953).
12) F. Bell, *J. Chem. Soc.*, **1930**, 1071.
13) G. T. Morgan and J. A. Pickard, *J. Chem. Soc.*, **97**, 48 (1910).
14) The following substituent constants are used. σ: *p*-CH_3O, −0.268; *p*-CH_3, −0.170; *p*-(*tert*-Bu), −0.197; *p*-Cl, 0.227; *p*-CF_3, 0.54; *p*-CN, 0.660; *p*-NO_2, 0.778; *m*-CH_3O, 0.115; *m*-Cl, 0.373; *m*-NO_2, 0.710. σ^+: *p*-CH_3O, −0.778; *p*-CH_3, −0.311; *p*-(*tert*-Bu), −0.256; *p*-Cl, 0.114 (L. P. Hammett, "Physical Organic Chemistry," 2nd ed., McGraw-Hill Kogakusha Ltd., Tokyo, 1970, p. 356). σ: *p*-isoPr, −0.151; *p*-CH_3S, −0.047 (H. H. Jaffé, *Chem. Rev.*, **53**, 191 (1953)). σ^+: *p*-isoPr, −0.276 (Y. Okamoto and H. C. Brown, *J. Org. Chem.*, **22**, 485 (1957)). σ^+: *p*-CH_3S, −0.604 (H. C. Brown, Y. Okamoto, and T. Inukai, *J. Am. Chem. Soc.*, **80**, 4964 (1958)). σ^-: *p*-CN, 0.983; *p*-NO_2, 1.239 (A. I. Biggs and R. A. Robinson, *J. Chem. Soc.*, **1961**, 388).
15) Y. Yukawa and Y. Tsuno, *Bull. Chem. Soc. Jpn.*, **32**, 965 (1959).
16) A. V. Willi, *Helv. Chim. Acta*, **39**, 46 (1956).
17) T. Okuyama, T. C. Pletcher, D. J. Sahn, and G. L. Schmir, *J. Am. Chem. Soc.*, **95**, 1253 (1973).
18) DeWolfe (R. H. DeWolfe, *J. Org. Chem.*, **36**, 162 (1971)) reported that the rate constants of the alkaline hydrolysis of ethyl *N*-arylformimidates were well correlated with σ of the aryl substituent with a ρ value of 1.7. In his experiments, however, substrates carrying a strongly electron-withdrawing substituent at the *para* position were not examined.
19) M. L. Bender, *J. Am. Chem. Soc.*, **73**, 1626 (1951).
20) W. P. Jencks and M. Gilchrist, *J. Am. Chem. Soc.*, **90**, 2622 (1968).
21) R. Heck and S. Winstein, *J. Am. Chem. Soc.*, **79**, 3432 (1957).
22) Another possible mechanism for the neutral alcoholysis would be based on the enhancement of the electrophilicity of the amidine central carbon by charge transfer from the imino nitrogen to the aromatic ring of the arenesulfonyl group. This mechanism accords well with the large negative ρ value for the substituent Y. However, this mechanism was ruled out by the fact that the neutral alcoholysis of N^1-mesyl-N^1-(*p*-nitrophenyl)-N^2-(*p*-methoxyphenyl)acetamidine (**31**) also proceeded with a rate constant of $5.78 \times 10^{-6}\,s^{-1}$ (see Experimental).
23) A. R. Fersht and A. J. Kirby, *J. Am. Chem. Soc.*, **89**, 4857 (1967).

Periandradulcins A, B and C: Phosphodiesterase Inhibitors from *Periandra dulcis* MART.

Yoshitaka IKEDA,[a] Masanori SUGIURA,[a] Chikara FUKAYA,*[,a] Kazumasa YOKOYAMA,[a] Yohei HASHIMOTO,[b] Kazuko KAWANISHI[b] and Midori MORIYASU[b]

Research Division, The Green Cross Corp.,[a] 2-1180-1 Shodai-ohtani, Hirakata, Osaka 573, Japan and Kobe Women's College of Pharmacy,[b] Kobe 658, Japan. *Received July 27, 1990*

During the course of our screening of bioactive natural products, three new saponins named periandradulcins A (1), B (2) and C (3) were isolated as phosphodiesterase (PDE, EC 3.1.4.17) inhibitors from 80% MeOH extract of the roots of *Periandra dulcis* MART. (Leguminosae) by a combination of column chromatography and reversed- and normal-phase high-performance liquid chromatography (HPLC). On the basis of ^{1}H-, ^{13}C- and two-dimensional nuclear magnetic resonance (NMR) spectral data and chemical evidence, their chemical structures were characterized as 3-*O*-*β*-[α-L-rhamnopyranosyl(1→2)-*β*-D-xylopyranosyl(1→2)-*β*-D-glucuronopyranosyl]-30-hydroxyl-25-formylolean-18-ene-22*β*-*O*-syringate, 3-*O*-*β*-[α-L-rhamnopyranosyl(1→2)-*β*-D-xylopyranosyl(1→2)-*β*-D-glucuronopyranosyl]-22*β*-hydroxyl-25-formylolean-12-ene and 3-*O*-*β*-[α-L-rhamnopyranosyl(1→2)-*β*-D-glucopyranosyl(1→2)-*β*-D-glucuronopyranosyl]-22*β*-hydroxyl-25-formylolean-18-ene, respectively.

The concentrations of periandradulcins A, B and C required to give 50% inhibition (IC_{50} values) of PDE from bovine heart, were 0.033, 7.6 and 7.7 μM, respectively. Compound 1 was the most potent among the known PDE inhibitors; it inhibited PDE-I (IC_{50}: 0.0022 μM) twenty and forty times more effectively than PDE-II and -III, respectively.

Keywords *Periandra dulcis*; Leguminosae; triterpenoid saponin; periandradulcin A; periandradulcin B; periandradulcin C; phosphodiesterase inhibitor

Since Sutherland found cyclic adenosine monophosphate (cAMP) as a second messenger inside cells,[1] compounds that act to alter cAMP metabolism have been studied with the aim of developing of new medicinal drugs. Various synthetic compounds[2] and natural products[3] have been reported as cAMP phosphodiesterase (PDE, EC 3.1.4.17) inhibitors.

During the course of our screening of bioactive constituents from crude drugs, three new triterpene glycosides, named periandradulcins A (**1**), B (**2**) and C (**3**), were isolated as potent PDE inhibitors from the roots of *Periandra dulcis* MART. (Leguminosae). Hashimoto *et al.* had reported the

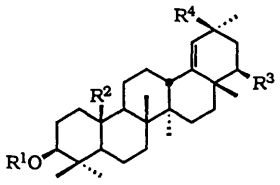

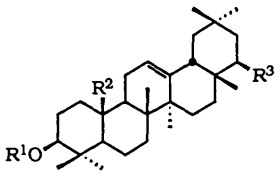

1: $R^1 = S_1$, R^2 = -CHO, R^3=-*O*-syringate, R^4 = $-CH_2OH$

2: $R^1 = S_1$, R^2 = -CHO, R^3 = -OH

3: $R^1 = S_2$, R^2 = -CHO, R^3 = -OH, R^4 = $-CH_3$

4: R^1 = H, R^2 = $-CH_3$, R^3 = -OH

5: R^1 = H, R^2 = $-CH_3$, R^3 = H, R^4 = $-CH_3$

6: R^1 = H, R^2 = $-CH_3$, R^3 = -OH, R^4 = $-CH_3$

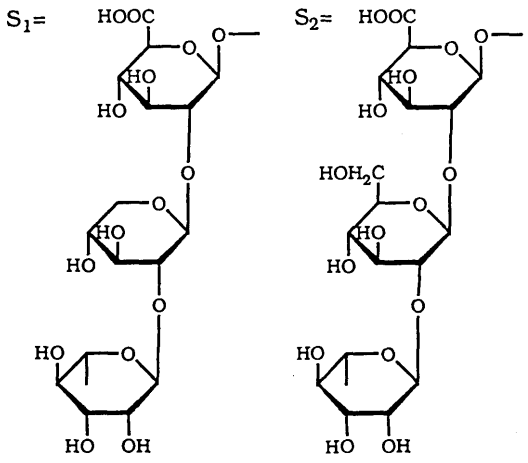

Chart 1

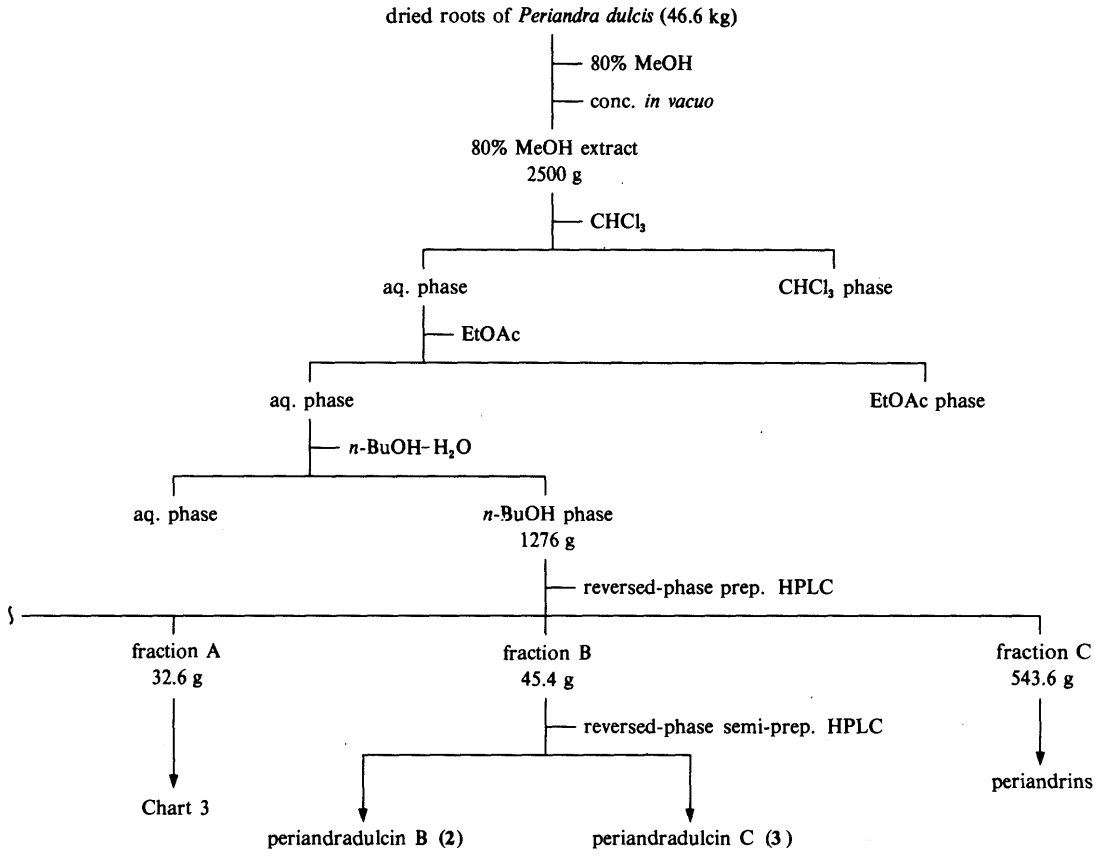

Chart 2. Isolation Procedure for Periandradulcins

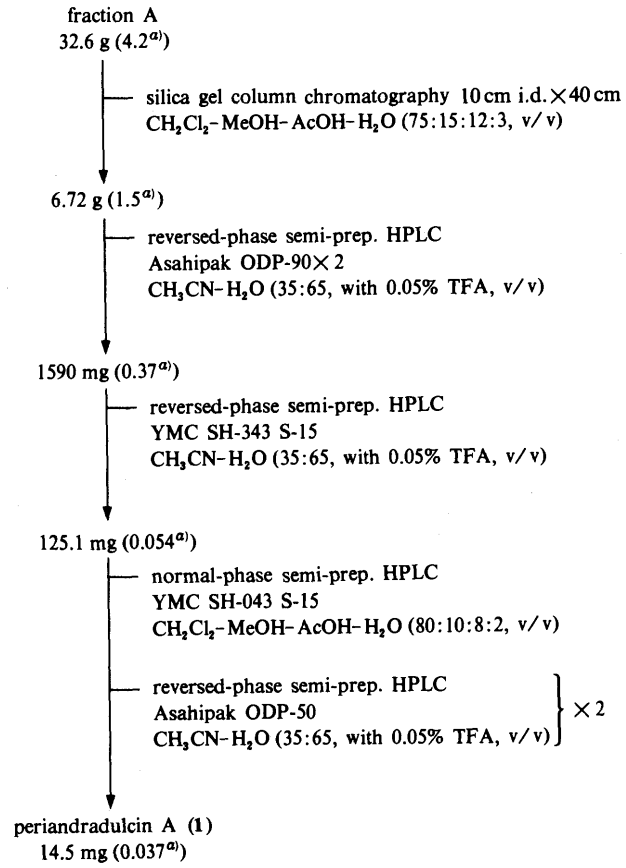

Chart 3. Isolation Procedure for Periandradulcin A (1) from Fraction A

a) IC_{50} values for PDE (μg/ml).

isolation and structural elucidation of four new saponins named periandrins I, II, III and IV as sweet constituents of this plant.[4]

In this paper, we describe the isolation, structural elucidation and PDE-inhibitory activities of periandradulcins A (**1**), B (**2**) and C (**3**).

The 80% MeOH extract from dried roots of *Periandra dulcis* was treated as shown in Chart 2 to give fractions A, B and C. Fraction A was further fractionated by column chromatography and reversed- and normal-phase high-performance liquid chromatography (HPLC) with the guidance of PDE inhibitory activity assay to obtain periandradulcin A (**1**) in 0.31 ppm yield (Chart 3). Fraction B was also fractionated by HPLC to give periandradulcins B (**2**) and C (**3**) in 25.8 and 19.2 ppm yield, respectively. Fraction C contained periandrins.[4]

The molecular weight of periandradulcin B (**2**), a white amorphous powder, was determined to be 910 by positive and negative secondary ion mass spectroscopy (SI-MS), from the peaks at *m/z* 933 for the $[M+Na]^+$ ion and at *m/z* 909 for the $[M-H]^-$ ion, respectively. The ^{1}H-nuclear magnetic resonance (^{1}H-NMR) spectrum of **2** showed signals due to seven angular methyl protons at δ 1.34, 1.27, 1.22, 1.14, 0.99, 0.98 and 0.90, one trisubstituted olefinic proton at δ 5.21 (br t), one formyl proton at δ 10.36 (br s) and three anomeric protons at δ 6.25 (d, J=1 Hz), 5.61 (d, J=7 Hz) and 5.04 (d, J=8 Hz). The ^{13}C-NMR spectrum showed two methine carbons bearing hydroxyl at δ 75.4 and a sugar moiety at δ 88.4, trisubstituted olefinic carbons at δ 144.6 (s) and 121.7 (d), a formyl carbon at δ 205.7 (d), a carbonyl carbon at δ 172.0

TABLE I. ^{13}C-NMR Chemical Shift Values (δ) of Aglycone Moieties of **1**, **2**, **3** and Related Compounds[a]

No.	2	4	3	6	5	1
1	32.5	39.2	33.5	39.0	38.5	33.6
2	27.3	28.2	27.6	27.0	27.4	27.7
3	88.4	78.1	88.7	79.0	79.0	88.5
4	39.6	39.5	40.2	39.0	39.0	39.5
5	54.1	55.9	54.4	55.5	55.7	54.4
6	17.4	18.9	17.7	18.5	18.3	17.7
7	33.1	33.3	34.0	34.5	34.7	34.7
8	39.9	40.1	40.5	39.5	40.8	40.5
9	49.9	48.1	53.6	51.2	51.3	53.5
10	52.6	37.3	52.8	37.0	37.3	52.8
11	23.9	23.9	21.9	21.1	21.2	21.7
12	121.7	122.5	26.8	26.6	26.2	26.5
13	144.6	144.9	38.5	38.4	39.0	38.5
14	42.2	42.5	42.8	42.5	43.4	42.7
15	26.7	26.5	28.1	27.4	27.6	27.8
16	28.6	28.7	35.1	34.4	37.7	33.9
17	37.8	38.0	40.1	40.6	34.4	34.7
18	45.3	45.4	142.5	141.5	142.8	143.6
19	46.6	46.9	129.4	129.3	129.8	127.0
20	30.8	30.9	33.7	33.5	32.3	40.1
21	42.2	42.3	42.3	41.1	33.4	33.6
22	75.4	75.6	75.4	76.5	37.4	78.4
23	26.5	28.8	26.8	28.0	28.0	26.8
24	15.4	15.9	15.8	15.4	15.4	15.8
25	205.7	16.6	205.6	16.1	16.1	205.6
26	19.3	17.3	18.4	16.7	16.7	18.3
27	25.6	25.8	14.9	14.7	14.6	15.0
28	28.6	28.8	21.4	21.0	25.3	19.7
29	33.1	33.3	32.1	31.8	31.3	25.1
30	21.0	21.2	30.1	29.9	29.2	72.1

a) Spectra were measured in pyridine-d_5 and assignment of the signals was performed by comparison with reference data.[6]

TABLE II. ^{13}C-NMR Chemical Shift Values (δ) of Sugar Moieties of **1**, **2** and **3**[a]

No.	1	2	3
Glucuronic acid-1	105.4	105.2	105.4
Glucuronic acid-2	79.2	78.5	78.8[b]
Glucuronic acid-3	76.3	76.4	76.6
Glucuronic acid-4	73.7	73.3	73.6
Glucuronic acid-5	78.4	78.9	78.8[b]
Glucuronic acid-6	172.8	172.0	173.4
Xylose-1	102.9	102.7	
Xylose-2	79.3	79.0	
Xylose-3	78.8	78.6	
Xylose-4	71.6	71.4	
Xylose-5	66.6	66.6	
Glucose-1			102.2
Glucose-2			79.5
Glucose-3			77.4
Glucose-4			72.4
Glucose-5			78.8
Glucose-6			63.4
Rhamnose-1	102.3	101.9	102.1
Rhamnose-2	72.4	72.1	72.4
Rhamnose-3	72.8	72.4	72.8
Rhamnose-4	74.4	74.1	74.3
Rhamnose-5	69.7	69.3	69.5
Rhamnose-6	19.0	18.8	19.0

a) Spectra were measured in pyridine-d_5. b) Overlapped.

and three anomeric carbons at δ 105.2, 102.7 and 101.9 (Tables I and II). These results suggested that **2** is a Δ^{12}-oleanene triterpene triglycoside with hydroxyl and formyl groups.

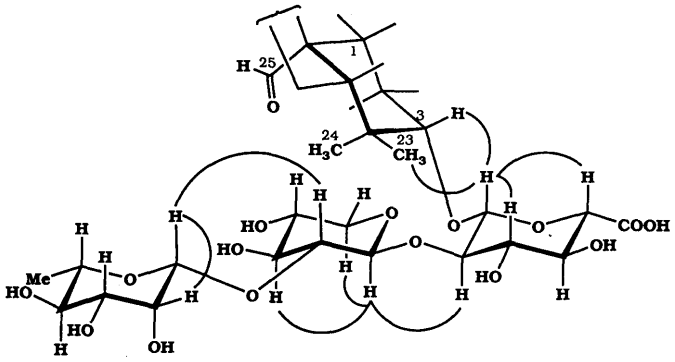

Fig. 1. NOE Correlations in the Sugar Moiety of **2** (Pyridine-d_5)

The product obtained by Huang-Minlon reduction of **2** was identical with sophoradiol (**4**) on ^{13}C-NMR comparison.[5]

A W-type long-range coupling between the formyl proton at δ 10.36 (br s) and 1α-H proton at δ 0.76 (br t), which was comfirmed by the ^{1}H-^{1}H correlation spectrum (^{1}H-^{1}H COSY), indicated that the position of the formyl group was at 25-C.

From the acidic hydrolysate of **2**, three sugars were identified as rhamnose, xylose and glucuronic acid by HPLC. Fragment ions at *m/z* 763 and 631 in the negative SI-MS of **2** were assumed to be due to $[M-\text{rhamnose}-H]^-$ and $[M-\text{rhamnose}-\text{xylose}-H]^-$, respectively, suggesting that **2** possesses a terminal rhamnosyl-xylosyl moiety in the carbohydrate residue. All proton and carbon signals of the sugar moiety were assigned on the basis of ^{1}H-^{1}H COSY and ^{1}H-^{13}C correlation (^{1}H-^{13}C COSY) spectroscopies (Table II). Glycosylation shifts which were observed at C-1—3 of glucuronic acid and xylose suggested that the linkage patterns of the sugars should be 1—2. These conclusions were supported by the nuclear Overhauser effect (NOE) correlations (Fig. 1) observed in the phase-sensitive nuclear Overhauser effect 2D spectroscopy (NOESY) spectra.

Therefore, the structure of **2** was concluded to be 3-*O*-β-[α-L-rhamnopyranosyl(1→2)-β-D-xylopyranosyl(1→2)-β-D-glucuronopyranosyl]-22β-hydroxyl-25-formyloleanan-12-ene.

Periandradulcin C (**3**) was a pale brown amorphous powder, of which the molecular weight was 940 as determined by positive and negative SI-MS, which showed peaks at *m/z* 963 for the $[M+Na]^+$ ion and at *m/z* 939 for the $[M-H]^-$ ion, respectively. Its ^{1}H- and ^{13}C-NMR spectra were similar to those of **2** except for the olefinic proton at δ 4.90 (br s) and the olefinic carbons at δ 142.5 (s) and 129.4 (d) which were similar to those of Δ^{18}-oleanene triterpenes such as geramanicol (**5**)[6] (Table I). Thus, **3** is a triglycoside of a Δ^{18}-oleanene triterpene having hydroxyl and formyl groups. The product (**6**) obtained by Huang-Minlon reduction showed an M^+ ion at *m/z* 442 in the electron impact mass spectrum (EI-MS). The ^{1}H-NMR spectrum of **6** showed signals of an olefinic proton as a broad singlet (δ 4.83), eight angular methyl protons as singlets (δ 1.07, 1.01, 1.00, 0.97, 0.96, 0.88, 0.77 and 0.73) and two methine protons on carbon equatorially bearing a hydroxyl group as double doublets [δ 3.63 (J=7, 10 Hz)

and 3.20 ($J=10$, 6 Hz)]. These assignments as well as the EI-MS fragmentations (*m/z* 220, 206, 205 and 175) suggested **6** to be 3β-hydroxylolean-18-ene with a hydroxyl group at 15α, 16β, 21α or 22β.[7] By ^{13}C-NMR comparison of **6** and **5**, signals due to 17-, 21- and 22-C were seen to be shifted downfield by 6.2, 7.7 and 39.1 ppm, respectively, and those due to 16-, 18- and 28-C were shifted upfield by 3.3, 1.3 and 4.3 ppm, while other carbon signals were not much changed (Table I). From these data, **6** was characterized as 3β,22β-dihydroxyolean-18-ene.

The position of the formyl group was suggested to be 25-C on the basis of ^{1}H–^{1}H COSY data similar to those for **2**. On acidic hydrolysis of **3**, the sugars were identified as rhamnose, glucose and glucuronic acid by HPLC. Fragment ions at *m/z* 793 and 631 in negative SI-MS, assumed to be due to $[M-\text{rhamnose}-H]^-$ and $[M-\text{rhamnose}-\text{glucose}-H]^-$, respectively, indicated that the sugar moiety of **3** was rhamnosyl, glucosyl and glucuronyl. From the NMR data (^{1}H-NMR, ^{1}H–^{1}H COSY, ^{1}H–^{13}C COSY and phase-sensitive NOESY), all carbon signals of the sugar moiety of **3** were assigned as shown in Table II.

Therefore, the chemical structure of **3** was concluded to be 3-*O*-β-[α-L-rhamnopyranosyl(1→2)-β-D-glucopyranosyl-(1→2)-β-D-glucuronopyranosyl]-22β-hydroxyl-25-formyl-olean-18-ene.

Periandradulcin A (**1**) was a pale brown amorphous powder, of which the molecular weight was 1106 as determined by positive and negative SI-MS, which showed peaks at *m/z* 1129 for the $[M+Na]^+$ ion and at *m/z* 1105 for the $[M-H]^-$ ion, respectively. The ^{1}H-NMR spectrum of **1** showed signals of six angular methyl protons at δ 1.42, 1.41×2, 1.08, 0.93 and 0.90, one trisubstituted olefinic proton as broad singlet at δ 5.21, one formyl proton at δ 10.38 (br s) and three anomeric protons at δ 6.42 (d, $J=1$ Hz), 5.72 (d, $J=7$ Hz) and 5.04 (d, $J=8$ Hz). The ^{13}C-NMR spectrum (Table I) showed signals of olefinic carbons at δ 143.6 (s) and 127.0 (d), a formyl carbon at δ 205.6 (d), two methine carbons bearing ester and sugar linkage at δ 78.4 and 88.5, a carbonyl carbon at δ 172.8 and three anomeric carbons at δ 105.4, 102.9 and 102.3. Besides these NMR signals, eight protons (except that of the hydroxyl group) and nine carbons were assignable as those of syringic acid.

Fragment ions at *m/z* 924 and 778, assumed to be due to $[M-\text{syringic acid}-H]^-$ and $[M-\text{syringic acid}-\text{rhamnose}-H]^-$, respectively, were observed in the negative SI-MS along with fragment ions at *m/z* 959 and 827, assumed to be due to $[M-\text{rhamnose}-H]^-$ and $[M-\text{rhamnose}-\text{xylose}-H]^-$, respectively. Methyl syringate was obtained from **1** by treatment with sodium methoxide, and was confirmed to be identical with an authentic specimen by HPLC, thin layer chromatography (TLC) and EI-MS. Therefore, **1** was suggested to be Δ^{18}-oleanene triterpene triglycoside syringate.

In the ^{1}H-NMR spectrum, a double doublet signal at δ 4.90 (22α-H) in **3** was observed at δ 5.63 in **1**. This downfield shift suggested that the ester linkage with syringic acid was at 22-C. The signals at δ 3.70 and 3.64 (hydroxymethyl, AB-quartet, $J=12$ Hz) showed NOE correlation with δ 5.21 (19-H), 2.33 (21α-H), 1.97 (21β-H) and 1.41 (29-H), and the signal at δ 1.41 (29-H) showed NOE correlation with δ 5.63 (22α-H) and 0.90 (27-H), as shown in Fig. 2. On ^{13}C-NMR

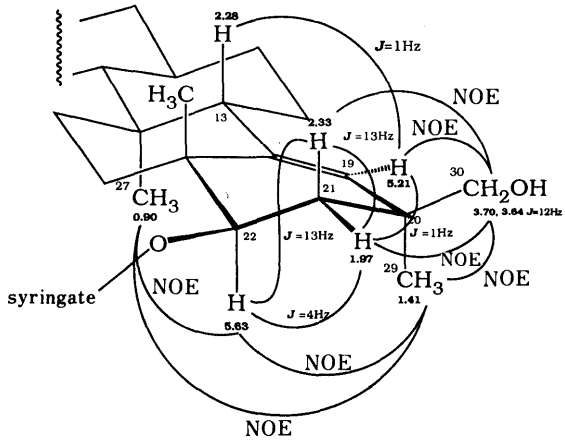

Fig. 2. ^{1}H-NMR Chemical Shift Values (δ), Spin Coupling Constants and NOE Correlation for the E-Ring of **1** (Pyridine-d_5)

comparison of **3** and **1** (Table I), signals due to 20-C, 22-C and 30-C were shifted downfield by 6.4, 3.0 and 42.0 ppm, respectively and those due to 17-C, 19-C, 21-C and 29-C shifted upfield by 5.4, 2.4, 8.7 and 7.0 ppm, respectively, while other carbon signals were almost unchanged. Thus, the hydroxymethyl carbon and the ester linkage position with syringic acid were concluded to be at 30-C and 22-C, respectively.

The position of the formyl group was suggested to be 25-C on the basis of ^{1}H–^{1}H COSY data, as in the case of **2**. On acidic hydrolysis of **1**, released sugars were identified as rhamnose, xylose and glucuronic acid by HPLC. The chemical shift values of all proton and carbon signals of the sugar moiety, which were assigned by ^{1}H–^{1}H COSY, ^{1}H–^{13}C COSY and phase-sensitive NOESY, were in good agreement with those of periandradulcin B (**2**) (Table II). Therefore, the chemical structure of **1** was characterized as 3-*O*-β-[α-L-rhamnopyranosyl(1→2)-β-D-xylopyranosyl-(1→2)-β-D-glucuronopyranosyl]-30-hydroxyl-25-formyl-olean-18-ene-22β-*O*-syringate.

Periandradulcin A (**1**) is the first example of a syringate of a saponin to be isolated from a natural source. This is also the first time that periandradulcins B (**2**) and C (**3**) have been found in nature.

The concentrations of **1**, **2** and **3** required to give 50% inhibition (IC_{50} values) of PDE from bovine heart were determined to be 0.033, 7.6 and 7.7 μM, respectively. Periandradulcin A (**1**) was thus two hundred times more potent than the others, and is the most potent among the known PDE inhibitors.

Three kinetically distinct PDEs PDE-I, PDE-II and PDE-III, were separated from bovine heart by diethylaminoethyl (DEAE)-cellulose chromatography.[8] Papaverine, which is a well known PDE inhibitor, was not specific for any of these PDEs. The novel vasodilating agent vinpocetine[9] specifically inhibited PDE-I, which was activated by Ca^{2+} and calmodulin. The novel positive inotropic agent milurinone was reported to inhibit most effectively PDE-III, which is a cAMP-specific PDE, among the three PDEs.[10] The IC_{50} value of **1** for PDE-I was 0.0022 μM, which is twenty and forty times less than those for the other PDEs (Table III). Thus, **1** is a specific inhibitor of PDE-I like vinpocetine, but the activity of the former was 500 times that of the latter. One of the important

TABLE III. IC_{50} Values (μM) of **1** and Typical Known Inhibitors for the PDEs Derived from Bovine or Guinea Pig Hearts[a]

	IC_{50} values (μM)			
	1[b]	Papaverine[b]	Vinpocetine[b]	Milurinone[c,d]
PDE-I	0.0022	11.7	22.8	310
PDE-II	0.042	2.26	71.3	220
PDE-III	0.083	1.75	>285	2.50

a) cAMP (1 μM) was used as a substrate. *b*) PDEs from bovine heart were used. *c*) PDEs from guinea pig heart were used. *d*) Reported data.[10]

vasodilating mechanisms of vinpocetine is thought to be specific inhibition of PDE-I.[9] So, **1** may be expected to show a vasodilating activity.

Experimental

Melting points were determined on a Yanagimoto micro melting point apparatus and are uncorrected. Ultraviolet (UV) spectra were recorded on a Shimadzu UV-240 spectrometer and optical rotations were measured on a JASCO DIP-181 digital polarimeter. NMR spectra were recorded on Bruker AM-500 (500 MHz for ^{1}H-NMR and 125 MHz for ^{13}C-NMR) and Bruker AC-200 (200 MHz for ^{1}H-NMR and 50 MHz for ^{13}C-NMR) instruments, using tetramethylsilane (TMS) as an internal standard. Chemical shifts are shown in δ (ppm) and multiplicities are indicated as follows: singlet=s, doublet=d, triplet=t, multiplet=m and broad=br. Coupling constants (J) are shown in Hz. All 1D and 2D plus sequences were run using Bruker standard software. EI-MS and SI-MS were taken on a Shimadzu QP-1000 mass spectrometer and a Hitachi M-2000 mass spectrometer, respectively. TLC analysis were performed on pre-coated Kieselgel 60 F_{254} plates (Merck) and spots were detected under UV irradiation (254 nm) and by spraying 10% H_2SO_4 solution followed by heating. Column chromatographies were carried out on Silica gel 60 (230—400 mesh, Nacalai Tesque Inc.) and YMC gel ODS-AQ S-50 (50 μm, YMC Co.). Preparative HPLC were carried out on two columns (47 mm i.d. × 300 mm) packed with YMC gel ODS-AQ S-50 (50 μm, YMC Co.) with a Waters System 500 Prep. LC System. Semi-preparative HPLC separations were carried out on a YMC SH-343 S-15 column (20 mm i.d. × 250 mm, ODS, 15 μm, YMC Co.), YMC SH-043 S-15 column (20 mm i.d. × 250 mm, silica gel, 15 μm, YMC Co.), YMC A023 column (10 mm i.d. × 250 mm, silica gel, YMC Co.) or Asahipack ODP-90 column (21.5 mm i.d. × 300 mm, octadecylpolymer, 9 μm, Asahi Chemical Industry Co., Ltd.) with a Waters M600 pump, Waters U6K injector and Shimadzu SPD-6AV ultraviolet-visual detector.

Isolation The dried roots of *Periandra dulcis* (46.6 kg) were extracted with 80% MeOH. The concentrated extract (2500 g) was dissolved in H_2O and extracted successively with $CHCl_3$, EtOAc and water-saturated *n*-BuOH. The *n*-BuOH layer was evaporated *in vacuo* to give the crude saponin (1276 g). The crude saponin fraction was subjected to preparative HPLC [conditions: column, as described above; mobile phase, CH_3CN–H_2O (35:65, v/v) containing 0.05% trifluoroacetic acid (TFA); flow rate, 150 ml/min; detector, refractive index] to give fractions A (32.6 g), B (45.4 g) and C (543.6 g) as shown in Chart 2. Fraction A was further subjected to silica gel column chromatography and normal- and reversed-phase semi-preparative HPLC as shown in Chart 3 to give periandradulcin A (**1**, 14.5 mg). A part of fraction B (4.54 g) was subjected to reversed-phase semi-preparative HPLC [conditions: column, YMC SH-343 S-15 column; mobile phase, CH_3CN–H_2O (35:65, v/v) containing 0.05% TFA; flow rate, 10 ml/min; detector, 207 nm UV absorbance] to give periandradulcin B (**2**, 120.0 mg) and periandradulcin C (**3**, 89.0 mg). Fraction C (543.6 g) mainly contained periandrin II, which was identified by HPLC and TLC comparisons with an authentic sample.

Periandradulcin A (1) A pale brown amorphous powder, $[\alpha]_D^{25}$ −55.0° (c=0.2, MeOH), mp 220—225 °C (dec.). UV λ_{max}^{MeOH} nm (log ε): 277 (3.88), 206 (4.21). ^{1}H-NMR (pyridine-d_5) δ: 10.38 (1H, br s, –CHO), 7.82 (2H, s, syringate-2), 6.42 (1H, d, J=1 Hz, Rha-1-H), 5.72 (1H, d, J=7 Hz, Xyl-1-H), 5.63 (1H, dd, J=13, 4 Hz, 22α-H), 5.21 (1H, br s, 19-H), 5.04 (1H, d, J=8 Hz, Glc.A-1-H), 5.02 (1H, dt, J=6, 9 Hz, Rha-5-H), 4.78 (1H, dd, J=1, 4 Hz, Rha-2-H), 4.70 (1H, dd, J=4, 9 Hz, Rha-H-3), 4.62 (2H, m, Glc.A-3-H overlapped with Glc.A-5-H), 4.49 (1H, dd, J=9, 10 Hz, Glc.A-4-H), 4.42 (1H, dd, J=9, 8 Hz, Glc.A-2-H), 4.36 (1H, t, J=9 Hz, Rha-4-H), 4.35 (1H, dd, J=4, 11 Hz, Xyl-5-H), 4.31 (1H, dd, J=7, 8 Hz, Xyl-2-H), 4.21 (2H, m, Xyl-3-H overlapped with Xyl-4-H), 3.91 (6H, s, syringate-OCH$_3$), 3.70 (1H, d, J=12 Hz, H-30), 3.64 (1H, d, J=12 Hz, H-30), 3.59 (1H, dd, J=11, 12 Hz, Xyl-5-H), 3.38 (1H, dd, J=4, 12 Hz, 3-H), 2.58 (1H, br d, J=14 Hz, 1β-H), 2.33 (1H, t, J=13 Hz, 21α-H), 2.28 (2H, 13-H overlapped with 2β-H), 1.97 (1H, ddd, J=13, 4, 1 Hz, 21β-H), 1.84 (3H, d, J=6 Hz, Rha-6-H), 1.42 (3H, s, 28-H), 1.41 (6H, s, 23-H overlapped with 29-H), 1.08 (3H, s, 24-H), 0.93 (3H, s, 26-H), 0.90 (3H, s, 27-H), 0.75 (1H, br t, J=12 Hz, 1α-H). ^{13}C-NMR (pyridine-d_5): Tables I and II.

Periandradulcin B (2) A white amorphous powder, $[\alpha]_D^{25}$ +12.0° (c=1.0, MeOH), mp 225—227 °C (dec.). UV λ_{max}^{MeOH} nm (log ε): 209 (3.56). *Anal.* Calcd for $C_{47}H_{74}O_{17}\cdot H_2O$: C, 60.76; H, 8.25. Found: C, 60.70; H, 8.45. ^{1}H-NMR (pyridine-d_5) δ: 10.36 (1H, br s, –CHO), 6.25 (1H, d, J=1 Hz, Rha-1-H), 5.61 (1H, d, J=7 Hz, Xyl-1-H), 5.21 (1H, br t, J=4 Hz, 11-H), 5.04 (1H, d, J=8 Hz, Glc.A-1-H), 5.02 (1H, dt, J=6, 9 Hz, Rha-5-H), 4.77 (1H, dd, J=1, 4 Hz, Rha-2-H), 4.69 (1H, dd, J=4, 9 Hz, Rha-H-3), 4.60 (2H, m, Glc.A-3-H overlapped with Glc.A-5-H), 4.49 (1H, dd, J=9, 10 Hz, Glc.A-4-H), 4.40 (1H, dd, J=9, 8 Hz, Glc.A-2-H), 4.35 (1H, t, J=9 Hz, Rha-4-H), 4.34 (1H, dd, J=4, 11 Hz, Xyl-5-H), 4.30 (1H, dd, J=7, 8 Hz, Xyl-2-H), 4.20 (2H, m, Xyl-3-H overlapped with Xyl-4-H), 3.72 (1H, dd, J=3, 7 Hz, 22α-H), 3.57 (1H, dd, J=11, 12 Hz, Xyl-5-H), 3.33 (1H, dd, J=4, 10 Hz, 3-H), 1.80 (3H, d, J=6 Hz, Rha-6-H), 1.34 (3H, s, 23-H), 1.27 (3H, s, 27-H), 1.22 (3H, s, 29-H), 1.14 (3H, s, 30-H), 0.99 (3H, s, 24-H), 0.98 (3H, s, 28-H), 0.90 (3H, s, 26-H), 0.76 (1H, br t, J=12 Hz, 1α-H). ^{13}C-NMR (pyridine-d_5): Tables I and II.

Periandradulcin C (3) A pale brown powder, $[\alpha]_D^{25}$ −17.4° (c=0.5, pyridine), mp 205—210 °C (dec.). UV λ_{max}^{MeOH} nm (log ε): 208 (3.70). *Anal.* Calcd for $C_{48}H_{76}O_{18}\cdot H_2O$: C, 59.17; H, 8.20. Found: C, 58.95; H, 8.45. ^{1}H-NMR (pyridine-d_5) δ: 10.30 (1H, br s, CHO), 6.29 (1H, d, J=1 Hz, Rha-1-H), 5.73 (1H, d, J=7 Hz, Glc-1-H), 4.90 (1H, br s, 18-H), 3.25 (1H, dd, J=4, 11, 3-H), 1.73 (3H, d, J=6 Hz, Rha-6-H), 1.34 (3H, s, 23-H), 1.24 (3H, s, 26-H), 1.10 (3H, s, 30-H), 1.03 (3H, s, 24-H), 1.01 (3H, s, 29-H), 0.93 (3H, s, 28-H), 0.86 (3H, s, 27-H), 0.71 (1H, br t, J=12 Hz, 1α-H). ^{13}C-NMR (pyridine-d_5): Tables I and II.

General Procedure of Acidic Hydrolysis The solution of pure saponin (1 mg) in 10% H_2SO_4 was refluxed for 3 h. After removal of the $CHCl_3$-soluble portion, the aqueous phase was neutralized with 1 N NaOH solution and analyzed by HPLC [column, TSKgel Sugar-AXI (4.6 mm i.d. × 150 mm, Tosoh Co.); mobile phase, FUNABEC-B solution (borate–ethanolamine complex, Funakoshi Pharmaceutical Co., Ltd.); detector, Shimadzu RF535 fluorescence detector (Ex=342 nm, Em=432 nm); flow rate, 0.4 ml/min; column temperature, 60 °C. Retention times: rhamnose, 14.92 min; xylose, 40.28 min; glucose, 49.82 min]. Glucuronic acid was identified by comparison with an authentic sample on another HPLC system [column, Carbopac PAI (4 mm i.d. × 250 mm, Dionex Co.); mobile phase, 100 mM NaOH–200 mM NaOH, 1.0 M NaOAc–200 mM NaOH (35:15:50, v/v); detector, Dionex PAD-2 plused amperometric detector; flow rate, 0.8 ml/min; column temperature, room temperature. Retention time: glucuronic acid, 12.34 min].

Huang-Minlon Reduction of Periandradulcin B (2) A solution of **2** (20 mg) in diethyleneglycol (20 ml) and 80% hydrazine hydrate (10 ml) with KOH (700 mg) was refluxed on an oil bath (160 °C) for 24 h. After the removal of excess hydrazine hydrate, the reaction mixture was refluxed at 210 °C for 24 h following by extraction with $CHCl_3$. The $CHCl_3$ extract was purified by semi-preparative HPLC [column, YMC-A023; mobile phase, hexane–iso-PrOH (95:5, v/v); flow rate, 5 ml/min; detection, 207 nm UV absorption] to furnish **4** (5.20 mg), of which the ^{13}C-NMR chemical shift values were identical with those of sophoradiol.[5]

Huang-Minlon Reduction of Periandradulcin C (3) A solution of **3** (20 mg) in diethyleneglycol (20 ml) and 80% hydrazine hydrate (20 ml) with KOH (700 mg) was refluxed on oil bath (160 °C) for 54 h. After removal of excess hydrazine hydrate, the reaction mixture was refluxed at 210 °C for 12 h following by extraction with $CHCl_3$. The $CHCl_3$ extract was purified by semi-preparative HPLC [column, YMC-A023; mobile phase, hexane–iso-PrOH (99:1, v/v); flow rate, 5 ml/min; detection, 207 nm UV absorption] to furnish **6** (5.30 mg).

3β,22β-Dihydroxyolean-18-ene (6) Colorless plates ($CHCl_3$–MeOH), $[\alpha]_D^{25}$ +8.0° (c=0.1, $CHCl_3$), mp 200—203 °C. EI-MS m/z: 442 (M^+). ^{1}H-NMR ($CDCl_3$) δ: 4.83 (1H, br s, 18-H), 3.63 (1H, dd, J=10, 7 Hz, 22α-H), 3.20 (1H, dd, J=10, 6, 3-H), 1.07, 1.01, 1.00, 0.97, 0.96, 0.88, 0.77, 0.73 (each 3H, s). ^{13}C-NMR ($CDCl_3$) Table I.

Cleavage of the Ester Linkage of Periandradulcin A (1) A solution of **1** (1 mg) in 10% sodium methoxide (1 ml) was kept at 70 °C for 12 h, then poured into ice-water, neutralized with AcOH and extracted with $CHCl_3$

(10 ml × 3). The product from the $CHCl_3$ extract was purified by preparative TLC [silica gel, hexane–EtOAc (2:1, v/v)] and confirmed to be identical with authentic methyl syringate in HPLC, TLC and EI-MS.

Preparation of Methyl Syringate Syringic acid (400 mg, Tokyo Kasei Co., Ltd.) was refluxed with consentrated H_2SO_4 (0.1 ml) and anhydrous MeOH (4 ml) for 5.5 h. The reaction mixture was poured into ice-water and extracted with Et_2O. The product from the Et_2O extract was purified by silica gel column chromatography [hexane–EtOAc (1:4, v/v)], to furnish methyl syringate (372.3 mg, 86.9% yield). Colorless needles ($CHCl_3$–MeOH), mp 104—105 °C. ^{1}H-NMR ($CDCl_3$) δ: 7.61 (2H, s, 2, 6-H), 3.88 (3H, s, $-COOCH_3$), 3.81 (6H, s, $-OCH_3$). ^{13}C-NMR ($CDCl_3$) δ: 167.0 (s, $-COOCH_3$), 148.5 (s, 3, 5-C), 142.6 (s, 4-C), 120.0 (s, 1-C), 107.8 (d, 2, 6-C), 56.2 (q, $-OCH_3$), 51.7 (q, $-COOCH_3$).

Assay of PDE-Inhibitory Activity Activity of PDE was determined by a modification of the method described by Thompson and Appleman[11] and Brooker *et al.*[12] The reaction mixture (400 μl), containing 50 mM Tris–HCl (pH 8.0), [^{3}H]cAMP or [^{3}H]cGMP and a sample dissolved in 4% dimethyl sulfoxide, was incubated with PDE derived from bovine heart (Boehringer Mannheim GmbH) for 10 min at 30 °C and then boiled for 5 min. In the assay for PDE-I, 0.1 mM Ca^{2+} and calmodulin (5 units, Sigma) were added to the reaction mixture. Snake vemon (5'-nucleotidase, Sigma) (20 μM, 0.2 U) was added to the boiled reaction mixture and the whole was incubated for another 10 min at 37 °C, then 1 ml of Dowex AG1 × 2 resin (200—400 mesh) was added. After the resin had absorbed unchanged [^{3}H]cAMP or [^{3}H]cGMP, it was precipitated by centrifugation, and the radioactivity of the supernatant containing [^{3}H]adenosine or [^{3}H]guanosine formed during the incubation was measured with a liquid scintillation counter. The IC_{50} value is concentration of the compound required to give 50% inhibition.

Fractionation of PDEs PDE derived from bovine heart (Boehringer Mannheim GmbH) was fractionated on a DEAE-cellulose (Seikagaku Kogyo Co., Ltd.) column (0—0.4 M sodium acetate linear gradient) to furnish PDE-II and PDE-III. PDE-I was obtained by purification of activator-deficient PDE derived from bovine heart (P-I fraction, Sigma) on a DEAE-cellulose column.

Acknowledgment We are grateful to Dr. T. Kusumi, Tsukuba University for the 500 MHz NMR measurement.

References and Notes

1) E. W. Sutherland and T. W. Rall, *J. Biol. Chem.*, **232**, 1077 (1958).
2) R. E. Weishear, M. H. Cain and J. A. Bristol, *J. Med. Chem.*, **28**, 537 (1985) and references cited therein.
3) U. Sankawa, *Farumashia*, **17**, 387 (1981); T. Nikaido, T. Ohmoto and U. Sankawa, *Chem. Pharm. Bull.*, **35**, 675 (1987) and references cited therein.
4) Y. Hashimoto, H. Ishizone, M. Ogura, K. Nakatsu and H. Yoshioka, *Phytochemistry*, **22**, 259 (1983) and references cited therein.
5) J. Kinjo, I. Miyamoto, K. Murakami, K. Kida, T. Tomimatsu, M. Yamasaki and T. Nohara, *Chem. Pharm. Bull.*, **33**, 1293 (1985).
6) A. G. Gonzalez, B. M. Furaga, P. Gonzalez, M. G. Hernandez and A. G. Ravelo, *Phytochemistry*, **20**, 1919 (1981).
7) *a*) A. G. Gonzalez, J. J. Mendoza, A. G. Ravelo and J. G. Luis, *J. Nat. Pro.*, **52**, 567 (1989); *b*) H. Budzikiewicz, J. M. Wilson and C. Djerassi, *J. Am. Chem. Soc.*, **85**, 3688 (1963); *c*) A. G. Gonzalez, J. L. Berton and B. M. Furaga, *An. Quim.*, **68**, 709 (1972).
8) M. L. Reeves, B. K. Leigh and P. J. England, *Biochem. J.*, **241**, 535 (1987).
9) M. Hagiwara, T. Endo and H. Hidaka, *Biochem. Pharmacol.*, **33**, 453 (1984).
10) R. E. Weishear, S. D. Burrows, M. M. Quade and D. C. Kobylarz, *Biochem. Pharmacol.*, **35**, 787 (1986).
11) W. J. Thompson and M. M. Appleman, *Biochemistry*, **10**, 311 (1971).
12) G. Brooker, L. J. Thomas and M. M. Appleman, *Biochemistry*, **7**, 4177 (1968).

Fischer Indolization and Its Related Compounds. XXIV.[1] Fischer Indolization of Ethyl Pyruvate 2-(2-Methoxyphenyl)phenylhydrazone

Hisashi ISHII,*[,a] Takao SUGIURA[a] (née HAGIWARA), Kimiko KOGUSURI,[a] Toshiko WATANABE,[b] and Yasuoki MURAKAMI*[,b]

Faculty of Pharmaceutical Sciences, Chiba University,[a] 1–33, Yayoi-cho, Chiba 260, Japan and School of Pharmaceutical Sciences, Toho University,[b] 2–2–1, Miyama, Funabashi, Chiba 274, Japan. *Received July 30, 1990*

In order to clarify the mechanism of Fischer indolization of 2-methoxyphenylhydrazones, Fischer indolization of ethyl pyruvate 2-(2-methoxyphenyl)phenylhydrazone (2) was carried out with hydrochloric acid in ethanol and zinc chloride in acetic acid. The reactions proceeded smoothly to give *N*-arylindoles (11—14) and some chlorinated diphenylamine derivatives (8—10) as by-products. Consideration of the indole products revealed that the Fischer indolization proceeded mainly at the unsubstituted phenyl nucleus rather than at the 2-methoxyphenyl nucleus. This result is inconsistent with the previous result that Fischer indolization of diarylhydrazones proceeded at the electron-richer nucleus. The structures of the diphenylamines were determined by chemical means and the mechanism of their formation is discussed.

Keywords Fischer indolization; *N*-arylphenylhydrazone; chlorinated diphenylamine; Ullmann–Goldberg reaction; *o*-quinone imine

In the previous paper[1] we reported the Fischer indolization of ethyl pyruvate 2-(2,6-dimethoxyphenyl)phenylhydrazone (**1**), in order to clarify the mechanism of abnormal Fischer indolization of 2-methoxyphenylhydrazones.[2] The result revealed that the cyclization proceeded mainly at the 2,6-dimethoxyphenyl nucleus rather than the unsubstituted phenyl one. However, the total amount of indoles formed was too small to allow a difinitive conclusion. Thus, we examined the Fischer indolization of ethyl pyruvate 2-(2-methoxyphenyl)phenylhydrazone (**2**) for the same purpose.[3] The results are presented here.

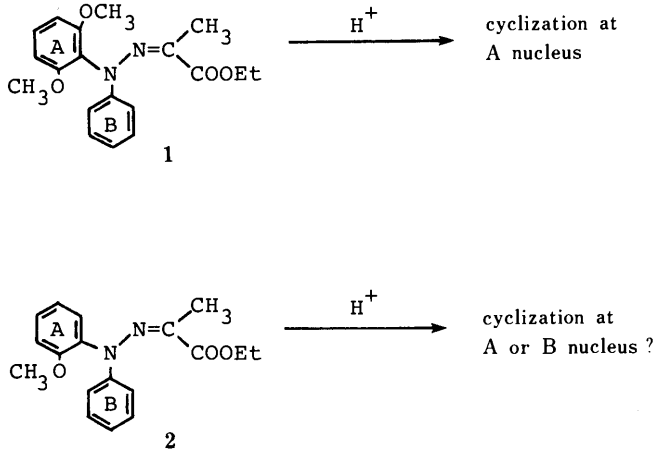

Chart 1

The (2-methoxyphenyl)phenylhydrazone (**2**) was synthesized from *o*-acetanisidide (**3**) by a similar route to that used for the synthesis of the (2,6-dimethoxyphenyl)phenylhydrazone[1] (**1**), as shown in Chart 2. Ullmann–Goldberg reaction[1] of *o*-acetanisidide (**3**) with bromobenzene gave the *N*-phenyl derivative (**4**), which was converted to *N*-phenyl-*o*-anisidine (**5**) by acid hydrolysis. Treatment of **5** with sodium nitrite in acidic media gave the *N*-nitroso derivative (**6**), which was converted to the hydrazine (**7**) by reduction with zinc and acetic acid. The crude hydrazine (**7**) was directly treated with ethyl pyruvate to give the desired hydrazone (**2**).

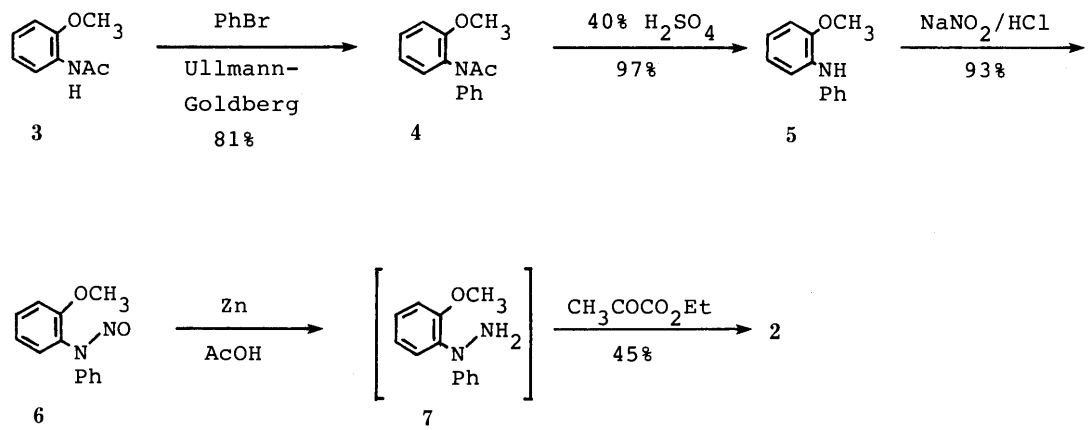

Chart 2

Result of Fischer Indolization

Ethyl pyruvate 2-(2-methoxyphenyl)phenylhydrazone (**2**) was allowed to react under Fischer indolization conditions with hydrochloric acid in ethanol to yield seven products (**8**, **9**, **5**, **10**, **11**, **12**, and **13**, in that order of elution on column chromatography).

The first (**8**), the second (**9**), and the fourth (**10**) products were oily. Their mass spectra (MS) showed the same molecular ion peak at *m/z* 233, with *m/z* 235 having 33% relative intensity, which indicated the molecular formula $C_{13}H_{12}ClNO$. The infrared (IR) spectra showed an NH absorption, and the ^{1}H-nuclear magnetic resonance

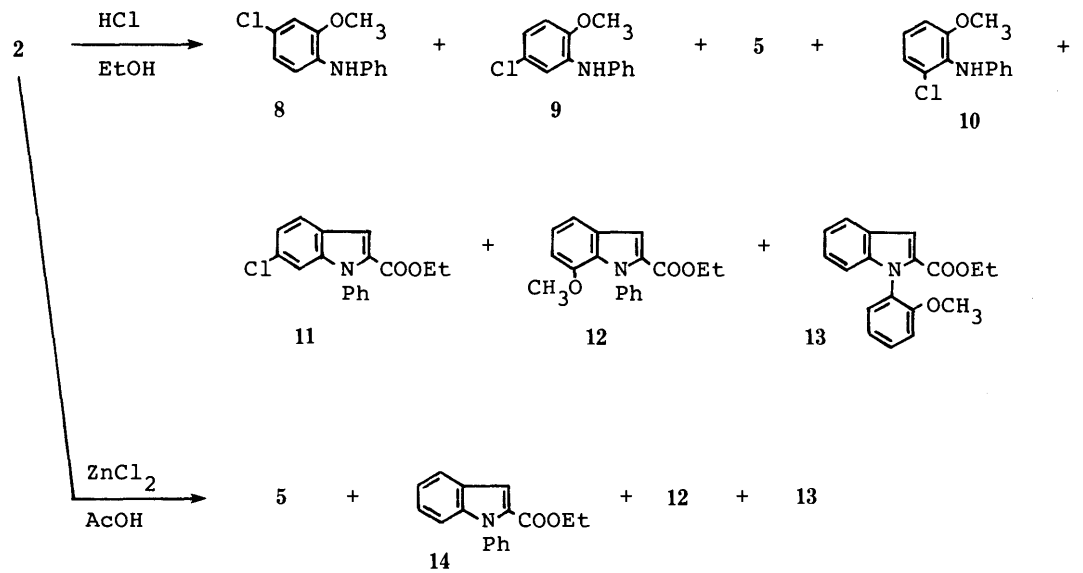

Acid catalyst	Product yields (%) Amines				Indoles			
	5	**8**	**9**	**10**	**11**	**12**	**13**	**14**
HCl/EtOH	1.5	7.1	14.9	2.5	1.3	2.8	34.5	0
$ZnCl_2$/AcOH	1.9	—	—	—	0	1.5	10.2	0.3
Cyclization direction on **2**					A	A	B	A

Chart 3

TABLE I. Mass Spectral Data for Chlorinated Diphenylamines (**8**—**10**)

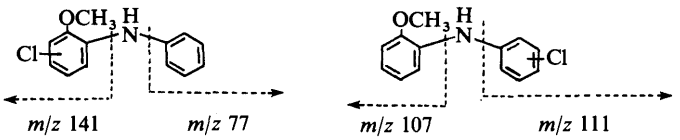

31 **32**

Compound	Relative intensities (%) with respect to base peak					
	m/z	77	141	107	111	Base peak
8		55	*ca.* 0	0	0	233
9		48	*ca.* 0	0	0	233
10		43	4.6	0	0	233

(^{1}H-NMR) spectra showed a methoxy group, and eight aromatic protons. These data showed that these three products (**8**—**10**) are structural isomers of chlorinated *N*-phenyl-*o*-anisidines. It was determined by mass spectral inspection, in the same manner as described previously,[1] which nucleus was chlorinated. Table I shows the fragment ions formed due to cleavage of the aryl–nitrogen bond. The fragment at *m/z* 77 was observed clearly, while fragments at *m/z* 107 and 111 were not observed at all. These data indicate that the structure of the chlorinated diphenylamines (**8**—**10**) is **31**, having a chlorine atom and a methoxy group on the same phenyl nucleus, but not **32**, having them on separate nuclei. Thus, the chlorinated diphenylamines (**8**—**10**) are three of the four possible isomers with respect to chlorine. As we could not discriminate the position of chlorine clearly by ^{1}H-NMR spectroscopy, we decided to determine the structures by means of alternative syntheses. We tentatively selected the 4-chloro (**8**), 5-chloro (**9**) and 6-chloro (**10**) compounds of the four as targets for synthesis. The 4-chloro (**8**) and 6-chloro (**10**) compounds were expected to have been formed, based on the previous results[1,4] that similar Fischer indolization of ethyl pyruvate 2-(4-methoxyphenyl)phenylhydrazone and the (2,6-dimethoxyphenyl)phenylhydrazone (**1**) gave diphenylamine derivatives in which the chlorine atom was introduced at the *meta* position with respect to the methoxy group. The third product should be the 3-chloro- or 5-chloro-diphenylamine, and the 5-chloro compound (**9**) was considered more likely, because it would be formed more easily than the 3-chloro one owing to steric hindrance to the attack of chlorine, although the formation mechanism was uncertain at that time.

Chart 4 shows the alternative syntheses of the three chlorinated diphenylamines (**8**—**10**). i) The Hofmann rearrangement of 4-chloro-2-methoxybenzoic acid (**15**) with diphenylphosphorylazide (DPPA), followed by treatment with ethanol gave the carbamate (**16**), which was led to 4-chloro-2-methoxyaniline (**17**) by alkaline hydrolysis. The amine (**17**) was converted to the acetanilide (**18**), which was allowed to react with bromobenzene (Ullmann–Goldberg reaction) to give 4′-chloro-*o*-(*N*-phenyl)acetanisidide (**19**), mp 103—105 °C. This diphenyl compound was identical with the sample, mp 103—105 °C, prepared from the Fischer product (**8**) by acetylation. ii) The Ullmann–Goldberg reaction of 5′-chloro-*o*-acetanisidide (**20**) with bromobenzene gave 5′-chloro-*o*-(*N*-phenyl)acetanisidide (**21**), mp 119—121 °C, which was identical with the sample, mp 121—123 °C, prepared from the Fischer product (**9**) by acetylation. iii) *o*-Chloroaniline (**22**) was converted to

alternative syntheses of chlorinated diphenylamines (**8**—**10**)

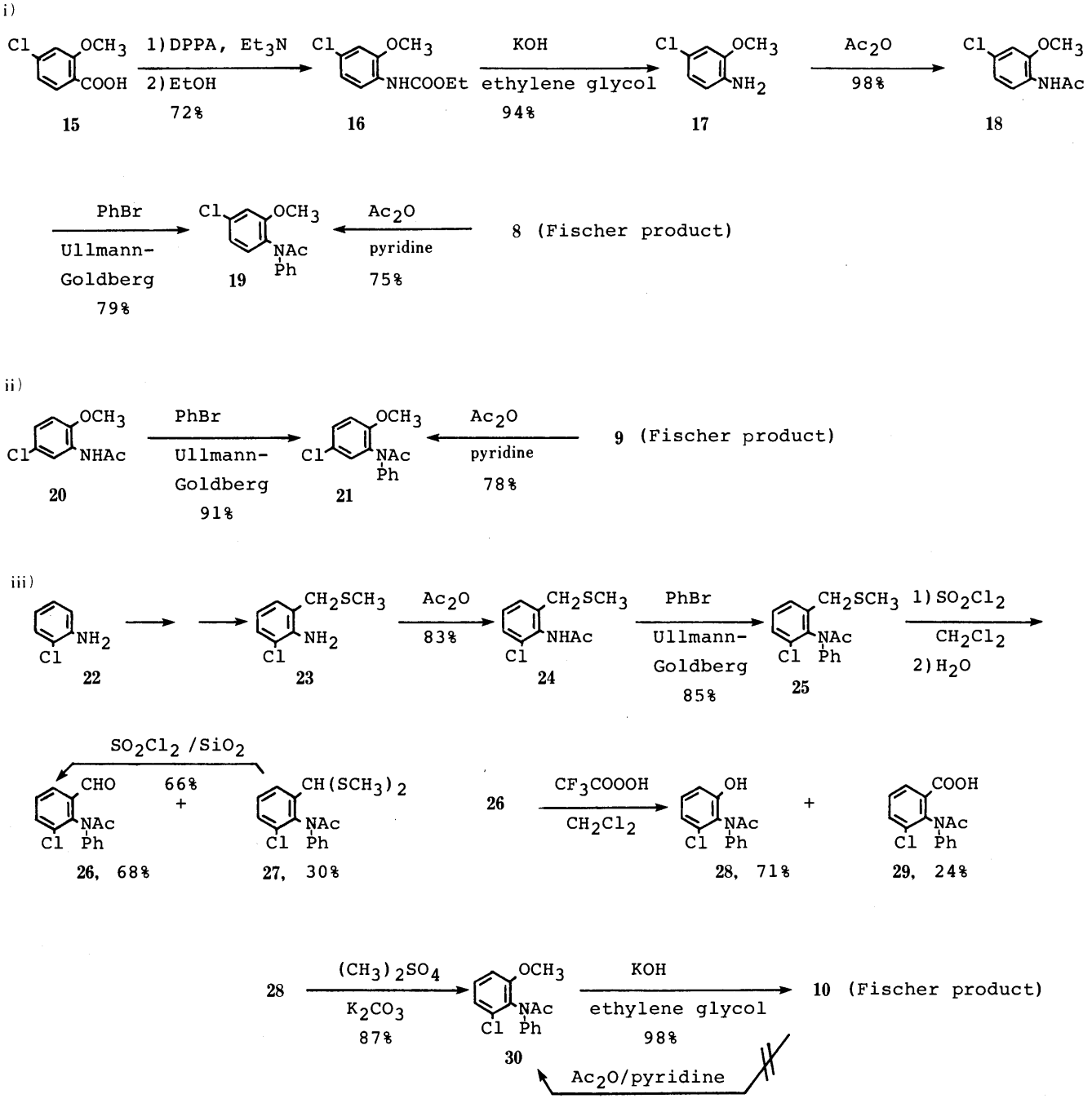

Chart 4

6-chloro-(α-methylthio)-*o*-toluidine (**23**) according to the known procedure.[5] The aniline (**23**) was converted to the *N*-acetyldiphenylamine (**25**) *via* **24** by acetylation followed by phenylation. Chlorination followed by hydrolysis of the *N*-acetyldiphenylamine (**25**) gave the expected aldehyde (**26**) with the thioacetal (**27**) as by-product. The latter (**27**) was easily converted to the former aldehyde (**26**) by hydrolysis using sulfuryl chloride and silica gel.

The Baeyer–Villiger reaction of the aldehyde (**26**) was unsuccessful with usual peracids, performic acid, peracetic acid, or *m*-chloroperbenzoic acid [the starting aldehyde (**26**) was recovered unchanged]. We next attempted this reaction with trifluoroperacetic acid by a modified procedure. Although the peracid has been prepared[6] from equimolar 90% hydrogen peroxide and trifluoroacetic anhydride, we prepared it safely from 6 eq of trifluoroacetic anhydride and 1 eq of 30% hydrogen peroxide. This reagent successfully gave the corresponding phenol (**28**) accompanied with a by-product, *N*-acetyl-3-chloro-*N*-phenylanthranilic acid (**29**). The phenol (**28**) was converted to the methoxy compound (**30**) with dimethyl sulfate. However, we were unable to acetylate the Fischer product (**10**) for identification, presumably because of steric hindrance. Thus, the acetyl compound (**30**) was hydrolyzed to 6-chloro-(*N*-phenyl)-*o*-anisidine (**10**), which was identical with the Fischer product.

The third product of Fischer indolization of the hydrazone (**2**) was *N*-phenyl-*o*-anisidine (**5**), which would be formed directly by degradation of the hydrazone (**2**).

The fifth compound (**11**), obtained in a minute amount, was positive to the Ehrlich reagent[7] and Beilstein's halogen test. The mass spectrum (MS) showed a molecular ion at *m/z* 299, corresponding to $C_{17}H_{14}ClNO_2$. These data suggested that **11** is ethyl 6-chloro-1-phenylindole-2-carboxylate formed as a result of *ortho*-C_6-abnormal Fischer indolization.[4] The structure was determined by alternative synthesis using the corresponding NH-indole (**33**) as shown in Chart 5.

Both the sixth (**12**) and the seventh (**13**) compounds showed positive Ehrlich reagent and had the same molecular ion at *m/z* 295, corresponding to $C_{18}H_{17}NO_3$, in the MS. Their ^{1}H-NMR spectra each showed a signal due to a methoxy group. These data suggested that these two compounds were ethyl 7-methoxy-1-phenyl- (**12**) and ethyl 1-(2-methoxyphenyl)- (**13**) -indole-2-carboxylate, expected to be formed by normal cyclization. Alternative syntheses of the two from the corresponding NH-indoles (**34** and **35**) as shown in Chart 5 revealed that the sixth product (**12**) was the former and the seventh (**13**) was the latter.

The result of this Fischer indolization (see the table in Chart 3) revealed that the cyclization proceeded at the electron-poorer B-nucleus of the hydrazone (**2**) (Chart 1). In order to confirm this, the Fischer indolization of the hydrazone (**2**) was also carried out by using anhydrous zinc chloride, a different kind of acid catalyst from hydrochloric acid in ethanol. The reaction gave four compounds, three (**5**, **12**, and **13**) of which were common to those obtained with hydrochloric acid in ethanol. The new compound (**14**) was identified as ethyl 1-phenylindole-2-carboxylate from the spectral data and finally by alternative synthesis as shown in Chart 5. The indolic compound (**14**) should be formed[3] by cyclization at the position occupied by the methoxy group, followed by reductive elimination of the

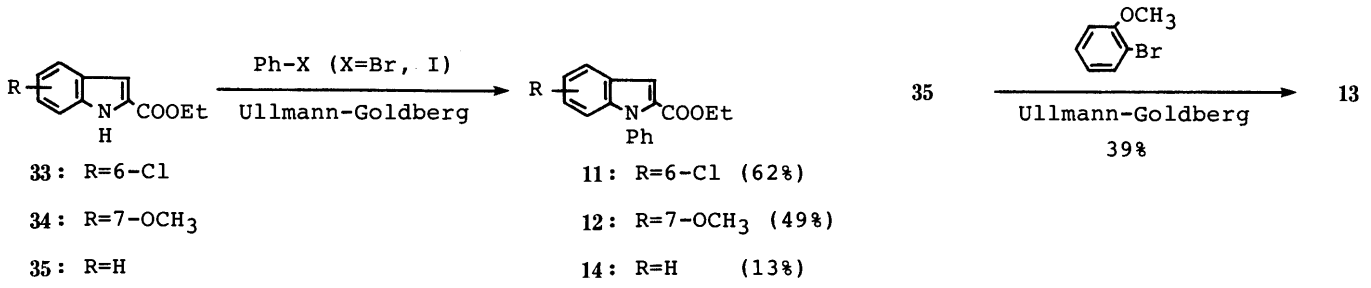

Chart 5

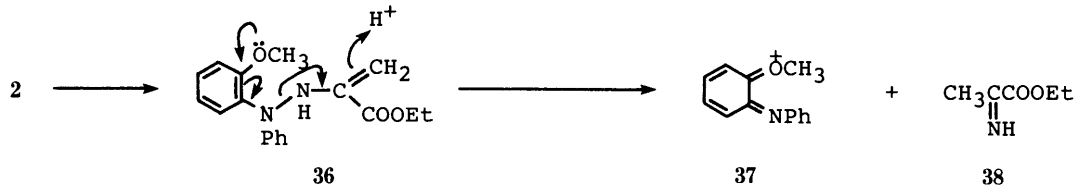

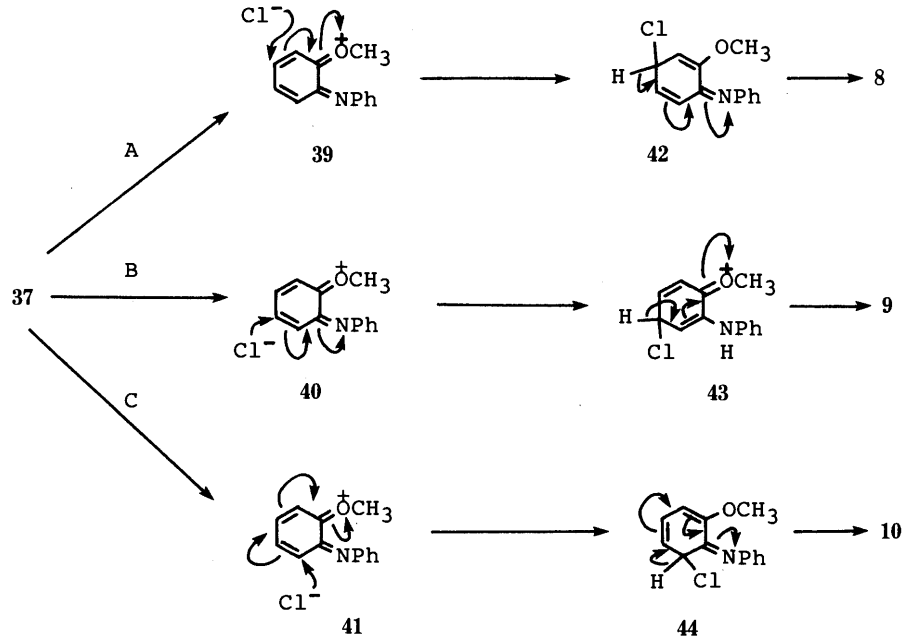

Chart 6

methoxy group.[2)]

Discussion

Cyclization Direction The result of the Fischer indolization of ethyl pyruvate 2-(2-methoxyphenyl)phenylhydrazone (**2**) is summarized in the table of Chart 3. Among the indolic products, the *N*-(2-methoxyphenyl)indole (**13**) is formed by cyclization toward the B-nucleus of the hydrazone (**2**). Other indoles (**11**, **12**, and **14**) should result from the cyclization toward the A-nucleus. The total amount of indoles obtained from the electron-poorer B-nucleus cyclization is much greater than that from the electron-richer A-nucleus cyclization. This tendency is common to the two reactions with hydrochloric acid in ethanol and zinc chloride in acetic acid. The present result is inconsistent with the previous finding[1,4)] that Fischer indolization proceeds through the electrophilic attack of the enhydrazine moiety on the aromatic nucleus. We cannot have any idea to explain all these results at this time. In order to obtain further information, we intend to carry out the Fischer indolization of the diarylhydrazone having an electron-attracting group at the 2-position on one of two nuclei.

Chlorinated Diphenylamines The formation mechanism of the chlorinated diphenylamines (**8**—**10**) could be as shown in Chart 6 on the basis of reported examples.[1,4)] The hydrazone (**2**) reacted with a proton and cleavage occurred at the nitrogen–nitrogen bond to generate an activated *o*-quinone imine intermediate (**37**) and pyruvate derivative (**38**). The quinone imine (**37**) reacted with chloride anion at the *meta* positions to the charged methoxy group to form the 4- or 6-chlorinated diphenylamine (**8** and **10**) in the same manner as reported,[1,4)] through route A or C. The formation of the 5-chlorodiphenylamine (**9**) was slightly different. The position of chlorine was *para* to the methoxy group. A chloride anion would react at the *meta* position to the imine moiety in the common intermediate (**37**) as shown by route B and would be aromatized to give the product (**9**). The formation of **9** would be consistent with the presence of the quinone imine intermediate (**37**).

Experimental

All melting points were measured on a micro melting point hot stage (Yanagimoto) and are uncorrected. IR spectra were recorded in Nujol mulls (unless otherwise stated) on Hitachi EPI-G3 and Shimadzu IR 400 instruments. ^{1}H-NMR spectra were recorded in $CDCl_3$ (unless otherwise stated) on JEOL JMN-4H-100 (100 MHz) and Hitachi R-24B (60 MHz) spectrometers. In the ^{1}H-NMR spectrum, chemical shifts are given in δ-values referred to internal tetramethylsilane, and the assignment of all NH and OH signals was confirmed by the disappearance of their signals after addition of D_2O. MS were measured by using the direct inlet system on a JEOL JMS-01-SG-2 spectrometer. For column chromatography, silicic acid (SiO_2) (100 mesh, Millinckrodt Chemical Works) and silica gel (Kiesel gel 60, 70—230 mesh, Merck), and for preparative thin layer chromatography (TLC), Kiesel gel GF_{254}, Merck, were used. The abbreviations used are as follows: s, singlet; d, doublet; dd, double doublet; t, triplet; q, quartet; m, multiplet; dif, diffused; br, broad; arom, aromatic. Distillation for elemental analysis of oily compounds was performed by using a micro distillation and sublimation apparatus (Miyamoto Riken Ind. Co., Ltd., Japan).

***N*-Phenyl-*o*-acetanisidide (4) General Procedure for Ullmann–Goldberg Reaction**[1,4)] A mixture of *o*-acetanisidide[8)] (**3**) (15.0 g), bromobenzene (19.5 ml), anhydrous K_2CO_3 (8.0 g), Cu powder (0.8 g), and a catalytic amount of I_2 in nitrobenzene (85 ml) was refluxed for 34 h under an Ar atmosphere. The reaction mixture was poured into H_2O, and steam distilled. The residue was extracted with Et_2O, then the extract was dried over anhydrous K_2CO_3, and evaporated to dryness *in vacuo*. The residue (25.0 g) was chromatographed over silicic acid using benzene, followed by AcOEt–benzene (1 : 8), to give a solid (17.66 g, 81%). Recrystallization from hexane–benzene gave pale brown plates (15.68 g), mp 108—109.5 °C. *Anal.* Calcd for $C_{15}H_{15}NO_2$: C, 74.66; H, 6.27; N, 5.81. Found: C, 74.93; H, 6.45; N, 5.76. IR ν_{max} cm^{-1}: 1665 (C=O). ^{1}H-NMR δ: 1.99 (3H, dif s, $COCH_3$), 3.85 (3H, s, OCH_3), 6.83—7.40 (9H, m, arom H). MS *m/z*: 241 (M^+).

***N*-Phenyl-*o*-anisidine (5)** A suspension of *N*-phenyl-*o*-acetanisidide (**4**) (15.676 g) in 40% H_2SO_4 (140 ml) was refluxed for 10 h under an Ar atmosphere. The reaction mixture was poured into H_2O, and extracted with Et_2O, then the extract was washed with 5% $NaHCO_3$, and dried over anhydrous K_2CO_3. Removal of the solvent *in vacuo* gave the residue (12.93 g), which was chromatographed over silicic acid using benzene to give a solid (12.09 g, 97%). Recrystallizations from hexane gave colorless plates, mp 36—37 °C [lit.,[9)] bp 158—160 °C (2 mmHg)]. *Anal.* Calcd for $C_{13}H_{13}NO$: C, 78.36; H, 6.58; N, 7.03. Found: C, 78.18; H, 6.74; N, 6.73. IR ν_{max} cm^{-1}: 3405 (NH). ^{1}H-NMR δ: 3.85 (3H, s, OCH_3), 5.60 (1H, br s, NH), 6.82—7.75 (9H, m, arom H). MS *m/z*: 199 (M^+).

***N*-Nitroso-*N*-phenyl-*o*-anisidine (6)** A solution of $NaNO_2$ (459 mg) in H_2O (2.5 ml) was added dropwise to a solution of *N*-phenyl-*o*-anisidine (**5**) (1.00 g) containing concentrated HCl (0.5 ml) at 0—4 °C, and the whole was stirred for 1 h. Then the reaction mixture was poured into H_2O, and extracted with Et_2O. The extract was washed with H_2O, dried over $MgSO_4$ and evaporated *in vacuo*. The residue (1.18 g) was chromatographed over silicic acid using benzene to give a solid (1.13 g). Recrystallizations from cyclohexane gave yellow needles (992 mg, 93%), mp 66—68 °C. *Anal.* Calcd for $C_{13}H_{12}N_2O$: C, 68.41; H, 5.30; N, 12.27. Found: C, 68.02; H, 5.33; N, 12.08. IR: no NH. ^{1}H-NMR δ: 3.72 (3H, s, OCH_3), 7.00—7.51 (9H, m, arom H). MS *m/z*: 199 ($M^+ - 29$).[4)]

Ethyl Pyruvate 2-(2-Methoxyphenyl)phenylhydrazone (2) Zn powder (12 g) was added portionwise to a solution of *N*-nitroso-*N*-phenyl-*o*-anisidine (**6**) (6.30 g) in a mixture of AcOH (35 ml) and H_2O (14 ml) under ice cooling, and the whole was stirred for 10 h. Then the reaction mixture was poured into H_2O, and filtered with suction to remove the unreacted Zn powder. The filtrate was basified with 10% NaOH, extracted with Et_2O. The extract was washed with H_2O, dried over anhydrous K_2CO_3, and evaporated to dryness. The residue (5.955 g), a crude 1-(2-methoxyphenyl)-1-phenylhydrazine (**7**), was dissolved in EtOH (30 ml). Ethyl pyruvate (2.26 g) and one drop of AcOH were added to this solution, and the whole was refluxed for 5 min. The reaction mixture was concentrated to dryness *in vacuo*. The residue (8.116 g) was chromatographed over silicic acid using benzene to give a solid (4.91 g). Recrystallizations from hexane gave pale yellow prisms (3.838 g, 45%), mp 102—103.5 °C. *Anal.* Calcd for $C_{18}H_{20}N_2O_3$: C, 69.21; H, 6.45; N, 8.97. Found: C, 69.13; H, 6.49; N, 8.95. IR ν_{max} cm^{-1}: 1690 (C=O). ^{1}H-NMR δ: 1.38 (3H, t, J=7.5 Hz, $CH_2\underline{CH}_3$), 1.52 (3H, s, CCH_3), 3.76 (3H, s, OCH_3), 4.31 (2H, q, J=7.5 Hz, $O\underline{CH}_2CH_3$), 6.95—7.50 (9H, m, arom H). MS *m/z*: 312 (M^+).

Fischer Indolization of Ethyl Pyruvate 2-(2-Methoxyphenyl)phenylhydrazone (2) with Saturated HCl in EtOH Ethyl pyruvate 2-(2-methoxyphenyl)phenylhydrazone (**2**) (1.801 g) was dissolved in absolute EtOH (90 ml) saturated with dry HCl gas and the whole was stirred at room temperature for 40 min. Then the reaction mixture was poured into H_2O, and extracted with Et_2O. The extract was washed with diluted $NaHCO_3$, and dried over anhydrous K_2CO_3. Removal of the solvent *in vacuo* gave the residue (1.44 g), which was chromatographed over silica gel using benzene to give the amine fraction (390 mg), and the indole fraction (707 mg) in that order of elution.

The amine fraction was repeatedly chromatographed over silica gel using benzene–hexane (1 : 1) to give three eluates, a mixture of **8** and **9**, **5**, and **10** in that order of elution. The mixture of **8** and **9** was separated into the two components by column chromatography over silica gel using Et_2O–hexane (1 : 10).

a) 4-Chloro-*N*-phenyl-*o*-anisidine (**8**): 96 mg (7.1%) yield. Oily compound. IR ν_{max}^{neat} cm^{-1}: 3420 (NH). MS *m/z*: 235 (M^+ + 2, 34%, intensity of M^+), 233 (M^+, base peak). *N*-Acetyl derivative (**19**) of the amine (**8**): prepared by reaction with Ac_2O–pyridine (75% yield). Colorless columns from hexane–benzene, mp 103—105 °C. This compound was identical with an authentic sample, whose preparation is described later.

b) 5-Chloro-*N*-phenyl-*o*-anisidine (**9**): 188 mg (14.0%) yield. Oily compound. IR ν_{max}^{neat} cm^{-1}: 3400 (NH). MS *m/z*: 235 (M^+ + 2, 35% intensity of M^+), 233 (M^+, base peak). *N*-Acetyl derivative (**21**) of the amine (**9**): prepared by the reaction with Ac_2O–pyridine (78% yield). Colorless prisms from benzene–hexane, mp 121—123 °C. This compound was identical with an authentic sample, whose preparation is described later.

c) *N*-Phenyl-*o*-anisidine (**5**): 17 mg (1.5%) yield. Colorless plates from

pentane, mp 36—37 °C. This compound was identical with an authentic sample.

d) 6-Chloro-*N*-phenyl-*o*-anisidine (**10**): 34 mg (2.5%) yield. Oily compound. IR ν_{max}^{neat} cm^{-1}: 3400 (NH). MS *m/z*: 235 ($M^+ + 2$, 37% intensity of M^+), 233 (M^+). This compound was identical with an authentic sample, whose preparation is described later.

The indole fraction was repeatedly chromatographed over silica gel using benzene–hexane (1 : 1) to give three indoles, **11**, **12**, and **13**, in that order of elution.

e) Ethyl 6-Chloro-1-phenylindole-2-carboxylate (**11**): 23 mg (1.3%) yield. Colorless prisms from pentane, mp 57.5—59 °C. IR ν_{max} cm^{-1}: 1710 (C=O). MS *m/z*: 301 ($M^+ + 2$, 36% intensity of M^+), 299 (M^+, base peak). This compound was identical with an authentic sample, whose preparation is described later.

f) Ethyl 7-Methoxy-1-phenylindole-2-carboxylate (**12**): 36 mg (2.8%) yield. Colorless needles from hexane, mp 58—60 °C. IR ν_{max} cm^{-1}: 1725 (C=O). MS *m/z*: 295 (M^+, base peak). This compound was identical with an authentic sample, whose preparation is described later.

g) Ethyl 1-(2-Methoxyphenyl)indole-2-carboxylate (**13**): 588 mg (34%) yield. Colorless prisms from hexane, mp 71—73.5 °C. IR ν_{max} cm^{-1}: 1710 (C=O). MS *m/z*: 295 (M^+, base peak). This compound was identical with an authentic sample, whose preparation is described later.

Fischer Indolization of Ethyl Pyruvate 2-(2-Methoxyphenyl)phenylhydrazone (2) with $ZnCl_2$–AcOH The hydrazone (**2**) (1.50 g) was added to a solution of anhydrous $ZnCl_2$ (1.18 g) in AcOH (15 ml) and the whole was refluxed for 35 min. The reaction mixture was poured into ice-water, and extracted with Et_2O, then the extract was washed with H_2O and 5% $NaHCO_3$, and dried over $MgSO_4$. Removal of the solvent *in vacuo* gave a crystalline residue (1.465 g). Column chromatography over silicic acid using benzene gave four eluates, A, B, C, D in that order of elution.

a) *N*-Phenyl-*o*-anisidine (**5**): A solid (20 mg) obtained from eluate A was recrystallized from pentane to give colorless plates (18.4 mg, 4.8%), mp 36—37.5 °C. IR ν_{max} cm^{-1}: 3400 (NH). This compound was identical with an authentic sample.

b) Ethyl 1-Phenylindole-2-carboxylate (**14**): A solid (5 mg) obtained from eluate B was recrystallized from pentane to give colorless plates (4 mg, 0.8%), mp 62.5—65.5 °C. IR ν_{max} cm^{-1}: 1710 (C=O). MS *m/z*: 265 (M^+, base peak). This compound was identical with an authentic sample, whose preparation is described later.

c) Ethyl 7-Methoxy-1-phenylindole-2-carboxylate (**12**): A solid (21 mg) obtained from eluate C was recrystallized from pentane to give colorless columns (21 mg, 3.6%), mp 58—60 °C. IR ν_{max} cm^{-1}: 1725 (C=O). This compound was identical with an authentic sample, whose preparation is described later.

d) Ethyl 1-(2-Methoxyphenyl)indole-2-carboxylate (**13**): A solid (148 mg) obtained from eluate D was recrystallized from pentane to give colorless prisms (145 mg, 25.5%), mp 66.5—67.5 °C. This compound was identical with an authentic sample, whose preparation is described later.

Preparation of Authentic 4'-Chloro-*N*-phenyl-*o*-acetanisidide (19) i) Ethyl 4-Chloro-2-methoxycarbanilate (**16**): DPPA[10] (3.46 ml) and Et_3N (3.0 ml) was added to a solution of commercial (Aldrich) 4-chloro-2-methoxybenzoic acid (**15**) (2.00 g) in dry dioxane (30 ml) and the mixture was refluxed for 4 h. Then absolute EtOH (5 ml) was added to it and the whole was refluxed for a further 6 h. After the reaction was over, the reaction mixture was concentrated to dryness *in vacuo* and the residue was dissolved in benzene. The organic layer was successively washed with 5% citric acid, H_2O, 5% $NaHCO_3$, and saturated NaCl, and dried over $MgSO_4$. Removal of the solvent *in vacuo* gave a pale yellow solid (2.64 g), which was chromatographed over silica gel using benzene, followed by benzene–AcOEt (10 : 1), to give colorless crystals (1.78 g, 72%). Recrystallization from Et_2O–hexane gave colorless prisms, mp 84—86 °C. *Anal.* Calcd for $C_{10}H_{12}ClNO_3$: C, 52.29; H, 5.27; N, 6.10. Found: C, 52.45; H, 5.26; N, 5.99. IR ν_{max} cm^{-1}: 3260 (NH), 1700 (C=O). ^{1}H-NMR δ: 1.31 (3H, t, J=8.0 Hz, $CH_2\underline{CH}_3$), 3.83 (3H, s, OCH_3), 4.21 (2H, q, J=8.0 Hz, $OC\underline{H}_2CH_3$), 6.79 (1H, d, J=2.0 Hz, C_3-H), 6.87 (1H, dd, J=8.0, 2.0 Hz, C_6-H), 7.08 (1H, br s, NH), 7.97 (1H, d, J=8.0 Hz, C_5-H). MS *m/z*: 231 ($M^+ + 2$, 41% intensity of M^+), 229 (M^+, base peak).

ii) 4'-Chloro-*o*-acetanisidide (**18**): A mixture of ethyl 4-chloro-2-methoxycarbanilate (**16**) (700 mg) and KOH (1.05 g) in ethylene glycol (7 ml) was heated at 160 °C (bath temperature) for 1.5 h. The reaction mixture was poured into H_2O, extracted with Et_2O. The extract was washed with saturated NaCl, and dried over anhydrous K_2CO_3. Removal of the solvent *in vacuo* gave 4-chloro-*o*-anisidine (**17**) (450 mg, 94%), mp 45—49 °C, which was recrystallized from EtOH–H_2O to give colorless needles, mp 48.5—49 °C (lit.,[11] mp 52 °C). A solution of the amine (**17**) (400 mg) in Ac_2O (2.0 ml) was stirred at room temperature for 1 h. The reaction mixture was poured into H_2O and basified with 28% NH_4OH. Precipitated crystals were collected with suction and air-dried to give colorless plates (495 mg, 98%), mp 147—151 °C. A part of this compound was recrystallized from H_2O–EtOH to give colorless plates, mp 149.5—150.5 °C (lit.,[11] mp 150 °C). IR ν_{max} cm^{-1}: 3270 (NH), 1660 (C=O). ^{1}H-NMR δ: 2.17 (3H, s, $COCH_3$), 3.84 (3H, s, OCH_3), 6.79 (1H, d, J=2.0 Hz, C_3-H), 6.87 (1H, dd, J=9.0, 2.0 Hz, C_5-H), 7.62 (1H, br s, NH), 8.24 (1H, d, J=9.0 Hz, C_6-H).

iii) 4'-Chloro-*N*-phenyl-*o*-acetanisidide (**19**): A mixture of 4'-chloro-*o*-acetanisidide (**18**) (200 mg), anhydrous K_2CO_3 (150 mg), and Cu_2Br_2 (37 mg) in bromobenzene (2 ml) was heated at 180—190 °C (bath temperature) under an Ar atmosphere for 5 h. The reaction mixture was worked up according to the general procedure of the Ullmann–Goldberg reaction. The crude product (279 mg) was recrystallized from benzene–hexane to give colorless prisms (217 mg, 79%), mp 103—105 °C. *Anal.* Calcd for $C_{15}H_{14}ClNO_2$: C, 65.34; H, 5.12; N, 5.08. Found: C, 65.68; H, 5.02; N, 5.11. IR ν_{max} cm^{-1}: 1670 (C=O). ^{1}H-NMR δ: 2.00 (3H, s, $COCH_3$), 3.83 (3H, s, OCH_3), 6.77—7.45 (8H, m, arom H).

Preparation of Authentic 5'-Chloro-*N*-phenyl-*o*-acetanisidide (21) A mixture of 5'-chloro-*o*-acetanisidide[12] (**20**) (500 mg), anhydrous K_2CO_3 (382 mg), Cu_2Br_2 (93 mg), and bromobenzene (5 ml) was heated at 180—190 °C (bath temperature) under an Ar atmosphere for 11 h. The reaction mixture was worked up according to the general procedure of the Ullmann–Goldberg reaction. The crude product (716 mg) was chromatographed over silica gel using benzene–AcOEt (10 : 1) to give a colorless solid (626 mg, 91%), mp 118—121 °C. Recrystallization from benzene–hexane gave colorless prisms, mp 119—121 °C. *Anal.* Calcd for $C_{15}H_{14}ClNO_2$: C, 65.34; H, 5.12; N, 5.08. Found: C, 65.51; H, 5.03; N, 5.16. IR ν_{max} cm^{-1}: 1670 (C=O). ^{1}H-NMR δ: 2.02 (3H, s, $COCH_3$), 3.85 (3H, s, OCH_3), 6.77—7.47 (8H, m, arom H).

Preparation of Authentic 6-Chloro-*N*-phenyl-*o*-anisidine (10) i) 6'-Chloro-(α-methylthio)-*o*-acetotoluidide (**24**): A solution of 6-chloro-(α-methylthio)-*o*-toluidine (**23**) (7.939 g), prepared from *o*-chloroaniline (**22**) according to Claus *et al.*'s method,[5] in Ac_2O (64 ml) was stirred at room temperature for 4 h. Then the reaction mixture was poured into H_2O, basified with NH_4OH, and extracted with AcOEt. The extract was washed with H_2O, and dried over anhydrous K_2CO_3. Removal of the solvent *in vacuo* gave a pale yellow solid (9.484 g, 87%), mp 119—121 °C. Recrystallization from benzene gave colorless leaflets (9.127 g, 83%), mp 123—124 °C. *Anal.* Calcd for $C_{10}H_{12}ClNOS$: C, 52.28; H, 5.27; N, 6.10. Found: C, 52.36; H, 5.21; N, 6.21. IR ν_{max} cm^{-1}: 3320 (NH), 1670 (C=O). ^{1}H-NMR δ: 1.96 (3H, s, SCH_3), 2.20 (3H, s, $COCH_3$), 3.64 (2H, s, CH_2S), 7.10—7.50 (4H, m, arom H and NH).

ii) 6'-Chloro-*N*-phenyl-(α-methylthio)-*o*-acetotoluidide (**25**): A mixture of 6'-chloro-(α-methylthio)-*o*-acetotoluidide (**24**) (101 mg), powdered anhydrous K_2CO_3 (67 mg), Cu_2Br_2 (6 mg), and bromobenzene (0.82 ml) was heated at 150—155 °C (bath temperature) under an Ar atmosphere for 2.5 h. The reaction mixture was worked up according to the general method of the Ullmann–Goldberg reaction. The crude product (128 mg) was recrystallized from benzene–hexane to give colorless prisms (114 mg, 85%), mp 131—134 °C. *Anal.* Calcd for $C_{16}H_{16}NOS$: C, 62.83; H, 5.27; N, 4.58. Found: C, 62.92; H, 5.16; N, 4.52. IR ν_{max} cm^{-1}: 1682 (C=O), no NH. ^{1}H-NMR δ: 1.90 (3H, s, SCH_3), 2.03 (3H, br s, $COCH_3$), 3.40, 3.57 (each 1H, d, J=14.0 Hz, $ArC\underline{H}_2S$), 6.98—7.66 (8H, m, arom H).

iii) (a) *N*-Acetyl-3-chloro-*N*-phenylanthranilaldehyde (**26**): A solution of SO_2Cl_2 (1.60 ml) in absolute CH_2Cl_2 (1.60 ml) was added to a solution of 6'-chloro-*N*-phenyl-(α-methylthio)-*o*-acetotoluidide (**25**) (5.436 g) in absolute CH_2Cl_2 (30 ml), and the whole was refluxed for 1 h. The reaction mixture was quenched with H_2O (50 ml), stirred at room temperature for 1 h, and extracted with $CHCl_3$. The organic layer was washed with H_2O, dried over $MgSO_4$, and evaporated to dryness *in vacuo*. The residue (6.265 g) was chromatographed over silica gel using benzene followed by benzene–AcOEt (10 : 1) to give two eluates, I (1.883 g, 30%) and II (3.290 g, 68%), in that order of elution.

Eluate II was recrystallized from benzene–hexane to give *N*-acetyl-3-chloro-*N*-phenylanthranilaldehyde (**26**) as colorless prisms, mp 92—94 °C. *Anal.* Calcd for $C_{15}H_{12}ClNO_2$: C, 65.82; H, 4.42; N, 5.12. Found: C, 65.94; H, 4.35; N, 5.18. IR ν_{max} cm^{-1}: 1670 (C=O). ^{1}H-NMR δ: 2.15 (3H, s, $COCH_3$), 7.07—7.99 (8H, m, arom H), 10.19 (1H, s, CHO). MS *m/z*: 275 ($M^+ + 2$, 41% intensity of M^+), 273 (M^+), 202 (base peak).

(b) 6'-Chloro-bis(α-methylthio)-*N*-phenyl-*o*-acetotoluidide (**27**): Eluate I was recrystallized from benzene–hexane to give colorless prisms, mp 116—118 °C. *Anal.* Calcd for $C_{17}H_{18}ClNOS_2$: C, 58.02; H, 5.16; Cl, 10.10; N, 3.98; S, 18.22. Found: C, 58.13; H, 5.10; Cl, 10.22; N, 4.05; S, 18.12.

IR ν_{max} cm^{-1}: 1685 (C=O). ^{1}H-NMR δ: 1.45 (3H, s, $COCH_3$), 2.10 (3H, s, SCH_3), 2.18 (3H, s, SCH_3), 4.89 (1H, s, CH(S)S), 7.00—7.80 (8H, s, arom H). MS *m/z*: 353 (M^++2, 43% intensity of M^+), 351 (M^+), 214 (base peak).

(c) Conversion of 6'-Chloro-bis(α-methylthio)-*N*-phenyl-*o*-acetotoluidide (**27**) to *N*-Acetyl-3-chloro-*N*-phenylanthranilaldehyde (**26**): The procedure followed that reported.[13] A solution of SO_2Cl_2 (0.04 ml) in CH_2Cl_2 (1 ml) was added dropwise to a mixture of 6'-chloro-bis(α-methylthio)-*N*-phenyl-*o*-acetotoluidide (**27**) (154 mg) and wet silica gel [a mixture of silica gel (0.2 g) and H_2O (0.2 g)] in CH_2Cl_2 (2 ml) under ice-cooling, and the whole was stirred at room temperature for 3 h. Powdered anhydrous K_2CO_3 (0.4 g) was added, and the reaction mixture was stirred for 5 min, then filtered. The filtrate was evaporated to dryness *in vacuo*. The oily residue (139 mg) was chromatographed over silica gel using benzene–AcOEt (10 : 1) to give two eluates.

The first eluate (53 mg, 34%) was found to be the starting thioacetal (**27**). The second eluate (79 mg, 66%) was recrystallized from benzene–hexane to give colorless prisms, mp 90—94 °C, this product was identical with *N*-acetyl-3-chloro-*N*-phenylanthranilaldehyde (**26**).

iv) 2'-Chloro-6'-hydroxy-*N*-phenylacetanilide (**28**): Pertrifluoroacetic acid was prepared by adding trifluoroacetic anhydride (2.3 ml, 16.3 mmol) to a suspension of 30% H_2O_2 (0.28 ml, 2.7 mmol) in CH_2Cl_2 (1 ml) under ice-cooling. This peracid solution was added dropwise to a solution of *N*-acetyl-3-chloro-*N*-phenylanthranilaldehyde (**26**) (500 mg, 1.8 mmol) in CH_2Cl_2 (3 ml) under ice-cooling, and the whole was stirred at room temperature for 2 h. The reaction was quenched with H_2O (1 ml) and Na_2SO_3 (1.1 g), and the reaction mixture was extracted with $CHCl_3$, washed with H_2O, and dried over $MgSO_4$. Removal of the solvent *in vacuo* left an oily residue (519 mg), which was chromatographed over silica gel using benzene–AcOEt (6 : 1) followed by $CHCl_3$–MeOH (10 : 1) to give two eluates.

The first eluate (341 mg, 71%) was recrystallized from MeOH–$CHCl_3$ to give colorless prisms of 2'-chloro-6'-hydroxy-*N*-phenylacetanilide (**28**), mp 185—187 °C. *Anal.* Calcd for $C_{14}H_{12}ClNO_2$: C, 64.25; H, 4.62; N, 5.35. Found: C, 64.24; H, 4.52; N, 5.55. IR ν_{max} cm^{-1}: 3125 (OH), 1645 (C=O). ^{1}H-NMR δ: 1.93 (3H, s, $COCH_3$), 6.60—7.55 (8H, m, arom H), 8.25 (1H, br s, OH). MS *m/z*: 263 (M^++2, 38% intensity of M^+), 261 (M^+), 219 (base peak).

The second eluate (127 mg, 24%) was recrystallized from benzene–MeOH to give colorless prisms, mp 157—160 °C, and this product was found to be *N*-acetyl-3-chloro-*N*-phenylanthranilic acid (**29**), based on the following spectral data. IR ν_{max} cm^{-1}: 1705 (CO_2H), 1630 ($NCOCH_3$). ^{1}H-NMR δ: 2.02, 2.19 (totally 3H, each s, $COCH_3$), 6.95—7.91 (8H, m, arom H), 9.07 (1H, br s, CO_2H). MS *m/z*: 291 (M^++2, 30% intensity of M^+), 289 (M^+), 247 (base peak).

v) 6'-Chloro-*N*-phenyl-*o*-acetanisidide (**30**): Dimethyl sulfate (0.28 ml) was added to suspension of 2'-chloro-6'-hydroxy-*N*-phenylacetanilide (**28**) (0.340 g) and K_2CO_3 (0.285 g) in xylene (7 ml) at 140 °C (bath temperature), and the whole was refluxed for 1 h. Then the reaction mixture was quenched with 5% NaOH (10 ml), stirred at room temperature for 1 h, and extracted with Et_2O. The ethereal layer was washed, dried over anhydrous K_2CO_3, and evaporated to dryness *in vacuo*. A crystalline residue (0.336 g) was recrystallized from benzene–hexane to give colorless prisms (0.312 g, 87%), mp 118—120 °C. *Anal.* Calcd for $C_{15}H_{14}ClNO_2$: C, 65.34; H, 5.12; N, 5.08. Found: C, 65.28; H, 5.12; N, 4.78. IR ν_{max} cm^{-1}: 1680 (C=O). ^{1}H-NMR δ: 1.98 (3H, dif s, $COCH_3$), 3.82 (3H, s, OCH_3), 6.60—7.55 (8H, m, arom H). MS *m/z*: 277 (M^++2, 31% intensity of M^+), 275 (M^+), 233 (base peak).

vi) Authentic 6-Chloro-*N*-phenyl-*o*-anisidine (**10**): A mixture of 6'-chloro-*N*-phenyl-*o*-acetanisidide (**30**) (101 mg) and powdered KOH (251 mg) in ethylene glycol (2 ml) was heated at 140 °C for 1 h under an Ar atmosphere. Then the reaction mixture was poured into H_2O, and extracted with Et_2O. The extract was washed with H_2O, and dried over $MgSO_4$. Removal of the solvent *in vacuo* left an oily residue (84 mg), which was chromatographed over silica gel using benzene–AcOEt (10 : 1) to give a colorless oil (84 mg, 98%), bp 115—120 °C (1 mmHg). *Anal.* Calcd for $C_{13}H_{12}ClNO$: C, 66.81; H, 5.12; N, 5.99. Found: C, 66.76; H, 5.18; N, 5.83. IR $\nu_{max}^{CHCl_3}$ cm^{-1}: 3400 (NH). ^{1}H-NMR δ: 3.77 (3H, s, OCH_3), 4.75 (1H, br s, NH), 6.58—7.41 (8H, m, arom H). MS *m/z*: 235 (M^++2, 34% intensity of M^+), 233 (M^+, base peak).

Preparation of Authentic *N*-Arylindoles by Ullmann–Goldberg Reaction

i) Ethyl 6-Chloro-1-phenylindole-2-carboxylate (**11**): A mixture of ethyl 6-chloroindole-2-carboxylate[3] (**33**) (200 mg), iodobenzene (0.2 ml), anhydrous K_2CO_3 (200 mg), Cu_2Br_2 (20 mg), and pyridine (0.4 ml) in nitrobenzene (2 ml) was refluxed for 9 h under an Ar atmosphere. The reaction mixture was worked up according to the general procedure. The crude product (308 mg) was chromatographed over silicic acid using benzene to give a solid (182 mg). Recrystallization from hexane–benzene gave colorless prisms (160 mg, 62%), mp 55—57.5 °C. *Anal.* Calcd for $C_{17}H_{14}ClNO_2$: C, 68.12; H, 4.71; N, 4.67. Found: C, 68.24; H, 4.64; N, 4.64. IR ν_{max} cm^{-1}: 1710 (C=O). ^{1}H-NMR δ: 1.15 (3H, t, J=7.5 Hz, $CH_2\underline{CH}_3$), 4.16 (2H, q, J=7.5 Hz, $OC\underline{H}_2CH_3$), 7.00—7.68 (9H, m, arom H).

ii) Ethyl 7-Methoxy-1-phenylindole-2-carboxylate (**12**): A mixture of ethyl 7-methoxyindole-2-carboxylate (**34**) (100 mg), bromobenzene (216 mg), anhydrous K_2CO_3 (100 mg), Cu_2Br_2 (10 mg), and pyridine (0.2 ml) in nitrobenzene (1 ml) was refluxed for 10 h under an Ar atmosphere. The reaction mixture was worked up according to the general procedure. The residue (265 mg) was chromatographed over silicic acid using benzene to give a solid (220 mg). Recrystallization from pentane gave colorless columns (130 mg, 49%), mp 58—59.5 °C. *Anal.* Calcd for $C_{18}H_{17}NO_3$: C, 73.20: H, 5.80; N, 4.74. Found: C, 73.34; H, 5.85; N, 4.75. IR ν_{max} cm^{-1}: 1725 (C=O). ^{1}H-NMR δ: 1.16 (3H, t, J=7.5 Hz, $CH_2\underline{CH}_3$), 3.52 (3H, s, OCH_3), 4.16 (2H, q, J=7.5 Hz, $OC\underline{H}_2CH_3$), 6.66 (1H, dd, J=7.5, 1.5 Hz, C_6-H), 7.07 (1H, t, J=7.5 Hz, C_5-H), 7.26—7.60 (7H, m, arom H).

iii) Ethyl 1-(2-Methoxyphenyl)indole-2-carboxylate (**13**): A mixture of ethyl indole-2-carboxylate[14] (**35**) (200 mg), 2-bromoanisole (800 mg), anhydrous K_2CO_3 (200 mg), Cu_2Br_2 (20 mg), and pyridine (0.4 ml) in nitrobenzene (2 ml) was refluxed for 12 h under an Ar atmosphere. The reaction mixture was worked up according to the general procedure. The residue (324 mg) was chromatographed over silicic acid using benzene to give a solid (240 mg). Recrystallization from pentane gave colorless prisms (123 mg, 39%), mp 66—68 °C. *Anal.* Calcd for $C_{18}H_{17}NO_3$: C, 73.20; H, 5.80; N, 4.74. Found; C, 72.99; H, 5.74; N, 4.89. IR ν_{max} cm^{-1}: 1710 (C=O). ^{1}H-NMR δ: 1.16 (3H, t, J=7.5 Hz, $CH_2\underline{CH}_3$), 3.65 (3H, s, OCH_3), 4.18 (2H, q, J=7.5 Hz, $OC\underline{H}_2CH_3$), 6.94—7.55 (8H, m, arom H), 7.69 (1H, dd, J=7.5, 2.0 Hz, C_4-H).

iv) Ethyl 1-Phenylindole-2-carboxylate (**14**): A mixture of ethyl indole-2-carboxylate (**35**) (300 mg), bromobenzene (750 mg), anhydrous K_2CO_3 (300 mg), Cu_2Br_2 (30 mg), and pyridine (0.6 ml) in nitrobenzene (3 ml) was refluxed for 15 h under an Ar atmosphere. The reaction mixture was worked up according to the general procedure. The residue (398 mg) was chromatographed over silicic acid using benzene to give a solid (67 mg). Recrystallization from pentane gave colorless plates (54 mg, 13%), mp 62.5—65.5 °C. *Anal.* Calcd for $C_{17}H_{15}NO_2$: C, 76.96; H, 5.70; N, 5.28. Found: C, 76.86; H, 5.67; N, 5.13. IR ν_{max} cm^{-1}: 1710 (C=O). ^{1}H-NMR δ: 1.16 (3H, t, J=7.5 Hz, $CH_2\underline{CH}_3$), 4.16 (2H, q, J=7.5 Hz, $OC\underline{H}_2CH_3$), 7.00—7.68 (10H, m, arom H).

References and Notes

1) Part XXIII: H. Ishii, T. Sugiura (née Hagiwara), Y. Akiyama, Y. Ichikawa, T. Watanabe, and Y. Murakami, *Chem. Pharm. Bull.*, **38**, 2118 (1990).
2) H. Ishii, Y. Murakami, K. Hosoya, H. Takeda, Y. Suzuki, and N. Ikeda, *Chem. Pharm. Bull.*, **21**, 1481 (1973).
3) In the NH-indole series, the total yield of indoles by Fischer indolization of ethyl pyruvate 2-(2-methoxyphenyl)hydrazone was higher to that in the case of the corresponding 2,6-dimethoxyphenyl hydrazone.[2]
4) Part XXI of this series: H, Ishii, H. Takeda, T. Hagiwara, M. Sakamoto, K. Kogusuri, and Y. Murakami, *J. Chem. Soc., Perkin Trans. 1*, **1989**, 2407.
5) P. Claus, W. Vycudilik, and W. Rieder, *Monatsh. Chem.*, **102**, 1571 (1971).
6) L. F. Fieser and M. Fieser, "Reagents for Organic Synthesis," Vol. I, John Wiley and Sons, Inc., New York, 1967, p. 821.
7) See reference 5 of Part XXIII.[1]
8) H. E. Ungnade, *J. Am. Chem. Soc.*, **76**, 5133 (1954).
9) F. Ullmann, *Justus Liebigs Ann. Chem.*, **355**, 312 (1907).
10) K. Ninomiya, T. Shioiri, and S. Yamada, *Tetrahedron*, **30**, 2151 (1974).
11) F. Herold, *Ber.*, **15**, 1684 (1882).
12) F. Reverdin and F. Eckhard, *Ber.*, **32**, 2622 (1899).
13) M. Hojo and R. Masuda, *Synthesis*, **1976**, 678.
14) W. E. Noland and F. J. Baude, "Organic Syntheses," Coll. Vol. V, ed. by H. E. Baumgarten, John Wiley and Sons, Inc., 1973, p. 567.

A Short and Convergent Synthesis of the Phytoalexins Vignafuran, 6-Demethylvignafuran, and Moracin M *via* Directed Lithiation Reaction

Mitsuaki WATANABE,*[,a] Kenji KAWANISHI,[b] and Sunao FURUKAWA[b]

Center for Instrumental Analysis,[a] Faculty of Pharmaceutical Sciences,[b] Nagasaki University, 1–14 Bunkyo-machi, Nagasaki 852, Japan.
Received July 30, 1990

2-Methyl-5-(*tert*-butyldimethylsilyloxy)phenyl *N,N,N',N'*-tetramethylphosphorodiamidate was lithiated with *sec*-BuLi in the presence of *N,N,N',N'*-tetramethylethylenediamine at −105 °C to generate the corresponding benzylic anion. This benzylic anion was reacted with various methyl benzoates to provide deoxybenzoin derivatives which, without purification, were treated with formic acid to give 2-aryl-6-hydroxybenzo[*b*]furans. The utility of this strategy has been demonstrated by its application to the short synthesis of phytoalexins, such as vignafuran, 6-demethylvignafuran, and moracin M.

Keywords lithiation; bis(dimethylamino)phosphoryl group; 2-arylbenzo[*b*]furan; phytoalexin; vignafuran; 6-demethylvignafuran; moracin M

In our previous papers, we reported a new and general synthetic method of 2-arylbenzo[*b*]furans, including naturally occurring neolignans, *via* regioselective lithiation of *ortho*-cresols using the bis(dimethylamino)phosphoryl group as a directing group.[1)] We report here the application of the above methodology to the total synthesis of several phytoalexins, including vignafuran (**1**), 6-demethylvignafuran (**2**), and moracin M (**3**) (Chart 1).

Recently, much attention has been given to antifungal compounds (phytoalexins) which are produced in plants after exposure to micro-organisms.[2)] These compounds include a series of 2-aryl-6-hydroxy- (or methoxy-)benzo[*b*]furan derivatives. Vignafuran (**1**) was isolated from the leaves of cowpea, *Vigna unguiculata* (L.) WALP., infected with *Colletotrichum lindemuthianum* and was identified as 6-methoxy-2-(2'-methoxy-4'-hydroxyphenyl)benzo[*b*]furan in 1975.[3)] Two total syntheses of **1** have been reported using two types of key reactions: i) the Hoesch reaction of 2-benzyloxy-4-methoxyphenylacetonitrile with 3-methoxyphenol in the presence of $ZnCl_2$ and $AlCl_3$ in low overall yield[3)]; ii) the reaction of copper(I) 4-benzyloxy-2-methoxyphenylacetylide with 2-bromo-5-methoxyphenol in 7.1% overall yield, starting from 4-benzyloxy-2-hydroxyphenyl methyl ketone.[4)] 6-Demethylvignafuran (**2**) was isolated from the leaves of *Tetragonolobus maritimus* (L.) ROTH inoculated with *Helminthosporium carbonum* ULLSTRUP. It was synthesized *via* deoxybenzoin derived from basic hydrolysis of 2'-benzyloxyisoflavone in 2.8% overall yield, the latter compound having been obtained from 4-benzyloxy-2-hydroxyphenyl methyl ketone.[5)] Moracin M (**3**) was isolated from the heartwood of *Morus laevigata* in 1975.[6)] The structure of **3** was elucidated as 2-(3',5'-dihydroxyphenyl)-6-hydroxybenzo[*b*]furan by Rama Rao *et al.* through synthesis starting from 2,4,3',5'-tetraacetoxystilbene, although in very poor overall yield.[6)] Recently, Widdowson *et al.* reported an attractive strategy for the synthesis of **3** which involved the palladium-catalyzed cross-coupling of 6-(*tert*-butyldiphenylsilyloxy)-2-trimethylstannylbenzo[*b*]-furan with 5-iodoresorcinolbis(triisopropylsilyl)ether as the key step, in 55.7% overall yield, starting from 6-methoxybenzo[*b*]furan.[7)] However, these total syntheses suffer from the disadvantages of lengthy synthetic routes and poor overall yields, except for the last one. We report here a new, convergent, and expeditious synthesis of vignafuran (**1**), 6-demethylvignafuran (**2**), moracin M (**3**), and related compounds from a common starting material, 2-methyl-5-(*tert*-butyldimethylsilyloxy)phenyl *N,N,N',N'*-tetramethylphosphorodiamidate (**4**).[1c)]

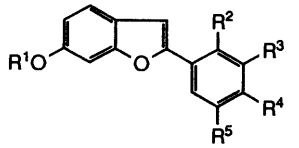

	R1	R2	R3	R4	R5
vignafuran(1):	Me	OMe	H	OH	H
6-demethylvignafuran (2):	H	OMe	H	OH	H
moracin M(3):	H	H	OH	H	OH

Chart 1

The requisite phosphorodiamidate **4** was regioselectively synthesized by the lithiation of 3-(*tert*-butyldimethylsilyloxy)phenyl tetramethyl phosphorodiamidate with *sec*-BuLi followed by reaction with MeI in 65% yield, as has been reported by us.[1c)] Compound **4** was converted to the methyl ether **5** (64% yield) in a one-step procedure according to Borchardt *et al.*[8)] First, we examined the lithiation behavior from the viewpoint of the regioselectivity of aromatic *vs. ortho*-methyl deprotonation in **4** and **5** (Chart 2).[1d)] Lithiation of **5** with 1.2 eq of *sec*-BuLi in tetrahydrofuran (THF) at −105 °C for 1 h followed by addition of MeI gave **6** in 61% yield, resulting from ring deprotonation; no product derived from the tolyl anion was isolated. In contrast, when **4** was lithiated under the same conditions described above and subsequently reacted with MeI, the ethyl compound **7** resulting from the benzylic anion was obtained in 51.8% yield. The significant difference in lithiation behavior between **4** and **5** may be attributed to the dual directing ability of the methoxy and the phosphorodiamidate groups, which direct the lithiation to the position between the two groups (for **5**), and to the steric hindrance of the bulky *tert*-butyldimethylsilyloxy and the phosphorodiamidate groups, which inhibit *ortho*-lithiation and thus generate the benzylic anion (for **4**).[1c,d,8,9)]

On the basis of the above results, lithiated **4** was reacted with methyl benzoates (**8a, b**) as model compounds (Chart 2). Lithiation of **4** with 1.2 eq of *sec*-BuLi in the presence of *N,N,N',N'*-tetramethylethylenediamine (TMEDA) in THF at −105 °C for 1 h resulted in the formation of the

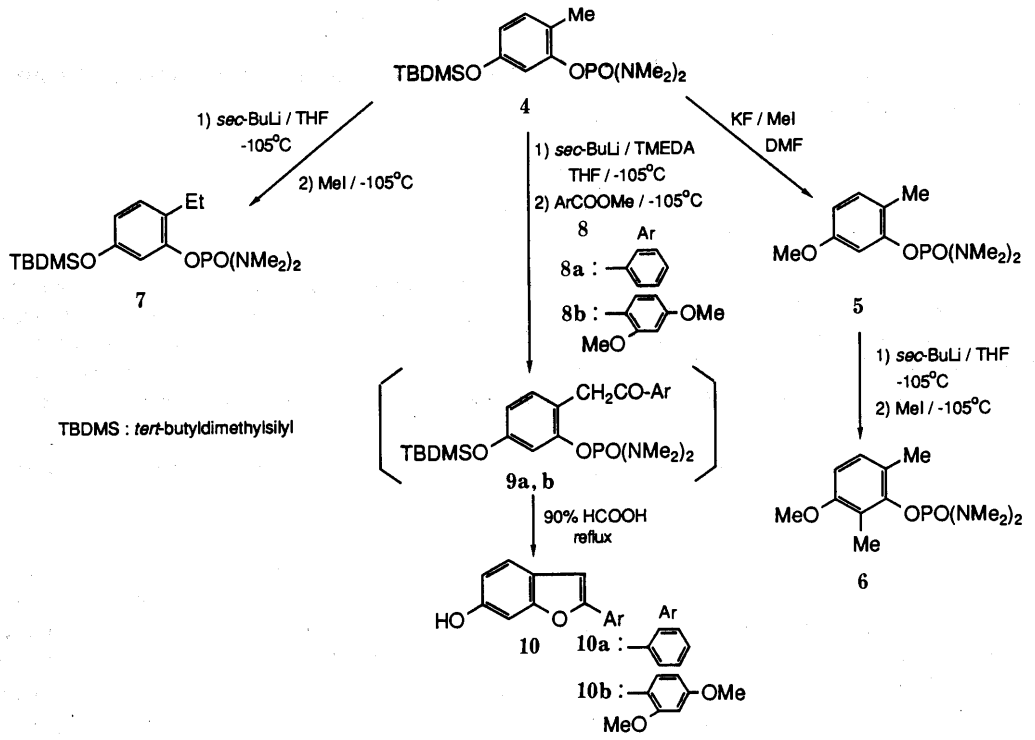

Chart 2

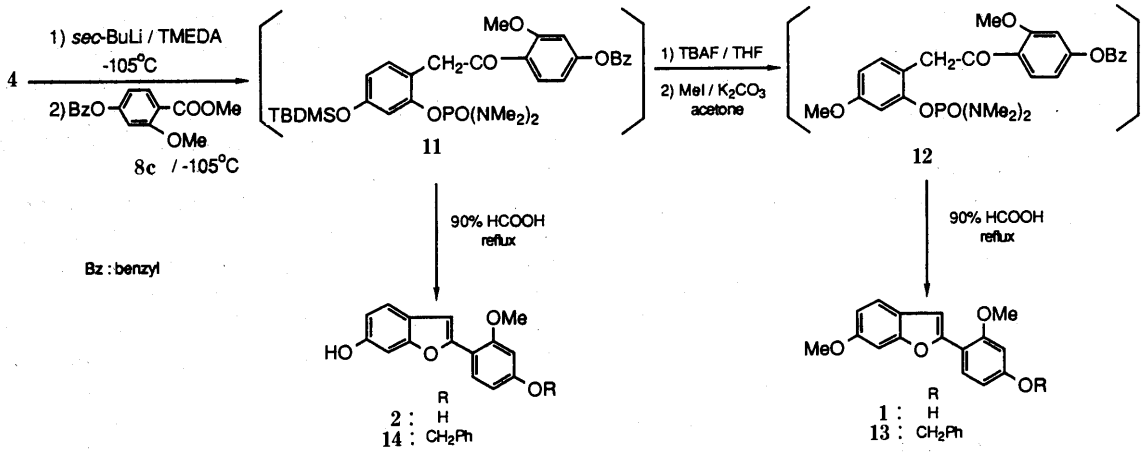

Chart 3

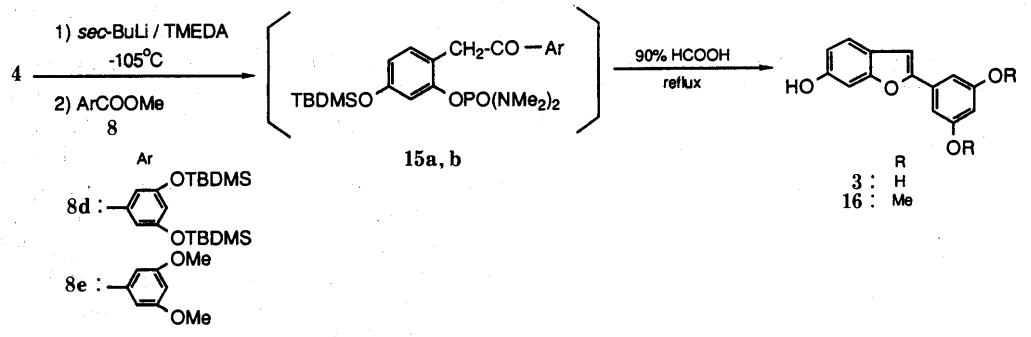

Chart 4

yellow benzylic anion, which, upon treatment with 2.0 eq of methyl benzoate (**8a**) at $-105\,^{\circ}C$ and quenching with saturated NH_4Cl solution at $-80\,^{\circ}C$ gave the deoxybenzoin derivative **9a** as a viscous oil in 63% yield after column chromatography. Although the structure of **9a** was confirmed by its proton nuclear magnetic resonance (^1H-NMR) spectrum, an analytically pure sample could not be obtained due to contamination by the starting material **4**. So, without

further purification, **9a** was treated with refluxing 90% formic acid[1b,d] for 1 h to give 6-hydroxy-2-phenylbenzo[*b*]-furan (**10a**)[2a] in 23.3% overall yield *via* dephosphorylation, desilylation, and subsequent cyclodehydration. Similarly, using methyl 2,4-dimethoxybenzoate (**8b**),[10] the corresponding product 2-(2',4'-dimethoxyphenyl)-6-hydroxybenzo[*b*]-furan (**10b**) was obtained in 59% overall yield. The structures of **10a** and **10b** were established by infrared (IR), ultraviolet (UV), ^{1}H-NMR, mass spectral (MS) data and elemental analyses (see Experimental).

Encouraged by these model studies, we turned our attention to the total synthesis of vignafuran (**1**) and 6-demethylvignafuran (**2**) along the lines shown in Chart 3. Compound **4** was lithiated and the benzylic anion was subsequently reacted with methyl 4-benzyloxy-2-methoxybenzoate (**8c**)[11] to give the deoxybenzoin derivative **11** in 75% yield after column chromatography. Without further purification, **11** was converted into the methoxy compound (**12**) *via* desilylation with tetrabutylammonium fluoride (TBAF) in THF followed by methylation with MeI in the presence of K_2CO_3 in refluxing acetone. Compound **12**, without isolation, was then treated with 90% formic acid at reflux for 4 h to give **1** and 2-(4'-benzyloxy-2'-methoxyphenyl)-6-methoxybenzo[*b*]furan (**13**)[4] in 22.5% and 6.5% overall yields, respectively, after standard work-up and chromatographic purification. Compound **13** had previously been converted into vignafuran (**1**).[4] Synthetic **1** and **13** were shown to be identical with vignafuran and benzylvignafuran on the basis of spectroscopic comparisons with reported data.[3,4] On the other hand, when **11** was refluxed in 90% formic acid for 4 h, compound **2**, which was identical with 6-demethylvignafuran by spectroscopic comparisons,[5] was directly obtained in 6% overall yield. When refluxing was stopped after 1 h, **2** and 2(4'-benzyloxy-2'-methoxyphenyl)-6-hydroxybenzo[*b*]furan (**14**) were obtained in 2% and 8% overall yields, respectively. The protecting benzyl group in **11** was removed during prolonged reaction under the above conditions. Alternatively, acidic treatment of **11** in refluxing 90% acetic acid for 11 h gave **14** in 22% yield (14% overall yield from **4**). For the synthesis of moracin M (**3**), lithiation of **4** followed by reaction with methyl 3,5-bis(*tert*-butyldimethylsilyloxy)benzoate (**8d**) gave the deoxybenzoin derivative **15a** in 57% yield after column chromatography. Without further purification, **15a** was treated with refluxing 90% formic acid for 1 h, affording moracin M (**3**) in 7% overall yield after chromatographic purification (Chart 4). When methyl 3,5-dimethoxybenzoate (**8e**)[12] was employed in the above reaction, similar treatment gave 2-(3',5'-dimethoxyphenyl)-6-hydroxybenzo-[*b*]furan (**16**) *via* **15b**, in 45% overall yield. Demethylation of **16** with an excess of boron tribromide (BBr_3) at room temperature for 20 d gave a mixture of **3** and 6-hydroxy-2-(3'- or 5'-hydroxy-5'-or 3'-methoxyphenyl)benzo[*b*]furan in 18% and 22% yields, respectively, after chromatographic purification. Complete demethylation was difficult to achieve under these conditions. The structure of **3** was established by the comparison of its spectral data with those of moracin M[6] and through conversion to moracin M trimethyl ether.[6]

In conclusion, the phytoalexins vignafuran (**1**), 6-demethylvignafuran (**2**), moracin M (**3**) and related compounds (**10a, b, 13, 14, 16**) were synthesized through lithiation of 2-methyl-5-(*tert*-butyldimethylsilyloxy)phenyl *N,N,N',N'*-tetramethylphosphorodiamidate (**4**) as a common starting compound followed by reaction with benzoates and subsequent acidic treatment. Although some of the steps are low-yielding, the poor yield may be compensated for by the easy accessibility of the starting material, the small number of steps, and the high degree of convergence.

Experimental

All melting points are uncorrected. The IR spectra were measured directly on an NaCl plate or in a KBr disk with a JASCO 810 spectrophotometer. The UV spectra were recorded in 95% ethanol on a Hitachi 323 spectrophotometer. The ^{1}H-NMR spectra were obtained with Hitachi R 600 (60 MHz) and JEOL JNM GX-400 (400 MHz) spectrometers using $CDCl_3$ or $(CD_3)_2CO$ as a solvent and tetramethylsilane as an internal reference. The MS and high-resolution MS (HRMS) were determined on a JEOL-DX 303 mass spectrometer. Elemental analyses were performed at the Microanalytical Laboratory of the Center for Instrumental Analysis in Nagasaki University. All solvents used for lithiation reaction were freshly distilled from sodium benzophenone ketyl before use. Flash chromatography was carried out on a column of Kieselgel 60 (230—400 mesh).

5-Methoxy-2-methylphenyl *N,N,N',N'*-Tetramethylphosphorodiamidate (5) This was prepared in 64% yield according to a literature procedure.[8] A colorless oil, bp 130 °C (0.5 mmHg). MS *m/z*: 272 (M^+). IR (neat): 2925, 1620, 1595, 1510, 1460, 1310, 1225, 1155, 1120, 1040, 990 cm^{-1}. UV nm (log ε): 221 (3.92), 279 (3.41), 284 (s) (3.35). ^{1}H-NMR δ: 2.22 (3H, s), 2.74 (12H, d, *J* = 10.3 Hz), 3.77 (3H, s), 6.57 (1H, dd, *J* = 8.2, 2.4 Hz), 6.88 (1H, br s), 7.05 (1H, d, *J* = 8.2 Hz). *Anal.* Calcd for $C_{12}H_{21}N_2O_3P$: C, 52.93; H, 7.77; N, 10.28. Found: C, 52.53; H, 7.71; N, 10.22.

2,6-Dimethyl-5-methoxyphenyl *N,N,N',N'*-Tetramethylphosphorodiamidate (6) A solution of *sec*-BuLi (0.95 M in cyclohexane, 2.5 ml, 2.4 mmol) was injected into a stirred solution of **5** (0.52 g, 1.9 mmol) in THF (50 ml) at −105 °C (liquid nitrogen–ethanol bath) under a nitrogen atmosphere. After stirring at −105 °C for 30 min, a solution of MeI (0.58 g, 2.4 mmol) in THF (10 ml) was injected to the yellow lithiated solution at −105 °C. Stirring was continued for an additional 1 h at −105 °C. The reaction mixture was quenched with saturated NH_4Cl solution at −90 °C and the solution was allowed to warm to room temperature. THF was removed under reduced pressure. The residue was extracted with CH_2Cl_2 and the organic layer was washed with 5% $Na_2S_2O_3$ solution, dried over Na_2SO_4, and then evaporated to give an oil, which was distilled to give **6** (0.33 g, 61%) as an oil, bp 125 °C (0.5 mmHg). MS *m/z*: 286 (M^+). IR (neat): 3450, 2925, 1615, 1590, 1490, 1460, 1305, 1260, 1225, 1160, 1110, 1100, 1000, 920 cm^{-1}. UV nm (log ε): 219 (4.00), 278 (3.36), 282 (s) (3.32). ^{1}H-NMR δ: 2.20 (3H, s), 2.30 (3H, s), 2.73 (12H, d, *J* = 9.6 Hz), 3.76 (3H, s), 6.55 (1H, d, *J* = 8.1 Hz), 6.94 (1H, d, *J* = 8.1 Hz). *Anal.* Calcd for $C_{13}H_{23}N_2O_3P \cdot 2/3H_2O$: C, 52.34; H, 8.22; N, 9.38. Found: C, 52.27; H, 7.90; N, 9.23.

2-Ethyl-5-(*tert*-butyldimethylsilyloxy)phenyl *N,N,N',N'*-Tetramethylphosphorodiamidate (7) This was prepared in 51.8% (0.26 g) yield by the lithiation of **4** (0.48 g, 1.3 mmol) with *sec*-BuLi (0.95 M in cyclohexane, 1.8 ml, 1.7 mmol) at −105 °C, followed by treatment with MeI (0.37 g, 2.6 mmol) according to a literature procedure.[1d] A colorless oil, bp 150 °C (0.6 mmHg). MS *m/z*: 386 (M^+). IR (neat): 3440, 2925, 2850, 1610, 1580, 1500, 1460, 1290, 1235, 1155, 1115, 990, 910 cm^{-1}. UV nm (log ε): 218 (3.97), 274.5 (s) (3.32), 279 (s) (3.28). ^{1}H-NMR δ: 0.20 (6H, s), 0.98 (9H, s), 1.19 (3H, t, *J* = 7.5 Hz), 2.22—2.57 (2H, m), 2.73 (12H, d, *J* = 9.6 Hz), 6.54 (1H, dd, *J* = 8.2, 2.1 Hz), 6.87—7.10 (2H, m). *Anal.* Calcd for $C_{18}H_{35}N_2O_3PSi \cdot 1/3H_2O$: C, 55.07; H, 9.15; N, 7.13. Found: C, 55.19; H, 9.12; N, 7.26.

General Procedure for the Synthesis of 2-Aryl-6-hydroxy-(or 6-methoxy)-benzo[*b*]furan Derivatives (10a, b, 1, 13, 2, 14, and 16) The following procedure for the synthesis of 6-hydroxy-2-phenylbenzo[*b*]furan (**10a**) is representative; the other arylbenzo[*b*]furans (**10b, 1, 13, 2, 14, 3,** and **16**) were obtained similarly.

1) 6-Hydroxy-2-phenylbenzo[*b*]furan (10a) A solution of *sec*-BuLi (0.95 M in cyclohexane, 3.8 ml, 3.6 mmol) was injected into a stirred solution of **4** (1.1 g, 3.0 mmol) and TMEDA (0.54 ml, 3.6 mmol) in THF (50 ml) at −105 °C under a nitrogen atmosphere. Stirring was continued at −105 °C for 20 min, then a solution of **8a** (0.82 g, 6.0 mmol) in THF (10 ml) was injected into the lithiated solution at −105 °C. The stirring was continued for an additional 1 h at −105 °C. The reaction mixture was quenched with

saturated NH_4Cl solution at −80 °C and the whole was allowed to warm to room temperature. Usual work-up and chromatographic purification using CH_2Cl_2–acetone (9 : 1) as an eluent gave crude 2-phenacyl-5-(*tert*-butyldimethylsilyloxy)phenyl *N,N,N',N'*-tetramethylphosphorodiamidate (**9a**, 0.9 g, 63%). ^{1}H-NMR: δ 0.21 (6H, s), 0.98 (9H, s), 2.62 (12H, d, J=10.2 Hz), 4.27 (2H, s), 6.47—6.67 (1H, m), 6.83—6.97 (2H, m), 7.27—7.50 (3H, m), 7.90—8.10 (2H, m). An analytically pure sample was not obtained owing to difficulty of separation of the product from the starting material **4**. Without further purification, the above crude material was used in the next step. A solution of this crude **9a** (0.68 g, 1.43 mmol) in 90% HCOOH (15 ml) was refluxed for 1 h. After removal of HCOOH under reduced pressure, the residue was washed with 5% $NaHCO_3$ solution and extracted with CH_2Cl_2. The organic layer was dried over Na_2SO_4 and evaporated to give the residue, which was chromatographed using benzene as an eluent and purified by recrystallization from ether–pentane to give **10a** as colorless crystals, mp 177—179 °C, 0.11 g, 37% yield, 23.3% overall yield from **4** (lit.[2a] mp 170—173 °C). MS *m/z*: 210 (M^+). IR (KBr): 3480, 3420, 1620, 1490, 1450, 1435, 1360, 1295, 1190, 1150, 1115, 1020, 915 cm^{-1}. UV nm (log ε): 222 (s) (4.11). 236 (s) (4.06), 287 (s) (4.06), 318 (4.48), 328 (4.42). ^{1}H-NMR ($(CD_3)_2CO$) δ: 6.89 (1H, d, J=9.0 Hz), 7.11 (2H, br s), 7.33—7.50 (4H, m), 7.75—7.88 (2H, m), 8.63 (1H, br s). *Anal.* Calcd for $C_{14}H_{10}O_2$: C, 79.98; H, 4.79. Found: C, 79.72; H, 4.98.

2) 2-(2',4'-Dimethoxyphenyl)-6-hydroxybenzo[*b*]furan (10b) The reaction of **4** (1.5 g, 4.0 mmol) with **8b** (1.6 g, 8.0 mmol) under the conditions described above gave crude **9b** (1.54 g, 72%). ^{1}H-NMR δ: 0.20 (6H, s), 0.96 (9H, s), 2.63 (12H, d, J=10.2 Hz), 3.81 (3H, s), 3.85 (3H, s), 4.24 (2H, s), 6.44—6.57 (3H, m), 6.90—7.06 (2H, m), 7.73—7.88 (1H, m). A solution of this crude **9b** (1.54 g, 2.87 mmol) in 90% HCOOH (20 ml) was refluxed for 1 h. Standard work-up and purification by chromatography using CH_2Cl_2–acetone (9 : 1) as an eluent gave **10b** as colorless crystals (ether), mp 113—116 °C (0.64 g, 82% yield, 59% overall yield from **4**). MS *m/z*: 270 (M^+). IR (KBr): 3290, 1620, 1585, 1500, 1480, 1285, 1210, 1155, 1140, 1105, 1045 cm^{-1}. UV nm (log ε): 225 (s) (4.14), 240 (s) (4.01), 249 (s) (3.91), 284 (4.13), 311 (s) (4.37), 322.5 (4.59), 337.5 (4.57). ^{1}H-NMR ($(CD_3)_2CO$) δ: 3.75 (3H, s), 3.89 (3H, s), 6.49—6.64 (2H, m), 6.91 (1H, dd, J=8.4, 2.4 Hz), 7.16—7.19 (2H, m), 7.47 (1H, d, J=9.0 Hz), 7.91 (1H, d, J=9.0 Hz), 8.49 (1H, br s). *Anal.* Calcd for $C_{16}H_{14}O_4$: C, 71.10; H, 5.22. Found: C, 70.96; H, 5.30.

3) 2-(4'-Hydroxy-2'-methoxyphenyl)-6-methoxybenzo[*b*]furan; Vignafuran (1) and 2-(4'-Benzyloxy-2'-methoxyphenyl)-6-methoxybenzo[*b*]furan (13) The reaction of **4** (1.12 g, 3.0 mmol) with **8c**[11] (1.36 g, 5.0 mmol) under the conditions described above gave the crude deoxybenzoin derivative **11** (1.38 g, 75%). ^{1}H-NMR δ: 0.20 (6H, s), 0.98 (9H, s), 2.63 (12H, d, J=9.6 Hz), 3.85 (3H, s), 4.25 (2H, s), 5.10 (2H, s), 6.52—6.66 (3H, m), 6.93—7.06 (2H, m), 7.39 (5H, s), 7.80 (1H, d, J=8.4 Hz). This crude **11** was used, without further purification, in the next step. A solution of TBAF (1.0 M in THF, 2.3 ml, 2.3 mmol) was added to a stirred solution of crude **11** (1.38 g, 2.25 mmol) in THF (20 ml) at room temperature. Stirring was continued for 10 min, then the THF was removed under reduced pressure to give a residue. A mixture of the residue, K_2CO_3 (0.69 g, 5.0 mmol), and MeI (0.71 g, 5.0 mmol) in acetone (100 ml) was refluxed for 4 h. After cooling to room temperature, the precipitated solid was filtered off. The filtrate was concentrated and usual work-up and chromatographic purification using CH_2Cl_2–acetone (9 : 1) as an eluent gave the crude deoxybenzoin derivative **12** (1.32 g). ^{1}H-NMR δ: 2.63 (12H, d, J=9.6 Hz), 3.77 (3H, s), 3.86 (3H, s), 4.25 (2H, s), 5.10 (2H, s), 6.52—6.64 (3H, m), 6.97—7.13 (2H, m), 7.39 (5H, s), 7.80 (1H, d, J=8.4 Hz). A solution of crude **12** (0.8 g, 1.6 mmol) in 90% HCOOH (10 ml) was refluxed for 4 h. Standard work-up gave a mixture of **1** and **13** which was chromatographed on silica gel. 2-(4'-Benzyloxy-2'-methoxyphenyl)-6-methoxybenzo[*b*]furan (**13**) was eluted faster than vignafuran (**1**) with CH_2Cl_2 as an eluent. 2-(4'-Benzyloxy-2'-methoxyphenyl)-6-methoxybenzo-[*b*]furan (**13**; 0.05 g, 8.7% yield, 6.5% overall yield from **4**). A colorless oil (lit.[4] mp 111—116 °C). IR (neat): 2940, 2840, 1620, 1585, 1500, 1450, 1290, 1260, 1200, 1155, 1030, 1010 cm^{-1}. UV nm (log ε): 228 (s) (4.21), 248 (s) (3.91), 284 (4.15), 310 (s) (4.37), 322 (4.59), 337.5 (4.56). ^{1}H-NMR δ: 3.81 (3H, s), 3.89 (3H, s), 5.05 (2H, s), 6.61—7.22 (6H, m), 7.39 (5H, s), 7.92 (1H, d, J=9.6 Hz). Vignafuran (**1**; 0.13 g, 30% yield, 22.5% overall yields from **4**). Oil (lit.[3,4] oil). MS *m/z*: 270 (M^+). IR ($CHCl_3$): 3600, 3320, 3020, 1620, 1595, 1510, 1495, 1470, 1310, 1155, 1110, 1035 cm^{-1}. UV nm (log ε): 224 (s) (4.17), 247 (s), (3.70), 283 (3.91), 309 (s) (3.99), 321 (4.17), 336.5 (4.11). ^{1}H-NMR (400 MHz) δ: 3.86 (3H, s), 3.91 (3H, s), 6.50 (2H, m), 6.84 (1H, dd, J=8.4, 2.2 Hz), 7.03 (2H, m), 7.41 (1H, d, J=8.4 Hz), 7.84 (1H, d, J=9.2 Hz).

4) 6-Hydroxy-2-(4'-hydroxy-2'-methoxyphenyl)benzo[*b*]furan; 6-Demethylvignafuran (2) and 2-(4'-Benzyloxy-2'-methoxyphenyl)-6-hydroxybenzo[*b*]furan (14) A solution of crude **11** (1.53 g, 2.5 mmol) obtained above was refluxed for 1 h in 90% HCOOH (20 ml). Standard work-up and chromatographic purification gave **14** (CH_2Cl_2 as an eluent) and **2** (CH_2Cl_2–acetone = 9 : 1 as an eluent). 2-(4'-Benzyloxy-2'-methoxyphenyl)-6-hydroxybenzo[*b*]furan (**14**; 0.09 g, 10.6% yield, 8.0% overall yield from **4**) was obtained as colorless crystals (from CH_2Cl_2/pentane), mp 107—110 °C. MS *m/z*: 346 (M^+). IR (KBr): 3250, 1610, 1580, 1495, 1420, 1285, 1195, 1150, 1110, 1025, 950 cm^{-1}. UV nm (log ε): 241.5 (s) (3.97), 249 (s) (3.88), 285 (4.10), 312 (s) (4.38), 323 (4.61), 338.5 (4.59). ^{1}H-NMR δ: 3.89 (3H, s), 5.09 (2H, s), 6.62—6.81 (3H, m), 6.98—7.03 (4H, m), 7.41 (5H, s), 7.91 (1H, d, J=9.6 Hz). HRMS *m/z* M^+ Calcd for $C_{22}H_{18}O_4$: 346.1205. Found: 346.1203. 6-Demethylvignafuran (**2**; 0.017 g, 2.7% yield, 2.0% overall yield from **4**). An oil (lit.[5] oil). MS *m/z*: 256 (M^+). IR ($CHCl_3$): 3600, 3300, 1620, 1595, 1505, 1450, 1475, 1445, 1305, 1255, 1150, 1115, 1060 cm^{-1}. UV nm (log ε): 225 (s) (4.07), 248.5 (s) (3.78), 284 (3.94), 309.5 (s) (4.14), 321.5 (4.34), 337 (4.29). ^{1}H-NMR δ: 3.93 (3H, s), 6.48—6.87 (2H, m), 7.01—7.43 (4H, m), 7.59 (1H, br s), 7.83 (1H, d, J=9.0 Hz), 7.86 (1H, br s). When a solution of crude **11** (0.38 g, 0.62 mmol) in 90% CH_3COOH (20 ml) was refluxed for 11 h, compound **14** (0.047 g, 22%) was obtained (14% overall yield from **4**). When a solution of crude **11** (1.08 g, 1.7 mmol) in 90% HCOOH (20 ml) was refluxed for 4 h, compound **2** (0.035 g, 8.0%) was obtained (6.0% overall yield from **4**).

5) Methyl 3,5-Bis(*tert*-butyldimethylsilyloxy)benzoate (8d) *tert*-Butyldimethylsilyl chloride (8.25 g, 55 mmol) was added to a stirred solution of imidazole (3.7 g, 55 mmol) and methyl 3,5-dihydroxybenzoate (4.2 g, 25 mmol) in *N,N*-dimethylformamide (20 ml) at room temperature. The reaction mixture was stirred at room temperature for 24 h. Water and *n*-hexane were added to the reaction mixture. The organic layer was separated, washed with 5% $NaHCO_3$ solution, and dried over Na_2SO_4. The solvent was removed to give a residue, which was distilled to give **8d** (8.09 g, 82%) as an oil, bp 160 °C (1.5 mmHg). IR (neat): 2955, 2940, 2860, 1730, 1590, 1450, 1340, 1255, 1170, 1030, 1015, 730, 835 cm^{-1}. UV nm (log ε): 247 (3.81), 303 (3.42). ^{1}H-NMR δ: 0.26 (12H, s), 1.04 (18H, s), 3.93 (3H, s), 6.55—6.63 (1H, m), 7.18—7.21 (2H, m). HRMS *m/z* M^+ Calcd for $C_{20}H_{36}O_4Si_2$: 396.2152. Found: 396.2152.

6) 2-(3',5'-Dihydroxyphenyl)-6-hydroxybenzo[*b*]furan; Moracin M (3) The reaction of **4** (1.1 g, 3.0 mmol) with **8d** (1.8 g, 4.5 mmol) under the conditions described above gave the crude deoxybenzoin **15a** (1.25 g, 57%). ^{1}H-NMR δ: 0.20 (18H, s), 0.98 (27H, s), 2.64 (12H, d, J=9.6 Hz), 4.21 (2H, s), 6.52—6.66 (2H, m), 6.95—7.13 (4H, m). A solution of this crude **15a** (1.25 g, 1.7 mmol) in 90% HCOOH (20 ml) was refluxed for 1 h. Standard work-up and purification by chromatography using CH_2Cl_2–acetone (4 : 1) as an eluent gave moracin M (**3**; 0.05 g, 12.3%, 7.0% overall yield from **4**) as crystals, mp 263—270 °C (acetone/ether) (lit.[6] mp 259—262 °C; lit.[7] mp 260—262 °C). MS *m/z*: 242 (M^+). IR (KBr): 3520, 3275, 1610, 1580, 1435, 1295, 1140, 1120, 1000, 965 cm^{-1}. UV nm (log ε): 218 (4.43), 251.5 (s) (3.74), 286 (s) (4.05), 296 (s) (4.13), 317.5 (4.46), 331 (4.39). ^{1}H-NMR ($(CD_3)_2CO$) δ: 6.38 (1H, t, J=3.0), 6.73—6.76 (1H, m), 6.89 (2H, d, J=1.8 Hz), 7.03 (2H, br s), 7.41 (1H, d, J=7.8 Hz), 8.41 (2H, br s). Moracin M trimethyl ether was obtained in 78% yield by the reaction of **3** with MeI in the presence of K_2CO_3 in refluxing acetone.

Moracin M Trimethyl Ether: Crystals, mp 70—72 °C (lit.[6] mp 80 °C). MS *m/z*: 284 (M^+). IR (KBr): 2960, 2940, 2835, 1600, 1570, 1490, 1450, 1415, 1360, 1275, 1205, 1150, 1110, 1065, 1025, 820 cm^{-1}. UV nm (log ε): 218 (4.47), 295 (s) (4.17), 317 (4.49), 330 (4.41), ^{1}H-NMR δ: 3.78 (6H, s), 3.86 (3H, s), 6.44 (1H, t, J=2.1 Hz), 6.85—7.04 (5H, m), 7.43 (1H, d, J=8.4 Hz).

7) 2-(3',5'-Dimethoxyphenyl)-6-hydroxybenzo[*b*]furan (16) The reaction of **4** (1.49 g, 4.0 mmol) with **8e** (1.57 g, 8.0 mmol) under the conditions described above gave the crude deoxybenzoin derivative **15b** (1.87 g, 87%). ^{1}H-NMR δ: 0.23 (6H, s), 0.90 (9H, s), 2.62 (12H, d, J=10.2 Hz), 3.70 (3H, s), 3.77 (3H, s), 4.23 (2H, s), 6.33—6.68 (4H, m), 6.93—7.20 (2H, m). A solution of this crude **15b** (1.87 g, 3.5 mmol) in 90% HCOOH (20 ml) was refluxed for 1 h. Standard work-up and purification by chromatography using CH_2Cl_2–acetone (9 : 1) as an eluent gave 2-(3',5'-dimethoxyphenyl)-6-hydroxybenzo[*b*]furan (**16**: 0.49 g, 52%, 45% overall yield from **4**) as colorless crystals (ether/pentane), mp 112—115 °C. MS *m/z*: 270 (M^+). IR (KBr): 3425, 1620, 1605, 1570, 1460, 1450, 1425, 1360, 1310, 1210, 1155, 1115, 1065, 1035, 960, 920 cm^{-1}. UV nm (log ε): 218 (4.49), 319 (4.53), 329 (s) (4.47). ^{1}H-NMR δ: 3.78 (6H, s), 6.40—6.48 (1H, m), 6.87—7.08 (5H, m), 7.36 (1H, d, J=8.4 Hz). *Anal.* Calcd for $C_{16}H_{14}O_4$: C, 71.10; H, 5.22. Found: C, 70.94; H, 5.38.

Demethylation of 16 Using BBr_3 A solution of BBr_3 (1 ml, 10.6 mmol)

in CH_2Cl_2 (5 ml) was injected into a solution of **16** (0.22 g, 0.81 mmol) in dry CH_2Cl_2 (50 ml) at −78 °C under a nitrogen atmosphere. The reaction mixture was allowed to warm to room temperature, stirred for 20 d, and then treated with 5% $NaHCO_3$ solution. The organic layer was separated, dried over Na_2SO_4 and evaporated to dryness. The residue was purified by chromatography to afford 6-hydroxy-2-(3′- or 5′-hydroxy-5′- or 3′-methoxyphenyl)benzo[*b*]furan (0.046 g, 22%) and moracin M (**3**; 0.035 g, 18%) using benzene–acetone (9 : 1) as an eluent.

6-Hydroxy-2-(3′- or 5′-hydroxy-5′- or 3′-methoxyphenyl)benzo[*b*]furan: Colorless crystals, mp 130—139 °C (acetone–ether). IR (KBr): 3290, 1620, 1580, 1440, 1425, 1380, 1320, 1295, 1190, 1155, 1140, 1120, 1050, 960 cm^{-1}. UV nm (log ε): 217.5 (4.43), 251 (s) (3.79), 286 (s) (4.05), 295 (s) (4.14), 317.5 (4.47), 330 (4.40). ^{1}H-NMR δ: 3.76 (3H, s), 6.41 (1H, t, J=4.2 Hz), 6.98—7.10 (4H, m), 7.34—7.50 (3H, m). HRMS m/z M^+ Calcd for $C_{15}H_{12}O_4$: 256.0736. Found: 256.0736.

Acknowledgement We are indebted to the staff of the Center for Instrumental Analysis in Nagasaki University for IR, UV, MS, HRMS, and NMR measurements and elemental analysis.

References and Notes

1) *a*) M. Watanabe, M. Date, K. Kawanishi, M. Tsukazaki, and S. Furukawa, *Chem. Pharm. Bull.*, **37**, 2564 (1989); *b*) M. Date, K. Kawanishi, T. Hori, M. Watanabe, and S. Furukawa, *ibid.*, **37**, 2884 (1989); *c*) M. Watanabe, M. Date, K. Kawanishi, T. Hori, and S. Furukawa, *ibid.*, **38**, 2637 (1990); *d*) *Idem*, *ibid.*, **39**, 41 (1991).
2) *a*) G. A. Carter, K. Chamberlain, and R. L. Wain, *Ann. Appl. Biol.*, **88**, 57 (1978); *b*) T. Masamune, M. Takasugi and A. Murai, *Yuki Gosei Kagaku Kyokai Shi*, **43**, 217 (1985).
3) N. W. Preston, K. Chamberlain, and R. A. Skipp, *Phytochemistry*, **14**, 1843 (1975).
4) R. P. Duffley and R. Stevenson, *J. Chem. Soc., Perkin Trans., 1*, **1977**, 802.
5) J. L. Ingham and P. M. Dewick, *Phytochemistry*, **17**, 535 (1978).
6) V. H. Deshpande, R. Spinivasan, and A. V. Rama Rao, *Indian J. Chem.*, **13**, 453 (1975).
7) J. M. Clough, I. S. Mann, and D. A. Widdowson, *Tetrahedron Lett.*, **28**, 2645 (1987).
8) A. K. Sinhababu, M. Kawase, and R. T. Borchardt, *Tetrahedron Lett.*, **28**, 4139 (1987).
9) *a*) B. M. Trost and M. G. Saulnier, *Tetrahedron Lett.*, **26**, 123 (1985); *b*) K. L. Kirk, O. Olubajo, K. Buchhold, G. A. Lewandowski, F. Gusovsky, D. McCulloh, J. W. Daly, and C. R. Creveling, *J. Med. Chem.*, **29**, 1982 (1986); *c*) D. C. Furlano, S. N. Calderon, G. Chen, and K. L. Kirk, *J. Org. Chem.*, **53**, 3145 (1988); *d*) M. Iwao, *ibid.*, **55**, 3622 (1990).
10) A. A. Shamshurin, *J. Gen. Chem. USSR.*, **19**, 1964 (1949).
11) D. W. Robertson, E. E. Beedle, J. H. Krushinski, G. D. Pollock, H. Wilson, V. L. Wyss, and J. S. Hayes, *J. Med. Chem.*, **28**, 717 (1985).
12) N. A. Valyashlso and A. E. Lutskii, *J. Gen. Chem. USSR*, **21**, 1069 (1951). Commercially available from Aldrich Chemical Company.

Amino Acids and Peptides. XIII.[1] Synthetic Studies on N-Terminal Tripeptide Amide Analogs of Fibrin α-Chain

Koichi KAWASAKI,*[,a] Toshiki TSUJI,[a] Katsuhiko HIRASE,[a] Masanori MIYANO,[a] Yoshinori IMOTO[a] and Masahiro IWAMOTO[b]

Faculty of Pharmaceutical Sciences, Kobe-Gakuin University,[a] Ikawadani-cho, Nishi-ku, Kobe 673, Japan and Research Institute, Daiichi Seiyaku Co., Ltd.,[b] 1-chome, Kitakasai, Edogawa-ku, Tokyo 134, Japan. *Received August, 8, 1990*

N-Terminal tripeptide analogs of fibrin α-chain were synthesized and their inhibitory effect on fibrinogen/thrombin clotting was examined. A new water-soluble active ester, 3-pyridinium ester, was used for the synthesis. Among the synthetic peptides, H-Gly-Pro-Arg-hexamethyleneimine exhibited the highest inhibitory effect on fibrinogen-thrombin clotting.

Keywords clotting; water-soluble active ester; peptide synthesis; fibrinogen–thrombin clotting; anticoagulant

The N-terminal tripeptide of fibrin α-chain (H–Gly–Pro–Arg–OH) and its analogs (H–Gly–Pro–Arg–Pro–OH and H–Gly–Pro–Arg–Sar–OH) were reported to be potent inhibitors of fibrin polymerization by Laudano and Doolittle[2]; the inhibitory effect of the latter two analogs was more potent than that of the former. The inhibitory effect was due to the binding of the peptides to fibrinogen, not to thrombin. Based on the mechanism of the inhibition, the development of a new type of anticoagulants should be possible. In the present study, various tripeptide analogs of the *N*-terminal portion of fibrin α-chain were synthesized to examine their inhibitory effect on fibrinogen–thrombin clotting (FTC). A new water-soluble active ester, methyl-pyridinium iodide ester was developed and used for synthesis of the peptides. Benzyloxycarbonyl (Z)[3] and *tert*-butoxycarbonyl (Boc)[4] groups were used as α-amino protecting groups and mesitylenesulfonyl (Mts)[5] and nitro groups[6] were used as guanidino protecting groups.

Since the fourth amino acids of the above inhibitors (H–Gly–Pro–Arg–Pro–OH and H–Gly–Pro–Arg–Sar–OH) have a secondary amine, various Gly–Pro–Arg amide analogs with such an amide were prepared. As the standard sample for comparison of the inhibitory effects of synthetic peptides on FTC, H–Gly–Pro–Arg–Pro–OH, the preparation of which by the solid-phase method was reported by Laudano and Doolittle,[2] was synthesized as shown in Fig. 1. The peptide was prepared by stepwise elongation from C-terminal H–Pro–OBzl.[7] The coupling reactions were done by the mixed anhydride method[8] and removals of Boc groups were done with trifluoroacetic acid (TFA). The final deblocking of the protected tetrapeptide was done by hydrogenation.

Tripeptide amide derivatives were prepared from Z–Gly–Pro–OH[9] and Arg amide derivatives by the mixed anhydride method followed by hydrogenation or trifluoromethanesulfonic acid (TFMSA)[10] treatment. For preparation of Z–Gly–Pro–OH, a new water-soluble active ester, pyridinium ester, was used as shown in Fig. 2. For preparation of pyridinium ester, 2-hydroxypyridine, 3-hydroxypyridine and 4-hydroxypyridine were treated with methyl iodide in methanol. Among them, 3-hydroxypyridine was converted to the corresponding pyridinium salt quantitatively, while 2- and 4-hydroxypyridines were not converted quantitatively even when a large excess of methyl

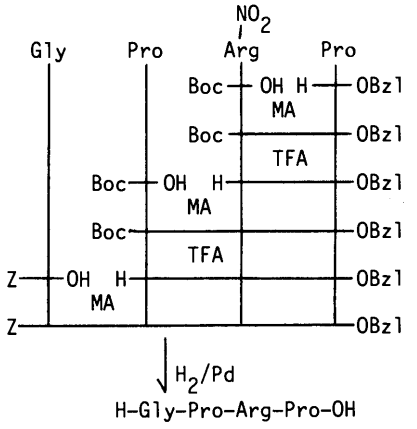

Fig. 1. Synthetic Scheme for the Tetrapeptide
MA: mixed anhydride method.

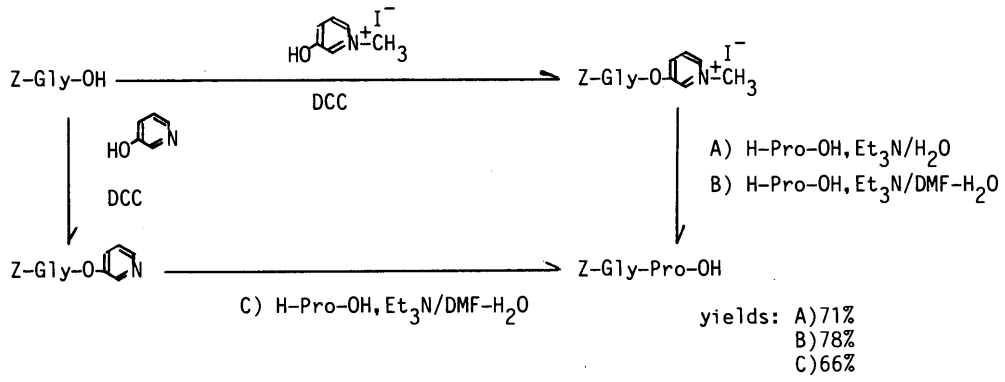

Fig. 2. Synthetic Scheme for Z–Gly–Pro–OH

iodide was used. 3-Hydroxypyridinium salt was thus used for preparation of a pyridinium ester. Z–Gly–OH was converted to the pyridinium ester by the dicyclohexylcarbodiimide (DCC) method[11] and the ester was reacted with H–Pro–OH in a mixture of DMF and water to give Z–Gly–Pro–OH in 78% yield. The same reaction proceeded even in water and the yield was 71%. The results suggested that the pyridinium ester method might be useful not only for peptide synthesis but also for acylation of compounds (such as proteins or sugars) in aqueous media. The 3-pyridine ester of Z–Gly–OH was also prepared by the DCC method to compare with the pyridinium ester. The pyridyl ester was reacted with H–Pro–OH to give Z–Gly–Pro–OH in 66% yield. The pyridinium ester was soluble in water and insoluble in organic solvents such as ethyl acetate and ether, but the pyridyl ester was soluble in the organic solvents and hardly soluble in water. Purification of the product (Z–Gly–Pro–OH) by the pyridinium ester method was achieved by washing the ethyl acetate extract with water. The occurrence of racemization during the coupling reaction was checked by nuclear magnetic resonance (NMR) spectroscopy according to the method reported by Weinstein *et al.*[12] For that purpose, Z–Ala–Phe–OMe was prepared by the pyridinium ester method and its NMR spectrum was measured. The methyl signal of Ala in the synthetic Z–Ala–Phe–OMe was compared with those of standard Z–L-Ala–L-Phe–OMe and Z–D-Ala–L-Phe–OMe.[12] As shown in Fig. 3, methyl signals of standard samples corresponding to D-Ala and L-Ala appeared at 1.28 and 1.33 ppm, respectively. The methyl signal of Ala in synthetic Z–Ala–Phe–OMe appeared at 1.33 ppm and no signal was observed at 1.28 ppm. These results indicate that the pyridinium ester method can be used for peptide synthesis.

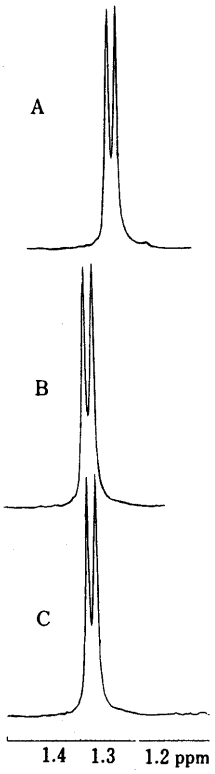

Fig. 3. NMR Spectrum Showing the Methyl Signals of Ala in Z–Ala–Phe–OMe

Solvent: $CDCl_3$. A, standard sample (D–L); B, standard sample (L–L); C, sample prepared by the pyridinium ester method.

Synthetic schemes for Gly–Pro–Arg–pyrrolidine and Gly–Pro–Arg–hexamethyleneimine are shown in Fig. 4 as examples of the synthetic methods used for various tripeptide amides. Boc–Arg(Mts)–OH and hexamethyleneimine were coupled by the mixed anhydride method, followed by TFA treatment to give H–Arg(Mts)–hexamethyleneimine. This was coupled with Z–Gly–Pro–OH by the mixed anhydride method followed by treatment with TFMSA to give H–Gly–Pro–Arg–hexamethyleneimine. Other tripeptide amides were prepared in a similar way, and hydrogenation was carried out for the final deprotection when N^G-nitroarginine[H–Arg(NO_2)–OH] was used instead of N^G-mesitylenesulfonylarginine.

The *p*-nitroanilide of the tripeptide was also prepared and the amide formation of Arg was achieved by the phosphazo

Table I. Relative Inhibitory Effects of Synthetic Peptides on FTC

Synthetic peptides	Relative activities
H–Gly–Pro–Arg–Pro–OH	1.00[a]
H–Gly–Pro–Arg–OH	0.33
H–Gly–Sar–OH	0.08
H–Gly–Pro–Arg–NH_2	0.14
H–Gly–Pro–Arg–$NHCH_3$	0.14
H–Gly–Pro–Arg–$N(CH_3)$	0.60
H–Gly–Pro–Arg–$N(C_2H_5)_2$	0.62
H–Gly–Pro–Arg–$N(C_3H_7)_2$	0.53
H–Gly–Pro–Arg–pyrrolidine	0.56
H–Gly–Pro–Arg–piperidine	0.93
H–Gly–Pro–Arg–4-hydroxypiperidine	1.20
H–Gly–Pro–Arg–3-methylpiperidine	1.29
H–Gly–Pro–Arg–hexamethyleneimine	1.85
H–Gly–Pro–Arg–cyclohexylamine	0.57
H–Gly–Pro–Arg–cyclooctylamine	0.48
H–Gly–Pro–Arg–aniline	0.20
H–Gly–Pro–Arg–*p*-nitroaniline	0.18

a) IC_{50} of H–Gly–Pro–Arg–Pro–OH: 28—65 μM.

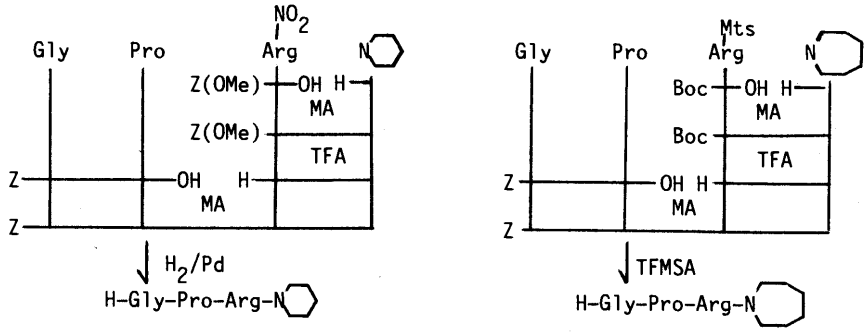

Fig. 4. Synthetic Schemes for the Tripeptides

TABLE II. Inhibitory Effects of Synthetic Peptides on Thrombin-Induced Hydrolysis of S-2238

Peptides	Concentration (mM)	% inhibition
H–Gly–Pro–Arg–piperidine	1.0	4.3
H–Gly–Pro–Arg–4-hydroxypiperidine	1.0	−2.5
H–Gly–Pro–Arg–3-methylpiperidine	1.0	1.8

method[13] instead of the mixed anhydride method.

Inhibitory effects of the synthetic peptides on fibrinogen–thrombin clotting[1a] were examined and the results are summarized in Table I. Since IC_{50} of each synthetic peptide varied when different lot of fibrinogen and thrombin were used, IC_{50} of H–Gly–Pro–Arg–Pro–OH was always measured for comparison when the inhibitory effect of the synthetic peptides was examined. Relative activities were calculated by dividing the IC_{50} of H–Gly–Pro–Arg–Pro–OH by that of each peptide.

As expected, the tripeptide amides with secondary amines were found to have a more potent inhibitory effect on FTC, compared with the carboxyl-free tripeptide or the tripeptide amide of a primary amine; the inhibitory effect of H–Gly–Pro–Arg–$N(CH_3)_2$ was more potent than those of H–Gly–Pro–Arg–OH and H–Gly–Pro–Arg–$NHCH_3$. The amide compounds of cyclic imines (such as piperidine, 4-hydroxypiperidine, 3-methylpiperidine and hexamethyleneimine) exhibited potent inhibitory effects and among them, the amide analog of hexamethyleneimine exhibited the highest inhibitory effect. Its inhibitory effect was more potent than that of H–Gly–Pro–Arg–Pro–OH, which was reported as a potent inhibitor by Laudano and Doolittle.[2] The inhibitory effect of the amide compound of piperidine was nearly equal to that of H–Gly–Pro–Arg–Pro–OH. The amide compounds of 4-hydroxypiperidine and 3-methylpiperidine were more effective than H–Gly–Pro–Arg–Pro–OH. Substitution of Pro with sarcosine (Sar) resulted in a decrease of the inhibition. The effect of the anilide was weaker than that of the cyclohexylamide and the introduction of a nitro group on the anilide did not cause any change.

Among the synthetic peptides, H–Gly–Pro–Arg–piperidine, H–Gly–Pro–Arg–4-hydroxypiperidine and H–Gly–Pro–Arg–3-methylpiperidine were examined for their antithrombin activities on thrombin/S-2238 (D-phenylalanylpipeconylarginine *p*-nitroanilide)[14] as shown in Table II. Since the peptides had almost no effect on the hydrolysis by thrombin, the inhibitory effects may result from their action on fibrin polymerization, but not on thrombin catalytic activity.

Experimental

Melting points are uncorrected. Solvent systems for ascending thin-layer chromatography on Silica gel G (type 60, E. Merck) are indicated as follows: Rf^1 = BuOH–AcOH–MeOH–H_2O (4:1:5, upper phase), Rf^2 = BuOH–pyridine–AcOH–H_2O (4:1:1:2), Rf^3 = $CHCl_3$–MeOH–H_2O (8:3:1, lower phase), Rf^4 = AcOEt–benzene (1:1), Rf^5 = $CHCl_3$–MeOH–AcOH (90:8:2). Inhibitory effect of the peptides on FTC and antithrombin activities of the peptides on thrombin/S-2238 system were examined as reported.[1a] NMR spectra were taken in $CDCl_3$ on a Brucker AM-400 (400 MHz). Chemical shifts are given in δ values (ppm) with tetramethylsilane as an internal standard. Amino acid compositions of acid hydrolysates were determined with a Hitachi 835 amino acid analyzer. Rotations were measured with a JASCO DIP-360 polarimeter.

Z–Gly–Pro–Arg(NO_2)–OBzl Prepared from Z–Gly–Pro–OH (1.5 g, 5 mmol) and H–Arg(NO_2)–OBzl·2TosOH[18] (3.2 g, 4.9 mmol) by the mixed anhydride method in the usual manner.[8] The product was purified by silica gel column (2.5 × 25 cm) chromatography using 1% MeOH–$CHCl_3$ as an eluent. Yield 1.52 g (52%), mp 68—71 °C, Rf^3 0.62, $[\alpha]_D^{22}$ −55.8° (c = 1.0, MeOH). *Anal.* Calcd for $C_{28}H_{35}N_7O_8$: C, 56.3; H, 5.9; N, 16.4. Found: C, 56.3; H, 6.0; N, 16.2.

H–Gly–Pro–Arg–OH Z–Gly–Pro–Arg(NO_2)–OBzl (500 mg, 0.8 mmol) was hydrogenated over a Pd catalyst in a mixture of AcOH (0.5 ml) and MeOH (20 ml) in the usual manner. The product was lyophilized from water to give a hygroscopic powder. Yield 263 mg (81%), Rf^2 0.10, $[\alpha]_D^{18}$ −55.2° (c = 1.0, H_2O). *Anal.* Calcd for $C_{13}H_{24}N_6O_4 \cdot AcOH \cdot 1/3H_2O$: C, 45.7; H, 7.3; N, 21.3. Found: C, 46.0; H, 7.4; N, 21.5. Amino acid ratios in an acid hydrolysate: Gly 1.00; Arg 0.90; Pro 1.14 (average recovery 87%).

Boc–Arg(NO_2)–Pro–OBzl Prepared from Boc–Arg(NO_2)–OH (3.5 g, 11 mmol) and HCl·H–Pro–OBzl (2.65 g, 11 mmol) in DMF by the mixed anhydride method in the usual manner. The product was purified by silica gel column chromatography using 1% MeOH–$CHCl_3$ as an eluent. Yield 3.6 g (59%), syrupy material, Rf^3 0.85, $[\alpha]_D^{21}$ −53.1° (c = 0.9, MeOH). *Anal.* Calcd for $C_{23}H_{34}N_6O_7$: C, 54.5; H, 6.8; N, 16.6. Found: C, 54.8; H, 6.6; N, 16.4.

Boc–Pro–Arg(NO_2)–Pro–OBzl Prepared from Boc–Pro–OH (2.67 g, 12.4 mmol) and H–Arg(NO_2)–Pro–OBzl [prepared from 6.3 g (12.4 mmol) of the corresponding Boc derivative by TFA treatment followed by Et_3N treatment] by the mixed anhydride method in the usual manner. The product was purified by silica gel column chromatography using 2% MeOH–$CHCl_3$ as an eluent. Yield 5.53 g (83%), mp 100—105 °C, Rf^5 0.58, $[\alpha]_D^{21}$ −96.2° (c = 0.9, MeOH). *Anal.* Calcd for $C_{28}H_{41}N_7O_8$: C, 55.7; H, 6.9; N, 16.2. Found: C, 55.7; H, 7.0; N, 16.1.

Z–Gly–Pro–Arg(NO_2)–Pro–OBzl Prepared from Z–Gly–OH (0.9 g, 4.3 mmol) and H–Pro–Arg(NO_2)–Pro–OBzl [prepared from 2 g (3.3 mmol) of the corresponding Boc derivative by TFA treatment followed by Et_3N treatment] by the mixed anhydride method in the usual manner. The product was purified by silica gel column chromatography using 3% MeOH–$CHCl_3$ as an eluent. Yield 1.83 g (77%), mp 103—107 °C, Rf^5 0.56, $[\alpha]_D^{21}$ −89.2° (c = 1.2, MeOH). *Anal.* Calcd for $C_{33}H_{42}N_8O_9$: C, 57.0; H, 6.1; N, 16.1. Found: C, 56.9; H, 6.2; N, 15.9.

H–Gly–Pro–Arg–Pro–OH The above protected tetrapeptide (500 mg, 0.7 mmol) was hydrogenated over a Pd catalyst in a mixture of MeOH and 1 N HCl in the usual manner. The product was lyophilized to give a hygroscopic powder. Yield 258 mg (78%), Rf^2 0.22, $[\alpha]_D^{21}$ −89.2° (c = 1.2, MeOH). *Anal.* Calcd for $C_{18}H_{31}N_7O_5 \cdot HCl \cdot 1/2H_2O$: C, 42.6; H, 6.8; N, 19.3. Found: C, 42.5; H, 7.0; N, 19.3. Amino acid ratios in an acid hydrolysate: Gly 1.00, Pro 2.24, Arg 0.93 (average recovery 77%).

3-Hydroxymethylpyridinium Iodide A solution of 3-hydroxypyridine (1 g, 11 mmol) and methyl iodide (19.5 ml, 220 mmol) in MeOH (4 ml) was refluxed at 45 °C for 6 h. After removal of the solvent *in vacuo*, the aqueous solution of the product was washed repeatedly with AcOEt and lyophilized. Yield 2.15 g (86%), mp 95—97 °C, Rf^2 0.70. *Anal.* Calcd for C_6H_8INO: C, 30.4; H, 3.4; N, 5.9. Found: C, 30.1; H, 3.4; N, 5.9.

3-(Z–Gly)-methylpyridinium Iodide Ester (Z–Gly–OMPI) DCC (2.27 g, 11 mmol) was added to a solution of Z–Gly–OH in DMF (10 ml) at 0 °C and the mixture was stirred for 20 min. A chilled solution of 1-methyl-3-hydroxypyridinium iodide (2.17 g, 9.2 mmol) in DMF (10 ml) was added to the above mixture and the whole was stirred overnight. The solvent was evaporated off, and the aqueous solution of the residue was washed with ethyl and lyophilzed. The residue was triturated with *n*-propanol. Yield 2.1 g (54%), amorphous powder, Rf^2 0.78. *Anal.* Calcd for $C_{16}H_{17}IN_2O_4 \cdot 5/3H_2O$: C, 41.9; H, 4.5; N, 6.1. Found: C, 41.9; H, 4.4; N, 6.0.

3-(Z–Gly)pyridyl Ester (Z–Gly–OPy) Prepared from Z–Gly–OH (5 g, 24 mmol) and 3-hydroxypyridine (2.27 g, 24 mmol) in DMF by the DCC method in the usual manner. The product was purified by silica gel column chromatography using 2% MeOH–$CHCl_3$ as an eluent. Yield 4.52 g (66%), syrupy material, Rf^4 0.42. *Anal.* Calcd for $C_{15}H_{14}N_2O_4 \cdot H_2O$: C, 59.2; H, 5.3; N, 9.2. Found: C, 58.9; H, 5.1; N, 8.9.

Z–Gly–Pro–OH a) Pyridinium Ester Method: A solution of Z–Gly–OMPI (0.3 g, 1 mmol), H–Pro–OH (0.12 g, 1 mmol) and *N*-methylmorpholine (NMM, 0.11 ml, 1 mmol) in H_2O (3 ml) was stirred overnight and acidified with citric acid. The AcOEt extract of the resulting precipitate was washed with H_2O and dried with Na_2SO_4. The solvent was evaporated off and the residue was recrystallized from AcOEt. Yield 0.22 g (71%). A 78% yield was obtained when the same reaction was done in a mixture

of DMF–H_2O, mp 153—156 °C, Rf^3 0.49, $[\alpha]_D^{22}$ −71.3° (c = 1.0, MeOH). *Anal.* Calcd for $C_{15}H_{18}N_2O_5 \cdot 1/4H_2O$: C, 58.0; H, 6.0; N, 9.0. Found: C, 57.8; H, 5.8; N, 9.2. Amino acid ratios in an acid hydrolysate: Gly 1.00, Pro 1.09 (average recovery 86%).

b) Pyridyl Ester Method: Z–Gly–OPy (1.2 g, 4.24 mmol) and H–Pro–OH (0.49 g, 4.24 mmol) were reacted in a mixture of DMF (10 ml), H_2O (3 ml) and Et_3N (0.59 ml, 4.3 mmol). After removal of the solvent, the product was purified as described above. Yield 0.85 g (66%), mp 150—152 °C, Rf^3 0.49, $[\alpha]_D^{28}$ −65.8° (c = 1.0, MeOH). Amino acid ratios in an acid hydrolysate: Gly 1.00, Pro 1.08 (average recovery 73%).

3-(Z-Ala)-methylpyridinium Iodide Ester (Z-Ala-OMPI) A solution of Z–Ala–OH (2 g, 9 mmol) and DCC (2.2 g, 10.8 mmol) in CH_2Cl_2 was stirred for 20 min at −5 °C and the resulting precipitate was removed by filtration. The filtrate was combined with a DMF solution of 1-methyl-3-hydroxypyridinium iodide (2.12 g, 9 mmol) and the mixture was stirred overnight. The solvent was evaporated off and the aqueous solution of the residue was washed with ether followed by lyophilization. Yield 3.51 g (88%), amorphous powder, Rf^2 0.73, $[\alpha]_D^{24}$ −13.1° (c = 1.0, MeOH). *Anal.* Calcd for $C_{17}H_{19}IN_2O_4 \cdot 2H_2O$: C, 42.7; H, 4.9; N, 5.9. Found: C, 43.1; H, 5.0; N, 6.1.

Z-Ala-Phe-OMe A mixture of Z–Ala–OMPI (1.98 g, 4.5 mmol), NMM (0.5 ml, 4.5 mmol) and H–Phe–OMe·HCl (0.97 g, 4.5 mmol) in DMF was stirred overnight and the solvent was evaporated off. The AcOEt extract of the residue was washed successively with 5% Na_2CO_3, 5% citric acid and H_2O, and concentrated. The product was recrystallized from AcOEt–petroleum ether. Yield 1.24 g (63%), mp 96—100 °C, Rf^4 0.76, $[\alpha]_D^{26}$ −10.4° (c = 1.0, EtOH) [lit.[19] mp 99—100 °C, $[\alpha]_D^{22}$ −9.3° (c = 1.0, EtOH)]. Amino acid ratios in an acid hydrolysate: Ala 1.00, Phe 1.03 (average recovery 95%). ^{1}H-NMR ($CDCl_3$) δ: 1.33 (3H, CH_3).

Z(OMe)-Arg(NO_2)-NH_2 Prepared from Z(OMe)–Arg(NO_2)–OH (3 g, 7.8 mmol) and 28% ammonia water (9.67 ml) in THF (60 ml) by the mixed anhydride method in the usual manner. The resulting precipitate was collected by filtration and washed with MeOH. Yield 2.08 g (70%), mp 220—223 °C, Rf^3 0.59, $[\alpha]_D^{26}$ −5.0° (c = 1.0, DMF). *Anal.* Calcd for $C_{15}H_{22}N_6O_6$: C, 47.1; H, 5.8; N, 22.0. Found: C, 47.4; H, 5.8; N, 21.7.

Z-Gly-Pro-Arg(NO_2)-NH_2 Prepared from Z–Gly–Pro–OH (0.56 g, 1.8 mmol) and H–Arg(NO_2)–NH_2 [prepared from the corresponding Z(OMe) derivative (0.53 g, 1.4 mmol) by TFA treatment followed by TEA treatment] were coupled by the diphenylphosphoryl azide (DPPA)[15] method in DMF. The DMF was removed *in vacuo* and the residue was extracted with BuOH followed by washing the extract with 10% Na_2CO_3, 0.5 N HCl and H_2O. The BuOH layer was concentrated and the product was precipitated by addition of ether. Yield 0.20 g (71%), amorphous powder, Rf^3 0.54, $[\alpha]_D^{26}$ −37.3° (c = 1.0, MeOH). *Anal.* Calcd for $C_{21}H_{30}N_8O_7$: C, 49.8; H, 6.0; N, 22.1. Found: C, 49.9; H, 5.9; N, 21.9.

Z(OMe)-Arg(NO_2)-$NHCH_3$ Prepared from Z–Arg(NO_2)–OH (4.03 g, 10 mmol) and 40% NH_2CH_3 (1.7 ml, 20 mmol) by the mixed anhydride method in DMF in the usual manner. The product was purified by silica gel column (2.7 × 15 cm) chromatography using 3% MeOH–$CHCl_3$ as an eluent. Yield 1.68 g (41%), amorphous powder, Rf^3 0.70, $[\alpha]_D^{19}$ −4.4° (c = 1.0, MeOH). *Anal.* Calcd for $C_{16}H_{24}N_6O_6$: C, 48.5; H, 6.1; N, 21.2 Found: C, 48.4; H, 6.2; N, 21.0.

Z-Gly-Pro-Arg(NO_2)-$NHCH_3$ Prepared from Z–Gly–Pro–OH (0.57 g, 1.86 mmol) and H–Arg(NO_2)–$NHCH_3$ (prepared from the corresponding Z(OMe) derivative by TFA treatment followed by TEA treatment) by the mixed anhydride method. The product was purified in the same manner as described for Z–Gly–Pro–Arg(NO_2)–NH_2. Recrystallized from AcOEt. Yield 0.66 g (69%), mp 98—101 °C, Rf^3 0.65, $[\alpha]_D^{19}$ −46.1° (c = 1.0, MeOH). *Anal.* Calcd for $C_{22}H_{32}N_8O_7$: C, 50.8; H, 6.2; N, 21.5. Found: C, 50.6; H, 6.4; N, 21.5.

H-Gly-Pro-Arg-$NHCH_3$ Prepared from Z–Gly–Pro–Arg(NO_2)–$NHCH_3$ (202 mg, 0.4 mmol) in a mixture of AcOH and MeOH by catalytic hydrogenation. The product was lyophilized from water to give a hygroscopic powder. Yield 147 mg (82%), Rf^2 0.28, $[\alpha]_D^{21}$ −70.0° (c = 1.0, H_2O). *Anal.* Calcd for $C_{14}H_{27}N_7O_3 \cdot 2AcOH \cdot 3/4H_2O$: C, 45.5; H, 7.8; N, 20.6. Found: C, 45.4; H, 7.5; N, 20.8. Amino acid ratios in an acid hydrolysate: Gly 1.00, Pro 1.17, Arg 0.97 (average recovery 77%).

Z(OMe)-Arg(NO_2)-N(CH_3)$_2$ Prepared from Z(OMe)–Arg(NO_2)–OH (3.04 g, 7.9 mmol) and 44% dimethylamine (0.81 ml, 7.9 mmol) in DMF by the mixed anhydride method in the usual manner. The product was purified by silica gel column chromatography using 3% MeOH–$CHCl_3$ as an eluent. Yield 1.03 g (32%), mp 68—70 °C, Rf^5 0.40, $[\alpha]_D^{20}$ −11.3° (c = 1.0, MeOH). *Anal.* Calcd for $C_{17}H_{26}N_6O_6 \cdot 1/3H_2O$: C, 49.0; H, 6.5; N, 20.2. Found: C, 48.9; H, 6.3; N, 20.4.

Z-Gly-Pro-Arg(NO_2)-N(CH_3)$_2$ Prepared from Z–Gly–Pro–OH (0.29 g, 0.95 mmol) and H–Arg(NO_2)–N(CH_3)$_2$ [prepared from the corresponding Z(OMe) derivative (0.39 g, 0.95 mmol) by TFA treatment followed by TEA treatment] in DMF by the mixed anhydride method in the usual manner. Yield 0.34 g (67%), amorphous powder, Rf^3 0.70, $[\alpha]_D^{23}$ −62.9° (c = 1.0, MeOH). *Anal.* Calcd for $C_{23}H_{34}N_8O_7$: C, 51.7; H, 6.4; N, 21.0. Found: C, 51.5; H, 6.5; N, 20.8.

H-Gly-Pro-Arg-N(CH_3)$_2$ Prepared from Z–Gly–Pro–Arg(NO_2)–N(CH_3)$_2$ (204 mg, 0.38 mmol) in MeOH by catalytic hydrogenation in the usual manner. Yield 146 mg (80%), amorphous powder, Rf^2 0.14, $[\alpha]_D^{20}$ −82.0° (c = 0.5, H_2O). *Anal.* Calcd for $C_{15}H_{29}N_7O_3 \cdot 2AcOH \cdot H_2O$: C, 46.2; H, 8.0; N, 19.9. Found: C, 46.5; H, 8.1; N, 20.2.

Z(OMe)-Arg(NO_2)-N(C_2H_5)$_2$ Prepared from Z(OMe)–Arg(NO_2)–OH (3 g, 7.8 mmol) and (C_2H_5)$_2$NH (1.08 ml, 10 mmol) by the mixed anhydride method in the usual manner. The product was purified by silica gel column chromatography using 3% MeOH–$CHCl_3$ as an eluent. Yield 1.62 g (47%), mp 56—59 °C, Rf^5 0.56, $[\alpha]_D^{17}$ −24.4° (c = 1.0, MeOH). *Anal.* Calcd for $C_{19}H_{30}N_6O_6$: C, 52.0; H, 6.9; N, 19.2. Found: C, 51.9; H, 6.8; N, 18.9.

Z-Gly-Pro-Arg(NO_2)-N(C_2H_5)$_2$ Prepared from Z–Gly–Pro–OH (0.55 g, 1.8 mmol) and H–Arg(NO_2)–N(C_2H_5)$_2$ [prepared from the corresponding Z(OMe) derivative (0.72 g, 1.6 mmol) by TFA treatment followed by TEA treatment] in DMF by the mixed anhydride method in the usual manner. Yield 0.47 g (51%), mp 77—79 °C, Rf^3 0.69, $[\alpha]_D^{19}$ −61.4° (c = 1.0, $CHCl_3$). *Anal.* Calcd for $C_{25}H_{38}N_8O_7$: C, 53.4; H, 6.8; N, 19.9. Found: C, 53.4; H, 6.8; N, 19.7.

H-Gly-Pro-Arg-N(C_2H_5)$_2$ Prepared from Z–Gly–Pro–Arg(NO_2)–N(C_2H_5)$_2$ (219 mg, 0.39 mmol) in a mixture of AcOH and MeOH by catalytic hydrogenation in the usual manner. Yield 154 mg (79%), hygroscopic powder, Rf^2 0.24, $[\alpha]_D^{18}$ −99.8° (c = 0.5, H_2O). *Anal.* Calcd for $C_{17}H_{33}N_7O_3 \cdot 2AcOH \cdot 1/2H_2O$: C, 49.2; H, 8.3; N, 19.1. Found: C, 48.9; H, 8.5; N, 19.4. Amino acid ratios in an acid hydrolysate: Gly 1.00; Pro 1.08; Arg 0.94 (average recovery 88%).

Z-(OMe)-Arg(NO_2)-N(C_3H_7)$_2$ Prepared from Z(OMe)–Arg(NO_2)–OH (2 g, 5.2 mmol) and NH(C_3H_7)$_2$ (1.42 ml, 10.4 mmol) in DMF by the mixed anhydride method in the usual manner. The product was purified by silica gel column chromatography using 3% MeOH–$CHCl_3$ as an eluent. Yield 2.96 g (61%), amorphous powder, Rf^3 0.67, $[\alpha]_D^{21}$ −22.4° (c = 1.0, MeOH). *Anal.* Calcd for $C_{21}H_{34}N_6O_6$: C, 54.1; H, 7.4; N, 18.0. Found: C, 53.9; H, 7.4; N, 18.0.

Z-Gly-Pro-Arg(NO_2)-N(C_3H_7)$_2$ Prepared from Z–Gly–Pro–OH (0.34 g, 0.88 mmol) and H–Arg(NO_2)–N(C_3H_7)$_2$ [prepared from its Z(OMe) derivative (0.43 g, 0.92 mmol) by TFA treatment followed by TEA treatment] by the mixed anhydride method in the usual manner. The product was purified by silica gel column chromatography using 3% MeOH–$CHCl_3$ as an eluent. Yield 0.41 g (76%), mp 79—82 °C, Rf^3 0.68, $[\alpha]_D^{20}$ −73.6° (c = 1.0, MeOH). *Anal.* Calcd for $C_{27}H_{42}N_8O_7$: C, 54.9; H, 7.2; N, 19.0. Found: C, 54.6; H, 7.4; N, 18.8.

H-Gly-Pro-Arg-N(C_3H_7)$_2$ Prepared from Z–Gly–Pro–Arg(NO_2)–N(C_3H_7)$_2$ (255 mg, 0.43 mmol) by catalytic hydrogenation in a mixture of MeOH and AcOH. Yield 172 mg (75%), hygroscopic powder, Rf^2 0.17, $[\alpha]_D^{20}$ −78.2° (c = 0.5, H_2O). *Anal.* Calcd for $C_{19}H_{37}N_7O_3 \cdot 2AcOH \cdot 2H_2O$: C, 48.7; H, 8.7; N, 17.3. Found: C, 48.4; H, 8.5; N, 17.3. Amino acid ratios in an acid hydrolysate: Gly 1.00; Pro 1.11; Arg 0.90 (average recovery 78.6%).

Z(OMe)-Arg(NO_2)-Pyrrolidine Prepared from Z(OMe)–Arg(NO_2)–OH (2.99 g, 7.8 mmol) and pyrrolidine (1.25 ml, 15 mmol) in DMF by the mixed anhydride method in the usual manner. The product was purified by silica gel column chromatography using 3% MeOH–$CHCl_3$ as an eluent. Yield 1.72 g (50%), mp 73—75 °C, Rf^5 0.40, $[\alpha]_D^{22}$ −10.4° (c = 1.0, MeOH). *Anal.* Calcd for $C_{19}H_{28}N_6O_6$: C, 52.3; H, 6.5; N, 19.3. Found: C, 52.1; H, 6.5; N, 19.2.

Z-Gly-Pro-Arg(NO_2)-Pyrrolidine Prepared from Z–Gly–Pro–OH (0.37 g, 1.2 mmol) and H–Arg(NO_2)–pyrrolidine [prepared from its Z(OMe) derivative (0.52 g, 1.2 mmol) by TFA treatment followed by TEA treatment] by the mixed anhydride method in the usual manner. The product was extracted with BuOH and the extract was washed successively with 10% Na_2CO_3, 0.5 N HCl, 5% $NaHCO_3$ and H_2O. The solvent was evaporated off and the residue was precipitated from EtOH–ether. Yield 0.31 g (46%), mp 105—108 °C, Rf^3 0.73, $[\alpha]_D^{17}$ −77.5° (c = 1.0, MeOH). *Anal.* Calcd for $C_{25}H_{36}N_8O_7 \cdot 1/4H_2O$: C, 53.1; H, 6.5; N, 19.8. Found: C, 53.1; H, 6.5; N, 19.5.

H-Gly-Pro-Arg-Pyrrolidine Prepared from Z–Gly–Pro–Arg(NO_2)–pyrrolidine (224 mg, 0.4 mmol) in a mixture of AcOH and MeOH by hydrogenation in the usual manner. Yield 178 mg (89%), hygroscopic powder, Rf^2 0.32, $[\alpha]_D^{21}$ −74.4° (c = 0.5, H_2O). *Anal.* Calcd for

$C_{17}H_{31}N_7O_3 \cdot 2AcOH \cdot 3/4H_2O$: C, 49.0; H, 7.9; N, 19.0. Found: C, 48.6; H, 7.9; N, 19.2. Amino acid ratios in an acid hydrolysate: Gly 1.00; Pro 1.12; Arg 0.91 (average recovery 78%).

Z(OMe)-Arg(NO_2)-Piperidine Prepared from Z(OMe)-Arg(NO_2)-OH (3 g, 7.8 mmol) and piperidine (1.38ml, 14 mmol) by the mixed anhydride method in the usual manner. The product was purified by silica gel column chromatography using 3% MeOH–$CHCl_3$ as an eluent. Yield 1.81 g (51%), amorphous powder, Rf^5 0.60, $[\alpha]_D^{23}$ −13.2° (c=1.0, MeOH). *Anal.* Calcd for $C_{20}H_{30}N_6O_6 \cdot H_2O$: C, 51.3; H, 6.9; N, 17.9. Found: C, 51.5; H, 6.6; N, 18.1.

Z-Gly-Pro-Arg(NO_2)-Piperidine Prepared from Z-Gly-Pro-OH (810 mg, 2.64 mmol) and H-Arg(NO_2)-piperidine [prepared from its Z(OMe) derivative (990 mg, 2.3 mmol) by TFA treatment followed by TEA treatment] by the mixed anhydride method in the usual manner. The product was purified by silica gel column chromatography using 3% MeOH–$CHCl_3$ as an eluent. Yield 0.66 g (52%), mp 107—110 °C, Rf^5 0.60, $[\alpha]_D^{19}$ −61.1° (c=1.0, MeOH). *Anal.* Calcd for $C_{26}H_{38}N_8O_7$: C, 54.3; H, 6.7; N, 19.5. Found: C, 54.2; H, 6.7; N, 19.2.

H-Gly-Pro-Arg(NO_2)-Piperidine Prepared from Z-Gly-Pro-Arg(NO_2)-piperidine (133 mg, 0.23 mmol) in a mixture of AcOH and MeOH by hydrogenation. Yield 94 mg (79%), hygroscopic powder, Rf^2 0.17, $[\alpha]_D^{20}$ −95.1° (c=0.5, H_2O). *Anal.* Calcd for $C_{18}H_{33}N_7O_3 \cdot 2AcOH \cdot 3/2H_2O$: C, 48.7; H, 8.2; N, 18.1. Found: C, 48.4; H, 8.4; N, 17.9. Amino acid ratios in an acid hydrolysate: Gly 1.00; Pro 1.10; Arg 0.98 (average recovery 91%).

Z(OMe)-Arg(NO_2)-4-Hydroxypiperidine Prepared from Z(OMe)-Arg(NO_2)-OH (5 g, 13 mmol) and 4-hydroxypiperidine (2.5 g, 25 mmol) in DMF by the DCC method. The DMF was evaporated off and the residue was dissolved in BuOH. This solution was washed successively with 10% Na_2CO_3, 5% citric acid and water. The BuOH was evaporated off and the residue was purified by silica gel column chromatography using 2% MeOH–$CHCl_3$ as an eluent. Yield 2.92 g (48%), amorphous powder, Rf^3 0.86, $[\alpha]_D^{26}$ −10.5° (c=1.0, MeOH). *Anal.* Calcd for $C_{20}H_{30}N_6O_7$: C, 51.5; H, 6.5; N, 18.0. Found: C, 51.2; H, 6.5; N, 17.7.

Boc-Gly-Pro-Arg(NO_2)-4-Hydroxypiperidine Prepared from Boc-Gly-Pro-OH[16] (0.68 g, 2.5 mmol) and H-Arg(NO_2)-4-hydroxypiperidine [prepared from its Z(OMe) derivative (1.29 g, 2.8 mmol) by TFA treatment followed by TEA treatmen] by the mixed anhydride method in the usual manner. The product was dissolved in BuOH and the solution was washed successively with 10% Na_2CO_3, 5% citric acid and water. The BuOH was evaporated off and the residue was precipitated from MeOH–ether and lyophilized from water. Yield 1.23 g (88%), amorphous powder, Rf^3 0.64, $[\alpha]_D^{29}$ −41.8° (c=1.0, DMF). *Anal.* Calcd for $C_{23}H_{40}N_8O_8$: C, 49.6; H, 7.2; N, 20.1. Found: C, 49.5; H, 7.3; N, 19.9.

H-Gly-Pro-Arg-4-Hydroxypiperidine Boc-Gly-Pro-Arg(NO_2)-4-hydroxypiperidine (600 mg, 1.1 mmol) was treated with HF at 0 °C for 1 h in the presence of anisole. The product was purified by CM-cellulose column chromatography using 0.01 M $AcONH_4$ containing an AcOH gradient (0—2%) as an eluent. Yield 0.39 g (75%), hygroscopic powder, Rf^1 0.22, $[\alpha]_D^{22}$ −30.5° (c=1.0, MeOH). *Anal.* Calcd for $C_{18}H_{33}N_7O_4 \cdot AcOH \cdot 1/2H_2O$: C, 50.0; H, 8.0; N, 20.4. Found: C, 49.8; H, 8.1; N, 20.0. Amino acid ratios in an acid hydrolysate: Gly 1.00; Pro 1.14; Arg 1.09 (average recovery 89%).

Z(OMe)-Arg(NO_2)-3-Methylpiperidine Prepared from Z(OMe)-Arg(NO_2)-OH (2 g, 5.2 mmol) and 3-methylpiperidine (0.62 g, 6.3 mmol) in DMF by the DCC-HOBt method[17] in the usual manner. The product was purified by silica gel column chromatography using 3% MeOH–$CHCl_3$ as an eluent. Yield 2.1 g (86%), mp 74—75 °C, Rf^5 0.76, $[\alpha]_D^{22}$ −11.8° (c=1.0, MeOH). *Anal.* Calcd for $C_{21}H_{32}N_6O_6$: C, 54.3; H, 6.9; N, 18.1. Found: C, 54.1; H, 6.9; N, 17.9.

Z-Gly-Pro-Arg(NO_2)-3-Methylpiperidine Prepared from Z-Gly-Pro-OH (790 mg, 2.6 mmol) and H-Arg(NO_2)-3-methylpiperidine [derived from its Z(OMe) derivative (1 g, 2.2 mmol) by TFA treatment] in DMF by the mixed anhydride method in the usual manner. The product was purified by silica gel column chromatography using 3% MeOH–$CHCl_3$ as an eluent. Yield 1.0 g (68%), mp 105—107 °C, Rf^3 0.67, $[\alpha]_D^{22}$ −70.2° (c=1.0, MeOH). *Anal.* Calcd for $C_{27}H_{40}N_8O_7$: C, 55.1; H, 6.8; N, 19.0. Found: C, 55.4; H, 6.7; N, 18.8.

H-Gly-Pro-Arg-3-Methylpiperidine Prepared from Z-Gly-Pro-Arg(NO_2)-3-methylpiperidine (800 mg, 1.36 mmol) by hydrogenation with a Pd catalyst in the usual manner. Yield 511 mg (71%), hygroscopic powder, Rf^2 0.23, $[\alpha]_D^{23}$ −62.0° (c=1.0, H_2O). *Anal.* Calcd for $C_{19}H_{35}N_7O_3 \cdot 2AcOH \cdot 3/2H_2O$: C, 49.6; H, 8.3; N, 17.6. Found: C, 49.4; H, 8.6; N, 18.0.

Boc-Arg(Mts)-Hexamethyleneimine Prepared from Boc-Arg(Mts)-OH (3 g, 6.6 mmol) and hexamethyleneimine (0.9 ml, 7.9 mmol) in DMF by the DCC–HOBt method in the usual manner. The product was purified by silica gel column chromatography using 2% MeOH–$CHCl_3$ as an eluent. Yield 2.33 g (66%), Rf^5 0.49, $[\alpha]_D^{24}$ −9.3° (c=1.0, MeOH). *Anal.* Calcd for $C_{26}H_{43}N_5O_5S \cdot 1/4H_2O$: C, 57.6; H, 8.1; N, 12.5. Found: C, 57.8; H, 8.1; N, 12.5.

Z-Gly-Pro-Arg(Mts)-Hexamethyleneimine Prepared from Z-Gly-Pro-OH (0.71 g, 2.3 mmol) and H-Arg(Mts)-hexamethyleneimine [prepared from its Boc derivative (1 g, 1.9 mmol) by TFA treatment followed by TEA treatment] by the mixed anhydride method in the usual manner. After purification by an extraction procedure with AcOEt, the product was precipitated from AcOEt–ether. Yield 1.08 g (78%), mp 98—101 °C, Rf^3 0.69, $[\alpha]_D^{24}$ −60.3° (c=1.0, MeOH). *Anal.* Calcd for $C_{36}H_{51}N_7O_7S$: C, 59.6; H, 7.1; N, 13.5. Found: C, 59.3; H, 7.2; N, 13.2.

H-Gly-Pro-Arg-Hexamethyleneimine Prepared from Z-Gly-Pro-Arg(Mts)-hexamethyleneimine (500 mg, 0.69 mmol) by 1 M TFMSA–TFA treatment[12] in the presence of thioanisole for 1 h at 0 °C and 1 h at room temperature. Cold ether was added to the reaction mixture to give a precipitate, which was treated with Amberlite IRA 400 resin (acetate form) in 5% AcOH. After lyophilization, the product was purified by HPLC (YMC R-ODS-5 column, 20 × 250 mm; gradient system of 0.1% TFA–H_2O: 0.1% TFA–CH_3CN, 80 : 20—50 : 50). The product was converted to its hydrochloride by lyophilization from a mixture of H_2O and 1 N HCl. Yield 230 mg (70%), hygroscopic powder, Rf^2 0.23, $[\alpha]_D^{27}$ −95.6° (c=1.0, H_2O). *Anal.* Calcd for $C_{19}H_{35}N_7O_3 \cdot 2HCl \cdot 7/4H_2O$: C, 44.4; H, 7.9; N, 19.1. Found: C, 44.4; H, 7.8; N, 19.0. Amino acid ratios in an acid hydrolysate: Gly 1.00; Pro 1.00; Arg 0.88 (average recovery 79%).

Boc-Arg(Mts)-Cyclohexylamine Prepared from Boc-Arg(Mts)-OH (1 g, 2.19 mmol) and cyclohexylamine (0.3 ml, 2.62 mmol) in DMF by the DCC–HOBt method[17] in the usual manner. Yield 1.11 g (94%), mp 99—105 °C, Rf^5 0.25, $[\alpha]_D^{24}$ +3.1° (c=1.0, MeOH). *Anal.* Calcd for $C_{26}H_{43}N_5O_5S$: C, 58.1; H, 8.1; N, 13.0. Found: C, 57.9; H, 8.1; N, 12.8.

Z-Gly-Pro-Arg(Mts)-Cyclohexylamine Prepared from Z-Gly-Pro-OH (0.76 g, 2.47 mmol) and H-Arg(Mts)-cyclohexylamine [prepared its Boc derivative (1.11 g, 2.06 mmol) by 4 N HCl–dioxane treatment followed by TEA treatment] by the DCC–HOBt method in the usual manner. Yield 1.26 g (84%), mp 115—120 °C, Rf^2 0.76, $[\alpha]_D^{24}$ −36.1° (c=1.0, MeOH). *Anal.* Calcd for $C_{36}H_{51}N_7O_7S$: C, 59.6; H, 7.1; N, 13.5. Found: C, 59.3; H, 7.3; N, 13.4.

H-Gly-Pro-Arg-Cyclohexylamine Z-Gly-Pro-Arg(Mts)-cyclohexylamine (0.6 g, 0.83 mmol) was treated with 1 M TFMSA–TFA in the presence of thioanisole at 0 °C for 1 h and at room temperature for 1 h. Ether was added to give a precipitate, which was treated with Amberlite IRA 400 (acetate form) in 5% AcOH. After lyophilization, the product was purified by HPLC (YMC R-ODS-5, 20 × 250 mm; gradient system of 0.1% TFA–H_2O: 0.1% TFA-CH_3CN, 80 : 20—50 : 50). The product was converted to its hydrochloride by lyophilization from a mixture of 1 N HCl and H_2O. Yield 0.19 g (49%), hygroscopic powder, Rf^2 0.21, $[\alpha]_D^{25}$ −80.8° (c=1.0, MeOH). *Anal.* Calcd for $C_{19}H_{35}N_7O_3 \cdot 2HCl \cdot 5/4H_2O$: C, 45.2; H, 7.9; N, 19.4. Found: C, 45.2; H, 7.9; N, 19.4. Amino acid ratios in an acid hydrolysate: Gly 1.00; Pro 1.05; Arg 1.08 (average recovery 92%).

Boc-Arg(Mts)-Cyclooctylamine Prepared from Boc-Arg(Mts)-OH (3 g, 6.75 mmol) and cyclooctylamine (1.09 ml, 7.92 mmol) by the DCC–HOBt method in the usual manner. Recrystallized from AcOEt–ether. Yield 3.37 g (90%), mp 96—102 °C, Rf^5 0.60, $[\alpha]_D^{26}$ −3.4° (c=1.0, MeOH). *Anal.* Calcd for $C_{28}H_{45}N_5O_5S$: C, 59.4; H, 8.5; N, 12.4. Found: C, 59.7; H, 8.7; N, 12.0.

Z-Gly-Pro-Arg(Mts)-Cyclooctylamine Prepared from Z-Gly-Pro-OH (0.65 g, 2.12 mmol) and H-Arg(Mts)-cyclooctylamine [prepared from the corresponding Boc derivative (1 g, 1.77 mmol) by HCl–dioxane treatment followed by TEA treatment] by the DCC-HOBt method in the usual manner. Recrystallized from AcOEt–ether. Yield 1.25 g (93%), mp 115—120 °C, Rf^1 0.77, $[\alpha]_D^{24}$ −34.6° (c=1.0, MeOH). *Anal.* Calcd for $C_{38}H_{55}N_7O_7S$: C, 60.5; H, 7.4; N, 13.0. Found: C, 60.8; H, 7.7; N, 12.8. Amino acid ratios in an acid hydrolysate: Gly 1.00; Pro 1.07; Arg 1.01 (average recovery 87%).

H-Gly-Pro-Arg-Cyclooctylamine Prepared from the corresponding protected peptide by treatment with 1 M TFMSA–TFA (13.3 ml)–thioanisole (0.8 ml) for 1 h at 0 °C and 1 h at room temperature. The product was precipitated by addition of ether, washed with ether and treated with Amberlite IRA-400 (acetate form) in 5% AcOH. After lyophilization, the product was purified by HPLC [YMC R-ODS-5; gradient system of (0.1% TFA–H_2O)/(0.1% TFA–CH_3CN), 80 : 20—50 : 50]. Yield 0.14 g (41%), hygroscopic powder, Rf^2 0.23, $[\alpha]_D^{26}$ −84.4° (c=1.0, H_2O). *Anal.* Calcd for $C_{21}H_{39}N_7O_3 \cdot 2HCl \cdot 3/2H_2O$: C, 46.9; H, 8.3; N, 18.2. Found: C, 47.1; H, 8.0; N, 18.2. Amino acid ratios in an acid hydrolysate: Gly 1.00; Pro

1.11; Arg 1.06 (average recovery 81%).

Boc-Arg(NO_2)-Aniline Prepared from Boc-Arg(NO_2)-OH (1.6 g, 5 mmol) and aniline (0.46 ml, 5 mmol) in DMF by the mixed anhydride method in the usual manner. Recrystallized from AcOEt–petroleum ether. Yield 1.77 g (90%), mp 77—80 °C, Rf^3 0.46, $[\alpha]_D^{28}$ −2.6° (c = 1.9, MeOH). *Anal.* Calcd for $C_{17}H_{26}N_6O_5$: C, 51.8; H, 6.6; N, 21.3. Found: C, 51.9; H, 6.8; N, 21.0.

Z-Gly-Pro-Arg(NO_2)-Aniline Prepared from Z-Gly-Pro-OH (0.77 g, 2.53 mmol) and H-Arg(NO_2)-NHC_6H_5 [prepared from its Boc derivative (1 g, 2.53 mmol) by TFA treatment followed by TEA treatment] by the mixed anhydride method in the usual manner. Recrystallized from AcOEt–petroleum ether. Yield 1.18 g (80%), mp 113—115 °C, Rf^3 0.67, $[\alpha]_D^{28}$ −49.6° (c = 1.0, MeOH). *Anal.* Calcd for $C_{27}H_{34}N_8O_7 \cdot 1/2H_2O$: C, 54.8; H, 5.8; N, 18.9. Found: C, 55.0; H, 5.9; N, 18.6.

H-Gly-Pro-Arg-Aniline Prepared from the protected peptide by hydrogenation in a mixture of MeOH and AcOH. The product was purified by CM-cellulose column (2.7 × 19.5 cm) chromatography using $AcONH_4$ buffer (pH 6.8). After repeated lyophilization, the product was converted to its HCl salt by lyophilization from a mixture of 1 N HCl and H_2O. Yield 0.25 g (51%), hygroscopic powder, Rf^2 0.35, $[\alpha]_D^{26}$ −85.0° (c = 1.0, H_2O). *Anal.* Calcd for $C_{19}H_{29}N_7O_3 \cdot 2HCl \cdot 7/4H_2O$: C, 44.9; H, 6.8; N, 19.3. Found: C, 44.6; H, 6.8; N, 18.9. Amino acid ratios in an acid hydrolysate: Gly 1.00; Pro 1.14; Arg 0.94 (average recover 78%).

Z-Arg(Mts)-*p*-Nitroaniline Prepared from Z-Arg(Mts)-OH (3 g, 5 mmol) and *p*-nitroaniline (0.69 g, 5 mmol) by the phosphazo method.[13] The product was purified by silica gel column (2.9 × 25 cm) chromatography using 2% MeOH–$CHCl_3$ as an eluent. Yield 1.65 g (53%), mp 95—97 °C, Rf^5 0.76, $[\alpha]_D^{28}$ +2.0° (c = 1.0, MeOH). *Anal.* Calcd for $C_{29}H_{34}N_6O_7S \cdot 1/2H_2O$: C, 56.2; H, 5.7; N, 13.6. Found: C, 56.7; H, 5.8; N, 13.2.

Z-Gly-Pro-Arg(Mts)-*p*-Nitroaniline Prepared from Z-Gly-Pro-OH (0.67 g, 2.17 mmol) and H-Arg(Mts)-*p*-nitroaniline [prepared from its Z derivative (1.33 g, 2.17 mmol) by HBr–AcOH treatment followed by TEA treatment] by the mixed anhydride method in the usual manner. The product was purified by silica gel column (1.9 × 14.5 cm) chromatography using 1% MeOH–$CHCl_3$ as an eluent. Yield 0.77 g (47%), mp 96—100 °C, Rf^5 0.80, $[\alpha]_D^{28}$ −30.5° (c = 1.0, MeOH). *Anal.* Calcd for $C_{36}H_{44}N_8O_8S \cdot H_2O$: C, 55.2; H, 5.9; N, 14.3. Found: C, 55.8; H, 5.8; N, 13.9.

H-Gly-Pro-Arg-*p*-Nitroaniline Prepared from the protected peptide (0.5 g, 0.64 mmol) by 1 M TFMSA–TFA (13 ml)–thioanisole (0.75 ml) treatment in the usual manner. The product was purified by CM-cellulose column (1.9 × 12 cm) chromatography using $AcONH_4$ buffer (pH 6.8) as an eluent. After repeated lyophilization, the material was converted to its HCl salt by lyophilization from a mixture of H_2O and 1 N HCl. Yield 0.21 g (64%), hygroscopic powder, Rf^2 0.45, $[\alpha]_D^{26}$ −33.4° (c = 1.0, H_2O). *Anal.* Calcd for $C_{19}H_{28}O_5N_8 \cdot 2HCl \cdot 3/2H_2O$: C, 41.6; H, 6.1; N, 20.4. Found: C, 41.3; H, 6.3; N, 20.2. Amino acid ratios in an acid hydrolysate: Gly 1.00; Pro 1.04; Arg 1.03 (average recovery 72%).

Z-Gly-Sar-OH Prepared from Z-Gly-ONp (2.16 g, 6.54 mmol) and H-Sar-OH (0.58 g, 6.54 mmol). The product was purified by silica gel column (1.8 × 21.3 cm) chromatography using 1% MeOH–$CHCl_3$ as an eluent. Yield 1.14 g (62%), amorphous powder, Rf^5 0.60. *Anal.* Calcd for $C_{13}H_{16}N_2O_5$: C, 55.7; H, 5.8; N, 10.0. Found: C, 55.4; H, 5.9; N, 9.7.

Z-Gly-Sar-Arg(NO_2)-OBzl Prepared from Z-Gly-Sar-OH (0.96 g, 3.42 mmol) and H-Arg(NO_2)-OBzl·TosOH (1.65 g, 3.42 mmol) in DMF by the mixed anhydride method in the usual manner. The product was purified by silica gel column (1.8 × 21 cm) chromatography using 3% MeOH–$CHCl_3$ as an eluent. Yield 1.04 g (53%), mp 72—75 °C, Rf^3 0.66, $[\alpha]_D^{25}$ −14.8° (c = 1.0, MeOH). *Anal.* Calcd for $C_{26}H_{34}N_7O_8$: C, 54.5; H, 6.0; N, 17.1. Found: C, 54.4; H, 6.1; N, 16.8.

H-Gly-Sar-Arg-OH Prepared from the protected peptide (0.5 g, 0.87 mmol) in MeOH by hydrogenation. The product was purified by CM-cellulose column (1.7 × 12 cm) chromatography using $AcONH_4$ buffer (pH 6.8) and converted to its HCl salt by lyophilization from a mixture of 1 N HCl and H_2O. Yield 0.17 g (54%), hygroscopic powder, Rf^2 0.33, $[\alpha]_D^{26}$ −9.6° (c = 1.0, H_2O). *Anal.* Calcd for $C_{11}H_{22}N_6O_4 \cdot 2HCl \cdot 3/2H_2O$: C, 32.8; H, 6.8; N, 20.9. Found: C, 32.7; H, 6.6; N, 21.0. Amino acid ratios in an acid hydrolysate: Gly 1.00; Sar 0.89; Arg 0.92 (average recovery 89%).

Acknowledgement This work was supported in part by The Science Research Promotion Fund of the Japan Private School Promotion Foundation.

References and Notes

1) *a*) Part XII: K. Kawasaki, K. Hirase, T. Tsuji, M. Miyano and M. Iwamoto, *Thrombosis Res.*, **56**, 757 (1989); *b*) Standard abbreviations for amino acids, protecting groups and peptides are used [*Eur. J. Biochem.*, **138**, 9 (1984)]; other abbreviations include DMF = dimethylformamide, Mts = mesitylenesulfonyl, TFA = trifluoroacetic acid, TFMSA = trifluoromethanesulfonic acid, TEA = triethylamine, DCC = dicyclohexylcarbodiimide, HOBt = 1-hydroxybenzotriazole, ONp = *p*-nitrophenyl, FTC = fibrinogen–thrombin clotting, N^G = the nitrogen of a guanidino group, NMM = *N*-methylmorpholine.
2) A. P. Laudano and R. F. Doolittle, *Proc. Natl. Acad. Sci. U.S.A.*, **75**, 3085 (1978).
3) M. Bergmann and L. Zervas, *Chem. Ber.*, **65**, 1192 (1932).
4) D. S. Tarbell, T. Yamamoto and B. M. Pope, *Proc. Natl. Acad. Sci. U.S.A.*, **69**, 730 (1972).
5) H. Yajima, M. Takeyama, J. Kanaki and K. Mitani, *J. Chem. Soc., Chem. Commun.*, **1978**, 482.
6) M. Bergmann, L. Zervas and H. Rinke, *Z. Physiol. Chem.*, **224**, 40 (1934).
7) J. Ramachandran and C. H. Li, *J. Org. Chem.*, **28**, 173 (1963).
8) J. R. Vaughan, Jr. and R. L. Osato, *J. Am. Chem. Soc.*, **74**, 676 (1952).
9) G. W. Anderson, J. E. Zimmerman and F. M. Callahan, *J. Am. Chem. Soc.*, **86**, 1839 (1964).
10) H. Yajima, N. Fujii, H. Ogawa and H. Kawatani, *J. Chem. Soc., Chem. Commun.*, **1974**, 107.
11) *a*) H. G. Khorana, *J. Chem. Soc.*, **1952**, 2081; *b*) J. C. Sheehan and G. P. Hess, *J. Am. Chem. Soc.*, **77**, 1067 (1955).
12) *a*) B. Halpern, L. F. Chew and B. Weinstein, *J. Am. Chem. Soc.*, **89**, 5051 (1967); *b*) B. Weinstein and A. E. Pritchard, *J. Chem. Soc., Perkin Trans. 1*, **1972**, 1015.
13) S. Goldschmidt and G. Rosculet, *Chem. Ber.*, **93**, 2387 (1960).
14) M. Iwamoto and B. Blombach, *Thrombo. Res.*, **33**, 427 (1984).
15) T. Shioiri, K. Ninomiya and S. Yamada, *J. Am. Chem. Soc.*, **94**, 6203 (1972).
16) *a*) T. Yamada, K. Suegane, S. Kuwata and H. Watanabe, *Bull. Chem. Soc. Jpn.*, **50**, 1088 (1977); *b*) K. Khodadadeh, K. Heppenheimer and E. R. Heidemann, *Makromol. Chem.*, **178**, 1897 (1977).
17) W. Konig and R. Geiger, *Chem. Ber.*, **103**, 788 (1970).
18) H. Otsuka, K. Inouye, M. Nakayama and F. Shinozaki, *Bull. Chem. Soc. Jpn.*, **39**, 882 (1966).
19) L. Zervas, D. Borovas and E. Gazis, *J. Am. Chem. Soc.*, **85**, 3660 (1963).

A Novel Glycoside Anomerization Catalyzed by Trimethylsilyl Bromide and Zinc Bromide in Combination

Kunio HIGASHI,* Kiyoshi NAKAYAMA, Kouichi UOTO, Emiko SHIOYA, and Tsuneo KUSAMA*

Research Institute, Daiichi Pharmaceutical Co., Ltd., 16–13, Kitakasai 1-chome, Edogawa-ku, Tokyo 134, Japan. *Received August 22, 1990*

A novel glycoside anomerization occurred when trimethylsilyl bromide (TMSBr) and zinc bromide were utilized in combination as a catalyst. Treatment of β-glycosides with TMSBr and zinc bromide in the presence of alcohols afforded anomerized products in good yields.

Keywords glycoside anomerization; trimethylsilyl halide; zinc halide; glucosamine; Lewis acid

In our preceding paper,[1] we reported the stereoselective glycosidation of **4** and **2a—d** to afford β-anomers (**1a—d**) by the combined use of trityl chloride (TrCl) and zinc chloride as an activator. When a zinc halide was used alone as an activator, only the α-anomers (**3a—d**) were obtained. These results suggest that the presence of TrCl may inhibit the anomerization of β-anomers (**1a—d**), and so we investigated the mechanism of the anomerization. We now report a novel glycoside anomerization catalyzed by a combination of trimethylsilyl bromide (TMSBr) and zinc bromide.

It is well known that glycoside anomerization proceeds in the presence of Lewis acids such as $TiCl_4$, $AlCl_3$, $ZnCl_2$, $SnCl_2$, $BF_3 \cdot Et_2O$, *etc.*[2] When the β-anomer (**1a**) was treated with Lewis acids such as $AgClO_4$, $ZnCl_2$ or $ZnBr_2$ in the presence of **2a**, however, no reaction occurred and the starting material was recovered (see Table I, run 1). Since the anomerization was thought to take place in the reaction system for the glycosidation of **4** and **2a** using $AgClO_4$, $ZnCl_2$ or $ZnBr_2$, we became interested in the anomerization mechanism.

Hydrogen bromide (HBr) would probably be formed during the glycosidation of **4** and **2a**, and so we anticipated that the resulting proton acid would participate in the anomerization.[2] Attempted anomerization of the β-anomer (**1a**) with HBr, however, resulted in the recovery of the starting material. After investigation of the reaction conditions, the anomerization was proved to take place in the presence of both HBr and Lewis acid. Thus, when the β-anomer (**1a**) was treated with $ZnBr_2$ in the presence of HBr in dichloromethane for 3 h at room temperature, the α-anomer (**3a**) was obtained in 50% yield along with the bromide (**4**)[3] in 34% yield (Table I, run 2). It must be emphasized that the presence of both HBr and Lewis acid is necessary for the anomerization to proceed. These results suggest that an active species generated from HBr and $ZnBr_2$ acts as a catalyst on the anomerization.[4]

Since the combination of HBr and Lewis acid was found to act as a catalyst on the anomerization, we searched for milder reaction conditions. We anticipated that TMSBr and $ZnBr_2$ in combination should also act as a catalyst.[5] Treatment of **1a** with TMSBr (1.5 eq) and $ZnBr_2$ (1.5 eq) in dichloromethane at room temperature for 20 h afforded the anomerized product (**3a**) in 54% yield along with the 1-bromo sugar (**4**) (Table I, run 3). When the reaction was carried out in the presence of 1 eq of the alcohol (**2a**) for

TABLE I. Anomerization of **1a—e** Catalyzed by the Combined Use of Trimethylsilyl Halide and Zinc Halide

Run	Substrate	Catalyst	Alcohol (eq)	Time[a] (h)	Products (% yield[b])
1	**1a**	$ZnBr_2$	**2a** (1.0)	24	—[c]
2	**1a**	$ZnBr_2$–HBr	**2a** (0)	3	**3a** (50), **4** (34)
3	**1a**	$ZnBr_2$–TMSBr	**2a** (0)	20	**3a** (54), **4** (10)
4	**1a**	$ZnBr_2$–TMSBr	**2a** (1.0)	4	**3a** (97)
5	**1a**	$ZnCl_2$–TMSCl	**2a** (1.0)	48	**3a** (34), **5** (38)
6	**1a**	TMSBr	**2a** (1.0)	24	—[c]
7	**1b**	$ZnBr_2$–TMSBr	**2b** (1.0)	1	**3b** (88)
8	**1c**	$ZnBr_2$–TMSBr	**2c** (1.0)	1	**3c** (88)
9	**1d**	$ZnBr_2$–TMSBr	**2d** (1.0)	24	**3d** (75), **4** (6)
10	**1e**	$ZnBr_2$–TMSBr	**2e** (1.0)	24	**3e** (71), **4** (5)

a) All reactions were carried out in dichloromethane at room temperature. *b*) Isolated yield. *c*) No reaction occurred, and the starting material (**1a**) was recovered.

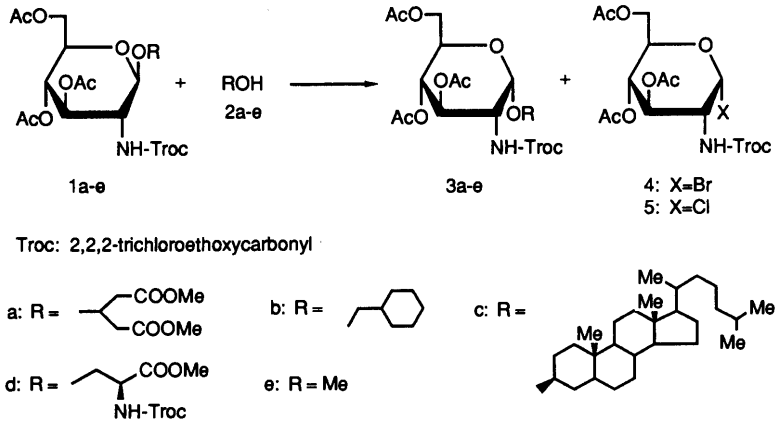

Chart 1

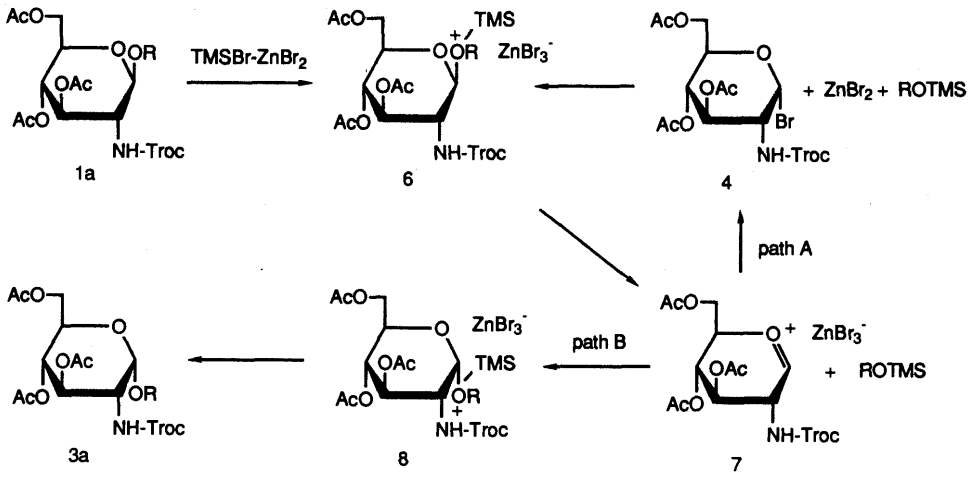

Chart 2

4h at room temperature, **3a** was obtained in 97% yield (Table I, run 4). Anomerization of **1a** with a large excess of $ZnCl_2$ and trimethylsilyl chloride (TMSCl) afforded **3a** and the 1-chloro sugar (**5**) in 34% and 38% yields, respectively (Table I, run 5). No reaction occurred when **1a** was treated with TMSBr alone (Table I, run 6).[6] Attempted anomerization of the α-anomer (**3a**) to the β-anomer (**1a**) by the combined use of TMSBr and $ZnBr_2$ resulted in the recovery of the starting material (**3a**).

A possible mechanism for the anomerization of **1a** to **3a** catalyzed by TMSBr and $ZnBr_2$ is shown in Chart 2. Thus, an oxonium salt (**6**), formed by the reaction of **1a** and the active species generated from TMSBr and $ZnBr_2$, collapses to **7** with liberation of the trimethylsilyl ether. Next, the reaction may proceed *via* two pathways. The bromide (**4**) was presumed to have been formed by bromination of the intermediate (**7**) with the resulting activated brominium anion (path A). Formation of the thermodynamically more stable anomerized compound (**3a**) would be accounted for by the conversion of **7** to an intermediate (**8**) by the attack of the ROTMS from the α side, followed by the liberation of TMSBr (path B). When the alcohol (**2a**) is present in the reaction system, path B is considered to be predominant from the above experimental results (Table I, run 4).

The success of the glycoside anomerization using TMSBr and $ZnBr_2$ prompted us to apply this methodology to other glycosides (**1b**—**e**).[1,7] The results are summarized in Table I. All the anomerization reactions of β-anomers (**1b**—**e**) with TMSBr and $ZnBr_2$ in the presence of alcohols (**2b**—**c**) afforded anomerized products (**3b**—**e**) in good yield (Table I, runs 7—10).

In summary, a novel anomerization occurred when the combination of TMSBr and $ZnBr_2$ was utilized as a catalyst. The reaction conditions were extremely mild, so this new method should be widely applicable in carbohydrate chemistry.

Experimental

Melting points were determined on a Yanagimoto melting point apparatus, and are uncorrected. Infrared (IR) spectra were taken on a Hitachi 270-30 infrared spectrophotometer. Proton nuclear magnetic resonance (^{1}H-NMR) spectra were obtained in deuteriochloroform on a JEOL GSX 500 spectrometer (500 MHz). Chemical shifts are reported in parts per million relative to tetramethylsilane (δ units) as an internal standard. Optical rotations were measured with a Horiba SEDA 200 polarimeter. Column chromatography was performed with Merck Silica gel 60 (70—230 mesh).

Anomerization of 1a with Combined Use of HBr and Zinc Bromide A mixture of **1a** (40 mg, 0.063 mmol), $ZnBr_2$ (14 mg, 0.063 mmol) and 0.17 N HBr–dichloromethane (1 ml) was stirred for 3 h at room temperature. The reaction mixture was diluted with AcOEt and washed with 5% $NaHCO_3$ and water, dried over $MgSO_4$, and concentrated *in vacuo*. The residue was chromatographed on silica gel (10 g) using chloroform–acetone (50 : 1) to give 12 mg (34%) of the bromide (**4**) and 20 mg (50%) of **3a**, as oils, in order of elution. The NMR spectra of **4** and **3a** were identical with those of authentic samples.[1]

Anomerization of 1a with Combined Use of TMSBr and Zinc Bromide A mixture of **1a** (85 mg, 0.13 mmol), TMSBr (30 mg, 0.20 mmol) and $ZnBr_2$ (44 mg, 0.20 mmol) in dichloromethane (2 ml) was stirred for 20 h at room temperature. The reaction mixture was diluted with AcOEt, washed with 5% $NaHCO_3$ and water, dried over $MgSO_4$, and concentrated *in vacuo*. The residue was chromatographed on silica gel (20 g) using chloroform–acetone (50 : 1) to give 46 mg (54%) of **3a**, as a colorless oil.

Anomerization of 1a with Combined Use of TMSCl and Zinc Chloride A mixture of **1a** (125 mg, 0.20 mmol), the alcohol **2a** (35 mg, 0.20 mmol), TMSCl (1 ml, 6.50 mmol) and zinc chloride (300 mg, 2.20 mmol) in dichloromethane (2 ml) was stirred for 24 h at room temperature. The reaction mixture was diluted with AcOEt, washed with 5% $NaHCO_3$ and water, dried over $MaSO_4$, and concentrated *in vacuo*. The residue was chromatographed on silica gel (20 g) using chloroform–acetone (50 : 1) to give 37 mg (38%) of **5** and 42 mg (34%) of **3a**, as colorless oils, in order of elution.

5: ^{1}H-NMR δ: 2.05 (3H, s, $OCOCH_3$), 2.08 (3H, s, $OCOCH_3$), 2.11 (3H, s, $OCOCH_3$), 4.13 (2H, m, H-5, H-2), 4.27 (1H, m, H-2), 4.33 (1H, dd, J=13.0, 4.0 Hz, H-6), 4.66 (1H, d, J=11.9 Hz, $COOCH_2CCl_3$), 4.81 (1H, d, J=11.9 Hz, $COOCH_2CCl_3$), 5.24 (1H, t, J=9.0 Hz, H-4), 5.37 (1H, m, H-3), 6.53 (1H, d, J=4.0 Hz, H-1), 6.80 (1H, br, NH).

Typical Procedure for Anomerization with Combined Use of TMSBr and Zinc Bromide in the Presence of the Alcohol A mixture of **1a** (125 mg, 0.20 mmol), the alcohol **2a** (27 mg, 0.15 mmol), TMSBr (46 mg, 0.31 mmol) and zinc bromide (75 mg, 0.31 mmol) in dichloromethane (2 ml) was stirred for 4 h at room temperature. The reaction mixture was diluted with AcOEt, washed with 5% $NaHCO_3$ and water, dried over $MgSO_4$, and concentrated *in vacuo*. The residue was chromatographed on silica gel (20 g) using chloroform–acetone (50 : 1) to give 121 mg (97%) of **3a**, as a colorless oil.

Compound **3e** was prepared from **1e**[7] according to the typical procedure described above. **3a**: mp 119—124 °C. $[\alpha]_D^{25}$ +64.7° (c=1.45, $CHCl_3$). *Anal.* Calcd for $C_{16}H_{22}Cl_3NO_{10}$: C, 38.85; H, 4.48; N, 2.83. Found: C, 38.90; H, 4.59; N, 2.97. IR (KBr): 3376, 1755, 1554, 1452, 1374, 1230, 1170 cm^{-1}. ^{1}H-NMR δ: 2.00, 2.03, 2.10 (each 3H, s, $OCOCH_3$), 3.43 (3H, s, OCH_3), 3.96 (1H, ddd, J=10.0, 4.0, 2.0 Hz, H-5), 4.06 (1H, dd, J=10.0, 3.0 Hz, H-2), 4.11 (1H, dd, J=12.0, 2.0 Hz, H-6), 4.26 (1H, dd, J=12.0, 4.0 Hz, H-6), 4.63 (1H, d, J=11.9 Hz, $COOCH_2CCl_3$), 4.78 (1H, d, J=3.0 Hz, H-1), 4.81 (1H, d, J=11.9 Hz, $COOCH_2CCl_3$), 5.11 (1H, t, J=10.0 Hz, H-4), 5.26 (1H, t, J=10.0 Hz, H-3), 5.26 (1H, d, J=10.0 Hz, NH).

References and Notes

1) K. Higashi, K. Nakayama, T. Soga, E. Shioya, K. Uoto, and T.

Kusama, *Chem. Pharm. Bull.*, **38**, 3280 (1990).
2) *a*) W. G. Overend, "The Carbohydrates," ed. by W. Pigman and D. Horton, Academic Press, New York, 1972, Vol. I, pp. 310—316, and references therein; *b*) R. U. Lemieux, *Adv. Carbohydr. Chem.*, **9**, 1 (1954); *c*) R. U. Lemieux and W. P. Shyluk, *Can. J. Chem.*, **33**, 120 (1955); *d*) E. Pacsu, J. Janson, and B. Lindberg, *Methods Carbohydr. Chem.*, **2**, 376 (1963); *e*) R. D. Guthrie and J. F. McCarthy, *Adv. Carbohydr. Chem.*, **22**, 11 (1967); *f*) J. Conchie, G. A. Levvy, and C. A. Marsh, *ibid.*, **12**, 157 (1957); *g*) C. T. Bishop and K. P. Cooper, *Can. J. Chem.*, **40**, 224 (1962); *h*) *Idem*, *ibid.*, **41**, 2743 (1963); *i*) I. Augstad and E. Berner, *Acta. Chem. Scand.*, **8**, 251 (1955); *j*) R. R. Schmidt and M. Stumpp, *Justus Liebigs Ann. Chem.*, **1984**, 680; *k*) R. R. Schmidt, *Angew. Chem., Int. Ed. Engl.*, **25**, 212 (1986).
3) M. Imoto, H. Yoshimura, T. Shimamoto, N. Sakaguchi, S. Kusumoto, and T. Shiba, *Bull. Chem. Soc. Jpn.*, **60**, 2205 (1987).
4) In the case of glycosidation of **4** and **2a—d** by the combined use of TrCl and zinc chloride, it was presumed that the generation of an active species from HBr and zinc chloride was inhibited by the presence of TrCl and hence on anomerization occurred, giving the β-anomers (**1a—d**) with high stereoselectivity.
5) *a*) N. Iwasawa and T. Mukaiyama, *Chem. Lett.*, **1987**, 463; *b*) Y. Ukaji, N. Koumoto, and T. Fujisawa, *ibid.*, **1989**, 1623.
6) J. Thiem and S. Kopper, *J. Carbohydr. Chem.*, **2**, 75 (1983), and references therein.
7) K. Higashi, K. Nakayama, E. Shioya, and T. Kusama, unpublished work. Compound **1e** was prepared in two steps from 2-deoxy-2-(2,2,2-trichloroethoxycarbonylamino)-D-glucose. The details of the synthesis of **1e** will be reported at a later date.

Constituents of *Ephemerantha lonchophylla*; Isolation and Structure Elucidation of New Phenolic Compounds, Ephemeranthol-A, Ephemeranthol-B, and Ephemeranthoquinone, and of a New Diterpene Glucoside, Ephemeranthoside[1)]

Yasuhiro TEZUKA,[a] Hiroyuki HIRANO,[a] Tohru KIKUCHI,*[,a] and Guo-Jun XU[b]

Research Institute for Wakan-Yaku (Oriental Medicines), Toyama Medical and Pharmaceutical University,[a] 2630 Sugitani, Toyama 930-01, Japan and China Pharmaceutical University,[b] 24 Tonjiaxian, Nanjing, China. *Received August 31, 1990*

Constituents of *Ephemerantha lonchophylla* (HOOK. f.) P. F. HUNT *et* SUMMERH, which is used as a source plant of the Chinese crude drug "Shi-Hu", were examined and four new phenolic compounds, 3-*O*-methylgigantol (2), ephemeranthoquinone (3), ephemeranthol-A (5), and ephemeranthol-B (7), and a new diterpene glucoside named ephemeranthoside (9) were isolated along with four known compounds, denbinobin (1), 4,7-dihydroxy-2,3-dimethoxyphenanthrene (4), erianthridin (6), and gigantol (8). The structures of the new compounds were determined on the basis of spectroscopic data.

Keywords *Ephemerantha lonchophylla*; Orchidaceae; 3-*O*-methylgigantol; ephemeranthol; ephemeranthoquinone; dihydrophenanthrene; dihydrophenanthraquinone; dihydrostilbene; ephemeranthoside; pimarane-type diterpene glucoside

The Chinese crude drug "Shi-Hu (石斛)" is prepared from the dried stems of *Dendrobium nobile* and several other *Dendrobium* species (Orchidaceae), and is used as a tonic and an antipyretic.[2)] *Ephemerantha lonchophylla* and *Pholidota yunnanensis* are also used as sources of "Shi-Hu".[3)] Constituents of *Dendrobium* plants have been examined by several groups of authors and sesquiterpene alkaloids,[4)] sesquiterpenes,[5)] steroid glycosides,[6)] fluorenones,[7)] phenanthrenes,[8)] dihydrophenanthrenes,[9)] and dihydrostilbenes[10)] have been identified so far. As to *Ephemerantha* species, however, only one report has been published by Niwa, *et al.*,[11)] who reported the isolation and structure elucidation of *cis*-clerodane-type diterpene lactones from *E. comata*. Recently, we have examined the constituents of *Ephemerantha lonchophylla* (HOOK. f.) P. F. HUNT *et* SUMMERH and isolated four new phenolic compounds, named 3-*O*-methylgigantol (**2**), ephemeranthoquinone (**3**), ephemeranthol-A (**5**), and ephemeranthol-B (**7**), and a new diterpene glycoside, ephemeranthoside (**9**), along with four known phenolic compounds (**1**, **4**, **6**, and **8**). This paper deals with the the isolation and the structure elucidation of these compounds.

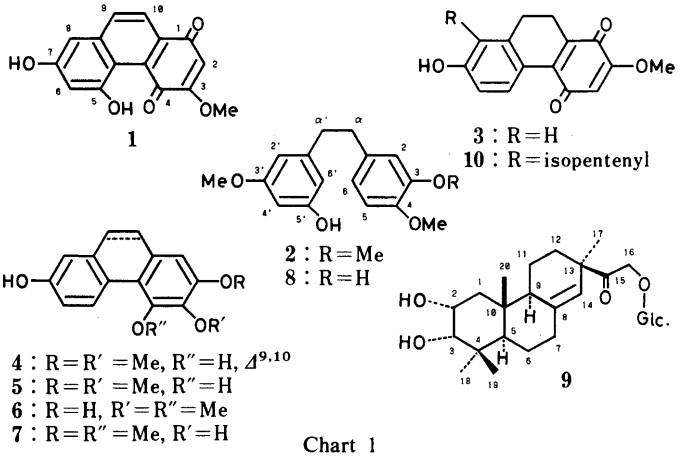

Chart 1

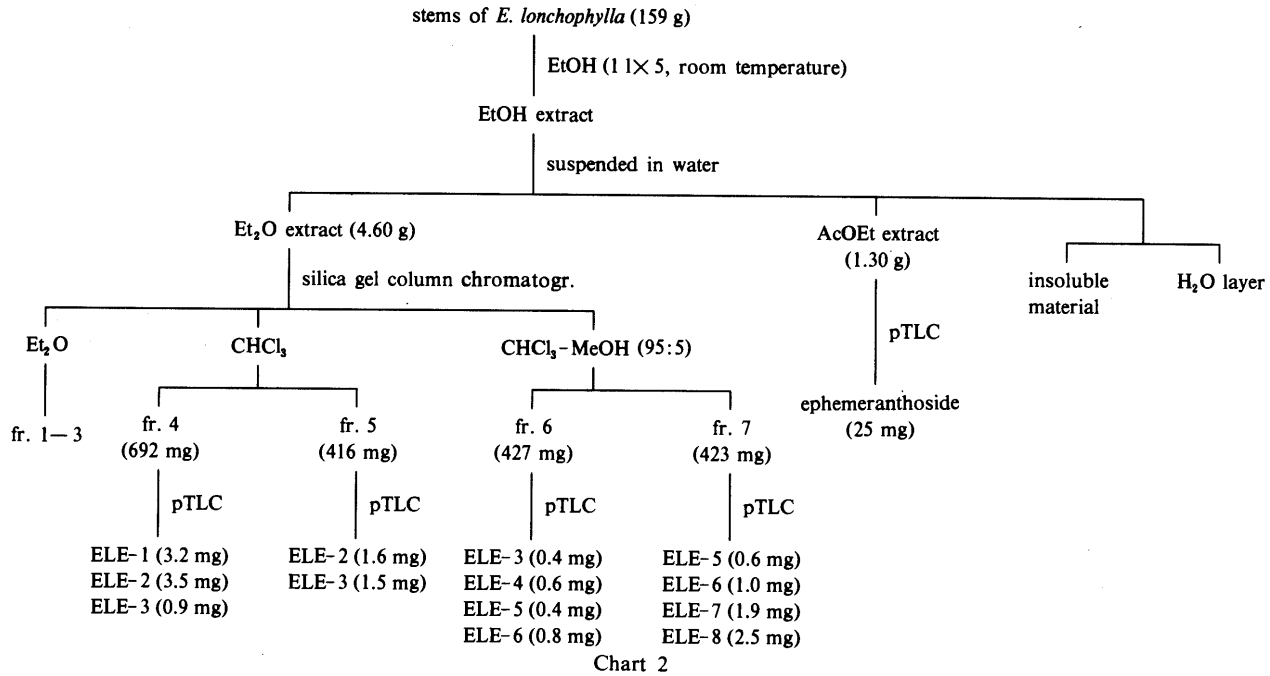

Chart 2

Stems of *Ephemerantha lonchophylla* were extracted with ethanol at room temperature and the extract was concentrated *in vacuo*, suspended in water, and extracted successively with ether and ethyl acetate (Chart 2). The ether extract was separated by a combination of silica gel column chromatography and preparative thin-layer chromatography (TLC) to give eight phenolic compounds (ELE-1 to ELE-8), while the ethyl acetate extract was subjected to preparative TLC to give a new diterpene glycoside designated as ephemeranthoside. Among these, four compounds, ELE-1, ELE-4, ELE-6, and ELE-8, were identified as denbinobin (5-hydroxy-3,7-dimethoxyphenanthrene-1,4-quinone, **1**),[8a] 4,7-dihydroxy-2,3-dimethoxyphenanthrene (**4**),[12] erianthridin (2,7-dihydroxy-3,4-dimethoxy-9,10-dihydrophenanthrene, **6**),[13] and gigantol (3',4-dihydroxy-3,5'-dimethoxydihydrostilbene, **8**),[14] respectively, based on the spectral data.

TABLE I. ^{1}H-NMR Data for Dihydrostilbenes Obtained from *E. lonchophylla* in $CDCl_3$

	Compd.	
	2	**8**
2-H	6.66 d (2)	6.62 d (2)
5-H	6.79 d (8)	6.83 d (8)
6-H	6.72 dd (8, 2)	6.68 dd (8, 2)
α,α'-H_4	2.82 m	2.81 m
2'-H	6.25 d (2)	6.25 d (2)
4'-H	6.32 t (2)	6.32 t (2)
6'-H	6.25 d (2)	6.25 d (2)
3-OCH_3	3.84 s	3.85 s
4-OCH_3	3.85 s	
3'-OCH_3	3.75 s	3.75 s
OH	—	4.71 s
		5.46 s

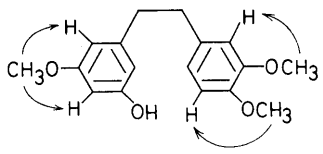

Chart 3

ELE-2 (**2**) was obtained as a colorless amorphous solid and determined to have the molecular formula $C_{17}H_{20}O_4$ (*m/z* 288) by mass spectral (MS) and high-resolution MS (HR-MS) measurements. Its ultraviolet (UV) and infrared (IR) spectra were closely similar to those of gigantol (**8**). The proton nuclear magnetic resonance (^{1}H-NMR) spectrum (Table I) was also almost superimposable on that of **8** except for the appearance of three methoxyl signals (δ 3.75, 3.84, and 3.85) instead of two in **8** (δ 3.75 and 3.85).

From these spectral data and the results of difference nuclear Overhauser effect (NOE) experiments (Chart 3), ELE-2 was determined to be 3-*O*-methylgigantol (5'-hydroxy-3,3',4-trimethoxydihydrostilbene) (**2**). Further, this conclusion was supported by the MS, which showed fragment ions at *m/z* 151 and 137 formed by benzylic fission.

Ephemeranthoquinone (ELE-3, **3**), a red amorphous solid, $C_{15}H_{12}O_4$, showed UV absorptions at λ 262, 330, and 495 nm (log ε 4.03, 3.73, and 3.39) and IR absorptions at ν 3576, 3386 (br, OH), 1645, 1631 (chelated quinone CO), 1611, 1560, and 1459 cm^{-1} (benzene ring). The ^{1}H-NMR spectrum of **3** showed a signal at δ 2.73 (m) corresponding to four protons, which were assignable to 9- and 10-H_2 of dihydrophenanthrenes,[15] and signals due to a 1,2,4-trisubstituted benzene ring, an isolated olefinic proton, a methoxyl group, and a hydroxyl group (Table II). Irradiation of the methyl protons at δ 3.85 gave an NOE enhancement of the olefinic proton signal at δ 5.92 and *vice versa*, indicating a vicinal orientation of these groups. These spectral data closely resembled those of spiranthoquinone (**10**),[1] obtained from *Spiranthes sinensis* var. *amoena* (Orchidaceae), and the ^{1}H-signals due to the methoxyl group and the isolated olefinic proton had the same chemical shifts as those of **10**. From these data, ephemeranthoquinone was concluded to be 7-hydroxy-2-methoxy-9,10-dihydrophenanthrene-1,4-quinone (**3**).

Ephemeranthol-A (ELE-5, **5**) and ephemeranthol-B (ELE-7, **7**) were obtained as amorphous solids and their molecular formulae were determined to be $C_{16}H_{16}O_4$ by MS and HR-MS measurements. They showed UV and IR spectra similar to those of erianthridin (**6**) and the ^{1}H-NMR spectra were also closely similar to that of **6** (Table II),

TABLE II. ^{1}H-NMR Data for the Phenolic Compounds Obtained from *E. lonchophylla* in $CDCl_3$

	1	**4**	**3**	**10**	**5**	**6**	**7**
1-H		7.07 s			6.39 s	6.62 s	6.57 s
2-H	6.16 s						
3-H			5.92 s	5.92 s			
5-H		9.33 d (9)	8.01 d (9)	7.82 d (8.9)	8.22 d (8.5)	8.13 d (8.5)	8.16 d (8)
6-H	6.94 d (2.5)	7.18 dd (9, 3)	6.76 dd (9, 2.5)	6.76 d (8.9)	6.74 dd (8.5, 3)	6.73 dd (8.5, 3)	6.74 dd (8, 3)
8-H	6.83 d (2.5)	7.21 d (3)	6.72 d (2.5)		6.71 d (3)	6.70 d (3)	6.71 d (3)
9-H(H_2)	8.08 d (8.5)	7.48 d (9)	2.73 m	2.76 m	2.74 m	2.69 m	2.72 m
10-H(H_2)	8.14 d (8.5)	7.57 d (9)		2.67 m			
2-OCH_3		4.05 s	3.85 s	3.85 s	3.89 s		3.91 s
3-OCH_3	3.96 s	3.95 s			3.93 s	3.97 s	
4-OCH_3						3.74 s	3.70 s
7-OCH_3	3.94 s						
OH	10.74 s	4.98 br s	5.16 br s	5.45 br s	—	4.70 br s	4.80 br s
		5.98 s				5.70 br s	5.58 s
1'-H_2				3.42 d			
2'-H				5.10 tqq			
4'-H_3				1.83 br s			
5'-H_3				1.72 d			

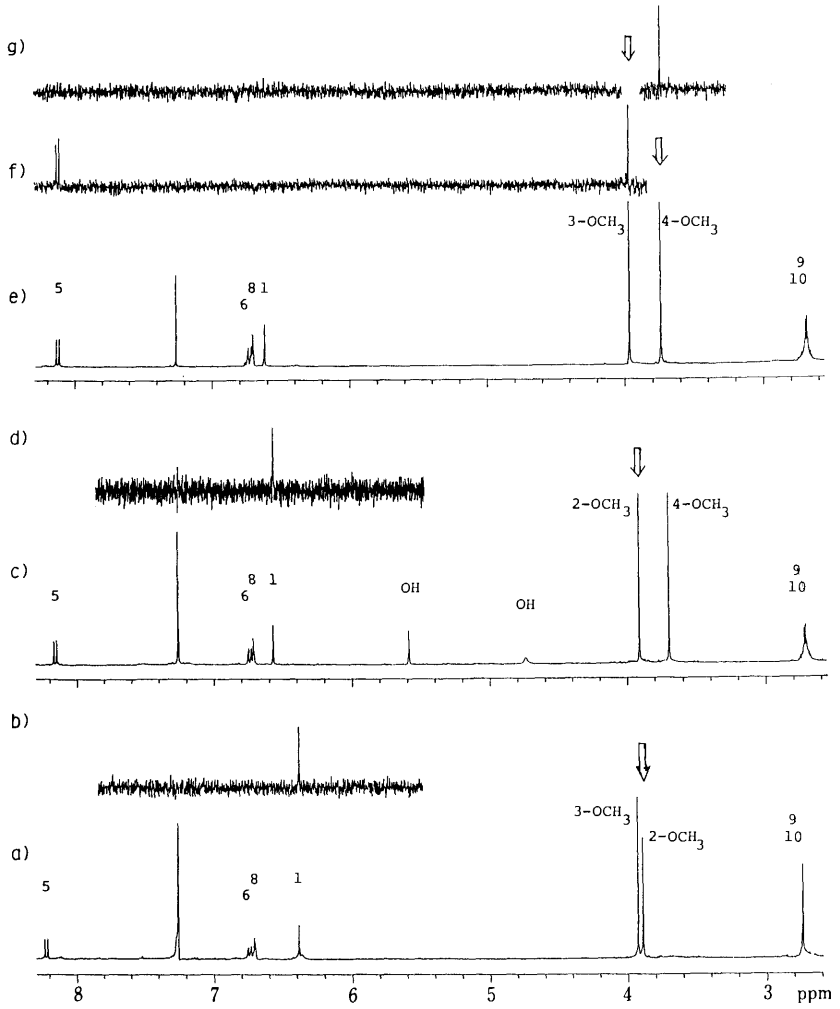

Fig. 1. Difference NOE Spectra of Ephemeranthol-A (**5**), Erianthridin (**6**), and Ephemeranthol-B (**7**)

a,c, e) Control spectra of **5**, **7**, and **6**, respectively. b) Difference NOE spectrum of **5**. d) Difference NOE spectrum of **7**. f, g) Difference NOE spectra of **6**.

suggesting that both **5** and **7** may be analogous compounds to **6**.

The location of the methoxyl groups was elucidated by means of difference NOE experiments. As shown in Fig. 1, irradiation of the methoxy protons at δ 3.89 in **5** and at δ 3.91 in **7** gave an NOE enhancement of 1-H (δ 6.39 in **5** and δ 6.57 in **7**), indicating the location of these methoxyl groups to be at the C-2 position. Although irradiation of the other methoxy protons in **5** and **7** caused no NOE enhancement, the positions of these methoxyl groups were determined to be at C-3 in **5** and at C-4 in **7** by comparison of their ^{1}H-chemical shifts with those of **6**, whose methoxyl signals could be unambiguously assigned on the basis of difference NOE experiments (Fig. 1).[16]

From the above spectral evidence, ephemeranthol-A and ephemeranthol-B were concluded to be 4,7-dihydroxy-2,3-dimethoxy-9,10-dihydrophenanthrene (**5**) and 3,7-dihydroxy-2,4-dimethoxy-9,10-dihydrophenanthrene (**7**), respectively.

Ephemeranthoside (**9**), colorless powder, $[\alpha]_D^{24}$ $-46.4°$ (MeOH), showed *quasi*-molecular ion peaks at *m/z* 521 $[C_{26}H_{42}O_9+Na]^+$ and 499 $[C_{26}H_{42}O_9+H]^+$ in the positive ion fast atom bombardment MS (FAB-MS) and at *m/z* 497 $[C_{26}H_{42}O_9-H]^-$ in the negative ion FAB-MS. In the IR spectrum, **9** showed strong absorptions due to hydroxyl (ν 3396 cm^{-1}) and carbonyl groups (ν 1716 cm^{-1}) and in the ^{1}H-NMR spectrum it showed signals due to four tertiary methyls (δ 0.73, 0.87, 1.01, and 1.21), an olefinic proton (δ 5.47, br s), and eleven oxygenated methine and/or methylene protons (Table III). The ^{13}C-NMR spectrum of **9** showed signals due to four methyls (δ 15.4, 22.4, 29.4, and 27.0), an olefin (δ 124.6, d and 141.9, s), a carbonyl (δ 210.5), thirteen methylenes, four methines, and three quaternary sp^3 carbons (Table III). Among these, the ^{1}H-signal at δ 5.01 (d, J=7.5 Hz) and the ^{13}C-signal at δ 104.3 (d) were suggestive of the presence of an anomeric methine group. Thus, **9** was thought to be a diterpene monoglycoside.

Detailed analyses of the ^{1}H- and ^{13}C-NMR spectra of **9** with the aid of the ^{1}H–^{1}H and ^{1}H–^{13}C shift correlation spectroscopy (COSY) led us to deduce the partial structures A—E shown in Chart 4.

Next, we measured the ^{1}H-detected heteronuclear multiple-bond multiple-quantum coherence (HMBC) spectrum[17] in order to clarify the connectivities of these partial structures. As shown in Fig. 2, the methyl protons at δ 0.73 (20-H$_3$) showed long-range correlations with the carbons at δ 39.7 (s, C-10), 40.5 (t, C-1), 47.6 (d, C-5), and 50.8 (d, C-9), indicating the carbons C-5, C-9, and C-20 to be connected with the quaternary carbon C-10. The methyl

protons at δ 0.87 (19-H_3) and at δ 1.21 (18-H_3) showed long-range correlations with the carbons at δ 29.4 (q, C-18), 38.7 (s, C-4), 47.6 (C-5), and 79.2 (d, C-3) and at δ 22.4 (q, C-19), 38.7 (C-4), 47.6 (C-5), and 79.2 (C-3), respectively. Thus, the carbons C-5, C-18, and C-19 should be connected with the quaternary carbon C-4. Moreover, the methyl protons at δ 1.01 (17-H_3) showed long-range correlations with the carbons at δ 32.9 (t, C-12), 47.6 (s, C-13), 124.6 (d, C-14), and 210.5 (s, C-15), and thus the carbons C-12, C-14, C-15, and C-17 must be connected with the quaternary carbon C-13. On the other hand, the oxygenated methylene protons at δ 4.95 and 5.06 (each d, J=18 Hz) showed long-range correlations with the carbonyl carbon at δ 210.5 (C-15) and thus it is reasonable to assign this methylene group to C-16. Also, these methylene protons showed long-range correlations with the anomeric carbon at δ 104.3, and, in turn, the anomeric proton at δ 5.01 (d, J=7.5 Hz) showed a long-range correlation with the methylene carbon at δ 71.5 (d, C-16). Therefore, the location of the glucose residue must be at the C-16 position. From these results and other long-range correlations depicted in the structural formula in Fig. 2 by arrows, the planar structure of ephemeranthoside was determined as **9**.

TABLE III. ^{1}H- and ^{13}C-NMR Data for Ephemeranthoside (**9**) in C_5D_5N

Position	δ_H	δ_C	Protons long-range-coupled[a]	
			$^3J_{CH}$	$^2J_{CH}$
1	1.72 dd (12, 4.5)	40.5 t	3, 20	
	1.93 t (12)			
2	4.18 ddd (12, 4.5, 2.5)	66.1 d		1, 3
3	3.73 d (2.5)	79.2 d	18, 19	
4		38.7 s		18, 19
5	1.75 dd (12, 2.5)	47.6 d	1,3,18,19,20	
6	1.27 m	22.0 t		
	1.52 m			
7	2.07 td (14, 5)	35.9 t	14	
	2.29 ddd (14, 4.5, 2)			
8		141.9 s		
9	1.84 dd (10, 7)	50.8 d	1, 14, 20	
10		39.7 s		1, 5, 20
11	1.31 dddd (13.5, 12.5, 10, 3.5)	20.5 t		
	1.54 ddt (13.5, 7, 3.5)			
12	0.97 td (12.5, 3.5)	32.9 t	17	
	2.37 dt (12.5, 3.5)			
13		47.6 s		17
14	5.47 br s	124.6 d	17	
15		210.5 s	17	16
16	4.96 d (18)	71.5 t	1′	
	5.06 d (18)			
17	1.01 s	27.0 q	14	
18	1.21 s	29.4 q	19	
19	0.87 s	22.4 q	5, 18	
20	0.73 s	15.4 q	1, 5	
1′	5.01 d (7.5)	104.3 d	16	
2′	4.11 t (7.5)	75.1 d	4′	
3′	4.23 m	78.3 d		4′
4′	4.26 m	71.3 d	2′	
5′	3.90 m	78.6 d	3′	
6′	4.36 dd (12, 5)	62.5 t		
	4.50 dd (12, 2)			

a) $^2J_{CH}$ and $^3J_{CH}$ indicate the protons coupled with the respective carbons through two and three bonds, respectively, observed in the HMBC spectrum.

In the difference NOE experiments involving irradiation of the methyl protons 17-H_3, 18-H_3, 19-H_3, and 20-H_3, NOE increases were observed at 16-H (δ 5.06) and 14-H (δ 5.47), at 19-H_3, 6-H (δ 1.52), 5-H, and 3-H, at 20-H_3, 18-H_3, 3-H, and 2-H, and at 19-H_3, 1-H (δ 1.72), 2-H, and 16-H (δ 4.96), respectively. From these results and the coupling constants of 2-H (ddd, J=12, 4.5, 2.5 Hz), 3-H (d, J=2.5 Hz), 5-H (dd, J=12, 2.5 Hz), and 9-H (dd, J=10, 7 Hz), the relative stereochemistry of ephemeranthoside (**9**) was determined to be as shown in Chart 1.

Based on the foregoing evidence, and assuming that the glucose residue has the D absolute configuration, the structure of ephemeranthoside was concluded to be 2,3,16-trihydroxy-15-ketopimara-8(14)-ene 16-*O*-β-D-glucopyranoside (**9**). This is the third example of a diterpenoid to have been found in *Orchidaceous* plants.[18]

Experimental

Optical rotation was measured on a JASCO DIP-4 automatic polarimeter at 24°C. UV spectra were obtained with a Shimadzu 202 UV

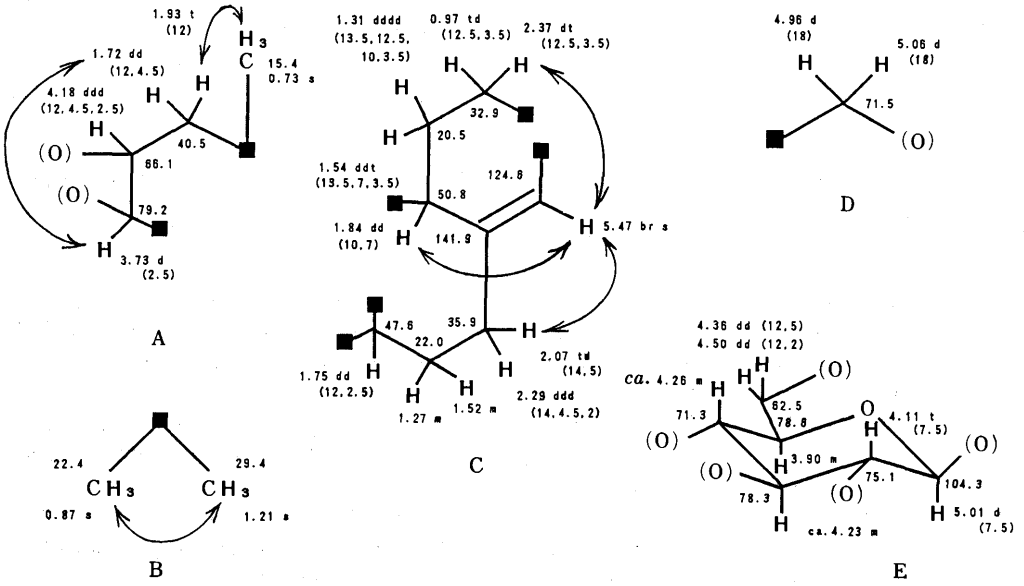

Chart 4. Partial Structures of **9** Obtained from ^{1}H–^{1}H and ^{1}H–^{13}C COSY Data

⌒: Long-range coupling observed in ^{1}H–^{1}H COSY.

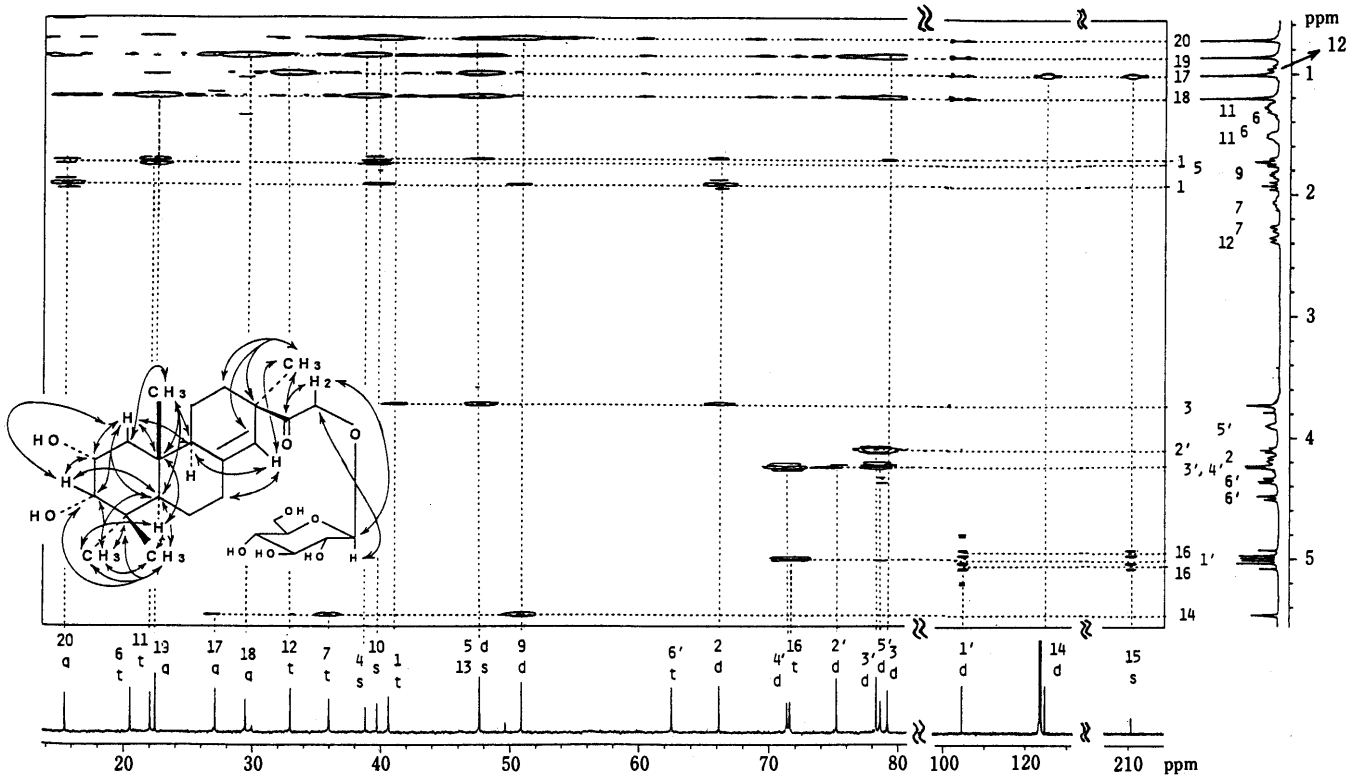

Fig. 2. HMBC Spectrum of **9** in C_5D_5N (Sample, 15 mg; Long-Range J_{CH} = 8.3 Hz; 12 h Run)

spectrometer in EtOH solutions and IR spectra were taken with a Nicolet 5DX FT-IR spectrometer in $CHCl_3$ solutions unless otherwise noted. NMR spectra were measured with a JEOL GX-400 spectrometer with tetramethylsilane as an internal standard, and chemical shifts are recorded in δ values. MS and HR-MS were taken with a JEOL JMS D-300 spectrometer (ionization voltage, 70 eV; accelerating voltage, 3 kV) using a direct inlet system. FAB-MS were measured with a JEOL JMS DX-300 spectrometer (accelerating voltage, 6 kV; neutral gas, Xe; matrix, glycerol) and high-resolution FAB-MS with a JEOL JMS-SX102 spectrometer (accelerating voltage, 10 kV; neutral gas, Xe; matrix, glycerol; standard, PEG-600). Column chromatography was done with Mallinkrodt silica gel and preparative TLC with Merck Kieselgel GF_{254} plates.

The crude drug "Shi-Hu" employed in this study was kindly provided by Tochimoto-tenkaido Co., Ltd. (collected in Guang-Xi Province, China and imported into Japan) and identified as *E. lonchophylla* by one of the present authors (G.-J. Xu).

Extraction and Isolation Air-dried stems of *Ephemerantha lonchophylla* (Hook. f.) P. F. Hunt *et* Summerh (159 g) were cut into small pieces and extracted with ethanol (1 l, 3 h, ×5) at room temperature. After concentration *in vacuo*, the residue was suspended in water and extracted successively with ether and ethyl acetate (each 300 ml ×6) to give an ether extract (4.60 g) and an ethyl acetate extract (1.30 g) along with an insoluble material (640 mg).

The ether extract was chromatographed on a silica gel column and eluted with ether, $CHCl_3$, and $CHCl_3$–MeOH (95:5) to give seven fractions. Fractions 4—7 were subjected separately to preparative TLC (MeOH:$CHCl_3$ = 2:98) to give phenolic compounds ELE-1 (**1**) to ELE-8 (**8**) (Chart 2). On the other hand, the ethyl acetate extract was subjected to preparative TLC (MeOH:$CHCl_3$ = 10:90) to give ephemeranthoside (**9**).

Denbinobin (ELE-1, 1) Dark green amorphous solid. UV λ_{max} nm (log ε): 236 (4.35), 310 (4.17), 408 (3.56). IR ν_{max} cm^{-1}: 3532 (OH), 1646, 1631 (chelated quinone CO), 1618, 1509, 1464, 1438 (benzene ring), 1323, 1239. ^{1}H-NMR: Table II. ^{13}C-NMR ($CDCl_3$) δ: 186.3 (s, C-4), 184.4 (s, C-1), 161.3 (s, C-3), 160.9 (s, C-7), 156.4 (s, C-5), 140.0 (s, C-4a), 137.4 (d, C-9), 132.5 (s, C-10a), 128.7 (s, C-8a), 122.7 (d, C-10), 117.2 (s, C-4b), 108.7 (d, C-8), 107.3 (d, C-2), 101.8 (d, C-6), 56.9 (q, 3-OCH_3), 55.5 (q, 7-OCH_3). MS *m/z* (%): 284 (M^+, 100), 269 (7), 255 (8), 241 (10), 229 (10), 213 (27), 124 (10). HR-MS: Found 284.0694, Calcd for $C_{16}H_{12}O_5$ (M^+) 284.0685.

3-*O*-Methylgigantol (ELE-2, 2) Colorless amorphous solid. UV λ_{max} nm (log ε): 224 (3.85), 265 (3.56), 279 (3.51). IR ν_{max} cm^{-1}: 3576, 3352 (br, OH), 1599, 1516, 1465 (benzene ring), 1156, 1062, 1029. ^{1}H-NMR: Table I. MS *m/z* (%): 288 (M^+, 44), 185 (15), 151 (100), 137 (2.4). HR-MS: Found 288.1375, Calcd for $C_{17}H_{20}O_4$ (M^+) 288.1362; Found 151.0755, Calcd for $C_9H_{11}O_2$ 151.0758; Found 137.0614, Calcd for $C_8H_9O_2$ 137.0603.

Ephemeranthoquinone (ELE-3, 3) Red amorphous solid. UV λ_{max} nm (log ε): 262 (4.03), 330 (3.73), 495 (3.39). IR ν_{max} cm^{-1}: 3576, 3386 (br, OH), 1645, 1631 (quinone CO), 1611, 1560, 1459 (benzene ring), 1359. ^{1}H-NMR: Table II. MS *m/z* (%): 256 (M^+, 100), 241 (39), 171 (28). HR-MS: Found 256.0734, Calcd for $C_{15}H_{12}O_4$ (M^+) 256.0735.

4,7-Dihydroxy-2,3-dimethoxyphenanthrene (ELE-4, 4) Colorless amorphous solid. UV λ_{max} nm (log ε): 233 (4.10), 258 (4.12), 306 sh (3.71). IR ν_{max} cm^{-1}: 3544, 3272 (br, OH), 1671, 1628, 1512, 1477, 1427 (benzene ring), 1292. ^{1}H-NMR: Table II. MS *m/z* (%): 270 (M^+, 100), 255 (65), 223 (17), 212 (12), 184 (17), 155 (17). HR-MS: Found 270.0898, Calcd for $C_{16}H_{14}O_4$ (M^+) 270.0892.

Ephemeranthol-A (ELE-5, 5) Colorless amorphous solid. UV λ_{max} nm (log ε): 212 (4.05), 232 sh (3.81), 280 (3.89), 290 sh (3.81). IR ν_{max} cm^{-1}: 3503, 3312 (br, OH), 1618, 1590, 1498, 1465 (benzene ring). ^{1}H-NMR: Table II. MS *m/z* (%): 272 (M^+, 100), 257 (16), 225 (11), 211 (7), 197 (9), 185 (6), 133 (59). HR-MS: Found 272.1048, Calcd for $C_{16}H_{16}O_4$ (M^+) 272.1049.

Erianthridin (ELE-6, 6) Colorless amorphous solid. UV λ_{max} nm (log ε): 212 (4.08), 281 (3.79). IR ν_{max} cm^{-1}: 3527, 3321 (br, OH), 1616, 1590, 1486, 1459, 1439 (benzene ring), 1355, 1288, 1277. ^{1}H-NMR: Table II. MS *m/z* (%): 272 (M^+, 100), 257 (16), 225 (14), 202 (40), 137 (25). HR-MS: Found 272.1054, Calcd for $C_{16}H_{16}O_4$ (M^+) 272.1049.

Ephemeranthol-B (ELE-7, 7) Colorless amorphous solid. UV λ_{max} nm (log ε): 230 (3.51), 259 (3.48), 273 (3.49), 282 (3.51), 296 sh (3.35), 309 sh (3.22). IR ν_{max} cm^{-1}: 3534, 3288 (br, OH), 1615, 1487, 1465 (benzene ring), 1218, 1078. ^{1}H-NMR: Table II. MS *m/z* (%): 272 (M^+, 100), 257 (25), 239 (4), 225 (8), 214 (8), 211 (7), 197 (13), 169 (5), 157 (6), 137 (8). HR-MS: Found 272.1056, Calcd for $C_{16}H_{16}O_4$ (M^+) 272.1049.

Gigantol (ELE-8, 8) Colorless amorphous solid. UV λ_{max} nm (log ε): 224 (4.21), 280 (3.86). IR ν_{max} cm^{-1}: 3544, 3288 (br, OH), 1600, 1515, 1465, 1432 (benzene ring). ^{1}H-NMR: Table I. MS *m/z* (%): 274 (M^+, 45), 185 (15), 137 (100). HR-MS: Found 274.1210, Calcd for $C_{16}H_{18}O_4$ (M^+) 274.1206; Found 137.0601, Calcd for $C_8H_9O_2$ 137.0602.

Ephemeranthoside (9) Colorless amorphous powder, $[\alpha]_D$ −46.4° (c = 1.0, MeOH). IR ν_{max} (KBr) cm^{-1}: 3396 (br, OH), 1716 (CO), 1078, 1044. ^{1}H- and ^{13}C-NMR: Table III. Positive ion FAB-MS *m/z* (%): 521

$[M+Na]^+$ (19), 499 $[M+H]^+$ (13), 337 [aglycone+H]$^+$ (100), 319 [M+H−glucose]$^+$ (80), 301 [M+H−glucose−H_2O]$^+$ (47). Negative ion FAB-MS *m/z* (%): 497 $[M-H]^-$ (100), 335 [aglycone−H]$^-$ (11). High-resolution FAB-MS: Found 499.2917, Calcd for $C_{26}H_{43}O_9$ $[M+H]^+$ 499.2907.

Acknowledgements The authors are grateful to Tochimoto-tenkaido Co., Ltd. for the gift of the crude drug "Shi-Hu", to Dr. M. Hattori and Mr. Y. Kawata of our Institute for FAB-MS measurements, and to Mr. A. Kusai of JEOL Ltd. for high-resolution FAB-MS measurements. This work was supported in part by a Grant-in-Aid for Scientific Research to T. K. (No. 63870090) from the Ministry of Education, Science and Culture of Japan.

References and Notes

1) This paper is the part X of the series, Studies on the Constituents of Orchidaceous Plants; Part IX: Y. Tezuka, L. Ji, H. Hirano, M. Ueda, K. Nagashima, and T. Kikuchi, *Chem. Pharm. Bull.*, **38**, 629 (1990).
2) Chiang Su New Medicinal College, "Dictionary of Chinese Crude Drugs," Shanghai Scientific Technologic Publisher, Shanghai, 1977, p. 586.
3) M.-F. Li, G.-J. Xu, L.-S. Xu, and R.-L. Jin, *Zhong Cao Yao*, **17**, 465 (1986).
4) S. Yamamura and Y. Hirata, *Nippon Kagaku Zasshi*, **85**, 377 (1964); K. Leander and B. Luning, *Tetrahedron Lett.*, **1968**, 905; Y. Inubushi, Y. Tsuda, T. Konita, and S. Matsumoto, *Chem. Pharm. Bull.*, **16**, 1014 (1968); T. Okamoto, M. Natsume, T. Onaka, F. Uchimaru, and M. Shimizu, *ibid.*, **20**, 418 (1972); and references cited therein.
5) L. Gawell and K. Leander, *Phytochemistry*, **15**, 1991 (1976); J. Dahmen and K. Leander, *ibid.*, **17**, 1949 (1978).
6) D. Behr and K. Leander, *Phytochemistry*, **15**, 1403 (1976).
7) S. K. Talapatra, S. Bose, A. K. Mallik, and B. Talapatra, *Tetrahedron*, **41**, 2765 (1985); P. L. Majumder and J. Chakraborti, *J. Indian Chem. Soc.*, **66**, 834 (1989).
8) *a*) B. Talapatra, P. Mukhopadhyay, P. Chaudhury, and S. K. Talapatra, *Indian J. Chem.*, **21B**, 386 (1982); *b*) P. L. Majumder and R. C. Sen, *ibid.*, **26B**, 18 (1987).
9) P. Veerraju, N. S. P. Rao, L. J. Rao, K. V. J. Rao, and P. R. M. Rao, *Phytochemistry*, **28**, 950 (1989).
10) P. L. Majumder and R. C. Sen, *Phytochemistry*, **26**, 2121 (1987); P. L. Majumder and S. Chatterjee, *ibid.*, **28**, 1986 (1989).
11) M. Niwa, N. Kihira, Y. Hirata, M. Tori, T.-S. Wu, and C.-S. Kuo, *Phytochemistry*, **26**, 3293 (1987).
12) J. Reisch, M. Bathory, K. Szendrei, I. Novak, and E. Minker, *Phytochemistry*, **12**, 228 (1973); R. M. Letcher and K.-M. Wong, *J. Chem. Soc., Perkin Trans. 1*, **1979**, 2449; R. Aquino, I. Behar, F. D. Simone, C. Pizza, and F. Senatore, *Biochem. Syst. Ecol.*, **13**, 251 (1985).
13) P. L. Majumder and M. Joardar, *Indian J. Chem.*, **24B**, 1192 (1985).
14) R. K. Juneja, S. C. Sharma, and J. S. Tandon, *Phytochemistry*, **24**, 321 (1985).
15) A. D. Cross, H. Carpio, and P. Crabbe, *J. Chem. Soc.*, **1963**, 5539; R. M. Letcher and L. R. M. Nhamo, *J. Chem. Soc. (C)*, **1971**, 3070; R. M. Letcher, L. R. M. Nhamo, and I. T. Gumiro, *J. Chem. Soc., Perkin Trans. 1*, **1972**, 206.
16) It was reported that the methoxy protons at C-4 or C-5 in dihydrophenanthrenes and phenanthrenes resonate at relatively higher field. See I. R. C. Bick, J. Harley-Mason, N. Sheppard, and M. J. Vernengo, *J. Chem. Soc.*, **1961**, 1896; M. J. Vernengo, *Experientia*, **19**, 294 (1963); K. Rajaraman and S. Rangaswami, *Indian J. Chem.*, **13**, 1137 (1975); R. Sunder, S. Rangaswami, and G. C. S. Reddy, *Phytochemistry*, **17**, 1067 (1978).
17) A. Bax and M. F. Summers, *J. Am. Chem. Soc.*, **108**, 2093 (1986); M. F. Summers, L. G. Marzilli, and A. Bax, *ibid.*, **108**, 4285 (1986).
18) *cis*-Clerodane-type diterpene lactones, ephemeric acid and ephemeroside, have been isolated from *Ephemerantha comata* (see reference 11). Ephemeranthoside (**9**) is the first example of a pimarane-type diterpenoid to have been found in Orchidaceous plants.

Studies on the Constituents of *Luffa acutangula* ROXB. I. Structures of Acutosides A—G, Oleanane-Type Triterpene Saponins Isolated from the Herb

Tsuneatsu NAGAO, Ryuichiro TANAKA, Yukiko IWASE, Hiroshi HANAZONO and Hikaru OKABE*

Faculty of Pharmaceutical Sciences, Fukuoka University, Nanakuma 8-19-1, Jonan-ku, Fukuoka 814-01, Japan. *Received September 10, 1990*

From the herb of *Luffa acutangula* ROXB. (Cucurbitaceae), seven oleanane-type triterpene saponins, acutosides A—G, were isolated and their structures were determined.

Acutoside A is oleanolic acid 3-*O*-β-D-glucopyranosyl-(1→2)-β-D-glucopyranoside. Acutosides B, D, E, F and G have a common prosapogenin structure, acutoside A, and only differ in the structures of the ester-linked sugar moieties. Acutoside B is a 28-*O*-[*O*-β-D-xylopyranosyl-(1→4)-*O*-α-L-rhamnopyranosyl-(1→2)-α-L-arabinopyranosyl] ester, D is a 28-*O*-[*O*-β-D-xylopyranosyl-(1→3)-*O*-β-D-xylopyranosyl-(1→4)-*O*-α-L-rhamnopyranosyl-(1→2)-α-L-arabinopyranosyl] ester, E is a 28-*O*-[*O*-α-L-arabinopyranosyl-(1→3)-*O*-β-D-xylopyranosyl-(1→4)-*O*-α-L-rhamnopyranosyl-(1→2)-α-L-arabinopyranosyl] ester, F is a 28-*O*-[*O*-β-D-xylopyranosyl-(1→3)-[*O*-β-D-xylopyranosyl-(1→4)]-*O*-α-L-rhamnopyranosyl-(1→2)-α-L-arabinopyranosyl] ester, and G is a 28-*O*-[*O*-β-D-xylopyranosyl-(1→3)-[*O*-α-L-arabinopyranosyl-(1→3)-*O*-β-D-xylopyranosyl-(1→4)]-*O*-α-L-rhamnopyranosyl-(1→2)-α-L-arabinopyranosyl] ester. Acutoside C is a machaelinic acid (=21β-hydroxyoleanolic acid) saponin having the same sugar moiety as that of acutoside B.

Keywords *Luffa acutangula*; Cucurbitaceae; triterpene saponin; 3,28-*O*-bisdesmoside; acutoside; oleanolic acid saponin; machaelinic acid; herb saponin

Luffa acutangula ROXB. (Cucurbitaceae) is a vine which is cultivated in the tropical and subtropical Asian region from India to the southern islands of Japan. The young fruits are eaten as a vegetable. The fruits are used in Ayurvedic medicine as an anthelmintic, stomachic and antipyretic, and the seeds are also used as an emetic and an expectorant.[1] The chemical constituents of this plant were first investigated by Barua *et al.*,[2] and they reported the isolation of cucurbitacin B and an oleanolic acid saponin from the seeds. However, the structure of the saponin has not been characterized. Takemoto *et al.* isolated tens of saponins from the herb of *Luffa cylindrica* ROEM.,[3] and we also isolated twelve triterpenoid saponins from the herb of *Luffa operculata* COGN.[4] The herb of *Luffa acutangula* was also expected to contain saponins, and our preliminary investigation indicated the presence of several kinds of triterpenoid saponins in the herb.

This paper deals with the isolation of seven saponins, named acutosides A—G, from the herb, and determination of their structures.

The dried herb was percolated with 50% MeOH and the aqueous solution after evaporation of MeOH was passed through a highly porous polymer Diaion HP 20 column. The saponin fraction was obtained by elution with MeOH after washing the column with water. The saponin fraction was repeatedly chromatographed on normal-phase and reversed-phase materials and seven saponins were isolated in a homogeneous state. They were designated as acutosides A—G in the order of increasing polarity. The physical data and the nuclear magnetic resonance (NMR) data are summarized in Tables I, II and III.

Acutoside A (I) showed an $[M+Na]^+$ ion at m/z 803 in the positive fast-atom bombardment mass spectrum (FAB-MS), and the molecular formula $C_{42}H_{68}O_{13}$ was obtained by high-resolution FAB-MS. Compound I gave D-glucose and oleanolic acid on acid hydrolysis, and the structure of I was determined to be oleanolic acid 3-*O*-β-D-glucopyranosyl-(1→2)-β-D-glucopyranoside by examination of the ^{1}H- and ^{13}C-NMR spectra of the methyl ester (II) of I. The spectral basis for determination of the structure of the sugar moiety is shown in Table IV.

Acutoside B (III), $C_{58}H_{94}O_{25}$, gave oleanolic acid, D-glucose, L-rhamnose, L-arabinose and D-xylose on acid hydrolysis, and the molecular weight (1190) and formula indicated that III is an oleanolic acid glycoside having 2 mol of D-glucose and 1 mol each of L-rhamnose, L-arabinose and D-xylose.

The ^{1}H-NMR signal of III at δ 6.45 (d, J=3 Hz) and the ^{13}C-NMR signals at δ 93.5 (the signals of the anomeric H and C of the ester-linked sugar) and δ 89.0 (C_3 of oleanolic

TABLE I. Physical Constants and MS Data of Acutosides

Acutoside		mp	$[\alpha]_D^{24}$	FAB-MS		Formula[c]
				Negative[a]	Positive[b]	
A (I)	Amorphous powder	265—270 °C (dec.)	36.5° (c=1.0, MeOH)	779	803.4543	$C_{42}H_{68}O_{13}$
B (III)	Amorphous powder	225—250 °C (dec.)	−18.3° (c=1.0, 80% MeOH)	1189	1213.5980	$C_{58}H_{94}O_{25}$
C (VI)	Amorphous powder	220—225 °C (dec.)	−15.5° (c=0.5, 80% MeOH)	1205	1229.5920	$C_{58}H_{94}O_{26}$
D (VII)	Amorphous powder	260—265 °C (dec.)	−21.4° (c=1.0, 80% MeOH)	1321	1345.6400	$C_{63}H_{102}O_{29}$
E (X)	Colorless needles	246—251 °C	−14.2° (c=1.0, 80% MeOH)	1321	1345.6390	$C_{63}H_{102}O_{29}$
F (XIII)	Amorphous powder	215—223 °C (dec.)	−25.3° (c=1.0, 80% MeOH)	1321	1345.6410	$C_{63}H_{102}O_{29}$
G (XVI)	Amorphous powder	250—252 °C (dec.)	−22.5° (c=1.0, H_2O)	1453	1477.6810	$C_{68}H_{110}O_{33}$

a) $[M-H]^-$ ion. *b*) $[M+Na]^+$ ion. Errors are within 2 mmu. *c*) Calculated by high-resolution FAB-MS measured by adding NaI.

TABLE II. NMR Chemical Shifts of Acutosides (Aglycone Moieties)

	Acut. A (I)		Acut. B (III)		Acut. C (VI)	
	^1H	^{13}C	^1H	^{13}C	^1H	^{13}C
1	*ca.* 0.85, 1.45	38.7	*ca.* 0.85, 1.40	38.8	*ca.* 0.85, 1.45	38.8
2	*ca.* 1.80, 2.19	26.6	*ca.* 1.80, 2.19	26.6	*ca.* 1.80, 2.19	26.6
3	3.29 (dd, 4, 12)	89.0	*ca.* 3.27	89.0	3.35 (dd, 4, 12)	89.0
4	—	39.5	—	39.5	—	39.5
5	0.75 (d, 11)	55.8	0.73 (d, 11)	55.8	0.75 (d, 12)	55.9
6	*ca.* 1.50	18.5	*ca.* 1.50	18.5	*ca.* 1.52	18.6
7		33.2		33.2	*ca.* 1.45	33.2
8	—	39.7	—	39.9	—	39.8
9	1.62 (t, 9)	48.0	*ca.* 1.60	48.0	*ca.* 1.60	48.0
10	—	36.9	—	36.9	—	37.0
11	1.91 (dd, 3, 9)	23.7	*ca.* 1.87	23.8	*ca.* 1.89	23.8
12	5.48 (t, 3)	122.5	5.45 (t, 4)	122.9	5.50 (t, 3)	122.9
13	—	144.9	—	144.2	—	143.4
14	—	42.0	—	42.1	—	42.2
15	*ca.* 1.20, 2.16	28.3		28.3	*ca.* 1.28, 2.03	28.5
16		23.7		23.2	*ca.* 2.19	24.6
17	—	46.7	—	47.3	—	49.2
18	3.29 (dd, 4, 12)	42.2	*ca.* 3.27	41.7	3.43 (dd, 4, 14)	41.4
19	*ca.* 1.30, 1.80	46.5	*ca.* 1.23, 1.80	46.3	*ca.* 1.44, 2.02	47.1
20	—	30.9	—	30.9	—	36.8
21	*ca.* 1.22, 1.45	34.2	*ca.* 1.17, 1.35	34.1	*ca.* 3.90	72.4
22		33.2		33.2	2.31 (d, 8)	41.1
23	1.30 s	28.2	1.29 s	28.2	1.29 s	28.2
24	1.10 s	16.8	1.10 s	16.8	1.10 s	16.8
25	0.84 s	15.4	0.84 s	15.5	0.85 s	15.5
26	1.00 s	17.4	1.06 s	17.4	1.25 s	17.7
27	1.30 s	26.2	1.27 s	26.0	1.29 s	25.9
28	—	180.2	—	176.2	—	175.4
29	0.96 s	33.2	0.93 s	33.1	1.25 s	29.7
30	1.02 s	23.7	0.99 s	23.7	1.06 s	17.4

The NMR chemical shifts of acutosides D (VII), E (X), F (XIII) and G (XVI) are almost the same as those of III and the chemical shifts are not shown.

acid) indicated that III is a 3,28-*O*-bisdesmoside of oleanolic acid. The selective cleavage of the ester-linked sugar moiety according to Ohtani's method[5] provided an anomeric mixture of a methyl glycoside and a prosapogenin, which was proved to be identical with I. The anomers of the methyl glycoside were separated by high performance liquid chromatography (HPLC). The faster-eluting anomer (IV) showed an $[M-H]^-$ ion at *m/z* 441, fragment ions at *m/z* 309 (441 − pentose) and *m/z* 163 (309 − rhamnose) in the negative FAB-MS, indicating that IV is a methyl pentosyl–rhamnosyl–pentoside. By the close examination of the NMR spectra, IV was presumed to be methyl *O*-*β*-D-xylopyranosyl-(1→4)-*O*-*α*-L-rhamnopyranosyl-(1→2)-*α*-L-arabinopyranoside and the other anomer (V), to be the *β*-anomer. The identity was established by comparison of the NMR data with those of a sample obtained from foetidissimoside isolated from the herb of *Aster tataricus* L.f. (Compositae).[6] The assignments of the ^1H- and ^{13}C-NMR signals are shown in Table V.

The structure of III is, therefore, 3-*O*-[*O*-*β*-D-glucopyranosyl-(1→2)-*β*-D-glucopyranosyl]-oleanolic acid 28-[*O*-*β*-D-xylopyranosyl-(1→4)-*O*-*α*-L-rhamnopyranosyl-(1→2)-*α*-L-arabinopyranosyl] ester. The configuration and conformation of the ester-linked arabinopyranosyl group in III were presumed to be *α*- and $^1C_4$ based on the $J_{H1,H2}$ (3 Hz) and $J_{C1,H1}$ (169 Hz) values[7] and splitting pattern (dd, $J=3$, 5 Hz) of the C_2-H signal (δ 4.55) which was observed by using the decoupling difference spectroscopy technique, irradiating at the frequency (δ 6.45) of the anomeric proton signal.

TABLE III. The NMR Signal Assignments of the Ester-linked Sugar Moieties of Acutosides

Sugar		B (III)		C (VI)		D (VII)		E (X)		F (XIII)		G (XVI)	
		^1H	^{13}C	^1H	^{13}C	^1H	^{13}C	^1H	^{13}C	^1H	^{13}C	^1H	^{13}C
28-*O*-Ara[1]	1	6.45 (d, 3)	93.5	6.45 (d, 3)	93.6	6.48 br s	93.3	6.48 br s	93.3	6.52 (d, 2)	93.3	6.53 (d, 2)	93.2
	2	4.55 (dd, 3, 5)	75.1	*ca.* 4.55	75.1	*ca.* 4.53	75.2	*ca.* 4.54	75.2	*ca.* 4.55		*ca.* 4.52	75.3
	5	*ca.* 3.90, 4.50	63.1	*ca.* 3.90, 4.50	63.2	*ca.* 3.90, 4.50	62.8		62.8	*ca.* 3.90, 4.50	62.5	*ca.* 3.90, 4.50	62.3
Rha(1—2A[1])	1	5.78 s	101.0	5.78 s	101.0	5.71 (d, 1)	100.9	5.73 br s	100.9	5.71 (d, 1)	100.6	5.66 br s	100.7
	2	*ca.* 4.57				*ca.* 4.51		*ca.* 4.54		4.77 (dd, 1, 3)	71.5	4.76 (dd, 1, 2)	71.4
	3									4.59 (dd, 3, 10)	82.3	*ca.* 4.57	82.3
	4	*ca.* 4.35	84.3	*ca.* 4.35	84.2	*ca.* 4.35	83.8	*ca.* 4.35	83.9	*ca.* 4.51	78.3	*ca.* 4.50	
	5	*ca.* 4.38	68.5	*ca.* 4.39	68.5	*ca.* 4.32	68.4	*ca.* 4.40	68.4	*ca.* 4.44	68.7	*ca.* 4.40	68.6
	6	1.78 (d, 6)	18.3	1.78 (d, 6)	18.3	1.74 (d, 5)	18.3	1.74 (d, 5)	18.3	1.79 (d, 6)	18.6	1.74 (d, 6)	18.6
Xyl[1](1—4R)	1	5.10 (d, 7)	107.2	5.10 (d, 7)	107.1	5.13 (d, 7)	106.4	5.09 (d, 8)	106.4	5.14 (d, 7)[a]	105.8	5.11 (d, 7)[a]	105.7
	2	*ca.* 4.03		*ca.* 4.03		*ca.* 4.02		*ca.* 3.90		*ca.* 3.90			
	3					*ca.* 4.03	87.0	*ca.* 4.05	86.3			*ca.* 4.05	86.7
	5	3.50 (t, 11), *ca.* 4.21	67.4	3.50 (t, 11), *ca.* 4.20	67.4	*ca.* 3.45, *ca.* 4.20 [a]	66.8[a]	3.43 (t, 11), *ca.* 4.20	66.8	3.40 (t, 10), *ca.* 4.14 [b]	67.1[b]	3.43 (t, 12), *ca.* 4.08 [b]	67.0[b]
Xyl[2](1—3X[1])	1					5.20 (d, 8)	105.9	—	—	—	—	—	—
	2					*ca.* 4.02		—	—	—	—	—	—
	5					3.66 (t, 11), *ca.* 4.30 [a]	67.2[a]	—	—	—	—	—	—
Ara[2](1—3X[1])	1							5.21 (d, 7)	105.5	—	—	—	—
	2							*ca.* 4.50		—	—	—	—
	5							3.77 (t, 11), *ca.* 4.30	67.1	—	—	—	—
Xyl[3](1—3R)	1									5.41 (d, 8)[a]	105.2[a]	5.45 (d, 8)[a]	104.6[a]
	2									*ca.* 3.90		*ca.* 3.90	
	5									3.44 (t, 11), *ca.* 4.06 [b]	67.0[b]	3.38 (t, 12), *ca.* 4.12 [b]	66.5[b]
Ara[3](1—3X[1])	1											5.17 (d, 7)	105.5
	5											3.51 (dd, 1, 12), *ca.* 4.20	66.7

The chemical shifts of the signals which were difficult to assign or ambiguous are not shown. *a, b*) The signals with the same superscripts in each column may be interchanged.

Acutoside C (VI) showed an $[M+Na]^+$ ion at *m/z* 1229, and an $[M-H]^-$ ion at *m/z* 1205 in the FAB-MS and the high-resolution FAB-MS gave the molecular formula $C_{58}H_{94}O_{26}$ for VI, having one more oxygen atom than III. On acid hydrolysis, VI gave D-glucose, L-rhamnose, L-arabinose and D-xylose, and the thin layer chromatography (TLC) showed a spot of an aglycone which is a little more polar than oleanolic acid. The ^{1}H- and ^{13}C-NMR spectra of the sugar moiety were almost superimposable on those of III, suggesting that VI is a glycoside of a hydroxy-oleanolic acid which has the same sugar moiety as that of III. The ^{1}H- and ^{13}C-NMR spectra of the aglycone moiety of VI were examined, and the data were compared with those of the reported compounds. The ^{13}C-NMR chemical shifts of the aglycone moiety were almost the same as those of lucyoside C (21β-hydroxyoleanolic acid 3,28-*O*-bis-β-D-glucopyranoside) isolated from the herb of *Luffa cylindrica* ROEM. by Takemoto *et al.*[3a] Therefore, acutoside C was concluded to be 3-*O*-[*O*-β-D-glucopyranosyl-(1→2)-β-D-glucopyranosyl]machaelinic acid 28-[*O*-β-D-xylopyranosyl-(1→4)-*O*-α-L-rhamnopyranosyl-(1→2)-α-L-arabinopyranosyl] ester.

Acutoside D (VII), $C_{63}H_{102}O_{29}$, gave oleanolic acid, D-glucose, L-rhamnose, L-arabinose and D-xylose on acid hydrolysis. The molecular weight (1322) indicated that the sugar moiety is composed of 2 mol of D-glucose, 1 mol of L-rhamnose and 3 mol of pentose, and the ^{1}H- and ^{13}C-NMR spectra suggested that VII is an oleanolic acid 3,28-*O*-bisdesmoside. On selective cleavage of the ester-linked sugar moiety, a prosapogenin and an anomeric mixture of a methyl glycoside were obtained. The former was proved to be identical with acutoside A (I). The latter was separated by HPLC on a reversed-phase material to give two anomers (VIII and IX) of the methyl glycoside. The faster-eluting anomer (VIII) showed an $[M+Na]^+$ ion at *m/z* 597 in the positive FAB-MS and the negative FAB-MS showed ions at *m/z* 573 ($[M-H]^-$), 441 (573−pentose), 309 (441−pentose) and 163 (309−rhamnose). This fragmentation pattern indicated that the sugar sequence in VIII is either a linear CH_3O–pentose(1)–rhamnose–pentose(2)–pentose(3) or a branched chain CH_3O–pentose(1)–rhamnose(pentose)$_2$.

In order to determine the number of the xylose and arabinose units in VIII, the ^{1}H-NMR spectrum was carefully examined. The ^{1}H-NMR spectrum of VIII showed the signals of the C_5-H (axial) of the pentosyl groups at δ 3.48 (dd, J=10, 11 Hz), 3.67 (dd, J=10, 11 Hz) and 3.68 (dd, J=3, 11 Hz), and the other anomer (IX) showed the

TABLE IV. The NMR Signal Assignments of the Sugar Moiety of II

	Inner glucose ^{1}H	Inner glucose ^{13}C	Outer glucose ^{1}H	Outer glucose ^{13}C
1	4.90 (d, 8)	105.0	5.35 (d, 8)	106.0
2	4.20 (dd, 8, 9)	83.5	4.09 (dd, 8, 9)	77.0
3	4.30 (t, 9)	78.3	4.21 (t, 9)	77.9
4	4.29 (t, 9)	71.7	4.13 (t, 9)	71.6
5	3.9 (m)	78.1[a]	3.9 (m)	77.9[a]
6	4.33 (dd, 6, 12)[b] 4.52 (dd, 3, 12)[b]	62.9[c]	4.43 (dd, 4, 12)[b] 4.47 (dd, 3, 12)[b]	62.8[c]

a—*c*) Assignments may be interchanged. The assignment of the anomeric proton signals was performed by examination of the NOE difference spectra. On irradiation at the frequency of δ 4.90, the NOE was observed at the signal of C_3-H of the aglycone.

TABLE V. The NMR Signal Assignments of Methyl Glycosides IV, V, VIII, IX, XI and XII

		IV ^{1}H	IV ^{13}C	V ^{1}H	V ^{13}C	VIII ^{1}H	VIII ^{13}C	IX ^{1}H	IX ^{13}C	XI ^{1}H	XI ^{13}C	XII[c] ^{1}H	XII[c] ^{13}C
OCH_3		3.49 s	56.0	3.39 s	55.1	3.50 s	56.0	3.40 s	55.1	3.50 s	55.9	3.39 s	55.3
Ara[1]	1	4.55 (d, 7)	103.6	5.29 (d, 3)	104.1	4.55 (d, 6)	103.6	5.27 (d, 4)	101.1	4.55 (d, 6)	103.6	5.26 (d, 4)	101.2
	2	4.45 (dd, 7, 8)	76.9	4.56 (dd, 3, 10)	78.6	4.45 (dd, 6, 7)	76.9	4.55 (dd, 4, 9)	78.7	4.44 (dd, 6, 8)	76.8	4.54 (dd, 4, 10)	78.8
	3	4.14 (dd, 8, 3)	69.2	4.46 (dd, 3, 10)	69.1	*ca.* 4.15		4.46 (dd, 4, 9)	69.1	*ca.* 4.14	69.0	4.44 (dd, 4, 10)	69.1
	4	*ca.* 4.17	74.2	4.28 m	70.7			*ca.* 4.29	70.6	*ca.* 4.17	74.4	*ca.* 4.30	70.6
	5	3.67 (d, 10) 4.20 (dd, 10, 4)	65.9	3.95 (2H, d, 2)	63.5	3.68 (dd, 2, 12) *ca.* 4.20	65.9	3.96 (2H, d, 2)	63.5	3.67 (d, 10) *ca.* 4.20	65.9	3.96 (2H, br s)	63.7
Rha(1—2A[1])	1	5.94 (d, 1)	102.1	5.61 s	101.1	5.93 (d, 2)	102.1	5.60 br s	101.1	5.94 (d, 1)	102.1	5.59 (d, 2)	104.3
	2	4.67 (dd, 1, 3)	72.0	4.63 br s	71.7	4.67 (dd, 2, 4)	72.0	4.55	71.7	4.66 (dd, 1, 3)	72.0	4.64 (dd, 2, 3)	71.7
	3	4.64 (dd, 3, 9)	72.8	4.63 br s	72.7	4.61 (dd, 4, 9)	72.7	4.55	72.6	4.60 (dd, 3, 10)	72.7	4.58 (dd, 3, 9)	72.8
	4	4.34 (t, 9)	84.8	4.32 (t, 9)	84.5	4.34 (t, 9)	84.3	*ca.* 4.35	84.0	4.33 (t, 10)	84.4	*ca.* 4.30	84.0
	5	*ca.* 4.56	67.9	*ca.* 4.40 m	68.1	*ca.* 4.54	67.8	*ca.* 4.35	68.0	*ca.* 4.44	67.8	*ca.* 4.30	68.2
	6	1.69 (d, 6)	18.2	1.67 (d, 6)	18.4	1.64 (d, 6)	18.2	1.63 (d, 6)	18.4	1.64 (d, 6)	18.2	1.60 (d, 5)	18.6
Xyl[1](1—4R)	1	5.12 (d, 7)	107.2	5.11 (d, 7)	107.1	5.20 (d, 8)[a]	105.8[a]	5.20 (d, 8)[a]	105.9[a]	5.13 (d, 8)	106.4	5.11 (d, 8)	106.2
	2	4.04 (t, 8)	76.1	4.02 (t, 9)	76.1	*ca.* 4.05		*ca.* 4.03		4.02 (t, 8)	75.0	*ca.* 4.00	75.0
	3	4.07 (t, 8)	78.6	4.06 (t, 9)	78.7	*ca.* 4.03	87.1	*ca.* 4.02	87.0	4.05 (t, 8)	86.4	*ca.* 4.05	86.6
	4	*ca.* 4.14	71.0	4.14 m	71.0	*ca.* 4.10				*ca.* 4.04	69.0	*ca.* 4.02	69.1
	5	3.52 (t, 11) 4.25 (dd, 5, 11)	67.5	3.51 (t, 10) 4.23 (dd, 10, 5)	67.5	3.48 (dd, 10, 11)[b] *ca.* 4.25	66.7[b]	3.48 (dd, 9, 11)[b] 4.23 (dd, 4, 11)	66.8[b]	3.46 (dd, 9, 11) *ca.* 4.21	66.8	3.45 (dd, 10, 11) 4.20 (dd, 5, 11)	66.8
Xyl[2](1—3X[1])	1	—	—	—	—	5.16 (d, 7)[a]	106.3[a]	5.14 (d, 7)[a]	106.3[a]				
	2	—	—	—	—	*ca.* 4.05		*ca.* 4.03		—	—	—	—
	3	—	—	—	—					—	—	—	—
	4	—	—	—	—					—	—	—	—
	5	—	—	—	—	3.67 (dd, 10, 11)[b] *ca.* 4.27	67.3[b]	3.67 (dd, 10, 11)[b] *ca.* 4.29	67.2[b]	—	—	—	—
Ara[2](1—3X[1])	1	—	—	—	—	—	—	—	—	5.20 (d, 7)	105.5	5.17 (d, 7)	105.5
	2	—	—	—	—	—	—	—	—	4.49 (dd, 7, 9)	72.7	4.50 (dd, 7, 9)	72.6
	3	—	—	—	—	—	—	—	—	4.16 (dd, 9, 3)		4.16 (dd, 3, 9)	74.4
	4	—	—	—	—	—	—	—	—	*ca.* 4.27	69.2	*ca.* 4.30	69.3
	5	—	—	—	—	—	—	—	—	3.77 (dd, 2, 12) 4.32 (dd, 3, 12)	67.1	3.77 (d, 11) *ca.* 4.32	67.2

a, b) The signals with the same superscripts in each column may be interchanged. *c*) The spectra were measured in pyridine-d_5–D_2O mixture. Abbreviations: A; arabinopyranosyl, R; rhamnopyranosyl, X; xylopyranosyl. Ara[2](1—3X[1]) means the second arabinopyranosyl group which is linked to the C_3-OH group of the first xylopyranosyl group.

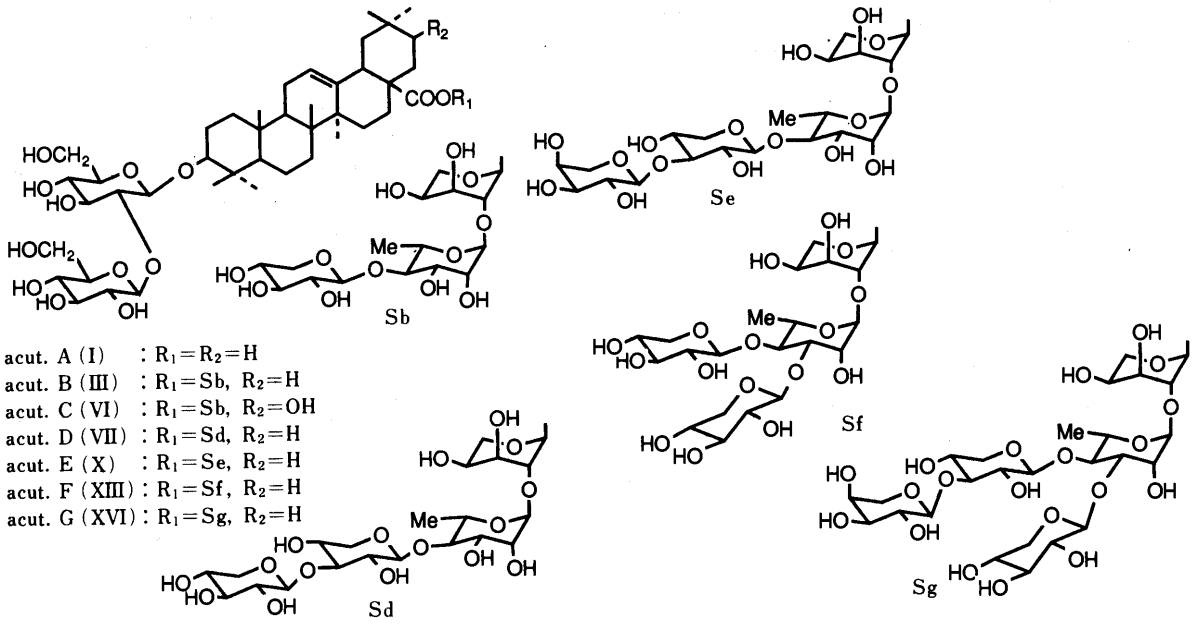

Chart 1

C_5-H signals at δ 3.48 (dd, axial, $J=9$, 11 Hz), 3.67 (dd, axial, $J=10$, 11 Hz) and δ 3.96 (2H, C_5-H_a, C_5-H_e, d, $J=2$ Hz). These signal patterns clearly indicate that VIII and IX have 1 mol of arabinose and 2 mol of xylose as the pentose units.

The identification of the pentose(1) and the determination of the position of the rhamnose linkage were performed by the examination of the ^{1}H- and ^{13}C-NMR spectra of VIII and IX. The ^{1}H-NMR signals of the C_1-H and C_2-H of the pentose (1) were observed at δ 4.55 (d, $J=6$ Hz) and δ 4.45 (dd, $J=6$, 7 Hz), respectively, but the signal of the C_3-H was overlapped by the signals of other sugar units and the splitting pattern could not be observed. On the other hand, the signal of the C_3-H of IX was fortunately separated from others and observed at δ 4.46 as a double doublet ($J=4$, 9 Hz). The splitting pattern of the C_3-H signal of IX clearly indicates that the pentose(1) is L-arabinose.

The chemical shifts of C_2 of the arabinosyl units in VIII and IX were 76.9 and 78.7, respectively, and these chemical shifts are in good agreement with the data for methyl *O*-α-L-rhamnopyranosyl-(1→2)-α- and β-L-arabinopyranosides reported by Mizutani *et al.*[8] Therefore, it is apparent that the rhamnopyranosyl group is linked to the C_2-hydroxyl group of the arabinosyl unit.

The position of the xylose linkage to the rhamnose unit was also determined by examination of the ^{1}H- and ^{13}C-NMR spectra of the rhamnosyl moieties in VIII and IX. Assignments of the ^{1}H- and ^{13}C-NMR signals are shown in Table V.

The ^{1}H-NMR signals of the rhamnosyl group overlapped and clear assignment could not be done in the case of IX. However, signals of the rhamnosyl group in VIII were clearly separated and could be easily assigned. The ^{13}C-NMR chemical shifts were determined from the C–H correlation spectroscopy (COSY) spectrum. As shown in Table V, only the C_4 signals were shifted to lower magnetic field, thus indicating that the xylobiose is linked to the C_4-OH group of the rhamnopyranosyl unit. The last problem on the structure of VIII is the position of the linkage of the terminal xylose unit. The signals of the C_2-H and C_3-H of the xylose units appeared at almost the same region, overlapped by the other sugar signals, and it was difficult to assign the ^{13}C-NMR signal at δ 87.1 to C_2 or C_3. The position of the terminal xylose linkage was unambiguously determined as C_3-OH by gas chromatography-chemical ionization-mass spectrometry (GC-CI-MS) identification of the methyl glycosides of 2,3,4-tri-*O*-methyl D-xylose, 2,4-di-*O*-methyl D-xylose, 3,4-di-*O*-methyl L-arabinose and 2,3-di-*O*-methyl L-rhamnose after methanolysis of the permethylate of IX. From the above-mentioned data, the structure of VIII is concluded to be methyl *O*-β-D-xylopyranosyl-(1→3)-β-D-xylopyranosyl-(1→4)-α-L-rhamnopyranosyl-(1→2)-α-L-arabinopyranoside and IX, to be its β-anomer.

Therefore, the structure of acutoside D (VII) was determined to be as shown in the chart. The configuration and conformation of the esterified L-arabinopyranosyl group were presumed to be α- and $^1C_4$ because the arabinosyl group showed almost the same NMR chemical shifts as those of III.

Acutoside E (X) showed an $[M+Na]^+$ ion at *m/z* 1345 and the high-resolution FAB-MS indicated the molecular formula $C_{63}H_{102}O_{29}$, the same formula as that of VII. The NMR spectra of X suggested that it is also an oleanolic acid 3,28-*O*-bisdesmoside. Compound X gave oleanolic acid, D-glucose, L-rhamnose, L-arabinose and D-xylose on acid hydrolysis, and the selective cleavage of the ester-linked sugar moiety provided acutoside A (I) along with an anomeric mixture of a methyl glycoside. The anomers (XI and XII) were preparatively separated by HPLC. The faster-eluting anomer (XI) showed an $[M-H]^-$ ion at *m/z* 573 and fragment ions at *m/z* 441 (573−pentose), 309 (441−pentose) and 163 (309−rhamnose) in the negative FAB-MS. From this fragmentation pattern, the sugar sequence of XI and the other anomer (XII) is either a linear CH_3O–pentose(1)–rhamnose–pentose(2)–pentose(3) or a branched chain CH_3O–pentose(1)–rhamnose–$(pentose)_2$.

The numbers of arabinose and xylose in XI were

determined by examination of the signal patterns of C_5-H of the pentosyl groups. Compound XI showed a doublet (1H, $J=10$ Hz) at δ 3.67, a double doublet (1H, $J=9$, 11 Hz) at δ 3.46 and a double doublet (1H, $J=2$, 12 Hz) at δ 3.77. These signals are those of the axial hydrogens at C_5 and the splitting patterns showed that XI has 1 mol of D-xylose and 2 mol of L-arabinose as the pentose units.

The pentose(1) was identified as L-arabinose by examination of the ^{1}H-NMR spectrum of XII measured in pyridine-d_5–D_2O mixture. The signal of the anomeric H appeared at δ 5.26 (d, $J=4$ Hz), C_2-H at δ 4.54 (dd, $J=4$, 10 Hz) and C_3-H at δ 4.44 (dd, $J=10$, 4 Hz). The site of rhamnose linkage was determined by examination of the ^{13}C-NMR chemical shifts of the arabinosyl unit. The C_2 signal of XI appeared at δ 76.8 and that of XII appeared at δ 78.8, and these data indicated that the rhamnopyranosyl group is linked to the C_2-OH group of the arabinopyranosyl group.

The position of the linkage of the pentose(2) to the rhamnosyl unit was determined from the ^{13}C-NMR glycosylation shifts of the carbons of the rhamnosyl unit after assignments of the ^{1}H-NMR signals. The results of assignments of ^{1}H- and ^{13}C-NMR signals are shown in Table V.

Only the signal of the C_4 was shifted downfield and this shift showed that the pentobiose is attached to the C_4-OH group of the rhamnosyl unit to form a linear methyl tetraglycoside.

The identification of the pentose(2) and the determination of the position to which the pentose(3) is linked were performed as follows. The ^{13}C-NMR signal at δ 86.4 in the spectrum of XI is correlated to the H signal at δ 4.05 (t, $J=8$ Hz). This proton signal showed in a ^{1}H–^{1}H COSY spectrum a cross peak with the signal at δ 4.02 (t, $J=8$ Hz), which showed a cross peak with the anomeric proton signal at δ 5.13 (d, $J=8$ Hz). These chemical shifts and splitting patterns of the C_1-H, C_2-H and C_3-H unambiguously indicated that the inner pentosyl unit is xylopyranose and, thus, the terminal one is arabinose, which is linked to the C_3-OH group of the xylopyranosyl group. From all the spectral evidence, the structure of XI was indicated to be methyl *O*-α-L-arabinopyranosyl-(1→3)-*O*-β-D-xylopyranosyl-(1→4)-*O*-α-L-rhamnopyranosyl-(1→2)-α-L-arabinopyranoside, and XII, to be the β-anomer of XI. The GC-CI-MS analysis of the methanolysis product of the permethylate of XII supported the above structure.

The structure of acutoside E (X) is, therefore, elucidated as shown in the chart.

Acutoside F (XIII), $C_{63}H_{102}O_{29}$, gave oleanolic acid, D-glucose, L-rhamnose, L-arabinose and D-xylose on acid hydrolysis, and acutoside A (I) was obtained together with an anomeric mixture of a methyl glycoside on heating XIII in 2,6-lutidine–MeOH mixture with LiI. The methyl glycoside fraction was separated by HPLC to give two anomers (XIV and XV). The faster-eluting anomer (XIV) showed an $[M-H]^-$ ion at m/z 573 and fragment ions at m/z 441, 309 and 163, suggesting that XIV is either a linear methyl tetraglycoside CH_3O–pentose(1)–rhamnose–pentose(2)–pentose(3) or a branched chain methyl tetraglycoside which has two terminal pentose units at the rhamnosyl unit. The ^{1}H-NMR spectrum (Table VI) of XIV showed the signals of the axial hydrogens on the C_5 of pentose units at δ 3.40 (2H, two triplets overlapped, $J=$ *ca.* 9 Hz) and at δ 3.63 (dd, $J=2$, 12 Hz). The ^{1}H-NMR spectrum of XV showed one broad singlet (δ 3.95) equivalent to two protons at C_5, and two triplets at δ 3.18 ($J=11$ Hz) and 3.41 ($J=10$ Hz) as the signals of the axial C_5-H. These signals indicated that XIV has 1 mol of L-arabinose and 2 mol of D-xylose as the pentose units.

In order to identify the pentose(1), the ^{1}H-NMR spectrum of XIV was examined. The anomeric proton signal appeared at δ 4.55 (d, $J=6$ Hz) and the C_2-H signal was assigned at δ 4.47 (dd, $J=6$, 8 Hz) from the ^{1}H–^{1}H COSY spectrum. However, the signal of C_3-H appeared at around δ 4.12 overlapped by signals of other sugar protons and the splitting pattern was not clearly observed. The decoupling difference spectrum was measured by irradiation at the frequency (δ 4.47) of the C_2-H, and the signal of the C_3-H was observed at δ 4.12 as a double doublet with coupling constants of 4 and 8 Hz. This splitting pattern indicates that the pentose(1) is L-arabinose.

The position of the rhamnose linkage was determined as the C_2-OH of the L-arabinosyl unit on the same basis as in the cases of the other methyl glycosides.

In order to determine the position(s) of the linkage(s) of a xylobiose or two xylose units, the NMR spectra of the rhamnosyl group were carefully examined. The assignments of the ^{1}H- and ^{13}C-NMR signals of XIV are summarized in Table VI. The down-field shifts of the C_3 and C_4 signals indicate that the two xylose units are linked to the C_3- and C_4-OH groups to form a branched-chain methyl tetraglycoside. The structures of XIV and XV are, therefore, methyl *O*-β-D-xylopyranosyl-(1→3)-[*O*-β-D-xylopyranosyl-(1→4)]-*O*-α-L-rhamnopyranosyl-(1→2)-α-L-arabinopyranoside and its β-anomer, respectively, and the structure of XIII was elucidated as shown in the chart.

Acutoside G (XVI) showed an $[M+Na]^+$ ion at m/z 1477 in the positive FAB-MS, and the high-resolution FAB-MS gave the molecular formula $C_{68}H_{110}O_{33}$. The ^{1}H-NMR spectrum suggested that XVI is also an oleanolic acid 3,28-*O*-bisdesmoside, and it gave oleanolic acid, D-glucose, L-rhamnose, L-arabinose and D-xylose on acid hydrolysis. On selective cleavage of the ester-linked sugar moiety, XVI gave acutoside A(I) and an anomeric mixture of a methyl glycoside. The anomers (XVII and XVIII) were separated by HPLC. The faster-eluting anomer (XVII) showed in the negative FAB-MS an $[M-H]^-$ ion at m/z 705 and fragment ions at m/z 573 (705−pentose), 441 (573−pentose), 309 (441−pentose) and 163 (309−rhamnose), indicating that XVII is a methyl pentaglycoside and has a similar sugar sequence to those of XI and XIV, having one more pentose unit than XI and XIV.

The numbers of xylose and arabinose units were determined by checking the ^{1}H-NMR signals of C_5-H of the pentose units. Compound XVII showed in its ^{1}H-NMR spectrum the signals of C_5-H at δ 3.40 (2H, t, $J=9$ Hz), δ 3.56 (1H, dd, $J=1$, 12 Hz) and δ 3.63 (1H, dd, $J=1$, 12 Hz). The ^{1}H-NMR spectrum of the other anomer (XVIII) showed two triplets at δ 3.18 ($J=11$ Hz) and δ 3.41 ($J=11$ Hz), one double doublet at δ 3.56 ($J=1$, 12 Hz) and one broad singlet equivalent to two protons at δ 3.94. These signal patterns of C_5-H indicated that XVII and XVIII have 2 mol each of L-arabinose and D-xylose as the pentose units.

Identification of the methyl glycosylated pentose was

performed as follows. The ^{1}H-NMR spectrum of XVII showed an anomeric proton signal at δ 4.54 (d, J=6 Hz) and the C_2-H signal appeared at δ 4.47 (dd, J=6, 8 Hz). The C_2-H signal is overlapped with the signal of the C_2-H of the other pentose, of which the anomeric H appeared at δ 5.16. The decoupling difference spectrum was measured to see the chemical shifts and splitting patterns of the C_3-H, irradiating at the frequency of the C_2-H signal (δ 4.47). The signals of the C_3-H of two pentose units appeared at δ 4.04 and 4.12 as double doublets with coupling constants of 3 and 8 Hz. The splitting pattern of the C_3-H signals indicated that the two pentoses in question are both arabinose.

The position of the rhamnose linkage was determined as the C_2-OH of the methyl arabinosyl unit by the fact that the signal (δ 4.57, dd, J=4, 10 Hz) of C_2-H of the arabinosyl group in XVIII was observed in the nuclear Overhauser effect (NOE) difference spectrum obtained by irradiation at the frequency (δ 5.62) of the anomeric proton of the rhamnosyl group. The chemical shifts of the C_2 signals of arabinosyl groups in XVII and XVIII were in good agreement with Mizutani's data.[8]

Determination of the positions in rhamnose to which the pentose is linked was accomplished by examination of the ^{1}H- and ^{13}C-NMR signals of the rhamnopyranosyl units of XVII and XVIII. The assignments of the ^{1}H- and ^{13}C-NMR signals are shown in Table VI.

The signals of C_3 and C_4 were shifted downfield as seen in the case of XIV. These glycosylation shifts indicate that a pentose unit and a pentobiose unit are linked to the C_3- and C_4-OH groups of the rhamnosyl unit to form a branched sugar chain.

In order to determine the positions of the linkages of one arabinose and two xylose units, the NOE difference spectra of XVIII were measured, irradiating at the frequencies at δ 5.45 [xylose(1)], 5.16 (arabinose) and 4.91 [xylose(2)]. When the signal at δ 5.45 was irradiated, the NOE was observed at a triplet at δ 4.45, and this proton signal was assigned to be that of C_4-H of the rhamnosyl group. On irradiation at the frequency (δ 4.91) of the other xylose anomeric proton, NOE was observed at the signal (δ 4.63, dd, J=3, 9 Hz) which was assigned as the signal of C_3-H of the rhamnosyl group. Therefore, xylose(1) and xylose(2) are linked to the respective C_4-OH and C_3-OH groups of the rhamnosyl unit, and the arabinosyl group is linked to one of the xylosyl units.

On irradiation at the signal (δ 5.16) of the anomeric proton of the arabinosyl group, the NOE difference spectrum showed a triplet (J=8 Hz) at δ 4.14 which was assigned to one of two C_3-H of xylosyl units. The assignment of the signal could not be done because the two C_2-H signals of the xylose units were very close and there was a risk of miss-assignment. Therefore, the HOHAHA spectra were measured, irradiating at the two xylose anomeric protons. The HOHAHA spectrum obtained by irradiation at the anomeric proton (δ 4.91) of xylose(2), showed the C_2-H signal at δ 3.90 (t, J=8 Hz), the C_3-H signal at δ 3.95 (t,

Table VI. The NMR Signal Assignments of Methyl Glycosides XIV, XV, XVII and XVIII

		XIV		XV		XVII		XVIII	
		^{1}H	^{13}C	^{1}H	^{13}C	^{1}H	^{13}C	^{1}H	^{13}C
MeO		3.50 s	55.8	3.39 s	55.0	3.51 s	55.8	3.40 s	55.0
Ara^1(1—OMe)	1	4.55 (d, 6)	103.5	5.30 (d, 3)	101.1	4.54 (d, 6)	103.5	5.29 (d, 4)	101.0
	2	4.47 (dd, 6, 8)	76.9	4.58 (dd, 3, 10)	78.8	4.47 (dd, 6, 8)	76.9	4.57 (dd, 4, 10)	78.8
	3	4.12 (dd, 4, 8)	70.9	*ca.* 4.45	69.0	4.12 (dd, 3, 8)[a]	70.9	*ca.* 4.48	
	4	*ca.* 4.18		*ca.* 4.26 br s	70.6	*ca.* 4.18		*ca.* 4.27	
	5	3.63 (dd, 2, 12) *ca.* 4.18	66.1	3.95 (2H, br s)	63.5	3.63 (dd, 1, 12)[b] *ca.* 4.18	66.1[b]	3.94 (2H, br s)	63.5
Rha(1—2A^1)	1	5.98 (d, 2)	102.0	5.63 (d, 2)	104.0	5.97 (d, 1)	102.0	5.62 (d, 1)	104.0
	2	4.91 br s	71.8	*ca.* 4.82	71.3	4.90 (dd, 1, 3)	71.8	4.82 (dd, 1, 3)	71.3
	3	4.61 (dd, 3. 9)	82.5	4.65 (dd, 3, 9)	82.4	4.69 (dd, 3, 9)	82.4	4.63 (dd, 3, 9)	82.4
	4	4.54 (t, 9)	78.8	*ca.* 4.46	78.6	4.53 (t, 9)	78.4	4.45 (t, 9)	78.2
	5	*ca.* 4.64 m	68.3	*ca.* 4.48	68.2	*ca.* 4.60	68.0	*ca.* 4.43	68.0
	6	1.69 (d, 6)	18.4	1.66 (d, 6)	18.6	1.64 (d, 6)	18.4	1.61 (d, 6)	18.6
Xyl^1(1—4R)	1	5.45 (d, 8)[a]	105.2[a]	5.41 (d, 8)[a]	105.2[a]	5.51 (d, 8)	104.5	5.45 (d, 8)	104.5
	2							3.95 (t, 8)	
	3						86.8	4.14 (t, 8)	86.8
	4							4.05 m	
	5	3.40 (t, 9) *ca.* 4.10	67.1	3.41 (t, 10) 4.18 (dd, 5, 10)[b]	66.9[b]	3.40 (t, 9)[c] *ca.* 4.15	66.4[c]	3.41 (t, 11) 4.16 (dd, 5, 11)	66.4
Xyl^2(1—3R)	1	5.31 (d, 8)[a]	105.8[a]	4.94 (d, 7)[a]	105.5[a]	5.18 (d, 7)	105.8	4.91 (d, 8)	105.5
	2							3.90 (t, 8)	75.3
	3							3.95 (t, 8)	
	4							*ca.* 4.05 m	
	5	3.40 (t, 9) *ca.* 4.10	67.1	3.18 (t, 11)[b] *ca.* 3.88	67.1[b]	3.40 (t, 9)[c] *ca.* 4.10	67.0[c]	3.18 (t, 11) *ca.* 3.95	66.8
Ara^2(1—3X^1)	1	—	—	—	—	5.16 (d, 7)	105.5	5.16 (d, 6)	105.4
	2	—	—	—	—	4.47 (dd, 7, 8)	72.7	*ca.* 4.48	
	3	—	—	—	—	4.04 (dd, 3, 8)[a]			
	4	—	—	—	—	*ca.* 4.21		*ca.* 4.20	
	5	—	—	—	—	3.56 (dd, 1, 12)[b] *ca.* 4.21	66.8[b]	3.56 (dd, 1, 12) *ca.* 4.20	66.8

The NMR spectra were taken in pyridine-d_5 and the chemical shifts of the signals which were difficult to assign or ambiguous are not shown. a—c) The signals with the same superscripts in each column may be interchanged. Abbreviations: A, arabinopyranosyl; R, rhamnopyranosyl; X, xylopyranosyl. Ara^2(1—3X^1) means the second arabonopyranosyl group which is linked to the C_3-OH group of the first xylopyranosyl group.

$J=8$ Hz) and the C_4-H signal at δ 4.05 (m), and on irradiation at δ 5.45 [the anomeric proton signal of xylose(1)], the signals of the C_2-H, C_3-H and C_4-H appeared at δ 3.95 (t, $J=8$ Hz), δ 4.14 (t, $J=8$ Hz) and δ 4.05 (m), respectively. The triplet at δ 4.14 is the signal of C_3-H of the xylose (1) which is linked to the C_4-OH group of the rhamnosyl unit, and from all the above-mentioned spectral evidence, the structure of XVIII was determined to be

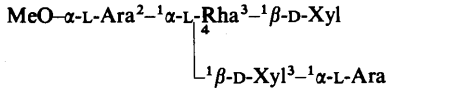

and XVII is the β-anomer of XVIII. The GC-CI-MS analysis of the component methylated sugars of the permethylates of XVII supported the above sugar sequence.

Thus, the structure of XVI was elucidated as shown in the chart.

Our preliminary examination of the saponin constituents in the seeds of this plant has indicated the presence of some oleanolic acid glucuronide saponins. The isolation and structures of these saponins will be reported in the next paper.

Experimental[9]

Extraction, Fractionation and Isolation of Acutosides from the Herb *Luffa acutangula* Roxb. was cultivated in the herbal garden of this Faculty and the herb was harvested in August, 1988. The dried and powdered herb (1 kg) was percolated with 50% MeOH (15 l). MeOH was evaporated off *in vacuo*, and the aqueous solution was filtered. The filtrate was passed through a column (1 l) of Diaion HP 20. After being washed with water (10 l), the column was washed with MeOH (10 l). The MeOH solution was concentrated *in vacuo* to give a saponin-containing fraction (fr. I, 29 g). Fraction I (29 g) was repeatedly chromatographed on silica gel using the solvent systems $CHCl_3$–MeOH–H_2O (15:4:0.5, 15:6:0.5, 15:6:1) and AcOEt–MeOH–H_2O (8:1:0.5, 8:2:0.5, 8:2:1, 6:2:1) and fractionated into seven fractions (fr. Ia—Ig).

Fraction Ia (820 mg) was chromatographed on an octadecyl silica (ODS) column (Fuji gel, 25 cm × 3 cm i.d.) using 85% MeOH as an eluent to give acutoside A (I) (365 mg). Fraction Ib (2.1 g) gave acutoside B (III, 1.56 g) by the same chromatography. Fraction Ic (258 mg) was chromatographed on the same Fuji gel column using 60% MeOH to give acutoside C (VI) (90 mg). Fraction Id (514 mg) was chromatographed on silica gel using AcOEt–MeOH–H_2O (8:2:0.3) to give acutoside D (VII) (311 mg). Fraction Ie (7 g) was almost pure acutoside E (X). Fraction If (3 g) contained a major amount of X and a minor amount of acutoside F (XIII). This fraction was chromatographed on an ODS column using 65% MeOH and 67.5% MeOH to give another crop of X (1.31 g) and XIII (308 mg). Fraction Ig (1.5 g) was almost pure acutoside G (XVI) with a small amount of other contaminants. This fraction was chromatographed on an ODS column using 65% MeOH as an eluant to give XVI (1.30 g). Acutoside E was obtained as colorless needles, but the others could not be crystallized and were obtained as amorphous white powders. The physical and analytical data are shown in Table I. The NMR data are summarized in Tables II and III.

Acid Hydrolysis of Acutosides, Identification of the Aglycone and Sugars The saponin (2 mg) was dissolved in 1 N HCl–MeOH and the solution was refluxed for 2 h. After neutralization with Ag_2CO_3 and filtration, the filtrate was bubbled through with H_2S, and the solvent was evaporated off. The residue was checked by TLC (silica gel, $CHCl_3$–MeOH, 95:5) for the aglycone. The remainder of the methanolysis product was treated with trimethylsilylimidazole and checked by gas-liquid chromatography (GLC) for the component sugars. Methyl glycosides were identified by comparison of the t_R values with those of the methanolysates of authentic sugar samples.

The absolute configurations of the sugars were determined in the same way as described in the previous paper from this laboratory.[10] The GLC conditions are as follows: column, Shimadzu capillary column HiCap (0.25 mm i.d. × 50 m); liquid phase, CBP-1; carrier gas, He at 0.7 ml/min (20 cm/s). Temperature: 190 °C for pentose and methylpentose derivatives, and 210 °C for hexose derivatives and for the determination of the absolute configuration.

The sugars identified for all acutosides are described in the text.

Selective Cleavage of the Ester-linked Sugar Moiety Acutoside B (III) (509 mg) and LiI (566 mg) were added to a mixture of 2,6-lutidine (5 ml) and dry MeOH (3 ml). The mixture was heated at 160 °C for 10 h, and allowed to cool. Then 50% MeOH (10 ml) was added and the diluted solution was passed through a column of Amberlite MB-3 (20 ml). The eluate was concentrated. The residue was suspended in water and chromatographed on a column of Diaion HP 20 (20 ml). The methyl glycoside fraction (278 mg) was eluted first with 30% MeOH (30 ml) and the prosapogenin fraction (385 mg) was eluted next with MeOH. The prosapogenin fraction was purified by chromatography on silica gel using $CHCl_3$–MeOH–H_2O (32:8:1) to give a thin-layer-chromatographically homogeneous prosapogenin (174 mg). The ^{1}H- and ^{13}C-NMR spectra were the same with those of acutoside A (I). The methyl glycoside fraction (278 mg) was chromatographed on an ODS column using 10% MeOH as an eluent to give 122 mg of a mixture of anomers, which were separated by HPLC [Shiseido Capcell Pak C18, 10% MeOH] to give an α-anomer (IV) (40 mg) and a β-anomer (V) (72 mg).

The same treatment of acutosides D (VII), E (X), F (XIII) and G (XVI) gave I as the prosapogenin, and VIII (11 mg) and IX (25 mg) (from 129 mg of VII), XI (36 mg) and XII (64 mg) (from 500 mg of X), XIV (9 mg) and XV (19 mg) (from 103 mg of XIII) and XVII (15 mg) and XVIII (28 mg) (from 524 mg of XVI) as the methyl glycosides.

IV: Amorphous powder. $[\alpha]_D^{26}$ −50.5° ($c=1.00$, MeOH). Negative FAB-MS *m/z*: 441 ($[M-H]^-$), 309 and 163.

V: Amorphous powder. $[\alpha]_D^{26}$ +39.3° ($c=0.90$, MeOH).

VIII: Amorphous powder. $[\alpha]_D^{26}$ −48.9° ($c=0.55$, MeOH). Negative FAB-MS *m/z*: 573 ($[M-H]^-$), 441, 309 and 163.

IX: Amorphous powder. $[\alpha]_D^{26}$ +13.9° ($c=0.95$, MeOH).

XI: Amorphous powder. $[\alpha]_D^{26}$ −38.3° ($c=1.10$, MeOH). Negative FAB-MS *m/z*: 573 ($[M-H]^-$), 441, 309 and 163.

XII: Amorphous powder. $[\alpha]_D^{26}$ +29.6° ($c=1.15$, MeOH).

XIV: Amorphous powder. $[\alpha]_D^{26}$ −58.0° ($c=0.45$, MeOH). Negative FAB-MS *m/z*: 573 ($[M-H]^-$), 441, 309 and 163.

XV: Amorphous powder. $[\alpha]_D^{26}$ +12.5° ($c=0.80$, MeOH).

XVII: Amorphous powder. $[\alpha]_D^{26}$ −41.7° ($c=0.65$, MeOH). Negative FAB-MS *m/z*: 705 ($[M-H]^-$), 573, 441, 309 and 163.

XVIII: Amorphous powder. $[\alpha]_D^{26}$ +10.3° ($c=1.45$, MeOH).

Methylation of Methyl Glycosides and Identification of the Component Methylated Sugars The major one of two anomers was used for analysis. Methylation was performed according to the method reported by Hakomori.[11]

The dimethyl sulfinyl carbanion solution (0.5 ml) (prepared from 30 mg of NaH in 1 ml of dimethylsulfoxide (DMSO) was added to the methyl glycoside (*ca.* 10 mg) and stirred at room temperature for 10 min. CH_3I (1 ml) was added to the solution and the mixture was stirred for 24 h. The reaction mixture was diluted with $CHCl_3$ (3 ml) and washed twice with water (3 ml). The organic solvent layer was dried over Na_2SO_4 and filtered. After evaporation of the solvent, the residue was chromatographed on silica gel (benzene–acetone, 4:1) to give a thin-layer-chromatographically homogeneous methylation product (*ca.* 10 mg). The product was dissolved in 1 N HCl–MeOH (0.5 ml) and the solution was refluxed for 1 h. The acid was neutralized with Ag_2CO_3, the precipitate was filtered off, and the filtrate was bubbled through with H_2S and concentrated to dryness. The methanolysate was acetylated in a usual manner and the acetylation product was analyzed by GC-CI-MS. Conditions were as follows.

Conditions for GC: Column, 2% OV-17 on Chromosorb AW DMCS glass column (1 m × 3 mm i.d.); column temperature, 130→190 °C (3 °C/min); carrier gas, He 20 ml/min.

Conditions for CI-MS: Reagent gas, isobutane; scan number, 1—300 (t_R 1.00—20.00); mass range, *m/z* 100—400; scan speed, 4 s (*m/z* 100—400); ion source temperature, 270 °C; ionization voltage, 150 eV; box current, 200 μA; ion accelerating voltage, 3.5 kV.

The permethylated and partially methylated and acetylated methyl glycosides identified by GC-CI-MS were as follows. Numbers in parentheses are retention times in minutes.

V: 2,3,4-Tri-*O*-methyl-β-D-xylopyranoside (2,3,4-M-β-Xyl) (1.2), 2,3,4-M-α-Xyl (1.6), 2,3-M-4-A-α-Rha (4.9), 3,4-M-2-A-α-Ara (6.0).

IX: 2,3,4-M-β-Xyl (1.2), 2,3,4-M-α-Xyl (1.6), 2,4-M-3-A-β-Xyl (4.5), 2,3-M-4-A-α-Rha (4.9), 2,4-M-3-A-α-Xyl (5.8), 3,4-M-2-A-α-Ara (6.0).

XII: 2,3,4-M-α-Ara (2.6), 2,4-M-3-A-β-Xyl (4.5), 2,3-M-4-A-α-Rha (4.9), 2,4-M-3-A-α-Xyl (5.8), 3,4-M-2A-α-Ara (6.0).

XV: 2,3,4-M-β-Xyl (1.2), 2,3,4-M-α-Xyl (1.6), 3,4-M-2-A-α-Ara (6.0), 2-M-3,4-A-α-Rha (7.5).

XVIII: 2,3,4-M-β-Xyl (1.2), 2,3,4-M-α-Xyl (1.6), 2,3,4-M-α-Ara (2.6), 2,4-M-3-A-β-Xyl (4.5), 2,4-M-3-A-α-Xyl (5.8), 3,4-M-2-A-α-Ara (6.0), 2-M-3,4-A-α-Rha (7.5).

Acknowledgements The authors are grateful to Dr. M. V. Chandravadana of the Indian Institute of Horticultural Research, Bangalore, India, for supplying the seeds of *Luffa acutangula*, and to Miss J. Honda for taking the NMR spectra.

References and Notes

1) K. S. Grewal and B. D. Kochhar, *Indian J. Med. Research*, **31**, 63 (1943).
2) A. K. Barua, S. K. Chakraborti and A. K. Ray, *J. Indian Chem. Soc.*, **35**, 480 (1958).
3) *a*) T. Takemoto, S. Arihara, K. Yoshikawa, K. Kusumoto, T. Yano and T. Hayashi, *Yakugaku Zasshi*, **104**, 246 (1984); *b*) T. Takemoto, S. Arihara, K. Yoshikawa, R. Tanaka and T. Hayashi, *ibid.*, **105**, 834 (1985).
4) K. Kusumoto, T. Nagao, H. Okabe and T. Yamauchi, *Chem. Pharm. Bull.*, **37**, 18 (1989); H. Okabe, T. Nagao, S. Hachiyama and T. Yamauchi, *ibid.*, **37**, 895 (1989).
5) K. Ohtani, K. Mizutani, R. Kasai and O. Tanaka, *Tetrahedron Lett.*, **25**, 4537 (1984).
6) R. Tanaka, T. Nagao, H. Okabe and T. Yamauchi, *Chem. Pharm. Bull.*, **38**, 1153 (1990).
7) K. Bock and C. Pederson, *J. Chem. Soc., Perkin Trans. 2*, **1974**, 293.
8) K. Mizutani, A. Hayashi, R. Kasai, O. Tanaka, N. Yoshida and T. Nakajima, *Carbohydr. Res.*, **126**, 177 (1984).
9) The instruments and materials used in this work were as follows. JASCO DIP-360 digital polarimeter (rotations), JEOL JNM GX-400 spectrometer (100 MHz for ^{13}C-NMR spectra and 400 MHz for ^{1}H-NMR spectra), JEOL DX-300 and HX-110 mass spectrometer (MS), Shimadzu gas chromatograph GC-8A (GC of sugar derivatives), Shimadzu Auto GCMS-6020 with GC-MSPAC 500 FDG data analyzer (GC-CI-MS of the methylated sugar derivatives), Kieselgel 60 (63—210 μm, E. Merck), Diaion HP 20 (Mitsubishi Chemical Industries Ltd.), Fuji gel prepacked ODS column (30 cm × 2.5 cm i.d.) (Wako Pure Chemical Industries, Ltd.), YMC Gel (ODS, 230/70 mesh, Yamamura Chemical Laboratories Co., Ltd.), precoated Kieselgel 60 F_{254} plate, RP-18 $F_{254}S$ plate (E. Merck), Capcell Pak C18 column (25 cm × 1 cm i.d.) (Shiseido Co., Ltd.). ^{1}H- and ^{13}C-NMR spectra were measured in pyridine-d_5 or pyridine-d_5 containing D_2O and chemical shifts were expressed on the δ scale using tetramethylsilane as an internal standard. The FAB-MS were obtained in a glycerol and/or thioglycerol matrix.
10) S. Hara, H. Okabe and K. Mihashi, *Chem. Pharm. Bull.*, **35**, 501 (1987).
11) S. Hakomori, *J. Biochem.*, **55**, 255 (1964).

Structure and Synthesis of an Immunoactive Lipopeptide, WS1279, of Microbial Origin[1)]

Yuko TSUDA,[a] Yoshio OKADA,*[,a] Miho TANAKA,[b] Nobuharu SHIGEMATSU,[b] Yasuhiro HORI,[b] Toshio GOTO[b] and Masashi HASHIMOTO[b]

Faculty of Pharmaceutical Sciences, Kobe-Gakuin University,[a] Nishi-ku, Kobe 651-21, Japan and Exploratory Research Laboratories, Fujisawa Pharmaceutical Co., Ltd.,[b] 5-2-3 Tokodai, Tsukuba, Ibaraki 300-26, Japan. *Received September 12, 1990*

The structure of WS1279, isolated from *Streptomyces* sp. as an immunoactive lipopeptide, has been deduced on the basis of chemical and physical evidence as *S*-[2,3-bis(palmitoyloxy)propyl]-*N*$^{\alpha}$-palmitoyl-Cys-Asn-Ser-Gly-Gly-Ser-OH. This was confirmed by synthesis.

Keywords *Streptomyces*; natural product; lipopeptide; *S*-2,3-dihydroxypropylcysteine; chemical synthesis; immunostimulating activity

Bacteria and cell wall components exhibit immunostimulating activity through proliferation of colony stimulating units in the bone marrow.[2,3)] In the course of our screening program for such immunoactive substances, we isolated from *Streptomyces willmorei* No. 1279 a new lipopeptide, WS1279, which stimulates the proliferation of bone marrow cells.[4)] Here, we report the structural elucidation and synthesis of this natural product.

WS1279 (I) was isolated as a mixture of lipopeptides in which the lipid part is composed of several kinds of fatty acids (Fig. 1). The fast-atom bombardment mass spectrum (FAB-MS) of I showed five main molecular ion peaks at *m/z* $(M+Na)^+$ 1306, 1320, 1334 (main), 1348 and 1362. The presence of the three fatty acid residues in I was corroborated by the ^{1}H-nuclear magnetic resonance (^{1}H-NMR) spectrum of I in $CDCl_3$–CD_3OD: δ 0.85 (9H, m, $3\times CH_3$), 1.25 (*ca.* 72H, m, $(CH_2)_n$), 1.60 (6H, m, $3\times\beta$-CH_2), 2.30 (6H, m, $3\times\alpha$-CH_2). Hydrolysis of I with 6 N HCl followed by methylation with diazomethane gave a mixture of fatty acid methyl esters. The total ion chromatogram of this mixture in gas chromatography–mass spectrum (GC-MS) showed five major peaks at 3 min 26 s, 3 min 31 s, 4 min 20 s, 4 min 42 s and 5 min 17 s (5:1:3:9:2), corresponding to *m/z* 256, 256, 270, 270 and 284, respectively, which were identified as methyl isopentadecanoate, methyl anteisopentadecanoate, methyl isopalmitate, methyl palmitate and methyl isoheptadecanoate, respectively, by comparison GC-MS with authentic samples. Alkaline hydrolysis of I (1 N NaOH) gave a product, whose FAB-MS showed the molecular ion at *m/z* 858 $(M+Na)^+$ due to loss of two fatty acid residues from the molecule of I, indicating that two of the three fatty acid residues are bonded somewhere to the peptide sequence by ester bonds and therefore the remaining one is linked by an amide bond. The latter amide-bonded lipophilic part was found to consist of a single fatty acid, because the molecular ion of the hydrolysis product appeared as a single peak.

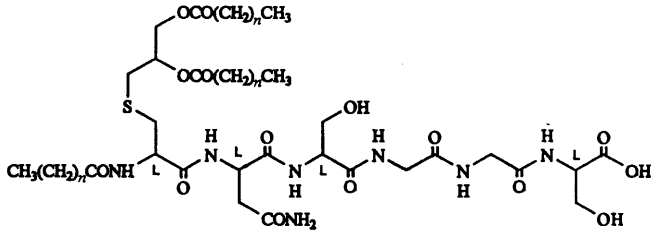

Fig. 1. Structure of WS1279

Amino acid analysis of the 6 N HCl hydrolysate of WS1279 (I) revealed the presence of Asp, Ser, Gly and NH_3 (1:2:2:1), plus two unknown compounds at 9.62 min (before Asp) and at 15.40 min (between Ser and Gly) in addition to the peak due to cystine (22.72 min). Asp and Ser were determined to be L by high performance liquid chromatography (HPLC) analysis using a chiral column (Chiralpak WH). L-Asp is presumed to have been derived from L-Asn, because an equimolar ratio of Asp and NH_3 was obtained in the amino acid analysis as described above and the C-terminal was shown to be a carboxylic acid but not a carboxamide as inferred from the result of hydrolysis with carboxypeptidase A (see below). The two unidentified peaks in the amino acid analysis were presumed to be *S*-glycerylcysteine and its degradation product.

The presence of *S*-glycerylcysteine in the molecule of WS1279 (I) was supposed on the following grounds. The ^{1}H-NMR spectrum of I showed signals at δ 2.75 (2H, m), 4.13 (1H, m), 4.37 (1H, m) and 5.18 (1H, m), and the ^{1}H–^{1}H correlation spectrum (^{1}H–^{1}H COSY) revealed that these signals are coupled to each other, indicating the partial structure shown in Fig. 2. The presence of one sulfur atom was identified by EMAX analysis [found, 2.2%; calcd. based on I ($n=14$), 2.4%]. The FAB-MS of WS1279 itself and the alkaline hydrolysis product both showed a fragment ion at *m/z* 751, which corresponds to the fragments formed by elimination of the $SCH_2CH(OR)CH_2OR$ units from the molecules. The final confirmation of the *S*-glycerylcysteine unit was obtained by comparison with a synthetic sample of *S*-[(2*RS*)-2,3-dihydroxypropyl]cysteine in amino acid analysis. The synthetic sample showed a peak corresponding to that at 9.62 min in the amino acid analysis of I, while, after hydrolysis with 6 N HCl, the synthetic sample showed an additional peak corresponding to that at 15.40 min. This material was deduced to be *S*-[(2*RS*)-2-chloro-3-hydroxypropyl]cysteine from the result of the GC-MS measurement (see below).

The stereochemistry of Cys in the *S*-glycerylcysteine

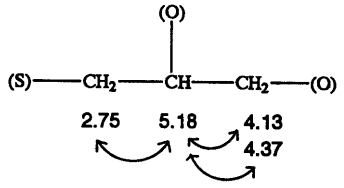

Fig. 2. Coupling in the ^{1}H–^{1}H COSY of WS1279

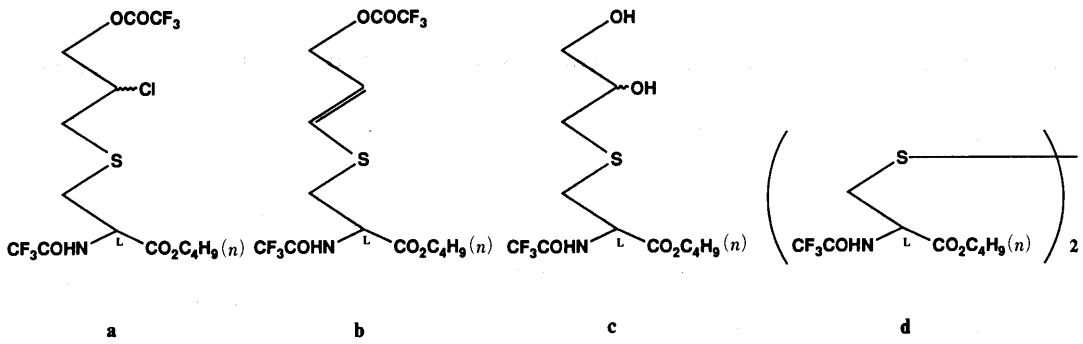

Fig. 3. Structure of Compounds (**a**, **b**, **c** and **d**) Derived from Hydrolysates of WS1279

moiety was deduced to be L as follows. The HCl hydrolysate of I was examined by HPLC on a chiral column [Crownpak CR(+)]. The hydrolysate showed peaks at 8.88, 9.49, 25.88 and 30.15 min. The former two peaks were identified as those of the diastereomeric *S*-[(2*RS*)-glyceryl]-L-cysteines by comparison with the synthetic sample. The corresponding D-cysteine derivatives, *S*-[(2*RS*)-glyceryl]-D-cysteines, were not separated and showed a peak at 4.94 min on Crownpak CR(+) under the same conditions. The degradation products of the synthetic *S*-[(2*RS*)-glyceryl]-L-cysteines also showed peaks at 25.88 and 30.15 min corresponding to the latter two peaks of the natural product under the same conditions. The structures of these products were deduced to be *S*-[(2*RS*)-2-chloro-3-hydroxypropyl]-L-cysteines as follows. The 6N HCl hydrolysate of *S*-[(2*RS*)-glyceryl]-L-cysteines was treated with 3N HCl in *n*-BuOH and then with TFAA in CH_2Cl_2 and subjected to GC-MS, which showed four main peaks in GC (scan numbers: 261, 284, 296 and 429). These peaks were estimated to show molecular weights of 461, 425, 347 and 544 from the MS data (see Experimental) and thus were assigned to have structures **a**, **b**, **c** and **d**, respectively. The peak at 15.40 min in the amino acid analysis and the peaks at 25.88 and 30.15 min in the chiral HPLC were assigned to the diastereoisomeric products **a**. Compound **b** was speculated to have been derived from during the treatments with HCl–*n*-BuOH and TFAA. Compound **c** was presumed to be a fragment ion of the tris(trifluoroacetyl) *n*-butyl ester of *S*-[(2*RS*)-glyceryl]-L-cysteine and compound **d** to be the *n*-butyl N^{α}-trifluoroacetylcystinate (cystine was observed at 22.72 min in the amino acid analysis of a hydrolysate of I). These results are summarized in Fig. 3.

In order to clarify the configuration at position 2 of the glyceryl moiety of *S*-glycerylcysteine, *S*-[(2*R*)-2,3-*O*-isopropylidene-2,3-dihydroxypropyl]-N^{α}-palmitoyl-L-Cys-OBu^t and its (2*S*) counterpart were synthesized. Although they showed single peaks on HPLC (Chiralcel OK) at 53.758 and 51.612 min, respectively, both showed, after treatment with 6N HCl, peaks identical with those at 9.62 and 15.40 min in the amino acid analysis and peaks corresponding to those at 8.88, 9.49, 25.88 and 30.15 min in the chiral HPLC [Crownpack CR(+)]. These results indicate that during the 6N HCl hydrolysis, the glyceryl moiety epimerized at position 2.

For determination of the amino acid sequence in WS1279 (I), an enzymatic degradation method was applied to I in combination with FAB-MS. After treatment of I with carboxypeptidase A, followed by alkaline hydrolysis for removal of the two palmitoyl ester groups, the resulting mixture was analyzed by FAB-MS. Cluster ions were observed at *m/z* 880, 793, 736, 679, 592 and 478 for $(M+2Na-H)^+$ and at *m/z* 858, 771, 714, 657, 570 and 456 for $(M+Na)^+$ as shown in Fig. 4. These data are consistent with the sequence Asn–Ser–Gly–Gly–Ser–OH. The hydrazine degradation of I further corroborated that Ser is the C-terminal in the sequence. The clusters at *m/z* 478 $(M+2Na-H)^+$ and 456 $(M+Na)^+$ correspond to N^{α}-palmitoyl-*S*-glycerylcysteine, which was thus found to be the N-terminal. Taking account of all the above chemical and physical data, we proposed the structure of WS1279 to be I, in which the fatty acid residues are composed mainly of palmitic acid ($n=14$).

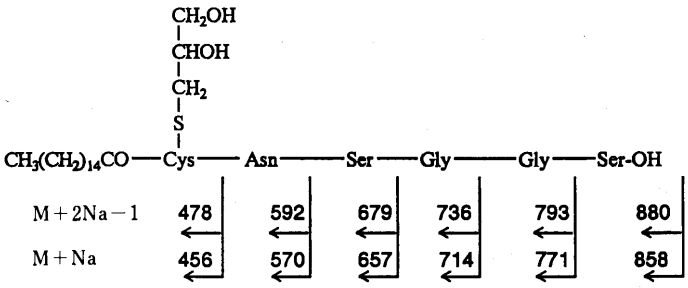

Fig. 4. Cluster Ions in the FAB-MS of the Mixture Obtained by Digestion of WS1279 with Carboxypeptidase A

A final confirmation of the structure I was obtained by a synthesis of I ($n=14$) as a diastereomeric mixture at position 2 of the glyceryl moiety as follows. The peptide part was prepared as shown in Fig. 5. Starting with H–Ser(Bu^t)–OBu^t,[5] Z–Gly–ONp[6] was coupled to give Z–Gly–Ser(Bu^t)–OBu^t. The Z group was removed by catalytic hydrogenation and the resulting amine was coupled with Z–Gly–ONp to give Z–Gly–Gly–Ser(Bu^t)–OBu^t. After removal of the Z group, Z–Ser(Bu^t)–OH[5] was coupled by the DCC–HOBt method[7] to afford Z–Ser(Bu^t)–Gly–Gly–Ser(Bu^t)–OBu^t. After removal of the Z group, the resulting peptide was coupled with Z–Asn–ONp[8] to give Z–Asn–Ser(Bu^t)–Gly–Gly–Ser(Bu^t)–OBu^t. Removal of the Z group afforded H–Asn–Ser(Bu^t)–Gly–Gly–Ser(Bu^t)–OBu^t in an analytically pure form. This peptide was coupled with *S*-[(2*RS*)-2,3-bis(palmitoyloxy)propyl]-N^{α}-palmitoyl–Cys–OH by the DCC–HOBt method described by Wiesmueller *et al.*,[9] to give *S*-[(2*RS*)-2,3-bis(palmitoyloxy)propyl]-N^{α}-palmitoyl–Cys–Asn–Ser(Bu^t)–Gly–Gly–Ser(Bu^t)–OBu^t. The final deprotection was carried out by treatment with

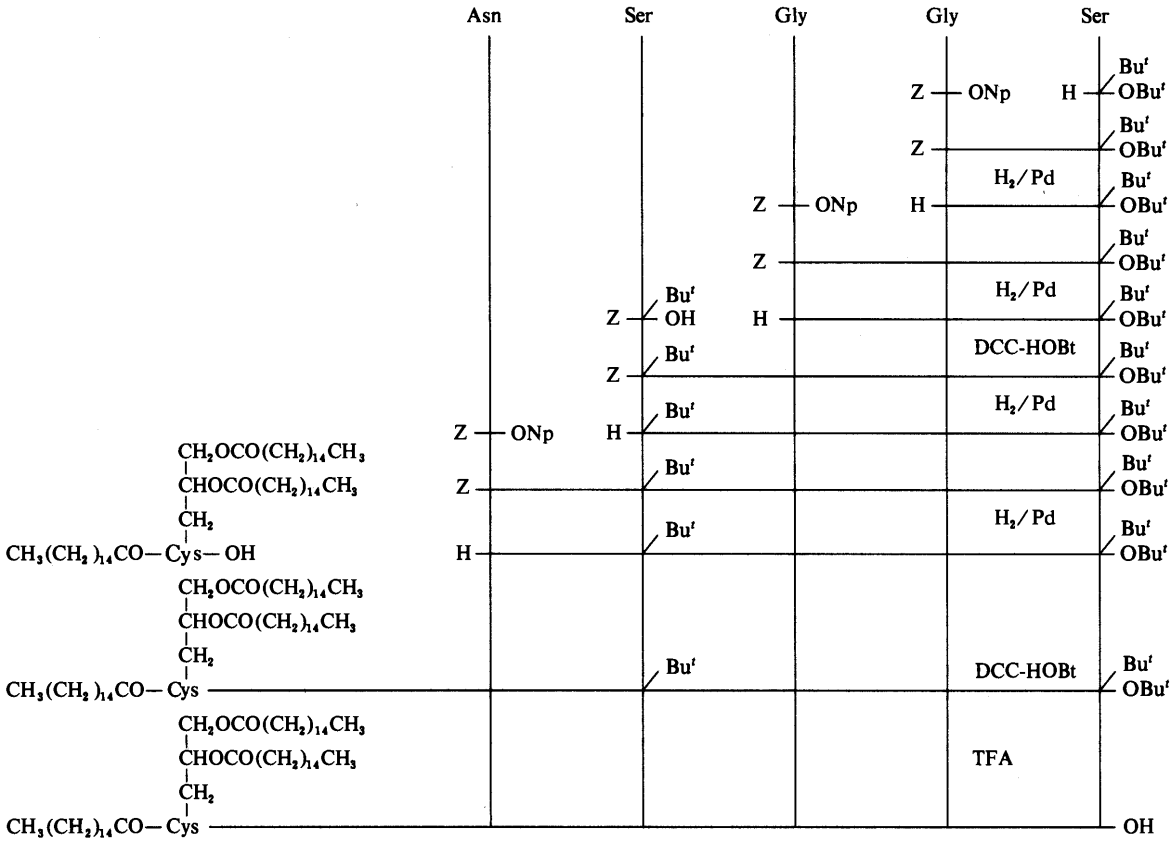

Fig. 5. Synthetic Route to WS1279

trifluoroacetic acid (TFA) to give *S*-[(2*RS*)-2,3-bis(palmitoyloxy)propyl]-N^{α}-palmitoyl–Cys–Asn–Ser–Gly–Gly–Ser–OH.

The synthetic sample was identical with the natural product on thin layer chromatography (TLC) and HPLC. It showed activity to stimulate the colony stimulating factor (CSF)-induced proliferation of bone marrow cells *in vitro* (concentration giving 50% increase: synthetic, 0.38 μg/ml; natural, 0.33 μg/ml). This discrepancy in activity between the synthetic sample and the natural product was probably due to the following reasons: 1) the synthetic sample was a diastereomeric mixture; 2) the synthetic sample was of higher purity and therefore was less soluble in H_2O.[10] Furthermore, it was revealed that the peptides Z–Asn–Ser–Gly–Gly–Ser–OH, H–Asn–Ser(Bu^t)–Gly–Gly–Ser(Bu^t)–OBu^t and H–Asn–Ser–Gly–Gly–Ser–OH did not exhibit any stimulating activity at the concentration of 50 μg/ml, although *S*-[(2*RS*)-2,3-bis(palmitoyloxy)propyl]-N^{α}-palmitoyl–Cys–OH exhibited stimulating activity at the concentration of 5 μg/ml. These results indicate that the lipid peptide structure with a certain chain length is required for manifestation of full stimulating activity. Full details of their activity will be reported elsewhere.

Experimental

The melting points are uncorrected. Optical rotations were measured with an automatic polarimeter, model DIP-360 (Japan Spectroscopic Co., Ltd.). Amino acid compositions of acid hydrolysates (6 N HCl, 110 °C, 18 h) were determined with an amino acid analyzer (K-101 AS, Kyowa Seimitsu). HPLC was conducted with a Shimadzu LC-4A instrument. ^{1}H-NMR spectra were measured with a Bruker AM 400 wb spectrometer, MS with a VG Analytical ZAB-SE and GC–MS with a ZAB-SE instrument equipped with a Hewlett Packard 5890 computer. For column chromatography, a Toyo SF-160 fraction collector was used, if necessary. In TLC (Kieselgel G, Merck), Rf^1, Rf^2, Rf^3, Rf^4 and Rf^5 values refer to the systems of $CHCl_3$, MeOH and H_2O (90 : 8 : 2), $CHCl_3$, MeOH and H_2O (89 : 10 : 1), $CHCl_3$, MeOH, H_2O (8 : 3 : 1, lower phase), *n*-BuOH, AcOH and H_2O (4 : 1 : 5, upper phase) and *n*-BuOH, AcOH, pyridine and H_2O, (1 : 1 : 1 : 1), respectively.

WS1279 (I) WS1279 was isolated as a powder from a fermentation broth of *Streptomyces willmorei* No. 1279.[4] TLC: Rf^3 0.10. HPLC: column, Ultrasphere (4.6 mm i.d. × 250 mm); eluant, MeOH–aq. $HClO_4$ (pH 2) (93 : 7); flow rate, 1 ml/min; temperature, 50 °C; detection, UV 210 nm; retention time, 15.4 min. Amino acid analysis of an acid hydrolysate: Asp (11.26 min), Ser (12.89 min), Gly (19.14 min), NH_3 (39.38 min) (1 : 2 : 2 : 1), cystine (22.72 min), plus two unknown peaks (9.62 and 15.40 min). FAB-MS *m/z*: $(M+Na)^+$ 1306, 1320, 1334 (main), 1348, 1362; fragment ion, *m/z* 751. ^{1}H-NMR ($CDCl_3$–CD_3OD) δ: 0.85 (9H, m, 3 × CH_3), 1.25 (*ca.* 72H, m, $(CH_2)_n$), 1.60 (6H, m, 3 × β-CH_2), 2.30 (6H, m, 3 × α-CH_2). EMAX analysis: Calcd 2.4% (n = 14 in I), Found: 2.2%.

Hydrolysis of WS1279 with 6 N HCl WS1279 (0.1 mg) was hydrolyzed with 6 N HCl (0.8 ml) at 110 °C in a sealed tube for 18 h. The reaction mixture was evaporated to dryness, and the residue was dissolved in 0.1 N HCl and the solution was extracted with AcOEt. The extract was evaporated and the residue was dissolved in MeOH and treated with CH_2N_2 in ether. This mixture was subjected to GC–MS. GC conditions: column, Quadrex (methyl silicone, 0.25 mm i.d. × 25 m × 0.25 μm film); oven temperature, 150—260 °C (10 °C/min); injection temperature, 270 °C; inlet pressure, 10 psi; carrier gas, He at 40 ml/min; retention times, 3 min 26 s, 3 min 31 s, 4 min 20 s, 4 min 42 s and 5 min 17 s (5 : 1 : 3 : 9 : 2), which were identified as those of methyl isopentadecanoate (*m/z* 256), methyl anteisopentadecanoate (*m/z* 256), methyl isopalmitate (*m/z* 270), methyl palmitate (*m/z* 270), and methyl isoheptadecanoate (*m/z* 284), respectively, by comparison with authentic samples. The 0.1 N HCl layer was evaporated and the residue was again dissolved in 0.1 N HCl (20 μl). A 10 μl portion of this solution was subjected to HPLC using Chiralpack WH (4 mm i.d. × 250 mm); eluant, 0.25 mM $CuSO_4$; flow rate, 1 ml/min; column temperature, 50 °C; detection, UV 254 nm; retention time, 43.33, 25.75 min (L-Asp, 43.33; D-Asp, 35.45; L-Ser, 25.75; D-Ser, 17.82 min). The remaining 10 μl portion of the 0.1 N HCl solution was subjected to HPLC using Crownpack CR(+) (4 mm i.d. × 150 mm); eluant, aq. $HClO_4$ (pH 1.0); flow rate, 0.4 ml/min; column temperature, 0 °C; detection, UV 200 nm; retention times, 8.88, 9.49, 25.88 and 30.15 min. The former two peaks

were identified as diastereomeric *S*-[(2*RS*)-glyceryl]-L-cysteines by comparison with a synthetic sample (see below). For identification of the latter two peaks, see the data on hydrolysis of *S*-[(2*RS*)-glyceryl]-L-cysteines with 6 N HCl.

Hydrolysis of WS1279 with NaOH WS1279 (1 mg) was hydrolysed with 1 N NaOH–MeOH (1 : 1, 0.5 ml) at room temperature for 2 h. A portion of the hydrolysate was subjected to FAB-MS *m/z*: 858 $(M+Na)^+$.

Enzyme Degradation of WS1279 with Carboxypeptidase A WS1279 (1 mg) was treated with carboxypeptidase A (0.2 mg) in 5% $NaHCO_3$ (1 ml, pH 7.0) at 20 °C for 10 d. A 1 N NaOH solution (0.2 ml) was added to the mixture and, after 2 h at room temperature, a portion of the mixture was subjected to FAB-MS *m/z*: 880, 793, 736, 679, 592 and 478 for $(M+2Na-H)^+$ and 858, 771, 714, 657, 570 and 456 for $(M+Na)^+$.

Degradation of WS1279 with Hydrazine WS1279 (0.1 mg) was hydrazinolyzed with dry hydrazine (0.8 ml) in a sealed tube at 100 °C for 6 h. The reaction mixture was lyophilized and the residue was dissolved in 0.1 N HCl and applied to an amino acid analyzer: the detected amino acid was Ser.

Hydrolysis of *S*-[(2*RS*)-Glyceryl]-L-cysteines with 6 N HCl *S*-[(2*RS*)-Glyceryl]-L-cysteines (0.1 mg) were hydrolyzed with 6 N HCl (0.8 ml) in the same manner as described above and then the mixture was evaporated to dryness. Amino acid analysis showed two peaks corresponding to those (9.62 and 15.40 min) seen in the amino acid analysis of WS1279. HPLC on Crownpack CR(+) under conditions similar to those for the 6 N HCl hydrolysate of I showed four peaks corresponding to those at 8.88, 9.49, 25.88 and 30.15 min. For identification of the former two peaks, see the data on hydrolysis of WS1279 with 6 N HCl. For identification of the latter two peaks, the following analysis was carried out. The hydrolysate was treated with 3 N HCl in *n*-BuOH (500 μl) at 100 °C for 15 min. The mixture was again evaporated to dryness and the residue was treated with TFAA (200 μl) in CH_2Cl_2 (600 μl) at 150 °C for 5 min. This reaction mixture was subjected to GC–MS: GC column, Ultra 1 (0.32 mm i.d. × 25 m × 0.1 μm film); oven temperature, 100—300 °C (10 °C/min); injection temperature, 270 °C; inlet pressure, 0.7 kgf/cm^2; reagent gas, NH_3(Cl): scan numbers, 261, 284, 296 and 429, which were assigned to be due to **a** [*m/z* 479 and 481 $(M+18)^+$], **b** [*m/z* 426 $(M+1)^+$, 443 $(M+18)^+$ and 461 $(M+36)^+$], **c** [*m/z* 347 M^+, 365 $(M+18)^+$ and 383 $(M+36)^+$] and **d** [*m/z* 544 M^+, 562 $(M+18)^+$]. The peaks at 25.88 and 30.15 min in the chiral HPLC were assigned to **a** (see the text, Fig. 3).

***S*-[(2*RS*)-2,3-Bis(palmitoyloxy)propyl]-*N*$^\alpha$-palmitoyl-Cys-OH** The title compound was prepared according to the method described by Wiesmueller *et al.*[9]

Z-Gly-Ser(Bu^t)-OBu^t (1) Z-Gly-ONp (7.4 g, 0.022 ml) and H-Ser(Bu^t)-OBu^t [prepared from Z-Ser(Bu^t)-OBu^t (13.7 g, 0.040 mol) by catalytic hydrogenation over a Pd catalyst] were dissolved in DMF (50 ml) and the reaction mixture was stirred at room temperature for 48 h. After removal of the solvent, the residue was extracted with AcOEt. The extract was washed with 5% Na_2CO_3, 10% citric acid and water, dried over Na_2SO_4 and evaporated down. Petroleum ether was added to the residue to give an oily material. The crude material in $CHCl_3$ (5 ml) was applied to a silica gel column (5 × 26 cm), equilibrated and eluted with $CHCl_3$. The eluate (2000—3000 ml) evaporated to dryness. Petroleum ether was added to the residue to provide the purified oily material, yield 8.2 g (89%), Rf^1 0.73, Rf^2 0.63. *Anal.* Calcd for $C_{21}H_{32}N_2O_6$: C, 61.7; H, 7.90; N, 6.86. Found: C, 61.7; H, 7.93; N, 6.79. Amino acid ratios in an acid hydrolysate: $Ser_{1.00}Gly_{1.00}$ (average recovery 85%).

Z-Gly-Gly-Ser(Bu^t)-OBu^t (2) The title compound was prepared from Z-Gly-ONp (6.3 g, 0.019 mol) and H-Gly-Ser(Bu^t)-OBu^t [prepared from **1** (8.2 g, 0.020 mol)] in the same manner as described for the synthesis of **1**. The crude material was recrystallized from AcOEt and ether, yield 5.7 g (64%), mp 92—98 °C, $[\alpha]_D^{22}$ +5.8° (*c* = 1.0, MeOH), Rf^1 0.50, Rf^2 0.44. *Anal.* Calcd for $C_{23}H_{35}N_3O_7$: C, 59.3; H, 7.58; N, 9.03. Found: C, 59.4; H, 7.66; N, 9.05.

Z-Ser(Bu^t)-Gly-Gly-Ser(Bu^t)-OBu^t (3) Z-Ser(Bu^t)-OH [prepared from Z-Ser(Bu^t)-OH·DCHA (5.7 g, 0.012 mol)], H-Gly-Gly-Ser(Bu^t)-OBu^t [prepared from **2** (5.6 g, 0.012 mol)] and HOBt (1.6 g, 0.012 mol) were dissolved in DMF (80 ml) and cooled with ice-salt. DCC (2.7 g, 0.013 mol) was added to the above cold solution. The reaction mixture was stirred at 4 °C overnight. After removal of dicyclohexylurea and the solvent, the residue was extracted with AcOEt. The extract was washed with 5% Na_2CO_3, 10% citric acid and water, dried over Na_2SO_4 and evaporated down. Petroleum ether was added to the residue to give a solid mass, which was collected by filtration. The crude material in $CHCl_3$ (5 ml) was applied to a silica gel column (4 × 34 cm), equilibrated with $CHCl_3$ and eluted with $CHCl_3$ (1500 ml), 0.5% MeOH in $CHCl_3$ (1200 ml) and then 1% MeOH in $CHCl_3$ (600 ml). The eluates with 0.5% MeOH in $CHCl_3$ (900—1200 ml) and 1% MeOH in $CHCl_3$ (600 ml) were evaporated to dryness. Petroleum ether was added to the residue to give a white powder, yield 4.7 g (64%), mp 148—151 °C, $[\alpha]_D^{22}$ +5.8° (*c* = 0.9, MeOH), Rf^1 0.57, Rf^2 0.46. *Anal.* Calcd for $C_{30}H_{48}N_4O_9$: C, 59.2; H, 7.95; N, 9.20. Found: C, 59.0; H, 8.05; N, 9.29.

Z-Asn-Ser(Bu^t)-Gly-Gly-Ser(Bu^t)-OBu^t (4) Z-Asn-ONp (1.5 g, 3.8 mmol) and H-Ser(Bu^t)-Gly-Gly-Ser(Bu^t)-OBu^t [prepared from **3** (2.3 g, 3.8 mmol)] were dissolved in DMF (20 ml) and the reaction mixture was stirred at room temperature for 48 h. After removal of the solvent, AcOEt was added to the residue to give a gelatinous precipitate, which was collected by filtration. The crude material in EtOH (5 ml) was applied to a Sephadex LH-20 column (3.5 × 127 cm), equilibrated and eluted with EtOH. Individual fractions (8 g each) were collected and the solvent of the effluent (tube Nos. 34—42) was evaporated off. Ether was added to the residue to give a white precipitate, which was collected by filtration, yield 1.9 g (69%), mp 142—145 °C, Rf^1 0.34, Rf^2 0.26, $[\alpha]_D^{22}$ −1.2° (*c* = 1.0, DMF). *Anal.* Calcd for $C_{34}H_{54}N_6O_{11}$: C, 56.5; H, 7.53; N, 11.6. Found: C, 56.3; H, 7.97; N, 11.3. Amino acid ratios in an acid hydrolysate: $Asp_{1.1}Ser_{2.0}Gly_{2.0}$ (average recovery 80%).

H-Asn-Ser(Bu^t)-Gly-Gly-Ser(Bu^t)-OBu^t (5) Z-Asn-Ser(Bu^t)-Gly-Gly-Ser(Bu^t)-OBu^t (**4**) (1.5 g, 2.5 mmol) in MeOH (50 ml) was hydrogenated over a Pd catalyst. After removal of Pd and the solvent, ether and petroleum ether were added to the residue to give a white precipitate, which was collected by filtration, yield 1.1 g (91%), mp 62—78 °C, $[\alpha]_D^{22}$ +0.2° (*c* = 0.5, DMF), Rf^3 0.11. *Anal.* Calcd for $C_{26}H_{48}N_6O_9$: C, 53.1; H, 8.21; N, 14.3. Found: C, 52.8; H, 8.26; N, 14.0.

S-[(2*RS*)-2,3-Bis(palmitoyloxy)propyl]-*N*$^\alpha$-palmitoyl-Cys-Asn-Ser(Bu^t)-Gly-Gly-Ser(Bu^t)-OBu^t (6) *S*-[(2*RS*)-2,3-Bis(palmitoyloxy)propyl]-*N*$^\alpha$-palmitoyl-cysteine (1.0 g, 1.0 mmol), HOBt (0.14 g, 1.0 mmol) in dichloromethane (20 ml) and DMF (3 ml) were cooled with ice-salt. DCC (0.24 g, 1.2 mmol) was added to the solution. After 30 min, compound **5** (0.58 g, 1.0 mmol) in dichloromethane (20 ml) and DMF (2 ml) was added to the above cold solution. The reaction mixture was stirred at room temperature for 15 h. After removal of the solvent and dicyclohexylurea, the residue was dissolved in $CHCl_3$ (4 ml) and MeOH (10 ml) and the solution was allowed to stand at −30 °C for 4 h. The resultant precipitate was collected by filtration. This material was dissolved in $CHCl_3$ (3 ml) and MeOH (6 ml). After 3 h at −30 °C, the colorless protected hexapeptide was collected by filtration and washed with $CHCl_3$ and MeOH, yield 1.2 g (80%), mp 179—187 °C, $[\alpha]_D^{22}$ −0.49° (*c* = 0.5, DMF), Rf^1 0.51. *Anal.* Calcd for $C_{80}H_{149}N_7O_{15}S\cdot 2H_2O$: C, 63.3; H, 10.2; N, 6.46. Found: C, 63.7; H, 10.1; N, 6.62. Amino acid ratios in an acid hydrolysate: $Asp_{1.1}Ser_{1.8}Gly_{2.0}$ (average recovery 83%); *S*-[(2*RS*)-2,3-dihydroxy]-Cys-OH appeared at a position before Asp.

***S*-[(2*RS*)-2,3-Bis(palmitoyloxy)propyl]-*N*$^\alpha$-palmitoyl-Cys-Asn-Ser-Gly-Gly-Ser-OH (7)** A solution of **6** (1.0 g, 0.70 mmol) in TFA (5.4 ml) was stored at room temperature for 3 h. After removal of the TFA, water (20 ml) was added and evaporated. The residue was dissolved in warm $CHCl_3$ (8 ml). Addition of MeOH (5 ml) afforded a precipitate. After 12 h at −30 °C, the colorless material was collected by filtration and washed with MeOH, yield 0.56 g (62%), mp 200.5—203.5 °C, Rf^3 0.10. *Anal.* Calcd for $C_{68}H_{125}N_7O_{15}S\cdot 3H_2O$: C, 59.8; H, 9.66; N, 7.17. Found: C, 59.6; H, 9.40; N, 7.41. Amino acid ratios in an acid hydrolysate: $Asp_{0.94}Ser_{2.0}Gly_{2.0}$ (average recovery 94%), *S*-[(2*RS*)-2,3-dihydroxypropyl]-Cys-OH appeared at a position before Asp.

Z-Asn-Ser-Gly-Gly-Ser-OH (8) A solution of **4** (350 mg, 0.48 mmol) in TFA (3.7 ml) containing anisole (0.52 ml) was stirred at 0 °C for 10 min and at room temperature for 90 min. Ether was added to the solution to give a precipitate, which was collected by filtration and washed with EtOH, yield 230 mg (89%), mp 161—164 °C, $[\alpha]_D^{22}$ −4.1° (*c* = 0.9, DMF), Rf^4 0.25. *Anal.* Calcd for $C_{22}H_{30}N_6O_{11}\cdot 1.5H_2O$: C, 45.4; H, 5.71; N, 14.4. Found: C, 45.8; H, 5.71; N, 14.1. Amino acid ratios in an acid hydrolysate: $Asp_{1.1}Ser_{2.0}Gly_{2.0}$ (average recovery 60%).

H-Asn-Ser-Gly-Gly-Ser-OH (9) Compound **8** (150 mg, 0.28 mmol) in 50% AcOH (20 ml) was hydrogenated over a Pd catalyst. After removal of the Pd, the solvent was removed by lyophilization to give an amorphous powder, yield 110 mg (78%), $[\alpha]_D^{22}$ −2.5° (*c* = 1.0, 1 N HCl), Rf^5 0.57. Amino acid ratios in an acid hydrolysate: $Asp_{1.0}Ser_{2.0}Gly_{1.9}$ (average recovery 73%).

(Boc-Cys-OBu^t)$_2$ Boc-ON (3.4 g, 14 mmol) in dioxane (20 ml) was added to a solution of $(H-Cys-OBu^t)_2$[9] (2.4 g, 6.8 mmol) in dioxane (10 ml) containing *N*-methylmorpholine (3.0 ml, 28 mmol). The reaction mixture was stirred at room temperature for 15 h. After removal of the solvent, the residue was extracted with AcOEt. The extract was washed with 10%

citric acid and water, dried over Na_2SO_4 and evaporated down. The crude material in $CHCl_3$ (3 ml) was applied to a silica gel column (2.5 × 34 cm), equilibrated and eluted with $CHCl_3$. The eluate (150—300 ml) was evaporated to dryness to give an oily material, yield 0.50 g (13%), Rf^1 0.74.

(Boc-D-Cys-OBu^t)$_2$ $(Boc)_2O$ (4.0 g, 19 mmol) in dioxane (20 ml) was added to a solution of (H-D-Cys-OBu^t)$_2$ (3.0 g, 8.2 mmol) [prepared from D-cystine (2.0 g, 8.2 mmol) according to the method previously described[9]] in dioxane (10 ml) containing *N*-methylmorpholine (2.0 ml, 19 mmol). The reaction mixture was stirred at room temperature for 15 h. After removal of the solvent, the residue was extracted with AcOEt. The extract was washed with 10% citric acid and water, dried over Na_2SO_4 and evaporated down. The crude material in $CHCl_3$ (3 ml) was applied to a silica gel column (2.5 × 25.5 cm), equilibrated and eluted with $CHCl_3$. The eluate (30—200 ml) was evaporated to dryness to give an oily material. Petroleum ether was added to the residue to give a white precipitate, yield 1.3 g (28%), mp 92.5—94 °C, $[\alpha]_D^{22}$ −15.4° (c=0.4, $CHCl_3$), Rf^1 0.74. *Anal.* Calcd for $C_{24}H_{44}N_2O_8S_2$: C, 52.2; H, 8.02; N, 5.06. Found: C, 51.9; H, 8.03; N, 5.10.

Boc-Cys-OBu^t (Boc-Cys-OBu^t)$_2$ (0.50 g, 0.90 mmol) in $CHCl_3$ (20 ml) was reduced with dithioerythritol (0.59 g, 3.8 mmol) in the presence of Et_3N (0.39 ml, 2.8 mmol). After being stirred at room temperature for 2 h under N_2, the solution was washed with 10% citric acid and water, dried over Na_2SO_4 and evaporated down. The oily residue was dried over P_2O_5 *in vacuo*, yield 0.50 mg (100%), Rf^1 0.60.

Boc-D-Cys-OBu^t The title compound was prepared from (Boc-D-Cys-OBu^t)$_2$ (0.50 g, 0.90 mmol) in the same manner as described above. The oily material was dried over P_2O_5 *in vacuo*. Petroleum ether was added to the residue to give a white precipitate, yield 0.33 g (67%), mp 46—49 °C, $[\alpha]_D^{22}$ −17.1° (c=1.0, $CHCl_3$), Rf^1 0.60. *Anal.* Calcd for $C_{12}H_{23}NO_4S$: C, 52.0; H, 8.35; N, 5.04. Found: C, 51.8; H, 8.46; N, 4.92.

***S*-[(2*RS*)-2,3-Dihydroxypropyl]-*N*$^\alpha$-Boc-Cys-OBu^t** 3-Bromo-1,2-propanediol (1.8 ml, 18 mmol) was added to a solution of Boc-Cys-OBu^t (0.50 g, 1.8 mmol) in DMF (10 ml) containing Et_3N (2.5 ml, 18 mmol). The reaction mixture was stirred at 80 °C for 1 h and at room temperature for 1 h. After removal of the solvent, the residue was extracted with AcOEt. The extract was washed with 10% citric acid and water, dried over Na_2SO_4 and evaporated down to give an oily material, which was dried over P_2O_5 *in vacuo*, yield 0.30 g (47%), Rf^1 0.48.

***S*-[(2*RS*)-2,3-Dihydroxypropyl]-*N*$^\alpha$-Boc-D-Cys-OBu^t** The title compound was prepared from Boc-D-Cys-OBu^t (0.32 g, 1.2 mmol) in the same manner as described above. The crude material in $CHCl_3$ (3 ml) was applied to a silica gel column (2.5 × 31.5 cm), equilibrated with $CHCl_3$ and eluted with $CHCl_3$ (600 ml) and then 1% MeOH in $CHCl_3$ (1000 ml). Individual fractions (10 g each) were collected and the solvent of the effluent (tube Nos. 90—180) was removed by evaporation. Petroleum ether was added to the residue to give an oily material, which was dried over P_2O_5 *in vacuo*, yield 0.20 g (47%), Rf^1 0.48.

***S*-[(2*RS*)-2,3-Dihydroxypropyl]-L-Cys-OH** *S*-[(2*RS*)-2,3-Dihydroxypropyl]-*N*$^\alpha$-Boc-Cys-OBu^t (0.30 g, 0.85 mmol) was dissolved in TFA (6.5 ml) containing thioanisole (1.0 ml) and the reaction mixture was stirred at room temperature for 1 h. Ether (25 ml) and petroleum ether (25 ml) were added to the reaction mixture under ice-cooling to yield an oily material. After removal of the solvent by decantation, the residue was dissolved in EtOH (10 ml). The pH of the solution was adjusted to 7 using Et_3N to yield a precipitate, which was collected by centrifugation, yield 26 mg (17%), mp 160—166 °C, $[\alpha]_D^{22}$ −8.6° (c=0.7, 0.1 N HCl), Rf^3 0.14, Rf^4 0.60. *Anal.* Calcd for $C_6H_{13}NO_4S$: C, 36.9; H, 6.70; N, 7.17. Found: C, 36.8; H, 6.81; N, 6.98. Chiral HPLC [Crownpack RC(+)] under the same conditions as those for the 6 N HCl hydrolysate of I showed two peaks corresponding to those at 8.88 and 9.49 min in the analysis of the hydrolysate of I.

***S*-[(2*RS*)-2,3-Dihydroxypropyl]-D-Cys-OH** The title compound was prepared from *S*-[(2*RS*)-2,3-dihydroxypropyl]-D-Cys-OBu^t (0.20 g, 0.57 mmol) in the same manner as described above, yield 11 mg (9.4%), mp 171—176 °C, $[\alpha]_D^{22}$ +4.5° (c=0.5, 0.1 N HCl), Rf^3 0.14, Rf^4 0.60. *Anal.* Calcd for $C_6H_{13}NO_4S$: C, 36.9; H, 6.70; N, 7.17. Found: C, 36.5; H, 6.72; N, 6.83. Chiral HPLC [Crownpack CR(+)] under the same conditions as those for the 6 N HCl hydrolysate of I: retention time, 4.94 min.

(2*S*)-1-*O*-Tosyl-2,3-*O*-isopropylideneglycerine Tosyl chloride (7.2 g, 38 mmol) was added to a solution of (2*S*)-2,3-*O*-isopropylideneglycerine (5.0 g, 38 mmol, Aldrich) in dry pyridine (30 ml) under cooling with ice. The reaction mixture was stirred at 4 °C overnight. After removal of the solvent, the residue was extracted with AcOEt. The extract was washed with 10% citric acid, 5% $NaHCO_3$ and water, dried over Na_2SO_4 and evaporated down to give an oily material, which was dried over P_2O_5 *in vacuo*, yield 10.3 g (95%), Rf^1 0.70. IR: 1170, 1375 (SO_2) cm^{-1}.

(2*R*)-1-*O*-Tosyl-2,3-*O*-isopropylideneglycerine The title compound was prepared from (2*R*)-2,3-*O*-isopropylideneglycerine (5.0 g, 38 mmol, Aldrich) in the same manner as described above, yield 10.1 g (93%), Rf^1 0.70. IR: 1170, 1375 (SO_2) cm^{-1}.

***S*-[(2*S*)-2,3-*O*-Isopropylidene-2,3-dihydroxypropyl]-*N*$^\alpha$-palmitoyl-Cys-OBu^t** *N*$^\alpha$-Palmitoyl-Cys-OBu^t (1.7 g, 4.1 mmol) and K_2CO_3 (0.56 g, 4.1 mmol) were added to a refluxing solution of (2*S*)-1-*O*-tosyl-2,3-isopropylideneglycerine (2.0 g, 7.1 mmol) in EtOH (50 ml). After 10 h, the EtOH was removed by evaporation. The residue was extracted with AcOEt. The extract was washed with H_2O, dried over Na_2SO_4 and evaporated down to give an oily product. The crude product in $CHCl_3$ (2 ml) was applied to a silica gel column (2.8 × 30 cm), equilibrated and eluted with $CHCl_3$. The eluate (800—900 ml) was evaporated to dryness to give an oily material, yield 0.10 g (4.6%), $[\alpha]_D^{22}$ +18.0° (c=1.7, $CHCl_3$), Rf^2 0.73. Exact MS Calcd for $C_{29}H_{55}NO_5S$+H: 530.3879. Found: 530.3865. Amino acid analysis of an acid hydrolysate showed peaks corresponding to those (9.63 and 15.40 min) in the amino acid analysis of the acid hydrolysate of WS1279. HPLC of the 6 N HCl hydrolysate on Crownpack CR(+) showed four peaks corresponding to those (8.88, 9.42, 25.88 and 30.15 min) in the HPLC of the 6 N HCl hydrolysate of WS1279.

***S*-[(2*R*)-2,3-*O*-Isopropylidene-2,3-dihydroxypropyl]-*N*$^\alpha$-palmitoyl-Cys-OBu^t** The title compound was prepared from *N*$^\alpha$-palmitoyl-Cys-OBu^t (1.0 g, 2.4 mmol) and (2*R*)-1-*O*-tosyl-2,3-isopropylideneglycerine (1.2 g, 4.1 mmol) in the same manner as described above, yield 50 mg (3.8%), $[\alpha]_D^{22}$ −5.3° (c=1.2, $CHCl_3$), Rf^2 0.73. Exact MS Calcd for $C_{29}H_{55}NO_5S$ +H: 530.3879. Found: 530.3886. Amino acid analysis and HPLC on Crownpack CR(+) of the 6 N HCl hydrolysate showed the same peaks as those of the 2*S* counterpart.

References and Notes

1) All amino acid residues are of L-configuration except in the case of glycine unless otherwise indicated. The abbreviations used are those recommended by the IUPAC-IUB Commission on Biochemical Nomenclature: *Biochemistry*, **5**, 3485 (1966); *ibid.*, **6** 362 (1967); *ibid.*, **11**, 1726 (1972). Other abbreviations used are: Boc, *tert*-butyloxycarbonyl; Z, benzyloxycarbonyl; OBzl, benzyl ester; OBu^t, *tert*-butyl ester; ONp, *p*-nitrophenyl ester; Bu^t, *tert*-butyl; DCC, *N*,*N*'-dicyclohexylcarbodiimide; HOBt, *N*-hydroxybenzotriazole; AcOEt, ethyl acetate; DMF, dimethylformamide; TFAA, trifluoroacetic anhydride.
2) R. S. Foster, B. R. McPherson and D. A. Browdie, *Cancer Res.*, **37**, 1349 (1977).
3) R. S. Foster, *Cancer Res.*, **38**, 2666 (1978).
4) M. Tanaka, Y. Hori, H. Ueda, H. Nakajima, T. Goto and M. Okuhara, *J. Antibiot.*, in preparation.
5) H. C. Beyerman and J. S. Bontekoe, *Rec. Trav. Chim. Pays-Bas*, **81**, 691 (1962).
6) Y. Wolman, D. Ladkang and M. Frankel, *J. Chem. Soc.*, (*C*), **1968**, 689.
7) W. Konig and R. Geiger, *Chem. Ber.*, **103**, 2024 (1970).
8) M. Bodansky and V. du Vigneud, *J. Am. Chem. Soc.*, **81**, 5688 (1959).
9) H. Wiesmueller, W. Bessler and G. Jung, *Z. Physiol. Chem.*, **364**, 593 (1983).
10) M. Tanaka, Y. Hori, H. Sakai, H. Ueda, T. Goto and M. Okuhara, *J. Antibiot.*, in preparation.

On the Repair of Thymine and Thymidine Bromohydrins: A Possible New Model for the Damage and Repair of Nucleic Acids

Takashi HARAYAMA,* Reiko YANADA, Taishin AKIYAMA, Mihoko TANAKA, Yuki FUJITA, and Fumio YONEDA*

Faculty of Pharmaceutical Sciences, Kyoto University, Sakyo-ku, Kyoto 606, Japan. *Received September 14, 1990*

Bromohydrins (2, 3, 4, and 5), oxidatively damaged products of thymine bases, were repaired on exposure to sunlight, heat, and/or some reagents to regenerate the thymine bases. A radical mechanism is proposed for the repair reaction with sunlight and heat. A hypothesis concerning the biological significance of thymidine in deoxyribonucleic acid is presented.

Keywords oxidatively damaged product; bromohydrin; repair reaction; sunlight; heat; thymine base; radical mechanism

Oxidative damage to nucleic acids and related compounds caused by active oxygen species, such as hydrogen peroxide, hydroxy radical, superoxide anion, singlet oxygen, and lipid hydroperoxides, has recently been receiving much attention, as it may play a role in mutagenesis, carcinogenesis, and aging.[1-6] In relation to the oxidative damage to nucleic acids and components, it has been revealed that *cis*-thymine and thymidine diols, oxidized thymidine derivatives, are released in human and rat urine as a result of the repair of oxidatively damaged deoxyribonucleic acid (DNA).[7] Moreover, it has recently been reported that haloperoxidases such as chloroperoxidase and bromoperoxidase obtained from living cells[8-12] activated halide anion to the halonium cation in the presence of hydrogen peroxide[13] and catalyzed the halogenation of nitrogen-containing aromatic heterocycles such as pyrazole, uracil, thymine, and cytosine to yield the respective halogenated (oxidized) products. Chloroperoxidase, in particular, catalyzed the oxidation of thymine (**1**) to thymine bromohydrin (**2**) in the presence of potassium bromide and hydrogen peroxide.[14] This finding strongly suggests that thymidine in living cells can be oxidized to thymidine bromohydrin with the aid of haloperoxidase. In spite of many investigations of oxidative damage to nucleic acids, there has been little study on the repair of oxidatively damaged nucleic acids from the viewpoint of organic chemistry. Therefore, we have investigated the repair of nucleosides subjected to oxidative damage,[15] especially thymine and thymidine bromohydrins, as model compounds of oxidatively damaged nucleic acids. We have briefly described the results.[16] The details are the subject of this paper.

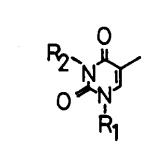

1 : $R_1=R_2=H$
6 : $R_1=R_2=Me$
10 : $R_1=Me$, $R_2=H$
11 : $R_1=H$, $R_2=Me$

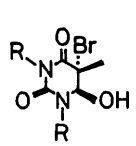

2 : R=H (*dl*)
3 : R=Me (*dl*)

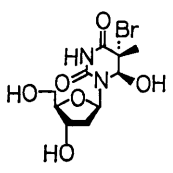

4

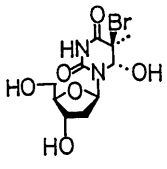

5

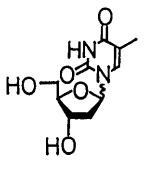

7

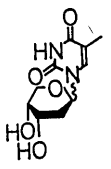

8

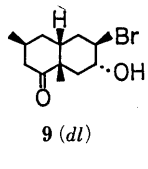

9 (*dl*)

Fig. 1

During our studies on the reactions of 1,3-dimethylthymine and thymidine epoxides with amines, L-amino acid derivatives, and other nucleophiles as model reactions for nucleic acid–protein cross-links,[17-20] we observed that heating of the bromohydrins (**3**, **4**, and **5**) in tetrahydrofuran (THF) with nucleophiles such as thiophenol, *N*-acetyl-L-cysteine, and L-ascorbic acid often gave thymine derivatives (**6**, **7**, and **8**), corresponding to the repaired products. However, the reproducibility of the reaction was very poor. After much sdudy, we found that the repair reaction proceeded without any reagent upon exposure of the compounds to either sunlight or heat. First, a suitable solvent for the repair reaction of the bromohydrin (**3**) was examined under the reaction conditions indicated in Table I. The results in Table I show that THF seems to be the most suitable solvent for this purpose. Therefore, using THF as a solvent, the repair reaction of bromohydrins (**3**, **4**, and **5**) with sunlight or heat was investigated. The results are summarized in Table II. As can be seen from Table II, the reaction proceeded with sunlight (3400 lux) or heat (entries 1 and 4), but not in the dark at room temperature. However, on adding a catalytic amount of azobisisobutyronitrile (AIBN), a radical initiator, the reaction in the dark at room temperature proceeded smoothly (entry 5) and that under sunlight was slightly accelerated (entry 2). The results also showed that galvinoxyl, a radical scavenger, could quench the reaction, with the starting material being recovered in good yield (entries 3 and 6). These results show that the repair reaction proceeds by a radical mechanism.[21-23] No epimerization of β-thymidine (β-7) to α-thymidine (α-7) and/or **8** occurred under the reaction conditions, indicating that α-thymidine (α-7) and **8** would be produced

TABLE I. Data on the Repair Reaction of the Bromohydrin (**3**) in Various Solvents

Entry	Solvent	Reaction temp.	Reaction time	(**6**) (%)	Recovery (%)
1	DMSO	130 °C	30 min	73.0	*ca.* 13
2	Diglyme	130 °C	45 min	88.4	—
3	THF	50 °C	1 h	95.6	—
4	Dioxane	Reflux	21 h	84.9	—
5	CCl_4	Reflux	20 h	25.2	*ca.* 47
6	Benzene	Reflux	20 h	7.2	*ca.* 59

Reaction conditions: addition of 1% AIBN under room light (70 lux).

TABLE II. Data on the Repair Reaction of Bromohydrins (3, 4, and 5)[a]

Entry	Conditions[b]	3 Reaction time (h)	3 6 (%)	3 Recovery (%)	4 Reaction time (h)	4 7 (%)	4 8 (%)	4 Recovery (%)	5 Reaction time (h)	5 7 (%)	5 8 (%)	5 Recovery (%)
1	A	2.5	81.7	—	1.5	42.7 (1:4.1)	16.1 (β)[c]	—	1.0	32.7 (1:2.8)	8.1 (1:1.4)	—
2	A, AIBN	1.0	89.3	—	1.0	37.0 (1:4.0)	13.0 (β)[c]	—	1.0	34.9 (1:3.0)	8.9 (1:1.7)	—
3	A, galvinoxyl	17.0	—	66.6	17.0	—	—	92.5	22.0	—	—	84.2
4	B	10.0	92.4	—	3.0	59.8 (1:2.4)	13.1 (β)[c]	—	3.0	66.8 (1:1.7)	22.4 (1:1.5)	—
5	C, AIBN	3.0	Quant.	—	4.0	50.0 (1:2.6)	18.2 (β)[c]	—	6.0	49.5 (1:2.9)	4.7 (β)[c]	—
6	B, galvinoxyl	10.0	—	81.0	6.0	—	—	90.0	8.0	—	—	91.7

a) Values in parentheses indicate the proportions of α- and β-isomers. Isomers were isolated by preparative TLC in entry 1. In other entries, proportions of α and β were determined by NMR spectroscopy. b) Reaction conditions: A; under sunlight irradiation at room temperature, B; in the dark under reflux, C; in the dark at room temperature. c) A trace amount of α-isomer (α-8) was present.

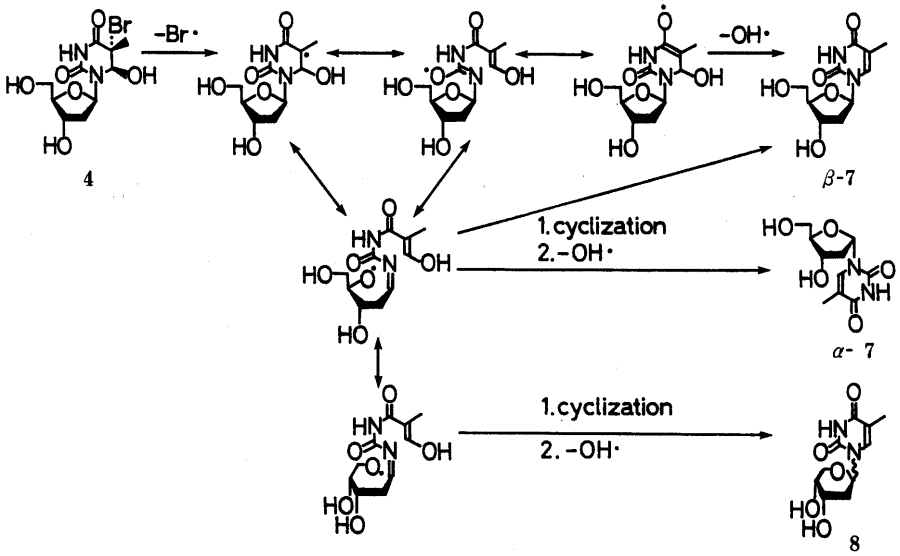

Fig. 2

concomitantly when the bromohydrins (**4** and **5**) were converted to thymidines (**7** and **8**). Furthermore, this repair reaction seems to be characteristic of bromohydrins having an aminal (α-carbinol amine) moiety, because exposure of the *trans*-bromohydrin (**9**)[24] to the same reaction conditions resulted in recovery of the starting material (**9**) quantitatively.

Subsequently, the repair reaction of thymine bromohydrin (**2**) to thymine (**1**) was investigated, the results being summarized in Table III. The repair reaction of **2**, as well as the bromohydrins (**3**, **4**, and **5**), with sunlight proceeded smoothly (entries 1 and 2), whereas the reaction of **2** in THF with heat scarcely proceeded (entries 3 and 4). The repair reaction with heat finally proceeded in dimethyl sulfoxide (DMSO) in the dark at 130 °C in the presence of a catalytic amount of AIBN (entry 5). The difference of reactivity between the bromohydrins **2** and **3**, **4**, and **5** seems to be attributable to the presence of the N-1 substituent. Therefore, we planned to synthesize bromohydrins of 1-methylthymine (**10**)[25] and 3-methylthymine (**11**)[26] and to investigate their repair reactions. However, the desired bromohydrins could not be isolated because of their instability.

Next, the repair reaction of the bromohydrin (**3**) with

TABLE III. Data on the Repair Reaction of Thymine Bromohydrin (2)

Entry	Reaction conditions[a]	Reaction time (h)	(1) (%)	Recovery (%)
1	A	4.5	82.3	—
2	A, AIBN	2.5	93.2	—
3	B	23.0	—	Quant.
4	B, AIBN	14.0	—	Quant.
5	C, AIBN	0.8	72.9	—

a) Reaction conditions: A; under sunlight irradiation at room temperature, B; in the dark under reflux, C; DMSO was used instead of THF in the dark at 130 °C.

TABLE IV. Data on the Repair Reaction of the Bromohydrin (3) with Heat and Reagents

Reagent	Equivalent	Reaction time (h)	(6) (%)
—	—	10—31	92—96
N-Ac-L-Cys–OMe	1.2	0.8	95
N-Ac-L-Cys	1.2	1.5	97
PhSH	2.4	2.3	96
Ascorbic acid	1.2	2.0	96
Ph_3P	1.2+1.2[a]	5.0	88

a) The reagent (1.2 eq) was added after 1 h.

TABLE V. Data on the Repair Reaction of the Bromohydrin (3) with Sunlight and Reagents

Reagent	Equivalent	Reaction time (h)	(6) (%)
—	—	2.5—6.5	81—96
N-Ac-L-Cys–OMe	1.2	6.0	81
N-Ac-L-Cys	1.2	6.5	87
PhSH	2.4	2.5	97

other reagents, especially biological compounds was examined. The results are summarized in Tables IV and V, indicating that addition of reagents affected the repair reaction in THF under heating in the dark (Table IV),[27] but did not affect the reaction under sunlight (Table V), although the reason for this remains to be clarified.

In Fig. 2, we propose a plausible mechanism for the repair reaction of the bromohydrin (**4**), initiated by radical scission of the C_5–Br bond. Thymidine having a vinylogous amide moiety is subject to oxidation, including halogenation, catalyzed by enzymes such as haloperoxidases as well as oxidants such as active oxygens to produce oxidized (damaged) thymidine derivatives such as thymidine diol and bromohydrin possessing an aminal moiety. These oxidized thymidine derivatives, especially thymidine bromohydrins, can be repaired by expoure to sunlight, heat, and/or other agents, regenerating the thymidines. We think that thymidine may protect other compounds *in vivo* by being oxidized (halogenated) itself and then readily undergoing repair. We consider that thymidine plays an important role, functionally and structurally, in the damage and repair process of nucleic acids.

Experimental

The proton nuclear magnetic resonance (^{1}H-NMR) spectra were obtained in $(CD_3)_2SO$-D_2O at 200 MHz on a JEOX FX 200 spectrometer with chemical shifts being reported in parts per million downfield from a tetramethylsilane internal standard, and coupling constants in hertz. Mass spectra (MS) were taken on a JEOL JMS 01SG-2 instrument (direct inlet) at 70 eV. Preparative thin layer chromatography (TLC) was run on 20 × 20 cm plates coated with a 0.25 mm layer of Merck silica gel PF_{254} and GF_{254}, using chloroform containing 4% methanol (solvent A) and ethyl acetate–propan-2-ol–water (75 : 16 : 5) (solvent B). A sunlight lamp (Toshiba, DR 250/TL, about 3400 lux) was used for the repair reaction. All reactions were carried out under an argon atmosphere unless otherwise stated. The reaction mixture was concentrated to dryness under reduced pressure. The residue was purified or separated by preparative TLC using solvent A (method A) or solvent B (method B). α-Thymidine (α-7) was purchased from Sigma Chemical Company and β-thymidine (β-7) from Wako Pure Chemical Industries, Ltd.

General Procedures for the Repair Reaction of the Bromohydrin (3) with Heat in Various Solvents (Table I) A solution of the bromohydrin (3) (1 mmol) with AIBN (0.01 mmol) in a dry solvent (20 ml) was heated under room light (about 70 lux) at the temperature indicated in Table I. The residue was purified by method A to give 1,3-dimethylthymine (**6**), mp 153—155 °C (needles from EtOH) (entries 2, 3, and 4), or 1,3-dimethylthymine (**6**) from the upper zone and the starting material (**3**) from the lower zone (entries 1, 5, and 6). Yields are given in Table I.

The Repair Reaction of Bromohydrins (3, 4, and 5) with Sunlight (Entry 1 in Table II) A solution of a bromohydrins (1 mmol) in dry THF (20 ml) was irradiated with a sunlight lamp at room temperature for the time indicated in Table II. Purification of the residue from **3** by method A gave 1,3-dimethylthymine (**6**). Separation of the residues from **4** and **5** by method B gave β-thymidine (β-**7**) from the first zone (highest zone), α-thymidine (α-**7**) from the second zone, β-**8** from the third zone, and α-8 from the fourth zone (lowest zone). Yields and ratios are indicated in Table II. The compounds (**6**, α-**7**, and β-**7**) were identified by comparison with authentic samples. 1-(2-Deoxy-β-D-*erythro*-pentopyranosyl)thymine (β-**8**), mp 218—220 °C (from isopropyl alcohol)[28]; ^{1}H-NMR (d_6-DMSO) δ: 1.77 (3H, d, J = 1.2 Hz, C_5-C<u>H</u>$_3$), 2.01—2.16 (2H, m, C_2-<u>H</u>$_2$), 3.57—3.66 (3H, br s, C_4-<u>H</u>, C_5-<u>H</u>$_2$), 3.99 (1H, br s, C_3-<u>H</u>), 5.84 (1H, dd, J = 11.2, 2.1 Hz, C_1-<u>H</u>), 7.57 (1H, q, J = 1.2 Hz, C_6-<u>H</u>). MS Calcd for $C_{10}H_{14}N_2O_5$: 242.09026. Found: 242.09033. 1-(2-Deoxy-α-D-*erythro*-pentopyranosyl)-thymine (α-**8**) mp 209—213 °C (from isopropyl alcohol)[28]; ^{1}H-NMR (d_6-DMSO) δ: 1.78 (3H, d, J = 1.2 Hz, C_5-C<u>H</u>$_3$), 1.88—2.08 (2H, m, C_2-<u>H</u>$_2$), 3.45—3.86 (4H, m, C_3-<u>H</u>, C_4-<u>H</u>, C_5-<u>H</u>$_2$), 5.50 (1H, dd, J = 11.2, 2.1 Hz, C_1-<u>H</u>), 7.56 (1H, q, J = 1.2 Hz, C_6-<u>H</u>). MS Calcd for $C_{10}H_{14}N_2O_5$: 242.09026. Found: 242.08967.

The Repair Reaction of Bromohydrins (3, 4, and 5) with Sunlight and AIBN (Entry 2 in Table II) A solution of a bromohydrin (1 mmol) and AIBN (0.01 mmol) in dry THF (20 ml) was irradiated with a sunlight lamp at room temperature for the time indicated in Table II. The residue from **3** was purified by method A to give 1,3-dimethylthymine (**6**). The residues from **4** and **5** were separated by method B to give a mixture of α- and β-thymidines (**7**) from the upper zone and a mixture of α- and β-**8** from the lower zone. Yields are given in Table II. The proportions of α- and β-**7**, and α- and β-**8** were determined from the C_6-H integral values in ^{1}H-NMR spectroscopy.

The Reaction of Bromohydrins (3, 4, and 5) with Sunlight and Galvinoxyl (Entry 3 in Table II) A solution of a bromohydrin (1 mmol) and galvinoxyl (1.2 mmol) in dry THF (20 ml) was irradiated with a sunlight lamp at room temperature for the time indicated in Table II. The residue was purified by method A for bromohydrin (**3**) and be method B for bromohydrins (**4** and **5**) to recover the starting materials (**3**, **4**, and **5**, respectively). Recovery yields are given in Table II.

The Repair Reaction of Bromohydrins (3, 4, and 5) with Heat (Entry 4 in Table II) A solution of a bromohydrin (1 mmol) in dry THF (20 ml) was refluxed in the dark for the time indicated in Table II. Each residue was purified in the same manner as for entry 3 in Table II mentioned above. Yields are given in Table II.

The Repair Reaction of Bromohydrins (3, 4, and 5) with AIBN at Room Temperature (Entry 5 in Table II) AIBN (0.01 mmol) in dry THF (1 ml) was refluxed for 1 min, then cooled, and a solution of a bromohydrin (1 mmol) in dry THF (19 ml) was added. The mixture was stirred at room temperature in the dark for the time indicated in Table II. Each residue was purified in the same manner as for entry 3 in Table II mentioned above. Yields are given in Table II.

Reaction of Bromohydrin (9) with Room Light and Heat A solution of the bromohydrin (**9**) (0.1 mmol) in dry THF (3 ml) was refluxed under room light for 10 h. The solvent was removed under reduced pressure to recover the starting material (**9**) quantitatively.

General Procedure for the Repair Reaction of Thymine Bromohydrin (2) (Table III) A solution of the bromohydrin (**2**) (1 mmol) or the bromohydrin (**2**) (1 mmol) with AIBN (0.01 mmol) in dry solvent (20 ml) was stirred under the reaction conditions indicated in Table III. The residue was washed three times with ether–acetone (10 : 1) by centrifugation (3000 rpm × 5 min) to afford thymine (**1**) in the yields given in Table III (entries 1, 2, and 5) or to afford the starting material (**2**) quantitatively (entries 3 and 4).

General Procedures for the Repair Reaction of the Bromohydrin (3) with Heat and Reagents (Table IV) A solution of the bromohydrin (**3**) (1 mmol) and a reagent [1.2, 2.4 or 1.2 + 1.2 (1.2 mmol of reagent was added first and a further 1.2 mmol of reagent was added after 1 h) mmol] in dry THF (20 ml) was refluxed in the dark for the time indicated in Table IV. The residue was purified by method A to afford 1,3-dimethylthymine (**6**). Yields are given in Table IV.

General Procedures for the Repair Reaction of the Bromohydrin (3) with Sunlight and Reagents (Table V) A solution of the bromohydrin (**3**) (1 mmol) and a reagent (1.2 or 2.4 mmol) in dry THF (20 ml) was irradiated with a sunlight lamp at room temperature for the time indicated in Table V. The residue was purified by method A to afford 1,3-dimethylthymine (**6**). Yields are given in Table V.

References and Notes

1) E. P. Burrows, H.-S. Ryang, and S. Y. Wang, *J. Org. Chem.*, **44**, 3736 (1979).
2) T.-J. Yu, R. G. Sutherland, and R. E. Verrall, *Can. J. Chem.*, **58**, 1909 (1980).
3) M. N. Schuchmann and C. von Sonntag, *J. Chem. Soc., Perkin Trans. 2*, **1983**, 1525.
4) M. Berger and J. Cadet, *Chemistry Letters*, **1983**, 435.
5) T. Kagiya, R. Kimura, C. Komuro, K. Sakano, and S. Nishimoto,

Chemistry Letters, **1983**, 1471.
6) T. Harayama, K. Mori, R. Yanada, K. Iio, Y. Fujita, and F. Yoneda, *J. Chem. Soc., Chem. Commun.*, **1988**, 1171.
7) R. Cathcart, E. Schwiers, R. L. Saul, and B. N. Ames, *Proc. Natl. Acad. Sci. U.S.A.*, **81**, 5633 (1984).
8) T. J. Ahren, G. G. Allan, and D. J. Medcalf, *Biochim. Biophys. Acta*, **616**, 329 (1980).
9) D. G. Baden and M. D. Corbett, *Biochem. J.*, **187**, 205 (1980).
10) J. A. Manthey and L. P. Hager, *J. Biol. Chem.*, **256**, 11232 (1981).
11) H. Yamada, N. Itoh, and Y. Izumi, *J. Biol. Chem.*, **260**, 11962 (1985).
12) H. Yamada, N. Itoh, S. Murakami, and Y. Izumi, *Agric. Biol. Chem.*, **49**, 2961 (1985).
13) R. D. Libby, J. A. Thomas, L. W. Kaiser, and L. P. Hager, *J. Biol. Chem.*, **257**, 5030 (1982).
14) N. Itoh, Y. Izumi, and H. Yamada, *Biochemistry*, **26**, 282 (1987).
15) T. Harayama, K. Kotoji, R. Yanada, F. Yoneda, T. Taga, K. Osaki, and T. Nagamatsu, *Chem. Pharm. Bull.*, **34**, 2354 (1986).
16) T. Harayama, R. Yanada, T. Akiyama, M. Tanaka, and F. Yoneda, *Biochem. Biophys. Res. Commun.*, **148**, 995 (1987).
17) T. Harayama, R. Yanada, T. Taga, and F. Yoneda, *Tetrahedron Lett.*, **26**, 3587 (1985).
18) T. Harayama, R. Yanada, T. Taga, K. Machida, and F. Yoneda, *J. Heterocycl. Chem.*, **23**, 283 (1986).
19) T. Harayama, R. Yanada, T. Taga, K. Machida, and F. Yoneda, *Chem. Pharm. Bull.*, **34**, 4961 (1986).
20) T. Harayama, R. Yanada, M. Tanaka, T. Taga, K. Machida, F. Yoneda, and J. Cadet, *J. Chem. Soc., Perkin Trans. 1*, **1988**, 2555.
21) M. Berger, J. Cadet, and J. Ulrich, *Can. J. Chem.*, **63**, 6 (1985).
22) R. Yanada, T. Akiyama, T. Harayama, K. Yanada, H. Meguri, and F. Yoneda, *J. Chem. Soc., Chem. Commun.*, **1989**, 238.
23) T. Akiyama, R. Yanada, O. Sakurai, T. Harayama, K. Tanaka, and F. Yoneda, *J. Chem. Soc., Chem. Commun.*, **1989**, 910.
24) T. Harayama, H. Cho, and Y. Inubushi, *Chem. Pharm. Bull.*, **25**, 2273 (1977).
25) T. B. Johnson and S. H. Clapp, *J. Biol. Chem.*, **5**, 49 (1908).
26) E. Wittenburg, *Chem. Ber.*, **99**, 2380 (1966).
27) The reaction of **3** with benzoic acid or boron trifluoride etherate in the dark also gave the repaired product (**6**) in good yield. In this connection, the repair reaction usually seems to involve a lag time and to occur more rapidly in a slightly acidic medium.
28) J. Cadet and R. Teoule, *Carbohydr. Res.*, **29**, 345 (1973).

Asymmetric Induction Reactions. IV.[1] Palladium-Catalyzed Asymmetric Allylations of Chiral Enamines Bearing Phosphine Groups[2]

Kunio HIROI* and Jun ABE

Department of Synthetic Organic Chemistry, Tohoku College of Pharmacy, 4-4-1 Komatsushima, Aoba-ku, Sendai, Miyagi 981, Japan.
Received September 17, 1990

The palladium-catalyzed asymmetric allylations of chiral enamines, derived from (*S*)-2-(diphenylphosphinomethyl)pyrrolidine, produced optically active α-allyl carbonyl compounds in high optical yields. The phosphino group in the chiral enamines presumably serves as a chiral ligand in these palladium-catalyzed reactions. In the transition states of π-allylpalladium complexes coordinated with the intramolecular phosphine group, the anionic counterparts or allylating reagents are considered to play an important role in controlling of the grade of the enantioselectivity.

Keywords asymmetric allylation; palladium catalyst; enantioselectivity; phosphine ligand; allylating reagent; chiral enamine

Recently much attention has been paid to the development of new methodologies for asymmetric induction with high enantioselectivity,[3] especially using transition metal catalysts.[4] Particular interest has been focused on the mechanisms of palladium-catalyzed reactions, especially in allylic systems with chiral models involving chiral sulfinates,[5] esters of chiral allylic alcohols,[6] and chiral phosphine ligands.[7] We have already explored new methods for asymmetric α-allylation of carbonyl compounds *via* π-allylpalladium complexes of chiral enamines,[8] imines,[9] or amides[10] derived from (*S*)-proline and other (*S*)-α-amino acid allyl esters, and suggested possible mechanisms of the asymmetric induction. Asymmetric alkylation with chiral enamines provides a useful method for preparation of optically active α-alkyl carbonyl compounds, as reported previously by one (K. H.) of us.[11] Accordingly, palladium-catalyzed reactions of chiral enamines involving phosphine groups have attracted much interest, since the phosphine groups would presumably serve as chiral ligands in the palladium catalysis and therefore different stereochemical results would be expected, compared with those obtained by the previous chiral enamine alkylation methods.[11]

As a chiral secondary amine with a phosphine group, we used (*S*)-2-(diphenylphosphinomethyl)pyrrolidine (**1**)[12] which was easily obtainable from (*S*)-proline. The chiral enamine (*S*)-**3a** was prepared by azeotropic dehydration of (*S*)-**1** and 2-phenylpropanal (**2a**) in refluxing benzene for 4 h using a Dean–Stark apparatus. Reaction of the chiral enamine (*S*)-**3a** with allyl acetate (**4a**) (2.0 eq) was carried out in tetrahydrofuran (THF) at room temperature or 66 °C for 45 or 19 h in the presence of tetrakis(triphenylphosphine)palladium [$Pd(PPh_3)_4$] (0.2 eq), followed by hydrolysis of the allylated enamine with 10% aqueous HCl–benzene (at 80 °C, for 1 h), giving (*R*)-(−)-2-methyl-2-phenyl-4-pentenal (**5a**) with 52 or 18% enantiomeric excess in 80 or 86% yield, respectively. The absolute configuration of the product (−)-**5a** has already been determined as (*R*)-(−)-**5a** by us.[8b] The enantiomeric excess (e.e.) of the product was determined by nuclear magnetic resonance (NMR) spectral analysis with a shift reagent, tris[3-(heptafluoropropylhydroxymethylene)-(+)-camphorato]europium (III) [$Eu(hfc)_3$].

In order to improve the chemical and optical yields of the product, stereochemical studies on this allylation have been attempted employing various other allylating reagents such as allyl carboxylates (**4a—e**), sulfonates (**4f, g**), and halides (**4h—j**). The results are summarized in Table I.

The direct reactions of (*S*)-**3a** with **4a—j** without the palladium catalyst, even in refluxing THF, gave none of the expected products. On the other hand, the direct reactions of (*S*)-**3a** with **4h—j** without the catalyst in refluxing THF produced (*S*)-(+)-**5a** in extremely lower optical yields (6—13%). However, the reactions at room temperature afforded no α-allylated aldehyde.

Therefore, the results listed in Table I indicate that the

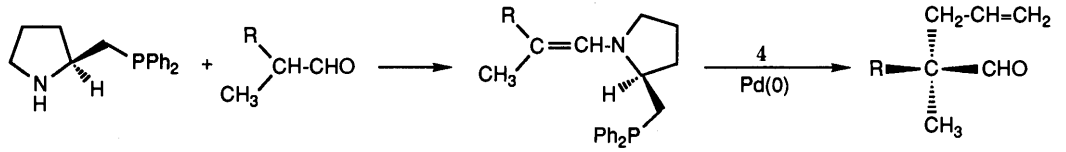

(*S*)-**1**

2a : R = C_6H_5
2b : R = *p*-$Bu^tC_6H_4CH_2$
2c : R = C_2H_5

(*S*)-**3a—c**

(*R*)-**5a** : R = C_6H_5
(*R*)-**5b** : R = *p*-$Bu^tC_6H_4CH_2$
(*S*)-**5c** : R = C_2H_5

CH_2=CH-CH_2-X

4a : X = AcO
4b : X = $C_6H_5CO_2$
4c : X = *p*-$NO_2C_6H_4CO_2$
4d : X = α-$C_{10}H_7CO_2$
4e : X = β-$C_{10}H_7CO_2$
4f : X = *p*-$CH_3C_6H_4SO_3$
4g : X = *o*-$CH_3C_6H_4SO_3$
4h : X = Cl
4i : X = Br
4j : X = I

Chart 1

anionic counterparts, presumably coordinated with the palladium catalyst, do affect the asymmetric induction in the palladium-catalyzed reactions. A remarkably large effect of the anionic counterparts of the allylating reagents on the asymmetric induction was observed. The optical yields increased with increasing steric bulkiness of the anionic counterparts (X) in allyl carboxylates and sulfonates. Exceptionally, allyl carboxylates having very large substituents such as α- or β-naphthoyl groups provided lower enantioselectivity. In the palladium-catalyzed reactions with allyl halides (**4i—j**), contrary to expectation, rather lower enantioselectivity was observed with the use of allyl iodide. Among the allylating reagents examined, the palladium-catalyzed reaction of (*S*)-**3a** with allyl bromide provided the highest optical yields of (*R*)-**5a**. This means that the steric character of the bromine atom is crucial for the asymmetric allylation in this system, and the reactivity of allylating reagents plays an important role in controlling the grade of the asymmetric induction. The effect of the anionic counterparts on the asymmetric induction can not be completely rationalized at this stage. It is presumably related to the coordinating ability of the anionic counterparts to the palladium catalyst, and also to the steric bulk.

It should be noted that the palladium catalysts have an important effect on the asymmetric induction: the use of bis(dibenzylideneacetone)palladium [$Pd(dba)_2$] resulted in a much lower optical yield of (*S*)-**5a** in the reaction of (*S*)-**3a** with allyl acetate than that obtained with $Pd(PPh_3)_4$.

Asymmetric allylations of other chiral aldehyde-enamines (*S*)-**3b, c**, derived from (*S*)-**1** and **2b, c**, were attempted using allylating reagents **4a, f, g, i**. The reactions of (*S*)-**3b, c** with **4a, f, g, i** were carried out in THF in the presence of Pd$(PPh_3)_4$ (0.2 eq), followed by heating in 10% aqueous HCl and benzene for 1 h, to produce (*R*)-(+)-**5b** and (*S*)-(−)-**5c**. The results are summarized in Table I. The absolute configurations of the aldehydes were deduced on the basis of the mechanistic pathway proposed later. The enantiomeric excess of the products was determined by NMR spectral analysis with a shift reagent [$Eu(hfc)_3$]. Higher enantiomeric excess of the products was observed on treatment with **4f, g, i**, as shown in Table I.

This method was applicable to chiral keto-enamines. The

TABLE I. The Palladium-Catalyzed Asymmetric Allylation of (*S*)-**3a—c**[a]

Enamine (*S*)-3	4	Reaction temp. (°C)	Reaction time (h)	Product	Yield (%)[b]	$[\alpha]_D$ (MeOH)	ee (%)[c]
3a	**4a**	66	19	(*R*)-**5a**	86	−6.2°	18
3a	**4a**	40	19	(*R*)-**5a**	74	−12.3°	35
3a	**4a**	r.t.	45	(*R*)-**5a**	80	−18.3°	52
3a	**4a**	66	19	(*S*)-**5a**	79[d]	+3.2°	8
3a	**4a**	40	19	(*S*)-**5a**	75[d]	+3.8°	10
3a	**4a**	r.t.	45	(*S*)-**5a**	61[d]	+5.8°	15
3a	**4b**	66	19	(*R*)-**5a**	83	−11.7°	31
3a	**4b**	40	19	(*R*)-**5a**	88	−14.0°	37
3a	**4b**	r.t.	45	(*R*)-**5a**	78	−21.0°	53
3a	**4c**	66	19	(*R*)-**5a**	82	−13.6°	36
3a	**4c**	40	19	(*R*)-**5a**	73	−16.7°	44
3a	**4c**	r.t.	45	(*R*)-**5a**	83	−27.0°	71
3a	**4d**	66	19	(*R*)-**5a**	71	−8.0°	21
3a	**4d**	40	19	(*R*)-**5a**	78	−12.0°	32
3a	**4d**	r.t.	45	(*R*)-**5a**	65	−17.2°	45
3a	**4e**	66	19	(*R*)-**5a**	70	−5.0°	13
3a	**4e**	40	19	(*R*)-**5a**	77	−11.9°	32
3a	**4e**	r.t.	45	(*R*)-**5a**	68	−20.3°	53
3a	**4f**	66	19	(*R*)-**5a**	77	−17.8°	47
3a	**4f**	40	19	(*R*)-**5a**	85	−22.9°	58
3a	**4f**	r.t.	45	(*R*)-**5a**	77	−30.0°	79
3a	**4g**	66	19	(*R*)-**5a**	83	−18.0°	47
3a	**4g**	40	19	(*R*)-**5a**	85	−21.3°	55
3a	**4g**	r.t.	45	(*R*)-**5a**	80	−32.0°	84
3a	**4h**	66	19	(*R*)-**5a**	92	−5.2°	14
3a	**4h**	r.t.	45	(*R*)-**5a**	90	−23.8°	63
3a	**4h**	66	19	(*S*)-**5a**	81[e]	+2.4°	6
3a	**4i**	66	19	(*R*)-**5a**	90	−8.0°	21
3a	**4i**	r.t.	45	(*R*)-**5a**	77	−33.3°	88
3a	**4i**	66	19	(*S*)-**5a**	60[e]	+3.3°	9
3a	**4j**	66	19	(*R*)-**5a**	91	−4.1°	11
3a	**4j**	r.t.	45	(*R*)-**5a**	94	−20.5°	54
3a	**4j**	66	19	(*S*)-**5a**	77[e]	+5.1°	13
3b	**4a**	66	19	(*R*)-**5b**	91	+1.9°	35
3b	**4a**	40	19	(*R*)-**5b**	84	+2.5°	46
3b	**4a**	r.t.	45	(*R*)-**5b**	82	+3.5°	64
3b	**4f**	66	19	(*R*)-**5b**	98	+2.3°	42
3b	**4f**	40	19	(*R*)-**5b**	87	+3.1°	56
3b	**4f**	r.t.	45	(*R*)-**5b**	88	+4.4°	80
3b	**4g**	66	19	(*R*)-**5b**	98	+2.0°	36
3b	**4g**	40	19	(*R*)-**5b**	81	+3.8°	69
3b	**4g**	r.t.	45	(*R*)-**5b**	85	+4.1°	75
3b	**4i**	66	19	(*R*)-**5b**	87	+2.7°	49
3b	**4i**	40	19	(*R*)-**5b**	90	+3.8°	69
3b	**4i**	r.t.	45	(*R*)-**5b**	85	+4.8°	87
3c	**4a**	66	19	(*S*)-**5c**	81	−4.0°	18
3c	**4a**	40	19	(*S*)-**5c**	79	−7.2°	33
3c	**4a**	r.t.	45	(*S*)-**5c**	85	−10.2°	46
3c	**4f**	66	19	(*S*)-**5c**	93	−6.7°	30
3c	**4f**	40	19	(*S*)-**5c**	89	−9.4°	43
3c	**4f**	r.t.	45	(*S*)-**5c**	88	−13.8°	52
3c	**4g**	66	19	(*S*)-**5c**	92	−10.1°	36
3c	**4g**	40	19	(*S*)-**5c**	85	−12.4°	47
3c	**4g**	r.t.	45	(*S*)-**5c**	81	−14.8°	60
3c	**4i**	66	19	(*S*)-**5c**	82	−7.4°	34
3c	**4i**	40	19	(*S*)-**5c**	79	−9.8°	44
3c	**4i**	r.t.	45	(*S*)-**5c**	83	−11.4°	52

a) The reactions of **3a—c** with **4a—j** were carried out in THF in the presence of $Pd(PPh_3)_4$(0.2 eq) followed by hydrolysis with 10% aqueous HCl–benzene for 1 h. *b*) The corrected yields based on the recovered starting materials are listed. *c*) The enantiomeric excess (ee %) was calculated by NMR analysis using a shift reagent [$Eu(hfc)_3$] and from the optical rotation of optically pure (*R*)-**5a**, $[\alpha]_D$ −38.0° (MeOH); (*R*)-**5b**, $[\alpha]_D$ +5.5° (MeOH) and (*S*)-**5c**, $[\alpha]_D$ −22.1° (MeOH). *d*) The reactions were carried out in the presence of $Pd(dba)_2$(0.2 eq). *e*) The reactions were carried out without palladium catalyst. r.t. = room temperature.

TABLE II. The Palladium-Catalyzed Asymmetric Allylations of (*S*)-**6** and **9**[a]

Enamine	4	Product	Yield (%)[b]	Product $[\alpha]_D$ (MeOH or $CHCl_3$)	ee (%)[c]
(*S*)-**6**	**4a**	(*S*)-7	77	−4.2°	27
(*S*)-**6**	**4b**	(*S*)-7	83	−4.4°	28
(*S*)-**6**	**4c**	(*S*)-7	70	−7.3°	46
(*S*)-**6**	**4f**	(*S*)-7	67	−10.3°	65
(*S*)-**6**	**4g**	(*S*)-7	62	−11.2°	71
(*S*)-**6**	**4i**	(*S*)-7	68	−9.6°	61
(*S*)-**9a**	**4a**	(*S*)-**10a**	77	−11.0°	37
(*S*)-**9b**	**4a**	(*S*)-**10b**	85	−17.4°	77
(*S*)-**9b**	**4b**	(*S*)-**10b**	84	−14.1°	62
(*S*)-**9b**	**4c**	(*S*)-**10b**	84	−15.2°	67
(*S*)-**9b**	**4f**	(*S*)-**10b**	89	−19.0°	84
(*S*)-**9b**	**4g**	(*S*)-**10b**	83	−19.3°	85
(*S*)-**9b**	**4i**	(*S*)-**10b**	78	−17.8°	78

a) The reactions of (*S*)-**6** or **-9a, b** with **4** were carried out in refluxing THF for 19 h in the presence of $Pd(PPh_3)_4$ (0.2 eq) followed by hydrolysis with aqueous AcONa–AcOH–H_2O–benzene. *b*) The corrected yields based on the recovered starting materials are listed. *c*) The enantiomeric excess (ee %) was determined on the basis of the optical rotation of optically pure (*S*)-**7** ($[\alpha]_D$ −15.8° (MeOH)),[15] (*S*)-**10a** ($[\alpha]_D$ −29.7° ($CHCl_3$)),[14] and (*S*)-**10b** ($[\alpha]_D$ −22.7° ($CHCl_3$)).

chiral keto-enamine (*S*)-**6**, prepared from (*S*)-**1** and cyclohexanone, was reacted with **4** in the presence of Pd $(PPh_3)_4$ (0.2 eq) in refluxing THF for 19 h, followed by hydrolysis with AcONa–AcOH–H_2O–benzene (at room temperature for 1 h), giving (*S*)-2-allylcyclohexanone (**7**).[8a,11] Rather high optical yields were observed in the reactions with allyl tosylates (**4f, g**) and bromide (**4i**), as shown in Table II. The chiral enamine (*S*)-**9a, b**, derived from (*S*)-**1** and ethyl or *tert*-butyl 2-methylacetoacetate (**8a**[13] or **8b**), was reacted with **4** under the same conditions as described above to give ethyl or *tert*-butyl (*S*)-2-allyl-2-methylacetoacetate (**10a**[14] or **10b**) in the optical yields listed in Table II. The absolute configuration of **10b** and the optical rotation of optically pure **10b** were determined by chemical correlation to (*S*)-(−)-**10a** of known absolute configuration[14] *via* 2-acetyl-2-methyl-4-pentenyl benzoate. High optical yields of (*S*)-**10b** were obtained when (*S*)-**9b** was reacted with **4f** and **4g** in refluxing THF.

The stereochemistry of these reactions was rationalized as follows. The palladium-catalyzed reaction of (*S*)-**3a** with **4a—j** provided (*R*)-**5a** of the same absolute configuration as that of the product *via* (*S*)-proline allyl ester enamine.[8b] Therefore, the allylation of (*S*)-**3a** is considered to proceed *via* a π-allylpalladium complex intramolecularly coordinated with the phosphine ligand.

The geometrical isomers **12** of the enamines (*S*)-**3** and (*S*)-**9** are preferred to the other isomers **11** because of the steric hindrance between the amino part and the large substituent (R^2) in **11**. The conformers **13** seem preferable to **12** from the viewpoint of steric interaction between the diphenylphosphinomethyl and the methyl groups in **12**. Therefore the preferred conformers **13** formed the π-allylpalladium complexes **14** coordinated with the phosphine group and the counterparts (X), and allylation then occurred *via* the palladium complexes from the bottom side as depicted in **14**, providing (*R*)-**5a, b**, (*S*)-**5c** or (*S*)-**10**. The steric effect of the anionic counterparts (X), presumably bonded to the palladium catalyst, is manifested at this stage. The allylating reagents (*e.g.* **4d** and **4e**) having overlarge anionic counterparts (X) could not be completely coordinated with the phosphine groups and therefore partial allylations *via* the π-allylpalladium complexes **14** would occur, along with the direct allylations from the back side of the chiral part in **13**, providing somewhat lower

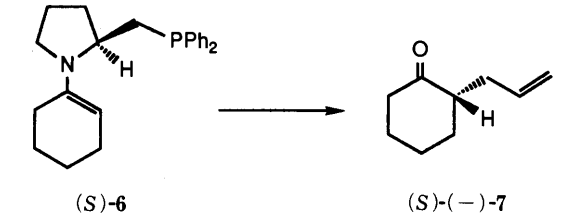

(*S*)-**6** (*S*)-(−)-**7**

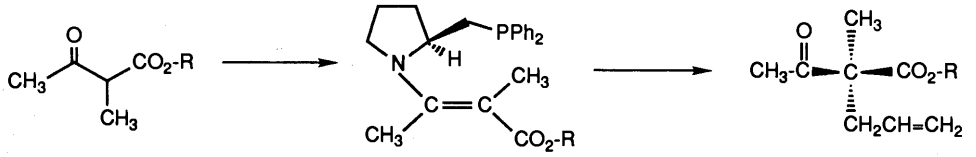

8a : R = CH_3CH_2
8b : R = *tert*-Bu

(*S*)-**9a, b**

(*S*)-(−)-**10a** : R = CH_3CH_2
(*S*)-(−)-**10b** : R = *tert*-Bu

Chart 2

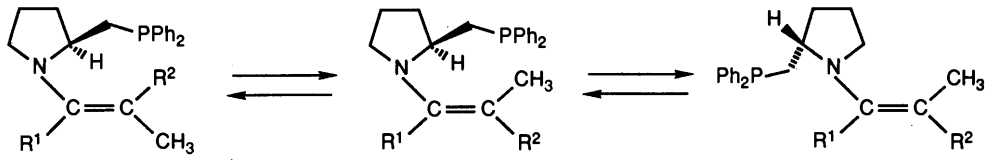

11 **12** **13**

a : R^1 = H , R^2 = C_6H_5
b : R^1 = CH_3, R^2 = $CO_2C_2H_5$
c : R^1 = CH_3, R^2 = CO_2Bu^t

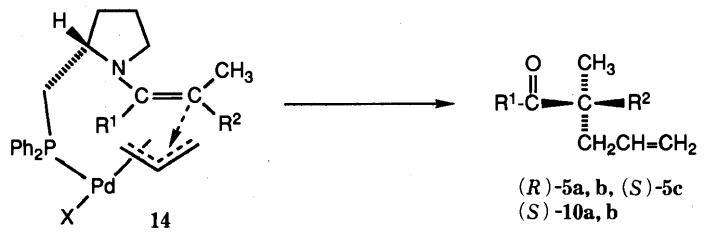

14

(*R*)-**5a, b**, (*S*)-**5c**
(*S*)-**10a, b**

Chart 3

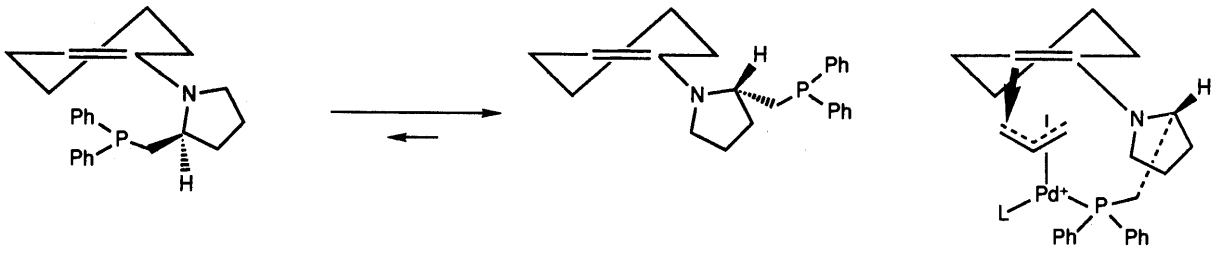

15a 15b 16

Chart 4

enantioselectivity in these palladium-catalyzed reactions. The allylations catalyzed by $Pd(dba)_2$ resulted in the formation of (*S*)-**5a** of reversed absolute configuration with lower enantioselectivity, since the formation of the π-allylpalladium complexes **14** coordinated by the phosphine ligand would not be easily attainable with $Pd(dba)_2$ and the direct allylation from the back side of the chiral part in **13** would be slightly preferable to that *via* **14**.

The great difference of the stereochemical results in the allylations with allyl halides can be rationalized in terms of the reactivity and the steric bulkiness of the halides. The high reactivity of allyl iodide allows partial direct allylation of the enamine without formation of the π-allylpalladium complexs **14** by coordination with the phosphine group, resulting in the lower enantioselectivity.

A similar explanation is applicable to the cyclohexanone enamine system (*S*)-**6**. The palladium-catalyzed reaction of (*S*)-**6** would proceed preferentially *via* the π-allylpalladium complex **16** coordinated with the phosphine group in the conformationally most stable from **15b**, producing (*S*)-**7** with the high enantioselectivity, since **15b** would be preferred to **15a** because of steric hindrance between the diphenylphosphinomethyl group and the olefinic hydrogen atom in **15a**.[11]

Thus, this method provides different stereochemical results, compared with those obtained by the previous method *via* chiral enamines.[11] Therefore we can control the stereochemistry of the products by selecting the amino moiety in chiral enamines. Accordingly, this method is useful for asymmetric α-allylation of carbonyl compounds and is also advantageous for organic synthesis, because the chiral auxiliary amine used as the starting chiral source can be efficiently recovered and recycled. Furthermore, it is noteworthy that the anionic counterparts of allylating reagents have a great effect on the asymmetric induction in these palladium-catalyzed reactions. This is the first demonstration of the importance of participation of anionic counterparts of allylating reagents in palladium-catalyzed asymmetric allylations.

Experimental

Thin-layer or preparative thick layer plates (preparative TLC) were made of Merck Silica gel 60PF-254 activated by drying at 140 °C for 3.5 h. Infrared (IR) spectra were obtained in the indicated state with a Hitachi 215 spectrometer and a JASCO DR-81 Fourier-transform infrared spectrometer. NMR spectra were determined in indicated solvent with a Hitachi R-24B high-resolution NMR spectrometer and a JEOL JNM-PMX 60si high-resolution NMR spectrometer (60 MHz); chemical shifts are given in ppm from tetramethylsilane as an internal standard. Splitting patterns are designated as s, singlet; d, doublet; q, quartet; m, multiplet. Mass spectra (MS) were taken on JEOL JMS-DX 303/JMA-DA 5000 system.

Synthesis of (*S*)-2-(Diphenylphosphinomethyl)pyrrolidine (1) (*S*)-*N*-*tert*-Butoxycarbonylproline Ethyl Ester: Potassium carbonate (6.4 g, 0.050 mol) was added to a solution of *N*-*tert*-butoxycarbonylproline (5.0 g, 0.025 mol) in 400 ml of acetone at room temperature. Ethyl iodide (18.6 ml, 0.250 mol) was added to the above suspension. The whole was stirred at room temperature for 16 h. The reaction mixture was filtered and the precipitates were washed with ether. The filtrates were combined and concentrated *in vacuo*. The residual oil was dissolved with ether. The solution was washed with saturated aqueous $NaHCO_3$ and saturated aqueous NaCl, dried over anhydrous Na_2SO_4, and concentrated *in vacuo*. The curde product was subjected to distillation under reduced pressure to give (*S*)-*N*-*tert*-butoxycarbonylproline ethyl ester (5.6 g, quantitative yield): bp 170 °C (4 mmHg), $[\alpha]_D^{23}$ −38.7° (c=2.3, EtOH). IR ν_{max}^{film} cm^{-1}: 1760 (ester), 1700 (C=O). NMR (CCl_4) δ: 1.03—1.63 (12H, m, $CH_2C\underline{H}_3$, $C(C\underline{H}_3)_3$), 1.70—2.53 (4H, m, CH_2CH_2), 3.16—3.86 (3H, m, CH_2N, NCH), 4.26 (2H, q, J=8, 8 Hz, $C\underline{H}_2CH_3$). MS *m/z*: 243 (M^+). Exact mass determination: 243.1479 (Calcd for $C_{12}H_{21}NO_4$: 243.1470).

(*S*)-*N*-*tert*-Butoxycarbonylprolinol: Lithium aluminum hydride (1.0 g, 0.033 mol) was added to a solution of (*S*)-*N*-*tert*-butoxycarbonylproline ethyl ester (4.8 g, 0.023 mol) in 100 ml of THF cooled to 0 °C. The reaction mixture was stirred at 0 °C for 16 h and then quenched with H_2O (3.0 ml) and 10% aqueous NaOH (0.9 ml). The mixture was diluted with ether and then refluxed for 1 h. The precipitates were filtered off and washed with ether. The filtrates were combined and concentrated *in vacuo*. The crude product was subjected to distillation under reduced pressure to give (*S*)-*N*-*tert*-butoxycarbonylprolinol (3.8 g, 96% yield): bp 150 °C (4 mmHg), $[\alpha]_D^{24}$ −30.8° (c=1.3, EtOH). IR ν_{max}^{film} cm^{-1}: 3370 (OH), 1700 (C=O). NMR (CCl_4) δ: 1.50 (9H, s, $C(CH_3)_3$), 1.66—2.33 (4H, m, CH_2CH_2), 3.00—4.66 (6H, m, CH_2NCH, CH_2OH). MS *m/z*: 201 (M^+). Exact mass determination; 201.1389 (Calcd for $C_{10}H_{19}NO_3$: 201.1364).

(*S*)-*N*-*tert*-Butoxycarbonylprolinol *p*-Toluenesulfonate: *p*-Toluenesulfonyl chloride (4.3 g, 0.023 mol) was added to a solution of (*S*)-*N*-*tert*-butoxycarbonylprolinol (3.8 g, 0.019 mol) in 10 ml of anhydrous pyridine at 0 °C. The reaction mixture was stirred at 0 °C for 4 h, and then diluted with ether. The solution was washed with 10% aqueous HCl, saturated aqueous $NaHCO_3$, and saturated aqueous NaCl, dried over anhydrous Na_2SO_4, and concentrated *in vacuo*. The crude product was subjected to preparative TLC (ether–hexane, 1:2) to give (*S*)-*N*-*tert*-butoxycarbonylprolinol *p*-toluenesulfonate (6.1 g, 91% yield): $[\alpha]_D^{28}$ −40.8° (c=1.8, EtOH). IR ν_{max}^{film} cm^{-1}: 1680 (C=O), 1600 (aromatic), 1180 (OSO_2). NMR (CCl_4) δ: 1.36 (9H, s, $C(CH_3)_3$), 1.60—2.23 (4H, m, CH_2CH_2), 2.43 (3H, s, $C_6H_4C\underline{H}_3$), 3.06—3.30 (2H, m, CH_2N), 3.60—4.26 (3H, m, NCH, CH_2O), 7.10—7.86 (4H, m, C_6H_4). MS *m/z*: 355 (M^+). Exact mass determination; 355.1439 (Calcd for $C_{17}H_{25}NO_5S$: 355.1452).

(*S*)-*N*-*tert*-Butoxycarbonyl-2-(diphenylphosphinomethyl)pyrrolidine: A mixture of sodium (0.8 g, 0.034 gatom) and chlorodiphenylphosphine (4.2 ml, 0.023 mol) in 20 ml of dioxane was refluxed for 15 h under a nitrogen atmosphere. After cooling, the solution was added to a solution of (*S*)-*N*-*tert*-butoxycarbonylprolinol *p*-toluenesulfonate (1.0 g, 0.003 mol) in THF (10 ml) at room temperature. The reaction mixture was stirred at room temperature for 19 h and then diluted with ether. The solution was washed with saturated aqueous NaCl, dried over anhydrous Na_2SO_4, and concentrated *in vacuo*. The crude product was subjected to preparative TLC (ether–hexane, 2:1) to give (*S*)-*N*-*tert*-butoxycarbonyl-2-(diphenylphosphinomethyl)pyrrolidine (0.9 g, 93% yield): $[\alpha]_D^{24}$ −45.8° (c=1.7, EtOH). IR ν_{max}^{film} cm^{-1}: 1680 (C=O), 1600 (aromatic). NMR (CCl_4) δ: 1.43 (9H, s, $C(CH_3)_3$), 1.60—2.30 (4H, m, CH_2CH_2), 2.50—4.60 (5H, m, CH_2NCH, CH_2P), 7.10—8.10 (10H, m, $P(C_6H_5)_2$). MS *m/z*: 369(M^+). Exact mass determination: 369.2119 (Calcd for $C_{22}H_{28}NO_2P$: 369.2108).

(*S*)-**1**: (*S*)-*N*-*tert*-Butoxycarbonyl-2-(diphenylphosphinomethyl)pyrrolidine (0.7 g, 0.019 mol) was dissolved in 10 ml of freshly distilled trifluoroacetic acid at 0 °C and the solution was stirred for 2 h. Then

trifluoroacetic acid was removed *in vacuo* to leave (*S*)-2-(diphenylphosphinomethyl)pyrrolidinium trifluoroacetate. The salt was dissolved in 20 ml of chloroform, followed by addition of 10% aqueous ammonia. The mixture was stirred for 10 min and then diluted with chloroform. The solution was washed with saturated aqueous NaCl, dried over anhydrous Na_2SO_4, and concentrated *in vacuo*. The crude product was subjected to distillation under reduced pressure to give (*S*)-2-(diphenylphosphinomethyl)pyrrolidine[12] (0.5 g, 93% yield) as a yellow oil: bp 220°C (4 mmHg), $[\alpha]_D^{25}$ −27.9° (*c*=2.9, EtOH) [lit.[12] bp 148 °C (0.06 mmHg), $[\alpha]_D$ −29.9° (*c*=4.6, EtOH)].

tert-Butyl 2-Methylacetoacetate (**8b**): *tert*-Butyl acetoacetate (4.6 ml, 0.030 mol) was added to a suspension of sodium hydride (50% oil dispersion, 1.7 g, 0.036 mol) in 10 ml of THF at 0 °C. The reaction mixture was stirred at 0 °C for 1 h, then a solution of methyl iodide (2.2 ml, 0.036 mol) in THF (10 ml) was added. The whole was stirred at room temperature for 16 h, and then diluted with ether. The solution was washed with 10% aqueous HCl, saturated aqueous $NaHCO_3$, and saturated aqueous NaCl, dried over anhydrous Na_2SO_4, and concentrated *in vacuo*. The crude product was subjected to distillation under reduced pressure to give **8b** (5.0 g, 78% yield): bp 50 °C (4 mmHg). IR ν_{max}^{film} cm^{-1}: 1745 (ester), 1725 (C=O). NMR (CCl_4) δ: 1.23 (3H, d, *J*=2 Hz, $CHC\underline{H}_3$), 1.43 (9H, s, $C(CH_3)_3$), 2.07 (3H, s, $COCH_3$), 3.20 (1H, q, *J*=7, 7 Hz, COCHCO). MS *m/z*: 172 (M^+). Exact mass determination: 172.0976 (Calcd for $C_9H_{16}O_3$: 172.1000).

Palladium-Catalyzed Asymmetric Allylations of Aldehyde- or Keto-enamines Allylating Reagents: Commercially available allyl acetate (**4a**) and allyl halides (**4h—j**) were used. Allyl benzoate (**4b**),[16] *p*-nitrobenzoate (**4c**),[17] and *p*-toluenesulfonate (**4f**)[18] were prepared according to the methods reported previously.

Allyl α- or β-Naphthoate (**4d** or **4e**): A solution of α- or β-naphthoic acid (1.0 g, 0.006 mol) and allyl alcohol (0.6 ml, 0.009 mol) in benzene (10 ml) was refluxed in the presence of a catalytic amount of concentrated sulfuric acid for 19 h using a Dean–Stark apparatus. After cooling, the reaction mixture was diluted with ether. The ethereal solution was washed with saturated aqueous $NaHCO_3$ and saturated aqueous NaCl, dried over anhydrous Na_2SO_4, and concentrated *in vacuo*. The crude product was subjected to preparative TLC (benzene–hexane, 1 : 2) to give **4d** (0.9 g, 72% yield) or **4e** (1.1 g, 87% yield).

4d: IR ν_{max}^{film} cm^{-1}: 1700 (ester), 1670 (C=C), 1580 (aromatic). NMR (CCl_4) δ: 4.86 (2H, d, *J*=6 Hz, $C\underline{H}_2CH=CH_2$), 5.10—6.56 (3H, m, $CH_2C\underline{H}=C\underline{H}_2$), 7.16—8.33 (7H, m, $C_{10}H_7$). MS *m/z*: 212 (M^+). Exact mass determination: 212.0893 (Calcd for $C_{14}H_{12}O_2$: 212.0887).

4e: IR ν_{max}^{film} cm^{-1}: 1700 (ester), 1620 (C=C), 1580 (aromatic). NMR (CCl_4) δ: 4.80 (2H, d, *J*=6 Hz, $C\underline{H}_2CH=CH_2$), 5.13—6.56 (3H, m, $CH_2C\underline{H}=C\underline{H}_2$), 7.10—8.70 (7H, m, $C_{10}H_7$). MS *m/z*: 212 (M^+). Exact mass determination: 212.0812 (Calcd for $C_{14}H_{12}O_2$: 212.0798).

Allyl *o*-Toluenesulfonate (**4g**): *o*-Toluenesulfonyl chloride (1.0 g, 0.005 mol) was added to a solution of allyl alcohol (0.6 ml, 0.008 mol) in 10 ml of pyridine at 0 °C. The reaction mixture was stirred at 0 °C for 4 h and then diluted with ether. The solution was washed with 10% aqueous HCl, saturated aqueous $NaHCO_3$, and saturated aqueous NaCl, dried over anhydrous Na_2SO_4, and concentrated *in vacuo*. The crude product was subjected to preparative TLC (ether–hexane, 1 : 2) to give **4g** (0.9 g, 86% yield). IR ν_{max}^{film} cm^{-1}: 1640 (C=C), 1600 (aromatic), 1370 (OSO_2). NMR (CCl_4) δ: 2.60 (3H, s, $C_6H_4C\underline{H}_3$), 4.43 (2H, d, *J*=6 Hz, $C\underline{H}_2CH=CH_2$), 5.00—6.50 (3H, m, $CH_2C\underline{H}=C\underline{H}_2$), 6.90—8.06 (4H, m, C_6H_4). MS *m/z*: 212 (M^+). Exact mass determination: 212.0502 (Calcd for $C_{10}H_{12}O_3S$: 212.0506).

Genaral Procedures: A solution of (*S*)-**1** (50 mg, 0.197 mmol) and an aldehyde (2-phenylpropional (**2a**), 3-(*p*-*tert*-butylphenyl)isobutanal (**2b**), or 2-methylbutanal (**2c**)) or a ketone (cyclohexanone or ethyl or *tert*-butyl 2-methylacetoacetate (**8a**[13] and **8b**)) (0.197 mmol) in 10 ml of benzene was refluxed for 4 h using a Dean–Stark apparatus. The solution was concentrated *in vacuo* to give the aldehyde- or keto-enamine ((*S*)-**3a—c**, (*S*)-**6**, or (*S*)-**8a, b**).

A dry 25 ml two-necked flask equipped with a septum inlet and magnetic stirring bar, and containing tetrakis(triphenylphosphine)palladium (46 mg, 0.039 mmol) or bis(dibenzylideneacetone)palladium (23 mg, 0.039 mmol) was flushed with nitrogen, and maintained under a positive pressure of nitrogen. A solution of an enamine (0.197 mmol) obtained above in 6 ml of THF was added to the above flask and the mixture was stirred at room temperature for 1 h and then a solution of an allylating reagent (**4a—j**) (2.0 eq) in 4 ml of THF was added. The whole was stirred at the temperature for the time shown in Tables I and II. The reaction mixture was treated with 10% aqueous HCl–benzene under reflux for 1 h (for **5a—c**) or with AcONa–AcOH–H_2O–benzene at room temperature for 1 h (for **7** and **10a, b**). The reaction mixture was diluted with ether. The ethereal solution was washed with 10% aqueous HCl, saturated aqueous $NaHCO_3$, and saturated aqueous NaCl, dried over anhydrous Na_2SO_4, and concentrated *in vacuo*. The crude product was subjected to preparative TLC to give the corresponding α-allyl carbonyl compound: (*R*)-(−)-2-methyl-2-allyl-4-pentenal (**5a**) (benzene–hexane, 1 : 2),[8b,19] (*R*)-(+)-2-(*p*-*tert*-butylphenyl)-methyl-2-methyl-4-pentenal (**5b**) (isopropyl ether–hexane, 1 : 3), (*S*)-(−)-2-ethyl-2-methyl-4-pentenal (**5c**), (isopropyl ether–hexane, 1 : 5),[20] (*S*)-(−)-2-allylcyclohexanone (**7**) (ether–hexane, 1 : 5),[8a,11] ethyl or *tert*-butyl (*S*)-(−)-2-allyl-2-methylacetoacetate (**10a**) (ether–hexane, 1 : 5)[14] or (**10b**) (ether–hexane, 1 : 3).[19] The yields, optical rotations, and the enantiomeric excess of the products are summarized in Tables I and II.

(*R*)-(−)-**5b**: IR ν_{max}^{film} cm^{-1}: 1730 (ester), 1645 (C=C), 1600 (aromatic). NMR (CCl_4) δ: 1.00 (3H, s, CH_3), 1.30 (9H, s, $C(CH_3)_3$), 1.86—2.36 (2H, m, $C\underline{H}_2C_6H_4$), 2.70 (2H, d, *J*=2 Hz, $C\underline{H}_2CH=CH_2$), 4.70—6.16 (3H, m, $CH_2C\underline{H}=C\underline{H}_2$), 6.70—7.43 (4H, m, C_6H_4), 9.46 (1H, s, CHO). MS *m/z*: 244 (M^+). Exact mass determination: 244.1834 (Calcd for $C_{17}H_{24}O$: 244.1827).

Conversion of (*S*)-(−)-10a,b into (*S*)-(−)-2-Acetyl-2-methyl-4-pentenyl Benzoate (*S*)-(−)-2-Acetyl-2-methyl-4-pentenyl Benzoate: Lithium aluminum hydride (22 mg, 0.578 mmol) was added to a solution of (*S*)-(−)-**10a** (90 mg, 0.489 mmol, $[\alpha]_D^{21}$ −13.5° (*c*=1.35, $CHCl_3$), 45% ee) in 10 ml of ether cooled to 0 °C. The reaction mixture was stirred at 0 °C for 1 h and then quenched with H_2O (0.1 ml) and 10% aqueous NaOH (0.06 ml). The mixture was diluted with ether and then refluxed for 1 h. The precipitates were filtered and washed with ether. The filtrates were combined and concentrated *in vacuo* to give 2-allyl-2-methyl-1,3-butanediol (70 mg) [IR ν_{max}^{film} cm^{-1}: 3300 (OH)].

Pyridine (77 mg, 0.978 mmol) and benzoyl chloride (83 mg, 0.586 mmol) were added to a solution of 2-allyl-2-methyl-1,3-butanediol obtained above in 10 ml of THF at 0 °C. The reaction mixture was stirred at 0 °C for 3 h and then diluted with ether. The solution was washed with 10% aqueous HCl, saturated aqueous $NaHCO_3$, and saturated aqueous NaCl, dried over anhydrous Na_2SO_4, and concentrated *in vacuo* to give 2-(1-hydroxyethyl)-2-methyl-4-pentenyl benzoate (121 mg) [IR ν_{max}^{film} cm^{-1}: 3300 (OH), 1740 (ester), 1580 (aromatic)].

The Jones reagent (0.5 ml) was added to a solution of the benzoate obtaine above in 2 ml of acetone at 0 °C. The reaction mixture was stirred at 0°C for 10 min and then quenched with isopropyl alcohol. The reaction mixture was concentrated *in vacuo*, and ether was added to the residue. The suspension was washed with saturated aqueous $NaHCO_3$ and saturated aqueous NaCl, and dried over anhydrous Na_2SO_4. The solution was concentrated *in vacuo*, and the crude product was subjected to preparative TLC (ether–hexane, 2 : 1) to give (*S*)-(−)-2-acetyl-2-methyl-4-pentenyl benzoate (118 mg, 98% yield), $[\alpha]_D^{21}$ −7.6° (*c*=2.5, $CHCl_3$). IR ν_{max}^{film} cm^{-1}: 1745 (ester), 1725 (C=O). NMR (CCl_4) δ: 1.13 (3H, s, CH_3), 1.20—1.53 (2H, m, $C\underline{H}_2CH=CH_2$), 2.32 (3H, s, $COCH_3$), 4.23 (2H, d, *J*=2 Hz, OCH_2), 4.68—5.35 (3H, m, $CH_2C\underline{H}=C\underline{H}_2$), 7.20—8.10 (5H, m, C_6H_5). MS *m/z*: 246 (M^+). Exact mass determination: 246.1371 (Calcd for $C_{15}H_{18}O_3$: 246.1360).

Treatment of (−)-**10b** (90 mg, 0.425 mmol, $[\alpha]_D^{24}$ −14.8° (*c*=1.6, $CHCl_3$)) under the same conditions led to (*S*)-(−)-2-acetyl-2-methyl-4-pentenyl benzoate (116 mg, 97% yield, $[\alpha]_D^{20}$ −10.9° (*c*=2,2, $CHCl_3$)).

On the basis of the above results, the optical rotation of cptically pure (*S*)-(−)-**10b** was calculated to be $[\alpha]_D$ −22.7°C ($CHCl_3$).

References and Notes

1) Part III: K. Hiroi and K. Makino, *Chem. Pharm. Bull.*, **36**, 1744 (1988).
2) For a preliminary report of this work see K. Hiroi and J. Abe, *Tetrahedron Lett.*, **31**, 3623 (1990).
3) S. Masamune, W. Choy, J. S. Petersen, and L. R. Sita, *Angew. Chem., Int. Ed. Engl.*, **24**, 1 (1985); M, Braun, *ibid.*, **26**, 24(1987); J. W. ApSimon and T. L. Collier, *Tetrahedron*, **42**, 5157 (1986).
4) H. Brunner, *Synthesis*, **1988**, 645; S. L. Blystone, *Chem. Rev.*, **89**, 1663 (1989).
5) K. Hiroi, *Yuki Gosei Kagaku Kyokai Shi*, **44**, 907 (1986); K. Hiroi, R. Kitayama, and S. Sato, *J. Chem. Soc., Chem. Commun.*, **1984**, 303; *idem, Chem. Lett.*, **1984**, 929; K. Hiroi and K. Makino, *ibid.*, **1986**, 617.
6) B. M. Trost and N. R. Schmuff, *Tetrahedron Lett.*, **22**, 2999 (1981); T. Hayashi, T. Hagihara, M. Konishi, and M. Kumada, *J. Am. Chem. Soc.*, **105**, 7767 (1983); *idem, J. Chem. Soc., Chem. Commun.*, **1984**, 107.

7) B. M. Trost and P. E. Strege, *J. Am. Chem. Soc.*, **99**, 1649 (1977); J. C. Fiaud, A. Hibon de Gournay, M. Larcheveque, and H. B. Kagan, *J. Organometal. Chem.*, **154**, 175 (1978); T. Hayashi, K. Kanehira, and M. Kumada, *J. Chem. Soc., Chem. Commun.*, **1982**, 1162; K. Yamamoto and J. Tsuji, *Tetrahedron Lett.*, **23**, 3089 (1982).
8) *a*) K. Hiroi, K. Suya, and S. Sato, *J. Chem. Soc., Chem. Commun.*, **1986**, 469; *b*) K. Hiroi, J. Abe, S. Suya, and S. Sato, *Tetrahedron Lett.*, **30**, 1543 (1989); *c*) K. Hiroi and J. Abe, *Heterocycles*, **30**, 283 (1990).
9) K. Hiroi, T. Koyama, and K. Anzai, *Chem. Lett.*, **1990**, 235.
10) K. Hiroi, K. Maezuru, M. Kimura, and N. Ito, *Chem. Lett.*, **1989**, 1751.
11) S. Yamada, K. Hiroi, and K. Achiwa, *Tetrahedron Lett.*, **10**, 4233 (1969); K. Hiroi, K. Achiwa, and S. Yamada, *Chem. Pharm. Bull.*, **20**, 246 (1972).
12) I. Kinoshita, Y. Yokota, K. Matsumoto, S. Ooi, K. Kashiwabara, and J. Fujita, *Bull. Chem. Soc. Jpn.*, **56**, 1067 (1983).
13) R. W. Hoffmann, W. Ladner, K. Steinbach, W. Massa, R. Schmidt, and G. Snatzke, *Chem. Ber.*, **114**, 2786 (1981).
14) G. Frater, *Helv. Chim. Acta*, **62**, 2825 (1979); K. Tomioka, K. Ando, Y. Takemasa, and K. Koga, *J. Am. Chem. Soc.*, **106**, 2718 (1984).
15) A. I. Meyers, D. R. Williams, G. W. Erickson, S. White, and M. Druelinger, *J. Am. Chem. Soc.*, **103**, 3081 (1981).
16) T. Migita, K. Nagai, and M. Kosugi, *Bull. Chem. Soc. Jpn.*, **56**, 2480 (1983).
17) L. Engman, *J. Am. Chem. Soc.*, **106**, 3977 (1989).
18) W. Szeja, *Synthesis*, **1979**, 822.
19) The physical properties of **5a** and **10b** will be reported in due course.
20) K. C. Brannock, *J. Am. Chem. Soc.*, **81**, 3379 (1959).

Novel Method for the Synthesis of 2′,3′-Unsaturated Nucleosides from 2′(3′)-Acetoxy-3′(2′)-halogeno Derivatives by Using Sodium Dithionite with Viologen as a Reductive Elimination Mediator

Yusuke AMINO* and Hisao IWAGAMI

Central Research Laboratories, Ajinomoto Co., Inc., 1–1, Suzuki-cho, Kawasaki-ku, Kawasaki 210, Japan. *Received September 18, 1990*

Reductive elimination of vicinal acetylated halohydrins with $Na_2S_2O_4$ as the reducing agent and viologen as the reduction mediator in a two-phase water–organic system is described. 2′,3′-Unsaturated nucleosides such as 1-(5-*O*-acetyl-2,3-dideoxy-β-D-*glycero*-pent-2-enofuranosyl)adenine, -hypoxanthine and -uracil were obtained from 2′(3′)-acetoxy-3′(2′)-halogeno derivatives in good yields by meanes of this procedure.

Keywords viologen; mediator; sodium dithionite; reductive elimination; 2′,3′-unsaturated nucleoside; 2′,3′-dideoxy nucleoside; 2′(3′)-acetoxy-3′(2′)-halogeno nucleoside

2′,3′-Dideoxy nucleosides and their 2′,3′-unsaturated analogues are known to be potent anti-human immunodeficiency virus (HIV) agents. Some of them are currently under clinical trial in patients with acquired immunodeficiency syndrome (AIDS) and AIDS-related complex. Therefore, general and economical methods for preparation of those substances are of interest.

Methods of olefin synthesis by deoxygenation of vicinal-diols have been studied in detail.[1] The conversion of the vicinal-diol functionality of ribonucleosides to 2′,3′-olefinic analogues represents one of the most general routes for the preparation of such unsaturated nucleoside analogues. For example, 2′,3′-unsaturated derivatives have been obtained through Barton deoxygenation of the bisxanthate or desulfurization of the cyclic thiocarbonate of 2′,3′-dihydroxy precursors.[2] They have also been obtained from 2′,3′-alkoxymethylidene cyclic orthoesters on heating at reflux in acetic anhydride in the case of pyrimidine nucleosides.[3] Unsaturated analogues can be hydrogenated to give 2′,3′-dideoxy analogues.

2′(3′)-Acetoxy-3′(2′)-halogeno derivatives (**2a, b**), readily obtained by following Moffatt *et al.*'s method[4] or its modification,[5] were also converted to 2′,3′-unsaturated derivatives (**3**) by reductive elimination on treatment with Zn[6] or $Cr(OAc)_2en_2$,[7] or *via* electrochemical reduction[8] (Chart 1). However, those methods have limited generality. When Zn is used, it forms a complex gel on treatment with water, making purification of the product extremely difficult, and the contaminating zinc complex significantly retards the subsequent catalytic reduction when the 2′,3′-dideoxy derivatives (**4**) are desired. In the case of $Cr(OAc)_2en_2$, various inseparable compounds, such as 3′(2′)-deoxy derivatives and 3′-deoxy-3′-olefinic derivatives, are obtained and special care is required in the preparation of the reagent. For electrolysis, a special apparatus would be necessary on an industrial scale.

We thought that 2′(3′)-acetoxy-3′(2′)-halogeno derivatives might be the best intermediates for transforming ribonucleosides to the corresponding olefins. A novel, more general method to synthesize 2′,3′-unsaturated derivatives starting from 2′(3′)-acetoxy-3′(2′)-halogeno derivatives was thus explored.

In the reaction with Zn or *via* electrolysis, reductive elimination is well understood to occur through a concerted electron transfer process. Viologens (*N*,*N*′-dialkyl-4,4′-bipyridinium salts) have been used as electron mediators in many reductions.[9] Application of viologens for the conversion of vicinal-dibromides to olefins by catalytic debromination under heterophase conditions has also been reported.[9d–f] These reports prompted us to examine the use of viologens with vicinal-acetoxyhalogeno derivatives.

We describe in this paper a novel and practical method for the synthesis of 2′,3′-unsaturated nucleosides *via* viologen-mediated reductive elimination of 2′(3′)-acetoxy-3′(2′)-halogeno derivatives in high yield.

Results and Discussion

Viologens (V^{2+}) are electron acceptors and carriers. They have generally been used in a two-phase water–organic system. Viologens undergo one-electron reduction by a reducing agent to produce the blue cation radicals ($V^{+\cdot}$) in the water phase and are extracted into the organic phase where they are easily reoxidized to V^{2+} by passing electrons to the substrate.

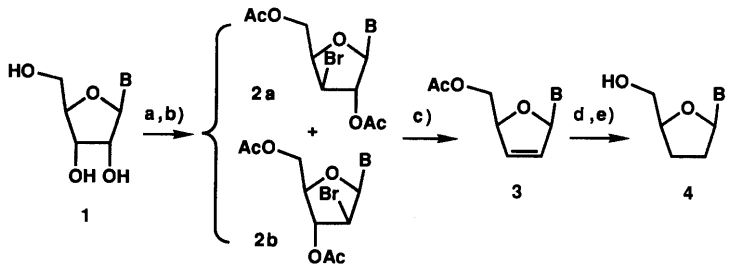

reagents : a) $(MeO)_3CCH_3$, Cl_3CCO_2H ; b) AcBr ; c) Zn-AcOH or $Cr(OAc)_2en_2$ or electrolysis ; d) H_2/Pd-C ; e) NaOH-H_2O

Chart 1

The general procedure for the transformation of 2′(3′)-acetoxy-3′(2′)-halogeno nucleosides to 2′,3′-unsaturated derivatives is as follows. A 2′(3′)-acetoxy-3′(2′)-halogeno nucleoside (**2a, b**) was dissolved in a two-phase water–organic system. Excess $Na_2S_2O_4$ (reducing agent) and K_2CO_3 were added to the mixture and the atmosphere was replaced with N_2 or Ar. Then viologen was added to the mixture and the mixture was stirred at room temperature. The reaction was monitored by reverse-phase high performance liquid chromatography (HPLC). The organic phase was separated and concentrated. We purified the product (**3**) by silica gel chromatography (Fig. 1).

In this reaction, $Na_2S_2O_4$ as well as glucose[9f] is available as an electron donor; however, they were not all effective for transforming acetoxyhalogeno derivatives to olefins without viologen. In order to neutralize the bromide and acetate anions formed in the reaction, K_2CO_3 was added as a base, because the resulting unsaturated nucleoside is very labile to acid. Epoxide (2′,3′-anhydro derivative) was not obtained so long as the reaction was carried out in a two-phase water–organic system, though the water phase was basic. To avoid the interference of oxygen, the reaction must be carried out under an inert gas. A small amount of 2′(3′)-hydroxy-3′(2′)-halogeno derivative (**5**) was detected by chromatography as a by-product(s).[10] The amount of it was constant throughout the reaction. The results suggest that compound **5** was formed in the initial stage of the reaction but was not consumed during the reaction. No appreciable amount of other products, such as the 2′(3′)-acetoxy-3′(2′)-deoxy derivative, except for the glycosidic cleavage product, was detected by HPLC.

Various organic solvents were tested in the reaction using 9-(2,5-di-*O*-acetyl-3-bromo-3-deoxy-β-D-xylofuranosyl)-adenine (**6**) as a substrate, and the results are shown in Table I. CH_2Cl_2 was found to be most suitable among

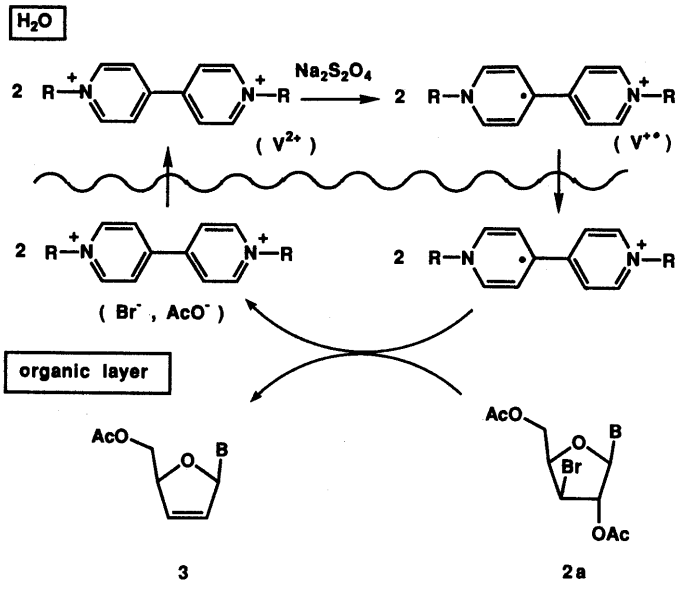

Fig. 1

TABLE I. Solvent Effect in the Reductive Elimination of Compound **6**

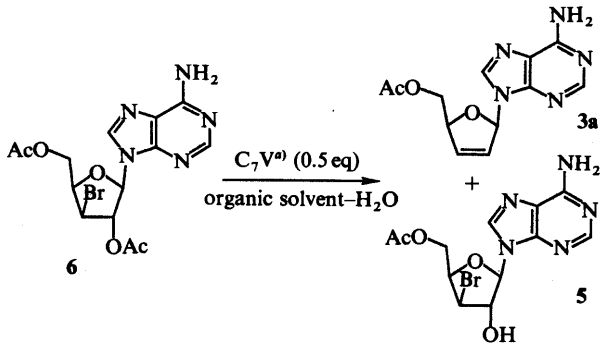

Organic solvent	Conversion (%)[b]	**3a** (%)[b]	By-product **5** (%)[b]
CH_2Cl_2	75	69	4
AcOEt	74	56	16
CH_3CN	28	3	23
CH_3OH	100[c]	Trace	Trace

Reaction conditions: organic solvent–H_2O (7:3 v/v; 24 mM), C_7V (0.5 eq), $Na_2S_2O_4$ (10 eq), K_2CO_3 (6 eq), room temperature, under Ar, 15 h. *a*) *N,N*′-Diheptyl-4,4′-bipyridinium dibromide. *b*) Calculated from the peak area in HPLC; see the experimental section. *c*) The substrate was completely hydrolyzed.

TABLE II. Molar Ratio of C_7V to the Substrate and Conversion of the Reaction

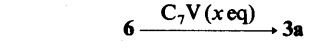

C_7V (eq)	Conversion (%)	**3a** (%)	By-product **5** (%)
0.1	40	35	4
0.5	75	69	4
1.0	96	92	3
1.5	99	94	4

The reaction was carried out in a two-phase water–CH_2Cl_2 system. Other notes are the same as in Table I.

TABLE III. Results of the Reductive Elimination of **6** Using Various Viologens

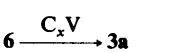

Viologen[a]	Conversion (%)[b]	Isolated yield of **3a** (%)
C_1V	86	75
C_3V	94	79
C_8V	93	72
$C_{12}V$	92	74

Reaction conditions: see the experimental section. *a*) C_1V, *N,N*′-dimethyl-4,4′-bipyridinium dichloride; C_3V, *N,N*′-dipropyl-4,4′-bipyridinium dibromide; C_8V, *N,N*′-dioctyl-4,4′-bipyridinium dibromide; $C_{12}V$, *N,N*′-didodecyl-4,4′-bipyridinium dibromide. *b*) Calculated from the peak area in HPLC.

TABLE IV. Reductive Elimination of 2′(3′)-Acetoxy-3′(2′)-halogeno Derivatives

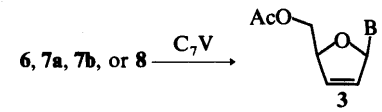

Substrate	B	Conversion (%)[a]	Product	Isolated yield (%)
6	Adenin-9-yl	94	**3a**	83
7a, 7b	Hypoxanthin-9-yl	96	**3b**	78
8	Uracil-1-yl	90	**3c**	64

Reaction conditions: see the experimental section. *a*) Calculated from the peak area in HPLC.

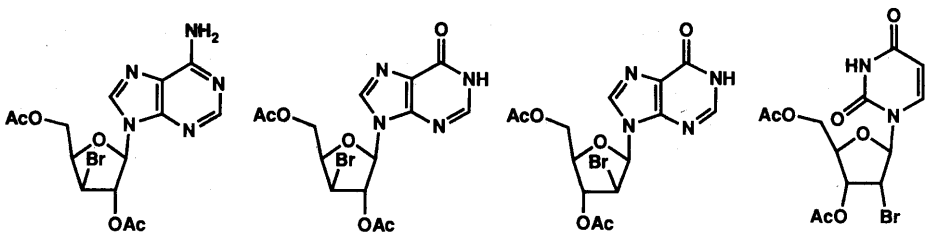

6 7a 7b 8

Fig. 2

them, so subsequent experiments were carried out using CH_2Cl_2 as the organic phase. In MeOH, the reaction mixture was homogeneous and the substrate was hydrolyzed completely. The results confirm the importance of using a two-phase system in the reaction with viologen.

Table II shows the relationship of the molar ratio of viologen to the substrate and the conversion of the reaction. Viologen is known to act as a catalyst in various reactions.[9] In our case, however, an equimolecular quantity of viologen to the substrate was necessary to complete the reaction. Nevertheless, it is noteworthy that the reaction proceeded to the extent of *ca.* 40% even in the presence of a 0.1 mol eq of viologen.

Viologens having various alkyl chains were tested and the results are summarized in Table III, which shows that the compounds have similar activity regardless of the length of the alkyl chain.

Table IV shows the results of the cases when various substrates were used in the reaction. Independently of the base structure, adenine, hypoxanthine or uracil, and the stereo- and/or regiochemistry at the 2′-3′-position (Figs. 2, **6**, **7a**, **b**, **8**), all substrates were transformed to the corresponding 2′,3′-unsaturated derivatives in good yields.

The mechanism of reductive elimination in this reaction is considered to be a two-electron reduction, as in the case of vicinal-dibromides. However, details of the mechanism, whether stepwise or concerted, have not yet been elucidated.

The reaction described here is useful because the substrates, vicinal-acetoxy halides, are readily available from vicinal-diols. 2′,3′-Unsaturated nucleosides, especially the inosine derivative (**3b**), are known to be unstable to protic solvents, due to deglycosylation.[2] It is worth noting that this reaction is applicable to labile nucleosides, so that 2′(3′)-acetoxy-3′(2′)-halogeno nucleosides could be transformed to 2′,3′-unsaturated nucleosides.

Experimental

Proton nuclear magnetic resonance (^{1}H-NMR) spectra were measured with a Varian VXR 300 spectrometer and chemical shifts are given as δ ppm relative to tetramethylsilane (TMS) as an internal standard. Infrared (IR) spectra were recorded on a Jasco IR-810 infrared spectrophotometer with samples in KBr disk. Mass spectra (MS) were recorded with a JEOL DX-300 instrument by using the fast-atom bomberdment (FAB) technique. Optical rotations were measured on a JASCO DPI-140 polarimeter. Melting points were determined with a Yanaco micro melting point apparatus and are uncorrected. The thin layer chromatographic system employed silica gel Merck Art. 7515. Preparative thin layer chromatography (PTLC) was performed with Whatman PLK 5F. HPLC was performed on a Hitachi L-6000 equipped with a YMC-Pack A312 (ODS 6 × 150 mm) column with a mobile phase composed of 20% CH_3CN–H_2O, at 25°C. The elution rate was 1.6 ml/min and detection was carried out in the ultraviolet (UV) at 260 nm.

N,*N*′-Dimethyl-4,4′-bipyridinium dichloride (C_1V) and *N*,*N*′-diheptyl-4,4′-bipyridinium dibromide (C_7V) were purchased from Aldrich Chemical Company, Inc. and Tokyl Kasei Kogyo Co., Ltd., respectively. *N*,*N*′-Dipropyl- (C_3V), *N*,*N*′-dioctyl- (C_8V) and *N*,*N*′-didodecyl-4,4′-bipyridinium dibromide ($C_{12}V$) were prepared according to Willner *et al.*'s method.[9f]

9-(2,5-Di-*O*-acetyl-3-bromo-3-deoxy-β-D-xylofuranosyl)adenine (**6**) and 9-[2(3),5-di-*O*-acetyl-3(2)-bromo-3(2)-deoxy-β-D-xylofuranosyl]hypoxanthine (**7a**, **b**) were prepared by a modification of the procedure of Norman and Reese.[5] 1-(3,5-Di-*O*-acetyl-2-bromo-2-deoxy-ribosyl)uracil (**8**) was prepared following the procedure of Marumoto and Honjo.[11] Compound **6** was recrystallized from AcOEt.

9-(2,5-Di-*O*-acetyl-3-bromo-3-deoxy-β-D-xylofuranosyl)adenine (6) ^{1}H-NMR (300 MHz, $CDCl_3$) δ: 2.13 (3H, s, CH_3), 2.18 (3H, s, CH_3), 4.43—4.54 (4H, m, CH_2, H-2′, H-4′ and H-5′), 5.75 (1H, dd, J=1.3, 2.3 Hz, H-3′), 6.02 (2H, br s, NH_2), 6.26 (1H, d, J=2.1 Hz, H-1′), 8.28 (1H, s, H-2 or H-8), 8.35 (1H, s, H-2 or H-8). IR (KBr): 3300, 3175, 1755 (C=O), 1665, 1605, 1230, 1215 cm^{-1}, FAB-MS *m*/*z*: 414, 416 (MH^+).

9-[2(3),5-Di-*O*-acetyl-3(2)-bromo-3(2)-deoxy-β-D-xylofuranosyl)hypoxanthine (7a, b) ^{1}H-NMR (300 MHz, $CDCl_3$) δ: major isomer: 2.13 (3H, s, CH_3), 2.19 (3H, s, CH_3), 4.40—4.58 (4H, m, CH_2, H-2′, H-4′ and H-5′), 5.73 (1H, dd, J=1.3, 2.3 Hz, H-3′), 6.18 (1H, d, J=2.1 Hz, H-1′), 8.15 (1H, s, H-2 or H-8), 8.30 (1H, s, H-2 or H-8); minor isomer: 2.16 (3H, s, CH_3), 2.19 (3H, s, CH_3), 4.29—4.34 (1H, m, H-3′ or H-4′), 4.40—4.58 (2H, m, CH_2, H-5′), 4.71 (1H, dd, J=2.3, 4.3 Hz, H-3′ or H-4′), 5.60 (1H, dd, J=2.7, 2.7 Hz, H-2′), 6.34 (1H, d, J=4.5 Hz, H-1′), 8.15 (1H, s, H-2 or H-8), 8.30 (1H, s, H-2 or H-8). IR (KBr): 1750 (C=O), 1695, 1220 cm^{-1}. FAB-MS *m*/*z*: 415, 417 (MH^+).

1-(3,5-Di-*O*-acetyl-2-bromo-2-deoxy-ribosyl)uracil (8) ^{1}H-NMR (300 MHz, $CDCl_3$) δ: 2.14 (3H, s, CH_3), 2.19 (3H, s, CH_3), 4.37—4.45 (3H, m, CH_2, H-4′ and H-5′), 4.58 (1H, t, J=5.7 Hz, H-2′), 5.14 (1H, t, J=5.4 Hz, H-3′), 5.78 (1H, dd, J=2.1, 8.1 Hz, H-5), 6.19 (1H, d, J=5.4 Hz, H-1′), 7.42 (1H, d, J=8.1 Hz, H-6). IR (KBr): 1765 (C=O), 1695 (C=O), 1460, 1380, 1230 cm^{-1}. FAB-MS *m*/*z*: 391, 393 $(MH)^+$.

Reaction of 9-(2,5-Di-*O*-acetyl-3-bromo-3-deoxy-β-D-xylofuranosyl)adenine (6) with Sodium Dithionite and Viologen 9-(2,5-Di-*O*-acetyl-3-bromo-3-deoxy-β-D-xylofuranosyl)adenine (**6**) (500 mg, 1.2 mmol), $Na_2S_2O_4$ (2.09 g, 12.0 mmol) and K_2CO_3 (995 mg, 7.2 mmol) were added to the mixture of CH_2Cl_2 (35 ml) and water (15 ml). A stream of Ar was passed through the apparatus with stirring to displace the air. *N*, *N*′-Diheptyl-4,4′-bipyridinium dibromide (308 mg, 0.6 mmol) was added and the reaction mixture was stirred for 15 h at room temperature under Ar. The stirring was continued under the same conditions for 24 h after the addition of $Na_2S_2O_4$ (418 mg, 2.4 mmol), K_2CO_3 (330 mg, 2.4 mmol) and *N*,*N*′-diheptyl-4,4′-bipyridinium dibromide (123 mg, 0.24 mmol). At this time, 96% consumption of the starting material was found by HPLC. The two phases were separated and the water phase was extracted with CH_2Cl_2 (50 ml). The combined organic layer was dried over $MgSO_4$ and concentrated. The residue was purified by silica gel PTLC developed with $CHCl_3$–MeOH (8/1, v/v) to give 1-(5-*O*-acetyl-2,3-dideoxy-β-D-*glycero*-pent-2-enofuranosyl)adenine (**3a**) (274 mg, 82.9%) as a white powder.

1-(5-*O*-Acetyl-2,3-dideoxy-β-D-*glycero*-pent-2-enofuranosyl)adenine (3a) ^{1}H-NMR (300 MHz, $CDCl_3$) δ: 2.07 (3H, s, CH_3), 4.27 (1H, dd, J=3.3, 12.3 Hz, H-5′), 4.33 (1H, dd, J=3.9, 12.3 Hz, H-5′), 5.15—5.20 (1H, m, H-4′), 5.79 (2H, br s, NH_2), 6.15 (1H, ddd, J=1.5, 2.4, 6.0 Hz, H-2′), 6.38 (1H, ddd, J=1.5, 1.8, 6.0 Hz, H-3′), 6.99—7.13 (1H, m, H-1′), 7.97 (1H, s, H-2 or H-8), 8.39 (1H, s, H-2 or H-8). IR (KBr): 3350, 3200, 1745 (C=O), 1665, 1605, 1255, 1235 cm^{-1}. FAB-MS *m*/*z*: 276 (MH^+). High mass (FAB) Calcd for $C_{12}H_{14}N_5O_3$+H: 276.1097. Found: 276.1119, mp 83—84 °C (from iso-PrOH), $[\alpha]_D^{22}$ −43.03 (*c*=0.5, MeOH).

1-(5-*O*-Acetyl-2,3-dideoxy-β-D-*glycero*-pent-2-enofuranosyl)hypoxanthine (3b) ^{1}H-NMR (300 MHz, $CDCl_3$) δ: 2.07 (3H, s, CH_3), 4.27 (1H, dd, J=3.3, 12.3 Hz, H-5'), 4.31 (1H, dd, J=3.6, 12.3 Hz, H-5'), 5.18 (1H, m, H-4'), 6.16 (1H, ddd, J=1.5, 2.4, 6.0 Hz, H-2'), 6.41 (1H, ddd, J=1.5, 1.8, 6.0 Hz, H-3'), 7.06 (1H, m, H-1'), 7.99 (1H, s, H-2 or H-8), 8.19 (1H, s, H-2 or H-8). IR (KBr): 3450, 3050, 2850, 1740 (C=O), 1715, 1700, 1600, 1555, 1240 cm^{-1}. FAB-MS m/z: 277 (MH^+). High mass (FAB) Calcd for $C_{12}H_{12}N_4O_4$+H: 277.0958. Found: 277.0937, mp >300 °C (dec.) (from $CHCl_3$–petroleum ether), $[\alpha]_D^{22}$ −38.87 (c=0.5, MeOH).

1-(5-*O*-Acetyl-2,3-dideoxy-β-D-*glycero*-pent-2-enofuranosyl)uracil (3c) ^{1}H-NMR (300 MHz, $CDCl_3$) δ: 2.08 (3H, s, CH_3), 4.25 (1H, dd, J=3.0, 12.3 Hz, H-5'), 4.36 (1H, dd, J=3.9, 12.3 Hz, H-5'), 5.06 (1H, m, H-4'), 5.72 (1H, dd, J=2.1, 8.1 Hz, H-5), 5.92 (1H, ddd, J=1.5, 2.1, 6.0 Hz, H-2'), 6.30 (1H, ddd, J=1.5, 1.8, 6.0 Hz, H-3'), 7.00 (1H, m, H-1'), 7.47 (1H, d, J=8.1 Hz, H-6), 8.54 (1H, br s, NH). IR (KBr): 3200, 3100, 1745 (C=O), 1700, 1625, 1470, 1390, 1260 cm^{-1}. FAB-MS m/z: 253 (MH^+). High mass (FAB) Calcd for $C_{11}H_{12}N_2O_5$+H: 253.0825. Found: 253.0865. mp 124—125 °C (from iso-PrOH), $[\alpha]_D^{22}$ −75.79 (c=0.5, MeOH).

Acknowledgement We are grateful to Dr. Toshihide Yukawa and Dr. Kunisuke Izawa in our laboratories for helpful discussions and advice.

References and Notes

1) E. Block, Organic Reactions, Vol. 30, John Wiley and Sons, New York, 1984, Chapter 2.
2) C. K. Chu, V. S. Bhadti, B. Daboszewski, Z. P. Gu, Y. Kosugi, K. C. Pullaiah and P. Van Roey, *J. Org. Chem.*, **54**, 2217 (1989) and references cited therein.
3) H. Shiragami, Y. Irie, H. Shirae, K. Yokozeki and N. Yasuda, *J. Org. Chem.*, **53**, 5179 (1988).
4) A. F. Russell, S. Greenberg and J. G. Moffatt, *J. Am. Chem. Soc.*, **95**, 4025 (1973).
5) D. G. Norman and C. B. Reese, *Synthesis*, **1983**, 304.
6) *a*) B. Classon, P. J. Garegg and B. Samuelsson, *Acta Chem. Scand.*, **B36**, 251 (1982); *b*) M. J. Robins, F. Hanske, N. H. Low and J. I. Park, *Tetrahedron Lett.*, **25**, 367 (1984); *c*) C. J. Welch, H, Bazin and J. Chattopadhyaya, *Acta Chem. Scand.*, **B40**, 343 (1986).
7) T. C. Jain, I. D. Jenkins, A. F. Russell, J. P. H. Verheyden and J. F. Moffatt, *J. Org. Chem.*, **39**, 30 (1974).
8) *a*) R. Mengel and J.-M. Siefert, *Tetrahedron Lett.*, **1977**, 4203; *b*) T. Adachi, T. Iwasaki, I. Inoue and M. Miyoshi, *J. Org. Chem.*, **44**, 1404 (1979).
9) *a*) T. Endo, Y. Saotome and M. Okawara, *Tetrahedron Lett.*, **26**, 4525 (1985); *b*) H. Tomioka, K. Ueda, H. Ohi and Y. Izawa, *Chem. Lett.*, **1986**, 1359; *c*) H. Shozenji, Y. Nakano and K. Yamada, *Chem. Lett.*, **1988**, 1033; *d*) Z. Goren and I. Willner, *J. Am. Chem. Soc.*, **105**, 7764 (1983); *e*) T. Endo, Y. Saotome and M. Okawara, *J. Am. Chem. Soc.*, **106**, 1124 (1984); *f*) R. Maidan, Z. Goren, J. Y. Becker and I. Willner, *J. Am. Chem. Soc.*, **106**, 6217 (1984); *g*) R. Maidan and I. Willner, *J. Am. Chem. Soc.*, **108**, 1080 (1986).
10) Compound **5** was very labile and easily transformed to 9-(5-*O*-acetyl-2,3-anhydro-β-D-ribofuranosyl)adenine (**9**) during the purification. The structure of **5** was confirmed by FAB-MS [m/z: 372, 374 (MH^+)] and examination of ^{1}H-NMR spectrum of the mixture of **5** and **9**.
11) R. Marumoto and M. Honjo, *Chem. Pharm. Bull.*, **22**, 128 (1974).

Quinazolin-2-ones Having a Spirohydantoin Ring. II. Synthesis of Several Spiro[imidazolidine-4,4′(1′*H*)-quinazoline]-2,2′,5(3′*H*)-triones *via* 5-Hydroxyhydantoin Derivatives[1,2]

Masafumi YAMAGISHI,[a] Yoshihisa YAMADA,[a] Ken-ichi OZAKI,[a] Junichi TANI,[b] and Mamoru SUZUKI*,[a]

Research Laboratory of Applied Biochemistry, Tanabe Seiyaku Co., Ltd.,[a] and Chemistry Technology Division, Tanabe Seiyaku Co., Ltd.,[b] 16–89, Kashima-3-chome, Yodogawa-ku, Osaka 532, Japan. *Received September 20, 1990*

Reaction of 1-ethoxycarbonylisatin (1b) with urea gave 5-(2-ethoxycarbonylaminophenyl)-5-hydroxyhydantoin (4b) in a good yield. Treatment of 4b with several amines directly gave the corresponding spiro[imidazolidine-4,4′(1′*H*)-quinazoline]-2,2′,5(3′*H*)-trione derivatives (7a—d) in moderate yields. 3-Unsubstituted and 3-methylspiroquinazolin-2-one derivatives 7a, b were also synthesized from 5-ethoxy and 5-ethylthiohydantoins 5a, d, which in turn were easily obtained by the reaction of either ethanol or ethylmercaptan with 4b in the presence of a catalytic amount of sulfuric acid.

Keywords 1-ethoxycarbonylisatin; urea; 5-(2-ethoxycarbonylaminophenyl)-5-hydroxyhydantoin; spirohydantoin; spiro[imidazolidine-4,4′(1′*H*)-quinazoline]-2,2′,5(3′*H*)-trione; spiroquinazolin-2-one

Several spirohydantoins which inhibit the enzyme aldose reductase are of potential value in the therapy of diabetic complications.[3–6] In connection with our interest in this field, we have studied the syntheses of quinazolin-2-ones having such a spirohydantoin ring.

In the previous paper,[1] we reported a new synthetic method for 3′-methylspiro[imidazolidine-4,4′(1′*H*)-quinazoline]-2,2′,5(3′*H*)-trione (**7b**) which involves the reaction of 1-methylcarbamoylisatin (**1a**) with urea followed by cyclization of resulting 3,4-dihydro-4-hydroxy-3-methyl-4-ureidocarbonyl-2(1*H*)-quinazolinone (**3**) with hydrochloric acid (HCl). We proposed the following mechanism for the formation of the key intermediate **3**: the ring opening of **1a** with urea yields the oxalylurea **2** (X=NHMe),[7] in which the amino group of the carbamoylamino residue attacks one of the carbonyl groups of the oxalylurea group through path A in Chart 1. Meanwhile, the hydantoin derivative **4a** which would be formed from **2** (X=NHMe) through path B was not obtained in this reaction. We then examined the reaction of urea with 1-alkoxycarbonylisatin, not including a nucleophilic moiety instead of the carbamoyl group, in the expectation of finding an alternative route to the spiroquinazolin-2-ones **7** through path B. In this paper, we describe the synthesis of the hydantoins **4** (X=OR), and their transformation to the spiroquinazolin-2-ones **7**.

On treatment of 1-ethoxycarbonylisatin (**1b**)[8] with urea under reflux in tetrahydrofuran (THF) for 15 h, the desired 5-hydroxyhydantoin **4b** was obtained in one step in 81% yield. The structural assignment of the product **4b** was based on the following spectroscopic and elemental analyses. The infrared (IR) spectrum of **4b** showed absorption bands at 1780, 1725, and 1690 cm^{-1} due to three carbonyl groups. In the carbon-13 nuclear magnetic resonance (^{13}C-NMR) spectrum of **4b**, three carbonyl carbon signals appeared at δ 153.10, 155.39 and 174.86, and one quaternary sp^3 carbon signal appeared at δ 86.38. In a similar manner, **4c** was obtained from **1c** and urea in 75% yield. Considering the fact that the 1-methylcarbamoylisatin (**1a**) did not react with urea under these conditions,[1] the carbonyl group at the 2-position of **1b** appears to be more reactive than that of **1a**.

We then attempted the cyclization of the resulting 5-hydroxyhydantoins **4b** and **4c** with several amines to convert them into the spiroquinazolin-2-ones **7**. When **4b** was heated with methylamine in a sealed tube at 120 °C, the desired 3′-methylspiro[imidazolidine-4,4′(1′*H*)-quinazoline]-2,2′,5(3′*H*)-trione (**7b**)[1] was obtained in 41% yield. Alternatively, compound **7b** was obtained by refluxing **4b** with methylamine in toluene–ethanol for 4 h. In the case of **4c**, however, the yield of **7b** was low.

In a similar manner, the reactions of **4b** with ammonia, hydrazine, and hydroxylamine gave the corresponding spiroquinazolin-2-ones **7a**, **c**, **d** as summarized in Table I. However, treatment of **4b** with benzylamine gave a complex mixture and the expected 3-benzylspiroquinazolin-2-one derivative was not isolated. A possible mechanistic interpretation for the formation of **7** is based on the assumption that **4b** is initially converted into the acyliminium ion

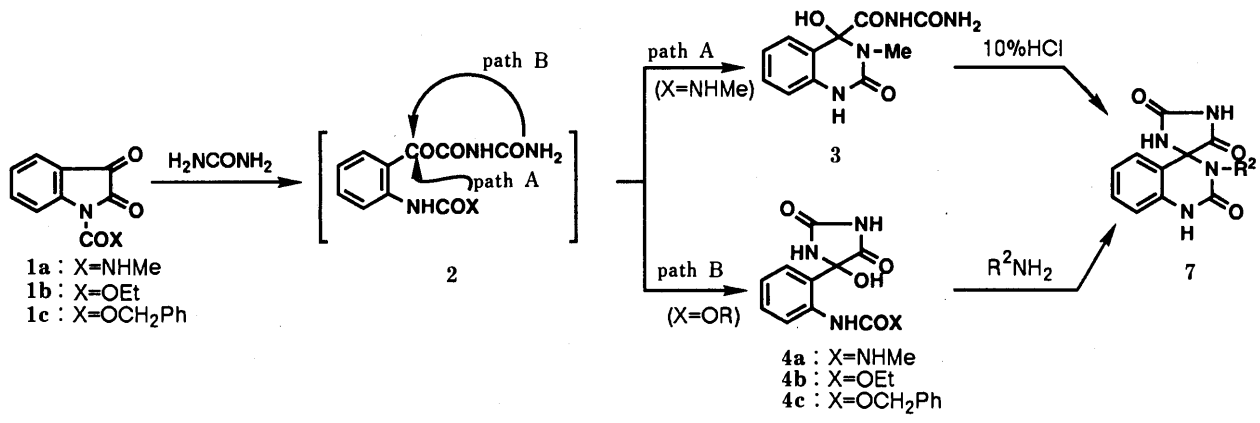

Chart 1

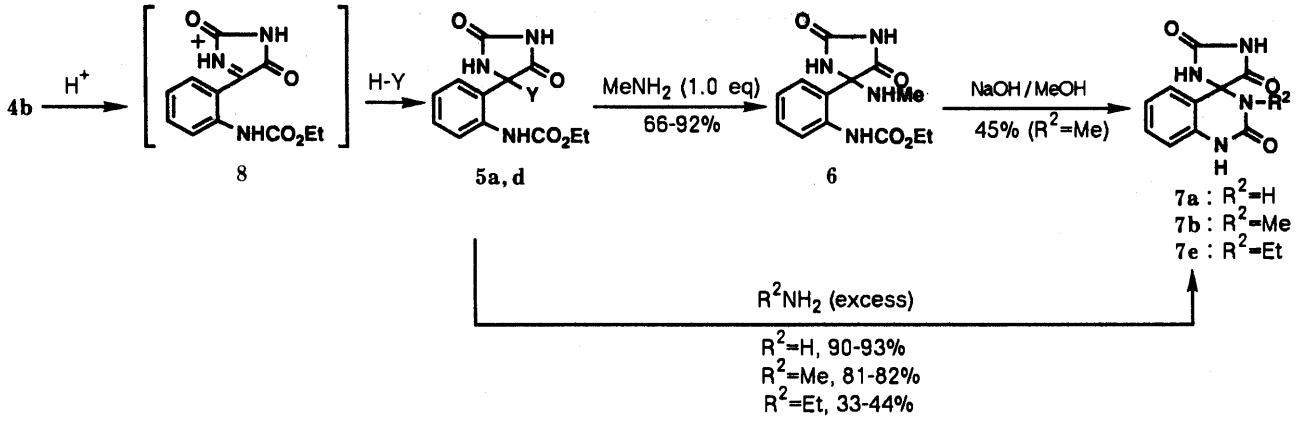

Chart 2

TABLE I. Reactions of 5-Hydroxyhydantoins **4** with Amines

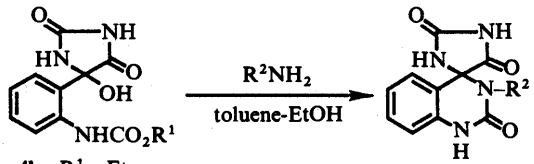

Run	R^1	R^2	Method	Product	Isolated yield (%)
1	Et	H	A	7a	59
2	Et	Me	A	7b	41
3	Et	Me	B	7b	37
4	CH_2Ph	Me	B	7b	17
5	Et	NH_2	B	7c	57
6	Et	OH	B	7d	15

A: in a sealed tube at 120 °C for 4 h. B: reflux for 4 h.

TABLE II. Replacement of the 5-Hydroxy Group of **4b** with an Alkoxy or Alkylthio Group

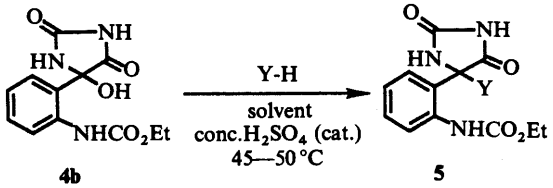

Run	Y	Solvent	Time (h)	Product	Isolated yield (%)
1	EtO	EtOH[a]	5	5a	0
2	EtO	EtOH	1	5a	77
3	iso-PrO	iso-PrOH	2	5b	85
4	$PhCH_2O$	THF[b]	15	5c	90
5	EtS	THF[b]	3	5d	96
6	$PhCH_2S$	THF[b]	5	5e	90

a) No addition of concentrated H_2SO_4. *b*) Y-H (1.2—3.0 eq).

intermediate **8**. This step is followed by attack of the amines to give the 5-amino derivatives, which then undergo cyclization to yield **7**. If this mechanism is correct, it is expected that the replacement of the 5-hydroxy group of the hydantoins **4** (X = OR) by more effective leaving groups, such as 5-alkoxy or 5-alkylthio groups, may lead to an improvement in the yields of **7**. When **4b** was heated in ethanol for 17 h, no reaction proceeded and the starting material **4b** was recovered. However, in the presence of a catalytic amount of sulfuric acid or HCl,[9] the expected reaction took place to give **5a** in a good yield. In a similar way, **4b** was treated with various alcohols and mercaptans in the presence of a catalytic amount of sulfuric acid at 45 °C to give the corresponding 5-alkoxy and 5-alkylthiohydantoins **5b—e** in good yields. These results are summarized in Table II.

When the resulting 5-ethoxy- and 5-ethylthiohydantoins **5a, d** were treated with one equivalent of methylamine at 45 °C, the exchange of the substituent at the 5-position proceeded to afford 5-methylaminohydantoin **6** in good yields as shown in Chart 2. Compound **6** was successfully cyclized to the desired spiroquinazolin-2-one **7b** by treatment with sodium hydroxide (NaOH) in methanol. Interestingly, treatment of 5-ethoxy- or 5-ethylthiohydantoins **5a, d** with an excess of ammonia at 45 °C gave directly the desired 3-unsubstituted spiroquinazolin-2-one **7a** in a high yield. Being encouraged by this result, we then examined the reaction of **5a, d** with other amines. Thus, the reaction of **5a** or **5d** with methylamine gave the desired 3-methylspiroquinazolin-2-one **7b** in a high yield. In the case of ethylamine, 3-ethylspiroquinazolin-2-one **7e** was obtained in 33—44% yield. In contrast, the reaction with benzylamine did not proceed, and the desired 3-benzylspiroquinazolin-2-one derivative was not isolated.

In summary, we have found a facile and practical synthetic method for 3-unsubstituted or various 3-substituted quinazolin-2-ones having a spirohydantoin ring *via* 5-substituted hydantoin derivatives which can be readily derived from 1-alkoxycarbonylisatin with urea. However, this method would be limited to the synthesis of the spiroquinazolin-2-ones having relatively less bulky groups at the 3-position for steric reasons. Further attempts to develop versatile synthetic methods for the spiroquinazolin-2-ones and the assay of the biological activities of the compounds thus obtained are in progress.

Experimental

All melting points were measured by the use of a Yamato MP-21 melting point apparatus and are uncorrected. IR spectra were recorded on a Shimadzu IR-420 spectrometer. The proton nuclear magnetic resonance (^{1}H-NMR) spectra were obtained using a Hitachi R-40 (90 MHz) spectrometer with tetramethylsilane (TMS) as an internal standard. ^{13}C-NMR spectra were determined on a Bruker AC-200 instrument (200 MHz) using TMS as an internal reference. Mass spectra (MS) were

taken with a Hitachi M-60 mass spectrometer at an ionizing potential of 30 eV. Column chromatography was carried out with Kieselgel 60 (230—400 mesh, E. Merck) and analytical thin-layer chromatography (TLC) was performed with precoated Kieselgel $60F_{254}$ plates (0.25 mm thickness, E. Merck).

Material 1-Ethoxycarbonylisatin (**1b**) was prepared from isatin according to the reported procedure.[8]

1-Benzyloxycarbonylisatin (1c) Benzyloxycarbonyl chloride (8.19 g, 48 mmol) was added dropwise to a suspension of isatin (5.88 g, 40 mmol) and triethylamine (4.86 g, 48 mmol) in THF (60 ml) at 0 °C and the mixture was stirred at the same temperature for 30 min, then concentrated under reduced pressure. Water was added to the residue and the resulting crystals were collected, washed with water, and recrystallized from *N,N*-dimethylformamide (DMF) to give **1c** (9.56 g, 85%), mp 153—154 °C. IR (Nujol): 1795, 1785, 1740 cm^{-1}. ^{1}H-NMR (DMSO-d_6) δ: 5.46 (2H, s, CH_2Ar), 7.33—7.55 (6H, m, ArH × 6), 7.70—7.81 (2H, m, ArH × 2), 8.00 (1H, d, J=8 Hz, ArH). MS *m/z*: 281 (M^+). *Anal.* Calcd for $C_{16}H_{11}NO_4$: C, 68.32; H, 3.94; N, 4.98. Found: C, 68.56; H, 4.07; N, 4.75.

5-(2-Ethoxycarbonylaminophenyl)-5-hydroxyimidazolidine-2,4-dione (4b) A suspension of **1b** (2.79 g, 12.7 mmol) and urea (1.15 g, 19.1 mmol) in THF (20 ml) was heated under reflux for 17 h. After cooling, the mixture was washed with water, and dried ($MgSO_4$). The solvent was evaporated off and the residue was chromatographed on silica gel using $CHCl_3$–methanol (9:1) as an eluent to give **4b** (2.88 g, 81%), mp 169—170 °C (dec.) (from AcOEt–*n*-hexane). IR (Nujol): 3300, 3200, 1780, 1725, 1690 cm^{-1}. ^{1}H-NMR (DMSO-d_6) δ: 1.20 (3H, t, J=7 Hz, $CH_2\underline{CH_3}$), 4.03 (2H, q, J=7 Hz, $\underline{CH_2}CH_3$), 6.8—7.35 (3H, m, ArH × 3), 7.70—7.90 (2H, m, ArH and OH), 8.90 (1H, s, NH), 9.10 (1H, s, NH), 10.70 (1H, s, NH). ^{13}C-NMR (DMSO-d_6) δ: 14.40 ($CH_2\underline{C}H_3$), 60.35 ($\underline{C}H_2CH_3$), 86.38 (C-5), 121.13 (C-3′), 122.51 (C-5′), 125.93 (C-1′), 126.54 (C-6′), 129.62 (C-4′), 137.67 (C-2′), 153.10, 155.39, 174.86 (CO × 3). *Anal.* Calcd for $C_{12}H_{13}N_3O_5$: C, 51.61; H, 4.69; N, 15.05. Found: C, 51.90; H, 4.97; N, 14.86.

5-(2-Benzyloxycarbonylaminophenyl)-5-hydroxyimidazolidine-2,4-dione (4c) This compound was synthesized from **1c** (5.0 g, 17.8 mmol) in the same manner as described for **4b**. Yield, 4.55 g (75%), mp 199—200 °C (dec.) (from AcOEt–*n*-hexane). IR (Nujol): 3300, 3230, 1790, 1730, 1705 cm^{-1}. ^{1}H-NMR (DMSO-d_6) δ: 5.17 (2H, s, CH_2Ar), 7.05—7.13 (1H, m, ArH), 7.31—7.44 (7H, m, ArH × 7), 7.98—8.04 (2H, m, ArH and OH), 9.16 (1H, s, NH), 9.45 (1H, s, NH), 10.97 (1H, s, NH). *Anal.* Calcd for $C_{17}H_{15}N_3O_5$: C, 59.82; H, 4.43; N, 12.31. Found: C, 59.52; H, 4.39; N, 11.99.

5-Ethoxy-5-(2-ethoxycarbonylaminophenyl)imidazolidine-2,4-dione (5a) Concentrated sulfuric acid (1.4 g) was added to a suspension of **4b** (27.9 g, 0.1 mol) in ethanol (100 ml) and the mixture was stirred at 45 °C for 1 h. After cooling, the resulting crystals were collected, washed with ethanol, and recrystallized from ethanol to give **5a** (23.6 g, 77%), mp 177—179 °C (dec.). IR (Nujol): 3400, 3210, 3110, 3080, 1790, 1740, 1720 cm^{-1}. MS *m/z*: 307 (M^+). ^{1}H-NMR (DMSO-d_6) δ: 1.18 (3H, t, J=7 Hz, $OCH_2\underline{CH_3}$), 1.23 (3H, t, J=7 Hz, $CO_2CH_2\underline{CH_3}$), 3.44 (2H, q, J=7 Hz, OCH_2), 4.14 (2H, q, J=7 Hz, CO_2CH_2), 7.00—8.00 (4H, m, ArH × 4), 9.03 (1H, s, NH), 9.41 (1H, s, NH), 11.38 (1H, s, NH). *Anal.* Calcd for $C_{14}H_{17}N_3O_5$: C, 54.72; H, 5.58; N, 13.68. Found: C, 54.66; H, 5.57; N, 13.72.

5-(2-Ethoxycarbonylaminophenyl)-5-isopropyloxyimidazolidine-2,4-dione (5b) This compound was synthesized from **4b** (0.56 g, 2 mmol) in isopropanol (10 ml) by a similar procedure to that described for **5a**. Yield, 0.55 g (85%), mp 217—218 °C (dec.) (from isopropanol–*n*-hexane). IR (Nujol): 3350, 3150, 3050, 1790, 1720 cm^{-1}. ^{1}H-NMR (DMSO-d_6) δ: 0.86—1.28 (9H, m, CH_3 × 3), 3.73—3.85 [1H, m, $C\underline{H}(CH_3)_2$], 4.05—4.21 (2H, m, CO_2CH_2), 7.08—7.16 (1H, m, ArH), 7.33—7.56 (2H, m, ArH × 2), 7.88—7.98 (1H, m, ArH), 9.13 (1H, s, NH), 9.41 (1H, s, NH), 11.34 (1H, s, NH). MS *m/z*: 321 (M^+). *Anal.* Calcd for $C_{15}H_{19}N_3O_5$: C, 56.07; H, 5.95; N, 13.08. Found: C, 55.80; H, 5.95; N, 13.08.

5-Benzyloxy-5-(2-ethoxycarbonylaminophenyl)imidazolidine-2,4-dione (5c) This compound was synthesized from **4b** (0.98 g, 3.5 mmol) and benzyl alcohol (1.07 g, 10.3 mmol) in THF (5 ml) by a similar procedure to that described for **5a**. Yield, 1.16 g (90%), mp 182—183 °C (dec.) (from methanol–water). IR (Nujol): 3150, 3070, 1780, 1730, 1705 cm^{-1}. ^{1}H-NMR (DMSO-d_6) δ: 1.18 (3H, t, J=7 Hz, $CH_2\underline{CH_3}$), 4.07 (2H, q, J=7 Hz, OCH_2), 4.43 (2H, s, CH_2Ar), 7.13—7.48 (8H, m, ArH × 8), 7.89—7.93 (1H, m, ArH), 9.10 (1H, s, NH), 9.61 (1H, s, NH), 11.49 (1H, s, NH). *Anal.* Calcd for $C_{19}H_{19}N_3O_5$: C, 61.78; H, 5.18; N, 11.38. Found: C, 61.86; H, 5.04; N, 11.47.

5-(2-Ethoxycarbonylaminophenyl)-5-ethylthioimidazolidine-2,4-dione (5d) This compound was synthesized from **4b** (1.4 g, 5 mmol) and ethanethiol (1.1 ml, 15 mmol) in THF (10 ml) by a similar procedure to that described for **5a**. Yield, 1.56 g (96%), mp 174—175 °C (dec.) (from AcOEt–*n*-hexane). IR (Nujol): 3280, 3150, 3050, 1775, 1740, 1705 cm^{-1}. ^{1}H-NMR (DMSO-d_6) δ: 1.14 (3H, t, J=7.5 Hz, $SCH_2\underline{CH_3}$), 1.23 (3H, t, J=7 Hz, $OCH_2\underline{CH_3}$), 2.42—2.64 (2H, m, SCH_2), 4.13 (2H, q, J=7 Hz, OCH_2), 7.16—7.68 (4H, m, ArH × 4), 9.42 (1H, s, NH), 9.56 (1H, s, NH), 11.57 (1H, s, NH). MS *m/z*: 262 (M^+ − SEt). *Anal.* Calcd for $C_{14}H_{17}N_3O_4S$: C, 52.00; H, 5.30; N, 12.99; S, 9.92. Found: C, 52.03; H, 5.31; N, 13.02; S, 9.76.

5-Benzylthio-5-(2-ethoxycarbonylaminophenyl)imidazolidine-2,4-dione (5e) This compound was synthesized from **4b** (0.98 g, 3.5 mmol) and benzylmercaptan (0.49 ml, 4.2 mmol) in THF (5 ml) by a similar procedure to that described for **5a**. Yield, 1.22 g (90%), mp 165—166 °C (dec.) (from AcOEt–*n*-hexane). IR (Nujol): 3180, 1770, 1730, 1705 cm^{-1}. ^{1}H-NMR (DMSO-d_6) δ: 1.22 (3H, t, J=7 Hz, $CH_2\underline{CH_3}$), 3.72—3.82 (2H, ABq, J=12 Hz, CH_2Ar), 4.12 (2H, q, J=7 Hz, OCH_2), 7.19—7.65 (9H, m, ArH × 9), 9.53 (1H, s, NH), 9.57 (1H, s, NH), 11.54 (1H, s, NH). *Anal.* Calcd for $C_{19}H_{19}N_3O_4S$: C, 59.20; H, 4.97; N, 10.90; S, 8.32. Found: C, 59.04; H, 4.97; N, 11.02; S, 8.33.

5-(2-Ethoxycarbonylaminophenyl)-5-methylaminoimidazolidine-2,4-dione (6) (a) From **5a**: A 40% aqueous solution of methylamine (3.9 g, 50 mmol) was added to a solution of **5a** (15.4 g, 50 mmol) in methanol (100 ml), and the mixture was stirred at 45 °C for 6 h, then concentrated under reduced pressure. The residue was crystallized from diethyl ether, and recrystallized from ethanol to give **6** (9.8 g, 66%), mp 185—186 °C (dec.). IR (Nujol): 3340, 3230, 3140, 3080, 1785, 1735, 1700 cm^{-1}. ^{1}H-NMR (DMSO-d_6) δ: 1.23 (3H, t, J=7 Hz, $CH_2\underline{CH_3}$), 2.18 (3H, d, J=6 Hz, $NHC\underline{H_3}$), 3.81 (1H, q, J=6 Hz, $N\underline{H}CH_3$), 4.12 (2H, q, J=7 Hz, $\underline{CH_2}CH_3$), 6.9—7.5 (3H, m, ArH × 3), 8.0—8.2 (1H, m, ArH), 8.95 (1H, s, NH), 10.7 (2H, s, NH × 2). MS *m/z*: 261 ($M^+ - NH_2CH_3$). *Anal.* Calcd for $C_{13}H_{16}N_4O_4 \cdot 1/4H_2O$: C, 52.61; H, 5.60; N, 18.88. Found: C, 52.96; H, 5.52; N, 18.62.

(b) From **5d**: A 40% aqueous solution of methylamine (0.1 g, 1.3 mmol) was added to a solution of **5d** (0.32 g, 1 mmol) in THF (10 ml), and the mixture was stirred at 45 °C for 1 h. Work-up as described above gave **6** (0.27 g, 92%), mp 185—186 °C (dec.).

Spiro[imidazolidine-4,4′(1′*H*)-quinazoline]-2,2′5(3′*H*)-trione (7a) (a) From **4b**: A solution of **4b** (5.59 g, 20 mmol) and 10% ethanolic ammonia (13.6 g, 80 mmol) in toluene (150 ml)–ethanol (15 ml) was heated at 120 °C for 4 h in a sealed tube. After cooling, the precipitates were collected, washed with ethanol, and dissolved in water. This solution was acidified with 10% HCl to pH 2. The resulting crystals were collected, washed with water, and recrystallized from DMF–water to give **7a** (2.74 g, 59%), mp > 280 °C. IR (Nujol): 3270, 1790, 1730, 1670, 1610 cm^{-1}. ^{1}H-NMR (DMSO-d_6) δ: 6.84—7.31 (4H, m, ArH × 4), 7.97 (1H, s, NH), 8.95 (1H, s, NH), 9.67 (1H, s, NH), 10.92 (1H, br, NH). MS *m/z*: 232 (M^+). *Anal.* Calcd for $C_{10}H_8N_4O_3$: C, 51.72; H, 3.47; N, 24.13. Found: C, 51.39; H, 3.47; N, 23.84.

(b) From **5a**: A 28% solution of ammonium hydroxide (1.28 g, 21 mmol) was added to a suspension of **5a** (1.07 g, 3.5 mmol) in methanol (10 ml), and the mixture was heated at 45 °C for 15 h, then concentrated under reduced pressure. The residue was diluted with water and acidified with 10% HCl to pH 2. The resulting crystals were collected, washed with water, and recrystallized from DMF–water to give **7a** (0.75 g, 93%), mp > 280 °C.

(c) From **5d**: According to method (b) described above, **7a** was synthesized from **5d** (0.65 g, 2 mmol) in THF (5 ml). Yield 0.42 g (90%), mp > 280 °C (DMF–water).

3′-Methylspiro[imidazolidine-4,4′(1′*H*)-quinazoline]-2,2′5(3′*H*)-trione (7b) (a) From **4b**: According to method (a) described for **7a**, **7b** was synthesized from **4b** (2.51 g, 9 mmol) and 40% methanolic methylamine (2.71 g, 35 mmol). Yield, 0.91 g (41%), mp > 280 °C (from DMSO).

(b) From **4b**: A mixture of **4b** (1.40 g, 5 mmol) and 40% methanolic methylamine (0.85 g, 11 mmol) in toluene (33 ml)–ethanol (3.3 ml) was heated under reflux for 15 min. Then, 40% methanolic methylamine (1.55 g, 20 mmol) was added dropwise to the mixture under reflux over 1 h, and refluxing was continued for an additional 2.5 h. After cooling, the resulting precipitates were collected, and dissolved in water. This solution was acidified with 10% HCl to pH 2. The resulting crystals were collected, washed with water, and recrystallized from DMSO to give **7b** (0.46 g, 37%), mp > 280 °C.

(c) From **4c**: According to method (b) described for **7b**, **7b** was synthesized from **4c** (6.82 g, 20 mmol). Yield 0.85 g, (17%), mp > 280 °C (from DMSO).

(d) From **5a**: According to method (b) described for **7a**, **7b** was synthesized from **5a** (1.73 g, 5.6 mmol) and 40% aqueous methylamine

(2.0 g, 26 mmol). Yield 1.14 g (82%), mp > 280 °C (from DMSO).

(e) From **5d**: According to method (b) described for **7a**, **7b** was synthesized from **5d** (0.65 g, 2 mmol) in THF (5 ml). Yield 0.40 g (81%), mp > 280 °C (DMSO).

(f) From **6**: A mixture of **6** (2.92 g, 10 mmol) and NaOH (0.8 g, 20 mmol) in methanol (50 ml) was heated at 40 °C for 5 h, then concentrated under reduced pressure. The residue was dissolved in water and the solution was acidified with 10% HCl to pH 2. The resulting crystals were collected, washed with water, and recrystallized from DMSO to give **7b** (1.1 g, 45%), mp > 280 °C.

3'-Aminospiro[imidazolidine-4,4'(1'*H*)-quinazoline]-2,2',5(3'*H*)-trione (7c) A mixture of **4b** (2.79 g, 10 mmol) and hydrazine monohydrate (2.0 g, 40 mmol) in toluene (50 ml)–ethanol (50 ml) was heated under reflux for 4 h. After cooling, the precipitates were collected. The precipitates were diluted with water and acidified with 10% HCl to pH 2. The resulting crystals were collected, washed with water, and dried to give **7c** (1.44 g, 57%), mp > 280 °C. IR (Nujol): 3310, 3150, 1742, 1720, 1680, 1605 cm^{-1}. ^{1}H-NMR (DMSO-d_6) δ: 4.47 (2H, s, NH_2), 6.6—7.3 (4H, m, ArH × 4), 8.61 (1H, s, NH), 9.82 (1H, s, NH), 10.5—11.2 (11H, br, NH). *Anal.* Calcd for $C_{10}H_9N_5O_3 \cdot 1/4H_2O$: C, 47.71; H, 3.80; N, 27.82. Found: C, 47.52; H, 3.46; N, 27.90.

3'-Hydroxyspiro[imidazolidine-4,4'(1'*H*)-quinazoline]-2,2',5(3'*H*)-trione (7d) A mixture of hydroxylamine hydrochloride (5.56 g, 80 mmol) and potassium hydroxide (4.49 g, 80 mmol) in ethanol (50 ml) was stirred at 40 °C for 10 min. A suspension of **4b** (5.59 g, 20 mmol) in toluene (150 ml) was added to the mixture, and the whole was heated under reflux for 4 h. After cooling, the precipitates were collected. The precipitates were dissolved in water and acidified with 10% HCl to pH 2. The resulting crystals were collected, washed with water, and dried to give **7d** (0.77 g, 15%), mp 253 °C (dec.). IR (Nujol): 3220, 3080, 1782, 1735, 1680, 1605 cm^{-1}. ^{1}H-NMR (DMSO-d_6) δ: 6.6—7.3 (4H, m), 8.74 (1H, s), 9.63 (1H, s), 9.77 (1H, s), 10.83 (1H, br). *Anal.* Calcd for $C_{10}H_8N_4O_4 \cdot 1/2H_2O$: C, 46.69; H, 3.53; N, 21.78. Found: C, 46.58; H, 3.37; N, 21.92.

3'-Ethylspiro[imidazolidine-4,4'(1'*H*)-quinazoline]-2,2',5(3'*H*)-trione (7e) (a) From **5a**: According to method (b) described for **7a**, **7e** was synthesized from **5a** (1.54 g, 5 mmol) and 70% aqueous ethylamine (2.00 g, 31 mmol). Yield, 0.43 g (33%), mp > 280 °C (from DMF–water). IR (Nujol): 3450, 3120, 1790, 1720, 1665, 1610 cm^{-1}. ^{1}H-NMR (DMSO-d_6) δ: 1.14 (3H, t, J = 7 Hz, CH_2CH_3), 2.8—3.6 (2H, m, CH_2CH_3), 6.7—7.5 (4H, m, ArH × 4), 9.13 (1H, s, NH), 9.84 (1H, s, NH), 11.17 (1H, s, NH). MS *m/z*: 260 (M^+). *Anal.* Calcd for $C_{12}H_{12}N_4O_3$: C, 55.38; H, 4.65; N, 21.53. Found: C, 55.22; H, 4.38; N, 21.72.

(b) From **5d**: According to method (b) described for **7a**, **7e** was synthesized from **5d** (0.65 g, 2 mmol) and 70% aqueous ethylamine (0.77 g, 12 mmol) in THF (5 ml). Yield 0.23 g (44%), mp > 280 °C (DMF–water).

Acknowledgement We are grateful to Dr. I. Chibata, President, and Dr. S. Saito, Research and Development Executive, for their encouragement and interest. Thanks are due to Drs. T. Tosa, S. Oshiro, I. Inoue, T. Oine, K. Matsumoto, and E. Yamato for their valuable comments during this study. We are also indebted to Mrs. K. Saito and O. Kanada for their skillful technical assistance.

References and Notes

1) Part I: M. Yamagishi, K. Ozaki, H. Ohmizu, Y. Yamada, and M. Suzuki, *Chem. Pharm. Bull.*, **38**, 2926 (1990).
2) A part of this work was presented at the 39th Annual Meeting of the Kinki Branch of the Pharmaceutical Society of Japan, Osaka, October 1989.
3) P. F. Kador, J. H. Kinoshita, and N. E. Sharpless, *J. Med. Chem.*, **28**, 841 (1985).
4) K. H. Gabbay, *Ann. Rev. Med.*, **26**, 521 (1975).
5) N. Sakamoto and N. Hotta, *Farumashia*, **19**, 43 (1983).
6) T. Tanimoto, *Farumashia*, **24**, 459 (1988).
7) It was reported that the ring opening of 1-acetylisatin with a nucleophile takes place at the 2-position in contrast to the reaction of isatin or 1-alkylisatin with a nucleophile at the 3-position; F. D. Popp, "Advances in Heterocyclic Chemistry," Vol. 18, ed. by A. R. Katritzky and A. J. Boulton, Academic Press, New York, 1975, pp. 1—58, and references cited therein.
8) G. Tacconi, P. P. Righetti, and G. Desimoni, *J. Pract. Chem.*, **315**, 339 (1973).
9) J. C. Hubert, J. B. P. A. Wijnberg, and W. N. Speckamp, *Tetrahedron*, **31**, 1437 (1975).

Tannins and Related Compounds. CV.[1] Monomeric and Dimeric Hydrolyzable Tannins Having a Dehydrohexahydroxydiphenoyl Group, Supinanin, Euphorscopin, Euphorhelin and Jolkianin, from *Euphorbia* Species

Seung-Ho LEE, Takashi TANAKA, Gen-ichiro NONAKA* and Itsuo NISHIOKA

Faculty of Pharmaceutical Sciences, Kyushu University 62, 3-1-1 Maidashi, Higashi-ku, Fukuoka 812, Japan. *Received September 21, 1990*

A chemical investigation of tannins in three *Euphorbia* species (*E. helioscopia*, *E. jolkini* and *E. supina*) has led to the isolation and characterization of four new hydrolyzable tannins, named supinanin (15), euphorscopin (16), euphorhelin (17) and jolkianin (18), together with fourteen known compounds (1—14). On the basis of chemical and spectroscopic evidence, the structures of supinanin and euphorscopin were established as 1,3,6-tri-*O*-galloyl-2,4-(*S*)-dehydrohexahydroxydiphenoyl-β-D-glucose (15) and 1,3-(*S*)-dehydrohexahydroxydiphenoyl-2-*O*-galloyl-4,6-(*S*)-hexahydroxydiphenoyl-β-D-glucose (16), respectively. Euphorhelin and jolkianin were characterized as dimeric hydrolyzable tannins (17 and 18, respectively), in which two glucopyranose units are linked *via* valoneoyl and dehydrodigalloyl groups, respectively, and each molecule possesses a dehydrohexahydroxydiphenoyl group.

Keywords *Euphorbia*; hydrolyzable tannin; supinanin; euphorhelin; euphorscopin; jolkianin; dehydrohexahydroxydiphenic acid; hexahydroxydiphenic acid; dehydrodigallic acid; tannin

In one[2] of the previous papers, we reported that *Euphorbia helioscopia* L., unlike other *Euphorbia* species so far examined, contains large amounts of novel ellagitannins, helioscopins A and B, which possess the 4,4',5,5',6,6'-hexahydroxydiphenoyl (HHDP) group at the 1,6-positions of the glucopyranose core. Further chemical study on tannins of this plant has led to the isolation of two minor hydrolyzable tannins named euphorscopin (**16**) and euphorhelin (**17**), together with eleven hydrolyzable tannins. Moreover, an extension of our examination to two other *Euphorbia* species, *E. supina* RAFIN and *E. jolkini* BOISS, has resulted in the isolation of ten and seven hydrolyzable tannins, respectively, among which two [supinanin (**15**) and jolkianin (**18**)] were found to be new. This paper deals with the isolation and characterization of these compounds.

A combination of Sephadex LH-20, MCI-gel CHP 20P, Prep-pak 500/C_{18}, Fuji-gel ODS G3 and Bondapak C_{18}/Porasil B chromatographies of the aqueous acetone extract of the fresh whole plants of *E. helioscopia* afforded compounds **1**, **2**, **4**—**12**, **16** and **17**, while on similar treatment, the aqueous acetone extract of *E. jolkini* gave compounds **1**, **2**, **5**—**11** and **18**. Furthermore, the extraction of *E. supina* yielded compounds **3**, **8**, **9** and **12**—**15**. Compounds **1**—**14** were identified as 1-*O*- (**1**),[3] 1,6-di-*O*- (**2**),[4] 1,2,3-tri-*O*- (**3**),[5], 1,2,6-tri-*O*- (**4**),[6] 1,2,3,6-tetra-*O*- (**5**),[7] 1,3,4,6-tetra-*O*- (**6**)[8] and 1,2,3,4,6-penta-*O*-galloyl-β-D-glucoses (**7**),[9] corilagin (**8**),[10] geraniin (**9**),[10] helioscopinin A (**10**),[2] carpinusin (**11**),[2] terchebin (**12**)[11] and rugosins

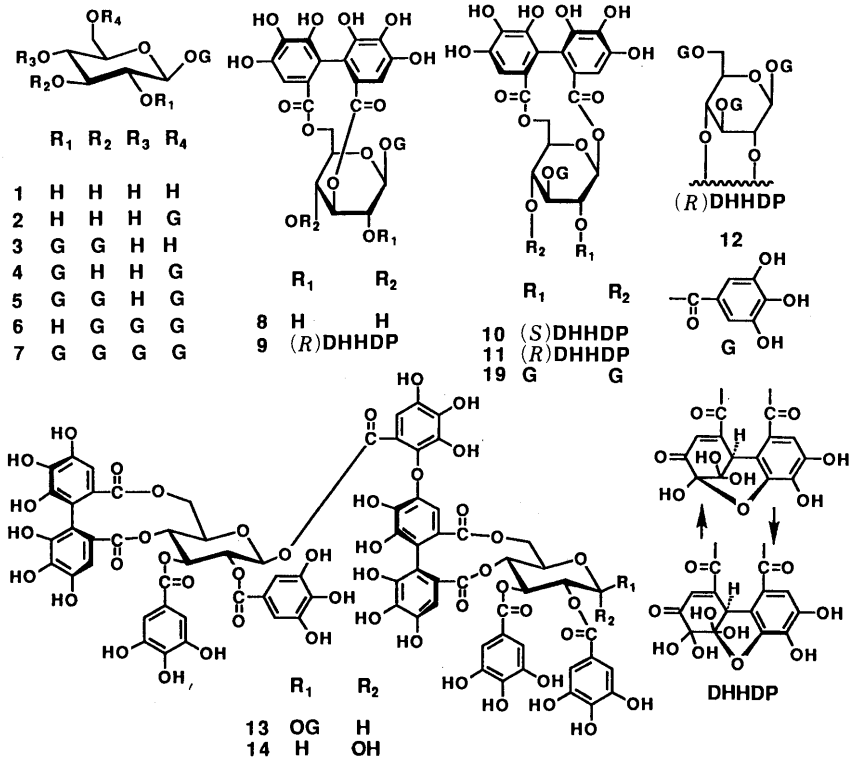

Chart 1

D (**13**)[12] and E (**14**),[12] by comparisons of their physical and spectral data with those of authentic samples.

Supinanin (**15**) was obtained as a pale yellow crystalline powder (H_2O). In the proton nuclear magnetic resonance (^{1}H-NMR) spectrum, the observation of signals at δ 7.11, 7.15 and 7.26 (each 2H, s) indicated the presence of three galloyl ester groups in the molecule, and a pair of benzylmethine signals [δ 5.03 (d, J=2 Hz) and 5.29 (s), 1H in total] and olefinic proton signals [δ 6.33 (d, J=2 Hz) and 6.63 (s), 1H in total] were characteristic of a dehydrohexahydroxydiphenoyl (DHHDP) ester group existing as an equilibrium mixture of five- and six-membered hemiketal forms.[10] The presence of the DHHDP ester group was also supported by carbon-13 nuclear magnetic resonance (^{13}C-NMR) spectral analysis.[2]

Upon treatment with *o*-phenylenediamine in an acidic solution, **15** yielded a phenazine derivative (**15a**). Subsequent methylation of **15a** with ethereal diazomethane, followed by alkaline hydrolysis and treatment with ethereal diazomethane, yielded methyl trimethoxybenzoate (**15b**) and a phenazine dimethyl ester (**15c**).[2] The negative sign of the optical rotation [$-29.0°$ ($CHCl_3$)] of **15c** established the chirality of the DHHDP group to be in the *S*-series.[2]

Partial hydrolysis of **15a** in hot water gave 1,3,6-tri-*O*-galloyl-β-D-glucose (**15d**), together with a phenazine bislactone (**15e**),[2] thus indicating that the DHHDP ester group is located at the glucose C-2 and C-4 hydroxyl groups. Furthermore, the orientation of the DHHDP ester group on the glucose moiety was determined chemically as follows. The treatment of **15** with triethylamine in acetonitrile[13] gave a product (**15f**), whose ^{1}H-NMR spectrum showed signals due to three galloyl groups [δ 7.04, 7.11, 7.15 (each 2H, s)] and a brevifolin carboxyl group[14] [δ 2.75 (1H, dd, J=7, 19 Hz), 4.50 (1H, br d, J=7 Hz), 7.17 (1H, s)]. The upfield shift of glucose H-4 [δ 4.05 (br d, J=8 Hz)], compared with that (δ 5.31) of the parent compound (**15**), indicated that the brevifolin carboxyl group is attached to the C-2 hydroxyl group of the glucose moiety, thus determining unequivocally the orientation of the DHHDP group.

On the basis of these findings, **15** was characterized as 1,3,6-tri-*O*-galloyl-2,4-(*S*)-DHHDP-β-D-glucose, in which the hydrated cyclohexenetrione ring in the DHHDP group is located at the glucose C-2 position.

Euphorscopin (**16**) was obtained as a pale yellow amorphous powder. The ^{1}H-NMR spectrum of **16** showed the presence of a galloyl ester group [δ 7.23 (2H, s)], an HHDP ester group [δ 6.47 and 6.80 (each 1H, s)] and a glucose moiety. The observation of a characteristic benzylmethine singlet [(δ 4.87 (1H)], an olefinic signal [δ 6.61 (1H, s)] and an aromatic one-proton singlet (δ 7.07) suggested the presence of a DHHDP ester group. Compound **16** gave a phenazine derivative (**16a**) on treatment with *o*-phenylenediamine in an acidic solution. Subsequent methylation of **16a** with ethereal diazomethane, followed by alkaline hydrolysis and ethereal diazomethane treatment, yielded methyl trimethyl gallate (**15b**), dimethyl hexamethoxydiphenoate[2] (**16b**) and the phenazine methylate (**15c**). The negative sign of the optical rotations of **16b** and **15c** established the chirality of the HHDP and DHHDP ester groups to be both in the *S*-series. These findings indicated that compound **16** contains a galloyl, an (*S*)-HHDP and an (*S*)-DHHDP ester group on the glucose core, which was supported by the observation of the intense $[M-H]^-$ ion

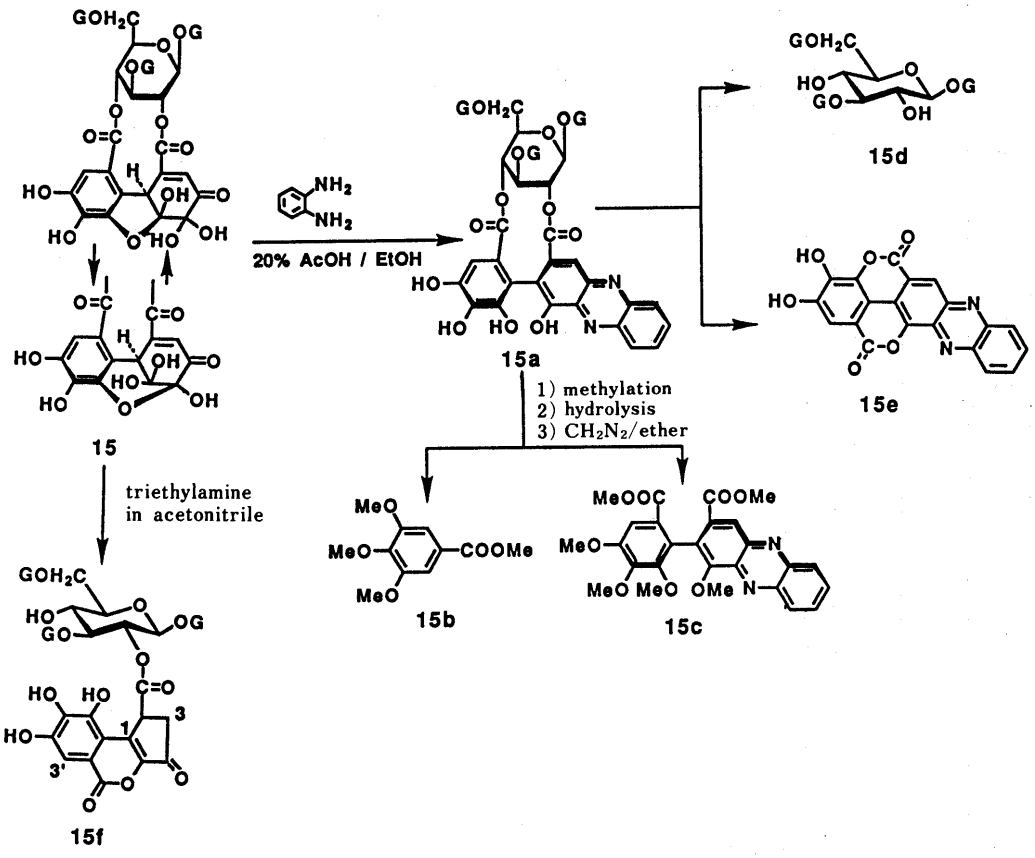

Chart 2

peak at m/z 951 in the negative fast atom bombardment mass spectrum (FAB-MS) of **16**.

The orientation and the location of each acyl group in the glucose moiety were determined as follows. The ^{1}H–^{13}C long-range shift correlation (COSY) spectrum (Fig. 1) of **16** clearly showed the correlation between the DHHDP aromatic one-proton singlet (δ 7.07) and a carboxyl carbon signal (δ 164.9) through a three-bond coupling, and this carboxyl carbon signal was also found to be correlated with the glucose C-1 proton signal (δ 6.54). Similarly, the glucose

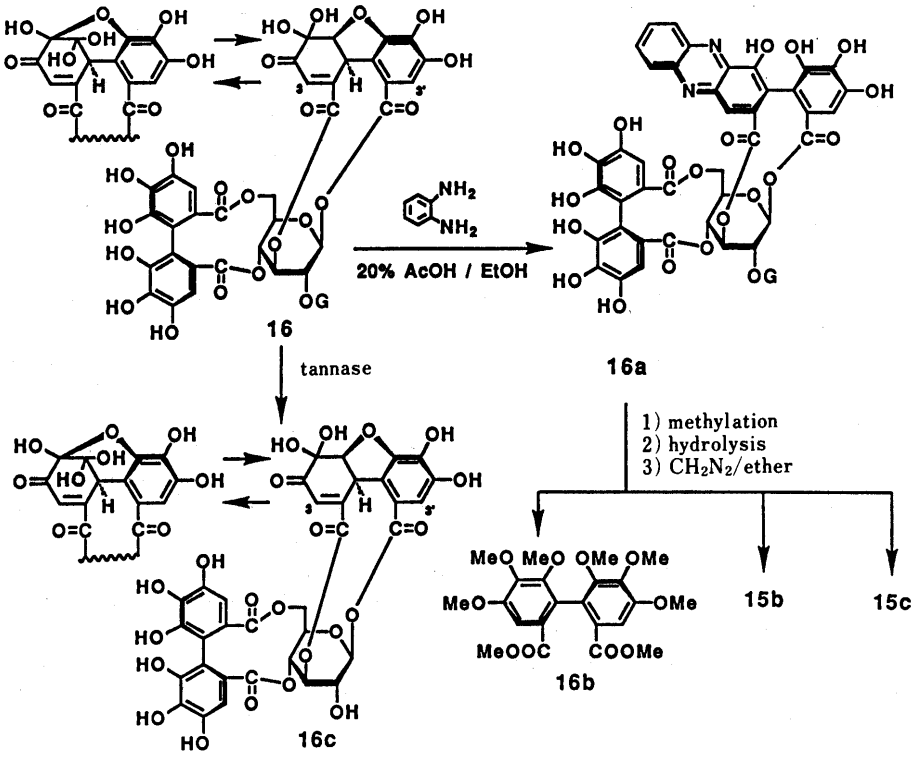

Chart 3

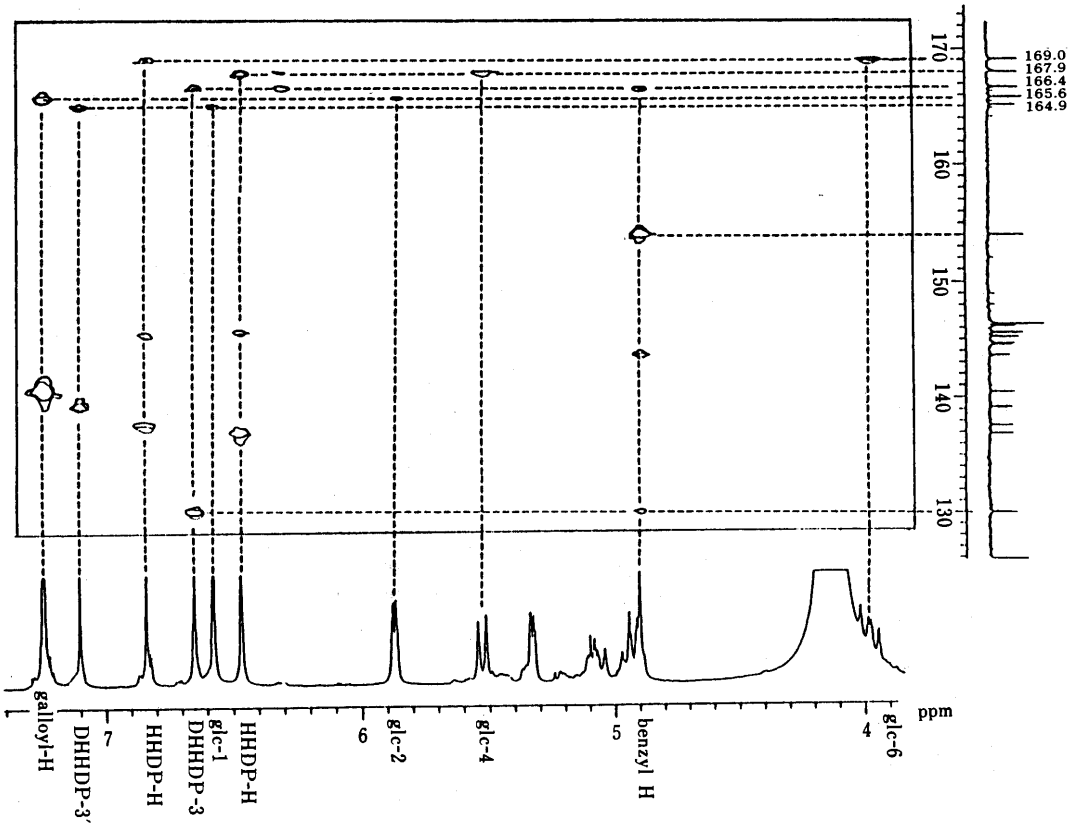

Fig. 1. The ^{1}H–^{13}C Long-Range COSY Spectrum of **16**

In acetone-d_6 + D_2O (J_{CH} = 10 Hz).

C-4 proton signal (δ 5.50) was shown to be correlated with the carboxyl carbon signal (δ 167.9), which also gave a cross peak with one (δ 6.47) of the HHDP proton signals. Furthermore, the glucose C-6 proton signal (δ 3.92) correlated with the carboxyl carbon signal (δ 169.0) also gave a cross peak with the HHDP proton signal (δ 6.83). These findings indicated that the HHDP ester group is located at the C-4 and C-6 positions of the glucose core, and the aromatic carboxyl of the DHHDP group is at the glucose C-1 position. Furthermore, treatment of **16** with tannase gave brevilagin II (**16c**)[14] and gallic acid, thus confirming that the galloyl ester group is located at the glucose C-2 position and the DHHDP ester group at the glucose C-1 and C-3 positions.

Examination of the Dreiding model showed that bridging of the (*S*)-DHHDP group over the glucopyranose C-1 and C-3 positions is possible only in the case of the β-configuration at the anomeric center. Thus, euphorscopin was characterized as 1,3-(*S*)-DHHDP-2-*O*-galloyl-4,6-(*S*)-HHDP-β-D-glucose (**16**).

Euphorhelin (**17**) was obtained as a pale yellow amorphous powder. In the ^{1}H-NMR spectrum of **17**, the observation of a pair of benzylmethine proton signals [δ 4.93 (d, J=1.5 Hz) and 5.81 (s), 1H in total] and olefinic proton signals [δ 6.20 (d, J=1.5 Hz) and 6.52 (s), 1H in total] showed the presence of an equilibrated DHHDP ester group in the molecule. The ^{1}H-NMR spectrum of the phenazine derivative (**17a**), obtained by treatment of **17** with *o*-phenylenediamine, indicated the presence of three galloyl groups [(δ 6.97, 7.12 and 7.13 (each 2H, s)] one valoneoyl group [(δ 6.22, 7.03 and 7.18 (each 1H, s) and one phenazine ester group [δ 7.50 (1H, s), 7.97—8.07, 8.27—8.35 (each 2H, m) and 8.33 (1H, s)]. In addition, two anomeric proton signals were observed at δ 5.83 (d, J= 8 Hz) and 6.12 (d, J=6 Hz), indicating the presence of two sugar moieties in the molecule.

Methylation of **17a** with ethereal diazomethane, followed by alkaline hydrolysis and diazomethane treatment, yielded the products (**17b** and **17c**), together with **15b**. The positive signs of the optical rotations of **17b** and **17c** established the chirality of the DHHDP and valoneoyl ester groups to be all in the *R*-series. The ^{13}C-NMR spectrum of **17a** showed twelve sugar carbon resonances, of which six (δ 63.9, 71.0, 73.8, 74.6, 75.4 and 93.7) were closely correlated with those found in 1,2,6-tri-*O*-galloyl-β-D-glucose (**4**), whereas the

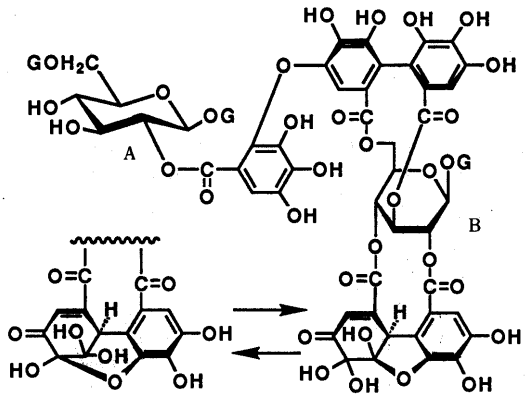

17

Chart 4

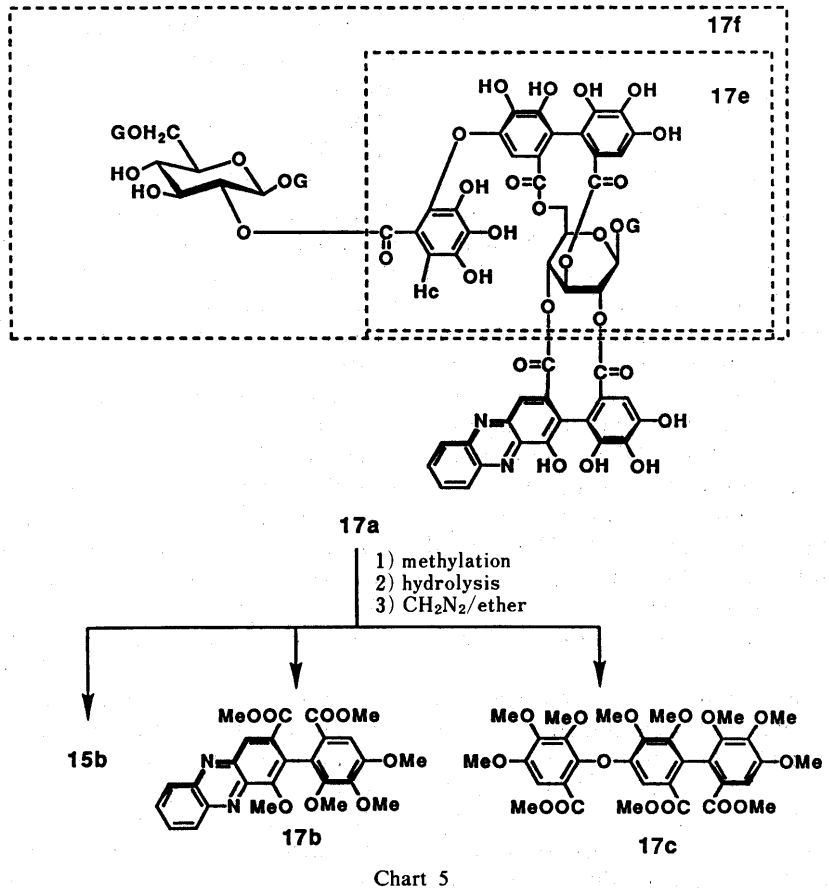

Chart 5

TABLE I. ^{1}H-NMR Data for Sugar Moieties in Compounds **4**, **9a**, **17a**, **19**, **10a** and **18a**

	4[a]	**9a**[a]	**17a**[b]	**19**[a]	**10a**[a]	**18a**[b]
Glucose						
A-1	5.98 (d, J=8)		5.83 (d, J=8)		6.25 (br s)	6.23 (br s)
A-2	5.28 (t, J=8)		5.20 (t, J=9)		5.26 (br s)	5.49 (br s)
A-3	3.97 (t, J=8)		—[c]		5.76 (br s)	5.71 (br s)
A-4	3.76 (t, J=8)		—[c]		5.08 (br s)	4.97 (br s)
A-5	4.10 (m)		3.93 (m)		4.45 (m)	4.03 (dd, J=5, 11)
A-6	4.67 (br d, J=12)		4.75 (dd, J=5, 12)		5.15 (t, J=11)	5.33 (t, J=11)
	4.47 (dd, J=4, 12)		4.46 (dd, J=4, 12)		4.20 (dd, J=5, 11)	4.44 (dd, J=5, 11)
Glucose						
B-1		6.16 (d, J=6)	6.12 (d, J=6)	6.12 (d, J=3)		6.15 (d, J=3)
B-2		5.69 (d, J=6)	5.70 (d, J=6)	5.52 (dd, J=3, 7)		5.53 (dd, J=3, 7)
B-3		5.50 (m)	5.55 (d, J=4)	5.79 (t, J=7)		5.86 (t, J=7)
B-4		5.50 (m)	5.42 (d, J=4)	5.20 (dd, J=2, 7)		5.25 (dd, J=3, 7)
B-5		4.69—5.09 (m)	4.95 (dd, J=4, 8)	4.58 (m)		4.56 (m)
B-6		4.69—5.09 (m)	4.78 (dd, J=8, 12)	4.85 (t, J=11)		4.76 (t, J=11)
			4.56 (dd, J=4, 12)	4.43 (dd, J=4, 11)		4.54 (dd, J=4, 11)

In Me_2CO-d_6 + D_2O, values, J values in Hz. *a*) Measured at 100 MHz. *b*) Measured at 270 MHz. *c*) Overlapped with HOD signals.

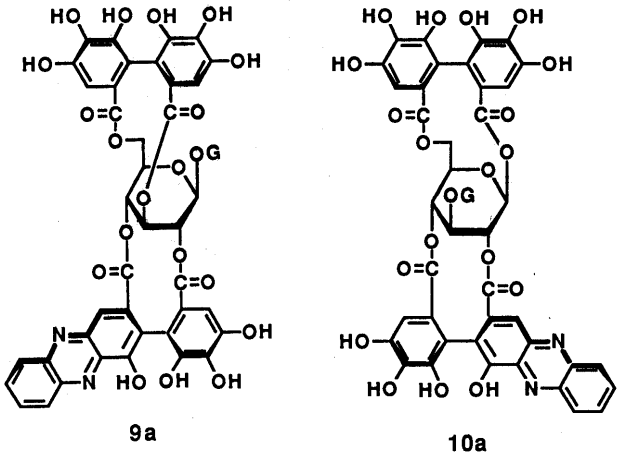

9a **10a**

Chart 6

chemical shifts of the remaining six signals [δ 65.8, 67.7, 68.6, 76.2 (×2) and 91.8] were almost identical with those of the phenazine derivative of geraniin (**9a**).[4] Similarly, the sugar signal pattern in the ^{1}H-NMR spectrum of **17a** closely resembles those of **9a** plus **4** (Table I).

From these findings, **17** was considered to be a dimeric ellagitannin composed of 1,2,6-tri-*O*-galloyl-β-D-glucose (**4**) and geraniin (**9**) units which are linked through the valoneoyl group. This was consistent with the negative FAB-MS data of **17**. The orientation of the 3,6-positioned valoneoyl group in **17** was determined by generation of isomallotinic acid (**17e**),[5] together with **15e** and **17f**, on partial hydrolysis of **17a**. The structure of **17f** followed from the negative FAB-MS [m/z 1267 $(M-H)^-$] and the observation of the significant high-field shift of the aromatic singlet (δ 6.22) due to the Hc proton[5] in the ^{1}H-NMR spectrum of **17f**.

Based on the above chemical and spectroscopic evidence, the structure of euphorhelin was determined to be as represented by the formula **17**. The ^{1}H-NMR spectrum of jolkianin (**18**) showed the presence of a DHHDP group [δ 4.93 (d, J=2 Hz) and 5.17 (s), 1H in total, δ 6.13 (d, J=2 Hz) 6.58 (s), 1H in total]. Treatment of **18** with *o*-phenylenediamine yielded the phenazine derivative (**18a**), whose ^{1}H-NMR spectrum exhibited two one-proton signals at δ 6.15 (d, J=3 Hz) and 6.23 (br s) attributable to the anomeric protons, suggesting the presence of two sugar moieties in **18**. The dimeric structure of **18** was also supported by the observation of twelve aliphatic resonances in the ^{13}C-NMR spectrum and of the prominent $(M-H)^-$ ion peak at m/z 1941 in the FAB-MS of **18a**. The ^{1}H-NMR spectrum of **18a** showed, in the aromatic region, two galloyl singlets at δ 7.11 and 7.12, five one-proton singlets at δ 6.68, 6.83, 6.84, 7.04 and 7.17 and two *meta*-coupled doublets at δ 6.35 and 7.12 (each J=2 Hz), together with signals arising from the phenazine moiety.

Methylation of **18a** with ethereal diazomethane, followed by alkaline hydrolysis and diazomethane treatment, yielded **15b**, **16b**, **15c** and dimethyl penta-*O*-methyldehydrodigallate (**18b**)[15] in the molar ratio of 2:2:1:1. Comparison of the ^{1}H-NMR spectrum of **18a** with those of 1,6-(*S*)-HHDP-2,3,4-tri-*O*-galloyl-β-D-glucose (**19**)[4] and the phenazine derivative of helioscopinin A (**10a**)[2] revealed a close structual relationship among these compounds. That is, in the ^{1}H-NMR spectrum of **18a**, the chemical shifts and coupling patterns of signals arising from the two glucose moieties were closely correlated with those of **19** plus **10a** (Table I).

These findings suggested that **18** is a dimeric ellagitannin consisting of moieties of 1,6-(*S*)-DHHDP-2,3,4-tri-*O*-galloyl-β-D-glucose (**19**)[4] and helioscopinin A (**10**), which are linked *via* the dehydrodigalloyl (DHDG) ester group.

To confirm the locations of each acyl group in the glucose moieties, partial hydrolysis of **18a** was attempted. Brief treatment of **18a** in hot water gave the hydrolysates (**18c** and **18d**), together with **15e**. Compound **18c** was characterized as a product formed by hydrolysis of the phenazine ester on the ground that the ^{1}H-NMR spectra of **18a** and **18c** showed a close similarity in the aromatic and sugar regions, except for the lack of signals due to the phenazine moiety and the upfield shifts of the glucose C-2 and C-4 proton signals. The ^{1}H-NMR spectrum of **18d** indicated the presence of two galloyl groups [δ 7.08 and 7.09 (each 2H, s)] and one DHHDP group [δ 6.75 and 7.19 (each 1H, d, J=2 Hz), 7.17 (1H, s)]. Although signals due

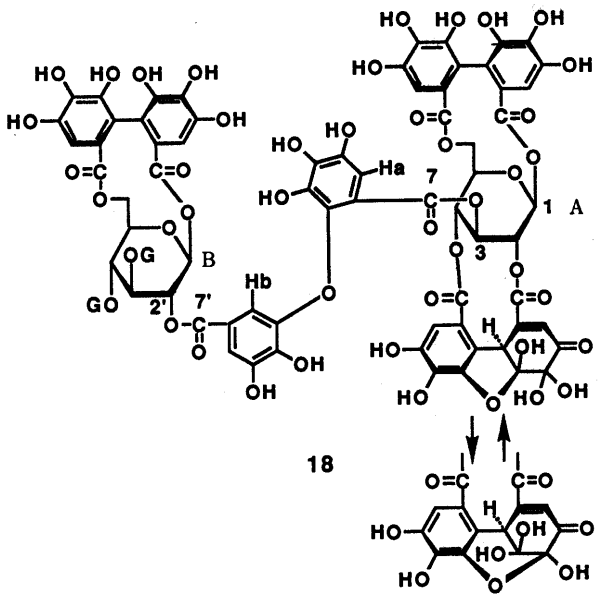

Chart 7

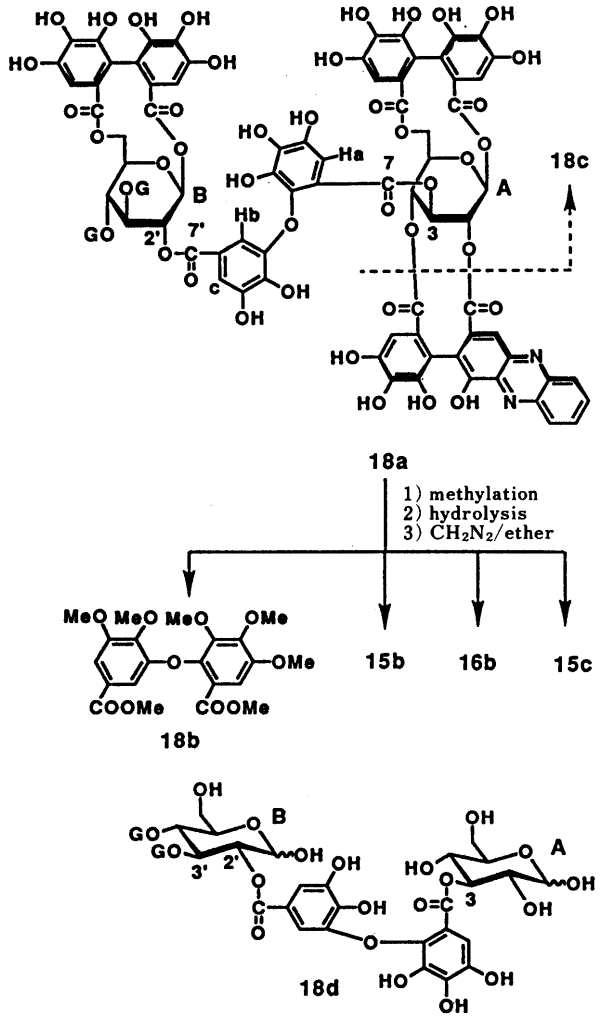

Chart 8

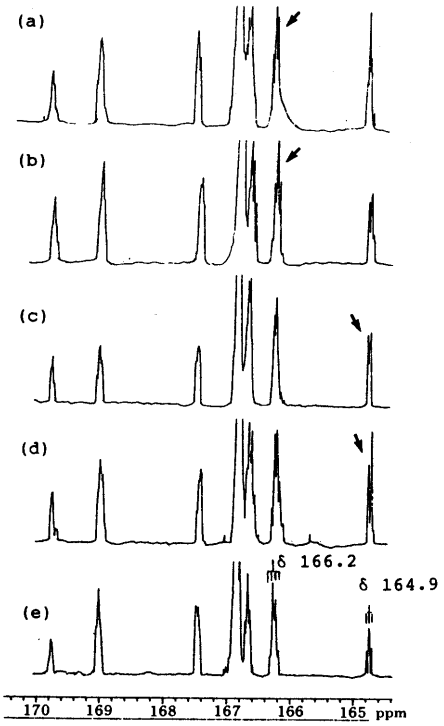

Fig. 2. LSPD Experiments in **18c**

(a) Irradiation at δ 7.28 (H_b), (b) irradiation at δ 5.50 (glc. H-2'), (c) irradiation at δ 7.16 (H_a), (d) irradiation at δ 5.13 (glc. H-3), (e) non-decoupling.

to the sugar moiety were found to be complicated owing to the anomerization at the C-1 position, the lowfield signals at δ 5.01 (dd, J=4, 10 Hz), 5.02 (t, J=10 Hz), 5.38 (t, J=10 Hz) and 6.00 (t, J=10 Hz) were assignable to the C-3, C-2', C-3' and C-4' protons from ^{1}H–^{1}H COSY spectral analysis, indicating that these positions were acylated.

These findings indicated that the DHHDP ester group is located at the C-2 and C-4 positions of the glucose A moiety and that the HHDP ester groups are at the C-1 and C-6 positions of the two glucose moieties. To confirm the location of the DHDG group, a long-range selective proton-decoupling (LSPD)[15] experiment on **18c** was performed. The ^{13}C-NMR spectrum of **18c** showed eight ester carbon signals. In the non-decoupling mode, the signal at δ 164.9 (C-7) was observed as a triplet, and this signal was changed into a doublet upon irradiation at δ 5.13 (glc. H-3) and δ 7.16 (DHDG-H_a). Accordingly, the C-7 ester group could be concluded to be located at the C-3 position of the glucose A moiety. On the other hand, the signal at δ 166.1 (C-7') was changed from a quartet into a sharp triplet on irradiation at δ 5.50 (glc. H-2') and δ 7.28 (DHDG-H_b). Accordingly, the location of the C-7' ester was shown to be at the C-2 position of the glucose B moiety.

Based on these findings, the structure of jolkianin was established to be as shown by the formula **18**.

Jolkianin (**18**) represents the first example of a dimeric hydrolyzable tannin possessing the HHDP group at the glucose 1,6-positions. The co-occurrence of hydrolyzable tannins having *R*- and *S*-DHHDP groups in these *Euphorbia* species is of great interest from the viewpoint of plant physiology.

Experimental

Melting points were determined on a Yanagimoto micro-melting point apparatus and are uncorrected. Optical rotations were measured with a JASCO DIP-4 digital polarimeter. ^{1}H- and ^{13}C-NMR spectra were recorded on JEOL FX-100 and JEOL GX-270 spectrometers, with

tetramethylsilane as an internal standard, and chemical shifts are given in δ (ppm). FAB-MS were taken with a JEOL JMS DX-300 instrument. Column chromatography was carried out with Sephadex LH-20 (25—100 μ, Pharmacia Fine Chemical Industry Co., Ltd.), MCI-gel CHP 20P (75—150 μ, Mitsubishi Chemical Industry Co., Ltd.), Fuji-gel ODS G3 (43—65 μ, Fuji-gel Hanbai Co., Ltd.), Prep-pak 500/C_{18} (37—75 μ, Waters Associates Inc.) and Bondapak C_{18}/Porasil B (37—75 μ, Waters Associates Inc.). Thin layer chromatgraphy (TLC) was conducted on precoated Silica gel 60 F_{254} plates (Merck) and precoated cellulose F_{254} plates. Spots were visualized under UV illumination and by spraying 1% $FeCl_3$ (EtOH) and 5% sulfuric acid.

Isolation of Tannins a) From *Euphorbia helioscopia*: The fresh whole plants (48.5 kg) of *E. helioscopia*, collected in Fukuoka city in April 1988, were extracted with 80% aqueous acetone at room temperature. The acetone was removed and the insolubles were filtered off. The filtrate was concentrated and applied to a column of Sephadex LH-20. Elution with H_2O containing increasing proportions of MeOH afforded five fractions; I (80 g), II (335 g), III (65 g), IV (20 g) and V (23 g). Fraction I was rechromatographed over MCI-gel CHP 20P, Sephadex LH-20 and Fuji-gel ODS G3 (H_2O–MeOH) to give 1-*O*-galloyl-β-D-glucose (**1**) (22 g) and 1,6-di-*O*-galloyl-β-D-glucose (**2**) (380 mg). Fraction II was repeatedly chromatographed over MCI-gel CHP 20P, Fuji-gel ODS G3, Bondapak C_{18}/Porasil B (H_2O–MeOH) and Sephadex LH-20 (EtOH) to give helioscopinin A (**10**) (8.4 g), carpinusin (**11**) (18 g), corilagin (**8**) (660 mg), euphorscopin (**16**) (3.4 g) and geraniin (**9**) (69 g). On similar chromatographies, fraction III gave 1,2,6-tri-*O*-galloyl-β-D-glucose (**4**) (48 mg) and euphorhelin (**17**) (340 mg), while fraction IV yielded 1,2,3,6-tetra-*O*-galloyl-β-D-glucose (**5**) (38 mg) and 1,3,4,6-tetra-*O*-galloyl-β-D-glucose (**6**) (2 g). 1,2,3,4,6-Penta-*O*-galloyl-β-D-glucose (**7**) (51 mg) and terchebin (**12**) (3 g) were obtained from fraction V by similar chromatographic separation.

b) From *E. jolkini*: The fresh whole plants (50 kg) of *E. jolkini*, collected in Yobuko, Saga prefecture in April 1989, were extracted with 80% aqueous acetone and the extract was treated in a manner similar to that described for *E. helioscopia* to afford three fractions; I (30 g), II (200 g) and III (60 g). Fraction I was rechromatographed over MCI-gel CHP 20P, Fuji-gel ODS G3, Prep-pak 500/C_{18} (H_2O–MeOH) and Sephadex LH-20 (EtOH) to give 1-*O*- (**1**) (410 mg) and 1,6-di-*O*-galloyl-β-D-glucoses (**2**) (55 mg). Fraction II was repeatedly chromatographed over MCI-gel CHP 20P, Bondapak C_{18}/Porasil B (H_2O–MeOH) and Sephadex LH-20 (60%, MeOH, EtOH) to give corilagin (**8**) (900 mg), geraniin (**9**) (9.5 g), helioscopinin A (**10**) (3.2 g), carpinusin (**11**) (1.3 g) and jolkianin (**18**) (340 mg). Similar chromatographies of fraction III gave 1,2,3,6-tetra-*O*- (**5**) (200 mg), 1,3,4,6-tetra-*O*- (**6**) (170 mg) and 1,2,3,4,6-penta-*O*-galloyl-β-D-glucoses (**7**) (94 mg).

c) From *E. supina*: The fresh whole plants (20 kg) of *E. supina*, collected in Fukuoka city in October 1989, were extracted with 80% aqueous acetone and the extract was treated in manner similar to that described for *E. helioscopia* to afford three fractions; I (120 g), II (14 g) and III (8 g). Fraction I was rechromatographed over MCI-gel CHP 20P, Fuji-gel ODS G3 (H_2O–MeOH) and Sephadex LH-20 (60% MeOH) to give corilagin (**8**) (18 g), supinanin (**15**) (400 mg) and geraniin (**9**) (20.4 g). On similar chromatographies, fraction II afforded 1,2,3-tri-*O*-galloyl-β-D-glucose (**3**) (293 mg). Terchebin (**12**) (120 mg) and rugosins D (**13**) (98 mg) and E (**14**) (340 mg) were obtained from fraction III by similar chromatographic separation.

Supinanin (15) A yellow crystalline powder (H_2O), mp 212—213 °C, $[\alpha]_D^{22}$ +38.2° (c=0.7, acetone). *Anal.* Calcd for $C_{41}H_{30}O_{27}\cdot 3/2H_2O$: C, 50.26; H, 3.08. Found: C, 49.94; H, 3.56. Negative FAB-MS m/z: 953 $[M-H]^-$. ^{1}H-NMR (acetone-d_6+D_2O, 100 MHz) ppm: 5.03 (d, J=2 Hz, DHHDP-1), 5.29 (s, DHHDP-1), 6.33 (d, J=2 Hz, DHHDP-3), 6.53 (1H, br s, glc-1), 6.57 (s, DHHDP-3), 7.12, 7.15 (each 2H, s, galloyl-H), 7.28 (1H, s, DHHDP-3'). ^{13}C-NMR (acetone-d_6+D_2O) ppm: 45.9, 51.7 (DHHDP-1), 62.3, 63.2, 65.1, 68.4, 69.3, 72.5, 73.1, 92.7 (glc-C), 92.1, 108.8 (DHHDP-6), 92.3, 96.2 (DHHDP-5), 110.0, 110.2 (galloyl-2, 6), 119.4, 119.5, 120.5 (galloyl-1), 125.8, 129.3 (DHHDP-3), 139.4, 140.1 (galloyl-4), 145.7, 145.9, 146.0 (galloyl-3,5), 148.6, 153.7 (DHHDP-2), 165.2, 165.5, 165.7, 167.3 (–COO–), 192.1, 194.9 (DHHDP-4).

Preparation of the Phenazine (15a) A mixture of **15** (100 mg), *o*-phenylenediamine (18 mg) and acetic acid (1.3 ml) in EtOH (5 ml) was left standing at room temperature for 15 h. The reaction mixture was diluted with water (2 ml), and evaporation of EtOH gave a yellow precipitate (**15a**) (64 mg). **15a**: A yellow powder (H_2O), mp > 300 °C, $[\alpha]_D^{24}$ −28.6° (c=0.7, acetone), *Anal.* Calcd for $C_{47}H_{32}N_2O_{24}\cdot H_2O$: C, 54.98; H, 3.14; N, 2.73. Found: C, 54.80; H, 3.42; N, 2.58. Positive FAB-MS m/z: 1009 $[M+H]^+$. ^{1}H-NMR (acetone-d_6+D_2O, 100 MHz) ppm: 4.34 (3H in total, m, glc-5, 6), 5.35 (1H, br d, J=4 Hz, glc-2), 5.42 (1H, br d, J=6 Hz, glc-4), 5.80 (1H, d, J=4 Hz, glc-3), 6.65 (1H, br s, glc-1), 6.90, 7.03, 7.28 (each 2H, s, galloyl H), 7.45 [1H, s, phenazine (phe)-3'], 7.93—8.07, 8.22—8.33 (each 2H, m, phe-2'', 3'', 4'', 5''), 8.33 (1H, s, phe-3). ^{13}C-NMR (acetone-d_6+D_2O) ppm: 65.1, 66.3, 71.4, 71.7, 73.1, 94.8 (glc-C), 109.9, 110.5, 110.8 (galloyl-2, 6), 112.7 (phe-3'), 116.1, 117.1 (phe-1, 1'), 119.8, 120.0, 120.7, 121.0 (galloyl-1, phe-3), 130.1, 132.3 (phe-2'', 3''), 136.0 (phe-2), 138.7, 138.9, 139.1, 139.6, 139.9 (galloyl-4, phe-5, 5'), 142.7, 142.9 (phe-1'', 6''), 145.9 (galloyl-3, 5), 152.2 (phe-6), 165.2, 165.6, 167.2, 168.1 (–COO–).

Methylation of 15a, Followed by Alkaline Hydrolysis A solution of **15a** (50 mg) in MeOH (2 ml) was methylated with ethereal diazomethane for 20 h at 0 °C. After removal of the solvent by evaporation, the residue was heated with 5% NaOH (2 ml) at 90 °C for 30 min. The solution was acidified with 1 N HCl and extracted with ether. The ether layer was washed with water, dried over Na_2SO_4 and concentrated to dryness. The residue was treated with ethereal diazomethane for 1 h. After evaporation of the solvent and the excess reagent, the residue was chromatographed over silica gel. Elution with benzene–acetone (25 : 1, v/v) yielded **15b** (5 mg) as a white powder (MeOH), mp 81 °C. Subsequent elution with benzene–acetone (25 : 2) afforded **15c** as a yellow amorphous powder (11 mg), $[\alpha]_D^{23}$ −29.0° (c=1.1, $CHCl_3$).

Partial Hydrolysis of 15a A solution of **15a** (50 mg) in H_2O–MeOH (1 : 1) (3 ml) was heated on a water bath for 3 h. The resulting red precipitate (**15e**) (7 mg) was collected by filtration. The filtrate was directly subjected to Sephadex LH-20 chromatography, and elution with 60% MeOH afforded **15d** (23 mg).

Treatment of 15 with Triethylamine A solution of **15** (70 mg) in acetonitrile (2 ml) was heated with triethylamine (0.2 ml) under reflux for 10 min. The solution was acidified with 2 N HCl. After concentration to *ca.* 2 ml, the solution was subjected to Sephadex LH-20 chromatography. Elution with 80% MeOH gave **15f** (8 mg). **15f**: A pale yellow amorphous powder, $[\alpha]_D^{23}$ −7.4° (c=0.8, acetone). *Anal.* Calcd for $C_{40}H_{30}O_{25}$: C, 52.74; H, 3.30. Found: C, 52.72; H, 3.39. Negative FAB-MS m/z: 909 $[M-H]^-$. ^{1}H-NMR (acetone-d_6+D_2O) ppm: 2.75 [(1H, dd, J=7, 19 Hz, brevifolin carboxyl (bre)-3)], 4.05 (1H, br d, J=8 Hz, glc-4), 4.50 (1H, br d, J=7 Hz, bre-2), 5.24 (1H, t, J=8 Hz, glc-2), 5.56 (1H, t, J=8 Hz, glc-3), 6.10 (1H, d, J=8 Hz, glc-1), 7.04, 7.11, 7.15 (each 2H, s, galloyl-H), 7.17 (1H, s, bre-3').

Euphorscopin (16) A pale yellow amorphous powder, $[\alpha]_D^{22}$ +128.3° (c=0.5, acetone). *Anal.* Calcd for $C_{41}H_{28}O_{27}\cdot 5H_2O$: C, 47.20; H, 3.64. Found: C, 47.34; H, 3.67. Negative FAB-MS m/z: 951 $[M-H]^-$. ^{1}H-NMR (acetone-d_6+D_2O, 270 MHz) ppm: 3.92 (1H, dd, J=8, 11 Hz, glc-6), 4.87 (1H, s, DHHDP-1), 4.90 (1H, t, J=8 Hz, glc-5), 5.06 (1H, dd, J=8, 11 Hz, glc-6), 5.30 (1H, dd, J=1, 4 Hz, glc-3), 5.50 (1H, d, J=8 Hz, glc-4), 5.84 (1H, dd, J=1, 4 Hz, glc-2), 6.54 (1H, d, J=1 Hz, glc-1), 6.47, 6.83 (each 1H, HHDP-H), 6.61 (1H, s, DHHDP-3), 7.07 (1H, s, DHHDP-3'), 7.23 (2H, s, galloyl-H). ^{13}C-NMR (acetone-d_6+D_2O) ppm: 45.9, 51.8 (DHHDP-1), 64.6, 65.5, 69.1 (×2), 71.3 (glc 2—6), 92.4, 96.2, 109.9 (DHHDP-5, 6), 93.3 (glc-1), 108.4, 109.0 (DHHDP-3, 3'), 110.6 (galloyl-2, 6), 112.7 (DHHDP-3'), 115.2 (DHHDP-1'), 115.8 (HHDP-1), 116.7 (HHDP-1'), 119.8 (DHHDP-2'), 120.1 (galloyl-1), 124.4, 125.4 (HHDP-2, 2'), 125.6, 129.7 (DHHDP-3), 136.5, 138.8 (HHDP-5, DHHDP-5'), 140.2 (galloyl-3, 5), 143.2, 144.7 (DHHDP-6'), 144.4 (DHHDP-4'), 144.9 (HHDP-4'), 145.3, 145.7 (HHDP-4, 6, 6'), 146.0 (galloyl-4), 148.5, 153.6 (DHHDP-2), 164.0, 165.0, 165.3, 165.6, 166.4, 167.9, 169.0 (–COO–), 192.1, 195.0 (DHHDP-4).

Preparation of the Phenazine (16a) A mixture of **16** (30 mg), *o*-phenylenediamine (56 mg) and acetic acid (4 ml) in EtOH (16 ml) was left standing at room temperature for 25 min. The reaction mixture was diluted with water (6 ml) and evaporation of EtOH gave a precipitate (**16a**) (120 mg). **16a**: A yellow powder (H_2O), mp > 300 °C, $[\alpha]_D^{23}$ +91.8° (c=1.0, acetone), *Anal.* Calcd for $C_{47}H_{30}N_2O_{24}\cdot 5/2H_2O$: C, 53.66; H, 3.33; N, 2.66. Found: C, 53.86; H, 3.23; N, 2.60. Positive FAB-MS m/z: 1007 $[M+H]^+$. ^{1}H-NMR (acetone-d_6+D_2O, 270 MHz) ppm: 3.87 (1H, dd, J=4, 13 Hz, glc-6), 4.80 (1H, dd, J=7, 10 Hz, glc-5), 5.13 (1H, dd, J=7, 13 Hz, glc-6), 5.32 (1H, dd, J=1, 4 Hz, glc-3), 5.41 (1H, br s, glc-2), 5.68 (1H, dd, J=4, 10 Hz, glc-4), 6.33 (1H, br s, glc-1), 6.63, 6.67 (each s, 1H, HHDP-H), 7.10 (1H, s, phe-3'), 7.17 (2H, s, galloyl-H), 7.92 (1H, s, phe-3), 7.94—8.03, 8.17—8.39 (each 2H, m, phe-2'', 3'', 4'', 5'').

Methylation of 16a, Followed by Alkaline Hydrolysis **16a** (50 mg) was methylated with ethereal diazomethane at 0 °C for 7 h. The tridecamethylate thus obtained was hydrolyzed with 5% NaOH (4 ml) at 90 °C for 1 h. Work-up as above gave a mixture of hydrolysates, which was treated with ethereal diazomethane. The methylates were separated as before to give **15b** (5 mg) and dimethyl-(*S*)-hexamethoxydiphenoate (**16b**) (11 mg) as a

yellow powder, $[\alpha]_D^{23}$ −27.6° (c=1.1, $CHCl_3$) and **15c** (11 mg).

Enzymatic Hydrolysis of 16 A solution of **16** (60 mg) in H_2O (3 ml) was incubated with tannase at room temperature for 40 min. The reaction mixture was subjected to MCI-gel CHP 20P chromatography with an H_2O–MeOH system to yield gallic acid and a hydrolysate (**16c**) (28 mg), which was identified as brevilagin II by comparison of the ^{1}H- and ^{13}C-NMR spectral data with reported values. **16c**: A pale yellow amorphous powder, $[\alpha]_D^{23}$ +71.3° (c=1.0, acetone). *Anal.* Calcd for $C_{34}H_{24}O_{23}\cdot 1/2H_2O$: C, 50.43; H, 3.09. Found: C, 50.40; H, 3.11. Negative FAB-MS m/z: 799 $[M-H]^-$. ^{1}H-NMR (acetone-d_6+D_2O, 270 MHz) ppm: 4.55 (1H, dd, J=1, 3 Hz, glc-2), 4.90 (1H, s, DHHDP-1), 4.91 (1H, dd, J=4, 6 Hz, glc-5), 4.96 (1H, dd, J=6, 9 Hz, glc-6), 5.09 (1H, br d, J=3 Hz, glc-3), 5.38 (1H, br d, J=4 Hz, glc-4), 6.35 (1H, d, J=1 Hz, glc-1), 6.53, 6.54, 6.74, 6.75, 7.08 (4H in total, each s, HHDP and DHHDP-3, 3′). ^{13}C-NMR (acetone-d_6+D_2O) ppm: 45.9, 51.7 (DHHDP-1), 63.8, 64.0, 64.4, 64.9, 68.1, 69.8, 74.2, 74.6 (glc 2—6), 95.3, 96.2 (glc-1), 92.5, 98.5, 108.9 (DHHDP-5, 6), 108.3, 109.7 (HHDP-3, 3′), 112.7 (DHHDP-3′), 115.0, 115.5 (HHDP-1, 1′), 115.7 (DHHDP-1′), 120.2 (DHHDP-2′), 125.3, 125.4 (HHDP-2, 2′), 126.1, 129.3 (DHHDP-3), 136.4, 136.9 (HHDP-5, 5′), 138.8 (DHHDP-5′), 143.3, 147.4 (DHHDP-6′), 145.0, 145.2 (HHDP-4, 4′), 145.8 (HHDP-6, 6′), 149.1, 154.2 (DHHDP-2), 164.5, 165.2, 166.6, 168.0, 168.1 (–COO–), 192.1, 194.9 (DHHDP-4).

Euphorhelin (17) A pale yellow amorphous powder, $[\alpha]_D^{20}$ −89.7° (c=1.0, acetone), *Anal.* Calcd for $C_{68}H_{50}O_{45}\cdot 7H_2O$: C, 47.66; H, 3.73. Found: C, 47.59; H, 3.73. Negative FAB-MS m/z: 1585 $[M-H]^-$. ^{1}H-NMR (acetone-d_6+D_2O, 270 MHz) ppm: 3.5—5.6 (12H in total, m, glc 2—6), 4.93 (d, J=1.5 Hz, DHHDP-1), 5.18 (s, DHHDP-1), 5.81 (1H, d, J=8 Hz, glc A-1), 6.20 (d, J=1.5 Hz, DHHDP-3), 6.52 (s, DHHDP-3), 6.56 (1H, d, J=7 Hz, glc B-1), 7.07, 7.11, 7.12, 7.13, 7.14, 7.16, 7.17, 7.22, 7.27 (11H in total, each s, aromatic H). ^{13}C-NMR (acetone-d_6+D_2O) ppm: 45.9, 51.8 (DHHDP-1), 62.7, 63.9, 65.9, 66.8, 69.8, 70.2, 71.0, 72.4, 73.1, 73.7, 74.7, 75.3, 91.3, 93.6 (glc-A, B), 92.3, 96.1, 108.8 (DHHDP-5, 6), 104.6, 109.9, 110.2, 110.5, 113.6, 114.6, 115.7, 116.7, 116.8, 117.1, 118.8, 119.7, 121.0, 123.6, 124.8, 125.0, 128.7, 135.9, 136.6, 137.5, 137.8, 139.0, 139.8, 140.1, 140.4, 143.1, 143.4, 144.7, 144.9, 145.3, 145.9, 146.9, 147.5, 148.9, 154.1 (aromatic C), 164.9, 165.4, 165.6, 165.9, 166.6, 167.2, 168.8 (–COO–), 192.0, 194.8 (DHHDP-4).

Preparation of the Phenazine (17a) A mixture of **17** (200 mg) and *o*-phenylenediamine (18 mg) in acetic acid–EtOH (1:4, v/v) (15 ml) was treated at room temperature for 10 h. The solution was diluted with water (5 ml) and evaporation of EtOH gave a yellow precipitate (**17a**) (170 mg). **17a**: A yellow powder (H_2O), $[\alpha]_D^{23}$ −12.0° (c=0.2, acetone). *Anal.* Calcd for $C_{74}H_{52}N_2O_{42}\cdot 2H_2O$: C, 52.90; H, 3.34; N, 1.67. Found: C, 53.13; H, 3.30; N, 1.69. ^{1}H-NMR (acetone-d_6+D_2O, 270 MHz) ppm: 3.86 (1H, dd, J=4, 12 Hz, glc A-6), 3.93 (1H, m, glc A-5), 4.37 (1H, dd, J=5, 12 Hz, glc A-6), 4.56 (1H, br d, J=12 Hz, glc B-6), 4.78 (1H, dd, J=8, 12 Hz, glc B-6), 4.95 (1H, dd, J=4, 8 Hz, glc B-5), 5.20 (1H, t, J=9 Hz, glc A-2), 5.42 (1H, d, J=3 Hz, glc B-4), 5.55 (1H, d, J=4 Hz, glc B-3), 5.70 (1H, d, J=6 Hz, glc B-2), 5.83 (1H, d, J=8 Hz, glc A-1), 6.12 (1H, d, J=6 Hz, glc B-1), 6.22, 7.03, 7.18, 7.50, 8.31 [valoneoyl (val), phe-H), 6.97, 7.12, 7.13 (each 2H, s, galloyl-H). ^{13}C-NMR (acetone-d_6+D_2O) ppm: 63.9 (glc A-6), 71.6 (glc A-4), 73.8 (glc A-2), 74.6 (glc A-3), 75.4 (glc A-5), 65.8, 67.7, 68.6, 76.6 (×2) (glc B 2—6), 91.8 (glc B-1), 93.7 (glc A-1), 105.3, 110.0, 110.3, 113.4, 114.7, 116.4, 116.5, 117.2, 119.4, 119.7, 120.1, 121.0, 123.7, 124.7, 129.8, 130.1, 132.7, 136.1, 136.7, 137.4, 139.0, 139.1, 139.6, 139.9, 140.2, 140.5, 142.9, 143.5, 144.7, 144.9, 145.9, 147.4, 152.2 (aromatic C), 165.2, 165.7, 166.1, 166.7 (×2), 167.4, 168.2, 169.1 (–COO–).

Methylation of 17a, Followed by Alkaline Hydrolysis A solution of **17a** (40 mg) in MeOH (3 ml) was methylated with ethereal diazomethane at 0 °C for 15 h to give a methylate, which was treated with 5% NaOH (4 ml) at 90 °C for 1 h. The hydrolysate mixture thus obtained was titrated with ethereal diazomethane and separated as described for **15a** to furnish **15b** (7 mg), the (*R*)-phenazine dimethyl ester (**17b**) (6 mg) [$[\alpha]_D^{24}$ +35.4° (c=0.6, $CHCl_3$)], and trimethyl octa-*O*-methyl-(*R*)-valoneate (**17c**) (5 mg) [$[\alpha]_D^{24}$ +14.7° (c=0.5, $CHCl_3$)].

Partial Hydrolysis of 17a A solution of **17a** (120 mg) in H_2O (6 ml) was heated on a water bath for 30 h. The resulting red precipitate (**15e**) (14 mg) was collected by filtration. The filtrate was directly subjected to MCI-gel CHP 20P chromatography and elution with H_2O–MeOH (1:0—0:1) gave 1,6-di-*O*-galloyl-β-D-glucose (**2**) (5 mg), isomallotinic acid (**17e**) (2 mg) and a hydrolysate (**17f**) (54 mg). **17f**: A pale brown amorphous powder, $[\alpha]_D^{23}$ −66.0° (c=0.6, acetone), *Anal.* Calcd for $C_{54}H_{44}O_{36}\cdot 2H_2O$: C, 49.69; H, 3.68. Found: C, 49.54; H, 3.47. Negative FAB-MS m/z: 1267 $[M-H]^-$. ^{1}H-NMR (acetone-d_6+D_2O, 270 MHz) ppm: 4.00—4.86 (11H in total, m, glc-H), 5.20 (1H, t, J=9 Hz, glc A-2), 5.82 (1H, d, J=9 Hz, glc A-1), 6.35 (1H, d, J=2 Hz, glc B-1), 6.23 (1H, s, val-3′), 6.85 (1H, s, val-3), 7.12 (1H, s, val-3″), 7.10, 7.15 (6H in total, each s, galloyl-H).

Jolkianin (18) A pale brown amorphous powder, $[\alpha]_D^{24}$ −0.8° (c=0.8, acetone). *Anal.* Calcd for $C_{82}H_{56}O_{53}\cdot 2H_2O$: C, 51.14; H, 3.11. Found: C, 50.89; H, 3.04. Negative FAB-MS m/z: 1887 $[M-H]^-$.

Preparation of the Phenazine (18a) A solution of **18** (100 mg) and *o*-phenylenediamine (9 mg) in 20% AcOH–EtOH (3 ml) was stirred at room temperature for 20 h. After removal of EtOH under reduced pressure, the aqueous solution was subjected to MCI-gel CHP 20P chromatography to give **18a** (67 mg). **18a**: A yellow powder (H_2O), mp>300 °C, $[\alpha]_D^{23}$ −68.3° (c=0.6, acetone). *Anal.* Calcd for $C_{88}H_{58}O_{50}N_2$: C, 54.37; H, 2.98; N, 1.44. Found: C. 54.21, H, 2.79; N, 1.43. Negative FAB-MS m/z: 1941 $[M-H]^-$. ^{1}H-NMR (acetone-d_6+D_2O, 270 MHz) ppm: 4.03 (1H, dd, J=5, 11 Hz, glc A-5), 4.44 (1H, dd, J=5, 11 Hz, glc A-6), 4.54 (1H, dd, J=4, 11 Hz, glc B-6), 4.56 (1H, m, glc B-5), 4.76 (1H, t, J=11 Hz, glc B-6), 4.97 (1H, br s, glc A-4), 5.49 (1H, br s, glc A-3), 5.25 (1H, dd, J=3, 7 Hz, glc B-4), 5.33 (1H, t, J=11 Hz, glc A-6), 5.53 (1H, dd, J=3, 7 Hz, glc B-2), 5.71 (1H, br s, glc A-3), 5.86 (1H, t, J=7 Hz, glc B-3), 6.15 (1H, d, J=3 Hz, glc B-1), 6.23 (1H, br s, glc A-1), 6.68, 6.74, 6.83, 6.84 (each 1H, s, HHDP-H), 6.85, 7.32 (each 1H, d, J=2 Hz, DHDG-H), 7.01 (1H, s, phe-3′), 7.11, 7.12 (each 2H, s, galloyl-H), 7.17 (1H, s, DHDG-H), 8.04 (1H, s, phe-3), 7.99—8.04, 8.28—8.33 (each 2H, m, phe-2″, 3″, 4″, 5″). ^{13}C-NMR (acetone-d_6+D_2O) ppm: 60.9, 64.0, 64.9, 67.7, 69.2, 70.7 (×2), 71.8, 72.7, 75.1, 90.1, 94.6 (glc A, B), 108.9, 109.4, 110.2, 111.3, 112.4, 114.8, 116.0, 116.2, 116.4, 116.6, 118.2, 118.6, 120.0, 120.1, 123.0, 124.7, 124.9, 125.3, 125.5, 130.1, 132.3, 135.7, 136.8, 137.0, 137.2, 137.9, 138.1, 138.5, 139.6, 140.5, 140.8, 142.9, 144.9, 145.0, 146.0, 146.3, 147.8, 152.6 (aromatic C), 162.0, 165.9, 166.2 (×2), 166.4 (×2), 166.8, 168.0, 168.5, 170.2 (–COO–).

Methylation of 18a, Followed by Alkaline Hydrolysis **18a** (70 mg) was treated with diazomethane in ether for 24 h at 0 °C. After evaporation of the solvent, the residue was hydrolyzed with 5% NaOH (3 ml) at 90 °C for 30 min. The reaction mixture was treated with ethereal diazomethane and separated as described before to give **15b** (13 mg), **16b** (16 mg), **15c** (11 mg) and dimethyl pentamethoxydehydrodigallate (**18b**) (13 mg). **18b**: An off-white amorphous powder. ^{1}H-NMR ($CDCl_3$) ppm: 3.74—4.05 (21H in total, each s, OCH_3), 6.80, 7.30 (each 1H, d, J=2 Hz), 7.27 (1H, s).

Partial Hydrolysis of 18a A solution of **18a** (100 mg) in H_2O–MeOH (4 ml) was heated at 90 °C for 5 h. After cooling, the reaction mixture was concentrated, and chromatographed over Sephadex LH-20 and MCI-gel CHP 20P (H_2O–MeOH) to afford **18c** (50 mg), **18d** (5 mg) and **15e** (7 mg). **18c**: A pale brown amorphous powder, $[\alpha]_D^{25}$ −47.0° (c=0.9, acetone). *Anal.* Calcd for $C_{68}H_{50}O_{44}$: C, 51.49; H, 3.37. Found: C, 51.89; H, 3.83. Negative FAB-MS m/z: 1569 $[M-H]^-$. ^{1}H-NMR (acetone-d_6+D_2O, 400 MHz) ppm: 3.67 (1H, dd, J=3, 6 Hz, glc A-4), 4.03 (1H, dd, J=6, 12 Hz, glc A-6), 4.21 (1H, dd, J=6, 12 Hz, glc A-5), 4.42 (1H, dd, J=5, 12 Hz, glc B-6), 4.54 (1H, dd, J=8, 12 Hz, glc B-5), 4.66 (1H, t, J=12 Hz, glc B-6), 4.73 (1H, t, J=12 Hz, glc A-6), 5.13 (1H, t, J=6 Hz, glc A-3), 5.22 (1H, dd, J=3, 8 Hz, glc B-4), 5.50 (1H, dd, J=3, 8 Hz, glc B-2), 5.81 (1H, d, J=3 Hz, glc A-1), 5.82 (1H, t, J=8 Hz, glc B-3), 6.08 (1H, d, J=3 Hz, glc B-1), 6.74, 6.83 (×2), 6.85 (each 1H, s, HHDP-H), 6.88, 7.28 (each 1H, d, J=2 Hz, DHDG-H), 7.10, 7.11 (each 2H, s, galloyl-H), 7.16 (1H, s, DHDG-H). ^{13}C-NMR (acetone-d_6+D_2O) ppm: 65.0, 68.1, 69.4, 70.7, 71.7, 73.1, 75.2, 76.2, 94.6, 96.1 (glc A, B), 108.3, 109.2, 109.5, 110.2, 110.3, 112.3, 114.3, 116.6, 119.8, 120.0, 124.7, 125.5, 125.9, 136.8, 137.0, 137.3, 139.6, 140.3, 140.6, 143.0, 144.7, 145.0, 146.0, 146.3, 148.1 (aromatic C), 164.9, 165.8, 166.1, 166.4, 167.1, 168.7, 169.4 (–COO–). **18d**: A pale brown amorphous powder, $[\alpha]_D^{25}$ 0° (c=0.5, acetone). *Anal.* Calcd for $C_{40}H_{38}O_{28}\cdot H_2O$: C, 48.78; H, 4.06. Found: C, 48.96; H, 4.23. Negative FAB-MS m/z: 965 $[M-H]^-$. ^{1}H-NMR (acetone-d_6+D_2O, 270 MHz) ppm: 3.14 (dd, J=8, 10 Hz, glc A-β-2), 4.60 (d, J=8 Hz, glc-A-β-1), 5.01 (dd, J=4, 10 Hz, glc B-α-2), 5.02 (t, J=10 Hz, glc A-β-3), 5.12 (d, J=4 Hz, glc B-α-3), 6.75, 7.17 (each 1H, m, DHDG-H), 7.18, 7.19 (1H in total, each s, DHDG-H), 7.08, 7.09 (each 2H, s, galloyl-H).

Acknowledgements The authors are indebted to Prof. K. Mihashi (Faculty of Pharmaceutical Sciences, Fukuoka University) for high-resolution (400 MHz) ^{1}H-NMR measurement, to Mr. Y. Tanaka, Miss Y. Soeda and Mr. K. Isobe for ^{1}H- and ^{13}C-NMR and MS measurements, and to the staff of the Central Analysis Room of this university for elemental analyses.

References

1) Part XIV: S.-H. Lee, T. Tanaka, G. Nonaka and I. Nishioka, *Phytochemistry*, "in press."

2) S.-H. Lee, T. Tanaka, G. Nonaka and I. Nishioka, *Chem. Pharm. Bull.*, **38**, 1518 (1990).
3) O. T. Schmidt and H. Schmadel, *Justus Liebigs Ann. Chem.*, **649**, 149 (1961).
4) E. A. Haddock, R. K. Gupta, S. M. K. Al-Shafi and E. Haslam, *J. Chem. Soc., Perkin Trans. 1*, **1982**, 2515.
5) S.-H. Lee, T. Tanaka, G. Nonaka and I. Nishioka, *Phytochemistry*, **29**, 3621 (1990).
6) G. Nonaka, I. Nishioka, T. Nagasawa and H. Oura, *Chem. Pharm. Bull.*, **29**, 2862 (1981).
7) M. Nishizawa, Y. Yamagishi, G. Nonaka and I. Nishioka, *J. Chem. Soc., Perkin Trans. 1*, **1983**, 2515.
8) O. T. Schmidt, W. Ebert and M. Koppe, *Justus Liebigs Ann. Chem.*, **729**, 251 (1969).
9) M. Nishizawa, T. Yamagishi, G. Nonaka and I. Nishioka, *J. Chem. Soc., Perkin Trans. 1*, **1982**, 2963.
10) E. A. Haddock, R. K. Gupta and E. Haslam, *J. Chem. Soc., Perkin Trans. 1*, **1982**, 2535.
11) O. T. Schmidt, J. Schulz and R. Wurmb, *Justus Liebigs Ann. Chem.*, **706**, 131 (1967).
12) T. Okuda, T. Hatano and N. Ogawa, *Chem. Pharm. Bull.*, **30**, 4234 (1982).
13) T. Tanaka, G. Nonaka and I. Nishioka, *Chem. Pharm. Bull.*, **38**, 2424 (1990).
14) O. T. Schmidt, R. Eckert, E. Gunther and H. Fisser, *Justus Liebigs Ann. Chem.*, **706**, 204 (1967).
15) M. Ishimatsu, T. Tanaka, G. Nonaka, I. Nishioka, M. Nishizawa and T. Yamagishi, *Chem. Pharm. Bull.*, **37**, 1735 (1989).

Tannins and Related Compounds. CVI.[1] Preparation of Aminoalditol Derivatives of Hydrolyzable Tannins Having α- and β-Glucopyranose Cores, and Its Application to the Structure Elucidation of New Tannins, Reginins A and B and Flosin A, Isolated from *Lagerstroemia flos-reginae* RETZ.

Ya-Ming XU,[a] Takashi SAKAI,[b] Takashi TANAKA,[b] Gen-ichiro NONAKA*,[b] and Itsuo NISHIOKA[b]

Shanghai Institute of Materia Medica, Academica Sinica,[a] 319 Yueyan Road, Shanghai, Peoples' Republic of China and Faculty of Pharmaceutical Sciences, Kyushu University 62,[b] 3-1-1 Maidashi, Higashi-ku, Fukuoka 812, Japan. *Received October 3, 1990*

To avoid tautomerism in the hydrolyzable tannins which lack an acyl group at the glucose C-1 position, a new method for the protection of the C-1 atom has been developed. That is reaction of the tannins with *p*-anisidine in the presence of acetic acid, followed by sodium cyanoborohydride reduction, afforded, without notable hydrolysis of ester bonds, the aminoalditol derivatives (1a—7a) in 50—80% yields. The proton and carbon-13 nuclear magnetic resonance (^{1}H- and ^{13}C-NMR) spectra of these derivatives exhibited much simpler signal patterns typical of an open-chain form of glucose, and almost all the signals could be assigned.

Application of this method to the structure elucidation of the new tannins, flosin A (22) and reginins A (23) and B (24), isolated from the leaves of *Lagerstroemia flos-reginae* RETZ. (Lythraceae), established their structures including the orientation of the 4,6-positioned valoneoyl group. In addition, the structure of a new hydrolyzable tannin, lagerstroemin (21), which was concomitantly isolated from the above species, was elucidated.

Keywords hydrolyzable tannin; aminoalditol derivative; reginin A; reginin B; flosin A; lagerstroemin; valoneic acid; *Lagerstroemia flos-reginae*; Lythraceae; tannin

Whilst considerable progress has been made on elucidation of the chemistry and structures of hydrolyzable tannins by employing proton and carbon-13 nuclear magnetic resonance (^{1}H- and ^{13}C-NMR) spectroscopic techniques, elucidation of the structures of hydrolyzable tannins based on a mixture of α- and β-glucopyranose cores has been severely hampered by the complexty of the signal patterns. In particular, when these tautomeric isomers exist in almost equal proportions, discrimination of signals arising from the α- and β-anomers is difficult from the signal intensities, and therefore the assignment of each signal is difficult. Moreover, in the cases of dimeric and trimeric hydrolyzable tannins having no acyl groups at the glucose C-1 position(s), the spectra are even more complicated owing to the occurrence of many tautomeric isomers. To overcome these difficulties, we have made several attempts to prepare derivatives in which tautomerism can not occur, and we found that reaction of these tannins with *p*-anisidine in ethanolic acetic acid, followed by sodium cyanoborohydride reduction,[2] affords, without notable hydrolysis of ester bonds, aminoalditol derivatives in relatively high yields. The ^{1}H- and ^{13}C-NMR spectra of these derivatives were found to be extremely simplified, showing signal patterns typical of an open-chain form of glucose. Subsequently, we have applied this method to the structure elucidation of a monomeric (flosin A) and two dimeric hydrolyzable tannins (reginins A and B) isolated from the Indonesian medicinal plant, *Lagerstroemia flos-reginae* RETZ. (Lythraceae), and unequivocally determined their structures, including the orientation of the valoneic acid ester group. This paper first describes the method for preparing aminoalditol derivatives of several structurally known hydrolyzable tannins and next deals with the structure elucidation of tannins in *L. flos-reginae*, together with their isolation.

Preparation of Aminoalditol Derivatives Many methods to protect the carbohydrate C-1 position have been reported,[3] but most of them are not applicable to the hydrolyzable tannins because of their instability to acids and bases. Formation of an *O*-alkyl ether or an *O*-acyl ester under mild conditions seems to be a simple and convenient method for the protection of the anomeric hydroxyl group, but separation of the α- and β-anomers produced is usually very difficult. We noticed that primary amines readily react with the carbohydrate C-1 atom in a weakly acidic medium to form a glycosyl amine,[2] and among various amines (monomethyl amine, benzylamine, aniline and *p*-anisidine) tested, *p*-anisidine was found to be the most satisfactory. Subsequent reduction with sodium cyanoborohydride afforded, without notable hydrolysis of the ester linkage, the aminoalditol derivatives in relatively high yields. The ^{1}H-NMR data for the aminoalditol derivatives (**1a—7a**) prepared from pedunculagin (**1**),[4] praecoxin A (**2**),[5] rugosin B (**3**),[5] camelliin A (**4**),[6] 1-desgalloyleugeniin (**5**),[7] gemin D (**6**)[8] and rugosin E (**7**)[9] are listed in Table I.

As is evident from this table, almost all the aminoalditol signals could be assigned unambiguously. It was found that among these signals, the H-3 signal invariably appears at the lowest magnetic field, whereas the H-1 methylene signals appear at the highest position (δ 3.3—3.7) as the AB-portions of typical ABX-type splitting patterns. The aromatic signals arising from the anisidine moiety were always observed as a four-proton singlet which was readily distinguishable from other aromatic signals, and from this signal coupled with the methoxyl signal, the number of

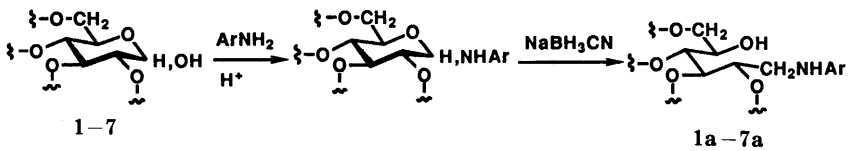

1—7 1a—7a

Chart 1

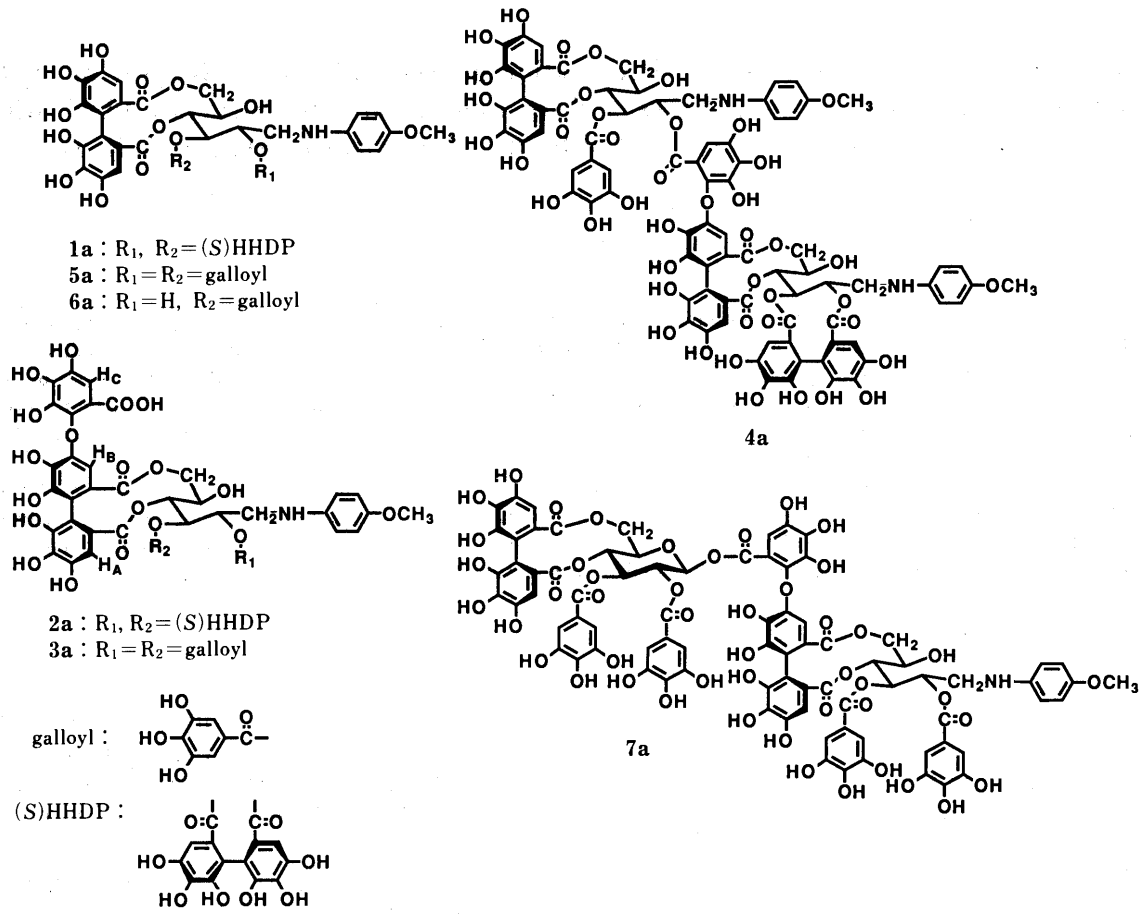

Chart 2

TABLE I. ^{1}H-NMR Spectral Data for Compounds **1a**, **2a**, **3a**, **4a**, **5a**, **6a**, **7a**, **22a**, **23a** and **24a**

		23a	**24a**[a,c]	**22a**[a,c]	**1a**[b]	**2a**[a]	**3a**[b]	**4a**[a,d]	**5a**[b]	**6a**[b]	**7a**[a,c]
4,6-HHDP	H_A	6.66		6.89	6.68	6.68	6.80	6.68	6.85	6.60	6.71
or valoneoyl	H_B	6.55	6.50—6.60[f]	6.63	6.54	6.21	6.15	6.16	6.47	6.53	6.10
	H_C	7.06		7.05		7.15	7.20	6.81			7.10
Aminoalditol	H-1	3.70[e]	3.64[e]	3.65[e]	3.30—3.70[e]	3.68[e]	3.40—3.70[e]	3.50—3.60[e]	3.30—3.70[e]	3.30—3.70[e]	3.30—3.70[e]
moiety		3.44 (dd, J=8, 12)	3.42 (dd, J=8, 15)	3.46 (dd, J=8, 13)		3.46 (dd, J=8, 12)		3.33 (dd, J=9, 13)			
	H-2	5.18 (ddd, J=2,8,9)	5.11 (ddd, J=2, 8, 8)	5.21 (m)	5.28 (m)	5.26 (m)	5.50 (m)	5.11—5.21[e]	5.51 (m)	4.28 (m)	5.54 (m)
	H-3	5.52 (dd, J=2, 9)	5.49 (dd, J=2, 9)	5.55 (dd, J=2, 10)	5.56 (dd, J=2, 10)	5.53 (dd, J=2, 10)	5.84 (t, J=5)	5.38—5.45[e]	5.89 (t, J=5)	5.54 (dd, J=5, 8)	5.86 (t, J=5)
	H-4	5.14 (dd, J=2, 9)	5.04 (dd, J=2, 8)	5.20 (dd, J=2, 8)	5.28 (m)	5.25 (dd, J=2, 8)	5.34 (dd, J=5, 8)	5.11—5.21[e]	5.38 (dd, J=5, 8)	5.38 (dd, J=5, 8)	5.35 (dd, J=5, 8)
	H-5	4.22 (dd, J=3, 9)	4.04 (dd, J=2, 8)	4.22 (dd, J=2, 8)	4.24 (br d, J=8)	4.25 (dd, J=2, 8)	4.05 (br d, J=8)	4.15 (br d, J=8)	4.06 (br d, J=8)	4.20 (dd, J=3, 8)	4.07 (br d, J=8)
	H-6	4.50 (dd, J=3, 12)	4.36 (dd, J=3, 13)	4.63 (dd, J=3, 12)	4.70 (dd, J=3, 13)	4.60 (dd, J=3, 13)	4.60 (dd, J=3, 12)	4.49 (dd, J=3, 13)	4.66 (dd, J=3, 12)	4.60 (dd. J=3, 12)	4.64 (dd, J=3, 12)
		4.02 (d, J=12)	3.69[e]	3.98 (d, J=12)	3.95 (d, J=13)	3.88 (d, J=13)	3.79 (d, J=12)	3.50—4.00[e]	3.83 (d, J=12)	3.88 (d, J=12)	3.82 (d, J=12)
Anisidine		6.71	6.69	6.70	6.69	6.70	6.71	6.58, 6.38	6.74	6.71	6.72
moiety		(4H)	(4H)	(4H)	(4H)	(4H)	(4H)	(4H) (4H)	(4H)	(4H)	(4H)
	OMe	3.68	3.67	3.67	3.66	3.67	3.67	3.45, 3.54	3.67	3.68	3.67

Acetone-d_6 + D_2O, ppm, Hz. *a*) Spectra measured at 270 MHz. *b*) Spectra measured at 100 MHz. *c*) Data for the aminoalditol moiety. *d*) Data for the aminoalditol of the praecoxin A moiety. *e*) Overlapped with other signals. *f*) Individual signals could not be assigned.

anisidino groups could be ascertained. Considering the coupling constants of the aminoalditol signals, substitution at the C-2 and C-3 positions with either a galloyl or a hexahydroxydiphenoyl (HHDP) ester group seems to affect, the conformation of the aminoalditol moiety as a whole. Namely, in the cases of 2,3-galloyl derivatives (**3a**, **5a** and **7a**), the coupling constants of H-2 and H-3 and of H-3 and H-4 were 5 Hz, whereas the 2,3-HHDP derivatives (**1a**, **2a** and **4a**) exhibited a larger coupling constant ($J=8$ Hz) of H-2 and H-3 and a smaller one ($J=2$ Hz) of H-3 and H-4. One of the characteristic features in the spectra of 4,6-valoneoyl derivatives (**2a**, **3a**, **4a** and **7a**) is the observation of the valoneoyl H_B signal at extremely high field (δ 6.10—6.21). This upfield shift was observed only in the compounds where the 'branched' gallic acid moiety (in the valoneoyl group) is attached to the aromatic ring at the glucose C-6 position (*vide infra*).

Isolation of Tannins from *Lagerstroemia flos-reginae* The dried leaves of *L. reginae*, collected in Indonesia, were extracted with aqueous acetone, and the concentrated extract was partitioned between water and ethyl acetate. The aqueous layer was subjected to Sephadex LH-20 chromatography with H_2O containing increasing proportions of methanol to give two fractions. Each fraction was repeatedly chromatographed over Sephadex LH-20, MCI-gel CHP 20P, TSK-gel Toyopearl HW-40F, TSK-gel Phenyl Toyopearl 650 M and various ODS-type gels to yield new tannins named lagerstroemin (**21**), flosin A (**22**) and reginins A (**23**) and B (**24**), together with 3-*O*-caffeoylquinic acid (**8**),[10] gentisic acid 5-*O*-β-D-glucopyranoside (**9**),[11] brevifolin carboxylic acid (**13**),[12] 4,6-(*S*)-HHDP-D-glucose (**11**),[13] pedunculagin (**1**),[4] 2,3-(*S*)-HHDP-D-glucose (**12**),[14] gentisic acid 5-*O*-β-D-(6′-*O*-galloyl)-glucopyranoside (**10**),[11] casuarinin (**15**),[15] casuariin (**14**),[15] stachyurin (**16**),[15] punicacortein A (**20**),[16] 5-desgalloyl stachyurin (**17**),[17] castalagin (**18**)[15] and vescalagin (**19**).[15] The known compounds were identified by direct comparisons of their chemical and physical data with those of authentic samples.

Structure Elucidation of New Tannins (21—24) Lagerstroemin (**21**) showed, in the ^{1}H-NMR spectrum, seven aliphatic proton signals whose chemical shifts and coupling patterns were similar to those of casuarinin (**15**).[15] In the aromatic field, the chemical shifts of three signals (δ 6.83, 6.59 and 6.41) out of six one-proton singlets were also correlated with those of **15**. Methylation of **21** with dimethyl sulfate and potassium carbonate in dry acetone yielded the octadecamethyl ether (**21a**). Subsequent alkaline methanolysis of **21a** gave three products (**21b**, **21c** and **21d**), of which compound **21b** was identified as dimethyl (*S*)-hexamethoxydiphenoate.[18] The ^{1}H-NMR spectrum of **21c** showed three aromatic one-proton singlets and seven methoxyl signals. These facts coupled with the observation of the intense molecular ion peak at m/z 568 in the electron impact mass spectrum (EI-MS) suggested that **21c** is valoneic acid

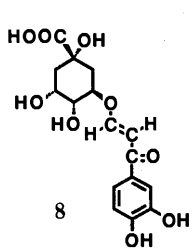

8

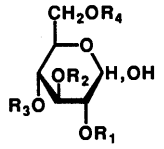

11 : $R_1=R_2=H$, R_3, $R_4=(S)$HHDP
12 : R_1, $R_2=(S)$HHDP, $R_3=R_4=H$
1 : R_1, $R_2=R_3$, $R_4=(S)$HHDP

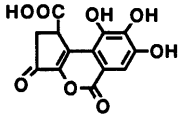

13

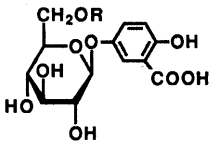

9 : R=H
10 : R=galloyl

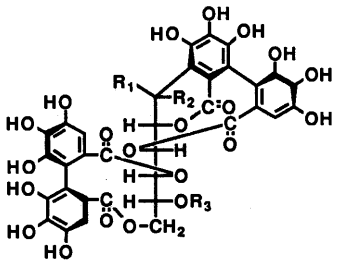

14 : R_1=OH, $R_2=R_3=H$
15 : R_1=OH, R_2=H, R_3=galloyl
16 : R_1=H, R_2=OH, R_3=galloyl
17 : $R_1=R_3=H$, R_2=OH

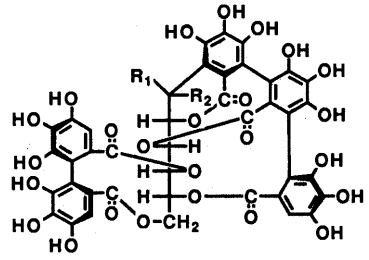

18 : R_1=OH, R_2=H
19 : R_1=H, R_2=OH

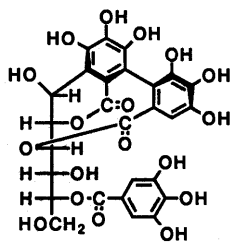

20

Chart 3

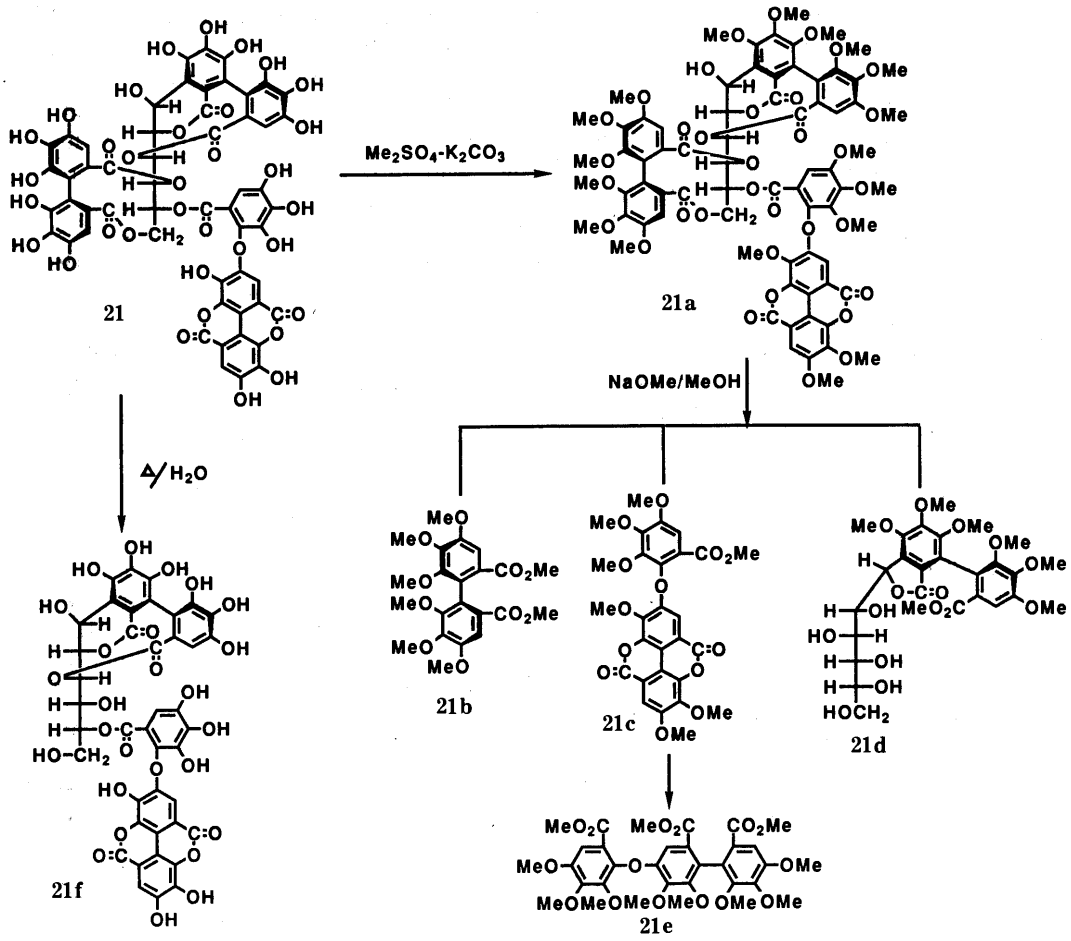

Chart 4

dilactone heptamethylate. The structure of **21c** was further confirmed by alkaline treatment, followed by methylation, yielding racemic trimethyl octa-*O*-methylvaloneate (**21e**).[19] The methanolysate (**21d**) was identical with the product obtained by similar methanolysis of casuarinin pentadecamethyl ether.[15]

To confirm the location of each acyl group, **21** was partially hydrolyzed in hot water to yield ellagic acid and a hydrolysate (**21f**). The ^{1}H-NMR spectrum of **21f** exhibited high-field shifts of the H-4 [δ 3.95 (dd, J=3, 8 Hz)] and H-6 signals (δ 3.80, m), indicating that the location of the HHDP group in **21** is at the C-4 and C-6 positions. On the basis of these findings, the structure of lagerstroemin was established to be as shown by the formula **21**.

The ^{1}H-NMR spectrum of flosin A (**22**) showed complicated signal patterns owing to the presence of α- and β-anomers, but the aliphatic signal patterns resembled those found in pedunculagin (**1**). The aromatic resonances all appearing as a singlet and corresponding to five protons in total suggested the presence of one HHDP and one valoneoyl group. The ^{13}C-NMR chemical shifts (Table II) of sugar carbon signals were in good accord with those of pedunculagin (**1**), suggesting that flosin A has a similar substitution pattern. The negative fast atom bombardment mass spectrum (FAB-MS)[20] exhibited the $[M-H]^-$ peak at m/z 951, which supports the presence of one HHDP and one valoneoyl group. Partial hydrolysis of **22** in hot water to yield 2,3-(*S*)-HHDP-D-glucose (**12**) indicated clearly that the valoneoyl and the HHDP groups are located at the glucose 4,6- and 2,3-positions, respectively. The atropisomerism of the valoneoyl group was determined to be *S* from the result of alkaline methanolysis of the hexadecamethyl ether (**22b**), which yielded trimethyl octa-*O*-methyl-(*S*)-valoneate (**22c**),[19] together with dimethyl (*S*)-hexamethoxydiphenoate (**21b**).

Treatment of **22** with *p*-anisidine in ethanolic acetic acid, followed by sodium cyanoborohydride reduction, yielded the aminoalditol derivative (**22a**). Comparison of the ^{1}H-NMR spectra (Table I) of **22a** and the praecoxin A aminoalditol (**2a**) clearly indicated that there are significant differences in the chemical shifts of the aromatic signals. As mentioned before, since the upfield shift of one of the valoneoyl signals was not observed in **22a**, the valoneoyl group was concluded to be located in the reverse direction. Thus, the structure of flosin A could be represented by the formula **22**.

Reginin A (**23**) was found to be a dimeric hydrolyzable tannin by the observation of the $[M-H]^-$ peak at m/z 1717 in the negative FAB-MS. The ^{1}H-NMR spectrum showed a duplicated signal pattern owing to the presence of α- and β-glucopyranose cores. The aromatic signals all appearing as singlets (see Experimental) corresponded to eight protons in total. The ^{13}C-NMR spectrum (Table II) exhibited eighteen aliphatic signals, among which those at δ 95.3 and 91.8 are typical of the β- and α-anomeric signals, respectively. Treatment of **23** with *p*-anisidine gave the aminoalditol derivative (**23a**), whose ^{1}H-NMR spectrum clearly showed the introduction of one anisidine moiety

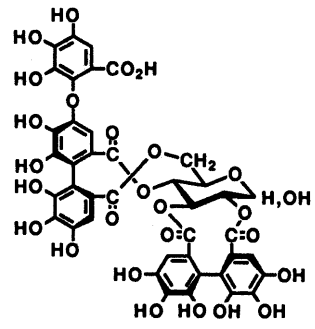

22

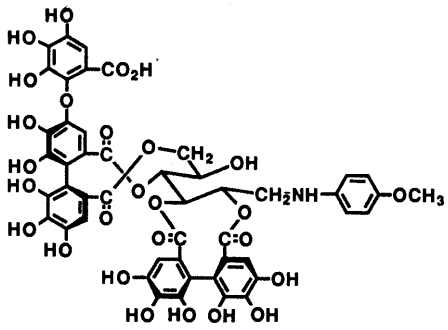

22a

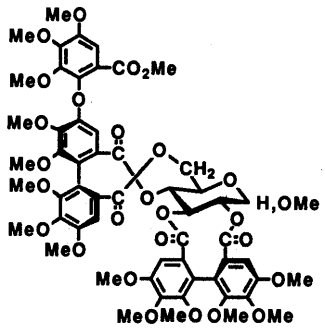

22b

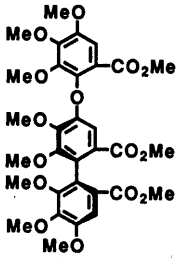

22c

Chart 5

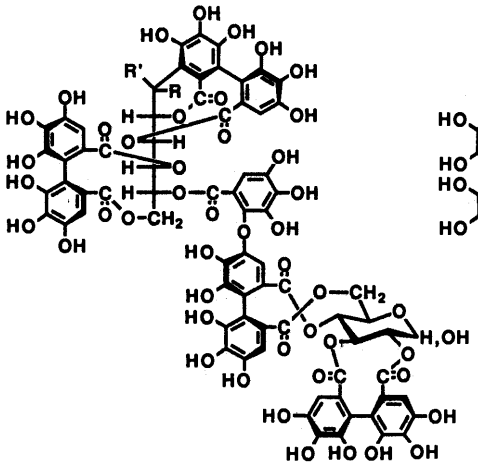

	R	R′
23 :	H	OH
24 :	OH	H

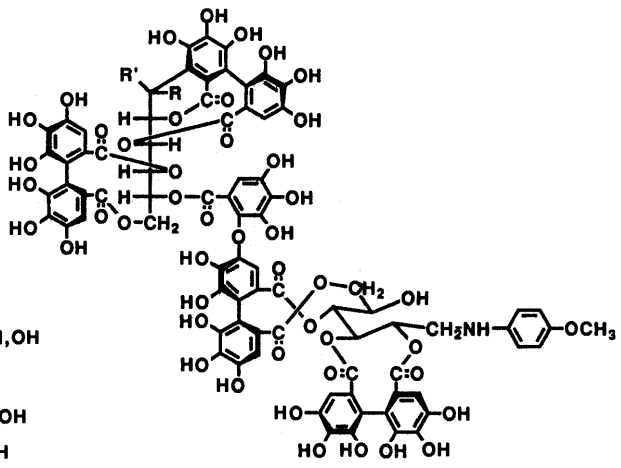

	R	R′
23a :	H	OH
24a :	OH	H

Chart 6

[δ 3.68 (3H, s, OMe) and 6.71 (4H, s)]. The aliphatic signals in the ^{1}H-NMR spectrum of **23a** were unequivocally assigned by ^{1}H–^{1}H shift correlation spectroscopy (COSY), and of these, signals arising from the aminoalditol moiety were closely correlated with those of **22a** and **2a** (Table I). On the other hand, the chemical shifts and the coupling patterns of the remaining aliphatic signals (see Experimental) were comparable to those of casuarinin (**15**). From these findings combined with the observation of eight aromatic one-proton singlets, **23** was considered to be a dimeric hydrolyzable tannin in which the galloyl group in casuarinin (**15**) and the HHDP group in pedunculagin (**1**) are linked through an ether bond, forming a valoneoyl group.

On heating in water, **23** yield 2,3-HHDP-D-glucose (**12**) and lagerstroemin (**21**), while methylation of **23** with dimethyl sulfate and potassium carbonate in dry acetone afforded many products, of which one was found to be identical with the flosin A hexadecamethyl ether (**22b**), thus establishing unambiguously the structure (**23**) of reginin A, including the configuration and the orientation of the valoneoyl group.

Reginin B (**24**) showed, in the negative FAB-MS, the same $[M-H]^-$ peak at m/z 1717 as that of reginin A (**23**). The ^{1}H-NMR spectrum of **24** was also complicated due to the existence of an equilibrium mixture of α- and β-anomers,

TABLE II. ^{13}C-NMR Spectral Data for Reginins A (**23**) and B (**24**), Flosin A (**22**), Pedunculagin (**1**), Casuarinin (**15**) and Stachyurin (**16**)

Glucose		23[a]	24[a]	22[b]	1[b]	15[c]	16[c]
Open-chain form	1′	67.8	64.7			67.8	65.3
	2′	77.5	81.6			77.4	81.8
	3′	70.3	72.3			70.3	72.6
	4′	74.6	73.7			74.6	73.8
	5′	71.5	71.1			71.6	71.5
	6′	65.0	64.4			65.0	65.0
Pyranose form	1 β	95.3	94.9	95.1	95.4		
	α	91.8	91.4	91.6	91.8		
	2 β	78.8	78.2	78.3	78.3		
	α	76.0	75.5	75.6	75.5		
	3 β	77.6	77.2	77.3	77.6		
	α	76.2	75.7	75.6	75.8		
	4 β	70.9	70.9	70.4	69.9		
	α	70.3	70.4	70.1	69.6		
	5 β	72.7	72.2	72.3	72.5		
	α	67.5	67.5	67.3	67.4		
	6 β	64.4	64.0	63.8	63.6		
	α	64.4	64.0	63.8	63.6		

Acetone-d_6 + D_2O, ppm. *a*) Spectra measured at 67.8 MHz. *b*) Spectra measured at 25.05 MHz. *c*) Spectra measured at 100 MHz.

but the ^{13}C-NMR spectrum (Table II) was similar to those of pedunculagin (**1**) plus stachyurin (**16**). Partial hydrolysis of **24** in hot water afforded 2,3-(*S*)-HHDP-D-glucose (**12**) and 5-desgalloyl stachyurin (**17**), and methylation of **24** with dimethyl sulfate and potassium carbonate in acetone, followed by alkaline methanolysis, gave dimethyl (*S*)-hexamethoxydiphenoate (**21b**) and trimethyl octa-*O*-methyl-(*S*)-valoneate (**22c**). From these findings, it was concluded that reginin B has the structure in which the galloyl group in the stachyurin moiety is connected with the 4,6-positioned HHDP group in the pedunculagin moiety through an (*S*)-valoneoyl group. To establish the structure of reginin B including the orientation of the valoneoyl group, the aminoalditol derivative (**24a**) was prepared. The ^{1}H-NMR spectrum (Table I and Experimental) of **24a** clearly showed signals arising from an open-chain form of the *C*-glucoside core and an aminoalditol moiety, and their chemical shifts and coupling patterns agreed well with those of stachyurin (**16**) plus pedunculagin (**1**). In the aromatic field, an upfield shift of H_B in the valoneoyl group, as observed in compounds **2a**, **3a** and **4a**, was not observed, thus confirming that the orientation of the valoneoyl group in reginin B is the same as that in flosin A (**22**) and reginin A (**23**). Accordingly, the structure of reginin B is represented by the formula **24**.

In conclusion, the preparation of the aminoalditol derivatives of hydrolyzable tannins which lack an acyl group at the glucose C-1 position was proved to be a useful tool for determining their structures. In particular, by using this method, the orientation of the valoneoyl group located at the glucose C-4 and C-6 positions was found to be readily determinable by observing the ^{1}H-NMR chemical shift of the H_B signal.

Experimental

Melting points were determined on a Yanagimoto micro-melting point apparatus and are uncorrected. Optical rotations were measured with a JASCO DIP-4 digital polarimeter (cell length: 0.5 dm). EI-MS were measured with a JEOL D-300 spectrometer, while field desorption mass spectrum (FD-MS) and FAB-MS were taken with a JEOL DX-300 instrument. ^{1}H (100 MHz)- and ^{13}C (25.05 MHz)-NMR spectra were recorded on JEOL PS-100 and JEOL FX-100 spectrometers, respectively, and ^{1}H (270 MHz)- and ^{13}C (67.8 MHz)-NMR spectra on a JEOL GX-270 spectrometer, with tetramethylsilane (TMS) as an internal standard, the chemical shifts being given in δ (ppm). Column chromatography was carried out with Sephadex LH-20 (25—100 μ, Pharmacia Fine Chemical Co., Ltd.), MCI-gel CHP 20P (75—150 μ, Mitsubishi Chemical Industries Co., Ltd.), TSK gel Toyopearl HW-40F (30—60 μ, Toso Co., Ltd.), TSK gel Phenyl Toyopearl 650 M (88 μ, Toso Co., Ltd.), Cosmosil 75 C_{18}-OPN (42—105 μ, Nacalai Tesque Inc.), Bondapak C_{18}/Porasil B (37—75 μ, Waters Associates Inc.) and Kieselgel 60 (70—230 mesh, Merck). Thin-layer chromatography (TLC) was conducted on precoated Silica gel 60 F_{254} plates (Merck, 0.20 mm thick) and precoated cellulose F_{254} plates (Merck, 0.10 mm thick). Spots were visualized under ultra violet light and by spraying $FeCl_3$ solution (for phenolics), $NaNO_2$–HOAc solution (for ellagitannins) or 10% sulfuric acid, followed by heating (for phenolics and methylates).

General Procedures for Preparing the Aminoalditol Derivatives (1a—7a) A mixture of a hydrolyzable tannin (**1**—**7**) (10—100 mg) and *p*-anisidine (2—20 mg) in 20% ethanolic acetic acid (1—5 ml) was stirred at room temperature for 2 h, and the mixture was treated with sodium cyanoborohydride (5—20 mg) at room temperature for 1 h. After addition of 1 N HCl, the product was purified by Sephadex LH-20 chromatography with EtOH–H_2O to give the corresponding aminoalditol derivative (**1a**—**7a**) in 50—80% yield.

Pedunculagin Aminoalditol (1a) An off-white amorphous powder, $[\alpha]_D^{13}$ +108.7° (*c* = 0.96, MeOH). *Anal.* Calcd for $C_{41}H_{33}NO_{22}\cdot 6H_2O$: C, 49.29; H, 4.54; N, 1.39. Found: C, 49.33; H, 4.34; N, 1.39. Negative FAB-MS *m/z*: 890 $[M-H]^-$. ^{1}H-NMR: see Table I.

Praecoxin A Aminoalditol (2a) An off-white amorphous powder, $[\alpha]_D^{30}$ +77.9° (*c* = 1.8, MeOH). *Anal.* Calcd for $C_{48}H_{35}NO_{27}$: C, 53.58; H, 3.50; N, 1.32. Found: C, 53.56; H, 3.54; N, 1.33. ^{1}H-NMR: see Table I.

Rugosin B Aminoalditol (3a) An off-white amorphous powder, $[\alpha]_D^{24}$ +53.8° (*c* = 0.9, MeOH), *Anal.* Calcd for $C_{48}H_{37}NO_{27}$: C, 54.39; H, 3.49; N, 1.32. Found: C, 54.20; H, 3.57; N, 1.35. ^{1}H-NMR (acetone-d_6 + D_2O, 100 MHz): 7.13 (2H, s, galloyl H), 7.12 (2H, s, galloyl H). For other signals, see Table I.

Camelliin A Aminoalditol (4a) An off-white amorphous powder, $[\alpha]_D^{20}$ +96.5° (*c* = 1.0, MeOH). *Anal.* Calcd for $C_{82}H_{66}N_2O_{44}\cdot 2H_2O$: C, 54.17; H, 3.88; N, 1.54. Found: C, 53.81; H, 3.68; N, 1.40. Negative FAB-MS *m/z*: 1781 $[M-H]^-$. ^{1}H-NMR (acetone-d_6 + D_2O, 270 MHz): 7.00 (2H, s, galloyl H), 6.87, 6.65, 6.63, 6.56 (each 1H, s, arom. H), 5.66 (1H, dd, *J* = 9, 2 Hz, H-3′), 5.38—5.45 (1H, m, H-2′), 5.11—5.21 (1H, m, H-4′), 4.35 (1H, dd, *J* = 12, 3 Hz, H-6′), 3.95 (1H, d, *J* = 9 Hz, H-5′), 4.50—3.60 (1H, m, H-1′), 2.99 (1H, dd, *J* = 14, 10 Hz, H-1′). For other signals, see Table I.

1-Desgalloyleugeniin Aminoalditol (5a) An off-white amorphous powder, $[\alpha]_D^{20}$ +78.9° (*c* = 0.8, MeOH). *Anal.* Calcd for $C_{41}H_{35}NO_{22}\cdot H_2O$: C, 51.02; H, 4.49; N, 1.45. Found: C, 51.04; H, 4.49; N, 1.45. Negative FAB-MS *m/z*: 892 $[M-H]^-$. ^{1}H-NMR (acetone-d_6 + D_2O, 100 MHz): 7.17 (2H, s, galloyl H), 7.22 (2H, s, galloyl H). For other signals, see Table I.

Gemin D Aminoalditol (6a) An off-white amorphous powder, $[\alpha]_D^{20}$ +80.7° (*c* = 2.0, MeOH). *Anal.* Calcd for $C_{34}H_{31}NO_{18}$: C, 55.06; H, 4.18; N, 1.89. Found: C, 54.83; H, 4.31; N, 1.77. ^{1}H-NMR (acetone-d_6 + D_2O, 100 MHz): 7.17 (2H, s, galloyl H). For other signals, see Table I.

Rugosin E Aminoalditol (7a) An off-white amorphous powder, $[\alpha]_D^{21}$ +85.8° (*c* = 1.0, acetone). *Anal.* Calcd for $C_{82}H_{63}NO_{48}\cdot H_2O$: C, 53.28; H, 3.52; N, 0.75. Found: C, 53.12; H, 3.65; N, 0.81. Negative FAB-MS *m/z*: 1828 $[M-H]^-$. ^{1}H-NMR (acetone-d_6 + D_2O, 270 MHz): 7.21, 7.17, 7.01, 6.97 (each 2H, s, galloyl H), 6.67, 6.46 (each 1H, s, arom. H), 6.09 (1H, d, *J* = 8 Hz, H-1′), 5.80 (1H, t, *J* = 10 Hz, H-3′), 5.53 (1H, dd, *J* = 4, 10 Hz, H-2′), 5.33 (1H, dd, *J* = 5, 12 Hz, H-6′), 5.16 (1H, t, *J* = 10 Hz, H-4′), 4.47 (1H, dd, *J* = 5, 10 Hz, H-5′), 3.78 (1H, d, *J* = 12 Hz, H-6′). For other signals, see Table I.

Isolation of Tannins Dried leaves of *L. flos-reginae*, collected in Java, Indonesia, in May, were extracted five times with 70% aqueous actone at room temperature. The extract was concentrated under reduced pressure, and the brown precipitates formed were filtered off with the aid of Celite 545. The filtrate was partitioned with ethyl acetate, and the aqueous layer was applied to a Sephadex LH-20 column, eluting with H_2O containing increasing proportions of MeOH to afford two fractions. Fraction 1 was repeatedly chromatographed over Sephadex LH-20 with EtOH–H_2O and MCI-gel CHP 20P with H_2O–MeOH to give 3-*O*-caffeoylquinic acid (**8**) (10 mg), gentisic acid 5-*O*-β-D-glucopyranoside (**9**) (132 mg), brevifolin carboxylic acid (**13**) (70 mg) and 4,6-(*S*)-HHDP-D-glucose (**11**) (110 mg). Fraction 2 was subjected to MCI-gel CHP 20P chromatography with

H_2O–MeOH to afford three fractions, 2-a, 2-b and 2-c. Fraction 2-a was repeatedly chromatographed over MCI-gel CHP 20P, Sephadex LH-20 and TSK gel Phenyl Toyopearl 650 M with H_2O–MeOH to give 2,3-(*S*)-HHDP-D-glucose (**12**) (70 mg), punicacortein A (**20**) (50 mg), 5-desgalloylstachyurin (**17**) (52 mg) and vascalagin (**19**) (80 mg). Fraction 2-b was repeatedly chromatographed over Sephadex LH-20 (H_2O–MeOH–50% acetone), TSK gel Toyopearl HW-40F (H_2O–MeOH–50% acetone), TSK gel Phenyl Toyopearl 650 M (H_2O–MeOH) and Cosmosil 75 C_{18}-OPN (H_2O–MeOH) to give reginins A (**23**) (500 mg) and B (**24**) (650 mg), flosin A (**22**) (98 mg), casuariin (**14**) (230 mg), stachyurin (**16**) (158 mg), castalagin (**18**) (170 mg) and pedunculagin (**1**) (1.35 g). Fraction 2-c was repeatedly chromatographed over Sephadex LH-20 (H_2O–MeOH–50% acetone), TSK gel Toyopearl HW-40F (MeOH, 50% acetone), TSK gel Phenyl Toyopearl 650 M (H_2O–MeOH) and Cosmosil 75 C_{18}-OPN (H_2O–MeOH) to give gentisic acid 5-*O*-β-D-(6′-*O*-galloyl)-glucopyranoside (**10**) (10 mg), casuarinin (**15**) (3.0 g) and lagerstroemin (**21**) (50 mg). Compounds **8**—**20** were identified by direct comparisons of their physical and spectral data with those of authentic samples.

Lagerstroemin (21) Colorless needles (H_2O), mp 230 °C (dec.), $[\alpha]_D^{20}$ +7.3° (*c* = 1.0, acetone), *Anal.* Calcd for $C_{55}H_{32}O_{34}\cdot 7H_2O$: C, 48.46; H, 3.55. Found: C, 47.98; H, 3.14. Negative FAB-MS *m/z*: 1235 $[M-H]^-$. ^{1}H-NMR (acetone-d_6 + D_2O, 270 MHz): 7.64, 7.20, 7.18 (each 1H, s valoneoyl H), 6.83, 6.59, 6.41 (each 1H, s, arom. H), 5.62 (1H, d, *J* = 5 Hz, H-1), 5.44 (1H, br s, H-3), 5.42 (1H, dd, *J* = 2, 9 Hz, H-4), 5.24 (1H, dd, *J* = 3, 9 Hz, H-5), 4.69 (1H, dd, *J* = 3, 13 Hz, H-6), 4.65 (1H, dd, *J* = 2, 5 Hz, H-2), 3.37 (1H, d, *J* = 13 Hz, H-6). ^{13}C-NMR (acetone-d_6, 67.8 MHz): 169.7, 169.3, 168.9, 165.6, 163.8 (–COO–), 160.7, 160.6 (δ-lactone), 149.9, 149.2, 145.9, 145.8, 145.3, 144.6, 144.5, 143.5, 141.6, 140.9, 140.4, 140.2, 139.0, 137.4, 137.3, 137.1, 137.0, 136.0, 135.0, 127.1, 126.6, 124.6, 119.8, 117.6, 116.4, 116.2, 116.1, 115.4, 115.1, 113.9, 113.1, 111.7, 109.8, 109.6, 108.7, 108.6, 108.4, 107.2, 105.5 (arom. C), 76.9 (C-2), 73.9 (C-4), 70.6 (C-5), 69.6 (C-3), 66.8 (C-1), 64.5 (C-6).

Methylation of 21 A mixture of **21** (200 mg), dimethyl sulfate (2 ml) and anhydrous potassium carbonate (2 g) in dry acetone (30 ml) was refluxed for 4 h. After removal of the inorganic salts by filtration, the filtrate was concentrated to a syrup and subjected to silica gel column chromatography [benzene–acetone (8 : 1)] to afford the octadecamethylate (**21a**) (94 mg), colorless needles (MeOH), mp 203—205 °C, $[\alpha]_D^{23}$ −35.2° (*c* = 0.6, acetone), *Anal.* Calcd for $C_{73}H_{68}O_{34}\cdot 1/2H_2O$: C, 58.51; H, 4.64. Found: C, 58.11; H, 4.64. FD-MS *m/z*: 1488 $[M^+]$. ^{1}H-NMR ($CDCl_3$, 270 MHz), 7.70, 7.31, 7.29, 7.04, 6.79, 6.50 (each 1H, s, arom. H), 5.52 (1H, dd, *J* = 2, 5 Hz, H-4), 5.42 (1H, d, *J* = 5 Hz, H-1), 5.33 (1H, t, *J* = 2 Hz, H-2), 4.79 (1H, dd, *J* = 3, 13 Hz, H-6), 4.27, 4.16, 4.04, 4.01, 4.00, 3.99, 3.98, 3.97, 3.96, 3.95, 3.93 (×2), 3.86, 3.84, 3.77, 3.71, 3.64, 3.44 (each 3H, s, OMe).

Alkaline Methanolysis of 21a **21a** (80 mg) was methanolyzed with 1% sodium methoxide in methanol (3 ml) at room temperature overnight. The reaction mixture was neutralized with Amberlite IR 120B (H^+ form), concentrated *in vacuo* and separated by silica gel chromatography. Elution with benzene–acetone (43 : 2) yielded dimethyl (*S*)-hexamethoxydiphenoate (**21b**) (12 mg) and valoneic acid dilactone heptamethylate (**21c**) (13 mg), colorless needles (MeOH), mp 264—265 °C, *Anal.* Calcd for $C_{28}H_{24}O_{13}$: C, 59.16; H, 4.26. Found: C, 59.28; H, 4.27. EI-MS *m/z*: 568 $[M]^+$. ^{1}H-NMR ($CDCl_3$, 100 MHz): 7.72, 7.35, 7.27 (each 1H, s, arom. H), 4.36, 4.20, 4.04, 3.99, 3.97, 3.80, 3.75 (each 3H, s, OMe). Further elution with benzene–EtOH (10 : 1) afforded the hydrolysate (**21d**) (10 mg), a white amorphous powder, $[\alpha]_D^{20}$ −40.4° (*c* = 0.6, acetone), FD-MS *m/z*: 598 $[M]^+$. ^{1}H-NMR (acetone-d_6, 270 MHz): 7.42 (1H, s, arom. H), 5.73 (1H, d, *J* = 2 Hz, H-1), 4.47 (1H, br d, *J* = 7 Hz, H-2), 4.15 (1H, d, *J* = 8 Hz, H-4), 4.05, 3.98, 3.95, 3.89, 3.59, 3.56 (×2) (each 3H, s, OMe).

Alkaline Treatment of 21c, Followed by Methylation A solution of **21c** (10 mg) in 5% NaOH [H_2O–MeOH (1 : 1)] (2 ml) was heated at 70 °C for 30 min. The reaction mixture was treated with dimethyl sulfate (1 ml) at 70 °C for 30 min. The solution was acidified with 1 N HCl (5 ml) and extracted three times with ether. The organic layer was dried over sodium sulfate, concentrated to dryness and treated with ethereal diazomethane. After evaporation of the solvent, the syrupy residue was chromatographed over silica gel with benzene–acetone (19 : 1) to give trimethyl octa-*O*-methyl valoneate (**21e**) (5 mg).

Partial Hydrolysis of 21 **21** (100 mg) in water was heated at 80 °C for 3 h. After filtration of the resulting precipitates (ellagic acid), the filtrate was directly subjected to Sephadex LH-20 chromatography with 60% MeOH to give the partial hydrolysate (**21f**) (23 mg), a tan amorphous powder, $[\alpha]_D^{20}$ −45.6° (*c* = 0.6, MeOH), Negative FAB-MS *m/z*: 933 $[M-H]^-$. ^{1}H-NMR (acetone-d_6 + D_2O, 270 MHz): 7.65, 7.19, 7.15, 6.21 (each 1H, s, arom. H), 5.55 (1H, d, *J* = 5 Hz, H-1), 5.23 (1H, dd, *J* = 2, 3 Hz, H-3), 4.98 (1H, dd, *J* = 3, 8 Hz, H-5), 4.78 (1H, dd, *J* = 2, 5 Hz, H-2), 3.95 (1H, dd, *J* = 3, 8 Hz, H-4), 3.80 (2H, m, H-6).

Flosin A (22) An off-white amorphous powder, $[\alpha]_D^{26}$ +32° (*c* = 1.1, MeOH), *Anal.* Calcd for $C_{41}H_{28}O_{27}$: C, 51.69; H, 2.96. Found: C, 51.82; H, 2.88. Negative FAB-MS *m/z*: 951 $[M-H]^-$. ^{1}H-NMR (acetone-d_6 + D_2O, 100 MHz): 7.07, 7.06 (1H in total, each s, valoneoyl H), 6.66, 6.65 (1H in total, each s, arom. H), 6.58 (1H, s, arom. H), 6.34, 6.26 (1H, in total, each s, arom. H), 6.30, 6.29 (1H in total, each s, arom. H), 3.50—5.50 (7H, m, glc. H). ^{13}C-NMR (acetone-d_6 + D_2O, 25.05 MHz): 169.3, 169.0, 168.8, 168.5, 168.1, 167.2 (–COO–). For other signals, see Table II.

Partial Hydrolysis of 22 A solution of **22** (10 mg) in water (2 ml) was heated on a water bath (90 °C) for 15 h. The reaction mixture was subjected to MCI-gel CHP 20P chromatography with 10% MeOH to yield 2,3-(*S*)-HHDP-D-glucose (**12**) (2 mg).

Methylation of 22 A mixture of **22** (20 mg), dimethyl sulfate (0.5 ml) and anhydrous potassium carbonate (1 g) in dry acetone (5 ml) was heated under reflux for 5 h. Work-up as described above afforded the hexadecamethylates as an inseparable mixture (**22b**) (11 mg), a white amorphous powder, FD-MS *m/z*: 1176 $[M]^+$. ^{1}H-NMR ($CDCl_3$, 270 MHz): 7.25, 7.21 (valoneoyl H_c), 6.78, 6.73, 6.72, 6.56 (valoneoyl H_a and HHDP-H), 6.47, 6.43 (valoneoyl H_b), 5.04 (t, *J* = 10 Hz, α, β-H-3), 4.96—5.19 (α, β-H-2, α, β-H-4, α, β-H-6), 4.91 (d, *J* = 5 Hz, α-H-1), 4.58 (d, *J* = 8 Hz, β-H-1), 4.23, 4.21 (each d, *J* = 9 Hz, α, β-H-5), 3.55—4.10 (OMe and α, β-H-6).

Alkaline Methanolysis of 22b **22b** (10 mg) was treated with 2% sodium methoxide in dry methanol (0.5 ml) at room temperature for 24 h. After neutralization with Amberlite IR 120B (H^+ form), the solution was concentrated *in vacuo* and the residue was chromatographed over silica gel with benzene–acetone (8 : 1) to furnish dimethyl (*S*)-hexamethoxydiphenoate (**21b**) (4 mg) and trimethyl octa-*O*-methyl-(*S*)-valoneate (**22c**) (3 mg).

Preparation of the Aminoalditol Derivative (22a) **22** (10 mg) was treated as described in the general procedure to furnish the aminoalditol (**22a**) as a brown amorphous powder, $[\alpha]_D^{30}$ +114.5° (*c* = 0.5, MeOH), *Anal.* Calcd for $C_{48}H_{35}NO_{27}$: C, 53.58; H, 3.50; N, 1.32. Found: C, 53.31; H, 3.57; N, 1.42. ^{1}H-NMR (acetone-d_6 + D_2O, 270 MHz): 6.70, 6.53 (each 1H, s, HHDP-H). For other signals, see Table I.

Reginin A (23) An off-white amorphous powder, $[\alpha]_D^{26}$ +62° (*c* = 0.9, MeOH), *Anal.* Calcd for $C_{75}H_{50}O_{48}$: C, 52.39; H, 2.91. Found: C, 52.20; H, 2.51. Negative FAB-MS *m/z*: 1717 $[M-H]^-$. ^{1}H-NMR (acetone-d_6 + D_2O, 100 MHz): 7.03, 7.02 (1H in total, each s, valoneoyl H_c), 6.82, 6.81 (1H in total, each s, arom. H), 6.65, 6.64 (1H in total, each s, arom. H), 6.58 (1H, s, arom. H), 6.58 (1H, s, arom. H), 6.56. 6.52 (1H in total, each s, arom. H), 6.31 (1H, s, arom. H), 6.35, 6.27 (1H in total, each s, arom. H), 5.60 (1H, d, *J* = 5 Hz, H-1′), 3.50—5.47 (13 H, m, glc. H). ^{13}C-NMR (acetone-d_6 + D_2O, 67.8 MHz): see Table II.

Methylation of 23 A mixture of **23** (50 mg), dimethyl sulfate (2 ml) and anhydrous potassium carbonate (2 g) in dry acetone (10 ml) was heated under reflux for 5 h. The reaction mixture was chromatographed over silica gel with benzene–acetone to afford among many uncharacterized products, a product (**3a**) (4 mg).

Partial Hydrolysis of 23 An aqueous solution (3 ml) of **23** (50 mg) was heated at 80—90 °C for 20 h. The reaction mixture was directly subjected to MCI-gel CHP 20P chromatography with H_2O–MeOH to afford lagerstroemin (**21**) (910 mg) and 2,3-(*S*)-HHDP-D-glucose (**12**) (5 mg).

Preparation of the Aminoalditol Derivative (23a) **23** (15 mg) was treated as described in the general procedure to give the aminoalditol (**23a**) (13 mg) as a brown amorphous powder, $[\alpha]_D^{30}$ +34.2° (*c* = 0.8, MeOH), *Anal.* Calcd for $C_{82}H_{57}NO_{48}\cdot H_2O$: C, 52.93; H, 3.28; N, 0.75. Found: C, 52.77; H, 3.50; N, 1.00. ^{1}H-NMR (acetone-d_6 + D_2O, 270 MHz): 6.88, 6.65, 6.62, 6.59, 6.58 (each 1H, s, arom. H), 5.61 (1H, d, *J* = 5 Hz, H-1′), 5.48 (1H, t, *J* = 2 Hz, H-3′), 5.40 (1H, dd, *J* = 2, 8 Hz, H-4′), 5.35 (1H, dd, *J* = 3, 8 Hz, H-5′), 4.82 (1H, dd, *J* = 3, 14 Hz, H-6′), 4.63 (1H, dd, *J* = 2, 5 Hz, H-2′), 3.86 (1H, d, *J* = 14 Hz, H-6′). For other signals, see Table I. ^{13}C-NMR (acetone-d_6 + D_2O, 25.05 MHz): 169.9, 169.8, 169.5 (×3), 169.1, 168.7 (×3) (–COO–), 165.2, 153.1 (anisidine moiety), 77.0 (C-2′), 76.2 (C-3), 74.2 (C-4), 73.8 (C-4′), 73.0 (C-2), 71.3 (C-5′), 70.1 (C-3′), 68.7 (C-5), 67.1 (C-1′), 65.0 (C-6′), 61.7 (C-6), 44.7 (C-1).

Reginin B (24) An off-white amorphous powder, $[\alpha]_D^{26}$ +26° (*c* = 1.3, MeOH), *Anal.* Calcd for $C_{75}H_{50}O_{48}\cdot 3H_2O$: C, 50.79; H, 3.27. Found: C, 50.87; H, 3.06. Negative FAB-MS *m/z*: 1717 $[M-H]^-$. ^{1}H-NMR (acetone-d_6 + D_2O, 270 MHz): 7.04, 7.03 (1H in total, s, valoneoyl H_c), 6.95, 6.94 (1H in total, s, arom. H), 6.65, 6.64 (1H in total, arom. H),

6.62, 6.61 (1H in total, s, arom. H), 6.60 (1H, s, arom. H), 6.55, 6.54 (1H, in total, s, arom. H), 6.31, 6.30 (1H in total, s, arom. H), 6.30, 6.25 (1H in total s, arom. H), 3.50—5.70 (14H, glc. H). ^{13}C-NMR (acetone-d_6+D_2O, 67.8 MHz): see Table II.

Methylation of 24, Followed by Alkaline Methanolysis A mixture of **24** (100 mg), dimethyl sulfate (2 ml) and anhydrous potassium carbonate (2 g) in dry acetone (20 ml) was heated under reflux for 7 h. The reaction mixture was worked up as before to afford a mixture of methylates (60 mg). A part (20 mg) of this methylate was treated with 2% sodium methoxide in dry MeOH (1 ml) at room temperature for 24 h. Separation of the reaction products as described for **22b** gave dimethyl (*S*)-hexamethoxydiphenoate (**21b**) (5 mg) and trimethyl octa-*O*-methyl-(*S*)-valoneate (**22c**) (3 mg).

Partial Hydrolysis of 24 A solution of **24** (50 mg) in water (5 ml) was heated at 80—90 °C for 20 h. The reaction products were separated by MCI-gel CHP 20P chromatography with H_2O–MeOH to afford 5-desgalloyl stachyurin (**17**) (5 mg) and 2,3-(*S*)-HHDP-D-glucose (**12**) (2 mg).

Preparation of the Aminoalditol Derivative (24a) **24** (50 mg) was treated as described in the general procedure to give **24a** (28 mg), a brown amorphous powder, $[\alpha]_D^{30}$ +73° (*c*=0.8, MeOH), *Anal.* Calcd for $C_{82}H_{57}NO_{48}$: C, 52.93; H, 3.28; N, 0.75. Found: C, 52.97; H, 3.28; N, 0.87. ^{1}H-NMR (acetone-d_6+D_2O, 270 MHz): 6.98, 6.60, 6.59, 6.58, 6.56, 6.54, 6.50 (each 1H, s, arom. H), 5.70 (1H, dd, *J*=2, 8 Hz, H-4'), 5.36 (1H, dd, *J*=3, 8 Hz, H-5'), 5.34 (1H, t, *J*=2 Hz, H-3'), 4.98 (1H, d, *J*=2 Hz, H-1'), 4.87 (1H, dd, *J*=3, 13 Hz, H-6'), 4.83 (1H, t, *J*=2 Hz, H-2'), 3.91 (1H, d, *J*=13 Hz, H-6'). For other signals, see Table I.

Acknowledgements The authors thank P. T. Eisai Indonesia for the supply of plant materials, Mr. Y. Tanaka and Miss Y. Soeda for ^{1}H- and ^{13}C-NMR measurements, Mr. R. Isobe for MS measurements and staff of the Central Analysis Room of this university for elemental analysis. One of us (Y.-M. Xu) wishes to express his gratitude to Nippon Mektron Co., for the award of a scholarship.

References

1) Part CV: S.-H. Lee, T. Tanaka, G. Nonaka and I. Nishioka, *Chem. Pharm. Bull.*, **39**, 630 (1991).
2) R. Oshima, J. Kumanotani and C. Watanabe, *J. Chromatogr.*, **259**, 159 (1983).
3) D. R. Knapp, "Handbook of Analytical Derivatization Reactions," John Wiley & Sons, Inc., New York, 1979, pp. 539—598.
4) O. T. Schmidt, L. Würtele and A. Harreus, *Justus Liebigs Ann. Chem.*, **690**, 150 (1965).
5) T. Okuda, T. Hatano, K. Yazaki and N. Ogawa, *Chem. Pharm. Bull.*, **30**, 4230 (1982).
6) T. Yoshida, Y. Maruyama and T. Okuda, The 103rd Annual Meeting of the Pharmaceutical Society of Japan, Tokyo, April 1985.
7) J.-H. Lin, T. Tanaka, G. Nonaka, I. Nishioka and I.-S. Chen, *Chem. Pharm. Bull.*, **38**, 2162 (1990).
8) T. Yoshida, Y. Maruyama, T. Okuda, M. U. Memon and T. Shingu, *Chem. Pharm. Bull.*, **30**, 4245 (1982).
9) T. Okuda, T. Hatano and N. Ogawa, *Chem. Pharm. Bull.*, **30**, 4234 (1982).
10) H. M. Barnes, J. R. Feldman and W. V. White, *J. Am. Chem. Soc.*, **72**, 4198 (1950).
11) K. Ishimaru, G. Nonaka and I. Nishioka, *Phytochemistry*, **26**, 1501 (1987).
12) O. T. Schmidt and R. Eckert, *Justus Leibigs Ann. Chem.*, **618**, 71 (1958); O. T. Schmidt, R. Eckert, E. Gunther and H. Filsser, *ibid.*, **706**, 24 (1967).
13) G. Nonaka, R. Sakai and I. Nishioka, *Phytochemistry*, **23**, 1753 (1984).
14) M. K. Seikel and W. E. Hillis, *Phytochemistry*, **9**, 1115 (1970).
15) G. Nonaka, T. Sakai, T. Tanaka, K. Mihashi and I. Nishioka, *Chem. Pharm. Bull.*, **38**, 2151 (1990).
16) T. Tanaka, G. Nonaka and I. Nishioka, *Chem. Pharm. Bull.*, **34**, 656 (1986).
17) S.-H. Lee, T. Tanaka, G. Nonaka and I. Nishioka, *Phytochemistry*, **29**, 3621 (1990).
18) G. Naonaka, T. Tanaka and I. Nishioka, *J. Chem. Soc., Perkin Trans. 1*, **1982**, 1067.
19) R. Saijo, G. Nonaka and I. Nishioka, *Chem. Pharm. Bull.*, **37**, 2063 (1990).
20) R. Isobe, T. Tanaka, G. Nonaka and I. Nishioka, *Chem. Pharm. Bull.*, **37**, 1748 (1989).

Tannins and Related Compounds. CVII.[1] Structure Elucidation of Three New Monomeric and Dimeric Ellagitannins, Flosin B and Reginins C and D, Isolated from *Lagerstroemia flos-reginae* RETZ.

Ya-Ming XU,[a] Takashi TANAKA,[b] Gen-ichiro NONAKA*,[b] and Itsuo NISHIOKA[b]

Shanghai Institute of Materia Medica, Academica Sinica,[a] 319 Yueyan Road, Shanghai, Peoples' Repulic of China and Faculty of Pharmaceutical Sciences, Kyushu University 62,[b] 3-1-1 Maidashi, Higashi-ku, Fukuoka 812, Japan. *Received October 3, 1990*

Further chemical work on tannins in the leaves of *Lagerstroemia flos-reginae* RETZ. (Lythraceae) has resulted in the isolation of new monomeric (flosin B) and dimeric ellagitannins (reginins C and D), together with pterocarinin A (1) and 5-desgalloylpterocarinin A (2). On the basis of chemical and spectroscopic evidence, the structure of flosin B was determined to be a *C*-glycosidic ellagitannin (3) possessing a valoneic acid dilactonyl group, while reginins C and D were characterized as dimeric ellagitannins (6 and 10, respectively), in which a pedunculagin moiety is connected to pterocarinin A and casuarinin [the C-1 epimer of stachyurin (5)] moieties, respectively, through a carbon-to-oxygen bond.

Keywords *Lagerstroemia flos-reginae*; Lythraceae; *C*-glycosidic ellagitannin; flosin B; reginin C; reginin D; biomimetic synthesis; L-ascorbic acid; tannin

In the preceding paper,[1] we reported the isolation and characterization of eighteen hydrolyzable tannins and related compounds, including four new hydrolyzable tannins [reginins A (**7**) and B (**8**), flosin A and lagerstroemin (**4**)], from the leaves of *Lagerstroemia flos-reginae* RETZ. (Lythraceae). Further chemical examination of tannins in this plant has resulted in the isolation of three new ellagitannins [flosin B (**3**) and reginins C (**6**) and D (**10**)], together with two known compounds [pterocarinin A (**1**) and 5-desgalloylpterocarinin A (**2**)]. This paper deals with the isolation and structure elucidation of these compounds.

A combination of Sephadex LH-20, MCI-gel CHP 20P, TSK gel Toyopearl HW 40F and TSK gel Phenyl Toyopearl 650M chromatographies of fraction 2, which was previously obtained from the aqueous acetone extract of the dried leaves, afforded flosin B (**3**), reginins C (**6**) and D (**10**), pterocarinin A (**1**),[2] and 5-desgalloylpterocarinin A (**2**).[2]

Flosin B (**3**), an off-white amorphous powder, $[\alpha]_D$ +65° (MeOH), gave positive ferric chloride and nitrous acid tests,[3] characteristic of ellagitannins. The negative fast atom bombardment mass spectrum (FAB-MS) gave the same $[M-H]^-$ peak at *m/z* 1235 as that of previously reported lagerstroemin (**4**). The proton nuclear magnetic resonance (^{1}H-NMR) spectrum showed six aromatic one-proton singlets, of which the chemical shifts of three signals (δ 7.50, 7.20 and 7.19) were similar to those (δ 7.64, 7.20 and 7.14) found in **4**, a finding consistent with the presence of a valoneic acid dilactonyl group. The aliphatic signal pattern was typical of a *C*-glycosidic ellagitannin, showing no anomeric proton signal, and the chemical shifts and coupling constants agreed well with those of stachyurin (**5**).[4] Among these signals, the small coupling constant of the *C*-glycosidic H-1 signal [δ 5.02 (d, J=1.5 Hz)] clearly indicated that **3** possesses the same configuration at the C-1 position as that of **5**. Furthermore, the chemical shifts of the aliphatic signals in the carbon-13 nuclear magnetic resonance (^{13}C-NMR) spectrum were almost in line with those of **5**, while among seven carboxyl carbon resonances, two upfield signals (δ 160.8 and 161.2) were characteristic of the δ-lactone carbons in the valoneoyl group. Thus, these findings suggested that flosin B has the same configuration in the *C*-glycoside moiety as that of **5**, and is the C-1 epimer of lagerstroemin (**4**).

Epimerization[5] at the *C*-glycosidic C-1 position was carried out by heating **4** in aqueous solution to give **3** in 15% yield. Accordingly, the structure of flosin B was unequivocally established as **3**.

Reginin C (**6**) was isolated as an off-white amorphous powder, $[\alpha]_D$ +53.8° (MeOH). The ^{1}H-NMR spectrum was extremely complicated. However, the chemical shifts of aromatic signals, although the signals were partly split, were found to be almost the same as those of the previously reported dimeric ellagitannin, reginin B (**8**). The aliphatic signal pattern between δ 4.0—6.7 was also closely correlated with that of **8**. The observation of additional complex signals at δ 3.5—4.0 indicated the existence of an extra polyalcohol

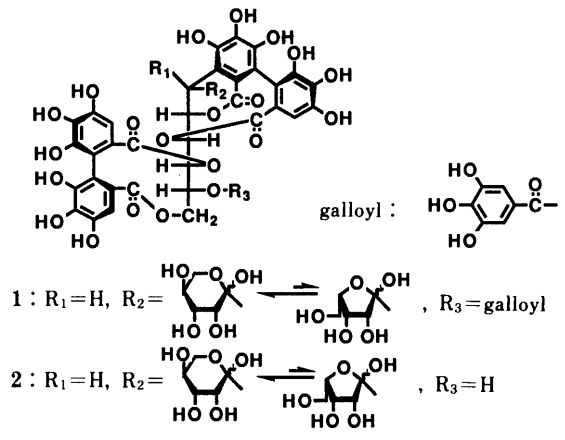

Chart 1

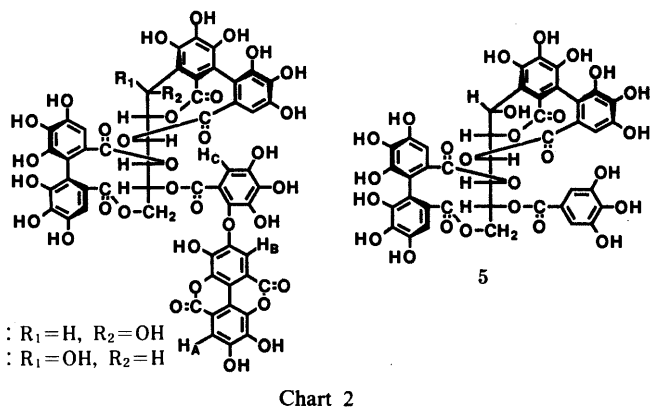

Chart 2

moiety carrying no acyl group. Although the aromatic signal pattern in the ^{13}C-NMR spectrum was complicated, the aliphatic signals arising from the major conformers could be assigned as shown in Table I by comparison with those of pterocarinin A(**1**) and pedunculagin (**9**). Among these, the signal at δ 102.1 was assignable to a ketal carbon, and the signal at δ 46.3 to the C-1 atom of an open-chain form of the glucose core to which the extra polyalcohol moiety is connected through a carbon-to-carbon bound. Furthermore, the observation of a pair of doublets at δ 95.0 and 91.5 was indicative of the presence of β- and α-forms of the glucopyranose cores. From these observations, reginin C was considered to be a dimeric ellagitannin in which pterocarinin A (**1**) and pedunculagin (**9**) moieties are linked through a carbon-to-oxygen bond. This consideration was also supported by the observation of the intense $[M-H]^-$ peak at *m/z* 1849 in the negative FAB-MS.

In order to confirm the structure, the synthesis of reginin C was carried out by condensation of L-ascorbic acid and reginin B (**7**),[2] giving reginin C in 20% yield. Therefore, the structure of reginin C was determined unambiguously to be as represented by the formula **6**.

Reginin D (**10**) was isolated as an off-white amorphous powder, $[\alpha]_D$ +82° (MeOH). The negative FAB-MS showed the same $[M-H]^-$ peak at *m/z* 1717 as those of reginins A (**7**) and B (**8**). The ^{1}H-NMR spectrum was duplicated owing to the presence of an α- and β-anomeric mixture. The aromatic signals all appearing as singlets corresponded to eight protons in total. The ^{13}C-NMR spectrum (Table II) of **10** showed aliphatic signal patterns similar to those of reginin A (**7**), and the signals at δ 94.8 and 91.3 were attributable to the β- and α-anomeric carbons in the glucopyranose moiety.

To avoid tautomerism, reginin D was treated with *p*-anisidine in ethanolic acetic acid, followed by sodium cyanoborohydride reduction.[1] The ^{1}H-NMR spectrum of the aminoalditol derivative (**14**) thus obtained was simplified, and clearly showed signal patterns closely correlated with those of the reginin A aminoalditol (**15**), although a moderate upfield shift (δ 6.25, ref. δ 6.58 in **15**) of one (H-B in the valoneoyl group) of the aromatic signals was observed in **14**.[1]

Partial hydrolysis of **10** in hot water afforded lagerstroemin (**4**) and 4,6-(*S*)-hexahydroxydiphenoyl(HHDP)-D-glucose (**13**). This result indicated that the valoneoyl group is located at the glucopyranose C-2 and C-3 positions in **10**. Furthermore, methylation of **10** with dimethyl sulfate and potassium carbonate in dry acetone, followed by alkaline methanolysis with 2% sodium methoxide, gave dimethyl (*S*)-hexamethoxydiphenoate (**11**) and trimethyl octa-*O*-methyl-(*S*)-valoneate (**12**). Thus, the atropisomerism of the valoneoyl ester group in **10** was established to be in the *S*-series. From these chemical and spectroscopic findings, the structure of reginin D was determined to be 10. The orientation of the valoneoyl group still remains to

Table I. ^{13}C-NMR Data for Reginin C (**6**), Pterocarinin A (**1**), Reginin B (**8**) and Pedunculagin (**9**)

	6[a,c]	1[a,c]	8[a]	9[b]
1″	102.1	102.0		
2″	72.2	72.2		
3″	72.2	72.2		
4″	66.9	66.9		
5″	63.2	63.2		
1′	46.3	46.4	64.7	
2′	75.5	75.3	81.6	
3′	74.3	74.2	72.3	
4′	73.9	73.5	73.7	
5′	70.7	71.1	71.1	
6′	64.4	64.5	64.4	
1 α	91.5		91.4	91.8
β	95.0		94.9	95.4
2 α	75.5		75.5	75.6
β	78.2		78.2	78.3
3 α	75.7		75.7	75.8
β	77.2		77.2	77.6
4 α	70.4		70.4	69.6
β	70.8		70.9	69.9
5 α	67.5		67.5	67.4
β	72.3		72.2	72.5
6 α	64.0		64.4	63.6
β	64.0		64.4	63.6

Acetone-d_6+D_2O, ppm, TMS. *a*) Spectra measured at 67.8 MHz. *b*) Spectrum measured at 25.05 MHz. *c*) Only the signals of major conformers are given.

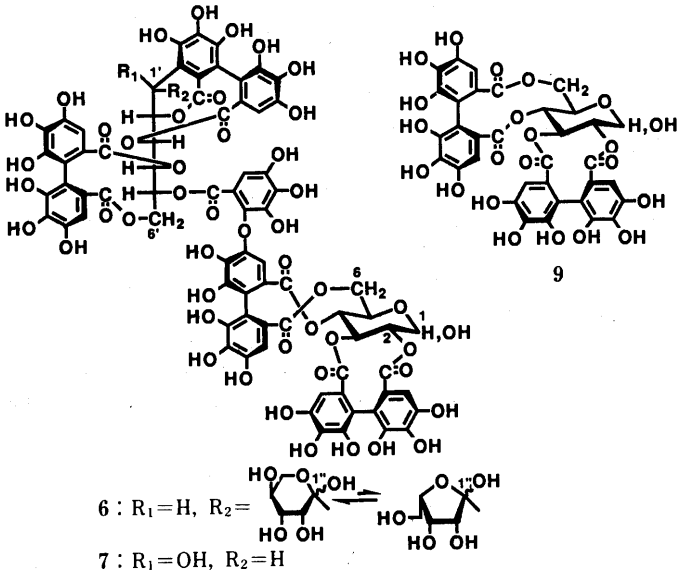

Chart 3

Table II. ^{13}C-NMR Data for Reginins D (**10**) and A (**7**)

		C-1	C-2	C-3	C-4	C-5	C-6	C-1′	C-2′	C-3′	C-4′	C-5′	C-6′
10	β	94.8	78.5	77.0	69.9	72.2	63.8	67.0	77.4	69.9	74.1	71.3	64.3
	α	91.3	75.6	75.6	69.8	67.2	63.8						
7	β	95.3	78.8	77.6	70.9	72.7	64.4	67.8	77.5	70.3	74.6	71.5	65.0
	α	91.8	76.0	76.2	70.3	67.5	64.4						

67.8 MHz, acetone-d_6+D_2O, ppm, TMS.

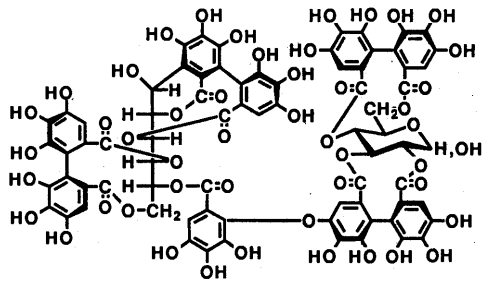

10

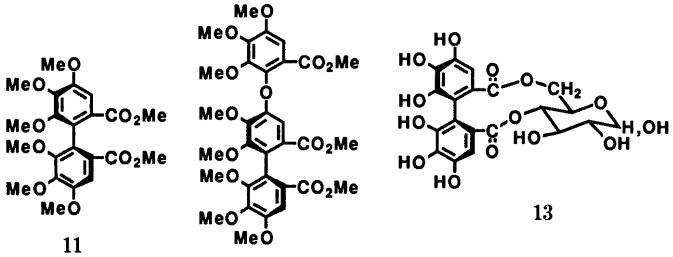

11 12 13

Chart 4

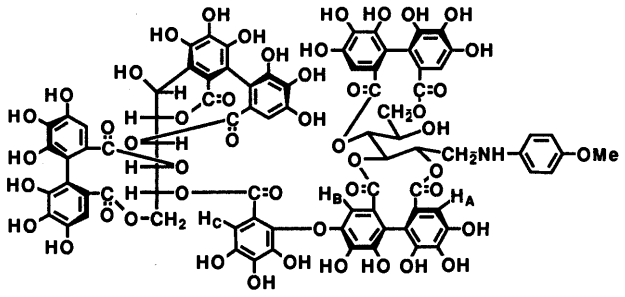

14

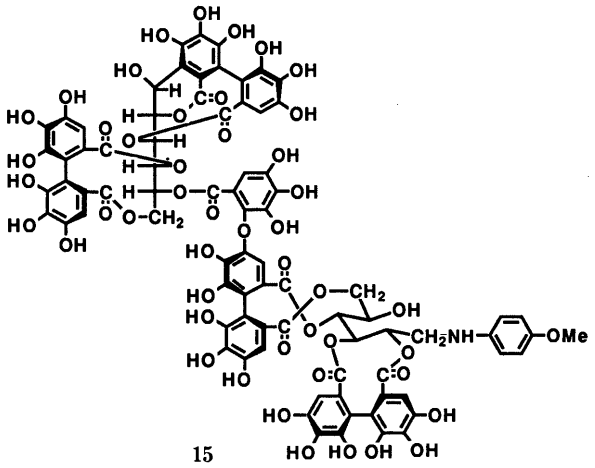

15

be proved.

Reginin C (**6**) is the first example of a dimeric ellagitannin containing a C_5-polyalcohol moiety at the C-1 position of the open-chain form of glucose.

Experimental

Details of the instruments and chromatographic conditions used throughout this work are the same as described in the previous paper.[1]

Isolation of Tannins Extraction and fractionation procedures were described in the preceding paper.[1] On chromatography over Sephadex LH-20, MCI-gel CHP 20P, TSK gel Toyopearl HW-40F and TSK gel Phenyl Toyopearl 650M with H_2O–MeOH, fraction 2-a yielded 5-desgalloylpterocarinin A (**2**) (50 mg) and reginin C (**6**) (70 mg), fraction 2-b afforded pterocarinin A (**1**) (70 mg) and fraction 2-c gave flosin B (**8**) (50 mg) and reginin D (**10**) (100 mg).

Flosin B (3) An off-white amorphous powder, $[\alpha]_D^{26}$ +65° (c=1.4, MeOH). *Anal.* Calcd for $C_{55}H_{32}O_{34}$: C, 51.72; H, 2.91. Found: C, 51.69; H, 3.09. Negative FAB-MS m/z: 1235 $[M-H]^-$. ^{1}H-NMR (270 MHz, acetone-d_6 + D_2O): 7.56 (1H, s, valoneoyl H-A), 7.20, 7.29 (each 1H, s, valoneoyl H-B and H-C), 6.88, 6.51, 6.40 (each 1H, s, arom. H), 5.57 (1H, dd, J=2, 8 Hz, glc. H-4), 5.21 (1H, dd, J=3, 8 Hz, glc. H-5), 5.02 (1H, d, J=1.5 Hz, glc. H-1), 5.01 (1H, t, J=2 Hz, glc. H-3), 4.80 (1H, dd, J=1.5, 2 Hz, glc. H-2), 4.75 (1H, dd, J=3, 13 Hz, glc. H-6), 3.77 (1H, d, J=13 Hz, glc. H-6). ^{13}C-NMR (25.05 MHz, acetone-d_6 + D_2O): 169.2 (×2), 168.7, 166.7, 164.4 (–COO–), 161.2, 160.8 (carboxyl C of δ-lactone), 150.1, 149.4 (arom. C), 81.4 (C-2), 72.9 (C-4), 72.0 (C-3), 70.9 (C-5), 64.7 (C-1), 64.4 (C-6).

Epimerization of Lagerstroemin (4) A solution of **4** (50 mg) in water was heated at 80 °C for 20 h. The reaction product was purified on an MCI-gel CHP 20P column with H_2O–MeOH to afford flosin B (**3**) (8 mg) and the starting material (**4**) (20 mg).

Reginin C (6) An off-white amorphous powder, $[\alpha]_D^{30}$ +53.8° (c=0.9, MeOH). *Anal.* Calcd for $C_{80}H_{58}O_{52}\cdot H_2O$: C, 51.39; H, 3.21. Found: C, 51.15; H, 3.24. Negative FAB-MS m/z: 1849 $[M-H]^-$. ^{1}H-NMR (270 MHz, acetone-d_6 + D_2O): 7.02, 7.01 (1H in total, each s, arom. H), 6.64, 6.63 (1H in total, each s, arom. H), 6.60 (1H, s, arom. H), 6.59, 6.58 (1H in total, each s, arom. H), 6.49, 6.48 (1H in total, each s, arom. H), 6.30 (1H, s, arom. H), 6.29, 6.24 (1H in total, each s, arom. H), 3.50—5.70 (19H, m, polyalcohol-H). ^{13}C-NMR (67.8 MHz, acetone-d_6 + D_2O): 169.5, 169.4, 169.3, 169.2, 168.8, 168.7, 167.1, 164.8, 164.7 (–COO–). For other signals, see Table I.

Condensation of Reginin B (7) with L-Ascorbic Acid, Giving Reginin C (6) A mixture of **7** (60 mg) and L-ascorbic acid (30 mg) in 0.1 M acetic acid was heated at 80 °C for 7 h. The reaction product was separated by MCI-gel CHP 20P chromatography with H_2O–MeOH (4:1) to give the crude product, which was further purified on a Cosmosil 75C_{18}-OPN column with H_2O–MeOH to yield reginin C (**6**) (12 mg).

Reginin D (10) An off-white amorphous powder, $[\alpha]_D^{26}$ +82° (c=1.8, MeOH). *Anal.* Calcd for $C_{75}H_{50}O_{48}\cdot 3H_2O$: C, 50.79; H, 3.27. Found: C, 50.83; H, 3.09. Negative FAB-MS m/z: 1717 $[M-H]^-$. ^{1}H-NMR (100 MHz, acetone-d_6 + D_2O): 7.04 (1H, s, valoneoyl H-C), 6.83, 6.80 (1H in total, each s, arom. H), 6.65 (1H, s, arom. H), 6.63, 6.61 (1H, in total, each s, arom. H), 6.57 (1H, s, arom. H), 6.54, 6.53 (1H in total, each s, arom. H), 6.32 (1H, s, arom. H), 6.25, 6.21 (1H in total, each s, arom. H), 3.50—5.70 (14H in total, m, polyalcohol-H). ^{13}C-NMR (25.05 MHz, acetone-d_6 + D_2O): 170.2, 169.8, 169.5, 168.8, 168.7, 168.4, 168.0, 165.2, 165.0, 164.5, 164.2 (–COO–). For other signals, see Table II.

Methylation of 10, Followed by Alkaline Methanolysis A mixture of **10** (50 mg), dimethyl sulfate (1 ml) and anhydrous potassium carbonate (1.0 g) in dry acetone (10 ml) was heated under reflux for 5 h. After removal of the inorganic salts by filtration, the filtrate was concentrated to dryness, and the oily residue was chromatographed over silica gel with benzene containing increasing proportions of acetone to afford a methylate mixture (25 mg), which was treated with 2% sodium methoxide in dry methanol at room temperature for 24 h. After neutralization with Amberlite IR 120B (H^+ form) and concentration *in vacuo*, the residue was chromatographed over silica gel with benzene–acetone to give dimethyl (*S*)-hexamethoxydiphenoate (**11**) (5 mg) and trimethyl octa-*O*-methyl-(*S*)-valoneate (**12**) (1 mg).

Preparation of the Aminoalditol Derivative (14) A mixture of **10** (20 mg) and *p*-anisidine (5 mg) in 20% ethanolic acetic acid (1 ml) was kept at room temperature for 2 h with stirring. The reaction mixture was treated with sodium cyanoborohydride (5 mg) at room temperature for 1 h. The product was purified by Sephadex LH-20 chromatography with EtOH–H_2O to furnish the aminoalditol (**14**). An off-white amorphous powder, $[\alpha]_D^{30}$ +79.3° (c=0.6, MeOH). *Anal.* Calcd for $C_{82}H_{57}O_{48}\cdot H_2O$: C, 52.93; H, 3.28; N, 0.75. Found: C, 52.92; H, 3.39; N, 0.79. ^{1}H-NMR (270 MHz, acetone-d_6 + D_2O): 7.02 (1H, s, valoneoyl H-C), 6.84, 6.69, 6.60, 6.58, 6.57 (each 1H, s, arom. H), 6.58 (5H, s, anisidine- and HHDP-H), 6.25 (1H, s, valoneoyl H-B), 5.58 (1H, d, J=5 Hz, glc. H-1'), 5.51 (1H, dd, J=1.5, 9 Hz, glc. H-3), 5.35—5.45 (3H, m, glc. H-2', 4', and 5'), 5.25 (1H, m, glc. H-2), 5.21 (1H, dd, J=8, 1 Hz, glc. H-4), 4.95 (1H, dd, J=2.5, 13 Hz, glc. H-6'), 4.70 (1H, dd, J=9, 13 Hz, glc. H-6), 4.64 (1H, dd, J=1.5, 5 Hz, glc. H-2'), 4.27 (1H, dd, J=2, 8 Hz, glc. H-5), 3.50—4.10 (overlapped with HOD signals, glc. H-6', 6 and 1), 3.61 (3H, s, OMe), 3.42 (1H, dd, J=8, 13 Hz, glc. H-1).

Partial Hydrolysis of 10 An aqueous solution (1 ml) of **10** (20 mg) was heated at 80 °C for 20 h. The reaction mixture was directly subjected to MCI-gel CHP 20P chromatography with H_2O–MeOH to give lagerstroemin (**4**) (5 mg) and 4,6-HHDP-D-glucose (**13**) (2 mg).

Acknowledgements The authors would like to thank P. T. Eisai Indonesia for the supply of plant materials, Mr. Y. Tanaka and Miss Y. Soeda for ^1H- and ^{13}C-NMR spectral measurements, Mr. R. Isobe for MS measurements and the staff of the Central Analysis Room of this University for elemental analysis. Y. M. Xu is grateful to Nippon Mektron Co., for the award of a scholarship.

References

1) Part CVI: Y.-M. Xu, T. Sakai, T. Tanaka, G. Nonaka and I. Nishioka, *Chem. Pharm. Bull.*, **39**, 1639 (1991).
2) G. Nonaka, K. Ishimaru, R. Azuma, M. Ishimatsu and I. Nishioka, *Chem. Pharm. Bull.*, **37**, 2071 (1989).
3) E. C. Bate-Smith, *Phytochemistry*, **11**, 1153 (1972).
4) G. Nonaka, T. Sakai, T. Tanaka, K. Mihashi and I. Nishioka, *Chem. Pharm. Bull.*, **38**, 2151 (1990).
5) W. Mayer, W. Babler, A. Riester and H, Korger, *Justus Liebigs Ann. Chem.*, **707**, 117 (1967); T. Tanaka, G. Nonaka and I. Nishioka, *Chem. Pharm. Bull.*, **34**, 656 (1986).

Synthesis and Platelet Aggregation Inhibitory Activity of Diphenylazole Derivatives. I. Thiazole and Imidazole Derivatives

Norihiko SEKO,* Kohichiro YOSHINO, Koichi YOKOTA and Goro TSUKAMOTO

Pharmaceuticals Research Center, Kanebo Ltd., 1–5–90, Tomobuchi-cho, Miyakojima-ku, Osaka 534, Japan. *Received July 26, 1990*

Diphenylimidazole and diphenylthiazole derivatives were synthesized and tested as inhibitors of platelet aggregation in *in vitro* experiments with the rabbit. Diphenylthiazole derivatives (10) were more potent than diphenylimidazole derivatives (4) in inhibiting arachidonic acid-induced platelet aggregation of rabbit platelet-rich plasma. Two diphenylimidazole and eight diphenylthiazole derivatives were evaluated for *ex vivo* arachidonic acid and collagen-induced platelet aggregation inhibitory activity using guinea pigs. In these compounds, 4,5-bis(4-methoxyphenyl)-2-(1,5-dimethyl-2-pyrrolyl)thiazole (10n) showed strong activity *in vitro* and *ex vivo*. The *ex vivo* activity of 10n was 200 times stronger than that of aspirin. The mechanism of the activity of 10n was the inhibition of cyclo-oxygenase.

Keywords platelet aggregation inhibitor; diphenylthiazole; diphenylazole; diphenylimidazole; anti platelet activity

In recent years, many compounds possessing platelet aggregation inhibitory activity have been discovered. The mechanisms of inhibition vary. For example, cyclo-oxygenase inhibitor (aspirin[1]), thromboxane synthetase inhibitor (ozagrel[2]), adenylate cyclase activator (ticlopidine[3]), phosphodiesterase inhibitor (dipyridamole[4] and cilostazole[5]) are known inhibitors and have been investigated for application to ischemic disease. Among these compounds, aspirin has been studied most extensively.

One of the causes of ischemic disease is platelet aggregation. Thromboxane A_2 is derived from arachidonic acid released from phospholipids and induces platelet aggregation. Another cause of ischemic disease is vasospasms, which can be induced by thromboxane A_2. Therefore, use of drugs that inhibit platelet function and suppress the synthesis of thromboxane A_2 should be effective in preventing and curing ischemic disease. The platelet aggregation inhibitory activity of aspirin is due to a decrease in thromboxane A_2 by the inhibition of cyclo-oxygenase[6] in platelets. In double blind trials, aspirin improved symptoms of ischemic disease. Aspirin was effective in myocardial infarction,[7–9] unstable angina,[10,11] and transition ischemic attack.[12–15] However, the platelet aggregation inhibitory activity of aspirin was weak. Moreover, aspirin has been known to induce stomach ulcers.[16,17] The stomach ulcerogenic activity of aspirin is based on a decrease in prostaglandin I_2 and prostaglandin E_1 due to the inhibition of cyclo-oxygenase. Prostaglandin I_2 and prostaglandin E_1 maintain stomach mucosa membrane blood flow and protect stomach cells.[18] We reported that a nonacidic 2-heteroarylbenzimidazole derivative, KB-1043, possessed anti-inflammatory activity.[19] Although one of the mechanisms of the activity of KB-1043 was the inhibition of cyclo-oxygenase, the ulcerogenic activity of KB-1043 was weak. We expected that a nonacidic cyclo-oxygenase inhibitor would eliminate the ulcerogenic activity. On the other hand, the idea of using a phenyl group or two phenyl groups attached to a ring system to mimic the corresponding benzo analog (fused phenyl moiety) has often been explored in medicinal chemistry.[20]

In a continuous investigation of 2-heteroarylazole derivatives, we synthesized a variety of 2-heteroaryl-4,5-diphenylazole and 2-heteroaryl-4-phenylazole derivatives as 2-heteroarylbenzimidazole derivative analog and screened them for platelet aggregation inhibitory activity.

Chemistry 4,5-Diphenylimidazole derivatives (**4a, f**) were prepared according to the literature.[21] 4,5-Bis(4-methoxyphenyl)imidazole derivatives (**4b, d, g—l**) were prepared by condensation of anisil (**2**) with aldehydes (**3**) and ammonium acetate in acetic acid as shown in Chart 1. In the case of **4c** and **4e**, because aldehydes were acid labile, dimethyl sulfoxide (DMSO) was used as a solvent instead of acetic acid. Anisil (**2**) was prepared by oxidation of anisoin (**1a**) with cupric sulfate in pyridine according to the literature.[22]

Diphenylthiazole derivatives (**10**) were synthesized by condensation of bromodeoxybenzoin derivatives (**9**)[23,24] and thioamides (**7**)[25–32] in acetonitrile as shown in Chart 3. Pyrrolecarbothioamides (**7k, l**) were prepared from pyrrolecarbaldehydes (**3k, l**) through 3-step reactions as shown in Chart 2. Pyrrolecarbaldehydes (**3k, l**) were condensed with hydroxylamine to give oximes (**5k, l**).[33] The oximes (**5k, l**) were dehydrated with acetic anhydride to give nitriles

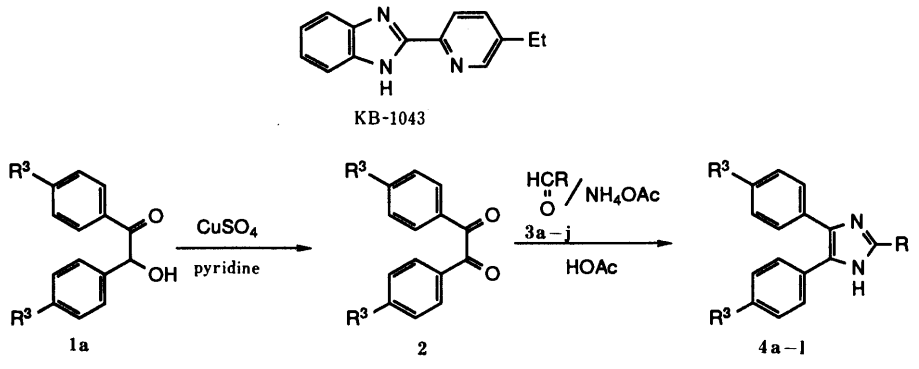

Chart 1

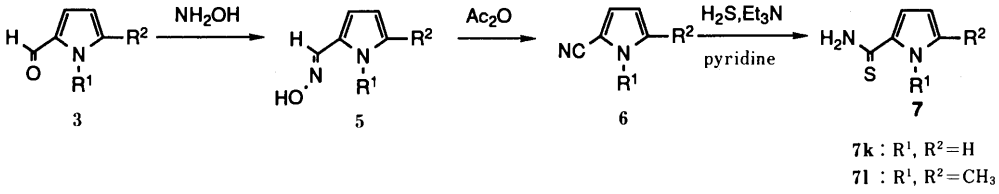

Chart 2

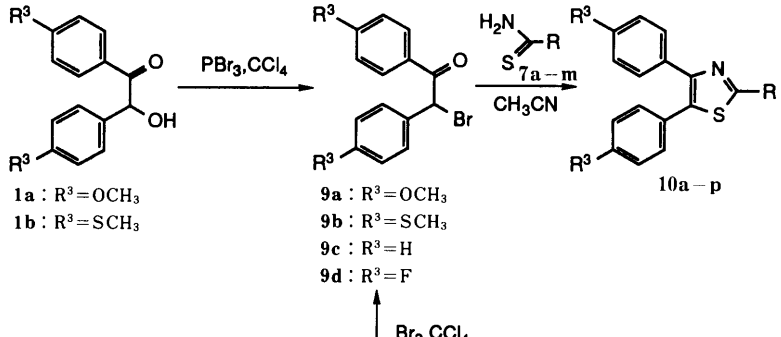

Chart 3

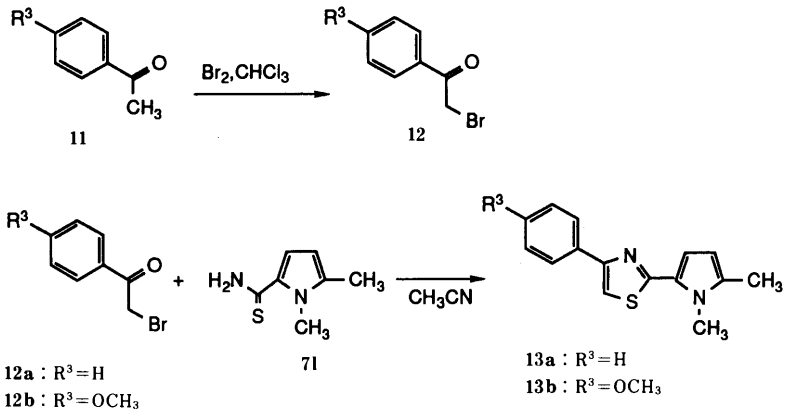

Chart 4

(**6k**, **l**).[34] The nitriles (**6k**, **l**) were treated with hydrogen sulfide in pyridine in the presence of triethylamine to give pyrrolecarbothioamides (**7k**, **l**).

Bromodeoxybenzoins (**9**) were prepared by two methods. Bromodeoxyanisoin (**9a**) and α-bromo-4,4′-dimethylthiodeoxybenzoin (**9b**) were obtained by the reaction of benzoin derivatives (**1a**, **b**) and phosphorous tribromide in carbon tetrachloride.[23] Bromodeoxybenzoin (**9c**) and α-bromo-4,4′-difluorodeoxybenzoin (**9d**) were obtained by bromination of deoxybenzoin derivatives (**8c**, **d**), in carbon tetrachloride.[24] These deoxybenzoin derivatives (**8c**, **d**) were easily obtained by the reduction of benzoin derivatives (**1c**, **d**). 4,4′-Difluorodeoxybenzoin (**8d**) was prepared by the reduction of 4,4′-difluorobenzoin (**1d**) with tin, hydrochloric acid, and cupric sulfate in ethanol.[34]

Phenylthiazole derivatives (**13**) were prepared by the condensation of phenacyl bromide derivatives (**12**) with pyrrolecarbothioamide derivative (**7l**) in acetonitrile as shown in Chart 4. Phenacyl bromide derivatives (**12**) were obtained by bromination of acetophenone derivatives (**11**).[35] The syntheses of these compounds are summarized in Tables I through VI.

Results and Discussion

The diphenylazole and phenylthiazole derivatives were evaluated for *in vitro* arachidonic acid-induced platelet aggregation inhibitory activity using rabbit platelet-rich plasma (PRP). Results are given in Tables VII and VIII.

Almost all of the examined diphenylazole derivatives exhibited excellent platelet aggregation inhibitory activity. Diphenylthiazole derivatives generally showed stronger inhibitory activity on the aggregation than the corresponding diphenylimidazole derivatives. Structure–activity relationships were different between the diphenylthiazole series and diphenylimidazole series.

Structure–Activity Relationships of Diphenylimidazole Series The substituent effects on the 4-position of the benzene rings and the 2-position of the imidazole ring were investigated and results are shown in Table VII.

TABLE I. Synthesis of 4,5-Bis(4-methoxyphenyl)imidazole Derivatives (4)

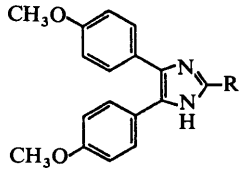

	R	Solvent	Yield (%)	Isolation[a]	mp (°C)
4b	3-Pyridyl·H_2O	AcOH	78	Benzene	188.0—190.5
4c	2-Pyridyl	DMSO	48	Benzene	190.0—191.0
4d[b]	6-Methyl-2-pyridyl	AcOH	10	Benzene	183.5—184.5
4e	4-Pyridyl	DMSO	33	CH_3CN	182.0—185.0
4g	2-Thienyl	AcOH	46	Benzene	195.0—196.0
4h	5-Methyl-2-thienyl	AcOH	19	Benzene	186.0—187.0
4i	3-Methyl-2-thienyl	AcOH	86	Benzene	185.5—186.5
4j	3-Thienyl	AcOH	64	Benzene	201.5—204.0
4k	2-Pyrrolyl	AcOH	37	Benzene	229.5—231.0
4l	1,5-Dimethyl-2-pyrrolyl	AcOH	30	Benzene	173.5—174.5

a) Recrystallization solvent. *b*) Diethyl acetal was used instead of aldehyde.

4,5-Bis(4-methoxyphenyl) derivatives (**4b, g**) showed stronger activity than diphenyl derivatives (**4a, f**). These results showed that the introduction of methoxy groups at the 4-position of the benzene rings enhanced the activity.

The activity of 4,5-bis(4-methoxyphenyl) derivatives were affected by a heteroaryl substituent at the 2-position of the imidazole ring. The 2-pyrrolyl group (**4k**) was the most active substituent. 3-Pyridyl (**4b**), 2-pyridyl (**4c**), and 2-thienyl (**4g**) derivatives were 2-fold less active than the 2-pyrrolyl derivative (**4k**). Substitution with the 3-thienyl group (**4j**) at the 2-position of the imidazole ring led to an 8-fold drop in the activity when compared with **4k**. The 4-pyridyl derivative (**4e**) exhibited only weak activity. Introduction of methyl groups at the 1- and 5-positions of the pyrrole ring (**4l**) decreased the activity. In the case of the thiophene ring, the substituent effect of a methyl group was not uniform. Introduction of a methyl group at the 5-position of the thiophene ring (**4h**) drastically decreased the activity. On the other hand, 3-methyl-2-thienyl derivative (**4i**) increased the activity 2-fold when compared with the 2-thienyl derivative (**4g**).

In the diphenylimidazole series, **4i** and **4k** exhibited strong activity. The 50% inhibitory concentration (IC_{50}) values of these derivatives were in 10^{-8} M order.

Structure–Activity Relationships of Diphenylthiazole Series The substituent effects on the 4-position of the benzene rings and the 2-position of the thiazole ring were investigated and the results are shown in Table VII.

Introduction of the methoxy groups at the 4-position of the benzene rings (**10n**) increased 500-fold platelet aggregation inhibitory activity compared with diphenyl derivative (**10l**). Substitution of the methoxy groups at the 4-position of the benzene rings with fluorine atoms (**10m**) decreased

TABLE II. Elemental Analysis of 4,5-Bis(4-methoxyphenyl)imidazole Derivatives (4)

	R	Formula	Analysis (%) Calcd			Found		
			C	H	N	C	H	N
4b	3-Pyridyl·H_2O	$C_{22}H_{21}N_3O_3$	70.38	5.60	11.19	69.98	5.61	11.24
4d	6-Methyl-2-pyridyl	$C_{23}H_{21}N_3O_2$	74.37	5.70	11.31	74.50	5.61	11.29
4e	4-Pyridyl	$C_{22}H_{19}N_3O_2$	73.93	5.36	11.76	74.19	5.26	11.86
4g	2-Thienyl	$C_{21}H_{18}N_2O_2S$	69.50	4.96	7.73	69.60	5.10	7.60
4h	5-Methyl-2-thienyl	$C_{22}H_{20}N_2O_2S$	70.19	5.35	7.44	70.17	5.37	7.39
4i	3-Methyl-2-thienyl	$C_{22}H_{20}N_2O_2S$	70.19	5.35	7.44	70.36	5.20	7.51
4j	3-Thienyl	$C_{21}H_{18}N_2O_2S$	69.50	4.96	7.73	69.24	5.18	7.69
4l	1,5-Dimethyl-2-pyrrolyl	$C_{23}H_{23}N_3O_2$	73.97	6.21	11.25	73.80	6.06	11.19

TABLE III. ^{1}H-NMR Spectra of 4,5-Bis(4-methoxyphenyl)imidazole Derivatives (4)

	R	^{1}H-NMR chemical shifts[a] (δ)
4b	3-Pyridyl·H_2O	3.7 (6H, s), 6.6—6.85 (4H, m), 6.9—7.4, (5H, m+1H, br)
4d	6-Methyl-2-pyridyl	2.4 (3H, s), 3.7 (6H, s), 6.4—8.1 (11H, m+1H, br)
4e	4-Pyridyl	3.8 (6H, s), 6.8—7.15 (2H, m), 7.35—7.6, (4H, m), 7.9—8.05 (2H, m), 8.55—8.7 (2H, m), 12.4—13.0 (1H, br)
4g	2-Thienyl	3.7 (6H, s), 6.45—6.8 (6H, m), 6.95—7.4 (5H, m), 8.0—8.4 (1H, br)
4h	5-Methyl-2-thienyl	2.45 (3H, s), 3.7 (6H, s), 6.55—6.85 (4H, m), 7.0—7.45 (6H, m), 8.9—9.4 (1H, br)
4i	3-Methyl-2-thienyl	2.5 (3H, s), 3.7 (6H, s), 6.5—6.85 (4H, m), 7.0—7.45 (6H, m), 8.4—8.9 (1H, br)
4j	3-Thienyl	3.7 (6H, s), 6.45—6.8 (4H, m), 7.0—7.55 (7H, m), 8.1—8.45 (1H, br)
4l	1,5-Dimethyl-2-pyrrolyl	2.15 (3H, s), 3.8 (6H, s), 4.0 (3H, s), 5.95 (1H, d, J=2), 6.3 (1H, d, J=2), 6.8—6.95 (4H, m), 7.3—7.55 (4H, m), 8.4—9.5 (1H, br)

a) Measured in $CDCl_3$.

the activity. Substitution of oxygen atoms at the methoxy groups of **10n** with sulfur atoms (**10o**) also decreased the activity. These results showed that the methoxy groups at the 4-position of the benzene rings are very important for platelet aggregation inhibitory activity.

In the 4,5-bis(4-methoxyphenyl) derivatives, 2-pyrrolyl (**10k**), 2-thienyl (**10f**), 3-thienyl (**10j**), and 2-pyridyl (**10b**) derivatives exhibited nearly equal inhibitory activity. The IC_{50} values of these derivatives were about 1×10^{-7} M. The 3-pyridyl derivative (**10a**) showed only weak activity. Pyrazinyl derivative (**10p**), possessing 2 nitrogen atoms in the 6-membered heteroaromatic ring, was 2-fold less active than the 2-pyridyl derivative (**10b**), possessing 1 nitrogen atom in the 6-membered heteroaromatic ring. The effects of introduction of a methyl, a chloro, and a methoxy group into the heteroaryl rings were examined. In the case of the pyrrole ring (**10n**), introduction of methyl groups enhanced the activity. The activity of (1,5-dimethyl-2-pyrrolyl) derivative (**10n**) was fairly strong compared with the unsubstituted pyrrolyl derivative (**10k**). On the other hand, in the thiophene or the pyridine ring, introduction of a methyl group reduced (**10i**) or had no effect (**10c, d, g**) on the activity. With introduction of a chlorine atom into the thienyl derivative (**10h**), the activity was nearly equal to the 2-thienyl derivative (**10f**). Introduction of a methoxy group into the 2-pyridyl derivative (**10e**) decreased the activity 4-fold when compared with the 2-pyridyl derivative (**10b**).

Among the diphenylthiazole derivatives, **10b—d, f—h, k,** and **10n** exhibited strong activity. The IC_{50} values of these derivatives were in 10^{-8} M order.

Platelet Aggregation Inhibitory Activity of 4-Substituted-Phenylthiazole Derivatives The substituent effect on the 5-position of the thiazole ring was investigated and results are shown in Table VIII.

4-Phenylthiazole derivatives (**13a, b**) did not exhibit any inhibitory activity. From these results, it seems that the 4,5-diphenylthiazole moiety is necessary for platelet aggregation inhibitory activity.

***Ex Vivo* Activity** Ten derivatives which showed strong activity (the IC_{50} values of these derivatives were in 10^{-8} M order) were evaluated for *ex vivo* arachidonic acid and collagen-induced platelet aggregation inhibitory activity using guinea pigs. Two compounds (**4i, k**) were diphenylimidazole derivatives. Eight other compounds (**10b—d, f—h, k, n**) were diphenylthiazole derivatives. The results are given in Table IX. All of the diphenylimidazole derivatives (**4i, k**) and all of the 2-unsubstituted-heteroaryl-diphenylthiazole derivatives (**10b, f, k**) showed no activity at a dose of 1 mg/kg. The introduction of substituents at the heteroaryl group, in some cases (**10d, h, n**), enhanced the activity. In these three compounds, 4,5-bis(4-methoxyphenyl)-2-(1,5-dimethylpyrrol-2-yl)thiazole (**10n**) showed the strongest *ex vivo* platelet aggregation inhibitory activity. The activity of **10n** in *ex vivo* was 200 times stronger than

TABLE IV. Synthesis of 4,5-Diphenylthiazole Derivatives (**10**)

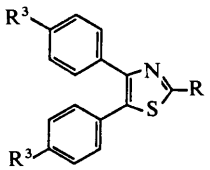

	R	R^3	Yield (%)	Isolation[a]	mp (°C)
10a	3-Pyridyl	MeO	40	Ligroin	138.5—140.0
10b	2-Pyridyl	MeO	69	Ligroin	144.0—146.0
10c	6-Methyl-2-pyridyl	MeO	60	Ligroin	90.0— 92.0
10d	4-Methyl-2-pyridyl	MeO	62	Ligroin	136.0—137.5
10e	6-Methoxy-2-pyridyl	MeO	50	EtOH	124.0—125.0
10f	2-Thienyl	MeO	61	EtOH	139.5—140.5
10g	5-Methyl-2-thienyl	MeO	59	Ligroin	148.5—149.5
10h	5-Chloro-2-thienyl	MeO	39	Ligroin	157.0—158.0
10i	3-Methyl-2-thienyl	MeO	43	EtOH	95.5— 98.5
10j	3-Thienyl	MeO	50	EtOH	133.5—134.5
10k	2-Pyrrolyl	MeO	86	Ligroin	131.5—134.0
10l	1,5-Dimethyl-2-pyrrolyl	H	91	Hexane	119.0—120.0
10m	1,5-Dimethyl-2-pyrrolyl	F	38	Hexane	135.0—136.0
10n	1,5-Dimethyl-2-pyrrolyl	MeO	75	Cyclohexane	116.5—117.5
10o	1,5-Dimethyl-2-pyrrolyl	MeS	64	Cyclohexane	112.0—113.5
10p	Pyrazinyl	MeO	42	AcOEt	148.0—149.0

a) Recrystallization solvent.

TABLE V. Elemental Analysis of 4,5-Diphenylthiazole Derivatives (**10**)

	R	R^3	Formula	Analysis (%) Calcd			Found		
				C	H	N	C	H	N
10a	3-Pyridyl	MeO	$C_{22}H_{18}N_2O_2S$	70.57	4.84	7.48	70.74	4.66	7.51
10b	2-Pyridyl	MeO	$C_{22}H_{18}N_2O_2S$	70.57	4.84	7.48	70.80	4.66	7.47
10c	6-Methyl-2-pyridyl	MeO	$C_{23}H_{20}N_2O_2S$	71.11	5.19	7.21	71.41	5.08	7.13
10d	4-Methyl-2-pyridyl	MeO	$C_{23}H_{20}N_2O_2S$	71.11	5.19	7.21	71.45	5.05	7.14
10e	6-Methoxy-2-pyridyl	MeO	$C_{23}H_{20}N_2O_3S$	68.30	4.98	6.93	68.55	4.91	6.78
10f	2-Thienyl	MeO	$C_{21}H_{17}NO_2S_2$	66.47	4.52	3.69	66.34	4.30	3.74
10g	5-Methyl-2-thienyl	MeO	$C_{22}H_{19}NO_2S_2$	67.15	4.87	3.56	67.15	4.63	3.49
10h	5-Chloro-2-thienyl	MeO	$C_{21}H_{16}ClNO_2S_2$	60.93	3.90	3.38	61.03	3.71	3.15
10i	3-Methyl-2-thienyl	MeO	$C_{22}H_{19}NO_2S_2$	67.15	4.87	3.56	67.36	4.80	3.56
10j	3-Thienyl	MeO	$C_{21}H_{17}NO_2S_2$	66.47	4.52	3.69	66.72	4.40	3.69
10k	2-Pyrrolyl	MeO	$C_{21}H_{18}N_2O_2S$	69.59	4.96	7.73	70.06	4.90	7.68
10l	1,5-Dimethyl-2-pyrrolyl	H	$C_{21}H_{18}N_2S$	76.33	5.49	8.48	76.64	5.25	8.48
10m	1,5-Dimethyl-2-pyrrolyl	F	$C_{21}H_{16}F_2N_2S$	68.84	4.40	7.65	68.61	4.26	7.51
10o	1,5-Dimethyl-2-pyrrolyl	MeS	$C_{23}H_{22}N_2S_3$	65.37	5.25	6.63	65.55	5.28	6.48
10p	Pyrazinyl	MeO	$C_{21}H_{17}N_3O_2S$	67.18	4.56	11.19	67.47	4.49	11.31

TABLE VI. ^{1}H-NMR Spectra of 4,5-Diphenylthiazole Derivatives (**10**)

	R	R^3	^{1}H-NMR chemical shifts[a] (δ)
10a	3-Pyridyl	MeO	3.8 (6H, s), 6.8—6.95 (4H, m), 7.2—7.6 (5H, m), 8.2—8.35 (1H, m), 8.55—8.7 (1H, m), 9.15—9.25 (1H, m)
10b	2-Pyridyl	MeO	3.7 (6H, s), 6.6—6.9 (4H, m), 7.0—7.8 (6H, m), 8.0—8.25 (1H, m), 8.35—8.55 (1H, m)
10c	6-Methyl-2-pyridyl	MeO	2.6 (3H, s), 3.8 (6H, s), 6.65—7.7 (10H, m), 7.85—8.1 (1H, m)
10d	4-Methyl-2-pyridyl	MeO	2.4 (3H, s), 3.7 (6H, s), 6.7—7.6 (9H, m), 7.9—8.05 (1H, m), 8.2—8.35 (1H, m)
10e	6-Methoxy-2-pyridyl	MeO	3.75 (6H, s), 3.95 (3H, s), 6.55—6.9 (5H, m), 7.1—7.8 (6H, m)
10f	2-Thienyl	MeO	3.75 (6H, s), 6.6—7.55 (11H, m)
10g	5-Methyl-2-thienyl	MeO	2.45 (3H, s), 3.75 (6H, s), 6.55—6.9 (5H, m), 7.1—7.55 (5H, m)
10h	5-Chloro-2-thienyl	MeO	3.7 (6H, s), 6.6—6.85 (5H, m), 7.0—7.5 (5H, m)
10i	3-Methyl-2-thienyl	MeO	2.5 (3H, s), 3.75 (6H, s), 6.65—7.0 (5H, m), 7.1—7.6 (5H, m)
10j	3-Thienyl	MeO	3.75 (6H, s), 6.6—6.85 (4H, m), 7.1—7.55 (5H, m), 7.65—7.8 (1H, m)
10k	2-Pyrrolyl	MeO	3.7 (6H, s), 6.05—6.15 (1H, m), 6.5—6.9 (6H, m), 7.1—7.5 (4H, m), 9.4—9.8 (1H, br)
10l	1,5-Dimethyl-2-pyrrolyl	H	2.3 (3H, s), 4.0 (3H, s), 5.95 (1H, d, J=4.0), 6.6 (1H, d, J=4.0), 7.15—7.4 (8H, m), 7.5—7.7 (2H, m)
10m	1,5-Dimethyl-2-pyrrolyl	F	2.25 (3H, s), 3.95 (3H, s), 5.9 (1H, d, J=4.0) 6.55 (1H, d, J=4.0), 6.85–7.7 (8H, m)
10o	1,5-Dimethyl-2-pyrrolyl	MeS	2.3 (3H, s), 2.5 (6H, s), 4.0 (3H, s), 5.95 (1H, d, J=4.0), 6.6 (1H, d, J=4.0), 7.1—7.3 (6H, m), 7.4—7.5 (2H, m)
10p	Pyrazinyl	MeO	3.85 (6H, s), 6.8—6.95 (4H, m), 7.2—7.65 (5H, m), 8.5—8.6 (2H, m), 9.4—9.5 (1H, m)

a) Measured in $CDCl_3$.

TABLE VII. *In Vitro* Platelet Aggregation Inhibitory Activity of 4,5-Diphenylazole Derivatives[a]

Imidazole (**4**)				Thiazole (**10**)			
	R	R^3	IC_{50}[b,c]		R	R^3	IC_{50}[b,c]
4a	3-Pyridyl	H	76.9				
4b	3-Pyridyl·H_2O	MeO	18.9	**10a**	3-Pyridyl	MeO	147
4c	2-Pyridyl	MeO	15.9	**10b**	2-Pyridyl	MeO	8.85
4d	6-Methyl-2-pyridyl	MeO	14.5	**10c**	6-Methyl-2-pyridyl	MeO	9.83
				10d	4-Methyl-2-pyridyl	MeO	7.50
4e	4-Pyridyl	MeO	2040	**10e**	6-Methoxy-2-pyridyl	MeO	33.9
4f	2-Thienyl	H	5140				
4g	2-Thienyl	MeO	20.0	**10f**	2-Thienyl	MeO	6.80
4h	5-Methyl-2-thienyl	MeO	720	**10g**	5-Methyl-2-thienyl	MeO	7.76
				10h	5-Chloro-2-thienyl	MeO	6.29
4i	3-Methyl-2-thienyl	MeO	9.42	**10i**	3-Methyl-2-thienyl	MeO	11.0
4j	3-Thienyl	MeO	60.4	**10j**	3-Thienyl	MeO	11.4
4k	2-Pyrrolyl	MeO	7.44	**10k**	2-Pyrrolyl	MeO	8.33
				10l	1,5-Dimethyl-2-pyrrolyl	H	3360
				10m	1,5-Dimethyl-2-pyrrolyl	F	66.4
4l	1,5-Dimethyl-2-pyrrolyl	MeO	86.5	**10n**	1,5-Dimethyl-2-pyrrolyl	MeO	6.42
				10o	1,5-Dimethyl-2-pyrrolyl	MeS	542
				10p	Pyrazinyl	MeO	18.5
	Aspirin		23200				

a) Rabbit PRP was used. b) Concentration of 4,5-bis(4-substituted-phenyl)azole required to inhibit 50% arachidonic acid-induced platelet aggregation. c) $\times 10^{-8}$ M. See Experimental section.

TABLE VIII. *In Vitro* Platelet Aggregation Inhibitory Activity of 4-(4-Substituted phenyl)thiazole Derivatives[a]

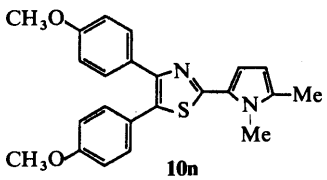

10n

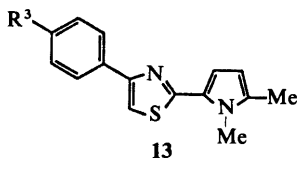

13

	R^3	IC_{50}[b,c]
10n	—	6.42
13a	H	>10000
13b	MeO	>10000

a) Rabbit PRP was used. b) Concentration of 4-(4-substituted-phenyl)thiazole or 4,5-bis(4-substituted phenyl)thiazole required to inhibit 50% arachidonic acid-induced platelet aggregation. c) $\times 10^{-8}$ M. See Experimental section.

that of aspirin.

Cyclo-oxygenase Inhibitory Activity **10n**, which showed the strongest *ex vivo* platelet aggregation inhibitory activity in these diphenylazole derivatives was evaluated as cyclo-oxygenase inhibitory activity. The IC_{50} value of **10n** was 3.6×10^{-7} M. This result indicated that the mechanism of the activity of **10n** was the inhibition of cyclo-oxygenase.

Conclusion

In *in vitro* experiments, diphenylthiazole derivatives (**10**) were more potent than the corresponding diphenylimidazole derivatives (**4**) in inhibiting platelet aggregation of rabbit platelet-rich plasma. In both the imidazole and the thiazole series, removal or substitution of the methoxy groups at the 4-position of the benzene ring (**4a, f, 10 l, m, o**) resulted in a drop in the activity. 4-Phenylthiazole deriv-

TABLE IX. *Ex Vivo* Platelet Aggregation Inhibitory Activity of 4,5-Bis(4-methoxyphenyl)azole Derivatives[a]

	ED_{50}[b,c]	
	A.A.[d]	Coll.[e]
4i	>1.0	>1.0
4k	>1.0	>1.0
10b	>1.0	>1.0
10c	>1.0	>1.0
10d	0.50	1.14
10f	>1.0	>1.0
10g	>1.0	>1.0
10h	0.44	0.84
10k	>1.0	>1.0
10n	0.22	0.29
Aspirin	38.2	58.9

a) Guinea pig PRP was used. *b*) Dose of tested compound required to inhibit 50% platelet aggregation. *c*) mg/kg. See Experimental section. *d*) Arachidonic acid-induced platelet aggregation. *e*) Collagen-induced platelet aggregation.

atives (**13**) did not exhibit any inhibitory activity. Two diphenylimidazole derivatives (**4i, k**) and eight diphenylthiazole derivatives (**10b—d, f—h, k, n**) were evaluated for *ex vivo* experiments. 4,5-Bis(4-methoxyphenyl)-2-(1,5-dimethylpyrrol-2-yl)thiazole (**10n**) showed the strongest activity in *ex vivo* experiments. The activity of **10n** in *ex vivo* was 200 times stronger than that of aspirin. The mechanism of the activity of **10n** was the inhibition of cyclo-oxygenase.

Experimental

Anisil (**2**),[22] 4,5-diphenyl-2-(3-pyridyl)imidazole (**4a**),[21] 4,5-diphenyl-2-(2-thienyl)imidazole (**4f**),[21] pyridine-3-carbothioamide (**7a**),[25] pyridine-2-carbothioamide (**7b**),[26] 6-methylpyridine-2-carbothioamide (**7c**),[27] 4-methylpyridine-2-carbothioamide (**7d**),[28] thiophene-2-carbothioamide derivatives (**7f—i**),[29] thiophene-3-carbothioamide (**7j**),[30] pyrrole-2-carbothioamide derivatives (**7k, l**),[31] pyrazine-2-carbothioamide (**7m**),[32] bromodeoxyanisoin (**9a**),[23] α-bromo-4,4'-dimethylthiodeoxybenzoin (**9b**),[23] bromodeoxybenzoin (**9c**),[24] α-bromo-4,4'-difluorodeoxybenzoin (**9d**),[24] phenacyl bromide (**12a**),[35] and 4-methoxyphenacyl bromide (**12b**),[35] were prepared according to the procedures in the literatures. Melting points were taken on a capillary melting point apparatus (Yamato MR-21). All melting points were uncorrected. The structures of all compounds were supported by their infrared (IR) (Hitachi 270-50) and 60 and 100 MHz proton nuclear magnetic resonance (^{1}H-NMR) (Hitachi R-24A and Nihon Denshi PS-100) spectra. All compounds were analyzed for C, H, N, and the results were within 0.4% of the calculated theoretical values. No attempt was made to maximize the yields.

Anisil (2) To a solution of cupric sulfate pentahydrate (173 g, 694 mmol) in pyridine (260 ml) and water (86 ml), anisoin (**1a**) (91 g, 333 mmol) was added. The mixture was refluxed for 2 h. The solution was poured into ice water. The above mixture was acidified with concentrated HCl (300 ml). The precipitated crystals were separated by filtration, washed with water, dried, and then recrystallized from benzene to give 74.6 g (yield 83%) of **2** as green needles: mp 132.0—134.0 °C. NMR ($CDCl_3$) δ: 3.8 (6H, s), 6.9 (4H, m), 7.9 (4H, m).

4,5-Bis(4-methoxyphenyl)-2-(2-pyridyl)imidazole (4c) A mixture of anisil (**2**) (2.7 g, 10 mmol) and ammonium acetate (11.5 g, 150 mmol) in DMSO (60 ml) was heated to 100 °C. Pyridine-2-carboxaldehyde (**3c**) (4.3 g, 40 mmol) was dissolved in DMSO and was added dropwise to the above solution over 90 min. The solution was cooled to room temperature and poured into ice water and aqueous ammonia. The precipitated crystals were separated by filtration, washed with water, and then dissolved in ethyl acetate, and washed twice with water. The ethyl acetate layer was dried over anhydrous magnesium sulfate, and evaporated *in vacuo*. The residue was chromatographed on a silica gel column with benzene : ethyl acetate = 10 : 1 as eluent. Recrystallization from benzene gave 1.7 g (yield 48%) of **4c** as colorless needles: mp 190.0—191.0 °C. NMR ($CDCl_3$) δ: 3.9 (6H, s), 6.7—6.9 (4H, m), 7.1—7.9 (6H, m), 8.2—8.4 (2H, m), 10.4—11.3 (1H, br). *Anal.* Calcd for $C_{22}H_{19}N_3O_2$: C, 73.93; H, 5.36; N, 11.76. Found: C, 74.18; H, 5.30; N, 11.76.

4,5-Bis(4-methoxyphenyl)-2-(2-pyrrolyl)imidazole (4k) To a mixture of anisil (**2**) (3.0 g, 11 mmol) and pyrrole-2-carboxaldehyde (**3k**) (2.4 g, 25 mmol) in acetic acid (60 ml), was added ammonium acetate (12.8 g, 165 mmol). The mixture was refluxed for 90 min. The solution was cooled to room temperature and poured into ice water. The precipitated crystals were separated by filtration, washed with water, dried, and chromatographed on a silica gel column with benzene : ethyl acetate = 4 : 1 as eluent. Recrystallization from benzene gave 1.4 g (yield 37%) of **4k** as pale purple needles: mp 229.5—231.0 °C. NMR (DMSO-d_6) δ: 3.7 (6H, s), 5.9—6.1 (1H, m), 6.5—6.8 (6H, m), 7.1—7.4 (4H, m), 8.1—8.8 (1H, br). *Anal.* Calcd for $C_{21}H_{19}N_3O_2$: C, 73.03; H, 5.54; N, 12.17. Found: C, 73.22; H, 5.51; N, 11.98.

1,5-Dimethylpyrrole-2-carbothioamide (7l) 1,5-Dimethylpyrrole-2-carbonitrile (**6l**)[33] (24.0 g, 200 mmol) was dissolved in a solution of triethylamine (10.1 g, 100 mmol) in pyridine (30 ml), and therein hydrogen sulfide was blown at 20 °C for 8 h. The reaction mixture was diluted with water (600 ml), and the precipitated crystals were separated by filtration, washed with water, dried, and then recrystallized from ligroin to give 24.8 g (yield 81%) of 7l as a pale yellow powder: mp 95.0—99.0 °C. NMR ($CDCl_3$) δ: 2.3 (3H, s), 4.0 (3H, s), 5.9—6.1 (1H, m), 6.4—6.6 (1H, m), 6.6—6.8 (1H, m).

Bromodeoxyanisoin (9a) A solution of phosphorus tribromide (22.3 g, 82 mmol) and carbon tetrachloride (40 ml) was added over 2 h to a reflux solution of anisoin (**1a**) (56 g, 206 mmol) in carbon tetrachloride (1 l). The solution was cooled to room temperature and poured into ice water. The organic layer was diluted with ethyl acetate (2 l), dried over anhydrous magnesium sulfate, and evaporated *in vacuo*. The residue was recrystallized from benzene to give 61.4 g (yield 89%) of **9a** as a colorless powder: mp 101—103.5 °C. NMR ($CDCl_3$) δ: 3.7 (3H, s), 3.8 (3H, s), 6.3 (1H, s), 6.7—6.9 (4H, m), 7.2—7.55 (2H, m), 7.65—7.9 (2H, m).

4,5-Bis(4-methoxyphenyl)-2-(1,5-dimethyl-2-pyrrolyl)thiazole (10n) 1,5-Dimethylpyrrole-2-carbothioamide (7 l) (4.6 g, 30 mmol) and bromodeoxyanisoin (**9a**)[23] (10.1 g, 30 mmol) were dissolved in acetonitrile (300 ml). The mixture was stirred at 60 °C for 50 min. After cooling the solution, the reaction mixture was evaporated *in vacuo*. The resulting residue was dissolved in chloroform (300 ml) and an aqueous solution of sodium carbonate (300 ml), and the mixture was shaken. The chloroform layer was taken, and the aqueous layer was further extracted with chloroform (300 ml). The chloroform layers were combined, dried over anhydrous magnesium sulfate, and evaporated *in vacuo*. The residue was recrystallized from cyclohexane to give 8.8 g (yield 75%) of **10n** as colorless needles: mp 115.5—117.5 °C. NMR ($CDCl_3$) δ: 2.3 (3H, s), 3.7 (6H, s), 4.0 (3H, s), 5.9—6.1 (1H, m), 6.4—6.8 (5H, m), 7.0—7.5 (4H, m). *Anal.* Calcd for $C_{23}H_{22}N_2O_2S$: C, 70.74; H, 5.68; N, 7.17. Found: C, 70.78; H, 5.57; N, 6.97.

2-(1,5-Dimethyl-2-pyrrolyl)-4-phenylthiazole (13a) 1,5-Dimethylpyrrole-2-carbothioamide (7 l) (1.54 g, 10 mmol) and phenacyl bromide (**12a**) (1.99 g, 10 mmol) were dissolved in acetonitrile (30 ml). The mixture was refluxed for 3 h. After cooling the solution, the reaction mixture was evaporated *in vacuo*. The resulting residue was poured into water (100 ml). The precipitated solid was washed with an aqueous solution of sodium carbonate. The solid was recrystallized from hexane to give 2.00 g (yield 79%) of **13a** as yellow needles: mp 114—116 °C. NMR ($CDCl_3$) δ: 2.3 (3H, s), 4.0 (3H, s), 5.9 (1H, d), 6.6 (1H, d), 7.2 (1H, s), 7.3—7.5 (3H, m), 7.8—8.0 (2H, m). *Anal.* Calcd for $C_{15}H_{14}N_2S$: C, 70.84; H, 5.55; N, 11.01. Found: C, 70.82; H, 5.42; N, 10.71.

2-(1,5-Dimethyl-2-pyrrolyl)-4-(4-methoxyphenyl)thiazole (13b) 1,5-Dimethylpyrrole-2-carbothioamide (7 l) (1.54 g, 10 mmol) and 4-methoxyphenacyl bromide (**12b**) (2.29 g, 10 mmol) were dissolved in acetonitrile (30 ml). The mixture was refluxed for 3 h. After cooling the solution, the reaction mixture was evaporated *in vacuo*. The resulting residue was poured into water (100 ml). The precipitated solid was washed with an aqueous solution of sodium carbonate. The solid was recrystallized from cyclohexane to give 2.70 g (yield 95%) of **13b** as pale yellow scales: mp 174—176 °C. NMR ($CDCl_3$): 2.4 (3H, s), 3.8 (3H, s), 4.0 (3H, s), 5.9 (1H, d), 6.5 (1H, d), 6.8—7.2 (3H, s), 7.7—7.9 (2H, m). *Anal.* Calcd for $C_{16}H_{16}N_2OS$: C, 67.58; H, 5.67; N, 9.85. Found: C, 67.43; H, 5.51; N, 9.76.

Preparation of Platelet-Rich Plasma (PRP) Platelet-rich plasma was prepared from citrated blood by centrifugation at 150 × *g* for rabbit (*in vitro*) and guinea pig (*ex vivo*) for 10 min. After PRP was withdrawn, the residual blood was centrifuged at 2000 × *g* for 15 min and platelet-poor plasma (PPP) was obtained from the supernatant.

Pharmacological Assay for Platelet Aggregation Inhibition *in Vitro*

Experiments Platelet aggregation was performed by the turbine methods of Born[36] using the Platelet Aggregation Profiler PAP-3 (Bio Data Inc.). A 450 μl sample of test drugs or DMSO was incubated for 3 min at 37 °C. After incubation, platelet aggregation was induced by the addition of 50 μl of arachidonic acid (A.A.). Changes in the light transmission of PRP after the addition of arachidonic acid were recorded. The maximum increase in light transmission determined from the aggregation curve for 3 min was defined as percentage of aggregation. Percentage of inhibition of aggregation was calculated as

$$\% \text{ inhibition} = \left(1 - \frac{\% \text{ aggregation (drug)}}{\% \text{ aggregation (control)}}\right) \times 100$$

The concentration of tested drug which caused a 50% inhibition of aggregation was determined by linear regression analysis and represented the IC_{50}.

Ex Vivo **Experiments** Guinea pigs weighing 350—450 g were orally given a test drug or the vehicle. At the scheduled time after oral administration of the drug, blood was collected and platelet aggregation was measured by the same method as *in vitro* experiments. The aggregating agent was 0.1 mM (final concentration) of A. A. and 10 μg (final concentration) of collagen. The inhibitory effects of the drugs were determined by calculating the percentage inhibition with respect to the control value. The dose of tested drug which caused a 50% inhibition of aggregation (ED_{50}) was determined by linear regression.

Cyclo-oxygenase Inhibitory Activity Cyclo-oxygenase inhibitory activity was measured by the method of Miyamoto.[37] 0.1 ml of 100 mM Tris–HCl buffer (pH 8.0) containing 2 μM hematin, 1 mM 4-(hydroxymercuri)benzoic acid, 5 mM L-tryptophan, sheep seminal vesicular gland microsomes (1.0 mg/ml, final concentration), and drugs were pre-incubated for 2 min at 24 °C. The reaction was started by the addition of 1 nmol [^{14}C]-arachidonic acid (125000 dpm) and incubated for 2 min at 24 °C. The reaction was stopped by the addition of a mixture of ether, methanol, and 0.2 M citric acid (30:4:1) which was pre-cooled to −20 °C. The reaction mixture was mixed with 0.5 g of sodium sulfate. A 100 μl aliquot of the organic phase was placed on a pre-coated silica gel glass plate with PGB_2 as a standard. Thin-layer chromatography was carried out to a height about 17 cm at −20 °C using solvent system ether, petroleum ether, and glacial acetic acid (85:15:1). Dried plates were subjected to autoradiography with X-ray film and the location of PGH_2 was confirmed. The chromatograms were divided into appropriate zones and silica gel was scraped into counting vials. The radio activity was determined by an Aloka liquid scintillation spectrophotometer, model LSC 1050, in a toluene solution containing 0.03% 1,4-bis[2-(5-phenyloxazolyl)]benzen and 0.5% 2,5-diphenyloxazole. Cyclo-oxygenase inhibitory activity was measured as the synthesis of PGH_2 and IC_{50} value was calculated by linear regression.

References

1) H. J. Weias, L. M. Aledort, and S. Kochwa, *J. Clin. Invest.*, **47**, 2169 (1968).
2) K. Iizuka, K. Akahana, D. Momose, M. Nakazawa, T. Tanouchi, M. Kawamura, and I. Ohyama, *J. Med. Chem.*, **24**, 1139 (1981).
3) S. Ashida, *Thromb. Haemostas.*, **40**, 542 (1979).
4) M. P. Cucuianu, E. E. Nishizawa, and J. F. Mustard, *J. Lab. Clin. Med.*, **77**, 958 (1971).
5) K. Watanabe, T. Kanbe, T. Igawa, and H. Hidaka, Abstracts of Papers, 8th International Congress of Pharmacology, 1981, p. 781.
6) M. Hamberg, J. Svensson, and B. Samuelsson, *Proc. Natl. Acad. Sci. U.S.A.*, **71**, 3824 (1974).
7) M. G. Bousser, E. Eschwege, M. Haguenau, J. M. Lefaucconier, K. Thibult, and P. J. Touboul, *Stroke*, **14**, 5 (1983).
8) P. S. Sorensene, H. Pedersene, J. Marquardsen, H. Petersson, A. Heltberg, N. Simonsen, O. Munch, and L. A. Andersen, *Stroke*, **14**, 15 (1983).
9) Antiplatelet Trialist Collaboration, *Br. Med. J.*, **296**, 320 (1988).
10) H. D. Lewis, J. W. Davis, D. G. Archibald, W. E. Steinke, T. C. Smitherman, J. E. Doeherty, H. W. Schnaper, M. M. LeWinter, E. Linares, J. M. Pouget, S. C. Sabharwel, E. Chesler, and H. Demost, *N. Engl. J. Med.*, **309**, 396 (1983).
11) J. Cairns, M. Gent, J. Singer, K. J. Finnie, G. M. Froggatt, D. A. Holder, G. Jablonsky, W. J. Kostik, L. J. Meledenz, M. G. Myers, L. D. Sackett, B. J. Sealey, and P. H. Tauser, *N. Engl. J. Med.*, **313**, 1369 (1985).
12) W. S. Feilds, N. A. Lemak, R. F. Frankowski, and R. J. Hardy, *Stroke*, **8**, 301 (1977).
13) Canadian Cooperative Study Group, *N. Engl. J. Med.*, **299**, 53 (1978).
14) American-Canadian Cooperative Study Group, *Stroke*,, **16**, 406 (1985).
15) M. Gent, *Stroke*, **18**, 541 (1987).
16) A. H. Douthwaite and G. A. M. Lintott, *Lancet*, ii, 1222 (1938).
17) L. T. F. L. Stubbe, *Br. Med. J.*, **2**, 1062 (1958).
18) A. Robert, "Advances in Prostaglandin and Thromboxane Research," Vol. 2, ed. by B. Samuelsson, and R. Paoletti, Raven Press, Inc., New York, 1976, p. 507.
19) G. Tsukamoto, K. Yoshino, T. Kohno, H. Ohtaka, H. Kagaya, and K. Ito, *J. Med. Chem.*, **23**, 734 (1980).
20) T. Y. Shen, "Medicinal Chemistry 13, Antiinflammatory Agent Chemistry and Pharmacology," Vol. 1, ed. by R. A. Scherrer, and M. W. Whitehouse, Academic Press, Inc., New York, 1974, p. 187.
21) J. G. Lombardino, U. S. Patent 3707475 (1972) [*Chem. Abstr.*, **77**, 101607*y* (1972)].
22) N. J. Leonard, R. T. Rapala, H. L. Herzog, and E. R. Blout, *J. Am. Chem. Soc.*, **71**, 2997 (1949).
23) J. Cymmerman-Craig, K. V. Martin, and P. C. Wailes, *Aust. J. Chem.*, **8**, 385 (1955).
24) P. E. Bender, D. T. Hill, P. H. Offen, K. Razgaitis, P. Lavanc, O. D. Stringer, B. M. Sutton, D. E. Griswold, M. DiMartino, D. T. Walz, I. Lantons, and C. B. Ladd, *J. Med. Chem.*, **28**, 1169 (1985).
25) R. I. Meltzer, A. D. Lewis, and J. A. King, *J. Am. Chem. Soc.*, **77**, 4062 (1955).
26) P. Karrer and J. Schukri, *Helv. Chim. Acta*, **28**, 820 (1945).
27) W. Walter, H. P. Kubersky, and D. Ahlquist, *Justus Liebigs Ann. Chem.*, **733**, 170 (1970).
28) R. Mayer, H. D. Eilhauer, and R. Keck, Ger. Offen. 54362 (1967) [*Chem. Abstr.*, **67**, 100016*m* (1967)].
29) A. E. S. Fairfull, J. L. Lowe, and D. A. Peak, *J. Chem. Soc.*, **1952**, 742.
30) J. Uhlendorf, S. Leyek, H. Friehe, and M. Probst, Ger. Offen. 3128453 (1983) [*Chem. Abstr.*, **98**, 160700*e* (1983)].
31) E. P. Papadopoulos, *J. Org. Chem.*, **38**, 667 (1973).
32) H. Foks and J. Sawlewicz, *Acta Pol. Pharm.*, **25**, 137 (1968).
33) H. J. Anderson, *Can. J. Chem.*, **37**, 2053 (1959).
34) A. Fischer, B. A. Grigor, J. Packer, and J. Vaughan, *J. Am. Chem. Soc.*, **83**, 4208 (1961).
35) R. M. Cowper and L. H. Davidson, "Organic Syntheses," Coll. Vol. II, ed. by John Wiley and Sons, Inc., New York, 1943, p. 480.
36) G. V. R. Born and M. J. Cross, *J. Physiol.*, **168**, 178 (1963).
37) T. Miyamoto, N. Ogino, S. Yamamoto, and O. Hayaishi, *J. Biol. Chem.*, **251**, 2629 (1975).

Carbapenem and Penem Antibiotics. V. Synthesis and Antibacterial Activity of 2-Functionalized-methyl 1-Methylcarbapenems Related to Asparenomycins[1)]

Mitsuru IMUTA,* Shoichiro UYEO* and Tadashi YOSHIDA

Shionogi Research Laboratories, Shionogi & Co., Ltd., Sagisu, Fukushima-ku, Osaka 553, Japan. *Received August 6, 1990*

The synthesis of 1α- and/or 1β-methylcarbapenems, 2-unsubstituted and 2-(5-methyl-1,3,4-thiadiazol-2-yl)thiomethyl derivatives having a 1-(hydroxy)methylethylidene or cyclic carbonate side chain at the C-6 position, is described. The *in vitro* antibacterial activities of these compounds and their corresponding 1-unsubstituted carbapenems are compared.

Keywords β-lactam antibiotic; carbapenem antibiotic; 1α-methyl carbapenem antibiotic; 1β-methyl carbapenem antibiotic; asparenomycin; 2-functionalized-methyl carbapenem antibiotic; Lewis acid mediated allylation; antibacterial activity

We previously reported that the chemical modification of asparenomycins[2)] at the C-2 position resulted in the finding of B-type carbapenems (Chart 1) with significantly enhanced activity compared to the parent compounds.[3)] We also reported that the novel A-type structure carbapenems with the carbonate side chain of 5*R**, 6*S**, 8*S** configuration (Chart 1) exhibited essentially the same antibacterial properties against both gram-positive and gram-negative organisms as the corresponding B-type counterparts bearing the 1-(hydroxymethyl)ethylidene side chain at the C-6 position, characteristic of asparenomycins ($R_1=R_2=H$, X=OAc, S-heteroaromatic ring).[3)] Specifically, this was observed in cases where the X=S-heteroaromatic ring in the A-type structure have led to a considerable increase in chemical and biological stability in comparison with imipenem as the reference compound.[1)]

It is now well recognized that the 1β-methylcarbapenem reported first by the Merck group has shown much improved stability toward dehydropeptidase-I (DHP-I) with high antibacterial potency.[4)] These properties of this structural variant have encouraged us to investigate the 1-methyl substituent effects of A- and B-type derivatives on their antibacterial activities. In this paper, we describe details of synthetic studies on the title compounds, as well as on corresponding 2-unsubstituted pairs. Their *in vitro* antibacterial properties will also be discussed.

Chemistry Our initial target was to synthesize the racemic 2-unsubstituted carbapenems (**7a**, **b**, and **9a**, **b**), considered to be the simplest structures, to examine the effect of the presence of a 1-methyl group on their activities. As a starting material we chose a 1:1 mixture of 4-(1-methylallyl)azetidinones (**2a** and **2b**), since we needed to test the activity of both 1α- and 1β-methylcarbapenems.

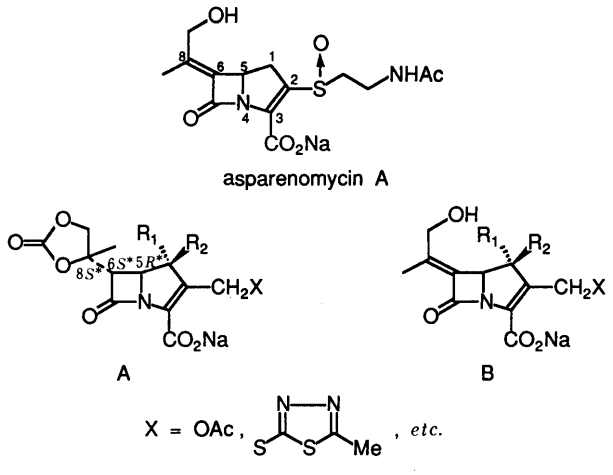

Chart 1

Although recently several methodologies for the introduction of an allylic moiety at the C-4 position of monocyclic azetidinones have been reported,[5)] we employed crotyltriphenylstannane as one of the most suitable reagents. Thus, treatment of 4-acetoxyazetidinone **1** with crotyltriphenylstannane in the presence of $BF_3\cdot Et_2O$ in CH_2Cl_2 at room temperature resulted in the formation of **2** as an inseparable mixture (*ca.* 1:1) in 93% yield. In this particular reaction, the choice of Lewis acid was crucial, so that $BF_3\cdot Et_2O$ was found to be superior to $TiCl_4$, $SnCl_4$ and ZnI_2.

The objective cyclic carbonates **4** as common intermediates having a 5*R**,6*S**,8*S** stereostructures (carbapenem structure numbering) were efficiently prepared according to our previously developed procedure.[3)] This sequence of reactions involves aldol type condensation between compound **3** and trimethylsilyloxyacetone, followed by treatment of the resulting glycols with phosgene and pyridine to afford the desired compound **4**. Although other isomers of compound **4** with carbonate side chains of 5*R**, 6*S**, 8*R** configuration could also be obtained at the same time, only the isomers of the 8*S** configuration were employed for the present studies. At this stage, fortunately, an approximate 1:1 mixture of the two diastereomers (**4a** and **4b**) isomeric at C-1 (carbapenem numbering) could be isolated by silica gel chromatography. Each isomer thus obtained was smoothly transformed into the carbapenem skeleton respectively, using the following sequence.

According to the standard method developed by Woodward,[6)] a stabilized phosphorane grouping was next built up on the azetidinone nitrogen atom of the compound **4**. The products of the thionyl chloride reaction proved to be unstable and were converted without purification into the ylides **5**. Subsequent ozonolysis and base-induced intramolecular Wittig condensation afforded the desired carbapenems (**6a** and **6b**) in fairly good yield (Chart 2).

The critical conversion of the cyclic carbonates **6** to the asparenomycin type derivatives **8** was accomplished by base-catalyzed E2 type elimination in a stereospecific manner as in the case of simpler 1-unsubstituted carbapenems[3)] and the corresponding penems.[7)] Thus, treatment of each carbonate derivative **6a** and **6b** in

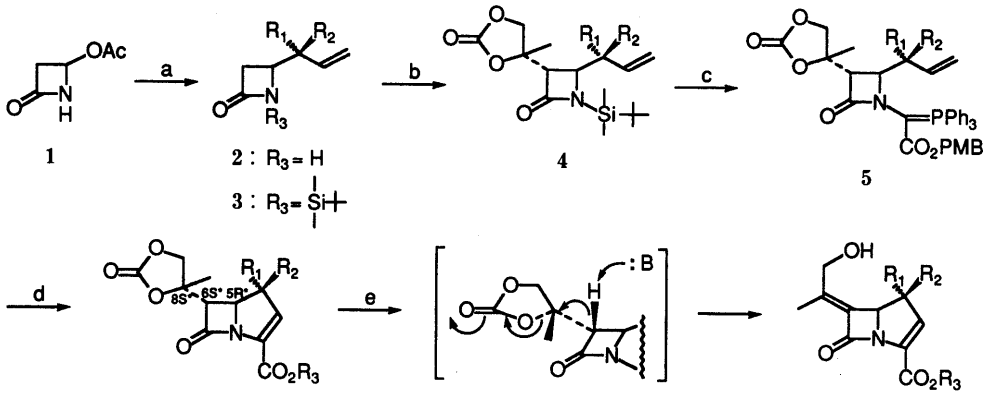

a) 1) $CH_3CH=CHCH_2SnPh_3$ / $BF_3 \cdot Et_2O$, 2) *tert*-$BuMe_2SiCl$ / Et_3N
b) 1) $MeCOCH_2OSiMe_3$ / LDA, 2) AcOH, 3) $COCl_2$
c) 1) *n*-Bu_4NF / AcOH, 2) $OHCCO_2PMB$ / Et_3N, 3) $SOCl_2$, 4) PPh_3
d) 1) O_3 / CF_3CO_2H, 2) $NaHCO_3$, 3) $AlCl_3$ / anisole
e) 1) DBU, 2) $AlCl_3$ / anisole

a : R_1 = Me, R_2 = H
b : R_1 = H, R_2 = Me
c : $R_1 = R_2$ = H

Chart 2

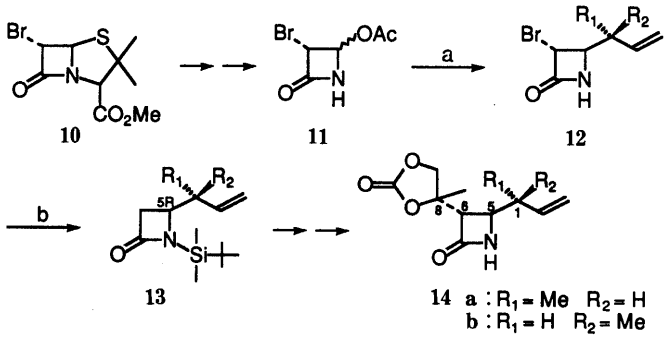

a) $CH_3CH=CHCH_2SnPh_3$ / $BF_3 \cdot Et_2O$
b) 1) *tert*-$BuMe_2SiCl$ / Et_3N, 2) Zn / AcOH

Chart 3

acetonitrile with a catalytic amount of 1,8-diazabicyclo[5.4.0]undec-7-ene (DBU) at room temperature for 20 min provided stereospecifically the trans allylic alcohols **8a** and **8b**, respectively.

Finally, the PMB esters of **6** and **8** were efficiently cleaved by the convenient method using $AlCl_3$ and anisole[8] to afford the sodium carboxylates **7** and **9**, respectively.

Unexpectedly, it turned out that the introduction of a 1-methyl group had little or no influence on antibacterial activity, as shown in Table I.

Our attention was therefore turned to the preparation of the optically active title carbapenems. As for the stereochemistry at the C-5 position of carbapenems, the *R* configuration is believed to be essential for antibacterial activity.[9] To this end, (3*R*)-4-acetoxy-3-bromoazetidinone **11** (*ca.* 1 : 1 mixture), readily prepared from 6-aminopenicillanic acid and used for our previous work,[7] was chosen as the key chiral synthon. By utilizing the facile crotylstannane procedure as described above, the 1-methylallyl group was introduced stereoselectively from the sterically less hindered face of the β-lactam ring, thus giving products (**12a** and **12b**) with an *R* configuration at the newly created chiral center C-4. The $J_{3,4}$ coupling constant of 2 Hz was consistent with the C-3,4 trans configuration of the resulting compounds, and no *cis* isomers were detected in this reaction (Chart 3).

After N-silylation, the bromine atom was reductively removed with zinc and acetic acid to afford the corresponding optically active key intermediates **13** (*ca.* 1 : 1 mixture) as shown in Chart 3. Elaboration to the cyclic carbonates with 5*R*, 6*S*, 8*S* configurations (**14a** and **14b**) was efficiently effected by the same sequences as the racemates. Separation of the two isomers could be achieved by silica gel chromatography.

X-Ray crystallographic analysis confirmed that **14a** (R_1 = Me, R_2 = H), possessing a sharp melting point (mp 121—122 °C, $[\alpha]_D$ +41.24° c = 0.43 ($CHCl_3$)), had a 1*R*, 5*R*, 8*S* stereo configuration (carbapenem structure numbering); therefore, the diastereoisomer **14b** (R_1 = H, R_2 = Me) should have a 1*S*,5*R*,8*S* structure.

Introduction of a thiadiazolylthio group at the C-2′ position was performed as detailed in Chart 4. Thus, epoxydation of each allylazetidinone **14a** and **14b** with *m*-chloroperbenzoic acid (MCPBA), followed by the same sequence described above for the formation of ylide, provided **15a** and **15b**, respectively. The epoxide ring was cleaved regiospecifically by the base-catalyzed nucleophilic attack of 5-methyl-1,3,4-thiadiazol-2-thiol, and subsequent oxidation of the resulting alcohol afforded the ketoylides **16a** and **16b**. It is noteworthy that these strongly basic reaction conditions did not effect epimerization of the 1-methyl groups of either the starting materials or the final products.

Thermolysis of the keto-ylides **16** in toluene gave rise to carbapenems **17**. Interestingly, it was observed that the 1α-methylcarbapenem **17a** was produced at a considerably lower temperature than the corresponding 1β-methyl derivative **17b**.

Transformation of the cyclic carbonate to trans allylic alcohol, and subsequent carboxy deprotection were suc-

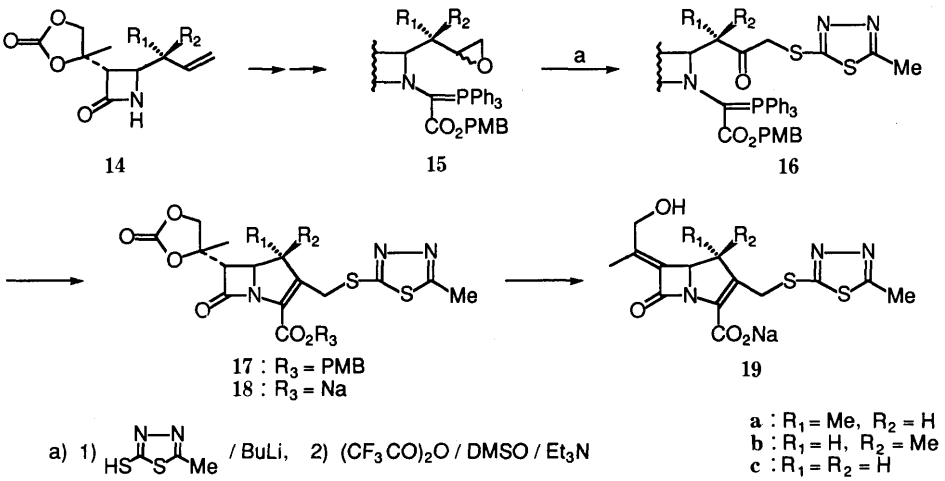

Chart 4

TABLE I. *In Vitro* Antibacterial Activity

Comp. No.	MIC (μg/ml)					
	S. aureus SR14	*S. pyogenes* C-203	*E. coli* EC-14	*K. pneumoniae* SR1	*P. vulgaris* CN-329	*S. marcescens* ATCC 13880
7a	6.3	12.5	25	50	>100	100
7b	25	50	50	100	>100	>100
7c	12.5	12.5	25	50	100	100
9a	1.6	3.1	12.5	12.5	50	50
9b	1.6	3.1	3.1	6.3	12.5	12.5
9c[a]	1.56	1.56	1.56	3.13	12.5	12.5
18a[b]	1.6	1.6	50	12.5	12.5	>100
18b	0.8	0.8	25	6.3	3.1	100
18c[c]	0.39	0.39	0.78	0.78	1.56	12.5
19b	0.1	0.1	0.1	0.4	0.2	12.5
19c[c]	0.2	0.2	0.78	0.78	0.78	12.5

a) The data taken from ref. 10. *b*) Compounds (**18a, b** and **19b, c**) are optically active. *c*) The data taken from ref. 3.

cessfully carried out using the procedures described above to produce the sodium carboxylates (**18a, b** and **19b**).

Although all these final products, as well as their intermediates, were stable enough to be isolated, compound **19a** could not be obtained as a pure sample to test antibacterial activity, probably due to its chemical instability.

Antibacterial Activity The minimum inhibitory concentration (MIC) values of these new carbapenems, together with the corresponding 1-unsubstituted derivatives against selected strains of gram-positive and gram-negative bacteria, are shown in Table I.

With regard to both 2-unsubstituted A- and B-type carbapenems (**7a, b,** and **9a, b**), no clear-cut structure activity relationships could be found.

In contrast to the above results, considerable differences were observed among the 2-functionalized-methyl carbapenem series. The 1β-methyl derivative of the B-type structure **19b** exhibited substantially increased potency relative to the corresponding 1-unsubstituted derivative **19c**.

Although the A-type and B-type carbapenems in the 1-unsubstituted series showed striking similarities in terms of their activities as exemplified by **18c** and **19c**, it is noteworthy that no such expected tendency has been observed in the 1-methyl series. On the contrary, the presence of either 1α- or 1β-methyl groups in the A-type counterparts induced a perceptible loss of activity. It seems likely that the A-type compound bearing no substituent at the C-1 position may be transformed to the B-type compound prior to interaction with the bacterial target enzyme (penicillin binding proteins). Our present observations seem to suggest that the presence of a 1-methyl group may inhibit this kind of eliminative transformation process in the biological system.

Experimental

All reactions involving air-sensitive reactants or products were carried out under N_2 using dry solvents. Melting points were determined on a Yanagimoto apparatus and are uncorrected. Infrared (IR) spectra were recorded on a Hitachi 260-10 spectrophotometer. Proton nuclear magnetic resonance (^{1}H-NMR) spectra were obtained on a Varian EM-390 (90 MHz). Chemical shifts are expressed in ppm downfield from tetramethylsilane (TMS) as an internal (in organic solvents) or external (in D_2O) standard. Ultraviolet (UV) spectra were taken on a Hitachi EPS-3T spectrometer. Specific optical rotations ($[\alpha]_D$) were taken at 25 °C on a Perkin–Elmer 241 Polarimeter. Medium pressure liquid chromatographies were performed on Merck 'Lobar' prepacked columns packed with LiChroprep Si 60; size A (240—10 mm, 40—60 μm), size B (310—25 mm, 40—60 μm) and size C (440—37 mm, 63—125 μm).

4-(1-Methylallyl)-2-azetidinone (2a and 2b) To a solution of **1** (12.2 g, 95 mmol) and crotyltriphenylstannane (46 g, 1.2 eq) in CH_2Cl_2 (150 ml) was added $BF_3 \cdot Et_2O$ (14 ml, 1.2 eq). The reaction mixture was stirred for 3 h and filtered. The filtrate was washed with 20% aq. $NaHCO_3$ solution and brine, then dried and concentrated. The residue was chromatographed on a Lobar column (size C, toluene–EtOAc 1 : 1) to give a 1 : 1 mixture of **2a** and **2b** as a white amorphous solid (11 g, 93%). IR ($CHCl_3$) cm^{-1}: 2900, 1740. ^{1}H-NMR ($CDCl_3$) δ: 0.99 (3H, d, J=7 Hz, CH_3), 1.05 (3H, d, J=7 Hz, CH_3), 2.23 (1H, m), 2.60 (1H, dd, J=2, 15 Hz), 3.00 (1H, dd, J=4, 15 Hz), 3.45 (1H, m), 5.10 (2H, m), 5.70 (1H, m), 6.60 (1H, br s, NH).

(3*S,4*R**)-1-*tert*-Butyldimethylsilyl-3-[(4*S**)-4-methyl-2-oxo-1,3-dioxolan-4-yl]-4-[(1*R**)-1-methylallyl]-2-azetidinone (4a)** Compound **2** (11 g, *ca.* 1 : 1 mixture of **2a** and **2b**) was silylated by the usual method to give **3** (*ca.* 1 : 1 mixture, 18 g, 87%). IR ($CHCl_3$) cm^{-1}: 2925, 1740. ^{1}H-NMR ($CDCl_3$) δ: 0.23 (3H, s, $SiCH_3$), 0.30 (3H, s, $SiCH_3$), 1.00 (9H, s), 1.01 (3H, d, J=7 Hz, CH_3), 1.06 (3H, d, J=7 Hz, CH_3), 2.00 (1H, m), 2.65 (1H, dd, J=2, 15 Hz), 2.95 (1H, dd, J=4, 15 Hz), 3.55 (1H, m), 5.10 (2H, m), 5.70 (1H, m). According to our previously established procedure,[3] **3** (8.5 g) was converted to the title compounds as follows.

A solution of *n*-butyllithium in hexane (1.6 N, 45 ml, 1.4 eq) was added to a solution of diisopropylamine (7.77 g, 1.5 eq) in (THF) (100 ml) at −70 °C. The mixture was stirred at 0 °C for 1 h then cooled to −70 °C. A solution of **3** (10.8 g, 45 mmol) in tetrahydrofuran (THF, 50 ml) was added dropwise to the above solution and the mixture was stirred for 40 min. To this mixture was added trimethylsilyloxyacetone (18 ml, 2 eq), and the combination was stirred for 30 min at the same temperature (−70 °C). The reaction mixture was diluted with brine and extracted with EtOAc (500 ml). The organic extracts were dried, filtered and evaporated to give an oily residue, which was dissolved in MeOH (200 ml) containing

acetic acid (10 ml). The solution was allowed to stand overnight at room temperature and then concentrated. The residue was chromatographed on a Lobar column (size C, benzene–EtOAc 1 : 1) to give the 8*R** isomer of glycol (9.5 g, 67%, 1 : 1 mixture at C-1) and the 8*S** isomer of glycol (4.3 g, 31%, 1 : 1 mixture at C-1). The 8*R** isomer: IR ($CHCl_3$) cm^{-1}: 3450, 3400, 2925, 2850, 1720. ^{1}H-NMR ($CDCl_3$) δ: 0.23 (3H, s), 0.30 (3H, s), 1.00 (9H, s), 1.01 (3H, d, J=7 Hz), 1.05 (3H, s), 1.07 (3H, d, J=7 Hz), 2.70 (1H, m), 2.90 and 3.00 (1H, d, J=2 Hz), 3.20—3.90 (3H, m), 4.27 (2H, br s, OH), 5.10 (2H, m), 5.70 (1H, m). The 8*S** isomer: IR ($CHCl_3$) cm^{-1}: 3450, 3400, 2925, 2850, 1720. ^{1}H-NMR ($CDCl_3$) δ: 0.23 (3H, s), 0.30 (3H, s), 1.00 (9H, s), 1.01 (3H, d, J=7 Hz), 1.07 (3H, d, J=7 Hz), 1.30 (3H, s), 2.70 (1H, m), 3.02 and 3.05 (1H, d, J=2 Hz), 3.30—3.80 (5H, m), 5.10 (2H, m), 5.70 (1H, m).

A solution of phosgene in toluene (3.3 M, 4.2 ml, 1.2 eq) was added to a solution of the above 8*S** glycol (3.7 g, 11.8 mmol) in CH_2Cl_2 containing pyridine (2.4 ml, 2.5 eq) under ice-cooling, and the mixture was stirred for 30 min, then diluted with EtOAc, washed with water, dried and concentrated. The residue was chromatographed on a Lobar column (size C, hexane–benzene–EtOAc 3 : 2 : 1) to give **4a** (1.71 g, 13%) and **4b** (1.74 g, 14%). **4a**: IR ($CHCl_3$) cm^{-1}: 2925, 1805, 1740. ^{1}H-NMR ($CDCl_3$) δ: 0.23 (3H, s), 0.30 (3H, s), 1.00 (9H, s), 1.13 (3H, d, J=7 Hz), 1.57 (3H, s), 2.70 (1H, m), 3.20 (1H, d, J=2 Hz), 3.62 (1H, m), 4.02 and 4.21 (2H, ABq, J=8 Hz), 5.10 (2H, m), 5.70 (1H, m).

(3*S,4*R**)-1-*tert*-Butyldimethylsilyl-3-[(4*S**)-4-methyl-2-oxo-1,3-dioxolan-4-yl]-4-[(1*S**)-1-methylallyl]-2-azetidinone (4b)** **4b**: IR ($CHCl_3$) cm^{-1}: 2925, 1805, 1740. ^{1}H-NMR ($CDCl_3$) δ: 0.23 (3H, s), 0.30 (3H, s), 1.00 (9H, s), 1.10 (3H, d, J=6 Hz), 1.55 (3H, s), 2.70 (1H, m), 3.20 (1H, d, J=2 Hz), 3.60 (1H, m), 4.04 and 4.24 (2H, ABq, J=8 Hz), 5.10 (2H, m), 5.70 (1H, m).

***p*-Methoxybenzyl (1*R**,5*R**,6*S**)-1-Methyl-6-[(4*S**)-4-methyl-2-oxo-1,3-dioxolan-4-yl]carbapen-2-em-3-carboxylate (6a)** Compound **4a** was converted to the ylide **5a** by the established procedure. **5a**: IR ($CDCl_3$) cm^{-1}: 1805, 1740, 1650, 1600. Ozone was passed through a solution of **5a** (1.10 g, 1.66 mmol) in CH_2Cl_2 (30 ml) containing trifluoroacetic acid (2 ml) at −60 °C until a blue color persisted. Excess ozone was removed by passing nitrogen gas through the reaction mixture, then dimethylsulfide (2 ml) was added and stirred for 1 h at room temperature. The solution was diluted with EtOAc (100 ml) and stirred with aqueous saturated $NaHCO_3$ (20 ml) for 1 h at room temperature. The organic layer was separated, washed with water, dried and concentrated. The residue was chromatographed on a Lobar column (size B, benzene–EtOAc 1 : 2) to give **6a** as an amorphous powder (392 mg, 61%). IR ($CHCl_3$) cm^{-1}: 1805, 1790, 1720. ^{1}H-NMR ($CDCl_3$) δ: 1.25 (3H, d, J=7 Hz), 1.64 (3H, s), 3.25 (1H, m), 3.61 (1H, d, J=2 Hz), 3.78 (3H, s), 4.10 (1H, m), 4.15 and 4.35 (2H, ABq, J=9 Hz), 5.18 (2H, s), 6.35 (1H, d, J=2 Hz), 6.85 and 7.35 (4H, A_2B_2q, J=8 Hz).

***p*-Methoxybenzyl (1*S**,5*R**,6*S**)-1-Methyl-6-[(4*S**)-4-methyl-2-oxo-1,3-dioxolan-4-yl]carbapen-2-em-3-carboxylate (6b)** The carbapenem **6b** was prepared by the same method as above. IR ($CHCl_3$) cm^{-1}: 1805, 1790, 1720. ^{1}H-NMR ($CDCl_3$) δ: 1.12 (3H, d, J=7 Hz), 1.66 (3H, s), 3.20 (1H, m), 3.62 (1H, d, J=2 Hz), 3.78 (3H, s), 4.20 (1H, m), 4.21 and 4.43 (2H, ABq, J=9 Hz), 5.18 (2H, s), 6.38 (1H, d, J=2 Hz), 6.85 and 7.35 (4H, A_2B_2q, J=8 Hz).

Sodium (1*R,5*R**,6*S**)-1-Methyl-6-[(4*S**)-4-methyl-2-oxo-1,3-dioxolan-4-yl]carbapen-2-em-3-carboxylate (7a)** The *p*-methoxybenzyl (PMB) ester **6a** (125 mg, 0.32 mmol) was added to a solution of $AlCl_3$ (172 mg, 4 eq) in a mixture of anisole (5 ml) and CH_2Cl_2 (2 ml) at −40 °C, and the mixture was stirred for 1 h at the same temperature. A solution of $NaHCO_3$ (390 mg, 12 eq) in a pH 7 phosphate buffer (0.02 M, 5 ml) and CH_2Cl_2 (20 ml) were added, and the reaction mixture was stirred under ice cooling for 30 min and filtered. The aqueous filtrate was chromatographed on an HP-20AG column (10 mm × 240 mm, H_2O) and the fractions containing the product were concentrated and freeze-dried to give **7a** as a white powder (17 mg, 18%). ^{1}H-NMR (D_2O) δ: 1.68 (3H, d, J=7 Hz), 2.15 (3H, s), 3.80 (1H, m), 4.35 (1H, d, J=2 Hz), 4.58 and 4.83 (2H, ABq, J=9 Hz), 5.00 (1H, m), 6.68 (1H, d, J=2 Hz).

Sodium (1*S,5*R**,6*S**)-1-Methyl-6-[(4*S**)-4-methyl-2-oxo-1,3-dioxolan-4-yl]carbapen-2-em-3-carboxylate (7b)** Similarly, **6b** (200 mg, 0.52 mmol) gave **7b** (113 mg, 76%). ^{1}H-NMR (D_2O) δ: 1.56 (3H, d, J=7 Hz), 2.19 (3H, s), 3.75 (1H, m), 4.35 (1H, d, J=2 Hz), 4.60 and 4.85 (2H, ABq, J=9 Hz), 5.00 (1H, m), 6.70 (1H, d, J=2 Hz).

***p*-Methoxybenzyl (1*R**,5*R**)-6-[(*E*)-1-(Hydroxymethyl)ethylidene]-1-methylcarbapen-2-em-3-carboxylate (8a)** A solution of DBU in toluene (1 M, 0.1 ml) was added to a solution of **6a** (250 mg, 0.65 mmol) in acetonitrile (2 ml) and the mixture was stirred at room temperature for 20 min, then diluted with EtOAc, washed with water, dried and concentrated. The residue was chromatographed on a Lobar column (size A, benzene–EtOAc 1 : 1) to give **8a** as a white powder (182 mg, 82%). IR ($CHCl_3$) cm^{-1}: 3400, 1750, 1710. ^{1}H-NMR ($CDCl_3$) δ: 1.24 (3H, d, J=7 Hz), 1.99 (3H, s), 3.20 (1H, m), 3.60 (1H, br, OH), 3.78 (3H, s), 4.20 (2H, s), 4.60 (1H, d, J=2 Hz), 5.18 (2H, s), 6.34 (1H, d, J=2 Hz), 6.85 and 7.35 (4H, A_2B_2q, J=8 Hz).

***p*-Methoxybenzyl (1*S**,5*R**)-6-[(*E*)-1-(Hydroxymethyl)ethylidene]-1-methylcarbapen-2-em-3-carboxylate (8b)** Similarly, **6b** (300 mg, 0.78 mmol) gave **8b** (210 mg, 79%). IR ($CHCl_3$) cm^{-1}:3400, 1750, 1710. ^{1}H-NMR ($CDCl_3$) δ: 0.99 (3H, d, J=7 Hz), 1.99 (3H, s), 3.10 (1H, m), 3.40 (1H, br, OH), 3.78 (3H, s), 4.18 (2H, s), 4.60 (1H, d, J=5 Hz), 5.18 (2H, s), 6.37 (1H, d, J=2 Hz), 6.85 and 7.35 (4H, A_2B_2q, J=8 Hz).

Sodium (1*R,5*R**)-6-[(*E*)-1-(Hydroxymethyl)ethylidene]-1-methylcarbapen-2-em-3-carboxylate (9a)** By the deprotection method described above, the PMB ester **8a** (200 mg, 0.58 mmol) gave **9a** (13 mg, 18%) as a white powder. ^{1}H-NMR (D_2O) δ: 1.68 (3H, d, J=7 Hz), 2.45 (3H, s), 3.70 (1H, m), 4.68 (2H, s), 5.30 (1H, d, J=2 Hz), 6.60 (1H, d, J=2 Hz).

Sodium (1*S,5*R**)-6-[(*E*)-1-(Hydroxymethyl)ethylidene]-1-methylcarbapen-2-em-3-carboxylate (9b)** Similarly, the PMB ester **8b** (150 mg, 0.44 mmol) gave **9b** (66 mg, 62%) as a white powder. ^{1}H-NMR (D_2O) δ: 1.40 (3H, d, J=7 Hz), 2.50 (3H, s), 3.60 (1H, m), 4.70 (2H, s), 5.30 (1H, d, J=5 Hz), 6.70 (1H, d, J=2 Hz). UV (H_2O) nm: 235, 307.

Preparation of the Optically Active Azetidinones. (4*R*)-1-*tert*-Butyldimethylsilyl-4-(1-methylallyl)-2-azetidinone (13a and 13b) According to our previously established procedure,[7] (3*R*)-4-acetoxy-3-bromo-2-azetidinone **11** (*ca.* 1 : 1 epimeric mixture) was prepared from 6α-bromopenicillanic acid methyl ester **10**. By the same method used for **2**, the azetidinone **11** (21 g, 100 mmol) gave 4(*R*)-(1-methylallyl)azetidinone **12** as a 1 : 1 mixture of **12a** and **12b** (17 g, 81%). IR ($CHCl_3$) cm^{-1}: 1750, 1610. **12a**: ^{1}H-NMR ($CDCl_3$) δ: 1.11 (3H, d, J=7 Hz), 2.35 (1H, m), 3.62 (1H, d, J=2 Hz), 3.95 (1H, m), 5.10 (2H, m), 5.70 (1H, m). **12b**: ^{1}H-NMR ($CDCl_3$) δ: 1.08 (3H, d, J=7 Hz), 2.35 (1H, m), 3.60 (1H, d, J=2 Hz), 5.10 (2H, m), 5.70 (1H, m).

After N-silylation, compound **12** (15 g, 73.5 mmol) was treated with zinc powder (6.9 g, 6.7 eq) in a mixed solvent of acetic acid (15 ml), MeOH (70 ml) and CH_2Cl_2 (100 ml). After 1 h of stirring at room temperature, the reaction mixture was filtered, concentrated and then chromatographed on Lobar columns (size C × 2, benzene–EtOAc 9 : 1) to give **13** as a 1 : 1 mixture of **13a** and **13b** (13 g, 72%). The NMR spectrum of **13** was identical to that of the racemate **3**.

(3*S*,4*R*)-3-[(4*S*)-4-Methyl-2-oxo-1,3-dioxolan-4-yl]-4-[(1*R*)-1-methylallyl]-2-azetidinone (14a) By the same procedure used for the racemates, **14a** and **14b** were prepared, respectively. **14a**: mp 121—122 °C (hexane–ether). $[\alpha]_D$ +41.24° (*c*=0.43, $CHCl_3$). IR ($CHCl_3$) cm^{-1}: 3410, 1775. ^{1}H-NMR ($CDCl_3$) δ: 1.11 (3H, d, J=7 Hz), 1.59 (3H, s), 2.40 (1H, m), 3.13 (1H, d, J=2 Hz), 3.38 (1H, m), 4.05 and 4.25 (2H, ABq, J=8 Hz), 5.10 (2H, m), 5.70 (1H, m), 7.10 (1H, br, NH). *Anal.* Calcd for $C_{11}H_{15}NO_4$: 6.71; N, 6.22; O, 28.41. Found: C, 58.58; H, 6.62; N, 6.27.

(3*S*,4*R*)-3-[(4*S*)-4-Methyl-2-oxo-1,3-dioxolan-4-yl]-4-[(1*S*)-1-methylallyl]-2-azetidinone (14b) **14b**: mp 120—121 °C (hexane–ether). $[\alpha]_D$ +15.91° (*c*=0.22, $CHCl_3$). IR ($CHCl_3$) cm^{-1}: 3410, 1810, 1775. ^{1}H-NMR ($CDCl_3$) δ: 1.09 (3H, d, J=7 Hz), 1.60 (3H, s), 2.40 (1H, m), 3.15 (1H, d, J=2 Hz), 3.38 (1H, m), 4.10 and 4.30 (2H, ABq, J=8 Hz), 5.10 (2H, m), 5.70 (1H, m), 7.10 (1H, br, NH). *Anal.* Calcd for $C_{11}H_{15}NO_4$: C, 58.66; H, 6.71; N, 6.22; O, 28.41. Found: C, 58.56; H, 6.65; N, 6.28.

***p*-Methoxybenzyl (1*R*,5*R*,6*S*)-1-Methyl-6-[(4*S*)-4-methyl-2-oxo-1,3-dioxolan-4-yl]-2-(5-methyl-1,3,4-thiadiazol-2-yl)thiomethylcarbapen-2-em-3-carboxylate (17a)** The above optically active azetidinone **14a** was transformed to the epoxy-ylide **15a** by our previously established procedure.[3] IR ($CHCl_3$) cm^{-1}: 3010, 1805, 1740, 1600. A solution of *n*-butyllithium in hexane (1.6 N, 1.25 ml, 0.5 eq) was added to a solution of 5-methyl-1,3,4-thiadiazolylthiol (787 mg, 3 eq) in THF (5 ml) under ice cooling. To this mixture was added a solution of the ylide **15a** (1.6 g, 2 mmol) in THF (10 ml), and the reaction mixture was stirred overnight at room temperature. It was then diluted with EtOAc, washed with aqueous $NaHCO_3$ solution and brine, dried and concentrated to give the hydroxy-ylide (1.73 g, 93%). A solution of dimethyl sulfoxide (DMSO) (0.422 ml, 3 eq) in CH_2Cl_2 (10 ml) was treated with trifluoroacetic anhydride (0.56 ml, 2 eq) at −70 °C for 30 min. To this mixture was added a solution of the above hydroxy-ylide in CH_2Cl_2 (3 ml) and the whole was stirred at −70 °C for 1 h. Triethylamine (1.16 ml, 4.2 eq) was added and stirred for 10 min and then diluted with EtOAc, washed with water, dried and concentrated to give the keto-ylide **16a** (1.7 g, 99%). IR ($CHCl_3$) cm^{-1}: 1805, 1740.

A solution of the above ylide **16a** (1.7 g, 1.8 mmol) in toluene (100 ml)

was heated at 81 °C for 2 h, then concentrated. The residue was chromatographed on a Lobar column (size B, CH_2Cl_2–acetonitrile 5 : 1) to give **17a** as an oil (75 mg, 8%). IR ($CHCl_3$) cm^{-1}: 1805, 1790, 1600. ^{1}H-NMR ($CDCl_3$) δ: 1.35 (3H, d, J=7 Hz), 1.55 (3H, s), 2.70 (3H, s), 3.30—3.55 (1H, m), 3.60 (1H, d, J=2 Hz), 3.80 (3H, s), 4.02 (1H, m), 4.15 and 4.40 (2H, ABq, J=8 Hz), 5.21 (2H, s), 6.85 and 7.35 (4H, ABq, J=9 Hz).

***p*-Methoxybenzyl (1*S*,5*R*,6*S*)-1-Methyl-6-[(4*S*)-4-methyl-2-oxo-1,3-dioxolan-4-yl]-2-(5-methyl-1,3,4-thiadiazol-2-yl)thiomethylcarbapen-2-em-3-carboxylate (17b)** Following the same procedure as described above, **17b** was synthesized from **14b** (intramolecular Wittig reaction proceeded at 100 °C). IR ($CHCl_3$) cm^{-1}: 1805, 1790, 1600. ^{1}H-NMR ($CDCl_3$) δ: 1.18 (3H, d, J=7 Hz), 1.60 (3H, s), 2.68 (3H, s), 3.30—3.55 (1H, m), 3.60 (1H, d, J=2 Hz), 3.79 (3H, s), 4.00 (1H, m), 4.16 and 4.47 (2H, ABq, J=8 Hz), 4.38 and 4.63 (2H, ABq, J=8 Hz), 5.20 (2H, s), 6.85 and 7.35 (4H, A_2B_2q, J=9 Hz).

The following compounds were prepared by the methods used for 2-unsubstituted derivatives.

Sodium (1*R*,5*R*,6*S*)-1-Methyl-6-[(4*S*)-4-methyl-2-oxo-1,3-dioxolan-4-yl]-2-(5-methyl-1,3,4-thiadiazol-2-yl)thiomethylcarbapen-2-em-3-carboxylate (18a) **18a**: $[\alpha]_D$ +26.1° (c=0.50, H_2O). ^{1}H-NMR (D_2O) δ: 1.75 (3H, d, J=7 Hz), 2.18 (3H, s), 3.20 (3H, s), 3.70—3.95 (1H, m), 3.85 (1H, d, J=2 Hz), 4.20 and 4.48 (2H, ABq, J=8 Hz), 4.50 and 4.71 (2H, ABq, J=8 Hz), 4.55 (1H, m). UV (H_2O) nm: 235, 276.

Sodium (1*S*,5*R*,6*S*)-1-Methyl-6-[(4*S*)-4-methyl-2-oxo-1,3-dioxolan-4-yl]-2-(5-methyl-1,3,4-thiadiazol-2-yl)thiomethylcarbapen-2-em-3-carboxylate (18b) **18b**: $[\alpha]_D$ −87.2° (c=0.50, H_2O). ^{1}H-NMR (D_2O) δ: 1.55 (3H, d, J=7 Hz), 2.18 (3H, s), 3.20 (3H, s), 3.70—3.95 (1H, m), 3.85 (1H, J=2 Hz), 3.50 and 4.22 (2H, ABq, J=8 Hz), 4.51 and 4.73 (2H, ABq, J=8 Hz), 4.60 (1H, m). UV (H_2O) nm: 235, 276.

Sodium (1*S*,5*R*)-6-[(*E*)-1-Hydroxymethyl)ethylidene]-1-methyl-2-(5-methyl-1,3,4-thiadiazol-2-yl)thiomethylcarbapen-2-em-3-carboxylate (19b) **19b**: $[\alpha]_D$ −336° (c=0.50, H_2O). ^{1}H-NMR (D_2O) δ: 1.43 (3H, d, J=7 Hz), 2.45 (3H, s), 3.18 (3H, s), 3.60—3.85 (1H, m), 4.63 and 4.80 (2H, ABq, J=8 Hz), 4.65 (2H, s), 5.30 (1H, d, J=5 Hz). UV (H_2O) nm: 230, 295.

Determination of MICs MICs were determined by the agar dilution method using sensitivity test agar (Eiken, Japan). An overnight culture of bacteria in tryptosoy broth (Eiken, Japan) was diluted to about 10^6 cells/ml with the same broth and inoculated with an inoculating device onto agar containing serial twofold dilutions of the test compounds. Organisms were incubated at 37 °C for 18—20 h. The MIC of a compound was defined as the lowest concentration that visibly inhibited growth.

Acknowledgment We wish to thank Dr. M. Shiro (X-ray crystallographic analysis), Mr. K. Motokawa and Mr. Y. Kimura (*in vitro* activity assay).

References

1) Carbapenem and Penem Antibiotics. IV. H. Ona, S. Uyeo, T. Fukao, M. Doi and T. Yoshida, *Chem. Pharm. Bull.*, **33**, 4382 (1985).
2) K. Tanaka, J. Shoji, Y. Terui, N. Tsuji, E. Kondo, M. Mayama, Y. Kawamura, T. Hattori, K. Matsumoto and T. Yoshida, *J. Antibiot.*, **34**, 909 (1981); J. Shoji, H. Hinoo, R. Sakazaki, N. Tsuji, K. Nagashima, K. Matsumoto, Y. Takahashi, S. Kozuki, T. Hattori, E. Kondo and K. Tanaka, *ibid.*, **35**, 15 (1982).
3) M. Imuta, H. Ona, S. Uyeo, K. Motokawa and T. Yoshida, *Chem. Pharm. Bull.*, **33**, 4361 (1985).
4) D. H. Shih, F. Baker, L. Cama and B. G. Christensen, *Heterocycles*, **21**, 29 (1984).
5) G. A. Kraus and K. Neuenschwanjder, *J. Chem. Soc., Chem. Commun.*, **1982**, 134; A. Martel, J-P. Davis, C. Bachand, M. Menard, T. Durst and B. Belleau, *Can. J. Chem.*, **61**, 1899 (1983); H. Fliri and C-P. Mak, *J. Org. Chem.*, **50**, 3438 (1985); M. Aratani, H. Hirai, K. Sawada and M. Hashimoto, *Heterocycles*, **23**, 1889 (1985); K. Fujimoto, Y. Iwano and K. Hirai, *Tetrahedron Lett.*, **26**, 89 (1985); *idem, Bull. Chem. Soc. Jpn.*, **59**, 1363 (1986).
6) H. R. Pfaendler, J. Gosteli and R. B. Woodward, *J. Am. Chem. Soc.*, **101**, 6306 (1979).
7) M. Imuta, S. Uyeo, M. Nakano and T. Yoshida, *Chem. Pharm. Bull.*, **33**, 4371 (1985).
8) M. Ohtani, F. Watanabe and M. Narisada, *J. Org. Chem.*, **49**, 5271 (1984).
9) R. W. Ratcliffe and G. Albers-Schönberg, "Chemistry and Biology of Beta-Lactam Antibiotics," Vol. 2, ed. by R. B. Morin and M. Gorman, Academic Press, New York, 1982, p. 227.
10) H. Ona, S. Uyeo, K. Motokawa and T. Yoshida, *Chem. Pharm. Bull.*, **33**, 4346 (1985).

Carbapenem and Penem Antibiotics. VI. Synthesis and Antibacterial Activity of 2-Heteroaromatic-thiomethyl and 2-Carbamoyloxymethyl 1-Methylcarbapenems[1)]

Mitsuru IMUTA,* Hikaru ITANI, Hisao ONA, Yoshinori HAMADA, Shoichiro UYEO* and Tadashi YOSHIDA

Shionogi Research Laboratories, Shionogi & Co., Ltd., Sagisu, Fukushima-ku, Osaka 553, Japan. *Received August 6, 1990*

The synthesis and antibacterial activity of the 1-methylcarbapenems, 2-heteroaromatic-thiomethyl and 2-carbamoyloxymethyl derivatives having a 6-[(*R*)-1-hydroxyethyl] side chain, are described. The introduction of a methyl substituent at the C-1 position was accomplished by a newly developed procedure using crotyl halides and zinc dust. The 2-hydroxymethyl carbapenems as key intermediates allowed an easy entry into the preparation of title carbapenems.

Keywords β-lactam antibiotic; carbapenem antibiotic; 1α-methyl carbapenem antibiotic; 1β-methyl carbapenem antibiotic; 1,1-dimethyl carbapenem antibiotic; 2-functionalized-methyl carbapenem antibiotic; Zn-promoted allylation; antibacterial activity; methicillin-resistant *S. aureus* (MRSA)

Since the first report on 1β-methyl carbapenem possessing unique biological properties by a Merck group in 1984,[2)] a considerable number of papers relevant to the analogous derivatives have appeared. However, only a few compounds have actually survived to be developed to date for clinical candidates.[3)] In recent years, we have been engaged in extensive studies on the synthesis of a series of 2-functionalized-methyl carbapenem[4)] and penem[5)] antibiotics, distinguishable from the well established 2-alkylthio derivatives as represented by imipenem.[6)] We have already reported that the 2-heteroaromatic thiomethyl as well as 2-acetoxymethyl carbapenems having a hydroxyethyl side chain at the C-6 position possessed potent and well-balanced antibacterial activity against both gram-positive and gram-negative bacteria except for *Pseudomonas aeruginosa*.[7)] This finding led us to extend our synthetic programs to the corresponding 1-methyl carbapenem congeners, including 2-carbamoyloxymethyl derivatives.

Our proposed synthetic strategy was to construct the desired 1-substituted carbapenems utilizing the crucial chiral synthons **2** as starting materials (Chart 2) and the 2-hydroxymethyl derivatives (**21** and **22b,c**) as ultimate precursors (Chart 4). The synthesis of 4(*R*)-(1-methylallyl)-azetidinones **2** was achieved by an allylation reaction of 4(*R*)-acetoxyazetidinone **1**[8)] with crotyl halides and zinc dust, which turned out to be effective for large scale preparation. The key compounds, both 2-hydroxymethyl-1β-methyl and corresponding 1-unsubstituted carbapenems (**20**, **21** and **22b,c**), were efficiently synthesized by the originally designed sequences.

After this study was completed and a patent concerning part of the work was filed,[9)] the syntheses of the 2-carbamoyloxymethyl derivative **25a** and related compounds[10)] as well as the 2-thiadiazolylthiomethyl **11a**[11)] and 2-tetrazolylthiomethyl **26a**[12)] derivatives have recently been reported.

With regard to antibacterial activity, all the 1β-methyl carbapenems exhibited considerable improvement compared to their 1-unsubstituted counterparts. In this paper, we now provide a full account of our synthetic studies on the title compounds. Their antibacterial properties will also be discussed.

Chemistry In the preceding paper we reported the establishment of an efficient reaction sequence for synthesizing the 2-functionalized-methyl 1-methylcarbapenems bearing the asparenomycin-type C-6 side chain starting from the 4-(1-methylallyl)azetidinones. In order to prepare the title carbapenems we therefore decided to use the corresponding azetidinones **2** as starting materials. Although Lewis acid-mediated allylations of the 4-acetoxyazetidinones by allylsilanes or allylstannanes have been recently studied,[13,14)] we have been interested in developing a more versatile and practical method, particularly from the industrial point of view.

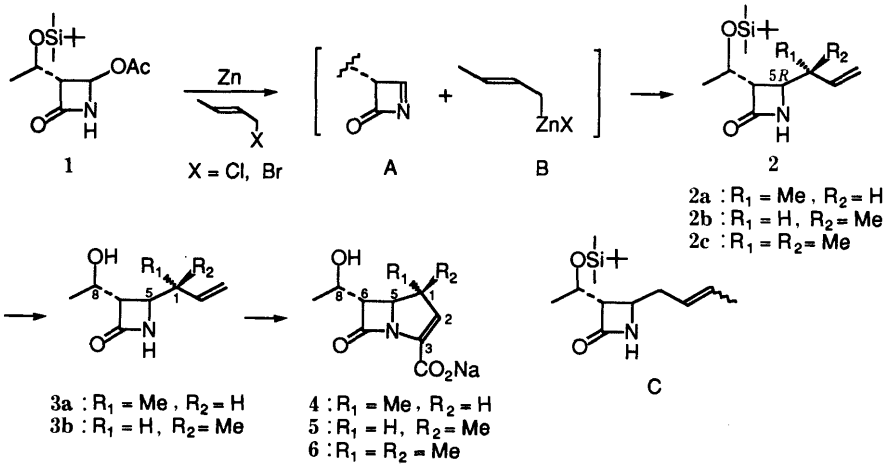

Chart 1

Since allylic zinc reagents are known to react with various electrophiles under relatively mild reaction conditions to afford allylation products,[15] we investigated the reaction of this class of reagents with 4-acetoxyazetidinone **1**.

Our initial approach, directed toward the preparation of the target compounds **2**, was quite successfully carried out as outlined in Chart 1. That is, treatment of the optically active 4-acetoxyazetidinone **1** with crotyl bromide (1.2 eq) and zinc dust (3 eq) in tetrahydrofuran (THF) at 35 °C (entry 1) resulted in the formation of 4(*R*)-(1-methylallyl)-azetidinone **2** in 90% yield. As far as the product stereospecificity at C-1 (carbapenem structure numbering) is concerned, approximately equal amounts of regioisomers (**2a** and **2b**) were detected by 200 MHz ^{1}H-NMR analysis. After considerable trials, it was found that this reaction in dimethylformamide (DMF) gave rise to a slightly higher ratio for the formation of **2b** (entry 2).[16] It is of particular note that the reaction proceeded regioselectively *via* complete allylic rearrangement of the zinc reagent leading to the C–C bond formation at the C-4 position of the azetidinone without contamination of any regioisomer C. Accordingly, the 1,1-dimethyl derivative **2c** was also obtained by the same procedure using prenyl bromide. Furthermore, this method was found to be effective with crotyl chloride, wherein the reagent behaved exactly the same way, albeit at a slow reaction rate (entry 4). Quite surprisingly, when 3-chloro-1-butene was used in this reaction, essentially the same result was observed (entry 5). This may be rationalized in terms of a facile isomerization of the initially formed zinc reagent to the type B structure giving rise to **2**, and not to the other isomer C (Chart 1). Since we needed first to test the activity of both 1α- and 1β-methylcarbapenems, the operational simplicity and high efficiency of the present method afforded significant advantages for large-scale preparation of the required common intermediates.

TABLE I. Reactions of Azetidinone **1** with Allylic Halides and Zinc

Entry	Allylic halide	Solvent	Time (h)	Yield (%)[a]	Ratio (**2a**/**2b**)[b]
1		THF	2	90	1/1
2		DMF	1.5	90	1/1.2
3	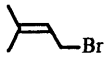	THF	2.5	95[c]	
4		DMF	10	80	1/1
5	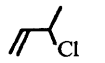	DMF	12	75	1/1

a) Isolated yields based on azetidinone **1**. *b*) The **2a**/**2b** ratios were determined by NMR of the crude product mixture. *c*) The product was **2c**.

The absolute configuration at C-1 of compound **2** was assigned unequivocally by the following sequence. The 1 : 1 regioisomeric mixture (**2a** and **2b**) thus obtained could not be separated by practical means. However, after deprotection of the silyloxy group, the resulting alcohols **3a** and **3b** could be readily separated by silica gel chromatography and purified by repeated recrystallization. X-Ray crystallographic analysis confirmed that the **3b** (mp 89—90.5 °C, $[\alpha]_D$ −31.2° (c = 1.0, $CHCl_3$)) had a 1*S*,5*R*,8*R* (carbapenem structure numbering) stereo configuration, and therefore the diastereoisomer **3a** should have a 1*R*,5*R*,8*R* structure.

To our knowledge, no detailed report on the bioactivity of 2-unsubstituted 1-methylcarbapenems has appeared since Shibuya *et al.* first reported the synthesis of 1,1-dimethyl derivative **6** in 1982.[17] Before getting into the synthetic studies on the title carbapenems, our initial work was therefore directed toward the synthesis of 2-unsubstituted derivatives (**4**, **5** and **6**) starting from **2a**, **b** and **2c**, respectively. To this end, both **3a** and **3b** were independently resilylated to give **2a** and **2b** as pure materials. The standard procedure involving the intramolecular Wittig cyclization developed by Woodward[18] has been used for the preparation of compounds **4**, **5** and **6**.

As for the final deprotection step, in all cases the *p*-methoxybenzyl (PMB) esters of the cyclized carbapenems were quite efficiently cleaved by the $AlCl_3$–anisole method[19] to give the corresponding sodium salts.

The structure activity relationship of the above synthesized carbapenems revealed that the 1β-methyl derivative **5** was superior to both the 1α **4** and 1,1-dimethyl **6** counterparts in terms of their antibacterial activity as shown in Table II. This observation agreed with that already

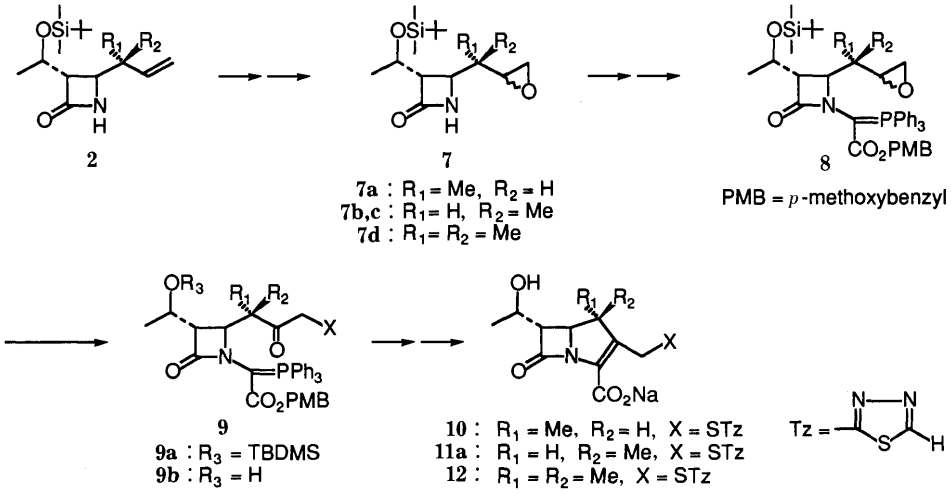

Chart 2

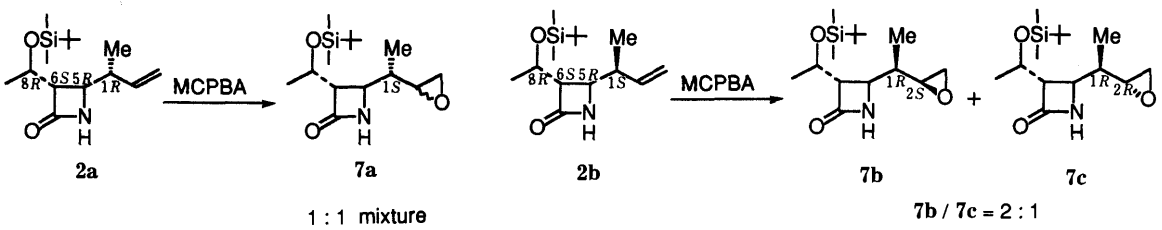

Chart 3

reported of other carbapenems by the Merck group.[2)]

Therefore, our attention was next focused on the preparation of the title carbapenems by utilizing the above regioisomeric mixture **2** ($\beta/\alpha = 1.2:1$, entry 2), which was found to be recrystallized from acetonitrile to produce a 2:1 mixture of β and α isomers **2b** and **2a** (Chart 2). Epoxidation of the resulting mixture with *m*-chloroperbenzoic acid (MCPBA) proceeded smoothly to afford the objective product **7**, which was directly recrystallized from acetonitrile to give a crystalline solid. Fortuitously, it was proven that this compound consisted primarily of a requisite β isomer **7b** in 90% purity contaminated with *ca.* 10% of **7a** and **7c** by comparison with the authentic compounds prepared alternatively as follows (Chart 3).

When the purified **2b** (1β-methyl carbapenem precursor) was epoxidized under the above reaction conditions, one stereoisomer, **7b**, with respect to the epoxide ring was formed more favorably (2:1) than the other isomer, **7c**. Each epoxide could be separated and purified by silica gel chromatography followed by recrystallization. The major isomer **7b** (mp 165—165.5 °C, $[\alpha]_D$ −30.7° ($c = 1.007$, $CHCl_3$)), unambiguously established by X-ray crystallographic analysis, was shown to possess a 1*R*,2*S* stereo configuration (carbapenem numbering). Therefore, the other isomer **7c** should have a 1*R*,2*R* structure. In the case of the purified **2a** isomer, however, the 1α-methyl group did not seem to affect the course of epoxidation reaction, giving rise to an inseparable mixture of two epoxides **7a** in a ratio of 1:1. With all four possible epoxides in hand, we were able to confirm that the isomers could, in fact, be distinguished by 200 MHz ^{1}H-NMR spectroscopy on the basis of the C-3 and C-4 (C-6 and C-5 of carbapenem) proton chemical shifts.

Using the standard procedure, the above resulting epoxide **7b** (90% purity) was converted to the corresponding epoxy-ylide **8**. The epoxide ring was cleaved regiospecifically by the base-catalyzed nucleophilic attack of a number of heteroaromatic thiols such as 1,3,4-thiadiazol-2-thiol, and subsequent oxidation of the resulting alcohols afforded the keto-ylides **9a**. All the 1β-methyl keto-ylides were found to be readily purified by silica gel chromatography at this stage.

In the case of the 1β-methyl intermediates thus obtained, further transformation to the carbapenem skeleton was successfully accomplished by the standard intramolecular Wittig reaction. Furthermore, the 1,1-dimethyl derivative **12** was alo prepared analogously starting from **2c**. On the other hand, it was observed that the 1α-methyl carbapenems and their intermediates were not so stable as those of the 1β-methyl and 1,1-dimethyl counterparts. The importance of the 1β-methyl substituent to the chemical stability of such structures was again recognized by these observations as emphasized in the preceding paper.[1)] Actually, to test the activity of an unstable sample, we could obtain only a 1:1 mixture of 1α- and 1β-methyl thiadiazolylthio derivatives (**10** and **11a**) by avoiding separation and purifications of the intermediates.

Although most of the target compounds were readily prepared by the above reaction sequence, elaboration of the C-2′ tetrazolylthio derivatives resulted in extremely low yields due to their concomitant thermal decomposition under the cyclization process, as observed in the case of the corresponding 1-unsubstituted derivative.[7)]

Since the penem antibiotic bearing a carbamoyloxymethyl side chain at the C-2 position has been advanced by the Farmitalia group as a broad spectrum, orally active, clinical candidate,[20)] there has been a particular interest to know the antibacterial properties of the corresponding carbapenem derivatives. Previous work from our laboratories had revealed that the preparation of **25a** by the procedure presented above *via* **9a** (X = $OCONH_2$) was unsuccessful.[21)] Therefore, we devised an alternative strategy for the synthesis of the 1β-methyl 2-hydroxymethyl carbapenem **21** in the hope of converting it into the desired compound.

For this purpose we chose the acetoxymethyl keto-ylide **14** as a suitable intermediate, and attempts were made to define conditions for selective hydrolysis of the acetoxy moiety. Elaboration of compound **14** began with a regiospecific ring opening reaction of the epoxide **7b** (90% purity) by acetic acid in the presence of a catalytic amount of $Ti(OiPr)_4$, wherein the choice of Lewis acids was found to be crucial. The usual procedure led to the objective 1β-methyl derivative **14** which could be purified by silica gel chromatography. After cleavage of the *tert*-butyldimethylsilyl (TBDMS) ether of **14**, the careful treatment of the resultant C-8 alcohol **15** with a catalytic amount of MeONa in MeOH at −20 °C afforded the desired diol **19a** in good yield (Chart 4). The conditions used above did not cause epimerization of the methyl group at the C-1 position. The critical cyclization of the diol **19a** to the carbapenem nucleus **21** by the internal Wittig reaction was successfully accomplished.

When the diol **21** was treated with trichloroacetyl isocyanate in CH_2Cl_2 at −20 °C, only the primary alcohol was selectively functionalized. Accordingly, subsequent utilization of the known procedure employed in the corresponding penem antibiotics,[22)] followed by the deprotection of the PMB ester, produced **25a**. Since the corresponding 1-unsubstituted derivative **24** had not yet been reported, we prepared this compound starting from **7e** by way of the carbapenem diol **20**. In addition, the 2-acetoxymethyl carbapenem **23a** was also prepared directly from the intermediate **14** in a parallel route.

Encouraged by the activity of **25a** as shown in Table II,

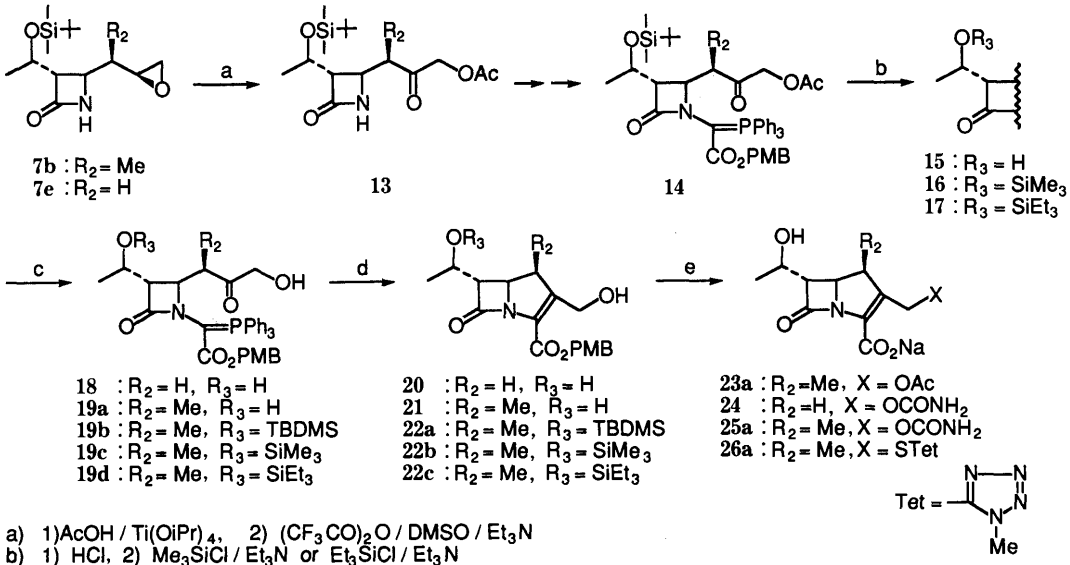

a) 1)AcOH / $Ti(OiPr)_4$, 2) $(CF_3CO)_2O$ / DMSO / Et_3N
b) 1) HCl, 2) Me_3SiCl / Et_3N or Et_3SiCl / Et_3N
c) MeONa / MeOH -20°C
d) *ca.* 100°C / toluene
e) 1) CCl_3CONCO, 2) MeOH, 3) $AlCl_3$ / anisole or 1) Mitsunobu reaction, 2) $AlCl_3$ / anisole

Chart 4

the modifications were extended to N-substituted derivatives. Unexpectedly, attempts to introduce N-substituted carbamoyl moieties into the diol **21** were unsuccessful because of poor selectivity. Although the corresponding 2-hydroxymethyl carbapenem bearing a C-8 TBDMS protective group **22a** could be readily functionalyzed at the C-2′ position, in many cases the standard desilylation procedures of the TBDMS group gave low yields and/or extensive decomposition once the carbapenem skeleton was constructed. This would in turn necessitate the use of a C-8 alcohol protecting group that would be readily removable in the presence of potentially more labile functionality. We eventually found that trimethylsilyloxy ether could be smoothly cleaved by the $AlCl_3$–anisole method in the final step when the PMB ester was deblocked. Therefore, desilylation and reprotection of the C-8 alcohol were carried out early in the synthetic sequence as shown in Chart 4.

Compound **22b** could be used successfully for preparation of several target derivatives; however, we often encountered an undesired cleavage of the C-8 trimethylsilyl ether during subsequent transformations, which gave rise to nonselective products. The use of a more stable triethylsilyl group as the C-8 alcohol protecting function allowed us to more easily manipulate further functionalization as well as final deprotection by the $AlCl_3$–anisole method.

The 1β-methyl 2-hydroxymethyl derivative **22c** thus obtained served as the common intermediate to provide the alternative method for introduction of the desired functional groups at the C-2′ position. The Mitsunobu reaction,[23] because of its mild reaction conditions, has been used for C-2′ functionalizations of the 2-hydroxymethylpenem.[24] By the same procedure, a number of other carbapenems bearing various heterocyclic-thiomethyl groups as well as originally designed N-substituted tetrazolylthiomethyl derivatives (**26a—d**) were analogously prepared in fair to good yields.

After our intensive efforts, it became possible to prepare the key intermediate **22c** on a hundredgram scale by the above described methodology, which involved chromatographic separations (silica gel) only twice throughout the sequence starting from the azetidinone **1**.

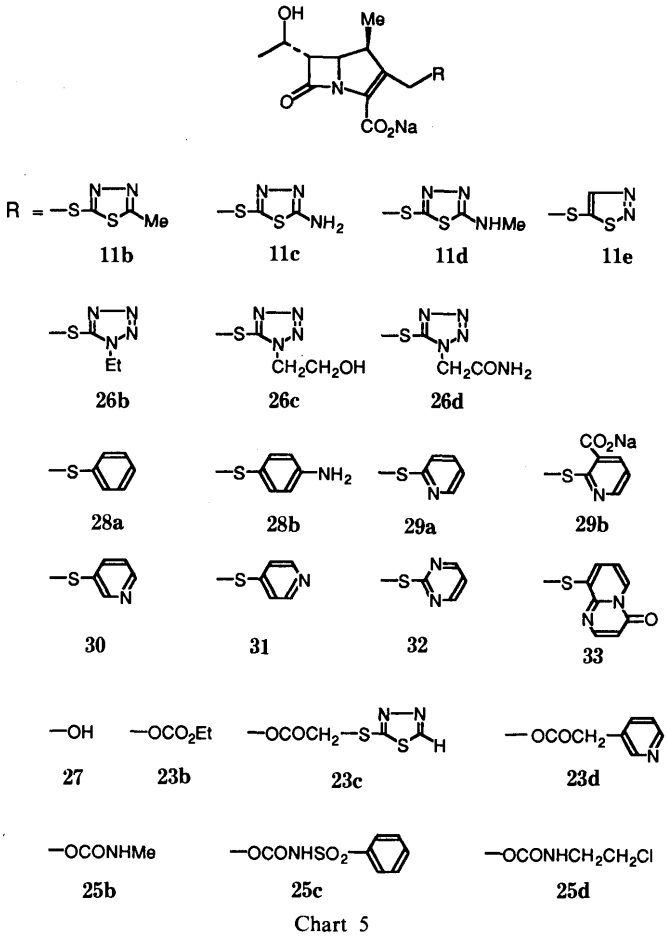

Chart 5

***In Vitro* Antibacterial Activity** The minimum inhibitory concentration (MIC) values of the synthesized carbapenems (Chart 5) against selected strains of gram-positive and gram-negative bacteria are shown in Table II. One general trend concerning the effect of 1-methyl substituents on the antibacterial activity was observed in the series of both

TABLE II. *In Vitro* Antibacterial Activity

Comp. No.	MIC (μg/ml)					
	S. aureus SR14	*S. pyogenes* C-203	*E. coli* EC-14	*K. pneumoniae* SR1	*P. vulgaris* CN-329	*S. marcescens* ATCC 13880
4	0.4	0.4	1.6	3.1	6.3	6.3
5	0.2	0.1	0.4	0.4	0.8	0.8
6	0.8	0.8	1.6	1.6	6.3	3.1
11a	0.02	0.006	0.1	0.1	0.05	0.8
10[a]	0.02	0.006	0.2	0.1	0.1	0.8
12	0.1	0.1	6.3	0.8	1.6	25
11b	0.1	0.1	12.5	3.1	3.1	25
11c	0.02	0.006	0.2	0.1	0.1	0.4
11d	0.05	0.006	0.8	0.2	0.1	3.1
11e	0.01	0.003	0.2	0.05	0.02	0.8
26a	0.1	0.01	0.2	0.1	0.1	0.8
26b	0.05	0.006	0.2	0.2	0.1	3.1
26c	0.1	0.02	0.1	0.1	0.2	0.4
26d	0.4	0.02	0.05	0.2	0.4	1.6
28a	0.01	0.003	12.5	6.3	0.2	50
28b	0.1	0.02	12.5	6.3	1.6	25
29a	0.02	0.006	3.1	0.8	0.2	12.5
29b	3.1	1.6	6.3	6.3	3.1	25
30	0.02	0.006	3.1	0.8	0.2	12.5
31	0.01	0.003	0.8	0.2	0.1	3.1
32	0.02	0.006	1.6	0.4	0.1	3.1
33	0.02	0.006	6.3	3.1	3.1	50
27	0.2	0.05	0.4	0.4	0.8	0.8
23a	0.05	0.01	0.1	0.1	0.1	0.8
23b	50	12.5	50	100	50	>100
23c	0.8	0.1	3.1	1.6	1.6	12.5
23d	0.05	0.01	0.8	1.6	0.2	12.5
24	0.1	0.02	0.1	0.2	0.4	0.8
25a	0.05	0.01	0.1	0.1	0.2	0.4
25b	0.1	0.02	0.1	0.1	0.2	0.4
25c	0.8	0.4	6.3	3.1	0.8	12.5
25d	0.05	0.01	0.2	0.4	0.1	3.1
Imipenem	0.025	0.013	0.1	0.2	0.78	0.39

a) This compound contained **11a** (50%).

2-unsubstituted and 2-thiadiazolylthio derivatives. The 1β-methyl carbapenems proved to be the most active, while the 1α-methyl and 1,1-dimethyl compounds led to significantly reduced activity in that order.

As for the 2-carbamoyloxymethyl series, the 1β-methyl derivative **25a** also provided better activity than the corresponding 1-unsubstituted compound **24**. Introduction of the N-substituents into the parent carbamoyl derivative had a negative effect on the activity (**25b, c** and **25d**). In this respect, more or less the same results were observed by the Merck group.[10]

Although the acetoxymethyl derivative **23a** showed activity similar to that of **25a**, all the modified compounds (**23b, c** and **23d**) were significantly less active.

In the tetrazole series, the N-methyl derivative **26a** exhibited high levels of activity against most gram-positive and gram-negative bacteria as we expected. Substitution of the methyl group in the parent compound **26a** with a more lipophilic group (Et) (**26b**), with a hydrophilic moiety (CH_2CH_2OH) (**26c**), and with a polar one (CH_2CONH_2) (**26d**) did not alter the activity to a great extent.

Among other heterocyclic-thiomethyl derivatives tested, the thiadiazolylthio derivatives (**11a, c** and **11e**) revealed quite high and well-balanced activity comparable to imipenem, except for *P. aeruginosa*. Interestingly, these thiadiazol derivatives were found to be more active than tetrazole analogues on the whole.

As a specific feature of these three derivatives (**11a, c** and **11e**), it should be noted that these compounds possessed a

TABLE III. *In Vitro* Antibacterial Activity

Compound No.	*S. aureus* SR2030 (L-MRSA)[a]	*S. aureus* SR3626 (H-MRSA)[b]	*E. faecalis* SR1004	*P. aeruginosa* SR1012
11a	0.2	3.1	0.8	25
11c	0.1	6.3	0.8	25
11e	0.1	3.1	0.8	12.5
Imipenem	0.2	50	1.6	1.6

a) Low-resistance groups of methicillin-resistant *S. aureus*. b) High-resistance groups of methicillin-resistant *S. aureus*.

TABLE IV. Protective Effect on Intraperitoneal Infection in Mice

Compound No.	ED_{50} (mg/kg/dose)/MIC (μg/ml)		
	S. aureus Smith	*S. pyogenes* C-203	*E. coli* EC-14
11a	0.24/0.02	0.42/0.006	0.42/0.1
11e	0.21/0.01	0.65/0.003	0.63/0.2
25a	0.13/0.1	1.38/0.01	0.55/0.1
Imipenem	0.021/0.01	0.028/0.013	0.36/0.1

ED_{50} was determined by survival rate 7 d after challenge.

fairly good activity against methicillin-resistant *Staphylococcus aureus* (MRSA) which is now being recognized as a recently increasing pathogen (Table III). Against low-resistance groups of methicillin-resistant *S. aureus* (L-MRSA),[25] these compounds showed about the same activity as that of imipenem. While imipenem had considerably weak activity against high-resistance groups of methicillin-resistant *S. aureus* (H-MRSA), the MIC values of the above compounds were in the range of 3.1 to 6.3 μg/ml. In addition, these derivatives exhibited a beneficial activity against *E. faecalis*, comparable to or better than that of imipenem.

***In Vivo* Activity** Because of their high *in vitro* antibacterial activity as described above, several compounds were examined for their *in vivo* activity. Quite unexpectedly, it turned out that in the mouse infection models, the ED_{50} values (sc) of all the compounds tested did not reflect the corresponding MIC values. The results of representative compounds together with the data of imipenem as reference are presented in Table IV. Therefore, further investigation to break through this critical barrier seems to be required.

Experimental

General Procedures All reactions involving air-sensitive reactants or products were carried out under a nitrogen atmosphere using dry solvents. Melting points were determined on a Yanagimoto apparatus and are uncorrected. Infrared (IR) spectra were recorded on a Hitachi 260-10 spectrophotometer. Proton nuclear magnetic resonance (^{1}H-NMR) spectra were obtained on a Varian EM-390 (90 MHz) and a VXR-200 (200 MHz). Unless otherwise stated, chemical shifts are expressed in ppm downfield from tetramethylsilane (TMS) as an internal (in organic solvents) or external (in D_2O) standard. Ultraviolet (UV) spectra were taken on a Hitachi EPS-3T spectrometer. Specific optical rotation ($[\alpha]_D$) were taken at 25 °C on a Prekin–Elmer 241 Polarimeter. Mass spectra (MS) were obtained on a Hitachi M-90 (SIMS) mass spectrometer. Medium pressure liquid chromatographies were performed on Merck 'Lobar' prepacked columns packed with LiChroprep Si 60; size A (240—10 mm, 40—60 μm), size B (310—25 mm, 40—60 μm) and size C (440—37 mm, 63—125 μm). Most of the new compounds reported here are either non-crystalline solids or foams or unstable. Hence, their analytical data could not be obtained.

Allylation of the azetidinone **1** using crotyl halides and zinc dust.

General Procedure I A suspension of commercially available optically active azetidinone **1** (28.7 g, 100 mmol) and zinc powder (19.6 g, 3 eq) in tetrahydrofuran (THF) (250 ml) was mixed for 5 min. To the vigorously stirred dispersion was added slowly crotyl bromide (16.2 g, 1.2 eq) in an ice bath at a rate sufficient to maintain the temperature of the solution under 35 °C. The reaction was allowed to proceed until thin layer chromatography (TLC) indicated consumption of starting material **1** (generally 2 h). To the mixture was added cold water (100 ml) and the mixture was then filtered. The filtrate was diluted with EtOAc (300 ml), washed with water, dried ($MgSO_4$) and concentrated. The ratio of the products, **2a** and **2b**,[14] was determined to be 1 : 1 by 200 MHz ^{1}H-NMR analysis of the resultant residue. Recrystallization from ether–hexane gave the compound **2** (12.8 g, 90%) as a 1 : 1 mixture of **2a** and **2b**.

General Procedure II A suspension of **1** (400 g, 1.39 mol), zinc powder (272.6 g, 3 eq) and $CuBr_2$ (31.1 g, 0.1 eq) in dimethylformamide (DMF) (1200 ml) was mixed for 20 min. To the vigorously stirred dispersion was added slowly crotyl bromide (225.2 g, 1.2 eq), and the temperature of the solution was kept at 35 °C until TLC indicated complete loss of starting material **1** (1.5 h). The reaction mixture was then cooled, quenched by addition of cold water (3600 ml) and filtered. The filtrate was diluted with EtOAc (3400 ml), washed with brine (700 ml), dried ($MgSO_4$) and concentrated to give the crude product **2** (374 g, 95%). The product ratio, **2a** and **2b**, was determined to be 1 : 1.2 by 200 MHz ^{1}H-NMR analysis. Recrystallization of the thus obtained product from acetonitrile (355 ml) gave the compound **2** (214 g, 54%) as a 1 : 2 mixture of **2a** and **2b**.

(3*S*,4*R*)-3-[(*R*)-1-Hydroxyethyl]-4-[(*R*)-1-methylallyl]-2-azetidinone (3a) To a solution of **2** (1 : 1 mixture, 1 g, 3.52 mmol) in acetonitrile (5 ml) was added $BF_3 \cdot Et_2O$ (0.54 ml, 1.2 eq) at room temperature, followed by stirring for 12 h. After the solvent was removed *in vacuo*, the residue was chromatographed on a Labor column (size A, EtOAc) to give **3a** (227 mg, 38%) and **3b** (233 mg, 39%). **3a**: mp 101—102.5 °C (acetone–hexane). $[\alpha]_D$ −2.3° (c = 1.005, $CHCl_3$). IR (Nujol) cm^{-1}: 3200, 2720, 2688, 1720, 1643, 1636. ^{1}H-NMR (200 MHz, $CDCl_3$) δ: 1.07 (3H, d, J = 6.8 Hz), 1.31 (3H, d, J = 6.3 Hz), 2.18—2.36 (2H, m), 2.86 (1H, ddd, J = 1.4, 2.2, 5.2 Hz), 3.44 (1H, dd, J = 2.2, 8.4 Hz), 4.10—4.28 (1H, m), 5.06 (1H, s), 5.13 (1H, dd, J = 1, 6 Hz), 5.60—5.77 (1H, m), 6.11 (1H, br). *Anal.* Calcd for $C_9H_{15}NO_2$: C, 63.88; H, 8.93; N, 8.28. Found: C, 63.64; H, 8.92; N, 8.14.

(3*S*,4*R*)-3-[(*R*)-1-Hydroxyethyl]-4-[(*S*)-1-methylallyl]-2-azetidinone (3b) **3b**: mp 89—90.5 °C (acetone–hexane). $[\alpha]_D$ −31.2° (c = 1.003, $CHCl_3$). IR (Nujol) cm^{-1}: 3328, 3208, 2476, 2400, 1715, 1643. ^{1}H-NMR (200 MHz, $CDCl_3$) δ: 1.09 (3H, d, J = 6.8 Hz), 1.26 (3H, d, J = 6.6 Hz), 2.25—2.43 (2H, m), 2.89 (1H, dd, J = 2.2, 5 Hz), 3.50 (1H, dd, J = 2.2, 7.8 Hz), 4.11—4.23 (1H, m), 5.08 (1H, d), 5.15 (1H, dd, J = 1, 6 Hz), 5.67—5.85 (1H, m), 6.27 (1H, br). *Anal.* Calcd for $C_9H_{15}NO_2$: C, 63.88; H, 8.93; N, 8.28. Found: C, 63.59; H, 8.88; N, 8.15.

(3*S*,4*R*)-3-[(*R*)-1-*tert*-Butyldimethylsilyloxyethyl]-4-[(*R*)-1-methylallyl]-2-azetidinone (2a) A solution of **3a** (300 mg, 1.77 mmol), *tert*-butyldimethylsilyl chloride (450 mg, 1.7 eq) and imidazole (300 mg, 2.5 eq) in DMF (1.5 ml) was stirred at room temperature for 12 h. To the solution was added water (1 ml) and the resulting solid was separated. The crude product was dissolved in CH_2Cl_2 (10 ml), washed with water (10 ml), dried and concentrated to give **2a** (482 mg, 96%). mp 124.5—126 °C (ether–hexane), (lit. 14, mp 120—123 °C). $[\alpha]_D$ −25.2° (c = 0.60, $CHCl_3$). IR (Nujol) cm^{-1}: 3190, 3080, 1757, 1715, 1640, 1250, 835, 773. ^{1}H-NMR (200 MHz, $CDCl_3$) δ: 0.07 (6H, s), 0.89 (9H, s), 1.06 (3H, d, J = 7 Hz), 1.23 (3H, d, J = 6.2 Hz), 2.13—2.31 (1H, m), 2.76 (1H, dt, J = 1.6, 4.8 Hz), 3.40 (1H, dd, J = 2.2, 8.8 Hz), 4.12—4.13 (1H, m), 5.05 (1H, s), 5.12 (1H, d, J = 6.2 Hz), 5.59—5.77 (1H, m), 5.88 (1H, br). *Anal.* Calcd for $C_{15}H_{29}NO_2Si$: C, 63.55; H, 10.31; N, 4.94. Found: C, 63.37; H, 10.33; N, 4.93.

(3*S*,4*R*)-3-[(*S*)-1-*tert*-Butyldimethylsilyloxyethyl]-4-[(*S*)-1-methylallyl]-2-azetidinone (2b) By the same procedure reported for the preparation of **2a**, **3b** (380 mg, 2.24 mmol) afforded **2b** (600 mg, 94%). mp 142.5—143 °C (acetonitrile), (lit. 14, mp 137—139 °C). $[\alpha]_D$ −34.4° (c = 1.00, $CHCl_3$). IR (Nujol) cm^{-1}: 3150, 3090, 1758, 1712, 1642, 1255, 830, 775. ^{1}H-NMR (200 MHz, $CDCl_3$) δ: 0.07 (6H, s), 0.88 (9H, s), 1.07 (3H, d, J = 6.8 Hz), 1.18 (3H, d, J = 6.2 Hz), 2.24—2.41 (1H, m), 2.81 (1H, ddd, J = 1.1, 2.2, 4.5 Hz), 3.50 (1H, dd, J = 2.2, 7.4 Hz), 4.11—4.23 (1H, m), 5.05 (1H, s), 5.12 (1H, dd, J = 1, 6 Hz), 5.69—5.86 (1H, m), 6.04 (1H, br). *Anal.* Calcd for $C_{15}H_{29}NO_2Si$: C, 63.55; H, 10.31; N, 4.94. Found C, 63.39; H, 10.36; N, 5.00.

(3*S*,4*R*)-3-[(*S*)-1-*tert*-Butyldimethylsilyloxyethyl]-4-(1,1-dimethylallyl)-2-azetidinone (2c) Following the general procedure I using prenyl bromide (8.9 g, 1.2 eq), the compound **1** (14.4 g, 50 mmol) was converted to the title compound **2c** (14.2 g, 94%). mp 158—160 °C (pet. ether). $[\alpha]_D$ −34.5° (c = 1.02, $CHCl_3$). IR (Nujol) cm^{-1}: 3360, 3090, 1758, 1713, 1638, 838. ^{1}H-NMR (200 MHz, $CDCl_3$) δ: 0.07 (6H, s), 0.88 (9H, s), 1.04 (6H, s), 1.21 (3H, d, J = 6.2 Hz), 2.79 (1H, m), 3.49 (1H, d, J = 2.2 Hz), 4.11—4.20 (1H, m), 5.05 (1H, d, J = 17 Hz), 5.08 (1H, d, J = 11 Hz), 5.78 (1H, br s), 5.83 (1H, dd, J = 11, 17 Hz). *Anal.* Calcd for $C_{16}H_{31}NO_2Si$: C, 64.59; H, 10.50; N, 4.71. Found: C, 64.62; H, 10.54; N, 4.82.

Sodium (1*R*,5*R*,6*S*)-6-[(*R*)-1-Hydroxyethyl]-1-methylcarbapen-2-em-3-carboxylate (4) According to our pre-established procedure detailed in the preceding paper, **4**, **5** and **6** were prepared from **2a**, **b** and **2c**, respectively. **4**: ^{1}H-NMR (90 MHz, D_2O) δ: 1.68 (3H, d, J = 7 Hz), 1.75 (3H, d, J = 6 Hz), 3.75 (1H, m), 3.85 (1H, dd, J = 2, 5 Hz), 4.20 (1H, dd, J = 2, 4 Hz), 4.65 (1H, m), 6.60 (1H, d, J = 2 Hz).

Sodium (1*S*,5*R*,6*S*)-6-[(*R*)-1-Hydroxyethyl]-1-methylcarbapen-2-em-3-carboxylate (5) **5**: ^{1}H-NMR (90 MHz, D_2O) δ: 1.49 (3H, d, J = 7 Hz), 1.75 (3H, d, J = 6 Hz), 3.70 (1H, m), 3.85 (1H, dd, J = 2, 5 Hz), 4.50—4.75 (2H, m), 6.62 (1H, d, J = 2 Hz).

Sodium (5*R*,6*S*)-1,1-Dimethyl-6-[(*R*)-1-hydroxyethyl]carbapen-2-em-3-carboxylate (6) **6**: ^{1}H-NMR (90 MHz, D_2O) δ: 1.57 (3H, s), 1.74 (3H, d, J = 6 Hz), 1.78 (3H, s), 3.82 (1H, dd, J = 2.9, 5.6 Hz), 4.28 (1H, dd, J = 5.6, 6.3 Hz).

(3*S*,4*R*)-3-[(*R*)-1-*tert*-Butyldimethylsilyloxyethyl]-4-[(1*R*,2*S*)-2,3-epoxy-1-methylpropyl]-2-azetidinone (7b) To a solution of **2b** (3 g, 10.6 mmol) in CH_2Cl_2 (10 ml) was added Na_2CO_3 (1.43 g, 1.6 eq), $MgSO_4$ (127 mg, 0.1 eq) and *m*-chloroperbenzoic acid (MCPBA) (3.66 g, 1.6 eq) at room temperature and the mixture was then stirred for 48 h. The reaction mixture was filtered and the filtrate was washed with aqueous $Na_2S_2O_3$, aqueous Na_2CO_3, water, then dried and concentrated. The residue was roughly chromatographed on a Lobar column (size B, toluene–EtOAc 1 : 1) to give the epoxides as a 2 : 1 mixture of **7b** and **7c** (2.87 g, 90.6%). The ratio of the products, **7b** and **7c**, was determined by 200 Hz ^{1}H-NMR analysis on the basis of the C-3 protons. In order to separate the two isomers, the mixture was again chromatographed on a Lobar column (size B, toluene–EtOAc 2 : 1) to give a less polar isomer **7c** (360 mg, 11.4%) and a polar one **7b** (1.89 g, 59.7%). Compound **7b** was first recrystallized from acetonitrile and then recrystallized from methanol to give a pure sample which was subjected to X-ray analysis. mp 165—165.5 °C. $[\alpha]_D$ −30.7° (c = 1.007, $CHCl_3$). IR (Nujol) cm^{-1}: 3144, 3086, 2712, 1759, 1709, 962, 829, 778. ^{1}H-NMR (200 MHz, $CDCl_3$) δ: 0.08 (6H, s), 0.89 (9H, s), 1.03 (3H, d, J = 6.6 Hz), 1.23 (3H, d, J = 6 Hz), 1.55—1.68 (1H, m), 2.60 (1H, dd, J = 2.8, 5 Hz), 2.76—2.87 (2H, m), 2.91 (1H, ddd, J = 1, 2.2, 4.8 Hz), 3.66 (1H, dd, J = 2.2, 7.2 Hz), 4.14—4.26 (1H, m), 6.14 (1H, br s). ^{1}H-NMR (200 MHz, CD_3OD) δ: 0.09 (6H, s), 0.90 (9H, s), 1.04 (3H, d, J = 7 Hz), 1.22 (3H, d, J = 6.2 Hz), 1.45—1.63 (1H, m), 2.65 (1H, dd, J = 2.6, 4.8 Hz), 2.76 (1H, dd, J = 4, 4.8 Hz), 2.86 (1H, ddd, J = 2.6, 4.8, 6.3 Hz), 2.97 (1H, dd, J = 2, 3.6 Hz), 3.62 (1H, dd, J = 2, 7.6 Hz), 4.18—4.28 (1H, m). *Anal.* Calcd for $C_{15}H_{29}NO_3Si$: C, 60.16; H, 9.76; N, 4.68. Found: C, 59.99; H, 9.66; N, 4.76.

A large scale preparation of **7b** (90% purity) was carried out as follows. By essentially the same procedure as described above, the compound **2** (α/β = 1 : 2, 214 g, 0.755 mol) afforded crude epoxidized products (225 g). Recrystallization of the mixture thus obtained (225 g) from acetonitrile (470 ml) gave rise to the compound **7b** in 90% purity contaminated with *ca.* 10% of **7a** and **7c** (112 g, 50%).

(3*S*,4*R*)-3-[(*R*)-1-*tert*-Butyldimethylsilyloxyethyl]-4-[(1*R*,2*R*)-2,3-epoxy-1-methylpropyl]-2-azetidinone (7c) **7c**: mp 117.5—118 °C (ether–*n*-hexane). $[\alpha]_D$ −19.5° (c = 1.006, $CHCl_3$). IR (Nujol) cm^{-1}: 3160, 3096, 3084, 2704, 1759, 1720, 963, 838, 774. ^{1}H-NMR (200 MHz, $CDCl_3$) δ: 0.08 (6H, s), 0.89 (9H, s), 1.03 (3H, d, J = 7 Hz), 1.26 (3H, d, J = 6.2 Hz), 1.40—1.55 (1H, m), 2.49—2.53 (1H, m), 2.76—2.82 (2H, m), 3.06 (1H, ddd, J = 1, 2.2, 4.2 Hz), 3.70 (1H, dd, J = 2.2, 7.4 Hz), 4.18—4.29 (1H, m), 5.93 (1H, br s). ^{1}H-NMR (200 MHz, CD_3OD) δ: 0.09 (6H, s), 1.04 (3H, d, J = 6.8 Hz), 1.25 (3H, d, J = 6.4 Hz), 1.31—1.42 (1H, m), 2.51 (1H, dd, J = 2.5, 5 Hz), 2.72—2.84 (2H, m), 3.04 (1H, dd, J = 2, 3.2 Hz), 3.68 (1H, dd, J = 2, 7.8 Hz), 4.19—4.30 (1H, m). *Anal.* Calcd for $C_{15}H_{29}NO_3Si$: C, 60.16; H, 9.76; N, 4.68. Found: C, 59.95; H, 9.69; N, 4.78.

(3*S*,4*R*)-3-[(*R*)-1-*tert*-Butyldimethylsilyloxyethyl]-4-[(1*S*)-2,3-epoxy-1-methylpropyl]-2-azetidinone (7a) By the same procedure as described above, the compound **2a** (94 mg, 0.33 mmol) afforded the epoxide **7a** as a 1 : 1 inseparable mixture (85 mg, 86%). The ratio of the products was determined by 200 MHz ^{1}H-NMR analysis on the basis of chemical shifts at the C-4 protons. ^{1}H-NMR (200 MHz, CD_3OD, 1 : 1 mixture) δ: 0.09 and 0.10 (6H, s), 0.09 (9H, s), 1.02 and 1.05 (3H, d, J = 6.8 Hz), 1.22 and 1.23 (3H, d, J = 6.2 Hz), 1.35—1.52 (1H, m), 2.51 (0.5 H, dd, J = 2.8, 5 Hz),

2.62 (0.5H, dd, J=2.7, 4.8 Hz), 2.71—2.87 (2H, m), 2.89 (0.5H, dd, J=2.2, 4 Hz), 3.03 (0.5H, dd, J=2.2, 3.7 Hz), 3.55 (0.5H, dd, J=2.2, 8.8 Hz), 3.69 (0.5H, dd, J=2.2, 6.6 Hz), 4.16—4.28 (1H, m).

Sodium (1*S*,5*R*,6*S*)-6-[(*R*)-1-Hydroxyethyl]-1-methyl-2-(1,3,4-thiadiazol-2-yl)thiomethylcarbapen-2-em-3-carboxylate (11a) and Related Compounds The above epoxide **7b** (90% purity) was transformed to the epoxy-ylide **8** (R_1=H, R_2=Me, 90% purity) by the known method.[4] IR ($CHCl_3$) cm^{-1}: 2950, 1740, 1600. A solution of *n*-butyllithium in hexane (1.6 N, 0.381 ml, 0.5 eq) was added to a solution of 1,3,4-thiadiazolylthiol (432 mg, 3 eq) in THF (3 ml) under ice cooling. To this mixture was added a solution of the ylide **8** (900 mg, 1.22 mmol) in THF (1 ml) and the reaction mixture was stirred at room temperature for 12 h. It was then diluted with EtOAc, washed with aqueous $NaHCO_3$ solution and brine, dried and concentrated to give the hydroxy-ylide (965 mg, 89%). A solution of dimethyl sulfoxide (DMSO) (0.24 ml, 3 eq) in CH_2Cl_2 (6 ml) was treated with trifluoroacetic anhydride (0.32 ml, 2 eq) at −70 °C for 30 min. To this mixture was added a solution of the above hydroxy-ylide (965 mg, 1.13 mmol) in CH_2Cl_2 (2 ml) and the whole was stirred at −70 °C for 1 h. Triethylamine (0.66 ml, 4.2 eq) was added and the mixture was stirred for 20 min, then diluted with EtOAc, washed with water, dried and concentrated. The residue was chromatographed on a Lobar column (size B, Benzene–EtOAc 2 : 1) to give **9a** (R_1=H, R_2=Me, 753 mg, 79%). To the keto-ylide **9a** (316 mg, 0.37 mmol) in acetonitrile (5 ml) was added conc. HCl (0.15 ml) at 0 °C. This mixture was stirred for 2 h, diluted with EtOAc (50 ml), washed with aqueous $NaHCO_3$ solution, dried and concentrated to give **9b** (R_1=H, R_2=Me, 268 mg, 98%). IR ($CHCl_3$) cm^{-1}: 3500, 1740, 1610. A solution of **9b** (250 mg, 0.34 mmol) in toluene (20 ml) was heated at 103 °C for 2 h then concentrated. The residue was chromatographed on a Lobar column (size B, CH_2Cl_2–EtOAc–acetonitrile 1 : 1 : 2) to give the corresponding carbapenem (89 mg, 57%). IR ($CHCl_3$) cm^{-1}: 3325, 1766, 1707, 1612, 1581. ^{1}H-NMR (90 MHz, $CDCl_3$) δ: 1.18 (3H, d, J=7.5 Hz), 1.27 (3H, d, J=6 Hz), 2.75 (1H, br s), 3.14—3.50 (1H, m), 3.25 (1H, dd, J=3.5, 6.5 Hz), 3.77 (3H, s), 3.98—4.32 (2H, m), 4.09 and 4.87 (2H, ABq, J=13.5 Hz), 5.20 (2H, s), 6.84 and 7.35 (4H, A_2B_2q, J=8.7 Hz), 8.97 (1H, s). The resulting carbapenem PMB ester (89 mg, 0.19 mmol) was added to a solution of $AlCl_3$ (101 mg, 4 eq) in a mixture of anisole (2 ml) and CH_2Cl_2 (1 ml) at −40 °C, and the mixture was stirred for 1 h at the same temperature. A solution of $NaHCO_3$ (192 mg, 12 eq) in pH 7 phosphate buffer (0.02 M, 2 ml) and CH_2Cl_2 (10 ml) were added, and the reaction mixture was stirred under ice cooling for 30 min, then filtered. The aqueous filtrate was chromatographed on an HP-20AG column (10 × 200 mm, H_2O) and the fractions containing the product were concentrated and freeze-dried to give **11a** as a white powder (49 mg, 70%). $[\alpha]_D$ −68.4° (c=1.015, H_2O). IR (KBr) cm^{-1}: 3410, 1777, 1595, 1260, 1227. ^{1}H-NMR (90 MHz, D_2O) δ: 1.58 (3H, d, J=7 Hz), 1.70 (3H, d, J=6 Hz), 3.70—3.90 (2H, m), 4.30—4.80 (2H, m), 4.44 and 4.72 (2H, ABq, J=8 Hz), 9.87 (1H, s). UV (H_2O) nm: 275. MS (SIMS, glycerol) m/z: 364 $(M+H)^+$, 386 $(M+Na)^+$. *Anal.* Calcd for $C_{13}H_{14}N_3O_4S_2Na \cdot H_2O$: C, 40.94; H, 4.23; N, 11.02; S, 16.81; Na, 6.03. Found: C, 41.17; H, 4.25; N, 11.19; S, 16.66; Na, 6.06.

By the same procedure, 1α-methyl carbapenem **10** was obtained as a 1 : 1 mixture containing **11a** from the epoxy-ylide **8** (α/β=1 : 1) which was derived from **2** (1 : 1 mixture of **2a** and **2b**). **10**: ^{1}H-NMR (90 MHz, D_2O) δ: 1.70 (3H, d, J=6 Hz), 1.72 (3H, d, J=7 Hz), 3.70—3.90 (2H, m), 4.30—4.80 (2H, m), 4.46 and 4.75 (2H, ABq, J=8 Hz), 9.87 (1H, s). UV (H_2O) nm: 277.

The following compounds were also prepared by the same method used for **11a**.

Sodium (5*R*,6*S*)-1,1-Dimethyl-6-[(*R*)-1-hydroxyethyl]-2-(1,3,4-thiadiazol-2-yl)thiomethylcarbapen-2-em-3-carboxylate (12) **12**: ^{1}H-NMR (90 MHz, D_2O) δ: 1.57 (3H, s), 1.73 (3H, d, J=5.3 Hz), 1.79 (3H, s), 3.78 (1H, dd, J=2.7, 6.3 Hz), 4.21 (1H, d, J=2.7 Hz), 4.21 (1H, m), 4.56 and 5.04 (2H, ABq, J=15.3 Hz), 4.6—4.8 (1H, m). MS (SIMS, glycerol) m/z: 378 $(M+H)^+$, 400 $(M+Na)^+$.

Sodium (5*R*,6*S*)-2-(5-Amino-1,3,4-thiadiazol-2-yl)thiomethyl-6-[(*R*)-1-hydroxyethyl]-1-methylcarbapen-2-em-3-carboxylate (11b) **11b**: $[\alpha]_D$ −88.7° (c=0.50, H_2O). ^{1}H-NMR (90 MHz, D_2O) δ: 1.56 (3H, d, J=7 Hz), 1.70 (3H, d, J=6 Hz), 3.17 (3H, s), 3.75 (1H, m), 3.85 (1H, dd, J=2, 6 Hz), 4.40 and 4.55 (2H, ABq, J=14 Hz), 4.45—4.70 (2H, m). UV (H_2O) nm: 278.

Sodium (5*R*,6*S*)-6-[(*R*)-1-Hydroxyethyl]-1-methyl-2-(5-methyl-1,3,4-thiadiazol-2-yl)thiomethylcarbapen-2-em-3-carboxylate (11c) **11c**: ^{1}H-NMR (90 MHz, D_2O) δ: 1.54 (3H, d, J=7 Hz), 1.73 (3H, d, J=6 Hz), 3.60—3.75 (1H, m), 3.86 (1H, dd, J=2, 6 Hz), 4.50—4.70 (2H, m), 4.52 and 4.70 (2H, ABq, J=14 Hz). UV (H_2O) nm: 278.

Sodium (5*R*,6*S*)-6-[(*R*)-1-Hydroxyethyl]-1-methyl-2-(5-methylamino-1,3,4-thiadiazol-2-yl)thiomethylcarbapen-2-em-3-carboxylate (11d) **11d**: $[\alpha]_D$ −115° (c=0.1, H_2O). ^{1}H-NMR (90 MHz, D_2O) δ: 1.55 (3H, d, J=7 Hz), 1.72 (3H, d, J=6 Hz), 3.39 (3H, s), 3.80 (1H, m), 3.85 (1H, dd, J=2, 6 Hz), 4.40 and 4.60 (2H, ABq, J=14 Hz), 4.50—4.70 (2H, m). UV (H_2O) nm: 280.

Sodium (5*R*,6*S*)-6-[(*R*)-1-Hydroxyethyl]-1-methyl-2-(1,2,3-thiadiazol-5-yl)thiomethylcarbapen-2-em-3-carboxylate (11e) **11e**: $[\alpha]_D$ −101° (c=0.1, H_2O), ^{1}H-NMR (90 MHz, D_2O) δ: 1.57 (3H, d, J=7 Hz), 1.70 (3H, d, J=6 Hz), 3.76 (1H, m), 3.87 (1H, dd, J=2, 6 Hz), 4.40 and 4.61 (2H, ABq, J=14 Hz), 4.50—4.80 (2H, m), 9.16 (1H, s). UV (H_2O) nm: 277. MS (SIMS, glycerol) m/z: 386 $(M+Na)^+$, 749 $(2M+Na)^+$.

(3*S*,4*R*)-4-[(1*R*)-3-Acetoxy-1-methyl-2-oxopropyl]-3-[(*R*)-1-*tert*-butyldimethylsilyloxyethyl]-2-azetidinone (13) To a solution of **7b** (90% purity, 50 g, 0.167 mol) in acetic acid (150 ml) was added slowly $Ti(OiPr)_4$ (29.8 ml, 0.6 eq) at room temperature. The temperature of the solution was kept at 32 °C and the mixture was stirred for 6 h. After removal of most of the solvent under reduced pressure, the mixture was diluted with CH_2Cl_2 (250 ml), washed with 1 N HCl (300 ml) and a 10% aq. $NaHCO_3$ solution, dried and concentrated to give the acetoxy alcohol (59 g, 98%). By the same procedure for **11a**, the resulting alcohol (59 g, 0.164 mol) was converted to acetoxymethyl ketone **13** which was purified by chromatography on Lobar columns (size C × 2, benzene–EtOAc 1 : 2) (34 g, 57% from **7b**). mp 54—55 °C (*n*-hexane). $[\alpha]_D$ −15.9° (c=0.996, $CHCl_3$). IR (KBr) cm^{-1}: 3440, 3180, 1766, 1752, 1737, 1730, 1230. ^{1}H-NMR (90 MHz, $CDCl_3$) δ: 0.83 (9H, s), 1.12 (6H, d, J=6 Hz), 2.08 (3H, s), 2.60—2.96 (1H, m), 2.84 (1H, dd, J=2, 4.8 Hz), 3.78 (1H, dd, J=2, 5.5 Hz), 3.93—4.20 (1H, m), 6.47 (1H, br). *Anal.* Calcd for $C_{17}H_{31}NO_5Si$: C, 57.11; H, 8.74; N, 3.92. Found: C, 57.01; H, 8.84; N, 4.02.

Sodium (1*S*,5*R*,6*S*)-2-Acetoxymethyl-6-[(*R*)-1-hydroxyethyl]-1-methylcarbapen-2-em-3-carboxylate (23a) By the established method, compound **13** (10 g, 27 mmol) was transformed to the keto-ylide **14**, which was then purified by chromatography on a Lobar column (size C, toluene–EtOAc 2 : 1) (6.2 g, 31%). IR ($CHCl_3$) cm^{-1}: 2920, 1740, 1610. After desilylation of the ylide **14** (796 mg, 1 mmol) by the standard method, the resulting alcohol **15** was heated in toluene (10 ml) at 98 °C for 2 h to give the corresponding PMB ester of 2-acetoxymethyl carbapenem (253 g, 63%). IR ($CHCl_3$) cm^{-1}: 3450, 1780, 1740, 1720. ^{1}H-NMR (90 MHz, $CDCl_3$) δ: 1.15 (3H, d, J=7 Hz), 1.30 (3H, d, J=6 Hz), 2.00 (1H, br), 2.07 (3H, s), 3.22 (1H, m), 3.28 (1H, dd, J=2, 6 Hz), 3.80 (3H, s), 4.05—4.35 (2H, m), 4.85 and 5.35 (2H, ABq, J=16 Hz), 5.21 (2H, s), 6.85 and 7.35 (4H, A_2B_2q, J=9 Hz). According to the $AlCl_3$–anisole method, the above PMB ester (253 mg, 0.63 mmol) afforded the title carbapenem **23a** (101 mg, 53%). $[\alpha]_D$ +67° (c=0.1, H_2O). ^{1}H-NMR (90 MHz, D_2O) δ: 1.55 (3H, d, J=7 Hz), 1.70 (3H, d, J=6 Hz), 2.58 (s, 3H), 3.72 (1H, m), 3.86 (1H, dd, J=2, 6 Hz), 4.55—4.70 (2H, m), 5.20 and 5.70 (2H, ABq, J=8 Hz). UV (H_2O) nm: 269.

The following compounds were also prepared by the same procedure.

Sodium (1*S*,5*R*,6*S*)-6-[(*R*)-1-Hydroxyethyl]-2-hydroxymethyl-1-methylcarbapen-2-em-3-carboxylate (27) **27**: ^{1}H-NMR (90 MHz, D_2O) δ: 1.55 (3H, d, J=7 Hz), 1.73 (3H, d, J=6 Hz), 3.68 (1H, m), 3.88 (1H, dd, J=2, 6 Hz), 4.50—4.80 (2H, m), 4.75 and 5.01 (2H, ABq, J=14 Hz).

Sodium (1*S*,5*R*,6*S*)-2-Ethyloxycarboxymethyl-6-[(*R*)-1-hydroxyethyl]-1-methylcarbapen-2-em-3-carboxylate (23b) **23b**: ^{1}H-NMR (90 MHz, D_2O) δ: 1.53 (3H, d, J=7 Hz), 1.72 (3H, d, J=6 Hz), 1.75 (3H, t, J=8 Hz), 3.20—3.30 (1H, m), 3.60—3.80 (1H, m), 4.40—4.60 (2H, m), 4.80 (2H, q, J=8 Hz), 5.10 and 5.80 (2H, ABq, J=14 Hz). UV (H_2O) nm: 274.

Sodium (1*S*,5*R*,6*S*)-6-[(*R*)-1-Hydroxyethyl]-1-methyl-2-(1,3,4-thiadiazol-2-yl)methylcarboxymethylcarbapen-2-em-3-carboxylate (23c) **23c**: ^{1}H-NMR (90 MHz, D_2O) δ: 1.55 (3H, dd, J=7 Hz), 1.70 (3H, d, J=6 Hz), 3.15—3.22 (1H, m), 3.85 (1H, dd, J=2, 6 Hz), 4.30—4.50 (2H, m), 4.40 and 4.70 (2H, ABq, J=13 Hz), 5.00 and 5.70 (2H, ABq, J=14 Hz), 9.80 (1H, s). UV (H_2O) nm: 268.

Sodium (1*S*,5*R*,6*S*)-6-[(*R*)-1-Hydroxyethyl]-1-methyl-2-(3-pyridyl)-methylcarboxymethylcarbapen-2-em-3-carboxylate (23d) **23d**: ^{1}H-NMR (90 MHz, D_2O) δ: 0.83 (3H, d, J=7.2 Hz), 1.07 (3H, d, J=6.4 Hz), 2.75—2.90 (1H, m), 3.20 (1H, dd, J=2, 6 Hz), 3.70 (2H, s), 3.90 (1H, dd, J=2.8, 9.4 Hz), 4.05 (1H, m), 4.60 and 5.15 (2H, ABq, J=13.6 Hz), 7.30—8.30 (4H, m).

***p*-Methoxybenzyl (1*S*,5*R*,6*S*)-6-[(*R*)-1-*tert*-Butyldimethylsilyloxyethyl]-2-hydroxymethyl-1-methylcarbapen-2-em-3-carboxylate (22a)** A solution of **14** (1 g, 1.3 mmol) in MeOH (20 ml) was treated with MeONa (0.1 eq) at −20 °C for 20 min. The reaction mixture was diluted with EtOAc (100 ml), washed with water, dried, and concentrated. The residue was chromatographed on a Lobar column (size B, benzene–EtOAc 1 : 1) to

give the alcohol-ylide **19b** (676 mg, 72%). A solution of this ylide (650 mg, 0.86 mmol) in toluene (20 ml) was heated at 98 °C for 2 h then concentrated. The residue was chromatographed on a Lobar column (size B, benzene–EtOAc 2:1) to give the carbapenem **22a** (312 mg, 76%). IR ($CDCl_3$) cm^{-1}: 3400, 1776. ^{1}H-NMR (90 MHz, $CDCl_3$) δ: 0.10 (6H, s), 0.90 (9H, s), 1.15 (3H, d, J=7 Hz), 1.20 (3H, d, J=6 Hz), 3.23 (1H, m), 3.32 (1H, dd, J=2, 6 Hz), 3.81 (3H, s), 4.03—4.32 (2H, m), 4.35 and 4.66 (2H, ABq, J=16 Hz), 4.42 (1H, br s), 5.20 (2H, s), 6.84 and 7.35 (4H, A_2B_2q, J=9 Hz).

***p*-Methoxybenzyl (1*S*,5*R*,6*S*)-6-[(*R*)-1-Hydroxyethyl]-2-hydroxymethyl-1-methylcarbapen-2-em-3-carboxylate (21)** To a solution of **14** (25 g, 31 mmol) in acetonitrile (63 ml) was added slowly conc HCl (7.9 ml) at 5 °C. The mixture was then stirred for 45 min at the same temperature. The mixture was diluted with EtOAc (240 ml), washed with aq. $NaHCO_3$ solution, dried and concentrated to give the C-8 alcohol **15** (21 g, 98%). IR ($CHCl_3$) cm^{-1}: 3300, 1730, 1620. By the same procedure, using MeONa (0.1 eq) in MeOH as described above, this alcohol (681 mg, 1 mmol) was converted to the diol **19a** (530 mg, 91%). IR ($CHCl_3$) cm^{-1}: 3400, 1735, 1620. A solution of **19a** (520 mg, 0.81 mmol) in toluene (20 ml) was heated at 90 °C for 1.5 h then concentrated. The residue was chromatographed on a Lobar column (size B, CH_2Cl_2–EtOAc–acetonitrile 1:1:2) to give the carbapenem **21** (152 mg, 52%). IR ($CHCl_3$) cm^{-1}: 3350, 2950, 1770, 1605. ^{1}H-NMR (90 MHz, $CDCl_3$) δ: 1.16 (3H, d, J=7 Hz), 1.30 (3H, d, J=6 Hz), 2.00 (2H, br s), 3.21 (1H, m), 3.27 (1H, dd, J=2, 6 Hz), 3.80 (3H, s), 4.10—4.35 (2H, m), 4.35 and 4.64 (2H, ABq, J=8 Hz), 5.21 (2H, s), 6.85 and 7.35 (4H, ABq, J=9 Hz).

***p*-Methoxybenzyl (1*S*,5*R*,6*S*)-2-Hydroxymethyl-1-methyl-6-[(*R*)-1-trimethylsilyloxyethyl]carbapen-2-em-3-carboxylate (22b)** To a solution of the C-8 alcohol **15** (4.9 g, 7.2 mmol) in CH_2Cl_2 (20 ml) was added trimethylsilyl chloride (2 ml, 2 eq) and Et_3N (2.4 ml, 2 eq) at 0 °C. This was then stirred for 30 min at the same temperature. The reaction mixture was diluted with EtOAc (50 ml), washed with water, dried and concentrated to give **16** (4.9 g, 90%). IR ($CHCl_3$) cm^{-1}: 1740. By the same method for **22a**, the compound **16** (4.5 g, 5.9 mmol) was transformed to the hydroxymethyl ketone **19c** (4 g, 94%). IR ($CHCl_3$) cm^{-1}: 3300, 1740. A solution of **19c** (3.8 g, 5.3 mmol) in toluene (200 ml) was heated at 100 °C for 1 h then concentrated. The residue was chromatographed on a Lobar column (size B, benzene–EtOAc 3:1) to give the carbapenem **22b** (1.7 g, 75%). IR ($CHCl_3$) cm^{-1}: 3400, 1775. ^{1}H-NMR (90 MHz, $CDCl_3$) δ: 0.06 (6H, s), 0.10 (9H, s), 1.16 (3H, d, J=7 Hz), 1.20 (3H, d, J=6 Hz), 3.25 (1H, m), 3.30 (1H, dd, J=2, 6 Hz), 3.80 (3H, s), 4.02—4.30 (2H, m), 4.35 and 4.61 (2H, ABq, J=8 Hz), 4.40 (1H, br s), 5.21 (2H, s), 6.85 and 7.35 (4H, A_2B_2q, J=9 Hz).

***p*-Methoxybenzyl (1*S*,5*R*,6*S*)-2-Hydroxymethyl-1-methyl-6-[(*R*)-1-triethylsilyloxyethyl]carbapen-2-em-3-carboxylate (22c)** To a solution of the C-8 alcohol **15** (27 g, 43 mmol) in CH_2Cl_2 (90 ml) was added triethylsilyl chloride (14.3 ml, 2 eq) and Et_3N (13 ml, 2.2 eq) at 5 °C, and the mixture was stirred for 30 min at the same temperature. The reaction mixture was diluted with EtOAc (200 ml), washed with water, dried, and concentrated to give **17** (39 g, 95%). By the same method for **19b**, compound **17** (8.43 g, 10.6 mmol) was transformed to the hydroxymethyl ketone **19d** (7.8 g, 98%). IR ($CHCl_3$) cm^{-1}: 3300, 1740. A solution of **19d** (7.8 g, 10 mmol) in toluene (800 ml) was heated at 105 °C for 30 min then concentrated. The residue was chromatographed on a Lobar column (size C, benzene–EtOAc 3:1) to give the carbapenem **22c** as pale yellow oil (3.65 g, 74%). $[\alpha]_D$ +69.7° (c=1.024, $CHCl_3$). IR ($CHCl_3$) cm^{-1}: 3500, 1770, 1700, 1615. ^{1}H-NMR (90 MHz, $CDCl_3$) δ: 0.53—0.65 (6H, m), 0.90—0.99 (9H, m), 1.18 (3H, d, J=7.4 Hz), 1.27 (3H, d, J=6 Hz), 3.10—3.28 (1H, m), 3.22 (1H, dd, J=3, 6 Hz), 3.80 (3H, s), 4.15 (1H, dd, J=3, 10 Hz), 4.36 and 4.48 (2H, ABq, J=8 Hz), 5.23 (2H, s), 6.89 and 7.39 (4H, A_2B_2q, J=8.9 Hz). UV (95% EtOH) nm: 226, 279. *Anal.* Calcd for $C_{25}H_{37}NO_6Si$: C, 63.13; H, 7.84; N, 2.95. Found; C, 63.01; H, 7.76; N, 2.89.

Sodium (1*S*,5*R*,6*S*)-2-Carbamoyloxymethyl-6-[(*R*)-1-hydroxyethyl]-1-methylcarbapen-2-em-3-carboxylate (25a) and Related Compounds A solution of the diol **21** (152 mg, 0.43 mmol) and trichloroacetyl isocyanate (0.051 ml, 1 eq) in CH_2Cl_2 (3 ml) was stirred at −20 °C for 1.5 h. The reaction mixture was diluted with EtOAc (20 ml), washed with water, dried and concentrated. The residue was dissolved in MeOH (5 ml) in the presence of silica gel (200 mg) and stirred overnight at room temperature. The reaction mixture was filtered and the filtrate was diluted with EtOAc (20 ml), washed with water, dried, concentrated and chromatographed on a Lobar column (size A, benzene–EtOAc 1:3) to give the desired PMB ester as an amorphous solid (52 mg, 31% from **21**). $[\alpha]_D$ +13.4° (c=1.027, $CHCl_3$). IR (KBr) cm^{-1}: 3450, 3380, 2840, 1770, 1715, 1670, 1615. ^{1}H-NMR (90 MHz, $CDCl_3$) δ: 1.12 (3H, d, J=6.5 Hz), 1.28 (3H, d, J=7 Hz), 2.50 (1H, br s), 3.05—3.40 (2H, m), 3.77 (3H, s), 3.99—4.31 (2H, m), 5.18 (2H, s), 6.86 and 7.35 (4H, A_2B_2q, J=8.4 Hz). UV (EtOH) nm: 227, 274. *Anal.* Calcd for $C_{20}H_{24}N_2O_7$: C, 59.48; H, 5.98; N, 6.93. Found: C, 59.28; H, 6.11; N, 6.83. According to the $AlCl_3$–anisole method, **25a** was prepared from the above PMB ester. **25a**: $[\alpha]_D$ +51° (c=0.1, H_2O). ^{1}H-NMR (90 MHz, D_2O) δ: 1.56 (3H, d, J=7 Hz), 1.72 (3H, d, J=6 Hz), 3.70 (1H, m), 3.87 (1H, dd, J=2, 6 Hz), 4.55—4.75 (2H, m), 5.18 and 5.65 (2H, ABq, J=14 Hz). UV (H_2O) nm: 269. MS (SIMS, glycerol) m/z: 307 $(M+H)^+$, 329 $(M+Na)^+$ *Anal.* Calcd for $C_{12}H_{15}N_2O_6Na \cdot 0.8H_2O$: C, 44.95; H, 5.22; N, 8.04; Na, 7.17. Found: C, 44.84; H, 5.42; N, 8.17; Na, 6.87.

Similarly, 1-unsubstituted derivative **24** was prepared from the corresponding acetoxy ylide **14** (R_2=H). **24**: $[\alpha]_D$ +28° (c=0.1, H_2O). ^{1}H-NMR (90 MHz, D_2O) δ: 1.73 (3H, d, J=6 Hz), 3.40 (2H, m), 3.85 (1H, m), 4.57—4.85 (2H, m), 5.20 and 5.66 (2H, ABq, J=14 Hz). UV (H_2O) nm: 270.

The following compounds were prepared from **22b** or **22c** by the same method as above.

25b: $[\alpha]_D$ +47° (c=0.1, H_2O). ^{1}H-NMR (90 MHz, D_2O) δ: 1.56 (3H, d, J=7 Hz), 1.73 (3H, d, J=6 Hz), 3.16 (3H, s), 3.70 (1H, m), 3.88 (1H, dd, J=2, 6 Hz), 4.50—4.75 (2H, m), 5.19 and 5.67 (2H, ABq, J=14 Hz). UV (H_2O) nm: 270.

25c: ^{1}H-NMR (90 MHz, D_2O, sodium 4,4-dimethyl-4-silapentanesulfonate (DSS) as standard) δ: 0.94 (3H, d, J=7.2 Hz), 1.26 (3H, d, J=6.2 Hz), 2.68—2.82 (1H, m), 3.34 (1H, dd, J=3, 6 Hz), 3.98 (1H, dd, J=2.8, 9.4 Hz), 4.15—4.28 (14H, m), 4.61 and 5.14 (2H, ABq, J=14 Hz), 7.54—7.88 (5H, m).

25d: ^{1}H-NMR (90 MHz, D_2O) δ: 0.96 (3H, d, J=7.2 Hz), 1.10 (3H, d, J=6.4 Hz), 3.05—3.15 (1H, m), 3.20 (1H, dd, J=2, 6 Hz), 3.22—3.38 (2H, m), 3.40—3.52 (2H, m), 3.95—4.10 (2H, m), 4.10 and 5.15 (2H, ABq, J=14 Hz).

Sodium (1*S*,5*R*,6*S*)-6-[(*R*)-1-Hydroxyethyl]-1-methyl-2-(1-methyl-1*H*-tetrazol-5-yl)thiomethylcarbapen-2-em-3-carboxylate (26a) and the Related Compounds To a solution of **22c** (404 mg, 1 mmol), triphenylphosphine (315 mg, 1.2 eq) and 1-methyltetrazole-5-thiol (139 mg, 1.2 eq) in THF (10 ml) was added diethyl azodicarboxylate (209 mg, 1.2 eq), and the mixture was then stirred at room temperature for 1 h. After the usual work up, the residue was chromatographed on a Lobar column (size B, benzene–EtOAc 4:1) to give the desired PMB ester (415 mg, 78%), then deprotected to give **26a** (119 mg, 42%). ^{1}H-NMR (90 MHz, D_2O) δ: 1.55 (3H, d, J=7 Hz), 1.68 (3H, d, J=6 Hz), 3.55—3.65 (1H, m), 3.85 (1H, dd, J=2, 6 Hz), 4.35 and 4.60 (2H, ABq, J=14 Hz), 4.48 (3H, s), 4.45—4.70 (2H, m).

The following compounds were prepared from **22c** by the same method as above.

Sodium (1*S*,5*R*,6*S*)-2-(1-Ethyl-1*H*-tetrazol-5-yl)thiomethyl-6-[(*R*)-1-hydroxyethyl]-1-methylcarbapen-2-em-3-carboxylate (26b) 26b: ^{1}H-NMR (90 MHz, D_2O) δ: 1.55 (3H, d, J=7 Hz), 1.67 (3H, d, J=6 Hz), 1.92 (3H, t, J=8 Hz), 3.56—3.66 (1H, m), 3.86 (1H, dd, J=2, 6 Hz), 4.32 and 4.65 (2H, ABq, J=14 Hz), 4.50—4.80 (2H, m), 4.85 (2H, q, J=8 Hz).

Sodium (1*S*,5*R*,6*S*)-6-[(*R*)-1-Hydroxyethyl]-2-[1-(2-hydroxy)ethyl-1*H*-tetrazol-5-yl]thiomethyl-1-methylcarbapen-2-em-3-carboxylate (26c) 26c: ^{1}H-NMR (90 MHz, D_2O) δ: 1.60 (3H, d, J=7.0 Hz), 1.75 (3H, d, J=6.4 Hz), 3.58—3.78 (1H, m), 3.89 (1H, dd, J=3, 6 Hz), 4.40—4.59 (2H, m), 4.60 and 5.48 (2H, ABq, J=14 Hz), 4.63—4.75 (1H, m), 4.91 (1H, dd, J=3, 9 Hz), 4.97—5.09 (2H, m).

Sodium (1*S*,5*R*,6*S*)-2-(1-Carbamoylmethyl-1*H*-tetrazol-5-yl)thiomethyl-6-[(*R*)-1-hydroxyethyl]-1-methylcarbapen-2-em-3-carboxylate (26d) 26d: ^{1}H-NMR (90 MHz, D_2O) δ: 1.56 (3H, d, J=7 Hz), 1.70 (3H, d, J=6 Hz), 3.55—3.72 (1H, m), 3.85 (1H, dd, J=2, 6 Hz), 4.27 (2H, s), 4.35 and 4.72 (2H, ABq, J=14 Hz), 4.50—4.80 (2H, m). UV (H_2O) nm: 279.

Sodium (1*S*,5*R*,6*S*)-6-[(*R*)-1-Hydroxyethyl]-1-methyl-2-phenylthiomethylcarbapen-2-em-3-carboxylate (28a) 28a: ^{1}H-NMR (90 MHz, D_2O) δ: 0.87 (3H, d, J=7.2 Hz), 1.05 (3H, d, J=6.4 Hz), 3.0—3.2 (2H, m), 3.23 and 4.52 (2H, ABq, J=14.4 Hz), 3.7—3.8 (1H, m), 3.85—4.05 (1H, m), 7.0—7.3 (5H, m).

Sodium (1*S*,5*R*,6*S*)-2-(4-Amino)phenylthiomethyl-6-[(*R*)-1-hydroxy]-ethyl-1-methylcarbapen-2-em-3-carboxylate (28b) 28b: ^{1}H-NMR (90 MHz, D_2O) δ: 0.86 (3H, d, J=7.2 Hz), 1.07 (3H, d, J=6.4 Hz), 3.0—3.2 (2H, m), 3.10 and 4.35 (2H, ABq, J=13 Hz), 3.48 (1H, dd, J=3, 9 Hz), 3.9—4.1 (1H, m), 6.58 and 7.05 (4H, A_2B_2q, J=8.4 Hz). UV (H_2O) nm: 279.

Sodium (1*S*,5*R*,6*S*)-6-[(*R*)-1-Hydroxyethyl]-1-methyl-2-(2-pyridyl)thiomethylcarbapen-2-em-3-carboxylate (29a) 29a: ^{1}H-NMR (90 MHz, D_2O)

δ: 1.57 (3H, d, J=7 Hz), 1.73 (3H, d, J=6 Hz), 3.51—3.69 (1H, m), 3.82 (1H, dd, J=2, 6 Hz), 4.20 and 5.10 (2H, ABq, J=14.5 Hz), 4.30—4.70 (2H, m), 7.65—8.90 (4H, m). UV (H_2O) nm: 279.

Sodium (1*S*,5*R*,6*S*)-6-[(*R*)-1-Hydroxyethyl]-1-methyl-2-(3-sodium-carboxy-2-pyridyl)thiomethylcarbapen-2-em-3-carboxylate (29b) 29b: ^{1}H-NMR (90 MHz, D_2O, DSS as standard) δ: 1.07 (3H, d, J=7.4 Hz), 1.24 (3H, d, J=6.2 Hz), 3.15—3.28 (1H, m), 3.33 (1H, dd, J=2.8, 6.2 Hz), 3.65 and 4.82 (2H, ABq, J=14 Hz), 4.00 (1H, dd, J=2.8, 9.8 Hz), 7.21 (1H, dd, J=4.6, 7.6 Hz), 7.82 (1H, dd, J=1.8, 7.6 Hz), 8.41 (1H, dd, J=1.8, 4.6 Hz).

Sodium (1*S*,5*R*,6*S*)-6-[(*R*)-1-Hydroxyethyl]-1-methyl-2-(3-pyridyl)thiomethylcarbapen-2-em-3-carboxylate (30) 30: ^{1}H-NMR (90 MHz, D_2O) δ: 0.90 (3H, d, J=7.4 Hz), 1.06 (3H, d, J=6.2 Hz), 3.0—3.3 (2H, m), 3.25 and 4.49 (2H, ABq, J=14 Hz), 3.82 (1H, dd, J=2.8, 9.4 Hz), 3.9—4.1 (1H, m), 7.1—7.3 (1H, m), 7.6—7.7 (1H, m), 8.2 (1H, m), 8.3 (1H, m). UV (H_2O) nm: 278.

Sodium (1*S*,5*R*,6*S*)-6-[(*R*)-1-Hydroxyethyl]-1-methyl-2-(4-pyridyl)thiomethylcarbapen-2-em-3-carboxylate (31) 31: ^{1}H-NMR (90 MHz, D_2O) δ: 1.53 (3H, d, J=7 Hz), 1.67 (3H, d, J=6 Hz), 3.55—3.75 (1H, m), 3.82 (1H, dd, J=2, 6 Hz), 4.15 and 4.82 (2H, ABq, J=14.5 Hz), 4.35—4.70 (2H, m), 7.76 and 8.77 (4H, A_2B_2q, J=8 Hz). UV (H_2O) nm: 276.

Sodium (1*S*,5*R*,6*S*)-6-[(*R*)-1-Hydroxyethyl]-1-methyl-2-(2-pyrimidinyl)-thiomethylcarbapen-2-em-3-carboxylate (32) 32: ^{1}H-NMR (90 MHz, D_2O) δ: 0.95 (3H, d, J=7.2 Hz), 1.07 (3H, d, J=6.4 Hz), 3.10 (1H, m), 3.21 (1H, dd, J=2.1, 6.2 Hz), 3.60 and 4.62 (2H, ABq, J=14 Hz), 3.87 (1H, dd, J=2.8, 9.4 Hz), 3.99 (1H, m), 7.03 and 8.38 (3H, m).

Sodium (1*S*,5*R*,6*S*)-6-[(*R*)-1-Hydroxyethyl]-2-(4-oxo-4*H*-pyrido-[1,2-*a*]pyrimidin-9-yl)thiomethylcarbapen-2-em-3-carboxylate (33) 33: ^{1}H-NMR (90 MHz, D_2O) δ: 1.15 (3H, d, J=7.4 Hz), 1.25 (3H, d, J=6.3 Hz), 3.33—3.50 (2H, m), 3.63 (1H, d, J=14.6 Hz), 4.03 (1H, dd, J=3.3, 10.5 Hz), 4.19 (1H, quint, J=6.4 Hz), 4.80 (1H, d, J=14.6 Hz), 4.82 (DHO), 6.50—6.60 (1H, m), 7.20—7.40 (1H, m), 7.80 (1H, d, J=7.5 Hz), 8.20—8.40 (1H, m), 8.78 (1H, d, J=7.5 Hz).

Determination of MICs MICs were determined by the agar dilution method using sensitivity test agar (Eiken, Japan). An overnight culture of bacteria in tryptosoy broth (Eiken, Japan) was diluted to about 10^6 cells/ml with the same broth and inoculated with an inoculating device onto agar containing serial twofold dilutions of the test compounds. Organisms were incubated at 37 °C for 18—20 h. The MIC of a compound was defined as the lowest concentration that visibly inhibited growth.

***In Vivo* Activity (Determination of ED_{50} Values)** Five-week-old male strain ICR mice weighing 19 to 23 g, in groups of 5—10 mice, were injected intraperitoneally with 10 to 100 times the 50% lethal dose of bacteria, which were suspended in heart infusion broth (HIB) or HIB containing 5% gastric mucin. The compounds were administered 1 and 5 h after infection. The 50% effective doses (ED_{50}, in milligram per killogram) were determined by the Probit method using survival rates at 7 d post-infection and expressed as a single dose.

Acknowledgment We wish to thank the following scientists for their contributions to this work: Mr. T. Yorifuji, Mr. S. Shinomoto, and Mr. F. Matsubara (large scale preparation of the compound **22c**), Dr. M. Shiro (X-ray analysis), Dr. Y. Nakagawa (mass spectroscopy), Mr. H. Miwa and Dr. S. Matsuura (*in vivo* activity assay), Mr. K. Motokawa, and Mr. Y. Kimura (*in vitro* activity assay).

References and Notes

1) Carbapenem and Penem Antibiotics. V. M. Imuta, S. Uyeo and T. Yoshida, *Chem. Pharm. Bull.*, **39**, 658 (1991).
2) D. H. Shih, F. Baker, L. Cama and B. G. Christensen, *Heterocycles*, **21**, 29 (1984).
3) T. F. Walsh, *Ann. Rep. Med. Chem.*, **23**, 121 (1988); R. C. Moellering, Jr, G. M. Eliopoulos and D. E. Sentochnik, *J. Antimicrobial Chemotherapy*, **24**, 1 (1989).
4) M. Imuta, H. Ona, S. Uyeo, K. Motokawa and T. Yoshida, *Chem. Pharm. Bull.*, **33**, 4361 (1985).
5) M. Imuta, S. Uyeo, M. Nakano and T. Yoshida, *Chem. Pharm. Bull.*, **33**, 4371 (1985).
6) For a review, see R. W. Ratcliffe and G. Albers-Schönberg, "Chemistry and Biology of β-Lactam Antibiotics," Vol. 2, ed. by R. B. Morin and M. Gorman, Academic Press, Inc., New York, 1982, p. 227.
7) H. Ona, S. Uyeo, T. Fukao, M. Doi and T. Yoshida, *Chem. Pharm. Bull.*, **33**, 4382 (1985).
8) This compound is now commercially available from Kanegafuchi Chemical Industry Co., Ltd.
9) Japan. Patent Appl. 201889/87, September 5, **1987** [*Chem. Abstr.*, **108**, 37494 (1988)].
10) S. M. Schmitt, T. N. Salzmann, D. H. Shih and B. G. Christensen, *J. Antibiot.*, **41**, 780 (1988).
11) J. Haruta, K. Nishi, K. Kikuchi, S. Matsuda, Y. Tamura and Y. Kita, *Chem. Pharm. Bull.*, **37**, 2338 (1989).
12) T. N. Salzmann, F. P. DiNinno, M. L. Greenlee, R. N. Guthikonda, M. L. Qesada, S. M. Schmitt, J. J. Herrmann and M. F. Woods, "Recent Advances in the Chemistry of Beta-Lactam Antibiotics," The Chemical Society, London, Special Publication 70, **1989**, p. 170.
13) G. A. Kraus and K. Neuenschwanjder, *J. Chem. Soc., Chem. Commun.*, **1982**, 134; A. Martel, J.-P. Davis, C. Bachand, M. Menard, T. Durst and B. Belleau, *Can. J. Chem.*, **61**, 1899 (1983); M. Aratani, H. Hirai, K. Sawada and M. Hashimoto, *Heterocycles*. **23**, 1889 (1985); K. Fujimoto, Y. Iwano and K. Hirai, *Tetrahedron Lett.*, **26**, 89 (1985); K. Fujimoto, Y. Iwano and K. Hirai, *Bull. Chem. Soc. Jpn.*, **59**, 1363 (1986).
14) H. Fliri and C.-P. Mak, *J. Org. Chem.*, **50**, 3438 (1985).
15) G. Courtois and L. Miginiac, *J. Organomet. Chem.*, **69**, 1 (1974); J. F. Ruppert and J. D. White, *J. Org. Chem.*, **41**, 550 (1976); G. P. Boldrini, D. Savoia, E. Tagliavini, C. Trombini and A. Umani-Ronchi, *ibid.*, **48**, 4108 (1983); H. M. R. Hoffmann and J. Rale, *Angew. Chem. Int. Ed. Engl.*, **24**, 94 (1985) and references cited therein.
16) Recently, it has been reported that the use of DMF as a solvent was highly effective in the Zn-promoted reaction of allyl bromide with carbonyl compounds in terms of reaction rate and yields. See T. Shono, M. Ishifune and S. Kashimura, *Chem. Lett.*, **1990**, 449.
17) M. Shibuya, M. Kuretani and S. Kubota, *Tetrahedron*, **38**, 2659 (1982).
18) M. Lang, K. Prasad, W. Holick, J. Gosteli, I. Ernest and R. B. Woodward, *J. Am. Chem. Soc.*, **101**, 6296 (1979).
19) M. Ohtani, F. Watanabe and M. Narisada, *J. Org. Chem.*, **49**, 5271 (1984).
20) R. Wise, J. M. Andrews and G. Danks, *Antimicrob. Agents Chemother.*, **24**, 909 (1983).
21) Y. Sendo and M. Yoshioka, unpublished results.
22) E. Perrone, M. Alpegiani, A. Bedeschi, F. Giudici, M. Foglio and G. Franceschi, *Tetrahedron Lett.*, **24**, 3283 (1983).
23) O. Mitsunobu, *Synthesis*, **1981**, 1.
24) M. Alpegiani, A. Bedeschi, E. Perrone, F. Zarini and G. Franceschi, *Heterocycles*, **23**, 2255 (1985).
25) For classification of L-MRSA and H-MRSA, see K. Murakami, K. Nomura, M. Doi and T. Yoshida, *Antimicrob. Agents Chemother.*, **31**, 1307 (1987).

Carbapenem and Penem Antibiotics. VII. Synthesis and Antibacterial Activity of 1β-Methyl-2-(Quaternary Heteroaromatic-thiomethyl) Carbapenems[1)]

Mitsuru IMUTA,* Hikaru ITANI, Hisao ONA, Toshiro KONOIKE, Shoichiro UYEO,* Yasuo KIMURA, Hideaki MIWA, Shinzo MATSUURA and Tadashi YOSHIDA

Shionogi Research Laboratories, Shionogi & Co., Ltd., Sagisu, Fukushima-ku, Osaka 553, Japan. *Received August 6, 1990*

The synthesis and antibacterial activity of a series of 1β-methylcarbapenems having quaternary heteroaromatic-thiomethyl groups at the C-2 position are described. Both 2-hydroxymethyl and 2-chloromethyl carbapenems (1 and 7) respectively served as the common key intermediates for the preparation of these compounds. Of these, the 4-pyridiniothiomethyl derivatives exhibited the best antibacterial properties and turned out to possess high *in vivo* efficacy as well.

Keywords β-lactam antibiotic; carbapenem antibiotic; 1β-methyl carbapenem antibiotic; 2-(quaternary heteroaromatic-thiomethyl) carbapenem antibiotic; antibacterial activity; methicillin-resistant *S. aureus* (MRSA)

In the preceding paper[1)] we described that the 1β-methyl 2-functionalized-methyl carbapenems, particularly 2-heteroaromatic-thiomethyl derivatives which are definitely distinguished from the well established 2-alkylthio carbapenems such as thienamycin family,[2)] exhibited high and well-balanced *in vitro* antibacterial activity except for *Pseudomonas aeruginosa*. The minimal inhibitory concentration (MIC) values of these compounds, however, were not reflected well in their protective effect on intraperitoneal infection in mice. In this respect, a similar tendency observed with some penem compounds has also been reported.[3)] To overcome this drawback, as well as to improve the activity against *P. aeruginosa*, we decided to continue our modification studies on 1β-methyl carbapenems by chemical manipulation at the C-2′ position.

In the field of cephalosporins, introduction of quaternary heterocyclic methyl groups at the C-3 position had led to a new class of cephalosporins such as ceftazidime[4)] and cefpirome,[5)] which are characterized by their potent activity against *P. aeruginosa*. Recently it has been reported that a successful application of this strategy for the 2-alkylthio carbapenems resulted in a high anti-pseudomonal activity.[6)] Since the 2-functionalized-methyl carbapenems might be regarded as a hybrid of the naturally occurring carbapenem and cephalosporin structures, we therefore became interested in the synthesis of a number of the title compounds to investigate the effect of quaternized heteroaromatic-thiomethyl groups on antibacterial properties.

Our synthetic route involves direct introduction of various heteroaromatic-thio groups into the C-2′ position of either 2-hydroxymethyl or 2-chloromethyl carbapenems (**1** and **7**) employed as the key intermediates.

Among these compounds prepared, the N-substituted 4-pyridinio-thiomethyl derivatives (**4a**, **b**, **c**, **e**, **k** and **4l**) exhibited the best balanced antibacterial spectrum. Furthermore, these derivatives were found to possess high *in vivo* activity against both gram-positive and gram-negative bacteria including *P. aeruginosa*. Of these, **4a** as a representative compound was subjected to pharmacokinetic investigations and proved to be more stable than imipenem in various kinds of kidney tissue homogenates, respectively. In this paper, we now describe details of the synthetic studies on this new class of carbapenems. Their antibacterial properties will also be discussed.

Chemistry Although the nature of a highly strained and reactive carbapenem nucleus requires that a minimum number of synthetic operations be performed on the carbapenem structure once it is formed, our synthetic strategy for the present modification studies was to introduce various C-2′ functional groups onto this constructed bicyclic system at a late stage of the synthesis. For this purpose, we employed the 2-hydroxymethyl carbapenem **1** as the key intermediate which can now be readily prepared in large quantity by our procedure reported in the preceding paper.[1)]

Since quaternization of pyridine ring nitrogen by a Menschutkin-type reaction[7)] has been well established, we first chose mercaptopyridines as reagents to react with the above compound **1**. As shown in Chart 1, incorporation of a variety of pyridylthio groups into the C-2′ position were readily carried out by either the Mitsunobu reaction[8)] or the analogous reaction[9)] in good yields, as exemplified by the synthesis of **2**.

Quaternary methylation at the pyridine nitrogen of the compound **2** and also in the case of the corresponding

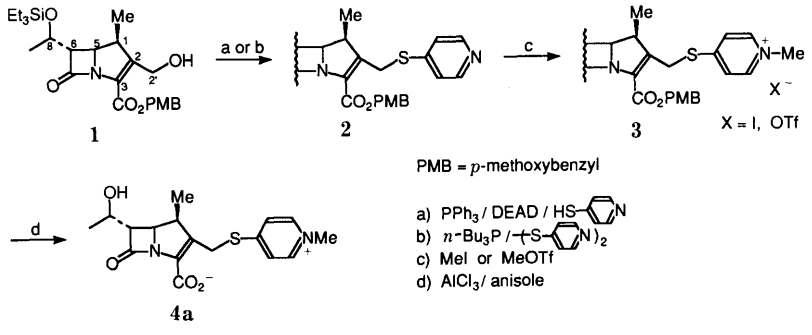

Chart 1

3-pyridyl (meta pyridine) ring was successfully accomplished by reaction with methyl iodide in acetonitrile at room temperature in almost quantitative yield. The same method, however, could not be applied to the 2-pyridyl (ortho pyridine ring) derivatives. This compound was found to be quaternized by treatment with methyl trifluoromethanesulfonate in CH_2Cl_2 under an ice-cooling condition. It should be noted that in both cases there was no detectable amount of product derived from alkylation at the sulfur atom of the C-2 side chains.

As far as the final deprotection step is concerned, the removal of the triethylsilyl (TES) group at the C-8 position, together with the *p*-methoxybenzyl (PMB) moiety, was successfully carried out by the conventional method using $AlCl_3$–anisole[10] to give the corresponding zwitterionic products as amorphous solids.

At this stage, the N-methyl-4-pyridinio-thiomethyl derivative **4a** thus obtained showed extremely potent overall activity as shown in Table I. Consequently, this derivative served as a lead compound and prompted us to explore the congeners in this area more extensively.

Therefore, we next attempted to examine the N-substituent effect on the activity of the pyridinio-thiomethyl derivatives. Quaternization of the pyridine moiety in such a carbapenem system by the Menschutkin-type reaction seemed to be limited, wherein only the simple alkyl halides as described above turned out to be applicable. This would in turn necessitate a more versatile strategy for introduction of the suitably functionalized substituents. Toward this end, our knowledge concerning cephalosporin chemistry[11] suggested that the reaction of the 2-chloromethyl carbapenem **7** with N-substituted thiopyridone would be one of the most efficient ways to generate the desired pyridinio-thiomethyl derivatives.

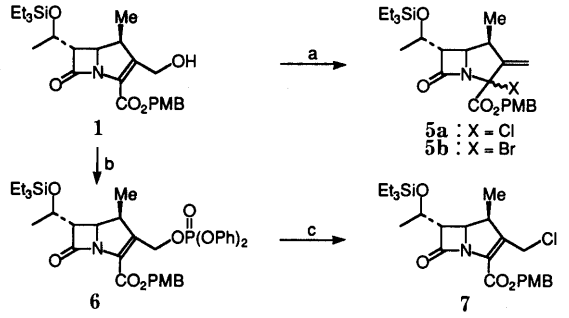

a) $SOCl_2$ / pyridine or PPh_3 / CCl_4 or $SOBr_2$ / pyridine
b) $ClPO(OPh)_2$ / DMAP
c) LiCl or Me_3SiCl

Chart 2

Chlorination of **1** by the ordinary method ($SOCl_2$/pyridine or PPh_3/CCl_4) as shown in Chart 2 gave rise to the undesired 3-chlorinated carbapenams **5a** in a regioselective manner. Similarly, bromination of **1** by the same kind of reaction ($SOBr_2$/pyridine) also afforded only the corresponding 3-brominated carbapenams **5b**. Our attempted elaborations to solve this problem finally resulted in the finding of an alternative route which involved the phosphonate intermediate **6**. Treatment of **1** with diphenylphosphoryl chloride in the presence of 4-dimethylaminopyridine at $-50\,°C$ generated the compound **6** as a pale yellow oil almost quantitatively. Subsequent treatment of this compound with either LiCl or Me_3SiCl in CH_2Cl_2 at room temperature gave rise to the desired 2-chloromethyl derivative **7** as a sole product in fairly good yield.[12] Although this compound was isolated as a relatively unstable form, it turned out that this ultimate intermediate could be utilized without purification to provide an entire series of target compounds. Thus, nucleophilic displacement of the chlorine by a variety of N-substituted thiopyridones such as **8** afforded the corresponding quaternized carbapenems in one step, as shown in Chart 3. According to this procedure, even bicyclic or tricyclic substrates such as **13** could be readily incorporated.

As for the synthesis of the unique tricyclic thiopyriridone **13**, we undertook an efficient synthetic route involving an intramolecular quaternization reaction of the trifluoromethane sulfonate intermediate (**11** to **12**) as depicted in Chart 3.

Finally, we investigated the antibacterial effect of a catechol moiety in the carbapenem molecule by synthesizing the compound **14**, since penicillin[13] and cephalosporin[14] derivatives containing a catechol residue are known to exhibit remarkable activity against *P. aeruginosa*. After several unsuccessful trials, we eventually synthesized the objective compound by the quaternization of **2** with 3,4-di-*p*-methoxybenzyloxybenzyl bromide, followed by the $AlCl_3$–anisole deblocking procedure under slightly acidic conditions (*ca.* pH 5), albeit in low yield. The derivative **14** displayed disappointingly reduced activity compared to the corresponding N-methyl compound **4a**, probably due to its chemical instability.

***In Vitro* Antibacterial Activity** The MIC values of these new carbapenems (Chart 5, 6 and 7) against selected strains of gram-positive and gram-negative bacteria are shown in Table I. As we expected, the positive charge in the quaternized heterocyclic ring resulted in significantly

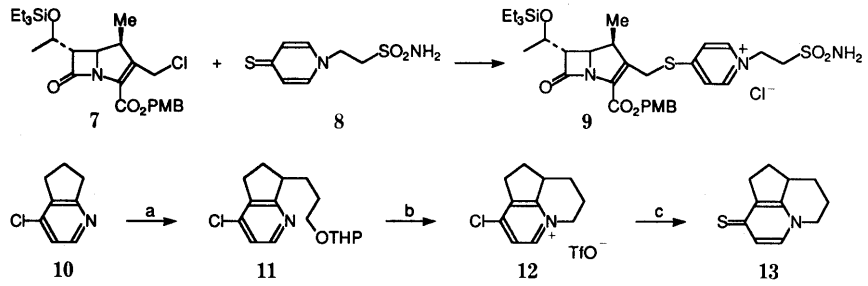

a) 1) BuLi, 2) $ICH_2CH_2CH_2OTHP$
b) 1) TsOH, 2) Tf_2O / Hünig base
c) 1) NaSH

Chart 3

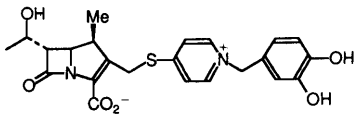

14

Chart 4

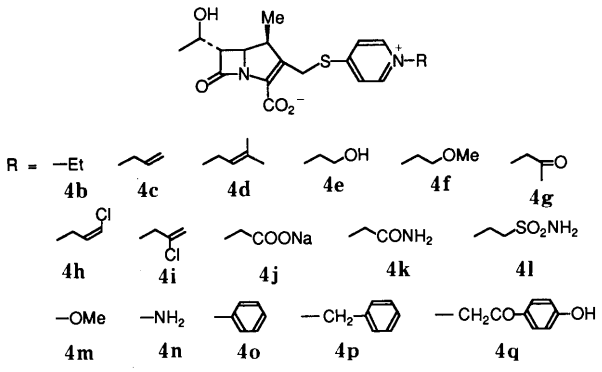

Chart 5

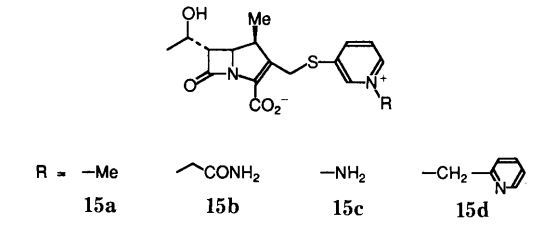

Chart 6

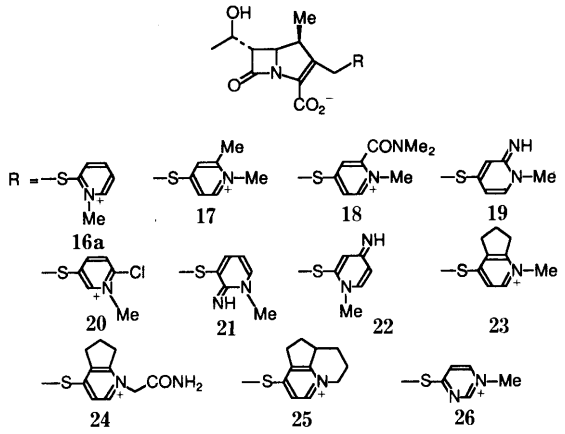

Chart 7

enhanced overall activity relative to their unquaternized partners.[1)]

The correlation between the structure of heterocyclic rings and their activity became clear. For example, additional substituents at various positions on the pyridine ring (Chart 7) had a negative effect on the activity in comparison with the parent derivatives (Chart 5 and 6), indicating that the electronic factor of the substituents seems to be less effective. With saturated rings fused to the pyridine moiety (**23**, **24** and **25**), the activity against gram-negative bacteria was reduced, thus implying that the steric bulkiness surrounding the cationic center and/or the increasing lipophilicity may reduce the permeability of the bacterial outer membrane.

TABLE I. *In Vitro* Antibacterial Activity

Comp. No.	MIC (μg/ml)					
	S. aureus SR14	*S. pyogenes* C-203	*E. coli* EC-14	*K. pneumoniae* SR1	*P. vulgaris* CN-329	*S. marcescens* ATCC 13880
4a	<0.01	<0.003	0.1	0.1	0.2	0.2
4b	0.01	0.003	0.1	0.1	0.2	0.2
4c	0.01	<0.003	0.1	0.2	0.2	0.2
4d	0.01	<0.003	0.2	0.2	0.4	0.8
4e	0.02	<0.003	0.1	0.2	0.4	0.4
4f	0.02	<0.003	0.2	0.2	0.4	0.4
4g	0.02	0.006	0.1	0.2	0.4	0.8
4h	0.01	<0.003	0.1	0.2	0.2	0.4
4i	0.01	<0.003	0.2	0.2	0.2	0.4
4j	0.05	0.01	0.1	0.1	0.2	0.4
4k	0.02	0.006	0.1	0.2	0.4	0.4
4l	0.02	<0.003	0.1	0.1	0.2	0.2
4m	0.8	0.2	12.5	6.3	6.3	50
4n	0.01	<0.003	0.1	0.1	0.2	0.4
4o	0.01	<0.003	0.2	0.2	0.2	0.8
4p	0.01	<0.003	0.2	0.2	0.4	0.8
4q	0.02	0.006	0.4	0.4	0.4	3.1
15a	0.02	0.006	0.2	0.2	0.4	0.8
15b	0.05	0.006	0.2	0.4	0.4	0.8
15c	0.02	0.006	0.2	0.4	0.4	0.8
15d	0.02	<0.003	0.4	0.4	0.4	1.6
16a	0.8	0.4	3.1	12.5	12.5	25
17	0.02	0.006	0.1	0.2	0.4	0.4
18	0.05	0.006	0.2	0.4	0.8	0.8
19	0.01	<0.003	0.2	0.2	0.4	0.8
20	0.02	0.006	0.4	0.4	0.4	0.8
21	0.05	0.01	0.8	0.8	0.8	1.6
22	0.02	0.006	0.4	0.4	0.8	1.6
23	0.01	<0.003	0.8	0.4	0.4	6.3
24	0.02	<0.003	0.8	0.4	0.4	6.3
25	0.01	<0.003	6.3	1.6	3.1	25
26	0.1	0.01	0.1	0.1	0.1	0.4
Imipenem	0.025	0.013	0.1	0.2	0.78	0.39

TABLE II. *In Vitro* Antibacterial Activity

Compound No.	Mean MIC (μg/ml)			
	L-MRSA[a)] (22 strains)	H-MRSA[b)] (22 strains)	*E. faecalis* (22 strains)	*P. aeruginosa* (21 strains)
4a	0.067	7.5	0.24	12.0
4b	0.069	10.6	0.25	17.3
4c	0.063	8.8	0.25	17.3
4e	0.11	12.5	0.34	16.2
4k	0.098	11.7	0.27	11.7
4l	0.13	11.7	0.31	9.28
Imipenem	0.095	48.4	0.83	1.41

a) Low-resistance groups of methicillin-resistant *S. aureus*. *b*) High-resistance groups of methicillin-resistant *S. aureus*.

Introduction of an additional nitrogen atom on the pyridine ring tended to decrease the activity against gram-positive bacteria, as exemplified by the N-methyl pyrimidine derivative **26**.

Among the N-substituted pyridinio-thiomethyl series bearing no substituents on the ring, the 4-pyridinio (*para* pyridinium ring) derivatives (Chart 5) proved to be the most active, while the 3-pyridinio (*meta* pyridinium ring) groups (Chart 6) were a little weak and the 2-pyridinio (*ortho* pyridinium ring) one (**16a**) had considerably diminished activity. Thus, the position of the positive charge on the pyridine ring played an important role in the activity on the whole. It is significant to note that the effect of variation of the N-substituents in the 4-pyridinio series (Chart 5) did

not influence the activity to a great extent. The MIC values (not including *P. aeruginosa*) of all the compounds except for **4m** in this group were comparable to those of imipenem.

Although the anti-pseudomonal activity of the quaternized derivatives has been enhanced to some extent as compared with the corresponding unquaternized counterparts, none of the compounds reached the same level as that of imipenem.

On the other hand, several derivatives (**4a**, **b**, **c**, **e**, **k** and **4l**) in the 4-pyridinio-thiomethyl series (Chart 5) were found to possess beneficial activity against methicillin-resistant *Staphylococcus aureus* (MRSA) which has recently been recognized as an increasing pathogen (Table II). Against low-resistance groups of methicillin-resistant *S. aureus* (L-MRSA),[15] these compounds showed about the same activity as that of imipenem in terms of the mean MIC values (22 strains). While imipenem showed considerably weak activity against high-resistance groups of methicillin-resistant *S. aureus* (H-MRSA), the above compounds exhibited mean MIC values of less than 12.5 μg/ml.

As another specific feature of these compounds, a fairly good activity against *E. faecalis* was demonstrated by the mean MIC values (22 strains) of less than 0.34 μg/ml.

***In Vivo* Activity** Because of the high levels of *in vitro* antibacterial activity against a wide variety of organisms, the above compounds were further examined for their *in vivo* activity. The ED_{50} values of these compounds in the mouse infection models against selected strains of gram-positive and gram-negative bacteria were determined and compared to those of imipenem, as shown in Table III. The *in vivo* activity of these compounds definitely reflected the corresponding *in vitro* antibacterial activity. Particularly against *P. aeruginosa*, these compounds exhibited much improved activity; thus, **4a** and **4k** became as active as imipenem on the basis of ED_{50} values (less than 1 mg/kg/dose). A good correlation between *in vitro* and *in vivo* activity of the quaternized heteroaromatic-thiomethyl derivatives was in marked contrast to the corresponding unquaternized compounds reported in the preceding paper.

TABLE III. Protective Effect on Intraperitoneal Infection in Mice

Compound No.	ED_{50} (mg/kg/dose)/MIC (μg/ml)			
	S. aureus SMITH	*S. pyogenes* C-203	*E. coli* EC-14	*P. aeruginosa* SR24
4a	0.0065/0.0125	0.012/<0.003	0.19/0.1	0.65/6.25
4b	0.0076/0.0125	— / 0.003	0.21/0.1	—/6.25
4c	0.011 /0.0125	0.016/<0.003	0.24/0.1	1.03/6.25
4e	0.009 /0.0125	0.016/<0.003	0.29/0.1	2.86/6.25
4k	0.0078/0.025	0.018/ 0.006	0.11/0.1	0.63/6.25
4l	0.009 /0.0125	0.016/<0.003	0.14/0.1	1.38/6.25
Imipenem	0.021 /0.0125	0.028/<0.013	0.36/0.1	0.98/1.56

ED_{50} was determined by survival rate 7 d after challenge.

TABLE IV. Stability in Kidney Tissue Homogenate

Compound No.	Remaining activity % in tissue homogenate[a]					
	Mouse	Rat	Rabbit	Dog	Monkey	Human
4a	54	43	46	59	46	70
Imipenem	37	32	33	36	33	54

a) Each compound was tested at a final concentration of 100 μg/ml and remaining activity % was determined after 1 h incubation at 37 °C.

Pharmacokinetic Properties of the Compound 4a As a representative of the above 6 compounds, **4a** was tested for stability in various kinds of kidney tissue homogenates respectively. In each species, this compound was found to be considerably more stable than imipenem (Table IV).

The urinary recovery of **4a** was next examined. In the case of mice (20 mg/kg, s.c.) and monkeys (10 mg/kg, i.v.), the average percentage of compound **4a** excreted for 24 h after dosing was 67% and 65%, respectively. These results were much better than those of imipenem (whose recovery values were in the range of about 25—30%) reflecting the above observed intrinsic stability of **4a** to mouse and monkey kidney enzyme preparations.

Experimental

General Procedures All reactions involving air-sensitive reactants or products were carried out under a nitrogen atmosphere using dry solvents. Infrared (IR) spectra were recorded on a Hitachi 260-10 spectrophotometer. Proton nuclear magnetic resonance (^{1}H-NMR) spectra were obtained on a Varian EM-390 (90 MHz) and VXR-200 (200 MHz). Unless otherwise stated, chemical shifts are expressed in ppm downfield from tetramethylsilane (TMS) as an internal (in organic solvent) or external (in D_2O) standard. Ultraviolet (UV) spectra were taken on a Hitachi EPS-3T spectrometer. Specific optical rotations ($[\alpha]_D$) were taken at 25 °C on a Perkin–Elmer 241 Polarimeter. Mass spectra (MS) were obtained on a Hitachi M-90 (SIMS) mass spectrometer. Medium pressure liquid chromatographies were performed on Merck 'Lobar' prepacked columns packed with LiChroprep Si 60; size A (240—10 mm, 40—60 μm), size B (310—25 mm, 40—60 μm) and size C (440—37 mm, 63—125 μm). Most of the new compounds reported here are either non-crystalline solids or forms, or unstable. Hence, their analytical data could not be obtained.

***p*-Methoxybenzyl (1*S*,5*R*,6*S*)-2-Hydroxymethyl-1-methyl-6-[(*R*)-1-triethylsilyloxyethyl]carbapen-2-em-3-carboxylate (1)** The title compound was prepared by essentially the same method described in the preceding paper.

***p*-Methoxybenzyl (1*S*,5*R*,6*S*)-1-Methyl-2-(4-pyridyl)thiomethyl-6-[(*R*)-1-triethylsilyloxyethyl]carbapen-2-em-3-carboxylate (2)** Method I: To a solution of **1** (476 mg, 1 mmol), triphenylphosphine (315 mg, 1.2 eq) and 4-mercaptopyridine (133 mg, 1.2 eq) in tetrahydrofuran (THF, 10 ml) was added diethyl azodicarboxylate (209 mg, 1.2 eq), and the mixture was stirred at room temperature for 1 h. After the usual work up, the residue was chromatographed on a Lobar column (size B, toluene–EtOAc 1 : 2) to give **2** (410 mg, 72%). IR ($CHCl_3$) cm^{-1}: 1780, 1615. ^{1}H-NMR (90 MHz, $CDCl_3$) δ: 0.52—0.68 (6H, m), 0.85—1.00 (9H, m), 1.15 (3H, d, J=8.7 Hz), 1.23 (3H, d, J=6 Hz), 3.18 (1H, dd, J=2.2, 6 Hz), 3.09—3.30 (1H, m), 3.46 and 4.91 (2H, ABq, J=14 Hz), 3.78 (3H, s), 4.09 (1H, dd, J=2.2, 13 Hz), 4.10—4.30 (1H, m), 5.21 (2H, s), 6.85 and 7.30 (4H, ABq, J=9 Hz), 7.06 and 8.30 (4H, ABq, J=6 Hz).

Method II: A solution of **1** (476 mg, 1 mmol), tributylphosphine (223 mg, 1.1 eq) and 4,4′-dipyridyl disulfide (242 mg, 1.1 eq) in CH_2Cl_2 (10 ml) was stirred at room temperature for 1 h. The reaction mixture was washed with aqueous $NaHCO_3$ solution, dried, concentrated and chromatographed as described above to give **2** (444 mg, 78%).

(1*S*,5*R*,6*S*)-6-[(*R*)-1-Hydroxyethyl]-1-methyl-2-(1-methyl-4-pyridinio)-thiomethylcarbapen-2-em-3-carboxylate (4a) and Related Compounds A solution of **2** (569 mg, 1 mmol) and iodomethane (1.42 g, 10 eq) in acetonitrile (10 ml) was stirred at room temperature for 2 h and then concentrated to give **3** (710 mg, 100%). The PMB ester **3** (710 mg, 1 mmol) was added to a solution of $AlCl_3$ (400 mg, 3 eq) in a mixture of anisole (7 ml) and CH_2Cl_2 (4 ml) at −40 °C, and the mixture was stirred for 1 h at the same temperature. A solution of $NaHCO_3$ (336 mg, 4 eq) in water (5 ml) and CH_2Cl_2 (20 ml) were added, and the reaction mixture was stirred under ice cooling for 10 min and filtered. The aqueous filtrate was chromatographed on an HP-20AG column (20 × 250 mm, H_2O) and the fractions containing the product were concentrated and freeze-dried to give **4a** as a yellow powder (233 mg, 67%). ^{1}H-NMR (90 MHz, D_2O) δ: 1.58 (3H, d, J=7 Hz), 1.65 (3H, d, J=6 Hz), 3.55—3.70 (1H, m), 3.85 (1H, dd, J=2, 6 Hz), 4.30 and 5.48 (2H, ABq, J=14 Hz), 4.35—4.75 (2H, m), 4.62 (3H, s), 8.20 and 8.75 (4H, A_2B_2q, J=8 Hz). UV (H_2O) nm: 231,

305. MS (SIMS, glycerol) *m/z*: 349 $(M+H)^+$, 697 $(2M+H)^+$. *Anal.* Calcd for $C_{17}H_{20}N_2O_4S \cdot 2H_2O$: C, 53.11; H, 6.29; N, 7.29; S, 8.34. Found: C, 52.94; H, 6.16; N, 7.50; S, 8.31.

The following compounds were prepared by the same or a slightly modified procedure.

(1*S*,5*R*,6*S*)-2-(1-Ethyl-4-pyridinio)thiomethyl-6-[(*R*)-1-hydroxyethyl]-1-methylcarbapen-2-em-3-carboxylate (4b) **4b**: ^{1}H-NMR (90 MHz, D_2O) δ: 1.62 (3H, d, J=7 Hz), 1.73 (3H, d, J=6 Hz), 2.02 (3H, t, J=8 Hz), 3.70—3.80 (1H, m), 3.88 (1H, dd, J=2, 6 Hz), 4.30 and 5.52 (2H, ABq, J=14 Hz), 4.50—4.90 (2H, m), 4.80 (2H, q, J=8 Hz), 8.25 and 8.95 (4H, A_2B_2q, J=8 Hz). UV (H_2O) nm: 232, 305.

(1*S*,5*R*,6*S*)-6-[(*R*)-1-Hydroxyethyl]-1-methyl-2-[1-(prop-2-enyl)-4-pyridinio]thiomethylcarbapen-2-em-3-carboxylate (4c) **4c**: ^{1}H-NMR (90 MHz, D_2O) δ: 1.55 (3H, d, J=7 Hz), 1.70 (3H, d, J=6 Hz), 3.70—3.90 (2H, m), 4.30 and 5.62 (2H, ABq, J=14 Hz), 4.40—4.80 (2H, m), 5.50 (1H, d, J=6 Hz), 5.91 (1H, m), 8.25 and 8.90 (4H, A_2B_2q, J=8 Hz). UV (H_2O) nm: 230, 307. MS (SIMS, glycerol) *m/z*: 375 $(M+H)^+$, 749 $(2M+H)^+$. *Anal.* Calcd for $C_{19}H_{22}N_2O_4S \cdot H_2O$: C, 58.15; H, 6.16; N, 7.14; S, 8.17. Found: C, 58.40; H, 6.27; N, 7.26; S, 8.09.

(1*S*,5*R*,6*S*)-6-[(*R*)-1-Hydroxyethyl]-1-methyl-2-[1-(3-methylbut-2-enyl)-4-pyridinio]thiomethylcarbapen-2-em-3-carboxylate (4d) **4d**: ^{1}H-NMR (200 MHz, D_2O, sodium 4,4-dimethyl-4-silapentanesulfonate (DSS) as standard) δ: 1.16 (3H, d, J=7.4 Hz), 1.25 (3H, d, J=6.4 Hz), 1.82 (3H, s), 1.84 (3H, s), 3.29—3.38 (1H, m), 3.42 (1H, dd, J=2.8, 6 Hz), 3.85 and 5.07 (2H, ABq, J=15 Hz), 4.12—4.28 (1H, m), 4.99—5.10 (2H, m), 5.43—5.51 (1H, m), 7.75 and 8.40 (4H, A_2B_2q, J=7.2 Hz).

(1*S*,5*R*,6*S*)-6-[(*R*)-1-Hydroxyethyl]-2-[1-(2-hydroxy)ethyl-4-pyridinio]-thiomethyl-1-methylcarbapen-2-em-3-carboxylate (4e) **4e**: ^{1}H-NMR (200 MHz, D_2O) δ: 0.98 (3H, d, J=7.4 Hz), 1.07 (3H, d, J=6.4 Hz), 3.10—3.25 (1H, m), 3.27 (1H, dd, J=2, 6 Hz), 3.69 and 4.90 (2H, ABq, J=14 Hz), 3.80—3.90 (2H, m), 3.92 (1H, dd, J=2, 9 Hz), 3.95—4.05 (1H, m), 4.30—4.40 (2H, m), 7.62 and 8.27 (4H, A_2B_2q, J=7.2 Hz). MS (SIMS, glycerol) *m/z*: 379 $(M+H)^+$, 757 $(2M+H)^+$.

(1*S*,5*R*,6*S*)-6-[(*R*)-1-Hydroxyethyl]-2-[1-(2-methoxy)ethyl-4-pyridinio]-thiomethyl-1-methylcarbapen-2-em-3-carboxylate (4f) **4f**: IR (KBr) cm^{-1}: 3450, 1749, 1630, 1592, 1546, 1104. ^{1}H-NMR (200 MHz, D_2O, DSS as standard) δ: 1.17 (3H, d, J=7.2 Hz), 1.26 (3H, d, J=6.4 Hz), 3.22—3.40 (1H, m), 3.43 (1H, dd, J=3, 6 Hz), 3.35 (3H, s), 3.87 and 5.08 (2H, ABq, J=15 Hz), 3.81—3.91 (2H, m), 4.07 (1H, dd, J=3, 10 Hz), 4.17—4.24 (1H, m), 4.58—4.62 (2H, m), 7.79 and 8.44 (4H, A_2B_2q, J=7 Hz). UV (H_2O) nm: 230.5, 307.

(1*S*,5*R*,6*S*)-2-(1-Acetylmethyl-4-pyridinio)thiomethyl-6-[(*R*)-1-hydroxyethyl]-1-methylcarbapen-2-em-3-carboxylate (4g) **4g**: ^{1}H-NMR (200 MHz, D_2O, DSS as standard) δ: 1.49 (3H, d, J=7.4 Hz), 1.58 (3H, d, J=6.4 Hz), 2.70 (3H, s), 3.6—3.8 (1H, m), 3.76 (1H, dd, J=3, 6 Hz), 4.21 and 5.41 (2H, ABq, J=13 Hz), 4.40 (1H, dd, J=3, 10 Hz), 4.5—4.6 (1H, m), 4.17—4.24 (1H, m), 5.88 (2H, s), 8.14 and 8.56 (4H, A_2B_2q, J=7.4 Hz).

(1*S*,5*R*,6*S*)-2-[1-(3-Chloroprop-2-enyl)-4-pyridinio]thiomethyl-6-[(*R*)-1-hydroxyethyl]-1-methylcarbapen-2-em-3-carboxylate (4h) **4h**: ^{1}H-NMR (200 MHz, D_2O, DSS as standard) δ: 1.16 (3H, d, J=7.2 Hz), 1.25 (3H, d, J=6.2 Hz), 3.26—3.38 (1H, m), 3.43 (1H, dd, J=2.4, 6 Hz), 3.87 and 5.08 (2H, ABq, J=15 Hz), 4.07 (1H, dd, J=2.4, 10 Hz), 4.14—4.27 (1H, m), 5.22—5.28 (2H, m), 6.16—6.28 (1H, m), 6.64—6.76 (1H, m), 7.79 and 8.44 (4H, A_2B_2q, J=6.8 Hz).

(1*S*,5*R*,6*S*)-2-[1-(2-Chloroprop-2-enyl)-4-pyridinio]thiomethyl-6-[(*R*)-1-hydroxyethyl]-1-methylcarbapen-2-em-3-carboxylate (4i) **4i**: ^{1}H-NMR (200 MHz, D_2O, DSS as standard) δ: 1.17 (3H, d, J=7.4 Hz), 1.26 (3H, d, J=6.4 Hz), 3.27—3.39 (1H, m), 3.43 (1H, dd, J=2.8, 6 Hz), 3.90 and 5.10 (2H, ABq, J=14.8 Hz), 4.08 (1H, dd, J=2.8, 9.8 Hz), 4.18—4.28 (1H, m), 5.26 (2H, s), 5.72 (1H, d, J=2.4 Hz), 5.83 (1H, d, J=2.4 Hz), 7.84 and 8.50 (4H, A_2B_2q, J=7.2 Hz).

(1*S*,5*R*,6*S*)-6-[(*R*)-1-Hydroxyethyl]-1-methyl-2-(1-sodiumcarboxymethyl-4-pyridinio)thiomethylcarbapen-2-em-3-carboxylate (4j) **4j**: ^{1}H-NMR (200 MHz, D_2O) δ: 1.00 (3H, d, J=7.0 Hz), 1.09 (3H, d, J=6.6 Hz), 3.1—3.3 (1H, m), 3.27 (1H, dd, J=2.8 and 5.8 Hz), 3.73 and 4.92 (2H, ABq, J=15 Hz), 3.9—4.2 (1H, m), 3.92 (1H, dd, J=2.8 and 8.8 Hz), 4.17—4.24 (1H, m), 4.86 (2H, s), 7.63 and 8.20 (4H, A_2B_2q, J=7 Hz).

(1*S*,5*R*,6*S*)-2-(1-Carbamoylmethyl-4-pyridinio)thiomethyl-6-[(*R*)-1-hydroxyethyl]-1-methylcarbapen-2-em-3-carboxylate (4k) **4k**: ^{1}H-NMR (200 MHz, D_2O) δ: 0.98 (3H, d, J=7.2 Hz), 1.07 (3H, d, J=6.4 Hz), 3.1—3.2 (1H, m), 3.24 (1H, dd, J=3, 6 Hz), 3.71 and 4.90 (2H, ABq, J=14.2 Hz), 3.88 (1H, dd, J=2.8, 8.8 Hz), 3.9—4.1 (1H, m), 5.12 (2H, s), 7.64 and 8.20 (4H, A_2B_2q, J=6.6 Hz).

(1*S*,5*R*,6*S*)-6-[(*R*)-1-Hydroxyethyl]-1-methyl-2-(1-methoxyl-4-pyridinio)thiomethylcarbapen-2-em-3-carboxylate (4m) **4m**: ^{1}H-NMR (200 MHz, D_2O, DHO as standard) δ: 1.16 (3H, d, J=7.4 Hz), 1.24 (3H, d, J=6.3 Hz), 3.10—3.30 (1H, m), 3.24 (1H, dd, J=2.9, 7.1 Hz), 3.72 (1H, d, J=15 Hz), 3.89 (1H, dd, J=2.8, 9.8 Hz), 3.90—4.10 (1H, m), 4.15 (3H, s), 4.62 (DHO), 4.89 (1H, d, J=15 Hz), 7.62 (2H, d, J=7.2 Hz), 8.59 (2H, d, J=7.2 Hz).

(1*S*,5*R*,6*S*)-2-(1-Benzyl-4-pyridinio)thiomethyl-6-[(*R*)-1-hydroxyethyl]-1-methylcarbapen-2-em-3-carboxylate (4p) **4p**: ^{1}H-NMR (200 MHz, D_2O, DHO as standard) δ: 0.94 (3H, d, J=7.4 Hz), 1.05 (3H, d, J=6.2 Hz), 3.05—3.19 (1H, m), 3.22 (1H, dd, J=2.8, 6 Hz), 3.64 and 4.85 (2H, ABq, J=14.6 Hz), 3.84 (1H, dd, J=2.8, 10 Hz), 3.93—4.25 (1H, m), 4.62 (DHO), 5.39 (2H, s), 7.24 (5H, s), 7.56 and 8.31 (4H, A_2B_2q, J=7.2 Hz).

(1*S*,5*R*,6*S*)-6-[(*R*)-1-Hydroxyethyl]-1-methyl-2-(1-methyl-3-pyridinio)-thiomethylcarbapen-2-em-3-carboxylate (15a) **15a**: IR (KBr) cm^{-1}: 3400, 1750, 1595, 1500, 1282, 1255. ^{1}H-NMR (200 MHz, D_2O) δ: 0.96 (3H, d, J=7.4 Hz), 1.08 (3H, d, J=6.4 Hz), 3.1—3.3 (1H, m), 3.22 (1H, dd, J=2.6, 6 Hz), 3.46 and 4.69 (2H, ABq, J=14 Hz), 3.87 (1H, dd, J=2.6, 9.8 Hz), 3.9—4.1 (1H, m), 4.14 (2H, s), 7.72 (1H, dd, J=6, 8.4 Hz), 8.25 (1H, d, J=8.4 Hz), 8.43 (1H, d, J=6.0 Hz), 8.59 (1H, s). MS (SIMS, glycerol) *m/z*: 349 $(M+H)^+$, 697 $(2M+H)^+$. *Anal.* Calcd for $C_{17}H_{20}N_2O_4S \cdot 0.7H_2O$: C, 56.56; H, 5.97; N, 7.76; S, 8.88. Found: C, 56.84; H, 6.23; N, 7.96; S, 8.75.

(1*S*,5*R*,6*S*)-2-(1-Carbamoylmethyl-3-pyridinio)thiomethyl-6-[(*R*)-1-hydroxyethyl]-1-methylcarbapen-2-em-3-carboxylate (15b) **15b**: ^{1}H-NMR (200 MHz, D_2O, DSS as standard) δ: 1.13 (3H, d, J=7.4 Hz), 1.25 (3H, d, J=6.4 Hz), 3.26—3.40 (2H, m), 4.03 (1H, dd, J=2.9, 9.6 Hz), 4.11—4.24 (1H, m), 3.69 and 4.92 (2H, ABq, J=14.8 Hz), 5.43 (2H, s), 7.98 (1H, dd, J=6, 8.4 Hz), 8.52 (1H, dd, J=6 Hz), 8.63 (1H, d, J=8.4 Hz), 8.85 (1H, s).

(1*S*,5*R*,6*S*)-2-(1-Amino-3-pyridinio)thiomethyl-6-[(*R*)-1-hydroxyethyl]-1-methylcarbapen-2-em-3-carboxylate (15c) **15c**: ^{1}H-NMR (200 MHz, D_2O, DSS as standard) δ: 1.14 (3H, d, J=7.4 Hz), 1.26 (3H, d, J=6.4 Hz), 3.23—3.47 (1H, m), 3.42 (1H, dd, J=3, 6.4 Hz), 3.64 and 4.84 (2H, ABq, J=14 Hz), 4.08 (1H, dd, J=3, 9.8 Hz), 4.17—4.23 (1H, m), 7.85 (1H, dd, J=6.4, 8 Hz), 8.26 (1H, d, J=8.4 Hz), 8.57 (1H, dd, J=2 Hz), 8.72 (1H, s).

(1*S*,5*R*,6*S*)-6-[(*R*)-1-Hydroxyethyl]-1-methyl-2-[1-(2-pyridyl)methyl-3-pyridinio]thiomethylcarbapen-2-em-3-carboxylate (15d) **15d**: ^{1}H-NMR (200 MHz, D_2O, DSS as standard) δ: 1.10 (3H, d, J=7.2 Hz), 1.25 (3H, d, J=6.2 Hz), 3.27—3.38 (2H, m), 3.66 and 4.94 (2H, ABq, J=14.7 Hz), 3.90 (1H, dd, J=2.8, 9.8 Hz), 4.15—4.21 (1H, m), 5.88 (2H, s), 7.45—7.59 (2H, m), 7.93—8.01 (2H, m), 8.48—8.52 (2H, m), 8.76 (1H, d, J=5.8 Hz), 8.91 (1H, m).

(1*S*,5*R*,6*S*)-6-[(*R*)-1-Hydroxyethyl]-1-methyl-2-(1-methyl-6-chloro-3-pyridinio)thiomethylcarbapen-2-em-3-carboxylate (20) **20**: ^{1}H-NMR (200 MHz, D_2O, DHO as standard) δ: 0.97 (3H, d, J=7.2 Hz), 1.07 (3H, d, J=6.2 Hz), 3.12—3.19 (1H, m), 3.24 (1H, dd, J=2.8, 6.2 Hz), 3.51 and 4.76 (2H, ABq, J=14.5 Hz), 3.87 (1H, dd, J=2.8, 9.8 Hz), 3.95—4.08 (1H, m), 4.14 (3H, s), 4.61 (DHO), 8.33 (1H, s), 8.57 (1H, s), 8.63 (1H, s).

(1*S*,5*R*,6*S*)-6-[(*R*)-1-Hydroxyethyl]-2-(2-imino-1-methyl-1,2-dihydropyridin-3-yl)thiomethyl-1-methylcarbapen-2-em-3-carboxylate (21) **21**: IR (KBr) cm^{-1}: 3400, 1748, 1645, 1585, 1515, 1240. ^{1}H-NMR (200 MHz, D_2O, DHO as standard) δ: 1.11 (3H, d, J=7.2 Hz), 1.27 (3H, d, J=6.3 Hz), 3.30—3.47 (1H, m), 3.33 and 4.49 (2H, ABq, J=13.4 Hz), 3.38 (1H, dd, J=2.8, 6 Hz), 3.84 (3H, s), 4.13 (1H, dd, J=2.8, 9.9 Hz), 4.15—4.28 (1H, m), 4.80 (DHO), 6.83 (1H, t, J=7 Hz), 7.87 (1H, dd, J=1.4, 6.6 Hz), 7.99 (1H, dd, J=1.4, 7.4 Hz).

(1*S*,5*R*,6*S*)-6-[(*R*)-1-Hydroxyethyl]-2-(4-imino-1-methyl-1,4-dihydropyridin-2-yl)thiomethyl-1-methylcarbapen-2-em-3-carboxylate (22) **22**: ^{1}H-NMR (200 MHz, D_2O, DHO as standard) δ: 0.98 (3H, d, J=7.2 Hz), 1.09 (3H, d, J=6.2 Hz), 3.12—3.21 (1H, m), 3.23 (1H, dd, J=3, 6.2 Hz), 3.35—3.49 (1H, m), 3.58 and 4.68 (2H, ABq, J=14.6 Hz), 3.70 (3H, s), 3.92 (1H, dd, J=3, 10 Hz), 4.00—4.10 (1H, m), 6.47 (1H, dd, J=2.6, 7.2 Hz), 4.62 (DHO), 6.56 (1H, d, J=2.6 Hz), 7.72 (1H, d, J=7.2 Hz).

(1*S*,5*R*,6*S*)-2-(1-Amino-4-pyridinio)thiomethyl-6-[(*R*)-1-hydroxyethyl]-1-methylcarbapen-2-em-3-carboxylate (4n) **4n**: ^{1}H-NMR (200 MHz, D_2O, DHO as standard) δ: 1.15 (3H, d, J=7.4 Hz), 1.25 (3H, d, J=6.3 Hz), 3.20—3.50 (1H, m), 3.45 (1H, dd, J=2.9, 7.1 Hz), 3.83 (1H, d, J=15.2 Hz), 4.06 (1H, dd, J=2.9, 9.9 Hz), 4.20 (1H, quintet, J=6.3 Hz), 4.81 (DHO), 5.06 (1H, d, J=15 Hz), 7.74 (2H, d, J=7.3 Hz), 8.41 (2H, d, J=7.3 Hz).

(1*S*,5*R*,6*S*)-6-[(*R*)-1-Hydroxyethyl]-1-methyl-2-(1-methyl-2-pyridinio)-thiomethylcarbapen-2-em-3-carboxylate (16a) **16a**: ^{1}H-NMR (200 MHz, D_2O) δ: 0.95 (3H, d, J=7.2 Hz), 1.11 (3H, d, J=6.4 Hz), 3.02—3.15 (1H, m), 3.24 (1H, dd, J=2, 6 Hz), 3.47 and 4.70 (2H, ABq, J=14 Hz), 3.80 (3H, s), 3.89 (1H, dd, J=3, 9.6 Hz), 3.9—4.2 (1H, m), 7.70—8.70 (4H, m).

(1*S*,5*R*,6*R*)-6-[(*R*)-1-Hydroxyethyl]-1-methyl-2-(1-methyl-4-pyrimidinio)thiomethylcarbapen-2-em-3-carboxylate (26) **26**: ^{1}H-NMR

(200 MHz, D_2O) δ: 0.96 (3H, d, J=7.2 Hz), 1.06 (3H, d, J=6.4 Hz), 3.05—3.14 (1H, m), 3.25 (1H, dd, J=2, 6 Hz), 3.78 and 4.80 (2H, ABq, J=14.2 Hz), 3.90 (1H, dd, J=2, 9 Hz), 3.94 (3H, s), 3.98—4.04 (1H, m), 7.67 (1H, d, J=7 Hz), 8.32 (1H, d, J=7 Hz), 8.90 (1H, s).

(1*S*,5*R*,6*S*)-2-[1-(3',4'-Dihydroxy)benzyl-4-pyridinio]thiomethyl-6-[(*R*)-1-Hydroxyethyl]-1-methylcarbapen-2-em-3-carboxylate (14) A solution of **2** (156 mg, 0.34 mmol) and 3,4-di-*p*-methoxybenzyloxybenzyl bromide (302 mg, 2 eq) in acetonitrile (5 ml) was stirred at room temperature for 12 h and then condensed to give a pyridinium salt which was washed with diethyl ether (284 mg, 92%). IR ($CHCl_3$) cm^{-1}: 2950, 1780, 1720, 1615. ^{1}H-NMR (90 MHz, $CDCl_3$) δ: 0.53—0.67 (6H, m), 0.85—1.00 (9H, m), 1.17 (3H, d, J=8.7 Hz), 1.23 (3H, d, J=6 Hz), 3.10 (1H, dd, J=2.2, 6 Hz), 3.15—3.30 (1H, m), 3.50 and 4.80 (2H, ABq, J=14 Hz), 3.75 (3H, s), 3.77 (3H, s), 3.80 (3H, s), 4.10 (1H, dd, J=2.2, 13 Hz), 4.15—4.30 (1H, m), 4.95—5.10 (4H, m), 5.20 (2H, s), 5.95 (2H, s), 6.80—7.45 (15H, m), 7.65—9.20 (4H, m).

The pyridinium salt (280 mg, 0.31 mmol) was added to a solution of $AlCl_3$ (186 mg, 4.5 eq) in a mixture of anisole (4 ml) and CH_2Cl_2 (3 ml) at −40 °C, and the mixture was stirred for 1 h at the same temperature. The mixture was poured into water and stirred under ice cooling for 10 min and filtered. The aqueous filtrate was chromatographed on an HP-20AG column (20 × 250 mm, H_2O) and the fractions containing the product were concentrated and freeze-dried to give **14** as yellow powder (13 mg, 9%). ^{1}H-NMR (90 MHz, D_2O) δ: 1.07 (3H, d, J=7.2 Hz), 1.12 (3H, d, J=6.4 Hz), 3.25—3.31 (1H, m), 3.45 (1H, dd, J=2, 6 Hz), 3.90 and 5.05 (2H, ABq, J=14 Hz), 4.00—4.18 (2H, m), 4.70 (2H, s), 6.80—8.50 (7H, m).

***p*-Methoxybenzyl (1*S*,5*R*,6*S*)-2-Diphenylphosphorylmethyl-1-methyl-6-[(*R*)-1-triethylsilyloxyethyl]carbapen-2-em-3-carboxylate (6)** To solution **1** (220 mg, 0.46 mmol) and 4-dimethylaminopyridine (62 mg, 1.1 eq) in CH_2Cl_2 (2 ml) was added chlorodiphenylphosphate (0.1 ml, 1.05 eq) at −50 °C, and the mixture was stirred for 30 min at the same temperature. The reaction mixture was washed with aqueous $NaHCO_3$ solution, 0.1 N HCl and water, and dried and concentrated to give **6** as a pale yellow oil (307 mg, 92%). IR ($CHCl_3$) cm^{-1}: 2900, 1770, 1700. ^{1}H-NMR (90 MHz, $CDCl_3$) δ: 0.53—0.68 (6H, m), 0.86—1.01 (9H, m), 1.18 (3H, d, J=7.2 Hz), 1.29 (3H, d, J=6.5 Hz), 3.05—3.31 (2H, m), 3.80 (3H, s), 4.00—4.30 (2H, m), 4.80 and 5.08 (2H, ABq, J=14 Hz), 5.18 (2H, s), 6.86 and 7.38 (4H, A_2B_2q, J=6.8 Hz), 6.90—7.50 (10H, m).

***p*-Methoxybenzyl (1*S*,5*R*,6*S*)-2-Chloromethyl-1-methyl-6-[(*R*)-1-trimethylsilyloxyethyl]carbapen-2-em-3-carboxylate (7)** To a solution of **6** (300 mg, 0.41 mmol) in CH_2Cl_2 (2 ml) was added LiCl (37 mg, 2 eq), followed by stirring at room temperature for 1 h. The reaction mixture was washed with aqueous $NaHCO_3$ solution. 0.1 N HCl and water, and dried and concentrated to give **7** as a colorless oil (178 mg, 78%). IR($CHCl_3$) cm^{-1}: 2950, 1770, 1620. ^{1}H-NMR (90 MHz, $CDCl_3$) δ: 0.54—0.65 (6H, m), 0.90—1.01 (9H, m), 1.02 (3H, d, J=7.2 Hz), 1.22 (3H, d, J=6.4 Hz), 2.71—2.82 (1H, m), 2.85—3.05 (1H, m), 3.80 (3H, s), 4.20—4.42 (2H, m), 5.15 and 5.40 (2H, ABq, J=14 Hz), 5.23 (2H, s), 6.87 and 7.39 (4H, A_2B_2q, J=6.8 Hz).

As for the direct chlorination of **1**, the following results were obtained. To a solution of **1** (128 mg, 0.27 mmol) and pyridine (0.052 ml, 2 eq) in THF (2 ml) at −30 °C was added thionyl chloride (0.082 ml, 1.2 eq). The mixture was stirred for 1 h at the same temperature. The reaction mixture was diluted with EtOAc (10 ml), washed with aqueous $NaHCO_3$ solution and water, and dried, concentrated and chromatographed on a Lobar column (size A, toluene–EtOAc 4 : 1) to give the 3-chloro-carbapenam **5a** as a 3 : 2 epimeric mixture (yellow oil, 92 mg, 68%). IR ($CHCl_3$) cm^{-1} of the mixture of two epimers: 1765, 1720, 1605. ^{1}H-NMR (200 MHz, $CDCl_3$) of the main epimer δ: 0.52—0.70 (6H, m), 0.85—1.00 (9H, m), 1.21 (3H, d, J=7.2 Hz), 1.36 (3H, d, J=7 Hz), 2.80—3.30 (2H, m), 3.80 (3H, s), 4.05—4.40 (2H, m), 5.20 (2H, s), 5.40 and 5.82 (2H, dd, J=2.5 Hz, vinyl H), 6.87 and 7.40 (4H, A_2B_2q, J=6.8 Hz).

When **1** (60 mg, 0.13 mmol) was treated with triphenylphosphine (80 mg, 2 eq) and CCl_4 (0.15 ml, 10 eq) in acetonitrile (2 ml) at room temperature, in this case also, only **5a** (3 : 2 epimeric mixture, 70%) was obtained.

Similarly, bromination of **1** (190 mg, 0.40 mmol) using thionyl bromide (0.041 ml, 1.2 eq) and pyridine (0.071 ml, 2 eq) afforded the 3-bromo-carbapenam **5b** as a 3 : 1 epimeric mixture (brownish oil, 138 mg, 62%). ^{1}H-NMR (200 MHz, $CDCl_3$) of the main epimer δ: 0.52—0.70 (6H, m), 0.85—1.00 (9H, m), 1.23 (3H, d, J=7.2 Hz), 1.38 (3H, d, J=7.0 Hz), 2.80—3.30 (2H, m), 3.80 (3H, s), 4.03—4.44 (2H, m), 5.20 (2H, s), 5.40 and 5.84 (2H, dd, J=2.5 Hz, vinyl H), 6.88 and 7.40 (4H, A_2B_2q, J=6.8 Hz).

(1*S*,5*R*,6*S*)-6-[(*R*)-1-Hydroxyethyl]-1-methyl-2-(1-sulfamoylethyl-4-pyridinio)thiomethylcarbapen-2-em-3-carboxylate (41) and Related Compounds To a solution of **7** (256 mg, 0.5 mmol) in acetonitrile (2 ml) was added **8** (131 mg, 1.2 eq), and the mixture was stirred for 2 h at room temperature. The reaction mixture was diluted with EtOAc (10 ml), washed with water, dried and concentrated to give tyhe pyridinio-thiomethyl derivative **9** (325 mg, 89%) which was converted to the titled compound by the $AlCl_3$–anisole method. **41**: ^{1}H-NMR (200 MHz, D_2O) δ: 1.15 (3H, d, J=7.4 Hz), 1.25 (3H, d, J=6.4 Hz), 3.37 (1H, m), 3.44 (1H, dd, J=2, 6 Hz), 3.80—3.95 (2H, m), 4.07 (1H, dd, J=2.4, 9 Hz), 4.20 (1H, m), 3.90 and 5.02 (2H, ABq, J=14 Hz), 4.85—4.95 (2H, m), 7.80 and 8.53 (4H, A_2B_2q, J=8 Hz).

The following compounds were also prepared by the same method.

(1*S*,5*R*,6*S*)-6-[(*R*)-1-Hydroxyethyl]-1-methyl-2-(1-phenyl-4-pyridinio)-thiomethylcarbapen-2-em-3-carboxylate (4o) 4o: ^{1}H-NMR (200 MHz, D_2O) δ: 0.99 (3H, d, J=7.2 Hz), 1.08 (3H, d, J=6.4 Hz), 3.12—3.20 (1H, m), 3.27 (1H, dd, J=2, 6 Hz), 3.78 and 4.96 (2H, ABq, J=14 Hz), 3.92 (1H, dd, J=2, 9 Hz), 4.01—4.10 (1H, m), 6.98—7.51 (5H, m), 7.76 and 8.51 (4H, A_2B_2q, J=7 Hz).

(1*S*,5*R*,6*S*)-2-[1-(4-Hydroxy)benzoylmethyl-4-pyridinio]thiomethyl-6-[(*R*)-1-hydroxyethyl]-1-methylcarbapen-2-em-3-carboxylate (4q) 4q: ^{1}H-NMR (200 MHz, D_2O, DHO as standard) δ: 1.05 (3H, d, J=7.0 Hz), 1.13 (3H, d, J=6.5 Hz), 3.10—3.30 (1H, m), 3.25 (1H, dd, J=2.8, 7.2 Hz), 3.65 (1H, d, J=14.8 Hz), 3.95 (1H, dd, J=2.8, 10 Hz), 4.00—4.20 (1H, m), 4.60—4.90 (3H, m), 4.61 (DHO), 6.50—6.60 (2H, m), 7.60—7.80 (4H, m), 8.10—8.20 (2H, m).

(1*S*,5*R*,6*S*)-2-(1,2-Dimethyl-4-pyridinio)thiomethyl-6-[(*R*)-1-hydroxyethyl]-1-methylcarbapen-2-em-3-carboxylate (17) 17: ^{1}H-NMR (200 MHz, D_2O, DHO as standard) δ: 0.96 (3H, d, J=7.4 Hz), 1.07 (3H, d, J=6.3 Hz), 2.45 (3H, s), 3.00—3.30 (1H, m), 3.22 (1H, dd, J=3.2, 5.2 Hz), 3.60 (1H, d, J=15 Hz), 3.86 (1H, dd, J=3.2, 9 Hz), 4.01 (1H, quintet, J=6.4 Hz), 4.61 (DHO), 4.88 (1H, d, J=15 Hz), 7.30—7.50 (2H, m), 8.10 (1H, d, J=6.8 Hz).

(1*S*,5*R*,6*S*)-2-(2-Dimethylcarbamoyl-1-methyl-4-pyridinio)thiomethyl-6-[(*R*)-1-hydroxyethyl]-1-methylcarbapen-2-em-3-carboxylate (18) 18: ^{1}H-NMR (200 MHz, D_2O, DHO as standard) δ: 0.97 (3H, d, J=7.2 Hz), 1.06 (3H, d, J=6.2 Hz), 2.79 (3H, s), 2.98 (3H, s), 3.00—3.30 (1H, m), 3.21 (1H, dd, J=2.8, 6.1 Hz), 3.68 (1H, d, J=15 Hz), 3.50—3.70 (1H, m), 3.87 (3H, s), 4.00 (1H, quintet, J=6.1 Hz), 4.61 (DHO), 4.99 (1H, d, J=15 Hz), 7.60—7.80 (2H, m), 8.26 (1H, d, J=6.8 Hz).

(1*S*,5*R*,6*S*)-6-[(*R*)-1-Hydroxyethyl]-2-(2-imino-1-methyl-1,2-dihydropyridin-4-yl)thiomethyl-1-methylcarbapen-2-em-3-carboxylate (19) 19: ^{1}H-NMR (200 MHz, D_2O, DHO as standard) δ: 0.94 (3H, d, J=7.2 Hz), 1.06 (3H, d, J=6.4 Hz), 3.00—3.30 (1H, m), 3.20 (1H, dd, J=2.9, 6.2 Hz), 3.48 (1H, d, J=14.8 Hz), 3.49 (3H, s), 3.87 (1H, dd, J=2.9, 9 Hz), 3.98 (1H, quintet, J=6.4 Hz), 4.61 (DHO), 4.70 (1H, d, J=14.8 Hz), 6.50—6.60 (2H, m), 7.42 (1H, d, J=7.7 Hz).

(1*S*,5*R*,6*S*)-2-(2,3-Cyclopenteno-1-methyl-4-pyridinio)thiomethyl-6-[(*R*)-1-hydroxyethyl]-1-methylcarbapen-2-em-3-carboxylate (23) 23: ^{1}H-NMR (200 MHz, D_2O) δ: 1.58 (3H, d, J=7.2 Hz), 1.72 (3H, d, J=6.4 Hz), 2.65—2.90 (2H, m), 3.40—3.55 (2H, m), 3.60—3.90 (4H, m), 4.20—4.50 (2H, m), 4.25 and 5.30 (2H, ABq, J=14 Hz), 4.51 (3H, s), 8.00 (1H, d, J=7 Hz), 8.68 (1H, d, J=7 Hz). MS (SIMS, glycerol) *m/z*: 389 $(M+H)^+$, 427 $(M+K)^+$.

(1*S*,5*R*,6*S*)-2-(1-Carbamoylmethyl-2,3-cyclopenteno-4-pyridinio)thiomethyl-6-[(*R*)-1-hydroxyethyl]-1-methylcarbapen-2-em-3-carboxylate (24) 24: ^{1}H-NMR (200 MHz, D_2O) δ: 0.98 (3H, d, J=7.4 Hz), 1.08 (3H, d, J=6.4 Hz), 2.12—2.20 (2H, m), 2.80—3.06 (4H, m), 3.22 (1H, dd, J=2, 6 Hz), 3.10—3.20 (1H, m), 3.70 and 4.92 (2H, ABq, J=14.6 Hz), 3.90 (1H, dd, J=2, 9 Hz), 4.00—4.10 (1H, m), 5.04 (2H, s), 7.40 (1H, d, J=6.6 Hz), 8.02 (1H, d, J=8.6 Hz).

(1*S*,5*R*,6*S*)-2-(1,9-Ethano-1,2,3,4-tetrahydroquinolizino-8-yl)thiomethyl-6-[(*R*)-1-hydroxyethyl]-1-methylcarbapen-2-em-3-carboxylate (25) 25: ^{1}H-NMR (200 MHz, D_2O) δ: 1.07 (3H, d, J=7.2 Hz), 1.12 (3H, d, J=6.4 Hz), 3.25—3.31 (1H, m), 3.45 (1H, dd, J=2, 6 Hz), 3.90 and 5.05 (2H, ABq, J=14 Hz), 4.00—4.18 (2H, m), 4.70 (2H, s), 6.80—8.50 (7H, m).

1,9-Ethano-6,7,8,9-tetrahydro-2-thioxo-2*H*-quinolizine (13) To a solution of 4-chloro-2,3-cyclopentenopyridine (614 mg, 4 mmol) in THF (4 ml), *n*-butyllithium (1.6 N, 2.75 ml, 4.4 mmol) was added dropwise at −78 °C, and after stirring for 10 min, hexamethyl phosphoric triamide (HMPA, 0.6 ml) was added. To the resulting mixture, 3-iodopropanol 2-tetrahydropyranyl (THP) ether (1.134 g, 4.2 mmol) in THF (2 ml) was added dropwise and the temperature was allowed to rise to 25 °C over a 1 h period. The mixture was poured into water and extracted with EtOAc. The organic layer was washed with water and dried over $MgSO_4$. The extracts was condensed and purified by chromatography (hexane–EtOAc 2 : 1) to give **11** (781 mg, 66%) as an oil. ^{1}H-NMR ($CDCl_3$) δ: 1.40—2.50

(12H, m), 2.80—3.10 (2H, m), 3.10—3.30 (1H, m), 3.40—3.60 (2H, m), 3.70—3.90 (2H, m), 4.50—4.60 (1H, m), 7.05 (1H, d, $J=5.4$ Hz), 8.25 (1H, d, $J=5.4$ Hz). *p*-Toluenesulfonic acid monohydrate (796 mg, 4.19 mmol) was added to a solution of **11** (739 mg, 3.49 mmol) in MeOH (10 ml). After stirring for 20 min, the mixture was poured into aqueous $NaHCO_3$ and extracted with EtOAc. The organic layer was washed with water, dried, and concentrated. The residue was chromatographed (EtOAc as eluent) to give an alcohol (432 mg, 58%). ^{1}H-NMR (200 MHz, $CDCl_3$) δ: 1.50—2.20 (5H, m), 2.30—2.50 (1H, m), 2.80—3.30 (3H, m), 3.71 (2H, t, $J=7.1$ Hz), 7.08 (1H, d, $J=5.4$ Hz), 8.24 (1H, d, $J=5.4$ Hz). Trifluoromethanesulfonic anhydride (0.293 ml, 1.74 mmol) was added dropwise to a solution of the above alcohol (351 mg, 1.66 mmol) and diisopropylethylamine (0.346 ml, 1.99 mmol) in CH_2Cl_2 (5 ml) at -78 °C. The temperature was raised to 25 °C and then refluxed for 1 h. The mixture was condensed under reduced pressure to give the pyridinium salt **12** as a yellow oil. ^{1}H-NMR (200 MHz, $CDCl_3$) δ: 1.20—3.90 (9H, m), 4.50—5.30 (2H, m), 7.65 (1H, d, $J=6.6$ Hz), 8.46 (1H, d, $J=6.6$ Hz). To the solution of the salt **12** in EtOH (7 ml), sodium hydrosulfide (531 mg) in water (3 ml) was added under ice cooling and then stirred for 30 min at room temperature. The resulting solution was extracted with $CHCl_3$, washed with water, dried and chromatographed to give **13** a yellow oil which was then triturated with ether to make a pale yellow solid (280 mg, 88%). ^{1}H-NMR (200 MHz, $CDCl_3$) δ: 1.40—2.50 (7H, m), 2.60—2.80 (1H, m), 2.80—3.20 (2H, m), 3.70—4.20 (2H, m), 7.03 (1H, d, $J=6.9$ Hz), 7.30 (1H, d, $J=6.9$ Hz).

Determination of MICs MICs were determined by the agar dilution method using sensitivity test agar (Eiken, Japan). An overnight culture of bacteria in tryptosoy broth (Eiken, Japan) was diluted to about 10^6 cells/ml with the same broth and inoculated with an inoculating device onto agar containing serial twofold dilutions of the test compounds. Organisms were incubated at 37 °C for 18—20 h. The MIC of a compound was defined as the lowest concentration that visibly inhibited growth.

***In Vivo* Activity (Determination of 50% Effective Doses (ED_{50}) Values)** Five-week-old male strain ICR mice weighing 19 to 23 g, in groups of 5—10 mice, were injected intraperitoneally with 10 to 100 times the 50% lethal dose of bacteria, which was suspended in heart infusion broth (HIB) or HIB containing 5% gastric mucin. The compounds were administered 1 and 5 h after infection. The ED_{50} (in milligram per killogram) were determined by the Probit method using survival rates at 7 days post-infection, and were expressed as a single dose.

Stability Test The kidneys were dissected out and each tissue homogenate was prepared at 10% final concentration with a phosphate buffer solution (pH 7.0, 0.1 M). A mixture of 0.1 mg of the test compound and 1 ml of tissue homogenate was incubated at 37 °C. Aliquots were collected at intervals, and after centrifugation the supernatant was subjected to bioassay.

Acknowledgment We wish to thank the following scientists for their contributions to this work: Dr. M. Shiro (X-ray analysis), Dr. Y. Nakagawa (mass spectroscopy), Mr. H. Nakashimizu (stability test) and Mr. K. Motokawa (*in vitro* activity assay).

References and Notes

1) Carbapenem and Penem Antibiotics. VI. M. Imuta, H. Itani, H. Ona, Y. Hamada, S. Uyeo and T. Yoshida, *Chem, Phem. Bull.*, **39**, 663 (1991).
2) For a review, see R. W. Ratcliffe and G. Albers-Schönberg, "Chemistry and Biology of β-Lactam Antibiotics," Vol. 2, ed. by R. B. Morin and M. Gorman, Academic Press, Inc., New York, 1982, p. 227.
3) G. Franceschi, M. Foglio, M. Alpegiani, C. Battistini, A. Bedeschi, E. Perrone, F. Zarini and F. Alcamone, *J. Antibiot.*, **36**, 938 (1983); G. Franceschi, M. Alpegiani, A. Bedeschi, M. Fuglio and E. Perrone, *ibid.*, **37**, 685 (1984).
4) L. Verbist and J. Verhanegen, *Antimicrob. Agents Chemother.*, **17**, 807 (1980).
5) J. R. Prous, *Drugs Future*, **9**, 242 (1984).
6) C. U. Kim, P. F. Misco, B. Y. Luh and M. J. M. Hitchcock, *J. Antibiot.*, **40**, 1707 (1987); C. U. Kim, B. Y. Luh, P. F. Misco and M. J. M. Hitchcock, *J. Med. Chem.*, **32**, 601 (1989).
7) F. Badea, "Reaction Mechanism in Organic Chemistry," Abacus Press, England, **1977**, p. 187.
8) O. Mitsunobu, *Synthesis*, **1981**, 1.
9) I. Nakagawa, K. Aki and T. Hata, *J. Chem. Soc., Perkin Trans. 1*, **1983**, 1315.
10) T. Ohtani, F. Watanabe and M. Narisada, *J. Org. Chem.*, **49**, 5271 (1984).
11) S. Shibahara, T. Okonogi, T. Yoshida, Y. Murai, T. Kudo, S. Inouye and S. Kondo, *J. Antibiot.*, **43**, 62 (1990).
12) For conversion of allylic alcohol to halides *via* allylic phosphates, see S. Araki, K. Ohmori and Y. Butsugan, *Synthesis*, **1984**, 841.
13) M. J. Basker, R. A. Edmondson, S. J. Knott, R. J. Ponsford, B. Slocombe and S. J. White, *Antimicrob. Agents Chemother.*, **26**, 734 (1984); W. Mandell and H. C. Neu, *ibid.*, **29**, 769 (1986); N. Ohi, B. Aoki, K. Moro, T. Kuroki, N. Sugimura, T. Noto, T. Nehashi, M. Matsumoto, H. Okazaki and I. Matsunaga, *J. Antibiot.*, **39**, 242 (1986).
14) H. Mochizuki, Y. Oikawa, H. Yamada, S. Kusakabe, T. Shihara, K. Murakami, K. Kato, J. Ishiguro and H. Kosuzume, *J. Antibiot.*, **41**, 377 (1988).
15) For classification of L-MRSA and H-MRSA, see K. Murakami, K. Nomura, M. Doi and T. Yoshida, *Antimicrob. Agents Chemother.*, **31**, 1307 (1987).

Design, Synthesis and Antiinflammatory Activity of a New Indomethacin Ester. 2-[*N*-[3-{3-(Piperidinomethyl)phenoxy}propyl]carbamoylmethylthio]ethyl 1-(*p*-Chlorobenzoyl)-5-methoxy-2-methylindole-3-acetate

Ikuo UEDA,*[a] Katsuyuki ISHII,[a] Heihachiro ARAI,[b] Shin-ichi IKEDA,[b] Yuji HITOMI[b] and Minoru HATANAKA[a]

The Institute of Scientific and Industrial Research, Osaka University,[a] Iḅaraki, Osaka 567, Japan and Central Research Laboratories, Zeria Pharmaceutical Co., Ltd.,[b] 2512–1, Oshikiri, Konan-machi, Osato-gun, Saitama 360–01, Japan. *Received August 8, 1990*

A novel indomethacin ester prodrug, 2-[*N*-[3-{3-(piperidinomethyl)phenoxy}propyl]carbamoylmethylthio]ethyl 1-(*p*-chlorobenzoyl)-5-methoxy-2-methylindole-3-acetate (1) was prepared from a new histamine H_2-receptor antagonist, *N*-[3-{3-(piperidinomethyl)phenoxy}propyl]-2-(2-hydroxyethylthio)acetamide (2) and indomethacin (3). The compound 1 was shown to be essentially similar to 3 in its antiinflammatory action and to almost completely inhibit carrageenin-induced hind-paw edema in the rat at a very high dose of 230 mg/kg (280 μmol/kg), which is comparable to that of 100 mg/kg (280 μmol/kg) of 3, without producing gastric lesions. On a molar basis, the acute gastric lesioning properties of 1 were near one-hundred times less than those of 3, resulting in over a twenty-fold improvement in the ratio of antiedema activity to ulcerogenicity. The effect of the co-administration of histamine H_2-receptor antagonists on antiedema activity and ulcerogenicity caused by 3 is also discussed.

Keywords indomethacin; ester prodrug; antiinflammatory activity; ulcerogenicity; histamine H_2-receptor antagonist; 2-[*N*-[3-{3-(piperidinomethyl)phenoxy}propyl]carbamoylmethylthio]ethyl 1-(*p*-chlorobenzoyl)-5-methoxy-2-methylindole-3-acetate

New nonsteroidal antiinflammatory drugs are needed for effective therapy in arthritic diseases in the absence of undesirable gastrointestinal side-effects. Indomethacin (**3**) is one of the most useful of the antirheumatic drugs but has the disadvantage typical of these agents, *i.e.*, that it may cause gastrointestinal ulceration and hemorrhage. Many attempts have been made to develop derivatives which would yield adequate antiinflammatory potency after oral administration without adversely affecting gastric mucosa.[1] In this paper, a novel approach to this problem is described, in which an antiinflammatory agent is administered as part of a histamine H_2-receptor antagonist. We report here design, synthesis and antiinflammatory activity of a new indomethacin ester prodrug, 2-[*N*-[3-{3-(piperidinomethyl)phenoxy}propyl]carbamoylmethylthio]ethyl 1-(*p*-chlorobenzoyl)-5-methoxy-2-methylindole-3-acetate (**1**). Additionally, the effect of the co-administration of histamine H_2-receptor antagonists on acute antiinflammatory activity and ulcerogenicity after the oral administration of **3** is described.

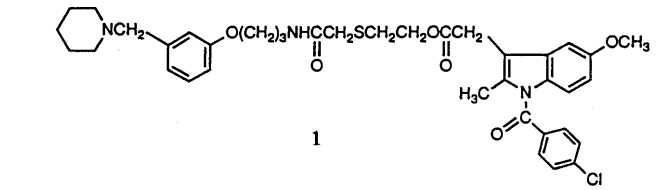

1

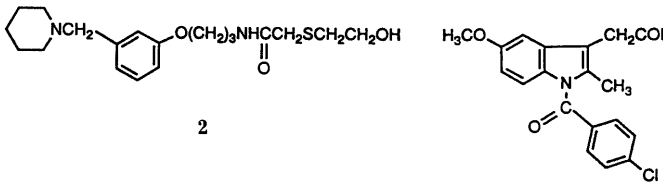

2

3 : R=OH, indomethacin
4 : R=Cl

Target Design Aspirin-like antiinflammatory drugs, which inhibit the synthesis of prostaglandins, prevent the formation of prostaglandins in the stomach and do not allow the normally-occurring prostaglandins' control mechanism to arrest secretions induced by increased levels of adenosine 3′,5′-cyclic monophosphate (cyclic AMP) or by vagal or histamine stimulation.[2] Vane postulated that continual synthesis of prostaglandins was necessary for the maintenance and integrity of the gastric mucosa.[3] Bommelaer *et al.* reported that both prostaglandins and cimetidine (**5**) protected against barrier disruption by aspirin and this might be a factor in the mechanism of their cytoprotective action.[4] Recently, it was reported in the patent literature that the formation of gastric lesions by aspirin-like antiinflammatory drugs was inhibited by the co-administration of a histamine H_2-receptor antagonist.[5]

Our approach toward the development of a drug which does not produce gastric lesions was to synthesize an ester prodrug prepared from **3** and a histamine H_2-receptor antagonist. First *N*-[3-{3-(piperidinomethyl)phenoxy}-propyl]-2-(2-hydroxyethylthio)acetamide (**2**),[6] which was shown to possess potential histamine H_2-receptor antagonist activity combined with cytoprotective activity, was selected as an ester function. As one of its features, compound **2** has a hydroxy function for preparing an ester prodrug. Compound **1** is prepared by the reaction of 1-(*p*-chlorobenzoyl)-5-methoxy-2-methylindole-3-acetyl chloride (**4**)[1b] with **2**. Compound **1** corresponds to one of the *O*-acyl derivatives of **2** which may fall into an ester prodrug and retain the original pharmacological properties of **2** itself. On the other hand, compound **1** is a typical indomethacin ester prodrug and is converted into **3** by enzymatic hydrolysis in an animal body, yielding **2**. From the standpoint of pharmacological properties, **1** may result in the improvement of the primary unwanted effect, which is direct gastric lesions due to contact of solid **3** (or of concentrated solutions of **3**) with the gastric mucosa. As **3** is administered as part of an ester prodrug of the histamine H_2-receptor antagonist, gastric lesions produced by **3** could be cured by both the ester prodrug **1** itself and the histamine H_2-receptor antagonist **2** produced by enzymatic hydrolysis of **1** in the animal body.

Chemistry Crude compound **1** was obtained as an oily

material by the reaction of **2** with **4** in the presence of pyridine in dry acetonitrile. The oil was treated with oxalic acid dihydrate to give oxalate dihydrate of **1** as crystals. The oxalate was treated with $NaHCO_3$ aqueous solution to give free base **1** as a crystalline material. The over-all yield of the crystalline free base **1** was 59% from **2**. Crystalline free base **1** was treated with maleic acid in a mixture of C_6H_6 and Et_2O to give maleate of **1** as an amorphous powder. Compound **1** and its salts were characterized by proton nuclear magnetic resonance (^{1}H-NMR), infrared (IR) and mass (MS) spectra and elemental analysis.

Biological Screening Methods Compound **1** was used as its maleate for biological screening tests. Two kinds of carrageenins were employed for rat carrageenin-induced hind-paw edema tests. This caused a difference in control values between the results shown in Tables I and II and results shown in Table III.

Antiedema Activity and Ulcerogenicity (1) Rat Carrageenin-Induced Hind-Paw Edema Test Compounds **1** and **3** were screened for acute antiinflammatory activity in the carrageenin-induced rat hind-paw edema assay, using a modification of the method described by Winter *et al.*[7] The compounds were administered orally 1 h prior to the carrageenin injection. Swellings were measured at 1 h intervals for 5 h after the carrageenin injection. The ED_{50} value of each compound represents micromole per kilogram (μmol/kg). The rats used for this test were killed 6 h after the carrageenin injection and the stomachs were separated for gastric ulcerogenicity studies.

(2) Gastric Ulcerogenicity Study in the Rat Compounds **1** and **3** were tested in the rats under two experimental conditions.

Experiment 1: The rats were killed 5 h after the oral administration of the test compound at the specified dose. All lesions on the gastric mucosa, regardless of size, were counted by visual examination under 8 × magnification. The ulcer index and ulcer incidence were calculated.

Experiment 2: The rats used for the antiedema test were used for the gastric ulcerogenicity study according to the procedure described in experiment 1.

(3) Gastric Acid Antisecretory Activity in the Rat Gastric acid antisecretory activity was evaluated in the conscious rat with fistula according to the procedure described in the previous paper.[6]

(4) Determination of Plasma Levels of 3 The plasma levels of free acid **3** following the oral administration of **1** and **3** itself as a reference compound were compared in the rats. Free acid **3** in plasma was measured by the procedure described in the literature, using high pressure liquid chromatography.[8]

Results and Discussion

The effects of the co-administration of **2** and reference compounds, cimetidine (**5**), ranitidine (**6**) and famotidine (**7**) on the antiedema activity and ulcerogenicity caused by **3** were estimated. The results are shown in Table I. The antiedema potency of **3** with the co-administration of **2** was less than that of **3** itself. The co-administration of **5** exhibited also reduced antiedema activity when compared to that of **3** without the co-administration of **5**. The co-administrations of **6** and **7** retained the activity which were comparable to that of **3** itself. The data on the ulcer indices and ulcer incidences showed that gastric lesions produced by **3** were improved by the co-administration of the histamine H_2-receptor antagonist as described in the patent literature.[5] The effect of **7**, in the dose range of 0.1 to 10 equimolars to **3**, on acute gastric mucosal lesions due to **3** is shown in Fig. 1. Control animals had an ulcer index of 0.62 ± 0.27. Doses of **7** significantly reduced lesion formation; the ulcer index was 0.24 ± 0.16, 0.08 ± 0.04 and 0.16 ± 0.08 with the co-administration of **7** at the 0.1, 1.0 and 10 equimolar doses, respectively. The results may provide evidence that the co-administration of a histamine

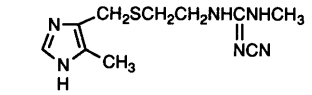

cimetidine (**5**)

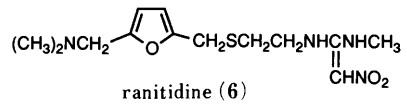

ranitidine (**6**)

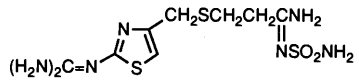

famotidine (**7**)

histamine H_2-receptor antagonist

TABLE I. Effect of Co-administration of Histamine H_2-Receptor Antagonists **2**, **5**, **6** and **7** on Acute Antiinflammatory Activity of **3** in the Carrageenin-Induced Hind-Paw Edema and Ulcerogenicity Caused by **3** in Rats

Compd. No.	Dose μmol/kg *p.o.*	Number of animals	Antiedema action (change in hind-paw volume due to swelling (% inhibition)[b]; time (h) after the carrageenin injection)		Ulcerogenic action[a] (acute gastric lesion at 6 h after the carrageenin injection)	
			2	4	Ulcer index	Ulcer incidence/total
3+**2**	8.4+8.4	10	47.5 ± 4.8[c] (26.4)	53.8 ± 4.6[c] (27.1)	0.19 ± 0.06[c]	4/10[c]
3+**5**	8.4+8.4	10	41.4 ± 5.8[d] (35.8)	49.6 ± 6.5[d] (32.8)	0.27 ± 0.17[c]	4/10[c]
3+**6**	8.4+8.4	10	32.6 ± 6.0[d] (49.5)	43.1 ± 4.3[d] (41.6)	0.54 ± 0.23[d]	5/10[d]
3+**7**	8.4+8.4	10	34.3 ± 5.3[d] (46.8)	42.8 ± 3.3[d] (42.0)	0.08 ± 0.04	3/10
3 only	8.4	10	32.6 ± 5.5[d] (49.5)	35.9 ± 2.8[d] (51.4)	0.62 ± 0.27[d]	6/10[d]
Control	—	10	67.0 ± 4.3	83.9 ± 5.2	0.00 ± 0.00	0/10

a) This was carried out under conditions described in experiment 2. *b*) ( ); % inhibition was calculated as follows: $\frac{\text{(control volume)} - \text{(change in hind-paw volume)}}{\text{(control volume)}} \times 100$.

c) $p < 0.05$, *d*) $p < 0.01$ (*t*-test comparing group mean with control group mean).

TABLE II. Antiedema Activity and Ulcergenicity Caused by **1**, **3** with Co-administration of **2** and **3** Itself

Comp. No.	Dose μmol/kg *p.o.*	Number of animals	Antiedema action (change in hind-paw volume due to swelling (% inhibition)[b]; time (h) after the carrageenin injection)			Ulcerogenic action[a] (acute gastric lesion at 6 h after the carrageenin injection)		
			2	4	ED_{50} μmol/kg	Ulcer index	Ulcer incidence /total	UD_{50} μmol/kg
1	8.4	10	52.1±6.7 (20.5)	75.1±5.5 (10.0)	42.5	0.00±0.00	0/10	>669
	28	10	32.8±4.3[d] (49.9)	44.9±4.5[d] (46.2)		0.02±0.02	1/10	
	84	10	39.7±5.8[d] (39.4)	43.6±7.6[d] (47.7)		0.03±0.02	2/10	
3+**2**	2.3+ 2.3	10	53.6±5.7[d] (18.2)	74.1±6.6[d] (11.2)	19.6	0.03±0.02	2/10	27.9
	8.4+ 8.4	10	29.0±3.9[d] (55.7)	44.9±5.5[d] (46.2)		0.10±0.05[d]	4/10[d]	
	28 +28	10	20.0±1.9[d] (69.5)	26.7±3.0[d] (68.0)		0.21±0.07[d]	6/10[d]	
3 only	8.4	10	37.4±4.1[d] (42.9)	47.5±4.7[d] (41.1)	23.4	0.17±0.06[d]	5/10[d]	5.85
	28	10	26.3±3.9[d] (55.9)	36.4±4.0[d] (56.4)		2.90±1.51[d]	10/10[d]	
Control		10	65.5±5.1	83.4±4.00		0.00±0.00	0/10	

a) This was carried out under conditions described in experiment 2. *b*) ( ); % inhibition was calculated as follows: $\frac{(\text{control volume}) - (\text{change in hind-paw volume})}{(\text{control volume})} \times 100$.
c) $p<0.05$, *d*) $p<0.01$ (*t*-test comparing group mean with control group mean).

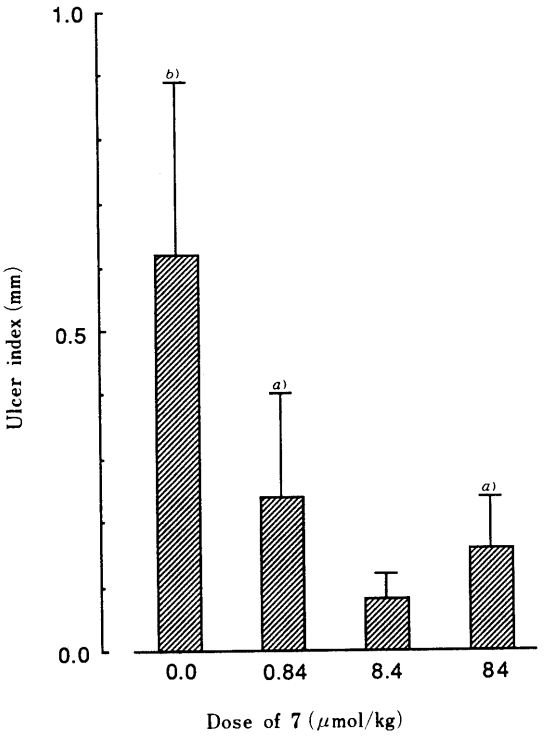

Fig. 1. Effect of Co-Administration of **7** on Ulcergenicity Caused by the 8.4 μmol/kg Dose of **3**

The vertical bars represent the mean value of ten animals. *a*) $p<0.05$, *b*) $p<0.01$ (*t*-test comparing group mean with control group mean).

H_2-receptor antagonist at approximately an equimolar dose to **3** effectively inhibits gastric lesions produced by **3**.

The effect of **2** on the antiedema activity and reduced ulcerogenicity of **3** were estimated. As seen in Table II, the ED_{50} values of **1**, **3** with the co-administration of **2** and **3** itself in the antiedema activity were 42.5, 19.6 and 23.4 μmol/kg, respectively. Compound **2** showed a tendency to enhance the potency of **3** in the antiedema activity. The potency of **1**, in terms of its ED_{50} value, was about one-third that of **3** with the co-administration of **2** and about one-half that of **3** itself. The UD_{50} values of **1**, **3** with the co-administration of **2** and **3** itself were over 669, 27.9 and 5.85 μmol/kg, respectively. These findings suggest

TABLE III. Effect of **1** and **3** on Carrageenin-Induced Hind-Paw Edema in Rats

Compd. No.	Dose μmol/kg *p.o.*	Number of animals	Antiedema action		
			Change in hind-paw volume due to swelling	Antiedema incidence /total	ED_{50} μmol/kg
1	8.4	10	191.90± 7.06[b]	0/10	28.0
	28	10	145.72±20.18[b]	5/10[b]	(13.3—59.0)
	84	10	84.87± 9.10[b]	9/10[b]	
	280	10	73.16± 6.29[b]	10/10[b]	
3	2.8	10	184.53±12.20[a]	1/10	
	8.4	10	126.57±12.47[b]	6/10[b]	8.10
	28	10	110.97± 6.09[b]	9/10[b]	(3.63—17.6)
	84	10	118.37±10.92[b]	6/10[b]	
Control	—	10	222.36± 6.30	0/10	—

a) $p<0.05$, *b*) $p<0.01$ (*t*-test comparing group mean with control group mean).

TABLE IV. Ulcerogenic Action of **1** and **3** in Rats

Compd. No.	Dose μmol/kg *p.o.*	Number of animals	Ulcerogenic action[a] (acute gastric lesion at 5 h after the administration of the drugs)		
			Ulcer index	Ulcer incidence /total	UD_{50} μmol/kg
1	84	10	0.0± 0.00	0/10	
	280	10	0.0± 0.00	0/10	>839
	560	10	0.0± 0.00	0/10	
	840	10	0.0± 0.00	0/10	
3	2.8	10	0.7± 0.47	2/10	
	14	10	17.4± 5.33[b]	6/10[b]	12.6
	28	10	46.5±15.00[b]	7/10[b]	(5.59—29.1)
	56	10	52.8±17.47[b]	7/10[b]	
	84	10	62.1±16.51[b]	8/10[b]	
Control	—	10	0.0± 0.00	0/10	—

a) This was carried out under conditions described in experiment 1.
b) $p<0.01$ (*t*-test comparing group mean with control group mean).

that compound **1** has a much better safety ratio whichever index is taken (difference between antiinflammatory activities and gastrodamaging effects or LD_{50}-activity ratio), compared to the co-administration of **2**. Alternative study

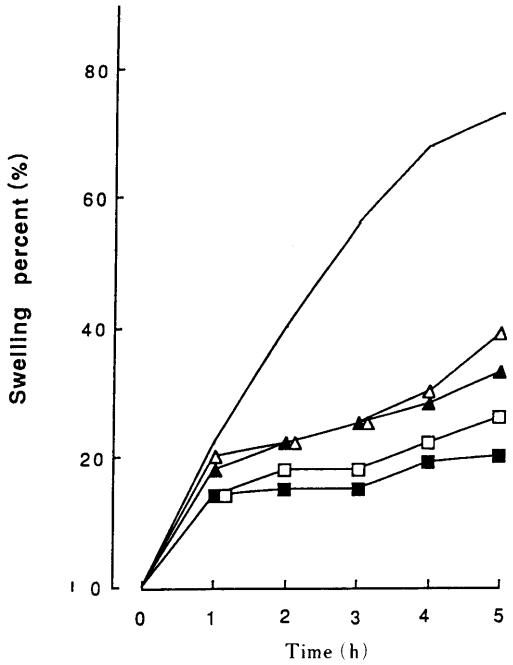

Fig. 2. Effects of **1** and **3** on Antiedema Activity in Carrageenin-Induced Hind-Paw Edema in Rats

—, control; —□—, 84 μmol/kg dose of **1**; —■—, 280 μmol/kg dose of **1**; —▲—, 28 μmol/kg dose of **3**; —△—, 84 μmol/kg dose of **3**. Data indicate the mean value of ten animals. All values were statistically significant ($p<0.01$) when compared with the control group mean.

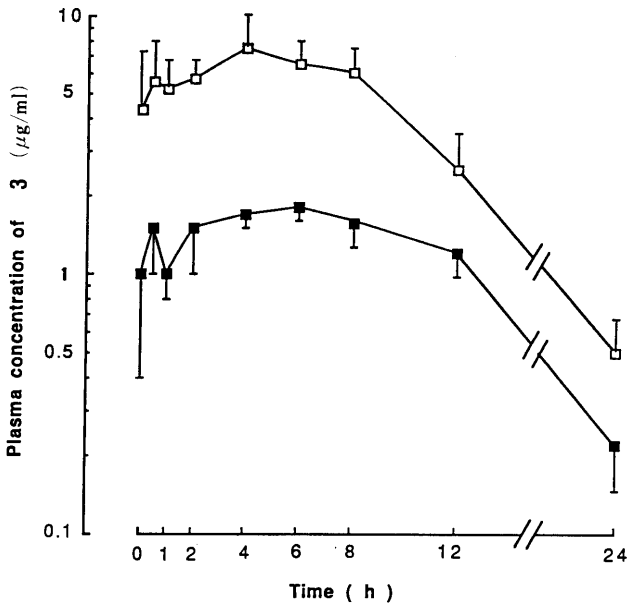

Fig. 3. Plasma Levels of **3** Following Oral Administration of **1** and **3** Itself

The animals received 5.3 μmol/kg of the drugs. The values represent the mean ± S.E. for five male rats at each time interval. —■—, **3** in plasma levels after dosing **1**; —□—, **3** in plasma levels after dosing **3** itself.

on the antiedema activity and ulcerogenic action of **1** was carried out. The results were shown in Tables III and IV. Table III shows the potency of **1**, in terms of its ED_{50} value, in reducing the carrageenin-induced edema. The ED_{50} values for **1** and **3** were 28.0 and 8.10 μmol/kg, respectively. Compound **3** was more effective than **1**. As seen in Table IV, compound **3** showed toxic effects at near dose levels which were active on experimental inflammation, whereas compound **1** did not show toxic effects at a very high dose of 840 μmol/kg. Thus, the antiinflammatory dose range of **1** was shown to be very much lower than the toxic range. As depicted in Fig. 2, compound **1** almost completely inhibited the edema 5 h after the administration of **1** at a very high dose of 230 mg/kg (280 μmol/kg), which was comparable to that of 100 mg/kg (280 μmol/kg) of **3**, without producing acute gastric lesions in the rats. The low toxicity of **1** may cause dose-related reduction in carrageenin-induced hind-paw edema in the rats. On a mole basis, the acute gastric lesioning properties of **1** were near one-hundred times less than those of **3**. Calculating the therapeutic index (UD_{50}/ED_{50}) of **1** gave a value of 30 for **1**, compared to 1.6 for **3**, based on the data shown in Tables III and IV. On the other hand, the therapeutic index of **1** calculated from the data shown in Table II was a value of 16 for **1**, compared to 0.25 for **3**. These values may represent a considerably high improvement (over a twenty-fold improvement) in the therapeutic index of **3** based on the acute antiinflammatory activity and ulcerogenicity.

The plasma levels of free acid **3** following the oral administrations of **1** and **3** itself were compared in rats. The compounds were administered at a dose of 5.3 μmol/kg. As seen in Fig. 3, free acid **3** in plasma from **1** and **3** itself reached the highest level (C_{max}) at 6 h for **1** and at 4 h for **3** after the administration of the drugs. The peak levels of free acid **3** from **1** was lower than the peak levels of free acid **3** after the administration of **3** itself. The value of the area under curve (AUC) of each compound was calculated as 27.7 μg·h/ml for **1** and 88.0 μg·h/ml for **3** itself, respectively. On comparing AUC values after dosing 5.3 μmol/kg of the drugs, the plasma levels after dosing **1** was approximately 30% that after dosing **3** itself. These data are compatible with the results on the antiedema activities of **1** and **3** as shown in Table III. These results indicate that the antiinflammatory action of **1** was probably due to the conversion of **1** to **3**. And compound **1** was presumed to produce a systemic antiinflammatory activity qualitatively similar to that of **3**.

Additionally, compound **1** was found to inhibit histamine-stimulated gastric acid secretion in the conscious rats with gastric fistula. The ED_{50} value of **1** was calculated as 26.8 μmol/kg, comparable to that of **2** as 26.5 μmol/kg.[6] From the comparison of each ED_{50} value of **1** for both the antiedema and gastric acid antisecretory activities with the UD_{50} value of **1** in the rat model, compound **1** may be a novel antiinflammatory drug which does not induce gastric hemorrhagic lesions at effective antiinflammatory and antiulcer doses with high safety.

Conclusion

The development of edema in the paw of the rat after carrageenin injection has been described as a biphase event. The initial phase of the edema has been attributed to the release of histamine and serotonin, the edema maintenance during the plateau phase to kinin-like substances, and the second phase of swelling to the release of prostaglandin-like substances.[9] Compound **1** was shown to inhibit gastric acid secretion stimulated by the histamine produced at the initial phase of edema. Although the antiinflammatory activity of **1** is probably related to **3** which inhibits the synthesis of

prostaglandins at the second phase of edema, the anti-inflammatory dose range of **1** was very wide and much lower than the toxic dose range. Compound **1** may accelate the healing of gastric lesions and prevent their formation along with the action of **2**. The effect of **1** on the gastrointestinal tract is now under study. Here we want only to point out the utility of **2** as a new type of ester function in ester prodrugs and lack of the gastric-stimulant activity of **1**. The antiinflammatory properties of **1** will be reported elsewhere in detail in the near future. At the present time, pharmacological and biological studies of **1** have been continued in order to confirm the clinical usefulness of **1** as an antiinflammatory agent.

Experimental

Melting points were measured in a Gallenkamp melting point apparatus and are uncorrected. IR spectra were recorded on a Hitachi 260-10 Model infrared spectrophotometer and ^{1}H-NMR spectra were measured on a Hitachi R-90H (90 MHz) spectrometer. MS spectra were obtained on a JMS-DX 300 spectrometer operating at an ionization potential of 70 eV. All spectra were consistent with the assigned structures. Combustion analyses were performed on a Perkin-Elmer Model 240C elemental analyzer and were within $\pm 0.4\%$ of the theoretical values.

Chemistry Compound **2** was prepared by the method described in the literature.[6] Indomethacin (**3**), cimetidine (**5**), ranitidine (**6**), and famotidine (**7**) were commercially available.

1-(*p*-Chlorobenzoyl)-5-methoxy-2-methylindole-3-acetyl Chloride (4) Compound **4** was prepared by the reaction of **3** with $SOCl_2$ according to the literature.[1b] Compound **4** (mp 125—126 °C; lit. 126—127 °C) was used for the following step without further purification.

2-[*N*-[3-{3-(Piperidinomethyl)phenoxy}propyl]carbamoylmethylthio]-ethyl 1-(*p*-chlorobenzoyl)-5-methoxy-2-methylindole-3-acetate (1) Compound **4** (5.70 g, 15.1 mmol) was added portionwise to a solution of **2** (5.13 g, 14.0 mmol) in 50 ml of dry acetonitrile under ice-water cooling. The resulting mixture was stirred at room temperature for 1 h. After removal of the solvent, the residue obtained was dissolved into 80 ml of CH_2Cl_2. The CH_2Cl_2 layer was washed with 50 ml of 3 N HCl, followed by saturated $NaHCO_3$ aqueous solution, and dried over $MgSO_4$. After removal of the solvent *in vacuo*, **1** was obtained as an oil. A solution of oxalic acid dihydrate (1.76 g) in 20 ml of acetonitrile was added to a solution of the oily material **1** in 65 ml of acetonitrile. The mixture was allowed to stand for 12 h at room temperature, giving a crystalline material, which was filtered and washed with a small amount of acetonitrile and dried *in vacuo* to give oxalate dihydrate of **1** (7.72 g, 66%), mp 102—103 °C. IR ν (KBr): 3290, 2800—2200, 1735, 1675, 1600 cm^{-1}. MS (EI) *m/z*: 705 (M^+). ^{1}H-NMR ($CDCl_3$) δ: 1.33—1.85 (2H, m, 2-CH_2 of piperidine), 1.94—2.03 (6H, br m, 3-CH_2 of piperidine and OCH_2-$\underline{CH_2}$-CH_2N), 2.36 (3H, s, CH_3), 2.58 (2H, br m, 2-CH_2 of piperidine), 2.82 (2H, t, J=6.5 Hz, SCH_2), 3.25 (2H, s, $COCH_2S$), 3.41—3.52 (2H, m, CH_2NH), 3.56—3.61 (2H, br m, 2-CH_2 of piperidine), 3.67 (2H, s, $COCH_2$), 3.83 (3H, s, OCH_3), 3.98 (2H, t, J=6.5 Hz, $ArOCH_2$), 4.12 (2H, s, $ArCH_2\overset{|}{N}^+$–), 4.28 (2H, t, J=6.5 Hz, CH_2O), 6.64—7.48 (8H, m, Ar-H), 7.47 (2H, d, J=8.4 Hz, 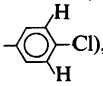), 7.66 (2H, d, J=8.4 Hz, ). *Anal.* Calcd for $C_{38}H_{44}ClN_3O_6S \cdot C_2H_2O_4 \cdot 2H_2O$: C, 57.72; H, 6.05; N, 5.05. Found: C, 57.95; H, 5.80; N, 4.87.

Free Base 1 from Oxalate Dihydrate A solution of oxalate dihydrate of **1** (12.2 g) in 150 ml of CH_2Cl_2 was washed with 5% $NaHCO_3$, dried over $MgSO_4$, filtered and evaporated to give an oil, which was dissolved into 60 ml of isopropyl ether (IPE) under heating. The resulting solution was allowed to stand at 5 °C for 12 h to give **1** (9.6 g, 89%) as crystalline powder: mp 81—83 °C. An analytical sample was obtained by recrystallization from IPE: mp 82—83 °C. IR ν (KBr): 3300, 1730, 1679 cm^{-1}. MS (EI) *m/z*: 705 (M^+). ^{1}H-NMR ($CDCl_3$) δ: 1.34—1.48 (2H, m, 4-CH_2 of piperidine), 1.36—1.61 (4H, m, 3-CH_2 of piperidine), 1.95—2.03 (2H, m, OCH_2-$\underline{CH_2}$-CH_2NH), 2.30—2.41 (4H, m, 2-CH_2 of piperidine), 2.37 (3H, s, CH_3), 2.77 (2H, t, S-$\underline{CH_2}$-CH_2O, J=6.4 Hz), 3.22 (2H, s, $COCH_2S$), 3.42 (2H, s, $ArCH_2N$), 3.42—3.50 (2H, m, CH_2-$\underline{CH_2}$-NH), 3.67 (2H, s, $COCH_2$), 3.83 (3H, s, OCH_3), 4.04 (2H, t, $ArOCH_2$, J=5.5 Hz), 4.26 (2H, t, SCH_2-$\underline{CH_2}$-O, J=6.4 Hz), 6.64—7.26 (8H, m, Ar-H), 7.46 (2H, d, J=8.4 Hz), 7.66 (2H, d, J=8.4 Hz). *Anal.* Calcd for $C_{38}H_{44}ClN_3O_6S$: C, 64.62; H, 6.28; N, 5.95. Found: C, 64.70; H, 6.36; N, 5.81.

Preparation of Maleate of 1 Saturated maleic acid in Et_2O solution was added to a solution of crystalline free base **1** (5.0 g, 7.1 mmol) in 300 ml of dry C_6H_6 until the precipitation of an oily material ceased. After removal of the solvent, the oil obtained was washed several times with dry Et_2O by decantation and dried under reduced pressure to give maleate **1** (4.1 g, 70%) as an amorphous powder. The maleate was used for biological screening tests. IR ν (neat): 3350, 2960, 2800—2300, 1730, 1670, 1590, 1460, 1350, 1318, 1261, 1220, 1162 cm^{-1}. ^{1}H-NMR ($CDCl_3$) δ: 1.38—1.51, 1.82—1.89 (1H and 5H, br, 3- and 4-CH_2 of piperidine), 1.95—1.99 (2H, m, OCH_2-$\underline{CH_2}$-CH_2N), 2.37 (3H, s, CH_3), 2.58—2.83 (2H, br, 2-CH_2 of piperidine), 2.81 (2H, t, J=6.0 Hz, SCH_2), 3.23 (2H, s, $COCH_2S$), 3.40—3.55 (4H, m, CH_2NH and 2-CH_2 of piperidine), 3.68 (2H, s, $COCH_2$), 3.83 (3H, s, OCH_3), 3.99 (2H, t, J=6.0 Hz, $ArOCH_2$), 4.09 (2H, s, $ArCH_2\overset{|}{N}^+$–), 4.28 (2H, t, J=6.0 Hz, CH_2O), 6.33 (2H, s, ), 6.63—7.31 (8H, m, Ar-H), 7.46 (2H, d, J=8.4 Hz), 7.66 (2H, d, J=8.4 Hz).

Determination of Free Acid 3 in Plasma Plasma levels of free acid **3** were determined according to the procedure described by H. B. Hucker *et al.*[8]

Biological Screening Methods Two kinds of carrageenins were employed for the rat carrageenin-induced hind-paw edema tests in this series. One, which was employed for the edema tests shown in Tables I and II, was purchased from Iwai Pharmaceutical Co., Ltd. The other, which was employed for the edema test shown in Table III, was purchased from Zushi Chemical Co., Ltd. This caused a difference in control values among the tests.

(1) Rat Carrageenin-Induced Hind-Paw Edema Test[7] The acute anti-inflammatory activity of **1** and **3** was determined by assay methods of carrageenin-induced hind-paw edema in the rat. Male rats weighing 133—155 g were arranged in groups of 10 and fasted 18 h. Inflammation was induced by a subcutaneous injection of 0.1 ml of 1% (w/v) carrageenin solution in 0.9% (w/v) saline into the right hind-paw. The compounds were administered orally 1 h prior to the carrageenin injection as a suspension in 0.5% (w/v) tragacanth. The volume of hind-paw was measured before the compound had been administered by a water displacement transducer. The swelling hind-paw volumes were measured every 1 to 5 h after the carrageenin injection. The effect of the compound was expressed as a percent increase in hind-paw volume due to swelling, as compared with the initial hind-paw volume. The results are summarized in Tables I, II and III.

The animals used for this test were killed 6 h after the carrageenin injection and the stomachs were separated and employed for the gastric ulcerogenicity study according to the procedure described in "Gastric Ulcerogenicity Study in the Rat."

(2) Gastric Ulcerogenicity Study in the Rat Gastric lesions were measured in male Wistar rats weighing 175—210 g.

Experiment 1: Rats were arranged in groups of 10 and fasted 18 h prior to experiments. The rats were killed 5 h after the administration of the compound. The stomachs were separated, everted and washed with tap water. All lesions on the gastric mucosa, regardless of size, were counted by visual examination under 8 × magnification. The UD_{50} value refers to the dose required to produce a 50% ulcerogenic response on an incidence. The results are summarized in Tables I and II with those of antiedema activity.

Experiment 2: The rats which were used for "Rat Carrageenin-Induced Hind-Paw Edema Test" were employed for this study. The ulcerogenicity was estimated according to the procedure described in Experiment 1. The results are summarized in Table IV.

(3) Gastric Acid Antisecretory Activity The gastric acid antisecretory activity of **1** was evaluated in the conscious rat with fistula according to the procedure described in the previous paper.[6]

(4) Statistical Evaluation Results shown in the text are expressed as mean values of $\pm$S.E.M. The significance of the compound's effects was determined by using the Student's t-test and $p<0.05$ was considered significant. The ED_{50} and UD_{50} were calculated according to the method of Litchfield and Wilcoxon.[10]

Acknowledgements We would like to express our deep thanks to the Material Analytical Center of ISIR, Osaka Univ., for spectral

measurements and microanalyses. We gratefully acknowledge support for pharmacological and biological studies by Zeria Pharmaceutical Co., Ltd. and are especially grateful to Drs. E. Tagashira and M. Seiki for valuable discussion of the pharmacological results.

References

1) *a*) A. L. Rovati, R. R. Vidal y Plana, P. L. Casula, D. Bizzarri, F. Makovec and I. Setnikar, *Arzneim.-Forsch.*, **29**, 1116 (1979); *b*) G. Y. Paris, D. L. Garmaise, D. G. Cimon, L. Swett, G. W. Carter and P. Young, *J. Med. Chem.*, **23**, 9 (1980); *c*) Von H. Vergin, H. Ferber, F. Brunner and W. R. Kukovetz, *Arzneim.-Forsch.*, **31**, 513 (1981); *d*) S. Kobayashi, H. Shirota, Y. Katoh, R. Hashida, J. Nagaoka, S. Abe and I. Yamatsu, *Oyo Yakuri*, **36**, 91 (1988); *e*) H. Betzing and S. Leyck, Eur. Patent Appl. EP 47358 (1982) [*Chem. Abstr.*, **97**, 23624*y* (1982)]; *f*) M. A. Los, C. A. Piccinali and E. L. Tosti, *Boll. Chim. Farm.*, **122**, 243 (1983) [*Chem. Abstr.*, **100**, 144924*k* (1984)]; *g*) Von K.-H. Boltze, O. Brendler, H. Jacobi, W. Opitz, S. Raddatz, P.-R. Seidel and D. Vollbrecht, *Arzneim.-Forsch.*, **30**, 1314 (1980).

2) *a*) A. Bennett and B. Fleschler, *Gastroenterology*, **59**, 790 (1970); *b*) M. Hamberg, *Biochem. Biophys. Res. Commun.*, **49**, 720 (1972).
3) J. R. Vane, *Nature New Biol.*, **231**, 232 (1971).
4) G. Bommelaer and P. H. Guth, *Gastroenterology*, **77**, 303 (1979).
5) J. L. LaMattina, Eur. Patent Appl. EP 178121 (1984) [*Chem. Abstr.*, **105**, 30073*e* (1986)].
6) *a*) I. Ueda, K. Ishii, K. Shinozaki, M. Seiki, H. Arai and M. Hatanaka, *Chem. Pharm. Bull.*, **38**, 3035 (1990); *b*) K. Shinozaki, K. Ishii and I. Ueda, Japan. Patent 63-165822 (1988) [*Chem. Abstr.*, **113**, 132008*v* (1990)].
7) C. A. Winter, E. A. Risley and G. W. Nuss, *J. Pharmacol. Exp. Ther.*, **141**, 369 (1963).
8) H. B. Hucker, A. G. Zacchei, S. V. Cox, D. A. Brodie and N. H. R. Cantwell, *J. Pharmacol. Exp. Ther.*, **153**, 237 (1966).
9) K. F. Swingle, "Antiinflammatory Agents," Vol. II, ed. by R. A. Scherrer and M. W. Whitehouse, Academic Press, New York, 1974, p. 43.
10) J. T. Litchfield and F. Wilcoxon, Jr., *J. Pharmacol. Exp. Ther.*, **96**, 99 (1949).

Design and Synthesis of Antitumor Compounds Based on the Cytotoxic Diterpenoids from the Genus *Rabdosia*

Kaoru FUJI,*[,a] Hai-Jian XU,[a] Hiroshi TATSUMI,[b] Hidekazu IMAHORI,[b] Nozomu ITO,[b] Manabu NODE,[c] and Makoto INABA[d]

Institute for Chemical Research, Kyoto University,[a] Uji, Kyoto 611, Japan, Research Laboratories, Nippon Shoji Kaisha, Ltd.,[b] Ibaraki, Osaka 567, Japan, Kyoto Pharmaceutical University,[c] Yamashina-ku, Kyoto 607, Japan, and Cancer Chemotherapy Center, Japanese Foundation for Cancer Research,[d] Toshima-ku, Tokyo 170, Japan. *Received September 17, 1990*

Two active sites responsible for antitumor activity, an oxirane ring and an α-methylene-cyclopentanone moiety, have been extracted from studies on the structure–activity relationship of the cytotoxic diterpenoids isolated from *Rabdosia shikokiana*. Series of the simplified cyclopentanone derivatives containing both of the two active sites in the molecule have been synthesized and evaluated for cytotoxicity against P 388 cells. The compounds possessing both of two active sites displayed cytotoxicity at a concentration of 1 μg/ml, while those possessing a single active site showed no activity.

Keywords diterpenoid; antitumor activity; drug design; *Rabdosia*; cytotoxity

Plants of the genus *Rabdosia* (Labiatae) are a treasury of biologically active diterpenoids. The potent cytotoxicity of *Rabdosia* diterpenoids against HeLa cells,[1,2] KB cells,[3] mammary cancer FM 3A/B cells,[4] and Ehrlich carcinoma cells,[5] has been reported. Some diterpenoids possess *in vivo* activity against Ehrlich ascites carcinoma,[2,6] Walker intramuscular carcinoma,[3c] and P 388 lymphocytic leukemia.[7] A clinical trial with oridonin, a major diterpenoid of *R. trichocarpa*, has been reported.[8] In a series of studies on the cytotoxic diterpenoids of the genus *Rabdosia*, we isolated antitumor diterpenoids of the 8,9-secokaurene-type from *R. shikokiana* var. *occidentalis*,[9] and report *in vivo* activity against Ehrlich ascites carcinoma in mice.[2a] In those studies, we found a remarkable increase in activity by converting shikoccin (**1**) into epoxyketone **2**.[10] This compound has both an α-methylene cyclopentanone moiety and an epoxide on the same 5-membered ring. An α,β-unsaturated carbonyl group has been claimed to be a Michael acceptor strong enough to react with bionucleophiles such as sulfhydryl groups to exert biological activities, including antitumor activity.[11] The oxirane ring has been known to open easily by attack of the nucleophiles. Thus, the marked increase in antitumor activity of epoxyketone **2** may be attributed to the intramolecular synergism[2b] of two active sites, an α,β-unsaturated ketone moiety a and the oxirane ring b.

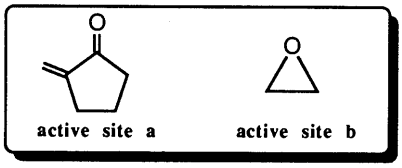

Chart 1. Two Active Sites Extracted from the Structure–Activity Relationship of Diterpenoids from *Rabdosia shikokiana*

The western parts of molecules **1** and **2**, shown by the thick line in Chart 2, are totally identical to each other, if C(6)–C(7) and C(12)–C(13) bonds are cleaved. In other words, all of the structural units necessary for antitumor activity are located on the 5-membered ring. Thus, we selected **7a** as a lead compound for a new type of antitumor agent, in which two key functional groups, a and b, are exquisitely deployed as in the eastern part of **2**. Here we describe syntheses of **7a** and its related compounds, and their *in vitro* activity against P 388 lymphocytic leukemia.

Synthesis Phenylselenylation of 2-methoxycarbonylcyclopentanone (**3a**) afforded **4a**, which was directly used for subsequent reactions. The oxidation, elimination of the resulting selenoxide, and the epoxidation were carried out in one pot to give the epoxide **5a**. The reaction of **5a** with formaldehyde provided the desired product **7a** in poor yield. An alternative two-step sequence *via* **6a** followed by the reduction with diisobutylaluminum hydride (DIBAH) increased the yield of **7a**. The related compounds **7b** and **7c** were prepared by the same route starting from **3b** and **3c**, respectively. Addition of ethanethiol and benzenethiol to **7a** gave **8** and **9**, respectively in high yield.

Aldol condensation of **3a** with benzaldehyde gave **10**,

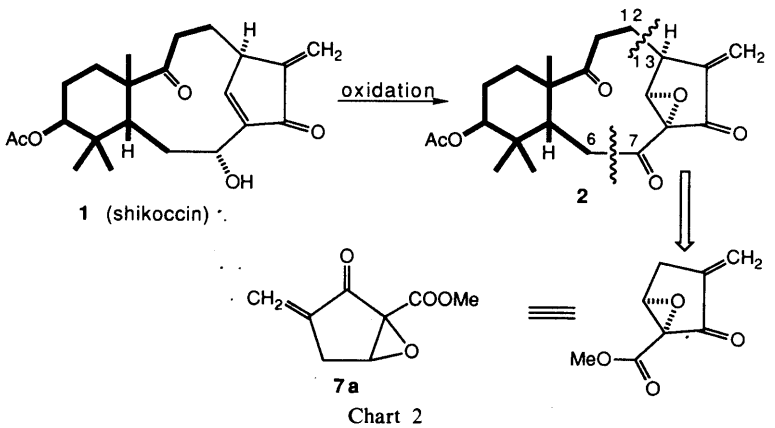

Chart 2

which was dehydrated with hydrochloric acid giving **12**. Phenylselenylation of **12** proceeded smoothly to afford **13**. A one-pot procedure involving hydrogen peroxide oxidation converted **13** into **14**. Compound **11** was prepared from **10** by phenylselenylation followed by oxidation. The reaction of **3a** with dimethylformamide dimethyl acetal afforded **15**. Compound **16** was prepared from **6a** by amidation with lithium benzylamide.

Transesterification of **3a** with ethylene glycol by Seebach's method[12] afforded **17**, which was condensed with **18** to give a symmetrical dimer **19**. Dimeric epoxide **20** and the corresponding α-methylenecyclopentanone **21** were obtained from **19** through a sequence of reactions similar to that for **3a**. Amidation of **18** with piperazine provided a dimeric amide **22** which was transformed to **23**, **24**, and **25** in a similar manner to that described for **3a**.

Phenylselenylation of β-estradiol derivative **26**, followed by oxidation with hydrogen peroxide in dichloromethane (CH_2Cl_2) provided **27**. Further oxidation of **27** with 30% hydrogen peroxide afforded an epoxide **28** which was converted to **29** through the two-step sequence described for **7a**. Syntheses of testosterone derivatives **31**, **32**, and **33** from **30** were similar to the preparation of β-estradiol derivatives.

Biological Evaluation The cytotoxicity of the monomeric and dimeric compounds against P 388 leukemia cells was determined and the results are listed Tables I and II. Compound **7a** displayed rather strong cytotoxicity as expected, since it possesses both of two active sites a and b. Other derivatives with two active sites, **7b**, **7c**, and **14**, were active at a concentration of 1 μg/ml. The compounds having an enaminoketone moiety displayed no activity, though both the two active sites a and b were present on the same 5-membered ring (entries 10—12 and 17, Table I). Electrophilicity at the β-carbon to the carbonyl group in these compounds decreases due to the electron-donation from the lone pair on the nitrogen atom, as shown in Chart 7, to suppress the Michael addition of bionucleophiles. It is worthy to note that compounds **8** and **9** showed strong activity. This may be ascribed to the regeneration of active site a by the elimination of thiol under physiological conditions.

The most active compound in the dimeric series was not **21** but **20**. This unexpected result may be due to the chemical instability of **21**. Dimeric compounds connected with amide

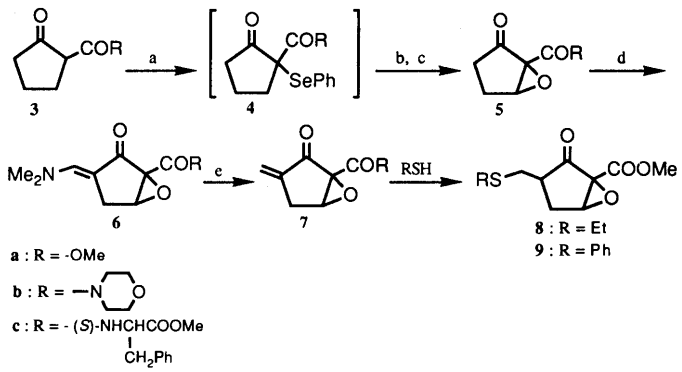

a) PhSeCl/pyridine/CH_2Cl_2, b) 15% H_2O_2/CH_2Cl_2, c) 15%H_2O_2/10% Na_2CO_3, d) $Me_2NCH(OMe)_2$, e) DIBAH/Et_3N

Chart 3

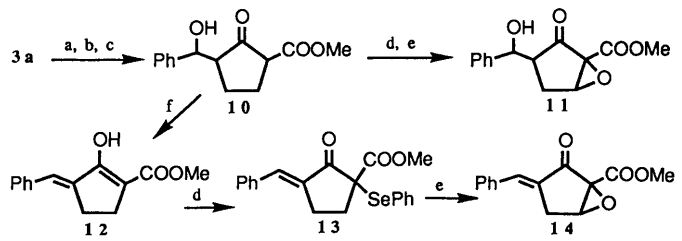

a) NaH, b) *n*-BuLi, c) PhCHO, d) PhSeCl/pyridine, e) 15%H_2O_2/10% Na_2CO_3, f) HCl

Chart 4

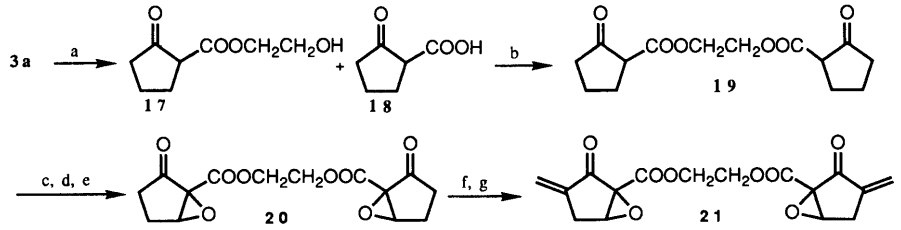

a) $HOCH_2CH_2OH$/$Ti(OEt)_4$, b) 1,1'-carbonyldiimidazole, c) PhSeCl/pyridine, d) 15%H_2O_2/CH_2Cl_2, e) 15%H_2O_2/10%Na_2CO_3, f) $Me_2NCH(OMe)_2$, g) DIBAH/Et_3N

Chart 5

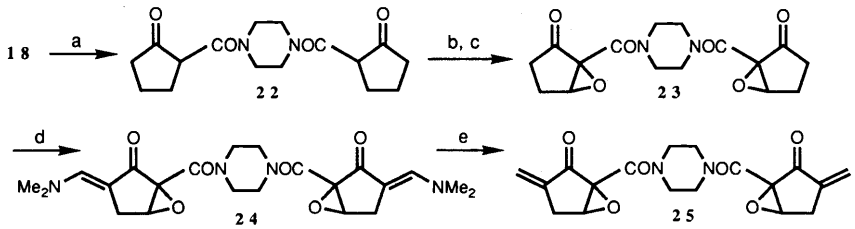

a) piperazine/DCC, b) PhSeCl/pyridine, c) 15%H_2O_2/10% Na_2CO_3, d) $Me_2NCH(OMe)_2$, e) DIBAH/Et_3N

Chart 6

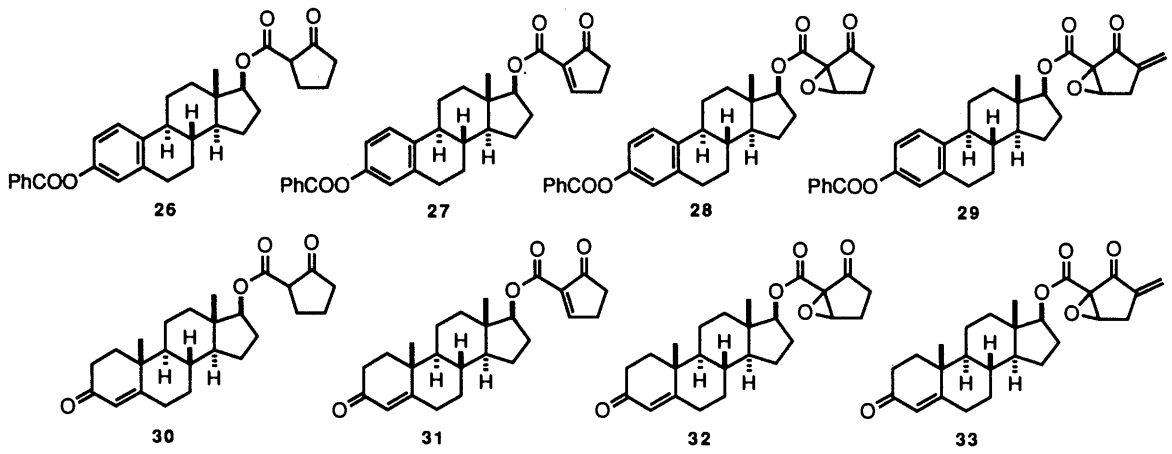

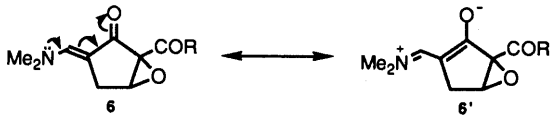

Chart 7

TABLE I. *In Vitro* Activity of the Monomeric Compounds against P388 Leukemia Cells

Entry	Compound	Growth rate (*T*/*C*%) Concentration μg/ml 10	1	0.1	Active site a	b
1	**5a**	26	105	110	No	Yes
2	**5b**	79	95	100	No	Yes
3	**5c**	0	63	91	No	Yes
4	**11**	0	23	72	No	Yes
5	**8**	0	4	66	No	Yes
6	**9**	0	0	62	No	Yes
7	**12**	36	93	102	Yes	No
8	**13**	0	73	98	Yes	No
9	**15**	100	101	104	Yes	No
10	**6a**	85	98	107	Yes	Yes
11	**6b**	85	100	108	Yes	Yes
12	**6c**	65	92	95	Yes	Yes
13	**7a**	0	0	69	Yes	Yes
14	**7b**	0	108	102	Yes	Yes
15	**7c**	0	52	44	Yes	Yes
16	**14**	0	57	101	Yes	Yes
17	**16**	54	94	93	Yes	Yes

TABLE II. *In Vitro* Activity of the Dimeric Compounds against P388 Leukemia Cells

Entry	Compound	Growth rate (*T*/*C*%) Concentration μg/ml 10	1	0.1
1	**20**	0	14	75
2	**21**	1	49	94
3	**22**	78	84	97
4	**23**	24	80	92
5	**24**	80	94	99
6	**25**	23	94	90

linkage displayed no significant activity (entries 3—6, Table II).

Estrogens and androgens have been clinically used for hormone dependent cancer. We synthesized **27**, **28**, and **29** from 17β-estradiol and **31**, **32**, and **33** from testosterone. Though *in vitro* antitumor activity was observed for all compounds at high concentrations, except for **27**, all compounds were inactive at the concentration of 1 μg/ml. Thus, further modification of the structures seems to be necessary for increasing the activity of those types of compound.

Though it is clear that more sophisticated chemical modifications are required, we have shown that our design of antitumor agents was successful in an *in vitro* system.

TABLE III. *In Vitro* Activity of Steroidal Derivatives

Compound	Dose (μg/ml)	Tumor cell GAC 3	GAC 4	MKN-28	Kato 3	P388
27	10	68.8	91.3	23.9	36.4	4.6
	1	132.3	115.7	110.2	105.3	102.7
	0.1	135.2	110.9	103.3	98.8	106.5
28	10	1.8	5.3	−0.5	0.0	−1.8
	1	64.1	92.2	24.7	28.5	4.8
	0.1	100.6	118.2	79.4	102.5	99.2
29	10	3.5	68.0	3.6	7.5	3.7
	1	99.5	101.2	68.7	90.5	84.4
	0.1	115.6	102.5	85.4	104.8	100.0
31	10	0.2	28.8	−1.3	−1.1	−2.1
	1	59.4	98.3	81.3	82.0	116.3
	0.1	89.5	103.5	73.7	100.3	93.1
32	10	3.4	22.3	5.2	2.7	4.6
	1	88.6	115.9	69.0	97.4	127.3
	0.1	92.5	104.0	83.2	106.6	106.1
33	10	3.3	33.6	−1.0	−0.3	−1.9
	1	85.8	103.5	34.6	93.8	4.9
	0.1	83.5	101.8	88.6	103.2	103.6

Experimental

General Method Melting points were determined on a Yanagimoto micro melting point apparatus and are uncorrected. Proton nuclear magnetic resonance (^{1}H-NMR) spectra were recorded on a JOEL JMN-GX 400 or JMN-FX 100 spectrometer. Infrared (IR) spectra were measured with a Jasco IR-180 spectrophotometer. Mass spectra (MS) were measured with a JEOL JMS-DX 300 mass spectrometer.

2,3-Epoxy-2-methoxycarbonylcyclopentanone (5a) To a solution of PhSeCl (7.4 g, 39 mmol) and pyridine (3.3 ml, 41 mmol) in anhydrous CH_2Cl_2 (150 ml) was added dropwise a solution of 2-methoxycarbonylcyclopentanone (**3a**) (4.8 g, 34 mmol) at 0 °C, and the mixture was stirred under N_2 at room temperature. The reaction mixture was washed successively with 10% HCl, saturated $NaHCO_3$ solution, and brine, dried, and evaporated to give 10.1 g of 2-methoxycarbonyl-2-

phenylselenocyclopentanone (**4a**). This was immediately dissolved in CH_2Cl_2 (350 ml), 14 ml of 15% H_2O_2 was added to this solution, and the mixture was stirred for 1.5 h at 0 °C. Vigorous stirring was continued for 20 min after the addition of another 14 ml of 15% H_2O_2 and 30 ml of 10% aq. Na_2CO_3. The mixture was washed with 10% aq. Na_2CO_3 and brine, dried, and evaporated. The residue was crystallized from AcOEt–hexane to yield 4.0 g (75%) of **5a**. An analytical sample was recrystallized from AcOEt–hexane, mp 50—50.5 °C. ^{1}H-NMR ($CDCl_3$) δ: 2.13—2.52 (m, 4H), 3.85 (s, 3H), 4.18 (s, 1H). *Anal.* Calcd for $C_7H_8O_4$: C, 53.84; H, 5.16. Found: C, 53.81; H, 5.16.

2,3-Epoxy-2-morpholinocarbonylcyclopentanone (5b) and *N*-(1,2-Epoxy-5-oxocyclopentylcarbonyl)-L-phenylalanine Methyl Ester (5c) Compounds **5b** and **5c** were prepared from **3b** and **3c** through a sequence similar to that for **5a** in 72 and 83% overall yields, respectively. **5b**: mp 75—77 °C (from AcOEt–hexane). *Anal.* Calcd for $C_{10}H_{13}NO_4$: C, 56.86; H, 6.20; N, 6.63. Found: C, 56.85; H, 6.17; N, 6.67. **5c**: Oil. *Anal.* Calcd for $C_{16}H_{17}NO_5$: C, 63.34; H, 5.65; N, 4.62. Found: C, 62.94; H, 5.65; N, 4.57.

5-Dimethylaminomethylene-2,3-epoxy-2-methoxycarbonylcyclopentanone (6a) A mixture of **5a** (4.7 g, 30 mmol) and dimethylformamide dimethylacetal (7.8 ml, 60 mmol) in dimethylformamide (DMF, 15 ml) was stirred at room temperature for 24 h. After the evaporation of the solvent, the residue was chromatographed over silica gel to yield 3.0 g (48%) of **6a**: mp 125.5—127 °C (from MeOH). ^{1}H-NMR ($CDCl_3$) δ: 2.84—3.31 (m, 2H), 3.07 (s, 6H), 3.85 (s, 3H), 4.05 (d, 1H, J=2.5 Hz), 7.31 (s, 1H). *Anal.* Calcd for $C_{10}H_{13}NO_4$: C, 56.86; H, 6.20; N, 6.63. Found: C, 56.86; H, 6.17; N, 6.63.

5-Dimethylaminomethylene-2,3-epoxy-2-morpholinocarbonylcyclopentanone (6b) and *N*-(4-Dimethylaminomethylene-1,2-epoxy-5-oxocyclopentylcarbonyl)-L-phenylalanine Methyl Ester (6c) Compounds **6b** and **6c** were prepared from **5b** and **5c** through a sequence similar to that for **6a** in 44 and 40% yields, respectively. **6b**: mp 199—200 °C (from EtOH). *Anal.* Calcd for $C_{13}H_{18}N_2O_4$: C, 58.63; H, 6.81; N, 10.52. Found: C, 58.58; H, 6.84; N, 10.62. **6c**: Oil. High resolution MS *m/z*: Calcd for $C_{19}H_{22}N_2O_5$: 358.1528. Found: 358.1529.

2,3-Epoxy-2-methoxycarbonyl-5-methylenecyclopentanone (7a) To a stirred solution of **6a** (870 mg, 4.1 mmol) in anhydrous tetrahydrofuran (THF, 60 ml) were added 3.3 ml of DIBAH (25 g/100 ml in hexane) and Et_3N (0.8 ml, 5.8 mmol) under N_2 at −78 °C, and the mixture was stirred for 2 h. After addition of 20 ml of saturated NH_4Cl solution, the mixture was extracted with CH_2Cl_2, and the combined CH_2Cl_2 phases were washed with saturated NH_4Cl solution, dried, and evaporated to afford an oily residue, which was chromatographed on silica gel to yield **7a** (525 mg, 76%), oil. ^{1}H-NMR ($CDCl_3$) δ: 2.94 (m, 2H), 3.88 (s, 3H), 4.18 (br s, 1H), 5.56 (t, 1H, J=2 Hz), 6.28 (t, 1H, J=3 Hz). *Anal.* Calcd for $C_8H_8O_4$: C, 57.14; H, 4.80. Found: C, 57.10; H, 4.80.

2,3-Epoxy-5-methylene-2-morpholinocarbonylcyclopentanone (7b) and *N*-(1,2-Epoxy-4-methylene-5-oxocyclopentylcarbonyl)-L-phenylalanine Methyl Ester (7c) Compounds **7b** and **7c** were prepared from **6b** and **6c** under conditions similar to those for **7a** in 39 and 36% yield, respectively. **7b**: Oil. ^{1}H-NMR ($CDCl_3$) δ: 2.95 (m, 2H), 3.46—3.92 (m, 8H), 4.18 (br s, 1H), 5.56 (t, 1H, J=2Hz), 6.25 (t, 1H, J=2 Hz). High resolution MS *m/z*: Calcd for $C_{11}H_{13}NO_4$: 223.0844. Found: 223.0845. **7c**: Oil. High resolution MS *m/z*: Calcd for $C_{17}H_{17}NO_5$: 315.1107. Found: 315.1106.

2,3-Epoxy-5-ethylthiomethyl-2-methoxycarbonylcyclopentanone (8) To a solution of **7a** (252 mg, 1.5 mmol) in 10 ml of anhydrous toluene were added EtSH (122 μl, 1.7 mmol) and Et_3N (230 μl, 1.7 mmol) and the mixture was stirred for 2.5 h. Evaporation of the solvent gave an oily residue, which was chromatographed on silica gel to yield 316 mg (92%) of oily **8**. ^{1}H-NMR ($CDCl_3$) δ: 1.25 (t, 3H, J=7 Hz), 2.32—3.08 (m, 5H), 2.53 (q, 2H, J=7 Hz), 3.85 (s, 3H), 4.16 (s, 1H). *Anal.* Calcd for $C_{10}H_{14}O_4S$: C, 52.16; H, 6.13. Found: C, 52.03; H, 6.09.

2,3-Epoxy-2-methoxycarbonyl-5-(phenylthiomethyl)cyclopentanone (9) Compound **9** was prepared in a similar manner to that described for **8** in 74% yield. **9**: mp 104—105 °C (from ether). *Anal.* Calcd for $C_{14}H_{14}O_4S$: C, 60.41; H, 5.07. Found: C, 60.26; H, 5.05.

5-α-Hydroxybenzyl-2-methoxycarbonylcyclopentanone (10) To a suspension of NaH (60% in mineral oil, 176 mg, 4.4 mmol) in anhydrous THF was added **3a** (570 mg, 4.0 mmol), and the mixture was stirred at room temperature for 15 min. After addition of *n*-BuLi (1.35 M in hexane, 3.3 ml, 4.4 mmol) and benzaldehyde (470 mg, 4.4 mmol), the mixture was stirred for 1 h at room temperature, poured into ice-water, acidified with 10% HCl, and extracted with ether. Combined ether phases were washed with brine, dried, and evaporated to give an oil, which was chromatographed on silica gel to yield **10** (452 mg, 46%) as a yellow oil. ^{1}H-NMR ($CDCl_3$) δ: 1.40—1.95 (m, 2H), 2.00—2.35 (m, 2H), 2.40—2.80 (m, 1H), 3.20 (t, J=10 Hz, 1H), 3.70 (s, 3H), 4.00 (s, 1H, OH), 4.70 (d, J=8.5 Hz, 1H), 7.22 (s, 5H). High resolution MS *m/z*: Calcd for $C_{14}H_{16}O_4$: 248.1048. Found: 248.1030.

2,3-Epoxy-5-α-hydroxybenzyl-2-methoxycarbonylcyclopentanone (11) Compound **11** was prepared from **10** through a sequence of the reactions similar to those for **5a** in 19% overall yield, mp 116—117 °C (from ether). *Anal.* Calcd for $C_{14}H_{14}O_5$: C, 64.11; H, 5.38. Found: C, 64.44; H, 5.43.

5-Benzylidene-2-methoxycarbonylcyclopentene-1-ol (12) A solution of 804 mg (3.2 mmol) of **10** in $CHCl_3$ (50 ml) saturated with HCl was stirred for 1 h, washed with aq.$NaHCO_3$ and brine, dried, and evaporated to give a residue, which was crystallized from AcOEt–hexane to yield **12** (497 mg, 67%), mp 114—115 °C. ^{1}H-NMR ($CDCl_3$) δ: 2.56—2.96 (m, 4H), 3.81 (s, 3H), 6.92 (t, 1H, J=2 Hz), 7.19—7.50 (m, 5H), 10.19 (s, 1H). IR ($CHCl_3$) ν: 3300, 1650, 1600, 1445, 1250 cm^{-1}. *Anal.* Calcd for $C_{14}H_{14}O_3$: C, 73.02; H, 6.13. Found: C, 72.82; H, 6.21.

5-Benzylidene-2-methoxycarbonyl-2-phenylselenylcyclopentanone (13) A solution of PhSeCl (934 mg, 4.7 mmol) in 25 ml of anhydrous CH_2Cl_2 was stirred with pyridine (415 μl, 5.2 mmol) for 15 min. After addition of a solution of **12** (990 mg, 4.3 mmol) in anhydrous CH_2Cl_2 (5 ml), the mixture was stirred for 2 h, washed with 10% HCl, aq.$NaHCO_3$ and brine, dried, and evaporated to afford an oil. Chromatography on silica gel yielded 1.5 g (87%) of **13**, oil. ^{1}H-NMR ($CDCl_3$) δ: 2.18 (m, 1H), 2.46 (m, 1H); 2.74—3.01 (m, 2H), 3.78 (s, 3H), 7.21—7.69 (m, 11H). IR ($CHCl_3$) ν: 1740, 1705, 1610 cm^{-1}. *Anal.* Calcd for $C_{20}H_{18}O_3Se$: C, 62.34; H, 4.71. Found: C, 62.09; H, 4.67.

5-Benzylidene-2,3-epoxy-2-methoxycarbonylcyclopentanone (14) To a solution of 1.4 g (3.7 mmol) of **13** in CH_2Cl_2 (50 ml) was added 15% H_2O_2 (1.5 ml) under ice-cooling and the mixture was stirred for 1.5 h. After addition of another 1.5 ml of 15% H_2O_2 and 6 ml of 10% aq.Na_2CO_3, the mixture was stirred vigorously for 2 h, washed with aq.Na_2CO_3 and brine, dried, and evaporated to give a residue, which was crystallized from MeOH to yield **14** (547 mg, 61%), mp 115—116 °C. ^{1}H-NMR ($CDCl_3$) δ: 3.04 (dt, 1H, J=18, 2.5 Hz), 3.37 (dd, 1H, J=18, 2 Hz), 3.90 (s, 3H), 4.28 (d, 1H, J=2 Hz), 7.27—7.06 (m, 6H). *Anal.* Calcd for $C_{14}H_{12}O_4$: C, 68.84; H, 4.95. Found: C, 69.11; H, 4.98.

2-Dimethylaminomethylene-5-methoxycarbonylcyclopentanone (15) Compound **15** was prepared from **3a** by a method similar to that described for **6a** in 43% yield, mp 89.5—90 °C (from AcOEt–hexane). *Anal.* Calcd for $C_{10}H_{15}NO_3$: C, 60.89; H, 7.67; N, 7.10. Found: C, 60.83; H, 7.79; N, 7.07.

2-Benzylcarbamoyl-5-dimethylaminomethylene-2,3-epoxycyclopentanone (16) To a solution of 634 mg (3.0 mmol) of **6a** in 30 ml of anhydrous THF was added under ice-cooling 3.3 mmol of lithium benzylamide in anhydrous THF (10 ml), and the mixture was stirred for 2 h. After addition of brine, the reaction mixture was extracted with CH_2Cl_2 and the combined phases were washed with brine, dried, and evaporated to afford a residue, which was chromatographed on silica gel to yield 405 mg (47%) of **16**, mp 135—136 °C (from AcOEt). ^{1}H-NMR ($CDCl_3$) δ: 2.84 (br s, 1H, J=16 Hz), 3.19 (d, 1H, J=16 Hz), 3.07 (s, 6H), 4.27 (d, 1H, J=2 Hz), 4.49 (br d, 2H, J=16 Hz), 7.28 (s, 1H), 7.31 (s, 5H), 8.72 (br s, 1H). *Anal.* Calcd for $C_{16}H_{18}N_2O_3$: C, 67.11; H, 6.34; N, 9.78. Found: C, 67.03; H, 6.35; N, 9.73.

2-(β-Hydroxyethyloxycarbonyl)cyclopentanone (17) A mixture of 2.3 g (16 mmol) of **3a**, 0.8 ml of Ti $(OEt)_4$, and 5 ml of ethylene glycol was stirred at 105 °C for 9 h. After addition of water at room temperature, the mixture was extracted with CH_2Cl_2. The combined organic layer was washed with aq.$NaHCO_3$ and brine, dried, and evaporated to give a residue which was purified by column chromatography on silica gel to yield 2.0 g of **17** (73%), oil. ^{1}H-NMR ($CDCl_3$) δ: 1.75—2.50 (m, 6H), 2.70 (m, 1H, OH), 3.25 (t, 1H, J=10 Hz), 3.85 (m, 2H), 4.25 (m, 1H), 4.48 (m, 1H). High resolution MS *m/z*: Calcd for $C_8H_{12}O_4$: 172.0736. Found: 172.0737.

1,2-Bis(2-oxocyclopentylcarbonyloxy)ethane (19) After a mixture of 550 mg (4.3 mmol) of **18** and 600 mg (3.7 mmol) of 1,1′-carbonyldiimidazole in CH_2Cl_2 (10 ml) was stirred for 30 min, a solution of 605 mg (3.5 mmol) of **17**, 0.5 ml of pyridine, and 0.6 ml (6 mmol) of sodium imidazole (1 M solution in dimethyl sulfoxide (DMSO) in CH_2Cl_2 (10 ml) was added and the mixture was stirred for 1 h at room temperature, washed with 10% HCl and water, dried, and evaporated to give a crude oil. Purification by column chromatography on silica gel yielded oily **19** (623 mg, 63%). ^{1}H-NMR ($CDCl_3$) δ: 1.70—1.95 (m, 4H), 2.00—2.40 (m, 8H), 3.15 (t, 2H, J=9 Hz), 4.33 (s, 4H). High resolution MS *m/z*: Calcd for $C_{14}H_{18}O_6$: 282.1102. Found: 282.1092.

1,2-Bis(1,2-epoxy-5-oxocyclopentylcarbonyloxy)ethane (20) and 1,2-Bis(1,2-epoxy-4-methylene-5-oxocyclopentylcarbonyl)ethane (21) Com-

pound **20** and **21** were prepared from **19** in a manner similar to those for **5a** and **7a** in 60 and 3% yields, respectively. **20**: Oil. ^{1}H-NMR ($CDCl_3$) δ: 2.10—2.50 (m, 8H), 4.25 (s, 2H), 4.50 (m, 4H). *Anal.* Calcd for $C_{14}H_{14}O_8$: C, 54.19; H, 4.55. Found: C, 53.76; H, 4.69. **21**: Unstable oil. ^{1}H-NMR ($CDCl_3$) δ: 2.82—3.10 (m, 4H), 4.25 (br s, 2H), 4.55 (m, 4H), 5.55 (s, 2H), 6.25 (s, 2H).

1,4-Bis(2-oxocyclopentylcarbonyl)piperazine (22) A mixture of **18** (955 mg, 7.5 mmol), dicyclohexylcarbodiimide (DCC, 2.3 g, 11.2 mmol), and piperazine (321 mg, 3.7 mmol) in CH_2Cl_2 (60 ml) was stirred at room temperature for 15 h. After filtration, an organic phase was washed with 5% HCl and brine, dried, and evaporated to give a residue, which was chromatographed on silica gel to yield 537 mg (47%) of **22**, mp 140—142 °C (from AcOEt). *Anal.* Calcd for $C_{16}H_{22}N_2O_4$: C, 62.72; H, 7.24; N, 9.14. Found: C, 62.74; H, 7.19; N, 9.16.

1,4-Bis(1,2-epoxy-5-oxocyclopentylcarbonyl)piperazine (23), 1,4-Bis(4-dimethylaminomethylene-1,2-epoxy-5-oxocyclopentylcarbonyl)piperazine (24), and 1,4-Bis(1,2-epoxy-4-methylene-5-oxocyclopentylcarbonyl)piperazine (25) Compounds **23**, **24**, and **25** were prepared through a sequence of reactions similar to **3a** to **7a** in 66, 41, and 46% yields, respectively. **23**: mp 237—240 °C (dec.) (from acetone). *Anal.* Calcd for $C_{16}H_{18}N_2O_6$: C, 57.48; H, 5.43; N, 8.38. Found: C, 57.87; H, 5.58; N, 8.55. **24**: mp > 300 °C (from CH_2Cl_2–MeOH). High resolution MS *m/z*: Calcd for $C_{22}H_{28}N_4O_6$: 444.2008. Found: 444.2009. **25**: mp > 300 °C (from CH_2Cl_2–acetone). *Anal.* Calcd for $C_{18}H_{18}N_2O_6$: C, 60.33; H, 5.06; N, 7.82. Found: C, 60.04; H, 5.05; N, 7.72.

3-Benzoyloxy-17-(5-oxocyclopentylcarbonyloxy)-$\Delta^{1,3,5}$-estratriene (26) A mixture of estradiol 3-benzoate (2.0 g, 2.7 mmol), **18** (1.0 g, 7.8 mmol), 1-ethyl-3-(dimethylaminopropyl)carbodiimide hydrochloride (2.2 g, 11.5 mmol), and 4-dimethylaminopyridine (DMAP, 0.1 g, 0.8 mmol) in CH_2Cl_2 (60 ml) was stirred at 0 °C for 3.5 h. The reaction mixture was washed with 10% HCl and brine, dried, and evaporated to give a residue. Chromatography on silica gel yielded 1.3 g (99%) of **26**, mp 155—156 °C (from AcOEt–hexane). High resolution MS *m/z*: Calcd for $C_{31}H_{34}O_5$: 486.2406. Found: 486.2418.

3-Benzoyloxy-17-(5-oxocyclopentenylcarbonyloxy)-$\Delta^{1,3,5}$-estratriol (27) A solution of PhSeCl (620 mg, 3.1 mmol) in 40 ml of anhydrous CH_2Cl_2 was stirred with pyridine (0.8 ml, 10 mmol) for 20 min. After addition of a solution of 1.3 g (2.6 mmol) of **26** in anhydrous CH_2Cl_2 (45 ml), the mixture was stirred for 20 h, washed with 10% HCl and brine, dried, and evaporated to give an oil which was chromatographed on silica gel. Elution with CH_2Cl_2 afforded an oil (980 mg), which was dissolved with CH_2Cl_2 (80 ml) and stirred with 3 ml of 15% H_2O_2 for 1 h. The reaction mixture was washed with H_2O, dried, and evaporated to afford a crystalline residue (768 mg, 61%), mp 177—179 °C (from CH_2Cl_2–hexane). High resolution MS *m/z*: Calcd for $C_{31}H_{32}O_5$: 484.2308. Found: 484.2279.

3-Benzoyloxy-17-(1,2-epoxy-5-oxocyclopentylcarbonyloxy)-$\Delta^{1,3,5}$-estratriol (28) and 3-Benzoyloxy-17-(1,2-epoxy-4-methylene-5-oxocyclopentylcarbonyloxy)-$\Delta^{1,3,5}$-estratriol (29) Compounds **28** and **29** were prepared from **26** in a manner similar to those for **5a** and **7a** in 66 and 69% yields, respectively. **28**: mp 179—180 °C (from AcOEt–hexane). *Anal.* Calcd for $C_{31}H_{32}O_6$: C, 74.38; H, 6.44. Found: C, 74.09; H, 6.29. **29**: Amorphous. *Anal.* Calcd for $C_{32}H_{32}O_6$: C, 74.97; H, 6.29. Found: C, 74.87; H, 6.27.

17-(5-Oxocyclopentylcarbonyloxy)-Δ^4-androstene-3-one (30) and 17-(5-Oxocyclopentenylcarbonyloxy)-Δ^4-androstene-3-one (31) Compounds **30** and **31** were prepared from testosterone as described for **26** and **27** in 99 and 71% yields, respectively. **30**: mp 118—119 °C (from AcOEt–hexane). *Anal.* Calcd for $C_{25}H_{32}O_4$: C, 75.34; H, 8.60. Found: C, 74.99; H, 8.48. **31**: mp 179—181 °C (from CH_2Cl_2–hexane). *Anal.* Calcd for $C_{25}H_{32}O_4$: C, 75.72; H, 8.14. Found: C, 75.37; H, 8.17.

17-(1,2-Epoxy-5-oxocyclopentylcarbonyloxy)-Δ^4-androstene-3-one (32) and 17-(1,2-Epoxy-4-methylene-5-oxocyclopentylcarbonyloxy)-Δ^4-androstene-3-one (33) Compounds **32** and **33** were prepared from **30** through a sequence of reactions similar to those for **28** and **29**, in 87 and 62% yields, respectively. **32**: mp 153—154 °C (from AcOEt–hexane). *Anal.* Calcd for $C_{25}H_{32}O_5$: C, 72.79; H, 7.82. Found: C, 72.60; H, 7.85. **33**: mp 174—177 °C (from AcOEt–hexane). *Anal.* Calcd for $C_{26}H_{32}O_5$: C, 73.56; H, 7.60. Found: C, 73.36; H, 7.60.

Assessment of the Activity of the Drug against Tumor Cells Growth Assay: RPMI 1640 supplemented with 10% fetal bovine serum, 10 μM 2-hydroxyethyldisufide and 100 μg/ml kanamycin was used as a culture medium. P388 cells were suspended in the culture medium containing the drug (final concentration: 0.1, 1 or 10 μg/ml), plated at a final cell density of 5×10^4 cells/ml, and incubated in a CO_2 incubator at 37 °C for 48 h. The number of cells was counted in a model ZBI Coulter Counter after a 5-min incubation with 0.25% trypsin to dissociate the cells. *T/C*(%) was calculated according to the equation: (treated cells − starting cells)/(untreated cells − starting cells) × 100.

MTT Assay: The above culture medium was also used in this assay. Human stomach cancer lines, GAC-3 and GAC-4, were kindly supplied by Dr. Morikawa, Shimane Medical College, Izumo. P388 and human stomach cancer (GAC-3, GAC-4, Kato-III and MKN-28) cells were plated at a cell density of 500 and 2000 cells/100 μl, respectively, in a 96-well microtiter plate on day 0, and 100 μl of the drug solution (final incubation in CO_2 incubator. On day 5, 50 μl of 3-(4,5-dimethylthiazol-2-yl)-2,5-phenyltetrazolium bromide (MTT) solution (1 mg/ml) was added and incubated for an additional 4 h. The MTT formazan formed was dissolved in 150 μl of DMSO after removing the culture medium, and its optimal density at 540 nm was measured. *T/C*(%) was calculated according to the equation: (OD of treated cells − OD of medium only)/(OD of untreated cells − OD of medium only) × 100.

Acknowledgment This work was supported by a Grant-in-Aid from the Tokyo Biochemical Research Foundation to K. F. and by a grant from the Ministry of Education, Science, and Culture, Japan (NO. 02152059 to M.N.).

References and Notes

1) T. Arai, Y. Koyama, T. Suenaga, and T. Morita, *J. Antibiot. Ser. A*, **16**, 132 (1963).
2) *a*) K. Fuji, M. Node, N. Ito, E. Fujita, S. Takeda, and N. Unemi, *Chem. Pharm. Bull.*, **33**, 1038 (1985); *b*) K. Fuji, M. Node, M. Sai, E. Fujita, S. Takeda, and N. Unemi, *ibid.*, **37**, 1472 (1989).
3) *a*) M. Yamaguchi, M. Taniguchi, I. Kubo, and T. Kubota, *Agric. Biol. Chem.*, **41**, 2475 (1977); *b*) I. Kubo, I. Miura, K. Nakanishi, T. Kamikawa, T. Isobe, and T. Kubota, *J. Chem. Soc., Chem. Commun.*, **1977**, 55; *c*) I. Kubo, I. Miura, T. Kamikawa, T. Isobe, and T. Kubota, *Chem. Lett.*, **1977**, 1289; *d*) I. Kubo, M. J. Pettei, K. Hirotsu, H. Tsuji, and T. Kubota, *J. Am. Chem. Soc.*, **100**, 628 (1978).
4) T. Fujita, Y. Takeda, and T. Shingu, *J. Chem. Soc., Chem. Commun.*, **1980**, 205; T. Fujita, Y. Takeda, T. Shingu, M. Kido, and Z. Taira, *ibid.*, **1982**, 162.
5) H.-D. Sun, T. Marunaka, and T. Fujita, *Chem. Lett.*, **1981**, 753.
6) *a*) E. Fujita, Y. Nagao, M. Node, K. Kaneko, S. Nakazawa, and H. Kuroda, *Experientia*, **32**, 203 (1976); *b*) E. Fujita, Y. Nagao, K. Kaneko, S. Nakazawa, and H. Kuroda, *Chem. Pharm. Bull.*, **24**, 2118 (1976); *c*) M. Node, M. Sai, K. Fuji, E. Fujita, S. Takeda, and N. Unemi, *ibid.*, **31**, 1433 (1983); *d*) M. Node, M. Sai, E. Fujita, and K. Fuji, *Heterocycles*, **22**, 1701 (1984) and ref. 3.
7) E. Fujita, N. Ito, I. Uchida, K. Fuji, T. Taga, and K. Osaki, *J. Chem. Soc., Chem. Commun.*, **1979**, 806; Y. Nagao, N. Ito, T. Khono, H. Kuroda, and E. Fujita, *Chem. Pharm. Bull.*, **30**, 727 (1982); J. Li, C. Lui, X. An, M. Wang, T. Zhao, S. Yu, and G. Zhao, *Yaoxue Xuebao*, **17**, 682 (1982) [*Chem. Abstr.*, **98**, 59801*p* (1983)].
8) H. Sun, C. Liu, J. Qin, J. Chao, and Q. Zhao, *Yunnan Chin Wu Yen Chiu*, **3**, 95 (1981) [*Chem. Abstr.*, **95**, 121032*g* (1981)].
9) M. Node, N. Ito, E. Uchida, E. Fujita, and K. Fuji, *Chem. Pharm. Bull.*, **33**, 1029 (1985).
10) K. Fuji, N. Ito, I. Uchida, and E. Fujita, *Chem. Pharm. Bull.*, **33**, 1034 (1985).
11) S. M. Kupchan, D. C. Fessler, M. A. Eakin, and T. J. Giacobbe, *Science*, **168**, 376 (1970).
12) D. Seebach, E. Hungerbühler, R. Naef, P. Schnurrenberger, B. Weidmann, and M. Züger, *Synthesis*, **1982**, 138.

Pharmacological Properties of Galenical Preparation. XIV.[1] Body Temperature Retaining Effect of the Chinese Traditional Medicine, "Goshuyu-to (呉茱萸湯)" and Component Crude Drugs

Yoshihiro KANO,* Qine ZONG and Ken-ichi KOMATSU

Hokkaido Institute of Pharmaceutical Sciences, 7–1 Katuraoka-cho, Otaru 047–02, Japan. *Received July 19, 1990*

We orally administered Goshuyu-to (呉茱萸湯) or Evodia fruit (呉茱萸) extract and Ginger (生姜) extract to untreated rats, and found a slight but not significant rise in their body temperature. In rats treated with chlorpromazine, the administration of Goshuyu-to prevented decrease in the body temperature. After administration of each extract of component crude drugs (Evodia fruit, Ginger, Ginseng: 人参, Jujube: 大棗), such an effect was recognized only by Evodia fruit, and other component crude drugs exhibited no body temperature retaining effect in this experiment system. We further studied the effect of Evodia fruit alkaloid hydroxyevodiamine, evodiamine, rutaecarpine and evocarpine used individually and confirmed that the body temperature retaining effect occurred mainly with evodiamine.

Keywords Goshuyu-to; Evodia fruit; *Evodia officinalis*; Rutaceae; evodiamine; body temperature; crude drug; alkaloid

The concept of a body temperature retaining action in a crude drug signifies a recovery action from the low body temperature state of the entrails. Specifically, a decrease in the metabolism rate will be followed by cause an insufficiency of thermogenesis, with the result that the temperature of internal organs will drop and their functions will be reduced; as a result, a characteristic syndrome (sho: 証) characteristic of cold hands and feet, a pale face, migraine, vomiting, *etc.* are observed.[2]

Goshuyu-to, known as a drug which maintains the body temperature, is a Chinese traditional medicine designed for the treatment of such symptoms. It is given to treat migraines and vomiting accompanying a cold.[3]

Hon-zo-kou-moku (本草綱目) mentions that Evodia fruit, the main drug of this prescription, warms the interior of the body and cures chills and fever.[4] According to Sho-kan-ron (傷寒論), it can be used to treat lesser yin disease (sho-yin-biyo: 少陰病),[5] cold hands and feet, and perennial chills. Thus, it seems that Evodia fruit affects body temperature. We studied the body temperature retaining effect of Goshuyu-to and component crude drugs.

Experimental

Animals We bred male Wistar rats (6 weeks old, weighing 150—200 g, purchased from Japan SLC) in a breeding room 24±1 °C temperature, and 50±5% humidity, with lighting from 6:00 to 18:00. During this time, they ate and drank freely.

Administered Drugs We purchased chlorpromazine hydrochloride, Tween 80 (polyoxyethylene (20) sorbitan monooleate) from Wako Co., Ltd. As component crude drugs for Goshuyu-to (Evodia fruit 3 g, Ginger 2 g, Ginseng 2 g, Jujube 4 g), were used those conforming to the Japanese pharmacopoeia XI. Evodia fruit alkaloids (I, hydroxyevodiamine: II, evodiamine; III, rutaecarpine and IV, evocarpine: Chart 1) to be used, were extracted from Evodia fruit. They were then refined and identified as standard samples.

Equipment We used a thermistor (Omron Digital Thermometer MC-14B, Tateishi Co., Ltd.).

Preparation of Sample Drugs We added water (about 20 times the weight of the crude drug) to Goshuyu-to or each crude drug, boiled it until its quantity was halved, and filtered it through 5-layer gauze. The boiled liquid was then freeze-dried and stored at 4 °C. Extract yield of Goshuyu-to, Evodia fruit, Ginger, Ginseng and Jujube per 1 g was 0.25, 0.09, 0.28, 0.27 and 0.68 g, respectively. Goshuyu-to (1.0 or 3.0 g) and each drug (0.2 or 1.0 g) in the crude drug equivalent was dissolved or suspended in 1.0 ml of 2% Tween 80, and orally administered to rats at a dose of 5 ml/kg body weight.

We prepared Evodia fruit alkaloid components so that each component concentration was 5 ml/kg as a dose (suspension with 2% Tween 80), and orally administered it to the rats.

Selecting the Preparation Conditions for Low Body Temperature Animal Models Rats were intraperitoneally administered with chlorpromazine at 4-stage dose of 2.0, 4.0, 8.0, 20.0 mg/kg, and their rectum temperature measured. The dose was 1.0 ml/kg, and the drug liquid to be administered was heated to the rats temperature prior to administration.

Measuring the Body Temperature We measured the rectum temperature of 10 rats in one group using a thermistor 0, 0.5, 1.0, 2.0, 3.0 and 4.0 h after oral administration (Chart 2).

In measuring the temperature of low body temperature animals, since chlorpromazine was administered 1.0 h after oral administration of the sample drug or 2% Tween 80, we also measured the rectum temperature 1.5 h after oral administration (Chart 2). A transitory rise in temperature observed with oral administration. Chlorpromazine was administered 1 h later when the influence of oral administration had disappeared.

Data Analysis Statistical analysis was performed by Student's *t*-test.

Results

Preparing the Low Body Temperature Models After the intraperitoneal injection of 2.0, 4.0, 8.0 and 20.0 mg/kg of chlorpromazine, the rats gradually became calm, and their body temperature dropped below normal level. Figure 1 shows the time course of this temperature drop induced by

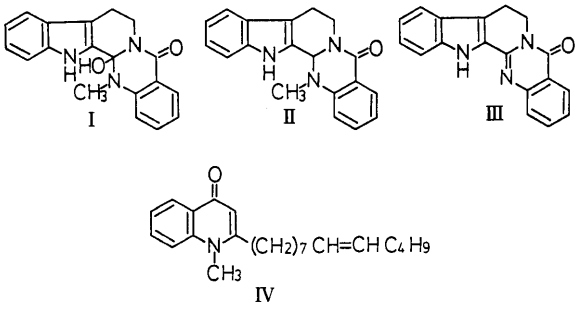

Chart 1

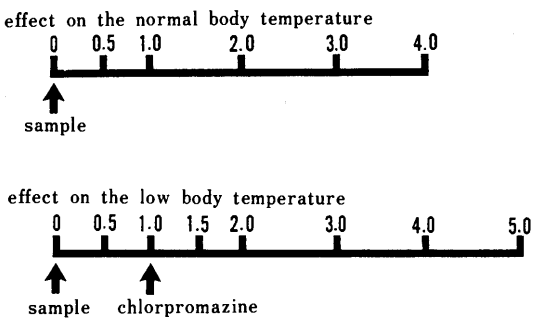

Chart 2

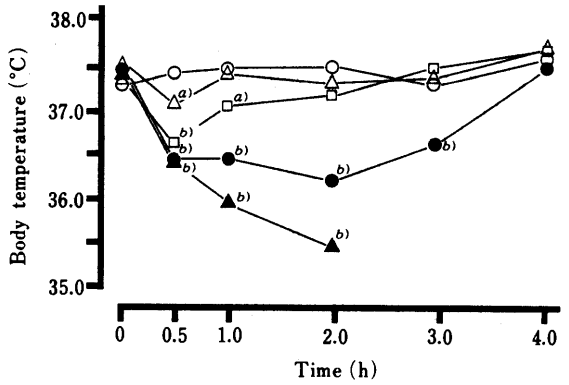

Fig. 1. Effect of Chlorpromazine on Rat Body Temperature ($n=10$)

○, control; △, 2.0 mg/kg; □, 4.0 mg/kg; ●, 8.0 mg/kg; ▲, 20.0 mg/kg.
Mean±S.D. at 2.0 h: ○, 37.50±0.37; △, 37.39±0.39; □, 37.17±0.43; ●, 36.18±0.35; ▲, 35.49±0.43.
a) $p<0.05$, *b*) $p<0.01$.

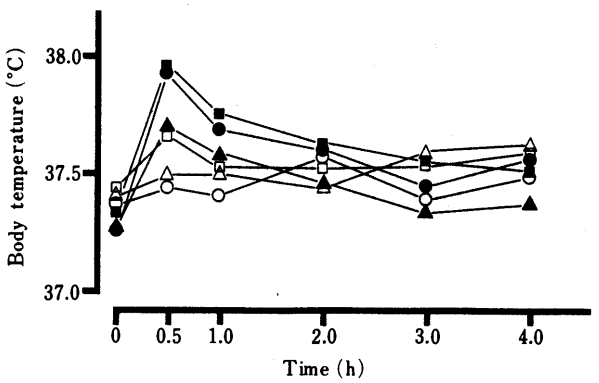

Fig. 2. Effect of Goshuyu-to, Evodia Fruit, Ginger, Ginseng and Jujube on Rectal Temperature of Normal Rats ($n=10$)

○, control; ■, Goshuyu-to (15 g/kg); ●, Evodia fruit (5.0 g/kg); ▲, Ginger (5.0 g/kg); □, Ginseng (5.0 g/kg); △, Jujube (5.0 g/kg).
Mean±S.D. at 0.5 h: ○, 37.44±0.52; ■, 37.92±0.59; ●, 37.89±0.61; ▲, 37.73±0.72; □, 37.66±0.58; △, 37.48±0.61.

each chlorpromazine dose and the time. With a 2.0 mg/kg chlorpromazine administration, the body temperature returned to normal within 1.0 h after injection, but with a 20.0 mg/kg injection, the body temperature was 35 °C or lower even, 3.0 h after administration. Thereafter, it became impossible to take measurements.

As a condition for producing a particular body temperature for subsequent experiments, we selected a chlorpromazine dose of 8.0 mg/kg. This value is preferable both for its reproducibility and for its effectiveness in lowering temperature.

Effects of Goshuyu-to and Its Component Crude Drugs on Body Temperature **A) Changes in Normal Body Temperature** After oral administration of 3.0 and 15.0 g/kg Goshuyu-to in the crude drug equivalent to untreated rats, there was a tendency for the animal's normal body temperature to rise, as shown in Fig. 2. The rise, however, did not depend on the dose and there was no significant difference. Meanwhile, after orally administering the sample drugs of Goshuyu-to component crude drugs Evodia fruit, Ginger, Ginseng and Jujube prepared at 1.0 and 5.0 g/kg in terms of crude drug weight, we measured normal body temperature. Evodia fruit and Ginger slightly raised temperature, but in this case, too, the reaction amount did not correlate to the dose, nor was there any significant difference.

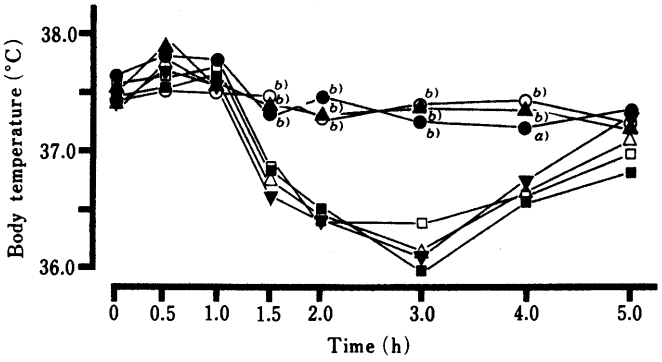

Fig. 3. Effect of Goshuyu-to, Evodia Fruit, Ginger, Ginseng and Jujube on Low Temperature Mode of Rats Induced by Chlorpromazine ($n=10$)

○, control; △, chlorpromazine (8.0 mg/kg): ●, Goshuyu-to (15 g/kg); ▲, Evodia fruit (5.0 g/kg); ■, Ginger (5.0 g/kg); ▼, Ginseng (5.0 g/kg); □, Jujube (5.0 g/kg).
Mean±S.D. at 3.0 h: ○, 37.43±0.33; △, 36.19±0.41; ●, 37.21±0.39; ▲, 37.38±0.37; ■, 36.04±0.44; ▼, 36.18±0.33; □, 36.49±0.35.
a) $p<0.05$, *b*) $p<0.01$.

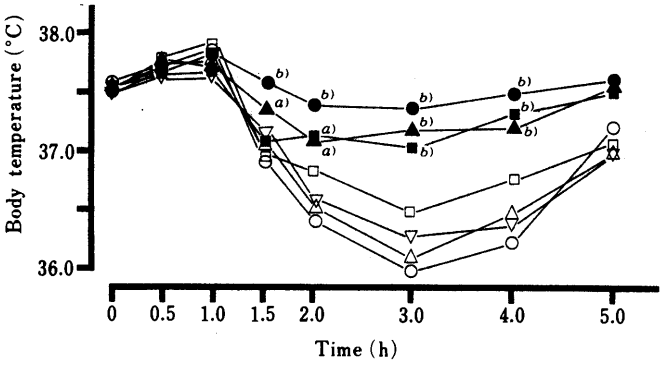

Fig. 4. Effect of Hydroxyevodiamine, Rutaecarpine, Evocarpine and Evodiamine on Low Temperature Mode of Rats Induced by Chlorpromazine ($n=10$)

○, chlorpromazine (8.0 mg/kg); ▲, evodiamine (5 mg/kg); ●, evodiamine (10.0 mg/kg); ■, *dl*-evodiamine (20.0 mg/kg); ▽, hydroxyevodiamine (10.0 mg/kg); □, rutaecarpine (10.0 mg/kg); △, evocarpine (10.0 mg/kg).
Mean±S.D. at 3.0 h: ○, 36.09±0.42; ▲, 37.23±0.29; ●, 37.46±0.41; ■, 37.08±0.34; ▽, 36.37±0.37; □, 36.50±0.52; △, 36.16±0.38.
a) $p<0.05$, *b*) $p<0.01$.

B) Changes in the Low Body Temperature State Intraperitoneally administering 8.0 mg/kg of chlorpromazine to rats 1.0 h after orally administering sample drugs, we measured body temperature in a time series (Fig. 3). As in the chlorpromazine administered control group, the 3.0 g/kg Goshuyu-to administered group showed a drop in body temperature, but no improvement in the low body temperature state. Meanwhile, in the 15.0 g/kg Goshuyu-to administered group, there was no drop in body temperature due to chlorpromazine, and instead the drug prevented such reduction, with the result that the group maintained a body temperature equal to that of the untreated normal rats.

Five g/kg of Evodia fruit proved to significantly prevent a drop in body temperature; the dose-dependence of what drop there was recognized. However, Ginger, Ginseng and Jujube showed no direct effect on the retention of temperature.

Effects of Alkaloid on Body Temperature **A) Changes in Normal Body Temperature** Since the body temperature retaining effect of Evodia fruit was recognized, we studied the main alkaloids in this component. First, we orally ad-

ministered to rats 10.0 mg/kg each of hydroxyevodiamine, evodiamine, rutaecarpine and evocarpine, and measured their normal body temperature. No alkaloid showed a significant effect on this temperature.

B) Changes in Low Body Temperature State Orally administering rats with hydroxyevodiamine (10.0 mg/kg), rutaecarpine (10.0 mg/kg) and evocarpine (10.0 mg/kg), evodiamine (2.0, 5.0 and 10.0 mg/kg) and intraperitoneally administering them with chlorpromazine (8.0 mg/kg) 1.0 h later, we sequentially measured their body temperature (Fig. 4). A body temperature retaining effect was recognized in the evodiamine (5.0 mg/kg) administered group, and a definite effect in preventing a drop in temperature was recognized in the 10.0 mg/kg administered group. However, no effect was observed with the other alkaloids.

Discussion

Goshuyu-to is a Chinese traditional medicine used for a syndrome characterized by cold hands and feet as a systemic symptom and migraines and vomiting as characteristic symptoms.

Evodia fruit and Ginger mixed with Toki-sigyaku-to can be used to treat chilblains and cold hands and feet. There is a strong possibility that the effect of Evodia fruit is related to thermogenesis and body temperature retention. Regarding this effect, Hon-zo-kou-moku mentions that it serves to warm the interior of the body and treats chills and fever.[4] Also, Sho-kan-ron mentions that it can be used for lesser yin disease, cold hand and feet, and for treating those who have felt cold for a long time.[4] Thus, there are expressions suggesting that it is concerned with retaining the temperature in the body's interior.

There have been reports[6] of a cardiotonic effect of Evodia fruit or alkaloids. It has further been reported that the methanol extract of Evodia fruit causes a slight rise in the body temperature of rabbits and that Toki-sigyaku-ka-goshuyu-shokyo-to causes a significant rise in the body temperature[7] of humans, but there have been no experiments clarifying improvements in the low body temperature state. The body temperature retaining action can be regarded as an intrinsic effect of Evodia fruit, and the authors confirmed this physiological action by low body temperature rat models, and searched for the substances responsible for this action.

We orally administered Goshuyu-to or Evodia fruit extract (the equivalent of 100 times the dose for an adult in terms of body weight), and Ginger extract (the equivalent of 150 times) to normally bred and untreated rats. A slight rise in body temperature was observed but it was not significant. On this point, we were unable to obtain experimental results which proved the conventional body temperature rise effect.

However, a significant body temperature retaining action (prevention of temperature reduction) was recognized when Goshuyu-to was administered to experimental low body temperature rats which had been given chlorpromazine. The action of Evodia fruit did not further raise the temperature when it was normal, but did affect it when it was low; only then was it effective. It is very interesting to have proven this fact and to have experimentally been able to understand the Chinese traditional medicine's effect. In addition, a similar effect was recognized in Evodia fruit alone, a component herbal medicine. No body temperature retaining effect was recognized in the other three component crude drugs, Ginger, Ginseng and Jujube. At least in these experiments, we were not able to prove the body temperature retaining action of these crude drugs.

Goshuyu-to prevents reduction in the body temperature of rats treated with chlorpromazine. The main cause of this effect is thought to be Evodia fruit, and the effect of the other compound crude drugs is believed to be indirect. Furthermore, each action of Evodia fruit alkaloid hydroxyevodiamine, evodiamine, rutaecarpine and evocarpine was studied during these experiments, and the body temperature retaining action recognized in Goshuyu-to and Evodia fruit was confirmed only in evodiamine. In a quantitative relation, while the 15.0 g/kg Goshuyu-to administration contained 4.1 g of Evodia fruit, a body temperature retaining effect was confirmed with the administration of 5.0 g/kg (almost the same weight as in the Evodia fruit extract administration). Since approximately 3 mg of evodiamine was contained in 5 g of the Evodia fruit aqueous extract in the crude drug equivalent, the body temperature retaining effect was confirmed in the 5.0 mg/kg of evodiamine used alone. This suggests that the main part of the retention effect of Goshuyu-to is due to evodiamine.

On the other hand, no marked effect was recognized in low temperature rats treated with chlorpromazine. The Ginger extract did, however, show a slightly higher body temperature than the normal rat body temperature. This suggests the involvement of a different action mechanism of the Ginger extract, which demonstrated the effect of slightly raising the normal rats body temperature. From the viewpoint of crude drug, Evodia fruit and Ginger which are believed to have body temperature production action, are involved with the improvement of the body temperature syndrome through independent and different action mechanisms. In this case, there is a possibility of developing a complex action, and this is now being studied.

We believe that the scientific endorsement of the efficacy of some crude drugs which these experiments have provided will contribute to the further scientific analysis of these drug.

References

1) Y. Kano, S. Kanemaki, M. Yasuda, K. Saito, K. Komatsu, *Shoyakugaku Zasshi*, **43**, 226 (1989).
2) Chui-kenkyuin, "Chugoku-Kampo-Igoziten," Chugoku-Kampo, Tokyo, 1983, p. 140.
3) Guang-zhou-zhong-yi-xiao-yuan, "Fang-ji-xiao," Shang-hai-ke-xiao-ji-zhu-zhuo-ban, Shanghai, 1979, p. 84.
4) K. Kimura, "Kokuyaku-honzokoumoku," Shun-yodo, Tokyo, 1975, p. 559.
5) Chui-kenkyuin, "Chokanlon," Chugoku-Kampo, Tokyo, 1978, p. 218.
6) J. Suzuki, S. Kanemaki, Y. Momose, K. Komatsu, Y. Kano, Abstract of Papers, 109th Annual Meeting of Pharmaceutical Society of Japan, Nagoya, April, 1989, IV, p. 121.
7) Y. Nishizawa and Y. Amakata, *Oriental Medicine and the Pain Clinic*, **17**, 162 (1987).

Structures and Cytotoxic Activity Relationship of Casearins, New Clerodane Diterpenes from *Casearia sylvestris* Sw.

Hiroshi MORITA,[a] Masahiko NAKAYAMA,[a] Hiroshi KOJIMA,[a] Koichi TAKEYA,[a] Hideji ITOKAWA,*[,a] Eloir Paulo SCHENKEL[b] and Mario MOTIDOME[c]

Department of Pharmacognosy, Tokyo College of Pharmacy,[a] Horinouchi 1432-1, Hachioji, 192-03 Tokyo, Japan, Faculdade Farmacia da UFRGS,[b] Ar. Ipiranga 90000 Port Alegre RGS, Brazil, and Instituto de Quimica, USP,[c] SP, Brazil. *Received July 23, 1990*

Casearins G—R, new cytotoxic clerodane diterpenes have been isolated from the leaves of *Casearia sylvestris* Sw. (Flacourtiaceae). Their structures have been elucidated by spectroscopic methods and chemical conversions, and their structure–activity relationships have been discussed.

Keywords *Casearia sylvestris*; Flacourtiaceae; cytotoxicity; clerodane diterpene; casearin; structure–activity relationship

Introduction

We have investigated antitumor substances contained in higher plants by the total packed cell volume method using Sarcoma 180 ascites in mice[1] and a cytotoxic test using Chinese hamster V-79 cells.[2] From *Casearia sylvestris*, one of the South American medicinal plants, antitumor and cytotoxic clerodane diterpenes, Casearins A—F were isolated and the structures reported in a previous paper.[3] In the process of isolating casearins A—F, the presence of many minor constituents presumed to be analogous clerodane diterpenes to casearins was revealed. Further investigation of *C. sylvestris* by the guidance of cytotoxic activity led to the isolation of minor cytotoxic clerodane diterpenes, named casearins G—R. These structures were elucidated by spectroscopic methods and chemical conversions. In this paper, the structures of casearins G—R and their structure–cytotoxic activity relationship are described.

Results and Discussion

The leaves of *Casearia sylvestris* Sw. (Flacourtiaceae) were extracted with hot ethanol (the extraction scale was set at 2.0 kg) and the extract showed strong antitumor activity reported in previous paper.[3] The *n*-hexane extract was prepared and purified by the procedure reported earlier.[3] Purification of fractions 5 and 6, as reported earlier, by high performance liquid chromatography (HPLC), whose fractions showed cytotoxic activity resulted in our isolating new cytotoxic clerodane diterpenes, named casearins G—R. The structures of the casearins isolated were revealed to possess the same basic *cis*-clerodane-type skeleton with various substituents as described below.

Casearin G, having the molecular formula, $C_{29}H_{42}O_8$ was obtained as colorless oil. The infrared (IR) spectrum of casearin G showed *exo*-methylene absorptions at 3100 and 920 cm^{-1} and ester carbonyl absorptions at 1770 and 1745 cm^{-1}. In the proton nuclear magnetic resonance (^{1}H-NMR) spectrum, the signals of two acetal protons (δ 6.67 and 6.41), a proton (δ 3.86) linked to methoxy-bearing carbon which was homoallylically coupled with one of the acetal protons and an olefinic proton (δ 5.99) which was allylically coupled with this acetal proton, appeared. Their presence was also characteristic of casearins A—F. Further, the presence of diene moiety was suggested by ^{1}H-NMR as shown in Table I and by ultraviolet (UV) (λ_{max} 233 nm, ε 13500) spectra. However, there was no other proton linked to oxygen-bearing carbon except for one (δ 4.90) linked to ester-bearing carbon. The position of this ester substituent was concluded to be at C-7 for the coupling pattern (triplet doublet), and the orientation of this ester must be equatorial because the coupling constants appeared at the value of 11.6 Hz (triplet) and 4.7 Hz (doublet). The ^{13}C-NMR spectrum (Table II) also corroborated with this structure as shown in Fig. 1. Casearins H and I were also disclosed to possess the structural features of casearin G. The site of ester substituents was elucidated by the ^{1}H–^{13}C long range coupling between the proton linked to ester-bearing carbon and the ester carbonyl carbon, and the nuclear Overhauser effect (NOE) observed between H-18 and acetyl methyl protons.

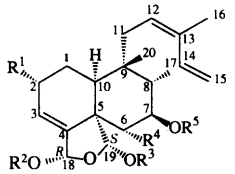

Casearins	R^1	R^2	R^3	R^4	R^5	IC_{50} (μmol/l)[a]
A	OMe	Ac	Ac[b]	OH	Bu[c]	1.0
B	OMe	Ac	Ac	OAc	Bu	8.5
C	OH	Ac	Ac	OAc	Dc[d]	0.77
D	OH	Bu	Ac	OH	Bu	1.8
E	OH	Et	Ac	OH	Dc	4.7
F	OH	Et	Ac	OH	Bu	29
G	OMe	Ac	Ac	H	Bu	0.17
H	OH	Ac	Ac	H	Bu	0.37
I	OH	Ac	Bu	H	Bu	0.51
J	OMe	Bu	Ac	OH	Bu	1.1
K	OAc	Ac	Ac	OH	Bu	0.52
L	OMe	Bu	Ac	OAc	H	1.6
M	OH	Bu	Bu	OAc	H	1.8
N	OMe	Ac	Bu	OAc	Bu	5.9
O	OMe	Bu	Ac	OAc	Bu	6.0
P	OMe	Ac	Ac	OAc	Ac	7.8
Q	OH	Ac	Ac	OAc	Bu	4.3
R	=O	Ac	Ac	OH	Bu	5.4
A_a	OMe	Ac	Ac	=O	Bu	0.55
A_b	OMe	Ac	Ac	OPr	Bu	17
A_c	OMe	Ac	Ac	OBu	Bu	38
D_a	=O	Bu	Ac	=O	Bu	19

a) Cytotoxic activities against V-79 cells, *b*) acetate, *c*) butylate, *d*) decanoate.

Fig. 1. Structures of Casearins and Their Derivatives and Cytotoxic Activities against V-79 Cells

TABLE I. ^{1}H Assignments of Casearins G—R, δ (ppm) from Tetramethylsilane in $CDCl_3$ (J/Hz in Parentheses, 400 MHz)

	Casearin G	H	I	J	K	L
H-2	3.86 (br s)	4.40 (br s)	4.39 (br s)	3.90 (br s)	5.45 (br s)	3.94 (br s)
H-3	5.99 (br d, J=4.2)	5.97 (br d, J=4.3)	5.95 (br d, J=4.3)	6.08 (br d, J=3.9)	6.00 (br d, J=4.0)	6.07 (br d, J=3.7)
H-6				3.65 (d, J=11.0)	3.66 (d, J=10.8)	5.05 (d, J=10.5)
H-7	4.90 (dt, J=4.7, 11.6)	4.90 (dt, J=4.7, 11.6)	4.91 (dt, J=4.7, 11.6)	4.98 (t, J=11.0)	4.97 (t, J=10.8)	3.63 (t, J=10.5)
H-10	2.22 (dd, J=2.3, 13.3)	a)	a)	a)	a)	2.36 (dd, J=3.0, 10.5)
H-11	2.51 (dd, J=16.2, 9.1)	a)	2.52 (dd, J=16.5, 9.5)	a)	2.51 (dd, J=16.2, 9.2)	2.53 (dd, J=16.1, 9.4)
H-12	5.31 (br d, J=10.1)	5.31 (br d, J=7.9)	5.31 (br d, J=6.3)	5.28 (br d, J=5.2)	5.23 (br d, J=9.2)	5.30 (br d, J=6.1)
H-14	6.64 (dd, J=10.8, 17.1)	6.63 (dd, J=10.9, 17.2)	6.63 (dd, J=10.8, 17.2)	6.62 (dd, J=11.0, 17.1)	6.61 (dd, J=10.8, 17.5)	6.62 (dd, J=10.9, 17.3)
H-15	5.11 (d, J=10.8)	5.12 (d, J=10.9)	5.12 (d, J=10.8)	5.11 (d, J=11.0)	5.11 (d, J=10.8)	5.11 (d, J=10.9)
	5.19 (d, J=17.1)	5.20 (d, J=17.2)	5.20 (d, J=17.2)	5.20 (d, J=17.1)	5.19 (d, J=17.5)	5.20 (d, J=17.3)
Me-16	1.80 (br s)	1.80 (br s)	1.80 (br s)	1.79 (br s)	1.79 (br s)	1.80 (br s)
Me-17	0.89 (d, J=6.4)	0.89 (d, J=6.5)	0.90 (d, J=6.2)	0.92 (d, J=7.2)	0.89 (d, J=6.7)	1.06 (d, J=6.7)
H-18	6.67 (t, J=1.3)	6.67 (t, J=1.5)	6.69 (t, J=1.5)	6.73 (t, J=1.7)	6.70 (t, J=1.6)	6.45 (t, J=1.7)
H-19	6.41 (s)	6.43 (s)	6.42 (s)	6.56 (s)	6.56 (s)	6.52 (s)
Me-20	0.90 (s)	0.90 (s)	0.90 (s)	0.87 (s)	0.81 (s)	0.89 (s)
MeO-	3.43 (s)			3.43 (s)		3.44 (s)
Me-Ac	1.98 (s)	1.99 (s)	1.98 (s)	1.98 (s)	1.98 (s)	1.99 (s)
	2.09 (s)	2.10 (s)			2.07 (s)	2.08 (s)
					2.08 (s)	
Me-Bu	0.94 (t, J=7.3)	0.94 (t, J=7.4)	0.94 (t, J=7.4)	0.94 (t, J=7.4)	0.98 (t, J=7.4)	0.96 (t, J=7.4)
			0.95 (t, J=7.4)	0.96 (t, J=7.4)		

	Casearin M	N	O	P	Q	R
H-2	4.47 (br s)	3.94 (br s)	3.95 (br s)	3.95 (br s)	4.49 (br s)	
H-3	6.01 (br d, J=3.4)	6.07 (br d, J=3.7)	6.08 (br d, J=3.8)	6.09 (br d, J=3.8)	6.05 (br d, J=3.4)	6.20 (d, J=1.5)
H-6	5.03 (d, J=10.7)	5.19 (d, J=10.5)	5.21 (d, J=11.0)	5.18 (d, J=10.4)	5.19 (d, J=10.6)	3.85 (t, J=10.5)
H-7	3.61 (t, J=10.7)	5.15 (t, J=10.5)	5.16 (t, J=11.0)	5.13 (t, J=10.4)	5.15 (t, J=10.6)	5.04 (t, J=10.5)
H-10	a)	2.39 (dd, J=3.4, 13.6)	2.39 (dd, J=3.1, 13.5)	2.40 (dd, J=3.4, 13.7)	2.43 (dd, J=4.0, 13.1)	a)
H-11	2.53 (dd, J=16.1, 9.4)	2.55 (dd, J=16.2, 9.4)	2.55 (dd, J=16.2, 9.3)	2.55 (dd, J=16.0, 9.1)	2.56 (dd, J=16.2, 9.3)	2.89 (dd, J=13.6, 6.0)
H-12	5.29 (br d, J=7.9)	5.29 (br d, J=3.9)	5.29 (br d, J=8.0)	5.29 (br d, J=8.0)	5.29 (br d, J=6.8)	5.22 (br d, J=10.4)
H-14	6.61 (dd, J=10.8, 17.1)	6.63 (dd, J=10.8, 17.2)	6.63 (dd, J=10.8, 17.2)	6.64 (dd, J=10.6, 17.4)	6.63 (dd, J=10.9, 17.3)	6.60 (dd, J=10.8, 16.7)
H-15	5.11 (d, J=10.8)	5.12 (d, J=10.8)	5.12 (d, J=10.8)	5.13 (d, J=10.6)	5.13 (d, J=10.9)	5.16 (d, J=10.8)
	5.19 (d, J=17.1)	5.20 (d, J=17.2)	5.20 (d, J=17.2)	5.21 (d, J=17.4)	5.20 (d, J=17.3)	5.24 (d, J=16.7)
Me-16	1.79 (br s)	1.79 (br s)	1.80 (br s)	1.80 (br s)	1.80 (br s)	1.81 (br s)
Me-17	1.05 (d, J=6.7)	0.89 (d, J=6.7)	0.89 (d, J=6.2)	0.91 (d, J=6.6)	0.88 (d, J=6.7)	0.96 (d, J=7.5)
H-18	6.45 (t, J=1.6)	6.43 (t, J=1.7)	6.41 (t, J=1.6)	6.42 (t, J=1.6)	6.40 (t, J=1.7)	6.85 (d, J=1.5)
H-19	6.52 (s)	6.60 (s)	6.60 (s)	6.60 (s)	6.61 (s)	6.68 (s)
Me-20	0.87 (s)	0.89 (s)	0.89 (s)	0.90 (s)	0.89 (s)	0.84 (s)
MeO-		3.43 (s)	3.44 (s)	3.44 (s)		
Me-Ac	1.97 (s)	1.98 (s)	1.99 (s)	2.00 (s)	2.00 (s)	2.02 (s)
		2.04 (s)	2.06 (s)	2.01 (s)	2.04 (s)	2.10 (s)
				2.06 (s)	2.07 (s)	
				2.08 (s)		
Me-Bu	0.93 (t, J=7.5)	0.93 (t, J=7.4)	0.92 (t, J=7.4)		0.92 (t, J=7.4)	0.97 (t, J=7.5)
	0.94 (t, J=7.5)	0.94 (t, J=7.4)	0.93 (t, J=7.4)			

a) The chemical shifts and coupling constants were not revealed because of the overlapping of the other protons. Me and Bu mean methyl and butyl groups, respectively.

Casearins J and K bore a marked structural resemblance to casearins A and D, especially at the point of possessing a hydroxyl moiety at C-6. The proton signal of H-7 (δ 4.98) in casearin J was coupled with the proton of H-6 (δ 3.65) attached to a hydroxyl-bearing carbon and the proton of H-8 at the value of 11.0 Hz, respectively. Further, the signal of H-6 was also coupled with a hydroxy proton at 9.0 Hz, which disappeared on addition of D_2O. In the case of casearin K, the presence of acetyl moiety at C-2 was suggested by the chemical shift (δ 5.45) of the proton linked at C-2. From this spectral evidence, the structures of casearins J and K were elucidated.

The structural characteristics of casearins L and M are represented by a hydroxyl moiety attached at C-7. The proton signal of triplet (δ 3.63) linked at C-7 in casearin L was shifted at high field compared with other casearins, and a hydroxy absorption band (3625 cm^{-1}) was also observed in the IR spectrum. This spectroscopic feature was consistent with the structures of casearins L and M.

The structures of casearins N, O, P and Q were characterized by their esteric functions of acetic acid or *n*-butylic acid at R^2—R^5.

Casearin R was obtained as a colorless oil having an UV absorption band at 233 nm ascribable to an α,β-unsaturated ketone and a diene moiety. The homoallyl long range coupling characteristic of H-18 disappeared and the IR absorption (1685 cm^{-1}) also indicated the presence of α,β-unsaturated ketone. The hydroxyl group attached at C-6 was found not to be esterificated such as in casearins J and K from the proton chemical shift of H-6 (δ 3.85).

In order to confirm the structural relationship among casearins, the structural conversion of each was carried out.

TABLE II. ^{13}C Assignments of Casearins G—R, δ (ppm) from Tetramethylsilane in $CDCl_3$ (100 MHz)

	Casearin G	H	I	J	K	L	M	N	O	P	Q	R
C-1	24.6	28.8	28.9	25.6	26.8	25.4	29.5	25.5	25.4	25.4	29.5	40.7
C-2	72.7	63.9	64.0	72.6	65.9	72.6	63.6	72.5	72.5	72.5	63.6	197.6
C-3	122.7	124.5	124.4	123.5	122.0	126.2	126.0	125.4	125.4	125.5	127.3	124.7
C-4	144.2	144.1	144.3	142.9	144.5	141.6	141.5	141.4	141.4	141.4	141.2	163.5
C-5	49.7	49.6	49.7	53.8	53.6	52.8	52.7	52.9	52.9	52.8	52.8	54.9
C-6	34.2	34.2	34.3	75.2	74.9	72.3	72.1	74.0	73.7	74.1	73.9	74.7
C-7	71.4	71.2	71.3	75.4	75.4	76.9	76.8	72.7	72.8	73.2	72.7	75.7
C-8	41.0	41.1	41.2	41.1	41.0	43.2	43.1	41.0	41.0	41.0	41.1	40.8
C-9	39.5	39.5	39.6	39.4	39.2	39.1	39.0	39.3	39.2	39.3	39.3	39.9
C-10	33.9	33.3	33.4	35.8	36.1	36.8	36.2	36.7	36.7	36.7	36.2	35.5
C-11	30.3	30.3	30.3	30.3	30.1	30.2	30.2	30.1	30.1	30.2	30.2	29.8
C-12	125.9	125.7	125.7	125.8	125.5	125.2	127.0	125.8	125.8	125.8	125.6	124.9
C-13	133.8	134.0	134.0	133.9	134.0	133.8	133.8	133.9	133.9	134.0	134.1	134.6
C-14	133.4	133.4	133.4	133.4	133.2	133.3	133.3	133.3	133.3	133.3	133.3	133.1
C-15	114.4	114.6	114.5	114.6	114.7	114.6	114.6	114.6	114.7	114.7	114.8	115.2
C-16	20.2	20.3	20.3	20.2	20.3	20.3	20.2	20.2	20.3	20.3	20.3	20.4
C-17	10.7	10.7	10.7	11.1	11.0	11.2	11.2	11.0	11.1	11.0	11.0	11.1
C-18	94.5	94.4	94.2	95.6	95.6	95.1	94.8	94.7	95.0	95.0	94.9	95.0
C-19	99.1	99.1	99.1	97.5	97.4	97.8	97.8	97.7	97.7	97.7	97.7	97.3
C-20	25.7	25.8	25.8	25.4	25.3	25.5	25.5	25.5	25.5	25.4	25.5	24.6
OMe	56.9			57.0		57.1		57.0	57.1	57.1		
Acetylate	21.2	21.2	21.2	21.3	20.9	21.3	21.3	21.1	21.3	20.6	21.0	21.0
	169.2	169.1	169.0	169.0	168.8	169.4	169.1	169.1	169.2	169.2	168.9	168.5
	21.2	21.3			21.1	21.5		21.4	21.4	21.0	21.2	21.2
	170.4	170.3			170.0	170.3		170.3	170.2	170.0	170.0	169.5
					21.2					21.3	21.4	
					171.5					170.1	170.2	
										21.4		
										170.3		
Butylate	13.7	13.7	13.7	13.5	13.5	13.7	13.5	13.5	13.8		13.7	13.7
	18.5	18.5	18.6	18.3	18.6	18.3	18.2	18.3	18.1		18.4	18.6
	36.4	36.4	36.4	36.3	36.4	36.5	36.3	36.1	36.1		36.1	36.3
	172.7	172.8	172.8	172.8	173.0	174.0	172.7	172.6	172.6		172.6	174.5
			13.6	13.7			13.6	13.8	13.8			
			18.3	18.6			18.2	18.4	18.4			
			36.3	36.4			36.4	36.3	36.3			
			172.7	174.3			174.0	172.8	172.9			

Acetylation of casearin J gave casearin O, which was also obtained by butylation of casearin L, and the same compound (**1**) was produced by acetylation of casearins Q and K. The oxidation of casearin Q by pyridinium dichlomate (PDC) and acetylation of casearin R also gave the same compound (**2**).

Further, the presence of each ^1H–^{13}C long range coupling between ester carbonyl carbon and the proton linked to ester-bearing carbon has provided powerful evidence in confirming the position of their esters.

Cytotoxic activities (IC_{50} value) against V-79 cells of these casearins A—R are listed in Fig. 1, and were classified in several groups; groups A, B, C and D, in particular, by remarking at the point of substituent at C-6. Group A which showed the strongest activity includes casearins G, H and I, whose structures were characterized by the lack of oxygen-bearing function at C-6. Casearins J and K, whose structures were characteristic of a hydroxy moiety at C-6 belong to the next group B and possess similar or slightly weaker activity than group A. The structures of casearins L and M are characterized by possession of a hydroxy moiety at not C-6 but C-7, and this group C had a little weaker activity than group B. The other casearins, N, O, P, Q and R belong to the last group D which showed only weak activity. Further, this activity was found to be little influenced by whether the substituents of R^1 were methoxyl, hydroxyl or oxygen. By this classification, casearins A and D belong to group B and casearin B belongs to group D. The only exception among these groups is casearin C, whose structural features include possession of decanoate substituent at C-7 and which belongs to group D. Casearin C exhibited about ten-fold more activity than the other casearins in group D and its hydrophobicity is considered to be remarkably larger than those of the other casearins. For this reason, affinity for the membrane of V-79 cells may increase and exhibit strong activity.

Then, to investigate the influence of substituents at C-6, derivatives A_a, A_b, A_c and D_a at R^4 were converted from casearins A and D. As shown in Fig. 1, inducement of acyl substituent at C-6 was found to cause marked weakness in the activity. These results support that bulkiness of the substituent at C-6 has the greatest influence on the activity.

Experimental

All melting points were recorded on a Yanagimoto micro melting apparatus and are uncorrected. Spectral data were obtained on the following instruments: optical rotation on a JASCO DIP-4, IR on a JASCO A-302, UV on a Hitachi 557, NMR on a Brucker AM 400 and MS on a Hitachi M-80. HPLC was carried out on a CIG column system (Kusano Scientific Co., Tokyo) with 10 μ silica gel as the stationary phase. Reversed phase HPLC was carried out on a YMC R and D column packed with

5 μ ODS.

Bioassay of Cytotoxic Activity against V-79 Cells Cloned Chinese hamster V-79 cells, supplied by Dr. S. Tsukagoshi of the Japan Foundation for Cancer Research, were maintained in RPMI-1640 medium (Mitsubishi Chemical Industry Co., Ltd.) and kanamycin (100 μg/ml). The cells (3×10^5 cells/well) were cultured in Corning disposable 6-well plates containing 2 ml of growth medium per well and were incubated at 37 °C in a humidified atmosphere of 5% CO_2. Various drug concentrations (10 μl) were added to the cultures at day 1 after the transplantation. The colonies were fixed with a 1% formaldehyde solution (2 ml) for 20 min and stained with 0.05% crystal violet (0.75 ml) at day 5. The cytotoxic activity of the drugs was assessed by determining the T (number of stained colonies of test groups)/C (those of control groups) $\times$ 100 values or IC_{50} (drug concentration that inhibits colony growth by 50%) in drug-containing medium relative to colony growth in 0.5% EtOH medium at day 5 after drug treatment.

Extraction and Isolation The leaves of *C. sylvestris* used in this investigation were collected on the grounds of the Universidade de Sao Paulo in August 1987. *Casearia sylvestris* was botanically identified by Prof. Dr. Sylvio Panizza, Departmento de Botanica in the Universidade de Sao Paulo and these leaves (2 kg) were extracted with hot ethanol three times and concentrated to give ethanolic extract (140 g). Then, this ethanolic extract was distributed to *n*-hexane, chloroform, ethyl acetate and water soluble fractions, respectively, and the activity was concentrated into *n*-hexane soluble fraction as described in a previous paper.[3] This *n*-hexane soluble fraction was subjected to silica gel column chromatography and separated into seven fractions. Chromatographic purification of fractions 5 and 6 by silica gel HPLC using the benzene–ethyl acetate solvent system and ODS HPLC using the acetonitrile–water solvent system led to the isolation of casearins A—R.

Casearin G: Colorless oil, $[\alpha]_D$ +29.5° (c=0.26, $CHCl_3$). MS m/z (%): 518 (M^+, 2), 398 (M^+ −2AcOH, 18), 370 (10), 310 (20), 186 (100). High MS: $C_{21}H_{26}O_2$ Calcd 310.1931. Found 310.1923. UV λ_{max}^{EtOH} nm (ε): 204 (7200), 233 (13500). IR ν_{CCl_4} cm^{-1}: 3100, 3000, 2960, 1770, 1745, 1460, 1380, 1230, 1220, 1180, 1090, 1050, 1030, 1020, 990, 970, 940, 920.

Casearin H: Colorless oil, $[\alpha]_D$ +32.2° (c=0.1, $CHCl_3$). MS m/z (%): 504 (M^+, 3), 384 (M^+ −2AcOH, 18), 296 (27), 186 (100). High MS: $C_{24}H_{32}O_4$ Calcd 384.2298. Found 384.2277. UV λ_{max}^{EtOH} nm (ε): 204 (8000), 233 (16000). IR ν_{CCl_4} cm^{-1}: 3640, 3500, 3100, 3000, 2950, 1765, 1745, 1545, 1380, 1230, 1185, 1050, 1020, 990, 970, 940, 915, 890.

Casearin I: Colorless oil, $[\alpha]_D$ +32.5° (c=0.1, $CHCl_3$). MS m/z (%): 532 (M^+, 2), 384 (35), 296 (45), 215 (88), 186 (100), 157 (89). High MS: $C_{24}H_{32}O_4$ Calcd 384.2298. Found 384.2277. UV λ_{max}^{EtOH} nm (ε): 203 (9700), 233 (15900). IR ν_{CCl_4} cm^{-1}: 3620, 3090, 2970, 2940, 1760, 1740, 1460, 1250, 1215, 1180, 1060, 1010, 985, 965, 940, 910.

Casearin J: Colorless oil, $[\alpha]_D$ +29.9° (c=1.0, $CHCl_3$). MS m/z (%): 502 (M^+ −AcOH, 2), 474 (3), 414 (7), 326 (13), 256 (20), 223 (30), 187 (55), 157 (75), 107 (100). High MS: $C_{22}H_{38}O_7$ Calcd 414.2614. Found 414.2609. UV λ_{max}^{EtOH} nm (ε): 204 (7800), 233 (12100). IR ν_{CCl_4} cm^{-1}: 3600, 3100, 2990, 2950, 1760, 1740, 1460, 1380, 1370, 1220, 1180, 1080, 1000, 960, 930.

Casearin K: Colorless oil, $[\alpha]_D$ +43.4° (c=0.10, $CHCl_3$). MS m/z (%): 502 (M^+ −AcOH, 4), 442 (M^+ −2AcOH, 12), 294 (25), 224 (100). High MS: $C_{28}H_{38}O_8$ (M^+ −AcOH), Calcd 502.2564. Found 502.2611. UV λ_{max}^{EtOH} nm (ε): 205 (10000), 233 (12600). IR ν_{CCl_4} cm^{-1}: 3500, 3090, 2980, 1760, 1740, 1540, 1370, 1220, 1170, 1140, 1080, 1030, 1000, 980, 960, 925.

Casearin L: Colorless oil, $[\alpha]_D$ +21.7° (c=0.06, $CHCl_3$). MS m/z (%): 474 (M^+ −AcOH, 8), 414 (M^+ −2AcOH, 25), 326 (26), 157 (100). High MS: $C_{27}H_{38}O_7$ Calcd 474.2507. Found 474.2507. UV λ_{max}^{EtOH} nm (ε): 203 (9600), 234 (14700). IR ν_{CCl_4} cm^{-1}: 3625, 3465, 3092, 2972, 2936, 1758, 1373, 1226, 1179, 1106, 1085, 1026, 994, 961, 926, 909, 892.

Casearin M: Colorless oil, $[\alpha]_D$ +26.2° (c=0.2, $CHCl_3$). MS m/z (%): 548 (M^+, 1), 532 (M^+ −18, 2), 460 (M^+ −butyric acid, 40), 400 (35), 312 (40), 231 (100). High MS: $C_{26}H_{36}O_7$ (M^+ −butyric acid), Calcd 460.2459. Found 460.2469. UV λ_{max}^{EtOH} nm (ε): 205 (11600), 233 (20000). IR ν_{CCl_4} cm^{-1}: 3640, 3000, 2970, 1760, 1545, 1380, 1220, 1180, 1070, 1040, 1010, 940.

Casearin N: Colorless oil, $[\alpha]_D$ +40.1° (c=0.2, $CHCl_3$). MS m/z (%): 544 (M^+ −AcOH, 2), 474 (3), 308 (35), 255 (27), 223 (32), 185 (54), 157 (100). High MS: $C_{21}H_{24}O_2$ Calcd 308.1775. Found 308.1778. UV λ_{max}^{EtOH} nm (ε): 204 (10000), 233 (20000). IR ν_{CCl_4} cm^{-1}: 3100, 2980, 2950, 1755, 1460, 1370, 1230, 1215, 1160, 1085, 1065, 1020, 990.

Casearin O: Colorless oil, $[\alpha]_D$ +36.4° (c=0.15, $CHCl_3$). MS m/z (%): 544 (M^+ −AcOH, 4), 484 (6), 396 (7), 308 (35), 256 (40), 186 (100), 157 (96). High MS: $C_{25}H_{32}O_4$ Calcd 396.2299. Found 396.2314. UV λ_{max}^{EtOH} nm (ε): 204 (9400), 233 (20600). IR ν_{CCl_4} cm^{-1}: 3100, 2990, 2950, 1765, 1750, 1460, 1370, 1230, 1185, 1090, 1030, 1000.

Casearin P: Colorless oil, $[\alpha]_D$ +32.1° (c=0.3, $CHCl_3$). MS m/z (%): 488 (M^+ −AcOH, 30), 428 (M^+ −2AcOH, 20), 368 (M^+ −3AcOH, 30), 308 (M^+ −4AcOH, 60), 228 (100). High MS: $C_{27}H_{36}O_8$ (M^+ −AcOH), Calcd 488.2407. Found 488.2400. UV λ_{max}^{EtOH} nm (ε): 204 (9200), 233 (20000). IR ν_{CCl_4} cm^{-1}: 3100, 2995, 2950, 1760, 1370, 1240, 1225, 1110, 1090, 1030, 990.

Casearin Q: Colorless oil, $[\alpha]_D$ +39.1° (c=0.3, $CHCl_3$). MS m/z (%): 502 (M^+ −AcOH, 8), 442 (10), 294 (38), 186 (80), 157 (100). High MS: $C_{28}H_{38}O_8$ (M^+ −AcOH), Calcd 502.2564. Found 502.2581. UV λ_{max}^{EtOH} nm (ε): 203 (8500), 234 (17500). IR ν_{CCl_4} cm^{-1}: 3640, 2990, 2955, 1765, 1755, 1375, 1235, 1220, 1180, 1095, 1035.

Casearin R: Colorless oil, $[\alpha]_D$ +12.5° (c=0.08, $CHCl_3$). MS m/z (%): 458 (M^+ −AcOH, 8), 398 (M^+ −2AcOH, 85), 310 (25), 201 (100). UV λ_{max}^{EtOH} nm (ε): 233 (17000). IR ν_{CCl_4} cm^{-1}: 3500, 3100, 3000, 2960, 1765, 1685, 1545, 1380, 1220, 1180, 1110, 1080, 1030, 1000.

Chemical Conversion from Casearins J and L to Casearin O Acetylation of casearin J by acetic anhydride in pyridine and butylation of casearin L by butyric anhydride in pyridine were carried out overnight at room temperature. By both reactions, a compound completely identical to casearin O by direct comparison was produced.

Acetylation of Casearins K and Q to Afford 1 Acetylation of casearins K and Q as described above afforded the same compound **1**: Colorless oil. ^{1}H-NMR ($CDCl_3$) δ: 0.86 (3H, s), 0.90 (3H, d, J=6.8), 1.00 (3H, t, J=7.4), 1.82 (3H, s), 2.00 (3H, s), 2.01 (3H, s), 2.06 (3H, s), 2.07 (3H, s), 5.13 (1H, t, J=10.5), 5.15 (1H, d, J=10.8), 5.19 (1H, d, J=10.5), 5.22 (1H, d, J=17.0), 5.51 (1H, br s), 6.03 (1H, br d, J=3.2), 6.42 (1H, t, J=1.6), 6.62 (1H, s), 6.64 (1H, dd, J=10.8, 17.0). IR ν_{CCl_4} cm^{-1}: 3090, 2966, 2934, 1757, 1550, 1371, 1260, 1238, 1223, 1171, 1101, 1075, 1027.

Oxidation of Casearin Q and Acetylation of Casearin R to Afford 2: Colorless oil. ^{1}H-NMR ($CDCl_3$) δ: 0.86 (3H, s), 0.93 (3H, d, J=6.8), for 4 h at room temperature. Then, dry ether (20 ml) was added, the reaction mixture was filtered and the filtrate was evaporated to afford **2**, which was also produced by acetylation of casearin R in the same way. Compound **2**: Colroless oil. ^{1}H-NMR ($CDCl_3$) δ: 0.86 (3H, s), 0.93 (3H, d, J=6.8), 0.95 (3H, t, J=7.4), 1.82 (3H, s), 2.02 (3H, s), 2.07 (3H, s), 2.08 (3H, s), 2.93 (1H, dd, J=6.3, 13.1), 5.17 (1H, d, J=10.9), 5.22 (1H, t, J=11.0), 5.24 (1H, d, J=16.0), 5.34 (1H, d, J=11.0), 6.18 (1H, d, J=1.6), 6.56 (1H, d, J=1.6), 6.62 (1H, dd, J=10.9, 16.0), 6.70 (1H, s). IR ν_{CCl_4} cm^{-1}: 2970, 2940, 1765, 1760, 1685, 1545, 1370, 1260, 1225, 1100, 1025.

Preparation of A_a and D_a Casearins A and D were treated with PDC in methylene chloride for 6 h at room temperature. Dry ether was then added, the reaction mixture was filtered and the filtrate was evaporated to afford crude oil, respectively. Chromatographic purification of this oil by silica gel afforded oxidative compounds A_a and D_a. Compound A_a: colorless oil. MS m/z (%): 532 (M^+, 4), 472 (M^+ −60, 15), 412 (M^+ −2AcOH, 25), 324 (45), 201 (100). ^{1}H-NMR ($CDCl_3$) δ: 0.97 (3H, s), 0.98 (3H, t, J=7.4), 1.05 (3H, d, J=6.7), 1.84 (3H, br s), 2.02 (3H, s), 2.08 (3H, s), 2.74 (1H, dd, J=9.3, 16.2), 3.84 (1H, br s), 3.42 (3H, s), 5.17 (1H, d, J=17.1), 5.37 (1H, br d, J=4.3), 6.19 (1H, d, J=4.3), 6.66 (1H, s), 6.67 (1H, dd, J=10.8, 15.6), 6.72 (1H, t, J=1.5). IR ν_{CCl_4} cm^{-1}: 3100, 2990, 2950, 1770, 1755, 1740, 1540, 1460, 1380, 1220, 1165, 1090, 1050, 1025, 985, 965, 935.

Compound D_a: Colorless oil. MS m/z (%): 396 (M^+ −AcOH−butyric acid, 20), 308 (55), 240 (100). ^{1}H-NMR ($CDCl_3$) δ: 0.93 (3H, s), 0.95 (3H, t, J=7.4), 1.10 (3H, d, J=6.6), 1.85 (3H, br s), 2.03 (3H, s), 5.21 (1H, d, J=10.8), 5.28 (1H, d, J=17.4), 5.29 (1H, d, J=8.3), 5.43 (1H, d, J=12.7), 6.26 (1H, d, J=1.6), 6.64 (1H, dd, J=10.7, 17.1), 6.79 (1H, s), 6.87 (1H, d, J=1.6). IR ν_{CCl_4} cm^{-1}: 3100, 2970, 2940, 1770, 1755, 1735, 1690, 1550, 1380, 1250, 1210, 1160, 1080, 1060, 1010, 960.

Preparation of A_b and A_c Casearin A was treated with propionic anhydride and butyric anhydride in pyridine, respectively, overnight at room temperature. After work-up in the usual manner, compounds A_b and A_c were obtained, respectively. Compound A_b: Colorless oil. MS m/z (%): 590 (M^+, 2), 530 (M^+ −AcOH, 25), 470 (M^+ −2AcOH, 30), 396 (10), 217 (100). ^{1}H-NMR ($CDCl_3$) δ: 0.88 (3H, d, J=6.5), 0.89 (3H, s), 0.93 (3H, t, J=7.4), 1.11 (3H, t, J=7.6), 1.80 (3H, br s), 1.99 (3H, s), 2.07 (3H, s), 2.55 (1H, dd, J=9.4, 16.3), 3.44 (3H, s), 3.95 (1H, br s), 5.12 (1H, d, J=10.7), 5.16 (1H, t, J=10.4), 5.20 (1H, t, J=10.4), 5.21 (1H, d, J=17.3), 5.29 (1H, br d, J=8.0), 6.08 (1H, br d, J=3.6), 6.39 (1H, t, J=1.6), 6.61 (1H, s), 6.64 (1H, dd, J=10.8, 17.2). IR ν_{CCl_4} cm^{-1}: 2990, 2950, 1765, 1750, 1540, 1460, 1370, 1225, 1190, 1090, 1030, 1010, 990, 960. Compound A_c: Colorless oil. MS m/z (%): 544 (M^+ −AcOH, 20), 484 (M^+ −2AcOH, 20), 396 (20), 308 (85), 256 (100). ^{1}H-NMR ($CDCl_3$) δ: 0.88 (3H, d, J=6.3), 0.89 (3H, s), 0.92 (3H, t, J=7.4), 0.93 (3H, t,

$J=7.4$), 1.80 (3H, br s), 1.99 (3H, s), 2.06 (3H, s), 2.55 (1H, dd, $J=9.3$, 16.1), 3.44 (3H, s), 3.95 (1H, br s), 5.12 (1H, d, $J=10.8$), 5.16 (1H, t, $J=10.0$), 5.20 (1H, d, $J=17.0$), 5.21 (1H, d, $J=10.0$), 5.29 (1H, br d, $J=6.4$), 6.08 (1H, br d, $J=3.4$), 6.41 (1H, t, $J=1.5$), 6.60 (1H, s), 6.64 (1H, dd, $J=10.9$, 17.3). IR ν_{CCl_4} cm^{-1}: 3100, 3000, 2960, 1770, 1755, 1545, 1460, 1375, 1230, 1190, 1095, 1035, 1005.

References

1) H. Itokawa, F. Hirayama, K. Funakoshi and K. Takeya, *Chem. Pharm. Bull.*, **33**, 3488 (1985); H. Itokawa, N. Totsuka, K. Nakahara, K. Takeya, J. P. Lepoittevin and Y. Asakawa, *ibid.*, **35**, 3016 (1987); H. Itokawa, H. Morita, T. Sumitomo, N. Totsuka and K. Takeya, *Planta Medica*, **53**, 32 (1987); H. Itokawa, S. Tsuruoka, K. Takeya, N. Mori, T. Sonobe, S. Kosemura and T. Hamanaka, *Chem. Pharm. Bull.*, **35**, 1660 (1987); H. Itokawa, Y. Ichihara, K. Watanabe and K. Takeya, *Planta Medica*, **55**, 271 (1989).
2) H. Itokawa, H. Morita, I. Katou, K. Takeya, A. J. Cavalheiro, R. C. B. de Oliveira, M. Ishige and M. Motidome, *Planta Medica*, **54**, 311 (1988); H. Itokawa, N. Totsuka, K. Nakahara, M. Maezuru, K. Takeya, M. Kondo, M. Inamatsu and H. Morita, *Chem. Pharm. Bull.*, **37**, 1619 (1989); H. Morita, E. Kishi, K. Takeya, H. Itokawa and O. Tanaka, *Chem. Lett.*, **1990**, 749.
3) H. Itokawa, N. Totsuka, K. Takeya, K. Watanabe and E. Obata, *Chem. Pharm. Bull.*, **36**, 1585 (1988); H. Itokawa, N. Totsuka, H. Morita, K. Takeya, Y. Iitaka, E. P. Schenkel and M. Motidome, *ibid.*, **38**, 3384 (1990).

Novel Polyhydroxylated Steroidal Saponins from *Allium giganteum*

Yutaka SASHIDA,* Kazuhiro KAWASHIMA and Yoshihiro MIMAKI

Tokyo College of Pharmacy, Horinouchi 1432-1, Hachioji, Tokyo 192-03, Japan. *Received August 3, 1990*

From the bulbs of *Allium giganteum*, three new steroidal saponins, (25*R*)-3-*O*-acetyl-5α-spirostan-2α,3β,5α,6β-tetraol 2-*O*-β-D-glucopyranoside (2), (25*R*)-5α-spirostan-2α,3β,5α,6β-tetraol 2-*O*-β-D-glucopyranoside (3) and (25*R*)-3-*O*-benzoyl-5α-spirostan-2α,3β,5α,6β-tetraol 2-*O*-β-D-glucopyranoside (4), have been isolated. The new saponins are unique in structure having the sugar moiety at the C-2 hydroxyl position on the steroidal skeleton.

Keywords *Allium giganteum*; Liliaceae; steroidal saponin; alliogenin; alliogenin 2-*O*-glucoside; bulb

Plants of the genus *Allium* have been used both as food and as a medicinal material.[1] The occurrence of steroidal saponins in the bulbs is well documented.[2] In this paper, we describe the isolation and characterization of three new steroidal saponins isolated from the bulbs of *Allium giganteum*, which is indigenous to Central Asia.

Commercially available fresh bulbs of *A. giganteum* (9.8 kg) were extracted with hot methanol. The concentrated methanol extract was partitioned between chloroform and H_2O, and then between *n*-butanol and H_2O. The *n*-butanol soluble phase was subjected to silica gel column chromatography to give three steroidal compounds, **1**, **2** and **3**, and the chloroform soluble phase to give one steroidal compound, **4**.

Compound **1** was obtained as colorless plates, recrystallized from methanol, mp 305.0—310.0 °C, $[\alpha]_D$ −80.4° (pyridine). The molecular formula of **1**, $C_{27}H_{44}O_6$ was confirmed from the molecular ion peak at *m/z* 464 in the electron impact mass spectrum (EI-MS) and elemental analysis. Compound **1** showed characteristic infrared (IR) absorption bands of the (25*R*)-spiroketal moiety at 980, 920, 895, 860 cm^{-1} (intensity, 920<895).[3] The proton nuclear magnetic resonance (^{1}H-NMR) and carbon-13 nuclear magnetic resonance (^{13}C-NMR) spectra were indicative of **1** being (25*R*)-5α-spirostanol derivative with three secondary hydroxyl groups and a tertiary hydroxyl group which were localized at the A and/or B rings. The ^{1}H-NMR spectrum exhibited two protons bearing hydroxyl groups at δ 4.85 and 4.22 in pyridine-d_5. The ^{13}C-NMR spectrum showed a total of 27 carbons and the signal at δ 75.8 (pyridine-d_5) which disappeared in the distortionless enhancement by polarization transfer (DEPT) 135° spectrum; this was assigned to the C-5 position with α-hydroxyl group. The double resonance experiment in the ^{1}H-NMR spectrum indicated the existence of a C–CH_2–CH(OH)–CH(OH)–CH_2–C moiety, and the hydroxyl groups were present in the equatorial orientations confirmed by coupling constants of the α-protons. Further, the downfield chemical shift of the H-19 methyl function (δ 1.69 in pyridine-d_5) accounted for the presence of the β-axial hydroxyl groups at the C-6 position. The above spectral data identified compound **1** as (25*R*)-5α-spirostan-2α,3β,5α,6β-tetraol, or alliogenin, previously isolated from *Allium giganteum* by Khristulas *et al.*[4]

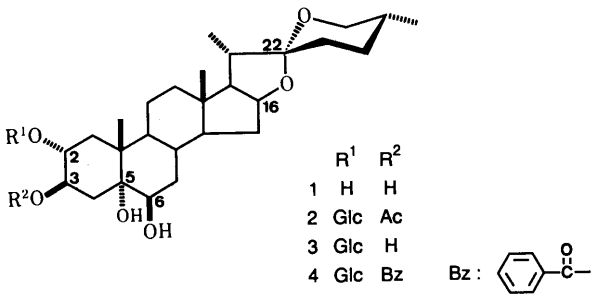

Compound **2** was obtained as a white amorphous powder, $[\alpha]_D$ −99.0° (methanol). The secondary ion mass spectrum (SI-MS) which showed a molecular ion peak at *m/z* 668 and elemental analysis confirmed the molecular formula of **2** as $C_{35}H_{56}O_{12}$. The IR spectrum proved the presence of a hydroxyl group(s) (3450 cm^{-1}), a carbonyl group (1720 cm^{-1}) and (25*R*)-spiroketal moiety (980, 920, 890 and 860 cm^{-1}; intensity 920<890). The ^{1}H-NMR spectrum (pyridine-d_5) showed the existence of two tertiary methyl groups (δ 1.54 and 0.88) and two secondary methyl groups [δ 1.12 (d, *J*=6.9 Hz) and 0.68 (d, *J*=5.8 Hz)]. In addition, signals for an acetyl group at δ 2.12 (3H, s) and an anomeric proton of hexose at δ 5.19 (1H, d, *J*=7.7 Hz) were indicated. The ^{13}C-NMR showed a total of 27 carbons arising from the aglycon moiety, six carbons from the hexose moiety

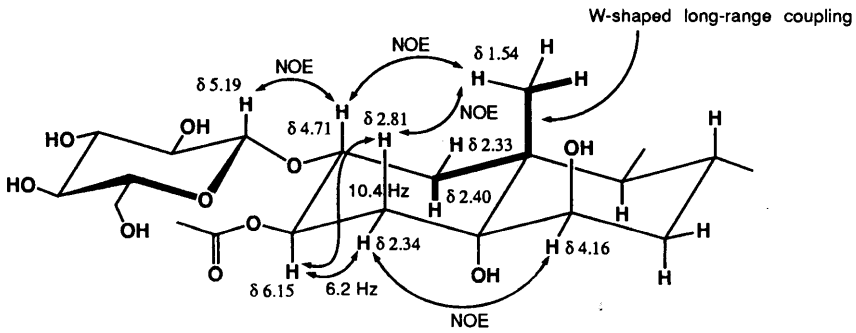

Fig. 1. ^{1}H-NMR Chemical Shifts, Spin-Coupling Constants and NOE Correlation of the A and B Rings (C_5D_5N) of **1**

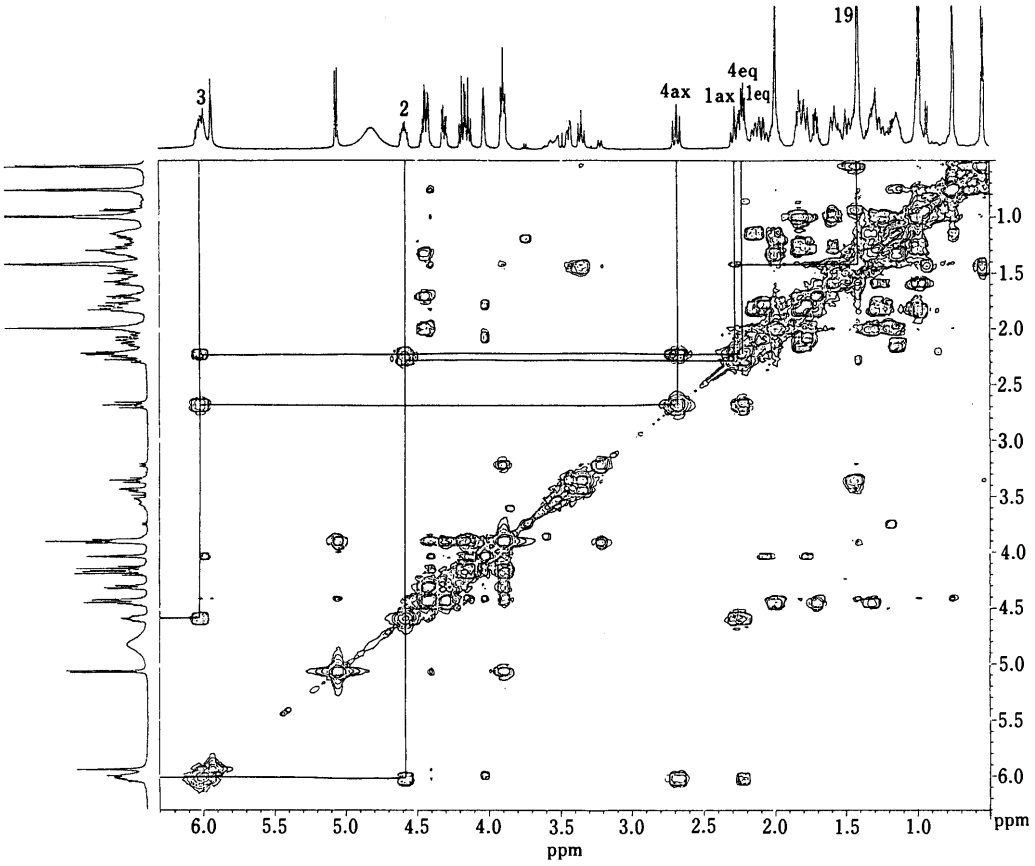

Fig. 2. ^1H–^1H Correlation 2D Spectrum of **2** in Pyridine-d_5 (400 MHz)

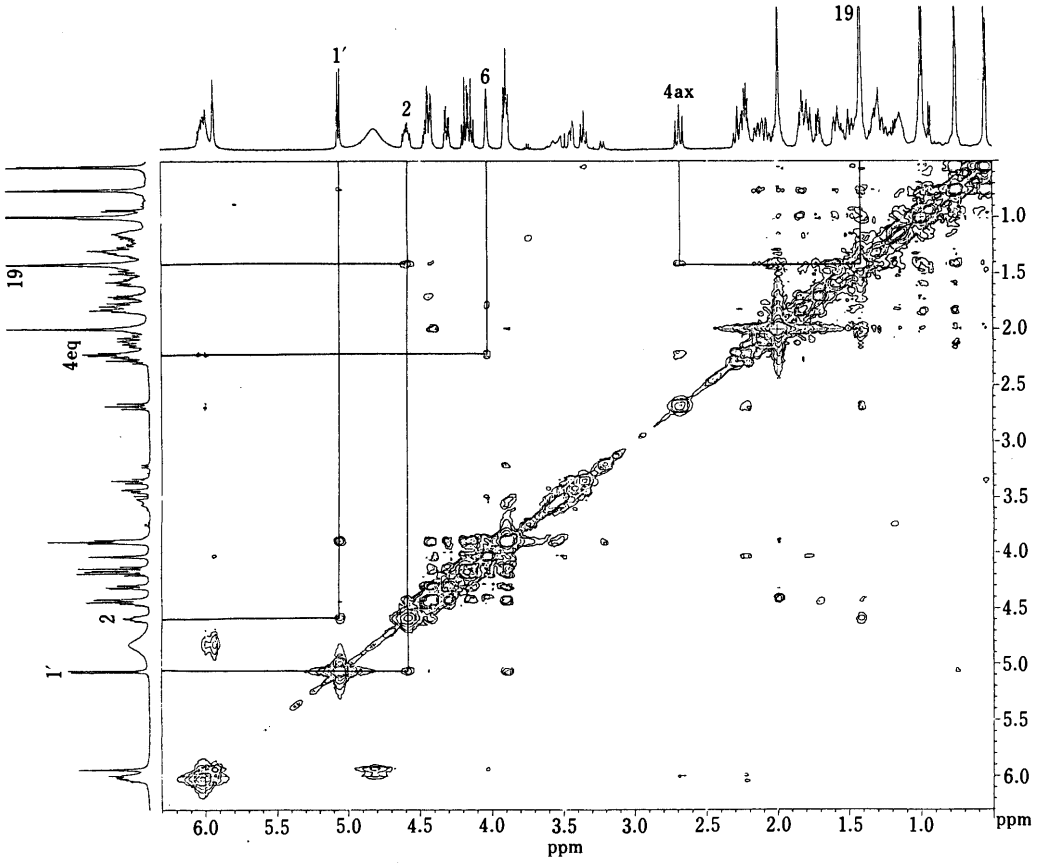

Fig. 3. NOE Correlation 2D Spectrum of **2** in Pyridine-d_5 (400 MHz)

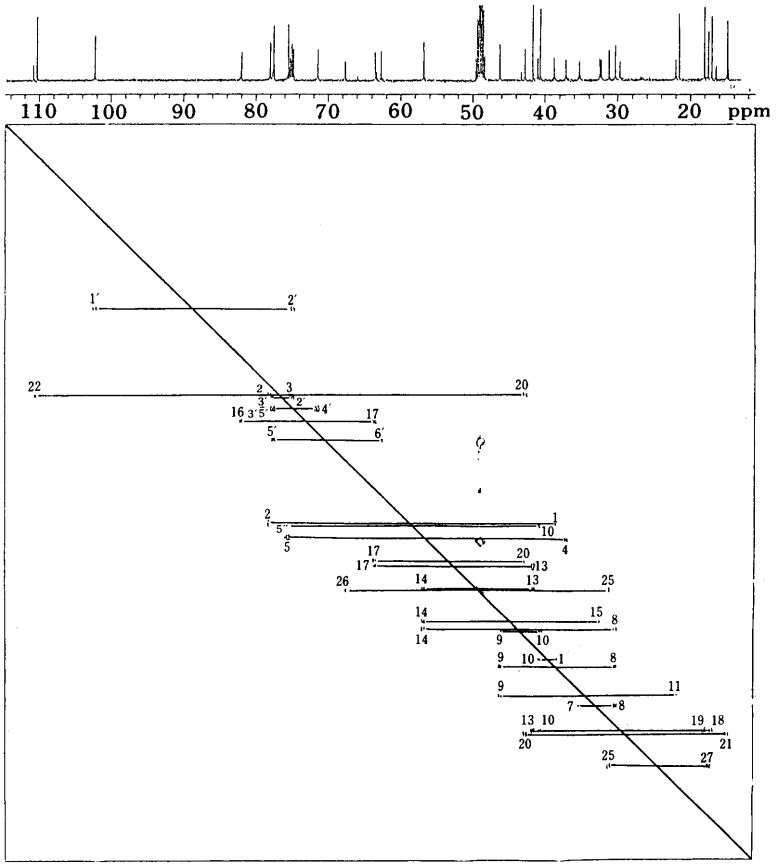

Fig. 4. 2D INADEQUATE Spectrum of **2** in Methanol-d_4 (400 MHz)

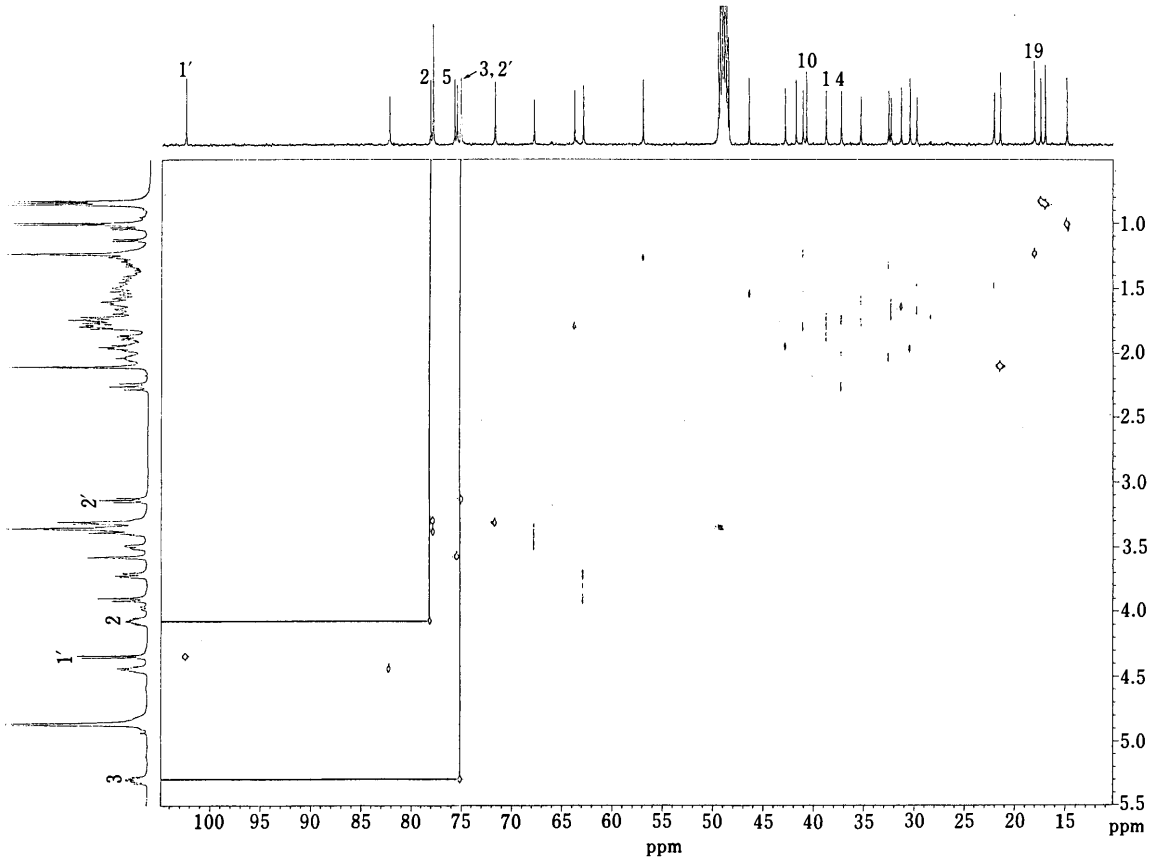

Fig. 5. ^1H–^{13}C Correlation 2D Spectrum of **2** in Methanol-d_4 (400 MHz)

and two carbons from the acetyl moiety. Treatment of **2** with acetic anhydride in pyridine introduced additional five acetyl groups (**2a**). On acid hydrolysis with 1 N hydrochloric acid, **2** liberated D-glucose and alliogenin (**1**). From the above data, **2** was alliogenin *O*-glucoside with an acetyl group. In order to determine the substituted positions, ^{1}H–^{1}H correlation spectroscopy (^{1}H–^{1}H COSY) and the two dimensional nuclear Overhauser effect (NOE) correlation spectroscopy (2D NOESY) were measured and examined in detail. The downfield signal at δ 6.15 (ddd, J=10.4, 10.2, 6.2 Hz) was assigned as the axial proton bearing the acetoxyl function and showed cross peaks at δ 4.71 (ddd, J=10.2, 10.1, 6.0 Hz), 2.81 (dd, J=12.3, 10.4 Hz) and 2.34 (1H, dd, J=12.3, 6.2 Hz, H-4 equatorial) in the ^{1}H–^{1}H COSY spectrum. The 2D NOESY spectrum showed the clear NOE correlation between signals at δ 2.81 and 1.54 (19-Me), and between δ 4.16 (br s, $W_{1/2}$=7.5 Hz, H-6 equatorial) and 2.34. Thus, the signals at δ 2.81 and 2.34 were concluded to be due to the H-4 axial and H-4 equatorial protons, and δ 6.15 to the H-3 axial proton. On the other hand, the signal at δ 4.71 was assigned as the axial proton bearing the glucosyloxyl group since the signal showed the NOE correlation at δ 1.54 (19-Me) and the anomeric proton signal at δ 5.19, and the spin-coupling cross peaks at δ 6.15, 2.40 (dd, J=12.1, 10.1 Hz) and 2.33 (overlapping). The *W*-shaped long-range coupling was observed between the signals at δ 2.40 and 1.54 (19-Me). Thus, the assignments of the signals at δ 2.40 and 2.33 to the H-1 axial and H-1 equatorial protons were carried out. Further, the two dimentional incredible natural abundance double quantum transfer experiment (2D INADEQUATE) spectrum (methanol-d_4) was measured to clarify the assignments of the carbon signals, and the signal at δ 78.2 was found assignable to C-2 carbon, and that at δ 75.1 to C-3 carbon (Fig. 4). In addition, we applied the ^{1}H–^{13}C correlation spectroscopy (^{1}H–^{13}C COSY) spectrum (methanol-d_4) (Fig. 5), in which the ^{1}H-signals at δ 5.25 (1H, ddd, J=11.4, 9.6, 6.0 Hz) and 4.02 (1H, m) showed correlations with the ^{13}C-signals at δ 75.1 (C-3) and 78.2 (C-2), respectively. From the discussion presented above, D-glucose moiety was unequivocally concluded to be localized at the C-2 hydroxyl group and the acetyl group at the C-3 hydroxyl group. The structure of **2** was characterized as (25*R*)-3-*O*-acetyl-5α-spirostan-2α,3β,5α,6β-tetraol 2-*O*-β-D-glucopyranoside, that is, 3-*O*-acetylalliogenin 2-*O*-β-D-glucopyranoside.

Compound **3** was obtained as colorless needles recrystallized from methanol, mp 253.0—256.0 °C, $[\alpha]_D$ −75.3° (pyridine). The SI-MS of **3** showed a pseudomolecular ion peak at m/z 627 $[M+H]^+$. No signal due to the acetyl group could be found in the IR, ^{1}H- and ^{13}C-NMR spectra. Compound **3** was identical with the deacetyl derivative of **2**, and the acetyl derivative of **3** which was prepared with acetic anhydride in pyridine was identical with **2a**. Compound **3** was a 3-deacetyl derivative of **2** and the structure was formulated as (25*R*)-5α-spirostan-2α,3β,5α,6β-tetraol 2-*O*-β-D-glucopyranoside, or alliogenin 2-*O*-β-D-glucopyranoside.

Compound **4** was obtained as a white amorphous powder, $[\alpha]_D$ −95.0° (methanol). The SI-MS of **4** showed a pseudomolecular ion peak at m/z 731 $[M+H]^+$ and the molecular formula was determined as $C_{40}H_{58}O_{12}$ with the help of elemental analysis. The spectral data of **2** and **4** were similar and suggestive of glucoside structure of the same type. The existence of a benzoyl group in the molecule was indicated by the IR [1700 cm^{-1} (carbonyl); 1600 and 710 cm^{-1} (aromatic ring)], ultraviolet (UV) (λ_{max} 230, 266 shoulder (sh), 273 and 280 sh nm), ^{1}H-NMR [δ 8.44 (2H) and 7.44 (3H)] and ^{13}C-NMR (δ 131.9, 130.3×2, 128.7×2, 132.9 and 166.8) spectra. Compound **4** was acetylated with acetic anhydride in pyridine to give a pentaacetate (**4a**), of which the EI-MS showed a molecular ion peak at m/z 940. Treatment of **4** with 3% sodium methoxide solution gave a methyl benzoate and a steroidal saponin, which was identified as **3**. In the ^{1}H-NMR spectrum of **4**, the signal for the H-3 position was shifted to downfield by 1.48 ppm compared with that of **3**. From the above discussion, the structure of **4** was characterized as (25*R*)-3-*O*-benzoyl-5α-spirostan-2α,3β,5α,6β-tetraol 2-*O*-β-D-glucopyranoside, or 3-*O*-benzoylalliogenin 2-*O*-β-

TABLE I. ^{13}C-NMR Spectral Data for **1**, **2**, **3** and **4**[a]

C	1	2[b]	2[c]	3	4
1	42.2[d]	38.8[d]	38.7	40.4[d]	37.9[d]
2	73.8	77.7	78.2	85.2	77.7
3	73.8	75.0	75.1	71.5	76.3
4	41.1[d]	37.8[d]	37.2	40.7[d]	38.9[d]
5	75.8	74.9	75.6	74.9	75.0
6	75.6	75.1	75.3	75.2	75.0
7	35.9	35.7	35.3	35.8	35.8
8	30.3	31.1	30.4	30.2	30.1
9	46.0	45.7	46.3	45.8	45.7
10	41.0	40.3	40.6	40.7	40.5
11	21.7	21.5	22.0	21.6	21.6
12	40.6	40.4	41.0	40.3	40.4
13	41.0	41.0	41.7	41.0	41.0
14	56.4	56.3	56.9	56.3	56.2
15	32.2	32.3	32.5	32.3	32.3
16	81.3	81.2	82.0	81.2	81.2
17	63.2	63.1	63.6	63.1	63.2
18	18.5	17.9	17.1	18.1	18.0
19	16.7	16.7	18.1	16.3	16.7
20	42.1	42.0	42.8	42.0	42.1
21	15.9	15.0	14.9	15.1	15.0
22	109.3	109.2	110.3	109.2	109.2
23	31.9	31.8	32.3	31.8	31.8
24	29.3	29.3	29.7	29.3	29.3
25	30.6	30.6	31.2	30.6	30.6
26	66.9	66.9	67.7	66.9	66.9
27	17.3	17.3	17.5	17.3	17.3
Glc					
1′		103.1	102.3	104.7	103.3
2′		75.3	74.8	75.3	75.3
3′		78.3[e]	77.6[e]	78.5[e]	78.2[e]
4′		71.8	71.5	71.9	71.8
5′		78.5[e]	77.6[e]	78.5[e]	78.4[e]
6′		63.0	62.8	62.0	63.0
Ac		170.9	173.1		
		21.6	21.5		
Benzoyl					
1″					131.9
2″					130.3
3″					128.7
4″					132.9
5″					128.7
6″					130.3
7″					166.8

a) Spectra of **1**, **2**[b], **3** and **4** were measured in C_5D_5N, and that of **2**[c] was measured in methanol-d_4 with TMS as internal standard. d, e) Signals with the same superscripts may be reversed in each column.

D-glucopyranoside.

Previously, alliogenin 3-*O*-*β*-D-glucopyranoside was isolated from the bulbs of *A. giganteum* and the linkage position of the sugar moiety was established by the circular dichroism (CD) spectrum.[5] In this study, we isolated alliogenin 2-*O*-*β*-D-glucopyranoside and its acetyl and benzoyl derivatives from the same source. The structures were confirmed by reliable high field NMR techniques. Unfortunately, the previous paper showed no detailed spectral data and we could not directly compare **3** with the previously reported compound, however, the alliogenin 3-*O*-glucoside reported seems to have been revised to alliogenin 2-*O*-glucoside. 2-*O*-Benzoylalliogenin 3-*O*-*β*-D-glucopyranoside was isolated from the bulbs of *A. karataviense* and its structure was established by comparison with alliogenin 3-*O*-glucoside from *A. giganteum*.[6] The 2-*O*-benzoylalliogenin 3-*O*-glucoside also seems to have been revised to 3-*O*-benzoylalliogenin 2-*O*-glucoside. To the best of our knowledge, **2**, **3** and **4** are the second examples of steroidal saponins carrying the sugar moiety at the C-2 hydroxyl position after yononin.[7]

Experimental

Melting points were determined with a Yazawa micro melting point apparatus and are uncorrected. Optical rotations were measured with a JASCO DIP-360 automatic polarimeter. IR spectra were recorded on a Hitachi 260-30 spectrometer and MS on a Hitachi M-80 machine. ^{1}H- and ^{13}C-NMR spectra were taken on a Bruker AM-400 or AM-500 spectrometer and 2D INADEQUATE spectrum on a JEOL JNM-GX400 spectrometer. Chemical shifts are reported in ppm (δ scale) with tetramethylsilane (TMS) as an internal standard, and the following abbreviations used: s, singlet; d, doublet; dd, doublet of doublets; m, multiplet; br, broad. ^{1}H–^{1}H COSY, ^{1}H–^{13}C COSY and 2D NOESY spectra were obtained with the standard Bruker softwear. Column chromatographies were done with Fuji Davison Silica gel BW-300 (200—400 mesh, Fuji Davison Co., Ltd.) and Sephadex LH-20 (25—100 μm, Pharmacia Fine Chemicals Co., Ltd.). Thin layer chromatography (TLC) was carried out on precoated Kiesel gel 60 F_{254} plates (0.25 mm thick, Merck). Spots were visualized under UV light (254 nm) irradiation and by spraying 10% H_2SO_4 solution followed by heating.

Extraction and Isolation Commercially available fresh bulbs of *A. giganteum* (9.8 kg) purchased from Heiwa-en Co. were extracted with hot MeOH and the extract was concentrated under reduced pressure. The crude residue was suspended in H_2O and extracted with $CHCl_3$ and then with *n*-BuOH. The *n*-BuOH phase was concentrated and chromatographed on silica gel with $CHCl_3$–MeOH (19:1, 9:1, 4:1, 2:1) and MeOH gradients to give ten fractions (1—10). Fraction 5 was concentrated to give precipitate, which was recrystallized from MeOH to yield **1** (250.0 mg). Fraction 5 was further subjected to a silica gel column with $CHCl_3$–MeOH (4:1) to give **2** with a few impurities, which was purified by silica gel column chromatography with AcOEt–MeOH (19:1) to yield **2** (280.0 mg). Fraction 7 was concentrated to give precipitate, which was recrystallized from MeOH to furnish **3** (700.0 mg). The $CHCl_3$ phase was concentrated and subjected to silica gel column using $CHCl_3$, $CHCl_3$–MeOH (19:1, 4:1) gradients to give five fractions (1—5). Fraction 4 was chromatographed on silica gel with $CHCl_3$–MeOH (19:1) to give **4** with a few impurities, which was further subjected to silica gel columns with AcOEt–MeOH (9:1) and AcOEt–Me_2CO (19:1) to yield **4** (93.0 mg).

Alliogenin (1) Colorless plates (MeOH), 250.0 mg, mp 305.0—310.0 °C, $[\alpha]_D^{24}$ −80.4° (c=0.1, pyridine). EI-MS m/z (rel. int.): 464 $[M]^+$ (16), 405 (9), 392 (36), 359 (6), 350 (12), 332 (44), 314 (30), 285 (24), 259 (7), 199 (4), 176 (10), 139 (100), 115 (51). *Anal.* Calcd for $C_{27}H_{44}O_6 \cdot 1/2H_2O$: C, 68.47; H, 9.57. Found: C, 68.71; H, 9.55. IR ν_{max}^{KBr} cm^{-1}: 3450 (OH), 2960 (CH), 2940, 2880, 1380, 1080, 1050, 980, 920, 895, 860 ((25*R*)-spiroketal, intensity 920<895). ^{1}H-NMR (C_5D_5N) δ: 4.85 (1H, ddd, J=11.3, 8.9, 5.6 Hz, H-2 or -3), 4.56 (1H, ddd, J=7.6, 7.2, 7.2 Hz, H-16), 4.45 (1H, ddd, J=11.3, 8.8, 5.2 Hz, H-2 or -3), 4.22 (1H, br s, $W_{1/2}$=8.0 Hz, H-6), 3.56 (1H, dd, J=10.6, 3.6 Hz, H-26a), 3.48 (1H, dd, J=10.6, 10.6 Hz, H-26b), 3.07 (1H, dd, J=13.2, 11.3 Hz, H-4 axial), 1.69 (3H, s, H-19), 1.12 (3H, d, J=6.9 Hz, H-21), 0.91 (3H, s, H-18), 0.67 (3H, d, J=5.7 Hz, H-27).

3-*O*-Acetylalliogenin 2-*O*-*β*-D-Glucopyranoside (2) A white amorphous powder, 280.0 mg, $[\alpha]_D^{27}$ −99.0° (c=0.1, MeOH). SI-MS m/z: 668 $[M]^+$. *Anal.* Calcd for $C_{35}H_{56}O_{12} \cdot H_2O$: C, 61.21; H, 8.51. Found: C, 61.23; H, 8.47. IR ν_{max}^{KBr} cm^{-1}: 3450 (OH), 2950 (CH), 1720 (carbonyl), 1375, 1260, 1070, 1040, 980, 920, 890, 860 ((25*R*)-spiroketal, intensity 920<890). ^{1}H-NMR (C_5D_5N) δ: 6.15 (1H, ddd, J=10.4, 10.2, 6.2 Hz, H-3), 5.19 (1H, d, J=7.7 Hz, H-1′), 4.71 (1H, ddd, J=10.2, 10.1, 6.0 Hz H-2), 4.43 (1H, dd, J=11.6, 4.8 Hz, H-6′a), 4.16 (1H, br s, $W_{1/2}$=7.5 Hz, H-6), 3.57 (1H, dd, J=10.5, 3.5 Hz, H-26a), 3.48 (1H, dd, J=10.5, 10.1, H-26b), 2.81 (1H, dd, J=12.3, 10.4 Hz, H-4 axial), 2.40 (1H, dd, J=12.1, 10.1 Hz, H-1 axial), 2.34 (1H, dd, J=12.3, 6.2 Hz, H-4 equatorial), 2.33 (1H, dd, J=12.1, 6.0 Hz, H-1 equatorial), 2.12 (3H, s, Ac), 1.54 (3H, s, H-19), 1.12 (3H, d, J=6.9 Hz, H-21), 0.88 (3H, s, H-18), 0.68 (3H, d, J=5.8 Hz, H-27); (methanol-d_4) δ: 5.25 (1H, ddd, J=11.4, 9.6, 6.0 Hz, H-3), 4.39 (1H, m, H-16), 4.29 (1H, d, J=7.8 Hz, H-1′), 4.02 (1H, m, H-2), 3.85 (1H, br d, J=11.4 Hz, H-6′a), 3.66 (1H, dd, J=11.4, 5.0 Hz, H-6′b), 3.08 (1H, dd, J=8.9, 7.9 Hz, H-4′), 2.19 (1H, dd, J=11.7, 11.7 Hz, H-4 axial), 2.06 (3H, s, Ac), 1.19 (3H, s, H-19), 0.96 (3H, d, J=6.9 Hz, H-21), 0.81 (3H, s, H-18), 0.79 (3H, d, J=6.3 Hz, H-27).

Acetylation of 2 Compound **2** (20.7 mg) was acetylated with acetic anhydride in pyridine and the crude acetate was chromatographed on silica gel with *n*-hexane–Me_2CO (2:1) to yield a hexaacetate (**2a**) (22.4 mg) as a white amorphous powder. IR ν_{max}^{KBr} cm^{-1}: 2960 (CH), 1760 (carbonyl), 1380, 1240, 1040, 980, 920, 900. EI-MS m/z (rel. int.): 880 $[M+2H]^+$ (13), 848 (1), 819 $[M-CH_3COO]^+$ (6), 806 (13), 746 (1), 686 (4), 626 (2), 559 (2), 531 $[M-$tetraacetylhexose$]^+$ (19), 504 (4), 471 (50), 429 (45), 393 (15), 357 (25), 331 [tetraacetylhexosyl]$^+$ (100), 271 (30), 169 (100), 139 (99), 109 (99). ^{1}H-NMR (C_5D_5N) δ: 5.98 (1H, m, H-3), 5.81 (1H, dd, J=9.7, 9.6 Hz, H-3′), 5.54 (1H, dd, J=10.0, 9.7 Hz, H-4′), 5.44 (1H, dd, J=9.6, 7.9 Hz, H-2′), 5.36 (1H, br s, $W_{1/2}$=6.7 Hz, H-6), 5.22 (1H, d, J=7.9 Hz, H-1′), 4.62 (1H, dd, J=12.3, 4.5 Hz, H-6′a), 4.47 (1H, dd, J=12.3, 2.5 Hz, H-6′b), 4.34 (1H, m, H-2), 4.22 (1H, ddd, J=10.0, 4.5, 2.5 Hz, H-5′), 3.57 (1H, dd, J=10.7, 3.4 Hz, H-26a), 3.47 (1H, dd, J=10.7, 10.7 Hz, H-26b), 2.18, 2.13, 2.06, 2.04 × 2, 2.01 (each 3H, s, Ac), 1.32 (3H, s, H-19), 1.15 (3H, d, J=6.9 Hz, H-21), 0.92 (3H, s, H-18), 0.67 (3H, d, J=5.7 Hz, H-27).

Acid Hydrolysis of 2 Compound **2** (46.0 mg) was dissolved in 2 N HCl in H_2O–dioxane (2:1) and the mixture was refluxed for 1 h. After being cooled, the reaction mixture was neutralized with 1 N NaOH and partitioned between AcOEt and H_2O. The AcOEt soluble phase was concentrated and subjected to silica gel column chromatography using AcOEt–MeOH (19:1) to give a steroidal sapogenin, which was identified as alliogenin (**1**) (13.3 mg) by the IR, EI-MS, ^{1}H- and ^{13}C-NMR spectra. The H_2O soluble phase was concentrated and examined by TLC with *n*-BuOH–Me_2CO–H_2O (4:5:1) to detect glucose (*Rf* 0.37). Further, the H_2O soluble phase was chromatographed with $CHCl_3$–MeOH–H_2O (20:10:1) to give D-glucose (5.5 mg), $[\alpha]_D^{24}$ +46.0° (c=0.1, H_2O).

Alkaline Methanolysis of 2 Compound **2** (20.3 mg) was treated with 3% NaOMe in MeOH at room temperature for 30 min. The reaction mixture was passed through a cation exchange resin (Amberlite IR-120B) and the eluate was concentrated to give residue. The residue was subjected to silica gel column chromatography with $CHCl_3$–MeOH (9:1) to give a steroidal saponin, which was identified as alliogenin 2-*O*-*β*-D-glucopyranoside (**3**) (13.9 mg) by the SI-MS, IR, ^{1}H- and ^{13}C-NMR spectra.

Alliogenin 2-*O*-*β*-D-Glucopyranoside (3) Colorless needles (MeOH), mp 253.0—256.0 °C, 700.0 mg. $[\alpha]_D^{23}$ −97.0° (c=0.1, MeOH), SI-MS m/z: 664 $[M+K-H]^+$, 627 $[M+H]^+$, 465 $[M+H-$hexosyl$]^+$. IR ν_{max}^{KBr} cm^{-1}: 3400 (OH), 2950 (CH), 2870, 1450, 1380, 1240, 1080, 1060, 980, 920, 900, 860 ((25*R*)-spiroketal, intensity 920<900). ^{1}H-NMR (C_5D_5N) δ: 5.17 (1H, d, J=7.8 Hz, H-1′), 4.83 (1H, ddd, J=11.5, 8.6, 5.9 Hz, H-3), 4.61 (1H, dd, J=11.6, 2.4 Hz, H-6′a), 4.40 (1H, ddd, J=11.4, 8.6, 5.4 Hz, H-2), 4.17 (1H, br s, $W_{1/2}$=6.5 Hz, H-6), 3.56 (1H, dd, J=10.7, 3.6 Hz, H-26a), 3.47 (1H, dd, J=10.7, 10.7 Hz, H-26b), 2.97 (1H, dd, J=13.4, 11.5 Hz, H-4 axial), 1.58 (3H, s, H-19), 1.12 (3H, d, J=6.9 Hz, H-21), 0.89 (3H, s, H-18), 0.67 (3H, d, J=5.8 Hz, H-27).

Acetylation of 3 Compound **3** (16.0 mg) was acetylated with acetic anhydride in pyridine and crude acetate was chromatographed on silica gel with *n*-hexane–Me_2CO (2:1) to yield a hexaacetate (17.5 mg) as a white amorphous powder, which was identical with **2a**.

3-*O*-Benzoylalliogenin 2-*O*-*β*-D-Glucopyranoside (4) A white amorphous powder (93.0 mg), $[\alpha]_D^{26}$ −95.0° (c=0.1, MeOH), SI-MS m/z: 731 $[M+H]^+$. *Anal.* Calcd for $C_{40}H_{58}O_{12} \cdot H_2O$: C, 64.15; H, 8.08. Found: C, 64.54; H, 8.15. IR ν_{max}^{KBr} cm^{-1} 3450 (OH), 2930 (CH), 1700 (carbonyl),

1600 (aromatic ring), 970, 920, 890, 860 ((25*R*)-spiroketal, intensity 920 <890), 710 (aromatic ring). UV λ_{max}^{MeOH} nm (ε): 230 (12460), 266 sh (1800), 273 (2000), 280 sh (1660). ^{1}H-NMR (C_5D_5N) δ: 8.44 (2H, H-2″, -6″), 7.44 (3H, H-3″, -4″, -5″), 6.31 (1H, m, H-3), 5.22 (1H, d, J=7.7 Hz, H-1′), 4.58 (1H, m, H-16), 4.41 (1H, dd, J=11.4, 2.0 Hz, H-6′a), 3.57 (1H, dd, J=10.7, 3.2 Hz, H-26a), 3.48 (1H, dd, J=10.7, 10.7 Hz, H-26b), 2.90 (1H, dd, J=12.2, 12.2 Hz, H-4 axial), 1.59 (3H, s, H-19), 1.13 (3H, d, J=6.8 Hz, H-21), 0.90 (3H, s, H-18), 0.68 (3H, d, J=5.5 Hz, H-27).

Acetylation of 4 Compound **4** (10.7 mg) was acetylated with acetic anhydride in pyridine and crude acetate was chromatographed on silica gel with *n*-hexane–Me_2CO (3 : 1) to yield a pentaacetate (**4a**) (9.0 mg) as a white amorphous powder. EI-MS *m/z* (rel. int.): 940 $[M]^+$ (0.4), 879 $[M-CH_3COOH-H]^+$ (1.3), 808 (0.8), 758 (0.4), 687 (0.3), 623 (0.4), 533 $[M-\text{tetraacetylhexose}-CH_3COO]^+$(6), 331 [tetraacetylhexosyl]$^+$(12), 139 (100). IR ν_{max}^{KBr} cm^{-1}: 2950 (CH), 1760 (carbonyl), 1600 (aromatic ring), 1430, 1370, 1270, 1230, 1030, 980, 920, 890, 860, 710 (aromatic ring). ^{1}H-NMR (C_5D_5N) δ: 8.36 (2H, dd, J=8.5, 1.4 Hz, H-2″, -6″), 7.53 (1H, dd, J=7.4, 1.4 Hz, H-4″), 7.47 (2H, dd, J=8.5, 7.4 Hz, H-3″, -5″), 6.17 (1H, m, H-3), 5.82 (1H, t, J=9.6 Hz, H-4′), 5.47 (1H, t, J=9.6 Hz, H-3′), 5.31 (1H, d, J=8.0 Hz, H-1′), 4.52 (1H, dd, J=12.2, 4.2 Hz, H-6′a), 4.24 (1H, dd, J=12.2, 2.2 Hz, H-6′b), 3.57 (1H, br d, H-26a), 3.48 (1H, dd, J=10.4, 10.4 Hz, H-26b), 2.14, 2.02, 2.00, 1.98, 1.96 (each 3H, s, Ac), 1.40 (3H, s, H-19), 1.16 (3H, d, J=6.9 Hz, H-21), 0.94 (3H, s, H-18), 0.68 (3H, d, J=5.5 Hz, H-27).

Alkaline Methanolysis of 4 Compound **4** (10.0 mg) was treated with 3% NaOMe solution at room temperature for 3 h. The reaction mixture was passed through an Amberlite IR-120B column and the eluate was concentrated. The residue was subjected to Sephadex LH-20 column chromatography with MeOH as an eluent to yield methyl benzoate and crude hydrolysate. Methyl benzoate was identified by TLC comparison with a commercially available authentic sample purchased from Tokyo Kasei Kogyo Co., Ltd. Methyl benzoate: TLC, *Rf* 0.23 (*n*-hexane–$CHCl_3$, 9 : 1); *Rf* 0.40 (*n*-hexane–AcOEt, 19 : 1). The crude hydrolysate was purified by silica gel column chromatography with $CHCl_3$–MeOH (4 : 1) to yield a steroidal saponin (4.6 mg), which was identified as **3** by the IR and ^{1}H-NMR spectra.

Acknowledgements We are grateful to Mr. T. Saito, Nippon Oil Company Ltd., Central Technical Research Laboratory, for the measurement of 2D INADEQATE spectrum. Our thanks are also due to Dr. Y. Shida and Mrs. Y. Kato for measurements of the SI-MS and EI-MS, to Mrs. C. Sakuma for measurements of the ^{1}H–^{1}H COSY, ^{1}H–^{13}C COSY and 2D NOESY spectra and to Mr. H. Fukaya for measurements of the elemental analysis.

References

1) M. Hotta, ed., "Useful Plants of the World," Heibonsha Ltd., Publishers, Tokyo, 1989, pp. 63—69.
2) S. B. Mahato, A. N. Ganguly and N. P. Sahu, *Phytochemistry*, **21**, 959 (1982).
3) *a*) M. E. Wall, C. R. Eddy, M. L. McClennan and M. E. Klumpp, *Anal. Chem.*, **24**, 1337 (1952); *b*) C. R. Eddy, M. E. Wall and M. K. Scott, *ibid.*, **25**, 266 (1953).
4) F. S. Khristulas, M. B. Gorovits, V. N. Luchnskaya and N. K. Abukakirov, *Khim. Prir. Soedin.*, **6**, 489 (1970) [*Chem. Abstr.*, **74**, 10356*n* (1971)].
5) *a*) M. B. Gorovits, F. S. Khristulas and N. K. Abubakirov, *Khim. Prir. Soedin.*, **1971**, 434 [*Chem. Abstr.*, **75**, 141102*v* (1971)]; *b*) *Idem, ibid.*, **1973**, 747 [*Chem. Abstr.*, **82**, 108809*c* (1975)].
6) F. S. Khristulas, M. B. Gorovits and N. K. Abubakirov, *Khim. Prir. Soedin.*, **1974**, 530 [*Chem. Abstr.*, **82**, 82955*v* (1975)].
7) *a*) T. Kawasaki and T. Yamauchi, *Yakugaku Zasshi*, **83**, 757 (1963); *b*) T. Kawasaki and K. Miyahara, *Tetrahedron*, **21**, 3633 (1965).

Metabolism of Aloesin and Related Compounds by Human Intestinal Bacteria: A Bacterial Cleavage of the *C*-Glucosyl Bond and the Subsequent Reduction of the Acetonyl Side Chain

Qing-Ming CHE,[a] Teruaki AKAO,[b] Masao HATTORI,*,[a] Kyoichi KOBASHI,[b] and Tsuneo NAMBA[a]

Research Institute for Wakan-Yaku (Traditional Sino-Japanese Medicines)[a] and Department of Pharmaceutical Sciences,[b] Toyama Medical and Pharmaceutical University, 2630 Sugitani, Toyama 930-01, Japan. *Received August 10, 1990*

By anaerobic incubation with a bacterial mixture from human feces, aloesin (aloeresin B; 1) was converted to 2-acetonyl-7-hydroxy-5-methylchromone (aloesone; 3) and *dl*-7-hydroxy-2-(2′-hydroxypropyl)-5-methylchromone (aloesol; 4a + 4b) through a cleavage of the *C*-glucosyl bond, followed by reduction of the acetonyl side chain. An analogous compound, aloeresin A (2), was converted to *p*-coumaric acid and aloesin (1), the latter being subsequently transformed to aloesone (3) and *dl*-aloesol (4a + 4b). On the other hand, 7-*O*-methylated derivatives (7, 5a and 5b) of aloesin and of 8-*C*-glucosylaloesol were not cleaved to the corresponding aglycones, suggesting the importance of a free hydroxy group adjacent to the *C*-glucosyl group in the molecule for the bacterial cleavage of aloesin derivatives. This is the first report on the cleavage of the *C*-glycosyl bond of chromone *C*-glucosides by intestinal bacteria.

Keywords aloe; aloesin; aloeresin A; aloesol; aloesone; *C*-glycosylchromone; *C*-glycosyls cleavage; human intestinal bacteria; metabolism

Five types of *C*-glycosyls, namely *C*-glycosides of anthrones, flavonoids, xanthones, chromones and gallic acids, are known to occur in a variety of plants, and they are resistant to acidic hydrolysis and enzymatic hydrolysis in contrast with the corresponding *O*-glycosyls.[1]

In the course of our studies on the metabolism of crude drug components by intestinal bacteria, we have found that barbaloin (anthrone *C*-glycoside),[2] homoorientin (flavonoid *C*-glycoside),[3] mangiferin (xanthone *C*-glycoside)[4] and bergenin (*C*-glycosylated gallic acid)[4] are transformed to the corresponding aglycones by human intestinal bacteria. In addition, we have isolated an *Eubacterium* species capable of transforming barbaloin to aloe-emodin-9-anthrone.[5]

In the present paper, we report the cleavage of the *C*-glycosyl bond of a chromone *C*-glycoside, aloesin (formerly aloeresin B, **1**) and aloeresin A (**2**) from aloe,[6-9] and the subsequent reduction of the acetonyl side chain by human intestinal bacteria.

Results

Analysis of Bacterial Metabolites of Aloesin (1) and Aloeresin A (2) by High-Performance Liquid Chromatography (HPLC) Aloesin (**1**) and its 2″-*O*-(*E*)-*p*-coumaroyl derivative, aloeresin A (**2**), were anaerobically incubated with a bacterial mixture from human feces. Five days after incubation, BuOH extracts of the respective incubation mixtures were analyzed by means of HPLC using an octadecyl silica (ODS) column. Figure 1 shows the typical elution profiles of the extracts. Aloesin (**1**) was converted to two metabolites, while aloeresin A (**2**) was converted to four metabolites including aloesin (**1**), two of which had identical retention times ($t_R = 4.3$ min and $t_R = 5.3$ min) with those obtained in the metabolism of aloesin (**1**).

Isolation and Identification of the Metabolites For the purpose of determining the structures of metabolites, aloesin (**1**) was anaerobically incubated in a large scale with a bacterial mixture from human feces in an anaerobic box, and the products were extracted with an organic solvent

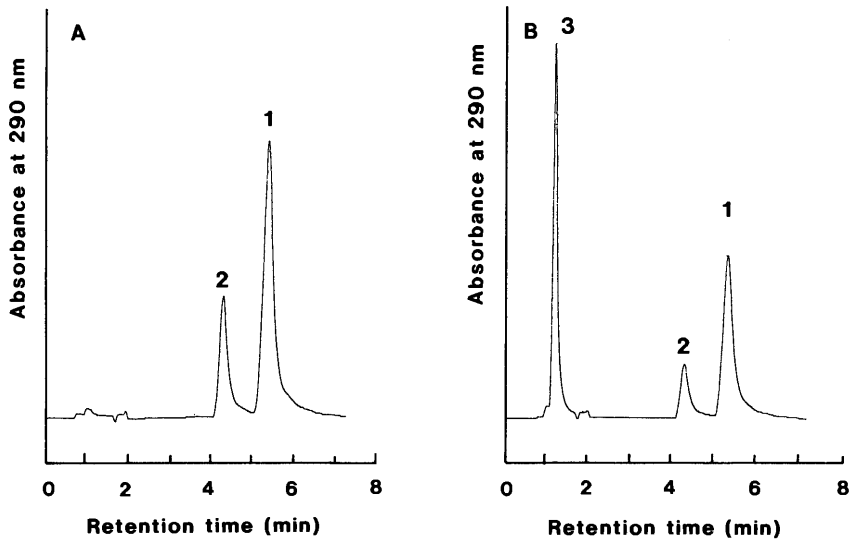

Fig. 1. Elution Profiles of the Metabolites of Aloesin (**1**) (A) and Aloeresin A (**2**) (B) Obtained by Anaerobic Incubation with a Bacterial Mixture from Human Feces

The metabolites were extracted with BuOH and analyzed by HPLC. HPLC was performed with an ODS-5 column (Nomura Chem. Co.) under conditions: mobile phase, CH_3CN–H_2O (1 : 3); flow rate, 1.0 ml/min; detection at 290 nm. 1, metabolite A (aloesone, **3**); 2, metabolite B (*dl*-aloesol, **4a** + **4b**); 3, metabolite C (*E*- and *Z*-*p*-coumaric acids).

TABLE I. ^{13}C-NMR Spectral Data for Metabolites and Aloesin Derivatives

Carbon	3[a]	4[b]	5a[a]	5b[a]	7[a]	8[c]
2	161.0 (s)	167.9 (s)	159.5 (s)	159.4 (s)	160.6 (s)	159.6 (s)[d]
3	112.9 (d)	113.3 (d)	111.1 (d)	111.0 (d)	112.4 (d)	113.7 (d)
4	178.1 (s)	182.7 (s)	178.6 (s)	178.6 (s)	178.7 (s)	179.1 (s)
5	141.6 (s)	144.5 (s)	140.0 (s)	139.9 (s)	141.1 (s)	144.1 (s)
6	116.6 (d)	118.8 (d)	116.2 (d)	116.2 (d)	115.8 (d)	118.5 (d)
7	160.5 (s)	163.8 (s)	164.4 (s)	164.4 (s)	160.2 (s)	159.0 (s)[d]
8	100.5 (d)	102.6 (d)	110.8 (s)	110.8 (s)	111.8 (s)	106.2 (s)
9	159.2 (s)	162.3 (s)	157.7 (s)	157.6 (s)	157.2 (s)	159.6 (s)[d]
10	114.3 (s)	116.8 (s)	114.7 (s)	114.6 (s)	113.0 (s)	113.9 (s)
5-$\underline{C}H_3$	22.3 (q)	23.9 (q)	22.5 (q)	22.4 (q)	22.8 (q)	23.1 (q)
7-O-$\underline{C}H_3$					56.4 (q)	
1′	47.4 (t)	45.0 (t)	43.0 (t)	43.0 (t)	47.7 (t)	48.2 (t)
2′	202.7 (s)	67.2 (d)	64.0 (d)	64.0 (d)	202.3 (s)	200.7 (s)
3′	29.8 (q)	24.3 (q)	23.6 (q)	23.3 (q)	29.8 (q)	30.2 (q)
1″			73.7 (d)	73.6 (d)	72.8 (d)	68.1 (d)
2″			71.1 (d)	71.1 (d)	71.0 (d)	73.7 (d)
3″			78.7 (d)	78.6 (d)	78.7 (d)	73.7 (d)
4″			70.5 (d)	70.4 (d)	70.5 (d)	70.2 (d)
5″			81.5 (d)	81.5 (d)	81.5 (d)	76.6 (d)
6″			61.4 (t)	61.4 (t)	61.7 (t)	61.6 (t)
O-$\underline{C}O$-CH_3						168.9 (s)
						169.4 (s)
						170.3 (s)
						170.6 (s)
O-CO-$\underline{C}H_3$						20.7 (q) (×4)

Measured at 22.5 MHz in *a*) DMSO-d_6, *b*) CD_3OD or *c*) $CDCl_3$. *d*) Assignments may be interchanged in each column.

and separated into two metabolites (metabolites A and B) by means of column chromatography.

Metabolite A, $t_R = 5.3$ min on HPLC, was obtained as colorless needles, mp 218—221 °C. Its mass spectrum (MS) showed a molecular ion at *m/z* 232, corresponding to the molecular formula $C_{13}H_{12}O_4$. The proton and carbon-13 nuclear magnetic resonance (^{1}H- and ^{13}C-NMR) spectra showed that the chromone nucleus and the acetonyl side chain were intact but the *C*-glucopyranosyl moiety was missing. The spectroscopic data agreed with those of aloesone (2-acetonyl-7-hydroxy-5-methylchromone, **3**).[10]

Metabolite B, $t_R = 4.3$ min on HPLC, was also obtained as colorless needles, mp 175—178 °C. Its MS showed a molecular ion peak at *m/z* 234, two mass units higher than that of metabolite A. The infrared (IR) spectrum showed no C=O stretching band due to the acetonyl group present in aloesin (**1**). The signals at δ 1.27 (3H, d, $J = 6.3$ Hz), 2.65 and 2.68 (each 1H, each dd, $J = 14.2$, 7.6 Hz and $J = 14.2$, 5.6 Hz, respectively), 4.19 (1H, m) in the ^{1}H-NMR spectrum indicated the presence of a CH_3–CH(OH)–CH_2– group in the molecule. On the basis of the above findings and the ^{13}C-NMR spectral data (Table I), the structure of metabolite B was determined as 7-hydroxy-2-(2′-hydroxypropyl)-5-methylchromone (aloesol). This compound was obtained as a racemic mixture ($[\alpha]_D$ 0°) though the optically active 2′*S*-form ($[\alpha]_D$ +38.4°) has been reported to occur in rhubarb.[11]

Similarly, anaerobic incubation of aloeresin A (**2**) with an intestinal bacterial mixture, followed by solvent extraction and column chromatography led to the isolation of four metabolites. These metabolites were identified as aloesin (**1**), aloesone (**3**), *dl*-aloesol (**4a**+**4b**) and *p*-coumaric acid on the basis of their spectral data. The last compound was determined to be a mixture of *E*- and *Z*-forms in a ratio of 9:1 by means of ^{1}H-NMR.

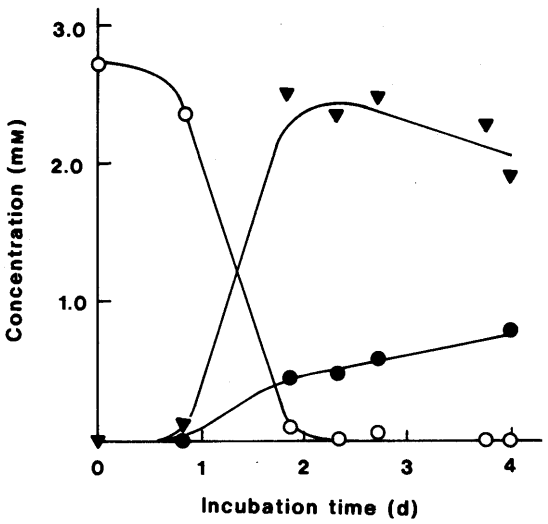

Fig. 2. Time Course of the Metabolism of Aloesin (**1**)

Aloesin (**1**) was anaerobically incubated with an intestinal bacterial mixture at 37 °C. The metabolites were analyzed by means of TLC-densitometry. (○) aloesin (**1**), (▼) aloesone (**3**), (●) *dl*-aloesol (**4a**+**4b**).

Time Courses of the Metabolisms of Aloesin (1) and Aloeresin A (2) by a Bacterial Mixture from Human Feces Figure 2 shows the time course of the bacterial transformation of aloesin (**1**). Aloesin (**1**) started to be converted to aloesone (**3**) and *dl*-aloesol (**4a**+**4b**) 20 h after incubation with the bacterial mixture, and disappeared completely within approx. 50 h as aloesone (**3**) reached a maximum concentration (*ca.* 80% in yield). Aloesone (**3**) then decreased in amount, while *dl*-aloesol (**4a**+**4b**) gradually increased. On further incubation, the amount of *dl*-aloesol (**4a**+**4b**) exceeded that of aloesone (**3**) as will be mentioned later. Transformation of aloesone (**3**) to *dl*-aloesol (**4a**+**4b**) was also confirmed by a separate

experiment; aloesone (3) itself was transformed slowly to *dl*-aloesol (**4a**+**4b**) through the entire time of incubation with an intestinal bacterial mixture in peptone yeast extract Fildes (PYF) broth, *ca.* 10% of the starting material being transformed to *dl*-aloesol (**4a**+**4b**) within 5 d. However, on anaerobic incubation with the bacterial suspension in phosphate buffer, *ca.* 60% of aloesone (3) was converted to *dl*-aloesol (**4a**+**4b**) within 3 d.

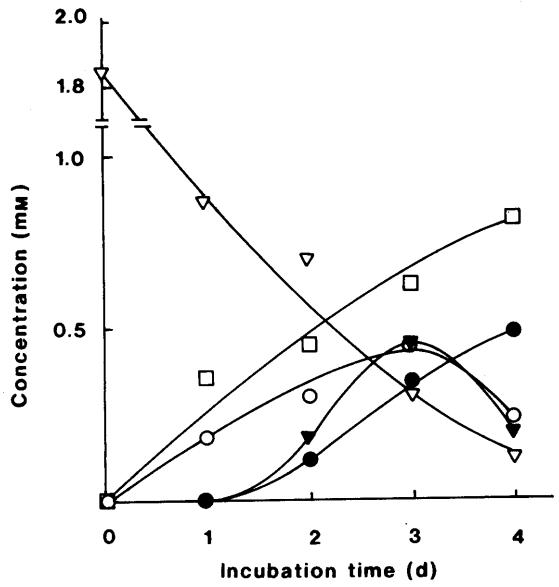

Fig. 3. Time Course of the Metabolism of Aloeresin A (2)

Aloeresin A (2) was anaerobically incubated with an intestinal bacterial mixture at 37 °C. The metabolites were analyzed by TLC-densitometry. (▽) aloeresin A (2), (□) *p*-coumaric acid, (○) aloesin (1), (▼) aloesone (3), (●) *dl*-aloesol (**4a**+**4b**).

TABLE II. Transformation of Aloesin (1) and Related Compounds by Human Intestinal Bacteria

Substrate	Yield of metabolite (%)	
	Aloesone	Aloesol
Aloesin (1)	17	43[a]
Aloeresin A (2)	27	59[a]
Aloesone (3)		9[a]
(2′*R*)-8-*C*-Glucocylaloesol (**5a**)		49[b]
(2′*S*)-8-*C*-Glucosylaloesol (**5b**)		44[c]
(2′*R*)-8-*C*-Glucosyl-7-*O*-methylaloesol (**6a**)	0	0
(2′*S*)-8-*C*-Glucosyl-7-*O*-methylaloesol (**6b**)	0	0
7-*O*-Methylaloesin (7)	0	0
Aloesin 2″,3″,4″,6″-tetra-*O*-acetate (**8**)	0	0

Aloesin (1) and related compounds (2—8) (2—6 mM) were anaerobically incubated with a bacterial mixture from human feces in PYF medium for 3 d at 37 °C. The products were extracted with BuOH and quantitatively analyzed by TLC densitometry. *a*) *dl*-form; *b*) 2′*R*-form; *c*) 2′*S*-form.

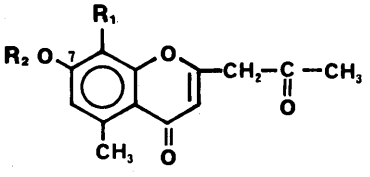

1: R_1 = *C*-Glc, R_2 = H
2: R_1 = *C*-Glc—(2)—*p*-Coum., R_2 = H
3: R_1 = R_2 = H
7: R_1 = *C*-Glc, R_2 = Me
8: R_1 = *C*-Glc (Ac)$_4$, R_2 = H

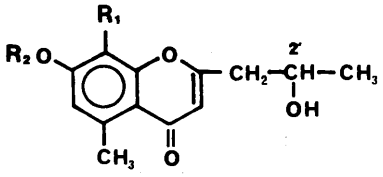

4a: R_1 = R_2 = H (2′*R*)
4b: R_1 = R_2 = H (2′*S*)
5a: R_1 = *C*-Glc, R_2 = H (2′*R*)
5b: R_1 = *C*-Glc, R_2 = H (2′*S*)
6a: R_1 = *C*-Glc, R_2 = Me (2′*R*)
6b: R_1 = *C*-Glc, R_2 = Me (2′*S*)

Chart 1. Structures of Aloesin (1) and Related Compounds (2—8)

Figure 3 shows the time course of the transformation of aloeresin A (2). One day after incubation, aloesin (1) and *p*-coumaric acid were produced but no aloesone (3) and *dl*-aloesol (**4a**+**4b**) were detected in the incubation mixture, indicating that enzymic hydrolysis of the *p*-coumaroyl moiety proceeded prior to the cleavage of the *C*-glucosyl in aloeresin A (2). After that, aloesone (3) and *dl*-aloesol (**4a**+**4b**) appeared gradually. Aloesone (2) became its maximal concentration (*ca.* 25% in yield) 3 d after incubation and then decreased on further incubation, while *dl*-aloesol (**4a**+**4b**) was continuously produced during the incubation. *p*-Coumaric acid was also continuously liberated, accompanied by a decrease in the amount of aloeresin A (2).

Screening of Intestinal Bacterial Strains for Ability of Metabolizing Aloesin (1) Twenty different kinds of defined bacterial strains from human feces were assayed for their ability to metabolize aloesin (1). However, none of the bacteria examined could cleave the *C*-glycosyl bond of aloesin (1) and the substrate was completely recovered 2 d after cultivation with each bacterium in general anaerobic medium (GAM) or PYF broth (data not shown).

Metabolism of Aloesin Derivatives by Human Intestinal Bacteria For comparing substrate specificity in the cleavage reaction of the *C*-glucosyls and in the reduction of the acetonyl side chain, aloesin (1), aloeresin A (2) and various aloesin derivatives synthesized chemically were incubated with a bacterial mixture from human feces under similar conditions. Both (2′*R*)- and (2′*S*)-8-*C*-glucosylaloesols (**5a** and **5b**) were transformed to (2′*R*)- and (2′*S*)-aloesols (**4a** and **4b**) in yields of 49 and 44%, respectively, 3 d after incubation, while (2′*R*)- and (2′*S*)-8-*C*-glucosyl-7-*O*-methylaloesols (**6a** and **6b**), 7-*O*-methylaloesin (7) and aloesin 2″,3″,4″,6″-tetra-*O*-acetate (**8**) were not metabolized (Table II).

Discussion

Anaerobic incubation of aloesin (1) with fecal flora of humans resulted in the cleavage of the *C*-glycosyl bond of aloesin (1) to give aloesone (3), which was subsequently reduced to *dl*-aloesol (**4a**+**4b**) (Chart 2).

On the other hand, aloeresin A (2) was first subjected to hydrolysis of the (*E*)-*p*-coumaroyl moiety by bacterial esterase to give aloesin (1) and *p*-coumaric acid. The latter was obtained as a mixture of (*E*)- and (*Z*)-forms. The aloesin (1) produced was further metabolized to aloesone (3), *dl*-aloesol (**4a**+**4b**). The products were essentially not altered by repeated experiments but their relative ratios or

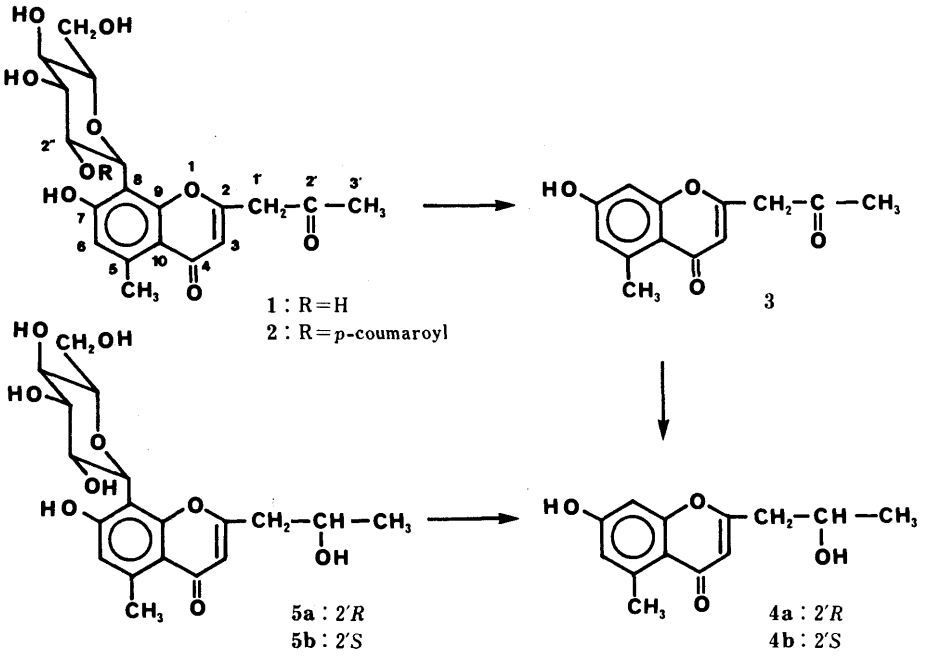

Chart 2. Metabolic Processes of Aloesin (**1**) and Aloeresin A (**2**) by Human Intestinal Bacteria

yields varied significantly with feces, incubation time and culture media.

(2'*R*)- and (2'*S*)-8-*C*-glucosylaloesols (**5a** and **5b**) were metabolized to (2'*R*)- and (2'*S*)-aloesols (**4a** and **4b**), respectively, by fecal flora. However, tetraacetylaloesin (**8**) was not metabolized, possibly due to its sparing solubility in the medium and its poor permeability to bacterial cells. Furthermore, 7-*O*-methylaloesin (**7**) and (2'*R*)- and (2'*S*)-8-*C*-glucosyl-7-*O*-methylaloesols (**6a** and **6b**) were not transformed to the corresponding aglycones, suggesting the necessity of a free hydroxyl group adjacent to the *C*-glucosyl group for cleaving the *C*-glycosyl bond.

During the incubation of aloesin (**1**), no 8-*C*-glucosylaloesols (**5a** and **5b**) were detected in the metabolic mixture when analyzed by means of HPLC and thin-layer chromatography (TLC). Further, reduction of aloesone (**3**) to *dl*-aloesol (**4a** + **4b**) proceeded quite slowly in the separate experiment. These findings indicate that the cleavage of the *C*-glycosyl bond of aloesin (**1**) occurrs prior to the reduction of the acetonyl group by intestinal bacteria.

On the isomerization of (*E*)-form to (*Z*)-form in *p*-coumaric acid, it is not clear whether the reaction was proceeded by the action of intestinal bacteria or not, because this type of isomerization may be effected by exposure to light during incubation and extraction procedures.

An attempt to find out bacteria capable of metabolizing aloesin (**1**) from our stock strains of intestinal bacteria was unsuccessful but a preliminary experiment to isolate such bacteria from human feces revealed that some bacteria had potent ability to cleave the *C*-glycosyl bond of aloesin (**1**). As reported previously,[5] *Eubacterium* sp. BAR has potent ability to transform barbaloin to aloe-emodin-9-anthrone by cleaving the *C*-glycosyl bond, but this bacterium had no ability to metabolize aloesin (**1**). This suggests that intestinal bacteria produce some *C*-glycosyl-cleaving enzymes specific for individual substrates as mentioned in the previous paper.[5]

Experimental

Instruments Melting points were determined on a Yanagimoto micro-melting point apparatus and uncorrected. ^{1}H- and ^{13}C-NMR spectra were measured with JEOL JNM-FX 270 (^{1}H, 270 MHz) and JEOL JNM-FX 90Q (^{13}C, 22.5 MHz) spectrometers and chemical shifts are represented as δ values relative to tetramethylsilane (TMS). MS were measured with a JEOL JMS DX 300 mass spectrometer at an ionization voltage of 70 eV. Densitometric profiles of TLC were recorded on a Shimadzu CS-910 dual wavelength TLC scanner. Optical rotations were measured with a Jasco DIP-4 automatic polarimeter at 21 °C.

Chromatography Wakogel 200 (Wako Pure Chem. Ind. Co., Osaka) was used for column chromatography and Merck Kieselgel 60 F_{254} (E. Merck, Darmstadt; layer thickness, 0.25 mm) for TLC.

Chemicals Aloesin (**1**) and aloeresin A (**2**) were isolated from crude aloin powder (Wako Pure Chem. Ind. Co.) and purified by column chromatography on silica gel followed by crystallization from EtOH. 7-*O*-Methylaloesin (**7**) was prepared by treating aloesin (**1**) with diazomethane.[6]

Culture Media PYF solution broth was prepared according to the procedure of Mitsuoka.[12] GAM was purchased from Nissui Co. (Tokyo, Japan).

Reduction of Aloesin (1) with $NaBH_4$ $NaBH_4$ (2.0 g) was added to a solution of aloesin (**1**) (1.0 g) in MeOH (20 ml). The mixture was stirred for 3 h at room temperature and acidified to pH 3 with 2 N HCl. The solution was extracted with BuOH. The BuOH solution was evaporated to dryness *in vacuo* and the residue was chromatographed on silica gel (column size, 30 cm × 2 cm i.d.; solvent, $CHCl_3$–MeOH (6:4)) to give a mixture of (2'*R*)- and (2'*S*)-8-*C*-glucosylaloesols (**5a** and **5b**) in a yield of 900 mg. The diastereomers were separated by preparative HPLC under the following conditions: column, ODS-10 (Nomura Chem. Co.); mobile phase, CH_3CN–H_2O (3:40); flow rate, 2.0 ml/min; detection, 290 nm.

(2'*S*)-8-*C*-Glucosylaloesol (**5b**): t_R = 7.0 min on HPLC (MeOH). EI-MS *m/z*: 397 ($M^+ + 1$). ^{1}H-NMR (270 MHz, DMSO-d_6) δ: 1.13 (3H, d, J = 6.1 Hz, 3'-H_3), 2.60 (1H, dd, J = 5.9, 13.7 Hz, 1'-H_a), 2.63 (3H, s, 5-Me), 2.65 (1H, dd, J = 7.3, 13.7 Hz, 1'-H_b), 3.1—5.0 (sugar-H), 4.10 (1H, m, 2'-H), 4.73 (1H, d, J = 9.5 Hz, 1''-H), 5.98 (1H, s, 3-H), 6.64 (1H, s, 6-H). In an anaerobic incubation with a bacterial mixture from human feces, the compound was converted to an aglycone, (2'*S*)-aloesol: $[\alpha]_D$ +39.1° (c = 0.11, MeOH). The optical rotation value was in agreement with that of the naturally occurring 2'*S*-form.[11]

(2'*R*)-8-*C*-Glucosylaloesol (**5a**): t_R = 8.1 min on HPLC. $[\alpha]_D$ −14.8° (c = 0.13, MeOH). EI-MS *m/z*: 397 ($M^+ + 1$). ^{1}H-NMR (270 MHz, DMSO-d_6) δ: 1.16 (3H, d, J = 6.1 Hz, 3'-H_3), 2.58 (2H, d, J = 6.1 Hz, 1'-H_2), 2.63 (3H, s, 5-Me), 3.1—5.0 (sugar-H), 4.13 (1H, m, 2'-H), 4.73 (1H, d, J = 9.5 Hz, 1''-H), 5.97 (1H, s, 3-H), 6.64 (1H, s, 6-H). In an anaerobic

incubation with a bacterial mixture from human feces, the compound was converted to an aglycone, (2′*R*)-aloesol: $[\alpha]_D$ −30° (*c*=0.31, MeOH).

Acetylation of Aloesin (1) Aloesin (**1**) was acetylated with acetic anhydride in pyridine to give 2″,3″,4″,6″-tetra-*O*-acetylaloesin (**8**). The physical and spectral data of **8** were as follows: EI-MS *m/z* (rel. int.): 562 (M^+, 20%), 340 (13%), 337 (30%), 261 (21%), 43 (100%). ^{1}H-NMR (270 MHz, $CDCl_3$) δ: 1.74 (3H, s, 3′-H_3), 2.03 (3H, s, OAc), 2.10 (3H, s, OAc), 2.17 (3H, s, OAc), 2.38 (3H, s, OAc), 2.78 (3H, br d, *J*=0.7 Hz, 5-H_3), 3.62, 3.70 (each 1H, AB q, *J*=16.2 Hz, 1′-H_2), 3.94 (1H, ddd, *J*=11.1, 2.2, 3.4 Hz, 5″-H), 4.16 (1H, dd, *J*=12.6, 2.2 Hz, 6″-H_a), 4.33 (1H, dd, *J*=12.6, 3.4 Hz, 6″-H_b), 5.2—5.4 (sugar-H), 6.07 (1H, s, 3-H), 6.69 (1H, d, *J*=0.7 Hz, 6-H).

Microorganisms The following intestinal bacterial strains from human feces were used for the screening of bacteria capable of metabolizing aloesin (**1**): *Bacteroides fragilis* ss. *thetaotus*, *Bifidobacterium adolescentis*, *B. breve* S-2 KZ 1287, *B. bifidum* a E319, *B. pseudolongum* PNC-2-9-G, *Clostridium butyricum*, *C. innocuum* ES 24-06, *C. perfringens* To-23, *Fusobacterium nucleatum* G-0470, *Gaffkya anaerobia* G-0608, *Klebsiella pneumoniae* ATCC 13883, *Lactobacillus acidophilus* ATCC 4356, *L. brevis* II-46, *L. fermentum* ATCC 9338, *L. plantarum* ATCC 14917, *L. xylosus* ATCC 155775, *Peptostreptococcus anaerobius* 0240, *P. intermedius*, *Proteus mirabilis* S2 and *Streptococcus faecalis* II-136.

Preparation of a Bacterial Mixture from Human Feces Fresh feces from a healthy man were thoroughly suspended in 50 volume of 0.2 M phosphate buffer (pH 7.2), filtered through layers of gauze to eliminate the sediment. The filtrate was used as an intestinal bacterial mixture in the following experiments.

Time Course of the Metabolism of Aloesin (1) by Intestinal Bacteria A tube containing **1** (10.7 mg) and an intestinal bacterial mixture (10 ml) was incubated at 37 °C in an anaerobic box. A portion (0.5 ml) of the mixture was taken out at intervals, and vigorously mixed with BuOH (0.5 ml). An aliquot of the BuOH layer was applied to a TLC plate and the plate was developed with $CHCl_3$–MeOH–H_2O (50 : 10 : 1). *Rf* values of aloesin (**1**), aloesone (**3**) and *dl*-aloesol (**4a**+**4b**) were 0.06, 0.59 and 0.44, respectively. The metabolites separated on the plate were quantitatively analyzed with a TLC scanner at 290 nm in the single scan mode. The calibration line was prepared with an authentic sample.

Time Course of the Metabolism of Aloeresin A (2) by Intestinal Bacteria Similar to the case of alosin (**1**), aloeresin A (**2**) was anaerobically incubated and the metabolites were extracted with BuOH. A portion of the extract was chromatographed on a silica gel plate with $CHCl_3$–MeOH–H_2O (50 : 10 : 1) and analyzed by densitometry. *Rf* values of the products were as follows: aloesone (**3**), 0.59; *dl*-aloesol (**4a**+**4b**), 0.44; *p*-coumaric acid, 0.20; aloesin (**1**), 0.06; aloeresin A (**2**), 0.13.

Incubation of Aloesin (1) with an Intestinal Bacterial Mixture Aloesin (1.0 g, **1**) was added to an intestinal bacterial mixture (500 ml) and incubated for 3 d at 37 °C in an anaerobic box. The mixture was extracted three times with BuOH (500 ml each). The combined BuOH solutions were evaporated *in vacuo* to give a residue (*ca.* 1.8 g). The residue was applied to a column of silica gel (20 cm × 3 cm i.d.; 45 g), which was eluted successively with $CHCl_3$, $CHCl_3$–MeOH (95 : 5) to give metabolites A and B (240 and 20 mg, respectively). The metabolites were further purified by crystallization from EtOH.

Metabolite A (2-Acetonyl-7-hydroxy-5-methylchromone, **3**): Colorless needles, mp. 218—221 °C, EI-MS *m/z* (rel. int.): 232 (M^+, 62%), 190 (86%), 161 (24%), 151 (42%), 43 (CH_3CO, 100%). IR ν_{max}^{KBr} cm^{-1}: 3450 (OH), 1650, 1545, 1360, 1280. ^{1}H-NMR (270 MHz, DMSO-d_6) δ: 2.22 (3H, s, 3′-H_3), 2.66 (3H, s, 5-Me), 3.86 (2H, s, 1′-H_2), 6.04 (1H, s, 3-H), 6.59 (1H, *J*=2.4 Hz, 8-H), 6.61 (1H, br d, *J*=2.4 Hz, 6-H), 10.58 (1H, s, 7-OH).

Metabolite B (7-Hydroxy-2-(2′-hydroxypropyl)-5-methylchromone): Colorless needles, mp 175—178 °C. $[\alpha]_D$ 0° (*c*=0.044, MeOH). IR ν_{max}^{KBr} cm^{-1}: 3400, 1630, 1540, 1360, 1285. EI-MS *m/z* (rel. int.): 234 (M^+, 65%), 190 (85%), 161 (20%), 151 (36%), 124 (15%), 91 (13%), 45 (42%), 18 (100%). ^{1}H-NMR (270 MHz, CD_3OD) δ: 1.27 (3H, d, *J*=6.3 Hz, 3′-H_3), 2.65 (1H, dd, *J*=14.2, 7.6 Hz, 1′-H_a), 2.68 (1H, dd, *J*=14.2, 5.6 Hz, 1′-H_b), 2.72 (3H, s, 5-Me), 4.19 (1H, m, 2′-H), 6.06 (1H, s, 3-H), 6.63 (1H, br d, *J*=2.0 Hz, 6-H), 6.66 (1H, d, *J*=2.0 Hz, 8-H).

Screening of Bacterial Strains for Ability to Metabolize Aloesin (1) A defined stock strain of intestinal bacteria was anaerobically cultured in GAM and PYF broth (2 ml) containing aloesin (2.0 mg, **1**) for 5 d at 37 °C. The culture was extracted with BuOH (1.0 ml) and the extract was analyzed by means of HPLC under the conditions described in the legend to Fig. 1.

Incubation of Aloeresin A (2) with an Intestinal Bacterial Mixture Aloeresin A (100 mg, **2**) in dimethyl sulfoxide (DMSO) (1.0 ml) was incubated with an intestinal bacterial mixture (100 ml) for 3 d at 37 °C in an anaerobic box. The incubation mixture was extracted three times with BuOH (100 ml each) and the BuOH layer was concentrated *in vacuo*. The residue (400 mg) was applied to a column of silica gel (300 mm × 20 mm i.d.; 45 g). The column was eluted successively with $CHCl_3$ and $CHCl_3$–MeOH (95 : 5 and 90 : 10) to give aloesone (**3**) (25 mg), *dl*-aloesol (**4a**+**4b**) (5 mg), a mixture of (*E*)- and (*Z*)-*p*-coumaric acids in a ratio of 9 : 1 and aloesin (**1**) (7.3 mg). The relative ratio of *p*-coumaric acids was determined by ^{1}H-NMR on the basis of the respective peak area of the vinyl proton signals which appeared at δ 6.28 and 7.60 (each d, *J*=16.0 Hz) in the *E*-form and at δ 5.76 and 6.73 (each d, *J*=12.7 Hz) in the *Z*-form.

Incubation of (2′*R*)- and (2′*S*)-8-*C*-Glucosylaloesols (5a and 5b) with an Intestinal Bacterial Mixture A mixture of 8-*C*-glucosylaloesols (**5a** and **5b**) (50 mg) prepared by the reduction of aloesin (**1**) with $NaBH_4$ was incubated with a bacterial mixture (50 ml) for 3 d at 37 °C in an anaerobic box. The reaction mixture was concentrated *in vacuo*. The residue (150 mg) was chromatographed on silica gel (45 g, $CHCl_3$–MeOH (95 : 5)) to give *dl*-aloesol (**4a**+**4b**) (20 mg). Similarly, each diastereomer (**5a** and **5b**) separated by HPLC was also converted to the corresponding optically active aglycones (**4a** and **4b**) as shown in Table II.

Incubation of Aloesone (3) with an Intestinal Bacterial Mixture Aloesone (30 mg, **3**) in DMSO (0.2 ml) was incubated with an intestinal bacterial mixture (30 ml) for 3 d at 37 °C in an anaerobic box. The incubation mixture was concentrated *in vacuo*, followed by preparative TLC on silica gel with EtOAc to give *dl*-aloesol (**4a**+**4b**) in a yield of 18 mg (59%).

References

1) G. Franz and M. Gruen, *Planta Medica*, **47**, 131 (1983).
2) M. Hattori, T. Kanda, Y. Shu, T. Akao, K. Kobashi, and T. Namba, *Chem. Pharm. Bull.*, **36**, 4462 (1988).
3) M. Hattori, Y. Shu, A. I. El-Sedawy, T. Namba, K. Kobashi, and T. Tomimori, *J. Nat. Prod*, **51**, 874 (1988).
4) M. Hattori, Y. Shu, T. Tomimori, K. Kobashi, and T. Namba, *Phytochemistry*, **28**, 1289 (1989).
5) Q. Che, T. Akao, M. Hattori, K. Kobashi, and T. Namba, *Planta Medica*, in press, (1991).
6) L. J. Haynes and D. K. Holdworth, *J. Chem. Soc.* (*C*), **1970**, 2582.
7) P. Gramatica, D. Monti, G. Speranza, and P. Manitto, *Tetrahedron Lett.*, **23**, 2423 (1982).
8) K. Makino, A. Yagi, and I. Nishioka, *Chem. Pharm. Bull.*, **22**, 1565 (1974).
9) J. M. Conner, A. I. Gray, T. Reynolds, and P. G. Waterman, *Phytochemistry*, **29**, 941 (1990).
10) G. Speranza, P. Gramatica, G. Dada, and P. Manitto, *Phytochemistry*, **24**, 1571 (1985).
11) Y. Kashiwada, G. Nonaka, and I. Nishioka, *Chem. Pharm. Bull.*, **32**, 3493 (1984).
12) T. Mitsuoka, "A Color Atlas of Anaerobic Bacteria," Shobunsha Co., Tokyo, 1980, p. 325.

New Aurone Glucosides and New Phenylpropanoid Glucosides from *Bidens pilosa*

Yutaka SASHIDA,* Kazunori OGAWA, Makoto KITADA, Hiroyuki KARIKOME, Yoshihiro MIMAKI, and Hiroko SHIMOMURA

Tokyo College of Pharmacy, 1432–1 Horinouchi, Hachioji-shi, Tokyo 192–03, Japan. *Received September 10, 1990*

Three new glucosides of (*Z*)-6,7,3',4'-tetrahydroxyaurone, (*Z*)-7-*O*-β-D-glucopyranosyl-6,7,3',4'-tetrahydroxyaurone, (*Z*)-6-*O*-(6-*O*-*p*-coumaroyl-β-D-glucopyranosyl)-6,7,3',4'-tetrahydroxyaurone, (*Z*)-6-*O*-(6-*O*-acetyl-β-D-glucopyranosyl)-6,7,3',4'-tetrahydroxyaurone, together with (*Z*)-6-*O*-β-D-glucopyranosyl-6,7,3',4'-tetrahydroxyaurone, and two new phenylpropanoid glucosides, 4-*O*-(6-*O*-*p*-coumaroyl-β-D-glucopyranosyl)-*p*-coumaric acid and 4-*O*-(2-*O*-acetyl-6-*O*-*p*-coumaroyl-β-D-glucopyranosyl)-*p*-coumaric acid, have been isolated from the fresh leaves of *Bidens pilosa*. These structures have been elucidated on the basis of spectral data and chemical correlation.

Keywords aurone glucoside; (*Z*)-6,7,3',4'-tetrahydroxyaurone; (*Z*)-6-*O*-β-D-glucopyranosyl-6,7,3',4'-tetrahydroxyaurone; (*Z*)-7-*O*-β-D-glucopyranosyl-6,7,3',4'-tetrahydroxyaurone; (*Z*)-6-*O*-(6-*O*-*p*-coumaroyl-β-D-glucopyranosyl)-6,7,3',4'-tetrahydroxyaurone; (*Z*)-6-*O*-(6-*O*-acetyl-β-D-glucopyranosyl)-6,7,3',4'-tetrahydroxyaurone; phenylpropanoid glucoside; 4-*O*-(6-*O*-*p*-coumaroyl-β-D-glucopyranosyl)-*p*-coumaric acid; 4-*O*-(2-*O*-acetyl-6-*O*-*p*-coumaroyl-β-D-glucopyranosyl)-*p*-coumaric acid; *Bidens pilosa*

Bidens pilosa L. (Compositae) was widely distributed in pantropical regions, and was also naturalized in Japan. The whole herb or the leaves are used as a folk medicine in China,[1] Hawaii[2] and other countries.[3] Chalcone glucosides were previously isolated from *B. pilosa*.[4] Our investigation of the chemical constituents of the fresh leaves of *B. pilosa* led to the isolation of three new aurone glucosides, (*Z*)-7-*O*-β-D-glucopyranosyl-6,7,3',4'-tetrahydroxyaurone (**1**), (*Z*)-6-*O*-(6-*O*-*p*-coumaroyl-β-D-glucopyranosyl)-6,7,3',4'-tetrahydroxyaurone (**2**), and (*Z*)-6-*O*-(6-*O*-acetyl-β-D-glucopyranosyl)-6,7,3',4'-tetrahydroxyaurone (**3**), and two new phenylpropanoid glucosides, 4-*O*-(6-*O*-*p*-coumaroyl-β-D-glucopyranosyl)-*p*-coumaric acid (**4**) and 4-*O*-(2-*O*-acetyl-6-*O*-*p*-coumaroyl-β-D-glucopyranosyl)-*p*-coumaric acid (**5**), together with known compounds, (*Z*)-6-*O*-β-D-glucopyranosyl-6,7,3',4'-tetrahydroxyaurone[5,6] (**6**), and okanin 4'-*O*-β-D-glucopyranoside[4d] (**7**) and quercetin 3-*O*-β-D-glucopyranoside[5] (**8**). The structures of these compounds are reported here.

Compound **1** was obtained as yellow needles. The secondary ion mass spectrum (SI-MS) of **1** showed the $[M+H]^+$ at *m/z* 449. The ^{1}H-nuclear magnetic resonance (^{1}H-NMR) spectrum (see Experimental) of **1** showed signals indicative of the presence of 2,5,6-related aromatic protons, *ortho*-related protons, and a β-anomer proton. In the ultraviolet (UV) spectrum of **1**, the main absorption appeared at 404 nm. These data closely related to those of the co-occurring aurone glucoside (**6**). Acid hydrolysis of **1** with 10% hydrochloric acid afforded an aglycon (**1a**) which was identical with (*Z*)-6,7,3',4'-tetrahydroxyaurone derived from **6** and D-glucose. No sugar was attached to the 3',4'-dihydroxyl position of the B-ring in **1**, because the 29 nm bathochromic shift on its UV spectrum in the presence of NaOAc with H_3BO_3 showed the existence of the free *ortho*-dihydroxyl group in the B-ring.[5] In the ^{13}C-NMR data of **1**, only signals corresponding to the A-ring changed

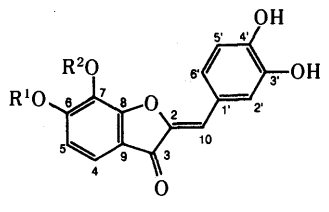

	R^1	R^2
1	H	β-D-glucopyranosyl
1a	H	H
2	6-*O*-*p*-coumaroyl-β-D-glucopyranosyl	H
3	6-*O*-acetyl-β-D-glucopyranosyl	H
6	β-D-glucopyranosyl	H

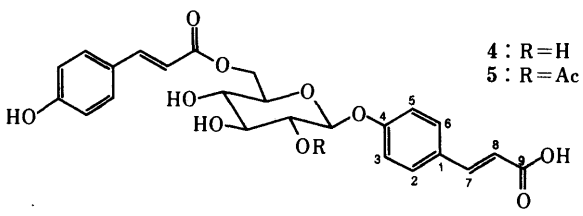

4: R=H
5: R=Ac

Chart 1

TABLE I. ^{13}C-NMR Data[a] of **1**, **1a**, **2**, **3**, and **6**

	1	**1a**	**2**	**3**	**6**
Aurone moiety					
2	147.6	147.9	147.4	147.4	147.3
3	183.8	184.9	185.1	185.1	184.9
4	122.1	116.8	115.6	115.5	115.7
5	115.0	113.7	113.6	113.6	113.7
6	160.2[b]	156.3[b]	153.5	153.5	153.6
7	131.1	131.7	134.6	134.5	134.4
8	160.7[b]	156.9[b]	156.2	156.2	156.0
9	116.3	116.3	119.1	119.2	119.0
10	114.9	114.3	115.3	115.4	115.4
1'	125.3	125.5	125.3	125.3	125.3
2'	119.5	119.4	119.4	119.4	119.4
3'	146.9	146.9	146.9	146.9	146.9
4'	149.7	149.5	149.8	149.8	149.8
5'	117.1	116.8	116.8	116.8	116.7
6'	126.8	126.2	126.9	126.7	126.5
Glucose moiety					
1	107.0		103.1	103.1	103.3
2	75.4		74.8	74.8	74.8
3	77.8		77.6	77.5	77.7
4	70.8		71.7	71.5	71.2
5	78.5		75.9	75.7	78.7
6	62.0		64.5	64.6	62.3
Acyl moiety					
1			126.7	172.6	
2,6			131.2	20.7	
3,5			117.0		
4			161.4		
7			146.6		
8			114.9		
9			165.6		

a) Spectra were measured at 100.6 MHz in CD_3OD–C_5D_5N (5 : 1). The data were given in δ value. *b*) These assignments in each column may be changed.

their positions compared with those of **6** and **1a** (see Table I). The combined spectral data indicated that the β-D-glucosyl moiety attached to the 7-hydroxyl position of **1a**. Thus, the structure of **1** was determined as (*Z*)-7-*O*-β-D-glucopyranosyl-6,7,3′,4′-tetrahydroxyaurone.

Compounds **2** and **3** were obtained as orange-red powder and as orange powder, respectively. Spectral data of **2** and **3** closely related to those of **6** except for the existence of a *p*-coumaroyl group in **2** and that of an acetyl group in **3**. Alkaline methanolysis of **2** with NaOMe (3% in MeOH) afforded **6** and methyl *p*-coumarate, and that of **3** gave **6**. In the ^{1}H-NMR spectra of **2**, the H_2-6 signals of the glucose moiety appeared at further downfield than those in **6**. In the ^{13}C-NMR spectra of the glucose moiety of **2**, the C-5 signal shifted to further highfield and that of the C-6 to further downfield compared with those of **6**. These nature of the NMR data was also observed in **3**. The above data indicated that the acyl groups in both **2** and **3** attached to the 6-hydroxyl position of the glucose. Thus, the structure of **2** was (*Z*)-6-*O*-(6-*O*-*p*-coumaroyl-β-D-glucopyranosyl)-6,7,3′,4′-tetrahydroxyaurone, and that of **3** was (*Z*)-6-*O*-(6-*O*-acetyl-β-D-glucopyranosyl)-6,7,3′,4′-tetrahydroxyaurone.

Compound **4** was obtained as colorless needles. The ^{1}H-NMR data of **4** showed two AB systems and two aromatic AA′BB′ systems and sugar protons. Treatment of **4** with 10% hydrochloric acid gave D-glucose and *p*-coumaric acid. Thus, **4** consisted of two *p*-coumaric acids and one glucose. Acetylation of **4** afforded the tetraacetate (**4a**). Its ^{1}H- and ^{13}C-NMR spectra (see Experimental and Table II) indicated that **4a** had three alcoholic and one phenolic acetyl groups. Methylation of **4** with diazomethane gave the dimethyl derivative (**4b**). The anomeric proton and carbon signals in the NMR data of **4** indicated the existence of β-glucosyl linkage in **4**. From the above results, **4** had the 4-*O*-β-D-glucopyranosyl-*p*-coumaric acid structure. This was confirmed by alkaline methanolysis of **4** with NaOMe (3% in methanol), followed by acetylation, giving the tetraacetate (**4c**) of the deacyl derivative of **4**. Location of the other *p*-coumaroyl group was decided at the 6-position of the glucose, because the ^{1}H-NMR signals due to the H_2-6 of the glucose moiety of **4** appeared at further downfield and the ^{13}C-NMR signals due to the C-5 and C-6 of that appeared, respectively, at higher field and lower field than those of methyl β-D-glucopyranoside. Thus, the structure of **4** was concluded to be 4-*O*-(6-*O*-*p*-coumaroyl-β-D-glucopyranosyl)-*p*-coumaric acid.

Compound **5** was obtained as colorless needles. The ^{1}H and ^{13}C-NMR spectra of **5** showed that the structure possessed the same components as **4** and an additional acetyl group. Acetylation of **5** yielding a derivative identical with **4a** revealed that **5** was the monoacetate of **4**. The anomeric carbon signal of **5** shifted further upfield than that of **1** in the ^{13}C-NMR spectrum and the H-2 signal of **5** appeared at downfield in the ^{1}H-NMR spectrum. These data were coincident with the fact that the 2-hydroxyl group of the glucose moiety was acetylated. Thus, the structure of **2** was determined to be 4-*O*-(2-*O*-acetyl-6-*O*-*p*-coumaroyl-β-D-glucopyranosyl)-*p*-coumaric acid.

TABLE II. ^{13}C-NMR Data[a] of **4**, **4a**, and **5**

	4	4a	5
Glucose moiety			
1	102.0	98.4	99.4
2	74.8[b]	72.7[b]	75.9[b]
3	78.4	72.3[b]	74.7[b]
4	71.5	71.2	71.5
5	75.7[b]	68.6	75.8[b]
6	64.4	62.2	64.0
p-Coumaroyl moiety			
1	129.4	131.8	129.9
	126.1	129.2	126.0
2,6	130.7	130.0	130.8
	130.0	129.4	130.1
3,5	117.5	122.3	117.5
	117.0	117.2	117.0
4	161.6	158.5	161.7
	159.9	152.4	159.2
7	145.4	145.9	145.5
	143.7	144.7	143.5
8	118.9	117.2	119.3
	115.1	116.0	114.9
9	169.4	169.3	169.3
	167.3	169.1	167.3
Acetyl moiety			
		171.2	170.1
		170.3	21.0
		169.5	
		166.2	
		21.2	
		20.7 (3C)	

a) Spectra were measured in C_5D_5N at 100.6 MHz. The data were given in δ value. b) These assignments in each column may be interchanged.

Experimental

Melting points are uncorrected. Measurements of optical rotation were carried out on a Jasco DIP-360 digital polarimeter. Infrared (IR) spectra were recorded on a Hitachi 260-36 and a Perkin-Elmer 1710. UV spectra were obtained with a Hitachi 557 spectrometer. Mass spectra (MS) were measured on a Hitachi M-80. One-dimentional NMR spectra were measured on a Bruker AM-400 spectrometer. Two-dimensional NMR spectra were obtained with an AM-500 spectrometer.

The leaves of *B. pilosa* were collected in Hino-shi, Tokyo in November, 1986. The concentrated MeOH extract of the fresh leaves (2.0 kg) of the plant was suspended in water. The suspension was successively extracted with $CHCl_3$ and BuOH. Chromatography of the BuOH phase (*ca.* 3.0 g) on silica gel (Fuji gel BM360, $CHCl_3$–MeOH system), ODS (Kusano CIG column, MeOH–H_2O system), and Diaion HP-20 (MeOH–H_2O system) afforded **1** (16 mg), **2** (60 mg), **3** (90 mg), **4** (90 mg), **5** (200 mg), **6** (195 mg),[5,6] **7** (13 mg),[4d] and **8** (24 mg).[5] Compounds **7** and **8** gave data identical with that described in the literature. No NMR spectral data for **6** were available. In order to confirm the structure of **6**, the ^{1}H- and ^{13}C-NMR spectral data combined with the results of the H–C correlation spectroscopy (H–CCOSY) and correlation spectroscopy *via* long-range coupling (COLOC) experiments were obtained. The NMR data and other spectral and physical data of **6** (see below) agreed with the structure of 6-*O*-β-D-glucopyranosyl-6,7,3′,4′-tetrahydroxyaurone. The geometry corresponding to the olefin portion of **6** was not referred to in the literature. On the basis of the chemical shift of the C-10 in the ^{13}C-NMR, the olefin was assumed to be a *Z*-isomer.[7]

(*Z*)-7-*O*-β-D-Glucopyranosyl-6,7,3′,4′-tetrahydroxyaurone (1) Yellow needles from MeOH–H_2O, mp 245—248 °C, $[\alpha]_D^{30}$ −93° (*c*=0.2, MeOH). SI-MS *m/z*: 449 $[M+H]^+$. EI-MS *m/z* (%): 286 (100), 152 (70). IR ν_{max}^{KBr} cm^{-1}: 3423, 2922, 1677, 1650, 1600, 1532, 1446, 1373, 1309, 1168, 1128, 1051, 1021. UV λ_{max}^{MeOH} nm (log ε): 208 (4.33), 245 (3.96), 257 (3.96), 268 sh (3.91), 340 sh (3.99), 404 (4.41); +NaOMe: 210, 253, 274 sh, 380 sh, 397, 466; +$AlCl_3$: 209, 259, 287, 343, 448; +$AlCl_3$–HCl: 207, 257, 271, 340 sh, 403; +NaOAc: 215, 244, 260 sh, 427; +NaOAc: 218, 249, 275, 433; +NaOAc–H_3BO_3: 217, 433. ^{1}H-NMR (400 MHz, CD_3OD–C_5D_5N (5:1)) δ: aurone moiety [7.84 (1H, d, *J*=2.1 Hz, H-2′), 7.45 (1H, d, *J*=8.4 Hz, H-4), 7.44 (1H, dd, *J*=8.4, 2.1 Hz, H-6′), 6.70 (1H, d, *J*=8.4 Hz, H-5), 6.81 (1H, d, *J*=8.4 Hz, H-5′), 6.78 (1H, s, H-10)]; glucose moiety [5.19 (1H, d, *J*=7.4 Hz, H-1), 3.93 (2H, m, H_2-6), 3.80—3.68 (5H,

overlapping, H-2, 3, 4, 5)].

Acid Hydrolysis of 1 Treatment of **1** (4 mg) with 5% HCl (4 ml) at 90 °C for 30 min gave D-glucose (0.8 mg), which was identical with an authentic sample, and **1a** (1.1 mg). **1a**: Red powder. EI-MS *m/z* (%): 286 $[M]^+$ (100), 153 (40), 152 (68), 134 (16). IR ν_{max}^{KBr} cm^{-1}: 3420. 1680, 1650, 1610, 1590, 1530, 1460, 1410, 1320, 1300. UV λ_{max}^{MeOH} nm (log ε): 208 (4.25), 246 sh (3.83), 270 sh (3.74), 350 (3.93), 410 (4.24); +NaOMe: 210, 253, 265, 388 sh, 403, 474; +$AlCl_3$: 209, 267, 286 sh, 390 sh, 454; +$AlCl_3$–HCl: 270, 246 sh, 255 sh, 272 sh, 350 sh, 410; +NaOAc: 217, 246 sh, 266, 390 sh, 434; +NaOAc–H_3BO_3: 213, 250 sh, 276 sh, 370 sh, 385 sh, 447. ^{1}H-NMR (400 MHz, CD_3OD–C_5D_5N (5:1)) δ: 7.63 (1H, d, *J*=2.0 Hz, H-2'), 7.41 (1H, dd, *J*=8.3, 2.0 Hz, H-6'), 7.24 (1H, d, *J*=8.3 Hz, H-4), 6.92 (1H, d, *J*=8.3 Hz, H-5), 6.80 (1H, d, *J*=8.3 Hz, H-5'), 6.76 (1H, s, H-10).

(*Z*)-6-*O*-(6-*O*-*p*-Coumaroly-β-D-glucopyranosyl)-6,7,3',4'-tetrahydroxyaurone (2) Red powder, $[\alpha]_D^{29}$ −96° (*c*=0.5, MeOH). EI-MS *m/z* (%): 286 (100), 147 (100). CI-MS *m/z* (%): 286 [aglycon]$^+$ (100), 153 (80), 152 (90), 147 (96), 120 (56). IR ν_{max}^{KBr} cm^{-1}: 3400, (4.51), 226 sh (4.27), 314 (4.36), 412 (4.25); +NaOMe; 206, 240 sh, 303 sh, 357, 488; +$AlCl_3$: 207, 300 sh, 310, 455; +$AlCl_3$–HCl: 205, 226 sh, 282 sh, 314, 414; +NaOAc: 205, 228, 310, 415. ^{1}H-NMR (400 MHz, CD_3OD–C_5D_5N (5:1)) δ: aurone moiety [7.65 (1H, d, *J*=2.0 Hz, H-2'), 7.37 (1H, dd, *J*=8.3, 2.0 Hz, H-6'), 7.22 (1H, d, *J*=8.3 Hz, H-4), 7.20 (1H, *J*=8.3 Hz, H-5), 6.91 (1H, d, *J*=8.3 Hz, H-5'), 6.77 (1H, s, H-10)]; glucose moiety [5.19 (1H, d, *J*=7.4 Hz, H-1), 4.71 (1H, dd, *J*=12.0, 2.1 Hz, H_A-6), 4.48 (1H, dd, *J*=12.0, 6.7 Hz, H_B-6), 3.93 (1H, ddd, *J*=9.2, 6.7, 2.1 Hz, H-5), 3.80—3.70 (2H, overlapping, H-2,3), 3.63 (1H, dd, *J*=9.2, 9.2 Hz, H-4)]; *p*-coumaric acid moiety [7.65 (1H, d, *J*=16.0 Hz, H-7), 7.44 (2H, AA'BB', *J*=8.6 Hz, H-2, 6), 6.89 (2H, AA'BB', *J*=8.6 Hz, H-3, 5), 6.36 (1H, d, *J*=16.0 Hz, H-8)].

Alkaline Methanolysis of 2 Alkaline methanolysis of **2** (10 mg) with NaOMe (3% in MeOH) at room temperature for 1 h gave methyl *p*-coumarate (1.3 mg) and **6** (1.6 mg).

(*Z*)-6-*O*-(6-*O*-Acetyl-β-D-glucopyranosyl)-6,7,3',4'-tetrahydroxyaurone (3) Orange-red powder, $[\alpha]_D^{30}$ −99° (*c*=0.5, MeOH). SI-MS *m/z*: 491 $[M+H]^+$. EI-MS *m/z* (%): 286 (286), 152 (50). IR ν_{max}^{KBr} cm^{-1}: 3450, 1700, 1640, 1610, 1520, 1450, 1370, 1260, 1170, 1126, 1070, 1040. UV λ_{max}^{MeOH} nm (log ε): 204 (4.46), 242 sh (3.97), 273 (3.84), 326 (4.07), 411 (4.36); +NaOMe: 204, 260, 245 sh, 350, 486; +$AlCl_3$: 205, 246 sh, 288, 330, 455; +$AlCl_3$–HCl: 204, 240 sh, 272, 326, 413; +NaOAc: 204, 253 sh, 380 sh, 420. ^{1}H-NMR (400 MHz, CD_3OD–C_5D_5N (5:1)) δ: aurone moiety [7.64 (1H, d, *J*=2.0 Hz, H-2'), 7.37 (1H, dd, *J*=8.3, 2.0 Hz, H-6'), 7.29 (1H, d, *J*=8.5 Hz, H-4), 7.14 (1H, d, *J*=8.5 Hz, H-5), 6.91 (1H, d, *J*=8.3 Hz, H-5'), 6.80 (1H, s, H-10)]; glucose moeity [5.13 (1H, d, *J*=7.4 Hz, H-1), 4.53 (1H, dd, *J*=11.9, 2.0 Hz, H_A-6), 4.35 (1H, dd, *J*=11.9, 6.5 Hz, H_B-6), 3.83 (1H, ddd, *J*=9.3, 6.5, 2.0 Hz, H-5), 3.72—3.67 (2H, overlapping, H-2, 3)], 3.54 (1H, dd, *J*=9.3, 9.2 Hz, H-4), 2.05 (3H, s, acetyl).

(*Z*)-6-*O*-β-D-Glucopyranosyl-6,7,3',4'-tetrahydroxyaurone (6) Orange powder, $[\alpha]_D^{23}$ −120° (*c*=0.10, MeOH). SI-MS *m/z*: 449 $[M+I]^+$. IR ν_{max}^{KBr} cm^{-1}: 3440, 1700, 1660, 1620, 1530, 1460, 1390, 1300, 1180, 1150, 1080, 1050. UV λ_{max}^{MeOH} nm (log ε): 207 (4.44), 240 sh (4.03), 271 (3.93), 330 (4.09), 412 (4.39); +NaOMe: 210, 263, 288 sh, 345, 490; +$AlCl_3$: 210, 248 sh, 289, 330, 452; +$AlCl_3$–HCl: 207, 243 sh, 274, 328, 414; +NaOAc: 215, 262, 363, 441. ^{1}H-NMR (400 MHz, CD_3OD–C_5D_5N (5:1)) δ: aurone moiety [7.65 (1H, d, *J*=2.0 Hz, H-2'), 7.38 (1H, dd, *J*=8.3, 2.0 Hz, H-6'), 7.26 (1H, d, *J*=8.5 Hz, H-4), 7.19 (1H, d, *J*=8.5 Hz, H-5), 6.92 (1H, d, *J*=8.3 Hz, H-5'), 6.80 (1H, s, H-10)]; glucose moiety [5.13 (1H, *J*=7.5 Hz, H-1), 4.04 (1H, dd, *J*=12.0, 1.8 Hz, H_A-6), 3.86 (1H, dd, *J*=12.0, 5.0 Hz, H_B-6), 3.75—3.59 (4H, overlapping, H-2, 3, 4, 5)].

Enzymatic Hydrolysis of 6 Enzymatic hydrolysis of **6** (20 mg) with β-glucosidase for 1 h at room temperature afforded D-glucose and **1a** (5.7 mg).

4-*O*-(6-*O*-*p*-Coumaroyl-β-D-glucopyranosyl)-*p*-coumaric acid (4) Colorless needles from $CHCl_3$–MeOH. mp 245—248 °C. $[\alpha]_D^{29}$ −96° (*c*=0.5, EtOAc–MeOH (1:1)). EI-MS *m/z* (%): 309 (9), 164 (100), 147 (100), 119 (88). IR ν_{max}^{KBr} cm^{-1}: 3420, 2920, 1680, 1670, 1630, 1600, 1510, 1240, 1170, 1090, 1070, 830. ^{1}H-NMR (400 MHz, C_5D_5N) δ: *p*-coumaric acid moiety [7.99, 7.94 (each 1H, d, *J*=15.9 Hz, H-7', 7''), 7.61, 7.56 (each 2H, AA'BB', *J*=8.7 Hz, H-2', 2'', 6', 6''), 7.34, 7.22 (each 2H, AA'BB', *J*=8.7 Hz, H-3', 3'', 5', 5''), 6.76, 6.65 (each 1H, d, *J*=15.9 Hz, H-8', 8'')]; glucose moiety [5.65 (1H, d, *J*=7.0 Hz, H-1), 5.18 (1H, br d, *J*=11.6 Hz, H_A-6), 4.92 (1H, dd, *J*=11.6, 6.4 Hz, H_B-6), 4.4—4.2 (4H, H-2, 3, 4, 5)].

Preparation of Tetraacetate (4a) from 4 Acetylation of **4** (20 mg) with Ac_2O and C_5D_5N in the usual manner afforded the tetraacetate (**4a**, 19 mg). Amorphous solid, $[\alpha]_D^{25}$ −50° (*c*=0.4, $CHCl_3$). EI-MS *m/z* (%): 477 (6.8), 435 (2.2), 315 (8.0), 273 (1.2), 220 (1.0), 189 (83), 147 (100). IR ν_{max}^{KBr} cm^{-1}: 3420, 2920, 1748, 1718, 1639, 1605, 1510, 1420, 1377, 1236, 1167, 1078, 838. ^{1}H-NMR (400 MHz, $CDCl_3$) δ: *p*-coumaric acid moiety [7.66, 7.64 (each 1H, d, *J*=16.0 Hz, H-7', 7''), 7.53, 7.44 (each 2H, AA'BB', *J*=8.7 Hz, H-2', 2'', 6', 6''), 7.16, 7.00 (each 2H, AA'BB', *J*=8.7 Hz, H-3', 3'', 5', 5''), 6.38, 6.24 (each 1H, d, *J*=16.0 Hz, H-8', 8'')]; glucose moiety [5.36—5.17 (3H, H-2, 3, 4), 5.17 (1H, d, *J*=7.4 Hz, H-1), 4.41 (1H, dd, *J*=12.3, 2.7 Hz, H_A-6), 4.92 (1H, dd, *J*=12.3, 5.8 Hz, H_B-6), 3.99 (1H, ddd, *J*=9.7, 5.8, 2.7 Hz, H-5)], 2.32 (3H, s, Ac), 2.07 (3H, s, Ac), 2.05 (3H, s, Ac), 2.03 (3H, s, Ac).

Preparation of the Methyl Derivative (4b) from 4 Methylation of **4** (9.2 mg) with CH_2N_2 in the usual manner gave **4b** (3.4 mg). Amorphous solid. EI-MS *m/z* (%): 469 (0.1), 340 (0.3), 323 (2.0), 309 (1.4), 220 (0.8), 193 (2.6), 178 (100), 161 (30), 147 (100), 119 (19). IR ν_{max}^{KBr} cm^{-1}: 3420, 2924, 1710, 1691, 1636, 1605, 1514, 1316, 1257, 1178, 826. ^{1}H-NMR (400 MHz, C_5D_5N) δ: *p*-coumaric acid moiety [7.89, 7.78 (each 1H, d, *J*=16.0 Hz, H-7', 7''), 7.56, 7.55 (each 2H, AA'BB', *J*=8.8 Hz, H-2', 2'', 6', 6''), 7.34, 7.02 (each 2H, AA'BB', *J*=8.8 Hz, H-3', 3'', 5', 5''), 6.67, 6.46 (each 1H, d, *J*=16.0 Hz, H-8', 8'')]; glucose moiety [5.67 (1H, d, *J*=7.4 Hz, H-1), 5.21 (1H, dd, *J*=11.7, 2.1 Hz, H_A-6), 4.92 (1H, dd, *J*=11.7, 7.2 Hz, H_B-6), 4.40—4.20 (4H, H-2, 3, 4, 5)], 3.74 (6H, s, Me×2).

Preparation of Tetraacetate (4c) of the Deacyl Derivative of 4 Alkaline methanolysis of **4** (10 mg) with 3% NaOMe (in MeOH, 2 ml) at room temperature for 1 h gave methyl *p*-coumarate, which was identical with an authentic sample, and a deacyl derivative. Acetylation of the deacyl derivative with Ac_2O and C_5D_5N in the usual manner afforded the tetraacetate (**4c**, 1 mg). **4c**: white powder. EI-MS *m/z* (%): 331 (10), 270 (2), 229 (3), 210 (28), 169 (100), 109 (80). IR ν_{max}^{KBr} cm^{-1}: 3440, 1760, 1640, 1610, 1530, 1380, 1265, 1230, 1040, 810. ^{1}H-NMR (400 MHz, $CDCl_3$) δ: *p*-coumaric acid moiety [7.71 (1H, d, *J*=16.0 Hz, H-7'), 7.50 (2H, AA'BB', *J*=8.7 Hz, H-2', 6'), 7.00 (2H, AA'BB', *J*=8.7 Hz, H-3', 5'), 6.36 (1H, d, *J*=16.0 Hz, H-8')]; glucose moiety [5.35—5.13 (4H, H-1, 2, 3, 4), 4.30 (1H, dd, *J*=12.3, 5.4 Hz, H_A-6), 4.18 (1H, dd, *J*=12.3, 2.4 Hz, H_B-6), 3.89 (1H, ddd, *J*=9.9, 5.4, 2.4 Hz, H-5)], 2.08 (3H, s, Ac), 2.06 (6H, s, Ac×2), and 2.04 (3H, s, Ac).

4-*O*-(2-*O*-Acetyl-6-*O*-*p*-coumaroyl-β-D-glucopyranosyl)-*p*-coumaric Acid (5) Colorless needles from $CHCl_3$–MeOH, mp 238—242 °C, $[\alpha]_D^{25}$ −60° (*c*=0.1, MeOH). EI-MS *m/z* (%): 351 (6), 164 (20), 147 (100). IR ν_{max}^{KBr} cm^{-1}: 3420, 2920, 1735, 1708, 1636, 1605, 1510, 1378, 1259, 1176, 1093, 1056, 830. ^{1}H-NMR (400 MHz, C_5D_5N) δ: *p*-coumaric acid moiety [7.97 and 7.91 (each 1H, d, *J*=15.9 Hz, H-7', 7''), 7.61 and 7.57 (each 2H, AA'BB', *J*=8.7 Hz, H-2', 6', H-2'', 6''), 7.33 and 7.21 (each 2H, AA'BB', *J*=8.7 Hz, H-3', 5', H-3'', 5''), 6.77 and 6.63 (each 1H, d, *J*=15.9 Hz, H-8', 8''); glucose moiety [5.86 (1H, dd, *J*=8.1, 9.0 Hz, H-2)], 5.69 (1H, d, *J*=8.1 Hz, H-1), 5.14 (1H, dd, *J*=11.8, 1.7 Hz, H_A-6), 4.89 (1H, dd, *J*=11.8, 6.4 Hz, H_B-6), 4.40 (1H, dd, *J*=9.0, 9.0 Hz, H-3), 4.37 (1H, ddd, *J*=9.0, 6.4, 1.7 Hz, H-5), 4.23 (1H, dd, *J*=9.0, 9.0 Hz, H-4)], 2.09 (3H, s, Ac). The tetraacetate of **5** obtained by acetylation with Ac_2O and C_5D_5N was completely identical with **4a**.

Acknowledgements We thank Dr. Y. Shida and Ms. Y. Kaneko for MS measurements, and Ms. C. Sakuma for NMR measurements.

References

1) Jiansu New Medical College, "Dictionary of Chinese Crude Drugs," Shanghai Scientific Technologic Publishing, Shanghai, 1986, pp. 1413, 1694, 2239.
2) B. H. Krauss, "Native Plants Used as Medicine in Hawaii," Harold L. Lyon Aboretum, University of Hawaii, Honolulu, 1981.
3) G. Dragendorff, "Die Heilpflanzen," Warner Fritsch, München, 1967, p. 672.
4) *a*) B. Hoffmann and J. Hölzl, *Phytochemistry*, **28**, 247 (1989); *b*) *Idem, ibid.*, **27**, 3700 (1988); *c*) *Idem, Planta Medica*, **54**, 450 (1988); *d*) *Idem, ibid.*, **54**, 52 (1988).
5) T. J. Mably, K. R. Markham, and M. B. Thomas, "The Systematic Identification of Flavonoids," Springer–Verlag, New York, 1970.
6) M. Shimokoriyama and T. A. Geissman, *J. Org. Chem.*, **25**, 1956 (1960).
7) A. Pelter and R. S. Ward, *J. Chem. Soc., Perkin Trans. 1*, **1979**, 328.

Cycloleonurinin, a Cyclic Peptide from Leonuri Fructus

Kaoru KINOSHITA,*[,a] Junko TANAKA,[a] Keiko KURODA (née YAMADA),[a] Kiyotaka KOYAMA,[a] Shinsaku NATORI[a] and Takeshi KINOSHITA[b]

Meiji College of Pharmacy,[a] Yato-cho, Tanashi-shi, Tokyo 188, Japan and Analytical and Metabolic Research Laboratories, Sankyo Co., Ltd.,[b] Hiro-machi, Shinagawa-ku, Tokyo 140, Japan. *Received September 10, 1990*

From Leonuri Fructus, a cyclic peptide composed of twelve amino acid residues was isolated. The sequence of the residues was established by mass spectroscopy and by the use of a protein sequencer for the partial hydrolysates obtained by α-chymotrypsin.

Keywords Leonuri Fructus; *Leonurus artemisia*; *Leonurus sibiricus*; cyclic peptide; FAB MS/MS; NMR

Leonuri Fructus (茺蔚子) is a traditional Chinese drug originating from the fruits of *Leonurus artemisia* S. Y. HU (*L. heterophyllus* SWEET) and *L. sibiricus* (Labiatae).[1,2] Also the terrestrial part of the plant (益母草) is used as a Chinese drug for invigorating blood circulation, regulating menstrual disturbance and to dispel edema.[1,2] In our course of studies on the pharmacological activities of some Chinese medicines, the extracts of the drug showed hypotensive and antiinflammatory effects as well as increased blood flow and relaxation of the aortic smooth muscle.[3,4] Further work revealed that the known guanidine alkaloid, leonurine, and several flavonol glycosides were the active constituents.[3,5] The fruit, Leonuri Fructus, has been alleged to exhibit nearly the same activities as the terrestrial part of the same plant but the constituents have not been characterized except for fatty oils, retinol derivatives, and an uncharacterized basic compound (leonurinine).[1,2] This work was conducted to make clear the alkaloidal constituent(s) and, as a result, the main Dragendorff-positive component of the seeds was found not to be an alkaloid such as leonurine but a cyclic peptide. The structural elucidation of the peptide will be reported in this paper.

The fruits were first defatted with hexane and then extracted with 70% methanol. The extract, after concentration, was partitioned successively with chloroform, ethyl acetate and butanol. Each fraction was checked by

TABLE I. ^{1}H-NMR Chemical Shifts of Cycloleonurinin

	α	β	γ	δ	OH	–NH–	$-CONH_2$	Arom.H
Thr[1]	4.95	4.40	1.00		5.45	7.60		
Thr[2]	4.60	4.00	1.10		5.20	7.40		
Tyr[1]	4.55	2.80, 3.28			9.13[a)]	8.60		6.62 (6H, dd)
Tyr[2]	4.80	2.63, 2.85			9.13[a)]	7.72		6.89 (2H, d)
Tyr[3]	4.58	2.51, 2.70			9.20[a)]	8.15		7.03 (4H,d)
Gly	3.72, 4.58					7.43		
Ala	4.31	1.22				7.43		
Gln	4.10	1.60, 1.95	2.45			8.20	7.18	
Pro[1]	5.00	1.80, 2.18	1.80[b)]	3.5—3.8				
Pro[2]	4.28	1.70, 2.35	1.98, 2.18[b)]	3.5—3.8				
Pro[3]	4.00	1.51, 1.90	1.92[b)]	3.70, 3.91				
Pro[4]	4.55	2.0, 2.1	1.98[b)]	3.00, 3.27				

δ ppm in DMSO-d_6. *a, b)* Assignments may be interchanged.

TABLE II. ^{13}C-NMR Chemical Shifts of Cycloleonurinin

	α	β	γ	δ	–CONH–	$-CONH_2$	Arom.C			
							C-1	C-2, 6	C-3, 5	C-4
Thr[1]	51.6	67.3	17.5		168.1[c)]					
Thr[2]	56.1	66.7	18.3		169.0[c)]					
Tyr[1]	58.1	32.5			169.4[c)]		127.1[d)]	130.1[e)]	114.7[f)]	155.3[g)]
Tyr[2]	54.1	38.3			169.8[c)]		127.3[d)]	130.1[e)]	114.8[f)]	155.7[g)]
Tyr[3]	55.5	35.8			170.1[c)]		128.1[d)]	130.0[e)]	114.9[f)]	155.9[g)]
Gly	40.8				170.3[c)]					
Ala	47.8	17.9			170.6[c)]					
Gln	53.7	26.5	30.1		170.6[c)]	173.7				
Pro[1]	59.2	29.9	21.3[a)]	46.4[b)]	170.7[c)]					
Pro[2]	61.7	29.0	24.2[a)]	45.7	171.5[c)]					
Pro[3]	60.8	27.6	24.5[a)]	47.8	171.8[c)]					
Pro[4]	58.1	31.6	25.3[a)]	46.5[b)]	171.9[c)]					

δ ppm in DMSO-d_6. *a—g)* Assignments may be interchanged.

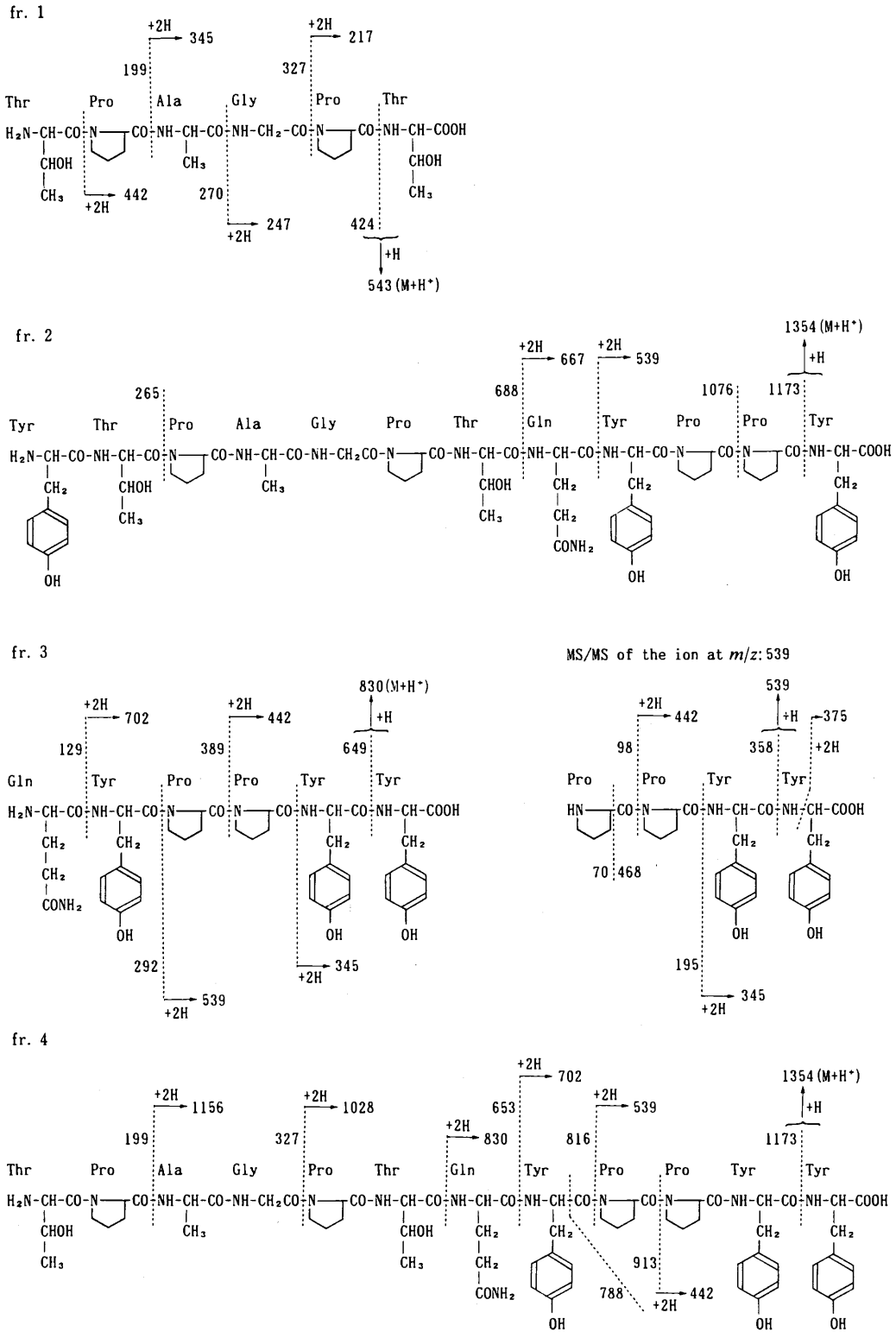

Fig. 1. FAB MS and MS/MS Spectra and Amino Acid Sequence of the α-Chymotrypsin Hydrolysates

Dragendorff's reagent for the presence of basic substances and the butanol fraction, showing the presence of such compounds, was further separated by column chromatography and high performance liquid chromatography (HPLC). Finally two compounds were isolated; one of them was identified as choline chloride and the other, named cycloleonurinin, was isolated as a colorless powder of mp 222—225 °C in a yield of 0.008%.

The elemental analysis of cycloleonurinin showed a high content of nitrogen and oxygen atoms and physical properties such as infrared (IR) absorptions (3400, 1650 (br) cm^{-1}) indicated that the compound might be a peptide. Since the compound is negative in ninhydrin reaction and is devoid of ester absorption in the IR spectrum, the compound was suggested not to be an acyclic peptide or a depsipeptide but a cyclic peptide.

Amino acid analysis of the peptide after hydrolysis with 6 N hydrochloric acid at 110 °C gave the composition:

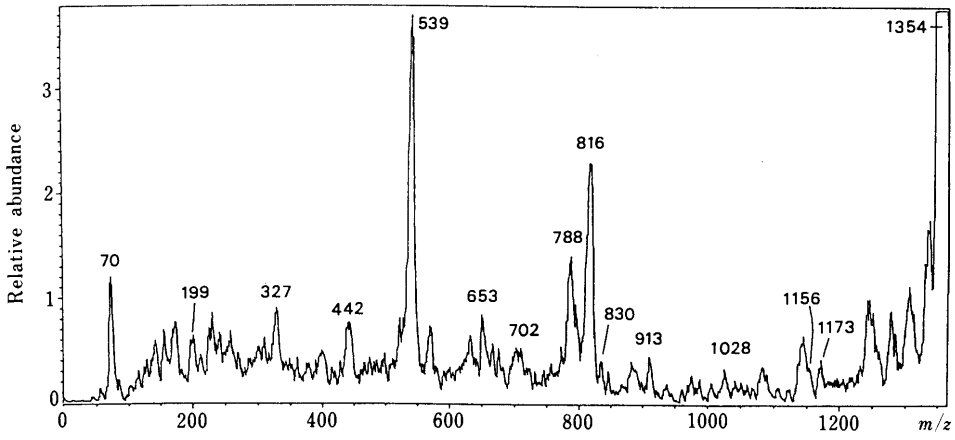

Fig. 2. MS/MS Spectrum of m/z 1354 ($M+H^+$) of fr. 4 by FAB MS

proline (Pro) (4 eq), tyrosine (Tyr) (3 eq), threonine (Thr) (2 eq), alanine (Ala) (1 eq), glutamic acid (Glu) (1 eq) and glycine (Gly) (1 eq). The presence of these amino acid units was also proved by ^{1}H- and ^{13}C-nuclear magnetic resonance (^{1}H- and ^{13}C-NMR) spectra including those by ^{1}H–^{1}H correlation spectroscopy (H–H COSY), ^{13}C–^{1}H COSY (C–H COSY), C–H long-range COSY, distortionless enhancement by polarization transfer (DEPT), and nuclear Overhauser effect spectroscopy (NOESY) as shown in Tables I and II.

The molecular formula of the peptide was established as $C_{65}H_{85}N_{13}O_{18}$ from fast atom bombardment mass spectrum (FAB MS) and secondary ion MS (SIMS) ($[M+H]^+$ ion at m/z 1336) together with the elemental analysis. The formula suggested the presence of one more acid amide group in the molecule, probably as that in glutamine (Gln), instead of glutamic acid (Glu) detected in the amino acid analysis. Eight –NH– and one $-NH_2$ groups shown in the ^{1}H-NMR spectra and thirteen amide carbonyl groups observed in the ^{13}C-NMR spectra gave support to the assumption. Thus, all the components in the cyclic peptide were proven to be four molecules of proline, three of tyrosine, two of threonine and one each of alanine, glycine and glutamine.

Our attempts to clarify the amino acid sequence by NOESY and C–H long-range COSY gave little success because of the presence of the same amino acid units in the molecules. However, digestion of the peptide with α-chymotrypsin[6] gave satisfactory results by specific cleavage at the aromatic amino acid units: Four hydrolysates (fr. 1—4) were obtained after reversed-phase HPLC and the FAB MS of the fractions indicated that fr. 2 and fr. 4 retained all the amino acid units ($[M+H]^+$ at m/z 1354), while fr. 1 and fr. 3 corresponded to the products formed by the cleavage at two peptide bonds ($[M+H]^+$ ion at m/z 543 and 830, respectively). The FAB MS and MS/MS spectra[7] of the four hydrolysates gave the results shown in Fig. 1. Figure 2 shows the MS/MS spectrum of m/z 1354 ($M+H^+$) of fr. 4 by FAB MS. The results obtained by a protein sequencer for the four peptides clearly showed the same results to indicate the sequence shown in Fig. 1. Thus, the structure of the cyclic peptide, cycloleonurinin, was established as shown in Fig. 3.

Enzymatic oxidations of the amino acids after complete hydrolysis indicated that all the amino acids were digested

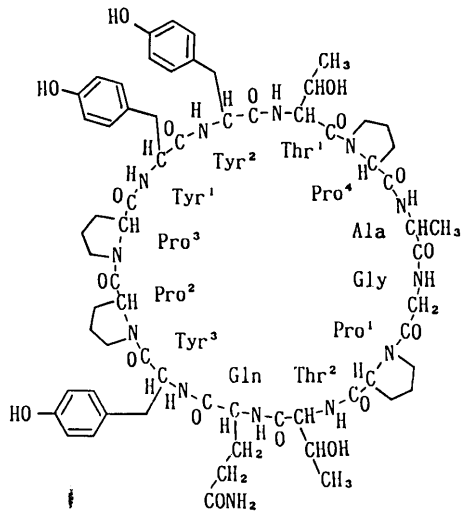

Fig. 3. The Structure of Cycloleonurinin

by L-amino acid oxidase but not by D-amino acid oxidase,[8] indicating that all the components are mainly of the L-amino acid series.

The hexane and methanol extracts of the fruits and hexane, chloroform, ethyl acetate, butanol and aqueous fractions of the methanol extract were subjected to pharmacological tests such as hypotensive action on rats and the increasing blood flow and aortic smooth muscle relaxing effects following the previous works.[3-5] However, obvious and reproducible effects were not observed in any fractions. Several pharmacological tests on the activity of cycloreonurin, the new cyclic peptide, were also carried out on the isolated guinea-pig ileum, and on the isolated rat aorta, as well as on blood pressure in urethane anesthetized rats. The peptide did not show any activity in the dose as high as 3×10^{-5} M on isolated organs, and 5 mg/kg, i.v. in the whole animals.[9]

Experimental

All melting points were determined on a Yanagimoto micromelting point apparatus. Ultraviolet (UV) and IR spectra were measured with a Shimadzu UV-240 spectrophotometer and a JASCO A-102 infrared spectrophotometer. The ^{1}H- and ^{13}C-NMR spectra were recorded using a JEOL GSX-400 spectrometer in dimethyl sulfoxide-d_6 with tetramethylsilane as an internal standard. The $[\alpha]_D$ values were determined with a JASCO DIP-140 digital polarimeter. Amino acid analysis was

carried out by a Hitachi amino acid analyser 835 and the amino acid sequence was determined by Protein Sequence 477A RTH Analyzer 120A (Applied Biosystem Co.).

FAB MS and FAB MS/MS spectra were obtained with a JEOL-HX 100 tandem mass spectrometer, which consists of a conventional geometry double-focusing mass spectrometer (MS-I) followed by an electrostatic analyzer used as MS-II. Xenon was used to provide the primary beam of atoms (6 keV). The liquid matrix used for FAB ionization was glycerol–1 N HCl (20 : 1). MS/MS spectra were obtained by activating the ions in the third field free region by collision with argon gas (sufficient to suppress the precursor ion beam by 25%) and by scanning MS-II.

Kieselgel 60 F_{254} (Merck) precoated plates were used for thin-layer chromatography (TLC) and the spots were detected with Dragendorff's and ninhydrin reagents. Column chromatography was carried out on 70—230 mesh silica gel (Merck). HPLC was performed using a SSC 3100-J pump with an Oyo-Bunko Uvilog 7 UV detector.

Extraction and Isolation of Cycloleonurinin and Choline Chloride Leonuri Fructus (Chinese origin, purchased from Tochimototenkaido, Osaka, on June 1986) (5 kg) was defatted with hexane (hexane extract, 542 g) and then extracted with 70% MeOH (2.4 l × 3). After removal of the solvent by evaporation, the residue (189 g) was treated with water and the water-insoluble portion was discarded. The aqueous solution was successively extracted with $CHCl_3$, AcOEt and BuOH saturated with H_2O to give the extracts (7.9, 5.0 and 53.1 g, respectively). The BuOH extract was chromatographed on silica gel ($CHCl_3$–MeOH (1 : 0→1 : 1)) and the fractions containing the substances positive to Dragendorff's reagent were further purified by HPLC (Nucleosil 50-5, eluting with CH_2Cl_2–MeOH (6 : 1)) to give cycloleonurinin (411 mg, 0.008%) and choline chloride, a pale yellow liquid (35 mg, 0.001%), ^{1}H-NMR δ ppm: 3.23 (9H, s), 3.52 (2H, t), 4.01 (2H, td), identified by ^{1}H-NMR and TLC.

Cycloleonurinin White powder of mp 222—225 °C (from MeOH), $[\alpha]_D$ −28.8° (MeOH, $c=0.79$). UV λ_{max}^{MeOH} nm: 225, 278. IR ν_{max}^{KBr} cm^{-1}: 3400, 2900, 1650 (br), 1520, 1440, 1220. MS (FAB and SIMS) *m/z*: 1336 $[M+H]^+$, 623, 493, 309, 195. MS (EIMS) *m/z*: 445, 339, 338, 308, 274, 260, 256, 242, 230, 220, 216, 212, 204, 202, 194, 168, 154, 107. ^{1}H- and ^{13}C-NMR (Tables I and II). *Anal.* Calcd for $C_{65}H_{85}N_{13}O_{18}\cdot 5H_2O$: C, 54.72; H, 6.71; N, 12.77. Found: C, 54.66; H, 6.39; N, 12.74.

Cycloleonurinin is slighty soluble in MeOH, sparingly soluble in EtOH, dimethylsulfoxide (DMSO) and water and insoluble in acetone and $CHCl_3$. It gives a positive reaction for Dragendorff's reagent but negative for ninhydrin reagent.

Complete Hydrolysis of Cycloleonurinin Cycloleonurinin (1 mg) in 6 N HCl (1 ml) was hydrolyzed at 110 °C for 24 h. The solution was evaporated and lyophilized to dryness and the hydrolysates were compared with standard amino acids on TLC developed by BuOH–AcOH–H_2O (7 : 1 : 2). The mixture was also applied to the analysis by an amino acid analyzer and the components, Thr, Glu, Gly, Ala, Tyr, Pro (1.86 : 1.04 : 1.0 : 1.0 : 2.84 : 3.78), were clarified.

Hydrolysis of Cycloleonurinin with α-Chymotrypsin To cycloleonurinin (10 mg) in NH_4HCO_3 solution (1%, 0.9 ml), α-chymotrypsin (500 μg dissolved in 50 μl of 0.001% HCl, Wako Pure Chemical Industries, substrate–enzyme ratio, 400 : 1) was added and the digestion was performed at 25 °C with the pH maintained at 8.0 by the manual addition of 0.1 N HCl.[6] After 4 h the reaction mixture showed a negative reaction for Dragendorff's reagent on TLC and the reaction was stopped by adjusting the solution to pH 2.2 with 1 N HCl. The digestion mixture showed the presence of four hydrolysates (fr. 1—4) by TLC (BuOH–AcOH–H_2O (7 : 1 : 2)) and, after lyophilization, the four peptides were separated by HPLC (Nucleosil ODS-5, 8 i.d. × 200 mm, eluted with 0.05% CF_3CO_2H–CH_3CN (4 : 1)). They were subjected to FAB MS/MS ($[M+H]^+$ ions at *m/z* 543, 1354, 830 and 1354, respectively) and to analyses by an automatic amino acid sequencer (Fig. 1).

Enzymatic Oxidation of the Componental Amino Acids[8] To the complete hydrolysates of cycloleonurinin (2.5 mg) in 0.1 M sodium pyrophosphate buffer (pH 8.2, 1 ml), catalase (5 μg, from bovine liver, Wako Pure Chemical Industries, 6.9 units/μg) and nicotineamide adenine dinucleotide (NADH) solution (5 mg/ml, 50 μl) were added and incubated at 37 °C for 1 h. After equilibration, D-amino acid oxidase (2 mg, from hog kidney, Tokyo Kasei Kogyo Co., 0.02 units/mg) was added and the mixture was incubated at 37 °C for 16 h.

The same amino acid mixture in 0.2 M Tris buffer (pH 7.7, 1 ml) and peroxidase (50 μg, from horseradish, Wako Pure Chemical Industries, 10 units/mg) were incubated at 37 °C for 1 h. After equilibration, L-amino acid oxidase (0.5 units, from snake venom, Tokyo Kasei Kogyo Co., 5 units/140 μl) was added and further incubated at 37 °C for 16 h.

The amino acids that remained in both digestion mixtures were subjected to TLC in the solvent system (phenol–H_2O (8 : 3)) to compare with the hydrolysate mixture and the amino acid standards.

Acknowledgement The authors thank Professor K. Watanabe of Chiba University for the pharmacological tests, Professor M. Suzuki, Meijo University, for the measurement of SIMS, Mr. N. Eguchi of this college for the amino acid analyses and Professor T. Morita of this college for his suggestions to this work. They are indebted to Mr. Y. Ogasawara, Mr. M. Sakaguchi and Miss J. Nakajima for their technical assistance.

References

1) Jiang Su New Medical College (ed.), "Zhong Yao Da Ci Dian," Vol. 2, Shanghai Science and Technology Press, Shanghai, 1977, pp. 1609—1610.
2) Chinese Academy of Medical Science and Others (eds.), "Zhong Yao Zhi," Vol. 3, People's Health Publisher, Beijing, 1984, pp. 513—516.
3) C.-E. Wang, S. Yano, K. Watanabe, S. Natori, K. Yamada and Y. Fujimoto, *J. Med. Pharm. Soc. Wakan-Yaku*, **3**, 446 (1986).
4) C.-E. Wang, S. Yano, K. Watanabe, K. Kuroda (née Yamada) and S. Natori, in preparation.
5) K. Kuroda (née Yamada), K. Kinoshita, S. Natori, C.-E. Wang, S. Yano and K. Watanabe, in preparation.
6) Biochemical Society of Japan (ed.), "Seikagaku Jikken Koza, 1, Protein Chemistry, II," Tokyo Kagaku Dojin, Tokyo, 1976, pp. 265—267.
7) T. Nakamura, H. Nagaki and T. Kinoshita, *Mass Spectroscopy*, **34**, 307 (1986); T. Kinoshita, K. Nakamura and H. Nagaki, *Nihon Kagaku Kaishi*, **1986**, 1665.
8) W. O. Godtfredson, S. Vangedal and D. W. Thomas, *Tetrahedron*, **26**, 4931 (1970).
9) Private communication from Professor K. Watanabe, Chiba University.

Isolation and Characterization of a New Abortifacient Protein, Karasurin, from Root Tubers of *Trichosanthes kirilowii* MAX. var. *japonicum* KITAM.

Shunsuke TOYOKAWA, Tadahiro TAKEDA and Yukio OGIHARA*

Faculty of Pharmaceutical Sciences, Nagoya City University, Tanabe-dori, Mizuho-ku, Nagoya 467, Japan. *Received September 25, 1990*

A new abortifacient protein, named karasurin, was isolated from fresh root tubers of *Trichosanthes kirilowii* MAXIMOWICZ var. *japonicum* KITAMURA (Cucurbitaceae, Japanese name: kikarasuuri) by the procedure involving acetone fractionation and ion-exchange chromatography on Toyopearlpak SP 650S. Homogeneity of Karasurin was demonstrated by sodium dodecyl sulfate (SDS)–polyacrylamide gel electrophoresis, and high performance liquid chromatography (HPLC). Karasurin was a highly basic protein of pI 10.1 and the molecular weight was estimated as 28000 by SDS–polyacrylamide gel electrophoresis. Karasurin showed a strong abortion effect in pregnant mice.

Keywords karasurin; *Trichosanthes kirilowii* var. *japonicum*; abortifacient protein; HPLC; amino acid sequencer; SDS–polyacrylamide gel electrophoresis

Trichosanthin, a protein from the root tubers of a Chinese medicinal herb *Trichosanthes kirilowii*, was found to be effective in inducing abortion in several mamalian models,[1-3] and in humans.[4] It has been used for abortion, and for therapy of choriocarcinoma and hydatiform moles in China. The isoelectric point of trichosanthin is 9.4 and the amino acid sequence has been determined. It is composed of 233 or 234 amino acid residues (molecular weight *ca.* 25700), and contains no cysteine or carbohydrate.[5-7] The sequence has revealed homology with the ricin A-chain. Trichosanthin was found to be a potent inhibitor of protein synthesis in a cell free translation system,[8,9] and also was found to selectively kill cells infected with human immunodeficiency virus (HIV), the virus causing aquired immune deficiency syndrome (AIDS).[10]

Besides trichosanthin, several abortifacient or ribosome-inactivating proteins were isolated from several species of Cucurbitaceae. β-Trichosanthin (from the roots of *Trichosanthes cucumeroides*),[11] trichokirin (from the seeds of *Trichosanthes kirilowii*),[12] α- and β-momorcharin (from the seeds of *Momordica charantia*)[13,14] and momorchochin (from the roots of *Momordica cochinchinensis*)[15] were basic proteins with molecular weights of 27000—32000.

In the light of these facts, we started to search for new abortifacient proteins in other varietas of Cucurbitaceae, collected in Japan. We report herein the purification and partial characterization of a new highly basic protein, which was found to be effective in inducing mid-term abortion in mice, from fresh root tubers of *Trichosanthes kirilowii* MAX. var. *japonicum* KITAM. (Japanese name is kikarasuuri). This newly isolated protein was designated karasurin. The physicochemical properties of karasurin were compared with other biologically active proteins obtained from the Cucurbitaceae family. Compared were the molecular weight, isoelectric point, amino acid composition and sequence of the N-terminal region.

Materials and Methods

Extraction and Acetone Fractionation Fresh root tubers (9.7 kg) of *Trichosanthes kirilowii* MAX. var. *japonicum* KITAM. were collected in the fall from our botanical garden. They were peeled, sliced and then homogenized with distilled water. After overnight at 4 °C, the homogenate was centrifugally filtered. The filtrate was adjusted to pH 4.0 with 2 N HCl, and then centrifuged at 2700 × *g* for 50 min at 6 °C. To the 12.5 l supernatant, 0.8 v/v of distilled acetone was added, and then centrifuged at 2700 × *g* for 50 min at 6 °C. The supernatant was concentrated *in vacuo* to 1 l. Thereafter, 1.2 l of distilled acetone was added, and then centrifuged at 2700 × *g* for 50 min at 6 °C to remove the precipitate. Finally proteins were precipitated with 0.5 l of distilled acetone, and collected by centrifugation at 2700 × *g* for 50 min at 6 °C. The precipitate was dissolved in a minimal volume of distilled water, and then dialyzed against distilled water at 4 °C for 1 d. The dialyzate was centrifuged at 13600 × *g* for 50 min at 4 °C to remove any precipitate following lyophilization and 16.5 g powder (fraction P1) was obtained.

Purification of Karasurin The fraction P1 (100 mg) was dissolved in 5 ml of 20 mM potassium phosphate buffer (pH 6.5), centrifuged to remove insoluble material, and applied on a column of Toyopearlpak SP 650S (2.2 × 20 cm, Tosoh), which was previously equilibrated with the same buffer used for dissolving the starting material. Proteins were then eluted with a linear gradient of 0—0.1 M NaCl in 20 mM potassium phosphate buffer (pH 6.5) at a flow rate of 4 ml/min. The main peak (P1-SP8) was collected and dialyzed against distilled water following lyophilization to yield 39 mg powder. The purified protein was designated karasurin.

Gel Filtration on High Performance Liquid Chromatography (HPLC) Karasurin was dissolved in 67 mM potassium phosphate buffer (pH 7.0) and applied on a column of Shimpack Diol 300 (0.79 × 50 cm, Shimadzu). The equilibration of the column and the elution (1 ml/min) was performed with the same buffer.

Sodium Dodecyl Sulfate (SDS)–Polyacrylamide Gel Electrophoresis The molecular weight of karasurin was determined by SDS–polyacrylamide gel electrophoresis according to the methods of Laemmli[16] with 15% gel using the molecular weight standards (Bio-Rad).

Isoelectric Focusing Isoelectric focusing was performed in a column (110 ml) with a sucrose density gradient (0—47%) containing 0.4% of LKB Ampholine (pH 3.5—10 *vs.* 9—11; 1:4, v/v) using LKB 8101 electric focusing column and LKB 8121 gradient mixer. The focusing was run for 48 h at 600 V. After focusing, each fraction (3.0 ml) was collected, and measured the pH and absorbance at 280 nm.

Amino Acid Composition Karasurin was hydrolyzed at 110 °C for 24 h in 6 N HCl containing phenol saturated with water *in vacuo* and the amino acid analysis was performed with a Hitachi amino acid analyzer (Hitachi Ltd.). The contents of cystine and tryptophan were determined by hydrolyses in 4 M methanesulfonic acid containing 0.2% (v/v) 3-(2-aminoethyl)indole.[17]

Amino Acid Sequence The amino acid sequence of the N-terminal region was determined by an automated Edman degradation process using a protein sequencer (Applied Biosystems 470A).

Assay of Mid-term Abortifacient Activity Mature ddY female mice (10 weeks old) weighing between 30 and 35 g were induced to ovulate by intraperitoneal injection of 3 international units of pregnant mare's serum gonadotropin (Serotropin, Teikokuzoki), followed 48 h later by an intraperitoneal injection of 5 international units of human chorionic gonadotropin (HCG, Mochida), both diluted with saline to a final volume of 0.1 ml. Seven and a half hours after the second injection, females were mated for 2 h with males. After this exposure, females with copulation plugs were separated. The post coitum (PC) interval was counted from the middle of the 2 h mating time, which was counted as zero.[18]

Karasurin in saline were administered intraperitoneally on day 12 PC. Mice were autopsied on day 14 PC. The total number of uterine implantation sites was recorded and their sizes measured. The numbers

of live fetuses, dead fetuses whose hearts had stopped pulsating, and resorbing fetuses were recorded.[19]

Results and Discussion

Fraction P1 was separated by ion-exchange chromatography on Toyopearlpak SP 650S into a number of peaks whose characters are to be described elsewhere. The eighth prominent peak (P1-SP8: karasurin), which comprised 60% of the total protein was eluted at a NaCl concentration of approximately 60 mM (Fig. 1).

Karasurin exhibited a single peak in HPLC with Shimpack Diol 300 column (Fig. 2), and also displayed a single band in SDS–polyacrylamide gel electrophoresis. Its molecular weight was estimated to be 28000 (Fig. 3).

The isoelectric focusing profile of karasurin showed a single peak at pH 10.1 (Fig. 4).

Thus, karasurin was shown to be a homogeneous highly basic protein with pI 10.1 and a molecular weight of *ca.*

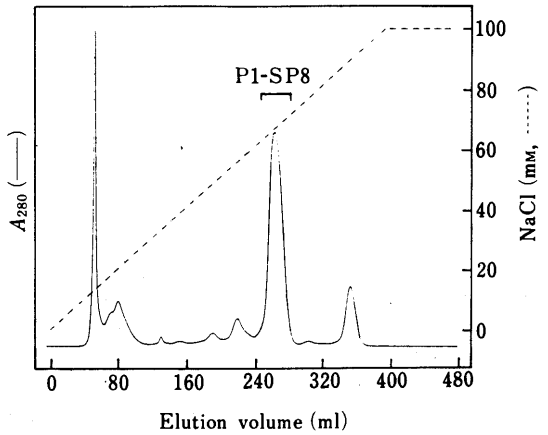

Fig. 1. Ion-Exchange Chromatography on Toyopearlpak SP 650S of Fraction P1

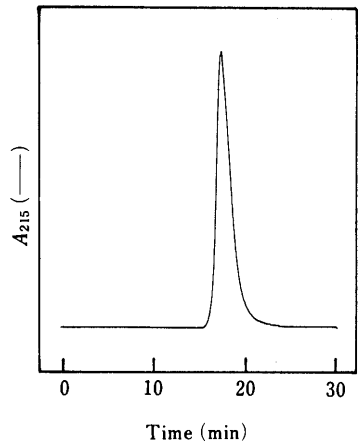

Fig. 2. Chromatogram on Shimpack Diol 300 of Karasurin

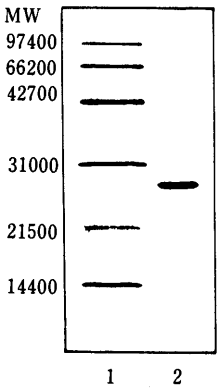

Fig. 3. SDS–Polyacrylamide Gel Electrophoresis of Karasurin

Samples were: lane 1, marker proteins [phosphorylase b (molecular weight (MW) 97400), bovine serum albumin (66200), ovalbumin (42700), carbonic anhydrase (31000), soybean trypsin inhibitor (21500) and lysozyme (14400)]; lane 2, karasurin. Samples were heated at 100 °C for 5 min in 1.6% SDS in the presence of 4% 2-mercaptoethanol. The gel was stained with Coomassie brilliant blue R-250.

TABLE I. Amino Acid Composition (mol%), Molecular Weight and Isoelectric Point of Karasurin and Other Abortifacient and Ribosome-Inactivating Proteins Isolated from Plant Members of Cucurbitaceae Family

	Amino acid composition						
	Karasurin	Trichosanthin[a]	β-Trichosanthin[b]	Trichokirin[b]	α-Momorcharin[b]	β-Momorcharin[b]	Momorchochin[b]
Asn/Asp	11.2	11.1	11.3	9.6	11.2	11.5	11.5
Thr	6.6	5.6	6.9	8.0	6.4	8.1	5.0
Ser	8.9	10.3	9.3	9.9	7.2	7.3	7.5
Gln/Glu	8.5	8.1	10.1	9.1	9.6	8.5	10.4
Pro	3.2	3.8	3.6	3.4	4.4	4.3	3.9
Gly	4.7	5.1	6.5	6.8	6.0	3.4	4.7
Ala	11.1	12.0	9.7	8.9	10.0	9.8	10.8
Cys	0.0	0.0	0.0	0.8	0.0	0.0	0.0
Val	6.1	5.1	5.3	5.3	6.0	5.6	6.1
Met	0.8	1.7	0.4	1.3	1.2	0.0	2.2
Ile	7.3	6.4	6.9	6.7	7.2	6.4	7.2
Leu	10.7	11.5	7.7	10.3	11.2	10.7	9.7
Tyr	5.9	5.6	6.1	5.1	5.2	6.0	8.2
Phe	3.8	3.8	4.5	4.3	3.6	6.0	3.2
Lys	4.8	3.4	5.3	7.4	4.0	6.0	5.0
His	0.3	0.4	0.4	0.5	0.8	1.3	0.7
Arg	5.7	5.6	6.1	2.6	6.4	5.1	3.9
Trp	0.4	0.4	—[c]	—[c]	—[c]	—[c]	—[c]
MW	28000	25682	28000	27000	29000	28000	32000
pI	10.1	9.4	>9.4	>9.0	8.5—9.0	8.5—9.0	—[c]

a) Composition was calculated from the sequence. *b*) Composition was calculated from the data revealed with mol/mol in the corresponding paper. *c*) Not determined. MW = molecular weight.

TABLE II. Comparison of the N-Terminal Sequence of Karasurin with These of Trichosanthin, Trichokirin and α-Momorcharin

	1	10	20	30
Karasurin	D V S F R L S G A T S S S Y G V F I S N L R K A L P	Y	E R K L Y D	I P L L
Trichosanthin	D V S F R L S G A T S S S Y G V F I S N L R K A L P	N	E R K L Y D	L P L I
Trichokirin	D V S F S L S G G G T A S Y E K			
α-Momorcharin	D V A F R L A G A D P R			

Boxes enclose identical residues.

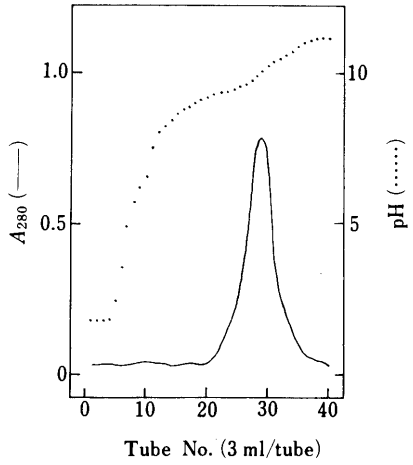

Fig. 4. Isoelectric Focusing Profile of Karasurin

28000. It is a new protein considering its characters dissimilar to other similar plant proteins.

Table I shows a comparison of the amino acid compositions of karasurin with other abortifacient and ribosome-inactivating proteins, which were isolated from the several kinds of Cucurbitaceae. Karasurin had no Cys. Furthermore, karasurin also had an abundance of Asn/Asp and Gln/Glu (19.7%) compared with His, Lys and Arg (10.8%). Since karasurin is a highly basic protein, a considerable high content of Asn and Gln is expected. On the whole, amino acid compositions of Cucurbitaceae proteins including karasurin were similar each other.

Automated Edman degradation was performed on intact karasurin and revealed an N-terminal sequence of 37-residues of the protein as shown in Table II. A comparison of the N-terminal sequences with trichosanthin, trichokirin and α-momorcharin showed 90%, 50% and 50% homology in the first 37, 16 and 12 amino acids, respectively, suggesting that these abortifacient or ribosome-inactivating proteins belong to a family.

The bioactivity of karasurin was achieved by an *in vivo* mid-term abortifacient assay in mice. The results presented in Table III show that a single intraperitoneal injection of a dose of 2.5 mg/kg of karasurin on day 12 PC induced abortion in all pregnant mice.

From the comparison of physicochemical properties (molecular weight, isoelectric point and amino acid composition) and the structural homology between karasurin and other Cucurbitaceae proteins, we have inferred that karasurin is an abortifacient or ribosome-inactivating protein. The ribosome-inactivating activity of karasurin remains to be tested. Karasurin shows a significantly high homology compared to trichosanthin, however the molecular weight, isoelectric point, amino acid composition and an amino acid sequence of the N-terminal with 37 residues are not identical to each other. These facts suggest that karasurin is a new protein homologous to abortifacient proteins in the Cucurbitaceae family. Recently, it has been reported that trichosanthin selectively kills cells infected with HIV,[10] in addition to the well-known biological activities. This finding will make the proteins having an abortifacient activity, including karasurin, important for clinical application.

TABLE III. Mid-term Abortifacient Activity of Karasurin

	Dose (mg/kg)	No. of mice	No. of aborted mice[a] / No. of treated mice
Control	0.2 ml saline	5	0/5 (0%)
Karasurin	0.75	5	2/5 (40%)
	1.5	5	4/5 (80%)
	2.5	5	5/5 (100%)

a) Mice were considered to be aborted when the number of dead fetuses was 50% or more of the total number of implantation sites on day 14PC.

Acknowledgements The authors are grateful to Dr. K. Wakabayashi and Dr. Y. Kato of the Gunma University and Dr. K. Sakamoto and Mr. Y. Waki of the Tsumura Research Institute for Pharmacology for their kind advice and encouragement.

References

1) I. F. Lau, S. K. Saksena and M. C. Chang, *Contraception*, **21**, 77 (1980).
2) M. C. Chang, S. K. Sanksena, I. F. Lau and Y. H. Wang, *Contraception*, **19**, 175 (1979).
3) Second Laboratory, Shanghai Institute of Experimental Biology, *Scientia Sinica*, **19**, 811 (1976).
4) C. Kuo-Fen, *Obstet. Gynecol.*, **59**, 494 (1982).
5) Y. Wang, R. Q. Qian, Z. W. Gu, S. W. Jin, L. Q. Zhang, Z. X. Xia, G. Y. Tian and C. Z. Ni, *Pure & Appl. Chem.*, **58**, 789 (1986).
6) Y. Wang, *Advances in Chinese Medical Materials Research*, **1985**, 289.
7) S. W. Jin, X. X. Sun, S. F. Wang, G. Y. Tian, Z. W. Gu, W. W. Qian, Y. Z. Liu, W. Y. She, R. Q. Qian and Y. Wang, *Acta Chimica Sinica*, **39**, 917 (1981).
8) J. M. Maraganore, M. Joseph and M. C. Bailey, *J. Biol. Chem.*, **262**, 11628 (1987).
9) X. J. Zhang and J. H. Wang, *Nature* (London), **321**, 477 (1986).
10) R. Buderi, *Nature* (London), **341**, 267 (1989).
11) H. W. Yeung and W. W. Li, *Int. J. Peptide Protein Res.*, **29**, 289 (1987).
12) P. Casellas, D. Dussossoy, A. I. Falasca, L. Barbieri, J. C. Guillemot,

P. Ferrara, A. Bolognesi, P. Cenini and F. Stirpe, *Eur. J. Biochem.*, **176**, 581 (1988).
13) H. W. Yeung, T. B. Ng, W. W. Li and W. K. Cheung, *Planta Medica*, 164 (1987).
14) H. W. Yeung, W. W. Li, Z. Feng, L. Barbieri and F. Stirpe, *Int. J. Peptide Protein Res.*, **31**, 265 (1987).
15) H. W. Yeung, T. B. Ng, N. S. Wong and W. W. Li, *Int. J. Peptide Protein Res.*, **30**, 135 (1987).
16) U. K. Laemmli, *Nature* (London), **227**, 680 (1970).
17) R. J. Simpson, M. R. Neuberger and T. Y. Liu, *J. Biol. Chem.*, **251**, 1936 (1976).
18) K. Suzumori, *Nagoya Medical Journal*, **22**, 135 (1977).
19) H. W. Yeung, W. W. Li, W. Y. Chan, L. K. Law and T. B. Ng, *Int. J. Peptide Protein Res.*, **28**, 518 (1986).

Evaluation of Hydrophobic Interaction between Acidic Drugs and Bovine Serum Albumin by Reversed-Phase High-Performance Liquid Chromatography

Atsunori KAIBARA, Misako HIROSE and Terumichi NAKAGAWA*

Faculty of Pharmaceutical Sciences, Kyoto University, Yoshidashimoadachi-cho, Sakyo-ku, Kyoto 606, Japan. *Received July 24, 1990*

The contribution of hydrophobic interaction to the protein binding of acidic drugs has been evaluated in terms of a new hydrophobic index (*r*-value), defined as the slope of the log–log plots of capacity factor *vs.* reciprocal of methanol concentration in an aqueous binary mobile phase, measured by the reversed-phase high-performance liquid chromatography. The logarithms of the binding constants (log K_1) of the selected acidic drugs and the related aromatic carboxylic acids indicated linear relationship with their *r*-values, suggesting that the effect of hydrophobicity on protein binding can be explained similarly to that on the retention onto the reversed-phase stationary ligand.

Keywords HPLC; hydrophobic index; bovine serum albumin; drug–protein binding; protein binding; hydrophobic interaction

Introduction

The protein binding of a drug exerts significant effect on its pharmacological and pharmacokinetic properties,[1-5] which is generally recognized as a combined effect of the specific and the non-specific interactions between drug molecule and the binding sites of protein. The binding force involves not only electrostatic interaction and hydrogen bonding but also hydrophobic interaction. Many drugs are known to have specific binding sites on an albumin molecule,[6-10] the specificity being a function of such various modes of interactions.

Hansch *et al.*[11-14] showed that the non-specific binding is solely a function of the hydrophobicity of a solute as expressed by

$$\log(1/C) = a \cdot \log P + b \quad (1)$$

where C is the molar concentration of a solute necessary to form a 1 : 1 complex with albumin, representing the bindability, and P is the 1-octanol/water partition coefficient of a solute widely used as a hydrophobic index. Hydrophobicity of a drug is also expected to play an important role in the specific albumin binding.

The coefficient a in Eq. 1 usually takes a value between 0.5 and 0.7.[13] This value is smaller than the coefficient (usually almost unity) for the correlation between log P and anesthetic[15] or hemolytic activities[16,17] of drugs where C in Eq. 1 presents the molar concentration of a drug causing the standard biological responses. These activities depend obviously on the partition to the biomembranes. This fact suggests that the hydrophobicity of a drug makes a smaller contribution to the protein binding than to the partition. It can be considered, therefore, that a drug binds with protein at its surface but not inside of the protein structure. Thus, it becomes necessary to evaluate the hydrophobic surface adsorbability of a drug to comprehend the protein binding. The partition coefficient (log P), however, does not necessarily reflect the surface hydrophobicity of a drug. For instance, the partition of a certain compound bearing strongly polar functional groups is much smaller than that expected from its hydrophobic adsorbability.[18]

In the previous papers, the authors evaluated the solute hydrophobicity in terms of the *r*-value measured by reversed-phase high-performance liquid chromatography (RP-HPLC) with methanol (MeOH)/water binary mobile phase.[19-21] The *r*-value, defined as a slope of the following equation,

$$\log k' = r \cdot \log(1/[\mathrm{MeOH}]) + q \quad (2)$$

is a hydrophobic index reflecting the adsorbability of a solute to the non-polar surface of the stationary ligand. It allows not only to evaluate the solute hydrophobicity but also to consider the molecular posture of the adsorbed solute and the surface properties of the stationary ligand.[19,21]

The present paper aims to correlate the *r*-value with the specific albumin binding of drugs. Several acidic drugs and the related aromatic carboxylic acids are selected as the model compounds bound specifically with serum albumin.

Experimental

Materials The clinically available acidic drugs used in this study were indomethacin (Nacalai Tesque Inc., Kyoto, Japan), ibuprofen (Kaken Seiyaku Co., Tokyo, Japan), ethacrynic acid (Sigma, St. Louis, U.S.A.), ketoprofen (Wako Pure Chemical Industries, Osaka, Japan), naproxen (Sigma) and salicylic acid (Nacalai Tesque). The structurally related aromatic carboxylic acids, biphenyl-4-carboxylic acid, naphthalene-2-carboxylic acid, 4-ethylbenzoic acids, naphthalene-1-carboxylic acid, 4-chlorobenzoic acid and 4-toluic acid were also used as supplied from Tokyo-Kasei Kogyo Co., Tokyo, Japan) and Nacalai Tesque. The chemical structures of these compounds are shown in Fig. 1. Bovine serum albumin (BSA) obtained from Sigma was fatty acid free.

Measurement of *r*-Value The retention time of a drug was measured on a Model LC-5A liquid chromatograph system (Shimadzu, Kyoto, Japan) equipped with a Model SPD-2A variable wave-length UV-detector (Shimadzu). The stationary phase used was a Nucleosil 5-C18 ODS silica (Macherey-Nagel, Duren, FRG) packed in a 15 cm × 4.6 mm i.d. stainless steel tubing. The column was kept at 40 °C in a thermostatic oven. The mobile phases were the binary mixtures of methanol and 10 mM KCl–HCl buffer solution (pH = 2.2). The methanol concentration was varied from 30% to 80% at an interval of 5%. The flow rate was fixed at 0.7 ml/min. The capacity factor (k') was calculated as

$$k' = (t_R - t_0)/t_0 \quad (3)$$

where t_R is the solute retention time, and t_0 is the retention time of nitrate ion. From the k' values obtained, log k' was plotted against log(1/[MeOH]), and the slope of the linear part of the plots was calculated by the least squares method.[19] In most cases, the linearity was observed between 45% and 65% of methanol concentration. The resulting *r*-values of the drugs are given in Table I.

Measurement of Free Drug Concentration The binding of a drug with BSA was determined as follows. A 3 ml portion of 10 or 50 μM BSA solution in the phosphate buffer (pH 7.4, ionic strength 0.17) was mixed with a 3 ml portion of the same phosphate buffer solution of a drug, and the mixture was incubated at 37 °C for 20 min. The drug concentration was varied to make the binding ratio, C_b/C_p (bound drug concentration/BSA concentration), to be in a range of 0.2 to 2.0. A 1.5 ml portion of the mixed solution was subjected to the ultrafiltration using Molcut II (UFP1 LGC, Millipore Co.) and a 0.1 ml portion of the filtrate was collected. For the drugs adsorbable to the filtration membrane, the first

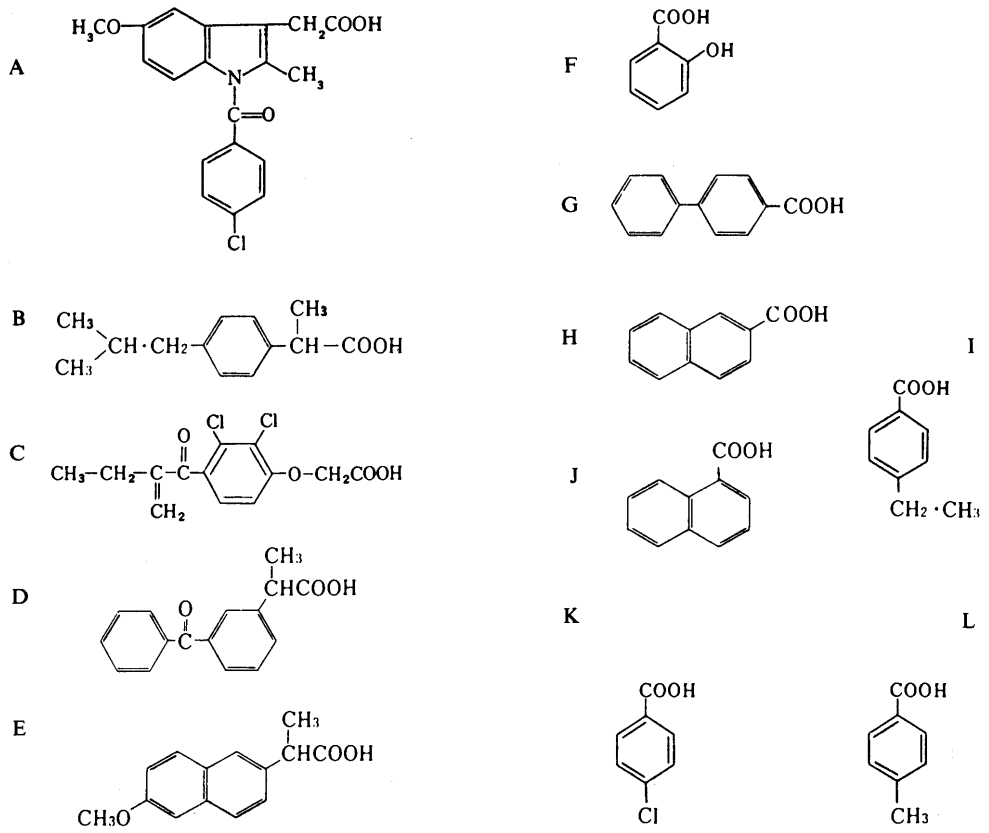

Fig. 1. Structures of the Acidic Drugs and the Related Aromatic Carboxylic Acids Used in This Study

The symbols, see Table I.

TABLE I. *r*-Values and BSA Binding Parameters Estimated by the Two-constant Equation and by the Klotz Equation

Solutes	*r*	*N*	Two-constant[a] K_1 [M^{-1}] (S.D.)	Klotz[b] K_1 [M^{-1}] (S.D.)
A. Indomethacin	6.76	10	321300 (10000)	[c]
B. Ibuprofen	6.42	15	1242000 (135000)	[c]
C. Ethacrynic acid	5.60	8	629200 (46000)	710500 (141700)
D. Ketoprofen	5.16	7	480400 (8600)	[c]
E. Naproxen	5.02	11	340100 (66500)	[c]
F. Salicylic acid	2.63	10	96600 (8800)	87500 (22300)
G. Biphenyl-4-carboxylic acid	5.33	10	640300 (77900)	711700 (236100)
H. Naphthalene-2-carboxylic acid	4.36	12	482400 (63500)	[c]
I. 4-Ethylbenzoic acid	4.03	14	238700 (29100)	262000 (38800)
J. Naphthalene-1-carboxylic acid	4.02	16	136400 (8300)	124800 (11100)
K. 4-Chlorobenzoic acid	3.56	6	138400 (22300)	[c]
L. 4-Toluic acid	3.28	7	129800 (3900)	121500 (3600)

r: hydrophobic index estimated by Eq. 2. *N*: Number of data for binding analysis. S.D.: standard deviation. *a*) Eq. 4. *b*) Eq. 5. *c*) Pertinent values, not obtained.

0.1 ml portion of the filtrate was discarded and the following 0.1 ml portion was collected. The drug concentration in the filtrate was determined by RP-HPLC under the following condition: Column, Capcell-pak C18 (Shiseido, Tokyo, Japan) packed in a 15 cm × 4.6 mm i.d. stainless tubing; mobile phase, acetonitrile/phosphate buffer solution (pH 4); detection, UV-210 nm. The mobile phase composition and the flow rate were selected appropriately.

Estimation of Binding Parameters The two-constant equation given by Larsen *et al.*[22] was adopted to estimate the binding parameters.

$$R = a \cdot \ln(b \cdot C_f + 1) \quad (4)$$

where R is the binding ratio (C_b/C_p), C_f is the free drug concentration, and a and b are the coefficients. This empirical equation has advantages over the Klotz (Adair) equation (Eq. 5)[23] derived based on the stepwise equilibrium and Scatchard equation[24] based on Langmuir type adsorption, because it involves a least number of the coefficients to be determined and does not show a plateau due to saturation.[22] Klotz equation is

$$R = \frac{K_1 \cdot C_f + 2 \cdot K_1 \cdot K_2 \cdot C_f^2 + \ldots + n \cdot K_1 \cdot K_2 \ldots K_n \cdot C_f^n}{1 + K_1 \cdot C_f + K_1 \cdot K_2 \cdot C_f^2 + \ldots + K_1 \cdot K_2 \ldots K_n \cdot C_f^n} \quad (5)$$

where $K_1, K_2, \ldots$ and K_n are the first, the second, ... and the n-th binding constants. The coefficients a and b in Eq. 4 are correlated with K_1 and K_2[22] as

$$a = \frac{K_1}{2(K_1 - 2 \cdot K_2)} \quad (6)$$

$$b = 2(K_1 - 2 \cdot K_2) \quad (7)$$

The pertinent values of a and b were estimated by the non-linear least squares fittings of Eq. 4 to the data obtained by the binding experiment mentioned above. From the results, the binding constants were calculated according to Eqs. 6 and 7.

Results and Discussion

The binding constants (K_1) for 12 acidic drugs, which reflect dominantly the binding to the primary specific sites on an albumin molecule, are listed in Table I. The values of the standard deviation given in parentheses indicate good fitness to the two-constant equation (Eq. 4). However, the

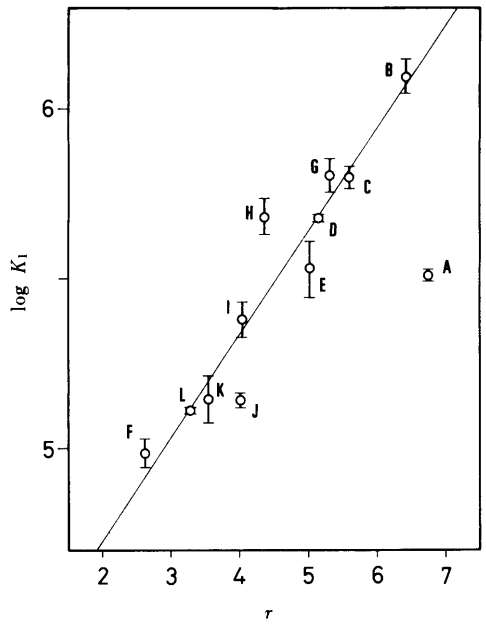

Fig. 2. Plots of $\log K_1$ *vs.* *r*-Value

The conditions for the measurements of *r*-values, see text. The symbols, see Table I.

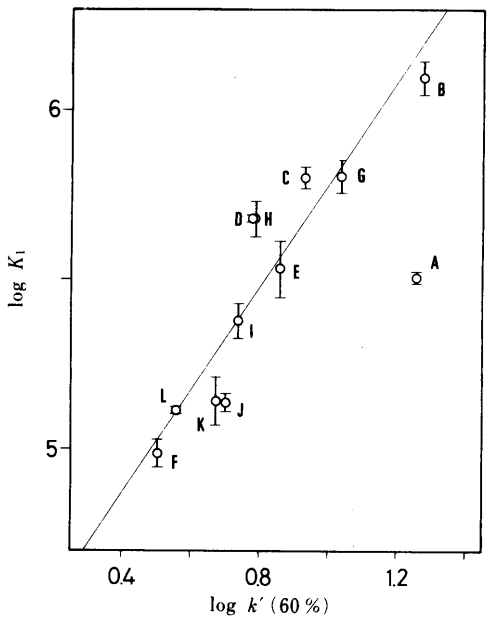

Fig. 3. Plots of $\log K_1$ *vs.* $\log k'$ Obtained by Using 60% Methanolic Mobile Phase

The symbols, see Table I.

fit with the Klotz equation (Eq. 5) did not give the pertinent values for some drugs (see Table I) which exhibited scattered or a small number of data points. In contrast, for the drugs which fit the Klotz equation, the results indicated good agreement with those obtained by the two-constant equation. This confirmed adequacy of the fit.

Figure 2 depicts the relationship between $\log K_1$ and *r*-value given in Table I. All the data points corresponding to the drugs and the related aromatic carboxylic acids except for indomethacin are almost linear. This fact suggests that among the various natures of drugs responsible for the specific binding to proteins, the hydrophobicity, represented by *r*-value, plays a predominant role in the prediction of protein binding ability of structurally related compounds (*e.g.* aromatic carboxylic acids in this study). The least squares analysis of the 11 data points (excluding indomethacin) in Fig. 2 gave a regression line

$$\log K_1 = 0.304 \cdot r + 4.121 \quad (8)$$

with the correlation coefficient 0.950.

Among the drugs used in this study, ibuprofen and ethacrynic acid are known to share the same primary binding site on albumin.[6,7] These compounds have electrostatic interaction with the basic functional group at the binding site and hydrophobic interaction with the surrounding non-polar moiety. It is interesting to note that the constant K_1, mainly reflecting the affinity to the primary site, is closely related with the hydrophobic adsorbability to the ODS ligand on the surface of the stationary phase of RP-HPLC. This fact suggests that the hydrophobicity of a drug makes a similar contribution to both the protein binding and the non-polar adsorption, and that these drugs show almost the same contribution of the non-hydrophobic interactions, such as electrostatic interaction and hydrogen bonding, to the protein binding. Therefore, it can be speculated that the related aromatic acids in Table I may also have the same primary binding site on albumin or a different binding site bearing similar specificity.

On the other hand, the point due to indomethacin in Fig. 2 is widely deviated downward from the straight line, showing weaker bindability than that expected from its hydrophobicity. That is, the hydrophobicity of indomethacin exerts a lower effect on the binding than that of other acidic drugs. This may imply that the primary binding site of indomethacin is different from those of others. Such a low affinity of indomethacin may be reasoned by the structural factors; the posture of indomethacin molecule bound to albumin will be restricted by the directional polar interactions and/or the dimension of hydrophobic circumstance around of the binding site, while the hydrophobic adsorption to the non-polar stationary ligand in RP-HPLC will occur to expose maximum surface area to contact with the ligand. Since indomethacin molecule has wider hydrophobic surface area than others as depicted in Fig. 1, this excess hydrophobicity may vainly contribute to the protein binding. This is why indomethacin gave the point deviating downward from the line in Fig. 2. This speculation agrees with the idea that the hydrophobic interaction at the binding site takes place on a limited area of "hydrophobic patch"[25] scattered on an albumin molecule.

When $\log K_1$ is plotted against $\log k'$ (capacity factor) instead of *r*-value, we obtain also a linear relationship. Figure 3 shows the result obtained from k' values of the acidic drugs and the related aromatic carboxylic acids in Table I, measured by using the binary mobile phase containing 60% methanol.

$$\log K_1 = 1.283 \cdot \log k'(55\%) + 4.232 \quad (9)$$

$$\log K_1 = 1.513 \cdot \log k'(60\%) + 4.272 \quad (10)$$

$$\log K_1 = 1.806 \cdot \log k'(65\%) + 4.304 \quad (11)$$

$$\log K_1 = 2.212 \cdot \log k'(70\%) + 4.330 \quad (12)$$

Equation 10 is the regression equation for the line in Fig. 3. Equations 9, 11 and 12 are those obtained with use of

the mobile phases containing 55%, 65% and 70% methanol, respectively. The correlation coefficients of Eqs. 9 to 12 are 0.932, 0.921, 0.906 and 0.889, respectively. As readily found from these results, the lower the methanol concentration of the mobile phase, the better the correlation, but all the values of correlation coefficients are lower than that (0.950) for the $\log K_1$ *vs.* r equation (Eq. 8). Therefore, the r-value is a better index than the capacity factor to evaluate contribution of the hydrophobicity to the protein binding. The low methanol concentration in the mobile phase gives rise to high contribution of the hydrophobicity to the non-polar adsorption, and hence results in relatively small effects of the non-hydrophobic interaction on k' value. Thus, the value of the correlation coefficient was increased with decreasing concentration of methanol. However, the excessive decrease causes the retention time of a hydrophobic drug to be impractically prolonged. For instance, the retention times of indomethacin and ibuprofen exceeded 1 h when 50% methanol was used as a mobile phase. The r-value is a convenient index of hydrophobicity, since it is easy to measure and is scarcely affected by non-hydrophobic forces.

References

1) C. Hansch, in "Drug Design," ed. by E. J. Ariens, Academic Press, New York, 1971, p. 271.
2) J. G. Wagner, *J. Pharmacokinet. Biopharm.*, **1**, 384 (1973).
3) W. J. Jusko and M. Gretch, *Drug Metab. Rev.*, **5**, 43 (1976).
4) J. J. Vallner, *J. Pharm. Sci.*, **66**, 447 (1977).
5) U. Kragh-Hansen, *Pharmacol. Rev.*, **33**, 17 (1981).
6) G. Sudlow, D. J. Birkett and D. N. Wade, *Mol. Pharmacol.*, **11**, 824 (1975).
7) G. Sudlow, D. J. Birkett and D. N. Wade, *Mol. Pharmacol.*, **12**, 1052 (1976).
8) I. Sjoholm, B. E. Ekman, A. Kober, I. Ljugstedt-Pahlman, B. Seiving and T. Sjodin, *Mol. Pharmacol.*, **16**, 767 (1979).
9) K. Ikeda, Y. Kurono, Y. Ozeki and T. Yotsuyanagi, *Chem. Pharm. Bull.*, **27**, 80 (1979).
10) Y. Ozeki, Y. Kurono, T. Yotsuyanagi and K. Ikeda, *Chem. Pharm. Bull.*, **28**, 535 (1980).
11) K. Kiehs, C. Hansch and L. Moore, *Biochemistry*, **5**, 2602 (1966).
12) F. Helmer, K. Kiehs and C. Hansch, *Biochemistry*, **7**, 2858 (1968).
13) A. Leo, C. Hansch and D. Elkins, *Chem. Rev.*, **71**, 525 (1971).
14) J. M. Vandenbelt, C. Hansch and C. Church, *J. Med. Chem.*, **15**, 787 (1972).
15) C. Hansch and W. J. Dunn, III, *J. Pharm. Sci.*, **61**, 1 (1972).
16) C. Hansch and W. R. Glave, *Mol. Pharmacol.*, **7**, 377 (1971).
17) R. G. Kirk, *Biochem. Biophys. Acta*, **464**, 157 (1977).
18) K. Miyake, K. Okumura and H. Terada, *Chem. Pharm. Bull.*, **33**, 769 (1985).
19) A. Kaibara, C. Hohda, N. Hirata, M. Hirose and T. Nakagawa, *Chromatographia*, **29**, 275 (1990).
20) A. Kaibara, T. Nakagawa, C. Hohda, N. Hirata and H. Tanaka, *J. Chromatogr. Sci.*, **27**, 716 (1989).
21) A. Kaibara, M. Hirose and T. Nakagawa, *Chromatographia*, **30**, 99 (1990).
22) C. G. Larsen, F. G. Larsen and R. Brodersen, *J. Pharm. Sci.*, **75**, 669 (1986).
23) I. M. Klotz and D. L. Hunston, *Arch. Biochem. Biophys.*, **193**, 314 (1979).
24) G. Scatchard, *Ann. N.Y. Acad. Sci.*, **51**, 660 (1949).
25) C. Tanford, "The Hydrophobic Effect," Wiley-Interscience, New York, 1973, p. 134.

7-Alkylaminocoumarin-4-acetic Acids as Fluorescent Probe for Studies of Drug-Binding Sites on Human Serum Albumin

Mitsuru IRIKURA,[a] Akira TAKADATE,[b] Shujiro GOYA*,[a] and Masaki OTAGIRI[a]

Faculty of Pharmaceutical Sciences,[a] Kumamoto University, 5-1, Ohe-honmachi, Kumamoto 862, Japan and Daiichi College of Pharmaceutical Sciences,[b] 22-1, Tamagawa-cho, Minami-ku, Fukuoka 815, Japan. *Received September 4, 1990*

7-Alkylaminocoumarin-4-acetic acids I—IX having alkylamino groups different in alkylchain length were synthesized as fluorescence probes for characterization of drug-binding sites on human serum albumin (HSA). The fluorescences of I—IX were quenched or enhanced in the presence of HSA with shifts of the emission maxima to shorter wavelength. The binding constants and the number of binding sites were determined by the spectral changes of the probes I—IX bound to HSA through analysis of Scatchard's and Job's plots. The primary binding sites of the tested probes were found to be site 2 (diazepam site) on HSA from the results of competitive displacement studies. The polarity of site 2 was estimated from the relationship between the emission maximum of the probe of IV and *Z*-values, and was found to be comparable to that of acetonitrile. Simple attempts to estimate the site 2 region from the molecular size of the probe of VIII obtained using the Corey-Pauling-Koltun molecular model suggest that the hydrophobic cleft at site 2 is about 21—25 Å in depth. The distance between the lone tryptophan residue in HSA and probes bound to site 2 was estimated to be 15—17 Å using Förster's equation on the basis of fluorescence energy transfer. The present data suggest that I—IX are useful as fluorescence probes for the characterization of site 2 on HSA.

Keywords 7-alkylaminocoumarin-4-acetic acid; human serum albumin; protein-binding fluorescence probe; binding parameter; binding site; binding site characterization

We previously reported that 7-anilinocoumarin-4-acetic acid (ACA)[1] and 7-anilino-4-methylcoumarin-3-acetic acid (AMCA)[2] are accessible as fluorescence probes selectively binding to the digitoxin site (site 3) on human serum albumin (HSA) and to the estrogen-binding site on α-globulin. The fluorescence of these aminocoumarins were quite sensitive to even slight changes of environment around their molecules.

In the course of our work, new nine 7-alkylaminocoumarin-4-acetic acids I—IX having alkylamino groups different in alkylchain length (Chart 1) were prepared as fluorescence probes, and the characteristics and applicability of I—IX to determine the environment at the drug-binding sites on HSA were examined.

Experimental

Material HSA (Lot. No. A-2386, M.W. 66500) was purchased from Sigma Chemical Co. (St. Louis, Mo. U.S.A.). Phenylbutazone (Ciba-Geigy Co., Takarazuka, Japan), ibuprofen, flufenamic acid (Kaken Pharmaceutical Co., Tokyo, Japan) and digoxin (Chugai Pharmaceutical Co., Tokyo, Japan) were gifts of the manufacturers. All other chemicals were of reagent grade, and deionized and distilled water was used throughout. The probes I—IX were synthesized according to the method described by Umemoto *et al.*[3] and a typical method was as follows.

7-Butylaminocoumarin-4-acetic Acid (I): A mixture of resorcinol (12.5 g, 0.11 mol), *n*-butylamine (25 g, 0.34 mol) and anhydrous calcium chloride (25.3 g, 0.23 mol) was heated at 220 °C for 8 h in an autoclave. The reaction mixture was extracted with acetone a few times. After evaporating the solvent, the residual oil was purified by distillation under reduced pressure to give 11.5 g of *m*-butylaminophenol as brown oil, bp 175—185 °C (3 mmHg). This compound (11 g, 0.07 mol) was refluxed with ethyl acetonedicarboxylate (20.2 g, 0.1 mol) in the presence of anhydrous zinc chloride (18.5 g, 0.14 mol) in absolute ethanol (70 ml) for 20 h. After cooling, the mixture was poured into ice-water. The resulting oil collected by separatory funnel was placed on the silica gel column and eluted with benzene–ethyl acetate (8 : 1, v/v). The crude product was recrystallized from ethanol to give 3.2 g of ethyl 7-butylaminocoumarin-4-acetate as pale yellow needles, mp 95—97 °C. This ester was heated at 100—110 °C for 4 h in a mixed solution (32 ml) of hydrochloric acid–acetic acid–water (1 : 1 : 1, v/v). The resulting precipitates were collected by filtration and recrystallized from ethanol to give 1.6 g of 7-butylaminocoumarin-4-acetic acid (I) as pale yellow needles, mp 171—174 °C. *Anal.* Calcd for $C_{15}H_{17}NO_4$: C, 65.44; H, 6.22; N, 5.09. Found: C, 65.50; H, 6.29; N, 5.04. Proton nuclear magnetic resonance (^{1}H-NMR) (dimethyl sulfoxide (DMSO)-d_6) δ: 0.85 (3H, t, $-CH_3$), 1.17—1.58 (4H, m, $-CH_2CH_2CH_3$), 3.08 (2H, m, C_7-$NHCH_2-$), 3.71 (2H, s, C_4-CH_2-), 5.96 (1H, s, C_3-H), 6.54—6.72 (3H, m, C_6-H, C_8-H and C_7-NH–), 7.37 (1H, d, C_5-H). All other compounds (II—IX) were recrystallized from ethanol to give pale yellow needles.

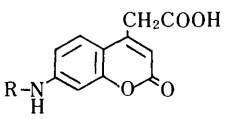

I : R = C_4H_9 IV : R = C_7H_{15} VII : R = $C_{10}H_{21}$
II : R = C_5H_{11} V : R = C_8H_{17} VIII : R = $C_{12}H_{25}$
III : R = C_6H_{13} VI : R = C_9H_{19} IX : R = $C_{13}H_{27}$

Chart 1

7-Pentylaminocoumarin-4-acetic Acid (II): mp 139—141 °C. *Anal.* Calcd for $C_{16}H_{19}NO_4$: C, 66.42; H, 6.62; N, 4.84. Found: C, 66.09; H, 6.92; N, 5.09. ^{1}H-NMR (DMSO-d_6) δ: 0.86 (3H, t, $-CH_3$), 1.32—1.57 (6H, m, $-CH_2(CH_2)_2CH_3$), 3.08 (2H, m, C_7-$NHCH_2-$), 3.74 (2H, s, C_4-CH_2-), 5.98 (1H, s, C_3-H), 6.40—6.69 (3H, m, C_6-H, C_8-H and C_7-NH–), 7.36 (1H, d, C_5-H).

7-Hexylaminocoumarin-4-acetic Acid (III): mp 164—167 °C. *Anal.* Calcd for $C_{17}H_{21}NO_4$: C, 67.31; H, 6.98; N, 4.62. Found: C, 67.20; H, 6.93; N, 4.80. ^{1}H-NMR (DMSO-d_6) δ: 0.85 (3H, t, $-CH_3$), 1.24—1.60 (8H, m, $-CH_2(CH_2)_3CH_3$), 3.07 (2H, m, C_7-$NHCH_2-$), 3.72 (2H, s, C_4-CH_2-), 5.97 (1H, s, C_3-H), 6.62—6.75 (3H, m, C_6-H, C_8-H and C_7-NH–), 7.37 (1H, d, C_5-H).

7-Heptylaminocoumarin-4-acetic Acid (IV): mp 165—167 °C. *Anal.* Calcd for $C_{18}H_{23}NO_4$: C, 68.12; H, 7.31; N, 4.41. Found: C, 68.46; H, 7.45; N, 4.62. ^{1}H-NMR (DMSO-d_6) δ: 0.86 (3H, t, $-CH_3$), 1.27—1.58 (10H, m, $-CH_2(CH_2)_4CH_3$), 3.07 (2H, m, C_7-$NHCH_2-$), 3.73 (2H, s, C_4-CH_2-), 5.98 (1H, s, C_3-H), 6.40—6.68 (3H, m, C_6-H, C_8-H and C_7-NH–), 7.36 (1H, d, C_5-H).

7-Octylaminocoumarin-4-acetic Acid (V): mp 156—158 °C. *Anal.* Calcd for $C_{19}H_{25}NO_4$: C, 68.86; H, 7.60; N, 4.23. Found: C, 69.24; H, 7.68; N, 4.43. ^{1}H-NMR (DMSO-d_6) δ: 0.86 (3H, t, $-CH_3$), 1.30—1.62 (12H, m, $-CH_2(CH_2)_5CH_3$), 3.10 (2H, m, C_7-$NHCH_2-$), 3.74 (2H, s, C_4-CH_2-), 5.98 (1H, s, C_3-H), 6.41—6.67 (3H, m, C_6-H, C_8-H and C_7-NH–), 7.31 (1H, d, C_5-H).

7-Nonylaminocoumarin-4-acetic Acid (VI): mp 146—149 °C. *Anal.* Calcd for $C_{20}H_{27}NO_4$: C, 69.54; H, 7.88; N, 4.05. Found: C, 69.85; H, 7.93; N, 4.23. ^{1}H-NMR (DMSO-d_6) δ: 0.85 (3H, t, $-CH_3$), 1.24—1.54

(4H, m, $-C\underline{H}_2(C\underline{H}_2)_6CH_3$), 3.07 (2H, m, C_7-NHC$\underline{H}_2$–), 3.73 (2H, s, C_4-CH_2–), 5.97 (1H, s, C_3-H), 6.39—6.68 (3H, m, C_6-H, C_8-H and C_7-NH–), 7.36 (1H, d, C_5-H).

7-Decylaminocoumarin-4-acetic Acid (VII): mp 120—123 °C. *Anal.* Calcd for $C_{21}H_{29}NO_4$: C, 70.17; H, 8.13; N, 3.90. Found: C, 70.28; H, 8.24; N, 3.66. ^{1}H-NMR (DMSO-d_6) δ: 0.85 (3H, t, $-CH_3$), 1.24—1.58 (16H, m, $-C\underline{H}_2(C\underline{H}_2)_7CH_3$), 3.07 (2H, m, C_7-NHC$\underline{H}_2$–), 3.73 (2H, s, C_4-CH_2–), 5.97 (1H, s, C_3-H), 6.39—6.68 (3H, m, C_6-H, C_8-H and C_7-NH–), 7.36 (1H, d, C_5-H).

7-Laurylaminocoumarin-4-acetic Acid (VIII): mp 144—146 °C. *Anal.* Calcd for $C_{23}H_{33}NO_4$: C, 71.29; H, 8.58; N, 3.61. Found: C, 71.69; H, 8.72; N, 3.77. ^{1}H-NMR (DMSO-d_6) δ: 0.86 (3H, t, $-CH_3$), 1.25—1.60 (20H, m, $-C\underline{H}_2(C\underline{H}_2)_9CH_3$), 3.09 (2H, m, C_7-NHC$\underline{H}_2$–), 3.73 (2H, s, C_4-CH_2–), 5.98 (1H, s, C_3-H), 6.40—6.71 (3H, m, C_6-H, C_8-H and C_7-NH–), 7.30 (1H, d, C_5-H).

7-Tridecylaminocoumarin-4-acetic Acid (IX): mp 139—142 °C. *Anal.* Calcd for $C_{24}H_{35}NO_4$: C, 71.79; H, 8.79; N, 3.49. Found: C, 71.67; H, 8.78; N, 3.57. ^{1}H-NMR (DMSO-d_6) δ: 0.58 (3H, t, $-CH_3$), 1.23—1.58 (22H, m, $-C\underline{H}_2(C\underline{H}_2)_{10}CH_3$), 3.07 (2H, m, C_7-NHC$\underline{H}_2$–), 3.73 (2H, s, C_4-CH_2–), 5.97 (1H, s, C_3-H), 6.39—6.65 (3H, m, C_6-H, C_8-H and C_7-NH–), 7.36 (1H, d, C_5-H).

Apparatus and Methods Melting points were measured with a Yanagimoto micro-melting point apparatus and are uncorrected. ^{1}H-NMR spectra were obtained with a JEOL FX 90Q FT-NMR spectrometer, employing tetramethylsilane as an internal standard. The abbreviations used are as follows: s, singlet; d, doublet; t, triplet; m, multiplet. Absorption and fluorescence spectra were measured with a Hitachi 150-20 spectrophotometer and a Hitachi 650-60 fluorescence spectrophotometer, respectively. Fluorescence quantum yields were determined according to the method of Parker and Rees[4] and quinine sulfate in 1 N H_2SO_4 was used as the standard. HSA and probe (I—IX) solutions were prepared in 0.1 M phosphate buffer (pH 7.4) at 25±1 °C. HSA solutions of 1.0×10^{-6}—5.0×10^{-5} M were used together with a wide concentration range of 5.0×10^{-7}—2.4×10^{-5} M probes.

Fuorometric Titrations: HSA solution at an appropriate concentration was titrated by successive additions of each solution of probe (the final probe concentration, 1.6×10^{-6} M) and the fluorescence intensity was measured (excitation at 360 nm and emission at 400 nm).

Data Treatment: The fraction of each probe, X was usually determined using Eq. 1,

$$X=\frac{F_p-F_o}{F_b-F_o} \tag{1}$$

where F_p and F_o are the fluorescence intensities of a given concentration of the probe in a solution of low HSA concentration and in a solution without HSA, respectively. F_b is the fluorescence intensity of the same concentration of fully bound probe. To determine the value of F_b for a given concentration of the probe, fluorescence titrations were carried out at several HSA concentrations. F_b is taken to be the fluorescence intensity of the probe in the presence of excess HSA. After values for the fraction of bound probe had been determined for all points along the titration curve, the results were plotted according to the Scatchard equation[5]:

$$r=\sum_{i=1}^{n}\frac{n_iK_iD_f}{1+D_f} \tag{2}$$

where r is the number of mol of the probe bound per mol of protein, n is the number of binding sites, K is the binding constant and D_f is the concentration of free probe.

Calculation of the Distance from the Lone Tryptophan Residue to the Bound Probe in HSA: The distance between the lone tryptophan residue (donor) and the probe (acceptor) bound to HSA was calculated using Förster's equation[6]:

$$R=R_0(E^{-1}-1)^{1/6} \tag{3}$$

$$R_0^6=8.785\times10^{-25}\kappa^2\phi_D\eta^{-4}J \tag{4}$$

where R is the distance between donor and acceptor, R_0 is the distance for 50% transfer, E is the efficiency of energy transfer, and κ^2 is the orientation factor. The values used for κ^2 and refractive index η were 2/3 and 1.4 as described in the literature,[7] respectively. The ϕ_D is the quantum yield arising from the lone tryptophan in HSA without acceptor, and its value was taken as 0.092, J represents the spectra overlap of the donor and acceptor:

$$J=\int\varepsilon_A(\lambda)f_D(\lambda)\lambda^4d\lambda \tag{5}$$

$$f_D(\lambda)d\lambda=\frac{F(\lambda)d\lambda}{\int_0^\infty F(\lambda)d\lambda} \tag{6}$$

where ε_A is the extinction coefficient of the acceptor at wavelength λ, $f_D(\lambda)$ is the normalized fluorescence spectrum of the donor determined from Eq. 6, and $F(\lambda)$ is the fluorescence intensities at wavelength λ.

Results and Discussion

Fluorescence Characteristics of I—IX The fluorescence spectral data of compounds I—IX measured in a variety of solvents are summarized in Table I. These compounds were highly fluorescent in both aqueous and organic solvents and their fluorescence quantum yields (0.979—0.181) increased with increase in the polarity of solvents. This indicates that the fluorescence characteristics of 7-alkylaminocoumarins I—IX were clearly different from those of 7-arylaminocoumarins (ACA and AMCA)[1,2] which were practically nonfluorescent in aqueous solution. The emission maxima of I—IX varied significantly with the polarity of solvents, that is, they shifted extremely to a shorter wavelength as the polarity of solvents was decreased. This suggests that the fluorescence intensities of I—IX bound to HSA vary greatly at a certain emission wavelength and that the compounds I—IX can serve as probes in protein binding studies. The influence of alkylchain length on the fluorescence in each solvent was not significant in the emission maxima and quantum yields.

Interaction between I—IX and HSA The fluorescence spectra of I—IX in the presence of HSA in pH 7.4 phosphate buffer were measured with excitation wavelength at 360 nm and their representative spectra (I, IV and VIII) are shown

Table I. Fluorescence Spectral Data of 7-Alkylaminocoumarin-4-acetic Acids in Various Solvents

Compound No.	$F\lambda_{max}$ nm (Quantum yield)[a]						
	Water	Methanol	Ethanol	*n*-Butanol	Acetonitrile	Chloroform	Benzene
I	468 (0.951)	452 (0.849)	443 (0.817)	443 (0.798)	435 (0.631)	423 (0.668)	416 (0.416)
II	466 (0.932)	448 (0.829)	445 (0.777)	439 (0.766)	433 (0.635)	421 (0.518)	412 (0.219)
III	468 (0.976)	452 (0.866)	444 (0.830)	442 (0.790)	434 (0.605)	423 (0.705)	416 (0.439)
IV	467 (0.979)	449 (0.895)	446 (0.843)	439 (0.826)	436 (0.651)	424 (0.678)	414 (0.181)
V	468 (0.961)	453 (0.858)	444 (0.831)	443 (0.790)	435 (0.607)	423 (0.717)	415 (0.410)
VI	468 (0.822)	448 (0.881)	450 (0.837)	444 (0.799)	435 (0.687)	423 (0.592)	414 (0.278)
VII	467 (0.831)	450 (0.866)	446 (0.819)	441 (0.791)	433 (0.703)	424 (0.639)	417 (0.434)
VIII	468 (0.846)	452 (0.860)	444 (0.830)	442 (0.794)	433 (0.625)	424 (0.697)	414 (0.407)
IX	468 (0.801)	451 (0.887)	450 (0.846)	442 (0.766)	435 (0.670)	423 (0.546)	415 (0.262)

a) Excitation at 360 nm.

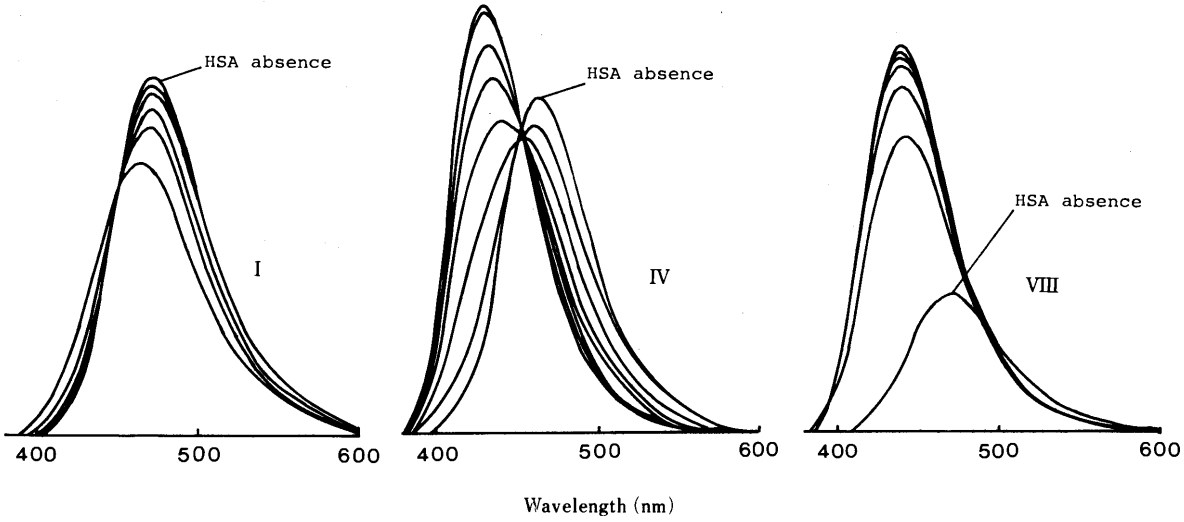

Fig. 1. Fluorescence Spectra of I, IV and VIII in the Absence and Presence of HSA

Concentration: I, IV and VIII, 1.0×10^{-6} M; HSA, 1.0×10^{-6}—5.0×10^{-5} M. Excitation wavelength: 360 nm.

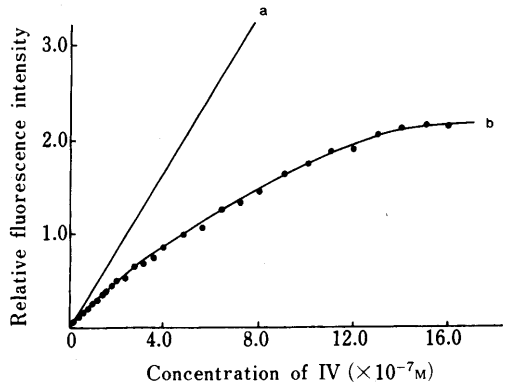

Fig. 2. Relative Fluorescence Intensity in the Probe-HSA Interaction Obtained by the Titration with IV

HSA concentration: a, 1.0×10^{-5} and 2.0×10^{-5} M; b, 1.0×10^{-6} M.

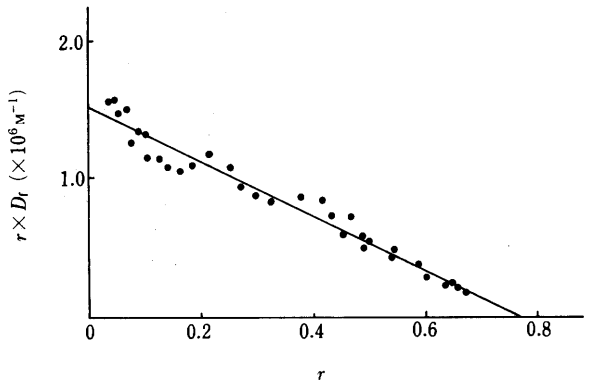

Fig. 3. Scatchard Plots of IV-HSA Interaction

in Fig. 1. The emission maxima on the spectra uniformly shifted toward a shorter wavelength with increasing HSA concentration, whereas the fluorescence intensity behavior was of three types according to the compound (Fig. 1). The intensity of I (the first type) decreased with the successive addition of HSA, that of IV (the second type including II, III and V) decreased at the beginning addition and thereafter increased, and that of VIII (the third type including VI, VII and IX) increased. Such fluorescence spectral changes are

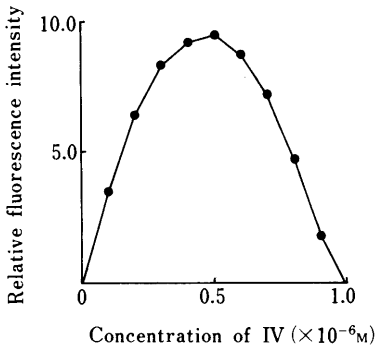

Fig. 4. Job's Plots of Relative Fluorescence Intensity for IV-HSA Interaction

The total concentration of [HSA]+[IV] was kept at 1.0×10^{-6} M.

of interest in connection with the binding character of I—IX to protein but are not yet clear.

To estimate the binding parameters for 7-alkylaminocoumarin-HSA interaction, the fluorometric titration curves were constructed by measuring the greatly differing fluorescence intensities at 400 nm, followed by the making of Scatchard plots from the results. Figures 2 and 3 show the titration curves and Scatchard plots of the IV-HSA system, respectively. The fluorescence intensities for the two titrations with high HSA concentration (1.0×10^{-5} and 2.0×10^{-5} M) were identical (straight line a in Fig. 2), suggesting that the added IV was fully bound to the protein. The plateau in the titration curve obtained at low HSA concentration indicates saturation of the binding sites in HSA. The linearity of Scatchard plots for the IV-HSA system obtained from the titration curves in Fig. 2 indicates that IV binds to one class of sites on HSA (Fig. 3). The binding constant, K and the n value estimated from Scatchard plots were 1.78×10^5 M^{-1} and 0.76, respectively. To check the maximum number of binding sites, Job's plots were also prepared for the IV-HSA system keeping the total concentration of IV and HSA at 1.0×10^{-6} M (Fig. 4). The inflection point for this plot is 0.5, the value expected for 1:1 complex formation. The binding parameters and binding ratios of the others to HSA were estimated in the

TABLE II. Binding Parameters of 7-Alkylaminocoumarin-4-acetic Acids to HSA

Compound No.	n_1	$K_1(M^{-1})$	n_2	$K_2(M^{-1})$	Molar ratio[a] (Probe : HSA)
I	0.28	1.55×10^5			1 : 2
II	0.34	4.75×10^5			1 : 2
III	0.74	5.20×10^5			1 : 1
IV	0.76	1.78×10^6			1 : 1
V	0.93	2.81×10^6			1 : 1
VI	0.83	5.85×10^6			1 : 1
VII	0.44	1.43×10^7	0.89	2.97×10^6	2 : 1
VIII	0.56	3.21×10^7	1.31	6.08×10^6	2 : 1
IX	0.62	2.09×10^7	1.48	4.71×10^6	2 : 1

a) From Job's plot analyses.

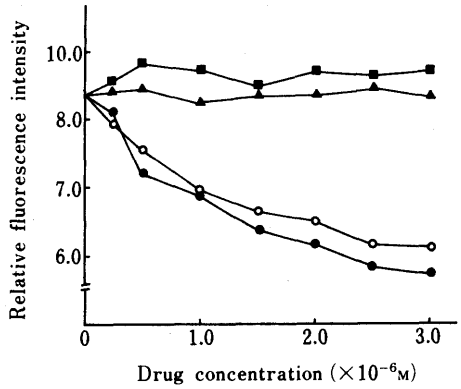

Fig. 5. Effects of Drugs on the Fluorescence Intensity of IV (5.0×10^{-7} M) in the Presence of HSA (1.0×10^{-6} M)

■, phenylbutazone; ▲, digoxin; ○, ibuprofen; ●, flufenamic acid.

same manner as that of the IV-HSA system and the results are shown in Table II. The n values (n_1, n_2) obtained by Scatchard analysis are in excellent agreement with the molar ratios of probe-HSA complexes found by Job's plots. Though the reason for small n values obtained for compounds I and II is not clear, it can well be understood from the data of binding affinity ($n\times K$) that these compounds may not be large enough to fit the binding site on HSA. As shown in Table II, the binding constants of I—IX in the primary binding site increased with lengthening of the alkylchain and the value was maximum for laurylamino-compound (VIII). This clearly indicates that the binding characters of I—IX depend upon the length of alkylchain, and these results thus suggest that the probe-binding sites have a hydrophobicity.

The effects of drugs on the fluorescence of I—IX bound to HSA were investigated for Sudlow's classification[8] of the binding sites. Figure 5 shows the changes in the fluorescence of the test compound IV bound to HSA on the addition of drugs. Compound IV was not displaced by phenylbutazone (site 1 drug) or digoxin (site 3 drug), whereas ibuprofen and flufenamic acid (site 2 drugs) caused significant displacement of IV at small molar ratios of drug to HSA. Similar displacements were also observed in the cases of other tested compounds in the presence of HSA. Thus, it was suggested on the basis of these results that the primary binding site of I—IX on HSA is site 2, differing from that of ACA and AMCA.

Further, attempts were made to estimate the environment

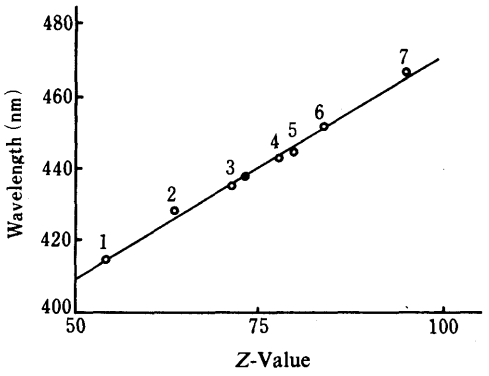

Fig. 6. Relationship between the Emission Maximum Wavelength of IV and Z-Value

○: 1, benzene; 2, chloroform; 3, acetonitrile; 4, n-butanol; 5, ethanol; 6, methanol; 7, water. ●, a plot of the wavelength of the emission maximum (438 nm) of IV (1.0×10^{-6} M) in HSA (2.0×10^{-5} M) solution.

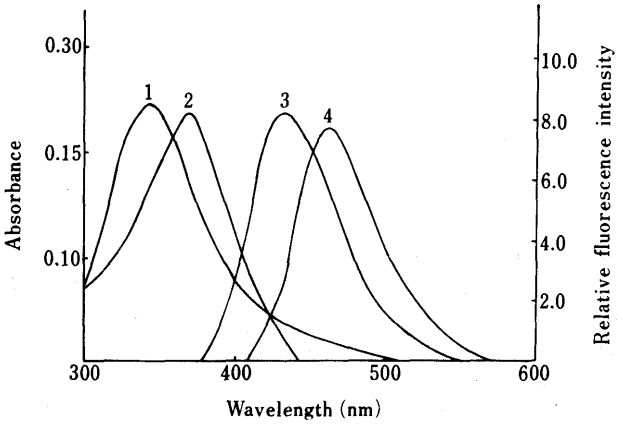

Fig. 7. Spectra of IV and HSA in Aqueous Solution (pH 7.4)

1, fluorescence spectrum of HSA tryptophan (1.0×10^{-4} M); 2, absorption spectrum of IV (1.0×10^{-5} M); 3, fluorescence spectrum of HSA tryptophan (5.0×10^{-6} M)–IV (1.0×10^{-6} M) complex; 4, fluorescence spectrum of IV (1.0×10^{-6} M). Fluorescence spectrum of HSA tryptophan was excited at 295 nm. The other fluorescence spectra were excited at 360 nm.

of site 2 using some of these probes. The relationship between the emission maximum wavelength of IV in various solvents and Z-values as a measure of the polarity of solvents afforded a good linearity, as can be seen in Fig. 6. From this relationship and the emission maximum (438 nm) in the HSA solution, the polarity of site 2 was 72.8 as Z-value which approximately corresponds to that of acetonitrile.

In addition, the binding constant, K usually has important implications for the fitness of a ligand to the binding site in proteins. K values shown in Table II became progressively greater as the alkylchain in probes lengthened. This suggests that the hydrophobicity of alkylamino group in probes contributes more predominantly to the binding to site 2 rather than does the coumarin ring character. The hydrophobic cleft at site 2 approximately 21—25 Å deep, because the binding patch can be estimated from the Corey–Pauling–Koltun molecular model of the probe molecule VIII as a whole which is maximal in K value among the tested probes.

Recently, the distance between the lone tryptophan residue at position 214 and the drug-binding sites (site 1 and site 2) in the HSA molecule was estimated for the characterization of the binding sites using Förster's equation based on the fluorescence energy transfer.[6] The absorption

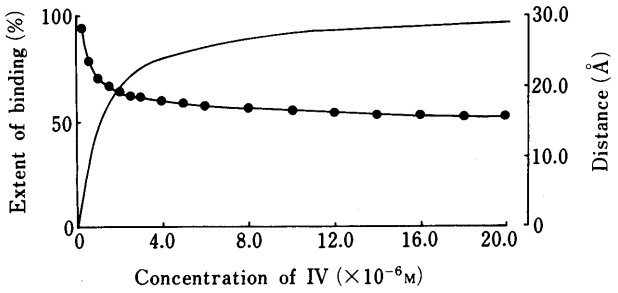

Fig. 8. Relationship between the Distance (—●—) from Site 2 to the Lone Tryptophan Residue in HSA and the Binding Extent (—) of IV at Its Site

The concentration of HSA was 5.0×10^{-7} M.

TABLE III. Apparent Distance (Å) between the Lone Tryptophan Residue and Probe in HSA Molecule

Compound No.	Extent of probe binding at primary binding site ($r/n \times 100\%$)			
	30%	50%	80%	≧90%
I	29.5	26.5	21.0	16.9
IV	24.8	21.2	18.6	16.2
VI	22.6	19.9	16.2	15.4
VIII	23.3	20.3	16.5	15.3

spectra of I—IX overlapped with the emission spectrum of the lone tryptophan residue in HSA excited at 295 nm, as shown in Fig. 7 for the case using IV. The fluorescence emission spectrum of the lone tryptophan residue was quenched by addition of I—IX. Therefore, the fluorescence energy transfer in the spectra may depend on the distance between the lone tryptophan residue and I—IX bound to site 2 in HSA. Figure 8 shows the relationship between the distance from the lone tryptophan residue to IV bound to site 2 and the extent of IV binding to the site. The extent of binding was determined from Eq. 2 using the binding parameters (n and K). The degree (%) of occupation of the binding site obtained for site 2 was plotted against the total concentration of IV. Distances between the lone tryptophan residue and IV bound to HSA were calculated from the fluorescence spectral data of HSA solution measured in the absence and presence of IV. The apparent distances obtained were plotted against the total concentration of IV. The values for distance decreased asymptotically with increase in the degree of the binding, and reached a constant value when the binding sites were saturated with IV. The distances obtained using several probes (I, IV, V and VIII) were in the range from 15.3—16.9 Å (Table III), which were comparable to the value (16.1 to 17.5 Å) estimated by Kasai *et al.*[7]

The results obtained here demonstrate that I—IX are useful as fluorescence probes for the characterization of drug-binding site 2 on HSA.

Acknowledgement The authors wish to thank the staff of the Analytical Center of this faculty for elemental analyses.

References

1) S. Goya, A. Takadate, H. Fujino, M. Otagiri and K. Uekama, *Chem. Pharm, Bull.*, **30**, 1363 (1982).
2) A. Takadate, Y. Ohkubo, M. Irikura, S. Goya, M. Otagiri and K. Uekama, *Chem. Pharm. Bull.*, **33**, 522 (1985); A. Takadate, M. Irikura, Y. Ohkubo, S. Goya and M. Otagiri, *ibid.*, **35**, 2104 (1987).
3) H. Umemoto, T. Kitao and K. Konishi, *Kogyo Kagaku Zasshi*, **73**, 1146 (1970).
4) C. A. Parker and W. T. Rees, *Analyst* (London), **85**, 587 (1960).
5) G. Scatchard, *Ann. N. Y. Acad. Sci.*, **51**, 660 (1949).
6) T. Förster, *Ann. Phys.*, **6**, 55 (1948).
7) S. Kasai, T. Horie, T. Mizuma and S. Awazu, *J. Pharm. Sci.*, **76**, 387 (1987).
8) G. Sudlow, D. J. Birkett and D. N. Wade, *Mol. Pharmacol.*, **11**, 824 (1975); *Idem, ibid.*, **12**, 1052 (1976).

Induction and Inhibition of a Novel Sulfotransferase in a Human Intestinal Bacterium, *Eubacterium* sp. A-44

Dong-Hyun KIM and Kyoichi KOBASHI*

Toyama Medical and Pharmaceutical University, 2630 Sugitani, Toyama-shi, Toyama 930-01 Japan. *Received July 27, 1990*

Induction and inhibition of a novel sulfotransferase produced by *Eubacterium* sp. A-44 isolated from human feces have been studied. Production of the enzyme was induced by phenylsulfate esters, sulfate donor substrates, but not by phenols, sulfate acceptor substrates, or inorganic sulfate.

***p*-Nitrophenylsulfate (PNS), a good donor substrate, stimulated enzyme production more than 10-fold. Sulfotransferase production was strongly inhibited by phenylphosphate esters. Enzyme activity was competitively inhibited by phenylphosphate esters, but not by inorganic phosphate. High yields of sulfotransferase from sonicated cells were obtained when the bacteria were grown in a media containing 0.6% (w/v) or less of glycine.**

Keywords sulfotransferase; *Eubacterium*; phenylsulfate ester; enzyme production

Introduction

The sulfoconjugation of phenolic compounds has been established to be an important detoxification process for phenolic compounds.[1] Recent studies have shown that among various posttranslationally modified proteins,[2-4] a large number of secretory proteins and peptides exist in sulfated form in tyrosine residues.[5,6] The role of tyrosine sulfation, however, is generally not yet understood.

Recently, we isolated a bacterium of *Eubacterium* sp. A-44 from human feces. The bacterium is an anaerobic, gram-positive, gas producing and non-spore forming rod which produces tyrosylprotein sulfotransferase but not arylsulfatases.[7,8] It was also discovered that the bacterium plays an important role in the metabolism of phenolic compounds.[9] It was therefore of interest to investigate the biological role of the enzyme in *Eubacterium* sp. A-44 and its regulatory mechanisms. The present study has been undertaken to investigate the induction of enzyme synthesis and its inhibition *in vitro* and *in vivo*.

Materials and Methods

Materials Bovine serum albumin (BSA), *p*-nitrophenylsulfate (PNS), 4-methylumbelliferyl 7-sulfate (MUS) and 4-methylumbelliferyl 7-phosphate (MUP) were purchased from Sigma Chemical Company (U.S.A.). Phenolphthalein disulfate (PPDS), *p*-nitrophenol, *p*-nitrophenylphosphate (PNP) and phenolphthalein diphosphate (PPDP) were bought from Nacalai Tesque, Ltd. (Japan). Phenylphosphate (PP) was obtained from Wako Pure Chemical Industry Ltd. (Japan) and General Anaerobic Medium (GAM) from Nissui Seiyaku Company (Japan). (^{35}S)Labeled PNS was synthesized by the method of Burchardt *et al.*[10] with minor modifications which were described in detail in our previous paper.[8] The crystallized (^{35}S)PNS was identified by thin-layer chromatography (TLC) and high performance liquid chromatography (HPLC) in comparison with an authentic PNS. Specific radioactivity of (^{35}S)PNS was 3×10^2 dpm per nmol. All other chemicals were of analytical reagent grade.

Growth of Bacteria and Preparation of the Enzyme The bacterium, *Eubacterium* sp. A-44 isolated from human feces,[11] was precultured in GAM broth with or without an inducer, an inhibitor and/or glycine. The culture medium (5 ml) was inoculated in 100 ml of GAM broth with or without an inducer, an inhibitor, and/or glycine, and cultivated at 37 °C for 18—20 h in an anaerobic box. After incubation, the culture was centrifuged at $5000 \times g$ for 20 min at 4 °C and the supernatant fluid discarded. All subsequent procedures were carried out under aerobic conditions. The harvested cells were washed twice with 0.9% saline. The resulting cell pellet was suspended in 5 ml of 20 mM acetate buffer, pH 5.7, and disrupted by sonication repeated five-times; at 60 W for 30 s of sonication and for a 1 min pause with a sonicator (Heat Systems-Ultrasonics, U.S.A.). After centrifugation ($20000 \times g$, 30 min) to remove cell debris, the supernatant fluid was retained as a crude enzyme solution and as a cytosol fraction. The cell debris was treated with the buffer containing 1% (w/v) Triton X-100 and centrifuged ($100000 \times g$, 30 min). The resulting supernatant fluid was used as a membrane extract.

Enzymatic Sulfation of Bacterial Proteins with (^{35}S) PNS A cytosol fraction or a membrane extract or their mixture (1 : 1 v/v) was incubated for 30 min at 37 °C with (^{35}S)PNS (1.0 mg, total 1.5×10^6 dpm) under the same protein concentrations (3.15 mg/ml) in 0.1 M Tris–HCl buffer, pH 8.0 in a final volume of 2.1 ml. The reaction mixtures were then applied on a Sephadex G-50 superfine column (0.9×30 cm) and eluted with 0.1 M Tris–HCl buffer, pH 8.0 (flow rate 9.0 ml/h). The protein fractions were combined and were analyzed by sodium dodecyl sulfate–polyacrylamide gel electrophoresis (SDS–PAGE)[12] with coomasie brilliant blue staining and X-ray film exposure.

Sulfotransferase Assay The assay mixture (total volume of 0.63 ml) contained 30 μl of 50 mM PNS, 0.29 ml of 20 mM tyramine or tyrosine methylester, 0.21 ml of 0.1 M Tris–HCl buffer, pH 8.0, and 0.1 ml of the enzyme solution. The assay mixture was incubated at 37 °C for 15 min. The reaction was stopped by the addition of 1 M NaOH (0.4 ml) and the absorbance at 405 nm was measured. Arylsulfatase activity was also measured under the assay conditions described above in which tyramine (an acceptor substrate) was omitted.

Definition of Activity One unit of enzyme activity was defined as the amount of enzyme required to catalyze the formation of 1.0 μmol of *p*-nitrophenol per min under standard assay conditions. Specific activity was defined in terms of units per mg protein.

Inhibition of Sulfotransferase Activity In order to determine the inhibitory effect of phenylphosphate esters such as PNP, MUP, PPDP and PP, the enzyme activity was measured according to the standard assay method described previously with the reaction mixture containing each inhibitor at various concentrations (final concentration 0—10 mM).

Determination of Protein Protein was determined by the method of Lowry *et al.*[13] using BSA as the standard.

Results and Discussion

Induction of Sulfotransferase Activity by Sulfate Donor Substrates When *Eubacterium* sp. A-44 was anaerobically cultivated in GAM broth, sulfotransferase was produced concomitantly with bacterial growth, reaching a plateau after 16—20 h cultivation (Fig. 1). Enzyme synthesis was stimulated by adding a sulfate-donor substrate (PNS) to the GAM broth, as shown in Fig. 2. When PNS was added, the stimulation of enzyme production was found to be concentration dependent, being 10 to 13-fold at 1 mM PNS. In addition to PNS, MUS which is a good donor substrate[11] was also a good inducer and the enzyme production at 0.5 mM MUS was 4 to 5-fold, but high concentrations of MUS interfered with the assay of enzyme (data not shown). *p*-Nitrophenol, which is a product of the enzyme reaction, and sodium sulfate were ineffective as inducers at

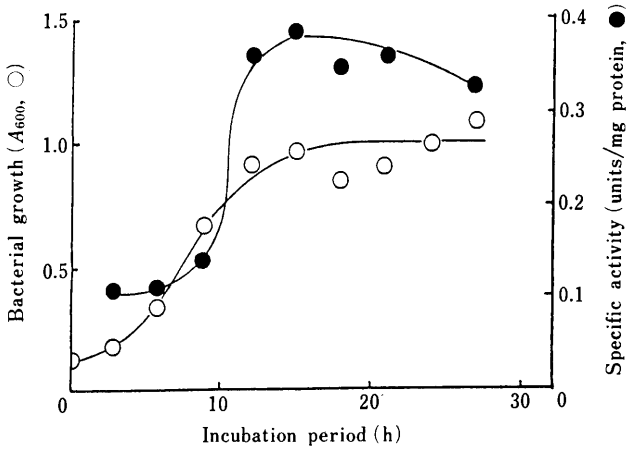

Fig. 1. Time Course of Bacterial Growth and Sulfotransferase Production

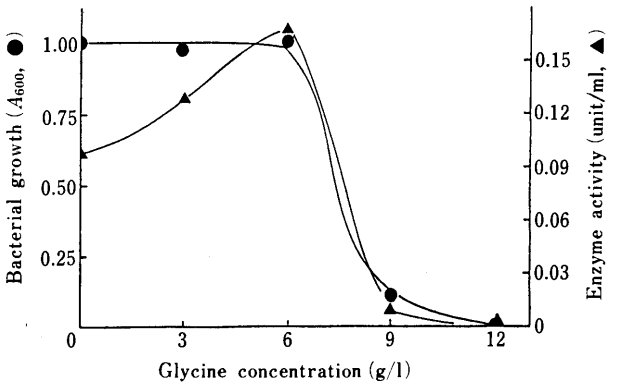

Fig. 3. Effect of Glycine Concentration on the Growth of *Eubacterium* A-44 and the Extraction Yield of Sulfotransferase Activity

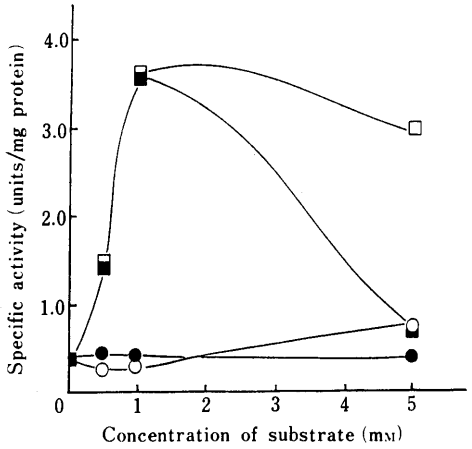

Fig. 2. Induction of Sulfotransferase by Donor Substrate in GAM Broth

□, *p*-nitrophenylsulfate; ●, *p*-nitrophenol; ■, *p*-nitrophenylsulfate and *p*-nitrophenol; ○, sodium sulfate. Specific activity of a crude enzyme solution was measured at 18 h cultivation under the same conditions as in Fig. 1.

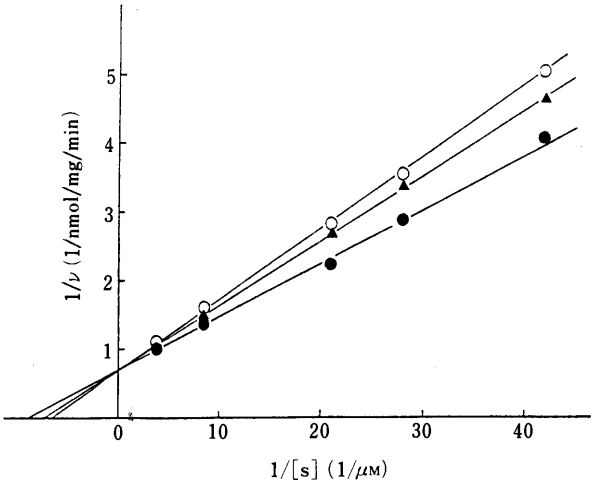

Fig. 4. Lineweaver–Burk Plots of Inhibition of Sulfotransferase by Phenylphosphate Esters

Inhibitors: ●, none; ▲, PNP (3.38 mM); ○, MUP (2.38 mM).

concentrations up to 5 mM. In the presence of 1 mM and 5 mM *p*-nitrophenol, the specific activity of the enzyme was not affected but the growth of the bacterium was inhibited. The simultaneous addition of PNS and *p*-nitrophenol at 1 mM induced sulfotransferase, but both enzyme production and bacterial growth were inhibited at 5 mM. During induction of the sulfotransferase by donor substrates, hydrolytic activity against the phenylsulfate esters was not induced. K_m values for donors and acceptors, and the pH optimum of the induced enzyme were the same as the values[8] obtained previously using the enzyme without induction.

When the cytosol fraction or the combined mixture of a cytosol fraction and a membrane extract were incubated with (^{35}S)PNS, several protein bands with (^{35}S)radioactivity were detected on SDS–PAGE.[12] The combined mixture incorporated more (^{35}S)radioactivity than each fraction (data not shown). These sulfated proteins and their function have not yet been identified, but they may be involved in the induction of the sulfotransferase. This induction may be important in the metabolism of phenolic compounds in the human intestine because various phenylsulfate esters are excreted into the intestine *via* the bile duct.[14]

Growth of *Eubacterium* sp. A-44 was sensitive to the glycine content in the medium (Fig. 3). While the bacterium did not grow in GAM broth containing more than 0.9% glycine, it grew well in media containing 0, 0.3 and 0.6% glycine. When the bacterium was cultivated in the medium containing 0.3 and 0.6% glycine, sulfotransferase activity (units/ml) extracted from the bacterium increased 1.3 and 1.7-fold, respectively over the control value, but the specific activity did not increase (data not shown). The increase of total activity in bacteria grown in the glycine-containing medium may be due to the fact that glycine was incorporated into the peptidoglycan of the cell wall and as a result of glycine incorporation, the cell wall became more labile and was easily disrupted by sonication.

Inhibition of Sulfotransferase by Phenylphosphate Esters A novel sulfotransferase was induced by phenylsulfate esters as described above and the activity was also stabilized by these compounds as reported previously.[8] However, phenylphosphate esters such as MUP and PNP competitively inhibited the enzyme activity (Fig. 4). MUP was the most potent inhibitor, followed by PNP, PP and PPDP. K_i values for MUP, PNP and PP, using PNS as a donor substrate and tyramine as an acceptor were 5.7, 10.2 and 12.7 mM, respectively. Among the phenylsulfate ester donor substrates, MUS, was a good substrate and PPDS was a poor substrate.[11] Thus, the degree of inhibition exerted by

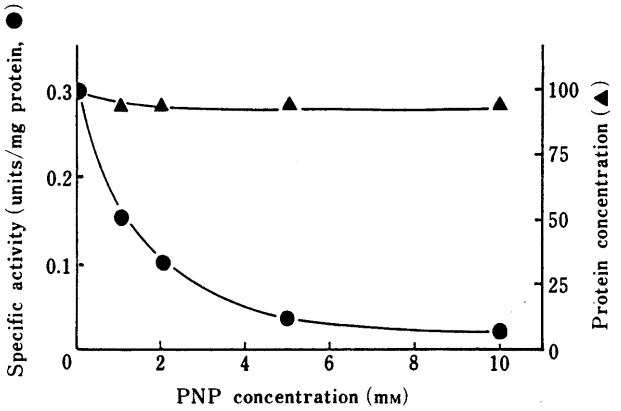

Fig. 5. *In Vivo* Inhibition of Sulfotransferase Production in *Eubacterium* A-44 by *p*-Nitrophenylphosphate

the phenylphosphate analogues paralleled the degree of substrate specificity of the corresponding phenylsulfate analogues. However, inorganic phosphate, inorganic borate and *p*-nitrophenol, one of the reaction products, did not inhibit the enzyme activity at the concentration of 5 mM.

The effect of phenylphosphate ester on sulfotransferase production was also examined. When the bacterium was grown in GAM broth containing PNP, enzyme production was strongly inhibited in a concentration-dependent manner (Fig. 5). At a concentration of 5 mM PNP, specific activity of the enzyme was 10% of the control, although bacterial growth was not affected. These results suggest that phenylphosphate esters inhibit not only activity but also production of sulfotransferase *in vivo*. Therefore, the formation of sulfoconjugates of phenolic compounds by the intestinal flora may be inhibited by phenylphosphate esters as well as by antibiotics.[9] When *Eubacterium* sp. A-44 was grown in GAM containing PNP and glycine, cell growth was similar to that occurring in the medium containing PNS and glycine. Total enzyme activity in a crude extract was increased by the addition of glycine to these media. These results also support the conclusion that glycine was incorporated into the cell wall rather than that glycine directly induced the enzyme.[15,16]

The induction of sulfotransferase by PNS and the inhibition of the enzyme by PNP will be of value in future studies on the physiological role of sulfated proteins. The glycine-containing medium will be useful for isolating proteins and enzymes from gram-positive organisms and for obtaining the protoplast preparations.

Acknowledgement The authors would like to thank Ms. S. Takayanagi for her secretarial assistance.

References

1) E. Baumann, *Pfluegers Arch. Gesamte Physiol. Menschen Tiere*, **13**, 285 (1876).
2) R. Uy and F. Wold, *Science*, **198**, 890 (1977).
3) F. Wold, *Annu. Rev. Biochem.*, **50**, 783 (1981).
4) P. Cohen, *Nature* (London), **296**, 613 (1982).
5) W. B. Huttner, *Nature* (London), **299**, 273 (1982).
6) P. A. Baeuerle and W. B. Huttner, *EMBO J.*, **3**, 2209 (1986).
7) K. Kobashi and D.-H. Kim, *Biochem. Biophys. Res. Commun.*, **140**, 38 (1986).
8) D.-H. Kim, L. Konishi and K. Kobashi, *Biochim. Biophys. Acta*, **872**, 33 (1986).
9) D.-H. Kim and K. Kobashi, *Biochem. Pharmacol.*, **35**, 3507 (1986).
10) G. N. Burchardt and A. Lapworth, *J. Chem. Soc.*, **1926**, 684.
11) K. Kobashi, Y. Fukaya, D.-H. Kim, T. Akao and S. Takebe, *Arch. Biochem. Biophys.*, **245**, 537 (1986).
12) U. K. Laemmli, *Nature* (London), **227**, 680 (1970).
13) O. H. Lowry, N. J. Rosebrough, A. L. Farr and R. J. Randall, *J. Biol. Chem.*, **193**, 265 (1951).
14) K. S. Dodgson and N. Tudball, *Biochem. J.*, **74**, 154 (1960).
15) D. A. Hopwood, *Annu. Rev. Microbiol.*, **35**, 237 (1981).
16) M. H. Jeynes, *Nature* (London), **180**, 867 (1957).

Potentiating Effect of Converting Enzyme Inhibitor Captopril to the Renal Responses of Magnesium Lithospermate B in Rats with Adenine-Induced Renal Failure

Takako YOKOZAWA,*[,a] Hae Young CHUNG,[b] Tae Woong LEE,[a] Hikokichi OURA,[a] Gen-ichiro NONAKA,[c] and Itsuo NISHIOKA[c]

Department of Applied Biochemistry, Research Institute for Wakan-Yaku, Toyama Medical and Pharmaceutical University,[a] Sugitani, Toyama 930-01, Japan, College of Pharmacy, Pusan National University,[b] Pusan, Korea, and Faculty of Pharmaceutical Sciences, Kyushu University,[c] Maidashi, Higashi-ku, Fukuoka 812, Japan. *Received July 30, 1990*

The renal responses of magnesium lithospermate B were investigated in the presence or absence of pretreatment with the converting enzyme (kininase II) inhibitor, captopril, in rats with adenine-induced renal failure. Magnesium lithospermate B (10 mg/kg body weight) caused a marked increase in the levels of the renal functional parameters (glomerular filtration rate, renal plasma flow and renal blood flow), accompanied by significant increases in urinary excretions of prostaglandin E_2 (PGE_2), kallikrein, sodium and creatinine. The administration of magnesium lithospermate B in combination with captopril (2 mg/kg body weight, 2 times) caused a further increase in renal functional parameters, urinary sodium and creatinine excretions. However, the kallikrein activity was similar to the control level. There were no significant changes between urinary PGE_2 following magnesium lithospermate B alone, or in combination with captopril. In addition, angiotensin converting enzyme activity did not change following the administration of magnesium lithospermate B alone, but was significantly decreased in rats given captopril, both alone and in combination with magnesium lithospermate B. The captopril administration group (captopril alone or in combination with magnesium lithospermate B) showed a significant decrease in blood pressure. From these results, it seems that the combination of magnesium lithospermate B and captopril induces a further increase in renal function by improving the renal circulatory state.

Keywords renal failure; magnesium lithospermate B; renal response; captopril; rat

Various conservative therapies are available for chronic renal failure, such as a low protein-high calorie diet, essential amino acid therapy, and administration of activated charcoal or lactulose.[1-3] We have been studying the actions of crude drugs in rats with experimental renal failure for several years as part of our research on drug therapy. Through such studies, we have shown that the administration of Salviae Miltiorrhizae Radix (a traditional Chinese medicinal herb known as "Dan Shen") is effective in improving renal function parameters, producing significant increases in the glomerular filtration rate, renal plasma flow and renal blood flow.[4] In addition, magnesium lithospermate B was isolated and identified as a biologically active component which improved renal function.[5] Studies on the mechanism of action of this compound, which is a new constituent of Salviae Miltiorrhizae Radix, are currently in progress in our laboratory.[6-10] In the previous paper, pretreatment with a kallikrein inhibitor (aprotinin) blunted magnesium lithospermate B-evoked renal responses as well as urinary excretions of prostaglandin E_2 (PGE_2) and kallikrein, which indicated that the kallikrein–kinin system is involved in renal responses to magnesium lithospermate B through activation of the prostaglandin system.[8] The present study is designed to confirm the precise mechanism by which magnesium lithospermate B improves renal function through the activation of the kinin–kallikrein and prostaglandin systems in kidney. For this purpose, the experiment was performed in the presence or absence of captopril, which has kinin-potentiating activity.

Materials and Methods

Animals and Treatment Male rats of the Wistar strain (SLC Ltd., Hamamatsu, Japan), with a body weight of 200—210 g, were placed in metabolic cages and kept at a temperature of 23±1 °C under a 12-h dark-light cycle. They were allowed an adaptation period of several days, during which they were fed on a commercial feed (type CE-2, Clea Japan Inc., Tokyo, Japan). They were then fed *ad libitum* on an 18% casein diet containing 0.75% adenine. It was previously confirmed that renal failure was present after 6 d of adenine ingestion.[11-18] On the 6th day of the experimental diet, four groups of studies were performed. In group 1, intraperitoneal administration of the vehicle saline for captopril was performed, followed 3 h later by intraperitoneal injection of saline (0.5 ml/kg body weight). In group 2, captopril was dissolved in saline immediately before use and injected at a dose of 2 mg/kg body weight into the rats, followed 3 h later by intraperitoneal injection of the vehicle for magnesium lithospermate B and captopril (2 mg/kg). In group 3, 3 h after administration of the vehicle for captopril the rats received magnesium lithospermate B (10 mg/kg body weight) dissolved in saline and the vehicle for captopril. In group 4, 3 h after captopril (2 mg/kg) administration, magnesium lithospermate B (10 mg/kg) and captopril (2 mg/kg) were given. Renal function was determined at about 6 h after intraperitoneal administration of magnesium lithospermate B and/or captopril. For determination of sodium, potassium, creatinine, PGE_2 and kallikrein, urine was collected 3—6 h after treatment. Both the angiotensin converting enzyme (ACE) activity in plasma and blood pressure were determined in rats that had 6 h of administration of the agent. Six rats were used for each experimental group. Values are expressed as means±S.E.

Chemicals Captopril was obtained from Squibb (Princeton, NJ, U.S.A.). [^{125}I]prostaglandin E_2 RIA kit was provided by New England Nuclear (Boston, MA, U.S.A.). DL-Val-Leu-Arg *p*-nitroanilide was obtained from Sigma Chemical Co., U.S.A.

Magnesium Lithospermate B Magnesium lithospermate B was isolated and purified from an extract of roots of Salviae Miltiorrhizae Radix (*Salvia Miltiorrhiza* BUNGE) produced in China, as described previously.[5] This compound gave a tan amorphous powder, $[\alpha]_D^{26}$ +147.7° (c=0.7, MeOH). The purity was checked by measuring its optical rotation and by thin-layer

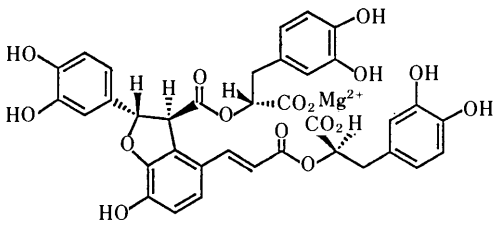

Fig. 1. Structural Formula of Magnesium Lithospermate B

chromatography [Kieselgel 60 F_{254}, benzene–ethyl formate–formic acid (2:7:1), *Rf* 0.3] and high-performance liquid chromatography [Cosmosil $5C_{18}$, 22% CH_3CN in 20 mM H_3PO_4, t_R 22.0 min]. The chemical structure is shown in Fig. 1.

Determination of Renal Function The glomerular filtration rate (*GFR*) and renal plasma flow (*RPF*) were measured by means of a renal clearance test using single intravenous administration of sodium thiosulfate or sodium *para*-aminohippurate, respectively, as an indicator.[19,20] At 25 min after intravenous administration of either of these agents, the bladder was reflexly emptied by having each rat inhale ether for 3—5 s. The urine thus voided was discarded. During the next 30 min urine was collected, and the collection was terminated after the bladder had again been emptied reflexly by ether inhalation. Blood samples were taken from conscious rats by heart puncture in the middle of the period used for the clearance test. Thiosulfate and *para*-aminohippurate concentrations in the plasma and urine were determined by titrimetry and colorimetry, respectively. Renal blood flow (*RBF*) was calculated on the basis of *RPF* and the hematocrit value (*Ht*) using the equation shown below. *Ht* was determined with a hematocrit measurement apparatus, model KH-120A (Kubota Co., Tokyo, Japan).

$$RBF=\frac{RPF}{1-Ht} \quad \text{(ml/min)}$$

Determination of Urinary Electrolytes Sodium and potassium were measured with an electrolyte measurement apparatus (AHS/Japan Corporation, Tokyo, Japan) based on the ion electrode method.

Determination of Urinary Creatinine Creatinine was measured by high-performance liquid chromatography using a step-gradient system.

Urinary PGE_2 Assay PGE_2 was measured by radioimmunoassay as reported elsewhere.[21,22]

Urinary Kallikrein Assay The activity of kallikrein was measured according to the method of Amundsen *et al.*[23]

Blood ACE Assay The assay of ACE (peptidyldipeptide hydrolase, EC 3.4.15.1) was estimated by colorimetric analysis.[24]

Blood Pressure Determination The systolic, mean and diastolic blood pressures of each conscious rat were determined by a tail-pulse pick-up method[25] and recorded with an MK-100 Automatic Sphygmotonograph (Muromachi Kikai Co., Ltd., Tokyo, Japan). Blood pressure was determined repeatedly throughout the experiment.

Statistics The significance of differences between the normal rats and those with renal failure treated or non-treated with magnesium lithospermate B and/or captopril was tested using the Student's *t*-test.

Results

Renal Function The *GFR* in rats given adenine significantly decreased (by 48%) compared to the level in normal rats. The *RPF* and *RBF* in the adenine-treated rats exhibited no significant differences when compared with those in normal rats. Intraperitoneal administration of magnesium lithospermate B increased the *GFR* in rats with renal failure. As shown in Table I, administration of magnesium lithospermate B significantly increased the *GFR* by about 68%, from 3.07 to 5.16 ml/min/kg. The combination of magnesium lithospermate B and captopril further increased the *GFR* to 6.29 ml/min/kg (a 105% change, $p<0.05$). Treatment with captopril alone also induced a significantly increased *GFR*. A significant increase in *RPF* and *RBF* was observed in response to administration of 10 mg/kg body weight of magnesium lithospermate B. Treatment with magnesium lithospermate B alone caused 42% and 34% increases in *RPF* and *RBF* as compared with the control rats, respectively (19.61 *vs.* 13.82 ml/min/kg and 34.78 *vs.* 25.97 ml/min/kg). After combined magnesium lithospermate B and captopril treatment, *RPF* and *RBF* were further augmented to 26.93 and 46.95 ml/min/kg, respectively (95% and 81% increases). Captopril alone also significantly increased *RPF* and *RBF*.

Urine Volume, Urinary Electrolyte and Creatinine Excretions As shown in Table II, urine volume, urinary electrolyte and creatinine excretions decreased on day 6 following adenine administration. Urine volume increased significantly, from 2.90 to 3.70 ml/3 h in the group treated with magnesium lithospermate B. Urinary sodium and creatinine excretions also exhibited a significant increase when compared with the respective control values. The combination of magnesium lithospermate B and captopril showed a further increase in urine volume, urinary sodium and creatinine excretions. In contrast, there were no significant differences in urinary potassium excretion between the control and magnesium lithospermate B-treated groups. The administration of magnesium lithospermate B and captopril combined also showed no significant increase. Further, a slight increase in urine volume, urinary sodium

TABLE I. Effect of Magnesium Lithospermate B on Renal Functional Parameters with and without Captopril Pretreatment

Group	Captopril	*GFR* (ml/min/kg)	*RPF* (ml/min/kg)	*RBF* (ml/min/kg)
Normal rats	–	5.90±0.28	16.85±1.11	29.51±1.27
Renal failure rats				
Control	–	3.07±0.20[b]	13.82±1.73	25.97±3.16
Control	+	5.22±0.92[c]	22.66±2.64[a,c]	44.63±6.24[a,c]
Magnesium lithospermate B	–	5.16±0.40[e]	19.61±1.81[c]	34.78±3.47[c]
Magnesium lithospermate B	+	6.29±1.13[c]	26.93±3.87[a,d]	46.95±6.74[a,c]

GFR, glomerular filtration rate; *RPF*, renal plasma flow; *RBF*, renal blood flow. Statistical significance: *a*) $p<0.05$, *b*) $p<0.001$ *vs.* normal rats, *c*) $p<0.05$, *d*) $p<0.01$, *e*) $p<0.001$ *vs.* renal failure control rats.

TABLE II. Effect of Magnesium Lithospermate B on Urine Volume, Urinary Electrolyte and Creatinine Excretions with and without Captopril Pretreatment

Group	Captopril	Urine volume (ml/3 h)	Na (μM/3 h)	K (μM/3 h)	Cr (μg/3 h)
Normal rats	–	3.38±0.10	367±29	155±17	944±23
Renal failure rats					
Control	–	2.90±0.09[b]	290±34	121±13	756±34[c]
Control	+	3.35±0.30	335±58	127±21	850±61
Magnesium lithospermate B	–	3.70±0.26[d]	407±18[d]	150±13	1002±19[e]
Magnesium lithospermate B	+	3.80±0.15[a,e]	486±36[d]	157±21	1069±64[a,e]

Statistical significance: *a*) $p<0.05$, *b*) $p<0.01$, *c*) $p<0.001$ *vs.* normal rats, *d*) $p<0.01$, *e*) $p<0.001$ *vs.* renal failure control rats.

TABLE III. Effect of Magnesium Lithospermate B on Urinary PGE_2 Excretion and Kallikrein Activity with and without Captopril Pretreatment

Group	Captopril	PGE_2 (ng/3 h)	Kallikrein activity (mU/3 h)
Normal rats	−	9.47±2.82	68.92±3.75
Renal failure rats			
Control	−	7.57±1.09	8.40±0.67[a]
Control	+	11.62±2.89	6.81±0.61[a]
Magnesium lithospermate B	−	13.29±2.12[b]	13.33±2.29[a,b]
Magnesium lithospermate B	+	14.37±2.13[b]	6.76±0.80[a]

PGE_2, prostaglandin E_2. Statistical significance: *a*) $p<0.001$ *vs.* normal rats, *b*) $p<0.05$ *vs.* renal failure control rats.

TABLE IV. Effect of Magnesium Lithospermate B on ACE Activity and Blood Pressure with and without Captopril Pretreatment

Group	Captopril	ACE (mU/ml)	Systolic blood pressure (mmHg)	Mean blood pressure (mmHg)	Diastolic blood pressure (mmHg)
Normal rats	−	27.55±1.85	139.4±3.1	113.8±2.3	100.7±2.3
Renal failure rats					
Control	−	29.24±1.17	150.0±3.7[a]	123.1±2.3[b]	109.3±2.0[a]
Control	+	22.73±2.52[c]	135.4±5.5[c]	108.9±2.9[d]	93.0±2.7[a,e]
Magnesium lithospermate B	−	28.67±1.39	147.6±4.8	115.2±2.4[c]	101.8±2.9[c]
Magnesium lithospermate B	+	25.38±1.09[c]	133.3±4.9[c]	108.5±6.7[c]	95.8±5.4[c]

ACE, angiotensin converting enzyme. Statistical significance: *a*) $p<0.05$, *b*) $p<0.01$ *vs.* normal rats, *c*) $p<0.05$, *d*) $p<0.01$, *e*) $p<0.001$ *vs.* renal failure control rats.

and creatinine excretions was observed in response to administration of captopril alone. No remarkable change was observed in potassium excretion.

Urinary PGE_2 and Kallikrein Excretions The changes in urinary excretion of PGE_2 and kallikrein following administration of magnesium lithospermate B and/or pretreatment with captopril are summarized in Table III. The urinary excretion of PGE_2 was decreased by 20% of the level in normal rats on the 6th day after adenine administration. A significant increase in PGE_2 was observed in response to administration of 10 mg/kg body weight of magnesium lithospermate B. Similar changes were obtained in rats following administration of magnesium lithospermate B and captopril. Captopril alone caused a 54% increase in PGE_2 excretion, but this variation was not statistically significant. On the other hand, the kallikrein activity in rats fed on the adenine diet decreased to 8.4 mU/3 h, compared to a level of 68.92 mU/3 h for the normal rats. Magnesium lithospermate B induced a marked enhancement of the urinary kallikrein (a 59% change, $p<0.05$). However, there were no significant changes in urinary kallikrein following magnesium lithospermate B administration in the group pretreated with captopril or administration of captopril alone.

ACE Activity and Blood Pressure As shown in Table IV, the ACE activity in adenine-treated rats was slightly higher when compared to the activity in normal rats. Intraperitoneal administration of captopril (captopril alone and in combination with magnesium lithospermate B) significantly decreased the ACE activity in rats with renal failure. However, magnesium lithospermate B alone did not change the ACE activity in renal failure. Furthermore, the systolic, mean and diastolic blood pressures in rats fed on the adenine diet were significantly higher than those for the normal rats; however, the captopril administration group (captopril alone and in combination with magnesium lithospermate B) induced a significant decrease in blood pressure. The levels of mean and diastolic blood pressure decreased also after treatment with magnesium lithospermate B alone, while the systolic blood pressure remained nearly unchanged.

Discussion

Several lines of evidence seem to indicate a close relationship between the renal prostaglandin and kallikrein–kinin systems: bradykinin is a potent stimulator of prostaglandin synthesis.[26] Urinary prostaglandin and kallikrein excretions have been shown to change in parallel in some experimental conditions, and prostaglandin production by the isolated perfused rabbit kidney seems to be dependent on endogenously produced kinin. Urinary kallikrein decreases in many forms of hypertension and renal disease both in man and laboratory animals.[27–30] Furthermore, inhibition of the kallikrein–kinin system by aprotinin has been found to reduce the aldosterone-induced increase in urinary PGE_2 excretion,[31] suggesting that enhanced prostaglandin production after administration of aldosterone might be mediated by the kallikrein–kinin system. In the preceding paper, it was reported that aprotinin, an inhibitor of kallikrein which therefore suppresses kinin generation, abolishes renal hemodynamic and prostaglandin-excretory responses to magnesium lithospermate B. This suggested that magnesium lithospermate B could act at least partly through activation of the kallikrein–kinin system in the kidney.[8] The same results were demonstrated by the present experiment. In rats with renal failure, the urinary excretion of PGE_2 (it has been shown by Frölich *et al.*[32] that PGE_2 in urine is mostly derived from the kidney), *GFR*, *RPF* and *RBF* increased significantly after magnesium lithospermate B administration, in proportion to the increase in kallikrein activity. In the present study, the extent to which endogenous kinin contributes to the manifestation of the action of magnesium lithospermate B was also investigated using captopril.

In rats with renal failure, captopril administration prior to magnesium lithospermate B caused a further increase in *GFR*, *RPF* and *RBF* in comparison to the increased levels of those administered with magnesium lithospermate B alone. On the other hand, the kallikrein activity was similar to the control level in the group given both captopril and magnesium lithospermate B. In this regard, Vinci *et al.*[33] reported that kallikrein excretion was decreased, while urinary kinin excretion was markedly increased by captopril in both sodium-replete and sodium-deplete patients; they discussed whether kallikrein may be influenced by many factors containing aldosterone. Margolius *et al.*[34] also reported that the release of kallikrein from a rat renal cortical cell suspension was increased after the addition of the aldosterone, yet decreased after the addition of the aldosterone antagonist, spironolactone, indicating that the generation or the release of renal kallikrein is regulated by aldosterone or some other sodium-retaining steroid hormone.

According to the report of Marks *et al.*,[35] the converting enzyme inhibitor, captopril, inhibits the physiological activity of the renin–angiotensin system by inhibiting the production of angiotensin II as well as by decreasing the production and release of aldosterone. Meanwhile, captopril also acts on the kinin decomposing enzyme, kininase II, enhancing the action of endogenous kinin. Since ACE activity decreased significantly after captopril administration in this study, it is clear that the decomposition of kinin into inactive peptides is suppressed. In the group given both captopril and magnesium lithospermate B, blood pressure and ACE activity significantly decreased, suggesting a decrease in angiotensin II. Inhibition of angiotensin II formation is probably the major mechanism by which captopril reduces blood pressure. However, other mechanisms may be involved. Bradykinin, like angiotensin II, also stimulates membrane phospholipase A_2 in various tissues, and thereby stimulates the production of depressive compounds such as PGE_2.[36,37] As mentioned above, the significant increase of renal functional parameters is associated with a significant increase of PGE_2 in rats pretreated with captopril compared to those given magnesium lithospermate B alone, and it is suggested that PGE_2 may be involved in the regulation of renal function by captopril. There is also interaction between the renal prostaglandins and renin–angiotensin system. McGiff *et al.*[38] reported that the intrarenal arterial infusion of angiotensin II was stimulated the release of prostaglandins from the kidney, counteracting the vasoconstricting effects of angiotensin II. On the other hand, several studies have demonstrated that the effect of kinin on renal function is associated with prostaglandin release. Bradykinin-induced natriuresis is also associated with an increase in renal PGE_2 synthesis.[36,39] Additionally, Kauker has reported that kinin exerts a direct action on uriniferous tubules to accelerate the excretion of sodium.[40] Therefore, a significant increase in renal function and urinary PGE_2 excretion, which occurs in response to captopril, is thus unlikely to result from the effect of captopril on the renin–angiotensin–aldosterone system, but might be related to a change in kinin metabolism following captopril pretreatment. In the present experiment, using a combination of captopril and magnesium lithospermate B, urinary excretion of sodium also increased, suggesting that endogenous kinin facilitates the excretion of sodium from the kidney. These effects were also noted after administration of captopril alone, indicating its involvement in the maintenance of renal function and hemodynamics and blood pressure regulation. However, the combination of magnesium lithospermate B and captopril was found to have an additive effect on improving the condition of renal failure.

The exact location in the kidney where the action of magnesium lithospermate B takes place remains to be elucidated in the future. Scicli *et al.*[41] found in an experiment using the stop flow method that kinin was produced in the distal uriniferous tubules. Using the micropuncture method, Farman *et al.*[42] demonstrated that most PGE_2 in urine was produced in the distal uriniferous tubules. Taking their data into account, the distal uriniferous tubules are most likely to be the site of the action of magnesium lithospermate B. Further studies with specific glandular kallikrein inhibitors and kinin receptor blockers will help to clarify the involvement of this system in the renal effect of magnesium lithospermate B.

Acknowledgement This work was supported in part by a Grant-in-Aid for Scientific Research (No. 02807209) from the Ministry of Education, Science and Culture, Japan.

References

1) W. E. Mitch and M. Walser, "The Kidney," ed. by B. M. Brenner and F. C. Rector, Saunders Company, Philadelphia, 1986, p. 1756.
2) K. Kumano, S. Takara, H. Izumi, T. Shimizu, T. Sakai, S. Kuwao, M. Iso, and H. Takahashi, *Jpn. J. Nephrol.*, **29**, 185 (1987).
3) M. Miyazaki, K. Aoyagi, and S. Tojo, *Jpn. J. Nephrol.*, **26**, 1091 (1984).
4) H. Y. Chung, T. Yokozawa, and H. Oura, *J. Med. Pharm. Soc. WAKAN-YAKU*, **4**, 59 (1987).
5) T. Yokozawa, H. Y. Chung, H. Oura, G. Nonaka, and I. Nishioka, *Jpn. J. Nephrol.*, **31**, 1091 (1989).
6) T. Yokozawa, H. Y. Chung, T. W. Lee, H. Oura, T. Tanaka, G. Nonaka, I. Nishioka, and A. Hirai, *Chem. Pharm. Bull.*, **37**, 1568 (1989).
7) T. Yokozawa, H. Y. Chung, T. W. Lee, H. Oura, T. Tanaka, G. Nonaka, and I. Nishioka, *Chem. Pharm. Bull.*, **37**, 2766 (1989).
8) T. Yokozawa, H. Y. Chung, T. W. Lee, H. Oura, G. Nonaka, and I. Nishioka, *Jpn. J. Nephrol.*, **32**, 893 (1990).
9) T. Yokozawa, H. Oura, T. W. Lee, G. Nonaka, and I. Nishioka, *Nephron*, **57**, 78 (1991).
10) T. Yokozawa, T. W. Lee, H. Y. Chung, H. Oura, G. Nonaka, and I. Nishioka, *J. Pharm. Pharmacol.*, **42**, 712 (1990).
11) T. Yokozawa, P. D. Zheng, H. Oura, and F. Koizumi, *Nephron*, **44**, 230 (1986).
12) T. Yokozawa, H. Y. Chung, and H. Oura, *Jpn. J. Nephrol.*, **29**, 1129 (1987).
13) T. Yokozawa and H. Oura, *Jpn. J. Nephrol.*, **29**, 1137 (1987).
14) T. Yokozawa, H. Oura, and T. Nakada, *Jpn. J. Nephrol.*, **29**, 1145 (1987).
15) T. Koeda, K. Wakaki, F. Koizumi, T. Yokozawa, and H. Oura, *Jpn. J. Nephrol.*, **30**, 239 (1988).
16) T. Yokozawa, Z. L. Mo, and H. Oura, *Nephron*, **51**, 388 (1989).
17) T. Yokozawa, N. Fujitsuka, and H. Oura, *Nephron*, **52**, 347 (1989).
18) T. Yokozawa, N. Fujitsuka, and H. Oura, *Nephron*, **56**, 249 (1990).
19) C. Brun, *J. Lab. Clin. Med.*, **35**, 152 (1950).
20) C. Brun, *J. Lab. Clin. Med.*, **37**, 955 (1952).
21) S. Ohki, T. Hanyu, K. Imaki, N. Nakazawa, and F. Hirata, *Prostaglandins*, **6**, 137 (1974).
22) J. Maclouf, M. Pradel, P. Pradelles, and F. Dray, *Biochim. Biophys. Acta*, **431**, 139 (1976).
23) E. Amundsen, J. Putter, P. Friberger, M. Knos, M. Larsbraten, and G. Claeson, *Adv. Exp. Med. Biol.*, **120A**, 83 (1979).
24) Y. Kasahara and Y. Ashihara, *Clin. Chem.*, **27**, 1922 (1981).
25) J. M. Pfeffer, M. A. Pfeffer, and E. D. Frohlich, *J. Lab. Clin. Med.*,

78, 957 (1971).
26) J. C. McGiff, N. A. Terragno, K. U. Malik, and A. J. Lonigro, *Circ. Res.*, **31**, 36 (1972).
27) H. R. Keiser, M. J. Andrews, R. A. Guyton, H. S. Margolius, and J. J. Pisano, *Proc. Soc. Exp. Biol. Med.*, **151**, 53 (1976).
28) J. A. Mitas, S. B. Levy, R. Holle, R. P. Frigon, and R. A. Stone, *N. Engl. J. Med.*, **299**, 162 (1978).
29) O. B. Holland, J. M. Chud, and H. Braunstein, *J. Clin. Invest.*, **65**, 347 (1980).
30) L. A. Arbeit and S. R. Serra, *Kidney Int.*, **28**, 440 (1985).
31) A. Nasjletti, J. C. McGiff, and J. Colina-Chourio, *Circ. Res.*, **43**, 799 (1978).
32) J. C. Frölich, T. W. Wilson, B. J. Sweetman, M. Smigel, A. S. Nies, K. Carr, J. T. Watson, and J. A. Oates, *J. Clin. Invest.*, **55**, 763 (1975).
33) J. M. Vinci, D. Horwitz, R. M. Zusman, J. J. Pisano, K. J. Catt, and H. R. Keiser, *Hypertension*, **1**, 416 (1979).
34) H. S. Margolius, J. Chao, and T. Kaizu, *Clin. Sci. Mol. Med.*, **51** (suppl. 3), 279s (1976).
35) E. S. Marks, R. F. Bing, H. Thurston, and J. D. Swales, *Clin. Sci.*, **58**, 1 (1980).
36) J. Colina-Chourio, J. C. McGiff, M. P. Miller, and A. Nasjletti, *Br. J. Pharmacol.*, **58**, 165 (1976).
37) R. K. Mayfield and H. S. Margolius, *Am. J. Nephrol.*, **3**, 145 (1983).
38) J. C. McGiff, K. Crowshaw, N. A. Terragno, and A. J. Lonigro, *Circ. Res.*, **26—27** (suppl. 1), I-121 (1970).
39) M. C. Blasingham and A. Nasjletti, *Am. J. Physiol.*, **237**, F182 (1979).
40) M. L. Kauker, *J. Pharmacol. Exp. Ther.*, **214**, 119 (1980).
41) A. G. Scicli, R. Gandolfi, and O. A. Carretero, *Am. J. Physiol.*, **234**, F36 (1978).
42) N. Farman, P. Pradelles, and J. P. Bonvalet, *Am. J. Physiol.*, **251**, F238 (1986).

Inhibitory Effect of Glutathione on the Generation of Hydroxyl Radicals in the Reaction System of Glutathione–Alloxan

Koichi SAKURAI* and Taketo OGISO

Hokkaido Institute of Pharmaceutical Sciences, 7–1 Katsuraoka-cho, Otaru 047–02, Japan. *Received August 13, 1990*

Deoxyribose (DOR) degradation, an indicator of hydroxyl radical (OH·) generation, was observed in the reaction system of glutathione (GSH)–alloxan in the presence of Fe^{3+}-ethylenediaminetetraacetic acid (EDTA). GSH had a biphasic action on the DOR degradation, *i.e.* GSH at low concentrations caused marked activation and at high concentrations had an inhibitory effect. GSH at high concentrations had an ability to scavenge OH· in the hypoxanthine–xanthine oxidase in the presence of Fe^{3+}-EDTA and to inhibit the oxygen consumption and the generation of the alloxan radical (AH·) and superoxide anion radical in the GSH–alloxan system. At GSH : alloxan ratio of 10 : 1 led to an immediate formation of dialuric acid. The autoxidation of dialuric acid was suppressed by GSH in a concentration-dependent fashion. These results indicate that autoxidation of dialuric acid is strongly suppressed by excess GSH in the alloxan–dialuric acid redox cycle, resulting in the decrease of AH· generation and oxygen consumption. On the other hand, the reduction of Fe^{3+}-EDTA to Fe^{2+}-EDTA by dialuric acid and AH· was scarcely inhibited by any concentrations of GSH. These results indicate that adding an excess of GSH suppresses the generation of OH· in the GSH–alloxan system through the inhibition of the redox cycling reaction between alloxan and dialuric acid independently on the reduction of Fe^{3+}-EDTA to Fe^{2+}-EDTA.

Keywords glutathione: alloxan; alloxan radical; dialuric acid; hydroxyl radical; iron reduction; redox-cycle

Alloxan shows a selective cytotoxicity on pancreatic β-cells and thus causes insulin-dependent diabetes.[1] The mechanism of action is not clearly understood, but since its actions are inhibited by superoxide dismutase (SOD), catalase and chemical scavengers of hydroxyl radicals (OH·), such as demethylurea, it has been suggested that the cytotoxic action of alloxan is initiated by OH· generated in a cyclic reaction involving alloxan and its reduction product, dialuric acid.[2-5]

In our previous works with a reaction system of glutathione (GSH)–alloxan in the presence of Fe^{3+}-ethylenediaminetetraacetic acid (EDTA), we demonstrated that OH· was generated by alloxan radicals (AH·) through a Fenton-type reaction.[6] Furthermore, we clearly demonstrated by electron spin resonance (ESR) spectrometry that the generation of AH· was enhanced depending on the concentrations of GSH in the reaction system, suggesting a possible participation of GSH in one electron reduction of alloxan.[6] However, the biphasic actions of GSH on the OH· generation in alloxan cytotoxicity have not been clearly elucidated yet.

During the course of our studies, we observed that an addition of GSH at a high concentration to the reaction system caused a marked inhibition of both the generation of AH· and OH·. These results indicate that GSH has either harmful or beneficial action depending on the concentration of GSH. The present work was undertaken to clarify the mechanism by which GSH inhibits the generation of OH· and protects against alloxan-induced diabetes.

Experimental

Materials Alloxan, GSH, 2-deoxy-D-ribose (DOR), hypoxanthine, mannitol and benzonate were purchased from Wako Pure Chemical Industries Ltd., Japan. SOD (from bovine erythrocytes), catalase (from bovine liver, thymol free), and lactoperoxidase (from bovine milk) were from Sigma Co., St. Louis, 5,5'-dimethyl-1-pyrroline-*N*-oxide (DMPO) was from Labotec Co., Japan, methylthiourea and dimethylthiourea were from Aldrich Chemical Co. and dialuric acid was from Tokyo Kasei Kogyo Co., Japan. Concentrations of the last compound were calculated from the absorption at 273 nm, based on a coefficient of $16000\,M^{-1}\cdot cm^{-1}$.[7] Xanthine oxidase was obtained from Biozyme, Great Britain, and its activity was assayed at 25 °C by measuring the absorption of uric acid at 293 nm. One unit of activity was defined as 1.0 μmol of xanthine converted to uric acid per min at pH 7.5. Other chemicals used in this experiment were of analytical grade from commercial suppliers.

DOR Degradation Thiobarbituric acid (TBA)-reactive oxidation products of DOR were determined according to the method of Halliwell *et al.* with a minor modification.[8] DOR (2.0 mM) was incubated in 3.0 ml of 10 mM phosphate buffer, pH 7.4, containing 1.0 mM alloxan, 50 μM Fe^{3+}-EDTA, 0.15 M NaCl and various concentrations of GSH. The degradation of DOR was terminated after incubation for 10 min at 37 °C by mixing with 0.03 ml of 30% trichloroacetic acid and then 0.5 ml of 0.6% TBA was added. The solution was heated for 10 min at 100 °C and cooled. The absorbance at 532 nm was measured with a spectrophotometer (Hitachi model U-2000).

ESR Measurements ESR measurements were made at room temperature with a JEOL model JES-RE1X. Samples were mixed outside of the cavity, then rapidly aspirated into the aqueous flat cell for ESR measurements. Spectrometer settings for DMPO/OH·adduct were 3365 G magnetic field, 8.0 mW microwave power, 9.455 GHz modulation frequency, 1.6 G field modulation width, 0.3 s time constant, 1000 gain and 25.0 G/min scan rate. The relative signal intensity of the DMPO/OH·adduct was evaluated by the peak height of the second signal of the quarted of DMPO/OH·. The *g*-value was measured using Mn^{2+} as a marker. Spectrometer settings for HA· were 3365 G magnetic field, 5.0 mW microwave power, 9.450 G Hz modulation frequency, 0.20 G field modulation width, 0.3 s time constant, 790 gain and 2.5 G/min scan rate. The peak height was determined by measuring at the center hyperfine line of the ESR spectrum of HA·.

Detection of Superoxide Anion Radical Production The superoxide anion radical (O_2^-) was detected by the production of compound III from lactoperoxidase.[9] Lactoperoxidase (10 μM) was incubated in 10 mM phosphate buffer, pH 7.4 containing 1.0 mM alloxan, 0.15 M NaCl and various concentrations of GSH. To avoid any effect of H_2O_2, catalase (420 U/ml) was added to all the reaction mixtures. The reaction was initiated by the addition of alloxan at 37 °C and continuously monitored at 588 nm.

Oxygen Consumption Oxygen consumption was measured polarographically at 37 °C with a Clark-type oxygen electrode (Yanaco model PO-100A). The reaction mixture consisted of 1.0 mM alloxan and various concentrations of GSH in 0.6 ml of 10 mM phosphate buffer, pH 7.4, containing 0.15 M NaCl.

Reduction of Fe^{3+}-EDTA Reaction mixtures consisted of 1.0 mM dialuric acid, 50 μM Fe^{3+}-EDTA, 1.0 mM bathophenanthroline sulfate, 0.15 M NaCl, various concentrations of GSH and 420 U/ml catalase. The reaction was initiated by the addition of dialuric acid at 37 °C and

continuously monitored at 534 nm. The amount of reduced iron was calculated from the increase in the absorption, based on a coefficient of 22140 $M^{-1} \cdot cm^{-1}$.[10] All data were corrected for by subtracting the value obtained in the blank that lacked dialuric acid.

Results

DOR Degradation in the GSH–Alloxan System Figure 1 shows the effect of GSH on DOR degradation, one of the indications of OH· generation, in the GSH–alloxan system in the presence of Fe^{3+}-EDTA. DOR degradation in response to GSH revealed a biphasic profile, *i.e.*, the addition of GSH up to 2.0 mM caused marked stimulation and increasing GSH beyond 2.0 mM had an inhibitory effect on DOR degradation. The maximum degradation of DOR was found to occur at a ratio of GSH to alloxan (2:1). These results suggest that GSH above 2.0 mM could inhibit OH· generation and/or directly scavenge OH· generated in the reaction system.

Action of GSH as Scavenger of OH· in the Hypoxanthine–Xanthine Oxidase System As the ESR signal due to the DMPO/OH· adduct could not be detected in the GSH–alloxan system, we attempted to detect it in the hypoxanthine–xanthine oxidase system in the presence of Fe^{3+}-EDTA. The ESR spectra obtained by aerobic incubation in the presence or absence of GSH are shown in Fig. 2(A). These resultant spectra obtained here agreed with that of the DMPO/OH· adduct reported by other workers. (hyperfine coupling constant: $A_N = A_H = 14.8$ G).[11,12] Omission of Fe^{3+}-EDTA from the reaction system resulted in a great decrease in the formation of the DMPO/OH· adduct. No ESR signals were observed in the absence of hypoxanthine or xanthine oxidase in the reaction system. As can be seen in Fig. 2(B), the signal intensity of the DMPO/OH· adduct decreased with the addition of GSH beyond a concentration of 2.0 mM, indicating that GSH can scavenge OH·. From these results, we presume that GSH above 2.0 mM acts as a scavenger of OH·, resulting in the inhibition of DOR degradation in the GSH–alloxan system (Fig. 1).

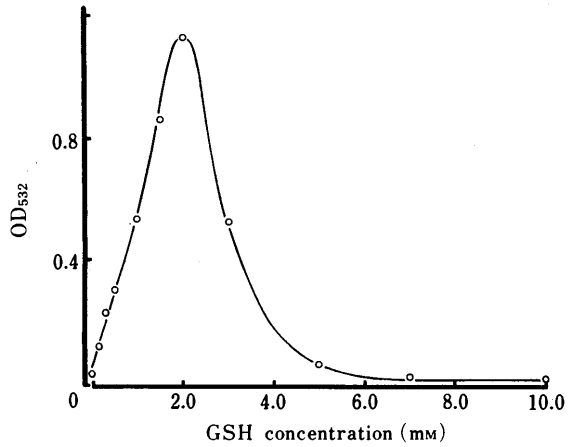

Fig. 1. Effect of GSH on the Degradation of DOR in the GSH–Alloxan System in the Presence of Fe^{3+}-EDTA

The reaction mixtures consisted of 1.0 mM alloxan, 2.0 mM DOR, 50 μM Fe^{3+}-EDTA, 0.15 M NaCl and various concentrations of GSH in 10.0 mM phosphate buffer, pH 7.4. Other conditions were described in Experimental. Each point represents the mean of triplicate experiments.

Generation of Alloxan Radicals The effect of varying concentrations of GSH on the generation of AH· in the GSH–alloxan system in the presence or absence of Fe^{3+}-EDTA was studied by ESR. The observed signal of AH· (hyperfine coupling constant: $A_N = A_H = 0.45$ G) was similar to that reported in the previous paper.[6] As shown in Fig. 3, the addition of GSH above 2.0 mM to the reaction system resulted in a marked decrease in the signal intensity of AH· in the presence or absence of Fe^{3+}-EDTA. In contrast, GSH below 2.0 mM caused an increase in the signal intensity of AH·. The signal intensity of AH· obtained in the presence of Fe^{3+}-EDTA was lower than that in the absence of Fe^{3+}-EDTA indicating that AH· directly reduced Fe^{3+}-EDTA as reported in the previous paper.[6] Next, we examined whether the generation of AH· is inhibited by SOD, catalase and several scavengers of OH·. As shown in Table I, none of them has any significant effect on the signal intensity of AH· in the presence or absence of Fe^{3+}-EDTA. These results indicate that AH· generation in the GSH–alloxan system is inhibited only at high concentrations of GSH but not by SOD, catalase and OH· scavengers.

Oxygen Consumption and O_2^- Generation As shown in Fig. 4, either oxygen consumption or O_2^- generation was rapidly initiated by the addition of GSH up to 2.0 mM to the reaction system in the absence of Fe^{3+} -EDTA. However, increasing the concentration of GSH up to 10.0 mM caused a marked decrease in the rate of oxygen consumption or O_2^- generation. No significant oxygen uptake and O_2^- generation were observed in the system of

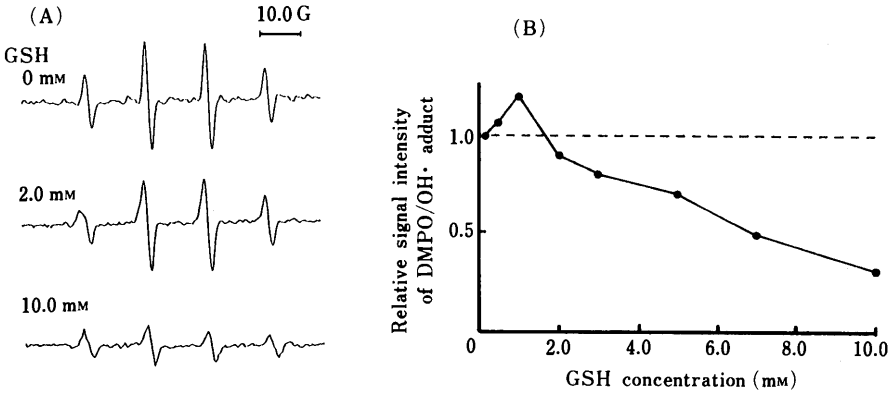

Fig. 2. Effect of GSH on the Generation of the DMPO/OH· Adduct in Hypoxanthine–Xanthine Oxidase in the Presence of Fe^{3+}-EDTA

The reaction mixtures contained 0.1 mM hypoxanthine, 0.025 U/ml xanthine oxidase, 0.15 M NaCl, 50 μM Fe^{3+}-EDTA, 0.2 M DMPO and various concentrations of GSH in 10.0 mM phosphate buffer, pH 7.4. Other conditions were described in Experimental. Each point indicates the mean of triplicate experiments.

alloxan alone. These results indicate that GSH beyond 2.0 mM acts not only as a scavenger of OH· but inhibits oxygen consumption and the generation of AH· and O_2^-.

Reduction of Alloxan to Dialuric Acid We next examined for the reduction of alloxan to dialuric acid in the GSH–alloxan system in the absence of Fe^{3+}-EDTA. As shown in Fig. 5 (A), the addition of GSH at a molar ratio of GSH to alloxan (10 : 1) led to an immediate increase in absorption at 273 nm, characteristic of dialuric acid as reported by other workers.[7] The intensity of the peak at 273 nm obtained here corresponded to about 65% reduction of alloxan to dialuric acid. These spectra chaged with time to an increase in absorption at 305 nm, which has been identified as due to formation of a GSH–alloxan adduct (compound 305), although the structure has not been determined.[14] The rate of dialuric acid formation appears to be faster than that of compound 305. As shown in Fig. 5 (B), the formation of both dialuric acid and compound 305 during incubation for 10 min progressively increased with increasing the concentrations of GSH. The reduction of alloxan to dialuric acid was scarcely observed in the absence of GSH.

Autoxidation of Dialuric Acid and Generation of Alloxan Radicals As shown in Fig. 6 (A), dialuric acid was oxidized rapidly in the absence of GSH. The autoxidation of dialuric acid was scarcely observed under anaerobic conditions. The increasing concentrations of GSH led to an inhibition of the autoxidation of dialuric acid. In the absence of GSH as shown in Fig. 6 (B), the addition of 1.0 mM dialuric acid to the reaction medium caused both rapid oxygen consumption and generation of AH·. O_2^- was also generated under the experimental conditions used (data not shown). With increasing concentrations of GSH, the oxygen consumption and generation of AH· were suppressed, reaching an extent of inhibition of about 70% and 85%, respectively, at a ratio of GSH to dialuric acid (10 : 1). These results indicate that the autoxidation of dialuric acid was strongly inhibited by excess GSH, resulting in the decrease of AH· generation

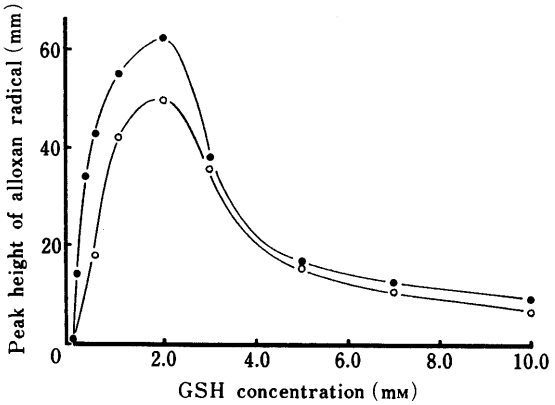

Fig. 3. Effect of GSH on Generation of Alloxan Radical

The reaction mixtures contained 1.0 mM alloxan, 0.15 M NaCl and various concentrations of GSH in the presence (○) or absence (●) of 50 μM Fe^{3+}-EDTA in 10.0 mM phosphate buffer, pH 7.4. Experimental conditions were described in Experimental. Each point represents the mean of triplicate experiments.

TABLE I. Effect of Oxygen Radical Scavengers on Generation of Alloxan Radical

Conditions	Peak height of alloxan radical (mm)			
	−EDTA-Fe^{3+}	Percent	+EDTA-Fe^{3+}	Percent
Alloxan system	73.0±4.4 (4)	100	61.6±3.0 (4)	100
+500 U/ml SOD	71.1±3.7 (3)	97	57.7±4.2 (3)	94
+500 U/ml catalase	73.1±4.1 (3)	100	60.4±5.5 (3)	98
+10 mM mannitol	69.8±5.9 (3)	96	63.7±3.3 (3)	103
+10 mM benzonate	73.0±6.0 (3)	100	60.0±6.3 (3)	97
+10 mM methylthiourea	70.7±5.7 (3)	97	57.7±6.5 (3)	94
+10 mM dimethylthiourea	68.0±4.2 (4)	93	61.7±2.2 (4)	100

The alloxan system consisted of 1.0 mM alloxan, 2.0 mM GSH and 0.15 M NaCl in the presence or absence of 50 μM Fe^{3+}-EDTA in 10 mM phosphate buffer, pH 7.4. Each value represents the mean±S.E. Numbers of experiments are given in parentheses.

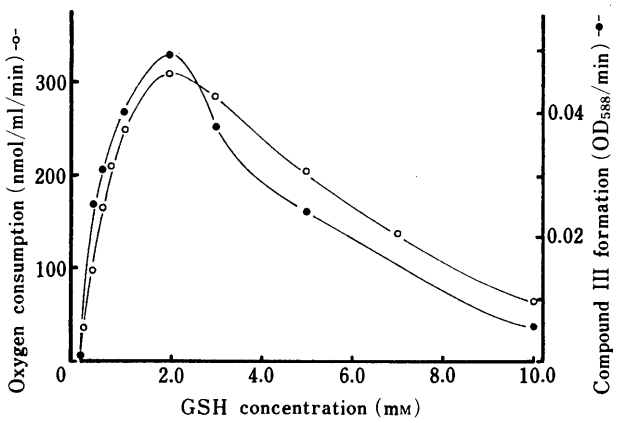

Fig. 4. Effect of GSH on Oxygen Consumption and Generation of O_2^- in Alloxan System

The reaction mixtures contained 1.0 mM alloxan, 0.15 M NaCl and various concentrations of GSH in 10.0 mM phosphate buffer, pH 7.4. Other conditions were described in Experimental. Each point represents the mean of triplicate experiments.

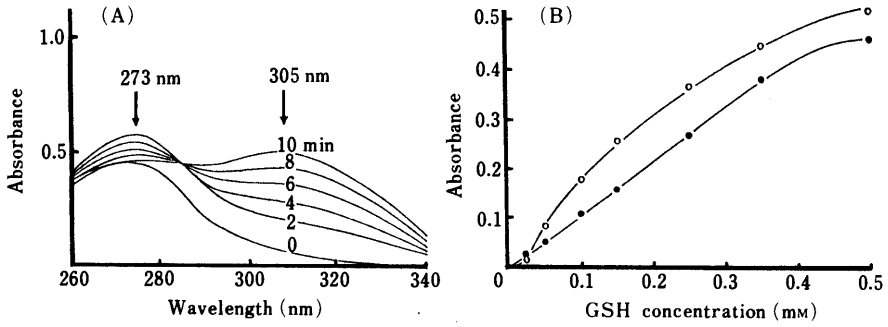

Fig. 5. Changes in the Spectrum of Alloxan in the Reaction with GSH

(A) The reaction mixtures contained 50 μM alloxan, 0.5 mM GSH and 0.15 M NaCl in 10.0 mM phosphate buffer, pH 7.4. The spectra between 260 and 340 nm were recorded at 2 min interval for 10 min starting immediately after addition of alloxan to the reaction medium at 37°C. (B) The experimental conditions were the same as given in (A), except for varying the concentration of GSH. The increases in the absorbance at 273 (●) and 305 (○) nm were plotted at 10 min after the addition of alloxan. Each point represents the mean of 3 to 4 experiments.

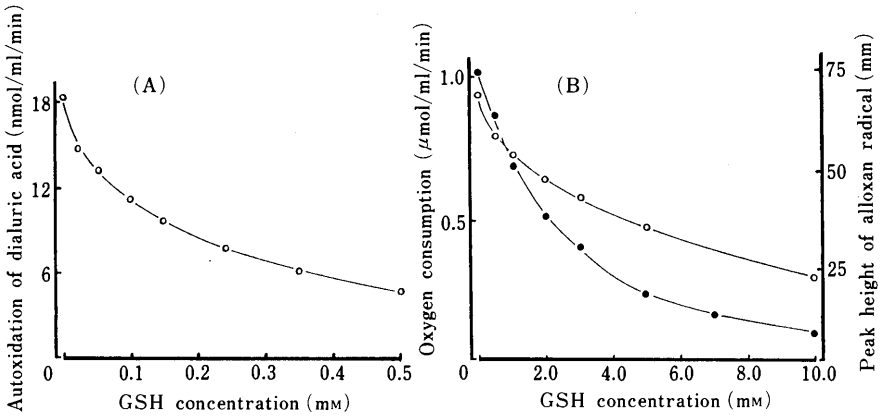

Fig. 6. Effect of GSH on Autoxidation of Dialuric Acid, Oxygen Consumption and Generation of Alloxan Radical

(A) The autoxidation of dialuric acid was recorded by following changes in absorbance at 273 nm. The reaction mixtures consisted of 50 μM dialuric acid, 0.15 M NaCl and various concentrations of GSH in 10.0 mM phosphate buffer, pH 7.4. (B) The reaction mixtures contained 1.0 mM dialuric acid, 0.15 M NaCl and various concentrations of GSH in 10.0 mM phosphate buffer, pH 7.4. Other conditions were the same as described in Experimental. Each point represents the mean of triplicate experiments.

TABLE II. Effect of GSH on Reduction of Fe^{3+}-EDTA by Dialuric Acid

Ratios of GSH to dialuric acid	Autoxidation of dialuric acid[a] (nmol/ml/min)	Inhibition (%)	Reduction of Fe^{3+}-EDTA[b] (nmol/ml/min)	Inhibition (%)
0:1	27.0±1.5	—	44.4±1.6	—
0.5:1	21.8±0.8	19	44.5±2.6	0
2:1	19.9±0.6	26	44.9±3.8	−1[c]
5:1	11.8±1.3	56	42.8±5.1	4
10:1	9.3±0.4	66	42.3±3.4	5

a) The autoxidation of dialuric acid (50 μM) was recorded by following the change in absorbance at 273 nm in the presence of various ratios of GSH to dialuric acid. The reaction mixtures were the same as described in the caption in Fig. 6, except in the presence of 2.5 μM Fe^{3+}-EDTA. *b*) The reduction of Fe^{3+}-EDTA was determined as described in Experimental. The reaction mixtures contained 1.0 mM dialuric acid, 1.0 mM bathophenanthroline sulfonate, 50 μM Fe^{3+}-EDTA, 0.15 M NaCl and varying concentrations of GSH in 10 mM phosphate buffer, pH 7.4. Each point represents the mean±S.E. of triplicate experiments. *c*) Activation of Fe^{3+}-EDTA reduction.

and oxygen consumption.

Reduction of Fe^{3+}-EDTA by Dialuric Acid As shown in Table II, dialuric acid was oxidized more rapidly in the presence of Fe^{3+}-EDTA (27 nmol/ml/min) than in the absence of Fe^{3+}-EDTA (18 nmol/ml/min). The addition of GSH at various ratios to dialuric acid resulted in an inhibition of the autoxidation of dialuric acid, reaching about 66% inhibition at a ratio of (10:1). On the other hand, Fe^{3+}-EDTA was rapidly reduced by the addition of dialuric acid but the reduction rate of Fe^{3+}-EDTA was scarcely affected by GSH. Under anaerobic conditions, the reduction rate of Fe^{3+}-EDTA was about 46 nmol/ml/min which was almost identical with that obtained under aerobic conditions. These results suggest that Fe^{3+}-EDTA is mainly reduced by dialuric acid independently in the concentrations of GSH.

Discussion

The diabetogenic action of alloxan is through to involve redox cycling between alloxan and dialuric acid, resulting in the generation of oxygen radicals which damage the insulin producing β-cells of the pancreas.[2,3,15] We reported previously that OH· was generated by the reaction of alloxan with low concentrations of GSH through the Fenton-reaction in which ferric iron is reduced by AH·.[6] In contrast, the present study demonstrated that the generation of OH· was strongly inhibited by GSH at high concentrations. Other workers have demonstrated that GSH at higher concentrations has an ability to scavenge OH· and that GSH at physiological concentrations could themselves produce OH· in the reaction system of hypoxanthine–xanthine oxidase in the presence of iron salts.[16] In accordance with their reports, the results obtained here by ESR methods also showed that GSH beyond 2.0 mM could scavenge OH·, while GSH slightly stimulated the formation of OH· at lower concentrations of GSH (Fig. 2). The reaction of GSH with OH· or O_2^- has been known to produce thiyl radicals (GS·) which are less reactive than OH· and the reaction of GSH with O_2^- is reported to be slow.[17] Further, the thiyl radicals were known to be converted to GSH disulfide (GSSG) by subsequent dimerization.[17]

$$GSH + OH\cdot \rightarrow GS\cdot + H_2O \quad (1)$$

$$GS\cdot + GS\cdot \rightarrow GSSG \quad (2)$$

Therefore, the inhibitory action of GSH observed in the degradation of DOR (Fig. 1), might be explained, in part at least, by the direct capability of GSH to scavenge OH·. As previously reported, however, GSH could reduce alloxan by one electron reduction to AH·, which mediated the OH· production through the reduction of chelated iron with a low redox potential such as Fe^{3+}-EDTA.[6] The results presented here show that GSH at high concentrations inhibited the AH· generation independently in the production of O_2^-, H_2O_2 and OH· (Fig. 3, Table I), and suggest that a more complex mechanism may be involved in the inhibitory action of GSH on DOR degradation.

When exposed to reducing substances (*e.g.* ascorbic acid) and oxygen, alloxan and dialuric acid have been

proposed to form a redox cycle in which O_2^- is generated during the autoxidation of dialuric acid.[15,18] The fact that oxygen consumption and O_2^- generation were practically inhibited by GSH at concentrations higher than 2.0 mM (Fig. 4) suggest that excess GHS may suppress oxygen uptake and O_2^- generation through the inhibition of the redox cycle between alloxan and dialuric acid. In accordance with an earlier report,[19] alloxan was reduced to dialuric acid dependently on the molar ratios of GSH to alloxan, accompanied with a concomitant formation of the compound characterized by an absorption at 305 nm (Fig. 5A). Since we reported that AH· were generated in the GSH–alloxan system,[6] the reaction of alloxan with GSH would be presented as follows; (A, alloxan: AH·, alloxan radicals: AH_2, dialuric acid)

$$A + GSH \rightarrow AH\cdot + GS\cdot \quad (3)$$

$$AH\cdot + GSH \rightarrow AH_2 + GS\cdot \quad (4)$$

$$A + GSH \rightarrow \text{compound 305} \quad (5)$$

The thiyl radicals formed (reaction 3, 4) are dimerizated to GSSG by the reaction 2.[17] The reaction of alloxan with GSH to form compound 305 (reaction 5) seems to be irreversible and slower than the reaction of 3 and 4. At a high ratio of GSH to alloxan, alloxan was rapidly reduced to dialuric acid and the formation of compound 305 increased with increasing concentrations of GSH (Fig. 5). Under these conditions, a total concentration of alloxan in the reaction system decreases, resulting in the increase in the relative concentration of dialuric acid, thereby, the reaction of redox cycling to generate AH· and O_2^- is almost inhibited. The reaction of redox cycling has been reported to require the autoxidation of dialuric acid.[19] The spectral changes of dialuric acid presented here showed that the autoxidation of dialuric acid was inhibited by GSH in the presence or absence of Fe^{3+}-EDTA in a concentration-dependent fashion (Fig. 6A and Table II). Moreover, the fact that the consumption of O_2 and the generation of AH· due to the autoxidation of dialuric acid were suppressed with increasing the concentration of GSH (Fig. 6B) provides evidence for the role of GSH to inhibit the redox cycling between dialuric acid and alloxan, and to inhibit the generation of OH· in the reaction system of GSH–alloxan. OH· has been reported to be generated during the autoxidation of dialuric acid only in the presence of Fe^{3+}-EDTA, suggesting that the formation of OH· was mediated through the reduction of Fe^{3+}-EDTA by dialuric acid and alloxan radicals.[6,20]

$$Fe^{3+}\text{-EDTA} + AH_2 \rightarrow Fe^{2+}\text{-EDTA} + AH\cdot + H^+ \quad (6)$$

$$Fe^{3+}\text{-EDTA} + AH\cdot \rightarrow Fe^{2+}\text{-EDTA} + A + H^+ \quad (7)$$

$$Fe^{2+}\text{-EDTA} + H_2O_2 \rightarrow Fe^{3+}\text{-EDTA} + OH\cdot + OH^- \quad (8)$$

The results presented here show that GSH at high concentrations inhibited the autoxidation of dialuric acid, generation of AH· and oxygen consumption, whereas the reduction of Fe^{3+}-EDTA was scarcely affected by GSH (Fig. 6 and Table II). These results indicate that GSH in excess suppresses the generation of OH· through the inhibition of the redox cycling reaction between alloxan and dialuric acid independently on the reduction of Fe^{3+}-EDTA to Fe^{2+}-EDTA.

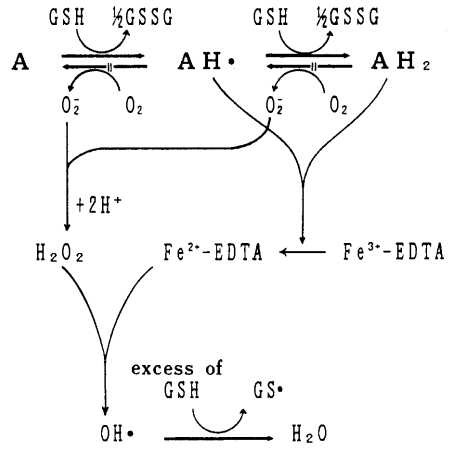

Chart 1. Proposed Mechanism for Effect of GSH on Generation of OH· in the Alloxan–Dialuric Acid Redox Cycle in the Presence of Fe^{3+}-EDTA
‖, site of inhibition by GSH at high concentrations.

At low concentrations of GSH, OH· must be continuously generated by the regeneration of AH· by redox cycling *via* the Fenton-reaction as previously reported.[6] The non-enzymatic formation of compound 305 possibly participates in the protective effect of GSH on cytotoxicity of alloxan *in vitro*. Therefore, the exact significance of this compound in physiological conditions must be clarified by further studies. Based on the present results and a previous report,[6] the biphasic action of GSH on the generation of OH· is proposed to occur as illustrated in Chart 1.

The injection of GSH has been reported to protect from the diabetogenic action of alloxan in rat.[21] On the other hand, treatments which lower GSH levels, such as fasting, ascorbic acid injection and a lower protein diet, have been reported to increase the susceptibility of animal to alloxan diabetes.[22] In rat islets, alloxan decreased the GSH content (34% decrease) and GSH/GSSG ratio (42% decrease).[23] Other workers have demonstrated that glucose increases the GSH levels in about 63% of isolated rat islets paralleled with a concomitant increase of the NADPH/NADP ratio.[24,25] These results suggest that glucose protects the islets from alloxan toxicity through the action of GSH, which are regenerated *via* the pentose phosphate pathway. Actually, the presence of glucose during incubation with alloxan prevents the cell from oxidative damages.[26] In view of these facts, the ability of GSH at high concentrations to scavenge OH· or to prevent the redox cycling between alloxan and dialuric acid may also explain why pretreatment with GSH can protect against alloxan diabetes in rats.

References

1) I. Lundquist and C. Rerup, *Eur. J. Pharmacol.*, **2**, 35 (1967).
2) L. J. Fischer and S. A. Hamburger, *Diabetes*, **29**, 231 (1980).
3) L. J. Fischer and S. A. Hamburger, *Life Sci.*, **26**, 1405 (1980).
4) K. Grankvist, S. Marklund and I. B. Täljedal, *Nature* (London), **294**, 158 (1981).
5) K. Sakurai, T. Miura and T. Ogiso, *Yakugaku Zasshi*, **106**, 1034 (1986).
6) K. Sakurai, T. Miura and T. Ogiso, *Chem. Pharm. Bull.*, **38**, 993 (1990).
7) J. J. Van Hemmen and W. J. A. Meuling, *Arch. Biochem. Biophys.*, **184**, 743 (1977).
8) B. Halliwell and J. M. C. Gutteridge, *FEBS Lett.*, **128**, 347 (1981).
9) I. Yamazaki and L. H. Piette, *Biochim. Biophys. Acta*, **77**, 115 (1963).

10) P. Cater, *Analyt. Biochem.*, **40**, 450 (1971).
11) C. M. Mansbach, G. M. Rosen, C. A. Rahn and K. E. Strauss, *Biochim. Biophys. Acta*, **888**, 1 (1986).
12) K. Sakurai and T. Ogiso, *Yakugaku Zasshi*, **109**, 102 (1989).
13) C. Langercrantz and M. Yhland, *Acta Chem. Scand.*, **17**, 1677 (1963).
14) W. W. Kay and K. C. Murfitt, *Biochem. J.*, **74**, 203 (1960).
15) G. Cohen and R. E. Heikkila, *J. Biol. Chem.*, **249**, 2447 (1974).
16) D. A. Rowley and B. Halliwell, *FEBS Lett.*, **138**, 33 (1982).
17) H. Wefers and H. Sies, *Eur. J. Biochem.*, **38**, 271 (1989).
18) D. W. Deamer, R. E. Heikkila, R. V. Panganamala, G. Cohen and D. G. Cornwell, *Physiol. Chem. Phys.*, **3**, 426 (1971).
19) C. C. Winterbourn and R. Munday, *Biochem. Pharm.*, **38**, 271 (1989).
20) R. Munday, *Biochem. Pharm.*, **37**, 409 (1988).
21) A. Razarow, *Proc. Soc. Exp. Biol. Med.*, **61**, 441 (1946).
22) C. C. Rerup, *Pharmacol. Rev.*, **22**, 485 (1970).
23) W. J. Malaisse, F. Malaisse-Lagae, A. Sener and D. G. Pipeleers, *Proc. Natl. Acad. Sci. U.S.A.*, **79**, 927 (1982).
24) H. P. T. Ammon, A. Gimm, D. Wagner-Tescher, E. J. Versorhl and M. Händel, *Diabetes*, **27** (suppl. 2), 142 (1978).
25) H. P. T. Ammon, A. Gimm, S. Lütz, D. Wagner-Tescher, E. J. Versorhl, M. Händel and I. Hagenlon, *Diabetes*, **29**, 803 (1980).
26) D. C. Weaver, M. L. McDaniel, S. P. Naber, D. Barry and P. E. Lacy, *Diabetes*, **27**, 1205 (1978).

Phospholipase D Modified with a Polyethylene Glycol Derivative

Haruyoshi MATSUYAMA, Ryo TAGUCHI and Hiroh IKEZAWA*

Faculty of Pharmaceutical Sciences, Nagoya City University, 3–1 Tanabe-dori, Mizuho-ku, Nagoya, Aichi 467, Japan. *Received August 16, 1990*

Phospholipase D from *Streptomyces* sp. AA586, PLDP, was modified with methoxypolyethylene glycol succinimidylsuccinate (ss-PEG), an active derivative of polyethylene glycol. By titration with trinitrobenzene sulfonate (TNBS), approximately 70% of the free amino groups in the enzyme protein were shown to be modified by treatment with ss-PEG. By this modification, the molecular weight of the enzyme was increased, judging from the results of sodium dodecyl sulfate-polyacrylamide gel electrophoresis, gel filtration with Toyopearl HW-55F and TNBS titration. Due to the loss of cationic charges, the enzyme protein became eluted faster in high performance liquid chromatography with CM-Toyopearl. By modification with ss-PEG, the enzyme became fairly thermostable, while pH-stability and optimal pH were not influenced. The value of K_m for phosphatidylcholine of the hydrolytic reaction increased 2-fold, whereas that of the transphosphatidyl reaction was not significantly altered.

Keywords phospholipase D; *Streptomyces*; chemical modification; polyethylene glycol modified protein

Phospholipase D (PLDP, phosphatidylcholine phosphatidohydrolase EC. 3.1.4.4) has been found in *Streptomyces*[1] as well as cabbage leaves[2] and peanuts.[3] Like plant enzymes, *Streptomyces* PLDP catalyzes not only hydrolysis of phosphatides into phosphatidic acid and component alcohols,[1] but also transphosphatidylation between alcohols.[4]

PLDP-catalyzed transphosphatidylation especially contributes to the *in vitro* enzymatic synthesis of new phosphatides such as phosphatidylnucleosides which cannot be found in natural products.[5] Also, enzymatic transphosphatidylation has been shown to proceed more effectively in organic solvents such as chloroform, benzene and ethyl acetate than in an aqueous medium.[1,6]

In the present study, PLDP from a strain of *Streptomyces* was modified by conjugation with methoxypolyethylene glycol succinimidylsuccinate (ss-PEG), which combines with free lysyl and N-terminal amino groups under neutral, mild conditions.

Generally, polyethylene glycol (PEG) has been known as an amphiphilic polymer, and those proteins or enzymes which are conjugated with PEG derivatives, reduce their antigenicity and prolong their half-lives when administered intravenously into animals.[7-12] Furthermore, PEG-modified enzymes become soluble in several organic solvents, retaining their catalytic activities even in these media and synthesizing hydrophobic compounds as the products in the reverse reaction of hydrolysis.[13] Also, in some cases, PEG-modified enzymes become more stable than native ones in an alkaline medium or upon heat treatment.[14] Thus in the present work, the properties of PEG-modified PLDP including pH and heat stabilities as well as catalytic parameters were investigated.

Materials and Methods

Materials A PLDP preparation from *Streptomyces* sp. AA586, PLDP, and a choline oxidase preparation from *Achromobacter globiformis* were kind gifts from Toyo Jozo Co., Ltd. The purity of PLDP preparation is 30 to 40%. Horseradish peroxidase, ss-PEG (Mw=5000) and 4-aminoantipyrine (4-AAP), were purchased from Sigma Chemical Co. All other chemicals used were of the purest commercial grade available.

Modification of PLDP with ss-PEG PLDP (20 mg) was dissolved in 10 mM phosphate buffer, pH 7.3, and dialyzed against 3 changes of the same buffer. After dialysis, 50 mg of solid ss-PEG were gradually added with stirring to the enzyme solution (*ca.* 1 ml) containing 3700 units of PLDP. Thereafter, the mixture was further stirred for 2 h at 25 °C. An equal volume of cold 10 mM acetate buffer, pH 5.0, was then added to the mixture in order to stop the reaction. From the reaction mixture, unreacted ss-PEG was removed by ultrafiltration with XM-50 membrane (Amicon Co., Ltd.) and by flushing the membrane with about 200 ml of the acetate buffer, pH 5.0.

The extent of PLDP modification with ss-PEG was estimated in terms of the decrease in free amino groups per mg protein, by titration of the remaining amino groups with trinitrobenzene sulfonate (TNBS), according to the method described by Habeeb[15] which involves spectrophotometric determination in terms of A_{335}.

The amount of protein was determined according to the biuret method.[16,17]

Assay of PLDP Activity The hydrolytic activity of native or modified PLDP was determined according to the method of Imamura and Horiuchi.[18] The reaction mixture (500 μl) containing 0.3% Triton X-100, 2 mM egg yolk phosphatidylcholine (PC), 1 mM $CaCl_2$ and enzyme in 40 mM 3,3-DMG buffer, pH 5.5, was incubated for 10 min at 37 °C. Then the reaction was terminated by the addition of 500 μl of 1 M Tris–HCl, pH 8.0, containing 10 mM ethylenediaminetetraacetic acid (EDTA) and 1% cetyl trimethylammonium bromide (CTAB). Then, an aliquot (200 μl) was withdrawn from the reaction mixture and added to 100 μl of chromogen solution containing 0.5 units of choline oxidase, more than 0.5 units of peroxidase, 0.02% phenol and 0.03% 4-AAP. The mixture was incubated for 30 min at 37 °C and then diluted with 300 μl of 1.5% Triton X-100 and the absorbance at 500 nm was determined.

In the measurement of the optimal pH, thermostability and kinetic parameters, the experimental conditions involving substrate concentration, pH, temperature and so forth were varied.

In the measurement of transphosphatidylation, the substrate solution was prepared by mixing various concentrations of PC in 1 ml of $CHCl_3$ with 50 μl of 4 M ethanolamine in 0.2 M acetate buffer, pH 6.0.

To this biphasic substrate, was added 50 μl of enzyme solution containing 1 unit of native or modified PLDP, then the mixture was incubated with vigorous shaking for 10 min at 37 °C.

Then, the enzyme reaction was stopped by adding 0.4 ml of 1 M HCl and 1.5 ml of extraction solvent ($CHCl_3$: CH_3OH : 1 M HCl = 26 : 33 : 1) to the mixture. The mixture was mixed well by a Vortex mixer and centrifuged at 3000 rpm for 5 min. After removal of the upper methanol–water layer, the lower chloroform layer was washed by the addition of 1 ml of Folch extraction solvent ($CHCl_3$: CH_3OH : H_2O = 3 : 48 : 47) and by subsequent centrifugation.

Thereafter, the lower layer was analyzed for the content of phosphatidylethanolamine (PE) by Thincrod-S-III (crystal rods coated with silica gel) thin layer chromatography (TLC) with $CHCl_3$: CH_3COCH_3 : CH_3OH : CH_3COOH : H_2O (10 : 4 : 2 : 2 : 1) and then by Iatroscan TH-10 TLC Analyzer containing FID-detector of high sensitivity (Iatron Laboratories, Inc., Tokyo).

Sodium Dodecyl Sulfate (SDS)-Polyacrylamide Gel Electrophoresis (PAGE) According to the method of Laemmli,[19] SDS-PAGE of native and modified PLDPs was carried out at room temperature. A molecular weight marker was purchased from Bio-rad laboratories.

High Performance Liquid Chromatography (HPLC) Analysis of Native

and Modified PLDPs The chromatographic behaviors of native and modified PLDPs was analyzed by HPLC columns of Toyopearl HW-55F (Toyo Soda Manufacturing Co., Ltd.) and CM-Toyopearl (Toyo Soda Manufacturing Co., Ltd.). In the size-exclusion chromatography, enzyme samples were applied to a Toyopearl HW-55F column (16 × 400 mm) and eluted with 10 mM Tris–HCl, pH 7.5, containing 5 mM $CaCl_2$ and 0.2 M NaCl; 2 ml fractions were collected at a flow rate of 2 ml/min. For molecular weight determinations of native and modified PLDPs, the reference proteins; aldolase (158 kilodaltons (kDa)), bovine serum albumin (68 kDa), ovalbumin (50 kDa) and cytochrome c (12.5 kDa) were applied to the same column in the same conditions.

In cation exchange column chromatography, enzyme samples were applied to a CM-Toyopearl column (13 × 100 mm) and eluted with two acetate buffers, A and B. Buffer A; 20 mM acetate, pH 3.5. Buffer B; 0.5 M NaCl in 20 mM acetate, pH 3.5.

The column was at first eluted with buffer A for 5 min, then with a NaCl gradient of 25 mM NaCl/min using buffer B for 10 min, and finally with buffer B.

Results

PLDP retained approx. 50% of its hydrolytic activity after modification with ss-PEG at pH 7.3 and 25 °C. As shown in Fig. 1, the molecular weight of the native enzyme was estimated by SDS-PAGE to be 52 kDa (lane 2), whereas modified PLDP seemed to have molecular weights ranging from 52 to 150 kDa (lane 3). Apparently, the native enzyme remained to some extent, but its major part might be removed by XM-50 ultrafiltration. In the subsequent experiments, the ultrafiltered preparation was used as the modified enzyme.

From size-exclusion HPLC using Toyopearl HW-55F, however, the molecular weights of native and modified PLDPs were calculated to be 25 and 89 kDa, respectively, since modified PLDP was eluted 10 min faster than the native one (Figs. 2A and 2B).

In cation-exchange HPLC using CM-Toyopearl, native PLDP was eluted at 0.45 M NaCl (Fig. 3A), whereas modified PLDP was mainly eluted at 0.15 and 0.25 M NaCl (Fig. 3B), in addition to the original eluting position. The first peak at 11 min in Fig. 3A might be another contaminating protein which had the same molecular weight as PLDP. Titration with TNBS showed the extent of modification with ss-PEG to be approximately 70% (Fig. 4) on the basis of this preparation. But the exact estimation of modification should be carried out with the homogeneously purified PLDP.

PLDP is fairly stable within a pH range of 2 to 9 at 37 °C incubation for 30 min, and the modified PLDP showed

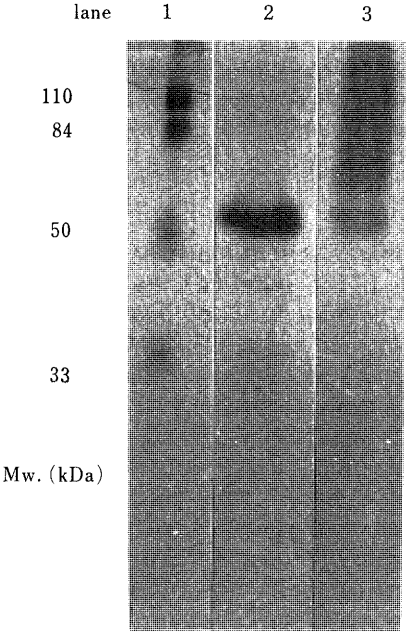

Fig. 1. SDS-PAGE

Electrophoresis was performed at a constant current (30 mA) for 30 min at room temperature using a gel of 12% polyacrylamide with a stacking gel of 3% acrylamide as described in Materials and Methods. lane 1: standard; phosphorylase b (110 kDa), bovine serum albumin (84 kDa), ovalbumin (50 kDa), carbonic anhydrase (33 kDa); lane 2: native PLDP; lane 3: modified PLDP.

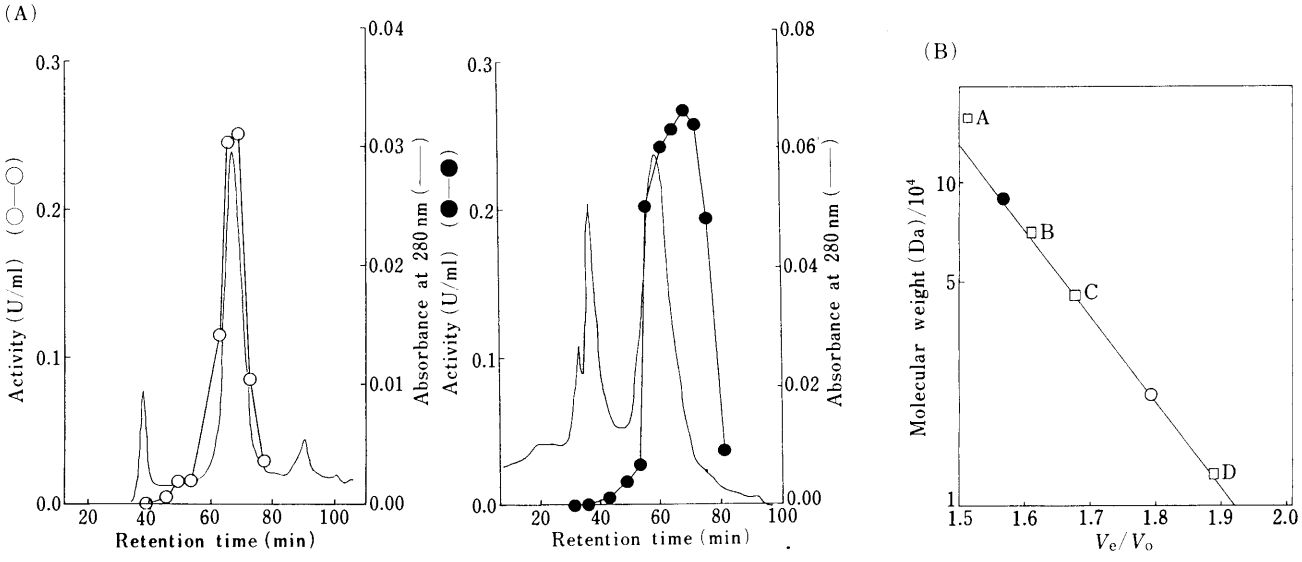

Fig. 2. Size-Exclusion Column HPLC

(A) Elution Patterns of Native and PEG Modified PLDP

The enzyme samples were applied to a Toyopearl HW-55F column (16 × 400 mm) and eluted with 10 mM Tris–HCl (pH 7.5) containing 5 mM $CaCl_2$ and 0.2 M NaCl in a flow rate of 1 ml/min. Solid lines stand for absorbance at 280 nm. ○—○, hydrolytic activity of native PLDP; ●—●, hydrolytic activity of modified PLDP.

(B) Calibration

Molecular weights of standard proteins were as follows. □ A, aldolase (158 kDa); □ B, bovine serum albumin (68 kDa); □ C, ovalbumin (50 kDa); □ D, cytochrome c (12.5 kDa); ○, native PLDP; ●, modified PLDP. Molecular weights of native and modified PLDP were calculated as 25 kDa and 89 kDa.

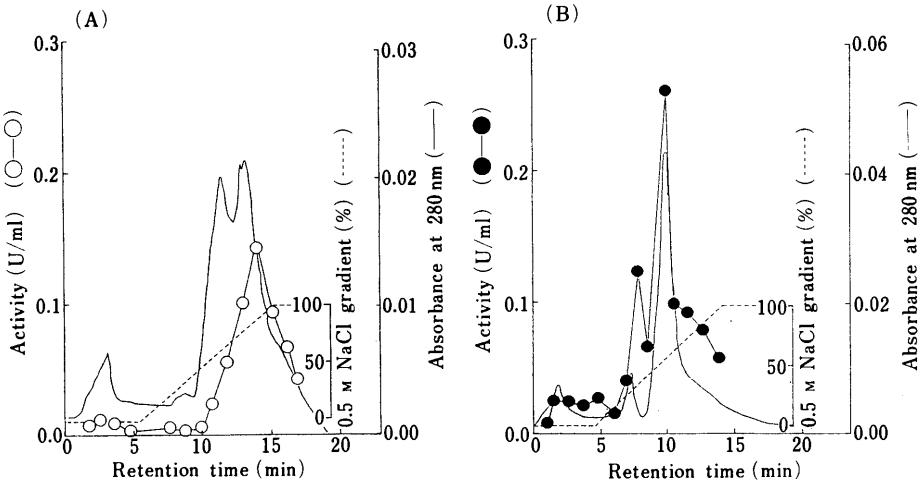

Fig. 3. Cation-Exchange Column HPLC

CM-Toyopearl column (13 × 100 mm) was used. Flow rate of elution was 2 ml/min. Linear gradient (25 mM/min) using 0.5 M NaCl was loaded as shown in dashed lines. Solid lines stand for absorbance at 280 nm. (A) ○—○, hydrolytic activity of native PLDP; (B) ●—●, hydrolytic activity of modified PLDP.

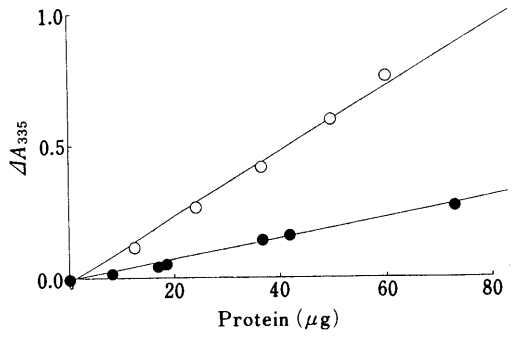

Fig. 4. TNBS-Titration

Protein concentration of native and modified PLDPs and the amounts of their residual amino groups were determined as described in Materials and Methods. From the ratio of the slopes of curves for modified (●) *versus* native (○) PLDPs, the extent of modification was estimated.

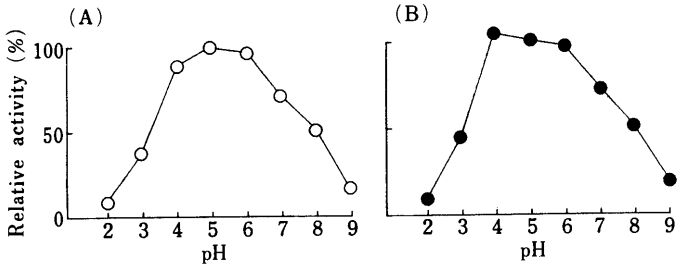

Fig. 5. pH-Activity Profiles

Phospholipase D activity of native (A) or modified (B) PLDP was determined with varying pH (2—9) of 0.2 M GTA buffer. The amount of enzyme used per assay were as follows. Native PLDP, 110 units/mg; modified PLDP, 63.2 units/mg.

similar pH stability. Also, the optimal pH of PLDP, around pH 5, was not significantly altered by modification with ss-PEG (Fig. 5). By heating at pH 5.5 and 50 °C for 10 min, native PLDP lost its activity by approximately 50%, while modified PLDP retained full enzyme activity under the same condition (data not shown).

Also, the effects of modification on catalytic properties were analyzed in terms of the K_m values in both hydrolytic and transphosphatidyl reactions. By modification with ss-PEG, the value of K_m for hydrolysis of PC by PLDP became 1.7 mM, twice as much as that by native PLDP, 0.8 mM, as shown in Fig. 6A. On the other hand, no

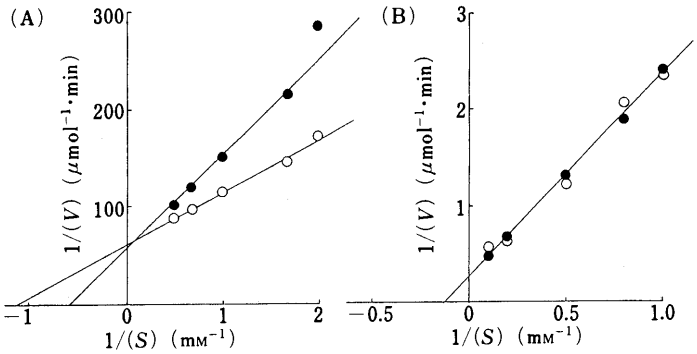

Fig. 6. K_m Determination in Hydrolytic and Transphosphatidyl Reactions

(A) For the determination of K_m values for hydrolysis of PC, phospholipase D activity was estimated by incubating 0.01 unit of native (○) or modified (●) PLDP with varying concentrations of PC (0.5—2 mM) for 10 min at 37 °C.

(B) In order to determine K_m values for PC in transphosphatidylation with ethanolamine, phospholipase D activity was estimated by incubating 1 unit of native (○) or modified (●) PLDP with varying concentrations of PC (1—10 mM) in $CHCl_3$ and 4 M ethanolamine in acetate buffer, pH 6.0, for 10 min at 37 °C with vigorous shaking. The relative activity of native or modified enzyme used for assay were as follows. Native PLDP (110 units/mg), modified PLDP (63.2 units/mg).

significant differences in the K_m values of transphosphatidylation for PC with ethanolamine, 8.0 mM, were observed between native and modified enzymes (Fig. 6B). Also, modification with ss-PEG did not significantly alter the values of V_{max} in both hydrolytic and transphosphatidyl reactions.

Discussion

From the present study, it was shown that modification of free amino groups existing in lysyl or N-terminal amino acid residues of PLDP with ss-PEG resulted in an increase of molecular weight, decrease of positive charges in the surface of the protein molecule, alteration of catalytic activity and change of thermostability. According to the results obtained by TNBS titration, SDS-PAGE and gel filtration, increase in the molecular weight of PLDP by modification with ss-PEG was estimated in three ways, as shown in Table I. From these three criteria, the molecular weight of PLDP increased with the introduction of bulky PEG into approximately 70% of the free amino groups

TABLE I. Molecular Weights of Native and Modified PLDPs

	Native PLDP	Modified PLDP
SDS-PAGE	52000	52000—150000
Gel filtration	25000	89000
TNBS titration	46000	81000

contained in the enzyme preparation, although, modification of the enzyme itself could not be determined because of its low purity.

The decrease in surface positive charges was demonstrated by cation-exchange HPLC. Modification of PLDP with ss-PEG brought about faster elution in HPLC with CM-Toyopearl, indicating a marked decrease in the cationic charges of lysyl or N-terminal amino groups which were combined covalently with the activated PEG.

By modification with ss-PEG, the value of K_m of PLDP for PC in the hydrolytic reaction increased 2-fold, whereas that in the transphosphatidyl reaction was not altered. Probably, modification of free amino groups must increase the hydrophobicity of the catalytic site in PLDP, lowering the affinity between the enzyme and PC in the completely aqueous medium. In the case of other enzymes, modification with an active PEG derivative also increases the values of K_m.[8] Apparently, PEG-modification of PLDP did not affect the enzyme–substrate affinity in the transphosphatidyl reaction, while such a modification decreased the enzyme substrate affinity in the hydrolytic reaction of PLDP. Therefore, if improvement in the modification procedure is achieved so as to block only the hydrolytic activity of the enzyme without effecting the transphosphatidyl activity, PEG-modified PLDP might become more useful than native PLDP for the synthesis of phosphatides. Both native and modified PLDPs were fairly stable in the wide pH range, while modified PLDP became more thermostable than the native enzyme. As reported with other enzymes,[10] introduction of active PEG into the enzyme molecule might stabilize the conformation of this enzyme against thermal denaturation through an increase in intramolecular, hydrophobic interactions maintaining the secondary structure of PLDP.

Generally speaking, the trials for modification of several phospholipases with active PEG derivatives must be fairly useful, because the substrates of these enzymes are highly amphiphilic and the increase in hydrophobicity in the enzyme proteins is not so fatally harmful against catalytic activity.

Modification of sphingomyelinase from *Bacillus cereus* using ss-PEG is now in progress in our laboratory (to be reported elsewhere).

Acknowledgments The authors are greatly indebted to Dr. Shigeyuki Imamura, Toyo Jozo Co., Ltd., for the kind gift of *Streptomyces* phospholipase D and to Mr. Yoshihiko Ohshima, Mr. Takayuki Mizutani and Mr. Haruo Morita for their kind cooperation. Also, the authors thank Dr. Yuji Inada, Yokohama University and Dr. Katsunobu Takahashi, Tokyo Institute of Technology for their kind technical advices.

References

1) S. Imamura and Y. Horiuchi, *J. Biochem.* (Tokyo), **85**, 79 (1979).
2) R. H. Quarles and R. M. C. Dawson, *Biochem. J.*, **112**, 795 (1969).
3) M. Heller, N. Mozes, I. Peri (Abramovitz) and E. Maes, *Biochim. Biophys. Acta*, **369**, 397 (1974).
4) S. Shuto, S. Imamura, K. Fukukawa, H. Sakakibara and J. Murase, *Chem. Pharm. Bull.*, **35**, 447 (1987).
5) S. Shuto, H. Itoh, S. Ueda, S. Imamura, K. Fukukawa, M. Tsujino, A. Matsuda and T. Ueda, *Chem. Pharm. Bull.*, **36**, 209 (1988).
6) L. R. Juneja, T. Kazuoka, N. Goto, T. Yamane and S. Shimizu, *Biochim. Biophys. Acta*, **1003**, 277 (1989).
7) A. Abuchowski, T. van Es, N. C. Palczuk and F. F. Davis, *J. Biol. Chem.*, **252**, 3578 (1977).
8) F. F. Davis, A. Abuchowski, T. van Es, N. C. Palczuk, K. Savoca, R. H-L. Chen and P. Pyatak, *Polymer Preprints, Am. Chem. Soc., Division of Polymer Chem.*, **20**, 357 (1979).
9) P. S. Pyatak, A. Abuchowski and F. F. Davis, *Res. Commun. Chem. Pathol. Pharmacol.*, **29**, 113 (1980).
10) A. Abuchowski, G. M. Kazo, C. R. Verhoest, Jr., T. van Es, D. Kafkewitz, M. L. Nucci, A. T. Viau and F. F. Davis, *Cancer Biochem. Biophys.*, **7**, 175 (1984).
11) N. V. Katre, M. J. Knauf and W. J. Laird, *Proc. Natl. Acad. Sci. U.S.A.*, **84**, 1487 (1987).
12) K. Miyata, Y. Nakagawa, M. Nakamura, T. Ito, K. Sugo, T. Fujita and K. Tomoda, *Agric. Biol. Chem.*, **52**, 1575 (1988).
13) Y. Inada, T. Yoshimoto, A. Matsushima and Y. Saito, *Trends Biotechnol.*, **4**, 68 (1986).
14) Y. Yamagata and E. Ichishima, *Current Microbiol.*, **19**, 307 (1989).
15) A. F. S. A. Habeeb, *Anal. Chem.*, **14**, 328 (1966).
16) A. G. Gornall, C. J. Bradawill and M. M. David, *J. Biol. Chem.*, **117**, 751 (1948).
17) E. E. Jacobs, M. Jacobs, D. R. Sanadi and J. B. Brandrey, *J. Biol. Chem.*, **223**, 147 (1956).
18) S. Imamura and Y. Horiuchi, *J. Biochem.* (Tokyo), **83**, 677 (1978).
19) U. K. Laemmli, *Nature* (London), **270**, 680 (1970).

The Effect of Staurosporine on Ca^{2+} Signals in Rat Basophilic Leukemia (RBL-2H3) Cells

Reiko TESHIMA,*[,a] Hideharu IKEBUCHI,[a] Tadao TERAO[a] and Mamoru NAKANISHI[b]

National Institute of Hygienic Sciences,[a] 1-18-1, Kamiyoga, Setagaya-ku, Tokyo 158, Japan and Faculty of Pharmaceutical Sciences,[b] Nagoya City University, Tanabe-Dori, Mizuho-ku, Nagoya 467, Japan. *Received September 5, 1990*

We examined the effect of staurosporine on cytosolic calcium response in rat basophilic leukemia (RBL-2H3) cells using fura-2 as a fluorescent indicator of calcium ion.

Staurosporine at a dose of 30 nM inhibited antigen-stimulated Ca^{2+}-influx into the cells from the extracellular environment. In contrast, the drug at this concentration inhibited neither the mobilization of Ca^{2+} from intracellular stores nor inositol 1,4,5-trisphosphate (IP_3) formation. At a high concentration (300 nM), however, staurosporine completely inhibited the cytosolic calcium responses as well as IP_3 formation. These results indicate that staurosporine, if used at an appropriate concentration, can be used to discriminate Ca^{2+}-influx from extracellular environment from mobilization of the ion from intracellular stores.

These results also suggest that protein kinases, possibly protein kinase C, are involved in the calcium influx of RBL-2H3 cells from the extracellular environment.

Serotonin release was strongly inhibited by the drug at 30 nM staurosporine. Since the inhibition of serotonin release and suppression of cytosolic calcium increase in response to the antigen were in parallel, we concluded that the inhibition of serotonin release from RBL-2H3 cells caused by the drug was elicited by the suppression of Ca^{2+} influx into the cells.

Keywords calcium ion signal; staurosporine; rat basophilic leukemia (RBL-2H3) cell; inositol trisphosphate (IP_3) formation

Introduction

The release of histamine and other inflammatory mediators from tissue mast cells and blood basophils is the primary event in a variety of acute allergic and inflammatory conditions.[1] The release of the mediators from these cells is an energy- and calcium-dependent process which is initiated by the interaction of antigen with membrane-bound immunoglobulin E (IgE) molecules.[2]

Like mast cells and blood basophils, rat basophilic leukemia (RBL-2H3) cells contain IgE receptors in their plasma membranes and can be stimulated to secrete histamine by aggregation of the receptor with antigen when cells are primed with the appropriate antigen-specific IgE.[3]

In these cells, the release of calcium from intracellular stores by inositol trisphosphate (IP_3) is prominent.[4,5]

Although the mechanism of Ca^{2+} influx into RBL-2H3 cells remains unclear, it is obvious that non-voltage activated calcium channels are involved in Ca^{2+} influx into these cells, since calcium influx is neither activated by depolarization[6,7] nor blocked by a variety of organic calcium channel antagonists.[8]

In this paper, we present a line of evidence which indicates that staurosporine inhibits Ca^{2+} entry into RBL-2H3 cells from the extracellular environment without affecting intracellular Ca^{2+} mobilization.

Materials and Methods

Reagents Fura-2-AM was obtained from Dojindo (Kumamoto, Japan). An IP_3 assay kit was obtained from Amersham Radiochemical Co. (Amersham, U.K.). Staurosporine was obtained from Kyowa Hakko Kogyo (Tokyo, Japan). Mouse anti-dinitrophenyl (DNP) monoclonal IgE antibody (IgE-53-569) and dinitrophenylated bovine serum albumin (DNP_7-BSA) and 1-(5-isoquinolin-sulfonyl)-2-methylpiperazine (H-7) were obtained as described in a previous paper.[9]

Cells All experiments were performed on a secreting subline of rat basophilic leukemia cells (RBL-2H3)[3] donated by Prof. T. Ishizaka (Johns Hopkins University School of Medicine, Baltimore, MD).

Buffer The following buffer was used; 140 mM NaCl, 5 mM KCl, 0.6 mM $MgCl_2$, 1.0 mM $CaCl_2$, 5.5 mM glucose, 0.1% BSA and 5 mM Piperazine-*N*-*N'*-bis(2-ethanesulfonic acid) (PIPES), pH 7.4.

Measurement of Serotonin Release from RBL-2H3 Cells The degranulation process was monitored by measuring [^{3}H]serotonin release according to the method described in a previous paper.[10] The cells were plated in a 24-well flat-bottom microtiter plate (Falcon, No. 3047) in 1 ml of MEM (Eagle's minimum essential medium) containing 10% fetal calf serum/well and incubated for 24 h at 37 °C. The supernatant was discarded and the cells (2×10^5/well) were incubated at 37 °C for 60 min with 2 μCi of [^{3}H]serotonin (26.3 Ci/mmol, New England Nuclear) and ascitic fluid containing DNP-specific monoclonal IgE antibody diluted 250-fold with MEM. Total [^{3}H]serotonin in the cells was $2-2.5 \times 10^5$ dpm/2×10^5 cells.

The supernatants were then removed and the cells were washed 3 times with the buffer to eliminate unbound IgE. We added 400 μl of the buffer to the cells and challenged them with 100 μl of DNP_7-BSA solution (100 μg/ml of the buffer) for 35 min at 37 °C. The supernatant was withdrawn from each well and mixed with Aquasol 2 (New England Nuclear) to determine [^{3}H]serotonin release from the cells.

To calculate total radioactivity present in the original cells, the [^{3}H]serotonin remaining in the cells after secretion was extracted with 500 μl of 2% $HClO_4$. The extract was removed and radioactivity was measured as described above.

To determine the effect of staurosporine on serotonin release, the cells were incubated with the drug for 2 min prior to stimulation with the antigen.

Measurement of Cytosolic Free Calcium Concentration ([Ca^{2+}]i) RBL-2H3 cells (6×10^5 cells/ml) were primed with anti-DNP-IgE (50 nM) and then loaded with fura-2-AM (6 μM) as described previously.[11] After removing both free dye and unbound IgE by centrifugation, the cells were resuspended in 1.5 ml of buffer. During these treatments, fura-2-AM was incorporated into the cytoplasm and converted to fura-2 by esterases, resulting in an average final intracellular accumulation of 100—150 μM of fura-2, based on the assumption that cell volume is 1.1 μl/10^6 cells. Fura-2-loading under the above conditions was adequate to monitor changes in [Ca^{2+}]i. Fluorescence measurements were made in a 1 cm quartz cuvette using a Shimazu RF-5000 spectrophotometer (excitation, 335 or 362 nm; emission, 500 nm) with stirring at 37 °C. During fluorescence monitoring, cells were stimulated by applying 20 μg/ml DNP_7-BSA. Estimation of [Ca^{2+}]i from fura-2 fluorescence data was based on the method described by Grynkiewicz *et al.*[12] When testing the effect of staurosporine on Ca^{2+} influx, the cells were incubated with the drug for 2 min prior to stimulation with the antigen.

Measurement of IP_3 Formation RBL-2H3 cells (8×10^6 cells/ml) were primed with anti-DNP-IgE (50 nM) for 15 min. After being washed with the buffer, the cells were challenged with 20 μg/ml of DNP_7-BSA for 20—200 s. To stop the reaction, 160 μl of cold 20% $HClO_4$ was added and the cells were allowed to stand at 4 °C for 20 min. After centrifugation, the supernatant (1.3×10^6 cells equivalent) was neutralized to pH 7.4 with 5 N KOH. After centrifugation, the IP_3 concentration in the supernatant was measured using an IP_3 assay kit (Amersham, U.K.).

When testing the effect of staurosporine on IP_3 formation, the cells were

incubated with the drug for 2 min prior to stimulation with an antigen.

Results

Effect of Staurosporine on Cytosolic Free Calcium Concentration As shown in Fig. 1, a rapid increase in $[Ca^{2+}]i$ occurred in response to the antigen. In this experiment we used fura-2 as an indicator of intracellular free calcium in RBL-2H3 cells. When fura-2 was complexed with Ca^{2+}, the maximum wavelength for excitation shifted from 362 to 335 nm. Therefore, we quantitated $[Ca^{2+}]i$ from the ratio of fluorescence intensity excited at 335 nm and 362 nm by changing the excitation wavelength every 2 s.[12] Figure 1B shows fluorescence intensities excited at 335 and 362 nm, and Fig. 1A shows the ratio of fluorescence intensities excited at 335 and 362 nm. As shown in Fig. 1B, the fluorescence intensity excited at 335 nm increased after antigen stimulation. On the other hand, the fluorescence intensity excited at 362 nm had a tendency to decrease after antigen stimulation. The 335/362 nm fluorescence ratio increased rapidly beginning 20 s after the antigen stimulation, reached its maximum by 60 s, and remained there for at least 5 min. $[Ca^{2+}]i$ before and after the antigen stimulation was 63 and 140 nM, respectively.

As shown in Fig. 1A, the increase of $[Ca^{2+}]i$ in RBL-2H3 cells after antigen stimulation was biphasic, that is, an initial rapid increase between 20—40 s followed by a gradual elevation (40—300 s). The pattern of $[Ca^{2+}]i$ change after antigen stimulation (Fig. 2a) in the presence of 3 nM of staurosporine was essentially the same as that without the drug. The result indicates that staurosporine at this concentration did not affect the $[Ca^{2+}]i$ of RBL-2H3 cells after antigen stimulation. In the presence of 30 nM of staurosporine, however, the second, gradual elevation after antigen stimulation almost completely disappeared. In this case, after the rapid increase between 20 and 40 s, the fluorescence ratio was rather low until 70—80 s after stimulation, then gradually increased again. This result suggests that staurosporine at a dose of 30 nM influenced the first, rapid increase in $[Ca^{2+}]i$ in RBL-2H3 cells only slightly or not at all, but severely suppressed the second gradual increase of $[Ca^{2+}]i$.

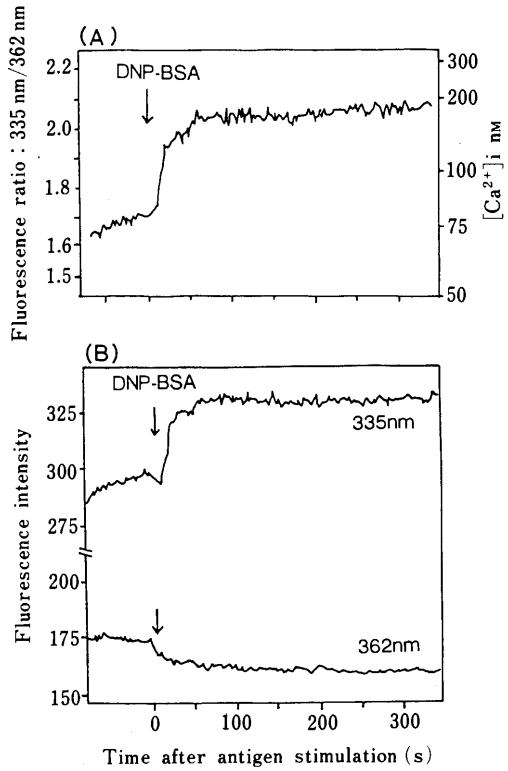

Fig. 1. Ca^{2+} Mobilization in Fura-2 Loaded RBL-2H3 Cells

Fura-2-loaded and IgE-primed 2H3 cells (final 6×10^5 cells/ml) were mixed with DNP_7-BSA (20 μg/ml) at 37°C. The fluorescence measurement (excitation, 335 or 362 nm; emission, 500 nm) were performed on fura-2 loaded cells. (A) Time course of fluorescence ratio of 335/362 nm. (B) Time course of fluorescence intensity excited at 335 or 362 nm.

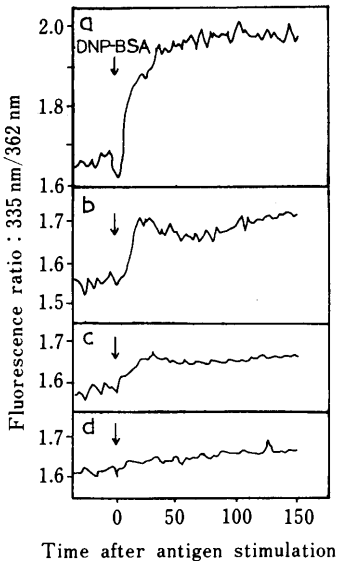

Fig. 2. Effect of Staurosporine on $[Ca^{2+}]i$ Increase in RBL-2H3 Cells Stimulated with the Antigen

Fura-2- loaded and IgE- primed 2H3 cells (final 6×10^5 cells/ml) were preincubated with various concentrations of staurosporine [a) 3 nM, b) 30 nM, c) 60 nM, d) 300 nM] for 2 min at 37°C and then mixed with DNP_7-BSA (20 μg/ml). The fluorescence measurements (excitation, 335 and 365 nm; emission, 500 nm) on fura-2- loaded cells were performed. These traces are representatives of typical experiments that were repeated at least 3 times.

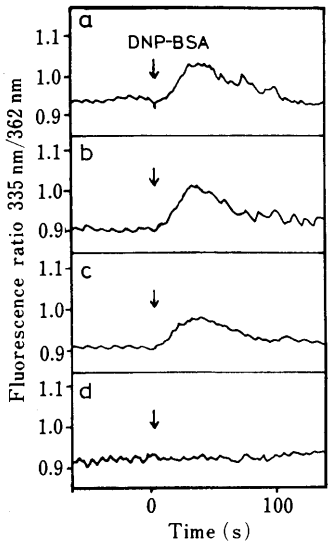

Fig. 3. Effect of Staurosporine on $[Ca^{2+}]i$ Increase in the Absence of External Free Ca^{2+}

Fura-2- loaded and IgE- primed 2H3 cells (final 6×10^5 cells/ml) were suspended in buffer including 1 mM EGTA instead of 1 mM Ca^{2+}, and preincubated with various concentrations of staurosporine [a) 0 nM, b) 30 nM, c) 60 n M, d) 300 nM] for 2 min and then mixed with DNP_7-BSA (20 μg/ml). The fluorescence measurements (excitation, 335 or 362 nm; emission, 500 nm) were performed on fura-2 loaded cells.

At higher concentration (more than 60 nM), staurosporine inhibited both phases (Fig. 2c and d).

$[Ca^{2+}]i$ is usually modulated by mobilization from intracellular stores and influx from the extracellular environment. To determine to which phase of the biphasic increase in $[Ca^{2+}]i$ (Fig. 1A) the intracellular mobilization of Ca^{2+} from its stores contributes, we investigated the $[Ca^{2+}]i$ increase by antigen stimulation in a free Ca^{2+}-depleted medium condition.

As shown in Fig. 3a, we were able to detect a rapid transient rise in $[Ca^{2+}]i$ after antigen stimulation in the presence of ethylene glycol bis(2-aminoethyl ether)-*N,N,N,N'*-tetraacetic acid (EGTA) (1 mM). Although total fluorescence intensity decreased,[13] this corresponded to the first, rapid increase in $[Ca^{2+}]i$ observed in Fig. 1A. Therefore, this first rapid rise in $[Ca^{2+}]i$ seemed to be caused by the release of calcium ions from intracellular calcium stores. As shown in Fig. 3b, RBL-2H3 cells pretreated with 30 nM staurosporine in the presence of EGTA (1 mM) underwent a similar, rapid, transient increase in $[Ca^{2+}]i$ with the antigen stimulation. This indicates that 30 nM of staurosporine did not inhibit the $[Ca^{2+}]i$ increase derived from intracellular calcium stores. Sixty nM of staurosporine slightly inhibited the increase in $[Ca^{2+}]i$ (Fig. 3c) and 300 nM staurosporine completely inhibited the increase in $[Ca^{2+}]i$ derived from intracellular calcium stores (Fig. 3d).

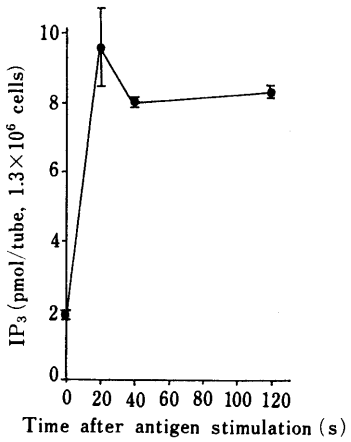

Fig. 4. Time Course of IP_3 Formation in RBL-2H3 Cells Stimulated with the Antigen

IgE-primed 2H3 cells (final 8×10^6 cells/ml) were mixed with DNP_7-BSA (20 μg/ml) and incubated for 20—200 s at 37 °C. After extraction, IP_3 concentration was measured by an IP_3 assay kit.

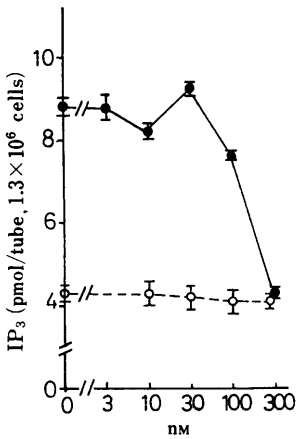

Fig. 5. Effect of Staurosporine on IP_3 Formation in RBL-2H3 Cells

IgE-primed 2H3 cells (final 8×10^6 cells/ml) were preincubated with various concentrations of staurosporine for 2 min at 37 °C and then mixed with DNP_7-BSA (20 μg/ml). After 20 s stimulation, IP_3 was extracted and IP_3 concentration was measured by an IP_3 assay kit. —●—, + antigen; —○—, − antigen.

Effect of Staurosporine on IP_3 Formation As shown in Fig. 4, a rapid increase in IP_3 formation was observed in response to the antigen. The IP_3 concentration reached its maximum 20 s after antigen stimulation and then decreased gradually. The time course of IP_3 formation after antigen stimulation is consistent with the reports of other authors who used ^3H-myoinositol to label phosphoinositol intrinsically.[14,15]

Figure 5 shows the effect of staurosporine on IP_3 formation after 20 s of stimulation. There was no obvious inhibition at concentrations of 3—30 nM, and IP_3 formation was slightly inhibited at the dose of 100 nM. At the maximum dose (300 nM), IP_3 formation was completely inhibited.

As IP_3 is known to release Ca^{2+} from intracellular stores, it is reasonable that 30 nM of staurosporine did not inhibit either IP_3 formation (Fig. 5) or $[Ca^{2+}]i$ increase from intracellular Ca^{2+} stores (Fig. 3b).

Effect of Staurosporine on Cytosolic Calcium Response and Serotonin Release We compared the effect of staurosporine on $[Ca^{2+}]i$ and serotonin release after stimulating RBL-2H3 cells with the antigen.

As shown in Table I, both serotonin release and $[Ca^{2+}]i$ elevation were decreased in a dose dependent manner. But the inhibition of serotonin release was slightly greater than that of the $[Ca^{2+}]i$ increase. At the 30 nM dose, 97% of the serotonin release was inhibited while 80% of the $[Ca^{2+}]i$ increase was inhibited. As shown in Fig. 3c, 30 nM staurosporine did not inhibit the $[Ca^{2+}]i$ increase derived from the intracellular stores. Therefore, it seems that only the $[Ca^{2+}]i$ increase from intracellular stores is not enough

TABLE I. Effect of Staurosporine on $[Ca^{2+}]i$ Response and Serotonin Secretion of RBL-2H3 Cells Stimulated with Antigen

Staurosporine (nM)	$[Ca^{2+}]i$ (nM)	Serotonin release (relative to maximum, %)
0	158±12	100
3	140± 8	88±1.3
15	106±12	35±0.7
30	80± 7	3±0.2
60	70± 4	1±0.1
300	60± 3	

Values are means±S.D. for three different experiments. $[Ca^{2+}]i$ was measured in suspensions of fura-2-loaded cells, and release of serotonin was measured in monolayer cultures. $[Ca^{2+}]i$ before stimulation was 60 nM.

TABLE II. Effect of H-7 on $[Ca^{2+}]i$ Response and Serotonin Secretion of RBL-2H3 Cells Stimulated with Antigen

H-7 (μM)	$[Ca^{2+}]i$ (nM)	Serotonin release (relative to maximum, %)
0	140±12	100
100	125± 8	88±2.0
500	85± 7	28±2.5
1000	65± 7	1±0.2

Values are means±S.D. for two different experiments. $[Ca^{2+}]i$ was measured in suspensions of fura-2 loaded cells, and release of serotonin was measured in monolayer cultures. $[Ca^{2+}]i$ before stimulation was 46 nM.

for serotonin secretion from RBL-2H3 cells.

At the 300 nM dose, $[Ca^{2+}]i$ increase as well as serotonin release was completely inhibited.

We then examined the effect of H-7, another protein kinase inhibitor,[15] on the $[Ca^{2+}]i$ increase and serotonin release after the antigen stimulation of RBL-2H3 cells.

As shown in Table II, both serotonin release and $[Ca^{2+}]i$ increase were decreased in a dose-dependent manner by this compound. Although the results were essentially the same as those obtained by staurosporine, H-7 was less effective than staurosporine.

Discussion

Changes in $[Ca^{2+}]i$ levels are associated with the secretion of mediators of immediate hypersensitivity by RBL-2H3 cells. In these cells, as well as in other non-excitable cells, the increase in cytoplasmic Ca^{2+} levels elicited by continuous receptor occupancy are governed by the following two mechanisms; (1) increased inositol 1,4,5-trisphosphate (IP_3)-induced release of Ca^{2+} from intracellular stores,[16-19] (2) entry of extracellular Ca^{2+} just after a rapid and transient rise in $[Ca^{2+}]i$ caused by (1).

Increases of cytoplasmic Ca^{2+} concentration caused by different stimuli in various cells is usually biphasic, that is, an initial rapid increase followed by a gradual elevation. The former is believed to be elicited by the mobilization of Ca^{2+} from intracellular stores by IP_3 and the latter by an influx of the ion from the extracellular environment. The mechanism by which extracellular Ca^{2+} enters the cell is not clear. In some non-excitable cells, IP_3 and IP_4 have been implicated in the control of Ca^{2+} entry.[18] In other non-excitable cells, Ca^{+} entry seems to be regulated by non-voltage-dependent calcium channels which are opened either directly through a receptor (receptor-opened channel)[20,21] or indirectly through some internal diffusible messenger (second messenger-opened channel).[22]

Staurosporine has been reported to be a highly effective inhibitor of protein kinase C[23,24] and its molecular and cellular effects on various cells have been reported.[25-27] However, there are few reports on its effects on the early Ca^{2+} signal. Ward *et al.*[28] and Kubbies *et al.*[29] have reported that staurosporine inhibited mitogen-induced calcium mobilization in T lymphocytes. The present report documents the effects of staurosporine on the early Ca^{2+}-flux signal in RBL-2H3 cells.

Staurosporine at a low dose (less than 30 nM) may cause a specific inhibitory action on protein kinases, especially on protein kinase C,[23] because protein kinase C obtained from RBL-2H3 cells was completely inhibited by 30 nM of staurosporine (data not shown). Therefore, we focused on the data obtained from the exposure of RBL-2H3 cells to low doses in order to understand the effects of the drug on the Ca^{2+} flux.

When RBL-2H3 cells were stimulated with the antigen, the resulting rapid increase in $[Ca^{2+}]i$ was sustained for more than 300 s after the stimulation (Fig. 1A). We examined the effect of staurosporine on $[Ca^{2+}]i$ in RBL-2H3 cells stimulated by the antigen. The results presented in Fig. 2 demonstrate that exposure to staurosporine resulted in a dose-dependent inhibition of $[Ca^{2+}]i$ increases in antigen-stimulated RBL-2H3 cells. On the other hand, staurosporine at a dose less than 30 nM did not show any effect of the formation of IP_3, a key compound for the mobilization of Ca^{2+} from intracellular stores (Fig. 5). Staurospoporine is used at a concentration lower than several tens nM for the inhibition of protein kinase C in cultured cells. Thus, the complete inhibition of IP_3 formation at 300 nM of staurosporine might be due to a non-specific action of this drug. Actually, incubation of RBL-2H3 cells in the presence of 300 nM of staurosporine showed a morphorogical change of the cells. These results suggest that the presence of this drug at a concentration lower than 30 nM does not affect the Ca^{2+} release from intracellular stores caused by the antigen stimulation of the cells. In fact, in the presence of 1 mM EGTA in the culture medium, the first rapid increase in $[Ca^{2+}]i$, which is thus attributed to the release of the ion from intracellular stores, was not inhibited by 30 nM of staurosporine (Fig. 3). In this case, $[Ca^{2+}]i$ reached a maximal level at 20—30 s and then decreased to the original Ca^{2+} level by 100 s after the antigen stimulation. These results indicate that, in RBL-2H3 cells, Ca^{2+} mobilization from intracellular stores contributes only to the transient increase in $[Ca^{2+}]i$, and to maintain an elevated $[Ca^{2+}]i$ concentration, influx of the ion from the extracellular environment is essential. Staurosporine at low doses (less than 30 nM) inhibits only the influx of Ca^{2+} from the extracellular environment.

Staurosporine is a potent inhibitor of protein kinases, especially protein kinase C. Thus it is probable that protein kinase C positively modulates the influx of Ca^{2+} from outside RBL-2H3 cells and the drug inhibits the enzyme to suppress the influx of Ca^{2+}. However, we cannot rule out the possibility that other protein kinases are involved in the modulation of Ca^{2+} influx.

Detailed mechanism of Ca^{2+} entry into RBL-2H3 cells is unknown. Stump *et al.*[13] have postulated that Ca^{2+} influx from culture medium into RBL-2H3 cells was mediated at least in part by Na^{+}/Ca^{2+} antiporter, and this system was associated with a protein kinase C-stimulated event. Similarly, a protein kinase C-activated Na^{+}/H^{+} exchange has been suggested to play a role in the regulation of Ca^{2+} influx in human platelets.[30]

Sagi-Eisenberg and Pecht[31] have demonstrated that the tumor-promoting phorbol ester 12-*O*-tetradecanoylphorbol-13-acetate, at a concentration between 1.5 and 75 nM, completely blocked the antigen-induced increase of $[Ca^{2+}]i$ in RBL-2H3 cells. They thus postulated that protein kinase C was involved in the closure of Ca^{2+} gates opened by antigen stimulation. They also demonstrated that protein kinase C is involved in both the activation and termination of an antigen-induced degranulation process, a typical Ca^{2+}-dependent event in RBL-2H3 cells.[32] Our data indicate that protein kinase C can exert a positive effect on the influx of Ca^{2+} into RBL-2H3 cells.

Ca^{2+} in the extracellular environments, the influx of extracellular Ca^{2+}, and the subsequent Ca^{2+}-dependent process (for example myosin light chain phosphorylation[33]) are known to be essential for the degranulation of RBL-2H3 cells in response to antigen stimulation. Since the present results indicated that staurosporine inhibited the influx of extracellular Ca^{2+}, we examined the effect of this drug on the degranulation of RBL-2H3 cells. The results shown in Table I indicated that the inhibition of serotonin release correlated with the inhibition of $[Ca^{2+}]i$ increase. Similar

results were obtained with H-7, another inhibitor of protein kinase C (Table II). HA1008, which is usually used as a negative control of H-7,[34] did not inhibit $[Ca^{2+}]i$ increase in RBL-2H3 cells (data not shown). From these results we conclude that staurosporine preferentially inhibits the influx of Ca^{2+} from the extracellular environment into RBL-2H3 cells and blocks the degranulation process.

Our preliminary investigation on fura 2-loaded individual cells using video-imaging techniques indicated that about 70% of RBL-2H3 cells showed an increased $[Ca^{2+}]i$ response to the antigen stimulation, regardless of the presence (30 nM) or absence of staurosporine (unpublished results). In the absence of the drug, all the responding cells sustained $[Ca^{2+}]i$ elevation for more than 200 s. In the presence of 30 nM of staurosporine, however, 80% of the responding cells showed only transient $[Ca^{2+}]i$ increase, and the original $[Ca^{2+}]i$ concentration was restored by 100 s. The remaining 20% of the responding cells sustained the increased $[Ca^{2+}]i$ level for more than 200 s, similar to cells stimulated by the antigen in the absence of the drug.

These results explain why, as shown in Fig. 2b, staurosporine could not completely abolish the Ca^{2+} influx from the outside of the cells.

In conclusion, staurosporine can be used to block most of the Ca^{2+} influx from the extracellular environment into RBL-2H3 cells without affecting mobilization of the ion from intracellular stores.

Acknowledgement The authors thank Dr. Yoji Arata of the University of Tokyo for his helpful discussions.

References

1) R. A. Lewis and K. F. Austen, *Nature* (London), **293**, 103 (1981).
2) H. Metzger, G. Alcaraz, R. Hohman, J. P. Kinet, U. Pribluda and R. Quarto, *Ann. Rev. Immunol.*, **4**, 419 (1986).
3) E. L. Barusumian, C. Isersky, M. G. Petrino and R. P. Siraganian, *Eur. J. Immunol.*, **11**, 317 (1981).
4) U. S. Pribluda and H. Metzger, *J. Biol. Chem.*, **262**, 11449 (1987).
5) T. Meyer, D. Holowka and L. Stryer, *Science*, **240**, 653 (1988).
6) B. I. Kanner and H. Metzger, *J. Biol. Chem.*, **259**, 10188 (1984).
7) F. C. Mohr and C. Fewtrell, *J. Cell Biol.*, **104**, 783 (1987).
8) E. Middleton, Jr., G. Drzewiecki and D. Triggle, *Biochem. Pharmacol.*, **30**, 2867 (1981).
9) R. Teshima, K. Suzuki, H. Ikebuchi and T. Terao, *Mol. Immunol.*, **23**, 279 (1986).
10) R. Teshima, H. Ikebuchi, S. Sekita, S. Natori and T. Terao, *Int. Arch. Allergy Appl. Immunol.*, **78**, 237 (1985).
11) K. Kato, M. Nakanishi, Y. Arata, R. Teshima, T. Terao and H. Miyamoto, *J. Biochem.* (Tokyo), **102**, 1 (1987).
12) G. Grynkiewicz, M. Poenie and R. Y. Tsien, *J. Biol. Chem.*, **260**, 3440 (1985).
13) R. F. Stump, J. M. Oliver, E. J. Cragoe, Jr. and G. G. Deanin, *J. Immunol.*, **139**, 881 (1987).
14) J. R. Cunha-Melo, N. M. Dean, J. D. Moyer, K. Maeyama and M. A. Beaven, *J. Biol. Chem.*, **262**, 11455 (1987).
15) H. Hidaka, M. Inagaki, S. Kawamoto and Y. Sasaki, *Biochemistry*, **23**, 5036 (1984).
16) H. Streb, R. F. Irvine, M. J. Berridge and I. Schulz, *Nature* (London), **306**, 67 (1984).
17) M. J. Berridge, *Biochem. J.*, **220**, 345 (1984).
18) M. J. Berridge and R. F. Irvine, *Nature* (London), **341**, 197 (1989).
19) G. M. Burgess, P. P. Godfrey, J. S. McKinney, M. J. Berridge, R. F. Irvine and J. W. Putney, Jr., *Nature* (London), **309**, 63 (1984).
20) N. Mazurek, P. Bashkin, A. Loyter and I. Pecht, *Proc. Natl. Acad. Sci. U.S.A.*, **80**, 6014 (1983).
21) A. Zschauer, C. van Breemen, F. R. Buhler and M. T. Nelson, *Nature* (London), **334**, 703 (1988).
22) R. Penner, G. Matthews and E. Neher, *Nature* (London), **334**, 499 (1988).
23) T. Tamaoki, H. Nomoto, I. Takahashi, Y. Kato, M. Morimoto and F. Tomita, *Biochem. Biophys. Res. Commun.*, **135**, 397 (1986).
24) R. V. K. Vegesna, H.-L. Wu, S. Mong and S. T. Crooke, *Mol. Pharmacol.*, **33**, 537 (1988).
25) S. P. Watson, J. McNally, L. J. Shipman and P. P. Godfrey, *Biochem. J.*, **249**, 345 (1988).
26) T. Sako, A. I. Tauber, A. Y. Jeng, S. H. Yuspa and P. M. Blumberg, *Cancer Res.*, **48**, 4646 (1988).
27) H. Nakano, E. Kobayashi, I. Takahashi, T. Tamaoki, Y. Kuzuu and H. Ibe, *J. Antibiot.*, **40**, 706 (1987).
28) S. G. Ward, D. Cantrell and J. Westwick, *FEBS Lett.*, **239**, 363 (1988).
29) M. Kubbies, B. Goller, E. Russmann, H. Stockinger and W. Scheuer, *Eur. J. Immunol.*, **19**, 1393 (1989).
30) W. Siffert and J. W. N. Akkerman, *Nature* (London), **325**, 456 (1987).
31) R. Sagi-Eisenberg and I. Pecht, *Immunol. Lett.*, **8**, 237 (1984).
32) R. Sagi-Eisenberg, H. Lieman and I. Pecht, *Nature* (London), **313**, 59 (1985).
33) R. Teshima, K. Suzuki, H. Ikebuchi and T. Terao, *Mol. Immunol.*, **26**, 641 (1989).
34) T. Asano and H. Hidaka, *J. Pharmacol. Exp. Ther.*, **231**, 141 (1984).

Synthesis of an Immunologically Active Fragment Analog of Prothymosin α with Enhanced Enzymatic Stability[1)]

Takashi ABIKO* and Hiroshi SEKINO

Kidney Research Laboratory, Kojinkai, 1-6 Tsutsujigaoka 2-chome, Miyagino-ku, Sendai 980, Japan. *Received September 10, 1990*

A fragment analog, [D-Arg^{30}]prothymosin α fragment 1—30, containing D-arginine in place of arginine residue at position 30 was synthesized by the liquid phase procedure and studied for immunological effect on the impaired blastogenic response of T-lymphocytes isolated from uremic patients after treatment of human serum. Deacetyl-thymosin α_1, a synthetic octaeicosapeptide corresponding to deacetyl-prothymosin α fragment 1—28, has restoration ability for the impaired blastogenic response of T-lymphocytes of uremic patients but is susceptible to proteolytic digestion. On the other hand, the fragment analog, [D-Arg^{30}]prothymosin α fragment 1—30 retained activity and was shown to exhibit a high degree of stability when incubated in human serum. These results indicate that N-terminal acetylation and the introduction of D-residue into the C-terminal residue of prothymosin α fragment 1—30 increase resistance to proteolytic degradation by exopeptidases.

Keywords [D-Arg^{30}]prothymosin α fragment 1—30 synthesis; trifluoromethanesulfonic acid deprotection; impaired T-lymphocyte blastogenic response; human serum treatment; restoration ability; enzymatic stability

Thymosin α_1, an N-terminal acetylated peptide containing 28 amino acid residues, was isolated from calf thymus by Goldstein and coworkers.[2)] Thymosin α_1 was found to be one of the factors that modulated steps in the maturation of T-lymphocytes.[3)]

We have demonstrated that not only deacetyl-thymosin α_1 but also C-terminal sequences (regions 14—28 and 19—28) exhibit partial activity when compared to the complete sequence in the restoration of E-rosette-forming ability of human peripheral T-lymphocytes of patients suffering from impaired immunological function due to minimal change nephrotic syndrome or chronic renal failure.[4-6)] In our previous paper,[7)] we suggested that the acetyl group at the N-terminal Ser residue of thymosin α_1 is not required for increasing the activity of E-rosette-forming lymphocytes.

In 1984, prothymosin α containing 113 amino acid residues with the thymosin α_1 sequence at its N-terminus was isolated from rat thymus.[8)] Preliminary observations indicated that prothymosin α was also active in impaired immunological functions.[8)] It is obvious that deacetyl-thymosin α_1 corresponding to the N-terminal octaeicosapeptide of deacetyl-prothymosin α reproduces all the immunological activity of thymosin α_1, yet its susceptibility to rapid degradation by proteolytic enzymes precludes oral dosage and the maintenance of significant blood levels. Those facts suggest that deacetyl-thymosin α_1 might be rapidly broken down by proteolytic enzymes in plasma, but slow infusion protocols were necessary to achieve an adequate immunological effect in many cases.

The practical difficulties of slow infusion could be overcome by design of an N-terminal prothymosin α fragment analog which contains an active region of thymosin α_1 having the identical spectrum of biological activity but with enhanced stability to enzymatic degradation.

Following our solution syntheses of thymosin α_1 fragments[4-6)] and deacetyl-thymosin α_1,[7)] we wish to report the solution synthesis of a prothymosin α fragment analog 1—30 in which the C-terminal arginine of the fragment is replaced by enzymatically stable D-arginine, and the *in vitro* effect of our synthetic deacetyl-thymosin α_1[7)] and [D-Arg^{30}]prothymosin α fragment 1—30 on the impaired blastogenic response of T-lymphocytes of uremic patient after treatment of human serum.

In contrast to our previous syntheses of thymosin α_1 fragments[4-6)] and deacetyl-thymosin α_1,[7)] the thioanisole-mediated trifluoromethanesulfonic acid (TFMSA) deprotection procedure[9,10)] was applied in the final step in place of catalytic hydrogenation or hydrogen fluoride.

The synthetic strategy for [D-Arg^{30}]prothymosin α fragment 1—30 was almost the same as for the previously reported deacetyl-thymosin α_1 and the synthetic route is outlined in Fig. 2. As shown, the TFA-labile Z(OMe) or Boc group for N$^{\alpha}$-protection and amino acid derivatives bearing protecting groups removable by 1 M TFMSA–thioanisole in TFA[9,10)] were employed, *i.e.*, Lys(Z), Glu(OBzl), Asp(OBzl) and D-Arg(Mts)OBzl. Ser and Thr residues were not protected. Of five fragments used in the present synthesis, fragments [2], [3] and [4] are identical with those employed for deacetyl-thymosin α_1 synthesis.[7)] The other two fragments, [1] and [5] were newly prepared.

The substituted hydrazine, Troc-NHNH$_2$,[11)] was employed for the preparation of fragments [4] and [5] containing the Asp(OBzl) and Glu(OBzl) residues. This Troc group is known to be cleaved by Zn[12)] in AcOH without affecting other functional groups.

Throughout the syntheses of these intermediates and fragments, the purity of every intermediate was checked by thin-layer chromatography (TLC), elemental analysis and amino acid analysis. The analytical results were within ±0.4% of theoretical values in all cases.

Starting from H–D-Arg(Mts)–OBzl, fragment [1], Z(OMe)–Val–Glu(OBzl)–Glu(OBzl)–Ala–Glu(OBzl)–Asn–Gly–D-Arg(Mts)–OBzl, was prepared by stepwise elongation using the Su active ester procedure[13)] except for

$$\overset{1}{\text{Ac–Ser}}\text{–Asp–Ala–Ala–}\overset{5}{\text{Val}}\text{–Asp–Thr–Ser–Ser–}\overset{10}{\text{Glu}}\text{–Ile–Thr–Thr–Lys–}\overset{15}{\text{Asp}}\text{–Leu–Lys–Glu–Lys–}\overset{20}{\text{Lys}}\text{–Glu–Val–Val–Glu–}\overset{25}{\text{Glu}}\text{–Ala–Glu–Asn–Gly–}\overset{30}{\text{Arg}}\text{–}$$

Fig. 1. N-Terminal Sequence of Prothymosin α 1—30

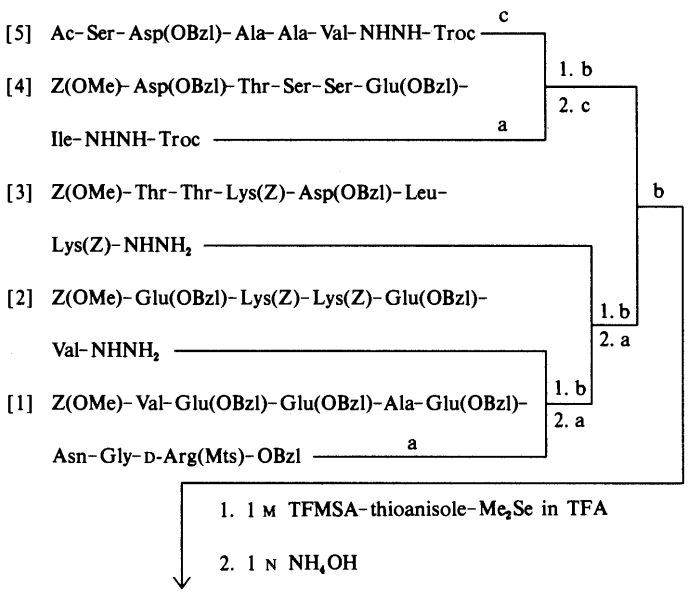

Fig. 2. Synthetic Route to [D-Arg^{30}]prothymosin α Fragment 1—30
a, TFA-anisole; b, azide; c, Zn-AcOH.

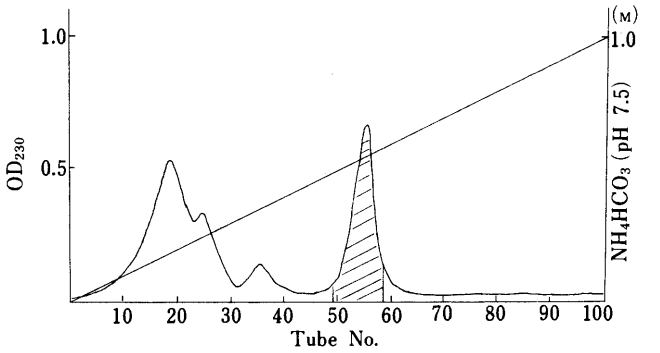

Fig. 3. Purification of Synthetic [D-Arg^{30}]prothymosin α Fragment 1—30 by Ion-Exchange Chromatography on a DEAE-Cellulose Column

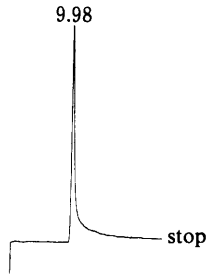

Fig. 4. HPLC of the Synthetic [D-Arg^{30}]prothymosin α Fragment 1—30

introduction of Asn residue, for which the NP active ester procedure[14] was employed. Fragment [5], Ac–Ser–Asp(OBzl)–Ala–Ala–Val–NHNH–Troc, was prepared by the HOBT–WSCI procedure[15] of Ac–Ser–OH with a TFA-treated sample of Z(OMe)–Asp(OBzl)–Ala–Ala–Val–NHNH–Troc.[7] Fragment [5] was treated with Zn[12] in AcOH and DMF to remove the Troc group, and the last trace of zinc acetate was removed by treatment with EDTA to give Ac–Ser–Asp(OBzl)–Ala–Ala–Val–$NHNH_2$ in analytically pure form. The hydrazine test on the thin-layer chromatogram and elemental analysis data were consistent with homogeneity of the desired product.

The five fragments were assembled successively from the C-terminal fragment to the N-terminal fragment by the azide procedure[16] according to the routes illustrated in Fig. 2. The amount of the acyl component in each fragment condensation was increased from 2 to 3 eq as the chain elongation progressed in order to secure complete condensation. Low solubility of the generating intermediates in DMF was overcome by use of additional DMSO and NMP.

First, protected C-terminal octapeptide ester [1] was condensed successively with [2] and [3]. Next, the Troc group of Ac–(1—5)–NHNH–Troc [5] was removed by treatment with Zn/AcOH. The hydrazide thus obtained was condensed with [4] by the azide procedure to yield Ac–(1—11)–NHNH–Troc. The Troc group of Ac–(1—11)–NHNH–Troc was removed by treatment with Zn/AcOH. The resulting hydrazide was condensed with the protected C-terminal nonadecapeptide ester by the azide procedure to yield Ac–(1—30)–OBzl.

Throughout this synthesis, Gly or Ile was selected as a diagnostic amino acid in acid hydrolysis.

In the final step of the synthesis, the protected triacontapeptide ester was treated with 1 M TFMSA–thioanisole in TFA in the presence of Me_2Se. Me_2Se was employed to facilitate acidic cleavage of protecting groups.[17] The deprotected peptide was next precipitated with dry ether, converted to the corresponding acetate with Amberlite IRA-400 (acetate form) and then treated with 1 N NH_4OH at pH 8.0 to reverse a possible N→O shift[18] at the Ser and Thr residues.

The crude peptide was purified by gel-filtration on Sephadex G-25, followed by ion-exchange column chromatography on a diethylaminoethyl (DEAE)-cellulose column with linear gradient elution using pH 7.5 NH_4HCO_3 buffer, followed by preparative TLC. Desalting on a Sephadex G-25 column gave a fluffy powder, which exhibited a single

Table I. Effect of the Synthetic [D-Arg^{30}]prothymosin α Fragment 1—30 and Deacetyl-thymosin α_1 on the Impaired PHA-Stimulation of T-Lymphocytes of Uremic Patients after Treatment of Human Serum

Peptide	Dose (μg/ml)	SI[a,b]
—[c]	—	279.5±50.1
—[d]	—	110.5±49.3[g]
Deacetyl-thymosin α_1[d,e]	5	219.6±51.4[h]
[D-Arg^{30}]prothymosin α fragment 1—30[d,e]	5	213.9±50.2[h]
Deacetyl-thymosin α_1[d,f]	5	108.1±48.9[h]
[D-Arg^{30}]prothymosin α fragment 1—30[d,f]	5	202.6±50.5[h]

a) Each value represents the mean±S.D. of triplicate measurements. *b*) SI (stimulation index) was calculated according to the following formula: $SI = ((I_2 - I_0)/(I_1 - I_0)) \times 100$, where I_2 = mean fluorescence intensity of PHA-activated lymphocytes, I_1 = fluorescence intensity of PHA-nonactivated lymphocytes and I_0 = fluorescence intensity of ethidium bromide. *c*) Normal venous lymphocytes. *d*) Patient's venous lymphocytes. *e*) Incubation was carried out at 37 °C in a humidified atmosphere of 5% CO_2 in air for 12 h using each synthetic peptide without treatment of human serum. *f*) Each synthetic peptide was incubated in human serum at 37 °C for 30 min and then lymphocytes were incubated with one of the human serum treated peptides at 37 °C for 12 h. *g*) $p<0.05$, when compared to the normal persons using Student's *t* test. *h*) $p<0.01$, when compared to the uremic patients using Student's *t* test.

chlorine–tolidine-positive spot on TLC in two different solvent systems and on paper electrophoresis (pH 7.4 pyridinium–acetate buffer). Its purity was further confirmed by amino acid analysis after acid hydrolysis. The peptide also exhibited a single peak on HPLC (Fig. 4).

The immunological effect of the synthetic [D-Arg^{30}]-prothymosin α fragment 1—30 and deacetyl-thymosin α_1[7] was examined by means of the JIMRO (Japan Immunoresearch Laboratories Co., Ltd.) fluorometric blast-formation test according to Itoh and Kawai.[19] Responses of T-lymphocytes to mitogenic stimulation were lower in uremic patients than those of normal persons. The *in vitro* effect of these two synthetic peptides after treatment of human serum on the impaired PHA response of T-lymphocytes from the uremic patients is shown in Table I.

Comparison of the stimulation index (SI) values of the blastogenic transformation of T-lymphocytes into lymphoblasts with mitotic activity upon PHA stimulation shows that restorative effect on both peptides, [D-Arg^{30}]prothymosin α fragment 1—30 and deacetyl-thymosin α_1, was approximately equal in potency without incubation with human serum. The synthetic [D-Arg^{30}]prothymosin α fragment 1—30, however, still demonstrated a restorative effect in the uremic patients investigated after treatment of human serum, although the restorative effect after incubation in human serum was a little weaker than that of the same peptide without incubation.

In contrast, *in vitro* addition of the synthetic deacetyl-thymosin α_1 after treatment of human serum had no effect on the mitotic activity induced by PHA stimulation under the same conditions.

These results seem to suggest that N-terminal acetylation and the introduction of D-Arg into the C-terminal residue of prothymosin α fragment 1—30 increase resistance to inactivation by enzyme degradation.

Experimental

General experimental procedures used were essentially the same as previously described.[4-7,20] Melting points are uncorrected. Rotations were measured with an Atago Polax machine (cell length: 10 cm). The amino acid compositions of the acid hydrolysates were determined with a Hitachi 835-50 type amino acid analyzer. Solutions were concentrated in a rotary evaporator under reduced pressure at a temperature of 30—45 °C. Z(OMe) or Boc groups of the protected peptides were removed by TFA–anisole treatment. The resulting amino components were chromatographed on silica gel plates (Kieselgel G, Merck) and Rf^1 values refer to the following solvent system: $CHCl_3$–MeOH–H_2O (8 : 3 : 1). The final product, [D-Arg^{30}]prothymosin α fragment 1—30, was chromatographed on cellulose plates (Merck). Rf^2 value refers to BuOH–AcOH–H_2O (4 : 1 : 5) and Rf^3 value refers to BuOH–pyridine–AcOH–H_2O (30 : 20 : 6 : 24).[21] Kits for the fluorometric blast-formation test were purchased from Japan Immunoresearch Laboratories Co., Ltd., Japan. Patient selection: Two uremic patients who were suffering from recurrent infectious diseases were selected. Examination of cellular immunocompetence of these patients revealed significant decrease in blast-formation by PHA. ^{3}H-Thymidine incorporation values of these patients were 12340 and 11639 cpm, respectively (normal values: 36480—38346 cpm). Venous blood was obtained from these uremic patients for the fluorometric blast-formation test. Venous blood samples from two healthy donors were used as a control and for stability studies for the synthetic peptides. The fluorescence excitation spectrum was measured with an Oyo-Bunko ULOG-FLOUSPEC 11 A fluorometer. HPLC was conducted with a Shimadzu LC-3A apparatus equipped with a YMC AM-312 column. Azides were prepared according to Honzl and Rudinger[16] with isoamyl nitrite. Preparations of protected intermediates were repeated several times in order to obtain sufficient quantities for the next step.

Z(OMe)–Gly–D-Arg(Mts)–OBzl [I] H–D-Arg(Mts)–OBzl (2.7 g) was dissolved in DMF (20 ml). To this solution, Z(OMe)–Gly–OSu (1.9 g) was added, and the mixture was stirred at room temperature for 6 h. The product was extracted with EtOAc and the extract was washed successively with 5% citric acid, H_2O, 5% $NaHCO_3$ and H_2O, dried over $MgSO_4$ and then concentrated *in vacuo*. The residue was reprecipitated from EtOAc with *n*-hexane: Yield 2.9 g (82%), mp 103—108 °C, $[\alpha]_D^{21}$ +9.8° (c=1.0, DMF), Rf^1 0.69, single ninhydrin-positive spot. *Anal.* Calcd for $C_{33}H_{41}N_5O_8S \cdot H_2O$: C, 57.80; H, 6.32; N, 10.21. Found: C, 57.51; H, 6.64; N, 10.38.

Boc–Asn–Gly–D-Arg(Mts)–OBzl [II] I (2.3 g) was treated with TFA–anisole (20 ml–4 ml) in an ice-bath for 40 min, and TFA was then removed by evaporation. The residue was washed with *n*-hexane, dried over KOH pellets *in vacuo* for 2 h, and then dissolved in DMF (20 ml) containing NMM (0.5 ml). To this solution, Boc–Asn–ONp (1.3 g) was added, and the mixture was stirred at room temperature for 7 h. The reaction mixture was diluted with 1 N NH_4OH (5 ml) with stirring to saponify the unchanged *p*-nitrophenyl ester. After 1 h, the mixture was extracted with EtOAc, and the extract was washed successively with 1 N NH_4OH, H_2O, 5% citric acid and H_2O, dried over $MgSO_4$ and then concentrated *in vacuo*. The residue was reprecipitated from EtOAc with *n*-hexane: Yield 2.1 g (84%), mp 110—117 °C, $[\alpha]_D^{21}$ −4.2° (c=1.0, DMF), Rf^1 0.59, single ninhydrin-positive spot. *Anal.* Calcd for $C_{33}H_{47}N_7O_9S \cdot 2H_2O$: C, 52.58; H, 6.82; N, 13.01. Found: C, 52.62; H, 7.13; N, 12.79.

Z(OMe)–Glu(OBzl)–Asn–Gly–D-Arg(Mts)–OBzl [III] II (1.9 g) was treated with TFA–anisole (19 ml–3.8 ml) as described above and the resulting powder was dissolved in DMF (19 ml) containing NMM (0.3 ml). To this solution, Z(OMe)–Glu(OBzl)–OSu (1.5 g) was added, and the solution was stirred at room temperature for 6 h. The mixture was extracted with EtOAc, and the extract was washed successively with 5% citric acid, H_2O, 5% $NaHCO_3$ and H_2O, dried over $MgSO_4$ and then concentrated *in vacuo*. The residue was reprecipitated from EtOAc with ether: Yield 2.2 g (85%), mp 134—139 °C, $[\alpha]_D^{21}$ −8.2° (c=1.0, DMF), Rf^1 0.65, single ninhydrin-positive spot. *Anal.* Calcd for $C_{49}H_{60}N_8O_{13}S \cdot 2H_2O$: C, 56.75; H, 6.22; N, 10.80. Found: C, 56.49; H, 6.45; N, 10.94.

Z(OMe)–Ala–Glu(OBzl)–Asn–Gly–D-Arg(Mts)–OBzl [IV] This compound was prepared in essentially the same manner as described for the preparation of III using III (2.1 g) and Z(OMe)–Ala–OSu (770 mg). The product was reprecipitated from EtOAc with ether: Yield 1.8 g (82%), mp 124—131 °C, $[\alpha]_D^{21}$ −12.4° (c=1.0, DMF), Rf^1 0.69, single ninhydrin-positive spot. *Anal.* Calcd for $C_{52}H_{65}N_9O_{14}S$: C, 58.25; H, 6.11; N, 11.75. Found: C, 57.90: H, 6.44; N, 11.89.

Z(OMe)–Glu(OBzl)–Ala–Glu(OBzl)–Asn–Gly–D-Arg(Mts)–OBzl [V] This compound was prepared from IV (1.5 g) and Z(OMe)–Glu(OBzl)–OSu (783 mg) essentially as described for the preparation of III. The product was reprecipitated from MeOH with ether: Yield 1.5 g (79%), mp 131—137 °C, $[\alpha]_D^{21}$ −15.4° (c=1.0, DMF), Rf^1 0.71, single ninhydrin-positive spot. *Anal.* Calcd for $C_{64}H_{78}N_{10}O_{17}S \cdot 3H_2O$: C, 57.31; H, 6.29; N, 10.41. Found: C, 56.88; H, 6.43; N, 10.26.

Z(OMe)–Glu(OBzl)–Glu(OBzl)–Ala–Glu(OBzl)–Asn–Gly–D-Arg(Mts)–OBzl [VI] V (1.4 g) was treated with TFA–anisole (14 ml–2.8 ml) as described above and the resulting powder was dissolved in DMF (14 ml) containing NMM (0.12 ml). To this solution, Z(OMe)–Glu(OBzl)–OSu (548 mg) was added, and the mixture was stirred at room temperature for 7 h. The mixture was poured into an ice-chilled 5% citric acid with stirring. The precipitate thereby formed was washed successively with 5% citric acid, H_2O, 5% $NaHCO_3$ and H_2O. The product was reprecipitated from AcOH with H_2O: Yield 1.3 g (81%), 146—152 °C, $[\alpha]_D^{21}$ −10.4° (c=1.0, DMF), Rf^1 0.65, single ninhydrin-positive spot. *Anal.* Calcd for $C_{76}H_{91}N_{11}O_{20}S \cdot 2H_2O$: C, 59.02; H, 6.19; N, 9.96. Found: C, 58.79; H, 6.34; N, 9.48.

Z(OMe)–Val–Glu(OBzl)–Glu(OBzl)–Ala–Glu(OBzl)–Asn–Gly–D-Arg(Mts)–OBzl [1] This compound was prepared in essentially the same manner as described for the preparation of VI using VI (1.2 g) and Z(OMe)–Val–OSu (320 mg). The product was recrystallized from hot EtOAc: Yield 1.1 g (85%), mp 139—147 °C, $[\alpha]_D^{21}$ −12.9° (c=1.0, DMF), Rf^1 0.72, single ninhydrin-positive spot. *Anal.* Calcd for $C_{81}H_{100}N_{12}O_{21}S \cdot 4H_2O$: C, 57.85; H, 6.47; N, 9.99. Found: C, 57.72; H, 6.79; N, 10.17.

Ac–Ser–Asp(OBzl)–Ala–Ala–Val–NHNH–Troc [5] Z(OMe)–Asp(OBzl)–Ala–Ala–Val–NHNH–Troc[7] (818 mg) was treated with TFA–anisole (8 ml–1.6 ml) as usual and the resulting powder was dissolved in DMF (8 ml) containing NMM (0.12 ml). To this ice-chilled solution, Ac–Ser–OH (129 ml), HOBT (149 mg) and WSCI (211 mg) were successively added. After having been stirred at 4 °C for 8 h, the mixture was extracted with

EtOAc, and the extract was washed successively with 5% citric acid, H_2O, 5% $NaHCO_3$ and H_2O, dried over $MgSO_4$, and then concentrated *in vacuo*. The residue was reprecipitated from EtOAc with ether: Yield 709 mg (87%), mp 106—114 °C, $[\alpha]_D^{21}$ −21.3° (c=1.0, DMF), Rf^1 0.60, single chlorine–tolidine-positive spot. *Anal.* Calcd for $C_{30}H_{42}Cl_3N_7O_{11}\cdot 2H_2O$: C, 43.99; H, 5.66; N, 11.97. Found: C, 43.72; H, 5.90; N, 12.28.

Ac-Ser-Asp(OBzl)-Ala-Ala-Val-NHNH$_2$ [VII] Ac-Ser-Asp(OBzl)-Ala-Ala-Val-NHNH-Troc (638 mg) in a mixture of AcOH (4 ml) and DMF (4 ml) was treated with Zn dust (540 mg) at 4 °C for 2 h and then at room temperature for 8 h. The solution was filtered, the filtrate was concentrated *in vacuo*, and the residue was treated with 3% EDTA to form a powder, which was washed with 5% $NaHCO_3$ and H_2O. The product was recrystallized from MeOH: Yield 502 mg (96%), mp 146—152 °C, $[\alpha]_D^{21}$ −17.6° (c=1.0, DMF), Rf^1 0.52, single hydrazine-test-positive spot. *Anal.* Calcd for $C_{27}H_{41}N_7O_9\cdot H_2O$: C, 51.83; H, 6.93; N, 15.67. Found: C, 51.59; H, 7.26; N, 15.92.

Ac-Ser-Asp(OBzl)-Ala-Ala-Val-Asp(OBzl)-Thr-Ser-Ser-Glu(OBzl)-Ile-NHNH-Troc [VIII] Z(OMe)-Asp(OBzl)-Thr-Ser-Ser-Glu(OBzl)-Ile-NHNH-Troc [4] (1.2 g) was treated with TFA–anisole (12 ml–2.4 ml) as described above. The N^a-deblocked peptide was dissolved in DMF (12 ml) containing NMM (0.12 ml). The azide [prepared from 1.3 g of VII (2 eq)] in DMF (7 ml) and NMM (0.31 ml) were added to the above ice-chilled solution and the mixture, after being stirred at −10 °C for 48 h, was acidified with a few drops of AcOH. The mixture was poured into ice-chilled 5% citric acid with stirring. The precipitate thereby formed was washed successively with 5% citric acid, H_2O, 5% $NaHCO_3$ and H_2O. The product was purified by column chromatography on silica gel (2.3 × 56 cm), equilibrated and eluted with $CHCl_3$–water-saturated BuOH (1 : 2). The desired fractions (4 ml each, tube Nos. 24—31) were combined and the solvent was removed by evaporation. Then, ether was added to the residue to obtain a precipitate: Yield 1.1 g (65%), mp 119—127 °C, $[\alpha]_D^{21}$ −13.3° (c=1.0, DMF), Rf^1 0.65, single chlorine–tolidine-positive spot. *Anal.* Calcd for $C_{69}H_{94}Cl_3N_{13}O_{24}\cdot 5H_2O$: C, 49.16; H, 6.22; N, 10.53. Found: C, 48.82; H, 6.51; N, 10.53. Amino acid ratios in a 6 N HCl hydrolysate: Ile 1.00, Ala 2.03, Val 0.93, Ser 2.87, Thr 0.93, Glu 0.92, Asp 1.97 (recovery of Ile 84%).

Ac-Ser-Asp(OBzl)-Ala-Ala-Val-Asp(OBzl)-Thr-Ser-Ser-Glu(OBzl)-Ile-NHNH$_2$ [IX] This compound was prepared from VIII (1 g) and Zn dust (385 mg) essentially as described for the preparation of VII. The product was recrystallized from MeOH: Yield 638 mg (72%), mp 138—146 °C, $[\alpha]_D^{21}$ +15.8° (c=1.0, DMSO), Rf^1 0.59, single hydrazine-test-positive spot. *Anal.* Calcd for $C_{66}H_{93}N_{13}O_{22}\cdot 4H_2O$: C, 53.11; H, 6.82; N, 12.20. Found: C, 52.73; H, 6.95; N, 12.49.

Z(OMe)-Glu(OBzl)-Lys(Z)-Lys(Z)-Glu(OBzl)-Val-Val-Glu(OBzl)-Glu(OBzl)-Ala-Glu(OBzl)-Asn-Gly-D-Arg(Mts)-OBzl [X] [5] (1 g) was treated with TFA–anisole (10 ml–2 ml) as usual and dissolved in DMF–DMSO (1 : 1, 10 ml) containing NMM (0.08 ml). The azide [prepared from 1.5 g of Z(OMe)-(18—22)-NHNH$_2$ (2 eq)] in DMF–DMSO (1 : 1, 10 ml) and NMM (0.14 ml) were added to the above ice-chilled solution and the mixture was stirred at −10 °C for 48 h until the solution became ninhydrin-negative. After addition of a few drops of AcOH, the mixture was poured into 5% citric acid with stirring. The resulting powder was washed with 5% citric acid, H_2O and MeOH and purified by gel-filtration on Sephadex LH-20 (3.0 × 90 cm) using DMF–DMSO (1 : 1) containing 2% H_2O as an eluent. The desired fractions (each 5 ml, tube Nos. 47—58) were combined, the solvent was evaporated off, and the residue was treated with MeOH to afford a power: Yield 1.2 g (71%), mp 159—167 °C, $[\alpha]_D^{21}$ −15.2° (c=1.0, DMSO), Rf^1 0.62, single ninhydrin-positive spot. *Anal.* Calcd for $C_{138}H_{171}N_{19}O_{34}S\cdot 7H_2O$: C, 59.24; H, 6.66; N, 9.51. Found: H, 58.90; H, 6.93; N, 9.28. Amino acid ratios in a 6 N HCl hydrolysate: Gly 1.00, Ala 1.04, Val 1.94, Glu 4.93, Asp 0.97, Lys 1.91, Arg 0.91 (recovery of Gly 83%).

Z(OMe)-Thr-Thr-Lys(Z)-Asp(OBzl)-Leu-Lys(Z)-Glu(OBzl)-Lys(Z)-Lys(Z)-Glu(OBzl)-Val-Val-Glu(OBzl)-Glu(OBzl)-Ala-Glu(OBzl)-Asn-Gly-D-Arg(Mts)-OBzl [XI] X (1 g) was treated with TFA–anisole (10 ml–2 ml) as usual and dissolved in DMF–DMSO (1 : 1, 10 ml) containing NMM (0.05 ml). The azide [prepared from 920 mg of Z(OMe)-(12—17)-NHNH$_2$ (2 eq)] in DMF–DMSO (1 : 1, 9 ml) and NMM (0.12 ml) were added to the above ice-chilled solution and the mixture was stirred at −10 °C for 48 h until the solution became ninhydrin-negative. After addition of a few drops of AcOH, the mixture was poured into 5% citric acid. The resulting powder was purified in the same manner as the preparation of X: Yield 957 mg (69%), mp 142—151 °C, $[\alpha]_D^{21}$ −26.1° (c=1.0, DMSO), Rf^1 0.73, single ninhydrin-positive spot. *Anal.* Calcd for $C_{191}H_{243}N_{27}O_{48}S\cdot 9H_2O$: C, 59.14; H, 6.79; N, 9.75. Found: C, 58.87; H, 6.96; N, 9.49. Amino acid ratios in a 6 N HCl hydrolysate: Gly 1.00, Ala 1.01, Val 1.92, Leu 0.94, Thr 1.88, Glu 4.96, Asp 1.94, Lys 3.93, Arg 0.92 (recovery of Gly 82%).

Ac-Ser-Asp(OBzl)-Ala-Ala-Val-Asp(OBzl)-Thr-Ser-Ser-Glu(OBzl)-Ile-Thr-Thr-Lys(Z)-Asp(OBzl)-Leu-Lys(Z)-Glu(OBzl)-Lys(Z)-Lys(Z)-Glu(OBzl)-Val-Val-Glu(OBzl)-Glu(OBzl)-Ala-Glu(OBzl)-Asn-Gly-D-Arg(Mts)-OBzl [XII] XI (388 mg) was treated with TFA–anisole (4 ml–0.8 ml) as usual and dissolved in DMF–NMP (1 : 1, 4 ml) containing NMM (0.01 ml). The azide [prepared from 299 mg of Ac-(1—11)-NHNH$_2$ (2 eq)] in DMF–NMP (1 : 1, 3 ml) and NMM (0.03 ml) were added to the above ice-chilled solution and the mixture was stirred at −10 °C for 48 h. Additional azide (1 eq) in DMF–NMP (1 : 1, 2 ml) and NMM (0.01 ml) were then added and stirring was continued for an additional 24 h until the solution became ninhydrin-negative. After addition of a few drops of AcOH, the mixture was poured into 5% citric acid with stirring. The resulting powder was purified in a manner similar to that described for the preparation of X: Yield 187 mg (37%), mp 167—175 °C, $[\alpha]_D^{21}$ −26.4° (c=1.0, DMSO), Rf^1 0.76, single chlorine–tolidine-positive spot. *Anal.* Calcd for $C_{248}H_{324}N_{38}O_{67}S\cdot 10H_2O$: C, 58.16; H, 6.77; N, 10.39. Found: C, 58.02; H, 6.95; N, 10.17. Amino acid ratios in a 6 N HCl hydrolysate: Gly 1.00, Ala 3.04, Val 2.92, Leu 0.94, Ile 0.95, Ser 2.92, Thr 2.93, Asp 4.03, Glu 5.87, Lys 4.03, Arg 0.96 (recovery of Gly 85%).

Ac-Ser-Asp-Ala-Ala-Val-Asp-Thr-Ser-Ser-Glu-Ile-Thr-Thr-Lys-Asp-Leu-Lys-Glu-Lys-Lys-Glu-Val-Val-Glu-Glu-Ala-Glu-Asn-Gly-D-Arg-OH [XIII] The protected triacontapeptide ester XII (100 mg) was treated with 1 M TFMSA–thioanisole in TFA (4 ml) in the presence of Me_2Se (100 μl) in an ice-bath for 110 min, then dry ether was added. The resulting powder was collected by centrifugation, dried over KOH pellets for 2 h and dissolved in 1 N AcOH (5 ml). After being stirred with Amberlite IRA-400 (acetate form, approximately 1 g) for 30 min, the solution was adjusted to pH 8.0 with 1 N NH_4OH and after 30 min to pH 6.0 with 1 N AcOH. The crude peptide was purified by gel-filtration on Sephadex G-25 (3.6 × 91 cm) using 2% AcOH as an eluent. The fractions (5 ml each) corresponding to the front main peak (tube Nos. 56—65, determined by ultraviolet absorption measurement at 230 nm) were combined and the solvent was removed by lyophilization to give a fluffy powder. The product was dissolved in H_2O (3 ml) and the solution was applied to a column of DEAE-cellulose (Brown, 2.3 × 14 cm), which was eluted with a linear gradient of 300 ml each of H_2O–0.1 M NH_4HCO_3 buffer at pH 7.5. Individual fractions (5 ml each) were collected and the absorbance at 230 nm was measured. Main peak fractions of the gradient eluates (tube Nos. 49—58) were combined and the solvent was evaporated *in vacuo*. Analysis by TLC revealed the presence of two chlorine–tolidine-positive spots with Rf^2 0.05 (main) and 0.29 (minor). The crude product was dissolved in a small amount of water and subjected to preparative TLC (cellulose plate, 20 × 40 cm) using the upper layer of BuOH–AcOH–H_2O (4 : 1 : 5) solvent system as a developing solvent. The zone corresponding to Rf^2 0.05 was separated and extracted with 2% AcOH. The extracts were concentrated to a small volume, applied to a column of Sephadex G-25 (3.6 × 91 cm) and eluted with 2% AcOH as described above and the solvent was removed by lyophilization: Yield 10.2 mg (15%), $[\alpha]_D^{21}$ −72.9° (c=0.3, 2% AcOH), Rf^2 0.05, Rf^3 0.11, single ninhydrin-positive spot. The synthetic peptide exhibited a single spot on a paper electrophoresis; Toyo Roshi No. 51 (2 × 40 cm), pyridinium–acetate buffer at pH 7.4, mobility 1.9 cm from the origin toward the anode after running at 2 mA, 650 V for 90 min. Amino acid ratios in a 6 N HCl hydrolysate: Gly 1.00, Ala 3.02, Val 2.96, Leu 0.98, Ile 1.03, Ser 2.92, Thr 2.94, Asp 3.97, Glu 6.05, Lys 3.92, Arg 0.94 (recovery of Gly 84%). The synthetic peptide exhibited a single peak on HPLC using an analytical YMC AM-312 column (6.0 × 150 mm) at a retention time of 9.98 min, when eluted with a gradient of acetonitrile 30 to 45% in 0.1% TFA at a flow rate of 1 ml per min (Fig. 4).

Stability Studies of the Two Synthetic Peptides 1. Treatment with Human Serum: The synthetic peptides were treated with human serum to evaluate the preservation of their immunological activity. Blood was collected from normal healthy volunteers in serum separation tubes (Beckton–Dickson SST vacutainer brand tubes No. 6572) and allowed to clot at room temperature. The tubes were then centrifuged at 2000 × *g* for 15 min and the serum immediately transferred to sterile conical centrifuge tubes (Corning No. 25310) and placed on ice. Peptide solutions (1.0 mg/ml) in 0.01 M sodium phosphate buffer (pH 7.4) were prepared. To 900 μl of serum in 1.5 ml polypropyrene centrifuge tubes equilibrated at 37 °C was added 50 μg of peptide solution. The mixture was incubated at 37 °C for 30 min and then the pH of the solution was adjusted to acidic area with dil. AcOH and lyophilized.

2. Fluorometric Blast-Formation Test: A 3-ml aliquot of venous blood from uremic patients was drawn into a syringe containing 25 U/ml of heparin and then mixed with 3 ml of PBS. Lymphocytes were isolated in Hypaque–Ficoll gradient.[22] Isolated lymphocytes were adjusted to 1.0×10^6/ml with PBS. The lymphocytes were cultured in 0.5 ml of RPMI 1640 (Gibco) with FCS (Dainippon Pharmaceutical Co.) in microplates. Cultures of each combination were incubated at 37 °C in the presence of the peptide in a humidified atmosphere of 5% CO_2 in air for 12 h and PHA (0.125%, 0.5 ml) was added to each well. Incubation was continued under the same conditions for 60 h. T-Lymphocytes in each well were transferred to a test tube and centrifuged for 10 min at 240 *g*, then the supernatant was removed. A 2 ml aliquot of 0.125% SDS was added to the residue and stirred for 20 min at room temperature; lymphocytes were completely destroyed and solubilized by this procedure. Ethidium bromide solution was added to the above solution and the mixture was stirred for 15 min at room temperature. The fluorescence excitation spectrum was measured according to Itoh and Kawai.[19]

References and Notes

1) Abbreviations used: TFA, trifluoroacetic acid; Z, benzyloxycarbonyl; OBzl, benzyl ester; Mts, mesityl-2-sulfonyl; Z(OMe), *p*-methoxybenzyloxycarbonyl; Ac, acetyl; Troc, β,β,β-trichloroethoxycarbonyl; NMM, *N*-methylmorpholine; OSu, *N*-hydroxysuccinimide ester; Su, *N*-hydroxysuccinimide; NP, *p*-nitrophenyl; ONP, *p*-nitrophenyl ester; DMF, dimethylformamide; DMSO, dimethylsulfoxide; AcOH, acetic acid; MeOH, methanol; EDTA, ethylenediaminetetraacetic acid; HOBT, *N*-hydroxybenzotriazole; WSCI, 1-ethyl-3-(3-dimethylaminopropyl)carbodiimide; EtOAc, ethyl acetate; HPLC, high-performance liquid chromatography; PHA, phytohemagglutinin; SDS, sodium dodecyl sulfate; PBS, phosphate-buffered saline; NMP, *N*-methyl-2-pyrrolidone; Boc, *tert*-butoxycarbonyl; E-rosette, a rosette with sheep erythrocytes; RPMI, Rosewell Park Memorial Institute.
2) J. A. Hooper, M. C. DcDaniel, G. B. Thurman, G. H. Cohen, R. S. Schulof and A. L. Goldstein, *Ann. N. Y. Acad. Sci.*, **249**, 125 (1975).
3) R. S. Schulof and A. L. Goldstein, *The Lymphokines*, **18**, 397 (1981).
4) T. Abiko, I. Onodera and H. Sekino, *Chem. Pharm. Bull.*, **27**, 3171 (1979).
5) T. Abiko, H. Sekino and H. Higuchi, *Chem. Pharm. Bull.*, **28**, 3411 (1980).
6) T. Abiko, I. Onodera and H. Sekino, *Chem. Pharm. Bull.*, **28**, 3542 (1980).
7) T. Abiko and H. Sekino, *Chem. Pharm. Bull.*, **30**, 1776 (1982).
8) A. A. Haritos, G. J. Goodall and B. L. Horecker, *Proc. Natl. Acad. Sci. U.S.A.*, **81**, 1008 (1984).
9) Y. Kiso, S. Nakamura, K. Ito, K. Ukawa, K. Kitazawa, T. Akita and H. Moritoki, *J. Chem. Soc., Chem. Commun.*, **1979**, 971; H. Yajima and N. Fujii, *J. Am. Chem. Soc.*, **103**, 5867 (1981).
10) H. Yajima, N. Fujii, H. Ogawa and H. Kawatani, *J. Chem. Soc., Chem. Commun.*, **1974**, 107.
11) H. Yajima and Y. Kiso, *Chem. Pharm. Bull.*, **19**, 420 (1971).
12) R. B. Woodward, K. Heusler, J. Gosteri, P. Naegeli, W. Oppolzer, R. Ramage, S. Rangnathan and H. Vorbrüggen, *J. Am. Chem. Soc.*, **88**, 852 (1966).
13) G. W. Anderson, J. E. Zimmerman and F. Callahan, *J. Am. Chem. Soc.*, **85**, 3039 (1963); *idem, ibid.*, **86**, 1839 (1964).
14) M. Bodanszky and V. du Vigneaud, *J. Am. Chem. Soc.*, **81**, 5688 (1959).
15) W. König and R. Gieger, *Chem. Ber.*, **106**, 3626 (1973).
16) J. Honzl and J. Rudinger, *Collect. Czech. Chem. Commun.*, **26**, 2333 (1961).
17) M. Shimokura, Y. Kiso, A. Nagata, M. Tsuda, H. Seki, N. Fujii and H. Yajima, *Chem. Pharm. Bull.*, **34**, 1841 (1986).
18) S. Sakakibara, "Chemistry and Biochemistry of Amino Acids, Peptides and Proteins," Vol. 1, ed. by B. Weinstein, Academic Press Inc., New York, 1971, p. 51.
19) Y. Itoh and T. Kawai, *Rinsho Kensa*, **27**, 982 (1983).
20) T. Abiko and H. Sekino, *Chem. Pharm. Bull.*, **37**, 391 (1989).
21) S. G. Walley and G. Watson, *Biochem. J.*, **55**, 328 (1953).
22) R. Harris and E. U. Ukaejiofo, *Br. J. Haematol.*, **18**, 229 (1970).

Barbaloin Stimulates Growth of *Eubacterium* sp. Strain BAR, a Barbaloin-Metabolizing Bacterium from Human Feces

Qing-Ming CHE,[a] Teruaki AKAO,[b] Masao HATTORI,[a] Yoshisuke TSUDA,[c] Tsuneo NAMBA,[a] and Kyoichi KOBASHI*,[b]

Research Institute for Wakan-Yaku (Traditional Sino-Japanese Medicines),[a] and Faculty of Pharmaceutical Sciences,[b] Toyama Medical and Pharmaceutical University, 2630 Sugitani, Toyama 930-01, Japan and Faculty of Pharmaceutical Sciences, Kanazawa University,[c] Takaramachi 13-1, Kanazawa 920, Japan. *Received September 10, 1990*

***Eubacterium* sp. strain BAR, isolated from human feces, transformed barbaloin to aloe-emodin anthrone in a basal medium lacking carbohydrate. Barbaloin remarkably stimulated the growth of strain BAR in the basal medium, the stimulative extent of the growth depending on the amount of barbaloin added. The addition of D-glucose, D-galactose, maltose, cellobiose, sucrose or D-amygdalin to the basal medium containing barbaloin caused a decrease of the growth stimulated by barbaloin to the growth level with each sugar, resulting in a complete inhibition of the barbaloin transformation. On the other hand, the addition of D-fructose, which itself stimulated the growth of strain BAR, further increased the growth in the presence of barbaloin and little inhibited barbaloin transformation. Nojirimycin bisulfite, a specific inhibitor of glucosidases, potently inhibited the growth with barbaloin, but did not affect the growth with glucose or cellobiose. Also, nojirimycin bisulfite completely inhibited the transformation of barbaloin to aloe-emodin anthrone.**

These results indicate that a unique enzyme capable of cleaving the *C*-glycosyl bond is induced in strain BAR by barbaloin and, consequently, strain BAR grows by utilizing as a nutrient the carbohydrate liberated from barbaloin. It is further suggested that the barbaloin-cleaving enzyme is inhibited by nojirimycin bisulfite and that the induction of the enzyme is repressed with D-glucose and D-galactose.

Keywords barbaloin; aloe-emodin anthrone; *Eubacterium* sp. strain BAR; intestinal bacteria; metabolism

Introduction

Barbaloin is a popular laxative from aloe, but is less purgative than sennosides, other popular laxatives from senna and rhubarb.[1-3] Aloe-emodin anthrone, an aglycone of barbaloin, shows weaker laxative action than rhein anthrone, the principal purgative of sennosides.[4,5] Therefore, aloe-emodin anthrone is considered to be the ultimate purgative of barbaloin. Intestinal flora play an important role in the transformation of sennosides to rhein anthrone.[6-15] We reported that barbaloin was also transformed to aloe-emodin anthrone by human intestinal flora.[16] However, the intestinal flora of rats and mice and 23 defined strains of human intestinal bacteria did not reveal any barbaloin-metabolizing activity.[16] The transformation of barbaloin to aloe-emodin anthrone seems to include a unique type of cleavage of the *C*-glycosyl bond. We isolated a new bacterium, called *Eubacterium* sp. strain BAR, capable of cleaving this bond of barbaloin from human feces.[17]

We describe here the stimulation of growth of strain BAR and the induction of a barbaloin-metabolizing enzyme by barbaloin.

Materials and Methods

Bacterium and Source *Eubacterium* sp. strain BAR capable of transforming barbaloin to aloe-emodin anthrone was isolated from human feces as described in a previous paper,[17] and maintained in a general anaerobic medium (GAM) or in a basal medium (PYF) containing barbaloin.

Cultivation *Eubacterium* sp. strain BAR precultured in PYF broth containing barbaloin was inoculated to PYF broth containing various compounds and then cultured at 37 °C in an anaerobic box. PYF broth contained 10 g of Trypticase (BBL Microbiology Systems, Cockeysville, Md.), 5 g of yeast extract, 40 ml of Fildes solution (peptic digest of human blood), 40 ml of salts solution (0.2 g of $CaCl_2$, 0.2 g of $MgSO_4$, 1 g of K_2HPO_4, 1 g of KH_2PO_4, 10 g of $NaHCO_3$, and 2 g of NaCl in liter) and 0.5 g of L-cysteine–HCl in 1 l, which was used as a basal medium for the growth experiment. Bacterial growth was monitored by measuring the absorbance at 540 nm.

Metabolism of Barbaloin by *Eubacterium* sp. Strain BAR *Eubacterium* sp. strain BAR was cultured anaerobically at 37 °C in PYF broth containing barbaloin with or without various carbohydrates. An aliquot (1 ml) of the culture was taken out at suitable intervals. One half was vigorously mixed with 0.5 ml of butanol and an aliquot (10 μl) of the butanol layer was analyzed for barbaloin and aloe-emodin anthrone by thin layer chromatography (TLC) as described below. The other half was mixed with 0.2 ml of 1% *N*,*N*'-dimethyl-*p*-nitrosoaniline in pyridine, and then mixed thoroughly with 0.5 ml of butanol. An aliquot (10 μl) of the butanol layer was analyzed for anil (adduct of aloe-emodin anthrone and *N*,*N*'-dimethyl-*p*-nitrosoaniline) by TLC as described below.

Thin Layer Chromatography TLC for barbaloin and aloe-emodin anthrone was performed on silica gel plates (silica gel F-254; layer thickness, 0.25 mm; Merck Co., Inc., Darmstadt, FRG) with the solvent system of chloroform–methanol–water (18:6:1). TLC for anil was performed on polyamide plates (Macherey-Nagel polyamide-6; layer thickness, 0.1 mm) with the solvent system of methanol–water (5:1). The amounts of barbaloin, aloe-emodin anthrone and anil were determined using calibration lines prepared with authentic samples as described previously.[17]

Protein Protein was determined by the method of Lowry *et al.*[18] Before the determination of bacterial proteins, *Eubacterium* sp. strain BAR cultured in broth containing barbaloin was harvested and then washed with ethanol to remove barbaloin and aloe-emodin anthrone.

Reagents Barbaloin was isolated from the powder of aloin which was purchased from Wako Pure Chemical Industries Ltd., Osaka, Japan, and purified by silica gel column chromatography, followed by repeated crystallization from ethanol. Nojirimycin bisulfite was synthesized as described.[19] D-Glucono-1,4-lactone was purchased from Sigma Chemical Co., St. Louis, MO., U.S.A. GAM was a product of Nissui Seiyaku Co., Tokyo, Japan. All other reagents were of the best available commercial quality.

Results

Stimulation of Growth of *Eubacterium* sp. Strain BAR by Barbaloin *Eubacterium* sp. strain BAR scarcely grew in PYF broth containing no carbohydrate, but its growth was stimulated remarkably by the addition of barbaloin, which was mostly transformed to aloe-emodin anthrone, as shown in Fig. 1. The transformation of barbaloin to aloe-emodin anthrone was in parallel to the growth. Moreover, the bacterial growth depended on the amount of barbaloin

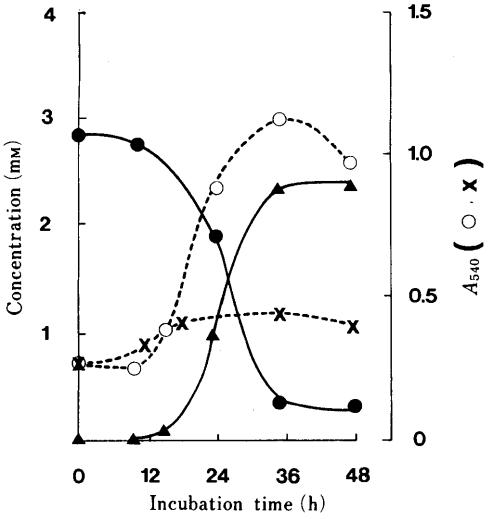

Fig. 1. Stimulation of Growth of Strain BAR by Barbaloin and Transformation of Barbaloin to Aloe-emodin Anthrone

Bacterial growth in PYF broth (×) and PYF broth containing 1 mg/ml barbaloin (○) was monitored by measuring turbidity at 540 nm. Concentrations of barbaloin (●) and aloe-emodin anthrone (▲) were measured as described in Materials and Methods.

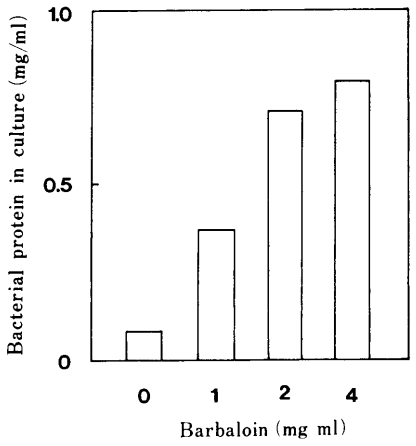

Fig. 2. Dose-Response of Growth Stimulation by Barbaloin

Barbaloin (0, 10, 20 and 40 mg) was added to 10 ml of PYF broth and then strain BAR was cultured for 2 d in an anaerobic box. After harvesting the cells by centrifugation, bacterial protein concentrations were measured.

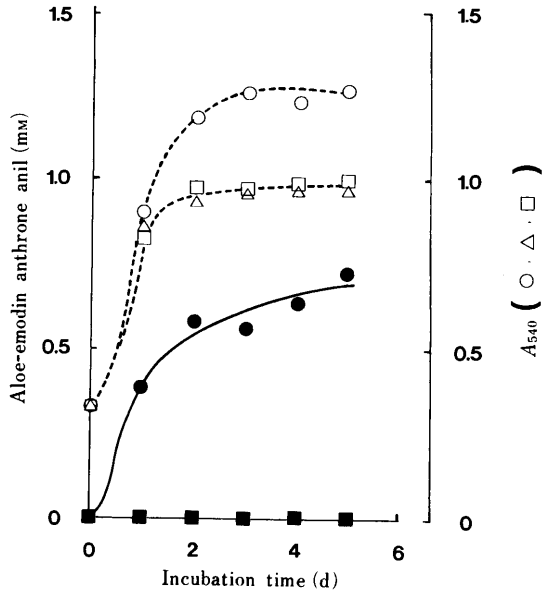

Fig. 3. Inhibition of Barbaloin-Stimulation of Growth and Barbaloin Transformation by Glucose

Strain BAR was cultured in PYF broth containing 0.5 mg/ml barbaloin (○), 0.5% glucose (△), or both of them (□), and the growth was monitored by measuring turbidity at 540 nm, respectively. Aloe-emodin anthrone anil in PYF broth containing barbaloin (●) or barbaloin + glucose (■), respectively, was measured as described in Materials and Methods.

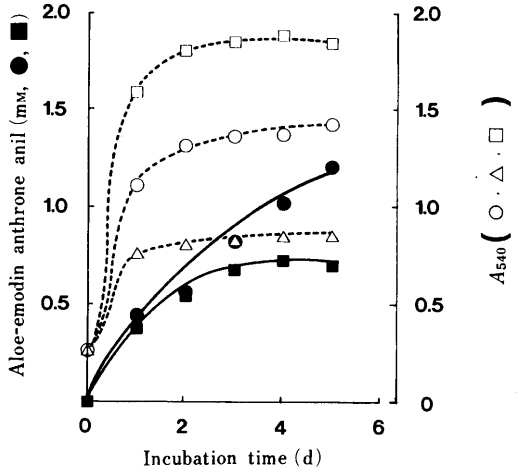

Fig. 4. Effect of Fructose on Barbaloin-Stimulation of Growth and Barbaloin Transformation

Strain BAR was cultured in PYF broth containing 0.5 mg/ml barbaloin (○, ●), 0.5% fructose (△) or both (□, ■). The experimental conditions were the same as in Fig. 3.

added to the medium (Fig. 2). These results suggest that *Eubacterium* sp. strain BAR utilizes barbaloin as a nutrient to grow.

Effects of Other Sugars on Barbaloin Metabolism *Eubacterium* sp. strain BAR in GAM broth, which contains D-glucose, grew well, but did not metabolize barbaloin at all as reported earlier.[17] Sugars such as D-glucose, D-galactose, D-fructose, maltose, cellobiose and sucrose stimulated the growth of strain BAR in PYF broth. D-Amygdalin also stimulated the growth, and barbaloin was the best stimulator of them all.

Addition of D-glucose, D-galactose, maltose, cellobiose, sucrose and D-amygdalin into PYF broth containing barbaloin inhibited the transformation of barbaloin to aloe-emodin anthrone, and also decreased the growth of strain BAR to the growth level found with the respective sugar. Figure 3 shows the effect of D-glucose as an example. D-Fructose, however, stimulated the growth in the presence of barbaloin but little inhibited the laxative's transformation (Fig. 4). Moreover, sugars such as D-xylose and L-rhamnose, which themselves hardly stimulated the growth of strain BAR in PYF broth, did not inhibit the barbaloin transformation (data not shown). These results suggest that barbaloin-metabolizing enzymes in strain BAR are induced by barbaloin and that their induction is repressed with D-glucose or D-galactose, but not with D-fructose.

Inhibition of Barbaloin Stimulation of Growth and of Barbaloin Metabolism by Nojirimycin Nojirimycin bisulfite, a specific inhibitor of glucosidases,[20] in a final concentration of more than 5×10^{-4} M completely inhibited the growth of strain BAR stimulated by barbaloin as shown in Fig. 5; the growth in broth containing D-glucose

or D-cellobiose was not affected by nojirimycin bisulfite at all, however, indicating that the inhibitor had no antibacterial action. I_{50} value of nojirimycin bisulfite against the growth was 8×10^{-6} M. The growth stimulated by barbaloin was not inhibited by D-glucono-1,4-lactone, a specific inhibitor of β-D-glucuronidases (data not shown).

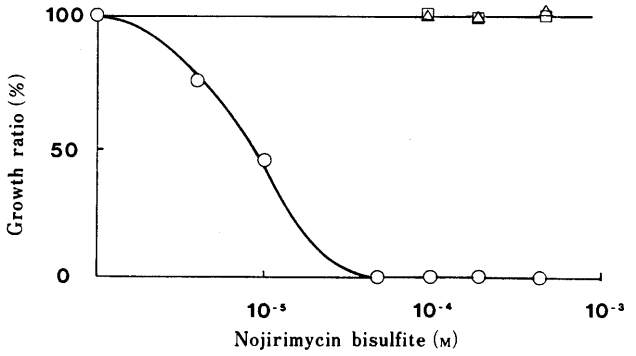

Fig. 5. Inhibition of Barbaloin-Stimulation of Growth by Nojirimycin

Strain BAR was cultured in the presence of various concentrations of nojirimycin bisulfite in PYF broth containing 0.5 mg/ml barbaloin (○), 0.5% glucose (△) or 0.5% cellobiose (□). The growth after cultivation for 2 d was monitored by measuring turbidity at 540 nm. The growth without nojirimycin bisulfite was indicated as 100%.

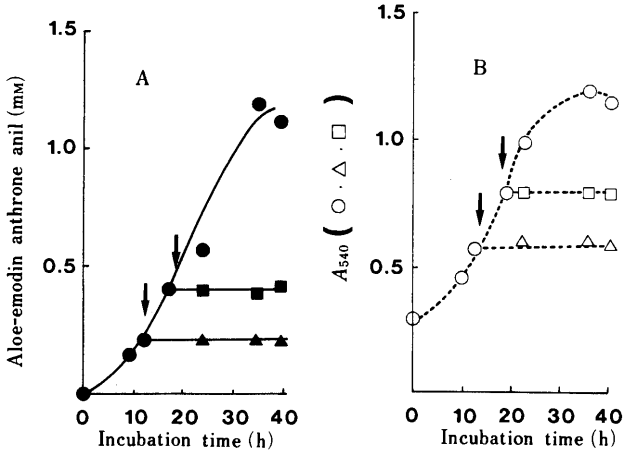

Fig. 6. Correlation of Barbaloin Cleavage and Growth

Strain BAR was cultured in PYF broth containing 0.5 mg/ml barbaloin. After cultivation for 11 h and 17 h (arrows), 2×10^{-4} mM nojirimycin bisulfite was added to the medium. Amount of anil (A) and turbidity at 540 nm (B) were measured as described in Materials and Methods.

Moreover, nojirimycin bisulfite completely inhibited the transformation of barbaloin to aloe-emodin anthrone in strain BAR as shown in Fig. 6. Thus, when nojirimycin bisulfite was added to the medium during the log phase of growth, both the growth of strain BAR and the barbaloin transformation were stopped. These results indicate that a barbaloin-metabolizing enzyme(s) capable of cleaving *C*-glycosyl bond is potently inhibited by nojirimycin and, consequently, the growth of strain BAR is interrupted. This enzyme cleaving the *C*-glycosyl bond may be a novel type of β-D-glucosidase.

Discussion

Barbaloin was reported to have appreciable purgative action in humans,[3] though weaker than sennoside. Human intestinal flora transformed barbaloin to aloe-emodin anthrone,[16] and *Eubacterium* sp. strain BAR having transforming capacity was isolated from human feces.[17] Aloe-emodin anthrone, which shows weak purgative action,[5] seems to be an ultimate purgative of barbaloin, in relation to the metabolic activation of sennoside.[6-15] This study indicated that barbaloin induced the metabolizing enzyme system and stimulated the growth of strain BAR. In general, rapidly growing bacteria seem predominant in the human intestine and strain BAR seems to be inferior in number because it grows very slowly (1—2 d, Fig. 1). However, when barbaloin is administered orally to humans as an aloe extract (an oriental medicine), the growth of barbaloin-metabolizing bacteria alone such as strain BAR may be stimulated. If human beings ingest barbaloin every day, barbaloin-transforming ability in a lower part of intestine will increase, because sugars such as D-glucose do not remain, being absorbed and metabolized in an upper part of intestine, and the bowels are gradually loosened due to the formation of aloe-emodin anthrone.

Many bacteria having potent β-D-glucosidase activities did not metabolize barbaloin at all,[17] and only *Eubacterium* sp. strain BAR cleaved the laxative's *C*-glycosyl bond. The barbaloin-cleaving enzyme in strain BAR was inhibited by nojirimycin bisulfite, a specific inhibitor of glucosidases (Fig. 6), and the induction of the enzyme was repressed by D-glucose. Accordingly, the enzyme cleaving *C*-glucosyl bond may be a novel type of β-D-glucosidase (Chart 1), but an attempt to identify the structure of liberated sugar from

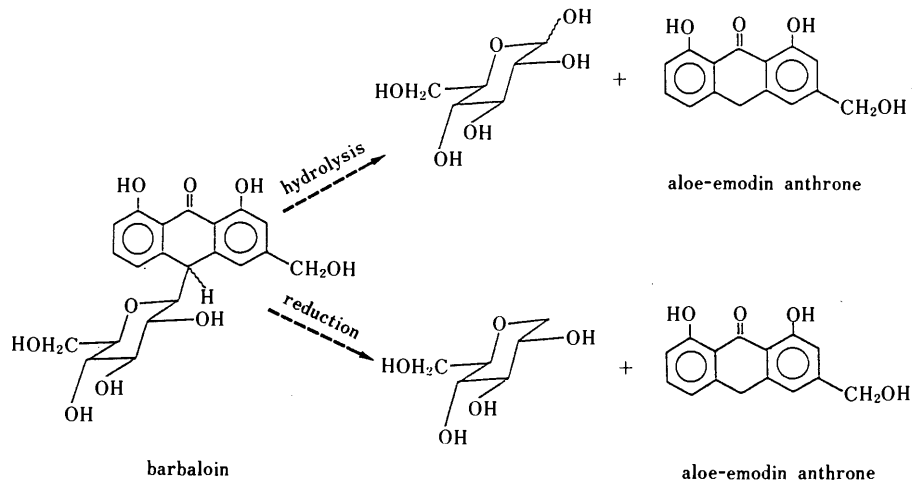

Chart 1. Two Possible Processes Cleaving *C*-Glycosyl Bond of Barbaloin

barbaloin was unsuccessful in this study. The possibility exists that the C(10)–C(1′) bond of barbaloin may be cleaved in a reductive manner similar to the cleavage of sennidine to rhein anthrone[14] (Chart 1).

Acknowledgement We are grateful to Nagase Science and Technology Foundation (Osaka, Japan) for partial financial support, and we thank Miss S. Takayanagi for her secretarial assistance.

References

1) J. W. Fairbairn, *Pharmacology*, **14** (Suppl. 1), 48 (1976).
2) F. H. L. Van Os, *Pharmacology*, **14** (Suppl. 1), 18 (1976).
3) Y. Ishii, H. Tanizawa, C. Ikemoto and T. Takino, *Yakugaku Zasshi*, **101**, 254 (1981).
4) K. Sasaki, K. Yamauchi and S. Kuwano, *Planta Med.*, **37**, 370 (1979).
5) D. D. Breimer and A. J. Baars, *Pharmacology*, **14** (Suppl. 1), 30 (1976).
6) J. W. Fairbairn and M. J. R. Moss, *J. Pharm. Pharmacol.*, **22**, 584 (1970).
7) J. W. Fairbairn, *Pharm. Weekbl.*, **100**, 1493 (1965).
8) H. Ippen and T. Montag, *Arch. Exp. Pathol. Pharmakol.*, **182**, 521 (1936).
9) J. Lemli and L. Lemmens, *Pharmacology*, **20**, 50 (1980).
10) M. Dressen, H. Eyssen and J. Lemli, *J. Pharm. Pharmacol.*, **33**, 679 (1981).
11) K. Kobashi, T. Nishimura, M. Kusaka, M. Hattori and T. Namba, *Planta Med.*, **40**, 226 (1980).
12) M. Hattori, G. Kim, S. Motoike, K. Kobashi and T. Namba, *Chem. Pharm. Bull.*, **30**, 1338 (1982).
13) T. Akao, T. Akao, K. Mibu, M. Hattori, T. Namba and K. Kobashi, *J. Pharmacobio-Dyn.*, **8**, 800 (1985).
14) T. Akao, K. Mibu, T. Erabi, M. Hattori, T. Namba and K. Kobashi, *Chem. Pharm. Bull.*, **35**, 1998 (1987).
15) M. Hattori, T. Namba, T. Akao and K. Kobashi, *Pharmacology*, **36**, (Suppl. 1), 172 (1988).
16) M. Hattori, T. Kanda, Y.-Z. Shu, T. Akao, K. Kobashi and T. Namba, *Chem. Pharm. Bull.*, **36**, 4462 (1988).
17) Q.-M. Che, T. Akao, M. Hattori, K. Kobashi and T. Namba, *Planta Med.*, in press (1991).
18) O. H. Lowry, N. J. Rosebrough, A. L. Farr and R. K. Randall, *J. Biol. Chem.*, **193**, 265 (1951).
19) Y. Tsuda, Y. Okuno and K. Kanemitsu, *Heterocycles*, **27**, 63 (1988).
20) T. Niwa, S. Inouye, T. Tsuruoka, K. Yoshihisa and T. Niida, *Agric. Biol. Chem.*, **34**, 966 (1970).

Pulmonary and Hepatic Disposition of Hippuryl-L-Histidyl-L-Leucine

Yusuke TANIGAWARA, Yan-Ling HE, Katsuhiko OKUMURA[1] and Ryohei HORI*

Department of Pharmacy, Kyoto University Hospital, Sakyo-ku, Kyoto 606, Japan. *Received July 16, 1990*

The pulmonary and hepatic clearances of the synthesized angiotensin converting enzyme (ACE) substrate, hippuryl-L-histidyl-L-leucine (HHL) were evaluated by applying the multiple sites of input method and the recirculation pharmacokinetic model. Rats received a constant rate infusion *via* the carotid artery, jugular vein or portal vein in the absence or presence of the ACE inhibitor, captopril. Blood samples were collected from the femoral artery. The organ extraction ratio was calculated from the steady-state plasma concentrations and the mean organ transit time was computed as the difference in the mean residence times for various administration routes. Pronounced elimination in the lung and liver was observed in the absence of captopril. Pulmonary metabolism was completely depressed in the presence of captopril while the hepatic elimination was little affected. This suggests that the pulmonary elimination was entirely ascribed to ACE while there exists an alternative elimination process in the liver. The mean cardiopulmonary transit time was very short, indicating the pulmonary elimination of HHL may take place on the surface of the vascular endothelium. The evaluation of the pulmonary elimination of HHL described in this paper indicates a simple *in vivo* method for assessing the pharmacological effect of ACE inhibitors. The present pharmacokinetic approach will be useful for the quantification of drug disposition in individual organs *in vivo*.

Keywords recirculation pharmacokinetics; moment analysis; mean transit time; multiple site input method; pulmonary metabolism; angiotensin converting enzyme; captopril

Introduction

Conventional pharmacokinetic studies are based on plasma concentrations in the peripheral veins following intravenous injection. It is well known, however, that drug disposition kinetics can be influenced by the sites of administration even when a drug is administered into the vessel, and that the venous plasma concentrations may be different from the arterial concentrations.[2,3] A pronounced arterial-venous difference was observed when pulmonary elimination took place.[4-6] Since in classical compartmental models, no distinction between arterial and venous blood has been taken into consideration and no attempt has been made to simulate the blood circulatory system, it has been impossible to analyze the influences of the injection or sampling sites. On the other hand, several investigators have described recirculation models in which drug concentration differences within the circulatory system were taken into account.[7-10] The recirculation model is useful for assessing individual organ clearance *in vivo* by the multiple sites of the input or sampling method, especially for drugs with short half-lives such as peptides or proteins.

Angiotensin I is converted to physiologically active angiotensin II primarily in pulmonary circulation.[11,12] The angiotensin converting enzyme (ACE) responsible for this hydrolysis is located along the luminal surface of the pulmonary vascular endothelial cells.[13,14] In this paper, we attempted to estimate ACE activity *in vivo* by application of the multiple sites of the input method and the recirculation pharmacokinetic model. A biologically inactive synthetic ACE substrate, hippuryl-L-histidyl-L-leucine (HHL) was used as a probe because biologically active substrates complicate the interpretation of the experimental results.[15] The clearance in the lung and liver was investigated in the absence or presence of the ACE inhibitor, captopril.

Materials and Methods

Materials HHL was obtained from Sigma Chemical Co., St. Louis, MO. and captopril was obtained from Sankyo Co., Tokyo. All other chemicals were of reagent grade.

Experiments Wistar male rats (250—280 g) were anesthetized with pentobarbital (40 mg/kg) administered i.p. Animals received heparin (1000 U/kg) and the right femoral artery was cannulated with polyethylene tubing (SP31, i.d. 0.50 mm, o.d. 0.80 mm, Natsume, Japan) for blood sampling. The protocol consisted of six separate experiments as follows.

Group A. Intra-arterial (i.a.) Administration ($n=7$): The left carotid artery was catheterized with SP31 polyethylene tubing so that the tip of the catheter lay near the aortic arch. Catheter placement was accomplished by placing the catheter tips a predetermined distance into the vessel. HHL in saline (8.15 mM) was infused at a constant rate of 2.77 μmol/min. Blood samples were withdrawn from the femoral artery at 1, 3, 5, 7, and 10 min after starting the infusion.

Group B. Intravenous (i.v.) Administration ($n=5$): The right jugular vein was catheterized with polyethylene tubing (PE10, i.d. 0.28 mm, o.d. 0.61 mm, Intramedic, Becton Dickinson & Co. N.J.) for the constant rate infusion of HHL solution (2.77 μmol/min). The tip of the jugular catheter laid near the entrance to the right atrium. The sampling schedule was the same as in group A.

Group C. Intra-portal vein (i.p.v.) Administration ($n=5$): The hepatoportal vein was catheterized with a straight needle (o.d. 0.4 mm, length 18 mm, Terumo, Japan), the other side of which was connected to SP31 tubing for the constant rate infusion of HHL solution (2.77 μmol/min). This catheterization avoided perturbation in the hepatoportal blood flow. Blood sampling was accomplished *via* a catheter placed in the femoral artery.

Group D. i.a. Administration in the Presence of Captopril ($n=5$): Rats received a priming dose of captopril (18.4 μmol/kg wt) *via* the femoral vein, followed by a constant rate i.v. infusion of captopril solution (5.06 μmol/h) throughout the experiment. This dose of captopril was determined according to the report of Koizumi and coworkers[16] to cause complete inhibition of ACE. 50 min after loading, an intra-arterial infusion of HHL was started and blood samples were collected as in group A.

Group E. i.v. Administration in the Presence of Captopril ($n=5$): Captopril was administered in the same manner as group D and HHL was infused intravenously as in group B.

Group F. i.p.v. Administration in the Presence of Captopril ($n=5$): Captopril was administered in the same manner as group D and HHL was infused into the hepatoportal vein as in group C.

Determination of HHL Concentration in Plasma Each blood sample was centrifuged at 10000 rpm for 1 min to separate the plasma (Eppendorf centrifuge 5415, FRG) immediately after sampling, then cooled to 0—5 °C in an ice-bath until assayed. The assay of HHL concentrations in plasma was carried out immediately after completing the animal experiments. 0.1 ml of plasma was transferred into centrifuge tubes and 0.2 ml of methanol was added for deproteinization. After vortex mixing, the samples were centrifuged at 3000 rpm for 20 min at 4 °C (Automatic refrigerated centrifuge 20 PR-52, Hitachi, Japan). 20 μl portions of supernatants were

subjected to the following analysis.

HHL concentrations were determined by reversed phase high performance liquid chromatography (HPLC). The chromatograph (Trirotar-II, Jasco, Japan) was equipped with a UV detector (UVIDEC-100 III, Jasco) adjusted to 235 nm. The stationary phase was octadecylsilane chemically bonded on silica gel (particle size 5 μm), packed in a 150 × 4.6 mm i.d. stainless steel column (Chemcosorb 5-ODS-H, Chemco, Japan). The mobile phase was a mixture of 10 mM phosphate buffer (pH 6.5) and acetonitrile (4 : 1, v/v) containing 12 mM tetra-*n*-butylammonium bromide (Nakarai Chemicals, Japan) and 1% (v/v) tetrahydrofuran. The flow rate was 1.0 ml/min and the retention times of HHL and the degradation product, hippuric acid were 11 min and 7.7 min, respectively. The peak area was quantified with an integrator (Chromatopac C-R1A, Shimadzu, Japan). The lower limit of the assay was 5 μM in plasma.

Pharmacokinetic Analysis The steady-state plasma concentration (C_{ss}) was computed by fitting the individual plasma concentration–time data to the following equation.

$$C_p = C_{ss}(1 - e^{-\lambda t}) \quad (1)$$

where λ is a parameter describing convex curves. The value of λ was converted to the mean residence time (MRT) using the relationship, $MRT = 1/\lambda$.[17]

A recirculation pharmacokinetic model has been developed to describe drug concentration differences within the circulatory system and to correlate the hemodynamics or individual organ extraction with clinically meaningful parameters such as total body clearance and volume of distribution. Figure 1 illustrates an outline of the blood circulation and the anatomical positions of several organs. Utilizing the network theory, the transfer function for the recirculating system ($H_{ix}(s)$) with administration into a site x is described as follows.[7]

$$H_{ix}(s) = H_x(s)/[1 - H(s)] \quad (2)$$

where $H(s)$ is the open loop transfer function of the circulatory system, which is the product of the transfer functions of the cardiopulmonary ($H_{pul}(s)$) and systemic circulations ($H_{sys}(s)$). $H_x(s)$ is the transfer function from the input site to the sampling site. The sampling site was fixed to the femoral artery in the present experiments. The transfer functions for the recirculating system following intraarterial ($H_{ia}(s)$), intravenous ($H_{iv}(s)$) or intra-portal vein ($H_{ipv}(s)$) administration are described as follows.

$$H_{ia}(s) = 1/[1 - H(s)] \quad (3)$$

$$H_{iv}(s) = H_{pul}(s)/[1 - H(s)] \quad (4)$$

$$H_{ipv}(s) = H_{hep}(s) \cdot H_{pul}(s)/[1 - H(s)] \quad (5)$$

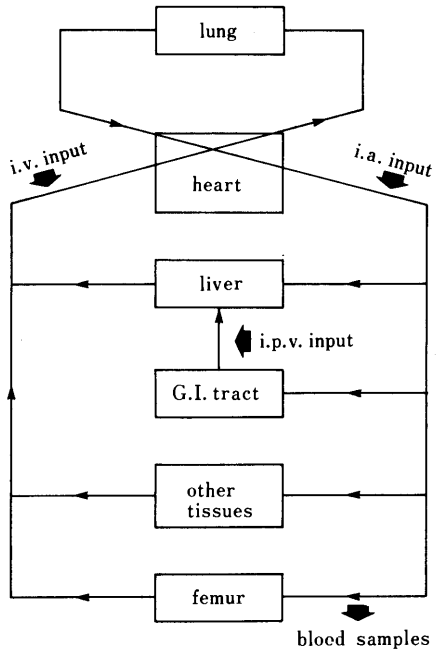

Fig. 1. Schematic Representation of the Circulatory System Showing the Sites of Drug Administration and Blood Sampling

i.v., intravenous; i.a., intra-arterial; i.p.v., intra-portal vein.

where $H_{hep}(s)$ is the transfer function for the hepatic circulation.

The basic pharmacokinetic characteristics (C_{ss} and MRT) evaluated from the plasma concentration profiles are related to the transfer function by the following equations.[7]

$$C_{ss,ix} = Ro/Q \lim_{s \to 0} H_{ix}(s) \quad (6)$$

$$MRT_{ix} = \lim_{s \to 0} -\mathrm{d}/\mathrm{d}s[\ln H_{ix}(s)] \quad (7)$$

where Ro and Q reveal the infusion rate and the cardiac output, respectively. The subscript ix denotes a specific input site. Substitution of Eqs. 3—5 into Eqs. 6—7 and rearrangement yield the following relationships.

$$E_{pul} = 1 - C_{ss,iv}/C_{ss,ia} \quad (8)$$

$$E_{hep} = 1 - C_{ss,ipv}/C_{ss,iv} \quad (9)$$

$$\bar{t}_{pul} = MRT_{iv} - MRT_{ia} \quad (10)$$

$$\bar{t}_{hep} = MRT_{ipv} - MRT_{iv} \quad (11)$$

where E_{pul} and E_{hep} are the extraction ratios for the cardiopulmonary and hepatic circulations, respectively, and $\bar{t}_{pul}$ and $\bar{t}_{hep}$ are the corresponding mean organ transit times. The pulmonary and hepatic clearances were calculated by multiplying the extraction ratio by the plasma flow rate. The volume of distribution at steady state (V_{ss}) was determined based on the i.a. data according to the non-compartmental method.[18,19]

Statistics Statistical analyses were performed by the one-way analysis of variance followed by the unpaired *t*-test. Differences between means were considered statistically significant if $p < 0.05$. All data calculations and statistical analyses were performed with the aid of a personal computer (PC-9801, NEC, Japan).

Results

Figure 2 illustrates the mean plasma concentration–time profiles during a constant rate infusion of HHL *via* i.a., i.v. and i.p.v. routes. A difference in plasma concentration was observed between i.v. and i.a. infusions, indicating substantial pulmonary elimination. Furthermore, a significant difference between i.v. and i.p.v. infusions was also observed, suggesting remarkable hepatic elimination at the first circulation through the liver.

The plasma concentration–time profiles in the presence of captopril are shown in Fig. 3. Unlike the control rats, the plasma concentration difference between i.a. and i.v. infusions disappeared, indicating that the pulmonary metabolism was completely inhibited by captopril. This effect indicates that the pulmonary metabolic activity is entirely attributable to ACE. The difference between i.v. and i.p.v., however, was not influenced by the presence of captopril. These results suggest that there is a difference between the lung and the liver in the metabolism of HHL.

Table I summarizes the disposition parameters of HHL.

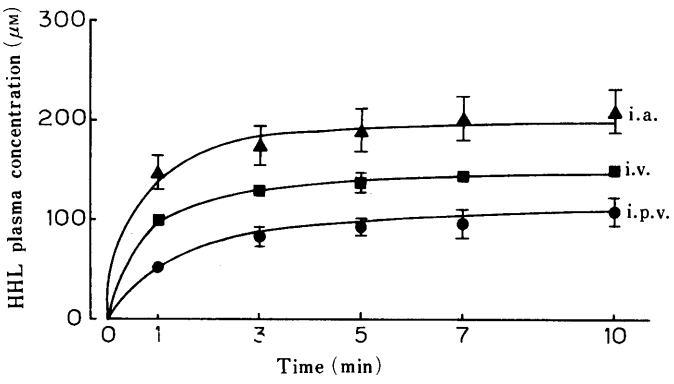

Fig. 2. Plasma HHL Concentrations during Constant Rate Infusion into the Carotid Artery (▲, $n=7$), Jugular Vein (■, $n=5$) or Portal Vein (●, $n=5$) in the Absence of Captopril

Data are reported as mean ± SEM.

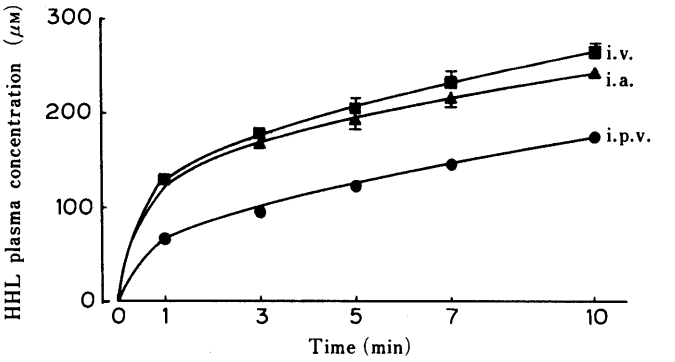

Fig. 3. Plasma HHL Concentrations during Constant Rate Infusion into the Carotid Artery (▲, $n=5$), Jugular Vein (■, $n=5$) or Portal Vein (●, $n=5$) in the Presence of Captopril

Data are reported as mean ± SEM.

TABLE I. Disposition Parameters of HHL following Continuous Infusion into the Carotid Artery, Jugular Vein or Portal Vein in the Absence and Presence of Captopril

	Control	Captopril-treatment
Steady-state plasma concentration (μM)		
i.a.	192.6 ± 28.1 ($n=7$)	218.4 ± 9.2 ($n=5$)
i.v.	138.0 ± 8.9 ($n=5$) [d) e)]	242.3 ± 12.4 ($n=5$)[g)] [e)]
i.p.v.	100.1 ± 14.9 ($n=5$)	189.5 ± 11.1 ($n=5$)[g)]
Extraction ratio[a)]		
Lung	0.284	
Liver	0.275	0.218
Organ clearance (ml/min)		
Lung[b)]	15.3	
Liver[c)]	2.45	1.94
Mean residence time (s)		
i.a.	49.6 ± 9.2 ($n=7$)	93.4 ± 10.6 ($n=5$)[f)]
i.v.	56.3 ± 4.6 ($n=5$) [d) e)]	112.3 ± 13.5 ($n=5$)[g)] [d)]
i.p.v.	99.6 ± 12.2 ($n=5$)	261.1 ± 50.2 ($n=5$)[f)]
Mean organ transit time (s)[a)]		
Lung	6.7	18.9
Liver	43.3	148.8

Values are means ± SEM. The number of animals for each group is represented in parenthesis. *a*) Estimated using the population mean of each group. *b*) 53.9 ml/min of cardiac output[33] was used to calculate the lung clearance. *c*) 8.9 ml/min of hepatic plasma flow[33] was used to calculate the hepatic clearance. *d*) Statistically different at $p<0.05$, *e*) $p<0.01$. *f*) Statistically different from control at $p<0.05$, *g*) $p<0.01$.

E_{pul} and E_{hep} were similar under the control conditions. In the presence of captopril E_{pul} vanished while E_{hep} remained unchanged. MRT_{ia}, MRT_{iv} and MRT_{ipv} were significantly prolonged by captopril treatment.

Discussion

The present study demonstrated that the biologically inactive synthetic ACE substrate, HHL, was significantly extracted at pulmonary and hepatic circulations. To confirm whether HHL was metabolized by the lung tissue or blood components, HHL was incubated at 37 °C with 10% lung homogenate or blood. No change in HHL concentration was observed during 60 min of incubation with rat blood. In contrast, when incubated with lung homogenate, HHL was metabolized rapidly and disappeared 30 min after incubation. Accordingly, the rapid elimination observed in this study is regarded as metabolism in the lung tissue rather than in the blood. Similar evidence that lung tissue can convert angiotensin I to angiotensin II has been reported.[20-24] Gillis and coworkers studied ACE activity *in vivo* by the double indicator dilution method.[25,26] Their approach was based on the direct determination of a single passage of a synthetic ACE substrate through the lung from the right atrium to the ascending aorta. In this paper, we applied the multiple sites of the input method and the recirculation pharmacokinetic model to evaluate *in vivo* organ clearance.

Although a statistical significance was not observed, the difference between MRT_{ia} and MRT_{iv} implied the mean cardiopulmonary transit time ($\bar{t}_{pul}$) of HHL. The value of 6.7 s was very short, suggesting that pulmonary extraction is a rapid process. This value of the mean cardiopulmonary transit time was similar to those reported for rabbits and lambs *in vivo* and for dogs *in vitro*.[26-28] In addition, comparable values of $\bar{t}_{pul}$ were obtained for HHL and T1824-labeled albumin in the preliminary experiment using the isolated perfused rat lung, which revealed that the volume of distribution of HHL was no larger than that of the vascular reference. This is consistent in that the V_{ss} of HHL (13.4 ml/rat) was almost similar to the plasma volume. Therefore, the pulmonary elimination of HHL is thought to occur on the surface of the vascular endothelium.

Since MRT_{ipv} was significantly different from MRT_{iv}, $\bar{t}_{hep}$ was obtained as a reliable value. The captopril treatment prolonged $\bar{t}_{hep}$ while there was little decrease in the E_{hep}. Previous studies on the distribution of ACE in the tissues of rat, rabbit, mouse and man, have shown that the enzyme is localized mainly on the surface of organ vascular endothelial cells.[29-32] In the absence of captopril, HHL may have been metabolized mainly by ACE on the surface of the hepatic vascular endothelium. On the other hand, in the presence of captopril, ACE was inhibited and HHL molecules were accessible to other enzymes. A prolonged $\bar{t}_{hep}$ suggests a change in plasma flow rate, and an unchanged E_{hep} implied that eliminating processes other than ACE contributed to the hepatic extraction of HHL in the presence of captopril.

The multiple sites of the input method and the recirculation pharmacokinetic model are theoretically applicable to both bolus injection and constant infusion study. However, no discussion has been attempted regarding the experimental design on applying this methodology. Since the plasma half-life of HHL was very short and its concentration fell quickly below the assay limit after bolus injection, only initial time profiles could be determined although a longer sampling time was necessary to evaluate the area under the curve or *MRT*. Furthermore, rapid injection often causes localized saturation because of incomplete mixing with the blood, though the maximal capacity of elimination is not reached. To overcome these shortcomings of the bolus study, the constant rate infusion experiment was performed for evaluating organ disposition of the drug with a short half-life.

In conclusion, the pulmonary and hepatic clearances of synthesized ACE substrate, HHL, were evaluated by applying the multiple sites of the input method and the recirculatory moment analysis. The evaluation of the pulmonary elimination of HHL described in this paper suggests a simple *in vivo* method for assessing the pharmacological effect of ACE inhibitors. The present pharmacokinetic approach will be useful for the quantifica-

tion of individual organ disposition *in vivo* of highly diffusible substances and further applicable for the evaluation of target organ directed drug delivery.

References

1) Present address: *Department of Pharmacy, Kobe University Hospital, Chuo-ku, Kobe 650, Japan.*
2) M. K. Cassidy and J. B. Houston, *Drug Metab. Dispos.*, **12**, 619 (1984).
3) M. Mistry and J. B. Houston, *Drug Metab. Dispos.*, **13**, 740 (1985).
4) W. L. Chiou, G. Lam, M. L. Chen and M. G. Lee, *Res. Commun. Chem. Pathol. Pharmacol.*, **32**, 27 (1981).
5) M.-L. Chen, G. Lam, M. G. Lee and W. L. Chiou, *J. Pharm. Sci.*, **71**, 1386 (1982).
6) R. M. Fieding, J. A. Waschek, D. J. Effeney, A. C. Pogany, S. M. Pond and T. N. Tozer, *J. Pharmacol. Exp. Ther.*, **236**, 97 (1986).
7) M. Weiss and W. Förster, *Eur. J. Clin. Pharmacol.*, **16**, 287 (1979).
8) M. Weiss, *J. Math. Biology.*, **15**, 305 (1982).
9) D. J. Cutler, *J. Pharmacokinet. Biopharm.*, **7**, 101 (1979).
10) D. P. Vaughan and I. Hope, *J. Pharmacokinet. Biopharm.*, **7**, 207 (1979).
11) K. K. F. Ng and J. R. Vane, *Nature* (London), **216**, 762 (1967).
12) P. Biron and C. G. Huggins, *Life Sci.*, **7**, 965 (1968).
13) J. W. Ryan, U. S. Ryan, D. R. Schultz, C. Whitaker, A. Chung and F. E. Dorer, *Biochem. J.*, **146**, 497 (1975).
14) U. S. Ryan, J. W. Ryan, C. Whitaker and A. Chiu, *Tissue & Cell*, **8**, 125 (1976).
15) H.-S. Cheung, F.-L. Wang, M. A. Ondetti, E. F. Sabo and D. W. Cushman, *J. Biol. Chem.*, **255**, 401 (1980).
16) M. Endoh, M. Suzuki, K. Katayama, M. Kakemi and T. Koizumi, *J. Pharmacobio-Dyn.*, **12**, 10 (1989).
17) K. Yamaoka, T. Nakagawa and T. Uno, *J. Pharmacokinet. Biopharm.*, **6**, 547 (1978).
18) M. Weiss, *J. Pharmacokinet. Biopharm.*, **12**, 167 (1984).
19) L. Z. Benet and R. L. Galeazzi, *J. Pharm. Sci.*, **68**, 1071 (1979).
20) Y. S. Bakhle, *Nature* (London), **220**, 919 (1968).
21) F. E. Dorer, J. R. Kahn, K. E. Lentz, M. Levine and L. T. Skeggs, *Biochim. Biophys. Acta*, **429**, 220 (1976).
22) T. Kokubu, E. Ueda, M. Ono, T. Kawabe, Y. Hayashi and T. Kan, *Eur. J. Pharmacol.*, **62**, 269 (1980).
23) K. Sakai, J. Aono, Y. Shiraki, Y. Hinohara, A. Akamatsu, S. Tanaka and K. Kuromaru, *Tohoku J. Exp. Med.*, **152**, 363 (1987).
24) B. Jackson, R. B. Cubela and C. I. Johnston, *J. Hypertension*, **6**, S51 (1988).
25) R. E. Howell, R. Moalli and C. N. Gillis, *J. Pharmacol. Exp. Ther.*, **228**, 154 (1984).
26) X. Chen, B. R. Pitt, R. Moalli and C. N. Gillis, *J. Pharmacol. Exp. Ther.*, **229**, 649 (1984).
27) B. R. Pitt and G. Lister, *J. Appl. Physiol.*, **57**, 1158 (1984).
28) B. L. Fanburg and J. B. Glazier, *J. Appl. Physiol.*, **35**, 325 (1973).
29) S. M. Danilov, A. I. Faerman, O. Y. Printseva, A. V. Martynov, I. Y. Sakharov and I. N. Trakht, *Histochemistry*, **87**, 487 (1987).
30) S. Antoniello, M. Auletta, V. Vatiero, C. Nigro and L. Cacciatore, *Enzyme*, **40**, 14 (1988).
31) P. Caldwell, B. Seegal, K. Hsu, M. Dos and R. Soffer, *Science*, **191**, 1050 (1976).
32) R. Auerbach, L. Alby, J. Grieves, J. Joseph, C. Lindgren, L. W. Morrissey, Y. A. Sidky, M. Tu and S. L. Watt, *Proc. Natl. Acad. Sci. U.S.A.*, **79**, 7891 (1982).
33) S. Ishise, B. L. Pegram, J. Yamamoto, Y. Kitamura and E. D. Frohlich, *Am. J. Physiol.*, **239**, H443 (1980).

Comparison of Cross-Reactivities of Imipenem and Other Beta-Lactam Antibiotics by Delayed-Type Hypersensitivity Reaction in Guinea Pigs

Naoki NAGAKURA,*[,a] Shinji SOUMA,[a] Tadayori SHIMIZU,[a] Katsuji UNO[b] and Yasutake YANAGIHARA[a]

Department of Microbiology, School of Pharmaceutical Sciences, University of Shizuoka,[a] 395 Yada, Shizuoka 422, Japan and Pharmacy, Suibarago Hospital,[b] Okayama-cho 13–23, Suibara-machi, Kitakanbara-gun, Niigata 959–21, Japan. *Received August 2, 1990*

The cross-reactivity of imipenem (IPM) in a delayed-type hypersensitivity (DTH) reaction was investigated by intradermal skin reaction, macrophage migration inhibition tests (MIT) and lymphocyte stimulation tests (LST) in guinea pigs. The animals were immunized with IPM, ampicillin (ABPC) or cephalexin (CEX) using Freund's complete adjuvant. Three sensitized-drugs exhibited the same immunogenicity in the skin reaction. The cross-reactivities in skin reaction among IPM, sulbactam, aztreonam, ABPC and 6-aminopenicillanic acid as penam, and CEX, ceftizoxime, 7-aminocephalosporanic acid as cephem were examined. IPM did not show cross-reactions with any of the tested drugs in three sensitized groups, indicating that the drugs possessed no cross-reactivity with tested beta-lactams in DTH.

In MIT, 4 or 5 of 6 animals reacted to be sensitized drugs in each group. The cross-reactivity of IPM- and ABPC-sensitized groups in MIT was similar to that of a skin reaction, however, the CEX-sensitized animals showed broad cross-reactions. Using a kind of test drug, one or two animals in the ABPC-sensitized group showed migration enhancement, but IPM- or CEX-sensitized animals did not exhibit migration enhancement. In LST, most of the animals tested exhibited lymphocyte prolifration by sensitized drugs but a cross-reaction was scarcely observed. The above results suggest that among beta-lactams, IPM has a very low cross-reactivity. LST is considered to be more a useful assay than MIT for *in vitro* identification of causative drugs in animal models.

Keywords beta-lactam; imipenem; delayed-type hypersensitivity; guinea pig; intradermal skin test; macrophage migration inhibition test; lymphocyte stimulation test

Introduction

Allergic reactions are known to be a common side effect of beta-lactam antibiotics. They are generally divided into two categories of immediate-type hypersensitivity (ITH) associated with humoral antibody-mediated immunity and delayed-type hypersensitivity (DTH), associated with cell-mediated immunity.[1,2] It has been shown that cellular immunity plays an important role in allergic reactions induced by beta-lactams.[2–4] We previously investigated the immunological properties of DTH reaction induced by a cephalexin such as beta-lactam in guinea pig[5] and examined the cross-reactivities among penams and cephems by intradermal skin reaction and the leucocyte migration test (LMT) using spleen cells.[6] However, the results of cross-reactivity of skin reaction and LMT showed some differences.

Recently, imipenem is widely used because of its high bactericidal potency. The cross-reactivity of imipenem and other beta-lactams in ITH has been reported,[7,8] however, that of imipenem in DTH has not been thoroughly studied. In this paper, we investigated the cross-reactivity of imipenem by an intradermal skin test as *in vivo* assay for DTH and by the macrophage migration inhibition test (MIT) and lymphocyte stimulation test (LST) as *in vitro* assay for DTH in guinea pig. Furthermore, we here report the difference in cross-reactivity among beta-lactams between MIT and LST.

Materials and Methods

Animals Male outbred Hartley guinea pigs weighing 400—500 g were purchased from the Japan SLC Co. (Hamamatsu).

Antigens Imipenem (IPM) was received from Banyu Pharmaceutical Co. (Tokyo). Aztreonam (AZT) was obtained from Eizai Co., Ltd. (Tokyo). Sulbactam (SBT) was given from Pfizer Pharmaceutical Co., Ltd. (Tokyo). Ampicillin (ABPC), 6-aminopenicillanic acid (6APA) and 7-aminocephalosporanic acid (7ACA) were purchased from Sigma Chemical Co. (St. Louis, MO., U.S.A.). Cephalexin (CEX) was obtained

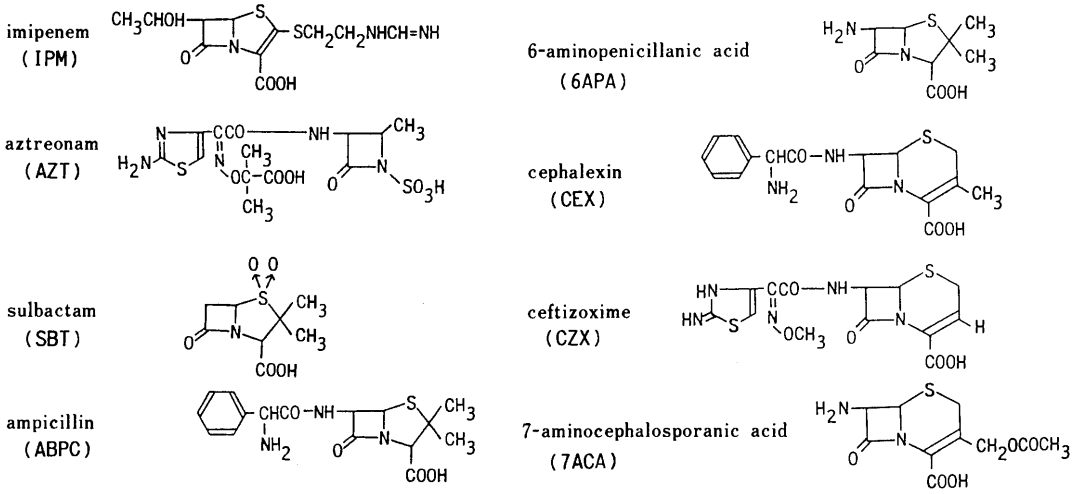

Fig. 1. Chemical Structures of Beta-Lactam Antibiotics Used

from Wako Pure Chemical Industries, Ltd. (Osaka). Ceftizoxime (CZX) was purchased from Fujisawa Pharmaceutical Co. (Osaka). Their chemical structures are shown in Fig. 1.

Immunization Each compound was dissolved in physiological saline (20 mg/ml) and emulsified with an equal volume of Freund's complete adjuvant (FCA) (Difco Laboratories, Detroit, MI., U.S.A.). Each footpad of the guinea pigs was injected intradermally (i.d.) with a total 0.5 ml of the emulsion on day 0. On day 14, each leg of the animals was injected intramuscularly (i.m.) with a total 0.4 ml of the emulsion.

Skin Test On day 20 or 27, one-tenth of a ml of pyrogen-free physiological saline of a non-irritating concentration (2 mg/ml) of tested drugs were injected i.d. into a shaved flank of the sensitized guinea pigs. At 24 h after the challenge, diameters of the erythematous area were measured with a caliper and mean values were obtained. Scoring was as follows: 0; ≤3 mm, 0.5; 3—5 mm, 1; 5—7 mm, 2; >7 mm.

Macrophage Migration Inhibition Test (MIT) MIT was performed according to the method of Mariam and Vaughan[9] with the following minor modifications. Peritoneal exudate cell (PEC) was induced by an i.p. injection of 20 ml of sterile paraffin-oil on day 25. The PEC was harvested on day 28 and washed with RPMI-1640 medium and suspended in TC-199 medium supplemented with kanamycin (60 μg/ml) and 10% horse serum. The cell viability was determined by trypan blue dye exclusion. Capillary tube (No. VCH075P, Terumo Co., Ltd., Tokyo) was filled with the cell suspension (1.5×10^7 cells/ml) by centrifugation and cut off at the boundary zone. The tube was placed into a chamber (leucocyte migration plate, Sterilin Ltd., Gelther, England). The chamber was filled with TC-199 medium supplemented with kanamycin, 10% horse serum and 5% guinea pig serum. Antigens were added to the medium at a concentration of 100 μg/ml. The chambers were sealed with a coverglass and incubated in an atmosphere of 95% air and 5% CO_2 at 37 °C for 24 h. The area of migration was measured and the migration index (M.I.) was calculated by the following formula.

$$\text{M.I.}(\%) = \frac{\text{(mean migration area with antigen)}}{\text{(mean migration area without antigen)}} \times 100$$

When a M.I. was 80 or less, it was interpreted as indicating the presence of a macrophage migration inhibition factor.[10] Also, when a M.I. was 120 or more, it was considered to be in the presence of a macrophage migration enhancement factor.[11]

Lymphocyte Stimulation Test (LST) LST was performed according to the method of Oort and Turk[12] with the following minor modification. Briefly, axial and inguinal lymph-nodes were removed from a sensitized animal on day 21. Single cell suspension was prepared by teasing the lymph-nodes apart with a slide glass. The lymphocytes were washed with RPMI-1640 medium and suspended in the medium supplemented with kanamycin (60 μg/ml) and 5% normal guinea pig serum. The cells (5×10^5/well) were cultured in a 96-well microplate (Falcon 3072, Becton Dickinson Co., Lincolin Park, N.J., U.S.A.) with or without antigen (50 μg/ml) in an atmosphere of 95% air and 5% CO_2 at 37 °C for 48 h. After an addition of 9.25 kBq (0.25 μCi) ^{3}H-thymidine (^{3}H-TdR: New England Nuclear Corp., Boston, MA., U.S.A.) to each well, the plate was further cultivated for 16 h. Lymphocytes were harvested with an automatic cell harvester. Radioactivity taken up by the cells was measured with a liquid scintillation counter and the stimulation index (S.I.) was calculated with the following formula.

$$\text{S.I.} = \frac{\text{mean cpm with antigen}}{\text{mean cpm without antigen}}$$

When a S.I. was 1.8 or more, it was considered to be a positive reaction.

Statistical Analysis Statistical differences were analyzed using unpaired Wilcoxon's test for skin reaction and Student's t test for LST and p-values of less than 0.05 were considered to be significant.

Results

Cross-Reactivities of IPM, ABPC and CEX by Intradermal Skin Test Cross-reactivities among the drugs were examined by a skin test. Each group showed almost the same score to the sensitized drug (Table I). The intensity of the skin reaction was somewhat stronger on day 28 than on day 21. IPM-sensitized animals reacted with IPM but did not exhibit the cross-reaction with other tested beta-lactams. The ABPC-sensitized group showed a weak cross-reaction with 6APA on day 21 and cross-reacted on day 28. The animals did not exhibit cross-reactivity with other tested drugs. CEX sensitized animals reacted with CEX on day 21 and 28. The animals showed a cross-reaction with 7ACA on day 28, but the score was insignificant.

TABLE I. Cross-Reactivities of Imipenem (IPM), Ampicillin (ABPC) and Cephalexin (CEX) by Intradermal Skin Test

Tested drugs	Sensitized drugs					
	IPM		ABPC		CEX	
	21[a]	28[a]	21[a]	28[a]	21[a]	28[a]
IPM	10[b]	11[b]	1	1	0	0
AZT	1	0.5	1	0	0	1
SBT	0.5	0	0.5	0	0	1
ABPC	0.5	0	11[b]	11[b]	1	1
6APA	2	0.5	2.5	4[b]	0	0
CEX	1	0	1	1.5	9[b]	10[b]
CZX	1.5	0.5	0.5	0	0	1
7ACA	0	0	0.5	0	1.5	7
Saline	1.0	0	0.5	0	0	0

Total score of each group ($n=6$) is expressed. *a*) The size of erythema was measured on the day. *b*) $p<0.01$.

TABLE II. Cross-Reactivities of Beta-Lactams by MIT in IPM-Sensitized Animals

Tested drugs[a]	Control migration (%)[b]	Animal number						No. of migration inhibition
		1	2	3	4	5	6	
IPM	94±11	58[c]	87	65[c]	81	73[c]	80[c]	4
AZT	95±13	79[c]	79[c]	97	108	111	88	2
SBT	90± 6	91	81	102	107	90	89	0
ABPC	102± 9	82	102	87	84	86	74[c]	1
6APA	94± 5	105	79[c]	93	83	87	106	1
CEX	100± 8	98	100	97	102	101	108	0
CZX	101±10	85	91	104	98	107	104	0
7ACA	93±17	76[c]	64[c]	89	91	101	82	2

a) Each drug was used at the dose of 100 μg/ml. *b*) Five FCA alone-injected animals were used as control. *c*) Migration inhibition, 80>. Migration enhancement was not observed.

Cross-Reactivity of IPM, ABPC and CEX by MIT Cross-reactivity of IPM, ABPC and CEX was examined by MIT. The percentage of the macrophage migration (control migration) by drugs tested in FCA alone-injected animals is shown in Table II. All beta-lactams did not affect the determination of the cross-reactivity at the concentration of 100 μg/ml. In the IPM-sensitized group, 4 of the 6 animals exhibited migration inhibition with IPM. Furthermore, two animals showed migration inhibition with AZT and 7ACA, and one animal cross-reacted with ABPC and 6APA. However, migration enhancement was not observed in the group.

In the ABPC-sensitized group, five animals reacted with ABPC (Table III). Four animals showed migration inhibition and one animal exhibited migration enhancement. SBT and 7ACA inhibited macrophage migration in 1 of 6 animals. IPM and CZX exhibited migration enhancement in 1 and 2 of 6 animals, respectively.

The CEX-sensitized group showed broad cross-reactivity with the tested drugs (Table IV), but migration enhancement was not observed. Five of 6 animals reacted with CEX and

TABLE III. Cross-Reactivities of Beta-Lactams by MIT in ABPC-Sensitized Animals

Tested drugs[a]	Animal number						No. of migration	
	1	2	3	4	5	6	Inhibition	Enhancement
IPM	101	130[c]	97	93	92	102	0	1
AZT	107	110	99	90	83	98	0	0
SBT	78[b]	104	99	89	103	105	1	0
ABPC	80[b]	65[b]	68[b]	88	121[c]	77[b]	4	1
6APA	94	92	89	98	114	101	0	0
CEX	99	97	91	109	119	114	0	0
CZX	127[c]	107	89	102	127[c]	101	0	2
7ACA	82	117	91	73[b]	90	113	1	0

a) See control M.I.(%) in Table II. *b*) Migration inhibition, 80>. *c*) Migration enhancement, 120<.

TABLE IV. Cross-Reactivities of Beta-Lactams by MIT in CEX-Sensitized Animals

Tested drugs[a]	Animal number						No. of migration inhibition
	1	2	3	4	5	6	
IPM	76[b]	75[b]	92	66[b]	78[b]	115	4
AZT	85	85	74[b]	83	102	73[b]	2
SBT	87	98	79[b]	85	84	86	1
ABPC	80[b]	81	92	93	98	73[b]	2
6APA	63[b]	90	101	77[b]	86	82	2
CEX	63[b]	56[b]	82	44[b]	69[b]	69[b]	5
CZX	77[b]	88	92	75[b]	89	78[b]	3
7ACA	70[b]	70[b]	87	42[b]	71[b]	55[b]	5

a) See control M.I.(%) in Table II. *b*) Migration inhibition, 80>. Migration enhancement was not observed.

TABLE V. Cross-Reactivities of Beta-Lactams by LST in IPM-Sensitized Animals

Tested drugs[a]	Animal number						No. of positive[c]
	1	2	3	4	5	6	
IPM	19.1[b,d]	17.4[d]	15.4[d]	26.3[d]	6.5[d]	5.9[d]	6
AZT	1.0	0.9	1.5[e]	1.2	0.8	0.7[e]	0
SBT	1.0	1.1	1.1	1.5[e]	0.8[e]	0.6[d]	0
ABPC	0.9	1.3[d]	1.8[e]	1.5[e]	0.9	0.8	1
6APA	0.7[d]	1.4	1.5[e]	1.6[e]	0.8[e]	0.9	0
CEX	0.7[e]	0.8	1.6[e]	1.3	0.8[e]	0.7[e]	0
CZX	0.7[e]	1.0	1.2	1.2	0.7[e]	0.7[e]	0
7ACA	0.6[d]	1.1	1.3	1.0	0.7	0.5[d]	0

a) Each drug was used at the dose of 50 μg/ml. *b*) Values show the stimulation index (S.I.). *c*) When a S.I. was 1.8 or more, it was considered to be a positive reaction. *d*) $p<0.01$. *e*) $p<0.05$.

cross-reacted with 7ACA. Four animals exhibited migration inhibition with IPM. Three animals showed cross-reaction with CZX. Furthermore, AZT, SBT, ABPC and 6APA inhibited macrophage migration of 1 or 2 animals.

Cross-Reactivities of IPM, ABPC and CEX by LST

Next, the cross-reactivity of beta-lactams was investigated by LST. As shown in Table V, the IPM-sensitized group, IPM was capable of increasing the ^{3}H-TdR incorporation of lymphocytes in all animals, but 1 of 6 animals exhibited lymphocyte stimulation induced by ABPC. Cross-reaction against other drugs tested was not observed.

In the ABPC-sensitized group, three animals showed

TABLE VI. Cross-Reactivities of Beta-Lactams by LST in ABPC-Sensitized Animals

Tested drugs[a]	Animal number						No. of positive[b]
	1	2	3	4	5	6	
IPM	2.4[a,c]	1.4[c]	1.6	2.2[d]	1.0	2.1[d]	3
AZT	1.3	0.9	0.9	1.5[d]	0.7	1.0	0
SBT	1.0	1.1	1.8	1.3	1.2	0.9	0
ABPC	3.1[c]	7.3[c]	5.1[c]	6.3[c]	2.9[c]	2.3[d]	6
6APA	1.1	1.2	1.3	1.8[d]	1.3	1.5[c]	1
CEX	0.8	0.9	0.6	1.5	2.3	1.4[c]	1
CZX	0.9	0.8	0.9	1.4	1.5	1.1	0
7ACA	1.7	1.2	0.9	2.3[c]	0.5[c]	1.3	1

a) Values show the stimulation index (S.I.). *b*) See legend *c*) for Table V. *c*) $p<0.01$. *d*) $p<0.05$.

TABLE VII. Cross-Reactivities of Beta-Lactams by LST in CEX-Sensitized Animals

Tested drugs[a]	Animal number						No. of positive[b]
	1	2	3	4	5	6	
IPM	1.2[a]	1.1	1.0	0.9	1.7[d]	1.5[c]	0
AZT	0.5[d]	0.6[c]	1.0	0.7	1.0	0.9	0
SBT	0.7	0.7[c]	1.1	0.7[d]	0.9	1.0	0
ABPC	1.0	0.9	0.9	0.8	1.5[d]	1.5[c]	0
6APA	1.0	1.0	0.8	0.9	1.3[d]	1.1	0
CEX	1.9[d]	2.0[c]	1.7[c]	1.9[c]	9.1[c]	16.5[c]	5
CZX	0.8	0.5[c]	0.6[c]	0.8	0.8	0.9	0
7ACA	1.0	1.4[d]	0.9	0.7	1.8[c]	2.5[d]	2

a) Values show the stimulation index (S.I.). *b*) See legend *c*) for Table V. *c*) $p<0.01$. *d*) $p<0.05$.

stimulation of the prolifrative response by IPM (Table VI). The positive response by 6APA, CEX and 7ACA occurred in 1 of 6 animals.

In the CEX-sensitized group, 5 animals reacted with CEX and 2 animals showed lymphocyte stimulation by 7ACA (Table VII). Other drugs did not elicit the stimulative reaction.

Discussion

Recently, Saxon *et al.*[7] reported that immediate hypersensitivity caused by IPM is of low incidence and penicillin allergic patients exhibit a cross-reaction with IPM in an immunoglobulin E (IgE)-mediated reaction. Maki *et al.*[8] demonstrated a low immunogenicity of IPM in the IgE antibody production system of mice and the cross-reactivity of rabbit anti-IPM sera with penams and cephems. We observed that the immunogenicity of IPM is lower than that of ABPC and CEX in the IgM and IgG production of mice (data not shown).

However, the antigenicity of IPM was almost the same as ABPC and CEX in delayed skin reaction, and IPM, ABPC and CEX did not show a cross-reaction to each other (Table I). Edwards *et al.*[13] also reported that a carbapenem, MM22383, shows the same immunogenicity as penicillin G in a contact sensitization test of guinea pig. Therefore, the above results indicate that IPM has lower immunogenicity than penams and cephems in humoral immunity, but the immunogenicity of carbapenems in cellular immunity appears not to be weak. Furthermore, we showed here that IPM does not show a cross-reaction with penams and

cephems in DTH.

In ITH, penams and cephems show a cross-reaction to each other.[14,15] However, we reported previously that ABPC-sensitized animals exhibit a cross-reaction with CEX in DTH, but CEX-sensitized animals do not.[6] In this study, we could not observe the cross-reaction between ABPC and CEX. It is well known that the impurities of beta-lactam antibiotics affect the immunogenicity and cross-reactivity.[16-18] The discrepancy of the above results seems to derive from the difference in the immune response of animals or in the manufacture of CEX.

We compared the suitability of MIT and LST as *in vitro* assay for DTH in this study. The control value of macrophage migration against 7ACA exhibited a somewhat wide standard deviation and similar results were obtained in the lymphocyte migration test (unpublished data). 7ACA (100 μg/ml) has some influence on macrophage migration, but cross-reactivity with 7ACA is no different from that with other tested drugs. The cross-reactivity of IPM- and ABPC-sensitized animals by skin reaction and MIT are similar to each other. The broad cross-reactivity in the CEX-sensitized group may result from the structural difference of degraded product(s). Major hydrolysis products of penam and IPM are shown to be stable. They have an acyl side chain and a five membered ring of nucleus.[19,20] On the other hand, the hydrolysed product(s) of CEX is unstable, therefore, the compound(s) further cleaves, and loses the dihydrothiazine ring of the nucleus.[21,22]

In LST, sensitized drugs caused stimulation of prolifrative responses of lymphocytes, but cross-reactivity was scarcely detected. LST is considered to be more useful for identification of causative drugs than MIT in the animal model, but the cross-reaction of beta-lactams appears not to be determined. Now, we will attempt a more useful *in vitro* assay for the determination of cross-reactivities.

References

1) A. Saxon, *Ann. Intern. Med.*, **107**, 204 (1987).
2) E. Livini, S. Halevy, B. Sthaland and H. Joshua, *J. Allergy Clin. Immunol.*, **80**, 843 (1987).
3) K. Uno and F. Yamasaku, *J. Antimicrob. Chemother.*, **24**, 241 (1989).
4) N. Nagakura, T. Shimizu, Y. Yanagihara and K. Uno, *Chemotherapy* (Tokyo), **38**, 910 (1990).
5) N. Nagakura, T. Kobayashi, T. Shimizu, T. Masuzawa and Y. Yanagihara, *Chem. Pharm. Bull.*, **38**, 3410 (1990).
6) N. Nagakura, T. Kobayashi, T. Shimizu, T. Masuzawa and Y. Yanagihara, *J. Pharmacobio-Dyn.*, **13**, 310 (1990).
7) A. Saxon, D. C. Adelman, A. Patel, R. Hajdu and G. B. Calandra, *J. Allergy Clin. Immunol.*, **82**, 213 (1988).
8) E. Maki, M. Kudo and T. Yoshida, *Chemotherapy* (Tokyo), **33**, S-4, 242, (1985).
9) G. Mariam and J. H. Vaughan, *Proc. Soc. Exp. Biol. Med.*, **111**, 514 (1962).
10) H. Bergstrand and B. Kallen, *Scand. J. Immunol.*, **2**, 173 (1973).
11) I. Takata, M. R. Gordon and Q. N. Myrvik, *Cell. Immunol.*, **95**, 137 (1985).
12) J. Oort and J. L. Turk, *Br. J. Exp. Pathol.*, **46**, 147, (1965).
13) R. G. Edwards, J. M. Dewdney, R. J. Dobranski and D. Lee, *Int. Arch. Allergy Appl. Immunol.*, **85**, 184 (1988).
14) M. Blanca, J. Fernandez, A. Miranda, S. Terrados, M. J. Torres, J. M. Vega, M. J. Avila, E. Perez, J. J. Garcia and R. Suau, *J. Allergy Clin. Immunol.*, **83**, 381 (1989).
15) H. Kawaji and M. Arakawa, *J. Takeda Res. Lab.*, **39**, 77 (1980).
16) A. L. de Weck, C. H. Schneider and J. Gutershon, *Int. Arch. Allergy*, **33**, 535 (1968).
17) S. Ahlstedt, A. Kristofferson, P. O. Svard and O. Strannegard, *Int. Arch. Allergy Appl. Immunol.*, **53**, 247 (1977).
18) J. Kuriyama, *Chemotherapy* (Tokyo), **34**, 8 (1986).
19) B. B. Levine, *N. Engl. J. Med.*, **275**, 1115 (1966).
20) R. W. Ratcliffe, K. J. Wildonger, L. Di Michele, A. W. Douglas, R. Hajdu, R. T. Goegelman, J. P. Springer and J. Hirshfield, *J. Org. Chem.*, **54**, 653 (1989).
21) J. M. T. Hamilton-Miller, G. G. F. Newton and E. P. Abraham, *Biochem. J.*, **116**, 371 (1970).
22) J. M. T. Hamilton-Miller, E. Richards and E. P. Abraham, *Biochem. J.*, **116**, 385 (1970).

Dissolution of Solid Dosage Form. II.[1] Equations for the Dissolution of Nondisintegrating Tablet under the Sink Condition

Yorinobu YONEZAWA,* Kenji SHIRAKURA, Akinobu OTSUKA and Hisakazu SUNADA

Faculty of Pharmacy, Meijo University, Yagoto-Urayama, Tempaku-cho, Tempaku-ku, Nagoya 468, Japan. *Received August 14, 1990*

An equation for dissolution from the whole surface of a nondisintegrating single component tablet under the sink condition was derived. Also, equations for several dissolution manners of the tablet under the sink condition were derived in the postulation of the dominant dissolution rate constant which determines the dissolution manner. The applicability or validity of these equations were examined by the dissolution measurements with nondisintegrating single component tablets. About one-tenth the amount of the amount needed to saturate the solution was used to prepare a tablet, and dissolution measurements were carried out with the tablet whose flat or side surface was masked with an adhesive tape in accordance with the conditions for derivation of equations.

Among the derived equations, dissolution from the whole surface of a tablet was expressed by a form similar to the cube root law equation for particles. Hence, a single component tablet compressed by the use of a suitable amount was thought to behave like a single crystal. Also, equations derived for several dissolution manners were thought to be applicable for the dissolution of a nonspherical particle and crystal concerning the crystal's habit and its dissolution property, and the extended applicability was examined by converting the crystal into a simplified or idealized form, *i.e.*, rectangle or plate.

Keywords tablet; dissolution; sink condition; rotating disk method; cube root law; simulation

Introduction

A rotating disk method is useful for determining the intrinsic dissolution rate constant. As is known, this method is carried out by keeping a tablet at constant surface area during the measurement. Also, the intrinsic dissolution rate constant can be obtained from the dissolution measurement of particles. However, these methods each give different values, and hence, as can be expected, the dissolution behavior with a whole tablet can not be predicted by these methods. Concerning the dissolution of a tablet composed of additives, an equation for estimation of an apparent dissolution rate constant was reported.[2] Hence, basic dissolution equations for nondisintegrating tablets without additives were derived.

An equation for dissolution from the whole surface of a nondisintegrating single component tablet under the sink condition was derived in the postulation of isotropic dissolution. Also, dissolution equation for various dissolution manners of the tablet under the sink condition were derived in the postulation of the dominant dissolution rate constant which defines the dissolution manner. Equations thus derived were examined by the dissolution measurement of a nondisintegrating single component tablet under the conditions in accordance with the derivation of the equations. Also, the equations derived, in a sense, were thought to be applicable for the dissolution of nonspherical particles and crystals, because conception of the dominant dissolution rate constant was taken into account for the derivation. Hence, these equations were also examined as an expanded application for the crystal's habit and its dissolution property by the use of simplified or idealized crystal form, *i.e.*, rectangle or plate, as necessary.[3]

Experimental

Materials Salicylic acid (guaranteed reagent grade, Wako Pure Chemical Ind., Ltd.: abbreviated as SA) was used.

Measurement of Solubility A suitable amount of 0.1 N HCl (pH 1) and a small excess of SA were added to a capped test tube and a saturated solution at 25 °C was prepared by shaking for 14 d in a thermocontrolled water bath. The concentration was determined from the absorbance at 296 nm measured with a type UV-160 spectrophotometer (Shimadzu Ind. Co.), and 1.70 g/l was obtained as a saturated concentration.

Dissolution Measurement of Tablet About 0.13 g of SA (about 8% of the amount needed to saturate the solution) was compressed at a pressure of 2 t (type clean press correct 12 HUK, Kikusui Ind. Co.) to make a model flat faced tablet of 0.80 cm diameter and 0.19 cm thickness. The model tablet and 1000 ml of 0.1 N HCl were put into a dissolution apparatus (type NTR-VS3, Toyama Sangyo Co., Ltd.) coupled to a flow cell in a type 200-20 spectrophotometer (Hitachi Ind. Co.) *via* a pump. The dissolution measurement was carried out at a rotation velocity of 250 rpm at 25 °C. The concentration of SA was estimated from the absorbance at 296 nm.

The model tablet whose flat or side surface was masked with an adhesive tape in accordance with the derivation condition of the dissolution equation was also used.

Results and Discussion

Dissolution Equations for Several Dissolution Manners Dissolution manners were simplified as illustrated in Fig. 1, and dissolution equations for tablets which dissolve without disintegration were derived as follows. Here, h_0 and d_0 are the initial thickness and diameter of the tablet, respectively. Also, k_h and k_d are the dissolution rate constants, and are defined by the dissolution from the side surface and flat surface of the tablet, respectively. Hence, these dissolution manners were classified in the terms of k_h and k_d.

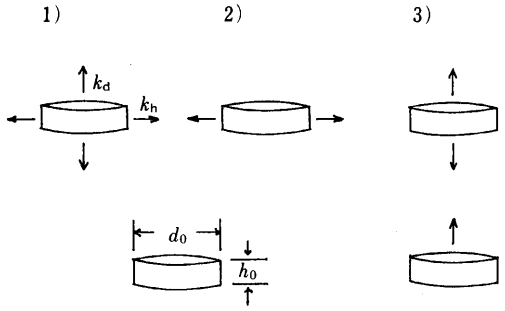

Fig. 1. Dissolution Manners of Tablet
1) $k=k_h=k_d$, 2) $k=k_h \gg k_d$, 3) $k=k_d \gg k_h$.

Denoting by W_0 the initial weight of the tablet, by $W(=W_0-w$, w is the dissolved amount) the weight of the tablet at time t and by V the solvent volume, the concentration (C) for the dissolution from the tablet is expressed by;

$$C=(W_0-W)/V \tag{1}$$

By differentiating Eq. 1, the following equation is obtained.

$$\mathrm{d}C=-(1/V)\mathrm{d}W \tag{2}$$

Denoting by k(= the diffusion constant/the thickness of the diffusion layer) the dissolution rate constant and by C_s the solubility, the dissolution rate under the sink condition is expressed by[4]:

$$\mathrm{d}C/\mathrm{d}t=(kC_s/V)S(t) \tag{3}$$

Here, $S(t)$ is the surface area of the tablet at time t.

Then the $S(t)$-value and dissolution equations were derived for each classified dissolution manner as follows.

1) $k=k_h=k_d$ In this case, dissolution of the tablet occurs isotropically from the whole surface, *i.e.*, the two flat and curved side surfaces. Since the size of the tablet was postulated to decrease isotropically, the diameter and thickness of the tablet keep the equation

$$h/h_0=d/d_0 \tag{4}$$

during dissolution. Here, h and d are the thickness and diameter of the tablet at time t, respectively. The surface area at time t is expressed by:

$$S(t)=2(\pi d^2/4)+\pi dh \tag{5}$$

When the relationship expressed by Eq. 4 is inserted into Eq. 5, $S(t)$ is given by the equation

$$S(t)=(1/2)\pi d_0^2(d/d_0)^2+\pi d_0^2(d/d_0)^2(h_0/d_0) \tag{6}$$

Here, the weight ratio at time t is defined by:

$$W/W_0=(\pi d^2h)/(\pi d_0^2h_0)=(d/d_0)^3 \tag{7}$$

Then $S(t)$ can be expressed by:

$$S(t)=(2S_d+S_h)(W/W_0)^{2/3} \tag{8}$$

where $S_d=\pi d_0^2/4$ and $S_h=\pi d_0h_0$, and $2S_d+S_h$ is the effective initial surface area (S_0) of the tablet. By inserting Eq. 8, Eq. 3 is transformed as:

$$\mathrm{d}C=(kC_s/V)(2S_d+S_h)(W/W_0)^{2/3}\mathrm{d}t \tag{9}$$

Then the following equation is obtained from Eqs. 2 and 9.

$$-(1/V)\mathrm{d}W=(kC_s/V)(2S_d+S_h)(W/W_0)^{2/3}\mathrm{d}t \tag{10}$$

Integrating Eq. 10, the following equations are obtained.

$$3W_0-3W_0(W/W_0)^{1/3}=kC_s(2S_d+S_h)t \tag{11}$$

$$(W/W_0)^{1/3}=1-(kC_s/3)\{(2S_d+S_h)/W_0\}t \tag{12}$$

On the other hand, the cube root law equation applied for spherical or cubic particles can be expressed by[5]:

$$(M/M_0)^{1/3}=1-(2kC_s/\rho fD)t \tag{13}$$

where M_0 is the initial amount, M is the residual amount, ρ is the density and f is Carman's shape factor. Using specific surface area ($S_{sp}=6/\rho fD$) and the effective surface area $S_0(=S_{sp}M_0)$, Eq. 13 can be transformed as follows.

$$(M/M_0)^{1/3}=1-(kC_sS_{sp}/3)t \tag{14}$$

$$(M/M_0)^{1/3}=1-(kC_s/3)(S_0/M_0)t \tag{15}$$

Thus, comparing Eqs. 12 and 15, it is obvious that the equation for the dissolution from the whole surface of the tablet is expressed by the same form as the Hixson–Crowell equation,[6] and it was thought that the tablet may behave like a large single crystal when it is dissolved isotropically without disintegration.

2) $k=k_h\gg k_d$ In this case, dissolution occurs more dominantly from the curved side surface than from the flat surface, and the diameter decreases with dissolution time, while the thickness (h_0) keeps constant. Then $S(t)$ is expressed as follows.

$$S(t)=\pi dh_0=\pi d_0h_0(d/d_0) \tag{16}$$

$$W/W_0=(\pi d^2h_0)/(\pi d_0^2h_0)=(d/d_0)^2 \tag{17}$$

$$S(t)=S_h(W/W_0)^{1/2} \tag{18}$$

Hence, the following equations are obtained.

$$\mathrm{d}C=(kC_s/V)S_h(W/W_0)^{1/2}\mathrm{d}t \tag{19}$$

$$-(1/V)\mathrm{d}W=(kC_s/V)S_h(W/W_0)^{1/2}\mathrm{d}t \tag{20}$$

$$W^{1/2}=W_0^{1/2}-(kC_s/2)S_hW_0^{-1/2}t \tag{21}$$

$$(W/W_0)^{1/2}=1-(kC_s/2)(S_h/W_0)t \tag{22}$$

Thus, the dissolution process is expressed in terms of the effective initial surface area ($S_0=S_h$) and the weight of the tablet.

3) $k=k_d\gg k_h$ (a) When dissolution occurs from both flat surfaces of the tablet, the thickness decreases with dissolution time while the diameter (d_0) of the tablet keeps constant. Then $S(t)$ remains constant, and is expressed by:

$$S(t)=2(\pi d_0^2/4)=2S_d \tag{23}$$

Then the following equations are obtained.

$$\mathrm{d}C=(kC_s/V)2S_d\mathrm{d}t \tag{24}$$

$$-(1/V)\mathrm{d}W=(kC_s/V)2S_d\mathrm{d}t \tag{25}$$

Integrating Eq. 25 and rearrangement, the following equation expressed in terms of the effective initial surface area ($S_0=2S_d$) and the weight is obtained.

$$W/W_0=1-kC_s(2S_d/W_0)t \tag{26}$$

(b) Dissolution from Single Flat Surface of Tablet In this case, $S(t)$ and dissolution equation are expressed as follows.

$$S(t)=\pi d_0^2/4=S_d \tag{27}$$

$$W/W_0=1-kC_s(S_d/W_0)t \tag{28}$$

Equations 26 and 28 are derived in the same derivation manner applied for Eqs. 12 and 22. However, these equations can be obtained from Eq. 3 when $2S_d$ or S_d is used in place of $S(t)$. For example, Eq. 3 is re-written as:

$$\mathrm{d}C=(kC_s/V)S_d\mathrm{d}t \tag{29}$$

and the following equations are obtained.

$$V\mathrm{d}C=\mathrm{d}w=kC_sS_d\mathrm{d}t \tag{30}$$

$$w=kC_sS_dt \tag{31}$$

Here, w is the amount dissolved. As W is given by W_0 minus w, Eq. 31 can be expressed in the same meaning of Eq. 28 as follows:

$$W=W_0-kC_sS_dt \tag{32}$$

Usually, this dissolution manner can be seen in the dissolution by the rotating disk method. Hence, when the dissolution measurement is carried out by the rotating disk method, a linear ralationship (Eq. 28) is expected independent of the optional W_0-value while dissolution follows Eq. 31.

Thus, various dissolution processes can be expressed in terms of the effective initial surface area (S_0) and the amount of the tablet (W_0).

Applicability of Equations Equations derived for various dissolution manners were examined by dissolution measurement.

1) $k=k_h=k_d$ Dissolution measurement was carried out by the use of a tablet without masking any surface in accordance with the derivation condition for Eq. 12. The result obtained was shown in Fig. 2, and the applicability of Eq. 12 was examined as shown in Fig. 3.

As can be seen in Fig. 3, dissolution up to 210 min was expressed as a straight line. The amount dissolved at that time was about half the amount of the tablet, and the concentration corresponded to about one-twentieth of the solubility. Hence, it was suggested that Eq. 12 may well express dissolution behavior when a suitable amount is used. The dissolution rate constant was estimated as 0.193 cm/min from the slope of the straight line.

2) $k=k_h\gg k_d$ The dissolution measurement was carried out with a tablet whose both flat surfaces were masked. The result obtained was shown in Fig. 2, and was treated by the use of Eq. 22 as was shown in Fig. 3.

It took about 10 h to dissolve half the amount of the tablet. The dissolution process up to about 400 min can be well expressed by Eq. 22, and the dissolution rate constant was estimated as 0.186 cm/min from the slope.

3) $k=k_d\gg k_h$ A tablet whose side and one flat surface were masked was used for dissolution measurement. The result and treatment by the use of Eq. 28 were shown in Figs. 2 and 3, respectively. The dissolution behavior fitted well with Eq. 28, and the dissolution rate constant was estimated as 0.196 cm/min from the slope.

Also, this dissolution method was thought to be a kind of rotating disk method, and the semilogarithmic treatment by means of equation

$$\ln\{C_s/(C_s-C)\}=k(S_d/V)t \tag{33}$$

was shown in Fig. 4. The dissolution rate constant obtained from the slope was 0.201 cm/min. As was expected from the previous description for the derivation of equations, the values are relatively close to each other.

Thus, equations derived for several dissolution manners could be expressed in terms of effective initial surface area (S_0) and weight (W_0), and were suggested to be reasonable, even though the whole process of dissolution could not be explained. When dissolution occurrs on the whole surface of the tablet, the dissolution process can be explained by the cube root law, and the tablet is expected to behave as if it were a single crystal. Also, an equation derived for

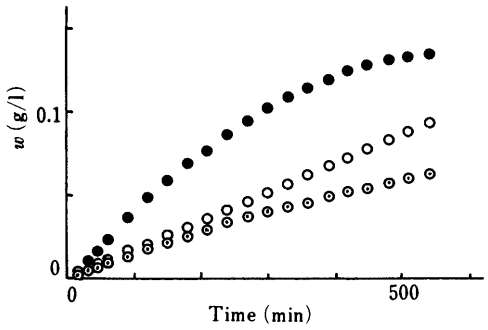

Fig. 2. Dissolution Curves for Various Dissolution Manners
●, $k=k_h=k_d$; ⊙, $k=k_h\gg k_d$, ○, $k=k_d\gg k_h$.

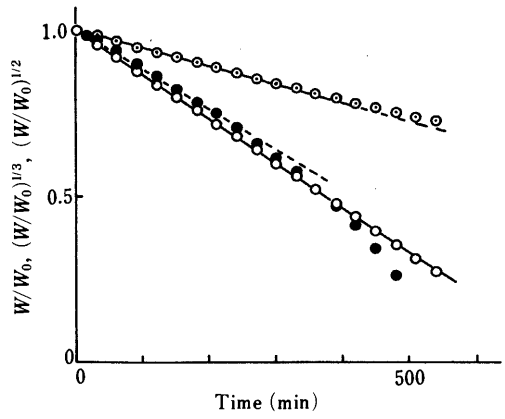

Fig. 3. Applicability of Derived Equations for Various Dissolution Manners
●, $k=k_h=k_d$, Eq. 12; ⊙, $k=k_h\gg k_d$, Eq. 22; ○, $k=k_d\gg k_h$, Eq. 28.

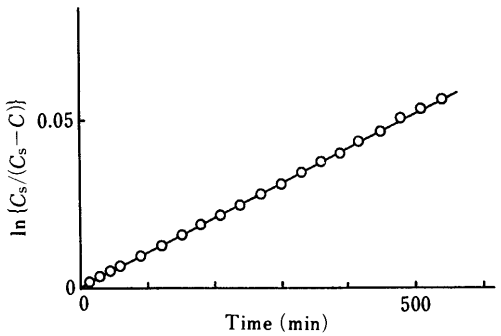

Fig. 4. Semilogarithmic Treatment of Dissolution from One Flat Surface of Tablet

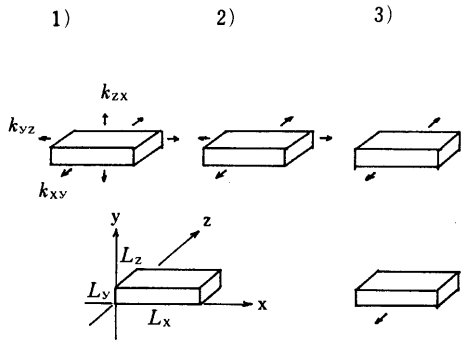

Fig. 5. Dissolution Manners of Idealized Crystal
1) $k=k_{xy}=k_{yz}=k_{zx}$, 2) $k=k_{xy}=k_{yz}\gg k_{zx}$, 3) $k=k_{xy}\gg k_{yz}$, k_{zx}.

the dissolution from a specific surface was thought to be useful for the examination of the crystal's habits and its dissolution property as an extended application.

Dissolution Equations for Idealized Crystal Dissolution manners and their equations for a single component tablet were confirmed before, and also, derived equations were suggested to be useful for the dissolution of crystals. Hence, the dissolution of an idealized plate, or rectangle crystal, was considered as a further application. Dissolution manners for idealized crystals were classified as illustrated in Fig. 5 in the postulation of crystal habits and dissolution properties. Here, L and l are the initial length and length at time t, respectively. Subscripts x, y and z show the directions.

1) $k=k_{xy}=k_{yz}=k_{zx}$ In this case, dissolution occurs isotropically, and it was postulated that the following equations were kept during dissolution.

$$l_x/L_x=l_y/L_y=l_z/L_z \tag{34}$$

$$l_xl_yl_z/L_xL_yL_z=W/W_0 \tag{35}$$

Effective initial surface area and surface area at time t are given as follows.

$$S_0=2(L_xL_y+L_yL_z+L_zL_x)=2(S_{xy}+S_{yz}+S_{zx}) \tag{36}$$

$$S(t)=2(l_xl_y+l_yl_z+l_zl_x)$$

$$S(t)=2(W/W_0)(S_{xy}L_z/l_z+S_{yz}L_x/l_x+S_{zx}L_y/l_y)$$

$$S(t)=2(S_{xy}+S_{yz}+S_{zx})(W/W_0)^{2/3} \tag{8'}$$

Then dissolution was expressed by:

$$(W/W_0)^{1/3}=1-(kCs/3)\{2(S_{xy}+S_{yz}+S_{zx})/W_0\}t \tag{12'}$$

2) $k=k_{xy}=k_{yz}\gg k_{zx}$ In this case, L_y remains constant, and the following equation is held.

$$W/W_0=l_xl_z/L_xL_z=(l_x/L_x)^2=(l_z/L_z)^2 \tag{37}$$

Hence, effective initial surface area, surface area at time t and dissolution equation were given as follows.

$$S_0=2(L_xL_y+L_yL_z)=2(S_{xy}+S_{yz}) \tag{38}$$

$$S(t)=2(l_xL_y+L_yl_z)$$

$$S(t)=2(W/W_0)(S_{xy}L_z/l_z+S_{yz}L_x/l_x)$$

$$S(t)=2(S_{xy}+S_{yz})(W/W_0)^{1/2} \tag{18'}$$

$$(W/W_0)^{1/2}=1-(kC_s/2)\{2(S_{xy}+S_{yz})/W_0\}t \tag{22'}$$

When $k=k_{xy}=k_{zx}\gg k_{yz}$ or $k=k_{yz}=k_{zx}\gg k_{xy}$, equation of the same form can be obtained.

3) $k=k_{xy}\gg k_{yz}, k_{zx}$ In the case of $S_0=2S_{xy}$, the following equations were obtained.

$$S(t)=2L_xL_y=2S_{xy} \tag{23'}$$

$$W/W_0=1-kC_s(2S_{xy}/W_0)t \tag{26'}$$

In the case of $S_0=S_{xy}$, the dissolution equation is to be expressed by:

$$W/W_0=1-kC_s(S_{xy}/W_0)t \tag{28'}$$

When $k=k_{yz}\gg k_{zx}, k_{xy}$ or $k=k_{zx}\gg k_{xy}, k_{yz}$, the equation is expressed by the same form.

Thus, simplified dissolution manners and their equations for idealized crystals correspond to those of the tablets.

Acknowledgements The authors wish to thank Mr. Kenji Kamiya for his technical assistance in preparing the samples.

References and Notes

1) Y. Yonezawa, I. Shinohara, A. Otsuka and H. Sunada, *Chem. Pharm. Bull.*, **38**, 3107 (1990).
2) Y. Kawashima, S. Y. Lin, A. Kasai, T. Handa and H. Takenaka, *Chem. Pharm. Bull.*, **33**, 2107 (1985).
3) N. Kitamori and K. Iga, *J. Pharm. Sci.*, **67**, 1674 (1978); J. T. Carstensen and M. Partel, *ibid.*, **64**, 1770 (1975); A. Watanabe, Y. Yamaoka and K. Takada, *Chem. Pharm. Bull.*, **30**, 2958 (1982).
4) W. Nernst, *Z. Phys. Chem.*, **47**, 52 (1904).
5) H. Sunada, I. Shinahara, A. Otsuka and Y. Yonezawa, *Chem. Pharm. Bull.*, **37**, 1889 (1989).
6) A. W. Hixson and J. H. Crowell, *Ind. Eng. Chem.*, **23**, 923 (1931).

Encapsulation of Doxorubicin into Liposomes by a Freeze-Thawing Method Using Buffer Solution

Eiji HAYAKAWA,* Masashi NAKAKURA, Yasuki KATO, Yuichi OKUBO, and Toshihito HOSOKAWA

Pharmaceutical Research Laboratories, Kyowa Hakko Kogyo Co., Ltd., 1188, Shimotogari, Nagaizumi-cho, Sunto-gun, Shizuoka 411, Japan.
Received September 6, 1990

When doxorubicin was encapsulated into liposomes by freeze-thawing, the percentage of encapsulated doxorubicin (*EN*%) was found to vary according to the type of buffer solution used. The reason for this was investigated in the present report. Drug-free liposomes prepared by hydration were mixed with doxorubicin dissolved in a certain type of buffer solution that shows a pH decrease on freezing, and this mixture was subjected to freeze-thawing. Doxorubicin was encapsulated by the liposomes due to the difference in pH between freezing and thawing. *EN*% depended on the pH of the buffer solution before freezing and increased significantly at over pH 7. About 60% of doxorubicin was encapsulated into liposomes after the 1st freeze-thawing cycle, and *EN*% was increased gradually with the number of freeze-thawing cycles. The addition of sugar to the experimental system was seen to affect doxorubicin encapsulation and the particle size of liposomes.

Keywords doxorubicin; liposome; freeze-thawing method; encapsulation efficiency; polycarbonate membrane

Introduction

Liposomes, vesicles comprising a phospholipid bilayer, have been broadly studied as drug carriers on the basis of their characteristics. The role of liposomes as drug carriers includes targeting of lesions, control of drug pharmacokinetics and improvement of protection from *in vivo* enzymatic degradation.[1-6]

In the preparation of liposomes, it is important to obtain high encapsulation efficiency (*EN*%). Generally, *EN*% of lipophilic drugs into liposomes is high while hydrophilic drugs are poorly encapsulated. Many attempts have been made to efficiently encapsulate hydrophilic drugs into liposomes. One procedure that has been employed is freeze-thawing.[4,7-10] In this study we made a further investigation into this method and observed that *EN*% varied according to the type of buffer solution used when doxorubicin was encapsulated into liposomes and we tried to clarify this mechanism.

In addition, it has been reported that during freeze-thawing cryoprotectants such as saccharides provided adequate protection against liposome aggregation or fusion.[10,11] Therefore, the effects of lactose on the encapsulation of doxorubicin into liposomes and on particle size during a freeze-thawing cycle were also investigated.

Experimental

Materials Doxorubicin (hydrochloride) was provided by Farmitalia Carlo Erba. Co. and egg phosphatidylcholine (Egg-PC) was purchased from Asahi Kasei Kogyo Co. All other reagents were special grade reagents from Kanto Kagaku Co.

Preparation of Liposomes Doxorubicin was encapsulated into liposomes by a freeze-thawing method as follows:

Drug-free liposomes were prepared in accordance with the hydration method described by Bangham *et al.*[12] in which 20 mg Egg-PC was dissolved in 5 ml chloroform in a 300 ml round-bottomed flask.

The chloroform was evaporated off in a rotary evaporator under reduced pressure to leave a thin film of Egg-PC on the surface of the flask. The residual solvent was removed under nitrogen gas flow. The thin film of Egg-PC was hydrated with 20 ml of various buffer solutions and subsequently shaken in a Vortex mixer for 20 min. The drug-free liposomes prepared by this hydration method were then filtered through a membrane filter 10 times (polycarbonate membrane, pore size 0.1 μm, Nomura Micro Science Co.) in order to size the liposomes.

Doxorubicin was dissolved in the same buffer solution as used in the preparation of drug-free liposomes described above to make 40 μg/ml. In the lactose experiment, lactose was dissolved (0.01—100 mg/ml) in the doxorubicin solution described above (40 μg/ml).

Ten ml of the drug-free liposomes were mixed gently by hand with an equal volume of the doxorubicin solution. Then the mixture was divided into 3 portions. A sample of 5 ml of each portion was put into a 10 ml glass vial and treated as follows.

The first portion was kept at 5 °C for 22 h in order to prepare liposomes without the freeze-thawing procedure as a control. The second portion was frozen at −20 °C for 20 h and thawed at room temperature (25 ± 1 °C) for 2 h and the third portion was subjected to repeated freeze-thawing cycles under the same conditions. The *EN*% and particle size of each portion were determined.

Calculation of *EN*% Free doxorubicin was removed from the liposomes by mixing the liposomes prepared as described above with a cation exchange resin (150 mg Dowex 50W-X4, 100—200 mesh per 40 μg doxorubicin) for 2 min with a mixer (model S-5N, Taiyo Kagaku Kogyo Co.). This cation exchange resin bound free doxorubicin and the encapsulated doxorubicin remained in the aqueous medium.

The liposomes were solubilized by the addition of a 10% aqueous solution of Triton X-100 at a 1 : 1 volume ratio.

EN% was calculated from the difference in doxorubicin concentration between liposomes containing free doxorubicin and liposomes after removal of free doxorubicin by the cation exchange resin.

The doxorubicin concentration was determined with a spectrophotometer (model U-3200, Hitachi Co.) at 497 nm.

EN% was calculated according to Eq. 1.

$$EN\% = \frac{CE}{CT} \times 100 \quad (1)$$

Where CT is the doxorubicin concentration in the solution before adding cation exchange resin (μg/ml) and CE is the doxorubicin concentration in the solution after adding cation exchange resin (μg/ml).

Determination of pH of the Liposome Solution in the Frozen State The pH of the liposome solution in the frozen state were determined according to the method described in the previous report.[13] A pH change was observed when using an indicator such as bromphenol blue between the liposome solution at 25 °C and the liposome solution in the frozen state at −20 °C when certain kinds of buffer were used to prepare the liposomes. This is thought to be due to the change of buffer components in the unfrozen regions. For this reason, −20 °C was adopted as the freezing temperature when comparing the effect of freeze-thawing on *EN*% among the various buffers.

Bromphenol blue (0.1 mg) dissolved in 50 μl H_2O was added to 1 ml of the equal volume mixture of the drug-free liposomes and the doxorubicin solution dissolved in various buffers and frozen at −20 °C for 20 h. The color of bromphenol blue dissolved in various buffer solutions in the frozen state was observed and the pH of the unfrozen regions were judged according to the color.

Measurement of Particle Size The liposome preparations were diluted with the same buffer used in the preparation of the liposomes. The mean particle size was determined by the use of a dynamic laser light scattering instrument (model DLS-700, Otsuka Electronics Co.).

In addition, the turbidity was measured as another index of mean particle size taking absorbance of each liposome suspension determined without

dilution at 650 nm at 25 °C in a 1 cm cuvette using a spectrophotometer as an index of turbidity. The measurement was repeated 3 times and the mean value was obtained.

Under the experimental procedures used here, chemical decomposition of doxorubicin was not observed from the high performance liquid chromatography (HPLC) chromatogram described previously.[13]

Results

Effect of Freeze-Thawing on *EN*% The effect of freeze-thawing on *EN*% among the three types of buffer, *i.e.* H_3BO_3/NaOH; NaH_2PO_4/K_2HPO_4; NaH_2PO_4/Na_2HPO_4 all at 20 mM, pH 7.5 and 25 °C was compared (Table I).

EN% of the control liposomes showed almost the same values for the three buffers. However, *EN*% of freeze-thaw liposomes showed significant differences. A high *EN*% of about 60% was observed for the NaH_2PO_4/Na_2HPO_4 buffer system.

When the three buffer systems were compared, a significant decrease in pH during freezing was also observed in the NaH_2PO_4/Na_2HPO_4 buffer.

Effect of the Number of Freeze-Thawing Cycles on *EN*% Doxorubicin liposomes were prepared using 20 mM NaH_2PO_4/Na_2HPO_4 buffer solution adjusted to pH 7.5 at 25 °C and subjected to repeated freeze-thawing cycles and the effect of the number of cycles on *EN*% was examined. The results are shown in Fig. 1.

About 60% of doxorubicin was encapsulated into liposomes after the 1st freeze-thawing cycle, and *EN*% was gradually increased with the number of freeze-thawing cycles.

The significant increase in *EN*% was achieved using only a single freeze-thawing cycle when compared with the liposomes prepared without the freeze-thawing procedure as a control. *EN*% of the control is similar to that reported by Gabizon *et al.*[14]

Effect of pH Adjusted before Freezing on *EN*% Doxorubicin liposomes were prepared using 20 mM NaH_2PO_4/Na_2HPO_4 buffer solution adjusted to pH 5.0—7.5 at 25 °C and subjected to one freeze-thawing cycle. The effect of pH on doxorubicin *EN*% in liposomes was examined and the results are shown in Fig. 2.

When compared with the control, the freeze-thawing procedure did not cause any change in *EN*% at a pH lower than 6.5. *EN*% of doxorubicin in liposomes prepared by freeze-thawing showed a tendency to increase with pH and significantly increased at a pH higher than pH 7.0.

Effect of Lactose on *EN*%, pH Change in the Frozen Solution, and Particle Size Doxorubicin liposomes were

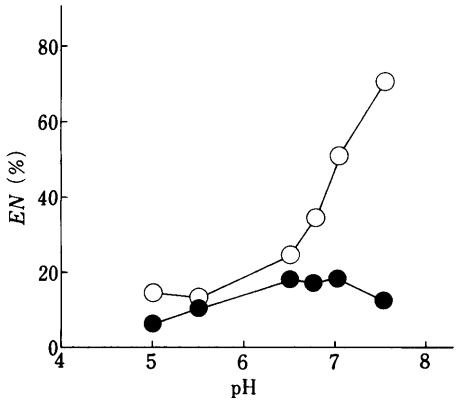

Fig. 2. Effect of Buffer Solution pH at 25 °C on the Encapsulation of Doxorubicin

Initial doxorubicin conc. = 20 μg/ml. Buffer solution = 20 mM NaH_2PO_4/Na_2HPO_4. ●, control; ○, prepared by freeze-thawing method. The number of freeze-thawing cycles = 1. Each point represents the mean of 3 experiments.

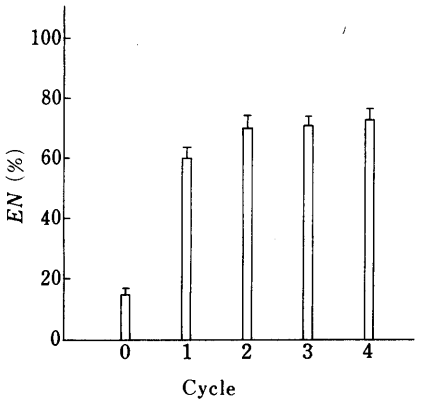

Fig. 1. Effect of Freeze-Thawing on the Encapsulation of Doxorubicin

Initial doxorubicin conc. = 20 μg/ml. Buffer solution = 20 mM NaH_2PO_4/Na_2HPO_4, pH 7.5 at 25 °C. The data are expressed as mean ± S.D. ($n = 5$).

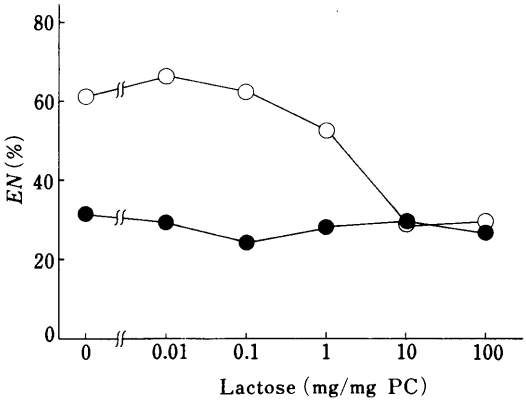

Fig. 3. Effect of Lactose on the Encapsulation of Doxorubicin

Initial doxorubicin conc. = 20 μg/ml. Buffer solution = 20 mM NaH_2PO_4/Na_2HPO_4, pH 7.5 at 25 °C. ●, control; ○, prepared by freeze-thawing method. The number of freeze-thawing cycles = 1. Each point represents the mean of 3 experiments.

TABLE I. The Relationship between the Components of Buffer Solutions and Color of Bromphenol Blue Dissolved in the Buffer Solution or Doxorubicin Encapsulation into Freeze-Thawed Liposomes

Buffer (20 mM, pH 7.5 at 25 °C)	Color (pH)[a]		*EN* (%)	
	Before freezing	During freezing	Control	After freeze-thawing
H_3BO_3/NaOH	Purple (7.5)	Purple (>4.6)	23.5±2.1	32.2±2.2
NaH_2PO_4/K_2HPO_4	Purple (7.5)	Purple (>4.6)	15.6±3.5	24.5±2.7
NaH_2PO_4/Na_2HPO_4	Purple (7.5)	Yellowish green (3.0—4.6)	14.1±2.3	59.7±3.5

Initial doxorubicin concentration = 20 μg/ml, number of freeze-thawing cycles = 1. *a*) Color/pH = yellow/<3.0, yellowish green—green/3.0—4.6, purple/>4.6. The data are expressed as mean ± S.D. ($n = 5$).

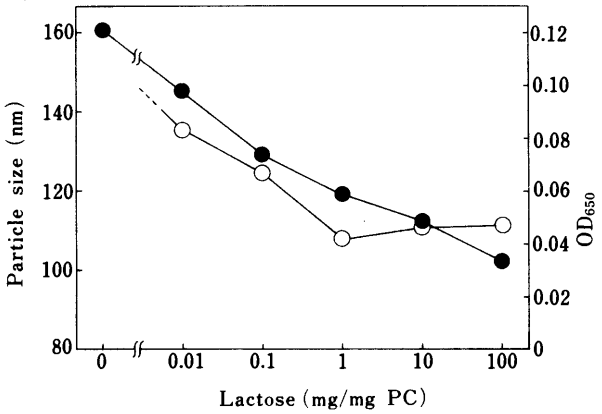

Fig. 4. Effect of Lactose on the Particle Size of Liposomes Prepared by Freeze-Thawing

Initial doxorubicin conc. = 20 μg/ml. Buffer solution = 20 mM NaH_2PO_4/Na_2HPO_4, pH 7.5 at 25 °C. The number of freeze-thawing cycles = 1. ○, particle size (nm); ●, OD 650 nm. Each point represents the mean of 3 experiments.

TABLE II. The Relationship between the Amount of Lactose and Color of Bromphenol Blue Dissolved in Buffer Solution[a] in the Frozen State

Lactose (mg/mgPC)	Color of bromphenol blue in the frozen state (pH)
0	Yellowish green (3.0—4.6)
0.01	Yellowish green (3.0—4.6)
0.1	Yellowish green (3.0—4.6)
1	Yellowish green (3.0—4.6)
10	Green (3.0—4.6)
100	Purple (>4.6)

Initial doxorubicin concentration = 20 μg/ml, number of freeze-thawing cycles = 1. *a*) Buffer solution = 20 mM NaH_2PO_4/Na_2HPO_4, pH 7.5 at 25 °C.

prepared by freeze-thawing using 20 mM NaH_2PO_4/Na_2HPO_4 buffer solution adjusted to pH 7.5 at 25 °C which contained various amounts of lactose. The influence of lactose on *EN*%, pH change and the particle size of liposomes were examined and the results are shown in Figs. 3, 4 and Table II.

When lactose was added at a ratio of more than 10 times the level of Egg-PC, the effect of freeze-thawing on the increase in *EN*% completely disappeared (Fig. 3). For the pH of the liposome solution in the frozen state at −20 °C, no decrease in pH was observed when lactose was added at a ratio of 100 times the level of Egg-PC.

However, a decrease in pH was observed when the amount of lactose added was less than 10 times that of Egg-PC (Table II). These pH change observations were consistent with the result of *EN*%. Both particle size and turbidity showed almost the same tendency to increase with a decrease in the amount of lactose added at a ratio of less than 1 mg/mg Egg-PC (Fig. 4).

Discussion

No significant effect of freeze-thawing on the increase in *EN*% of doxorubicin in liposomes was observed in 2 buffer systems, *i.e.* H_3BO_3/NaOH and NaH_2PO_4/K_2HPO_4 but a remarkable response was seen in the NaH_2PO_4/Na_2HPO_4 buffer system. Figure 5 shows the outline of the encapsulation mechanism.

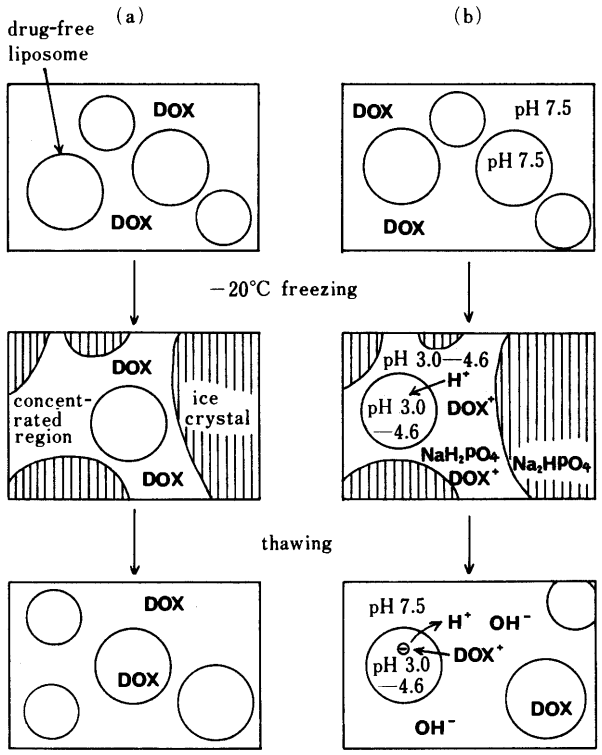

Fig. 5. Schematic Representation of the Proposed Encapsulation Mechanism for Freeze-Thawing Method using Buffer

(a) Conventional freeze-thawing method; (b) freeze-thawing method using the NaH_2PO_4/Na_2HPO_4 buffer system adjusted to pH 7.5 at 25 °C. DOX, doxorubicin.

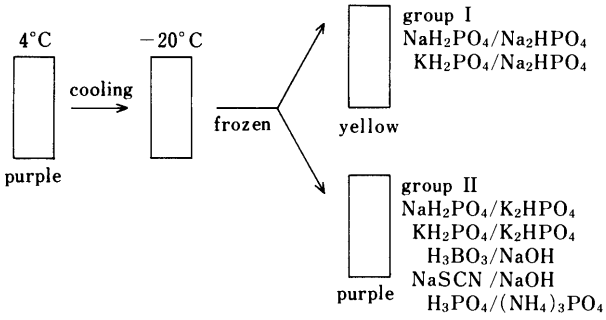

Fig. 6. Relationship between the Buffer Components and Color Change of Bromphenol Blue before and after Freezing

Color change of bromphenol blue as pH indicator dissolved in various buffer solutions (0.1 M, pH 7.0 at 25 °C) was measured. Color of bromphenol blue; over pH 4.6, purple; below pH 3.0, yellow.

It is already known that freeze-thawing can increase drug encapsulation into liposomes.[4,7-10] This mechanism has been explained by the theory in which phospholipids and drugs are concentrated into the unfrozen region at −20 °C (concentrated region) (Fig. 5a). But this theory did not satisfactorily explain the difference in *EN*% between these 3 buffer systems which were observed in our study.

We previously reported (as shown in Fig. 6) that various buffers were divided into 2 groups according to the pH change of the unfrozen region at −20 °C. Group I buffer systems showed a difference in pH between the solution state and the frozen state at −20 °C.[13]

Mayer *et al.*[15] described that transmembrane pH

gradients produced by the change of buffer systems at room temperature during drug loading into the drug-free liposomes result in the efficient entrapment of the drugs into the liposomes. We also reported[13] that on the basis of DSC measurements the eutectic point of the buffer system components played an important role in the pH change during the freezing process. For example, when the NaH_2PO_4/Na_2HPO_4 buffer system, adjusted to pH 7.0 at 25 °C, was frozen at −20 °C, alkaline Na_2HPO_4 was phased out as a result of eutectic solidification and accordingly the concentrated region became acidic due to the NaH_2PO_4 solution whose pH was 3.0—4.6 or lower (Figs. 6 and 7). This phenomenon was not observed in two other buffer systems (H_3BO_3/NaOH, NaH_2PO_4/K_2HPO_4).

When doxorubicin liposomes were prepared with a NaH_2PO_4/Na_2HPO_4 buffer adjusted to pH 7.5 at 25 °C and were frozen at −20 °C, a decrease in pH occurred in the concentrated region. Therefore, the pH inside the liposome is lowered to 3.0—4.6 during freezing at −20 °C (Table I). During the thawing process, the Na_2HPO_4 portion that solidified thaws and the pH outside the liposome only returns to the pre-freezing value (pH 7.5—9.0). Therefore, transmembrane pH gradients are produced (Fig. 5b).

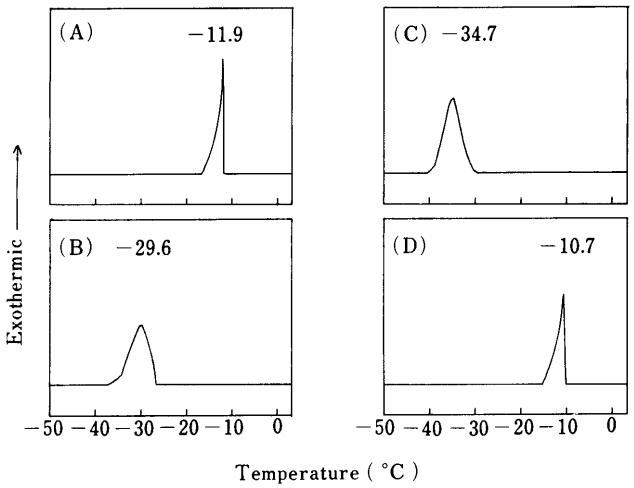

Fig. 7. Eutectic Point of the Buffer Components by Differential Scanning Colorimetry (DSC)

Cooling rate = 2 °C·min^{-1}. Each pH value of saturated solutions was measured at 25 °C. (A) Na_2HPO_4 (pH 9.0), (B) NaH_2PO_4 (pH 4.5), (C) K_2HPO_4 (pH 9.0), (D) H_3BO_3 (pH 5.5). The eutectic point of NaOH is −28 °C.[17]

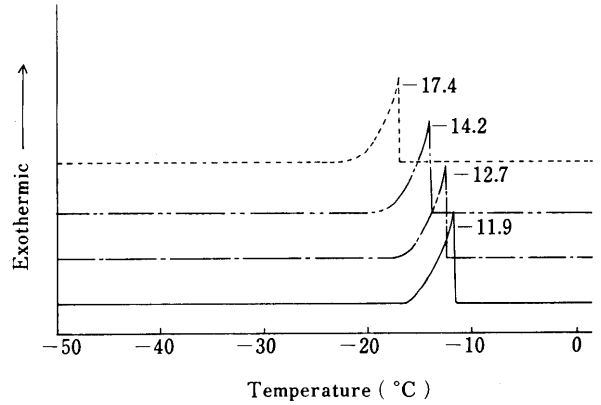

Fig. 8. Decrease in Eutectic Point of Na_2HPO_4 by the Addition of Lactose

Eutectic point was measured by DSC. Cooling rate = 2 °C·min^{-1}. [Na_2HPO_4] = 0.1 M. [Lactose], 0 mg/mg PC (—); 0.5 mg/mg PC (— — —); 5 mg/mg PC (— — — — —); 100 mg/mg PC (– – –).

It can be suggested from a recent report[15] that the pH gradients produced by the mechanism mentioned above allow doxorubicin to cross lipid bilayers and this results in a significant increase in the *EN*% of doxorubicin in liposomes after freeze-thawing. Mayer *et al.*[15] also reported that a favorable change in the *EN*% according to the pH gradient could be obtained when the pH difference between the inside and the outside of the liposomes exceeded 3.0. This supports our observation that a significant effect of freeze-thawing on the increase in *EN*% was obtained only in the NaH_2PO_4/Na_2HPO_4 buffer system adjusted to a pH of more than 7.0 at 25 °C in which we anticipated a pH difference exceeding 3 between before and after freeze-thawing.

In the effect of the number of freeze-thawing cycles on the *EN*%, it was suggested that sufficient drug uptake into the liposomes can be achieved using only a single freeze-thawing cycle.

Crommelin *et al.*[16] found that saccharides were effective protectants in terms of preserving the original particle size. According to the results of our present study involving the addition of lactose, an excessive amount of lactose was found to inhibit the encapsulation of doxorubicin induced by the pH gradient (Fig. 3) but the particle size remained unchanged. This inhibition of encapsulation may have resulted from the decrease in the eutectic point because the addition of lactose lowered the eutectic point of Na_2HPO_4 (Fig. 8). The addition of excess lactose caused a decrease in the eutectic point in the whole solution and prevented eutectic solidification of Na_2HPO_4 which resulted in a smaller decrease in pH at −20 °C and this led to a lower transmembrane pH gradient.

From the view point of maintaining high *EN*% and preventing liposomes from coagulation during freeze-thawing, a lactose/Egg-PC ratio of about 1 : 1 is suggested.

References

1) J. N. Weinstein, *Cancer Treatment Reports*, **68**, 1, 127 (1984).
2) J. D. Crapo and S. L. Young, *Fed. Proc.*, **44**, 10, 2591 (1985).
3) R. L. Juliano and D. Stamp, *Biochem. Pharmacol.*, **27**, 21 (1978).
4) T. Ohsawa, Y. Matsukawa, Y. Takakura, M. Hashida, and H. Sezaki, *Chem. Pharm. Bull.*, **33**, 11, 5013 (1985).
5) M. Ueno, T. Nakasaki, I. Horikoshi, and N. Sakuragawa, *Chem. Pharm. Bull.*, **30**, 6, 2245 (1982).
6) N. Das and M. K. Das, *Indian J. Biochem. Biophys.*, **23**, 242 (1986).
7) M. Kasahara and P. C. Hinkle, *J. Biol. Chem.*, **252**, 20, 7384 (1977).
8) T. Ohsawa, H. Miura, and K. Harada, *Chem. Pharm. Bull.*, **33**, 7, 2916 (1985).
9) T. Ohsawa, H. Miura, and K. Harada, *Chem. Pharm. Bull.*, **33**, 9, 3945 (1985).
10) T. Ohsawa, H. Miura, and K. Harada, *Chem. Pharm. Bull.*, **33**, 12, 5474 (1985).
11) E. M. G. Van Bommel and D. J. A. Crommelin, *Int. J. Pharmaceut.*, **22**, 299 (1984).
12) A. D. Bangham, M. M. Standish, and J. C. Watkins, *J. Mol. Biol.*, **13**, 238 (1965).
13) E. Hayakawa, K. Sugiyama, K. Furuya, and T. Kuroda, *Yakuzaigaku*, **49**, 4, 289 (1989).
14) A. Gabizon, A. Dagan, D. Goren, Y. Barenholz, and Z. Fuks, *Cancer Res.*, **42**, 4734 (1982).
15) L. D. Mayer, M. B. Bally, M. J. Hope, and P. R. Cullis, *Chem. Phys. Lipids*, **40**, 333 (1986).
16) D. J. A. Crommelin and E. M. G. Van Bommel, *Pharm. Res.*, **4**, 159 (1984).
17) S. Senba, *Jpn. J. Freezing and Drying*, **15**, 76 (1969).

Synthesis and Absolute Configuration of Optically Active 2,3-Disubstituted 2,3-Dihydro-1,3,4-thiadiazoles

Kouhei TOYOOKA,* Yoshiyuki TAKEUCHI, Hiroyuki OHTO, Masayuki SHIBUYA, and Seiju KUBOTA

Faculty of Pharmaceutical Sciences, University of Tokushima, Shomachi, Tokushima 770, Japan. *Received August 3, 1990*

Optically active 3-substituted 2,3-dihydro-1,3,4-thiadiazoles (2—5) were synthesized by the reaction of aldehyde methylthio(thiocarbonyl)hydrazones (1) and chiral 5-substituted 1,3-dioxolane-2,4-diones. The absolute configurations of compounds 2—5 were deduced from their circular dichroism spectra.

Keywords 2,3-dihydro-1,3,4-thiadiazole; absolute configuration; circular dichroism; methylthio(thiocarbonyl)hydrazone; chiral 1,3-dioxolane-2,4-dione; cyclization

Circular dichroism (CD) spectroscopy is one of the generally applicable methods for the analysis of optically active compounds. Among CD techniques, the exciton chirality method[1] is useful for the determination of absolute configurations of organic compounds. Kakimura and co-wokers have applied this method for determining the absolute configuration of asukamycin, having a polyene-amide chromophore.[2]

In a previous communication,[3] we reported that the acylation of 4-bromobenzaldehyde methylthio(thiocarbonyl)hydrazone (**1a**) with chiral 5-phenyl-1,3-dioxolane-2,4-dione gave novel chiral 2-(4-bromophenyl)-3-mandelyl-2,3-dihydro-1,3,4-thiadiazoles (**2a**—**5a**) which have extremely high optical rotations. We determined their absolute configurations by single-crystal X-ray analysis (for compound **2a**) and by analysis of the optical rotations (for **3a**—**5a**). Here we report the application of this new synthetic route to the synthesis of several optically active 3-substituted 2,3-dihydro-1,3,4-thiadiazole analogues and the assignment of their absolute configurations by the CD method.

Reaction of 4-bromobenzaldehyde methylthio(thiocarbonyl)hydrazone (**1a**) and (*S*)-(+)-5-methyl-1,3-dioxolane-2,4-dione[4] in the presence of trifluoroacetic acid (TFA) at room temperature for 3 h gave the optically active compounds **2b** (25%), $[\alpha]_D^{20}$ +437.2°, and **3b** (56%), $[\alpha]_D^{20}$ −511.7° after separation by column chromatography. In view of our previous results,[3] this acylation reaction was assumed to proceed without isomerization at the lactyl moiety.[5] Compounds **2b** and **3b** were both found to be diastereoisomers of 2-(4-bromophenyl)-3-[(*S*)-lactyl]-5-methylthio-2,3-dihydro-1,3,4-thiadiazoles on the basis of the following spectral data. The elemental analyses of both compounds were consistent with the molecular formula $C_{12}H_{13}BrN_2O_2S_2$. The mass spectra (MS) of the 2,3-dihydro-1,3,4-thiadiazoles (**2b** and **3b**) showed the same molecular ion peak at *m/z* 362 ($M^+ + 1$). Compounds **2b** and **3b** showed infrared (IR) absorption due to a carbonyl group at 1645 and 1650 cm^{-1}, respectively. The proton nuclear magnetic resonance (^{1}H-NMR) spectra of compounds **2b** and **3b** showed C-2 proton absorptions at δ 6.97 and 7.01 with an upfield shift of 0.83 and 0.79 ppm from

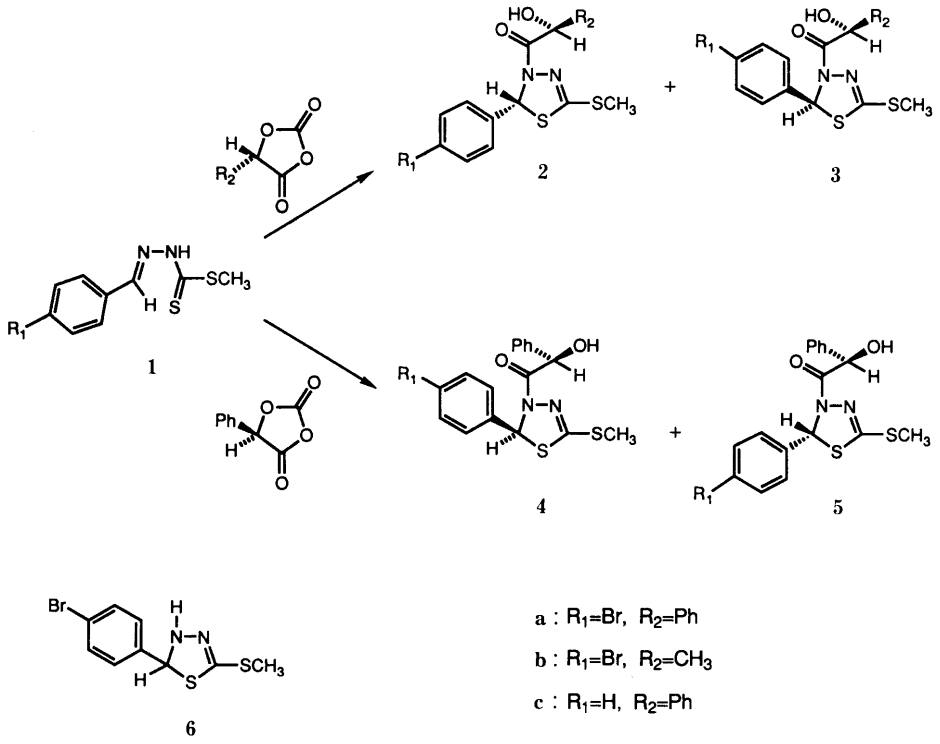

Chart 1

that of the methine proton of the starting material (**1a**), respectively. Those shift values are in good agreement with those reported for 2,3-dihydro-1,3,4-thiadiazole derivatives.[6]

Benzaldehyde methylthio(thiocarbonyl)hydrazone (**1c**) was acylated with (*S*)-(+)-5-phenyl-1,3-dioxolane-2,4-dione[4] in a similar manner to that used for compounds **2b** and **3b** to give the optically active compounds **2c** (17%), $[\alpha]_D^{20}$ +465.2°, and **3c** (47%), $[\alpha]_D^{20}$ −540.2°, after separation by column chromatography. Compounds **2c** and **3c** were both found to be diastereoisomers of 3-[(*S*)-mandelyl]-5-methylthio-2-phenyl-2,3-dihydro-1,3,4-thiadiazoles on the basis of their spectral data. The elemental analyses of both compounds were consistent with the molecular formula $C_{17}H_{16}N_2O_2S_2$. MS of 2,3-dihydro-1,3,4-thiadiazoles (**2c** and **3c**) showed the same molecular ion peak at *m/z* 344 (M^+). Compounds **2c** and **3c** showed IR absorption due to a carbonyl group at 1650 and 1660 cm^{-1}, and the ^{1}H-NMR signal due to the C-2 protons at δ 6.98 and 7.04, respectively.

Similarly, acylation of the methylthio(thiocarbonyl)-hydrazone (**1c**) with (*R*)-(−)-5-phenyl-1,3-dioxolane-2,4-dione[4] afforded the optically active compounds **4c** (17%), $[\alpha]_D^{20}$ −456.6° and **5c** (54%), $[\alpha]_D^{20}$ +543.1° as diastereoisomers of 3-[(*R*)-mandelyl]-5-methylthio-2-phenyl-2,3-dihydro-1,3,4-thiadiazoles. The optical purity of the 2,3-dihydro-1,3,4-thiadiazoles (**2c**—**5c**) was confirmed by chiral phase high performance liquid chromatography (HPLC) (CHIRAL OC, EtOH at 0.5 ml/min for compounds **2c** and **4c**, EtOH at 0.05 ml/min for compounds **3c** and **5c**, ultraviolet (UV) detector set at 254 nm) to be >99.9% in each case.

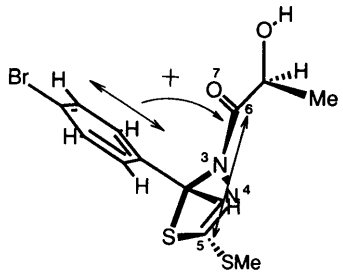

Fig. 1. A Stereochemical View of (+)-**2b**

TABLE I. UV and CD Data for **2**—**5**

Compound	UV[a] λ_{max} nm (ε)	CD[a] λ nm ($\Delta\varepsilon$)	Absolute configuration
2a	265 (9500), 235 (17450), 211 (17100)	250 (+40.5), 226 (−46.8)	2*R*
2b	262 (7150), 234 (12100), 208 (9650)	245 (+36.4), 218 (−39.0)	2*R*
2c	269 (10350), 230 (13950), 209 (20450)	245 (+29.6), 219 (−35.1)	2*R*
3a	265 (12800), 235 (21050), 211 (19600)	249 (−32.7), 222 (+40.7)	2*S*
3b	261 (6900), 234 (11600), 208 (9300)	245 (−35.7), 218 (+38.9)	2*S*
3c	266 (7400), 228 (9250), 210 (11600)	248 (−24.3), 220 (+31.3)	2*S*
4a	265 (10600), 235 (19400), 211 (18400)	250 (−40.7), 226 (+46.5)	2*S*
4c	266 (10400), 230 (14050), 209 (21100)	245 (−29.6), 219 (+36.9)	2*S*
5a	265 (14450), 235 (24000), 211 (22300)	249 (+32.4), 222 (−37.9)	2*R*
5c	268 (7000), 228 (8700), 210 (11100)	248 (+24.6), 220 (−31.3)	2*R*

a) Compounds **2**—**5** in EtOH.

The CD spectra of (+)-**2b** and (−)-**3b** were studied as models for 3-acyl-2,3-dihydro-1,3,4-thiadiazoles. The acylhydrazino moiety, O(7)–C(6)–N(3)–N(4)–C(5), of the 3-acyl-2,3-dihydro-1,3,4-thiadiazole nucleus is assumed to be almost planar and the 4-bromophenyl group on C-2 would be located below (α) or above (β) the 2,3-dihydro-1,3,4-thiadiazole ring on the basis of the results of X-ray analysis reported previously.[3,7] If the 4-bromophenyl group is located below (α) the thiadiazole ring, the exciton dipoles should have the directions shown in Fig. 1, and positive induced Cotton effects would be expected, based on exciton chirality method. The CD spectrum of (+)-**2b** exhibited a distinct positive split Cotton effect owing to exciton coupling with a maximum at 245 nm ($\Delta\varepsilon$ +36.4) and a minimum at 218 nm ($\Delta\varepsilon$ −39.0). The positive sign of the longer wavelength peak indicates that the two chromophores have a clockwise helicity (Table I). Therefore, the absolute configuration at C-2 of (+)-**2b** was assigned as *R*. The CD spectrum of (−)-**3b** showed a negative Cotton effect at 245 nm ($\Delta\varepsilon$ −35.7) (Table I), indicating that the two chromophores have a counterclockwise helicity. Therefore, the absolute configuration at C-2 of (−)-**3b** was assigned as *S*. Further support for the absolute configurations of (+)-**2b** and (−)-**3b** was obtained by comparison of the CD spectra with those of similar compounds, (+)-**2a** and (−)-**3a**, having known absolute configurations, respectively. The CD curves of compounds **2b**, **3b** were similar to those of compounds **2a**, **3a** in the sign, shape, and position of the Cotton effect, respectively, reflecting the similarity in their absolute configurations at C-2 (Fig. 2). This result also suggests that the absolute configurations of (+)-**2b** and (−)-**3b** are 2*R* and 2*S*, respectively.

The CD spectra of the two diastereoisomers (+)-(**2c**) and (+)-(**5c**) showed positive Cotton effects while the two diastereoisomers (−)-(**3c**) and (−)-(**4c**) showed negative Cotton effects at longer wavelengths in accordance with (+)-**2b** and (−)-**3b** having 2*R* and 2*S* configurations, respectively (Table I). The CD signs of compounds **2c**—**5c** are also in agreement with those of the similar compounds **2a**—**5a** (Table I) and with the rule described above for compounds **2b** and **3b**.

From our results and the above facts, it was concluded

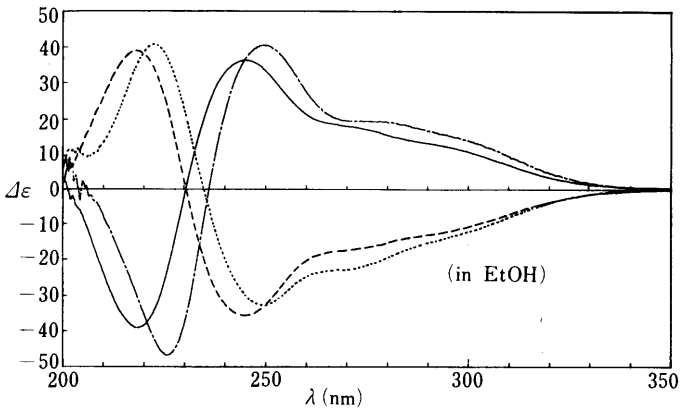

Fig. 2. CD Spectra of 2,3-Dihydro-1,3,4-thiadiazole Derivatives
(+)-**2a**, ———; (+)-**2b**, —; (−)-**3a**, - - -; (−)-**3b**, — —.

that the absolute configurations of 3-lactyl- or 3-mandelyl-2,3-dihydro-1,3,4-thiadiazoles can be determined from the CD sign independently of the nature and chirality of the 3-acyl moiety.

Experimental

Melting points were determined by the capillary method and are uncorrected. IR spectra were recorded on a Hitachi 215 spectrometer. ^{1}H-NMR spectra were recorded on a JEOL PS-100 spectrometer or a JEOL JNM-FX 200 spectrometer using tetramethylsilane as an internal standard. The optical rotations were measured with a Union Giken PM-201 polarimeter, and CD spectra were measured with a JASCO J-600 spectropolarimeter. UV spectra were recorded with a Shimadzu UV-200 spectrometer. MS were measured with a JEOL D-300 instrument. Column chromatography was performed on silica gel (K-100-S, from Katayama Chemicals). HPLC was performed on a CHIRAL OC column (4.6 i.d. × 250 mm) using an EtOH solvent system.

Aldehyde Methylthio(thiocarbonyl)hydrazones (1) Compounds **1a**[8] and **1c**[9] were prepared by literature methods.

(2*R*)-(4-Bromophenyl)-3-[(*S*)-lactyl]-5-methylthio-2,3-dihydro-1,3,4-thiadiazole (2b) and (2*S*)-(4-Bromophenyl)-3-[(*S*)-lactyl]-5-methylthio-2,3-dihydro-1,3,4-thiadiazole (3b) A solution of (*S*)-(−)-5-methyl-1,3-dioxolane-2,4-dione (322 mg, 2.78 mmol) in CH_2Cl_2 (10 ml) was added to a stirred solution of 4-bromobenzaldehyde methylthio(thiocarbonyl)hydrazone (**1a**) (800 mg, 2.77 mmol) and TFA (0.21 ml, 2.82 mmol) in CH_2Cl_2 (15 ml) at 0 °C. After being stirred at room temperature for 3 h, the reaction mixture was concentrated under reduced pressure. The residue was chromatographed on silica gel with $CHCl_3$–acetone (50 : 1) as the eluent to give two fractions containing diastereomeric products. Evaporation of the first fraction gave a solid, which was recrystallized from isopropyl ether to give **2b** (249 mg, 25%), mp 95—96 °C. $[\alpha]_D^{20}$ +437.2° (c=0.99, $CHCl_3$). IR (KBr): 3100—3600 (OH), 1645 (C=O) cm^{-1}. ^{1}H-NMR ($CDCl_3$) δ: 1.40 (3H, d, J=8 Hz, CH_3), 2.62 (3H, s, SCH_3), 2.70—3.15 (1H, br, OH), 4.79 (1H, q, J=8 Hz, CH), 6.97 (1H, s, C_2-H), 7.21 (2H, dd, J=2, 8 Hz, ArH), 7.49 (2H, dd, J=2, 8 Hz, ArH). MS m/z: 362 (M^+ +1). *Anal.* Calcd for $C_{12}H_{13}BrN_2O_2S_2$: C, 39.90; H, 3.63; N, 7.75. Found: C, 39.84; H, 3.55; N, 7.54. Evaporation of the second fraction gave a solid, which was recrystallized from isopropyl alcohol to give **3b** (564 mg, 56%), mp 98—99 °C. $[\alpha]_D^{20}$ −511.7° (c=0.983, $CHCl_3$). IR (KBr): 3100—3600 (OH), 1650 (C=O) cm^{-1}. ^{1}H-NMR ($CDCl_3$) δ: 1.43 (3H, d, J=8 Hz, CH_3), 2.62 (3H, s, SCH_3), 2.70—3.10 (1H, br, OH), 4.69 (1H, q, J=8 Hz, CH), 7.01 (1H, s, C_2-H), 7.19 (2H, dd, J=2, 8 Hz, ArH), 7.49 (2H, dd, J=2, 8 Hz, ArH). MS m/z: 362 (M^++1). *Anal.* Calcd for $C_{12}H_{13}BrN_2O_2S_2$: C, 39.90; H, 3.63; N, 7.75. Found: C, 39.84; H, 3.47; N, 7.61.

3-[(*S*)-Mandelyl]-5-methylthio-(2*R*)-phenyl-2,3-dihydro-1,3,4-thiadiazole (2c) and 3-[(*S*)-Mandelyl]-5-methylthio-(2*S*)-phenyl-2,3-dihydro-1,3,4-thiadiazole (3c) A solution of (*S*)-(+)-5-phenyl-1,3-dioxolane-2,4-dione (609 mg, 3.42 mmol) in CH_2Cl_2 (16 ml) was added dropwise to a stirred solution of benzaldehyde methylthio(thiocarbonyl)hydrazone (**1c**) (600 mg, 2.86 mmol) and TFA (0.25 ml, 3.36 mmol) in CH_2Cl_2 (20 ml) at 0 °C. After being stirred at room temperature for 1 h, the reaction mixture was concentrated under reduced pressure. The residue was chromatographed on silica gel with $CHCl_3$–acetone (50 : 1) as the eluent to give two fractions of diastereomeric products. Evaporation of the first fraction gave a solid, which was recrystallized from isopropyl ether to give **2c** (162 mg, 17%), mp 155—157 °C. $[\alpha]_D^{20}$ +465.2° (c=1.01, $CHCl_3$). IR (KBr): 3300—3600 (OH), 1650 (C=O) cm^{-1}. ^{1}H-NMR ($CDCl_3$) δ: 2.44 (3H, s, SCH_3), 4.00 (1H, d, J=8 Hz, OH), 5.62 (1H, d, J=8 Hz, CH), 6.98 (1H, s, C_2-H), 7.31 (10H, s, ArH). MS m/z: 344 (M^+). *Anal.* Calcd for $C_{17}H_{16}N_2O_2S_2$: C, 59.28; H, 4.68; N, 8.13. Found: C, 59.15; H, 4.47; N, 8.09. Evaporation of the second fraction gave a solid, which was recrystallized from diethyl ether to give **3c** (463 mg, 47%), mp 82—83 °C. $[\alpha]_D^{20}$ −540.2° (c=1.02, $CHCl_3$). IR (KBr): 3150—3550 (OH), 1660 (C=O) cm^{-1}. ^{1}H-NMR ($CDCl_3$) δ: 2.54 (3H, s, SCH_3), 4.05 (1H, d, J=8 Hz, OH), 5.56 (1H, d, J=8 Hz, CH), 7.04 (1H, s, C_2-H), 7.28 (5H, s, ArH), 6.84—7.38 (5H, m, ArH). MS m/z: 344 (M^+). *Anal.* Calcd for $C_{17}H_{16}N_2O_2S_2$: C, 59.28; H, 4.68; N, 8.13. Found: C, 59.28; H, 4.64; N, 8.12.

3-[(*R*)-Mandelyl]-5-methylthio-(2*S*)-phenyl-2,3-dihydro-1,3,4-thiadiazole (4c) and 3-[(*R*)-Mandelyl]-5-methylthio-(2*R*)-phenyl-2,3-dihydro-1,3,4-thiadiazole (5c) Compounds **4c** and **5c** were obtained from (*R*)-(−)-5-phenyl-1,3-dioxolane-2,4-dione (760 mg, 4.27 mmol), the methylthio(thiocarbonyl)hydrazone (**1c**) (600 mg, 2.86 mmol), and TFA (0.32 ml, 4.31 mmol) in a similar manner to that described for compounds **2c** and **3c**. The minor diastereoisomer (**4c**) (171 mg, 17%) showed the same IR and ^{1}H-NMR spectra as those of **2c**, mp 154—156 °C, $[\alpha]_D^{20}$ −456.6° (c=1.01, $CHCl_3$). MS m/z: 344 (M^+). *Anal.* Calcd for $C_{17}H_{16}N_2O_2S_2$: C, 59.28; H, 4.68; N, 8.13. Found: C, 59.14; H, 4.56; N, 8.03. The major diastereoisomer (**5c**) (527 mg, 54%) showed the same IR and ^{1}H-NMR spectra as those of **3c**, mp 83—84 °C, $[\alpha]_D^{20}$ +543.1° (c=0.99, $CHCl_3$). MS m/z: 344 (M^+). *Anal.* Calcd for $C_{17}H_{16}N_2O_2S_2$: C, 59.28; H, 4.68; N, 8.13. Found: C, 59.28; H, 4.75; N, 8.09.

Acknowledgement This work was supported in part by a grant from the Ministry of Education, Science and Culture, Japan.

References and Notes

1) N. Harada and K. Nakanishi, "Circular Dichroic Spectroscopy Exciton Coupling in Organic Stereochemistry," University Science Books, Mill Valley, CA, 1983.
2) K. Kakimura, N. Ikekawa, A. Nakagawa, and S. Omura, *J. Am Chem. Soc.*, **101**, 3402 (1979).
3) K. Toyooka, Y. Takeuchi, Z. Taira, and S. Kubota, *Heterocycles*, **29**, 1233 (1989).
4) K. Toyooka, Y. Takeuchi, and S. Kubota, *Heterocycles*, **29**, 975 (1989).
5) The hydrazone (**1a**) presumably exists as an equilibrium mixture with the cyclic form (**6**) under these conditions. The kinetically preferred product (**3b**) would be formed predominantly by acylation of the intermediate (**6**) with (*S*)-(+)-5-methyl-1,3-dioxolane-2,4-dione.
6) *a*) S. Kubota, Y. Ueda, K. Fujikane, K. Toyooka, and M. Shibuya, *J. Org. Chem.*, **45**, 1473 (1980); *b*) K. H. Mayer and D. Lauerer, *Justus Liebigs Ann. Chem.*, **731**, 142, (1970); *c*) S. H. Askari, S. F. Moss, and D. R. Taylor, *J. Chem. Soc., Perkin Trans. 1*, **1981**, 360; *d*) S. F. Moss and D. R. Taylor, *ibid.*, **1982**, 1981; *e*) *Idem*, *ibid.*, **1982**, 1987; *f*) *Idem*, *ibid.*, **1982**, 1993; *g*) S. Kubota, K. Toyooka, J. Ikeda, N. Yamamoto, and M. Shibuya, *ibid.*, **1983**, 967; *h*) S. Kubota, K. Toyooka, H. K. Misra, M. Kawano, and M. Shibuya, *ibid.*, **1983**, 2957; *i*) S. Andreae, E. Schmitz, and H. Seeboth, *J. Prakt. Chem.*, **328**, 205 (1986).
7) S. Kubota, K. Toyooka, M. Shibuya, and Z. Taira, *J. Chem. Soc., Perkin Trans. 1*, **1986**, 1357.
8) J. Korosi, Ger. Patent 1934809 (1970) [*Chem. Abstr.*, **72**, 100334 (1970)].
9) M. Busch and M. Stark, *J. Prakt. Chem.*, **93**, 59 (1916).

Studies on Chlorinated α-Santonin. V.[1] Conformation of the Cyclohexenone Ring in 6β-Santonin Derivatives

Hiroaki TAKAYANAGI,[a] Rieko IRIMAJIRI,[a] Haruo OGURA*,[a] and T. Brian H. McMURRY[b]

School of Pharmaceutical Sciences, Kitasato University,[a] Shirokane, Minato-ku, Tokyo 108 and University Chemical Laboratory, Trinity College,[b] Dublin 2, Ireland. *Received August 10, 1990*

The conformations of 1α,2β-dichloro-1,2-dihydro-6β-santonin (5), 1,2,4,5-tetrachloro-6β-santonin (6), 1α,2β-dibromo-1,2-dihydro-6β-santonin (8), and 1,2-dihydro-6β-santonin (9) were elucidated by proton nuclear magnetic resonance spectrometry and X-ray crystallographic analysis. Among these derivatives (5, 6, 8, and 9), only 1α,2β-dichloroenone (5) shows a difference in the conformation of the cyclohexenone ring between solution (half-chair form) and crystal (half-boat form) states.

Keywords 6β-santonin; 1α,2β-dichloro-1,2-dihydro-6β-santonin; 1α,2β-dibromo-1,2-dihydro-6β-santonin; 1α,2β,4α,5β-tetrachloro-1,2-dihydro-6β-santonin; half-chair conformation; half-boat conformation; X-ray diffraction; 1,2-dihydro-6β-santonin

Inayama *et al.*[2] have investigated the conformation of the cyclohexenone ring of α-santonin derivatives by means of proton nuclear magnetic resonance (^{1}H-NMR) spectroscopy, X-ray analysis, and molecular mechanics calculations. In their report, the cyclohexenone rings of 2α-chloro-1,2-dihydro-α-santonin (**1**) and 1,2-dihydro-α-santonin (**2**) were concluded to take a half-chair form, while those of 2β-chloro-1,2-dihydro-α-santonin (**3**) and 1α,2β-dichloro-1,2-dihydro-α-santonin (**4**) take a half-boat conformation.

We wish to report here on the stereochemistry of the cyclohexenone ring in 6β-santonin derivatives. 6β-Santonin is an epimer of α-santonin and is easily prepared from α-santonin.[3] During our studies on α-santonin derivatives, we obtained 1,2-dichloro-1,2-dihydro-6β-santonin (**5**) as a sole product of chlorination of 6β-santonin (**7**) in $CHCl_3$ for 20 min, while 1,2,4,5-tetrachloro-6β-santonin (**6**) was obtained by chlorination of **5** in a mixture of $CHCl_3$ and MeOH for 1 h. We determined the stereochemistry of these products by X-ray crystallographic analysis. Fractional coordinates for the crystals of **5** and **6** are given in Table II, perspective views of the molecules of **5** and **6** are given in Fig. 1, and a perspective drawing of the cyclohexenone ring of **5** viewed along the carbonyl group is given in Fig. 2. Selected dihedral angles and bond lengths of compounds **5** and **6** are given in Table IV.

As demonstrated in Figs. 1 and 2, the configurations of the chlorine substituents in **6** are 1α, 2β, 4α, 5β, where the dihedral angle 1βH–C(1)–C(2)–2αH is 170° (Table IV). In the nuclear magnetic resonance (NMR) spectrum of **6**, the coupling constant between the 1- and 2-hydrogens is 12.0 Hz, suggesting that the two hydrogens are diaxial. The 1- and 2-chlorine substituents in both the solid state and in solution are diequatorial.

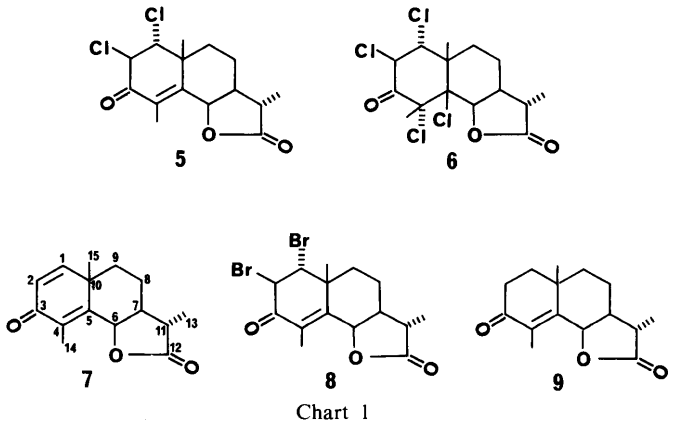

Chart 1

The stereochemistry of **5** is 1α,2β-dichloro-1,2-dihydro-6β-santonin, where the cyclohexenone ring exists in a half-boat form (Fig. 2), in which the 1- and 2-chlorines are diequatorial. This is the same as that of 1α,2β-dichloro-1,2-dihydro-α-santonin (**4**).[2] However, the NMR spectrum of **5** shows a 1H, 2H coupling constant of 4.0 Hz, whereas the corresponding coupling constant of **4** is 11 Hz. This suggests that in solution the conformation of the cyclohexenone ring of **5** is different from that of **4**, and, indeed, that in solution the cyclohexenone ring in **5** adopts a half-chair conformation, with both chlorines axial. As for the relationship between the 1H, 2H coupling constant and the dihedral angle of 1H–C(1)–C(2)–2H, **5** can be compared with the rigid 1α,2α,5β-trichloro-4α-methoxy-α-santonin.[1] For this compound, in solution, the 1,2-coupling constant is 6 Hz, while the crystal structure shows a 1H–C(1)–C(2)–2H dihedral angle of 75°.[1]

We wished to determine whether the finding that **5** has a half-boat form in the crystal structure, and a half-chair form in solution could be generalized for other derivatives of 6β-santonin. Accordingly, we synthesized 1α,2β-dibromo-1,2-dihydro-6β-santonin (**8**) and 1,2-dihydro-6β-santonin (**9**), and we carried out X-ray analysis to elucidate their stereochemistry. Fractional coordinates for the crystals of **8** and **9** are given in Tale III, perspective views of the molecules of **8** and **9** are given in Fig. 1, and perspective drawings of the cyclohexenone ring in **8** and **9** viewed along the carbonyl group are given in Fig. 2. Selected dihedral angles and bond lengths of compounds **8** and **9** are given in Table IV.

As shown in Fig. 2, compound **9** has a half-chair form in the crystal structure, which is the same as that of **2**.[2] It must have the same conformation in solution because the coupling constant between the 1β and 2α hydrogen atoms is 2.0 Hz. Compound **8** also has a half-chair form in the crystal structure, with the two bromine atoms axially orientated. For this compound, the coupling constant between the 1- and 2-hydrogen atoms is 2.0 Hz, and the dihedral angle (1H–C(1)–C(2)–2H) is 88° (Table IV). These data clearly indicate that compound **8** takes a half-chair form both in solution and in the crystal structure. As

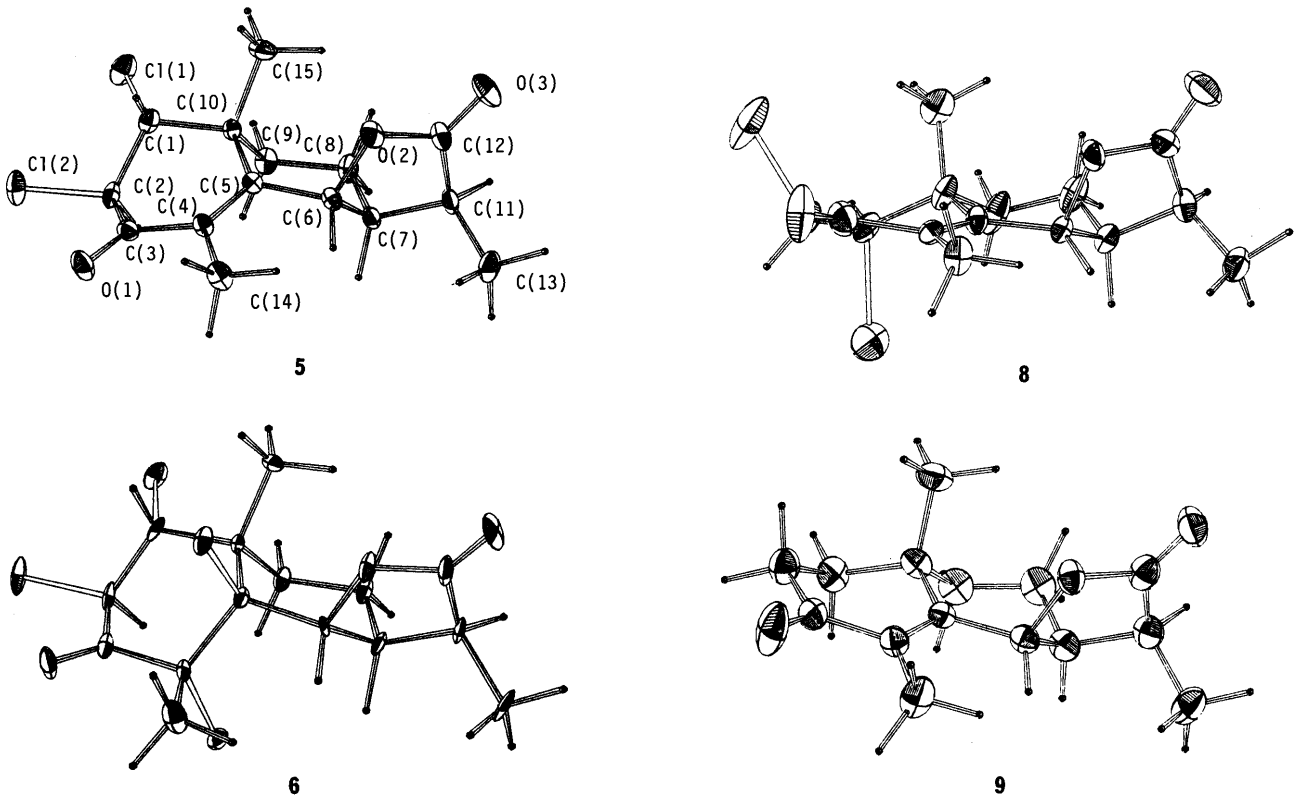

Fig. 1. Perspective Views of the Molecules of **5**, **6**, **8**, and **9**

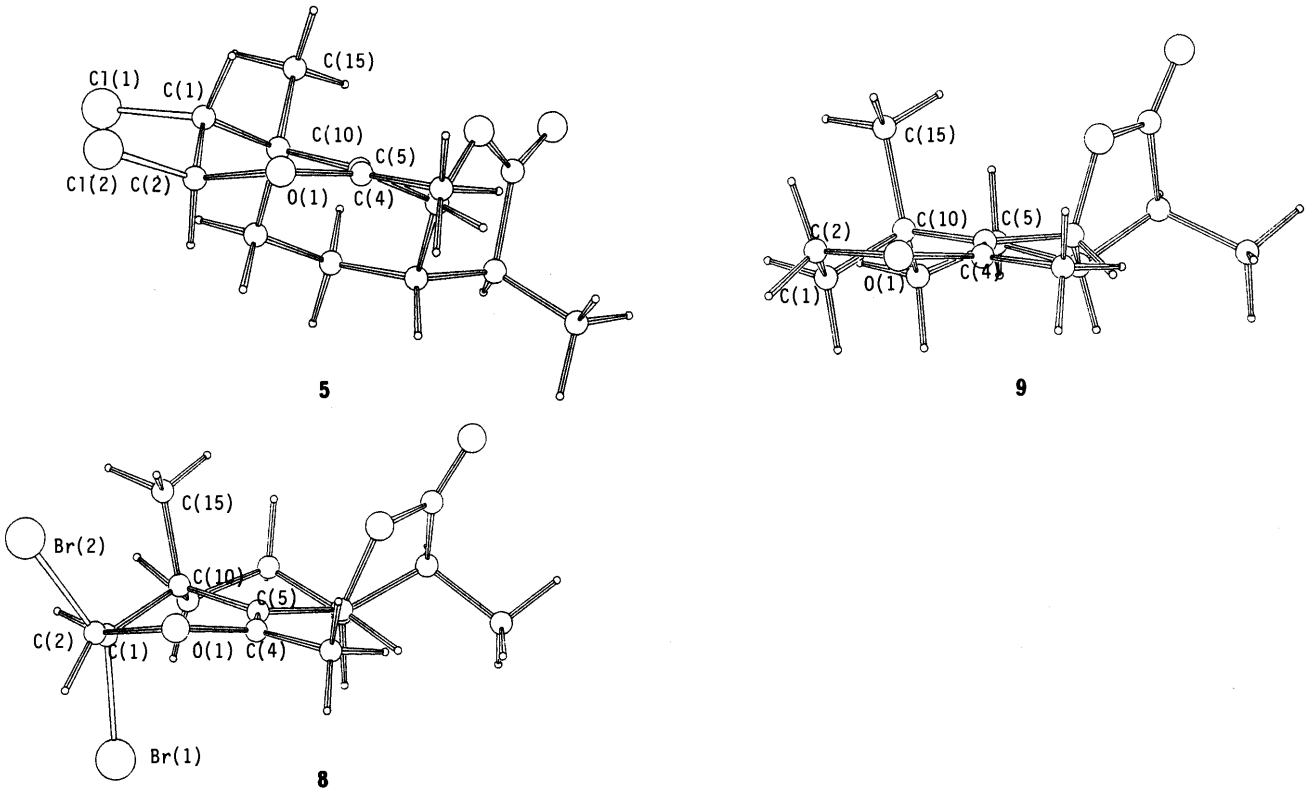

Fig. 2. Perspective Drawings of the Cyclohexenone Ring of **5**, **8**, and **9** Viewed along the Carbonyl Group

compounds **5** and **8** have a similar coupling constant between the 1- and 2-hydrogen atoms in $CDCl_3$ solution, compounds **5** and **8** should adopt similar half-chair forms in solution, and this conformation must be very similar to that adopted by **8** in the crystal structure.

In conclusion, among α-santonin derivatives, as mentioned before, 1α,2β-dichloro-1,2-dihydro-α-santonin and 2β-chloro-1,2-dihydro-α-santonin take a half-boat con-

TABLE I. Crystal Data and Experimental Details

	5	6	8	9
Formula	$C_{15}H_{18}Cl_2O_3$	$C_{15}H_{18}Cl_4O_3$	$C_{15}H_{18}Br_2O_3$	$C_{15}H_{20}O_3$
Formula weight	317.19	388.09	406.09	248.31
Crystal system	Orthorhombic	Orthorhombic	Orthorhombic	Orthorhombic
Space group	$P2_12_12_1$	$P2_12_12_1$	$P2_12_12_1$	$P2_12_12_1$
a (Å)	10.881 (5)	13.666 (5)	11.295 (2)	10.536 (3)
b (Å)	14.434 (6)	13.988 (7)	12.671 (4)	15.048 (4)
c (Å)	9.253 (7)	8.572 (6)	10.984 (2)	8.572 (2)
V (Å^3)	1453.2	1638.6	1572.0	1359.1
z	4	4	4	4
D_c (g cm^{-3})	1.415	1.573	1.716	1.214
$\mu(CuK_\alpha)$ (cm^{-1})	4.496	7.333	51.100	0.777
Crystal size (mm)	0.2 × 0.3 × 0.2	0.3 × 0.4 × 0.2	0.3 × 0.4 × 0.2	0.3 × 0.3 × 0.2
No. of unique reflections	1537	1498	1601	1235
No. of observed reflections	1363	1478	1187	1148
$F(000)$	2656	3200	3232	2144
R	0.055	0.064	0.062	0.067
$2\theta_{max}$ (°)	150	150	150	150

TABLE II. Fractional Coordinates (× 10^4) and Equivalent Isotropic Thermal Parameters (B_{eq}) of Non-hydrogen Atoms, with Estimated Standard Deviations in Parentheses for **5** and **6**

Atom	5				Atom	6			
	x	y	z	B_{eq} (Å^2)		x	y	z	B_{eq} (Å^2)
Cl(1)	4380 (2)	−2013 (1)	5923 (2)	3.5	Cl(1)	3741 (3)	305 (2)	2249 (4)	3.0
Cl(2)	2427 (2)	−1666 (1)	3419 (2)	3.7	Cl(2)	4218 (3)	−803 (2)	5422 (5)	3.5
O(1)	3168 (4)	−155 (3)	1575 (5)	3.4	Cl(3)	5092 (2)	2350 (2)	6808 (4)	2.5
O(2)	7699 (4)	1013 (3)	4403 (5)	2.9	Cl(4)	1962 (2)	2020 (2)	6232 (4)	2.2
O(3)	9350 (4)	1519 (4)	5642 (8)	5.7	O(1)	3734 (8)	387 (6)	8043 (12)	3.2
C(1)	4665 (6)	−1164 (4)	4541 (6)	2.2	O(2)	2320 (6)	3888 (5)	5123 (12)	2.2
C(2)	3484 (5)	−783 (4)	3954 (7)	2.3	O(3)	1777 (8)	5226 (7)	4072 (15)	4.3
C(3)	3804 (6)	−171 (4)	2646 (7)	2.1	C(1)	3457 (10)	814 (8)	4130 (15)	2.0
C(4)	4859 (5)	453 (4)	2841 (6)	2.0	C(2)	4168 (10)	453 (8)	5300 (17)	2.2
C(5)	5596 (5)	393 (4)	4030 (6)	1.7	C(3)	3909 (9)	858 (8)	6938 (16)	2.0
C(6)	6363 (5)	1214 (4)	4433 (7)	2.0	C(4)	3837 (9)	1954 (8)	7029 (15)	1.7
C(7)	6123 (6)	1578 (4)	5958 (7)	2.0	C(5)	3189 (8)	2372 (8)	5632 (14)	1.4
C(8)	5944 (6)	801 (4)	7077 (7)	2.4	C(6)	3233 (8)	3477 (7)	5645 (14)	1.4
C(9)	5073 (6)	39 (4)	6559 (6)	2.1	C(7)	4023 (9)	3966 (8)	4537 (16)	1.9
C(10)	5519 (5)	−390 (4)	5130 (6)	1.7	C(8)	4197 (9)	3436 (8)	3019 (17)	2.2
C(11)	7310 (5)	2114 (4)	6259 (7)	2.4	C(9)	4306 (9)	2351 (8)	3233 (15)	1.9
C(12)	8242 (6)	1541 (5)	5458 (8)	3.2	C(10)	3382 (8)	1910 (8)	3974 (14)	1.4
C(13)	7313 (7)	3116 (5)	5680 (8)	3.4	C(11)	3539 (10)	4932 (9)	4253 (17)	2.5
C(14)	4947 (6)	1185 (5)	1674 (7)	3.1	C(12)	2453 (10)	4740 (8)	4417 (17)	2.6
C(15)	6803 (6)	−853 (5)	5343 (7)	2.9	C(13)	3863 (13)	5750 (9)	5336 (23)	4.2
					C(14)	3487 (12)	2265 (10)	8672 (16)	3.1
					C(15)	2476 (9)	2110 (9)	2861 (16)	2.3

formation, and 2α-chloro-1,2-dihydro-α-santonin has a half-chair conformation both in solution and in the solid state.[2] On the other hand, among 6β-santonin derivatives, 1α,2β-dibromo-1,2-dihydro-6β-santonin (**8**) adopts a half-chair form both in solution and in the crystal, but 1α,2β-dichloro-1,2-dihydro-6β-santonin (**5**) takes a half-chair form in solution and a half-boat form in the crystal state. Among the 6β-santonin derivatives (**5**, **8** and **9**), only the dichloroenone **5** exhibits a difference in the conformation of the cyclohexenone ring between solution and the solid state. The reason is not clear. There is no doubt that the *cis* lactone ring makes ring B flexible. As shown in Table IV, the bond lengths between O(2) and C(15) are 3.05 and 3.50 Å for **5** and **8**. In the case of **5**, the value is within the van der Waals radii, thus introducing repulsion between the two substituents. Moreover, it is well known that the energy difference is very small between the two conformations of α-halocyclohexanones, in which the halogen is equatorial and axial, respectively.[4] Indeed, the position of the equilibrium between them is solvent-dependent.[5]

Experimental

General Methods Unless otherwise stated, the following procedures were adopted. Melting points were taken on a Yanagimoto micro hot-stage apparatus and are uncorrected. Infrared (IR) spectra were taken in $CHCl_3$ or KBr with a Hitachi 260-10 spectrometer and are given in cm^{-1}. Ultraviolet (UV) spectra were recorded in EtOH with a Hitachi 200-10 spectrophotometer. ^{1}H-NMR (100 MHz) spectra were measured in $CDCl_3$ solution with tetramethylsilane (TMS) as an internal standard on a JEOL FX-100 spectrometer. High-resolution mass spectra (MS) were recorded on a JEOL JMS-D300 mass spectrometer. For column chromatography, silica gel (Wako-gel C-200) was used.

1α,2β-Dichloro-1,2-dihydro-6β-santonin (5) Dry chlorine gas was passed into a solution of 6β-santonin (**7**, 1.0 g) in $CHCl_3$ (12 ml) for 20 min

TABLE III. Fractional Coordinates ($\times 10^4$) and Equivalent Isotropic Thermal Parameters (B_{eq}) of Non-hydrogen Atoms, with Estimated Standard Deviations in Parentheses for **8** and **9**

Atom	**8**				Atom	**9**			
	x	y	z	B_{eq} (Å^2)		x	y	z	B_{eq} (Å^2)
Br(1)	675 (2)	1770 (1)	1403 (2)	5.9	O(1)	2163 (6)	5802 (3)	7108 (5)	7.6
Br(2)	2552 (2)	−683 (1)	3661 (3)	8.8	O(2)	2703 (3)	8931 (2)	9931 (4)	3.7
O(1)	4382 (10)	625 (8)	2114 (12)	6.6	O(3)	3572 (4)	10145 (3)	10966 (6)	5.5
O(2)	3598 (8)	4000 (6)	4621 (8)	3.6	C(1)	1000 (6)	6114 (4)	11039 (4)	4.6
O(3)	3903 (11)	5143 (9)	6114 (10)	6.7	C(2)	1737 (6)	5621 (4)	9776 (7)	4.8
C(1)	1315 (11)	1227 (9)	2979 (13)	3.4	C(3)	1850 (6)	6147 (4)	8307 (7)	4.3
C(2)	2315 (12)	524 (9)	2582 (13)	3.7	C(4)	1643 (6)	7136 (3)	8374 (6)	3.5
C(3)	3518 (14)	1083 (11)	2453 (14)	4.4	C(5)	1506 (5)	7558 (4)	9727 (6)	3.0
C(4)	3554 (10)	2254 (9)	2676 (11)	2.3	C(6)	1406 (5)	8559 (4)	9732 (6)	3.4
C(5)	2681 (10)	2733 (8)	3305 (11)	2.6	C(7)	631 (5)	9007 (4)	11031 (7)	4.0
C(6)	2827 (9)	3897 (8)	3561 (12)	2.4	C(8)	745 (6)	8520 (5)	12589 (7)	5.0
C(7)	1689 (10)	4509 (9)	3960 (11)	2.8	C(9)	490 (6)	7546 (5)	12367 (7)	4.6
C(8)	852 (12)	3834 (10)	4714 (16)	4.4	C(10)	1460 (5)	7078 (4)	11284 (6)	3.6
C(9)	538 (13)	2833 (10)	4079 (16)	5.1	C(11)	1253 (6)	9936 (4)	11095 (7)	4.2
C(10)	1641 (11)	2112 (9)	3836 (14)	3.5	C(12)	2639 (7)	9727 (4)	10709 (7)	4.3
C(11)	2278 (12)	5413 (9)	4712 (13)	3.6	C(13)	739 (7)	10590 (4)	9877 (9)	5.6
C(12)	3349 (15)	4883 (11)	5249 (13)	4.5	C(14)	1712 (8)	7584 (4)	6763 (7)	5.6
C(13)	2651 (13)	6345 (9)	3962 (14)	4.3	C(15)	2815 (6)	7076 (4)	12023 (7)	4.9
C(14)	4679 (11)	2775 (10)	2190 (13)	3.6					
C(15)	1990 (13)	1626 (12)	5040 (14)	4.8					

TABLE IV. Selected Dihedral Angles (ϕ (°)) and Bond Lengths (Å) of **5**, **6**, **8**, and **9**

	5	**6**	**8**	**9**
1βH–C(1)–C(2)–2αH	160 (5)	170 (11)	88 (1)	61 (9)
1αH–C(1)–C(2)–2βH				170 (4)
Cl(1)–C(1)–C(2)–Cl(2)	51 (1)	56 (1)		
Br(1)–C(1)–C(2)–Br(2)			148 (6)	
C(15)–O(2)	3.02	3.17	3.55	3.32

at room temperature. The solvent was removed by evaporation under reduced pressure. The residue was washed with water. Crystallization from $CHCl_3$–MeOH gave **5** as colorless plates in 81% yield (1.2 g), mp 165—167 °C (dec.). IR ($CHCl_3$): 1745 (lactone C=O), 1675 (C=O) cm^{-1}. UV λ_{max} nm (ε): 249 (2.0×10^4). CD (MeOH) $[\theta]_{max}$ (nm): 2044 (332), −35240 (252). ^{1}H-NMR ($CDCl_3$) δ: 5.43 (1H, d, $J_{2,1}$=4.0 Hz, 2-H), 4.68 (1H, d, $J_{1,2}$=4.0 Hz, 1-H), 4.38 (1H, d, $J_{6,7}$=4.0 Hz, 6-H), 2.05 (3H, s, 4-CH_3), 1.60 (3H, s, 10-CH_3), 1.37 (3H, d, J=11.0 Hz, 11-CH_3). *Anal.* Calcd for $C_{15}H_{18}Cl_2O_3$: C, 56.92; H, 5.75; Cl, 22.22. Found: C, 56.92; H, 5.75; Cl, 22.25. MS *m/z*: 318 (M$^+$).

1α,2β,4α,5β-Tetrachloro-1,2-dihydro-6β-santonin (6) Dry chlorine gas was passed into a solution of 1α,2β-dichloro-1,2-dihydro-6β-santonin (**5**, 1.0 g) in $CHCl_3$ (20 ml) and MeOH (10 ml) with stirring at room temperature for 1 h. The solvent was removed under reduced pressure. The precipitate was washed with water. Crystallization from MeOH–$CHCl_3$ gave **6** as colorless plates in 84% yield (1.02 g), mp 222—225 °C (dec.). UV λ_{max} nm (ε): 245 (1.48×10^3). IR ($CHCl_3$): 1745 (lactone C=O), 1700 (C=O) cm^{-1}. ^{1}H-NMR ($CDCl_3$) δ: 5.45 (1H, d, $J_{2,1}$=12.0 Hz, 2-H), 4.95 (1H, d, $J_{6,7}$=5.0 Hz, 6-H), 4.30 (1H, d, $J_{1,2}$=12.0 Hz, 1-H), 2.11 (3H, s, 4-CH_3), 1.52 (3H, s, 10-CH_3), 1.32 (3H, d, $J_{7,11}$=7.0 Hz, 11-CH_3). CD (MeOH) $[\theta]_{max}$ (nm): 7890 (290), −1480 (250). *Anal.* Calcd for $C_{15}H_{18}Cl_4O_3$: C, 46.42; H, 4.67; Cl, 36.54. Found: C, 46.64; H, 4.68; Cl, 36.25. MS *m/z*: 387 (M$^+$).

6β-Santonin (7) This was prepared as described in the literature.[6] mp 102—103 °C.

1α,2β-Dibromo-1,2-dihydro-6β-santonin (8) Bromine was added to a mixture of 6β-santonin (**7**) (1.0 g), $CHCl_3$ (10 ml), and CCl_4 (10 ml), at 0 °C. The mixture was stirred at room temperature for 2 h, and the solvent was removed under reduced pressure. The residue was crystallized from ethyl acetate and petroleum-ether to give **8** as colorless needles in 26.4% yield (0.5 g), mp 88—89 °C (dec.). IR (Nujol): 1775 (lactone C=O), 1679 (C=O) cm^{-1}. UV λ_{max} nm (ε): 228 (1.37×10^3). CD (MeOH) $[\theta]_{max}$ (nm): −43300 (230). ^{1}H-NMR ($CDCl_3$) δ: 5.42 (1H, d, $J_{6,7}$=4.0 Hz, 6-H), 5.18 (1H, d, $J_{2,1}$=2.0 Hz, 2-H), 4.64 (1H, d, $J_{1,2}$=2.0 Hz, 1-H), 2.10 (3H, s, 4-CH_3), 1.80 (3H, s, 10-CH_3), 1.42 (3H, d, $J_{7,11}$=8.0 Hz). *Anal.* Calcd for $C_{15}H_{18}Br_2O_3$: C, 44.23; H, 4.52; Br, 38.68. Found: C, 44.30; H, 4.41; Br, 38.89. MS *m/z*: 404 (M$^+$).

1,2-Dihydro-6β-santonin (9) This was prepared as described in the literature.[6] ^{1}H-NMR ($CDCl_3$) δ: 5.54 (1H, d, $J_{6,7}$=5.5 Hz, 6-H), 2.70 (1H, ddd, $J_{1\beta,2\beta}$=5.5, $J_{1\alpha,2\beta}$=14.8, $J_{2\alpha,2\beta}$=17.9 Hz, 2β-H), 2.50 (1H, ddd, $J_{2\alpha,1\beta}$=2.0, $J_{2\alpha,2\beta}$=17.9, $J_{1\alpha,2\alpha}$=4.8 Hz, 2α-H), 2.57 (1H, m, 11-H), 2.22 (1H, m, 7-H), 1.90 (1H, ddd, $J_{1\alpha,1\beta}$=13.2, $J_{1\alpha,2\alpha}$=4.8, $J_{1\alpha,2\beta}$=14.8 Hz, 1α-H), 1.73 (1H, ddd, $J_{1\beta,1\alpha}$=13.2, $J_{1\beta,2\beta}$=5.5, $J_{1\beta,2\alpha}$=2.0 Hz, 1β-H), 1.62 (3H, s, 4-CH_3), 1.38 (3H, d, J=7.5 Hz, 11-CH_3), 1.25 (3H, s, 10-CH_3).

Structure Determination and Refinement Crystal data and intensity data were collected on a Rigaku automated four-circle diffractometer using CuK_α radiation (λ=1.5479 Å) monochromated by a graphite plate. Of the unique reflections measured, those observed with $|F_O|>3\sigma(|F_O|)$ were used. The intensities were corrected for Lorentz, polarization, but not for absorption and extinction. The structure was solved by the direct method (MULTAN78),[7] and was refined by the block-diagonal least-squares method. Crystal data and details of the refinement are summarized in Table I. Scattering factors were taken from "International Tables for X-Ray Crystallography."[8] Computations were performed on Hitachi M-680H and M-682H computers in the Computer Centre of the University of Tokyo, using a local version of the UNICS program.[9]

References

1) Part IV: H. Takayanagi, H. Ogura, and T. B. H. McMurry, *Chem. Pharm. Bull.*, **38**, 581 (1990).
2) *a*) S. Inayama, N. Shimizu, H. Hori, T. Ohsaka, T. Hirose, T. Shibata, and Y. Iitaka, *Chem. Pharm. Bull.*, **30** 3856 (1982); *b*) Y. Ohta, C. Jaime, E. Osawa, Y. Iitaka, N. Shimizu, S. Nishihara, T. Ohsaka, H. Hori, T. Shibata, and S. Inayama, *Chem. Pharm. Bull.*, **33**, 400 (1985).
3) H. Ishikawa, *Yakugaku Zasshi*, **76**, 504 (1956).
4) E. T. Corey, *J. Am. Chem. Soc.*, **75**, 2301 (1953).
5) C. Djerassi, *Proc. Chem. Soc.*, **314** (1964).
6) A. E. Green, J.-C. Muller, and G. Ourisson, *J. Org. Chem.*, **39**, 186 (1974).
7) P. Main, S. E. Hull, L. Lewssinger, G. Germain, J. P. Declercq, and M. M. Woolfson, "A Computer Program for the Automatic Solution of Crystal Structures from X-Ray Diffraction Data," Univ. of York, England and Louvain, Belgium, 1978.
8) "International Tables for X-Ray Crystallography," Vol. IV, Kynoch Press, Birmingham, 1974.
9) "Universal Crystallographic Computation Program System (UNICS)," ed. by T. Sakurai, Crystallographic Society of Japan, Tokyo, 1967.

A Practical Synthesis of Arylthiocyanates from Arenesulfinates or Arenesulfonyl Chlorides with Cyanotrimethylsilane[1)]

Shinzo KAGABU,*,[a] Keisuke SAWAHARA,[a] Masaki MAEHARA,[a] Sachiko ICHIHASHI,[a] and Katsuhiro SAITO[b]

Department of Chemistry, Faculty of Education, Gifu University,[a] Yanagido, Gifu, 501-11, Japan and Department of Applied Chemistry, Nagoya Institute of Technology,[b] Gokiso-cho, Showa-ku, Nagoya 466, Japan. *Received August 27, 1990*

Preparation of arylthiocyanates by simply mixing aromatic sulfinates with cyanotrimethylsilane (TMSCN) was achieved in good to moderate yields. The thiocyanates were also obtained directly from sulfonyl chloride using TMSCN, sodium sulfite, and potassium carbonate.

Keywords sodium arenesulfinate; arenesulfinic acid; arenesulfonyl chloride; arylthiocyanate; cyanotrimethylsilane

Thiocyanates have attracted much attention as potential synthetic intermediates for thiazoles or thiols as well as from pharmacological viewpoint.[2)] Several methods have been devised and improved to synthesize thiocyanates. Arylthiocyanates have traditionally been prepared from diazonium salts with metal thiocyanate.[3)] This Gattermann–Sandmeyer reaction, however, requires careful control of reaction conditions and tedious separation procedures of the thiocyanate from the by-produced isothiocyanate. Arylthallium salts readily produce the thiocyanates with potassium thiocyanate by photolysis[4)] or in the presence of copper(II) ion.[5)] Thiocyanogen or halothiocyan provides arylthiocyanate by substitution on electron-rich (hetero) aromatic rings.[6)] The transformation of sulfenyl chlorides to thiocyanates with cyanide ion has long been known and was recently improved by using cyanotrimethylsilane (TMSCN).[7)] As an alternative method, Harusawa and Shioiri reported a simple thiocyanate synthesis from sulfinates with diethyl phosphorocyanidate (DEPC).[8)]

In a study on nitrile synthesis by thermolysis of tosylhydrazone and TMSCN with sodium hydride in diethylene glycol dimethyl ether (diglyme),[9)] we observed the formation of a small amount of tolylthiocyanate. We traced its origin to the reaction of sodium *p*-toluenesulfinate formed by the decomposition of the tosylhydrazone with excess TMSCN. In order to develop a new synthetic method for arylthiocyanates we attempted to improve this reaction.[1)] In this paper we present the details.

In order to find the optimal conditions for the transformation of sulfinates to the thiocyanates we have examined the effects of molar ratio of TMSCN with respect to the chosen standard substrates *p*-toluenesulfinate, and the solvents (Table I). The best choice was three molar equivalents of TMSCN in hexamethylphosphoramide (HMPA) at 0 °C, under whose conditions *p*-tolylthiocyanate was formed in 80% yield as estimated by gas liquid partition chromatography (GLC). Other sulfinates were also transformed to the corresponding thiocyanates under these conditions (Table II). Unsubstituted, halo- and alkyl-substituted benzenesulfinates gave the corresponding arylthiocyanates in satisfactory yields. Despite the steric hindrance, 2,4,6-triisopropylbenzenesulfinate and naphthalenesulfinate were also effective. Although the yield was moderate in the case of the heteroaromatic quinoline derivative, considering the simple procedure for the conversion, the present method may be still valuable.

Although the transformation of sulfinates to thiocyanates mentioned above involves a facile procedure, there remains the problem that sulfinic acids are not always accessible and their unstable and hygroscopic nature often causes difficulty in handling. Thus, in an attempt to transform sulfonyl chlorides directly to the thiocyanates we have admixed a reducing agent of sulfonyl chlorides to sulfinic acids with TMSCN. Among the frequently employed agents such as Zn, Na_2S, $SnCl_2$, KI, PPh_3, $NaBH_4$, $P(OEt)_3$, Na_2SO_3, and $Na_2S_2O_4$,[11)] the combination of sodium sulfite and

TABLE I. Effects on the Transformation of Sodium *p*-Toluenesulfinate to *p*-Tolylthiocyanate of Using TMSCN at Various Molar Ratios and Various Solvents

Molar ratio[a)]	Solvent	Temp. (°C)	Time (h)	Yield[b)] (%)
1	HMPA	0	1	27
2	HMPA	0	1	56
3	HMPA	0	0.5	80
4	HMPA	0	0.5	63
3	Diglyme	105	4	50
3	DMF	0	0.5	70

a) Molar ratio of TMSCN to sulfinate. *b*) Yields were calculated by GLC (Silicon OV-1, 5%) using phenylthiocyanate as the standard substance. DMF = *N*,*N*-dimethylformamide.

TABLE II. Preparation of Thiocyanates from RSO_2Na or RSO_2Cl[a)]

Substrate R	Reaction temp. (°C)	Reaction time (h)	SO_2Na[b)] Yield[d)] (%)	SO_2Cl[c)] Yield[d)] (%)	IR ν_{max}^{KBr} SCN (cm^{-1})
Phenyl	0	6.0	51	38	2150[e)]
4-Methylphenyl	0	6.0	64	41	2155[e)]
4-Methoxyphenyl	0	6.0	52	42	2150
4-Chlorophenyl	0	6.0	51	41	2155
4-Bromophenyl	0	6.0	67	49	2155
4-Acetylaminophenyl	0	6.0	38		2160
2,5-Dimethylphenyl	70	2.0	52	38	2150
2,4,6-Triisopropylphenyl	70	0.5	52	40	2145
2-Naphthyl	0	6.0	69	80	2150
4,4'-Biphenyldi				38	2140
1,3-Phenyldi				10	2150
Benzyl	0	6.0	0	7	2145[e)]
8-Quinolyl	70	0.5	20	18	2150

a) Molar ratio of TMSCN to substrates was 1:3. *b*) In HMPA. *c*) With Na_2SO_3/K_2CO_3 in 2.7/4.0 molar ratio to the substrate in refluxing acetonitrile for 10 min except for 40 min in the case of 4,4'-biphenyldisulfonyl dichloride. *d*) Isolated yields. *e*) ν_{max}^{neat}.

TABLE III. Effects of Reducing Agent on Transformation of Benzenesulfonyl Chloride to Phenylthiocyanate Using TMSCN[a]

Reducing agent/base (molar ratio)[b]	Solvent	Temp. (°C)	Time (h/min)	Yield[c] (%)
Na_2SO_3/NaOH	Acetonitrile	[d]	8	16
Na_2SO_3/$(C_2H_5)_3N$	Acetonitrile	[d]	3	20
Na_2SO_3/K_2CO_3	Acetonitrile	[d]	/5	47
Na_2SO_3/K_2CO_3	Diglyme	105	4	28
Na_2SO_3/K_2CO_3	THF	[d]	8	22
Na_2SO_3/K_2CO_3	HMPA	20	/5	28

a) Molar ratio of TMSCN to sulfonyl chloride was 1:3. *b*) Molar ratio of additives to sulfonyl chloride was 2:1, but that of Na_2SO_3/bases was 2.7/4.0:1.[10] *c*) Yields were calculated from GLC (Silicon OV 1, 5%) data based on *p*-tolylthiocyanate as the standard substance. *d*) Reflux temperatures of the solvents.

potassium carbonate in acetonitrile as the solvent gave the best result (Table III). The application of the phosphorus compounds, Na_2S, or $NaBH_4$ gave the thiocyanate only in trace amounts. The transformation of sulfonyl chlorides to thiocyanates using TMSCN and the finely powdered reducing reagent was completed in most cases within 10 min. Arylthiocyanates were generally obtained in preparatively satisfactory yields, free from the isothiocyanates (Table II). Bifunctional 4,4'-biphenyldithiocyanate and *m*-phenyldithiocyanate could also be prepared by this method.

Experimental

Melting points were recorded on a Yanagimoto micro melting point apparatus and are uncorrected. Infrared (IR) spectra were determined on a JASCO A-100 spectrometer. Nuclear magnetic resonance (NMR) spectra were recorded by using a JNMGX-270 spectrometer in $CDCl_3$ solution with tetramethylsilane as an internal standard. GLC was measured by using a Shimadzu GC 14A with a C-R 5A Calculator (5% OV-1, 2 m glass column). Acetonitrile and HMPA were purified by distillation from phosphorus pentoxide and calcium hydride, respectively. Sulfonyl chlorides and TMSCN were purchased from Aldrich Chem., Milwaukee, and were used without further purification. Sulfinic acids and the sodium salts were prepared according to the standard procedures.[12] Potassium carbonate and sodium sulfite were finely powdered immediately before use. Plates for preparative thin-layer chromatography were prepared with Merck Silica gel PF-254.

Reaction of Sulfinates with TMSCN Typical Procedure A: A solution of TMSCN (297 mg, 3 mmol) in HMPA (1 ml) was added to an ice-cold suspension of sodium 4-chlorobenzenesulfinate (198 mg, 1 mmol) in HMPA (2 ml). After being stirred for 6 h at 0 °C, the mixture was diluted with water and extracted with diisopropyl ether and then the organic layer was washed with 5% Na_2CO_3 solution and dried over anhydrous sodium sulfate. The solvent was evaporated off, and the residue was chromatographed on silica gel using carbon tetrachloride as the eluent to give 4-chlorophenylthiocyanate as crystals (86 mg, 51%), mp 32—34 °C (lit.[7] 34—35 °C). The following thiocyanates were similarly prepared; the oily compounds were identified by comparison of the retention times on GLC with those of authentic samples. Phenylthiocyanate (oil)[7]; *p*-tolylthiocyanate (oil)[7]; *p*-methoxyphenylthiocyanate, mp 47—48 °C (lit.[13] 48 °C); *p*-bromophenylthiocyanate, mp 53 °C (lit.[14] 56 °C); 2,5-dimethylphenylthiocyanate (oil)[6c]; acetylaminophenylthiocyanate, mp 183—185 °C (lit.[15] 181 °C); *m*-dithiocyanobenzene, mp 52—54 °C (lit.[16] 54 °C); 2-naphtylthiocyanate, mp 38—39 °C (lit.[7] 43—44 °C); benzylthiocyanate, mp 41 °C (lit.[7] 39—40 °C); 8-quinolylthiocyanate, mp 88—89 °C (lit.[17] 89 °C).

Reaction of Sulfonyl Chloride with TMSCN/Na_2SO_3/K_2CO_3 Typical Procedure B: A solution of benzenesulfonyl chloride (1.77 g, 10 mmol) in acetonitrile (10 ml) was added to a stirred suspension of TMSCN (3.00 g, 30 mmol), sodium sulfite (3.43 g, 27 mmol), and potassium carbonate (4.28 g, 40 mmol) in acetonitrile (15 ml). Stirring was continued under reflux. The reaction was quenched by diluting with diisopropyl ether (*ca.* 30 ml) and insoluble materials were filtered off. The filtrate was poured into ice-cold water and the aqueous phase was extracted with ether. The combined ether extract was washed once with water and dried over anhydrous sodium sulfate. After evporation of the solvent, the residue was chromatographed on silica gel using diisopropyl ether as the eluent to give phenylthiocyanate as a pale yellow oil (513 mg, 38%).

Preparation of 2,4,6-Triisopropylphenylthiocyanate[8] by Procedure A A solution of TMSCN (297 mg, 3 mmol) in HMPA (1 ml) was added to a stirred solution of sodium 2,4,6-triisopropylbenzenesulfinate (290 mg, 1 mmol) in HMPA (3 ml) at room temperature. After being stirred for 30 min at 70 °C, the mixture was diluted and worked up as described in typical procedure A. Chromatography using benzene as the eluent gave the thiocyanate (136 mg, 52%), mp 73—74 °C. MS *m/z* (%): 262 ($M^+ + 1$, 11), 261 (M^+, 95), 246 ($M^+ - CH_3$, 100), 218 ($M^+ - CH(CH_3)_2$, 8). ^{1}H-NMR ($CDCl_3$) δ: 1.26 (d, 6H, J=7 Hz), 1.31 (d, 12 H, J=7 Hz), 2.92 (m, 1H), 3.78 (m, 2H), 7.13 (s, 2H). ^{13}C-NMR ($CDCl_3$) δ: 23.6, 23.7, 32.3, 34.3, 112.1, 117.6, 123.0, 152.7, 152.8.

Preparation of 4,4'-Biphenyldithiocyanate by Procedure B 4,4'-Biphenyldisulfonyl dichloride (1.76 g, 5 mmol) was added portionwise to a stirred solution of TMSCN (3.00 g, 30 mmol), sodium sulfite (3.43 g, 27 mmol), and potassium carbonate (5.57 g, 40 mmol) in acetonitrile (15 ml) and then HMPA (0.5 ml) was added. The mixture was heated under reflux for 40 min. The reaction mixture was poured into cold water and extracted with benzene. The benzene solution was washed with saturated Na_2CO_3 solution and with water and dried over anhydrous sodium sulfate. After evaporation of the solvent, the residue was chromatographed on silica gel using benzene as the eluent to give 4,4'-biphenyldithiocyanate as pale yellow needles (509 mg, 38%), mp 129.5—130.5 °C. ^{1}H-NMR ($CDCl_3$) δ: 7.62 (br s). ^{13}C-NMR ($CDCl_3$) δ: 109.8, 124.4, 128.7, 130.3, 140.6. MS *m/z* (%): 270 ($M^+ + 2$, 10), 269 ($M^+ + 1$, 18), 268 (M^+, 100), 210 ($M^+ - SCN$, 25), 153 ($M^+ - 2SCN - 1$, 25). *Anal.* Calcd for $C_{14}H_8N_2S_2$: C, 62.66; H, 3.00; N, 10.44; S, 23.90. Found: C, 62.82; H, 2.91; N, 10.38; S, 24.02.

Acknowledgement We are grateful to Bayer AG and Nihon Tokushu Noyaku Seizo Co. for providing of some of the sulfonyl chlorides and sulfinates.

References and Notes

1) A preliminary communication describing part of this work has appeared: S. Kagabu, M. Maehara, K. Sawahara, and K. Saito, *J. Chem. Soc., Chem. Commun.*, **1988**, 1485.
2) B. Schulze, M. Mülstädt, and J. Schubert, *Z. Chem.*, **19**, 41 (1979); E. E. Reid, "Organic Chemistry of Bivalent Sulfur," Vol. 6, Chemical Pub. Co., N.Y. 1966, Chap. 1.
3) R. G. Guy, "The Chemistry of Cyanates and Their Thio Derivatives," ed. by S. Patai, Wiley, Chichester, 1977, Chap. 18; S. Harusawa and T. Shioiri, *Yuki Gosei Kagaku Kyokai Shi*, **39**, 741 (1981).
4) E. C. Taylor, F. Kienzle, and A. McKillop, *Synthesis*, **1972**, 38.
5) S. Uemura, S. Uchida, M. Okano, and K. Ichikawa, *Bull. Chem. Soc. Jpn.*, **46**, 3254 (1973).
6) *a*) J. L. Wood, "Organic Reactions," Vol. 3, 1946, Chap. 6; *b*) F. Söderbäck, *Acta Chem. Scand.*, **8**, 1851 (1954); *c*) S. Uemura, A. Onoe, H. Okazaki, and M. Okano, *Bull. Chem. Soc. Jpn.*, **48**, 619 (1975).
7) D. N. Harpp, B. T. Friedlander, and R. A. Smith, *Synthesis*, **1979**, 181.
8) S. Harusawa and T. Shioiri, *Tetrahedron Lett.*, **23**, 447 (1982).
9) K. Saito, S. Kagabu, Y. Horie, and K. Takahashi, *Org. Prep. Proced. Int.*, **21**, 354 (1989).
10) In this transformation the best molar ratio of benzenesulfonyl chloride, TMSCN, sodium sulfite, and potassium carbonate was 1:3:2.7:4; K. Sawahara, unpublished result.
11) F. Muth, "Methoden der Organischen Chemie," Vol. 9, ed. by E. Müller, Houben-Weyl, Thieme, Stuttgart, 1955, pp. 303—331; K. K. Andersen, "In Sulphur, Selenium, Silicon, Boron, Organometallic Compounds," ed. by D. N. Jones, Vol. 3 of "Comprehensive Organic Chemistry," ed. by D. Barton and D. Ollis, Pergamon, 1979, p. 363; E. Wenschu and K. Polling, *Z. Chem.*, **20**, 122 (1980); A. Nose and T. Kudo, *Chem. Pharm. Bull.*, **35**, 1770 (1987).
12) M. Uchino, K. Suzuki, and M. Sekiya, *Chem. Pharm. Bull.*, **26**, 1837 (1978).
13) J. W. Dienske, *Rec. Trav. Chim.*, **50**, 165 (1931).
14) F. Challenger and A. D. Collins, *J. Chem. Soc.*, **1924**, 1379.
15) H. P. Kaufmann and E. Weber, *Arch. Pharm.*, **267**, 192 (1929).
16) S. Gabriel, *Chem. Ber.*, **10**, 184 (1877).
17) A. Edinger, *Chem. Ber.*, **41**, 938 (1908).

Synthesis and Anti-inflammatory Activities of Some *N*-[Pyridyl(phenyl)carbonylamino]-*tert*-butyl/phenyl-1,2,3,6-tetrahydropyridines

Kinfe K. REDDA,* Kode N. RAO, Ann S. HEIMAN, Folakemi Y. ONAYEMI and Janine B. CLARK

College of Pharmacy and Pharmaceutical Sciences, Florida A & M University, Tallahassee, Florida 32307, U.S.A. *Received June 11, 1990*

Nucleophilic attack of *tert*-butyl/phenylpyridines 3 on 1-chloro-2,4-dinitrobenzene 4 results in the formation of *tert*-butyl/phenyl substituted 2,4-dinitrophenylpyridinium chlorides 5. Benzoyl hydrazide and pyridyl acid hydrazides 6 were reacted with the pyridinium chlorides 5 furnishing the 2,4-dinitroanilino derivatives 7, which were subsequently hydrolyzed with water: *p*-dioxane to yield *N*-[pyridyl(phenyl)carbonylimino]-*tert*-butyl/phenylpyridinium ylides 8. The title compounds 9, *N*-[pyridyl(phenyl)carbonylamino]-*tert*-butyl/phenyl-1,2,3,6-tetrahydropyridines, were obtained by sodium borohydride reduction of the pyridinium ylides 8. The anti-inflammatory activities of compounds 9a—p were determined using the carrageenan-soaked sponge model of inflammation in Sprague Dawley rats. All compounds tested showed moderate to good anti-inflammatory effects compared to indomethacin. Compounds 9b, 9c and 9p were the most active analogs of the group in this model.

Keywords pyridinium *N*-aroylimide; sodium borohydride reduction; *N*-aroylamino-1,2,3,6-tetrahydropyridine; anti-inflammatory activity; carrageenan

Several compounds consisting of reduced pyridine, like the 1,2,3,6-tetrahydropyridine (THP) **1** ring systems shown in Fig. 1, are known to exhibit a variety of biological activities.[1,2] Our interest[3,4] along with Knaus *et al.*[5,6] and Coutts *et al.*[7] in the 1,2,3,6-tetrahydropyridines is due to their hypotensive, analgesic, anti-inflammatory and antipyretic activities. 1-Methyl-4-phenyl-1,2,3,6-tetrahydropyridine (MPTP) **2** was recently found to be neurotoxic, causing persistent parkinsonism in humans and other animal species.[8-11] Aspects of the MPTP mechanism of action,[12,13] bioactivation pathways[14] and structural modifications[15,16] are well documented. The pharmacological activities of the compounds bearing a THP ring system appear to be greatly dependent on the nature and position of alkyl and/or aryl substituents. Previously, we synthesized a series of *N*-amino-1,2,3,6-tetrahydropyridines which showed significant anti-inflammatory, analgesic and hyperglycemic activities with no observed toxicity, even at high dose levels on preliminary pharmacological screening.[17,18] We have renewed interest in the THP ring system substituted with appropriate alkyl and/or aryl groups. In the present paper, we describe the synthesis of 1,2,3,6-tetrahydropyridines, substituted with phenyl or *tert*-butyl groups, and their anti-inflammatory activities.

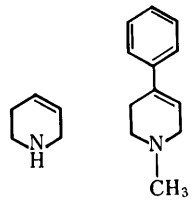

1 2

Fig. 1

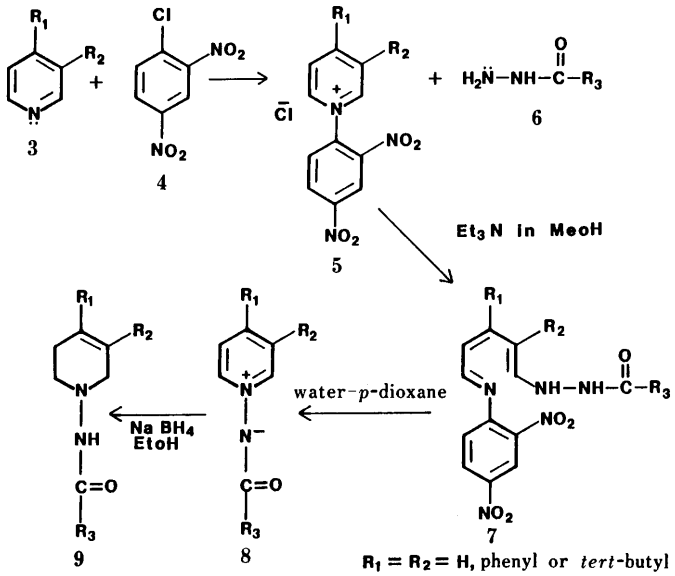

Chart 1

Chemistry Appropriate molar amounts of *tert*-butyl or phenyl substituted pyridines **3** are reacted with 1-chloro-2,4-dinitrobenzene **4** in dry acetone at reflux for 12 h to furnish the *N*-(2,4-dinitrophenyl)pyridinium chlorides **5**. Reaction of **5** with benzoyl or pyridyl acid hydrazides **6** in methanol containing triethylamine at room temperature for 12 h results in the ring-opened products, 2,4-dinitroanilino derivatives **7**. The *N*-[pyridyl(phenyl)carbonylimino]-*tert*-butyl/phenylpyridinium ylides **8** are obtained by hydrolysis of **7** with water : *p*-dioxane mixture (1 : 4, v/v) for 12 h under reflux along with 2,4-dinitroaniline. $NaBH_4$ reduction of **8** in absolute ethanol at 0 °C for 4 h afforded *N*-[pyridyl(phenyl)carbonylamino]-1,2,3,6-tetrahydropyridines **9** (Chart 1).[19,20] The proton nuclear magnetic resonance (^{1}H-NMR) spectra of the pyridinium ylides **8** and the title compounds **9** show well resolved splitting patterns.[21,22] The ^{1}H-NMR spectrum of *N*-(2′-pyridyl)carbonylamino-3-phenyl-1,2,3,6-tetrahydropyridine **9g** [Figs. 2a and 2b, c (expanded)] recorded in $CDCl_3$ shows signals at δ 2.52 (2H, m, C_3-H), 3.18 (2H, t, J = 5.49 Hz, C_2-H), 3.90 (2H, m, C_6-H), 6.18 (1H, m, C_4-H, olefinic), 7.21—7.34 (5H, complex m, $C_{2''}$-H to $C_{6''}$-H of phenyl), 7.43 (1H, m, $C_{5'}$-H), 7.84 (1H, td, $J_{4',3'} = J_{4',5'} = 7.78$ Hz, $J_{4',6'} = 1.83$ Hz, $C_{4'}$-H), 8.23 (1H, dt, $J_{3',4'} = 7.78$ Hz, $J_{3',5'} = 1.38$ Hz, $J_{3',6'} = 0.91$ Hz, $C_{3'}$-H), 8.52 (1H, m, $C_{6'}$-H), 9.07 (1H, NH, D_2O exchangeable) in agreement with the structure.

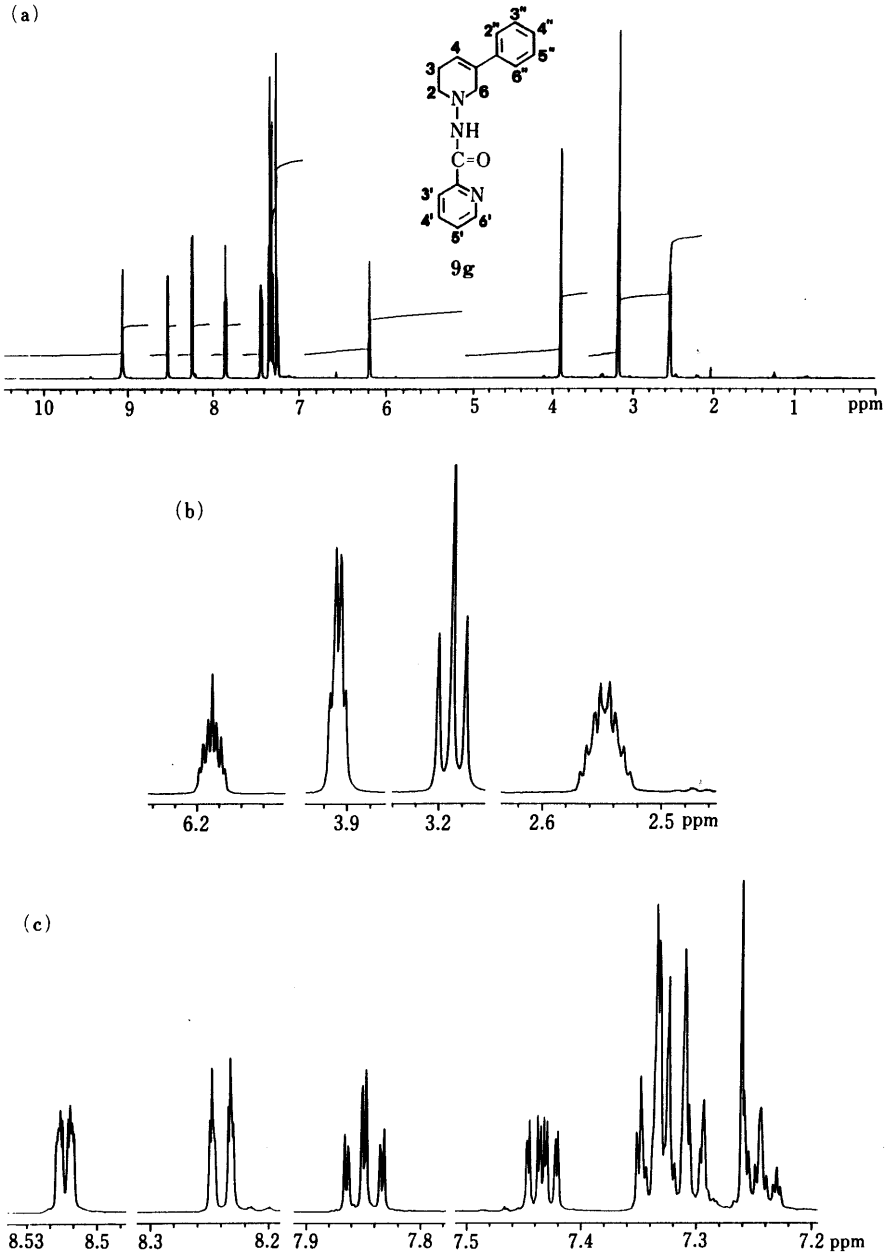

Fig. 2

The synthetic data of the pyridinium ylides **8a**—**l** and the tetrahydropyridines **9a**—**l** are shown in Table I and Table II, respectively.

Biological Activity The pharmacological testing data of **9a**—**p** are summarized in Table II. Sponge implantation is a convenient system for providing ready access to cells and fluids involved in an ongoing inflammatory response. Using this technique, it has been shown that indomethacin reduces leukocyte migration into subcutaneously implanted carrageenan-impregnated sponges with an ID_{50} of 2 mg/kg when administered orally.[23] In the present investigation, we find that following intraperitoneal administration, indomethacin has an ID_{50} of 2.9 mg/kg for leukocyte accumulation while the dose required to reduce the volume of exudates by 50% is approximately 4.5-fold higher. Indomethacin, at 2.9 mg/kg, was used at the standard against which inhibition of cell accumulation was assessed as a measure of anti-inflammatory activity for the new tetrahydropyridine derivatives.

ID_{50} values of anti-inflammatory activities are depicted in Table II. All compounds tested inhibited leukocyte accumulation in a dose-dependent manner although none were as potent as the reference compound, indomethacin. When ID_{50}'s of the phenyl and *tert*-butyl derivatives **9a**—**l** are compared with their respective unsubstituted compounds **9m**—**p**, it can be seen that for the 4-, 3- and 2-pyridyl series, the greatest increases in activity are seen following treatment with 4-*tert*-butyl derivatives **9a**—**c**. In contrast, the 3- or 4-phenyl substituents **9e**—**k** generally did not increase anti-inflammatory activity in this model. The 4-phenyl and *tert*-butyl derivatives of compound **9p** showed 3.5 to 4.5-fold losses of anti-inflammatory activity.

Taken together, these pharmacological testing results indicate that a 1.8 to 6.5-fold increase in anti-inflammatory activity can be achieved by 4-*tert*-butyl substitution of the 2-, 3- or 4-pyridyl compounds.

TABLE I. *N*-[Pyridyl(phenyl)carbonylimino]-*tert*-butyl or Phenyl Pyridium Ylides (**8a—l**)

Compound	R_1	R_2	R_3	mp (°C)	Yield (%)	Formula	Analysis (%) Calcd (Found)		
							C	H	N
8a	*tert*-Butyl	H	4′-Pyridyl	201—203	43	$C_{15}H_{17}N_3O$	70.56 (70.51	6.71 6.73	16.45 16.43)
8b	*tert*-Butyl	H	3′-Pyridyl	145—147	36	$C_{15}H_{17}N_3O$	70.56 (70.34	6.71 6.60	16.45 16.33)
8c	*tert*-Butyl	H	2′-Pyridyl	224—226	50	$C_{15}H_{17}N_3O$	70.56 (70.48	6.71 6.74	16.45 16.50)
8d	*tert*-Butyl	H	Phenyl	184—186	32	$C_{16}H_{18}N_2O$	75.56 (75.34	7.13 7.33	11.01 11.07)
8e	H	Phenyl	4′-Pyridyl	144—145	54	$C_{17}H_{13}N_3O$	74.16 (73.92	4.75 4.67	15.26 15.09)
8f	H	Phenyl	3′-Pyridyl	112—114	41	$C_{17}H_{13}N_3O$	74.16 (74.27	4.75 4.81	15.26 15.23)
8g	H	Phenyl	2′-Pyridyl	Semi-solid	52	$C_{17}H_{13}N_3O$	74.16 (74.45	4.75 4.60	15.26 15.15)
8h	H	Phenyl	Phenyl	123—125	72	$C_{18}H_{14}N_2O$	78.81 (78.92	5.14 5.34	10.21 10.09)
8i	Phenyl	H	4′-Pyridyl	245—247	42	$C_{17}H_{13}N_3O$	74.16 (74.12	4.75 4.76	15.26 15.24)
8j	Phenyl	H	3′-Pyridyl	207—209	33	$C_{17}H_{13}N_3O$	74.16 (74.16	4.75 4.78	15.26 15.23)
8k	Phenyl	H	2′-Pyridyl	195—197	51	$C_{17}H_{13}N_3O$	74.16 (74.10	4.75 4.80	15.26 15.30)
8l	Phenyl	H	Phenyl	209—211	39	$C_{18}H_{14}N_2O$	78.81 (78.78	5.14 5.18	10.21 10.21)

TABLE II. Synthetic and Pharmacological Data of *N*-[Pyridyl(phenyl)carbonylamino]-*tert*-butyl or Phenyl-1,2,3,6-tetrahydropyridine (**9a—p**)

Compound	R_1	R_2	R_3	mp (°C)	Yield (%)	Formula	Analysis (%) Calcd (Found)			Anti-inflammatory[a] ID_{50} (mg/kg)
							C	H	N	
9a	*tert*-Butyl	H	4′-Pyridyl	184—186	51	$C_{15}H_{21}N_3O$	69.46 (69.43	8.16 8.14	16.20 16.13)	10
9b	*tert*-Butyl	H	3′-Pyridyl	141—143	35	$C_{15}H_{21}N_3O$	69.46 (69.52	8.16 7.76	16.20 16.04)	6.7
9c	*tert*-Butyl	H	2′-Pyridyl	125—127	26	$C_{15}H_{21}N_3O$	69.46 (69.02	8.16 8.23	16.20 15.92)	7.9
9d	*tert*-Butyl	H	Phenyl	126—128	45	$C_{16}H_{22}N_2O$	74.38 (74.24	8.58 8.65	10.84 10.96)	20.6
9e	H	Phenyl	4′-Pyridyl	158—160	45	$C_{17}H_{17}N_3O$	73.09 (72.90	6.13 6.13	15.04 14.99)	17.4
9f	H	Phenyl	3′-Pyridyl	159—161	35	$C_{17}H_{17}N_3O$	73.09 (72.67	6.13 6.10	15.04 14.56)	42.7
9g	H	Phenyl	2′-Pyridyl	78—80	66	$C_{17}H_{17}N_3O$	73.09 (73.04	6.13 6.14	15.04 15.08)	18.2
9h	H	Phenyl	Phenyl	170—172	25	$C_{18}H_{18}N_2O$	77.67 (77.54	6.51 6.49	10.06 10.08)	23.1
9i	Phenyl	H	4′-Pyridyl	191—193	48	$C_{17}H_{17}N_3O$	73.09 (73.10	6.13 6.12	15.04 15.00)	24.3
9j	Phenyl	H	3′-Pyridyl	172—174	32	$C_{17}H_{17}N_3O$	73.09 (73.14	6.13 6.14	15.04 15.00)	13.5
9k	Phenyl	H	2′-Pyridyl	140—142	38	$C_{17}H_{17}N_3O$	73.09 (73.14	6.13 6.14	15.04 15.00)	14.6
9l	Phenyl	H	Phenyl	177—179	20	$C_{18}H_{18}N_2O$	77.67 (77.63	6.51 6.54	10.06 10.06)	19.2
9m	H	H	4′-Pyridyl	142—144	(lit. 143)[3,4]					17.9
9n	H	H	3′-Pyridyl	119—121	(lit. 120)[3,4]					43.6
9o	H	H	2′-Pyridyl	82—83	(lit. 82)[3,4]					13.8
9p	H	H	Phenyl	138—140	(lit. 138)[3,4]					5
Indomethacin										2.9

a) Anti-inflammatory ID_{50}s represent doses required to inhibit accumulation of leukocytes by 50% in the 5 h carrageenan-soaked sponge model of inflammation in the rat.

Further efforts to introduce bifunctional substituents to these tetrahydropyridines and to study cycloaddition reactions are in progress.

Experimental

^{1}H-NMR spectra were recorded on a Brucker 270 MHz NMR instrument, except **9g**, which was recorded on a varian 500 MHz instrument in $CDCl_3$ while using chloroform as an internal standard. Infrared (IR) spectra were recorded on a Perkin Elmer 1430 Instrument equipped with a 7500 professional computer. Melting points were recorded on Electrothermal R apparatus and are uncorrected. C, H, N analytical data was provided by Galbraith Laboratories, Inc., Knoxville, Tennessee. Sprague Dawley rats were purchased from Harlan Inc., Indianapolis, IN. Lambda carrageenan was purchased from Sigma Chemical Co., St. Louis, MO. Leukocytes were quantitated in Neubauer chambers from Fisher Scientific Co., and/or counted electronically with a CBC5 Coulter Counter purchased from Coulter Electronics, Hialeah, Florida. All the other chemicals and solvents used were purchased from Aldrich Chemical Company, Inc., Milwaukee, Wisconsin, and Fisher Scientific Company, Orlando, Florida. Compounds were tested for anti-inflammatory activity in the carrageenan-soaked sponge model of inflammation[24] in 140—170 g male rats randomly divided into groups of five. Sponge implants (1.0 cm square) were sterilized by autoclaving; then, just prior to implantation, they were injected with 0.3 ml of sterilized 1% lambda carrageenan in saline. Drugs were freshly prepared by dissolving them in 5% dimethyl sulfoxide (DMSO) and 95% propylene glycol (v/v).

Sponges (two per animal) were implanted subcutaneously in rats lightly anesthetized with methoxyfluorane inhalation anesthesia, and their abdomens washed thoroughly with 70% ethanol in water (v/v). A small incision was made through the ventral skin and a subcutaneous pocket formed near each axilla by gently prying the skin loose from the underlying body wall. Following insertion of a sponge into each pocket, the incision was closed with 9 mm stainless steel autoclips and drugs administered by intraperitoneal injection.

Sponges were left *in situ* for 5 h, then carefully removed and placed into the barrel of a 10 ml syringe. Inflammatory exudates were recovered by adding 1 ml phosphate buffered saline containing 10 U/ml heparin and gently compressing the syringe plunger. Exudate volumes were measured by weighing on a Mettler balance, and total leukocyte contents were determined by counting diluted aliquots of cells in Neubauer chambers and/or with a Coulter Counter.[25]

ID_{50} (the dose needed to inhibit leukocyte accumulation by 50%) values were calculated from best fit linear regression lines relating dose to response where response was expressed as percent inhibition compared to untreated controls.

***N*-(4′-Pyridylcarbonylimino)-4-*tert*-butylpyridinium Ylide (8a): General Procedure A** 4-*tert*-Butylpyridine **3a** (25.7 g, 190.08 mmol) was added to a stirring solution of 1-chloro-2,4-dinitrobenzene (35.0 g, 172.79 mmol) in 400 ml anhydrous acetone dropwise and the contents refluxed for 12 h. The reaction mixture was cooled to 10 °C for 1 h and filtered. The residue was washed thoroughly with hexane (3 × 100 ml) and dried *in vacuo* at room temperature to furnish *N*-(2′,4′-dinitrophenyl)-4-*tert*-butylpyridinium chloride **5a** as a pale yellow crystalline solid (37.5 g, 58%), mp 154—156 °C (dec.). Compound **5a** (6.0 g, 17.76 mmol) was reacted with isonicotinic acid hydrazide (2.44 g, 17.79 mmol) in 100 ml methanol containing 1.0 ml triethylamine for 12 h at room temperature. The dark brown precipitate formed was filtered, then washed successively with 60 ml each of hexane and ether. The residue was immediately refluxed in water: *p*-dioxane (1 : 4, v/v) for 12 h. The reaction medium was evaporated under reduced pressure and the brownish residue obtained was chromatographed on a column of neutral alumina (2.5 × 25 cm) using ether : methanol (20 : 1, v/v, and 10 : 1, v/v) as an eluent. The product **8a** was crystallized from ethyl acetate : methylene chloride : hexane (2 : 1 : 1, v/v) as pale yellow needles (1.96 g). ^{1}H-NMR ($CDCl_3$) δ: 1.37 (9H, s, C_4-*tert*-butyl) 7.6 (2H, d, J=5 Hz, $C_{3'}$-H, $C_{5'}$-H), 7.93 (2H, d, J=5 Hz, C_3-H, C_5-H), 8.57—8.67 (4H, m, C_2-H, C_6-H, $C_{2'}$-H, $C_{6'}$-H).

***N*-(3′-Pyridylcarbonylimino)-4-*tert*-butylpyridinium Ylide (8b)** Compound **8b** was prepared by following the procedure for **8a**. ^{1}H-NMR ($CDCl_3$) δ: 1.37 (9H, s, C_4-*tert*-butyl), 7.30 (1H, m, $C_{5'}$-H), 7.62 (2H, d, $J_{3,2}=J_{5,6}$=5 Hz, C_3-H, C_5-H), 8.37 (1H, dt, $J_{4',5'}$=8 Hz, $J_{4',6'}=J_{4',2'}$= 2 Hz, $C_{4'}$-H), 8.60—8.67 (3H, m, C_2-H, C_6-H, $C_{6'}$-H), 9.32 (1H, dd, $J_{2',4'}=J_{2',6'}$=2 Hz, $C_{2'}$-H).

***N*-(2′-Pyridylcarbonylimino)-4-*tert*-butylpyridinium Ylide (8c)** Compound **5a** (16.0 g, 47.37 mmol) was reacted with picolinic acid hydrazide (7.99 g, 58.26 mmol) in 110 ml methanol containing 7.38 ml triethylamine at 0 to 10 °C for 2 h, and the yellow precipitate obtained was washed with 100 ml each of hexane followed by ether and then hydrolyzed with water: *p*-dioxane (1 : 4, v/v, 500 ml) for 12 h at reflux temperature. The reaction medium evaporated to nearly half the volume, was cooled to −10 °C for 2 h and filtered. The yellow residue was found to be exclusively the dinitroaniline and was rejected. The filtrate was concentrated and azeotroped with benzene (3 × 100 ml). The residue was crystallized from ethyl acetate : methylene chloride (1 : 1, v/v, 150 ml) as pale yellow prisms (6.05 g). ^{1}H-NMR ($CDCl_3$) δ: 1.33 (9H, s, *tert*-butyl), 7.27—7.34 (1H, m, $C_{5'}$-H), 7.6 (2H, d, J=7 Hz, C_3-H, C_5-H), 7.77 (1H, m, $C_{4'}$-H), 8.16 (1H, d, J=7 Hz, $C_{3'}$-H), 8.65 (3H, m, C_2-H, C_6-H and $C_{6'}$-H).

***N*-(Benzoylimino)-4-*tert*-butylpyridinium Ylide (8d)** Compound **8d** was similarly prepared by following the procedure for **8a**. ^{1}H-NMR ($CDCl_3$) δ: 1.32 (9H, s, C_4-*tert*-butyl), 7.33—7.45 (3H, m, $C_{3'}$-H, $C_{4'}$-H, $C_{5'}$-H of phenyl), 7.53 (2H, d, $J_{2',3'}=J_{6',5'}$=7 Hz, $C_{2'}$-H, $C_{6'}$-H of phenyl), 8.10—8.20 (2H, m, C_3-H, C_5-H), 8.6—8.67 (2H, d, $J_{2,3}=J_{6,5}$=7 Hz, C_2-H, C_6-H).

***N*-(4′-Pyridylcarbonylimino)-3-phenylpyridinium Ylide (8e)** Equimolar amounts of 3-phenylpyridine (24.0 g, 154.64 mmol) and 1-chloro 2,4-dinitrobenzene (31.33 g, 154.67 mmol) were refluxed in 350 ml of anhydrous acetone for 12 h. The contents were cooled to 0 °C for 1 h, filtered and washed with hexane (2 × 100 ml). The residue was crystallized from ethyl acetate : methanol (4 : 1, v/v, 200 ml) to give *N*-(2′,4′-dinitrophenyl)-3-phenylpyridinium chloride **5e** as a brown solid (29.9 g). **5e** (6.0 g, 16.77 mmol) was reacted with isonicotinic acid hydrazide (2.53 g, 18.45 mmol) and the reaction was worked up as described in general procedure A to furnish **8e** (2.5 g). ^{1}H-NMR ($CDCl_3$) δ: 7.48—7.66 (5H, complex m, $C_{2''}$-H to $C_{6''}$-H of phenyl), 7.73 (1H, m, C_5-H), 7.97 (2H, d, J=4.5 Hz, $C_{3'}$-H, $C_{5'}$-H), 8.11 (1H, m, C_4-H), 8.67 (2H, d, J=4.5 Hz, $C_{2'}$-H, $C_{6'}$-H), 8.75 (1H, dt, J=1.5, 6 Hz, C_6-H), 9.05 (1H, m, C_2-H).

***N*-(3′-Pyridylcarbonylimino)-3-phenylpyridinium Ylide (8f)** Nicotinic acid hydrazide (1.53 g, 11.18 mmol) was reacted with **5e** (4.0 g, 11.18 mmol) in 100 ml methanol containing 1.0 ml triethylamine at 0 to 10 °C for 12 h, and the reaction was worked up as described under the general procedure A. The resulting product was chromatographed on a column of neutral alumina (2.5 × 25 cm) employing ether : methanol (10 : 1, v/v) as the eluent, and then crystallized from ethyl acetate as brown needles, **8f** (1.27 g). ^{1}H-NMR ($CDCl_3$) δ: 7.30 (1H, m, $C_{5'}$-H), 7.41—7.61 (5H, complex m, $C_{2''}$-H to $C_{6''}$-H of phenyl), 7.70 (1H, m, C_5-H), 8.06 (1H, m, $C_{4'}$-H), 8.40 (1H, dt, J=2, 8 Hz, C_4-H), 8.62 (1H, dd, J=1.5, 5 Hz, $C_{6'}$-H), 8.72 (1H, m, C_6-H), 9.03 (1H, t, J=1.5 Hz, $C_{2'}$-H), 9.36 (1H, br s, C_2-H).

***N*-(2′-Pyridylcarbonylimino)-3-phenylpyridinium Ylide (8g)** Compound **8g** was similarly prepared by following the general procedure A. ^{1}H-NMR ($CDCl_3$) δ: 7.47—7.67 (5H, complex m, phenyl), 7.72—7.87 (2H, m, C_5-H, $C_{5'}$-H), 8.12 (1H, d, $J_{4,5}$=8 Hz, C_4-H), 8.26 (1H, d, $J_{6',5'}$=7.5 Hz, $C_{6'}$-H), 8.82 (1H, d, $J_{6,5}$=6 Hz, C_6-H), 9.11 (1H, s, C_2-H).

***N*-(Benzoylimino)-3-phenylpyridinium Ylide (8h)** Compound **5e** (4.0 g, 11.18 mmol) was reacted with benzoylhydrazide (1.53 g, 11.23 mmol) in 120 ml of methanol containing 2.0 ml of triethylamine for 3 h at 0 to 10 °C and the reaction was worked up as described under the general procedure A. The product obtained was chromatographed on a column of neutral alumina (2.5 × 25 cm) using ether : methanol (35 : 1, v/v) as eluent when a semi-solid was obtained on evaporation. It was crystallized from ethyl acetate: hexane (2 : 1, v/v, 150 ml) to give pale yellow needles, **8h** (2.21 g). ^{1}H-NMR ($CDCl_3$) δ: 7.39—7.63 (8H, complex m, $C_{3'}$-H, $C_{4'}$-H, $C_{5'}$-H and $C_{2''}$-H to $C_{6''}$-H of phenyl), 7.7 (1H, m, C_5-H), 8.06 (1H, m, C_4-H), 8.17 (2H, m, $C_{2'}$-H, $C_{6'}$-H of phenyl), 8.76 (1H, m, C_6-H), 9.07 (1H, t, J=1.5 Hz, C_2-H).

***N*-(4′-Pyridylcarbonylimino)-4-phenylpyridinium Ylide (8i)** 4-Phenylpyridine (25.0 g, 161.08 mmol) and 1-chloro 2,4-dinitrobenzene (32.63 g, 161.09 mmol) were refluxed in 400 ml of anhydrous acetone under stirring for 12 h. The contents were cooled to 10 °C for 1 h, filtered, and the residue was washed thoroughly with hexane (3 × 100 ml). The product was dried at room temperature under vacuum to furnish *N*-(2′,4′-dinitrophenyl)-4-phenylpyridinium chloride **5i** as a pale yellow shining crystalline solid (30.0 g, 52.05%), mp 182—184 °C. Compound **5i** (6.0 g, 16.77 mmol) was reacted with isonicotinic acid hydrazide (2.30 g, 16.78 mmol) in 125 ml methanol containing 1.5 ml of triethylamine for 12 h at room temperature and the reaction was worked up as described under the general procedure A. The resulting product was chromatographed on a column of neutral alumina (2.5 × 30 cm) using ether : methanol (10 : 1, v/v and 5 : 1, v/v) as eluent. The product was collected as a brown solid after evaporation. An analytical sample was obtained by crystallization from methylene chloride : ethyl acetate : methanol (4 : 1 : 0.1, v/v) as brownish white prisms

of **8i** (1.94 g). ^{1}H-NMR ($CDCl_3$) δ: 7.53 (3H, m, $C_{3''}$-H, $C_{4''}$-H, $C_{5''}$-H of phenyl), 7.8—7.95 (4H, m, C_3-H, C_5-H and $C_{2''}$-H, $C_{6''}$-H of phenyl), 8.01 (2H, d, J=7 Hz, C_3-H, C_5-H), 8.56 (2H, d, J=6 Hz, $C_{2'}$-H, $C_{6'}$-H), 8.85 (2H, d, J=7 Hz, C_2-H, C_6-H).

***N*-(3'-Pyridylcarbonylimino)-4-phenylpyridinium Ylide (8j)** Compound **8j** was prepared by following the general procedure A. ^{1}H-NMR ($CDCl_3$) δ: 7.33 (1H, m, $C_{5'}$-H), 7.55 (3H, m, $C_{3''}$-H, $C_{4''}$-H, $C_{5''}$-H of phenyl), 7.71 (2H, m, $C_{2''}$-H, $C_{6''}$-H of phenyl), 7.87 (2H, d, $J_{3,2}=J_{5,6}$=7 Hz, C_3-H, C_5-H), 8.43 (1H, dt, $J_{4',5'}$=7.5 Hz, $J_{4',6'}=J_{4',2'}$=2 Hz, $C_{4'}$-H), 8.67 (1H, dd, $J_{6',5'}$=5 Hz, $J_{6',4'}$=2 Hz, $C_{6'}$-H), 8.87 (2H, d, $J_{2,3}=J_{6,5}$=7 Hz, C_2-H, C_6-H), 9.38 (1H, m, $C_{2'}$-H).

***N*-(2'-Pyridylcarbonylimino)-4-phenylpyridinium Ylide (8k)** Compound **5i** (6.0 g, 16.77 mmol) was reacted with picolinic acid hydrazide (2.3 g, 16.77 mmol) in 125 ml methanol containing 1.5 ml triethylamine at 0 to 10 °C for 2 h, and the reaction was worked up as described under the general procedure A. The product obtained was chromatographed on a neutral alumina column (2.5 × 30 cm) while eluting with ether : methanol (10 : 1, v/v, 5 : 1, v/v), and then crystallized from ethyl acetate : methylene chloride : hexane (1 : 1 : 1, v/v, 100 ml) to give light yellow feathery flakes of **8k** (2.37 g). ^{1}H-NMR ($CDCl_3$) δ: 7.35 (1H, m, $C_{5'}$-H), 7.55 (3H, m, $C_{3''}$-H to $C_{5''}$-H of phenyl), 7.71 (2H, m, $C_{2''}$-H and $C_{6''}$-H of phenyl), 7.81 (1H, td, J=1.5, 7.5 Hz, $C_{4'}$-H), 7.86 (2H, d, J=7.5 Hz, C_3-H, C_5-H), 8.24 (1H, d, J=7.5 Hz, $C_{3'}$-H), 8.72 (1H, d, J=5 Hz, $C_{6'}$-H), 8.89 (2H, d, J=7.5 Hz, C_2-H, C_6-H).

***N*-(Benzoylimino)-4-phenylpyridinium Ylide (8l)** Compound **8l** was prepared by following the general procedure A. ^{1}H-NMR ($CDCl_3$) δ: 7.45 (3H, m, $C_{3''}$-H, $C_{4''}$-H, $C_{5''}$-H of phenyl), 7.55 (3H, m, $C_{3'}$-H, $C_{4'}$-H, $C_{5'}$-H of phenyl), 7.7 (2H, m, $C_{2''}$-H, $C_{6''}$-H of phenyl), 7.84 (2H, $C_{2'}$-H, $C_{6'}$-H of phenyl), 8.2 (2H, m, C_3-H, C_5-H), 8.85 (2H, d, $J_{2,3}=J_{6,5}$=7 Hz, C_2-H, C_6-H).

***N*-(4'-Pyridylcarbonylamino)-4-*tert*-butyl-1,2,3,6-tetrahydropyridine (9a): General Procedure B** Sodium borohydride (0.6 g, 15.86 mmol) was added to an ice-cold strirring solution of **8a** (1.0 g, 3.92 mmol) in 100 ml absolute ethanol. The stirring was continued for 4 h at 0 °C during which time the reduction was completed as monitored by TLC. The excess sodium borohydride was treated with ice (25 g) and allowed to warm up to room temperature. It was then extracted with chloroform (3 × 150 ml). The combined chloroform extract was dried over sodium sulfate, filtered and concentrated under reduced pressure. The residue obtained was chromatographed on a column of neutral alumina (2.5 × 25 cm) using ether : methanol (40 : 1, v/v) as an eluent. The resulting product was crystallized from ethyl acetate as an amorphous white powder **9a** (0.52 g). IR (KBr): 3305 (NH), 1660 (C=O) cm^{-1}. ^{1}H-NMR ($CDCl_3$) δ: 1.22 (9H, s, C_4-*tert*-butyl), 2.33 (2H, br s, C_3-H), 3.07 (2H, t, J=5.5 Hz, C_2-H), 3.50 (2H, s, C_6-H), 5.37 (1H, m, C_5-H, olefinic), 7.27—7.37 (1H, br s, NH, D_2O exchangeable), 7.58 (2H, d, J=5 Hz, $C_{3'}$-H, $C_{5'}$-H), 8.70 (2H, d, J=5 Hz, $C_{2'}$-H, $C_{6'}$-H).

***N*-(3'-Pyridylcarbonylamino)-4-*tert*-butyl-1,2,3,6-tetrahydropyridine (9b)** Compound **9b** was prepared by following the general procedure B. IR (KBr): 3280 (NH), 1655 (C=O) cm^{-1}. ^{1}H-NMR ($CDCl_3$) δ: 1.02 (9H, s, C_4-*tert*-butyl), 2.35 (2H, m, C_3-H), 3.10 (2H, t, J=5 Hz, C_2-H), 3.51 (2H, br s, C_6-H), 5.39 (1H, m, C_5-H, olefinic), 7.17—7.27 (1H, br s, NH, D_2O exchangeable), 7.35 (1H, t, J=7 Hz, $C_{5'}$-H), 8.18 (1H, d, J=7 Hz, $C_{4'}$-H), 8.70 (1H, weakly split d, $C_{6'}$-H), 8.91 (1H, br s, $C_{2'}$-H).

***N*-(2'-Pyridylcarbonylamino)-4-*tert*-butyl-1,2,3,6-tetrahydropyridine (9c)** An ice-cold stirring solution of **8c** (3.0 g, 11.75 mmol) in 150 ml of absolute ethanol was reduced with sodium borohydride (1.78 g, 47 mmol) as described under the general procedure B. The resulting product was chromatographed on a neutral alumina column (2.5 × 35 cm) using ether : methanol (40 : 1, v/v and 30 : 1, v/v) as an eluent. The product was crystallized from ethyl acetate : hexane (2 : 1, v/v, 150 ml) as off white flakes, **9c** (0.78 g). IR (KBr): 3300 (NH), 1690 (–C=O) cm^{-1}. ^{1}H-NMR ($CDCl_3$) δ: 1.05 (9H, s, 4-*tert*-butyl), 2.36 (2H, m, C_3-H), 3.06 (2H, t, J=6 Hz, C_2-H), 3.50 (2H, m, C_6-H), 5.49 (1H, m, C_5-H, olefinic), 7.4 (1H, m, $C_{5'}$-H), 7.82 (1H, td, J=1.5, 8 Hz, $C_{4'}$-H), 8.21 (1H, d, J=8 Hz, $C_{3'}$-H), 8.51 (1H, m, $C_{6'}$-H), 8.82 (1H, br s, NH, D_2O exchangeable).

***N*-(Benzoylamino)-4-*tert*-butyl-1,2,3,6-tetrahydropyridine (9d)** Compound **9d** was prepared by following the general procedure B. IR (KBr): 3300 (NH), 1650 (C=O) cm^{-1}. ^{1}H-NMR ($CDCl_3$) δ: 1.02 (9H, s, C_4-*tert*-butyl), 2.33 (2H, br s, C_3-H), 3.04 (2H, t, J=5.5 Hz, C_2-H), 3.5 (2H, br s, C_6-H), 5.36 (1H, m, C_5-H, olefinic), 7.1 (1H, br s, NH, D_2O exchangeable), 7.32—7.52 (3H, complex m, $C_{3'}$-H, $C_{4'}$-H, $C_{5'}$-H of phenyl), 7.72 (2H, d, $J_{2',3'}=J_{6',5'}$=7.5 Hz, $C_{2'}$-H, $C_{6'}$-H of phenyl).

***N*-(4'-Pyridylcarbonylamino)-5-phenyl-1,2,3,6-tetrahydropyridine (9e)** Compound **9e** was prepared by following the general procedure B. IR (KBr): 3230 (NH), 1650 (C=O) cm^{-1}. ^{1}H-NMR ($CDCl_3$) δ: 2.51 (2H, m, C_3-H), 3.22 (2H, t, J=5.5 Hz, C_2-H), 3.91 (2H, br s, C_6-H), 6.15 (1H, m, C_4-H, olefinic), 7.05—7.20 (1H, br s, NH, D_2O exchangeable), 7.2—7.40 (5H, complex m, $C_{2''}$-H to $C_{6''}$-H of phenyl), 7.61 (2H, overlapping d(s), $J_{3',2'}=J_{5',6'}$=5 Hz, $C_{3'}$-H, $C_{5'}$-H), 8.71 (2H, d, $J_{2',3'}=J_{6',5'}$=5 Hz, $C_{2'}$-H, $C_{6'}$-H).

***N*-(3'-Pyridylcarbonylamino)-5-phenyl-1,2,3,6-tetrahydropyridine (9f)** Sodium borohydride (0.55 g, 14.53 mmol) was added to a stirring solution of **8f** (1.0 g, 3.63 mmol) in 100 ml of absolute ethanol at 0 °C. The reduction was completed and the crude product was isolated as described under the general procedure B. It was then chromatographed on a column of neutral alumina (2.5 × 25 cm) using ether : methanol (10 : 1, v/v) as an eluent, and then crystallized from ethyl acetate : methylene chloride : hexane (3 : 1 : 1, v/v, 100 ml) to collect **9f** as shining cream colored plates (0.36 g). IR (KBr): 3230 (NH), 1645 (C=O) cm^{-1}. ^{1}H-NMR ($CDCl_3$) δ: 2.51 (2H, br s, C_3-H), 3.21 (2H, t, J=5.5 Hz, C_2-H), 3.92 (2H, br s, C_6-H), 6.13 (1H, m, C_4-H, olefinic), 7.2—7.45 (6H, $C_{5'}$-H (pyridyl), $C_{2''}$-H to $C_{6''}$-H of phenyl), 7.5 (1H, br s, NH, D_2O exchangeable), 8.12 (1H, br d, J=8 Hz, $C_{4'}$-H), 8.71 (1H, m, $C_{6'}$-H), 8.96 (1H, s, $C_{2'}$-H).

***N*-(2'-Pyridylcarbonylamino)-5-phenyl-1,2,3,6-tetrahydropyridine (9g)** Compound **9g** was prepared by following the general procedure B. IR (KBr): 3220 (NH), 1675 (C=O) cm^{-1}. ^{1}H-NMR was described in the text.

***N*-(Benzoylamino)-5-phenyl-1,2,3,6-tetrahydropyridine (9h)** Sodium borohydride (1.2 g, 31.72 mmol) was added to a stirring solution of **8h** (2.0 g, 7.29 mmol) in 200 ml of absolute ethanol at 0 °C. The reaction was worked up as described under the general procedure B. The resulting product was chromatographed on a column of neutral alumina (2.5 × 25 cm) using ether : methanol (35 : 1, v/v) as an eluent. The product obtained was further crystallized from ethyl acetate : hexane (4 : 1, v/v, 150 ml) as pale yellow granules, **9h** (0.51 g). IR (KBr): 3230 (NH), 1648 (C=O) cm^{-1}. ^{1}H-NMR ($CDCl_3$) δ: 2.5 (2H, m, C_3-H), 3.2 (2H, t, J=6 Hz, C_2-H), 3.92 (2H, br s, C_6-H), 6.13 (1H, m, C_4-H, olefinic), 7.22—7.35 (5H, complex m, $C_{2''}$-H to $C_{6''}$-H of phenyl), 7.35—7.55 (3H, complex m, $C_{3'}$-H $C_{4'}$-H, $C_{5'}$-H of phenyl), 7.76 (2H, d, J=7 Hz, $C_{2'}$-H, $C_{6'}$-H of phenyl).

***N*-(4'-Pyridylcarbonylamino)-4-phenyl-1,2,3,6-tetrahydropyridine (9i)** An ice-cold stirring solution of **8i** (1.63 g, 5.92 mmol) was reduced with sodium borohydride (0.9 g, 23.79 mmol) in 100 ml absolute ethanol and the reaction was worked up as described under general procedure B. The resulting product was chromatographed on a column of neutral alumina (2.5 × 30 cm) using ether : methanol (20 : 1, v/v; 15 : 1, v/v and 10 : 1, v/v) as an eluent. The product obtained was crystallized from ethyl acetate : methylene chloride : hexane (3 : 1 : 1 v/v, 100 ml) as a light yellow powder, **9i** (0.8 g). IR (KBr): 3225 (NH), 1645 (C=O) cm^{-1}. ^{1}H-NMR ($CDCl_3$) δ: 2.19 (2H, br s, C_3-H), 2.7 (2H, t, J=5.5 Hz, C_2-H), 3.16 (2H, m, C_6-H), 5.51 (1H, m, C_5-H, olefinic), 6.67—6.95 (5H, $C_{2''}$-H to $C_{6''}$-H of phenyl), 7.21 (2H, d, J=5 Hz, $C_{3'}$-H, $C_{5'}$-H), 8.16 (2H, d, J=5 Hz, $C_{2'}$-H, $C_{6'}$-H), 9.13 (1H, s, NH, D_2O exchangeable).

***N*-(3'-Pyridylcarbonylamino)-4-phenyl-1,2,3,6-tetrahydropyridine (9j)** Compound **9j** was prepared by following general procedure B. IR (KBr): 3210 (NH), 1650 (C=O). ^{1}H-NMR δ: 2.73 (2H, m, C_3-H), 3.29 (2H, t, J=5.5 Hz, C_2-H), 3.72 (2H, br s, C_6-H), 6.00 (1H, m, C_5-H, olefinic), 7.27 (1H, m, $C_{5'}$-H), 7.30—7.46 (5H, complex m, $C_{2''}$-H to $C_{6''}$-H of phenyl), 7.55 (1H, s, NH, D_2O exchangeable), 8.11 (1H, d, $J_{4',5'}$=8 Hz, $C_{4'}$-H), 8.70 (1H, br d, $J_{6',5'}$=5 Hz, $C_{6'}$-H), 8.96 (1H, s, $C_{2'}$-H).

***N*-(2'-Pyridylcarbonylamino)-4-phenyl-1,2,3,6-tetrahydropyridine (9k)** To an ice-cold stirring solution of **8k** (1.5 g, 5.44 mmol) in 125 ml of absolute ethanol, sodium borohydride (0.83 g, 21.94 mmol) was added and the reaction was worked up as described under general procedure B. The product obtained was chromatographed on a neutral alumina column (2.5 × 30 cm) while eluting with ether : methanol (20 : 1, v/v and 10 : 1, v/v) and then crystallized from ethyl acetate as a cream white powder, **9k** (0.58 g). IR (KBr): 3260 (NH), 1660 (C=O) cm^{-1}. ^{1}H-NMR ($CDCl_3$) δ: 2.76 (2H, m, C_3-H), 3.28 (2H, t, J=5.5 Hz, C_2-H), 3.70 (2H, m, C_6-H), 6.05 (1H, m, C_5-H, olefinic), 7.26—7.50 (6H, complex m, $C_{5'}$-H and $C_{2''}$-H to $C_{6''}$-H of phenyl), 7.82 (1H, td, J=2, 8 Hz, $C_{4'}$-H), 8.21 (1H, dt, J=1, 1.5, 8 Hz, $C_{3'}$-H), 8.52 (1H, m, $C_{6'}$-H), 8.96 (1H, s, NH, D_2O exchangeable).

***N*-(Benzoylamino)-4-phenyl-1,2,3,6-tetrahydropyridine (9l)** Compound **9l** was prepared by following the general procedure B. IR (KBr): 3225 (NH), 1645 (C=O) cm^{-1}. ^{1}H-NMR ($CDCl_3$) δ: 2.23 (2H, br s, C_3-H), 2.76 (2H, t, J=5 Hz, C_2-H), 3.20 (2H, br s, C_6-H), 5.55 (1H, m, C_5-H, olefinic), 6.67—7.12 (8H, $C_{3'}$-H, $C_{4'}$-H, $C_{5'}$-H of phenyl and $C_{2''}$-H–$C_{6''}$-H of phenyl), 7.35 (2H, d, J=7 Hz, $C_{2'}$-H, $C_{6'}$-H of phenyl), 8.67 (1H, s, NH, D_2O exchangeable).

Acknowledgements We are grateful to the National Institutes of Health,

National Institute of General Medical Sciences, MBRS funding program No. 08111 and NIH's RCMI Grant # 03020. We are also grateful to Dr. Tom Gedris and Dr. Richard Rosanaske of the Chemistry Department, NMR unit, Florida State University, Tallahassee, Florida, for providing all the NMR spectra.

References

1) R. T. Coutts and A. F. Casay, "Pyridine and Its Derivatives: A Supplement," Vol. 14, ed. by R. A. Abramovitch, Interscience Publishers, New York, 1975.
2) M. Ferles and J. Pliml, "Advances in Heterocyclic Chemistry," Vol. 12, ed. by A. R. Katritzky and A. J. Boultin, Academic Press, New York, 1970.
3) E. E. Knaus and K. K. Redda, *J. Heterocycl. Chem.*, **13**, 1237 (1976).
4) K. K. Redda, L. A. Corleto and E. E. Knaus, *J. Med. Chem.*, **22**, 1079 (1979).
5) J. M. Yeung, L. A. Corleto and E. E. Knaus, *J. Med. Chem.*, **25**, 191 (1982).
6) J. M. Yeung, L. A. Corleto and E. E. Knaus, *J. Med. Chem.*, **25**, 720 (1982).
7) R. T. Coutts and J. R. Scott, *Can. J. Pharm. Sci.*, **6**, 78 (1971).
8) J. W. Langston, P. Ballard, J. W. Tetrud and I. Irwin, *Science*, **219**, 979 (1983).
9) J. W. Langston, *Life Sci.*, **36**, 201 (1985).
10) C. C. Chiueh, R. S. Burns, S. P. Markey, D. M. Jacobowitz and I. J. Kopin, *Life Sci.*, **36**, 213 (1985).
11) J. W. Langston, L. S. Forno, C. S. Rebert and I. Irwin, *Br. Res.*, **292**, 390 (1984).
12) I. Irwin and J. W. Langston, *Life Sci.*, **36**, 207 (1985).
13) G. Cohen and C. Mytilineou, *Life Sci.*, **36**, 237 (1985).
14) N. Castagnoli, Jr., K. Chiba and A. J. Trevor, *Life Sci.*, **36**, 225 (1985).
15) W. Gessner, A. Brossi, R. Shen and C. W. Abell, *J. Med. Chem.*, **28**, 311 (1985).
16) D. S. Fries, J. de Vries, B. Hazelhoff and A. S. Horn, *J. Med. Chem.*, **29**, 424 (1986).
17) E. E. Knaus, L. A. Corleto and K. K. Redda, Can. Patent 1120930 (1982) [*Chem. Abstr.*, **97**, 566 (1982)].
18) K. K. Redda, E. E. Knaus and L. A. Corleto, U. S. Patent 4338445 (1982) [*Chem. Abstr.*, **91**, 22 (1979)].
19) Y. Tamura, Y. Miki, T. Honda and M. Ikeda, *J. Hetrocycl. Chem.*, **9**, 865 (1972).
20) Y. Tamura and N. Tsujimoto, *Chem. Ind.* (London), **926** (1970).
21) K. K. Redda, H. Melles and K. N. Rao, *J. Heterocycl. Chem.*, **27**, 1041 (1990).
22) K. K. Redda, K. N. Rao, A. S. Heiman and H. Melles, *J. Pharm. Sci.*, **1990**, submitted.
23) A. Blackham, A. A. Norris and F. A. M. Woods, *J. Pharm. Pharmacol.*, **37**, 787 (1985).
24) P. J. Bailey, *Methods Enzymol.*, **162**, 327 (1988).
25) S. J. Foster, M. E. McCormick, A. Howarth and D. Aked, *Biochem. Pharmacol.*, **35**, 1709 (1986).

Formation of Pyrazine Derivatives from D-Glucosamine and Their Deoxyribonucleic Acid (DNA) Strand Breakage Activity

Kunihiro SUMOTO,*[,a] Michiko IRIE,[a] Nobuko MIBU,[a] Seiji MIYANO,[a] Yukihiko NAKASHIMA,[a] Kenji WATANABE,*[,a] and Tadatoshi YAMAGUCHI[b]

Faculty of Pharmaceutical Sciences, Fukuoka University,[a] Nanakuma, Jonan-Ku, Fukuoka, 814–01, Japan and Department of Hygiene, Miyazaki Medical College,[b] Kiyotake, Miyazaki, 889–16, Japan. *Received July 30, 1990*

Two pyrazine derivatives [fructosazine (3) and deoxyfructosazine (6)] were simultaneously formed in a solution of D-glucosamine hydrochloride under various conditions. They showed deoxyribonucleic acid (DNA) strand breakage activity in plasmid pBR322 comparable to that of D-glucosamine. The DNA strand breakage by fructosazine (3) was stimulated by Cu^{2+}.

Keywords pyrazine; fructosazine; deoxyfructosazine; DNA strand breakage; plasmid pBR322; D-glucosamine; L-cysteine; aminosugar; copper ion

Previously, we found that some aminosugars caused single-strand breakage of pBR322 covalently closed circular (ccc)-deoxyribonucleic acid (DNA),[1] and that the pre-heated sample of D-glucosamine (**1**) in solution had higher DNA breakage activity than that without heating (unpublished data). These findings led us to focus on a study of the chemical transformation of aminosugars in order to obtain more effective agents in terms of DNA breakage activity.

In this paper, we have reported the formation of pyrazine derivatives from D-glucosamine and their DNA strand breakage activity in plasmid pBR322.

Chemistry Under neutral (TE buffer) to basic (in aqueous ammonia) conditions, we isolated two pyrazine derivatives (**3** and **6**) as the sole products, the formation ratios (**6**/**3**) of which were dependent on the reaction conditions (Table I). We also detected formation of a small amount of the aldehyde, 5-(hydroxymethyl)-2-furaldehyde (**7**)[2-4] by high performance liquid chromatography (HPLC) analysis of the reaction mixture in some runs (see Experimental). Under acidic condition, the formation of the aldehyde (**7**) was increased, however, the formation of pyrazines (**3** and **6**) were greatly decreased. Although these pyrazines were already reported independently in the literature and named for fructosazine and deoxyfructosazine (**3** and **6**, respectively),[5-10] to the best of our knowledge, no report describing the simultaneous formation of these pyrazine derivatives has appeared, so far.

The formation process for the two pyrazine derivatives

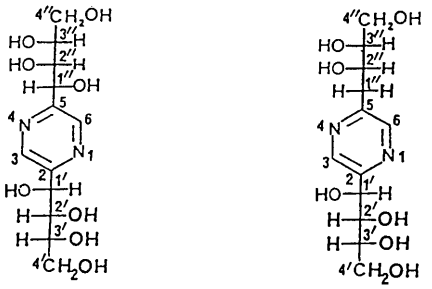

3 **6**

Fig. 1

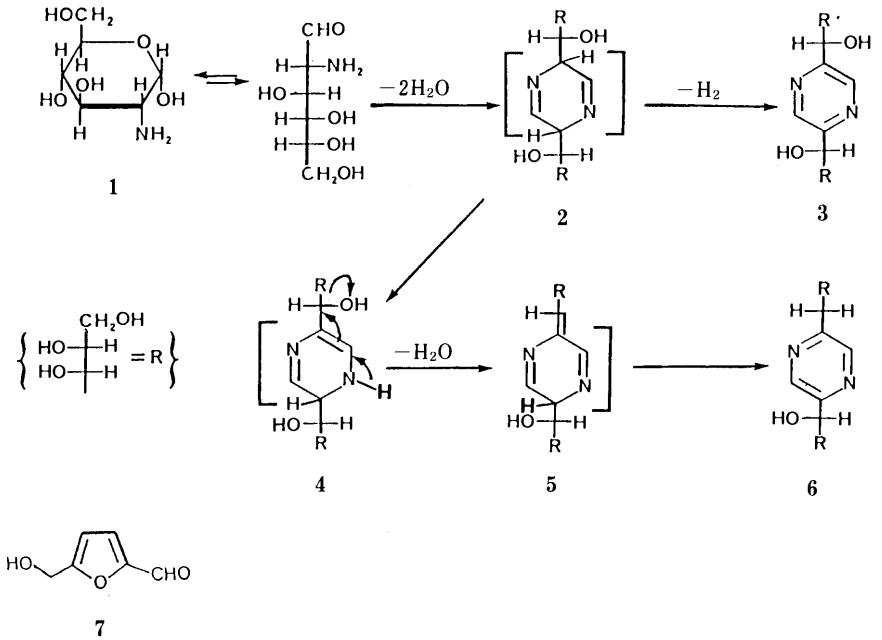

1 **2** **3** **4** **5** **6** **7**

Chart 1

TABLE I. Ratios of the Products (**3**, **6**, and **7**) in the Reaction of **1** under Various Conditions[a]

Conditions[b]	Product ratio 3 : 6 : 7
TE buffer 130 °C/4.5 h[c]	1 : 28 : 13
H_2O–pyridine 120 °C/16 h	1 : 1.74 : 0
H_2O–MeOH–pyridine–L-cysteine 120 °C/16 h	1 : 21 : 0
H_2O–IRA410 r.t./3 w	1 : 0.81 : <0.2
H_2O–Tris (1 eq mol) r.t./10 min	1 : 0.55 : Trace
H_2O–NaOH (1 eq mol) r.t./18 d	1 : 0.33 : Trace
28% aq.NH_3 r.t./3 w	1 : <0.01 : 0

a) Ratios were determined by HPLC monitering. *b*) Abbreviations: w; weeks, r.t.; room temperature, and Tris; tris(hydroxymethyl)aminoethane. *c*) Other unknown products were also detectable but the structures could not be established.

TABLE II. Relative Amounts of Remaining ccc-DNA

Incubation time (h)	**3**	**6**	[**3**+Cu^{2+}][a]	**1**[b]
0	100.0	100.0	100.0	100.0
1	86.4	81.9	69.2	96.7
3	75.1	67.7	50.6	80.1
5	71.1	61.6	34.9	44.5

a) This experiment was carried out with 2 mM of **3** (1/50-fold amount compared to other runs) in the presence of 1 mM $CuCl_2$. *b*) Used as hydrochloride.

mentioned above would be rationalized as shown in Chart 1, in which an oxidative (dehydrogenation) process leading to fructosazine (**3**) and a dehydration stage, followed by isomerization, (**2**→**4**→**5**) for deoxyfructosazine (**6**) from a proposed intermediate dihydropyrazine (**2**) takes place competitively.[8,9] This hypothesis is well supported by the following experiment. Thus, the reaction of D-glucosamine carried out in the presence of a reducing agent (SH group) such as L-cysteine, afforded deoxyfructosazine in good yield, together with L-cystine having disulfide (-SS-) bond (see Experimental).

The fact that eight of the observed ^{13}C-resonances for the product (**3**) coincide, *i.e.*, the chemical shift of C1′, C2′, C3′, and C4′ overlap with those of C1″, C2″, C3″, and C4″ respectively, indicates that the molecule is symmetrical and that no epimerization at those chiral centers took place. Therefore, regarding the absolute configuration [C1′(1″), C2′(2″), and C3′(3″)] of two polyhydroxyalkyl substituents on the pyrazine ring, we are considering the possibility that products should have the same absolute configurations as those (C3, C4, and C5) in the starting aminosugar (**1**).

DNA Strand Breakage Activity The results with isolated pyrazines (**3** and **6**) of DNA strand breakage activity are shown in Table II, where relative activity was expressed as the ratio of ccc-DNA. The results obtained with D-glucosamine (**1**) used as a reference compound is also presented for comparison. As Table II shows, the pyrazine derivatives (**3** and **6**) possessed a DNA strand breakage activity, comparable to that of D-glucosamine. Compound **7** showed no activity. Since Cu^{2+} accelerated the ccc-DNA breakage activity of D-glucosamine, we examined the effect of Cu^{2+} on the compound **3**. As the same Table shows, Cu^{2+} was found to stimulate the ccc-DNA breakage. Cu^{2+} is known to catalyze the autoxidation of some reducing compounds to generate active oxygens and certain radicals in aqueous solutions containing oxygens.[11] Thus, these radicals might be involved in the pyrazines-induced DNA strand breakage. The elucidation of the mechanism of DNA strand breakage by pyrazines and the synthesis of more active compounds by chemical modification of these pyrazines are currently being investigated.

Experimental

Melting points were determined with a Yanaco micro melting point apparatus or a Yamato melting point apparatus, and uncorrected. Infrared (IR) spectra were obtained on a Hitachi 250 spectrometer. ^1H- and ^{13}C-nuclear magnetic resonance (NMR) spectra were recorded on a JEOL GX-400 spectrometer, with 3-(trimethylsilyl) propionic acid-d_4 sodium salt (TSP) as an internal standard. High-resolution mass spectra were obtained with a JEOL JMX-DX300 instrument. Assignment for ^{13}C-resonances of the products were supported by 2D homo- or heteronuclear shift correlation spectra with a JEOL GX-400 spectrometer.

HPLC analyses were carried out on a Shimadzu LC-8A system consisting of a refractive index detector Shimadzu RID-6A with a data module Shimadzu C-R4A chromatopac. The columns used are mentioned below.

Fructosazine (3)[5-9] The following procedure is conventional for the preparation of fructosazine (**3**): D-Glucosamine hydrochloride (1.0 g, 0.0046 mol) was dissolved in 28% aqueous ammonia (10 ml) (pH 11), and the resulting solution was stirred at room temperature for 3 weeks.

After neutralization with 1N-HCl, evaporation of the solvent gave solid material. Purification of the products with HPLC [Hibar Lichrosorb RP-18 (7 μm) 250 × 25/water as solvent] afforded fructosazine (**3**) in 47% yield, in addition to small amounts of deoxyfructosazine (**6**).

Compound **3** had mp 234 °C (dec.) [lit.[8] mp 237 °C (dec.)]. $[\alpha]_D^{23.5}$ −82.2° (c=0.2, H_2O) [lit.[8] $[\alpha]_D^{20}$ −84.1° (c=1.0, H_2O)]. IR (KBr): 3300 (polymeric hydrogen bonded OH), 1035 (primary OH), 1090 (secondary OH) cm^{-1}. ^1H-NMR (D_2O) δ: 8.76 (2H, s, pyrazine ring protons), 5.19 [2H, d, J=2.44 Hz, C(1′ and 1″)-H], 3.92—3.84 [2H, m, C (2′ and 2″)-H], 3.92—3.84 [2H, m, C(3′ and 3″)-H], 3.92—3.67 [4H, m, C (4′ and 4″)-H]. ^{13}C-NMR (D_2O) δ: 65.84 (C4′ and C4″), 73.98 (C3′ and C3″), 74.32 (C1′ and C1″), 76.33 (C2′ and C2″), 144.82 (C3 and C6), 157.90 (C2 and C5). FAB-MS m/z: 321.1289 [$(M+H)^+$, $C_{12}H_{21}N_2O_8$]. The IR (Nujol) and Ultraviolet (UV) (in H_2O) data of the product were identical with the values reported previously.[8] *Anal.* Calcd for $C_{12}H_{20}N_2O_8$: C, 45.00; H, 6.29; N, 8.75. Found: C, 44.72; H, 6.38; N, 8.52.

Ratios of the two pyrazines (**3**/**6**) in the crude reaction mixture under various reaction conditions (monitered by HPLC analysis) are summarized in Table II. In some runs, a small amount of compound **7** which was identified with an authentic sample,[2] was isolated.

Deoxyfructosazine (6)[10] **(Reaction of D-Glucosamine in the Presence of L-Cysteine)** A solution of D-glucosamine hydrochloride (1.075 g, 0.005 mol), L-cysteine monohydrochloride monohydrate (0.878 g, 0.005 mol) and pyridine (39.5 g, 0.5 mol) in 45 ml of MeOH–H_2O (8 : 1) was refluxed for 32 h. After cooling, the precipitates were collected by filtration and washed with water to afford L-cystine (*ca.* 37%), which was identified with the commercially available sample. The filtrate was concentrated to a syrup and subjected to purification by HPLC [Prep PAK C18 cartrige/water as solvent] to give a light yellow powder, mp 130—141 °C. The product in the crude form was calculated at 76% by the internal standard method, however the isolated yield was 45%. Compound **6** had mp 156—158 °C (EtOH), [lit.[10] mp 161—162 °C]. $[\alpha]_D^{23.5}$ −79.8° (c=0.2, H_2O) [lit.[10] $[\alpha]_D^{23}$ −78° (c=0.6, H_2O)]. IR (KBr): 3290 (polymeric hydrogen bonded OH), 1040, 1055 (primary OH), 1075, 1100 (secondary OH) cm^{-1}. ^1H-NMR (D_2O) δ: 8.72 [1H, s, pyrazine ring C(3)-H], 8.55 [1H, s, pyrazine ring C(6)-H], 5.16 [1H, d, J=2.44 Hz, C(1′)-H], 3.25—2.96 [2H, m, C(1″)-methylene H], 4.08—4.03 [1H, m, C(2″)-H], 3.91—3.80 [1H, m, C(2′)-H], 3.91—3.80 [1H, m, C(3′)-H], 3.75—3.65 [1H, m, C(3″)-H), 3.91—3.50 [4H, m, C (4′ and 4″)-H]. ^{13}C-NMR (D_2O) δ: 40.38 (C1″), 65.37 (C4″), 65.82 (C4′), 74.01 (C3′), 74.20 (C2″), 74.23 (C1′), 76.36 (C2′), 77.25 (C3″), 145.04 and 146.95 (C3 and C6), 156.12 and 156.75 (C2 and C5). FAB-MS m/z: 305.1348 [$(M+H)^+$, $C_{12}H_{21}N_2O_7$]. *Anal.* Calcd for $C_{17}H_{20}N_2O_7$: C, 47.36; H, 6.63; N, 9.21. Found: C, 47.18; H, 6.72; N, 9.11.

Assay of DNA Strand Breakage Activity The reaction mixture (100 μl) containing 1 μg of plasmid pBR322 ccc-DNA, 0.1 M of sample compound, and 50 mM of Tris–HCl buffer (pH 7.4) was incubated at 37 °C. ccc-DNA of pBR322 was isolated from *Escherichia coli* W3350/pBR322 as described by Kupersztoch-Portony *et al.*[12] At intervals, 10 μl of the reaction mixture

was mixed with 3 μl of 22.5 mM ethylenediaminetetraacetic acid (EDTA) (pH 8.2) containing 1.5% (w/v) sodium dodecyl sulfate (SDS), 25% (w/v) sucrose, and 0.22% (w/v) bromophenol blue, to stop the reaction. The resulting mixture was analyzed directly by agarose-gel electrophoresis as described in a previous paper.[1] After electrophoresis, the gels were stained with ethidium bromide (0.5 μg/ml) for 0.5 h, and washed with running water for 30 s. The stained DNA bands, ccc-DNA, nicked open circular (oc)-DNA and linear DNA, were made visible using an ultraviolet lamp (302 nm) and then photographed with Polaroid film. For quantitative analysis of DNA on the gel, the photographic negatives were scanned with a Shimadzu CS-920 TLC scanner for the OD measurement. The relative amounts of remaining ccc-DNA by this procedure are summarized in Table II.

Acknowledgment We thank Miss K. Watanabe for her technical assistance in some of the experiments.

References

1) K. Watanabe, K. Kashige, Y. Nakashima, M. Hayashida, and K. Sumoto, *Agric. Biol. Chem.*, **50**, 1459 (1986).
2) W. Alberda van Ekenstein and J. J. Blanksma, *Ber.*, **43**, 2355 (1910).
3) F. H. Newth, *Adv. Carbohydr. Chem.*, **6**, 83 (1951).
4) M. L. Mednick, *J. Org. Chem.*, **27**, 398 (1962).
5) C. A. Lobry de Bruyn, *Rec. Trav. Chim.*, **18**, 72 (1899).
6) C. A. Lobry de Bruyn, *Ber.*, **31**, 2476 (1898).
7) M. I. Taha, *J. Chem. Soc.*, **1961**, 2468.
8) S. Fujii, R. Kikuchi, and H. Kushida, *J. Org. Chem.*, **31**, 2239 (1966).
9) S. Fujii and Y. Kosaka, *J. Org. Chem.*, **47**, 4772 (1982).
10) R. Kuhn, G. Kruger, H. J. Haas, and A. Seeliger, *Justus Liebigs Ann. Chem.*, **644**, 122 (1961).
11) *a*) E. S. G. Barron, E. B. Miller, and G. Kalnitsky, *Biochem. J.*, **41**, 62 (1974); *b*) Y. Kono, *Arch. Biochem. Biophys.*, **186**, 189 (1978).
12) Y. M. Kupersztoch-Portony, M. A. Lovett, and D. R. Helinski, *Biochemistry*, **13**, 5484 (1974).

Studies on Antiatherosclerotic Agents.[1] Synthesis of 7-Ethoxycarbonyl-4-formyl-6,8-dimethyl-1(2*H*)-phthalazinone Derivatives and Related Compounds

Yukuo EGUCHI,*[,a] Fujinori SASAKI,[b] Yoshimi TAKASHIMA,[a] Masako NAKAJIMA,[a] and Masayuki ISHIKAWA[a]

Institute for Medical and Dental Engineering, Tokyo Medical and Dental University,[a] 2-3-10, Surugadai, Kanda, Chiyoda-ku, Tokyo 101, Japan and Banyu Pharmaceutical Co., Ltd.,[b] 2-9-3, Shimomeguro, Meguro-ku, Tokyo 153, Japan. *Received August 7, 1990*

Derivatives of 7-ethoxycarbonyl-4-formyl-6,8-dimethyl-1(2*H*)-phthalazinone and closely related compounds were synthesized using Wittig and epoxidation reactions. Ring opening amination of the epoxides were carried out using dimethylaluminum amide reagents under mild reaction conditions. β-Keto ester and β-diketone moieties were introduced through diazo derivatives. These moieties were reacted with hydrazine hydrate to produce 4-pyrazolyl derivatives. The derivatives were tested for their inhibitory effect on platelet aggregation, and their relaxing effect on blood vessels.

Keywords synthesis; 7-ethoxycarbonyl-4-formyl-6,8-dimethyl-1(2*H*)-phthalazinone; Wittig reaction; epoxidation; dimethylaluminum amide reagent; rhodium(II) acetate; inhibitory effect; platelet aggregation

In the preceding paper,[1] we reported the synthesis of 7-ethoxycarbonyl-4-hydroxymethyl-6,8-dimethyl-1(2*H*)-phthalazinone (**1**) which showed potent inhibitory activities both on platelet aggregation and edematous arterial reaction, and compared the activity to closely related compounds, such as 4-formyl (**2**) and 4-methyl (**3**) in order to obtain insights into the structure–activity relationship.

We wish to report herein on the synthesis of derivatives of **1**, starting from **2** and **3** by applying the known methods to construct the expected bioactive side chain.

First of all, introduction of a cinnamic moiety[2,3] in the compound was carried out by Wittig reaction, with carboethoxymethylene triphenylphosphorane in tetrahydrofuran (THF), **2**, gave 4-unsaturated ester (**4**) in a 68% yield. The transformed structure of **4** was predominant according to the determination of proton nuclear magnetic resonance (^{1}H-NMR) assignments: each vinyl proton resonated at 6.80 and 8.00 ppm with a coupling constant of 16 Hz. Although **4** reacted with hydrazine hydrate to afford acid hydrazide (**5**), when direct aminolysis on **4** with secondary amines was performed, no corresponding products were obtained. However by means of trimethylaluminum with amines,[4] **4** produced amides (**6**—**8**) in moderate yields.

In order to construct a β-blocking side chain, an amino alcohol moiety which was often familiar to cardiovascular agents was introduced by ring opening amination of the epoxide. As reported,[5] **2** reacted with dimethylsulfonium methylide at −10 °C to afford a 4-epoxidated product (**9**).

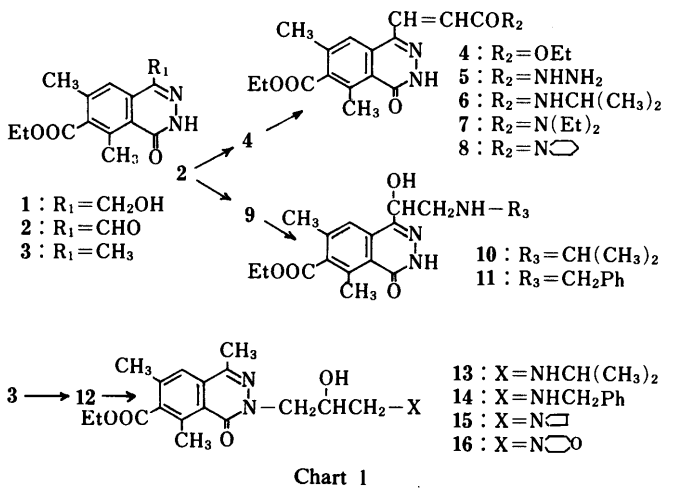

Chart 1

Upon refluxing the epoxide in benzene with amines, the corresponding aminoethyl alcohols (**10**, **11**) were obtained without any difficulty. On the other hand, the sodium salt of **3** was reacted with epichlorohydrin in dimethylformamide (DMF) to afford a sole product of *N*-epoxypropyl compound (**12**). Unfortunately, **12** was inert to secondary amines under refluxing conditions in benzene to open the ring, but was converted following treatment with dimethylaluminum amides in methylenechloride at room temperature to the corresponding products (**13**—**16**). Dimethylaluminum amide reagents[4] functioned well to produce ring opened compounds under very mild reaction conditions in this case.

Meanwhile, they reported[6-8] a condensation reaction of acyldiazomethanes with aldehydes or ketones to provide α-diazo-β-hydroxycarbonyl compounds, as well as an efficient procedure for the transformation of α-diazo-β-hydroxy esters into the corresponding β-keto esters using $Rh_2(OAc)_4$.[9] Keeping these reports in mind, we carried out condensation reactions of **2** with ethyl diazoacetate[10] and diazoacetone[11] under cooled conditions in a similar manner,[7] followed by treatment with $Rh_2(OAc)_4$ in dimethoxyethane in the same way.[8] Upon condensation of **2** with ethyl diazoacetate in ethanolic KOH at around 5 °C, a pale yellow crystalline product of diazo compound (**17**) was obtained. The infrared (IR) spectrum showed a typical absorption band due to a N≡N group at 2100 cm^{-1}. While carrying out the reaction in methanolic KOH, considerable trans esterification (ethyl to methyl) of the product at the 4 position was observed. Through reaction with diazoacetone, **2** was converted to diazoacetyl compound (**18**) in a 48% yield. In the reaction, an equilibration depicted in Chart 2 may have occured, depending on the reaction temperature. The yield lowered drastically when the temperature of the reaction mixture was not maintained at less than −10 °C. Addition of a catalytic amount of $Rh_2(OAc)_4$ to a stirred solution of **17** or **18** at room temperature resulted in rapid and quantitative evolution of nitrogen with a formation of β-keto ester (**19**) and β-diketone (**20**) in good yields, respectively. Hydrolysis accompanied with decarboxylation while refluxing in alcoholic KOH, converted **19** to 4-acetyl derivative (**19a**), whose ^{1}H-NMR spectrum displayed acetyl methyl protons at 2.88 ppm. Compound **19** was easily reacted with hydrazine hydrate in ethanol to afford a 4-pyrazolyl

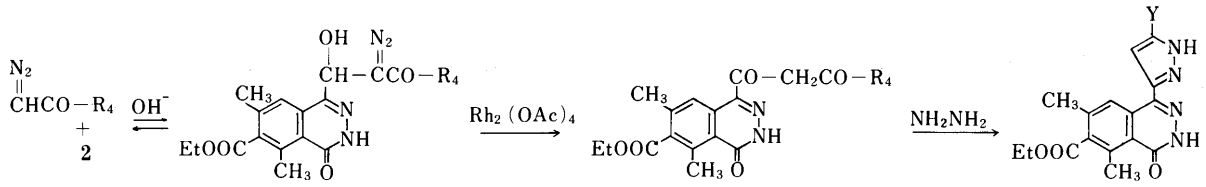

17 : R_4=OEt
18 : R_4=CH_3

19 : R_4=OEt
20 : R_4=CH_3

21 : Y=OH
22 : Y=CH_3

Chart 2

TABLE I. Biological Activities of Compounds

Compd.	Inhibition of platelet aggregation (%) ADP (10 μM)	AA (137 μM)	Relaxing effect of blood vessel (%) Concentration 3×10^{-5} M
Papaverine			62
1	70	92	
3	72	88	
4	20	12	
5	14	42	
6	16	20	
7	13	32	
8	8	16	
10	8	16	34
11	10	18	42
13	27	45	48
14	18	30	30
15	17	18	37
16	20	32	48
21	22	40	
22	42	70	

derivative (**21**). Analysis of the ^{1}H-NMR spectra suggested almost exclusively the enolized structure of **21** shown in Chart 2, in which appeared the pyrazolyl ring proton at 5.76 ppm and the enolized hydroxy proton at 8.26 ppm. From β-diketone, **20** afforded a 4-(5-methyl-3-pyrazolyl) derivative (**22**), which was converted to HCl salt with high solubility in water.

Biological Results The biological activities assessed in this study were inhibitory effects on platelet aggregation[1,12] induced by both adenosine diphosphate (ADP) (10 μM) and arachidonic acid (AA) (137 μM). In addition, several compounds were tested for hypotensive activity for relaxing effects[13] on the blood vessels of spontaneously hypertensive rats.

In the results listed in Table I, compounds **5**, **13** and **22** showed high activity in the platelet aggregation test, especially **22**, whose pyrazolyl ring exhibited relatively potent activity. On the other hand, compounds having amino alcohol in their side chains, such as **13** and **16**, showed modest activity compared to its papaverine. Consequently, compounds **13**, **16** and **22** showed a relatively good balance of biological activity for further pharmacological evaluation.

Experimental

All melting points were determined in a capillary tube and were uncorrected. IR spectra were determined with a Hitachi model 285 spectrometer, mass spectra (MS) were recorded by a Hitachi RMU-7L spectrometer, ultraviolet (UV) spectra with a Hitachi model 323 spectrometer, and ^{1}H-NMR spectra with a JEOL-C-60HL machine. Merck Silica gel 60 was used for column chromatography.

7-Ethoxycarbonyl-4-(2-ethoxycarbonylethenyl)-6,8-dimethyl-1(2*H*)-phthalazinone (4) A mixture of NaH (54%, 400 mg) and dimethyl sulfoxide (DMSO) (7 ml) was warmed at 70 °C under nitrogen until evolution of the gas had ceased. The mixture was diluted with THF (50 ml) then treated with carboethoxymethylene triphenylphosphonium bromide (3.8 g) at 0 °C. To the stirred mixture was added **2** (2.44 g) at room temperature, and the new mixture was refluxed for 2 h. Decomposition by water and working-up afforded 1.6 g of **4**, mp 170—172 °C (EtOAc). *Anal.* Calcd for $C_{18}H_{20}N_2O_5$: C, 62.78; H, 5.85; N, 8.14. Found: C, 62.77; H, 5.82; N, 8.11. ^{1}H-NMR ($CDCl_3$) δ: 1.30 (3H, t, J=7 Hz), 1.40 (3H, t, J=7 Hz), 2.45 (3H, s), 2.90 (3H, s), 4.30 (2H, q, J=7 Hz), 4.45 (2H, q, J=7 Hz), 6.80 (1H, d, J=16 Hz), 7.65 (1H, s), 8.00 (1H, d, J=16 Hz), 11.25 (1H, s).

Compound **5** was obtained from **4**: mp 235—237 °C (EtOH). ^{1}H-NMR (DMSO-d_6) δ: 1.35 (3H, t, J=7 Hz), 2.41 (3H, s), 2.77 (3H, s), 4.48 (2H, q, J=7 Hz), 7.63 (1H, d, J=10 Hz), 7.87 (1H, d, J=10 Hz), 9.01 (1H, s), 11.12 (1H, s), 12.26 (1H, s).

Compounds **6**—**8** were obtained from **4** in the described manner.[4]

6: mp 285—287 °C (MeOH). ^{1}H-NMR (DMSO-d_6) δ: 1.08 (3H, s), 1.17 (3H, s), 1.48 (3H, t, J=7 Hz), 2.48 (3H, s), 2.75 (3H, s), 3.94 (1H, br), 4.40 (2H, q, J=7 Hz), 6.82 (1H, d, J=15 Hz), 7.76 (1H, d, J=15 Hz), 7.86 (1H, s), 12.70 (1H, s).

7: mp 193—195 °C (MeOH). IR ν_{max}^{KBr} cm^{-1}: 3400, 2910, 1730, 1650, 1430, 1260, 1140.

8: mp 186—188 °C (MeOH). ^{1}H-NMR ($CDCl_3$) δ: 1.84 (3H, t, J=7 Hz), 1.63—1.88 (6H), 2.47 (3H, s), 2.90 (3H, s), 3.67 (4H, br), 4.47 (2H, q, J=7 Hz), 7.75 (1H, s), 7.58 (1H, d, J=16 Hz), 8.03 (1H, d, J=16 Hz), 10.82 (1H, br).

7-Ethoxycarbonyl-4-epoxyethyl-6,8-dimethyl-1(2*H*)-phthalazinone (9) A mixture of NaH (54%, 800 mg) and DMSO (12 ml) was heated at 65 °C under nitrogen, then was diluted with THF (40 ml) and cooled to −10 °C. To the stirred mixture was added dropwise a solution of trimethylsulfonium iodide (3.68 g) in THF (20 ml) and DMSO (10 ml), followed by **2** (2.74 g) in THF (20 ml) and DMSO (5 ml). The mixture was stirred vigorously at −10 °C for 30 min then allowed to warm at room temperature. The mixture was decomposed by addition of water, and acidified by dil. H_2SO_4 to afford an oil, which was purified by column chromatography with benzene : EtOAc (12 : 3). Yield: 1.46 g. mp 154—156 °C (acetone). *Anal.* Calcd for $C_{15}H_{16}N_2O_4$: C, 62.49; H, 5.59; N, 9.72. Found: C, 62.44; H, 5.54; N, 9.80. MS *m/z*: 288, 273, 260, 243, 232. ^{1}H-NMR ($CDCl_3$) δ: 1.45 (3H, t, J=7 Hz), 2.50 (3H, s), 2.90 (3H, s), 3.25 (2H, br), 4.20 (1H, t, J=3 Hz), 4.45 (2H, q, J=7 Hz), 7.75 (1H, s), 10.80 (1H, s).

Compounds **10** and **11** were obtained from **9**.

10: mp 235—237 °C (acetone). MS *m/z*: 316, 302, 288. ^{1}H-NMR (DMSO-d_6) δ: 1.25 (3H, s), 1.40 (3H, s), 1.40 (3H, t, J=7 Hz), 2.45 (3H, s), 2.75 (3H, s), 3.25 (2H, br), 4.40 (2H, q, J=7 Hz), 5.45 (1H, s), 8.05 (1H, s), 12.55 (1H, s), HCl salt: mp 242—244 °C (acetone).

11: 155—157 °C (EtOAc). ^{1}H-NMR ($CDCl_3$) δ: 1.40 (3H, t, J=7 Hz), 2.45 (3H, s), 2.80 (3H, s), 3.10 (2H, d, J=5 Hz), 3.80 (2H, s), 4.45 (2H, q, J=7 Hz), 5.10 (1H, t, J=5 Hz), 7.30 (5H, s), 7.65 (1H, s). HCl salt: mp 248—250 °C (acetone).

7-Ethoxycarbonyl-2-(2,3-epoxypropyl)-4,6,8-trimethyl-1(2*H*)-phthalazinone (12) A clear solution of **3** (5.2 g), NaOH (800 mg) in water (12 ml) and MeOH (20 ml) was dried *in vacuo* to make sodium salt. To a stirred solution of epichlorohydrin (2.2 g) in DMF (20 ml) was added portionwise the salt (5.5 g) at 70 °C over a period of 2 h. The reaction mixture was poured into water. Working-up with EtOAc gave an oil. Purification by chromatography with benzene : EtOAc (4 : 1) afforded 3.2 g of **12**. mp 80—82 °C (EtOH). *Anal.* Calcd for $C_{17}H_{20}N_2O_4$: C, 64.54; H, 6.37; N, 8.86. Found: C, 64.54; H, 6.34; N, 8.88. IR ν_{max}^{KBr} cm^{-1}: 3450, 3000, 1740, 1640, 1430. MS *m/z*: 316, 287, 285, 273, 271. ^{1}H-NMR ($CDCl_3$) δ: 1.39 (3H, t, J=7 Hz), 2.44 (3H, s), 2.51 (3H, s), 2.75 (2H, m),

2.89 (3H, s), 3.45 (1H, br), 4.25 (2H, m), 4.48 (2H, q, $J=7$ Hz), 7.40 (1H, s), 11.32 (1H, s).

7-Ethoxycarbonyl-2-(2-hydroxy-3-isopropylaminopropyl)-4,6,8-trimethyl-1(2*H*)-phthalazinone (13) To a stirred solution of isopropylamine (260 mg) in CH_2Cl_2 was added trimethylaluminum in hexane (25%, 0.8 ml) (Alfa Inorganics) under nitrogen. After 30 min, **12** (316 mg) was added and the mixture was stirred at room temperature for 10 h. The mixture was decomposed by careful addition of water and extracted with CH_2Cl_2. Working-up afforded semi-solid crystals, which were recrystallized from EtOAc–ether to give **13**, mp 111—112 °C in 210 mg. *Anal.* Calcd for $C_{20}H_{29}N_3O_4$: C, 63.97; H, 7.79; N, 11.19. Found: C, 63.90; H, 7.83; N, 11.23. ^{1}H-NMR ($CDCl_3$) δ: 1.00 (3H, s), 1.11 (3H, s), 1.41 (3H, t, $J=7$ Hz), 2.46 (3H, s), 2.53 (3H, s), 2.72 (2H, s, 1H, s), 2.87 (3H, s), 4.25 (2H, s), 4.45 (2H, q, $J=7$ Hz), 7.41 (1H, s).

Compounds **14**—**16** were obtained from **12** in a similar manner.

14: mp 135—136 °C (EtOAc–ether). ^{1}H-NMR ($CDCl_3$) δ: 1.41 (3H, t, $J=7$ Hz), 2.45 (3H, s), 2.51 (3H, s), 2.79 (2H, br), 2.86 (3H, s), 3.35 (2H, s), 3.84 (2H, s), 4.27 (2H, s), 4.44 (2H, q, $J=7$ Hz), 7.29 (5H, s), 7.40 (1H, s).

15: mp 115—116 °C (EtOAc). ^{1}H-NMR ($CDCl_3$) δ: 1.40 (3H, t, $J=7$ Hz), 1.75 (4H, m), 2.47 (3H, s), 2.55 (3H, s, 4H, m), 3.86 (3H, s), 3.87 (1H, br), 4.25 (4H, m), 4.45 (2H, q, $J=7$ Hz), 7.40 (1H, s).

16: mp 137—138 °C (EtOAc–ether). ^{1}H-NMR ($CDCl_3$) δ: 1..41 (3H, t, $J=7$ Hz), 2.45 (3H, s), 2.53 (10H, s), 2.87 (3H, s), 3.71 (4H), 4.24 (2H, s), 4.43 (2H, q, $J=7$ Hz), 7.40 (1H, s).

4-(2-Diazo-2-ethoxycarbonyl-1-hydroxyethyl)-7-ethoxycarbonyl-6,8-dimethyl-1(2*H*)-phthalazinone (17) To a mixture of **2** (1.64 g) and ethyl diazoacetate (1.37 g) in EtOH (30 ml) was added dropwise aq. NaOH [(480 mg) in water (10 ml)] at 0 °C. It was then allowed to stir at 0—5 °C for 5 h. While stirring, the reaction mixture became clear and crystals began to fall. Crystals were filtered and washed with cold EtOH on a filter to afford 1.3 g of **17**. mp 155—156 °C (EtOAc–ether). *Anal.* Calcd for $C_{18}H_{20}N_4O_6$: C, 55.66; H, 5.19; N, 14.43. Found: C, 55.53; H, 5.22; N, 14.21. MS *m/z*: 350 ($M^+ - N_2$), 331, 316. IR ν_{max}^{KBr} cm^{-1}: 3380, 2100, 1720, 1650. ^{1}H-NMR ($CDCl_3$) δ: 1.26 (3H, t, $J=7$ Hz), 1.39 (3H, t, $J=7$ Hz), 2.38 (3H, s), 2.85 (3H, s), 4.27 (2H, q, $J=7$ Hz), 4.40 (2H, q, $J=7$ Hz), 4.41 (1H, br), 6.11 (1H, d, $J=6$ Hz), 7.52 (1H, s), 10.76 (1H, s).

Compound **18**: mp 157—158 °C (EtOAc). IR ν_{max}^{KBr} cm^{-1}: 3350, 2100, 1730, 1640. ^{1}H-NMR ($CDCl_3$) δ: 1.38 (3H, t, $J=7$ Hz), 2.25 (3H, s), 2.38 (3H, s), 2.81 (3H, s), 4.36 (1H, s), 4.47 (2H, q, $J=7$ Hz), 6.25 (1H, d, $J=5$ Hz), 7.50 (1H, s), 10.56 (1H, s).

7-Ethoxycarbonyl-4-(2-ethoxycarbonyl-1-oxoethyl)-6,8-dimethyl-1(2*H*)-phthalazinone (19) To a stirred solution of **17** (388 mg) in dimethoxyethane (10 ml) was added portionwise $Rh_2(OAc)_4$ (8.0 mg). Nitrogen (about 23 ml) evolved. Inorganics were filtered off and the filtrate was concentrated at reduced pressure to afford semi-solid. Recrystallization from EtOAc–ether afforded 260 mg of **19** as pale yellow needles melted at 137—138 °C. *Anal.* Calcd for $C_{18}H_{20}N_2O_6$: C, 59.99; H, 5.59; N, 7.77. Found: C, 59.87; H, 5.60; N, 7.64. IR ν_{max}^{KBr} cm^{-1}: 3150, 3000, 1740, 1660, 1650. MS *m/z*: 360, 331, 315. ^{1}H-NMR ($CDCl_3$) δ: 1.25 (3H, t, $J=7$ Hz), 1.44 (3H, t, $J=7$ Hz), 2.48 (3H, s), 2.86 (3H, s), 4.10 (2H, s), 4.19 (2H, q, $J=7$ Hz), 4.48 (2H, q, $J=7$ Hz), 8.69 (1H, s), 10.73 (1H, s).

Compound **20**: mp 154—155 °C (EtOAc–ether). ^{1}H-NMR ($CDCl_3$) δ: 1.38 (3H, t, $J=7$ Hz), 2.15 (3H, s), 2.42 (3H, s), 2.87 (3H, s), 4.18 (1H, s), 4.41 (2H, q, $J=7$ Hz), 6.25 (1H, s), 8.41 (1H, s), 10.41 (1H, br).

Compound **19a**: mp 158—159 °C (EtOAc). ^{1}H-NMR ($CDCl_3$) δ: 1.43 (3H, t, $J=7$ Hz), 2.47 (3H, s), 2.66 (3H, s), 2.88 (3H, s), 4.44 (2H, q, $J=7$ Hz), 8.67 (1H, s), 10.87 (1H, s).

Compounds **21** and **22** were obtained from **19** and **20**, respectively.

21: Did not melt at 280 °C. UV λ_{max}^{EtOH} nm: 228, 305. ^{1}H-NMR (DMSO-d_6) δ: 1.31 (3H, t, $J=7$ Hz), 2.30 (3H, s), 2.75 (3H, s), 4.38 (2H, d, $J=7$ Hz), 5.76 (1H, s), 8.20 (1H, br), 10.30 (1H, br), 12.68 (1H, s).

22: mp 230—231 °C (EtOH). UV λ_{max}^{EtOH} nm: 229, 306. ^{1}H-NMR ($CDCl_3$ + DMSO-d_6) δ: 1.37 (3H, t, $J=7$ Hz), 2.31 (3H, s), 2.34 (3H, s), 2.79 (3H, s), 4.38 (2H, q, $J=7$ Hz), 6.29 (1H, s), 8.48 (1H, s), 12.22 (1H, s). HCl salt: mp 239—240 °C (EtOH–acetone).

References

1) M. Ishikawa, Y. Eguchi, and A. Sugimoto, *Chem. Pharm. Bull.*, **28**, 2770 (1980); S. Kaneko, Y. Eguchi, Y. Takashima, M. Nakajima, and M. Ishikawa, *Blood and Vessel*, **12**, 433 (1981).
2) J. R. Sorenson, *J. Med. Chem.*, **19**, 135 (1976); B. R. McAuslan and W. Reilly, *Exp. Cell Res.*, **130**, 147 (1980).
3) K. Tanaka, K. Maruto, A. Nakanishi, T. Hatano, H. Izeki, Y. Ishida, and W. Mori, *Chem. Pharm. Bull.*, **31**, 2810 (1983).
4) A. Basha, M. Lipton, and S. M. Weinreb, *Tetrahedron Lett.*, **48**, 4171 (1977).
5) E. J. Corey and M. Chaykovsky, *J. Am. Chem. Soc.*, **87**, 1353 (1965).
6) E. Wenkert and C. A. McPherson, *J. Am. Chem. Soc.*, **94**, 8084 (1972).
7) N. F. Woolsy and M. H. Khalil, *J. Org. Chem.*, **40**, 3521 (1975).
8) R. Pellicciari, P. Fringuelli, P. Ceccherelli, and E. Sisani, *J. Chem. Soc., Chem. Commun.*, **1979**, 959.
9) P. Legzdins, R. W. Mitchell, G. L. Rempel, J. D. Ruddick, and G. Wilkinson, *J. Chem. Soc. (A)*, **1970**, 3322.
10) E. B. Womack and A. B. Nelson, "Organic Syntheses," Coll. Vol. 3, ed. by E. C. Horning, Academic Press, New York, 1955, p. 392.
11) F. Arndt and J. Amende, *Chem. Ber.*, **1928**, 1123.
12) Born, G. V. R., *Nature* (London), 1962, **194**, 927.
13) M. Ishikawa, Y. Eguchi, and A. Sugimoto, *Heterocycles*, **16**, 21 (1981).

Polysaccharides in Fungi. XXVI.[1] Two Branched (1→3)-β-D-Glucans from Hot Water Extract of Yũ ěr

Tadashi KIHO,[a] Miho SAKUSHIMA,[a] Shuru WANG,[b] Katsuyuki NAGAI,[a] and Shigeo UKAI*,[a]

Gifu Pharmaceutical University,[a] Mitahora-higashi 5-chome, Gifu 502, Japan and China Pharmaceutical University,[b] 24 Tongjia Xiang, Nanjing 210009, China. *Received September 10, 1990*

Two water-insoluble glucans, U-3-N ($[\alpha]_D$ +1.0°, 0.5 M sodium hydroxide) and U-3-AP$_1$ ($[\alpha]_D$ +2.5°, 1 M sodium hydroxide) were isolated from hot-water extract of the fruiting bodies of Yũ ěr (Chinese name) (*Auricularia* sp.). U-3-N and U-3-AP$_1$ were investigated by a combination of chemical and spectroscopic methods. The results indicated that U-3-N (molecular weight, 6.1×10^5) was similar to β-(1→6)-branched (1→3)-β-D-glucan (N-5P: molecular weight, 5.6×10^5) isolated from the alkaline extract of the fruiting bodies, and U-3-AP$_1$ (molecular weight, 6.3×10^4) was β-(1→6)-branched (1→3)-β-D-glucan containing β-(1→6)-linked D-glucopyranosyl residues. U-3-N showed potent antitumor activity against the solid form of sarcoma 180, although U-3-AP$_1$ had little effect on the tumor.

Keywords branched (1→3)-β-D-glucan; Yũ ěr (*Auricularia* species); polysaccharide structure; antitumor activity; ^{13}C-NMR

We have isolated the acidic polysaccharide (U-3-A)[2] from the hot water extract and β-D-glucan (N-5-P)[3] from the alkaline extract of the fruiting bodies of Yũ ěr (*Auricularia* species) belonging to Auriculariaceae. We reported on the structural characterizations and the biological activities such as antiinflammatory activity[2] and antitumor activity.[4] Since we found the presence of the neutral polysaccharides (U-3-N and U-3-AP$_1$) together with U-3-A in the hot water extract of the fruiting bodies, the present paper deals with the structural characterization and the antitumor activity of U-3-N and U-3-AP$_1$.

The fruiting bodies were successively extracted with methanol and 70% aqueous ethanol, in a boiling water bath. The residue was extracted 4 times with water (1 l) in a boiling water bath. The crude polysaccharides obtained from the hot water extract were fractionated with cetyltrimethylammonium bromide (CTAB) to provide the precipitate of the acidic polysaccharide (U-3-A) and the supernatant, as described in a previous paper.[2] The supernatant was purified by addition of ethanol and anion-exchange chromatography on diethylaminoethyl (DEAE)-Toyopearl 650 M. The neutral fraction was lyophilized to give a neutral polysaccharide (U-3-N) in 1.24% yield. The fraction eluted by the gradient elution with aqueous sodium chloride afforded a polysaccharide (U-3-AP$_1$) in 0.63% yield. The polysaccharides thus obtained were insoluble in water, and soluble in an alkaline solution. Each polysaccharide showed a symmetrical elution pattern in gel filtration on Toyopearl HW-65 with 0.5 M sodium hydroxide solution. Gas-liquid chromatography (GLC) and paper chromatography (PPC) showed that both polysaccharides were composed solely of D-glucosyl residues. The polysaccharides showed characteristic absorbance at 890 cm^{-1} in the infrared (IR) spectra and had low specific rotations $[\alpha]_D$ +1.0° (c=0.13, 0.5 M NaOH) for U-3-N; $[\alpha]_D$ +2.5° (c=0.13, 1 M NaOH) for U-3-AP$_1$, suggesting the presence of the β-D configuration. The molecular weights of U-3-N and U-3-AP$_1$ were estimated by gel filtration to be *ca.* 6.1×10^5 and *ca.* 6.3×10^4, in an alkaline solution, respectively.

Each glucan was methylated, and the fully methylated glucans were hydrolyzed, then converted into the partially methylated alditol acetates. As shown in Table I, GLC and GLC-mass spectrometry (GLC-MS) revealed that U-3-N was (1→6) branched (1→3)-linked glucan and U-3-AP$_1$ was (1→6) branched (1→3)-linked glucan containing (1→6) linked residues. On periodate oxidations, U-3-N and U-3-AP$_1$ consumed 0.50 and 0.70 mol of periodate per hexosyl residue, respectively. Sequential borohydride reduction of each oxidized polysaccharide, and acid-hydrolysis (Smith degradation) gave glycerol and glucose. The results were consistent with the data obtained from the methylation analysis.

The carbon-13 nuclear magnetic resonance (^{13}C-NMR) spectra of U-3-N and U-3-AP$_1$ were recorded. The spectrum of U-3-AP$_1$ (see Fig. 1) was very similar to that of U-3-N except for the relative intensities of the signals. The values of chemical shifts and characteristic triplet signals at substituted C-3[5] showed that U-3-N and U-3-AP$_1$ were β-(1→6) branched (1→3)-β-D-glucans. β-D-Configrations of glucopyranosyl residues were supported by the $^1J_{CH}$ value of 163.0 Hz.[6]

The glucan (U-3-N) was digested with *exo*-(1→3)-β-D-glucanase (Lysing enzyme) from *Rhizoctonia solani*, and enzymic degradation products of U-3-N were examined by gel filtration on Bio-gel P-2, only two peaks, corresponding

TABLE I. GLC[a] and GLC-MS of Partially Methylated Alditol Acetates

Methylated sugar (as alditol acetate)	Relative retention time[b]	Main mass-fragments (m/z)	Molar ratios		Mode of linkage
			U-3-N	U-3-AP$_1$	
2,3,4,6-Me$_4$–Glc	1.00	43, 45, 71, 87, 101, 117, 129, 145, 161, 205	1.00	1.00	[Glc$p$] 1→
2,4,6-Me$_3$–Glc	1.51	43, 45, 87, 101, 117, 129, 161, 233	2.16	1.29	→3 [Glc$p$] 1→
2,3,4-Me$_3$–Glc	1.72	43, 87, 99, 101, 117, 129, 161, 189, 233	Trace	0.38	→6 [Glc$p$] 1→
2,4-Me$_2$–Glc	2.69	43, 87, 117, 129, 189	1.03	0.91	→3 →6 [Glc$p$] 1→

a) Conditions: 3% ECNSS-M on Gaschrom Q at 170 °C. *b*) Relative to authentic 1,5-di-*O*-acetyl-2,3,4,6-tetra-*O*-methyl-D-glucitol.

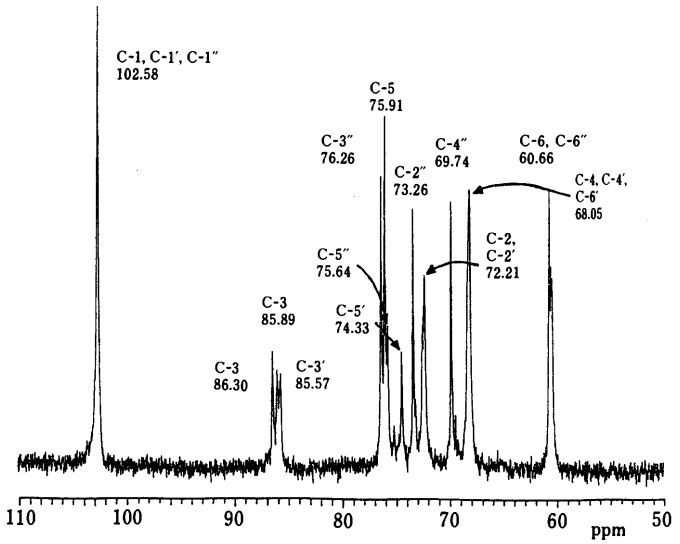

Fig. 1. ^{13}C-NMR Spectrum of U-3-AP$_1$ in DMSO-d_6 at 60 °C

to mono- and disaccharide, were revealed. The molar ratio of disaccharide to monosaccharide reached a constant value (0.45) at 24 h.

The foregoing data indicated that polysaccharide U-3-N was a branched glucans composed of a (1→3)-β-D-glucopyranosyl main chain, and had single, β-(1→6)-linked D-glucopyranosyl groups attached as side chains. The side chain attached, on average, to every third residue of the backbone. The data also indicated that U-3-AP$_1$ was β-(1→6)-branched (1→3)-β-D-glucan containing β-(1→6)-linked residues, and higher branched and smaller molecular-weight glucan than U-3-N.

The comformational behavior of linear, and branched (1→3)-β-D-glucans has been discussed in regard to changes in the visible absorption spectra of the complexes formed with Congo red, as previously reported.[3] The values of the visible absorption maximum (λ_{max}) of Congo red were largely shifted to a longer wavelength in the presence of U-3-N (501 nm) and U-3-AP$_1$ (495 nm), at a low concentration (0.1 M) of sodium hydroxide, whereas at high concentrations (0.25 M and 0.50 M) of sodium hydroxide, no λ_{max} shifts were observed. The results suggested that U-3-N has an ordered, triple-helical structure in a weakly alkali solution, and has single chains in a highly alkaline solution, and U-3-AP$_1$ may have a partially triple-helical structure.

Branched (1→3)-β-D-glucans having side chains of single D-glucosyl group at *O*-6 have been known to exhibit antitumor activity against sarcoma 180 implanted in mice, as previously reported.[3] The antitumor activity of the polysaccharides against sarcoma 180 in mice is listed in Table II. U-3-N showed antitumor activity at doses of 1 and 5 mg/kg, although U-3-AP$_1$ had little effect on the tumor. The difference of the activity may be due to that of structure. Many (1→3)-β-D-glucans in the fruiting bodies of fungi are usually extracted by an alkaline solution, but the glucans (U-3-N and U-3-AP$_1$) in Yū ěr were also extracted with hot water. The reason may be explained by the following results. Each glucan was an alkali-soluble, but the solution neutralized with acid was dialyzed against water to yield a water-insoluble material of the glucan. The neutral polysaccharides (U-3-N and U-3-AP$_1$) were dissolved, together with the acidic polysaccharide (U-3-A), in 0.5 M sodium hydroxide, and the neutralized solution was dialyzed against water. The polysaccharides were yet soluble in water. The results suggested an interaction of the glucan with the acidic polysaccharide in the solution.

TABLE II. Antitumor Activity of the Polysaccharides against Sarcoma 180 Solid Tumor

Sample	Dose (mg/kg/d × 10)	Mean tumor wt. ±S.D.[a] (g)	Inhibition ratio (%)	Complete regression
Exp. 1				
U-3-N	0.5	5.29±2.98[b]	51	0/8
	1	1.78±1.78[c]	84	2/8
	5	3.24±2.21[c]	70	1/8
Control	—	10.86±4.79	—	0/8
Exp. 2				
U-3-AP$_1$	0.5	6.50±5.16	30	0/10
	1	8.50±6.64	8	0/9
	5	7.78±7.09	16	1/9
PSK	200	1.31±1.24[d]	86	0/8
Control	—	9.22±5.51	—	0/10

a) Significant difference from the control [*b*) $p<0.05$, *c*) $p<0.01$, *d*) $p<0.005$].

As described in the earlier articles,[2,3] the residue of hot-water extract was successively extracted with 5% sodium carbonate[7] and with 1 M sodium hydroxide, at room temperature. Antitumor β-(1→6)-branched (1→3)-β-D-glucan N-5-P was isolated from the sodium hydroxide extract, its properties were as follows (U-3-N in parentheses): $[\alpha]_D$ +2.3° (+1.0°); molecular weight, 5.6×10^5 (6.1×10^5); branched ratio, 1/3 (1/3); max of complex with Congo red, 510 nm (501 nm); yield, 1.2% (1.24%). Thus, U-3-N was similar to N-5-P, although high-order structure may be slightly different. The work revealed that antitumor, branched (1→3)-β-D-glucan (U-3-N) was able to isolate from hot-water extract before alkaline extraction.

These findings are of interest in connection with a physiological role of these polysaccharides in the fruiting body of this fungus. The water-soluble mixture of U-3-N and U-3-AP$_1$ together with U-3-A may occur as cell-surface glycans, whereas N-5-P extracted with alkaline solution might arise from an intracellular component, or be present as a component of the cell wall.[8]

Experimental

Materials The dried fruiting bodies of Yū ěr (*Auricularia* sp.) are commercially available in Hong Kong.[3] Lysing enzyme was purchased from Sigma Chemical Company. Toyopearl HW-65 and DEAE-Toyopearl 650 M were purchased from Tosoh Industry Co., and standard dextrans and Bio-gel P-2 were purchased from Pharmacia Fine Chemicals and Bio-Rad Laboratories, respectively.

General All evaporations were conducted under diminished pressure at bath temperatures not exceeding 40 °C. Specific rotations were measured with a JASCO DIP-4 automatic polarimeter. IR spectra were recorded with a JASCO A-102 spectrometer. PPC was performed by the double-ascending method, using ADVANTEC TOYO No. 51B filter-paper and the following solvent system (v/v): 1-butanol–pyridine–water (6 : 4 : 3). Sugars were detected with an alkaline silver nitrate reagent.[9] GLC was performed in a Shimadzu GC-4CM apparatus equipped with a flame-ionization detector, using a glass column (0.3 × 200 cm) packed with 3% ECNSS-M on Gaschrom Q (100—120 mesh). Peak areas were measured with a Shimadzu Chromatopac C-R3A. GLC-MS was conducted with a JEOL JMS-D 300 apparatus equipped with a glass column (0.2 × 100 cm) packed with 3% ECNSS-M, at 190 °C, at a pressure of helium of 1.2 kg/cm^2. The MS were recorded at an ionizing potential of 70 eV, an ionizing current of 50 μA, and a temperature of the ion source

of 210 °C.

Isolation of the Polysaccharides After the successive extraction of the dried, pulverized fruiting bodies (85 g) with methanol (1 l, 20 h) and 70% aqueous ethanol (7 times, 2 l, 5 h), in a boiling water bath, the residue was extracted 4 times with water (1 l) for 5 h in a boiling water bath. The extracts were deproteinized, and the solution was precipitated by 2% CTAB to give the acidic polysaccharide (U-3-A), as reported previously.[2] The supernatant was precipitated by addition of 3 volumes of EtOH, and the precipitate was dissolved in water, then dialyzed against distilled water. Non-dialyzable solution was applied to a column of DEAE-Toyopearl 650 M (3 × 42 cm). The neutral fraction was precipitated by addition of 1 volume of EtOH. The precipitate was dispersed in water, and lyophilized to afford the purified polysaccharide (U-3-N), in 1.24% yield. The acidic fraction of DEAE-Toyopearl 650 M was dialyzed, lyophilized, and applied to a column of DEAE-Toyopearl 650 M, then the column was eluted by the gradient elution with NaCl solution (0 to 1 M). The peak 1 (No. 31—40) was dialyzed, and lyophilized to afford the purified polysaccharide (U-3-AP_1), in 0.63% yield.

Gel Filtration and Estimation of Molecular Weight Gel filtration of U-3-N and U-3-AP_1 on a column of Toyopearl HW-65 was performed with 0.5 M sodium hydroxide as the eluent, and the molecular weight was estimated by a calibration curve constructed by the use of standard dextrans as previously reported.[3]

Analysis of Component Sugar The polysaccharides (U-3-N and U-3-AP_1) were hydrolyzed with 2 M trifluoroacetic acid for 8 h at 100 °C. The hydrolyzates were evaporated to remove the acid, and analyzed by PPC and GLC of alditol acetates, as previously described.[3]

Methylation Analysis The polysaccharides (U-3-N and U-3-AP_1) was methylated 4 times by Hakomori's method[10] until they showed no hydroxyl absorption in the IR spectra, as previously described.[11] The fully methylated glucans were heated successively with 90% formic acid for 6 h at 100 °C, and with 0.25 M sulfuric acid for 15 h at 100 °C. After neutralization of the acid with barium carbonate, the partially methylated sugars were converted into the alditol acetates. The resulting, partially methylated alditol acetates were analyzed by GLC and GLC-MS.[12]

Periodate Oxidation and Smith Degradation Each sample (10 mg) was dissolved in 0.5 M NaOH (1 ml) and neutralized with 0.5 M HCl (1 ml), and water (18 ml) and 20 mM $NaIO_4$ (20 ml) were added. They were kept in the dark, with stirring, for 7 d at 4 °C. An aliquot (1 ml) was taken at various times, and the periodate consumption was determined by an arsenite method.[13] The oxidized polysaccharides were reduced with sodium borohydride to give the polyalcohols as described previously.[3] They were treated successively with 90% formic acid for 6 h at 100°C and with 0.25 M sulfuric acid for 15 h at 100°C. The hydrolyzates were analyzed by GLC as the alditol acetates, using a programmed rise in temperature of 6°C/min from 60 to 185 °C. The retention times of glycerol acetate and glucitol acetate were 13.8 and 39.5 min, respectively.

^{13}C-NMR Spectroscopy The ^{13}C-NMR spectra were recorded with a JEOL-GX 270 spectrometer in the Fourier-transform mode, with complete proton-decoupling for solutions in Me_2SO-d_6 (*ca.* 100 mg/ml) at 60 °C.

Enzymic Hydrolysis U-3-N (8.5 mg) was treated with *exo*-(1→3)-β-D-glucanase (Lysing enzyme; 4.0 mg) in 17 mM McIlvaine buffer, pH 4.88 (30 ml), at 37 °C.[3] A portion (4 ml) of the reaction mixture was taken at various times (5, 10, 24, 48, and 72 h), and each was heated for 15 min at 100 °C. Then, the solution was evaporated to *ca.* 0.5 ml, and applied to a column (1.5 × 97 cm) of Bio-gel P-2. The column was eluted with water, and fractions (1.3 ml each) were collected, and analyzed by the phenol–sulfuric acid method.[14] The molar ratio (G_2/G_1) of products was calculated from the peak area.

Interaction with Congo Red in Aqueous Sodium Hydroxide Each Sample (0.2 mg/ml) was dissolved in sodium hydroxide (0.10, 0.25, and 0.50 M) containing Congo red (50 μM), and λ_{max} was measured using a Hitachi 323 spectrophotometer.

Antitumor Activity The antitumor activity against the solid form of sarcoma 180 in mice was tested as described in a previous report.[3] The inhibition ratios were calculated by use of the formula: inhibition ratio (%) = $[(A-B)/A] \times 100$, where A is the average tumor weight of the control group, and B is that of the tested group.

References and Notes

1) Part XXV: T. Kiho, K. Nagai, I. Miyamoto, T. Watanabe, and S. Ukai, *Yakugaku Zasshi*, **110**, 286 (1990).
2) T. Kiho, M. Sakai, S. Ukai, C. Hara, and Y. Tanaka, *Carbohydr. Res.*, **142**, 344 (1985).
3) T. Kiho, M. Ito, K. Nagai, C. Hara, and S. Ukai, *Chem. Pharm. Bull.*, **35**, 4286 (1987).
4) S. Ukai, T. Kiho, C. Hara, M. Morita, A. Goto, N. Imaizumi, and Y. Hasegawa, *Chem. Pharm. Bull.*, **31**, 741 (1983).
5) N. Ohno, I. Suzuki, and T. Yadomae, *Chem. Pharm. Bull.*, **34**, 1362 (1986).
6) K. Bock, I. Lundt, and C. Pedersen, *Tetrahedron Lett.*, **1973**, 1037.
7) The carbonate extract contained very small amounts of other unknown polysaccharides.
8) D. J. Manners, A. J. Masson, and J. C. Patterson, *Biochem. J.*, **135**, 19 (1973); Y. Ueno, M. Abe, R. Yamauchi, and K. Kato, *Carbohydr. Res.*, **87**, 257 (1980).
9) W. E. Trevelyan, D. P. Procter, and J. S. Harrison, *Nature* (London), **166**, 444 (1950).
10) S. Hakomori, *J. Biochem.* (Tokyo), **55**, 205 (1964).
11) C. Hara, T. Kiho, and S. Ukai, *Carbohydr. Res.*, **117**, 201 (1983).
12) H. Björndall, C. G. Hellerqvist, B. Lindberg, and S. Svensson, *Angew. Chem., Int. Ed. Engl.*, **9**, 610 (1970).
13) P. F. Fleury and J. Lange, *J. Pharm. Chim.*, **17**, 196 (1933).
14) M. Dubois, K. A. Gilles, J. K. Hamilton, P. A. Rebers, and F. Smith, *Anal. Chem.*, **28**, 350 (1956).

Formation of O^6,7-Dimethylguanine Residues in Calf Thymus Deoxyribonucleic Acid Treated with Carcinogenic *N*-Methyl-*N*-nitrosourea *in Vitro*

Kohfuku KOHDA,* Noriaki SAWADA and Yutaka KAWAZOE

Faculty of Pharmaceutical Sciences, Nagoya City University, Tanabedori, Mizuho-ku, Nagoya 467, Japan. *Received September 10, 1990*

Treatment of calf thymus deoxyribonucleic acid (DNA) *in vitro* with a methylating carcinogen, *N*-methyl-*N*-nitrosourea (MNU), in phosphate buffer (pH 7.2) resulted in formation of O^6,7-dimethylguanine residues in DNA besides the well-known methylated DNA adducts, 7-methylguanine, O^6-methylguanine and 3-methyladenine. The product ratio (%) of O^6,7-dimethylguanine versus 7-methylguanine was 0.32 after one MNU treatment. The significance of formation of O^6,7-dimethylguanine residues in DNA is discussed briefly in relation to the carcinogenicity of MNU.

Keywords DNA damage; O^6,7-dimethylguanine; O^6-methylguanine; 7-methylguanine; DNA; methylation; *N*-methyl-*N*-nitrosourea; carcinogen; repair

Introduction

It is well known that the treatment of deoxyribonucleic acid (DNA) with methylating carcinogens *in vitro* and *in vivo* results in formation of varieties of methylated nucleobase and phosphate residues in DNA.[1] Among these methylated products, O^6-methylguanine and O^4-methylthymine residues are considered to cause the DNA damage most responsible for induction of mutation and/or cancer.[2,3] In our previous study on the reactivity of N-9 substituted O^6-methylguanine derivatives we revealed that their N-7 position is susceptible to further methylation resulting in formation of O^6,7-dimethylguanine derivatives.[4] In this paper we report the formation of O^6,7-dimethylguanine residues in calf thymus DNA treated with a carcinogenic *N*-methyl-*N*-nitrosourea (MNU) *in vitro*.

Experimental

Preparation of O^6,7-Dimethylguanine Our previously reported procedure[4] was modified. Briefly, O^6-methylguanine[5] was treated with CH_3I–K_2CO_3 in dimethylformamide to form a mixture of O^6,7-dimethylguanine and O^6,9-dimethylguanine. O^6,7-Dimethylguanine thus formed was separated by aluminum column chromatography eluted with $CHCl_3$: MeOH = 5 : 2. mp 252—253 °C. ^{1}H-NMR (DMSO-d_6) δ: 3.83 (s, 3H, N-CH_3), 3.97 (s, 3H, O-CH_3), 6.06 (br s, 2H, NH_2), 7.99 (s, 1H, H-8). UV λ_{max} nm (ε): 235 (sh) (6300) and 287 (11300) (pH 1), 240 (sh) (7500) and 288 (6700) (H_2O and pH 12). *Anal.* Calcd for $C_7H_9N_5O$: C, 46.93; H, 5.03; N, 39.11. Found: C, 46.86; H, 5.06; N, 39.13. MS *m/z*: 179 (M^+).

Other Materials 7-Methylguanine, 3-methyladenine and calf thymus DNA were purchased from Sigma Co., Ltd. O^6-Methylguanine was prepared by the method reported.[5]

Treatment of DNA with MNU, and Separation of Methylated Purines Fifty-five mg of MNU dissolved in 200 μl of dimethyl sulfoxide (DMSO) was added to a DNA solution (10 mg of calf thymus DNA in 10 ml of 80 mM phosphate buffer (pH 7.2)). The mixture was incubated at 37 °C for 3 h. Then, 20 ml of cold EtOH was added to the mixture and the resulting fibrous DNA was collected by centrifugation (3000 rpm, 10 min). After the DNA was re-dissolved in 10 ml of a solution (10 mM phosphate buffer (pH 7.2)–100 mM NaCl), it was heated at 100 °C for 30 min. Then the DNA solution was dialyzed against 300 ml of H_2O at 4 °C for 6 h, and the solution of outside the dialysis bag was collected and lyophilized. The lyophilizate was dissolved in a small amount of H_2O and was used as a sample (sample 1) for high-performance liquid chromatography (HPLC) analysis. The dialysate (DNA solution in the dialysis bag) was lyophilized and dissolved in 10 ml of 80 mM phosphate buffer (pH 7.2). To this solution, 55 mg of MNU in 200 μl of DMSO was again added and the mixture was incubated at 37 °C for 3 h. After repeating the above procedure, a sample (sample 2) was obtained as the lyophilizate of the solution of outside the dialysis bag. The experimental protocol is shown in Fig. 1.

Analyses of Methylated Purines A Shimadzu LC-9A HPLC system equipped with photodiode ultraviolet (UV) detector was employed. The column was TSK-gel ODS 80TM (4.6 × 250 mm) and the solvent system was 10 mM NaH_2PO_4–15% CH_3OH at a flow rate of 0.7 ml/min. The yields of the products were calculated from their UV intensity and ε value.

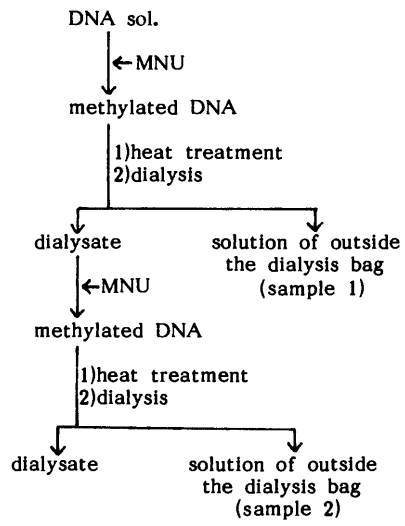

Fig. 1. Protocol for the Experiment

Results and Discussion

Figure 2 shows the HPLC chromatogram of sample 1. Large peaks were observed around retention time (t_R) of 8 to 14 min and two small peaks with longer t_R followed. Peaks 1 and 2 were those of 3-methyladenine and 7-methylguanine, respectively. Peak 3 observed at t_R 51 min was identified as O^6,7-dimethylguanine by comparison of the t_R and UV absorption with those of an authentic sample. UV spectra of peak 3 and its authentic sample are shown in Fig. 3. The other small peak (peak 4) observed

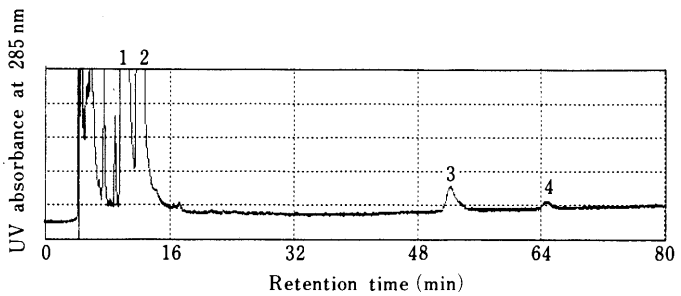

Fig. 2. Analysis of Methylated Purines
HPLC chromatogram of sample 1.

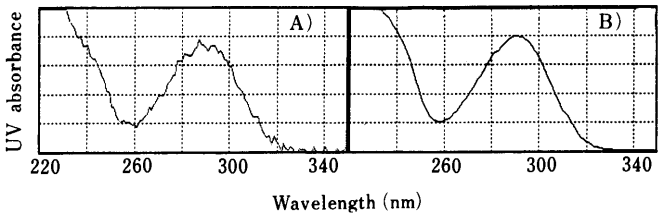

Fig. 3. UV Spectrum of O^6,7-Dimethylguanine
(A) Peak 3 in Fig. 2., (B) authentic sample.

TABLE I. Product Ratio of Methylated Purines[a]

Product	Ratio (%)	
	Sample 1	Sample 2
7-Methylguanine	100	100
O^6,7-Dimethylguanine	0.34	0.92
3-Methyladenine	12	11
O^6-Methylguanine	(9.4)[b]	

a) Expressed as % of 7-methylguanine. *b*) Determined separately by acid hydrolysis of the dialysate.

after peak 3 was not identified. The product ratio of methylated purines is shown in Table I. The percent ratio of O^6,7-dimethylguanine versus 7-methylguanine was 0.34 after the first MNU treatment (sample 1), and the ratio was increased to 0.92 by the second MNU treatment (sample 2). Since O^6,7-dimethylguanine is formed by the N-7 methylation of O^6-methylguanine residues,[4] the increased rate of O^6,7-dimethylguanine is due to the accumulated O^6-methylguanine residues in DNA by the first MNU treatment.

The existence of several unidentified minor components in DNA treated with methylating carcinogens was reported.[6] In this work we formulated the structure of one of them. The identification of O^6,7-dimethylguanine residues in cellular DNA treated with MNU is in progress.

The biological significance of O^6,7-dimethylguanine is an interesting subject to study, because the substance includes two well-known modifications, methylations at the O-6 and N-7 positions. O^6-Methylguanine residues in DNA are considered to cause the DNA damage most responsible for mutation and/or cancer, and are known to be reparable by an enzyme, O^6-methylguanine-DNA methyltransferase.[7] 7-Methylguanine residues are considered to cause damage related to the cell killing, and are known to be reparable by the enzyme, DNA glycosylase.[7] Could O^6,7-dimethylguanine formed in cellular DNA be repaired by these repair enzymes? If not, this modified portion would be a serious detriment in terms of initiation of mutation and/or cancer, even if its amount were extremely low.

References

1) B. Singer, *Prog. Nucleic Acid Res. Mol. Biol.*, **15**, 219 (1975).
2) B. Singer, *Cancer Investigation*, **2**, 233 (1984).
3) B. Singer, *Cancer Res.*, **46**, 4879 (1986).
4) K. Kohda, K. Baba and Y. Kawazoe, *Tetrahedron Lett.*, **28**, 6285 (1987).
5) R. W. Balsiger and J. A. Montgomery, *J. Org. Chem.*, **25**, 1573 (1960).
6) R. Valencia, H. N. Cong and O. Bertaux, *J. Chromatogr.*, **325**, 207 (1985).
7) T. Lindahl, B. Sedgwick, M. Sekiguchi and Y. Nakabeppu, *Ann. Rev. Biochem.*, **57**, 133 (1988).

Further Study on Two Chemical Races of *Salix sachalinensis* Fr. Schmidt

Mizuo Mizuno,*[,a] Masaya Kato,[a] Munekazu Iinuma,[a] Toshiyuki Tanaka,[a] Arika Kimura,[b] Hiroyoshi Ohashi,[b] Hideki Sakai,[b] and Tadashi Kajita[b]

Department of Pharmacognosy, Gifu Pharmaceutical University,[a] 6–1 Mitahorahigashi 5 chome, Gifu 502, Japan, and Department of Botany, Faculty of Science, Tohoku University,[b] Aoba, Aramaki, Sendai 980, Japan. *Received November 5, 1990*

Chemical constituents in the bark of two chemical races (flavonoid race and phenylpropanoid race) in *Salix sachalinensis*, the existance of which had been proposed on the basis of the secondary metabolites in the leaves, were qualitatively and quantitatively compared. The results showed the comparison of secondary metabolites in the leaves between two races is efficient for Salicaceous plants chemotaxonomy.

Keywords *Salix sachalinensis*; Salicaceae; chemical race; bark chemical constituent

In our preliminary chemotaxonomic studies on the Salicaceous plants,[1,2] we have made clear the presence of two intraspecific chemical races in *Salix sachalinensis* on the basis of the chemical constituents in their leaves.[3] In the present paper, comparison of two races by means of the chemical constituents in the bark is described.

Experimental

Plant Material The bark of *Salix sachalinensis* used for high performance liquid chromatography (HPLC) analysis in the present study was collected from 18 individuals (sample number: 25, 27—43) in Takane-mura, Ohno-gun, Gifu pref. in May 1989, and 14 individuals (96, 98—102, 106, 109, 116—118, 120, 122 and 125) in Kawauchi, Sendai, Miyagi pref. Japan in March 1988. The bark was obtained from the same individuals which had been used for the analysis of their leaves. The sample numbers shown in parentheses correspond to those in reference.[3] Voucher specimens are deposited in the Herbarium of Gifu Pharmaceutical University and of Biological Institute of Tohoku University (TUS).

Chemical Constiuents in the Barks By repeated column chromatography on silica gel and Sephadex LH20, (+)-catechin (**1**), sachaliside I (**2**),[4] taxifolin (**3**) and vimalin (**4**)[5] were isolated from a methanolic extract of *S. sachalinensis* (sample number 18). Their structures shown in Fig. 1 were elucidated by spectroscopic analysis.

Preparation of Sample Solutions The dried and powdered bark (about 300 mg) was weighed with accuracy and extracted with 50% MeOH in ultrasonification for 10 min. The extract was diluted with 50% MeOH up to 10 ml.

HPLC Analysis The sample solution was subjected to HPLC analysis using a Shimadzu LC-6A system with a Cosmosil $5C_{18}$ (4.0 mm × 250 mm, Nakarai Chemicals, Japan) column. A linear gradient elusion system was applied as follows: an aqueous solution (A), containing acetic acid (25 ml) and 5% phosphoric acid (2.5 ml) in water (1000 ml), and acetonitrile (B) were used as the mobile phase. The ratio of A and B was kept at 9 : 1 for 10 min after injection. The ratio was increased to 6 : 4 linearly for 30 min, kept at the same ratio for 10 min (50 min total time), and finally reverted to 9 : 1. The flow rate of mobile phase was 1 ml/min, and 10 μl of sample solution was injected. Phenolic constituents were detected at 270 nm by a ultraviolet spectrophotometer. The contents of bark chemical constituents were calculated by comparing the peak area (**2**) and by the peak height (**1**, **3** and **4**) with the respective calibration curves.

Test of Significant Differences Mann-Whitney U test were used for the contents of the bark phenolics (**1**—**4**) in the flavonoid race (group 1) and in the phenylpropanoid race (group 2).

Results and Discussion

The HPLC profile of *S. sachalinensis* (sample number 35) is shown in Chart 1. Four main components (**1**—**4**) were observed at the retention time (t_R) of *ca.* 7, 9, 20 and 23 min, respectively as well as some minor unidentical peaks. The contents of four components in 32 individuals were calculated and the values are listed in Table I. The histograms of two chemical races in an average amount are drawn in Fig. 2. Though the contents of four components in the barks were considerably varied on the whole, each of 18 individuals belonging to group 1 showed a similar profile to 14 individuals belonging to group 2. (+)-Catechin (**1**), sachaliside I (**2**) and taxifolin (**3**) exhibited rather higher contents in the bark of the flavonoid race, whereas the phenylpropanoid race have a trend to accumulate vimalin (**4**). To qualify the difference between two chemical races, the Mann-Whitney U test was applied to respective contents.

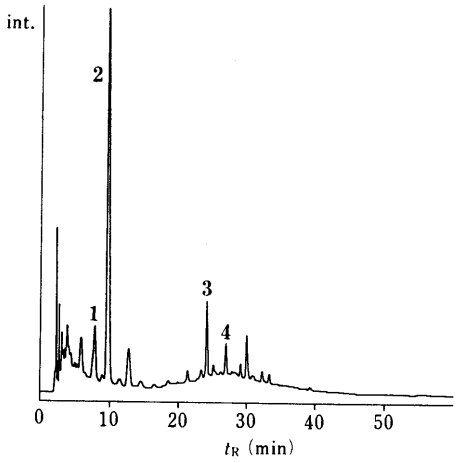

Chart 1. HPLC Chromatogram of the Bark of *Salix sachalinensis*

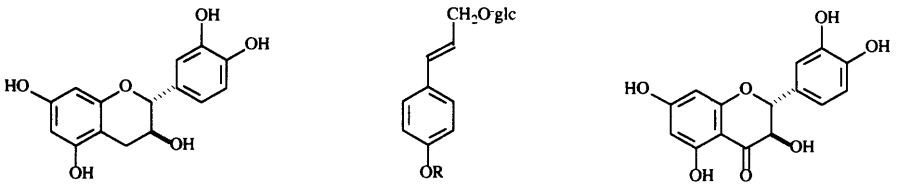

1 : (+)-catechin **2** : R=H, sachaliside I **3** : taxifolin

4 : R=CH_3, vimalin

Fig. 1. Structures of Compounds **1**—**4**

TABLE I. Contents of Phenolics in the Bark of *Salix sachalinensis*

Sample no.	Content (mg/g) 1	2	3	4
25	8.09	4.26	0.37	0.08
27	5.43	4.62	0.35	0.09
28	3.68	3.62	0.20	0.06
29	5.94	8.62	0.12	0.03
30	6.07	2.60	0.72	0.07
31	3.68	7.85	5.46	0.11
32	4.76	12.78	7.51	0.11
33	4.87	9.87	3.96	0.11
34	3.87	2.74	0.10	0.03
35	2.85	2.77	1.72	0.18
36	4.35	2.50	0.20	0.39
37	3.58	3.56	0.46	0.07
38	2.66	3.42	0.90	0.07
39	2.98	2.86	0.86	0.06
40	3.77	3.77	1.50	0.07
41	3.80	4.45	0.49	0.08
42	2.50	6.99	4.43	0.05
43	4.47	3.76	0.29	0.45
96	4.21	2.66	0.94	2.53
98	2.01	1.06	1.88	2.18
99	3.57	3.63	0.03	1.45
100	1.73	1.82	0.23	0.94
101	1.93	2.73	0.00	0.15
102	0.94	1.42	0.10	0.04
106	1.98	2.24	0.31	0.05
109	2.96	2.18	0.51	2.11
116	3.56	2.23	0.00	0.14
117	2.81	1.71	0.36	0.50
118	2.99	2.01	0.00	0.04
120	3.26	2.17	0.08	0.09
122	3.94	2.89	0.14	0.18
125	2.61	2.37	0.00	0.08
Average (S.E.)				
No. 25—43	4.30	5.06	1.64	0.12
	(0.33)	(0.69)	(0.51)	(0.03)
No. 96—125	2.75	2.22	0.33	0.75
	(0.25)	(0.17)	(0.14)	(0.25)

The significant differences were found at the level of significance $p<1\%$ in the contents of (+)-catechin (**1**) sachaliside 1 (**2**) and taxifolin (**3**), and $p<5\%$ in that of vimalin (**4**).

These results indicated that two chemical races in *S. sachalinensis* based on the secondary metabolites in the leaves have identical chemical components in their bark

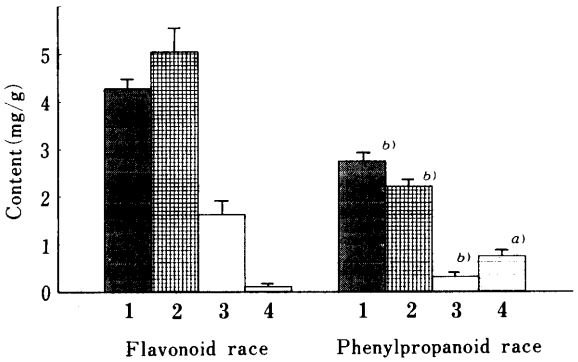

Fig. 2. Average Contents (**1**—**4**) in the Bark of Two Chemical Races in *Salix sachalinensis*

Level of significancy *a*) $p<0.05$, *b*) $p<0.01$.

regarding quality, but that the races were quantitatively nonidentical. Consequently, the two chemical races in *S. sachalinensis* were also distinct based on the chemical profile in the bark, and were regarded as having a significantly different ability to produce phenolic compounds. On the other hand, the leaf chemical profile of *S. sachalinensis* is clearly divided into two races—flavonoid race and phenylpropanoid race—. This evidence proved the investigation on flavonoid or phenylpropanoid in the leaf to be an efficient basis for Salicaceous plants chemotaxonomy. In another of our studies,[6] no intraspecific chemical variation was observed in other *Salix* species, for example, *S. gracilistyla*, *S. integra*, *S. gilgiana*, *S. bakko*, *S. pierotii*, *S. chaenomeloides etc.* Therefore, the chemical profiles of the leaf in the genus are reliable characters to clarify not only the interspecific relationship but also the relation among the sections of Salicaceous plants.

References

1) M. Mizuno, M. Kato, M. Iinuma, T. Tanaka, A. Kimura, H. Ohashi, and H. Sakai, *Phytochemistry*, **26**, 2418 (1987).
2) M. Mizuno, M. Kato, M. Iinuma, T. Tanaka, A. Kimura, H. Ohashi, and H. Sakai, *Asian J. Plant Sci.*, **1**, 1 (1989).
3) M. Mizuno, M. Kato, M. Iinuma, T. Tanaka, A. Kimura, H. Ohashi, H. Sakai, and T. Kajita, *Bot. Mag. Tokyo*, **102**, 403 (1989).
4) M. Mizuno, M. Kato, N. Hosoi, M. Iinuma, T. Tanaka, A. Kimura, H. Ohashi, H. Sakai, and T. Kajita, *Heterocycles*, **31**, 1409 (1990).
5) H. Thieme, *Naturwissenschaften*, **51**, 217 (1964).
6) M. Kato, unpublished data.

THE INHIBITORY EFFECT OF 3,3',4,5'-TETRAHYDROXYSTILBENE, A CONSTITUENT OF *CASSIA GARRETTIANA*, ON ANTI-IgE-INDUCED HISTAMINE RELEASE FROM HUMAN BASOPHILS *IN VITRO*[1)]

Yoshihiko INAMORI,*,[a] Masafumi OGAWA,[a] Hiroshi TSUJIBO,[a] Kimiye BABA,[a] Mitsugi KOZAWA[a] and Hideo NAKAMURA[b]

Osaka University of Pharmaceutical Sciences,[a] Kawai, Matsubara-shi, Osaka 580, Japan, and Dainippon Pharmaceutical Co., Ltd,[b] Enoki, Suita-shi, Osaka 564, Japan

3,3',4,5'-Tetrahydroxystilbene (I), a constituent of *Cassia garrettiana*, strongly inhibited the anti-IgE-induced histamine release from human basophils *in vitro* at concentrations of 3 to 30 μM. Considering that disodium cromoglycate showed no significant inhibitory activity in this assay method, the strong effect of I should be emphasized.

KEYWORDS 3,3',4,5'-tetrahydroxystilbene; *Cassia garrettiana*; histamine release; human basophil; disodium cromoglycate; theophylline; oxystilbene derivative

3,3',4,5'-Tetrahydroxystilbene (I, Chart 1),[2)] a constituent of *Cassia garrettiana*, and 3,4-*O*-isopropylidene-3,3',4,5'-tetrahydroxystilbene, a chemical derivative of I, have been reported to show antifungal activity,[3-5)] coronary vasodilator action in the isolated guinea pig heart,[5,6)] and hypotensive effect in rats.[5,6)] Although caffeic acid,[7)] chlorogenic acid[7)] and di-*O*-caffeoylquinic acid[7)] having a common moiety of I in the molecule have been reported to inhibit histamine release from rat peritoneal mast cells, no work has been done on the inhibitory effect of I on histamine release. Therefore, to develop the range of biological activity of I, the effect of I on anti-IgE-induced histamine release from human basophils was examined. As a result, it was found that I strongly inhibited histamine release from this cell. In this paper, we report the inhibitory effect of I.

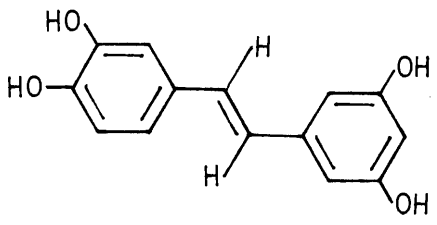

I

Chart 1

The results are summarized in Table I. Compound I strongly inhibited anti-IgE-

induced histamine release from this cell. Namely, I at 30 μM inhibited histamine release 90% more than the vehicle control did. Compound I also showed 17.7% inhibition of histamine release even at a concentration of 3 μM. In conclusion, the 50% inhibitory concentration (IC_{50}) of I was 7.3 μM. The inhibitory activity of I was stronger than that of theophylline used as a positive control. On the other hand, disodium cromoglycate (DSCG) did not inhibit histamine release even at a high concentration of 1000 μM.

Table I. Inhibition by 3,3',4,5'-Tetrahydroxystilbene (I) of Anti-IgE-Induced Histamine Release from Human Basophils *in Vitro*

Compound	Concentration (μM)	No. of[a] donors	Histamine release		IC_{50} (μM)
			Mean (%) ± S.E.	Inhibition (%)	
Vehicle		3	51.5± 2.8		
I	1	3	49.7± 3.8	3.5	
	3	3	42.4± 4.1	17.7	
	10	3	23.6± 4.4[b]	54.2	7.3
Vehicle		3	45.9± 6.4		
I	30	3	3.0± 2.1[b]	93.5	
Vehicle		3	52.2±11.8		
DSCG[c]	1000	3	63.0±14.2	-20.7	>1000
Vehicle		2	40.8± 7.4		
Theophylline	300	2	12.2± 4.0	70.1	< 300

a) Each concentration consisted of 2 to 3 tubes per donor. b) $P<0.01$, significantly different from the vehicle control (the mean ± S.E. of total histamine levels of 3 donors: 45.2±1.7 ng/ml). c) Disodium cromoglycate. The leukocyte fraction containing basophils (Alcian blue staining), separated from the whole blood of a healthy donor by the dextran sedimentation method, was used as basophil samples. Leukocytes were suspended in Tris-ACM buffer (25 mM Tris, 120 mM KCl, 0.6 mM $CaCl_2$, 1 mM $MgCl_2$ and 0.03% human albumin, pH 7.6) to yield concentrations of 1-10 X 10^6 cells/ml. Of these suspensions, 1-ml portions were incubated with various concentrations of a test compound solution of 0.1 ml for 15 min at 37°C. Thereafter, 0.1 ml of anti-human-IgE (1 : 1.2 X 10^4; affinity purified from goat anti-serum; International Immunology Corporation, USA) was added and incubation was continued for another 45 min. Histamine was measured by the fluorometric method.[8,9] The IC_{50}-value was calculated from a regression equation plotted for the mean inhibitory rate from 3 donors versus concentraion. Compound I alone did not release histamine.

As mentioned above, 3,3',4,5'-tetrahydroxystilbene (I) strongly inhibited anti-IgE-induced histamine release from human basophils. It should be emphasized that although DSCG had no significant effect, I was strongly inhibitory (IC_{50}: 7.3 μM). The inhibitory mechanism of I is suggested by the reports that caffeic acid,[7] chlorogenic acid,[7] di-*O*-caffeoylquinic acid[7] and tranilast,[10] which have a common moiety of I in their molecules,

inhibit histamine release from rat peritoneal mast cells. The inhibition by an oxystilbene derivative such as **I** of histamine release is reported for the first time in this paper.

Further studies on **I** and other oxystilbene derivative in relation to antiallergic activity are in progress, together with mechanisms of histamine release inhibition.

REFERENCES AND NOTES

1) This work was presented at the 110th Annual Meeting of the Pharmaceutical Society of Japan, Sapporo, August 1990.
2) K. Hata, K. Baba and M. Kozawa, *Chem. Pharm. Bull.*, **27**, 984(1979).
3) Y. Inamori, Y. Kato, M. Kubo, M. Yasuda, K. Baba and M. Kozawa, *Chem. Pharm. Bull.*, **32**, 213(1984).
4) Y. Inamori, M. Kubo, Y. Kato, M. Yasuda, K. Baba and M. Kozawa, *Chem. Pharm. Bull.*, **32**, 801(1984).
5) Y. Inamori, M. Kubo, Y. Kato, M. Yasuda, H. Tsujibo K. Baba and M. Kozawa, *Chem. Pharm. Bull.*, **33**, 2904(1985).
6) Y. Inamori, M. Kubo, Y. Kato, M. Yasuda, K. Baba and M. Kozawa, *Yakugaku Zasshi*, **104**, 819(1984).
7) Y. Kimura, H. Okuda, T. Okuda, T. Hatano, I. Agata and S. Arichi, *Chem. Pharm. Bull.*, **33**, 690(1985).
8) P. A. Shore, A. Burkhaltar and V. H. Cohn, *J. Pharmacol. Exp. Ther.*, **127**, 182(1959).
9) R. P. Siraganian, *Anal. Biochem.*, **57**, 383(1974).
10) K. Sakano and T. Yoshimura, *Allergy*, **26**, 385(1977).

(Received December 20, 1990)

CONTINUOUS MONITORING OF UNBOUND FLOMOXEF LEVELS IN RAT BLOOD USING MICRODIALYSIS AND ITS NEW PHARMACOKINETIC ANALYSIS

Yutaka SAISHO* and Tsuneji UMEDA
Shionogi Research Laboratories, Shionogi & Co., Ltd., Fukushima-ku, Osaka 553 Japan

Microdialysis sampling method coupled to high-performance liquid chromatography with UV detection was applied to continuous monitoring of *in vivo* unbound flomoxef concentration in rat blood. By comparison with ultrafiltration method, it was demonstrated that it gave reliable results for the unbound drug monitoring in blood. Furthermore, a new method was presented for the calculation of pharmacokinetic parameters from the data obtained by the microdialysis method.

KEYWORDS microdialysis; flomoxef; high-performance liquid chromatography; ultrafiltration; pharmacokinetic parameter

Microdialysis, which was first introduced by Tossman and Ungerstedt in 1981,[1] has been developed to sample the extracellular space of brain[2] and other tissues.[3,4] In recent years, its several applications to the analysis of exo- and endogenous substances in blood have been reported.[5,6] The present investigation was undertaken (a) to monitor the unbound flomoxef concentration in blood of individual rat after i.v. administration of its sodium salt[7] by the combination of microdialysis and high-performance liquid chromatography (HPLC) with UV detection, (b) to evaluate the reliability for results of the microdialysis method by comparison with those of the established ultrafiltration method, and (c) to propose a new method to calculate pharmacokinetic parameters from the product of concentration and sampling time obtained by the microdialysis method.

As shown in Fig. 1, a microdialysis probe (Bioanalytical Systems, Inc./Carnegie Medicin, West Lafayette, IN) equipped with a dialysis membrane (10×0.5 mm I.D., molecular cut-off 20,000) was introduced inside a 19-gage needle cannula into the jugular vein of 260-320 g male rats under pentobarbital anesthesia, and was perfused with saline at a speed of 2 μl/min by a microinjection pump. After i.v. administration of flomoxef sodium, sample dialysates were collected every 10 minutes, and were directly subjected to HPLC analysis. As illustrated in Fig. 2, the chromatogram was free from interferences. Time courses of the concentrations of unbound flomoxef in blood of individual six rats were monitored continuously until 90 minutes after i.v. administration (20, 40, 80 mg/kg). Unbound flomoxef levels in blood were corrected for the mean of *in vitro* recoveries (*ca.* 50%) that were tested at 37°C both before and after in vivo operation using a well-stirred standard solution of flomoxef sodium.

The ultrafiltration method established for the sampling of unbound fraction in blood was examined to evaluate the reliability for in vivo drug monitoring by the microdialysis method. The six blood samples were collected through femoral vein at each time point of 5, 10, 30, 60 and 90 minutes, respectively, after i.v. administration of flomoxef sodium. Unbound fractions of plasma were prepared under centrifugation at 37°C by use of MPS-3 micropartition system (amicon. Lexington, MA). There was no need to adjust the pH of plasma, because the protein binding of flomoxef in plasma was little influenced in the range of pH 6.5-8.0. As shown in Fig. 3 with comparative illustration, good correlations were appeared for the unbound levels of flomoxef between both methods of microdialysis and ultrafiltration. These results would imply that the mass transport resistance[8] in blood is as low as that in a well-stirred aqueous medium, and that the blood fluid is under ideal surroundings for its microdialysis due to its continuous fast replacement. Therefore, microdialysis of blood would be applicable to the quantitation of individual unbound drug levels in small animals such as rats with satisfactory reliability.

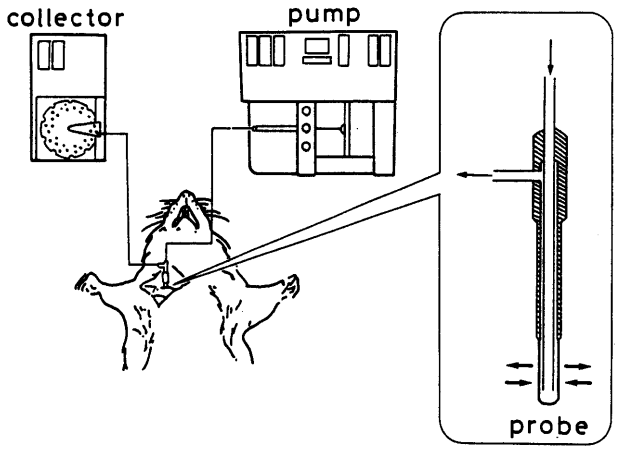

Fig. 1. Microdialysis System

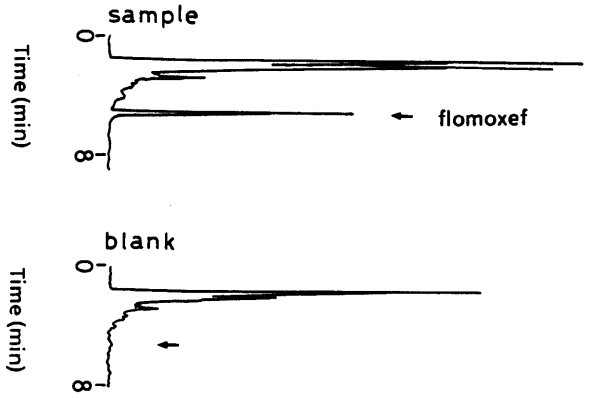

Fig. 2. HPLC of Drug-Free (Lower) and Flomoxef-Containing (Upper) Rat Blood Dialysate. Conditions: column, Nucleosil 5 C_{18} (150×4.6 mm I.D.); mobile phase, CH_3CN: 50 mM tetra-n-butylammonium bisulfate = 1 : 3 (v/v); flow rate, 1.0 ml/min; UV detection, 270 nm.

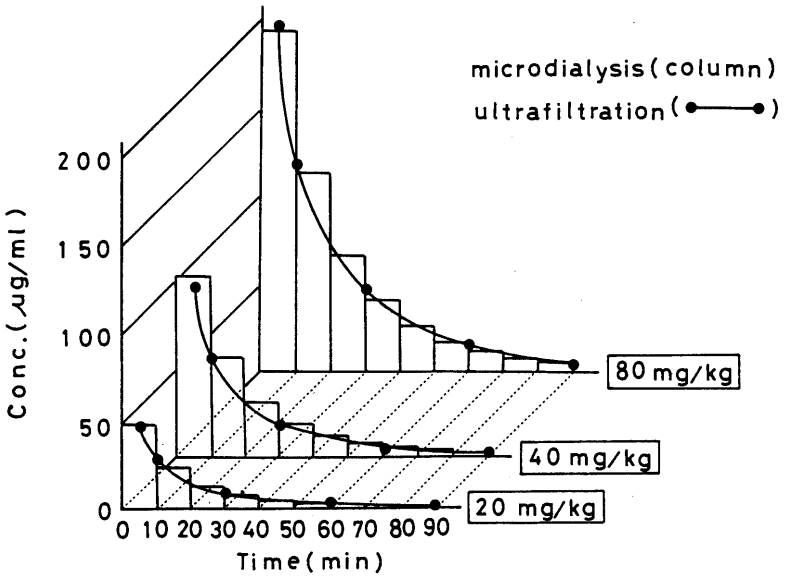

Fig. 3. Mean Concentrations of Unbound Flomoxef in Rat Blood Treated with Microdialysis and Ultrafiltration Methods after i.v. Administration of 20, 40 and 80 mg/kg of Flomoxef Sodium
Dialysate values are corrected for *in vitro* recovery.

Since microdialysis method needs a time period to collect the blood dialysate, it is unable to give the concentration at a time point. Instead of the measured concentration itself, the product of it and the sampling time is more likely to be a significant response variable, first proposed by us, for pharmacokinetic analysis of *in vivo* drug level monitoring by the microdialysis method. The product that is the each column area shown in Fig. 3, is corresponding to the area, in a time period, under the concentration-time curve which is ordinarily obtained by the discontinuous sampling method to withdraw blood. By use of the non-linear curve-fitting program NONLIN,[9] pharmacokinetic analysis was undertaken according to the one-compartment model to which the product was fitted as a function described by the following equation;

$$P = A \int_{t_1}^{t_2} e^{-k_e \cdot t} dt$$

where P is the product of concentration and sampling time during the interval t_1 to t_2, A is initial unbound drug concentration and k_e is first-order elimination rate constant. Comparative pharmacokinetic analysis was likewise carried out for the concentration-time data of the ultrafiltration method. As shown in Table I, the analyzed pharmacokinetic parameters gave good agreements between both the methods.

Table I. Pharmacokinetic Parameters for Unbound Flomoxef

Parameter		Microdialysis	Ultrafiltration
k_e	(min^{-1})	0.0648 ± 0.0082	0.0756
A	($\mu g \cdot ml^{-1}$)	66.0 ± 12.0	65.2
$t_{1/2}$	(min)	10.9 ± 1.7	9.2
V_d	($l \cdot kg^{-1}$)	314 ± 62	307
AUC_∞	($\mu g \cdot ml^{-1} \cdot min$)	1020 ± 150	860
CL	($ml \cdot kg^{-1} \cdot min^{-1}$)	20.0 ± 3.2	23.2

Dose: 20 mg/kg. Microdialysis data express mean ± S.D. (n = 6).

In the present study, microdialysis has been shown to be reliably applied to *in vivo* determination of unbound drug levels in blood. Furthermore, we have presented a new method for pharmacokinetic analysis from the data obtained by the microdialysis method. In conclusion, microdialysis of blood has been also evaluated to be a unique and useful sampling method for continuous drug monitoring in individual rats. Further studies are in progress on the application of the method to monitoring other drugs.

ACKNOWLEDGEMENT The authors express their sincere thanks to Dr. K. Matsunaga for giving his technical advices on operation of rat and to Dr. T. Tasaki and Mr. M. Zaizen for the pharmacokinetic analysis of the data.

REFERENCES AND NOTES

1) U. Tossman and U. Ungerstedt, Neurosci. Lett. Suppl., 7, S479 (1981).
2) H. Benveniste, J. Neurochem., 52, 1667 (1989).
3) O. Meirieu, M. Pairet, J. F. Suruta and M. Ruckebusch, Life Sci., 38, 827 (1986).
4) H. Jarry, M. Dietrich, A. Barthel, A. Giesler and W. Wuttke, Endocrinology, 125, 624 (1989).
5) R. M. Caprioli and Shen-Nan Lin, Proc. Natl. Acad. Sci., USA, 87, 240 (1990).
6) D. O. Scott, L. R. Sorensen and C. E. Lunte, J. Chromatogr., 506, 461 (1990).
7) A new parenteral oxacephem antibiotic which was synthesized in our laboratories; T. Tsuji, H. Satoh, M. Narisada, Y. Hamashima and T. Yoshida, J. Antibiot., 38, 466 (1985).
8) P. M. Bungay, P. F. Morrison, R. L. Dedrick, Life Sci., 46, 105 (1990).
9) C. M. Metzler, G. R. Elfring and A. J. Mcewen, Biometrics, 130, 560 (1974).

(Received January 10, 1991)

MEISENHEIMER REARRANGEMENT OF 2-ETHENYL-1,4,5,10b-TETRAHYDRO-2H-AZETOPYRIDO[3,4-b]INDOLE N-OXIDES: NEW ROUTE TO THE 12(S)CARBA-EUDISTOMIN SKELETON

Takushi KURIHARA,* Miki DOI, Kayo HAMAURA, Hirofumi OHISHI, Shinya HARUSAWA, and Ryuji YONEDA

Osaka University of Pharmaceutical Sciences, 2-10-65, Kawai, Matsubara, Osaka 580, Japan

Oxidation of 1,2-cis- and 1,2-trans-2-ethenyl-1,4,5,10b-tetrahydro-2H-azetopyrido[3,4-b]indoles **4** and **5** with m-chloroperbenzoic acid (mCPBA) gave tetrahydropyridooxazepine **7**, which has a 12(S)carba-eudistomin skeleton, and tetrahydropyridoisoxazole **8** by Meisenheimer rearrangement.

KEYWORDS 3,4-dihydro-β-carboline; tetrahydroazetopyridoindole; tetrahydropyridooxazepine; tetrahydropyridoisoxazole; Meisenheimer rearrangement; m-chloroperbenzoic acid; carbaeudistomin; X-ray analysis

Meisenheimer rearrangement of cyclic and heterocyclic amine oxides has been used to prepare cyclic 1,2-oxazine derivatives.[1] But in general, thermal conditions are necessary for this rearrangement. A number of azeto[2,1-a]isoquinolines have recently been synthesized in view of the interest in the chemical aspects as well as the potential biological activity.[2] From these points of view, we report here the preparation of a unique ring system of 1,2-cis- and 1,2-trans-2-ethenylazetopyridoindoles (**4** and **5**) and the Meisenheimer rearrangement of their N-oxides under very mild conditions.[3]

Based on the method of Nakagawa and Hino,[4] N-methyl-3,4-dihydro-β-carboline **1**[5] was alkylated with lithio methyl acetate (3 eq.) in the presence of $BF_3 \cdot OEt_2$ (1.1 eq.) followed by quenching with di-tert-butyldicarbonate (Boc_2O) (4 eq.) to give methyl N-Boc-tetrahydro-β-carboline-1-acetate **2** in 90% yield in a one-pot operation. Aldol condensation of **2** (LDA/-78°C) with acrolein gave allyl alcohol **3** in quantitative yield as a mixture of diastereomers. This was sequentially treated with methanesulfonyl chloride (MsCl)/Et_3N, dry HCl gas in EtOAc for de-Boc group, then DBU in DMSO at room temperature. Purification of the resulting reaction mixture by SiO_2 column chromatography afforded in turn cis-azetidine **4** (mp 97-98 °C),[6] trans-azetidine **5** (mp 117-119 °C), and 2-oxo-tetrahydro-1,3-oxazine **6**[7] in 54%, 6% and 9% overall yields from allyl alcohol **3**. The stereostructures of **4** [δ 3.13 (1H, dd, J=8 and 3 Hz, 1-H), 4.30 (1H, t, J=8 Hz, 2-H), and 5.10 (1H, br s, 10b-H)] and **5** [δ 2.88 (1H, t, J=4 Hz, 1-H), 4.54 (1H, dd, J=10 and 4 Hz, 2-H) and 5.02 (1H, br s, 10b-H)] was determined from the ^1H NMR spectral data, based on the general rule[2b] in which the vicinal coupling constants of the azetidines $^3J(H,H)_{cis}$ are larger than $^3J(H,H)_{trans}$.

When cis-azetidine **4** was treated with mCPBA in CH_2Cl_2 at 0°C, oxazepine **7** (mp 111-112 °C) was obtained in 80% yield. The structure of **7** was supported by spectral and analytical data[8], and unambiguously confirmed by X-ray analysis[9] of the corresponding alcohol **9** [mp 141-142 °C (EtOH)] obtained by reduction of **7** with $LiAlH_4$, as shown in

Fig. 1. On the other hand, trans-azetidine **5** was converted to isoxazolidine **8**[8] by the same treatment with mCPBA, in 45% yield. Measurement of NOE, which enhances 2-H (4.0%) by irradiation of 10b-H, strongly supported the stereostructure. From these results, it was clear that the N-oxidation of **4** and **5** takes place from the α-side followed by the Meisenheimer [2,3] rearrangement of the former and [1,2] rearrangement of the latter, which lead to **7** and **8**, respectively.

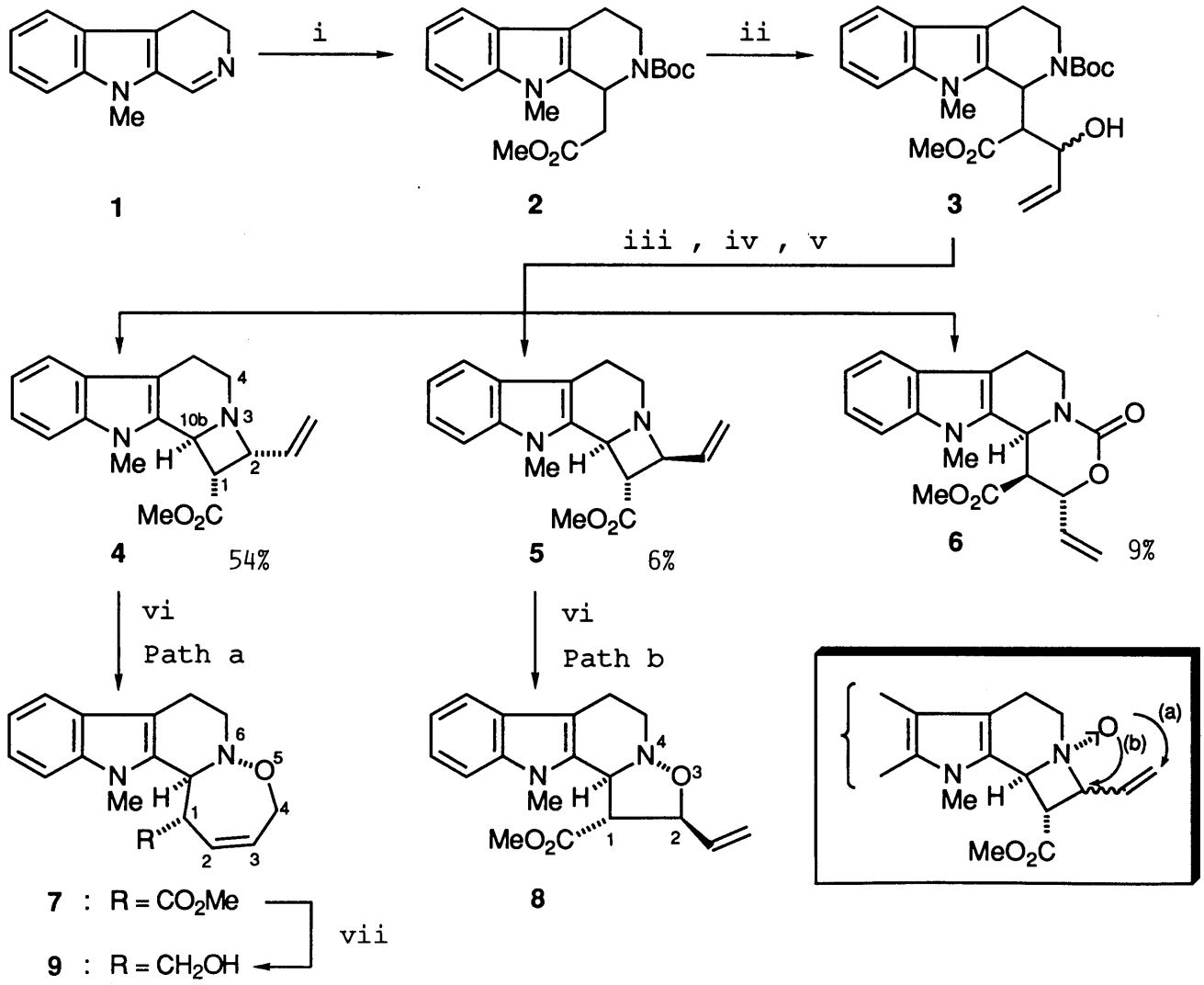

Chart.1
Reagents and conditions: i, LDA/$MeCO_2Me$, $BF_3 \cdot OEt_2$, -23°C, then Boc_2O, r.t.; ii, LDA, acrolein, -78°C; iii, MsCl/TEA, r.t.; iv, 2.3N HCl-EtOAc, r.t.; v, DBU/DMSO, r.t.; vi, mCPBA, 0°C; vii, $LiAlH_4$

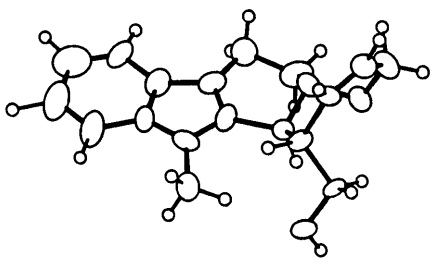

Fig. 1. Perspective View of Compound **9**

The framework of tetrahydro-4H-indolo[2,3-c]pyrido[1,2-b][1,2]oxazepine **7** corresponds to that of 12(S)carba-analog of eudistomins.[10] These are antiviral marine natural products. This work will provide a promising route for the synthesis of carbaeudistomin analogs.[11]

REFERENCES AND NOTES

1) J.B. Bremner,"Studies in Natural Products Chemistry," Vol.6, ed. by Atta-ur-Rahman, Elsevier, Inc., Amsterdam, 1990, pp. 467-502.

2) a) G. Bernáth, J. Kóbór, F. Fülöp, P. Sohar, G. Argay and A. Kálmán, Tetrahedron, **42**, 5139 (1986); b) J. Kóbór, F. Fülöp, G. Bernáth, and P. Sohár, ibid., **43**, 1887 (1987).

3) a) M. Nakagawa, K. Yoshikawa, and T. Hino, J. Am. Chem. Soc., **97**, 6496 (1975); Q.-S. Yu, H.J.C. Yeh, and A. Brossi, J. Nat. Prod., **52**, 332 (1989).

4) M. Nakagawa, T. Kawata, H. Yamazaki, and T. Hino, J. Chem. Soc., Chem. Commun., **1990**, 991.

5) R. Zo Andriamialisoa, N. Langlois, and Y. Langlois, J. Org. Chem., **50**, 961 (1985).

6) Satisfactory spectroscopic and analytical data were obtained for all new compounds.

7) The structure of **6** (mp 170-172°C), IR (Nujol) 1720, 1680 (CO) cm^{-1}; ^1H NMR ($CDCl_3$) δ 2.7-3.1 (3H, m), 3.33 (3H, s), 3.41 (1H, dd, J=2, 4 Hz), 4.68 (3H, s), 4.76 (1H, br d, J=12 Hz), 5.11 (1H, br d, J=4 Hz), 5.18 (1H, m), 5.49 (1H, d, J=10 Hz), 5.55 (1H, d, J=16 Hz), 5.98 (1H, ddd, J=16, 10, 4 Hz), 7.19 (3H, m), and 7.50 (1H, d, J=7.5 Hz)] was finally established by X-ray crystallographic analysis, the results of which will be published soon. The mechanistic proposal of its formation is illustrated in our previous paper, Y. Matsubara, R. Yoneda, S. Harusawa, and T. Kurihara, Heterocycles, **27**, 667 (1988).

8) **7**: IR ($CHCl_3$) 1720 (CO) cm^{-1}; ^1H NMR ($CDCl_3$) δ 2.7-3.2 (3H, m), 3.56 (3H, s), 3.56 (4H, m), 3.72 (3H, m), 3.90 (1H, t, J=6 Hz), 4.39 (1H, d, J=16 Hz), 4.53 (1H, d, J=16 Hz), 5.05 (1H, d, J=6 Hz), 5.61-5.79 (2H, m), 7.0-7.27 (3H, m), and 7.45 (1H, d, J=7.5 Hz); ^{13}C NMR ($CDCl_3$) δ 21.5 (t), 31.5 (q), 49.5 (d), 52.9 (q), 53.0 (t), 65.5 (d), 72.0 (t), 109.5 (s), 109.7 (d), 118.8 (d), 120.0 (d), 122.2 (d), 123.5 (d), 126.7 (s), 131.0 (d), 135.7 (s), 139.5 (s), and 174.5 (s); HRMS Calcd for $C_{18}H_{20}N_2O_3$: 312.1473. Found: 312.1478.
8: IR ($CHCl_3$) 1725 (CO)cm^{-1}; ^1H NMR ($CDCl_3$) δ 2.7-3.3 (3H, m), 3.20 (1H, dd, J=7.5, 5 Hz), 3.59 (3H, s), 3.65 (1H, m), 3.82 (3H, s), 4.76 (1H, t, J=7.5 Hz), 5.10 (1H, d, J=5 Hz), 5.19 (1H, d, J=10 Hz), 5.35 (1H, d, J=17 Hz), 5.78 (1H, ddd, J=17, 10, 7.5 Hz), 7.19 (3H, m), and 7.51 (1H, d, J=7.5 Hz); HRMS Calcd for $C_{18}H_{20}N_2O_3$: 312.1473. Found: 312.1476.

9) Crystal data for **9**: $C_{17}H_{20}N_2O_2$, M = 284.358, momoclinic, space group Pc, a = 18.499(4), b = 6.2149(9), c = 26.45(1), β= 103.16(3) Å, V = 2961(1) $Å^3$, Z = 4, unit cell contents = 4, D_c = 1.28 g cm^{-3}, (Cu-Kα) = 6.38 cm^{-1}, θ range = 1-130°. The final conventional R-factor was 0.0443 for 4547 independent reflections [F>2σ(F)] and 1078 parameters.

10) M. Nakagawa, J. Liu and T. Hino, J. Synth. Org. Chem. Jpn., **48**, 891 (1990), and references cited therein.

11) M.P. Kirkup, B.B. Shankar, S. McCombie, A.K. Granguly, and A.T. McPhail, Tetrahedron Lett., **30**, 6809 (1989).

(Received January 10, 1991)

EFFECT OF LASER IRRADIATION ON SURFACE HARDNESS OF SELF-SETTING HYDROXYAPATITE CEMENT

Makoto OTSUKA,*,[a] Yoshihisa MATSUDA,[a] Jeffery L. FOX,[b] G. LYNN POWELL[c] and William I. HIGUCHI[b]

Kobe Women's College of Pharmacy,[a] Motoyama Kitamachi, Higashi-Nada, Kobe 658, Japan, and Department of Pharmaceutics[b] and Department of Dental Education,[c] University of Utah, and Salt Lake City, Utah 84112, U.S.A.

A novel approach to the use of self-setting hydroxyapatite cement in a dental cement system uses CO_2 laser irradiation is proposed to solve the problem of the insufficient hardness of the cement. After setting, the cement is transformed to hydroxyapatite which has a high affinity for hard tooth and bone tissuess. The Vickers hardness of the cement system is significantly increased by CO_2 laser irradiation.

KEYWORDS CO_2 laser; artificial hard tissue; Vickers hardness; hydroxyapatite; self-setting cement; biomaterial

For use in implanting artificial hard tissue, hydroxyapatite (HAP) has a high affinity to hard tissue in situ and can be molded to fill up spaces created by accident or by surgical operation on bones or teeth. It can also be used as a bonding material between bones or between bone and a prosthesis.[1] Brown and Chow reported that a patented self-setting hydroxyapatite cement,[2] $Ca_{10}(PO_4)_6(OH)_2$ (Mw = 1004.62), which has the same elementary chemical composition as bone and teeth, is proposed as a new dental and bioconvertible material. But in practical applications, the hydroxyapatite cement does not have adequate mechanical strength after setting. This is the most serious problem with this cement system. But now currently, the surgical laser has proved to be a valuable treatment modality in many special surgical applications.[3] Stern *et al.*,[4] Yamamoto *et al.*[5] and Wong *et al.*[6] reported that enamel exposed to a CO_2 laser or an yttrium aluminum garnet laser is highly acid-resistant. In this study, we tested the effect of CO_2 laser irradiation on the hydroxyapatite cement formation. The formation was accelerated by the CO_2 laser irradiation, and it also hardened the cement.

EXPERIMENTAL SECTION

Hydroxyapatite Cement The patented hydroxyapatite cement was prepared by the procedure described by Brown *et al.*,[2] except for the addition of HAP seed crystals.[7] The hydroxyapatite cement powder consisted of a mixture of 1.83 g of tetracalcium phosphate, $Ca_4(PO_4)_2O$ (TTCP); 0.86 g of dicalcium phosphate dihydrate, $CaHPO_4\ 2H_2O$ (DCPD); and 1.79 g (40%) or 0.13 g (3%) of hydroxyapatite $Ca_{10}(PO_4)_6(OH)_2$ seed crystals. Five hundred milligrams of the HAP powder was mixed with 0.25 ml of 20 mM H_3PO_4. The mixed paste was poured into a mold with a diameter of 13 mm, and stored at 37°C and 100% RH for 24 h. After the cement was fixed, it was irradiated

with a CO_2 laser (Model 60Z, Nippon Infrared Ind.) at 50 W for 2 s. The laser beam width was 14 mm in diameter. The hardness of the cement was measured by a Vickers hardness tester (model M, Shimadzu). A load of 1.0 kg was applied to the cement for 10 s, then the diagonal length of the indentation was measured.

Characterization

X-ray powder diffraction profiles and infrared spectra (KBr disk method) of the HAP cement were measured using a powder X-ray diffraction analysis system (XD-3A, Cu radiation, 15 mA, 35 kV, Shimadzu) and FT-IR spectrophotometer (type 1600, Perkin Elmer), respectively.

RESULTS AND DISCUSSION

Figure 1 shows the effect of CO_2 laser irradiation on the X-ray diffraction profiles of the HAP cement. The fixed HAP cement samples before and after laser irradiation exhibited typical HAP patterns. After laser irradiation the diffraction peaks of the cement became somewhat sharper than those before irradiation. However, the diffraction peaks of the cements were broader than those of the synthetic HAP. Munemiya et al.[8] reported that low-crystallinity HAP, which had a broader X-ray diffraction profile, had a higher affinity to hard tissue than the high crystallinity HAP. It is thought that the HAP transformed from the cement system has a high affinity to hard tissue.

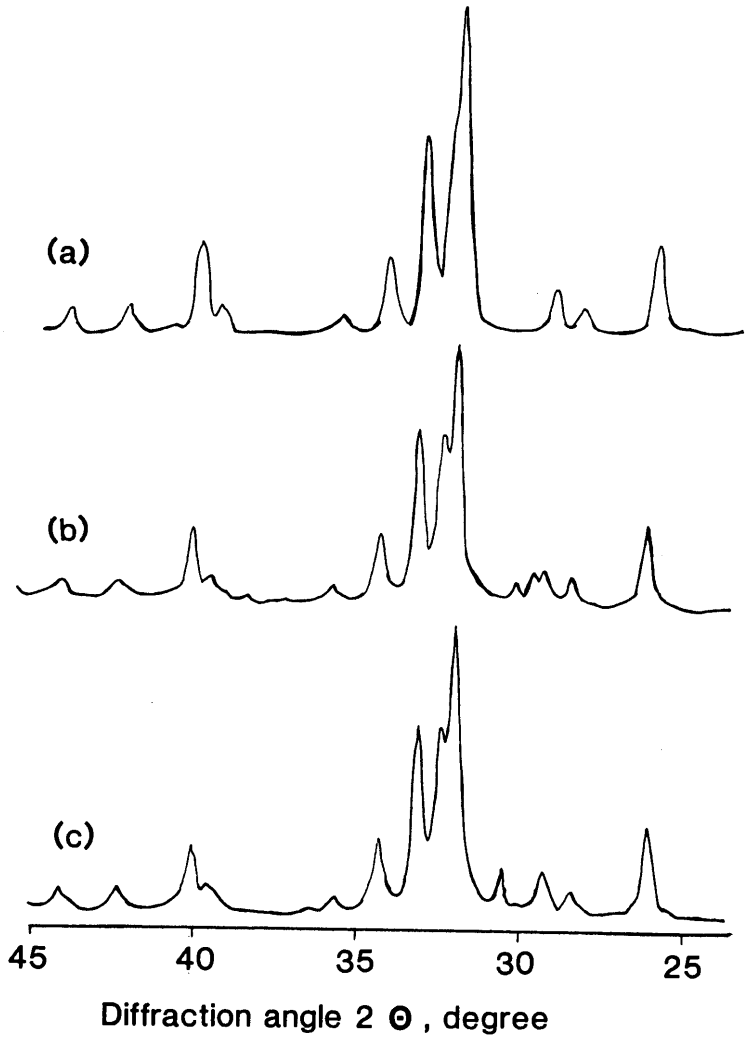

Fig. 1. Effect of Laser Irradiation on X-Ray Powder Diffraction Profiles of Hydroxyapatite Cement (a) Synthetic hydroxyapatite; (b) hydroxyapatite cement; (c) laser-irradiated cement.

Table I. Effect of Laser Irradiation on the Vikers Hardness of Hydroxyapatite Cement

	Vickers hardness of hydroxyaptite cement system	
	3% seed crystal ± S.D. (kg/cm^2)	40% seed crystal ± S.D.(kg/cm^2)
Intact	294±8	295±2
50 W, 2 s, 1 time	407±4	344±21
50 W, 2 s, 3 times	602±56	362±42
50 W, 2 s, 5 times	493±27	387±13

S.D.; standard deviation (n=4).

The effect of CO_2 laser irradiation on the IR spectra of HAP cement was studied using FT-IR spectroscopy. The HAP cements before and after irradiation showed the typical IR spectrum of HAP. HAP crystals absorbed CO_2 laser light energy very well because the wave number of the CO_2 laser light was 10.6 um (943 cm^{-1}) and adjusted to the IR absorption band of the phosphate group at 930- 1100 cm^{-1}.[9] The surface mechanical strength of the fixed HAP cements are shown in Table I. The tooth enamel surfaces irradiated at low energy densities (10-60 J/cm^2) had reduced subsurface acid demineralization compared with unirradiated controls,[10] but the teeth were decomposed by irradiation energy higher than 100 J/cm^2.[11] Therefore, the irradiation density of 64.9 J/cm^2 (50W, 2 s) was used in the laser irradiation to prevent damaging the of surrounding hard tissue. The Vicker's hardness of laser-irradiated HAP cement containing 3% or 40% seed crystals noticeably increased with the number of laser irradiations. The laser-irradiated HAP cement containing 3% seed crystals was harder than that containing 40% seed crystals. This showed that the cement system containing a lower percentage of seed crystals was hardened to a greater extent by the CO_2 laser irradiation. Munemiya et al.[8] reported that the low crystallinity of HAP was transformed the to high crystallinity of that after heat-treatment at 250 - 1250°C. It is thought that part of the HAP with the lower crystallinity, which was transformed from TTCP and DCPD, was recrystallized to a high crystallinity by the laser energy.

REFERENCES

1) F. Magee, 12th Annual Meeting of the Society for Biomaterials, **1986**, 135.
2) W. E. Brown and C. L. Chow, U.S.Patent 4,612,053 (1986).
3) D. B. Apfelberg, M. R. Maser, and H. Lash, Ann. Plast Surg., **12**, 355 (1984).
4) R. H. Stern and R. E. Sognnaes, J. Am. Dent. Assoc., **73**, 838 (1966).
5) H. Yamamoto and K. Sato, J. Dent. Res., **59**, 2171 (1980).
6) J. Wong, M. Otsuka, W. I. Higuchi, G. L. Powell, and J. L. Fox, J. Pharm. Sci., **79**, 510 (1990).
7) Y. Doi, Y. Takezawa, S. Shibata, N. Wakamatsu, H. Kamemizu, T. Goto, M. Ijima, Y. Moriwaki, K. Uno, and Y. Haeuchi, J. Jpn. Soc. Dental Materials and Devices, **6**, 53 (1987).
8) M. Munemiya, S. Niwa, K. Sawai, T. Mitsui, S. Takahashi, M. Kuroda, Y. Sugitou, F. Takayanagi, M. Sato, S. Yamazaki, H. Tagai, M. Ono and K. Fukuda, Central Jpn. J. Orthopaedic and Traumatic Surgery, **24**, 1267 (1981).
9) D. G. A. Nelson, M. Shariati, R. Glena, C. P. Shields, and J. D. B. Featherstone, Caries Res., **20**, 289 (1986).
10) H. Yamamoto and K. Ooya, J. Oral. Path., **3**, 7 (1974).
11) T. Shimizu, Dental Materials and Devices, **3**, 95 (1984).

(Received January 10, 1991)

STUDIES ON SIALIC ACIDS XXIV. SYNTHESIS OF 2,7-ANHYDRO-*N*-ACETYLNEURAMINIC ACID

Kimio FURUHATA, Kazuyoshi TAKEDA, and Haruo OGURA*

School of Pharmaceutical Sciences, Kitasato University, 5-9-1 Shirokane, Minato-ku, Tokyo 108, Japan

The first synthesis of 2,7-anhydro-*N*-acetylneuraminic acid, a sialic acid, has been completed efficiently by intramolecular glycosidation of the *S*-(1-phenyl-1*H*-tetrazol-5-yl) glycoside derivative of *N*-acetylneuraminic acid (5) using silver triflate - bis(acetonitrile)palladium(II) chloride as a promoter.

KEYWORDS sialic acid; 2,7-anhydro-*N*-acetylneuraminic acid; intramolecular glycosidation; silver triflate; bis(acetonitrile)Pd(II) chloride; benzoylation; *S*,*S*'-bis(1-phenyl-1*H*-tetrazol-5-yl) dithiocarbonate

Sialic acid containing intramolecular glycoside, 2,7-anhydro-*N*-acetylneuraminic acid (1), was isolated in a free form from cerumen of the wet type by Suzuki *et al.*[1] Moreover, Li *et al* recently found that leeches contain a novel sialidase which releasses 1 almost quantitatively from α-sialosylglycoconjugate.[2] Because it is available only in a small quantity from natural sources, 1 has to be synthesized in order to study its biological activities. As a part of the research program on glycosylation of sialic acid, we now report the first synthesis of 2,7-anhydro-*N*-acetylneuraminic acid and the confirmation of its structure.

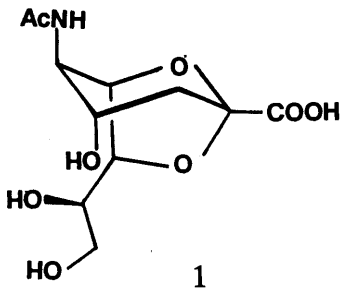

1

Several methods are available for preparing 1,6-anhydrohexopyranoses,[3,4,5] but it is very difficult to synthesize 1 by those methods. We have developed a facile method for the synthesis of 1 by the treatment of *S*-(1-phenyl-1*H*-tetrazol-5-yl) glycoside with silver triflate and palladium(II) as a promoter.[6] This procedure gave a satisfactory yield of 1. The starting material, methyl 5-acetamido-3,5-dideoxy-8,9-isopropylidene-β-D-*glycero*-D-*galacto*-2-nonulopyranosonate (2) was prepared as reported in a previous paper.[7] Benzoylation of 2 using benzoic anhydride in pyridine gave regioselectively 4-*O*-benzoyl derivative of 2 (3),[8] colorless needles, mp 151-153°C, $[\alpha]_D^{19}$ -4.6° (c=1 MeOH), $C_{22}H_{29}NO_{10}$, in 85% yield. The sterically hindered 2- or 7-OH of 2 was not benzoylated owing to low reaction with benzoic anhydride.[9] The treatment of 3 with *S*,*S*'-bis(1-phenyl-1*H*-tetrazol-5-yl) dithiocarbonate (4)[10] in acetonitrile in the presence of 4-*N*,*N*-dimethylaminopyridine gave the stable *S*-glycoside, methyl [*S*-(1-phenyl-1*H*-tetrazol-5-yl) 5-acetamido-4-benzoyl-3,5-dideoxy-8,9-isopropylidene-β-D-*glycero*-D-*galacto*-2-nonulopyranosid]onate (5),[11] colorless prisms, mp 177-178°C, $[\alpha]_D^{19}$ -187.6° (c=1 MeOH), $C_{29}H_{33}N_5O_9S$, in 75% yield. The gated proton-decoupled ^{13}C-NMR experiments evidenced the β-configuration of the anomeric center of 5 as the coupling constant $J_{1\text{-}C,3\text{-}H_{ax}}$=1.0 Hz was observed at δ 166.7 (1-C).[12]

Intramolecular glycosidation of 5 was performed in dichloromethane in the presence of silver triflate - bis(acetonitrile)palladium(II) chloride, and molecular sieves 4A to give methyl (5-acetamido-2,7-anhydro-4-*O*-benzoyl-3,5-dideoxy-8,9-isopropylidene-α-D-*glycero*-D-*galacto*-2-nonulopyranosid)onate (6),[13] white powder, $[\alpha]_D^{19}$ +91.4° (c=1 MeOH), $C_{22}H_{27}NO_9$, in 45% yield and 2-deoxy-2,3-dehydro derivative of 3 (7), colorless

needles, mp 224-225°C, $[\alpha]_D^{19}$+123.5° (c=1 MeOH), in 40% yield. In this reaction, the yield of 6 in the presence of palladium(II) was higher than that in only silver triflate. The structure of 6 was deduced from a comparison of the ^{1}H-NMR data of 3 and 6. The vicinal coupling constants on the pyranose ring in 6 were all small (1-4.5 Hz), reflecting the structural change in 3, that is, the conversion of the pyranose ring in 6 from $^2C_5$(D) to $^5C_2$(D). These results indicated that the intramolecular glycosyl linkage was formed between 2-C and 7-OH.

After removal of the isopropylidene group in 6 with 80% AcOH-H_2O at 40°C for 2 h, the product was subjected to debenzoylation with 2% MeONa-MeOH at 25°C for 4 h and the reaction mixture was neutralized at pH 5.0 with Dowex-50 (H^+) to provide a methyl ester derivative of 1 (8),[14] colorless needles, mp 95-96°C, $[\alpha]_D^{19}$ +77.8° (c=1 MeOH), $C_{12}H_{19}NO_8$ H_2O, in 90% yield. After saponification of 8 with 0.5N NaOH at 35°C for 3 h, subsequent treatment with Dowex-50 (H^+) afforded 2,7-anhydro-*N*-acetylneuraminic acid (1, 5-acetamido-2,7-anhydro-3,5-dideoxy-α-D-*glycero*-D-*galacto*-2-nonulopyranosonic acid),[15] white powder, CD(MeOH) $[\theta]_{235}^{23}$ +3550, $[\theta]_{213}^{23}$ -350, $C_{11}H_{17}NO_8$, in 95% yield, which was identified as 2,7-anhydro-*N*-acetylneuraminic acid by comparing its negative-ion (matrix; ethanolamine) FAB-MS, GC-MS,[16] and its chromatographic behavior (TLC)[1] with those of an authentic sample of 1.

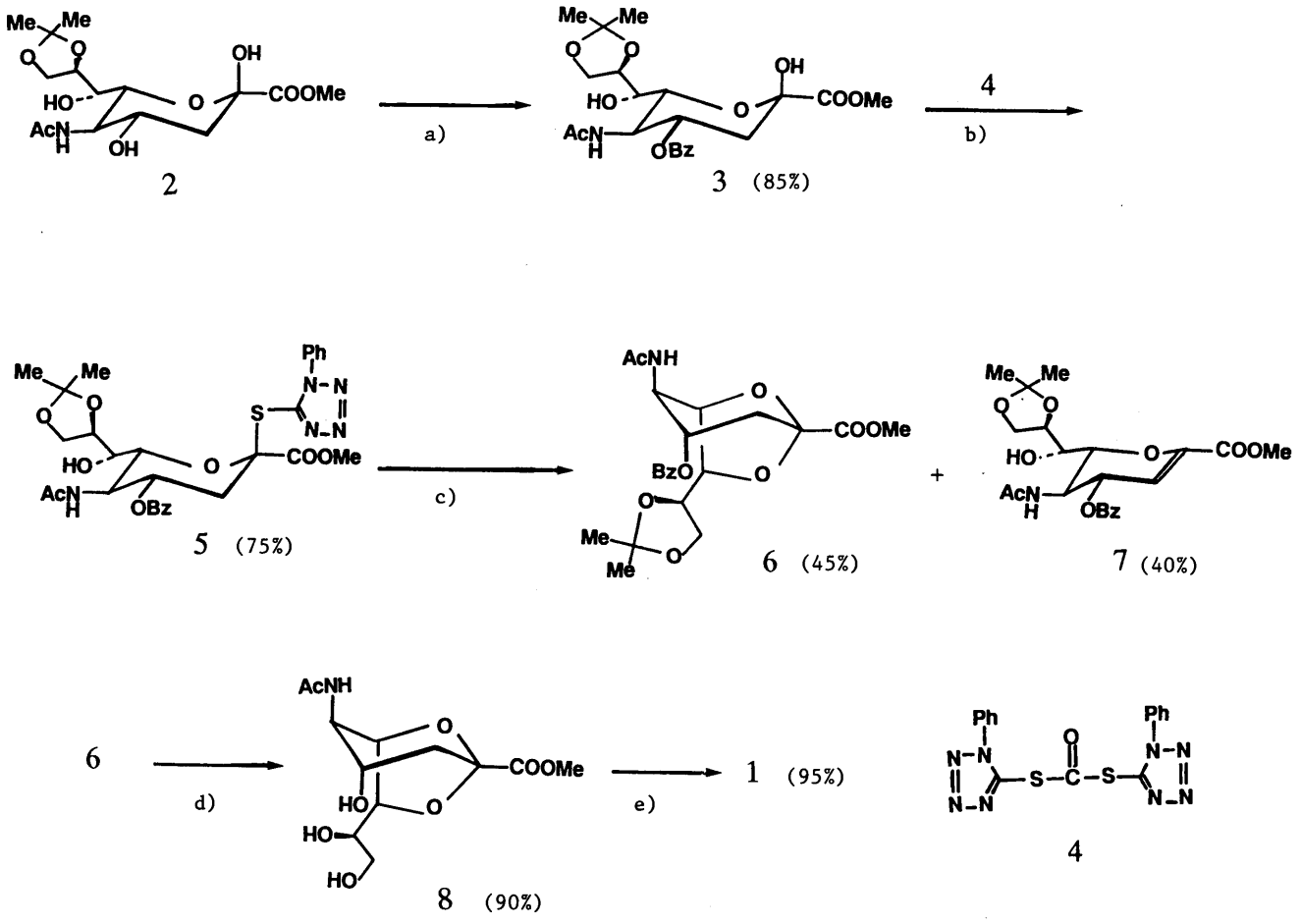

a) benzoic anhydride / pyrididne b) DMAP / MeCN c) AgOTf (2 eq) / $(MeCN)_2Pd(II)Cl_2$ (1 eq) / MS 4A / CH_2Cl_2 d) 80% AcOH-H_2O ; 2% MeONa-MeOH e) 0.5N NaOH ; Dowex-50 (H^+)

ACKNOWLEDGEMENTS We thank Dr. M. Suzuki of Tokyo Methropolitan Institute of Medical Science for the MS measurement of synthetic 1 and an authentic natural sample to identify synthetic 1.

This work was supported in part by a Grant-in-Aid for Scientific Research (63470129) from the Ministry of Education, Science and Culture, and by a grant from Suzuken Memorial Foundation.

REFERENCES AND NOTES

1) M. Suzuki, A. Suzuki, T. Yamakawa, and E. Matsunaga, J. Biochem., 97, 509 (1985).

2) Y.-T. Li, H. Nakagawa, S. A. Ross, G. C. Hansson, and S.-C. Li, J. Biol. Chem., 265, 21629 (1990).

3) M. Akagi, S. Tejima, and M. Haga, Chem. Pharm. Bull., 10, 1039 (1962).

4) I. Fujimaki, Y. Ichikawa, and H. Kuzuhara, Carbohydr. Res., 101, 148 (1982).

5) M. A. Zottola, R. Alonso, G. D. Vite, and B. Fraser-Reid, J. Org. Chem., 54, 6123 (1989).

6) The details of mechanistic aspects of this glycosylation using AgOTf - $(MeCN)_2PdCl_2$ will be reported in due course.

7) H. Ogura, K. Furuhata, S. Sato, K. Anazawa, M. Itoh, and Y. Shitori, Carbohydr. Res., 167, 77 (1987).

8) 3: ^{1}H-NMR (400MHz, $CDCl_3$) δ; 1.34 and 1.40(both 3H, s, isopropylidene), 1.95(3H, s, NHAc), 2.43(1H, t, J=12.0Hz, 3-H_{ax}), 2.33(1H, dd, J=5.0, 12.5Hz, 3-H_{eq}), 3.49(1H, br dd, J=4.5, 8.5Hz, 7-H), 3.52(3H, s, COOMe), 4.05(1H, br.d, J=8.5Hz, 6-H), 4.15(1H, dd, J=8.0, 10.0Hz, 5-H), 4.15(2H, d, J=5.5Hz, 9-H_2), 4.20 (1H, dt, J=5.5, 8.5Hz, 8-H), 4.59(1H, d, J=5.0Hz, 7-OH), 5.64(1H, dt, J=5.0, 11.0Hz, 4-H), 6.35(1H, d, J=8.0Hz, NH), and 7.42-7.98(5H, phenyl group).

9) S. Sato, K. Furuhata, and H. Ogura, Chem. Pharm. Bull., 36, 4678 (1988).

10) K. Takeda, K. Tsuboyama, K. Torii, K. Furuhata, N. Sato, and H. Ogura, Carbohydr. Res., 203, 57 (1990).

11) 5: ^{1}H-NMR (300MHz, $CDCl_3$) δ; 1.33, 1.38(both 3H, s, isopropylidene), 2.06(3H, s, NAc), 2.34(1H, dd, J= 11.0, 14.0Hz, 3-H_{ax}), 2.79(1H, dd, J=5.0, 14.0Hz, 3-H_{eq}), 3.35(3H, s, COOMe), 3.74(1H, dd, J=6.5, 8.5Hz, 9-H), 3.85(1H, br t, J=4.0Hz, 7-H), 3.99(1H, dd, J=5.5, 8.5Hz, 9-H'), 4.32(1H, dd, J=4.2, 10.0Hz, 6-H), 4.33(1H, q, J=10.5Hz, 5-H), 4.51(1H, ddd, J=4.0, 5.5, 6.5Hz, 8-H), 4.57(1H, d, J=4.8Hz, 7-OH), 5.66(1H, dt, J=5.0, 11.0Hz, 4-H), 6.82(1H, d, J=7.5Hz, NH), 7.36-7.90(10H, two phenyl groups). ^{13}C-NMR (75MHz, $CDCl_3$) δ; 22.9(NCOMe), 37.0(3-C), 50.6(6-C), 53.3(COOMe), 64.9(9-C), 68.7(4-C), 69.0(7-C), 75.9(5-C), 76.0(8-C), 108.2(2-C), 147.4(5'-C), 124.8x2, 128.4, 128.5x2, 129.6x2, 130.4x2, 133.5, 133.8(two phenyl groups), 166.7(1-C), and 173.1(NCOMe). Proton assignments were made by ^{1}H-^{1}H COSY, and carbon shifts were assigned by DEPT, ^{1}H-^{13}C COSY, and LSPD techniques.

12) H. Hori, T. Nakajima, Y. Nishida, H. Ohrui, and H. Meguro, Tetrahedron Lett., 29, 6317 (1988).

13) 6: ^{1}H-NMR (300Hz, $CDCl_3$) δ; 1.33, 1.42(both 3H, s, isopropylidene), 2.03(3H, s, NAc), 2.28(1H, dd, J= 4.5, 15.5Hz, 3-H_{ax}), 2.33(1H, dd, J=1.5, 15.5Hz, 3-H_{eq}), 3.82(3H, s, COOMe), 4.12(1H, dt, J=3.0, 8.5Hz, 9-H), 3.96-4.20(2H, m, 8-H, 9-H'), 4.36(1H, br d, J=9.0Hz, 5-H), 4.50(1H, br dt, J=3.0, 7.9Hz, 7-H), 4.65(1H, br s, 6-H), 5.17(1H, br.s, 4-H), 6.24(1H, d, J=9.0Hz,NH), and 7.45-7.98(5H, two phenyl groups).

14) 8: ^{1}H-NMR (400MHz, D_2O) δ; 1.92(3H, s, NAc), 1.98(1H, br.d, J=15.5Hz, 3-H_{ax}), 2.14(1H, dd, J=5.5, 15.5 Hz, 3-H_{eq}), 3.44(1H, ddd, J=2.5, 6.0, 7.5Hz, 8-H), 3.47(1H,dd, J=6.0, 11.0Hz, 9-H), 3.62(1H, dd, J=2.5, 11.0Hz, 9-H'), 3.74(3H, s, COOMe), 3.85(1H, br s, 5-H), 3.87(1H, br d, J=5.5Hz, 4-H), 4.43(1H, d, J=7.5 Hz, 7-H), and 4.56(1H, br s, 6-H).

15) 1: ^{1}H-NMR (400MHz, D_2O) δ; 1.91(3H, s, NAc), 1.95(1H, d, J=15.5Hz, 3-H_{ax}), 2.10(1H, dd, J=5.5, 15.5Hz, 3-H_{eq}), 3.43(1H, ddd, J=2.5, 6.0, 7.5Hz, 8-H), 3.48(1H, dd, J=7.5, 11.0Hz, 9-H), 3.63(1H, dd, J=2.5, 6.0, 7.5Hz, 9-H'), 3.84(1H, br.s, 5-H), 3.87(1H, d, J=5.5Hz, 4-H), 4.38(1H, d, J=7.5Hz, 7-H), and 4.51(1H, br s, 6-H). ^{13}C-NMR(75MHz, D_2O) δ; 22.0(NCOMe), 35.2(3-C), 52.0(5-C), 62.3(9-C), 66.7(4-C), 71.9(8-C), 77.1(7-C), 77.7(6-C), 104.8(2-C), 171.9(1-C), and 173.7(NCOMe).

16) This sample, methyl ester-trimethylsilyl derivative, of synthetic 1 was prepared as described in ref. 1.

17) The molecular composition of the compound was determined either by elemental analysis or by high resolution mass spectrometry.

(Received January 22, 1991)

CHARACTERIZATION OF CONTAMINANTS IN EMS-ASSOCIATED L-TRYPTOPHAN SAMPLES BY HIGH-PERFORMANCE LIQUID CHROMATOGRAPHY

Toshimasa TOYO'OKA, Takeshi YAMAZAKI, Tsuyoshi TANIMOTO, Kyoko SATO, Michio SATO, Masatake TOYODA, Mumio ISHIBASHI, Kunitoshi YOSHIHIRA and Mitsuru UCHIYAMA*

National Institute of Hygienic Sciences (NIHS), 1-18-1 Kamiyoga, Setagaya-ku, Tokyo 158, Japan

To identify chemical contaminant(s) associated with eosinophilia-myalgia syndrome (EMS), case and control lots of tryptophan were analyzed by HPLC with both UV and FL detection. Numerous contaminant peaks appeared on the chromatograms and some of them were identified as 5-hydroxytryptophan, indol aldehyde, indol, etc. from the retention time of authentic compounds. Among these, three peaks were significantly associated with case lots. One corresponds to di-tryptophan aminal of aldehyde (peak E). Others are unknown contaminants, UV-5 (FL-7) and UV-28 (FL-36). The structural elucidation and toxicological implication of UV-5 (FL-7) are currently in progress.

KEYWORDS eosinophilia-myalgia syndrome (EMS); tryptophan; high-performance liquid chromatography (HPLC); UV detection; FL detection

INTRODUCTION

The eosinophilia-myalgia syndrome (EMS) associated with the consumption of tryptophan products has been recognized recently.[1] The tryptophan products had been sold in tablet, capsule and powder form as a food supplement. Many patients of the EMS were located in United States of America (U.S.A.) especially in Minnesota, Oregon and some other states.[2-5] In Japan, two patients were also diagnosed as the EMS from epidemiological serveillance. However, it is still obscure whether the syndrome is caused from the consumption of excess amount of tryptophan itself or trace chemical contaminant(s) introduced by the manufacturing process.[6] According to a recent report,[7] most of the patients (97%) in U.S.A. had consumed the tryptophan products that were derived from bulk tryptophan powder manufactured between October 1988 and June 1989 by single company, Showa Denko K.K. (SDK). Recently, we obtained the storage samples of tryptophan manufactured at different time from SDK, including case lots which have been identified to be associated with EMS by case-control study. This communication describes the high-performance liquid chromatography (HPLC) analysis on case and control lots of tryptophan to identify chemical contaminants which might associate with the EMS.

RESULTS AND DISCUSSION

HPLC analysis of tryptophan samples manufactured by SDK was performed by a reversed-phase ODS column with both UV and FL detection. For accurate retention time of individual peaks, a simple linear gradient elution was selected in this work. Carboxylic acid (COOH) functional groups in the structures of tryptophan and its chemical contaminants dissociate in neutral and alkaline solutions to COO^- and H^+. The dissociation equilibria sometimes interfered with chromatographic peak separation. Therefore, the mobile phase solutions were adjusted below pH 3 with trifluoroacetic acid to suppress ionization.

Figure 1A and 1B show the typical chromatograms obtained from one of the case lots. The tryptophan was demonstrated as a large peak at 7.5-9 min. Numerous peaks besides tryptophan appeared on the chromatogram. The concentration of each peak obtained by UV detection was lower than 0.1% based upon comparison of the peak area of the contaminant with the total area of all the peaks including tryptophan in the chromatogram. The number of contaminant peaks identified was greater with FL detection; therefore, the peak number designations differ in the two types of chromatograms. The difference in the retention time of the corresponding peaks is due to the arrangement of the detectors. Some of the contaminant peaks were identified from the retention time of authentic compounds, e.g. 5-hydroxytryptophan corresponds to UV peak 3 and FL peak 4, indole aldehyde is UV peak 13, indole is UV peak 27 and FL peak 35, etc. Four other peaks, UV peaks 18, 22, 24 and 25, have been designated as peaks D, C, B and A, respectively, by the Center for Disease Control (CDC) in U.S.A. and assigned as the tryptophan analogues by the instrumental comparison of synthetic compounds. The details will be reported elsewhere by the SDK research group. Similar

chromatograms were obtained from the control lots of tryptophan.

When 30-min chromatograms with UV detection were compared between case and control lots, three peaks were significantly associated with case lots (Fig. 2). One corresponds to peak E (UV peak 15 and FL peak 21, hereafter designated as "UV-15" and "FL-21") and was assigned as a di-L-tryptophan aminal of acetaldehyde by research groups at CDC[8] and SDK.[9] The concentration of this peak in each lot is shown in Fig. 3. The others are UV-5 (FL-7) and UV-28 (FL-36). The former, UV-5, is a peak eluted before the large peak of tryptophan, the concentration of which in each lot is illustrated in Fig. 4. The lots containing UV-5 were restricted to the lots associated with the case lots (sample No. 21-26), the lots which were produced by *Bacillus amyloliquefacience* Strain V (sample No. 28, 29 and 40), and two feed grade tryptophan lots. In contrast, it does not appear in the chromatograms of control lots (Fig. 4). The presence of peak E was also identified mainly in the case lots manufactured by Strain V[7] (Fig. 3). Similar results were also obtained by the comparison of FL peaks derived from case and control lots. The latter, UV-28, was not investigated because of its lower content and far longer retention time among contaminants. Since UV-5 exhibited relatively high fluorescence intensity compared to peak E (FL/UV=7.9 versus 1.9) and was eluted earlier than tryptophan, it may be an aromatic compound with a lower molecular weight derived from intermediate steps of tryptophan production. No contaminants associated with EMS were identified from the comparison between control and case tryptophan by other analyses such as ion chromatography and gel-permeation chromatography. The structural elucidation of UV-5 is currently in progress and will be reported elsewhere. Though the amount of UV-5 in case lots is less than peak E, the possibility of associated constituent toward the EMS will be investigated further in animal experiments.

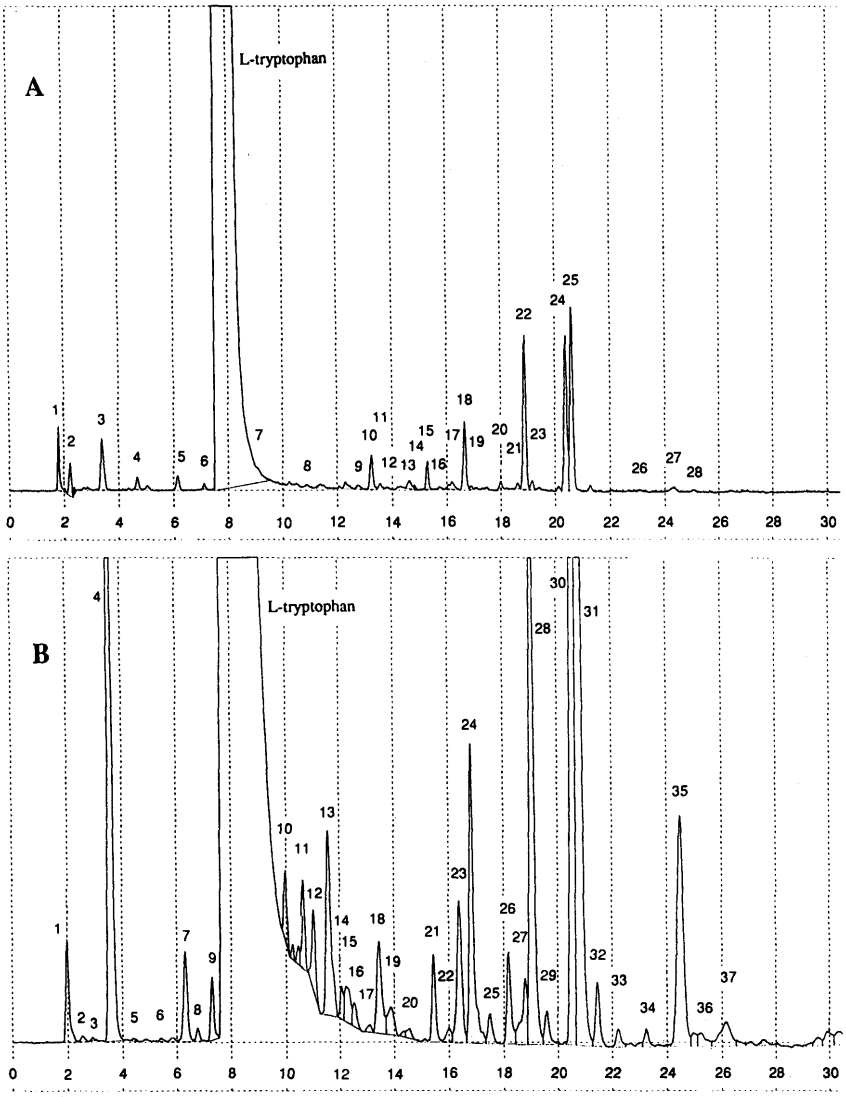

Fig. 1. Typical Chromatograms Obtained from Case Lot of Tryptophan
A: UV detection at 280nm, B: FL detection at 360nm (excitation at 290nm)

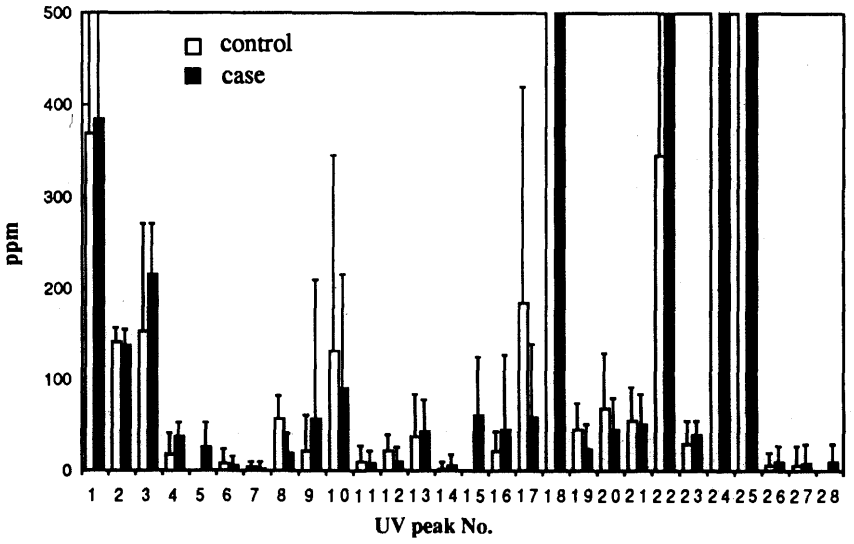

Fig. 2. Comparison of Mean Concentration of Individual UV Peaks Appeared on Case and Control Lots
Each column and bar indicate the mean and S.D., respectively (n=12 for case, n=16 for control).

MATERIALS AND METHODS

Forty storage samples of tryptophan manufactured between January 1986 and December 1989 were donated by SDK. They consisted of case, control, feed grade and other lots as illustrated in Figs. 3 and 4. The tested samples were dissolved in deionized and distilled water at 1000 ppm concentration (1 mg/ml).

High-performance liquid chromatograph (HPLC) consists of two LC-9A pumps (Shimadzu Co., Kyoto, Japan) and an SCL-6B system controller (Shimadzu). All samples (50μl each) were injected using an SIL-6B auto injector (Shimadzu). The gradient elution was controlled by an SCL-6B system controller. The analytical column used in this work was a 5-μm Inertsil ODS-2 (150 x 4.6 mm, i.d.) (GL Science, Tokyo, Japan). The column was maintained at 40°C with a 655A-52 column oven (Hitachi, Tokyo, Japan). A Hitachi 655A UV monitor equipped with an 18-μl flow cell and a Shimadzu RF-550 fluorescence (FL) monitor equipped with a 12-μl flow cell were used to detect the eluent from the column. The UV detector was placed between the analytical column and the FL detector. All mobile phases were de-gassed with an on-line degasser (DGU-3A) (Shimadzu). The flow rate of the eluent was fixed at 1.0 ml/min. A linear gradient elution from 90% A (mobile phase A = 0.1% trifluoroacetic acid in H_2O) to 90% B (mobile phase B = 0.1% trifluoroacetic acid in CH_3CN) over a period of 60 min was adopted for the separation of tryptophan and its related chemical constituents. The eluate was monitored with both UV (at 280nm) and FL (excitation at 290nm and emission at 360nm) detection. The individual peak areas, obtained from both UV and FL detectors, were calculated by a C-R4A chromatopac (Shimadzu) and compared with each other for all tryptophan samples.

ACKNOWLEDGMENT

This work was supported by a Grant-in-Aid from the Ministry of Health and Welfare in Japan. The authors thank Dr. Y. Takeda, Dr. Y. Saito, Dr. A. Nakamura, Dr. A. Tanaka, Dr. T. Maitani and Dr. T. Yamada, National Institute of Hygienic Sciences (NIHS), for their valuable suggestions and discussion. Thanks are also due to Dr. Charles R. Warner, Food and Drug Administration (FDA) in U.S.A., for his valuable suggestions on the manuscript, and Showa Denko K.K. for the donation of tryptophan samples.

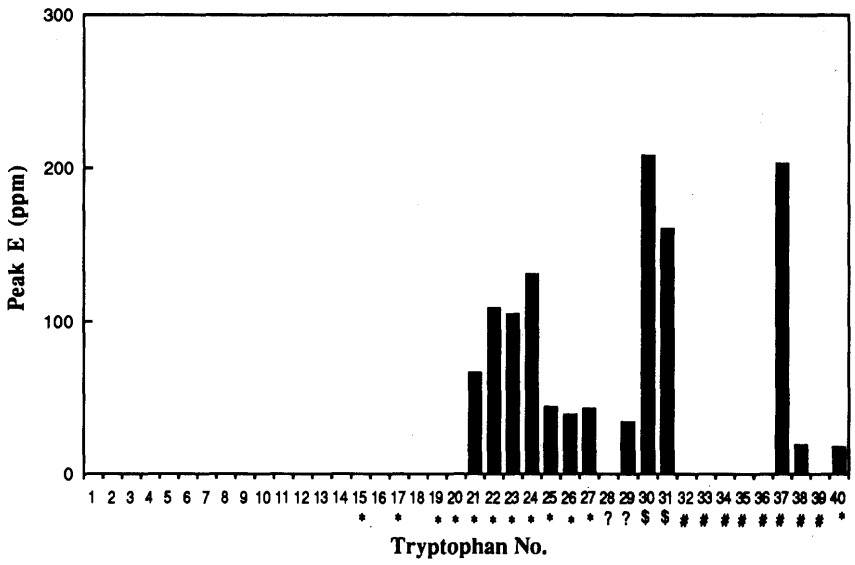

Fig. 3. Concentration of Peak E Obtained from UV Detection in Various Lots of Tryptophan
Control: no mark, case: *, feed grade: $, and others (produced by strain V: ? and produced by strain III: #).

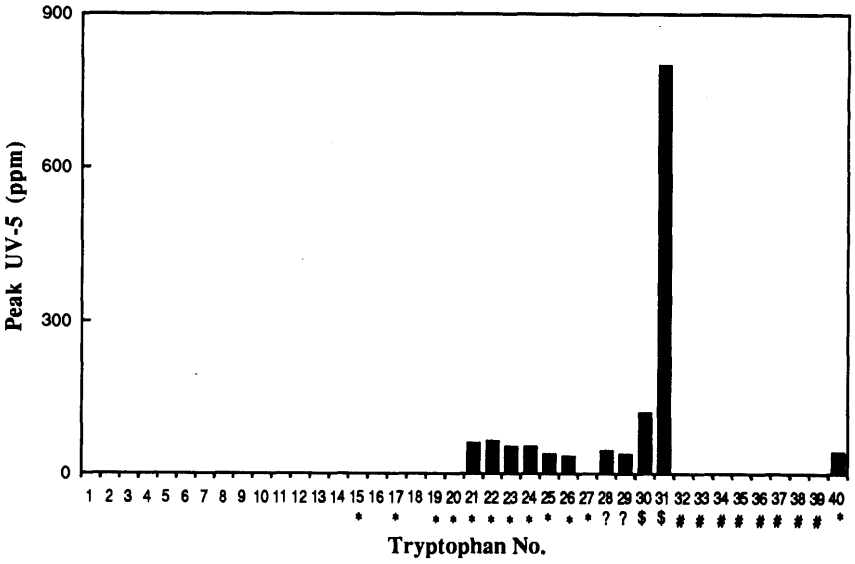

Fig. 4. Concentration of Unknown UV Peak in Various Lots of Tryptophan
The marks (no mark, *, $, ? and #) are the same as those of Fig. 3.

REFERENCES

1) P.A. Hertman, W.L. Blevins, J. Mayer, B. Greenfield, M. Ting and G.J. Gleich, *N. Engl. J. Med.*, **322**, 869-873 (1990).
2) M.T. Flannery, P.M. Wallach, L.R. Espinoza, M.P. Dohrenwend and L.C. Moscinski, *Ann. Intern. Med.*, **112**, 300-301 (1990).
3) W.D. Travis, M.E. Kalafer, H.S. Robin and F.J. Luibel, *Ann. Intern. Med.*, **112**, 301-303 (1990).
4) B. Amor, G. Rajzbaum, S. Poiraudeau, C. Haas and A. Kahan, *Lancet*, **335**, 420 (1990).
5) Eosinophilia-myalgia syndrome and L-tryptophan-containing products - New Mexico, Minnesota, Oregon, and New York. *MMWR*, **38**, 785-788 (1989).
6) E.R. Bernhart, V.L. Maggio, L.R. Alexander, W.E. Turner, D.G. Patterson Jr., L.L. Needham, M.H. Reilly and L.T. Gelbaum, *Lancet*, **336**, 742 (1990).
7) E.A. Belongia, C.W. Hedberg, G.J. Gleich, K.E. White, A.N. Mayeno, D.A. Loegering, S.L. Dunnette, P.L. Pirie, K.L. MacDonald and M.T. Osterholm, *N. Engl. J. Med.*, **323**, 357-365 (1990).
8) Update: Analysis of L-tryptophan for the etiology of eosinophilia-myalgia syndrome. *MMWR*, **39**, 789-790 (1990).
9) K. Sakimoto, *N. Engl. J. Med.*, **323**, 992-993 (1990).

(Received January 23, 1991)

SYNTHESIS OF CHIRAL 3-SUBSTITUTED γ-LACTONES AND 9-FURANOSYL-ADENINE FROM (*R*)-2-(2,2-DIETHOXYETHYL)-1,3-PROPANEDIOL MONOACETATE PREPARED BY LIPASE-CATALYZED REACTION

Yoshiyasu TERAO, Minoru AKAMATSU, and Kazuo ACHIWA*
School of Pharmaceutical Sciences, University of Shizuoka, 395 Yada, Shizuoka 422 ,Japan

A chiral building block, (*R*)-2-(2,2-diethoxyethyl)-1,3-propanediol monoacetate was synthesized in high optical and chemical yields by lipase-catalyzed transesterification. From this compound, we synthesized chiral 3-substituted γ-lactones and a new nucleoside with antiviral activity.

KEYWORDS lipase; asymmetric synthesis; γ-lactone; nucleoside; A-factor

Enzyme-catalyzed asymmetric synthesis has become one of the practical methods for production of useful chiral molecules because of the development of enzyme preparation and the advantages of enzymatic reactions such as the high stereospecificity of enzyme and mild reaction conditions.[1] In particular, the reaction in organic media is an extremely convenient procedure.[2] In this paper we describe the efficient synthesis of optically pure (*R*)-2-(2,2-diethoxyethyl)-1,3-propanediol monoacetate (**1b**) by lipase-catalyzed transesterification in a noneaqueous system and its utility for the syntheses of optically active 3-substituted γ-lactones and a unique nucleoside with antiviral activity.

We have reported that lipase-catalyzed transesterification of 2-substituted 1,3-propanediols in vinyl acetate gave optically active monoesters in high optical and chemical yields,[3] where lipase P (*pseudomonas fluorescens*) and lipase B (*Pseudomonas fragi*) were well adapted to the substrates.[4] When 2-(2-benzyloxyethyl)-1,3-propanediol was allowed to react in vinyl acetate, the corresponding (*R*)-monoacetate (**1a**) was obtained in moderate optical yield. However, lipase P in the 2-(2,2-diethoxyethyl)-1,3-propandiol showed extremely high enantioselectivity (entry 3 in Table I). The absolute configuration of both products were determined as the *R* form by conversion into the (*S*)-(-)-2-methyl-1,4-butanediol reported previously.[5] (*R*)-2-(2,2-Diethoxyethyl)-1,3-propanediol monoacetate (**1b**)[6] is a useful chiral building block with three easily convertible functional groups at an asymmetric carbon even though it is a simple molecule.

Table I. Lipase-Catalyzed Transesterification[a]

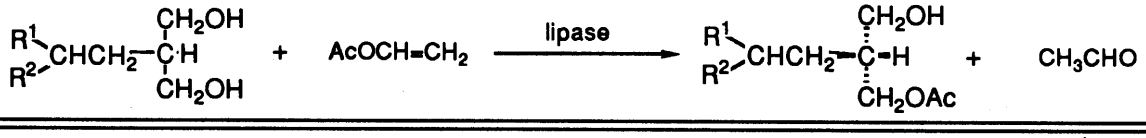

Entry	Substrate R^1	Substrate R^2	Lipase	Reaction time(h)	Product No.	Yield (%)	Optical yield[b] (%ee)
1	$PhCH_2O$	H	lipase P	1.0	**1a**	90	81
2	$PhCH_2O$	H	lipase B	0.5	**1a**	82	55
3	C_2H_5O	C_2H_5O	lipase P	1.0	**1b**	95	98
4	C_2H_5O	C_2H_5O	lipase B	1.0	**1b**	89	82

a) All reactions were carried out with substrate (5 mmol), vinyl acetate (7.5mmol), and lipase P (100mg) or lipase B (50mg) at 20°C. *b)* Optical yields were determined by HPLC analyses (after benzoylation in entries 3 and 4) using a column packed with Chiralcel OD (2-propanol / n-hexane system).

(*S*)-3-Methyl-γ-lactone, from which the side chain of α-tocopherol was prepared[7], was synthesized as shown in Chart 1. The reaction and isolation procedures in each step were carried out in the usual manner. The structure of the final product (**5**) was determined by its spectral data and the specific rotation was in agreement with the reported value.[8]

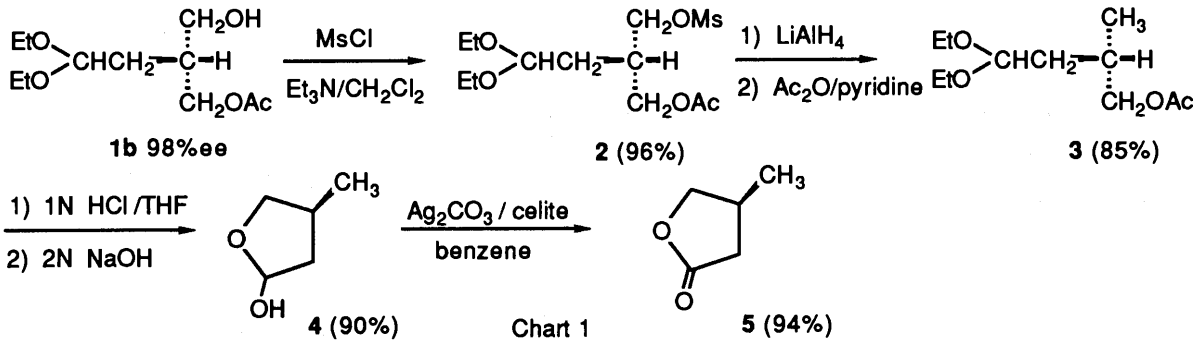

Chart 1

Our next synthesis target was A-Factor which had been isolated from *Streptmyces griseus* as the inducer for the production of streptomycin by Khokhlov.[9] By using **1b**, A-factor was successfully synthesized according to the route described in Chart 2.

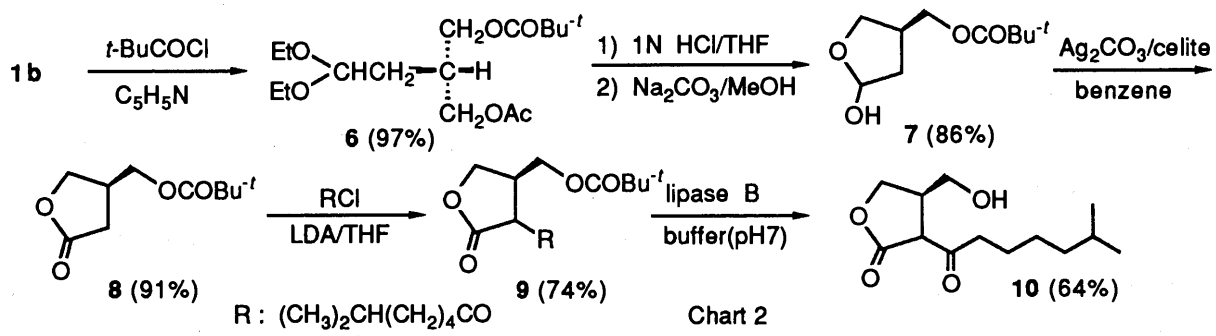

Chart 2

After hydrolysis of the acetal moiety of **6**, treatment with 10% aqueous Na_2CO_3 in methanol gave the required (2-hydroxy-4-(*S*)-tetrahydrofuranyl)methyl pivalate (**7**). The lactone **8** obtained by Fetizon's oxydation of **7** was acylated with 7-methylheptanoyl chloride in the presence of LDA at -70°C. Because of the lability of the final product (**10**) the hydrolysis of the pivalic acid ester group of **9** was carried out with lipase B catalyst in a neutral buffer solution. The spectral data[10] and specific rotation of product **10** were quit like those reported.[11]

In the course of this work, we focused on hemiacetal (**7**) because the nucleosides with various sugar moeties showed antiviral activities [12] and **7** seems to be a unique sugar moiety which does not exist in nature. The protected 6-[2,3,4-trideoxy-3-hydroxymethyl)furanosyl]adenine (**12**) was synthesized according to the reported method[13] from the fully silylated N^6-benzoyladenine prepared *in situ* and the acetate of **7** in the presence of stannic chloride.

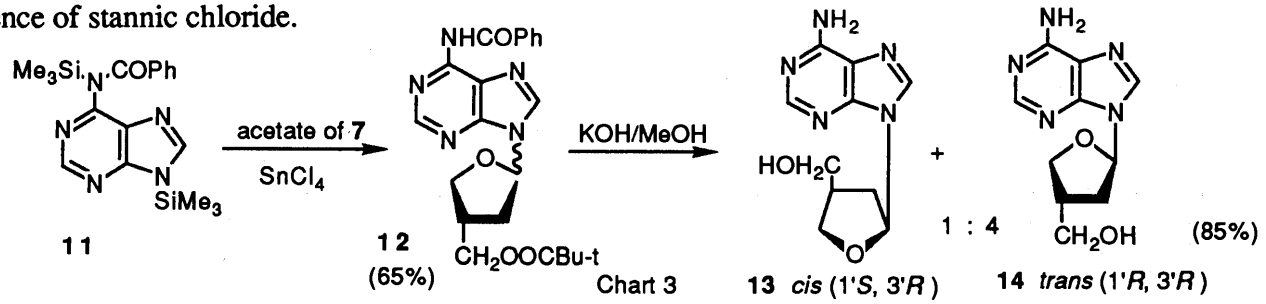

Chart 3

13 *cis* (1'*S*, 3'*R*) 14 *trans* (1'*R*, 3'*R*)

After deprotection with alkaline methanol, the adenosine obtained was a 1:4 mixture of 1,3-*cis* (**13**) and 1,3-*trans* isomer (**14**).[14] The preliminary examination of their biological activities indicated that the 1,3-*cis* isomer (**13**) had anti-HIV activity in MT-4 cells, and no cytotoxicity.

ACKNOWLEDGEMENT This work was supported in part by a Grant-in-Aid for Scientic Research from Suzuken Memorial Foundation.

REFERENCES AND NOTES

1) J. B. Jones, *Tetrahedron*, **42**, 3351 (1986); H. Yamada and S. Shimizu, *Angew. Chem. Int.Ed.Engl.*,**27**, 622 (1988); M. Ohno and M. Otsuka, *Organic Reactions*, Vol. **37**, pp. 1-51, John Wiley & Sons, Inc., New York 1989.

2) For a recent review: A. M. Klibanov, *Acc. Chem. Res.*, **23**, 114 (1990).

3) Y. Terao, M. Murata, K. Achiwa, T. Nishio, M. Akamatsu, and M. Kamimura, *Tetrahedron Lett.*, **29**, 5173 (1988); K. Tsuji, Y. Terao, and K. Achiwa, *ibid.*,**30**, 6189 (1989).

4) Lipase P and lipase B were kindly supplied by Amano Pharmaceutical Co. and Sapporo Breweries Ltd., respectively.

5) R. Rossi, P. Diversi, and G. Ingrosso, *Gazz. Chim. Ital.*, **98**, 1391 (1971).

6) **1b**: IR(neat)cm^{-1}: 3410, 1730, ^{1}H-NMR($CDCl_3$) δ: 1.12(6H, t, J=7.0Hz, 2xCH_3), 1.55-1.85 (3H, m, -CH_2CH<), 2.02(3H, s, $COCH_3$), 2.30(1H, br.s, OH), 3.30-3.60(6H, m, -C$\underline{H_2}$OH, 2xC$\underline{H_2}$O-), 4.05(2H, d, J=6Hz, CH_2OAc), 4.65(1H, t, J=5.5Hz, -$CH(OEt)_2$).

7) H. Leuenberger, R. Barnar, W. Boguch, M. Schmid, and R. Zell, *Helv.*, **62**, 455 (1979).

8) **6**: $[a]_D^{20}$ -25.4°(*c*=1.0, MeOH), [*lit.*[7], $[a]_D^{20}$ -24.7°(*c*=4.0, MeOH)], IR(neat)cm^{-1}: 1765, ^{1}H-NMR ($CDCl_3$) δ: 1.16(3H, d, J=6.4Hz, CH_3), 2.13(1H, dd, J_1,J_2=10.2Hz, -C$\underline{H_A}H_B$CO), 2.61-2.68(2H, m, . >CH-, -CH_AC$\underline{H_B}$CO), 3.87(1H, dd, J=6.2, 9.2Hz, -C$\underline{H_A}H_B$-), 4.41(1H, dd, J=6.9, 9.2Hz, -O$CH_A\underline{H_B}$-), ^{13}C-NMR($CDCl_3$) δ: 17.9, 30.4, 36.1, 74.7, 177.3, Ms(*m/z*): 100(M^+).

9) E. M. Kleiner, S. A. Pliner, U. S. Soiber, V. V. Onoprienko, T. A. Balashova, B. V. Rosynov, and A. S. Khokhlov, *Bioorg. Khim.*, **2**, 1142 (1976).

10) **10:** $[a]_D^{20}$ -12.7°(c=1.0, $CHCl_3$), [lit.[11], $[a]_D^{20}$ -13.1°(c=1.18, $CHCl_3$) or -12.5°(c=1.10, $CHCl_3$)], IR(neat)cm^{-1}: 3640, 1765, 1720, ^{1}H-NMR($CDCl_3$) δ: 0.86(6H, d, J=6.9Hz), 1.1-1.8(9H, m), 2.5-3.3(3H, m), 3.5-3.85(2H, m), 4.0-4.3(2H, m), ^{13}C-NMR($CDCl_3$) δ: 22.5, 23.5, 26.5, 27.8, 38.6, 39.1, 42.5, 54.9, 61.8, 69.0, 172.4, 202.9, MS(*m/z*): 242 (M^+).

11) K. Mori and K. Yamane, *Tetrahedron*, **38**, 2919 (1982); K.Mori and N. Chiba, *Ann.*, **1990**, 31.

12) H. Mitsuya, K. J. Weinhold, P. A. Furman, M. H. St. Clair, S. N. Lehrman, R. C. Gallo, D. Bolognesi, D. W. Barry, and S. Broder, *Proc. Natl. Acad. Sci., U.S.A.*,**82**, 7096 (1985); J. A. Warshaw and K. A. Watanabe, *J. Med. Chem.*, **33**, 1663 (1990) and see refferences cited therein.

13) M. Yamashita, Y. Kawai, I. Uchida, T. Komori, M. Kohsaka, H. Imanaka, K. Sakane, H. Setoi, and T. Teraji, *J. Antibiot.*, **37**, 1284 (1984).

14) The ^{1}H- as well as the ^{13}C-NMR spectra of **13** and **14** were similar to each other and their elemenents were satisfactorily analysed. The isomeric structures were also supported by the results of the nuclear Overhauser effect (NOE).

(Received February 1, 1991)